Proceedings of

Finnish Center of Excellence in 'Physics, Chemistry, Biology and Meteorology of Atmospheric Composition and Climate Change', and Nordic Center of Excellence in 'Cryosphere-Atmosphere Interactions in a Changing Arctic Climate'

Annual Meetings 2012

Editors: Markku Kulmala, Hanna K. Lappalainen, Michael Boy, Magdalena Brus and Tuomo Nieminen

Helsinki 2012

TABLE OF CONTENTS

FINNISH CoE IN PHYSICS, CHEMISTRY, BIOLOGY AND METEOROLOGY OF ATMOSPHERIC COMPOSITION AND CLIMATE CHANGE RESULTS AND ACTIVITIES IN 2011-2012

MARKKU KULMALA[1], HANNA K. LAPPALAINEN[1,3] JAANA BÄCK[1,2], ARI LAAKSONEN[3,4], EERO NIKINMAA[2], MARJA-LIISA RIEKKOLA[5], TIMO VESALA[1], YRJÖ VIISANEN[3], MICHAEL BOY[1], MIIKKA DAL MASO[1], HANNELE HAKOLA[3], PERTTI HARI[2], KARI HARTONEN[5], VELI-MATTI KERMINEN[1,3], ANTTI LAURI[1], TUOMAS LAURILA[3], HEIKKI LIHAVAINEN[3], TUUKKA PETÄJÄ[1], JANNE RINNE[1], SAMI ROMAKKANIEMI[4], SANNA SORVARI[1,3], HANNA VEHKAMÄKI[1] + the FCoE TEAM

[1]Department of Physics, University of Helsinki, Finland
[2]Department of Forest Sciences, University of Helsinki, Finland
[3]Finnish Meteorological Institute, Finland
[4]Department of Physics, University of Eastern Finland, Kuopio Unit, Finland
[5]Department of Chemistry, University of Helsinki, Finland

BACKGROUND AND SCOPE

The ongoing Finnish Center of Excellence (FCoE$_2$) in *Physics, Chemistry, Biology and Meteorology of Atmospheric Composition and Climate Change* is a research activity targeted for the years 2008-2013. It is originated from work of the FCoE$_1$ in "*Physics, Chemistry and Biology of Atmospheric Composition and Climate change*" for 2002-2007 and is based on the supra-disciplinary research approach by the research teams from Departments of Physics, Chemistry and Forest Sciences at the University of Helsinki, Finnish Meteorological Institute and Department of Physics at the University of Eastern Finland.

The ongoing FCoE$_2$ has set its objectives on creating a deep understanding on the dynamics of aerosol particles and ion and neutral clusters in the lower atmosphere. This scientific approach emphasizes the role of biogenic formation mechanisms and their linkage to biosphere-atmosphere interaction processes, biogeochemical cycles and trace gases. Furthermore, the scientific scope of the FCoE$_2$ has moved towards an all scale concept, while the objectives of the previous FCoE$_1$ (2002-2007) where targeted to understanding the couplings between CO_2 concentrations, photosynthesis, biogenic volatile organic compounds (BVOCs) and aerosols particle concentrations (Kulmala et al. 2004). The relevance and usage of the FCoE$_2$ results starting from the molecular scale modeling is targeted to improve global scale predictions of the climate change (Fig.1).
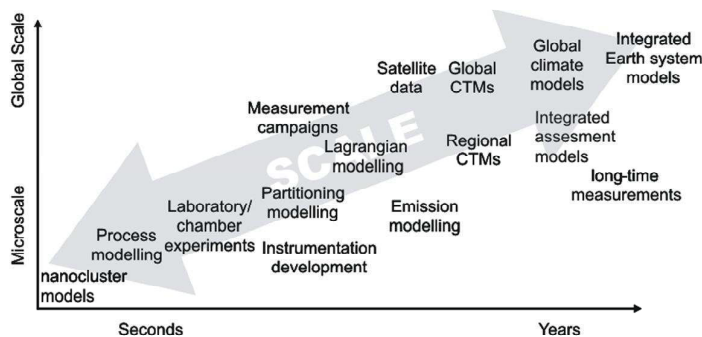
Figure 1. The FCoE$_2$ scientific approach is based on the all scale approach providing new knowledge at process level to be implemented into Earth system models at the global scale.

Here we summarise the activities and scientific highlights of FCoE$_2$ for the period 1.Jun.2011-31.Aug.2012. This overview identifies the most important (i) methodological developments and new data pools, (ii) scientific approach & scientific highlights, (iv) research collaboration and training and (v) climate policy and public outreach activities of the reporting period. Also the vision of the future prospects for the FCoE is outlined.

DEVELOPMENT OF NOVEL METHODS AND DATA POOLS

The key strength of the FCoE$_2$ approach has been a successful combination of new methods, instrument development, and comprehensive measurements, which have been used to improve fundamental process understanding and to develop parameterizations to various models. As a synthesis of a long-span instrument development on aerosol measurement the team published this year a scientific protocol on the measurement of the nucleation of atmospheric aerosol particles in Nature Protocols (Kulmala et al. 2012). The protocol describes the procedures for identifying new-particle-formation (NPF) events, and the methods for determining the nucleation, formation and growth rates during such events under atmospheric conditions. Also the descriptions of the present instrumentation, best practices and other tools used to investigate the atmospheric nucleation and the NPF at a certain mobility diameter (1.5, 2.0 or 3.0 nm) are addressed. Furthermore, the reliability of the methods used and requirements for the proper measurements and data analysis are discussed (Kulmala et al. 2012 and Petäjä et al., this issue). This work provides a summary of methodology development within the FCOE$_2$ during the last two decades. It will be used as a benchmark, to which future research on the experimental nanoparticle formation in the atmosphere will be compared to.

Furthermore, in 2011 and 2012 we have made several important breakthroughs in the laboratory and field measurement techniques. We have generated (i) new laboratory techniques to analyse the atmospheric aerosol particle composition and developed (ii) systems measuring different types of biological activity and ecosystem emissions. To ensure the state of the art data pools also in the future, we have continued our (iii) active and visible participation of the large (European scale) integrated field and laboratory experiments. Furthermore, the FCoE groups have been intensively involved with a super-site concept development in Europe and outside Europe. In spring 2012, the Chinese research bodies introduced a SMEAR-type station near Nanjing (Petäjä et al., this issue). In addition, the co-operation to establish atmospheric measurement stations in Estonia, South Africa and Saudi Arabia is on the way. We are also involved in a collaboration to establish a state of the art, long term measurement station to Siberia (Tiksi) in Russia (Asmi et al. 2012), especially to attain year-round observations of important climate forcing agents within the Russian side of the Arctic (Lihavainen et al., this issue). These collaborations are a direct consequence of the FCoE$_2$ activities.

(i)   New laboratory techniques on aerosol composition

The new laboratory techniques for analyzing the atmospheric aerosol particle composition cover the identification of organic compounds in different size atmospheric aerosol particles as well as determination of aliphatic and aromatic amines in atmospheric aerosol particles and vapor pressures of several atmospherically relevant compounds. Comprehensive two-dimensional gas chromatography coupled to time-of-flight mass spectrometry has been used for the screening and quantitation of semi-volatile organic compounds in different size atmospheric aerosol particles: ultrafine 30 nm, 50 nm and total suspended particles. The air samples have been collected at the Hyytiälä Station for Measuring Forest Ecosystem-Atmosphere Relations (SMEAR II). The exploitation of the mass spectra and retention index information has allowed the identification of more than 400 organic compounds. Two different classifications of the samples have been developed. One is based on the distribution of the main functional groups, and another on the specific element present in the molecule of the identified compounds. These classifications enable the successful clarification of the aerosol particle composition and the influence of

the aerosol size on the chemical composition of the particles. DMA was used for the separation of 50 nm aerosol particles prior to quartz/Teflon filter sampling (Riekkola et al., this issue).

Furthermore, a complete methodology was developed for the determination of ten aliphatic and nine aromatic amines in atmospheric aerosol particles. The developed methodology was successfully applied to the determination of the target analytes in eight size separated ultrafine particulate (Dp = 30 ± 4 nm) samples and in eight total suspended particulate samples collected at the SMEAR II station. 13 amines were quantified for the first time in 30 nm aerosol particles (Riekkola et al., this issue).

A novel gas chromatographic methodology for the determination of vapour pressures of compounds in mixtures was developed and utilized in aerosol studies. Vapor pressures of several atmospherically relevant compounds were determined for the first time. The method proved to be superior over all the existing techniques in terms of time, sensitivity, precision and sample preparation (Riekkola et al., this issue).

(ii)   Proper accounting for measurement uncertainties on particle size distribution from multiple simultaneous measurements

We have worked on a long-standing question in aerosol science about how to combine the measurement data from several instruments. Current methods possess limiting assumptions concerning the overlapping measurement ranges and have difficulties in properly accounting for measurement uncertainties. For this purpose, we have implemented an Extended Kalman Filter (EKF) and applied it to generate state estimates of the particle size distribution from multiple simultaneous measurements, namely from Differential Mobility Particle Sizer (DMPS), Aerodynamic Particle Sizer (APS) and nephelometer (Viskari et al, 2012a, b). The results indicate that the EKF is a very promising alternative to the instrument-specific inversion techniques and seems to alleviate many deficiencies of the current techniques, such as unrealistic solutions in the overlapping measurement ranges. The increased physical realism is due to the fact that a detailed microphysical aerosol model, the so-called UHMA model, is used to propagate the state estimation in time (Lihavainen et al., this issue).

(iii)   Systems measuring different types of biological activity and ecosystems

The measurements on biological activity of living biota and on the biosphere-atmosphere interface are crucial links in the FCoE scientific scope. During 2011 and 2012 the teams have made major progress in tree related physiological analysis, measuring aquatic ecosystem gas exchange, peatland methane emissions and detecting biogenic VOC (amines, sesquiterpenes) compounds in field conditions.

A new understanding on tree scale structures and functions can be based on a method, which we have developed to estimate sugar transport in phloem that is based on diurnal variation of xylem and phloem thickness. The optimal carbon usage and pit size structure of water transporting cells explains the structure of tree vascular system (Hölttä et al. 2012). Furthermore, a theory to explain tree structure has been published (Hölttä et al. 2011, Mencuccini et al. 2011). New understanding on coupling xylem and phloem transport (Sevanto et al. 2011) based on structural-functional models was published. Further, a method to combine process based modelling and measured ecophysiological data to analyse the effects of nitrogen nutrition on tree growth has been developed. The model was applied to hybrid poplar in Quebec. The model showed that changes in photosynthetic capacity are the most important determinants of growth in the poplars, whereas changes in allocation were less (Bäck et al., this issue).

We have started the first measurements on aquatic ecosystem gas exchange and analyzed the related methodological aspects of these measurements (Vesala et al., this issue, Bäck et al., this issue). There are only seven articles reporting eddy-covariance EC measurements of CO_2 fluxes over lakes (see Vesala et

al., 2012), and none over rivers, and the lengths of the records are rather short. We conducted the first long-term, ecosystem level CO_2 flux measurements with eddy covariance technique in a boreal lake within a natural state catchment, covering 5 years. On average, the lake emitted ca 10% of the terrestrial net ecosystem production of the surrounding old growth forest and the main immediate drivers behind the fluxes were physical rather than biological. Our results suggest that lakes are an integral part of terrestrial carbon cycling (Huotari et al. 2011). In 2011–2012 we address the gas transfer coefficients for water-air exchange and their dependence on environmental variables and possible site-specific factors. We formulate new parameterizations to be tested against earlier ones and other data sets. There is an urgent need for more flux data from lakes and rivers of different size and type (like trophic status and water colour) over varying meteorological conditions and different seasons. We organised two campaigns with measurements of water velocities and turbulence accompanied by EC for CH_4 and two campaigns where aquatic VOC exchange was measured. We carried out two EC campaigns over rivers (one large river and one smaller one) for CO_2.

The knowledge of the relative importance of different methane transport/release mechanisms is crucial, since it affects how much CH_4 may be oxidized before escaping to the atmosphere. In 2011–2012 we have addressed the description of the methane transport and release processes based on the fundamental physical principles coupled with the characteristics of vegetation and bacterial metabolic processes. The comparisons of the model results to broad range of available observations are performed. We are establishing a long-term CO_2 and CH_4 EC measurement site at a boreal wetland, a raised bog with a strong characteristic pattern of hummocks and hollows with open water pools. Thus, together with data set from the nearby fen site, two long-term data sets from the same boreal wetland become available. New measurement methods for *in-situ* detection of methane bubbles in peat matrix will be developed and tested (Vesala et al., this issue).

In 2011 an ozone removal technique (heated stainless steel inlet) which enabled in situ sesquiterpene measurements was developed. Using this technique, we also conducted in situ VOC concentration measurements in Hyytiälä throughout the growing season. Sesquiterpenes have not been measured earlier in boreal forest air. We also collected aerosol samples for the analysis of organic acids in Hyytiälä and were able to detect the acids formed from α-pinene, β-pinene, 3-carene, limonene and β-caryophyllene. The organic acids were measured in a course of a whole year and the concentrations peaked concomitant with the emission peak, but small amounts were detected also in other seasons. We also developed a method for amine analysis using impregnated filters and collected samples for amine analysis during the whole year. The major amines detected in air were ethylamine+dimethylamine, triethylamine and diethylamine (Hakola et al., this issue). Our preliminary results indicate also that there are substantial amounts of bound amines in boreal forest soil and fungal biomass, which supports our hypothesis that amines are produced through protein-amino acid pathway also in soil. The liberation of these amines from soil could explain the measured amine concentrations in the air at a forest environment (Kieloaho et al., this issue).

(iv)   Participation in large scale, integrated field and laboratory experiments

The backbones of our research activities have been data products from our SMEAR and GAW station network. The access to global and European scale aerosol and other climate data pools have been attained by the active coordination or participation to European Union FP6 projects such as EUCAARI (European Integrated project on aerosol, cloud, climate and air quality interactions) (Kulmala et al. 2011) and Integrated Infrastructures Initiatives project EUSAAR (European Supersites for Atmospheric Aerosol Research). In order to ensure the access to best data pools in the field of atmospheric sciences and biosphere–atmosphere interface the FCoE teams have continued active participation to the ongoing European FP7 research and infrastructure projects. The most crucial projects here are the four-year projects FP7-ACTRIS-I3 (**A**erosols, **C**louds, and Trace gases Research Infra**S**tructure Network, see Kulmala et al., this issue) and FP7-PEGASOS (The Pan-European Gas-AeroSOls Climate Interaction Study; see Manninen et al this issue), FP7- EXPEER-I3 (Experimentation in Ecosystem Research), and

the recently concluded FP7-MarieCurie-ITN-CLOUD representing a leading edge laboratory experiments at CERN. In June–July 2012 the FCoE teams participated in the PEGASOS intensive field campaign at the San Pietro Capofiume (SPC) measurement station where a large number of different quantities were measured by several international research groups.

These projects provide standardized quality checked controlled data products, but also bring good visibility and active use of the SMEAR- data products. To ensure the continuous development of national data products and the research infrastructures used by the FCoE teams the data product development is networked to the ongoing EU-FP7-projects: FP7-ENVRI-project "Common Operations of Environmental Research Infrastructures" in Europe and FP7-COOPEUS-project "Transatlantic cooperation in the field of environmental research infrastructures" between Europe and USA. The aim of these research infrastructure projects is the identification of next generation user friendly data structures and formats (Sorvari et al. this issue).

The FCoE$_2$ serves as the core for the partners for contributing the European Research Area initiatives. FCoE partners are active in ESFRI infrastructures (European Strategy Forum on Research Infrastructures) via ICOS (Integrated Carbon Observation System, see Kaukolehto et al., this issue), ANAEE (Infrastructure for Analysis and Experimentation on Ecosystems) and via strategic planning of European aerosol and atmospheric chemistry infrastructure (ACTRIS-I3). Members of the FCoE have been active in preparing the Joint Programming Initiative (JPI) on decadal climate predictability and developing of better climate services for end-users (Connecting Climate Knowledge for Europe, Clik'EU (see Sorvari et al., this issue). In 2012 it was decided that ICOS headquarters will be established in Helsinki. Furthermore, in 2012 University of Helsinki in collaboration of the main European ACTRIS-I3- partners, has set the roadmap for the future actions for establishing long-term aerosol-cloud-trace gases research infrastructure in Europe as a part of the ESFRI process.

The FCoE teams will also be heavily involved with planning (Science Plan) of the "Pan EurasianExperiment – Towards a new multinational environment and climate research effort in Eurasia" (PEEX). PEEX can be listed as one of the most potential experiment initiatives providing new data on the climate change problematic of the cryosphere and arctic areas. University of Helsinki (FCoE) is coordinating the first PEEX workshop in Helsinki in October 2012, where the key Russian partners will meet the leading European partners (Kulmala et al., this issue).

SCIENTIFIC APPROACH

Molecular scale

The research on molecular scale is focussed on theoretical aspects of the formation of new particles in the atmosphere, specifically the role of ions. At the moment there are no consistent theoretical approaches capable of explaining and predicting atmospheric neutral particle formation rates using realistic trace gas concentrations. Vehkamäki and Riipinen (2012) have made a tutorial review summarizing current key questions in atmospheric particle formation. In 2011-2012 we have started the extensive analysis and compared the computational results with CLOUD experiments and Hyytiälä field data. The work is aimed to provide theoretical support for experiments and instrument development and seek to improve and test our model by comparing to a wide selection of experiments (Vehkamäki et al., this issue). We have also made a major scientific outcome of the CLOUD experiment on formation of aerosol particles both via neutral and ion induced pathways. Kirkby et al. (2011) have shown that sulphuric acid – water system is not capable of reproducing the atmospheric new particle formation in the boundary layer. The role of ammonia in concentrations less than 100 pptv was crucial enhancing the nucleation rate considerably (Petäjä et al., this issue).

Another major scientific outcome of the reporting period is related to the discovery of a new atmospherically relevant oxidant of sulphur dioxide by Mauldin et al. (2012). The new pathway can potentially contribute to the atmospheric oxidation and budgets of various compounds. This can have large consequences to current knowledge on atmospheric oxidation capacity as well as on new particle formation (Petäjä et al., this issue).

Understanding the relation between aerosols and their precursor emissions, atmospheric aerosol particle populations, clouds and, eventually, climate is not possible without quantification of the sources responsible for atmospheric cloud condensation nuclei (CCN) (Andreae and Rosenfeld 2008, Carslaw et al. 2010). We have provided a synthesis of the existing knowledge on CCN production associated with atmospheric nucleation by Kerminen et al. (2012) (see also Kerminen et al. this issue). In addition we have conducted both theoretical and experimental studies on the ability of particles to act as CCN in the atmospheric conditions (Laaksonen et al., this issue; Lihavainen et al., this issue). The work has included theoretical studies on insoluble, wettable, particles as a cloud condensation nuclei and the description of the hygroscopic behavior by adsorption theory. Furthermore, we have studied the dependence on cloud droplet number concentration (N_d) on aerosol number concentration (N_a) both from experimental data and by modeling the aerosol effect on cloud. Kuopio and FMI teams have developed aerosol modules that can be used in large scale applications.

Linking the biological activity of the forest to atmospheric chemistry processes

Emission of HONO from soil is a good example of how soil processes are linked with atmospheric chemistry. It also links the trace amounts of reactive nitrogen and the nitrogen and sulfur cycles with the biogeochemical water and carbon cycles. The future needs to document all the ecosystem-atmosphere cycles including the soil, atmospheric oxidation, and aerosol particles and their links and feedback loops to fully understand how the biosphere affects the atmosphere and the global climate were reviewed by Kulmala and Petäjä (2011). In order to do this, both extensive global modelling and continuous, comprehensive field measurements are necessary. In addition to HONO emissions, the soil-originating volatile organic compound (VOC) emissions are relevant for atmospheric chemistry. The sources of VOC emissions in soil and understorey vegetation are poorly understood, but litter quantity and quality, soil microbial activity and the physiological stages of plants are linked with these fluxes (Aaltonen et al. 2011). Soil is an efficient VOC source even during winter, and natural or human disturbance can increase forest floor VOC fluxes substantially (Aaltonen et al. 2012) (Bäck et al., this issue).

We have linked the role of the soil fungi to increased temperature, CO_2 levels and photosynthesis. Different fungi in soil contain large quantities of amines, and same compounds can be found in the air in boreal forests. For example, *Tricholoma matsutake* produces enzymes that are capable of degrading soil organic matter (SOM), suggesting that *T. matsutake* lives mainly as an ectomycorrhizal symbiont but can also feed as a saprotroph. The finding that ectomycorrhizal fungi plays a role also in SOM decomposition is important when the effects of increased temperature, CO_2 levels and photosynthesis in boreal forest zone are evaluated (Bäck et al. this issue).

Also the soil related meteorological aspects are important. The canopy snow substantially increases the forest albedo. However, the difference in total amount of shortwave radiation reflected from a forest on an average winter and on one simulated snow free was 55 MJ m^{-2}, which is less than the inter-annual variation in solar irradiance. Based on these results, we concluded that the positive feedback on climate warming in case of potential snow free winters and lower albedos would not be considerable in the studied forest (Kuusinen et al. 2012). Furthermore, we found that the soil temperature affects photosynthesis and biomass allocation in Scots pine, Norway spruce and Silver birch, but net CO_2 was not changed due to concomitant increase in respiration. Different soil temperatures did not alter the ECM fungi species composition and the below-ground carbon sink strength did not seem to be directly related to ECM biomass and species composition (Pumpanen et al. 2012). We have also measured soil CO_2 fluxes in

stands formerly dominated by Norway spruce (*Picea abies* L. Karst.) with total or partial canopy destruction. Removal of wind-damaged material decreased instantaneous CO_2 flux from the soil surface. New wind-thrown stands where residues are left on site would most likely turn to sources of CO_2 for several years until forest regeneration reaches to substantial assimilation rates (Köster et al. 2011) (Bäck et al., this issue).

In addition to these most important findings of aerosols physics we have new insight linking the biological activity of the forest to atmospheric chemistry processes. The VOC production by terrestrial vegetation is related to biological activity, mainly photosynthesis, which is reflected in the high atmospheric concentrations of VOCs especially during the spring recovery period (Lappalainen et al. 2012). We analyzed the chemical composition of monoterpenes from individual Scots pines in a homogeneous stand. The chemical composition of monoterpenes from Scots pines varies significantly between individual trees, levels of carene dominating the intraspecific variation, chemotype. Based on this result, parameterisations based on volatiles emitted from single trees may be misleading and yield large biases in atmospheric chemistry models (Bäck et al. 2012). A comparison of emission model approaches show that there is room for improvement in the stand-level description of VOC sources, as well as in the temporal description of driving factors (Smolander et al., this issue).

The biomass of evergreen species in the ground vegetation is highest at poor sites and below canopies, whereas grasses and herbs predominated at fertile sites and open areas in a boreal pine forest. This influences the seasonal productivity of below-canopy compartment: photosynthetic activity increased earlier and decreased later in evergreen species than in deciduous species, whereas photosynthesis of ground vegetation was highest in deciduous species, resulting in notably higher photosynthetic production at fertile sites than at poor clear-cut sites. The photosynthetic production of ground vegetation decreased with stand age (Kulmala et al. 2011). We have also improved the new methodologies for the study of seasonal processes in Scots pine needles: Photorespiration measurements, protein extractions and fluorescence spectroscopy (Porcar-Castell 2011, Bäck et al., this issue).

It is yet unknown whether the temperature dependence of ecosystem respiration varies systematically between aquatic and terrestrial environments. In the recent Nature paper by Yvon-Durocher et al. (2012) the largest database of respiratory measurements yet compiled (9 ecosystem types encompassing 373 measurement sites) was used to show that the sensitivity of ecosystem respiration to seasonal changes in temperature is remarkably similar for diverse environments encompassing lakes, rivers, estuaries, the open ocean and forested and non-forested terrestrial ecosystems. The annual ecosystem respiration in aquatic ecosystems showed a substantially greater temperature response compared to those of terrestrial ecosystems whereas the short term temperature responses fitted over seasonal scale were remarkably similar between the ecosystem types.

Mesoscale biosphere-aerosol modelling

The understanding of the whole process of formation of secondary aerosols, starting from the emissions of precursors from the canopy up to their activation to form cloud droplets is in the core of the models predicting climate behavior (e.g. Boy et al., this issue). Our results show that in atmospheric conditions, clustering of H_2SO_4 can possibly produce a pool of clusters that are later activated for growth to climatically relevant particle sizes by e.g., sulfuric acid or supersaturated organic vapors (Petäjä et al. 2011). In 2011 we have also produced the first version of a sulphuric acid model and proxy. The new SOSA simulates the concentrations of organic vapours and sulphuric acid inside the atmospheric boundary layer (Boy et al. 2011). A statistical proxy for sulphuric acid uses global solar radiation, SO_2 concentration, condensation sink and relative humidity as predictor variables, yielding a correlation measure (R) of 0.87 between observed concentration and the proxy predictions (Mikkonen et al. 2011).

Mesoscale studies in 2011–2012 have been especially focused on the phenomenology of Northern and arctic areas. We have analysed air mass transport and pollution trends in connection with aerosols in Northern Finland (Väänänen et al. 2012, Kyrö et al. 2012) and observations of aerosol formation at Antarctica (Kyrö et al. 2012). These analyses are contributing the research approach of the CRAICC Nordic Center of Excellence. Furthermore, long-term analyses of aerosol properties as a function of the air mass temperature history has been performed (Liao et al. this issue) and studies of satellite data concerning atmospheric humidity and its connection to aerosol concentrations (Riuttanen et al., this issue). Efforts a statistical model of boreal BVOC concentrations has continued (Karsisto et al., this issue), as well as analyses of CCNC data (Paramonovet al., this issue) (Dal Maso et al., this issue).

Global climate models

The studies of semivolatile and surface active compound effects on cloud droplet activation have been continued. Furthermore, global scale simulations in which different methods to take account surface active species on cloud droplet formation were compared. Previously we have constructed a parameterization describing the nitric acid effect on cloud droplet number concentration (Romakkaniemi et al. 2005) and now we have used the parametererization in global modeling framework (Makkonen et al. 2012a) (Laaksonen et al. this issue).

In addition to studies of SOA phase, we have carried out plant chamber experiments to investigate mass yields of SOA from the oxidation of α-pinene and real plant emissions (Hao et al. 2011) and the effect of biotic stress on SOA formation and aerosol forcing of climate (Joutsensaari et al. 2012). Laboratory and field experiments showed that biotic stress (i.e. insect herbivory) increase VOC emissions significantly (ca. 10-fold). The results from field and laboratory experiments, global modelling (GLOMAP), and satellite observations suggest that more frequent insect outbreaks in a warming climate could result in ample increase in biogenic SOA formation in the boreal zone and affect both aerosol direct and indirect forcing of climate at regional scales. The effect of insect outbreaks on VOC emissions and SOA formation should be considered in future climate model calculations (Joutsensaari et al. 2012) (Laaksonen et al., this issue).

The role of nucleation in atmospheric CCN formation and associated indirect radiative effects as a result of complex interactions between anthropogenic and biogenic emissions was investigated for both present day and future conditions using the ECHAM5-HAM climate model (Makkonen et al., 2012b, c). It was shown that incorporating atmospheric nucleation is crucial for realistic estimation of the aerosol indirect forcing. The magnitude of the forcing seems not, however, to be extremely sensitive to the exact details of the nucleation mechanism. Over the next century, a large fraction of the anthropogenic climate benefit (the negative radiative forcing) due to atmospheric aerosols is expected to be lost as a result of emission regulations. We showed that natural aerosols resulting from continental biogenic emissions act to the opposite direction, but the magnitude of this climatically beneficial effect remains to be quantified.

Scientific highlights

During the reporting period (May 2011 – Aug 2012) we have published altogether 7 papers in Nature, Nature Geosciences, Nature Protocols or Science. The total number of all peer reviewed publications by members of the FCoE in 2011–12 (until August 30th) is more than 150. In 2011–2012 our most important scientific results are on the new sights on the atmospheric nucleation phenomena (Kirkby et al. 2011) and the related processes (Mauldin et al. 2012, Riipinen et al. 2012) and on the linking processes and factors in the land- atmosphere interface (Kulmala and Petäjä 2011, Yvon-Durocher et al. 2012). We have also attributed the hot spot of the current climate policy debate on the role of black carbon in the climate system by presenting results on radiative absorption features of black carbon (Cappa et al. 2012).

Abstract by Petäjä et al. (this issue) represents the overview of the highlight results of FCoE related to atmospheric oxidation, atmospheric nucleation, nanoparticle growth, aerosol climatic effects and advances on measurements techniques.

List of FCoE Nature / Nature Geosciences / Nature Protocols and Science papers published in 2011-2012:

1. Kirkby, J., Curtius, J. Almeida, J. Dunne, E., Duplissy, J., Ehrhart, S., Franchin, A., Gagné, S., Ickes, L., Kürten, A., Kupc, A., Metzger, M., Riccobono, F., Rondo, L., Schobesberger, S., Tsagkogeorgas, G., Wimmer, D., Amorim, A., Bianchi, F., Breitenlechner, M., David, A., Dommen, J., Downard, A, Ehn, M., Flagan, R. C., Haider, S., Hansel, A., Hauser, D., Jud, W., Junninen, H., Kreissl, F., Kvashin, A., Laaksonen, A., Lehtipalo, K., Lima, J., Lovejoy, E. R., Makhmutov, V., Mathot, S., Mikkilä, J., Minginette, P., Mogo, S., Nieminen, T., Onnela, A., Pereira, P., Petäjä, T., Schnitzhofer, R., Seinfeld, J. H., Sipilä, M., Stozhkov, Y., Stratmann, F., Tomé, A., Vanhanen, J., Viisanen, Y., Vrtala, A., Wagner, P. E., Walther, H., Weingartner, E., Wex, H., Winkler, P. M., Carslaw, K. S., Worsnop, D. R., Baltensperger, U. and Kulmala, M.: **The role of sulfuric acid, ammonia and galactic cosmic rays in atmospheric aerosol nucleation**, Nature, 476, 429-433, doi:10.1038/nature10343, 2011.
2. Kulmala, M. and Petäjä, T.: Soil nitrites influence atmospheric chemistry, Science, 333, 1586-1587, doi:10.1126/science.1211872, 2011.
3. R.L. Mauldin III, T. Berndt, M. Sipilä, P. Paasonen, T. Petäjä, S. Kim, T. Kurtén, F. Stratmann, V.-M. Kerminen and M. Kulmala: **A new atmospherically relevant oxidant of sulphur dioxide.** 2 0 1 2 4 8 8 | 1 9 3- 197. doi:10.1038/nature11278
4. Yvon-Durocher G., Caffrey J.M, Cescatti A., Dossena M., del Giorgio P., Gasol J.M, Montoya J.M, Pumpanen J., Staehr P.A, Trimmer M., Woodward G. & Andrew A.P.: **Reconciling the temperature dependence of respiration across timescales and ecosystem types**. doi:10.1038/nature11205
5. Riipinen I., Yli-Juuti T., Pierce J.R, Petäjä T., Worsnop D.R., Kulmala, M.& Donahue N.M.:**The contribution of organics to atmospheric nanoparticle growth.** Nature Geoscience 5, 453–458 (2012) doi:10.1038/ngeo1499
6. Cappa, C.D., Onasch, T.B., Massoli, P., Bates, T.S., Gaston, C.J., Hakala, J., Petäjä, T., Hayden, K., Kolesar, K.R., Lack, D.A., Mellon, D., Li, S.-M., Nuaaman, I., Prather, K.A., Quinn, P.K., Song, C., Subramanian, R., Vlasenko, A., Worsnop, D.R. and Zaveri, R.A., **Radiative Absorption Enhancements Due to the Mixing State of Atmospheric Black Carbon**, Science, 337, 1078-1081 DOI: 10.1126/science.1223447
7. Kulmala, M., Petäjä, T., Nieminen, T., Sipilä, M., Manninen, H.E., Lehtipalo, K., Dal Maso, M., Aalto, P.P., Junninen, H., Paasonen, P., Riipinen, I., Lehtinen, K.E.J., Laaksonen, A. and Kerminen V.-M. (2012) **Measurement of the nucleation of atmospheric aerosol particles**, Nature Protocols 7, 1651-1667, doi:10.1038/nprot.2012.091.

RESEARCH COLLABORATION AND TRAINING

In 2011-2012 FCoE has continued the collaboration among the two Nordic centers of excellence CRAICC (Cryosphere-Atmosphere Interactions in a Changing Arctic Climate) and DEFROST. In 2011-2012 FCoE researchers have participated to Earth System Modelling - CRAICC-SVALI-DEFROST workshop in June 2012 at the University of Helsinki, Finland, Black Carbon workshop June 2012 at the Lund University, Sweden and the Ice Nucleation workshops in February 2012 at ETHZ, Zurich, Switzerland.

Altogether over 27 MSc's and 13 PhD's finalized their theses within the FCoE during 2011-2012 (until August 30th 2012). The education and knowledge transfer of the Centre of Excellence is formalized in the National ACCC Doctoral Programme (Atmospheric Composition and Climate Change: From Molecular Processes to Global Observations and Models). Altogether the ACCC Programme has more than 140 doctoral students, and it is one of the approximately 130 doctoral programmes of the Academy of Finland. The ACCC Programme holds 15 out of the 1600 doctoral student positions directly funded by the Ministry

of Education and Culture, set under competition for the doctoral programmes. The funding scheme will change in 2013. The Academy of Finland doctoral programmes will cease to exist, and the funding will be transferred to the budget funding of the Finnish universities.

Between June 2011 and August 2012 the ACCC Programme organized a total of seven intensive graduate courses. In total, more than 150 students participated in these courses. The intensive courses were usually organized in collaboration with several international projects and programmes, e.g. iLEAPS, CLOUD-ITN, the Nordic Master's Degree Programme ABS, and the Nordic Centres of Excellence CRAICC, DEFROST and SVALI. The annual seminar of the ACCC Programme, held in January 2012, attracted more than 50 students to present their research work - all the oral and poster presentations of the seminar were given by ACCC students. The seminar also included a session about entrepreneurship.

As a part of the ongoing development of working atmosphere within the FCoE, an Equality task group was established at the Division of Atmospheric Sciences (Univ of Helsinki). The group works towards identifying and prevention of any kind of inequality or discrimination of the personnel. The task group planned and executed an Equality Questionnaire in summer 2012. The questionnaire was aimed at screening the work atmosphere and attitudes, and it gathered up over 100 replies. The results will be dealt with at departmental meetings during fall and winter 2012–13.

CLIMATE POLICY AND PUBLIC OUTREACH

The main channels for the European and global climate policy impact for the FCoE activities are the IGBP iLEAPS, Integrated Land Ecosystem – Atmosphere Processes Study and participation to the IPCC panels (Suni et al. this issue). Helsinki University is hosting the iLEAPS international project office at Helsinki and prof. Kulmala is a co-chair of the iLEAPS Scientifc Steering Committee. In 2011 iLEAPS organized the science conference in Garmisch-Partenkirchen, where the FCoE research was presented, altogether 8 presentations and 50 posters.

FCoE PIs prof. V-M-Kerminen and prof. T. Vesala are participating in the IPCC Fifth Assessment Report (AR5, years 2010–2014) processes and future developments of the global research programmes (IGBP/WCRP). Prof. Kerminen is a lead author of the chapter "Cloud and Aerosols" in Working Group 1 (WG1) of AR5, and Prof. Vesala is a Review Editor of the chapter "Carbon and other biogeochemical cycles" in WG1 of AR5.

The Finnish Ministry of Environment established a national Climate Panel in December 2011 and nominated Prof. Kulmala as the chair of the panel for the period 1.12.2011 – 31.12.2013. The national climate panel is collating climate change research for politicians. The panel consists of 13 members, who are senior scientists in the fields of natural sciences, economics and other social sciences, engineering and international politics. One of the first tasks of the national Climate Panel is to mediate the insights of the science community for the preparation process of Climate law of Finland. During this year Prof. Kulmala as a chair of the panel has given a great number of TV and radio interviews providing publicity and visibility to the FCoE research.

A modern approach to get the public attention to science was launched by Helsinki University in 2011. FCoE research was presented at the "Think Corner"–science cafe, as a part of the Helsinki Design year activities (http://blogs.helsinki.fi/wdc-2012/think-corner/). During one week in June 2012, the FCoE researchers gave 15 presentations to public audience, and a scientific exhibition showing e.g. measurement tools and the interactive Carbon tree software were included in the program of the week. All the presentations and discussions were recorded for a wider audience via the "Think Wall" facebook site (http://www.helsinki.fi/thinkwall/).

The non-scientific end-users of the data are informed using distributed written material and press conferences, which generates interviews and articles in popular science magazines and in domestic and

international newspapers as well as in the television and radio. FCoE teams are active players in several platforms for outreach, such as Hiukkastieto (www.hiukkastieto.fi/) for aerosol information, Hiilipuu (www.hiilipuu.fi, see Kulmala L. et al. this issue) for illustration of CO_2 fluxes of boreal tree and Ympäristötiedon foorumi (www.ymparistotiedonfoorumi.fi), which is a collaborative network of actors in environmental science to promote dialogue between scientists and decision makers at different levels.

RESPONSE TO REMARKS PRESENTED BY FCoE SCIENTIFC ADVISORY BOARD (SAB)

In the last FCoE Annual Workshop in Luosto, May 18-20, 2011, the SAB listed several valuable remarks (R 1–12) on the previous work and results of FCoE. Here we report, how we have taken into account the SAB remarks during the period 1. Jun. 2011 – 31. Aug. 2012.

R-1: There is an interesting approach to calculate the CCN concentration in historic times. As an effect of industrialization, globally the calculations resulted in the global CCN concentration to roughly double. This could have consequences to the climate of the earth, since clouds do affect the albedo. This consequence should be explored further.

- The work is in on-going. As the first estimate, Makkonen et al. (2012b) explored the role new particle formation to the global CCN in pre-industrial, present day and by 2100. The results indicated that including the nucleation mechanism increased considerably the present-day anthropogenic aerosol forcing. In the future, the modelling data also showed that a strong decrease in the aerosol forcing is foreseen, based on reductions of primary aerosols and SO2 emissions. This also links to the brightening of the clouds in the future, assuming the decrease in SO_2 emissions and the increased role of nitric acid (Makkonen et al. 2012a).

R-2: One area to improve is to continue to broaden the international collaboration and exchange at all levels. The FCoE should continue to strongly encourage its doctoral graduates to travel abroad for postdoctoral work around the world. In addition the FCoE could benefit from more aggressive recruitment of postdoctoral researchers from other leading groups around the world. This same exchange could be extended to doctoral students, where exchange programs of 6–12 months could become a highly effective means of broadening the perspective of doctoral students.

- The unit has been active in proposing programmes and research projects involving mobility between countries. Erasmus Mundus Joint Doctoral Programmes (currently no such programmes within FCoE), Marie Curie Initial Training Networks (CLOUD-ITN, CLOUD-TRAIN, HEXACOMM), and Nordic Centres of Excellence (CRAICC, DEFROST, SVALI) are examples of programmes involving systematic mobility.
- The unit has recruited prominent scientists in all levels from the key collaborators worldwide. A non-exhaustive short list is provided below, which only shows a part of the recruitments and the related activity
1) Professor Joel Thornton from Washington State University will spend the academic year 2012/2013 in Helsinki providing insights into chemical ionization methods of nanoparticles and gases. His expertise is complementary to the FCoE knowledge and there are mutual benefits of this sabbatical year. This is a new opening in our collaboration.
2) Adjunct Professor Roy L. Mauldin III has been visiting the $FCoE_2$ on a regular basis spending 1-2 months per year in Helsinki. His contributions to our understanding of atmospheric radical measurements (incl. OH and stabilized Criegee intermediates, Mauldin et al. 2012, Sipilä et

al. 2012, Petäjä et al. 2012, this issue) has opened us an opportunity to probe novel and yet unexplored field of atmospheric chemistry with potentially global consequences.

The post-doctoral researchers have been recruited e.g. from:

3) University of Innsbruck (PhD. Gerhard Steiner, high resolution mobility analysis in connection with mass spectrometric analysis).

4) University of Crete (PhD. Nikos Kalivitis), comparison of new particle formation events between Hyytiälä and Finokalia). This collaboration connects the $FCoE_2$ to work conducted by the group led by ERC advanced grant holder Prof. Spyros Pandis.

5) University of Frankfurt (PhD. Daniela Wimmer, February 2013), development of condensation particle counters,

6) University of Stockholm (PhD Mathias Vogt, aerosol and water flux between the atmosphere-ecosystem-anthropocene interfaces)

7) Paul Scherrer Institute and ETH Zurich (PhD. Arnaud Praplan, gas phase amine measurements). This collaboration brings new knowledge regarding the amine measurements and process level understanding of the nanoparticle growth both in the CLOUD chamber as well as in the atmosphere.

8) University of Chemistry, Helsinki (PhD. Alexey Adamov), development of ionization techniques for atmospheric applications

9) CERN (PhD. Jonathan Duplissy), CLOUD experiments, data interpretation and technological development

10) Estonian Agricultural University, Tartu (PhD Kajar Köster), expertise on forest ecosystem functioning and soil sciences has provided novel insights to e.g. ecosystem disturbance dynamics

Several researchers from the $FCoE_2$ are post-doctoral researchers in various research facilities around the world, such as:

11) PhD. Mikael Ehn at the Reseach Center Julich, Germany. He is concentrating on understanding the production of low-volatile organic compounds from biogenic VOCs.

12) PhD. Hanna Manninen at University of Tartu, Estonia. She integrates the available atmospheric ion and electrical conductivity measurement data worldwide and contributes to the development of SMEAR-type station in Estonia.

13) PhD. Erik Herrmann, University of Nanjing, China has been responsible for sub-micron aerosol measurements and data analysis in SMEAR-type station at Nanjing.

14) PhD. Eija Asmi, University Clermont Ferrand, France. She worked e.g. at Puy de Dome research station gathering expertise regarding high-altitude atmospheric measurements.

15) PhD. Risto Makkonen, University of Oslo, Norway. He is working on global modeling of aerosol particles.

16) PhD. Pauli Paasonen is currently a guest researcher at International Institute of Applied Systems (IIASA), Laxenburg, Austria. His efforts in aims to add a module estimating the aerosol particle number emissions into the GAINS model and thus to improve the applicability of the model in predicting the health and climate effects of the aerosol particles.

17) PhD. Stephanie Gagne is a post-doctoral fellow at Dalhousie University in Halifax, Canada working with atmospheric aerosol measurements.

Student exchange between the core groups worldwide has been active. As an example,

18) MSc. Tuija Jokinen will spend up to a year at Institute of Tropospheric Research, Leipzig, Germany. She will contribute to the flow tube experiments exploring the role of stabilized Criegee intermediates to the oxidation of a variety of atmospherically relevant trace gases.

19) MSc. Silja Häkkinen is currently a visiting PhD student at the University of Columbia in New York supported by a Fullbright scholarship. She is working with Prof. Vivian Faye McNeill on chemical ionization of atmospheric samples.

20) During the forthcoming Marie Curie ITN CLOUD-TRAIN project, two new international PhD students will be hired at Helsinki. We are also actively promoting the recruitment of MSc. students from the FCoE2 by the other CLOUD-TRAIN partners, which will connect our activities more tightly to the international education of the next generation of scientists.

R-3: The wider public and policy impact of the work would benefit to be more clearly demonstrated. At present, the results are highly "policy relevant", should also be shown to be "policy applied". Some percentage of the resources should be used to a) engage in dialogue with policy users of the research and to b) clearly record highlight examples of this dialogue.

- Prof. Kulmala has been nominated as the Chair of the national Climate Panel for the period 1.12.2011 – 31.12.2013. This position provides a direct link to ministry level policy makers.
- FCoE hosted a three day event open to the public in Helsinki (Tiedekulma) presenting e.g. the aspects of climate change, atmosphere-forest interactions, connections to international climate policies, air quality and the need of collaborative scientific activity to resolve these issues.
- ATM has provided a course in "Scientific outreach and international partnership", spring 2012.

R-4: There remain major challenges in quantifying the sources of amine emissions and the dynamics of their biosphere atmosphere exchange, e.g. in relation to nitrogen supply, photosynthesis, agricultural emissions etc. This needs to be a future priority.

- The work is in progress. Within the $FCoE_2$ we have formed a working group around the amines, which is aiming at a comprehensive view of the amine emissions, sources, processes and atmospheric chemistry and their role in secondary aerosol formation. This collaborative effort has already started and will continue and intensify during the coming years.

R-5: There was currently little visibility in the work presented of the wider role that HNO_3 is playing in aerosol growth processes, which is surprising given the increasing atmospheric ratio NO_3/SO_4 in Europe, as SO_2 emissions decline. In particular, the role of mixed acid chemistry (i.e. H2SO4 and HNO_3 mixtures) in aerosol formation and growth remains a challenge for further analysis.

- An assessment of the nitric acid / sulphuric acid on the initial nucleation process is work in progress. However, as a general direction and as the SAB indicated, the sulphate emissions are declining world-wide. The importance of nitric acid in the future is now also illustrated by work of Makkonen et al. 2012b as part of global modelling efforts of the $FCoE_2$. Makkonen et al. 2012b showed that assuming the present day nitric acid concentrations while the SO2 emissions are declining will have a strong increase in the modelled cloud droplet concentrations leading to an increase in aerosol indirect effect. Furthermore, assuming a decreasing trend in the aerosol concentrations will lead into enhanced effect due to nitric acid brightening the clouds in the future.

R-6: In Aerosol biochemisty and biology, we did not see much attention given to the role of biological processing of aerosol (as mentioned in the previous SAB report). The focus on secondary aerosols should be complimented by primary biological aerosols. First steps have been made, but it needs a greater drive (and not only cooperation) to dig into that.

- The work is in progress. H. Manninen et al will soon submit a manuscript analyzing the SMEAR II pollen and spore data and the connections of these with other measurements. The tentative title is "Annual cycle of airborne pollen, fungal spores and particle mass in boreal forest", which will include the detailed analysis of a long-time series of bioaerosol, seasonal cycles and long-range transport of the bioaerosol.
- We hosted MPI instrument (UV-APS) at SMEAR II station in Hyytiälä for more than 1 year. This data set is currently being analysed with the aim to show the annual, seasonal and diurnal cycles of super-micron bioaeosol with a relatively high time resolution (10 minutes).

R-6: The work at the SMEAR stations would benefit from further integration of the role of ozone chemistry, particularly given the context of increasing global ozone background concentrations. Example questions include addressing the extent to which increasing ozone concentrations alter BVOC emissions, alter net ecosystem exchange of CO_2 of forest, alter aerosol formation and growth rates (e.g. via altering sulphate oxidation rates in the presence of increasing base availability).

- Also this work is in progress. A manuscript (Rannik et al.) analyzing a decade-long series of ozone deposition measurements is in review in ACPD. This analysis will enable the evaluation of O_3 effects on BVOC production and CO_2 uptake, as well as on the signature and relevance of the different deposition processes in the coniferous forest stand.
- As a brand new opening, we will also continue to explore the role of stabilized Criegee intermediates to the atmospheric chemistry. This process is initiated by the ozone reacting with alkenes (Mauldin et al. 2012, Sipilä et al. 2012, Petäjä et al. 2012, this issue). The interesting issue with the sCI is that the source of the radical is linked to the BVOC concentrations, which has been directly linked with the growth of the atmospheric nanoparticles (Dal Maso et al. 2012, in preparation).

R-7: There is scope for further integration of the SMEAR station results on biosphere atmosphere exchange into these models, in particular on the role of within-canopy air chemistry interactions on atmospheric chemistry processes. However, modelers are advised to update themselves, how experiments are done and what is experimentally possible. So they are not living in an isolated world.

- See the reply above. The Rannik et al manuscript also attempts to analyze and model the various O_3 deposition processes, including the chemical sink within canopy, created by mono- and sesquiterpenes.
- We have also conducted modelling efforts to estimate the effect of reactivity within the canopy to the measured VOC fluxes (Rinne et al. 2012). We used a stochastic Lagrangian transport model in which the chemical degradation was described as first order decay in order to study the effect of the chemical degradation on above canopy fluxes of chemically reactive species. We used the results of the simulations together with oxidant data measured during HUMPPA-COPEC-2010 campaign at a Scots pine site to estimate the effect of the chemistry on fluxes of three typical biogenic VOCs, isoprene, alpha-pinene, and beta-caryophyllene. Of these, the chemical degradation had a major effect on the fluxes of the most reactive species beta-caryophyllene, while the fluxes of alpha-pinene were affected during nighttime.

R-8: The analytical chemistry group should be encouraged on the strongest possible terms to grapple with the very challenging problem of quantifying these vapor contributions and not simply constraining the artifact as an interference to be quantified, subtracted, and then neglected

- Since spring 2012 the tests on the applicability of the improved version of the DMA based collection system on the quantification of organic compounds in gas and particle phases have been initiated. The success of the system has not yet been proved, but the analysis will be carried out during fall 2012. In addition, collection system including phosphoric acid denuder and filter sampling has been implemented in the studies. The suitability of solid-phase microextraction for the collection of gas phase sample will be clarified.
- Analytical methods to resolve the vapour concentrations are ongoing (see, e.g. Jokinen et al. this issue). We have also actively looking into collaborations with the gap filling knowledge (see recruitment of e g. Arnaud Praplan).

R-9: collection times. Up to now 100 h are needed. The chemistry group is aware that this is too long and must be reduced. Otherwise an interpretation of the results in connection to physical results remains questionable.

- This work is currently in progress. The instrumentation developed within the FCoE now is in a routine use to collect the aerosol samples and we are in the process of determining the minimum collection time needed.
- So far the studies have been concentrated on the development of size selective collection and sensitive and reliable analysis methods for the elucidation of the chemical composition of ultrafine atmospheric aerosols (<50 nm) and for the analysis of specific target compounds like amines in ultrafine aerosol particles. Even as long as 100–300 h sampling times have been needed to make sure that the amount of sample material is enough also for the analyses carried out by other instrumental techniques, used for the comparison and confirmation of the results. After the successful validation of the sample pretreatment and analysis methods developed, the next step is to decrease the sampling time. For certain target analysis (e.g. amines), it can be easily shortened at least 10-100 times. In addition, e.g. a new portable gas chromatography-mass spectrometry equipped with the special sampling valve developed for aerosol collection, will allow almost the simultaneous analysis of the sample material collected.

R-10: The team should continue to host intensive campaigns. Additional measurements of VOC oxidation products would provide an excellent additional constraint.

- We hosted the HUMPPA-COPEC 2010 activity, where the scientific findings are now being published (e.g. Williams et al. 2011, Mauldin et al. 2012, , Rinne et al 2012, Yassaa et al 2012). This was a large campaign with a strong participation by the MPI.
- Forthcoming activities include the PEGASOS project, where the Zeppelin will be flying around Hyytiälä providing both transects as well as vertical profiles of both radical (OH) data, air ion chemical composition and aerosol particle data. These efforts are conducted within the PEGASOS project. See Manninen et al. 2012, this issue.
- Large EU-funded infrastructure projects such as ACTRIS, EXPEER and ANAEE (see Lappalainen et al. 2012, this issue) will provide Trans-national access to Hyytiälä. Already we have had visitors from University of Arhus, Denmark, conducting research on organosulphates in the particulate phase, an intercomparison of GC-and PTR-MS systems to quantify the oxidized Volatile Compound concentrations (OVOC), which was done in collaboration with EMPA, UHEL and FMI. We are also collecting aerosol samples with MPI to probe the properties of aerosol particles with TEM.

- Currently a US Department of Energy proposal has been submitted, which would bring ARM mobile facility to Hyytiälä for the year 2014. The project is looking into Biogenic Aerosols and how they will effect clouds and climate. The ARM facility is complementary to SMEAR II providing in-situ observations on aerosol-cloud interactions with active remote sensing instruments. This activity is coordinated by PI Tuukka Petäjä

R-11: Statistics, presentations (95% condifence intervals). Further attention should be given to presenting results using more sophisticated metrics. For example, results should go beyond looking at aerosol formation rates in response to single ppb concentrations (such as ammonia or DMA) and look at results as a function of chemical equivalent ratio, also considering the role of mass of the input compounds when expressing results as particle mass and number.

- A lot of the expertise regarding statistical analysis is already within the group, and in future it will be further utilised. . E.g. just after the FCoE meeting we will host a workshop providing advanced statistical analysis tools for the students and researchers.

R-12: Web pages

- After the last FCoE meeting in Luosto, May 2011, we re-constructed the www-page setup in a way that it would be more informative about the ongoing activities of the FCoE related events. The current pages are in www.atm.fi/FCoE.

FUTURE PROSPECTS

The $FCoE_2$ has taken the world leading position in building up scientific understanding related to the dynamics of aerosols, ions, and neutral clusters in the lower atmosphere and their links to biosphere-atmosphere interaction processes, biogeochemical cycles and trace gases. Current knowledge on formation and growth mechanisms of atmospheric aerosols, aerosol and air ion dynamics, the effect of secondary biogenic aerosols on global aerosol load, aerosol-cloud-climate interactions, air pollution-climate interactions and the relationships between the atmosphere and different ecosystems, particularly boreal forest is largely based on scientific approach by the $FCoE_1$ and the ongoing $FCoE_2$.

However, it is already seen that in spite of the improved understanding on the aerosol formation process and related dynamics, there is still a great challenge in the assessment and prediction of climate change and the analyses of the related processes in a global scale. The future vision of the $FCoE_2$ is a solution oriented approach, which will provide reliable prediction tools for the society in order to cope with environmental impacts of climate change. There is an urgent need to integrate the improved description of processes and parametrisations in the Earth System Models (ESMs). The efficient integration of process understanding and parameterisation of the next generation EMSs requires more efficient use of Earth system observations. The Earth Observation (EO) techniques (space-borne remote sensing) are the only methods providing spatially continuous, frequent observational data sets. EO-data can be applied to the validation of the climate model predictions for the large scale, to the trend analyses of essential climate variables, to the analyses of spatially distributed processes in biosphere and to develop further the physical models through improvement of the model parameterisation or static background fields.

The research focus of the $FCoE_2$ has been to develop a holistic understanding on the global climate change, biosphere-atmosphere interactions, climate – air quality interactions and the complex, non-linear system of atmospheric new aerosol formation. During the last year of $FCoE_2$, several benchmarking results from WP5 "Global modeling" will be anticipated. This will prepare the FCoE teams to be ready for a more focused approach of improving the regional and global scale Earth System models and to apply for the third period of Center of Excellence (2014-2019).

ACKNOWLEDGEMENTS

REFERENCES

Aaltonen H., Pumpanen J., Pihlatie M., Hakola H., Hellén H., Kulmala L., Vesala T. & Bäck J. (2011) Boreal pine forest floor biogenic volatile organic compound emissions peak in early summer and autumn. Agricultural and Forest Meteorology 151: 682–691.

Aaltonen H., Pumpanen J., Hakola H., Vesala T., Rasmus S. & Bäck J. (2012). Snowpack concentrations and estimated fluxes of volatile organic compounds in a boreal forest. Biogeosciences 9: 2033–2044.

Andreae M. O. and Rosenfeld, D. (2008) Aerosol-cloud-precipitation interactions. Part 1. The nature and sources of cloud-active aerosols. Earth Sci. Rev. 89: 13–41.

Asmi E, T. Laurila, H. Lihavainen, D. Brus, M. Aurela1, A. Hyvärinen, J.Hatakka1, Y. Viisanen, V. Kondratyev, V. Ivakhov, A. Reshetnikov, T. Uttal, and A. Makshtas (2012) Measurement of erosol particles and greenhouse gases in Arctic Russia,

Boy, M., Sogachev, A., Lauros, J., Zhou, L., Guenther, A. and Smolander, S. (2011) SOSA - a new model to simulate the concentrations of organic vapours and sulphuric acid inside the ABL - Part I: Model description and initial evaluation, Atmos. Chem. Phys. 11: 43–51.

Bäck J., Aalto J., Henriksson M., Hakola H., He, Q. & Boy, M. (2012) Chemodiversity of a Scots pine stand and implications for terpene air concentrations. Biogeosciences 9: 689–702.

Cappa, C. D., Onasch, T. B., Massoli, P., Bates, T. S., Gaston, C. J., Hakala, J., Petäjä, T., Hayden, K., Kolesar, K. R., Lack, D. A., Mellon, D., Li, S.-M., Nuaaman, I., Prather, K.A., Quinn, P.K., Song, C., Subramanian, R., Vlasenko, A., Worsnop, D.R. and Zaveri, R.A. (2012) Radiative absorption enhancements due to the mixing state of atmospheric black carbon, Science, 337: 1078–1081, DOI: 10.1126/science.1223447.

Carslaw, K. S., Boucher, O., Spracklen, D. V., Mann, G. W., Rae, J. G. L., Woodward, S., and Kulmala, M. (2010) A review of natural aerosol interactions and feedbacks within the Earth system. Atmos. Chem. Phys. 10: 1701–1737.

Hao, L. Q., Romakkaniemi, S., Yli-Pirilä, P., Joutsensaari, J., Kortelainen, A., Kroll, J. H., Miettinen, P., Vaattovaara, P., Tiitta, P., Jaatinen, A., Kajos, M. K., Holopainen, J. K., Heijari, J., Rinne, J., Kulmala, M., Worsnop, D. R., Smith, J. N., and Laaksonen, A. (2011) Mass yields of secondary organic aerosols from the oxidation of alpha-pinene and real plant emissions. Atmos. Chem. Phys., 11, 1367–1378.

Huotari J., Ojala A., Peltomaa E., Nordbo A., Launiainen S., Pumpanen J., Rasilo T., Hari P. and Vesala T. (2011). Long-term direct CO_2 flux measurements over a boreal lake: Five years of eddy covariance data. Geophys. Res. Lett. 38, doi: 10.1029/2011GL048753.

Hölttä, T., Mencuccini, M., Nikinmaa, E. (2011) A carbon cost–gain model explains the observed patterns of xylem safety and efficiency. Plant, Cell & Environment. 34, 1819–1834.

Joutsensaari, J., P. Yli-Pirilä, H. Korhonen, A. Arola, J. D. Blande, J. Heijari, M. Kivimäenpää, L. Hao1, P. Miettinen, P. Lyytikäinen- Saarenmaa, A. Laaksonen, J. K. Holopainen (2012). Biotic stress accelerates formation of climate-relevant aerosols in boreal forests. Nature Climate Change (submitted).

Kerminen, V.-M., Paramonov, M., Anttila, T., Riipinen, I., Fountoukis, C., Korhonen, H., Asmi, E.,Laakso, L., Lihavainen, H., Swietlicki, E., Svenningsson, B., Asmi, A., Pandis, S. N., Kulmala, M., and Petäjä, T. (2012) Cloud condensation nuclei production associated with atmospheric nucleation: a synthesis based on existing literature and new results. Atmos. Chem. Phys. Discuss. 12: 22139–22198.

Kirkby, J., Curtius, J. Almeida, J. Dunne, E., Duplissy, J., Ehrhart, S., Franchin, A., Gagné, S., Ickes, L., Kürten, A., Kupc, A., Metzger, M., Riccobono, F., Rondo, L., Schobesberger, S., Tsagkogeorgas, G., Wimmer, D., Amorim, A., Bianchi, F., Breitenlechner, M., David, A., Dommen, J., Downard, A, Ehn, M., Flagan, R. C., Haider, S., Hansel, A., Hauser, D., Jud, W., Junninen, H., Kreissl, F., Kvashin, A., Laaksonen, A., Lehtipalo, K., Lima, J., Lovejoy, E. R., Makhmutov, V., Mathot, S., Mikkilä, J., Minginette, P., Mogo, S., Nieminen, T., Onnela, A., Pereira, P., Petäjä, T., Schnitzhofer, R., Seinfeld, J. H., Sipilä, M., Stozhkov, Y., Stratmann, F., Tomé, A., Vanhanen, J., Viisanen, Y., Vrtala, A., Wagner, P. E., Walther, H., Weingartner, E., Wex, H., Winkler, P. M., Carslaw, K. S., Worsnop, D. R., Baltensperger, U. and Kulmala, M. (2011) The role of sulfuric acid, ammonia and galactic cosmic rays in atmospheric aerosol nucleation, Nature 476: 429-433, doi:10.1038/nature10343.

Kulmala M., Suni T., Lehtinen K.E.J., Dal Maso M., Boy M., Reissell A., Rannik Ü., Aalto P., Keronen P., Hakola H., Bäck J., Hoffmann T., Vesala T. & Hari P. (2004) A new feedback mechanism linking forests, aerosols, and climate. - Atmospheric Chemistry and Physics 4: 557–562.

Kulmala, M. et al. (2011) General overview: European Integrated project on Aerosol Cloud Climate and Air Quality interactions (EUCAARI) – integrating aerosol research from nano to global scales, Atmos. Chem. Phys., 11, 13061–13143.

Kulmala L. Pumpanen J., Hari P., and Vesala T. (2011). Photosynthesis of ground vegetation in different aged pine forests: Photosynthesis of ground vegetation in different aged pine forests: Ef¬fect of environmental factors predicted with a process-based mode. Journal of Vegetation Science 22: 96–110.

Kulmala L., Pumpanen J., Kolari P., Muukkonen P., Hari P. and Vesala T. (2011). Photosynthetic production of ground vegetation in different aged Scots pine forests. Canadian Journal of Forest Research 41: 2020-2030, 10.1139/x11-121.

Kulmala, M. and Petäjä, T. (2011) Soil nitrites influence atmospheric chemistry. Science 333: 1586–1587, doi:10.1126/science.1211872.

Kulmala, M., Petäjä, T., Nieminen, T., Sipilä, M., Manninen, H.E., Lehtipalo, K., Dal Maso, M., Aalto, P.P., Junninen, H., Paasonen, P., Riipinen, I., Lehtinen, K.E.J., Laaksonen, A. and Kerminen V.-M. (2012) Measurement of the nucleation of atmospheric aerosol particles, Nature Protocols 7, 1651-1667, doi:10.1038/nprot.2012.091.

Kuusinen, N., Kolari, P., Levula, J., Porcar-Castell, A., Stenberg, P., & Berninger, F. (2012). Seasonal variation in boreal pine forest albedo and effects of canopy snow on forest reflectance. Agricultural and Forest Meteorology 164: 53-60.

Kyrö, E.-M., Virkkula, A., Kerminen, V.-M., Dal Maso, M., Parshintsev, J., Ruiz-Jimenez, J., Forsström, L., Manninen, H., Heinonen, P., Riekkola, M.-L., and Kulmala, M. Antarctic aerosol formation from continental biogenic sources this collection.

Kyrö, E.-M., Dal Maso, M., Virkkula, A., Nieminen, T., Aalto, P.P., Keronen, P., Hari, P. and

Kulmala, M. Long-term trends in air pollution and new particle formation in Eastern Lapland, Finland

Köster, K. Puttsepp U & Pumpanen J. et al. .(2011) Comparison of soil CO2 flux between uncleared and cleared windthrow areas in Estonia and Latvia. Forest Ecology and Management 262, 65-70.

Makkonen, R., Romakkaniemi, S., Kokkola, H., Stier, P., Räisänen, P., Rast, S., Feichter, J., Kulmala, M., and Laaksonen, A. (2012a). Brightening of the global cloud field by nitric acid and the associated radiative forcing, Atmos. Chem. Phys. 12: 7625–7633.

Makkonen, R., Asmi, A., Kerminen, V.-M., Boy, M., Arneth, A., Hari, P. and Kulmala, M. (2012b) Air pollution control and decreasing new particle formation lead to strong climate warming. Atmos. Chem. Phys. 12: 1515-1524.

Makkonen, R., Asmi, A., Kerminen, V.-M., Boy, M., Arneth, A., Guenther, A.. and Kulmala, M. (2012c) BVOC-aerosol-climate interactions in the global aerosol-climate model ECHAM5.5-HAM2. Atmos. Chem. Phys. Discuss. 12: 9195–9246.

Mencuccini, M., Hölttä, T., Martinez-Vilalta, J. 2011. Comparative Criteria for Models of the Vascular Transport Systems of Tall Trees. *Size- and Age-Related Changes in Tree Structure and Function*, (R. Meinzer, B. Lachenbruch, T. Dawson, Editors). Springer books, in press.

Mikkonen, S., Romakkaniemi, S., Smith, J. N., Korhonen, H., Petäjä, T., Plass-Duelmer, C., Boy, M., McMurry, P. H., Lehtinen, K. E. J., Joutsensaari, J., Hamed, A., Mauldin III, R. L., Birmili, W., Spindler, G., Arnold, F., Kulmala, M., and Laaksonen, A. (2011) A statistical proxy for sulphuric acid concentration. Atmos. Chem. Phys. 11: 11319–11334.

Petäjä, T., Sipilä, M., Paasonen, P., Nieminen, T., Kurten, T., Ortega, I. K., Stratmann, F., Vehkamäki, H., Berndt, T., and Kulmala, M. (2011) Experimental observation of strongly bound dimers of sulphuric acid nucleating in the atmosphere, Phys. Rev. Lett., 106, 228302, doi:10.1103/PhysRevLett.106.228302.

Porcar-Castell A. (2011). A high-resolution portray of the annual dynamics in photochemical and non-photochemical quenching in needles of Pinus sylvestris. Physiologia Plantarum 143: 139-153.

Mauldin III, R. L., Berndt, T., Sipilä, M., Paasonen, P., Petäjä, T., Kim, S., Kurten, T., Stratmann, F., Kerminen, V.-M., and Kulmala, M. (2012) A new atmospherically relevant oxidant for sulphur dioxide. Nature 488: 193–197, doi:10.1038/nature11278.

Riipinen I., Yli-Juuti T., Pierce J.R, Petäjä T., Worsnop D.R., Kulmala, M. & Donahue N.M. (2012) The contribution of organics to atmospheric nanoparticle growth. Nature Geoscience 5: 453–458, doi:10.1038/ngeo1499.

Romakkaniemi S., Kokkola H. and Laaksonen A. (2005) Parameterization of the nitric acid effect on CCN activation. Atmos. Chem. Phys. 5: 879-885.

Sevanto S., Hölttä T. & Holbrook M. (2011) Effects of the hydraulic coupling between xylem and phloem on diurnal phloem diameter variation. Plant, Cell and Environment. 34, 690–703.

Vehkamäki, H. and Riipinen, I. (2012) Thermodynamics and kinetics of atmospheric aerosol particle formation and growth. Chemical Society Reviews 41: 5160.

Vesala T et al. Eddy Covariance Measurements over Lakes, in: Eddy Covariance, Eds. Aubinet M et al., Springer 2012.

Viskari, T., Asmi, E., Kolmonen, P., Vuollekoski, H., Petäjä, T., and Järvinen, H. (2012a) Estimation of aerosol particle distributions with Kalman Filtering – Part 1: Theory, general aspects and statistical validity. Atmos. Chem. Phys. Discuss. 12: 18853–18887.

Viskari, T., Asmi, E., Virkkula, A., Kolmonen, P., Petäjä, T., and Järvinen, H. (2012b) Estimation of aerosol particle number distribution with Kalman filtering – Part 2: Simultaneous use of DMPS, APS and nephelometer measurements. Atmos. Chem. Phys. Discuss. 12: 18889–18925.

Yvon-Durocher G., Caffrey J.M, Cescatti A., Dossena M., del Giorgio P., Gasol J.M, Montoya J.M, Pumpanen P., Staehr P.A, Trimmer M., Woodward G. & Andrew A.P. (2012) Reconciling the temperature dependence of respiration across timescales and ecosystem types. doi:10.1038/nature11205

Väänänen, R., Nieminen, T., Dal Maso, M., Virkkula, A., Svenningson, B., Kivekäs, N., Holst, T., Arneth, A., Kerminen, V.-M., and Kulmala, M (2012) Analysis of aerosol dynamics between three sites in Northern Scandinavia (manucript in preparation).

GENERAL OVERVIEW: AEROSOLS, CLOUDS, AND TRACE GASES RESEARCH INFRASTRUCTURE NETWORK (ACTRIS)

M. KULMALA[1], H.K.LAPPALAINEN[1,2,], T.PETÄJÄ[1], and ACTRIS-Finland teams

[1]University of Helsinki, Department of Physics, 00014 Helsinki, Finland
[2]Finnish Meteorological Institute, Research and Development, 00101 Helsinki, Finland

Keywords: atmospheric aerosols, clouds, trace gases, research infrastructures.

INTRODUCTION

The ACTRIS-I3 "Aerosols, Clouds, and Trace gases Research InfraStructure Network" project is an European Commission FP-7-Project aiming at integrating European ground-based stations equipped with advanced atmospheric probing instrumentation for aerosols, clouds, and short-lived gas-phase species. ACTRIS-I3 will be active for a period of 4 years in 2011 - 2015. The project is coordinated by CNR (Italy) and CNRS (France) and has 29 partners. ACTRIS consortium represents 35 infrastructures in 24 European countries. In addition, more than 60 sites are reporting ACTRIS labeled data. The ACTRIS-I3-project is an essential pillar of the EU ground-based observing system that provides the long-term observations information required to understand current variability of the atmospheric aerosol components and better predict their impact on climate and air quality in a changing climate. University of Helsinki (UHEL) is a partner and Finnish Meteorological Institute (FMI) is an associated partner in the ACTRIS-I3 consortium. As a part of the European ACTRIS framework University of Helsinki, Finnish Meteorological Institute and University of Eastern Finland have established ACTRIS-Finland research collaboration network (http://www.atm.helsinki.fi/multisites/actris/).

METHODS

The Project is organized into three activities: networking (i), transnational access (ii) and joint research (iii). Networking activities (i) are designed to improve the quality and the standardization of pan-European atmospheric measurements on aerosol vertical distribution, in-situ chemical, physical and optical properties of aerosols, volatile organic carbon and nitrogen oxides and the clouds and aerosol quality controlled observations. Transnational access activity (ii) is based eleven high-quality measurement stations around Europe providing access to the data and the facility and allows to conduct experiments with the support of the permanent technical staff. ACTRIS is also constructing the ACTRIS Data Centre, which will give open access to all data resulting from the activities of the ACTRIS-listed infrastructures with a user-friendly interface for the different end-user communities.

ACTRIS Joint research activities (iii) are related to developing novel observation performances, new data products and studying methodology for the simultaneous real-time data products of chemical composition of aerosols and trace gases. The research activity includes the integration of currently operating aerosol observation networks, the European Aerosol Research Lidar Network (EARLINET) and the European part of the Aerosol Robotic Network (AERONET), development of standardized measurement techniques of oxygenated volatile organic compounds (OVOC), mass closure experiments by combined measurements of organic carbon compounds in the gas and particle phases and the physical characterization of clouds and aerosols in the context of cloud formation and its impact on climate change.

RESULTS

University of Helsinki (UHEL) and Finnish Meteorological Institute (FMI) contribute to several the work packages (WPs) of the ACTRIS-project related to networking actions (In-situ chemical, physical and optical properties of aerosols, trace gases, clouds and aerosol quality controlled observations, clouds and aerosol quality controlled observations) and joint research action of comprehensive gas phase and aerosol chemistry. There WPs are also an integral part of the FCoE research approach, especially data products and measurement techniques. SMEAR-II in Hyytiälä, the core of the Finnish Centre of Excellence (FCoE) datapool, is listed as ACTRIS transnational access site and is proving SMEAR-datasets and measurement infrastructure for open use of the ACTRIS research community. The during the first year of operation ACTRIS has opened permanent call researcher and research teams for free access to any of the 11 advanced experimental atmospheric research stations, including SMEAR-II, in a frame of ACTRIS listed sites. Furthermore free access to the AERONET-EUROPE Calibration and Maintenance Centre offering the scientific community the use of a unique sun photometer calibration facility in the frame of AERONET. As a part of networking actions ACTRIS has performed first internal quality checks of the hardware of remote sensing of vertical aerosol distribution. Networking actions for improving the in-situ data on aerosols properties has started by implementing of the EUSAAR standardization protocol for mobility size spectrometers. Also standardized operating procedures (SOPs) for VOC and NOxy measurements have drafted.

University of Helsinki is leading the strategic work package (WP6) on "Integration, outreach, and sustainability" and has released the ACTRIS Roadmap to mark out the actions to be taken for the long-term continuation of advanced measurements on aerosols, clouds and reactive gases in Europe in a coordinated and cost-efficient way and set the framework and, how ACTRIS would be part of the European Union research infrastructure landscape ensuring Europe's competitiveness in "frontier" research. The estimated schedule for the steps from the ACTRIS-I3 project to ACTRIS world-class European Research Infrastructure (RI) in operation would be in 8 years.

During the first twelve months of the ACTRIS-I3 project the joint research on lidar and sunphotometers has been targeted to determination of database structure for combined lidar and sunphotometer observations and evaluation of Raman lidar techniques for daytime extinction measurements. The work on comprehensive gas phase and aerosols chemistry has started by the definition of experimental design for mass closure experiments and mapping the existing cloud, aerosol, water vapour, retrieval techniques.

ACKNOWLEDGEMENTS

REFERENCES

ACTRIS Description of Work

PAN EURASIAN EXPERIMENT (PEEX) –

TOWARDS A NEW MULTINATIONAL ENVIRONMENT AND CLIMATE RESEARCH EFFORT IN EURASIA

MARKKU KULMALA[1], HANNA K. LAPPALAINEN[1,2], TUUKKA PETÄJÄ[1], MIKKO SIPILÄ[1], SANNA SORVARI[1], PAVEL ALEKSEYCHIK[1], MIKHAIL PARAMONOV[1], VELI-MATTI KERMINEN[1] AND SERGEJ ZILITINKEVICH[1,2]

[1]University of Helsinki, Department of Physics, P.O. Box 64, FI-00014 University of Helsinki, Finland

[2]Finnish Meteorological Institute, Erik Palménin aukio 1, 00560 Helsinki, Finland

INTRODUCTION

Boreal forests are the major source of greenhouse gases, biogenic volatile organic compounds (BVOCs) and natural aerosols, the critical atmospheric components related to climate change processes. Major fraction of the boreal forests of the world is situated in Siberian region. Representative measurements of carbon dioxide (CO_2) and methane (CH_4) concentrations, BVOC emissions and aerosols production from the Siberian region are of special importance when estimating global budgets of climate change relevant factors. As a whole new knowledge is needed on the interactions of physical, chemical and biological processes of the land-atmosphere interface in order to understand the climate change problematic in a global and regional scales. The process based understanding is crucial basis for the Earth system models, which are the best tools for analysing the effect of different environmental changes on future climate.

Kulmala et al. 2011 has already addressed the need for coordinated Pan Siberian research program and has listed several research questions effecting the land-atmosphere interface processes incl. the impact of land use changes in boreal forest areas and it's consequences on the amount of aerosols precursors, greenhouse gases and BVOC emissions. The other area of research focus is on the ongoing changes in cryosphere. The permafrost area in Siberia is extensive and scientific valid estimates are needed on the progress of permafrost thaw and smelt.

The reliable research results covering the Siberian region could only be based on the coherent, regionally representative research infrastructure. The selection of station sites should represent the large variation of vegetation zones and type of ecosystems in Siberia such as boreal forest (taiga), a tundra belt on the northern fringe, and a temperate forest zone in the south. The recent reviews by Kulmala et al. 2011 and Kulmala et al. 2012 show that of the Siberian aerosol and gas data is mostly based on temporary field campaigns. However, already existing research stations and other infrastructure (Global Atmospheric Watch sites (WMO), Zotino Tall tower, Japan-Russia Siberian Tall Tower Inland Observation Network, Total Carbon Column Observing Network, TROICA experiments on board the trans-Siberian railway, Tiksi measurement site, GOSAT) serves as good basis for further development of the measurement network. In an ideal case each of the major ecosystem types should have a supersite type of measurement stations like SMEAR (Station for Measuring Forest Ecosystem - Atmosphere Relations) station network in Finland (Kulmala et al. 2011).

A new concept of the Pan Eurasian Experiment (PEEX) has just recently introduced in part from an the concept of Pan Siberian Experiment by Kulmala et al., 2011. The scope of PEEX is expanded to a large-scale experiment approach, which aims to connect and collaborate with as many Eurasian states as possible. The

size of experiment demands the interdisciplinary research collaboration between Russian and European research teams and the support the European Union research infrastructure instruments for establishing new stations network to cover the Eurasian regions.

METHODS

The scope of the planed experiment is to set up a process for planning of a large-scale, long-term, coordinated observations and modeling experiment in the Pan Eurasian region, especially to cover ground base, airborne and satellite observations together with global and regional models to find out different forcing and feedback mechanisms in the changing climate. University of Helsinki together with Finnish Meteorological institute has taken an active role in organizing the Pan-Eurasian Experiment and to gather all the European and Russian key players in the field of climate and Earth system science to plan jointly in coordinated manner the future research activities in the Pan-Eurasian region. The Russian contribution consists of several Russian institutes of Russian Academy of Sciences; Institute of the Cryosphere of the Earth, Siberian Branch of RAS, Institute of Atmospheric Physics RAS, Russian State Hydrometeorological University. The approach starts with the series of workshops in October 2012 and drafting the overall Science Plan for Pan-Eurasian experiment.

This series of workshops is linked to several national and international research actions and projects. In the European scale PEEX is part of the JPI Climate Fast Track Activity 1.3. "Changing cryosphere in the climate system – from observations to climate modeling" which was approved by the JPI Climate GB in May 2012. The coordinated science plan for Pan Siberian large scale Experiment has been listed as output from FTA-1.3 activity.

PEEX research topics are closely related the NordForsk's Top Research Initiative project CRAICC – Cryosphere – atmosphere interaction in the changing Arctic climate coordinated by University of Helsinki. The CRAICC-research will focus our attention on short-lived climate forcers (SLCF) and clouds and their linkages with cryospheric changes due to their significant relevance in Arctic warming. PEEX is also a central part of the ongoing the Finnish Cultural Foundation – Earth System modeling Working Group activity (2012-2013). Working group will identify scientific uncertainties in current Earth System Models and aims to create a deep understanding on several processes associated with biosphere-atmosphere interactions, biogeochemical cycling of climatically relevant compounds and soil processes.

PEEX scientific aims and future actions to develop Pan Eurasian research infrastructure can be linked to several EC and ESA funded activities such as EU-FP7 project aiming to develop research infrastructures and data products. ACTRIS-I3 (Aerosols, Clouds, and Trace gases Research InfraStructure Network-project 2011-2015) and is aiming at integrating European ground-based stations equipped with advanced atmospheric probing instrumentation for aerosols, clouds, and short-lived gas-phase species. ICOS is a research infrastructure to decipher the greenhouse gas balance of Europe and adjacent regions. EU-FP-7 e-infra project ENVRI "Common Operations of Environmental Research Infrastructures" is a collaboration effort of the ESFRI Environment Cluster and to develops common e-science components and services for their facilities. Furthermore, The Pan-Eurasian Experiment will be supported iLEAPS (Integrated Land Ecosystem – Atmosphere Processes Study) bringing the PEEX under umbrella of the International Geosphere-Biosphere Programme (IGBP).

CONCLUSIONS

The permafrost regions and boreal forests of the Pan Eurasian area can be identified as a hot spot of climate change research in a global scale. PEEX experiment can be considered as a crucial part of the strategic aims of several international and national roadmaps for climate change research and the development of next-generation research infrastructures.

ACKNOWLEDGEMENTS

REFERENCES

Kulmala M., Alekseychink P., Paramonov M., Laurila T., Asmi E., Arneth A., Zilitinkevich S. & Kerminen V-M. 2011. On measurements of aerosol particles and greenhouse gases in Siberia and future research needs. *Boreal Env. Res.* 16: 337–362. http://www.borenv.net/BER/pdfs/ber16/ber16-337.pdf

Kulmala et al. 2012. Pan Eurasian EXperiment (PEEX) – towards a new multinational environment and climate research effort in Eurasia. Manuscript in preparation.

CRYOSPHERE-ATMOSPHERE INTERACTION IN A CHANGING ARCTIC CLIMATE - CRAICC
WHAT HAS BEEN ACHIEVED IN THE FIRST TWO YEARS

Markku Kulmala, Michael Boy, Jaana Bäck, Antti Lauri, Andreas Stohl, Merete Bilde, Margareta Hansson, Ingibjorg Jónsdóttir and the CRAICC Science Team

Coordination office: University of Helsinki, Finland

Background

Climate change is proceeding fastest at the Arctic, its near-surface warming being about twice the global average during the recent decades. Simultaneously, the Arctic cryosphere has experienced notable changes: the sea-ice area has been decreasing at record rates, and precipitation and river discharges into the Arctic Ocean have been increasing. The changes have dramatic impacts on the Arctic ecology and societies.

There is no consensus on the reasons why climate changes so fast in the Arctic, and whether the amplified warming will continue. It is clear, however, that the Arctic surface radiation balance regulates the melting and freezing of the pack ice, a key climate regulator. Simulations of Arctic clouds are particularly deficient, impeding correctly simulated radiative fluxes. Important, yet poorly-quantified players in this context are short-lived climate forcers (SLCF): natural and anthropogenic aerosols, ozone and methane.

The climate impacts of SLCFs are tightly connected with cryospheric changes and associated human activities. Transport of black carbon aerosols into high latitudes and their deposition on snow decrease the surface albedo. Together with decreased sulfate aerosol emissions it has probably contributed to the observed Arctic warming. Melting of the pack ice and sea ice is likely to result in increased numbers of aerosol particles and CCN from sources in the high Arctic, which increase the reflectivity of clouds. Properties of high-latitude clouds may also be affected by the changing biogenic aerosol formation associated with warming and snow-cover changes over boreal forest regions. Emissions of methane from thawing permafrost and coupling of atmospheric methane oxidation with ozone formation affect Arctic greenhouse gas forcing. Finally, cryospheric changes alter human activities in Arctic and Nordic regions, which changes anthropogenic emissions of SLCFs over these areas.

The Nordic Center of Excellence Cryosphere-Atmosphere interactions in a changing Arctic Climate (CRAICC) started in autumn 2010. The goals of CRAICC are i) to identify and quantify the major processes controlling Arctic warming and related feedback mechanisms, ii) to outline strategies to mitigate Arctic warming, and iii) to develop Nordic Earth System modeling. The project includes 23 partners from all Nordic countries (Finland, Norway, Sweden, Denmark and Iceland) and is coordinated by Prof. Kulmala from the Division of Atmospheric Science at the University of Helsinki.

RESULTS FROM THE SECOND YEAR

During the second year the CRAICC community has initiated several workshops and courses related to the scientific topics in CRAICC, which were all announced on the web-page of the project and other related places. The activities in CRAICC-fellowships increased dramatically during the last 12 month and involved are nearly all CRAICC-partners through doctoral, post-doctoral and visiting scientist fellowships. In 2012, the education and knowledge transfer activities in CRAICC included three summer schools and one winter school. More specific information on the single CRAICC-actions are presented below.

The first CRAICC-annual meeting was arranged in October 2011 in Iceland. An abstract book including all 50 abstracts submitted to this meeting was published under the Report Series in Aerosol Science (No: 128, 2011). The picture below shows the 76 participants on a field trip to glaciers, volcanoes and other interesting sites in Iceland.

1. Fellowships

Since the start of the project altogether 25 proposals for fellowships were submitted to the CRAICC-coordination office in Helsinki. Out of these 22 were accepted by the Scientific Steering Committee (SSC). At the end of the second year of the CRAICC-project two fellowships had already ended, 13 are on-going and 7 will start in the next months. The fellowship-projects are distributed over all scientific objectives and work packages from CRAICC and involve until now all partners beside two (Norwegian Meteorological Institute and the Centre for International Climate and Energy Research in Oslo - CICERO). A table including the project topic, the selected fellow, the start and duration of the project and the institutes and PI's responsible is presented at the end of the abstract. Two of the fellowships are shared between the CRAICC and Defrost NCoEs.

2. Networking

In 2011, four workshops with different scientific themes related to one or more work packages were organized under CRAICC, partly in cooperation with the other Nordic Centres of Excellence.

Earth System Modelling - CRAICC-SVALI-DEFROST initiative
This workshop was a common initiative by all three Nordic Centres of Excellence and took place in **June 2012 at the University of Helsinki, Finland**. The main topics were the cross-cutting themes among the NCoEs, the involvement of observation and process based studies into ESM activities and planned actions of collaborations. The discussions showed that there exists a long list of themes important and crucial in all NCoEs, like the ocean land-ice interface or the deposition of aerosols on glaciers. Related to available data sets it was recognized that all NCoEs provide data as open access, but a common database for all Centers does not exist until now. The data should be reported and documented well with standardized data format for easy comparison between observations and models (ESM and others). Recommendations for data-format and metadata should be provided by the NCoEs as already exist in other projects like ICOS, AeroCom or EBAS. For a better future collaboration the participants of the workshop suggested many possible action items, like a data-workshop which concentrates on what kind of data is needed and what can be provided by each NCoE, hands-on workshops on ESMs with details on different models, and a common course on running an ESM model for people from different fields with different interests.

Black Carbon
The workshop on the formation, life cycle, impacts, co-benefits, policy, mitigation and response measures of black carbon was organized in **June 2012 at the Lund University, Sweden**. Soot (or BC: "Black Carbon") is one of the short-lived climate forcers. The Swedish Minister of the Environment, Lena Ek, together with the US Secretary of State Hillary Clinton and others in Washington, recently launched a global initiative in order to decrease emissions of SLCF including soot. The purpose of the workshop was to summarize the state of knowledge regarding the effects of black carbon on climate and human health and map the fields of research, within and across disciplines, which need to be addressed in order to fulfill the requirements of the society. It was discussed to establish a dialogue between scientists in relevant disciplines and the stakeholders of our society and to outline a roadmap for how research on the climate and health effects of soot should be conducted and financed.

Ice Nucleation
Three workshops were organized, the first one already during the first year of the CRAICC-project in **April 2011 in Copenhagen, Denmark**, the second **theory workshop in Helsinki in August 2011** and the third in **February 2012 at ETHZ, Zurich, Switzerland.** The talks in Copenhagen represented different aspects of ice nucleation: including theoretical and experimental studies on molecular level, laboratory studies on aerosols and ice, instrument development, as well as global modelling of the importance of ice nucleation.

The second theoretical workshop gathered 27 scientists from 7 institutes to discuss the state of art of the ice nucleation theory for three days. The presentations outlined the basic concepts and theoretical framework of 1) homogeneous gas-to-liquid and liquid-to-ice nucleation 2) heterogeneous gas-to-liquid, liquid-to-solid and gas-to-solid nucleation. Concepts and main features of different types of homogeneous and heterogeneous nucleation were compared to each other.

The last workshop focused on technical aspects of ice nuclei measurements and in particular the goals for the CRAICC community in terms of establishing ice nuclei (IN) measurement and monitoring capacity within the Nordic countries. In this regard the main focus was to discuss and examine specific instrumental options for CRAICC collaborators to pursue in regard to establishing Nordic based measurement instruments. Modelling was also discussed with the idea of maintaining open communication with the modelling community with the desire those measurements serve as functional input for weather and climate modelling at a range of scales. Within the workshop multiple talks from outside collaborators focused on current measurement instruments. After re-examining the CRAICC proposal and discussions regarding the potential for high levels of contribution to the IN research community it was evident that the place for the best synthesis is for CRAICC to support technology development that enables continuous IN monitoring of Arctic sites. A second goal of any Nordic based instrumentation must be that it can be utilized for controlled laboratory measurements. This may necessarily be a two stage process because even the most advanced INCs currently have difficulty measuring both continuously and very low concentrations.

Eddy-covariance fluxes
The training course/workshop on Eddy-covariance fluxes was jointly organized by the NORDFLUX network and the two Nordic Centers of Excellence CRAICC and DEFROST in **January 2012 at the University of Helsinki, Finland**. The training course focused on eddy covariance flux (EC) measurements technique and on the software EddyUH (a software for eddy covariance flux calculation), recently developed by the Micrometeorology group of the Division of Atmospheric Sciences at the University of Helsinki, Department of Physics. The course consisted of lecture and practical work sessions, and it was intended to those students/researchers with scientific background in atmospheric surface layer and eddy covariance technique.

3. Education

Within CRAICC, education and knowledge transfer have been given a special emphasis. Following the CBACCI Education Structure (CBACCI, 2003), determined work has been carried out to develop the multidisciplinary training on all levels (master students, doctoral students, postdoctoral scientists, professors).

In 2012, the education and knowledge transfer activities in CRAICC included three summer schools and one winter school:

- Advanced analysis of atmospheric processes and feedbacks and biosphere-atmosphere interactions, Hyytiälä, Finland, February 27 - March 8, 2012

- Measurements of atmospheric aerosols: aerosol physics, sampling and measurement techniques, Hyytiälä, Finland, May 5-12, 2012
- Arctic air pollution, Lund, Sweden, June 11-20, 2012
- Formation and growth of atmospheric aerosols, Hyytiälä, Finland, August 14-24, 2012

Altogether, more than 100 students participated in these courses. Some of the courses were given in collaboration with the other NCoEs in Interaction between the Cryosphere and Climate Change (ICCC), DEFROST and SVALI. Furthermore, the education strategy was discussed during a special working group session during the annual meeting in Iceland in October 2011, and the education collaboration with DEFROST and SVALI was discussed in a joint meeting during the ICCC meeting in Oslo in November 2011.

4. Other activities

The CRAICC partners were actively presenting their research results in several Cryosphere-related international meetings. These included e.g. the Committee on River Ice Processes and the Environment (CRIPE) conference (Manitoba), the 3rd iLEAPS Science Conference (Garmisch-Partenkirchen), Bert Bolin Climate Center annual meeting (Stockholm), American Geophysical Union (San Francisco), the International Polar Year conference (Montreal, Canada), European Geosciences Union General Assembly 2012 (Vienna), and the European Aerosol Conference (Granada) 2012.

5. On Research Activities and Publications

As one common activity by the three Nordic Centers a new special issue entitled "Interactions between climate change and the Cryosphere: SVALI, DEFROST, CRAICC" was established for the three EGU journals: The 'Cryosphere', 'Atmospheric Chemistry and Physics' and 'Biogeosciences'. The special issue was launched in 2012 and will be open for submission until the end of 2016.

The first manuscript partly based on the results of the fellowship by Dr. Tjarda Roberts 'Linking Svalbard ice core records to atmosphere measurements at Zeppelin station' which ended in December 2011 was published (Kuhnel et al., 2011). And a second manuscript by Carsten Ambelas Skjoth, also a CRAICC-fellow ('Tree species inventories in the northern hemisphere') ended in February 2012 is in preparation.

The ongoing activities in the NCoE in the different work packages are reflected by the research projects of the CRAICC-fellow which will be summarized below. Most of the projects will provide valuable contributions to several WPs but listed in the WP were their expected results have the highest impact.

In **WP 2** various aspects related to cryosphere changes are investigated. The trend of northern hemisphere seasonal snow mass and albedo for the period of 29 years was studied with satellite data in combination with albedo modelling. The results reveal that albedo changes show in general a negative trend with the most pronounced changes at areas with melting conditions (Atlaskina et al., this issue).

The under ice carbon dioxide dynamics and the implications for a changing cryosphere was investigated and preliminary results show that lake water pCO_2 under ice cover is primarily dependent on lake morphology and hydrological conditions (Denfeld et al., this issue). The research on the energy exchange and dissolve organic matter (DOM) production in boreal forest in relation to cryosphere processes will clarify the role of runoff changes in the framework of boreal-arctic climate change (Kasurinen et al., this issue).

Natural emissions, their fate in the atmosphere and their relation to warming and cryospheric changes are the topics under **WP 3**. A global data base of forests and tree species and for atmospheric modelling of BVOCs has been established and it could concluded that for global or near global usage, modelers need to be able to deal with data spare areas or areas without any information at all (Skjøth et al., this issue). The long-term arctic tree-line changes are investigated by model-data comparison in the European tree-line region. The simulated tree-line appears to be too sensitive to climate, suggesting the current model may need to include potential ecological factors of, for example, microclimate conditions generated by forest (Fang et al., this issue).

The evaluation of sea spray aerosol source functions in Lagrangian particle dispersion model FLEXPART was investigated and preliminary results indicate that there is more than an order of magnitude difference in mass produced by the different source functions and similar differences in the resulting concentrations (Grythe et al., this issue). The influence of microbiology on sea spray production at low temperatures will be investigated experimental in a new sea spray simulation tank incorporating a number of design features to enable systematic investigation of the physical, chemical, and biological parameters that control SSA production (Salter et al., this issue).

WP4 will measure aerosol chemical composition, physical parameters and optical properties as well as ozone and other gases concentrations at the Arctic and sub-Arctic stations. Impurities in snow, such as black carbon (BC), have been known for some time to have negative effects on snow albedo, hence perturbing the climatic system, especially in the vast snow-covered Arctic. Snow samples were collected along a transect ranging from western Sweden to eastern Finland. This pilot study showed some promising results with an east-west gradient and also a potential north-south gradient (Svensson et al., this issue). New particle formation statistics at Puijo measurement station in central Finland indicate that air masses associated with nucleation events arrive mostly from Arctic, the northern Atlantic and the Arctic Ocean (Baranizadeh et al., this issue).

In **WP 5** the cryosphere-aerosol-cloud-climate interactions are investigated. One primary aspect of the ice nucleation studies in the CRAICC framework is the development of continuous Ice Nuclei Counters (INCs) for use by CRAICC partners in both laboratory and filed measurement campaigns. Currently, a detailed production plan for CRAICC INCs is expected to be completed shortly after the technology sharing agreement has been fully implemented and CRAICC partners receive technical specifications (Thomson et al., this issue).

Hygroscopic and condensation nuclei properties of nucleation, Aitken and accumulation mode particles in sub- and supersaturating condition were analysed in a boreal forest environment during the summer of 2010. The parameters determined were compared

with each other, and their information were coupled with the aerosol chemical composition data from an aerosol mass spectrometer (Hong et al., this issue). The CCN activation of insoluble silica aerosols coated with soluble pollutants was examined. Results showed that the size distributions of pure particles formed unimodal distribution curves, while the coated particles distributions behave as bimodal distribution curves. (Dalirian et al., this issue).

WP 6 concentrates on the atmosphere-cryosphere-societal interactions. We have implemented new particle formation mechanisms in the NorESM (Norwegian Earth System Model). Compared to the original bulk nucleation scheme in NorESM, mechanistic nucleation implementations increase global average number concentrations by 10-20% below 700 hPa height. Due to active binary nucleation in the upper troposphere, the number concentrations between 200 and 500 hPa are increased globally by over 50%, compared to the original NorESM without mechanistic nucleation scheme. Future work will include quantification of the effect of nucleation on cloud properties and aerosol indirect effect, and also studying the climate feedback mechanisms related to secondary aerosol formation (Makkonen et al., this issue).

Past long term changes in the Arctic is the topic in **Wp7**. The long-term accumulation of black carbon in the European Arctic will be studied by comparing the BC concentration of four lakes from continental northern Europe with BC concentrations from a lake sediment core in Svalbard for the industrial era. This project will strengthen our understanding on the past variations in BC concentrations in the Arctic, test new methods for BC quantification from different matrices and thereby enhance comparability of BC concentration results from different kind of studies (Ruppel et al., this issue).

WP8 will address cross-cutting issues between the different components of the Earth system. These issues include interactions between the atmosphere and the cryosphere, including various feedback mechanisms. Most of the projects will provide valuable contributions to the last and crucial work package.

References:

CBACCI, 2003: CBACCI education structure. Annex of the Steering Committee memorandum of the meeting 5.5.2003 in Oslo.

Kuhnel, R. **T. J. Roberts**, M. P. Björkman, E. Isaksson, W. Aas, K. Holmén, J. Ström. 2011. 20 years climatology of N_O^{3-} and N_H^{4+} wet deposition at Ny-Ålesund, Svalbard. *Advances in Meteorology* Volume 2011 (2011), Article ID 406508, 10 pages doi:10.1155/2011/406508.

Table: List of past, active and already funded fellowships under CRAICC

Name of person and title of the proposal	Form	Duration	Start	WP contrib.	Inst.	Name of Pis from the CRAICC-partners
Carsten Ambelas Skjoth - Tree species iventories in the northern hemisphere	PhD	6	1.9.2011	3	4 A	Henrik Skov
Dr. Tjarda Roberts - Linking Svalbard ice core records to atmosphere measurements at Zeppelin station	PD	4	1.9.2011	4 + 7	7 14 A	Elisabeth Isaksson Johan Ström
Blaize Denfeld - Carbon fluxes from freshwaters under a changing climate	PhD	48	1.9.2011	2	15	Gesa Weyhenmeyer
Ksenia Atlaskina - Satellite retrieval of aerosol properties over the Arctic and impacts on climate (SAAC)	PhD	36	1.7.2011	2	1A 2 13	Gerrit de Leeuw Pekka Kolmonen Erik Swietlicki
Jonas Svensson - Depostion of absorbing aerosol on snow and its climate effects	PhD	24	28.11.2011	2 + 4	2 14 A	Heikki Lihavainen Johan Ström
Ville Kasurinen - Energy exchange and DOC production in boreal forests in relation to cryosphere processes	PhD	36	15.4.2012	2 + 3 + 7	1 B 10 15	Frank Berninger Knut Alfredsen Gesa Weyhenmeyer
Dr. Mathew Salter - Sea spray sources at low temperatures	PD	18	1.1.2012	3 + 5	14 A 5	Douglas Nilson Merete Bilde
Henrik Grythe - Source, fate and transport of SLCF in polar regions	PhD	48	1.11.2011	3 + 4	14 A 8 1A	Radovan Krejci Andreas Stohl Aki Virkkula
Elham Baranizadeh - Data Analysis and Regional Scale Modeling of Arctic Aerosol	PhD	36	1.6.2012	4	3 14 A	Ari Laaksonen Ilona Riipinen
Juan Hong - Cloud formation in the arctic region: laboratory and filed observations	PhD	24	1.1.2012	4 + 5	1A 14 A 5	Tuukka Petäjä Ilona Riipinen Merete Bilde
Dr. Erik Thomson - Heterogeneous Ice Nucleation	PD	24	1.1.2012	5	16 5 13	Jan Pettersson Merete Bilde Erik Swietlicki
Maryam Dalirian - Ice and Liquid-phase Cloud Activation and Gas-Aerosol Interactions of Insoluble and Slightly Soluble Particles	PhD	48	1.3.2012	5	14 A 2	Ilona Riipinen Ari Laaksonen
Meri Ruppel - Linking past black carbon variations in lake sediments and Svalbard ice core data	PhD	12	1.1.2012	7	7 1 D	Elisabeth Isaksson Atte Korhola
Dr. Keyan Fang - Past-long-term changes in the Arctic	PD	24	1.9.2011	7	1 C 14 B	Heikki Seppä Margareta Hansson
Dr. Risto Makkonen - The sensitivity of aerosol direct and indirect effects to aerosol nucleation	PD	12	1.7.2012	8	9 1A	Jon Egill Kritjansson Markku Kulmala

Name of person and title of the proposal	Form	Duration	Start	WP contrib.	Inst.	Name of Pis from the CRAICC-partners
The effect of sea-ice loss and climate change on the natureal sulphur cycle and radiative forcing	PD	4	1.9.2012	6 + 8	14 C	Annica Ekman
					14 C	Oyvind Sland
Formation, occurrence and climate effects of organosulfates in Nordic and Arctic aerosols	PhD	48	1.10.2012	3, 4 + 5	4 B	Marianne Glasius
Long-range transported aerosols to the high Arctic	VSS	1.5	1.10.2012	4	4 A	Henrik Skov
					9	Jon Egill Kritjansson
Aerosols from ship traffic in the Arctic	PD	6	1.11.2012	4 + 5	13	Erik Swietlicki
					2	Gerrit de Leeuw
					5	Merete Bilde
Quantification of VOC emissions from periodically ice-covered aquatic sources (iceVOC)	PD	12	1.1.2013	2, 3 + 8	1 B	Jaana Bäck
						Anne Ojala
					16	Jan Pettersson
Measurements and modeling of the atmospheric boundary layer sturcture in high-Arctic	VSS	3	not decided	2	6	Sven-Erik Gryning
					4A	Henrik Skov
					2	Gerrit de Leeuw
The impact of aerosols deposition on radiative forcing in the Arctic and speed up of snow and glacier melt	PhD	36	not decided	2 + 3	17	Throstur Thorsteinsson
					8	Andreas Stohl
					2	Gerrit de Leeuw
					1A	Aki Virkkula

red = ongoing fellowships
green = funded but not yet started
blue = past fellowships

Partners and PI's in CRAICC:
1. University of Helsinki: A) Dept. of Physics (Prof. Kulmala); B) Dept. of Forest Sciences – Prof. Nikinmaa; C) Dept. of Geosciences and Geography – Prof. Seppä; D) Dept. of Environmental Sciences – Prof. Korhola
2. Finnish Meteorological Institute - Prof. de Leeuw
3. University of Eastern Finland - Prof. Laaksonen
4. University of Aarhus: A) Dept. of Atmospheric Environment - Prof. Skov, Dr. Massling; B) Dept. of Chemistry - Dr. Glasius
5. University of Copenhagen - Prof. Bilde
6. Technical University of Denmark - Prof. Gryning
7. Norwegian Polar Institute - Dr. Isaksson
8. Norwegian Institute for Air Research - Dr. Stohl
9. University of Oslo - Prof. Kristjánsson
10. Norwegian University of Science and Technology - Prof. Alfredsen
11. Norwegian Meteorological Institute - Dr. Iversen
12. Center for International Climate and Environmental Research - Prof. Myhre
13. Lund University - Prof. Swietlicki
14. Stockholm University: A) Dept. of Physical Geography and Quaternary Geology - Prof. M. Hansson; B) Institute of Applied Environmental Research - Prof. HC Hansson; C) Dept. of Meteorology - Dr. Leck
15. Uppsala University - Prof. Weyhenmeyer
16. University of Gothenburg - Prof. Pettersson
17. University of Iceland - Prof. Jónsdóttir

OVERVIEW ABOUT THE ACTIVITIES IN THE ATMOSPHERE MODELLING GROUP

M. BOY, N. BABKOVSKAIA, R. GIERENS, K.V. GOPALKRISHNAN, D. MOGENSEN, A. RUSANEN, S. SMOLANDER, L. ZHOU, P. ZHOU

Department of Physics, University of Helsinki, P.O.Box 64,FI-00014 University of Helsinki, Finland

Keywords: ATMOSPHERE MODELLING, VOC'S, AEROSOSLS, CLOUDS

INTRODUCTION

Today it is crucial to point out in any statement given from the scientific community to politicians that many of our future climate predictions are based on simplified and more or less empirical achieved parameterizations without knowing the detailed processes. In general the activities of the Atmosphere Modelling Group are to improve our knowledge in several atmosphere relevant topics focused to decrease the uncertainties in future climate predictions. One important goal in the group is to understand the formation of secondary aerosols starting from the emissions of precursors from the canopy up to their activation to form cloud droplets.

OBJECTIVES

The Atmosphere Modelling Group in the Division of Atmospheric Sciences at the University of Helsinki, was established in the beginning of 2009. The group currently includes beside Dr. Boy who is leading the group two post-doctoral scientists, three PhD- and three Master students. The main objectives of the group activities are:

- to quantify the emissions of volatile organic compounds (VOCs) from different ecosystems and to pinpoint the fraction of organic compounds which are not identified by novel instrumentation up today

- to study different not complete solved chemical reaction mechanisms important in the formation of new particles (e.g. OH and H_2SO_4 closures)

- to improve our capability in modelling the formation of SOA in the atmosphere and their ability to act as cloud condensation nuclei (CCN)

- to gain a better understanding in the cloud formation processes and the influence of turbulence on the aerosol dynamic and vice versa

- to parameterize the new achieved results on a more process-based understanding and implement them in large-scale models

METHODS

The tools used are several models reaching from process-based models like the University of Helsinki Multi-component Aerosol Model UHMA up to the general circulation model of the atmosphere ECHAM-HAM. A detailed description with references from all models used inside the group is available at the group website: http://www.physics.helsinki.fi/tutkimus/atm/english/research/atmosphere_modelling.html.

RESULTS

Figure 1 shows the place in time and space of the individual models. The scientific goal of each model and flow of information between the models are presented by thin black lines and blue arrows, respectively. Although each activity by itself contributes valuable information to the scientific community an overall outstanding achievement can only be reached when a strong and barrier-less cooperation between all group-members is guaranteed.
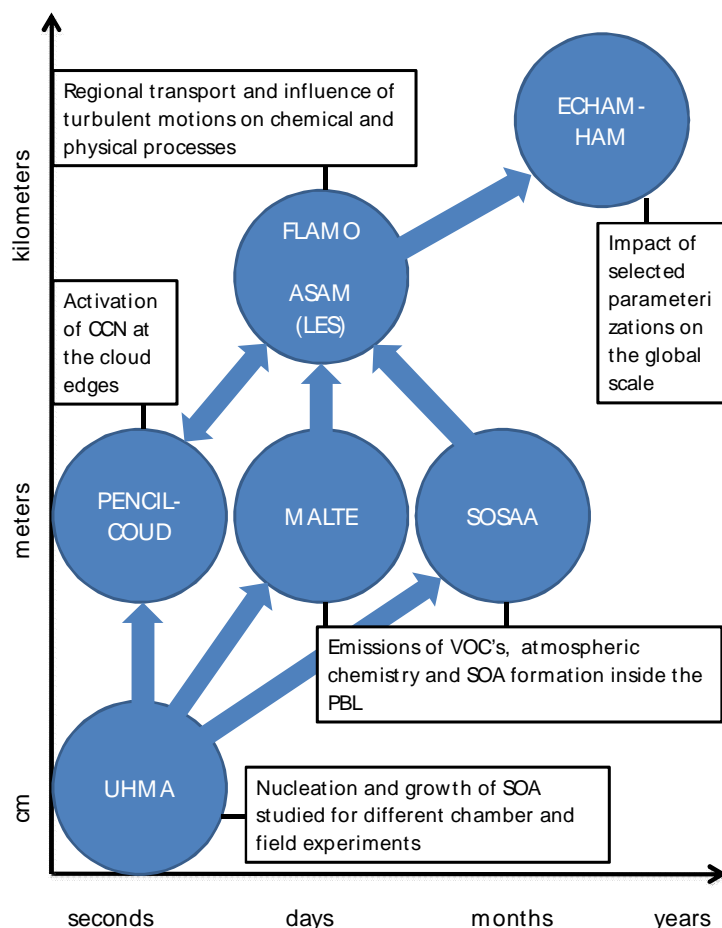
Figure 1: The used models and activities of the group in time and space

In the following we present specific discussions of new results by the group in the fields of emissions of organic vapours from the biosphere, the sulphuric acid closure, activation of cloud condensation nuclei (CCN) at the cloud edge and the BVOC- aerosol-climate interactions in the global model ECHAM-Ham.

Emissions of VOC's

Biogenic volatile organic compounds (BVOCs) are essential in atmospheric chemistry because of their chemical reactions to produce and destroy tropospheric ozone, their effects on aerosol formation and growth, and their potential influence on global warming. As one of the important BVOC groups, monoterpene has been drawing more and more scientific attention in atmospheric research. Detailed

regional measurements and model estimates are urgently encouraged to study emission controls and monoterpene budget on a global scale. However, since physical and biological factors such as genetic variation, temperature and light, water availability, seasonal changes, and environmental stresses have complex impacts on monoterpene emissions, comprehensive inventories are not so often reliably defined.

To further track monoterpene concentrations and their chemical transformations, the model SOSA (Boy et al., 2011) was applied to investigate Scots pine (Pinus sylvestris) emissions in the boreal coniferous forest at SMEAR II in Hyytiälä, Finland. Monoterpene emissions in the boreal pine forest at SMEAR II with the consideration of meteorological transport and atmospheric chemistry have been modelled in this study. We found that chemodiversity matters when constructing input inventories and parameters for emission models (Bäck et al., 2012). Better understandings of chemotypic characterization variability could reduce the model uncertainties. The three emission modules implemented in SOSA give reasonable simulations of monoterpene concentrations in comparison with measurement data. Monoterpenes emitted from conifers were identified as specific storage in resin canals, or resin ducts, and the emissions did continue during the night. The available forest floor emission data were included in our model for several months as well, and we found that the high forest floor emission seasons were spring and autumn with active microbes and increased litterfall. The modelled dominant compounds of monoterpene composition were α-pinene, followed by $\triangle^3$–carene and β-pinene, which is compatible with our measurements. Prominent seasonal variations with the highest concentrations in summer and small cycles throughout the year were reported by the model as well as the observations. The diurnal maximum monoterpene emissions appeared during the afternoon hours, whereas the monoterpene concentrations in ambient air were small at daytime. The vertical concentrations were found at very low values near ground but to reach their maximum in canopy region and then to decrease with height.

Atmospheric chemistry

According to several studies (e.g. Paasonen et al., 2010; Sipilä et al., 2010; Lauros et al., 2011) sulphuric acid is one of the initial or required molecules in the atmospheric nucleation mechanism(s). In order to quantify future atmospheric sulphuric acid concentrations a complete understanding of the sink and source terms is crucial. Although the precursors for sulphuric acid (at least some of them), as well as the main sink term (condensation on atmospheric aerosols) have been measured in several places, the closure between measured and calculated sulphuric acid concentrations has rarely been investigated (Eisele et al., 1993; Weber et al., 1997; Boy et al., 2005).

New atmospheric observations supported by laboratory experiments and theoretical considerations point to the existence of compounds (most probably stabilized Criegee Intermediate radicals – CI's) which have significant capacities to oxidize atmospheric trace gases like sulphur dioxide (Welz et al., 2012; Mauldin III et al., 2012). In this work we investigated the effect of increased reaction rates of SO_2 with Criegee Intermediate radicals on the atmospheric concentrations of sulphuric acid for two different stations: SMEAR II, Hyytiälä, Finland and Hohenpeissenberg, Germany. The results showed that oxidation of SO_2 by stabilized Criegee Intermediate radicals can be a crucial source for atmospheric sulphuric acid production in VOC rich environments. Depending on the concentrations of several investigated organic compounds (reaction products from ozone oxidation of isoprene and monoterpenes) their contribution via the reaction of stabilized Criegee Intermediates to atmospheric sulphuric acid gas phase concentrations could be as high as 50 % at ground level. Taking into account that most of the H_2SO_4 measurements are performed at ground level, the inclusion of this new oxidation mechanism is crucial in regional, as well as, global models.

Our model investigations of the boundary layer in Hyytiälä showed that the contribution from the sCI to sulphuric acid production is, as expected, most important in the canopy where the concentration of organic compounds are highest. However, our overall results show that the effect of sCI's up to 100 m is very important to consider when calculating the sulphuric acid concentration. Figure 2 shows sulphuric acid production ratio for two different height intervals (500 m and 50 m) averaged over the whole year 2010 at the SMEAR II station. We define the H_2SO_4 production ratio as the ratio between H_2SO_4 produced only by

OH oxidation of SO$_2$ divided by H$_2$SO$_4$ produced both by OH oxidation of SO$_2$ and also by reactions of stabilized Criegee intermediates with SO$_2$.
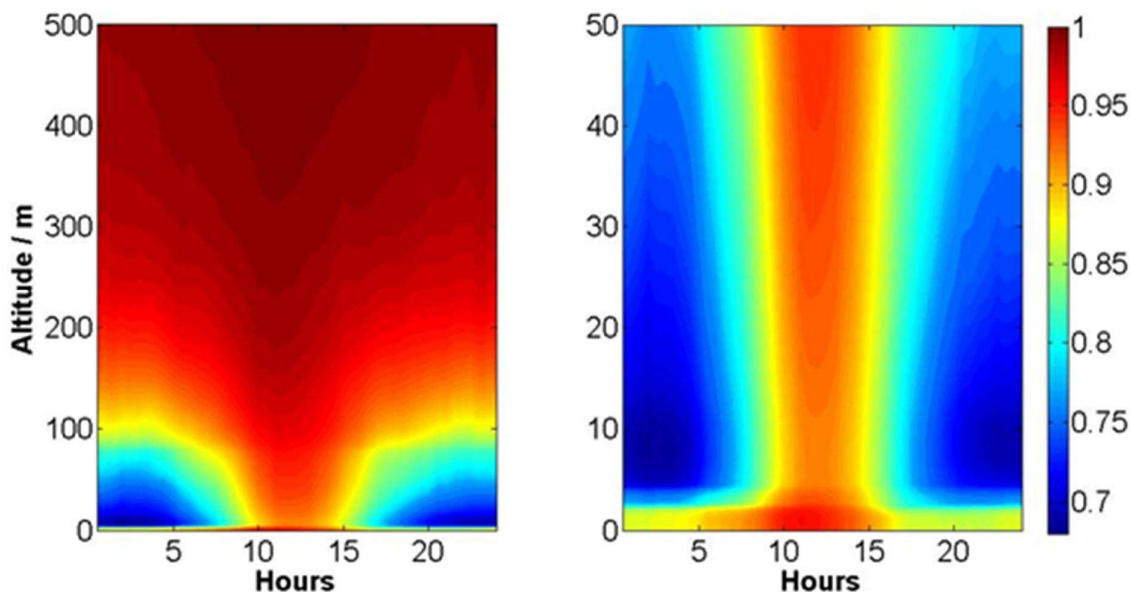
Figure 2: Yearly average sulphuric acid production ratio for 50 and 500 m above the surface at SMEAR II station in Hyytiälä, Finland.

Activation of CCN

Direct numerical simulations (DNS) are used to study the structure of the cloud edge area. In this study we used the direct numerical simulation high-order public domain finite-difference PENCIL Code for compressible hydrodynamic flows. The code is highly modular and comes with a large selection of physics modules. It is widely documented in the literature and used for many different applications (W. Dobler et al., 2006; Pensil Code, 2001). Recently, a detailed chemistry module has been implemented, including an accurate description of all necessary quantities, such as diffusion coefficients, thermal conductivity, reaction rates etc. (N. Babkovskaia et al., 2011). The new developed aerosol-module coupled to the PENCIL Code now is prepared for calculating an evaporation and condensation processes of aerosol particles, which consists of a solid core covered by liquid water.

Depending on different conditions in the investigated area the particles are evaporated or grow because of condensation. We study the effect of the air mixing on the aerosol dynamics and vise versa. The results show that due to interaction of air fluxes with different properties the final particle distribution is crucially changed. In turn, the influence of aerosol dynamics on the fluid dynamics is negligibly small in proposed model (a manuscript is in preparation).

BVOC-aerosol-climate interactions

In the study by Makkonen and co-workers (2012) we used the global aerosol-climate model ECHAM5.5-HAM2 to explore the effect of BVOC emissions on new particle formation, clouds and climate. Two BVOC emission models, MEGAN2 and LPJ-GUESS, are used to estimate the effect of BVOC-aerosol climate coupling.

The change of shortwave cloud forcing from year 1750 to 2000 ranges from -1.4 to -1.8Wm^{-2} with 5 different nucleation mechanisms. We showed that the change in shortwave cloud forcing from the year 2000 to 2100 ranges from 1.0 to 1.5Wm^{-2}. Although increasing future BVOC emissions provide 3–5% additional CCN, the effect on the cloud albedo change is modest. Due to simulated decreases in future cloud cover, the increased CCN concentrations from BVOCs cannot provide significant additional cooling in the future.

ACKNOWLEDGEMENTS

REFERENCES

Babkovskaia, N., Haugen, N., Brandenburg, A.: A high-order public domain code for direct numerical simulations of turbulent combustion, J. of Computational Physics, 230, 1, 2011.

Boy, M., Kulmala, M., Ruuskanen, T. M., Pihlatie, M., Reissell, A., Aalto, P. P., Keronen, P., Dal Maso, M., Hellen, H., Hakola, H., Jansson, R., Hanke, M. and Arnold, F.: Sulphuric acid closure and contribution to nucleation mode particle Growth, Atmos. Chem.. Phys,, 5, 863–878, 2005.

Boy, M., Sogachev, A., Lauros, J., Zhou, L., Guenther, A. and Smolander, S.: SOSA - a new model to simulate the concentrations of organic vapours and sulphuric acid inside the ABL - Part I: Model description and initial evaluation, Atmos. Chem. Phys. 11, 43-51, 2011.

Boy, M., Mogensen, D., Smolander, S., Zhou, L., Nieminen, T., Paasonen, P., Plass-Dülmer, C., Sipilä, M., Petäjä, T., Mauldin, L., Berresheim H. and Kulmala, M.: Oxidation of SO_2 by stabilized Criegee Intermediate (sCI) radicals as a crucial source for atmospheric sulphuric acid concentrations, Atmos. Chem. Phys. Disc., submitted 09/2012.

Bäck, J., Aalto, J., Henriksson, M., Hakola, H., He., Q. and Boy, M.: Chemodiversity in terpene emissions at a boreal Scots pine stand, Biogeosciences, 9, 689-702, 2012.

Dobler W., Stix M., Brandenburg, A.: Magnetic field generation in fully convective rotating spheres Astrophys. J., 638, 336, 2006.

Eisele F. L. and Tanner D. J.: Measurement of the gas phase concentration of H2SO4 and methane sulfonic acid and estimates of H2SO4 production and loss in the atmosphere, J. Geophys. Res., 98(D5), 9001—9010, 1993.

Lauros, J., Sogachev, A., Smolander, S., Vuollekoski, H., Sihto, S.-L., Laakso, L., Mammarella, I., Rannik, U. and Boy, M.: Particle concentration and flux dynamics in the atmospheric boundary layer as the indicator of formation mechanism, Atmos. Chem. Phys. 11, 5591-5601, 2011.

Makkonen, R., Asmi, A., Kerminen, V.-M., Boy, M., Arneth, A., Guenther, A. and Kulmala, M.: BVOC-aerosol-climate interactions studied with the global aerosol model ECHAM5.5-HAM2, Atmos. Chem. Phys. Discuss., 12, 9195-9246, 2012.

Mauldin III, R.L., Berndt, T., Sipilä, M., Paasonen, P., Petäjä, T., Kim, S., Kurtén, T., Stratmann, F., Kerminen, V.-M. and Kulmala, M.: A new atmospherically relevant oxidant, Nature, 488, 193, 2012.

Paasonen, P., Nieminen, T., Asmi, E., Manninen, H. E., Petäjä, T., Plass-Dülmer, C., Flentje, H., Birmili, W., Wiedensohler, A., Hörrak, U., Metzger, A., Hamed, A., Laaksonen, A., Facchini, M. C., Kerminen, V.-M., and Kulmala, M.: On the roles of sulphuric acid and low-volatility organic vapours in the initial steps of atmospheric new particle formation, Atmos. Chem. Phys., 10, 11223–11242, doi:10.5194/acp-10-11223-2010, 2010.

PENCIL Code, http://pencil-code.googlecode.com, 2001.

Sipilä, M., Berndt, T., Petäjä, T., Brus, D., Vanhanen, J., Stratmann, F., Patokoski, J., Mauldin III, R. L., Hyvärinen, H., Lihavainen, H., and Kulmala, M.: The Role of Sulphuric Acid in Atmospheric Nucleation, Science, 327, 1243–1246, 2010.

Weber, R. J., Marti, J. J., McMurry, P. H., Eisele, F. L., Tanner, D. J., and Jefferson, A.: Measurements of new particle formation and ultrafine particle growth rates at a clean continental site, J.Geophys. Res., 102, 4375–4385, 1997.

Welz, O., Savee, J.D., Osborn, D.L., Vasu, S.S., Percival, C. J., Shallcross, D. E. and Taatjes, C. A.: Direct kinetic measurements of Criegee Intermediate (CH_2OO) formed by reaction of CH_2I with O_2, Science, 335, 204-207, 2012.

OVERVIEW OF ECOLOGICAL RESEARCH ON FOREST-ATMOSPHERE INTERACTIONS

J. BÄCK[1,2], E. NIKINMAA[1], J. PUMPANEN[1], F. BERNINGER[1], P. HARI[1], T. HÖLTTÄ[1,] E. JUUROLA[1,2], P. KOLARI[1,2], A. MÄKELÄ[1], A. PORCAR-CASTELL[1], H. HAKOLA[3], J. RINNE[2], M. KULMALA[2] and T. VESALA[2]

[1]Dept. of Forest Sciences, P. O. Box 27, 00014 University of Helsinki, Finland

[2]Dept. of Physics, P.O. Box 64, FI-00014 University of Helsinki, Finland.

[3]Finnish Meteorological Institute, P.O. Box 503, FI-00101 Helsinki, Finland

Keywords: BOREAL FORESTS AND WATERSHEDS, CARBON AND NITROGEN DYNAMICS, VOLATILE ORGANIC COMPOUNDS, TRACE GASES, TREE-SOIL INTERACTIONS, STRUCTURAL-FUNCTIONAL RELATIONSHIPS, PHOTOSYNTHESIS, CHLOROPHYLL FLUORESCENCE, UPSCALING, PROCESS MODELS

INTRODUCTION

The forest ecological research at the SMEAR stations (Stations for Measuring forest Ecosystem-Atmosphere Relations) has continued to develop towards a comprehensive understanding of the feedbacks and linkages between different compartments in the ecosystem and the surroundings. This has been possible due to rapid developments in many research methods (e.g. in soil carbon and nitrogen dynamics, VOC exchange, upscaling), as well as due to a long-lasting and insightful development of both personnel and expertise. The SMEAR station network and the research philosophy were described by Hari & Kulmala (2005) as: 'The major coupling mechanisms between atmosphere and land surface are the fluxes of energy, momentum, water, carbon dioxide, atmospheric trace gases and atmospheric aerosols. Understanding of couplings and feedbacks is the basis for the prediction of changes in the system formed by atmosphere, vegetation and soil.'

Simultaneous, well planned and continuous measurements of several processes and phenomena in a forest ecosystem enable the understanding of feedbacks and connections, joining the ecosystem compartments and the surrounding atmosphere, lithosphere and hydrosphere in a dynamic manner. These include (i) carbon and nitrogen fluxes (photosynthesis, respiration, growth), (ii) trace gas exchange (reactive carbon compounds, N-compounds, ozone), and (iii) hydrological fluxes.

Below the forest ecological research at the SMEAR stations (mainly at SMEAR II) is described, along with recent new openings that have emerged from previous work.

BOREAL FORESTS AS MODIFIERS OF ATMOSPHERIC CHEMISTRY (J. Bäck et al)

Compared to tropical areas, the boreal forests are relatively inefficient as volatile organic compound (VOC) sources, but due to their large aerial coverage, their contributions are both regionally and globally important. The reactive VOCs are influencing the atmospheric O_3 and NO_x budgets, acting as precursors for secondary organic aerosols (SOA) and influencing methane lifetime. They are considered to be secondary compounds in the plant metabolism, implying that their role is in defence and signalling instead of being directly related to growth processes. However, physiologically they have many linkages to important primary processes, such as photosynthesis and transpiration.

VOC's are emitted from vegetation as mixtures of a variety of compounds, depending on plant metabolic activity both seasonally and diurnally. The most important compounds with respect to atmospheric reactions are terpenoids, i.e. isoprene, mono- and sesquiterpenes, but also several oxygen containing compounds such as methanol, acetone and acetaldehyde are emitted in variable quantities from vegetation. Field measurements on VOC exchange between ecosystems and atmosphere at the SMEAR II site have

been conducted for over 10 years, and they have provided us understanding on how the boundary layer atmospheric chemistry is influenced by vegetation under the boreal forested setting. Yet, many new processes are being recognized to contribute to the fluxes, when the long time series are analyzed in detail.

Isoprene is the dominant biogenic VOC globally (e.g. Guenther et al., 1995, Arneth et al., 2011) and its emissions from boreal forests are also significant. The main sources for isoprene in SMEAR II are Norway spruce (Picea abies), trembling aspen (Populus tremula) and willow (Salix sp.) (e.g. Hakola et al., 1998, Hakola et al., 2003). The ecosystem scale measurements of isoprene show that emissions increase in spring-time, stay rather constant in summer and decline again in fall (Hakola et al., 2003).

The most important group of VOCs in boreal forests is monoterpenes. They form the main emissions from Norway spruce and Scots pine (Pinus sylvestris), as well as from several other, deciduous species (e.g. Betula pendula, Betula pubescens and Alnus incana) (Hakola et al., 1998, 1999, 2001, 2006, Tarvainen et al., 2005). Monoterpenes are a large group of compounds with different reaction coefficients in the atmosphere, and thus it is important to know also the compound specification in emissions. Based on enclosure measurements, the two most important compounds in pine emissions are α-pinene and Δ^3 carene, followed by β-pinene, myrcene and camphene, and several minor compounds. Interestingly, the pine individuals emit a specific, inherited monoterpene blend, and thus the concentrations at the top of the canopy can differ significantly from those at the shoot level (Bäck et al., 2012, Yassaa et al., 2012). This has important implications for emission models, which are normally parameterized using information from one tree individual only (Smolander et al., this issue).

Sesquiterpenes are a very reactive group of terpenoids, emitted during summer months from pine and birch, among others (Tarvainen et al., 2005, Hakola et al., 2001, 2006). Most important compounds in pine emissions are β-caryophyllene and α-farnesene (Hakola et al., 2006, Yassaa et al., 2012). In recent years, with the novel online measurement technique PTR-MS (proton-transfer reaction mass spectrometer), also fluxes of other volatile compounds have been measured from boreal forests (Lappalainen et al., 2009, 2012). These include the short-chained alcohols, aldehydes and ketones such as methanol, ethanol, acetaldehyde and acetone. Also one larger alcohol, methyl butenol (MBO) was detected in Scots pine emissions.

We have also succeeded to measure sesquiterpene concentrations in addition to isoprene and monoterpenes in boreal pine forest air, using an in situ gas chromatograph mass-spectrometer (Hakola et al., 2012). The measurements covered the whole year, at least one week every month. During the winter months, and still in March, the concentrations of all biogenic compounds were very low, most of the time below detection limits, but in April they started to increase and show diurnal variability with maxima during night and minima during day. The diurnal variation was affected by the friction velocity, high concentrations being found with low friction velocities and low concentrations being observed high friction velocities. The main sesquiterpenes were longifolene and isolongifolene. Sesquiterpenes had a similar diurnal cycle to that of monoterpenes and contrary to isoprene suggesting temperature dependent source of sesquiterpenes.

The dynamic enclosure system (Kolari et al., 2012) has enabled the detailed analyses of factors driving the trace gas exchange under field conditions. The setup enables measurement of VOC emissions with good accuracy while minimising the disturbance caused by the chamber to the object being measured. The system underestimates the isoprene, monoterpene and many oxygenated VOC fluxes by 5-30%, mainly due to the enclosure itself. The systematic error is higher at high relative humidity than in drier conditions, which suggests that the thickness of the water film adsorbed on the chamber inner surfaces (and thus transpiration) contributes to the VOC loss rate in the chamber. This method has been applied to study fluxes of biogenic VOCs, as well as ozone and nitrogen oxides (e.g. Joensuu et al., this issue).

In short term, the biogenic emissions of VOCs show clear temperature dependence, owing to the exponential relationship between volatility and temperature (e.g. Guenther et al., 1993, Tarvainen et al., 2004, Aalto et al., this issue). Isoprene emissions are also closely connected to irradiance, as a result of the direct link between isoprene emission and synthesis from photosynthetic products. Further, the observed de novo synthesis of monoterpenes indicates that prevailing light conditions can also be important for their

biosynthesis even in terpene-storing species such as e.g. pine and spruce (Bäck et al., 2005, Ghirardo et al., 2010). In addition to the short term drivers, emissions are responsive to medium-term changes in growth conditions, which may affect the emission capacity, the shape of the light response as well as the temperature optimum of emission (Guenther et al., 2006, Arneth et al., 2008, Lappalainen et al., 2012). Large seasonal variability in monoterpene-producing enzyme activities (Juurola et al., this issue) reflects the plant's dynamic, inherent emission capacity and strong relationships with other processes and incident emission rates

In addition to emissions from green tissues, VOCs are also originating from other sources in boreal ecosystems. The below-canopy compartment, both the ground vegetation, decaying litter, and soil processes, is important as source of VOCs in particular during spring and fall, when fresh litter is creating a large source (Aaltonen et al., 2011, 2012b). The forest floor plays a substantial role (from a few per cents to several tens of per cents, depending on the season) in the total VOC emissions of the boreal forest ecosystem. Somewhat surprisingly, the wintertime fluxes within the snowpack can be equal to those from the soil during warmer periods, especially after strong winter storms when large amounts of litter are accumulating in the snow (Aaltonen et al., 2012a). The common forest soil fungal species are potential contributors for the soil VOC fluxes, especially the oxygenated compounds (methanol and acetone) (Bäck et al., 2010). Also the woody stems and branches contribute to the total VOC flux considerably (Vanhatalo et al., this issue). In a recent study (Sjöblom 2011) we observed that the lake water was a substantial source of many VOCs. Their chemical composition and also the flux rates were rather similar to that measured in the nearby forest (Aaltonen et al. 2011). Aquatic fluxes were largest during night-time, indicating either a specific nocturnal source for VOCs or an effect of transport phenomena. The research is continued with a campaign by the lake in fall 2012.

Estimates of emissions from vegetation are traditionally obtained for mature leaves under standard (constant) conditions to yield standard emission potential values ('Guenther approach'), which then are used as model parameters. However, seasonality (aside from direct temperature effect) has been recognized to strongly influence isoprene and monoterpene emission rates as well as the emission capacity. A particular feature in boreal regions is that evergreen vegetation is dormant in winter, but recovers from dormancy when temperatures rise in spring. Our measurements show that the growth processes induce high emissions of VOCs from buds and shoots. New shoots make up a small biomass in the beginning, but their absolute contribution to the emissions from foliage is 50-75% for monoterpenes, 25-50% for methanol, 25% for acetone and 25-50% for isoprene/MBO. The maximum emission rates for monoterpenes are observed before growth even starts. During the most active growth period, the normalized emissions from growing shoots are larger during morning hours and less in the afternoon than those of the old (mature) foliage, showing clearly that these emissions originate from growth processes. This will be further analyzed using our continuous field data, to reveal potential circadian controls over emission rates and their links to other physiological processes.

Canopy density influences the chemical degradation of VOC flux from forest floor (Rinne et al., 2012) by hindering transport and thus prolonging the transport time, in addition to affecting the lifetimes of VOCs by influencing the concentrations of oxidants. For isoprene the above-canopy flux closely corresponds the emission, whereas for more reactive compounds such as caryophyllene the effect of chemistry is considerable especially at nighttime, and the calculated fluxes are seriously underestimating the actual emissions.

INFLUENCE OF TREE STRUCTURE ON FLUXES ON FOREST ATMOSPHERE-INTERFACE
(Nikinmaa et al)

Material fluxes at forest atmosphere boundary occur predominantly through leaf surfaces. The rate across the surface depends on its total (leaf) area and the surface specific exchange rate. In flux studies the former is often considered to be fairly constant and the latter to be driven by the properties of the atmosphere next to and radiation reaching the leaf. The largest fluxes between canopies and atmosphere

are those of CO_2 and water vapor and thus the most influential atmospheric properties are the concentrations of those gases along the components of the radiation balance.

In reality the situation is much more complex than described above as trees exert considerable control on both the total leaf area and the leaf area specific exchange rate. For most of the time at tree stand level the leaf area is in fact quite constant as the stand becomes fully stocked relative to resource availability (often the light) but there are important deviations from this situation after disturbances when the leaf area becomes zero. The dynamics how trees grow and leaf area develops depends on the structural development and resource allocation, that is an important factor determining the competitive status of tree individuals. Carbon capture and its allocation by individuals determine how quickly stand becomes fully stocked and after that which individuals continue growing and how much and which individuals die. They also determine the longevity of captured carbon in the organic matter as there are hundred times difference in maximal carbon residence time between foliage and stemwood. We have been successfully studying and modeling forest dynamics since early 1980´s as described below. In this analysis one key aspect has been the functional balance between different structural components of trees.

Similarly as structure exerts strong influence on the leaf area dynamics, it has strong impact on the leaf area specific exchange rate. Under conditions that allow photosynthesis, parallel flows of carbon dioxide into leaf and water vapor out of the leaf are driven by opposite concentration gradients of these gases. By adjusting the size of the pores (stomata) through which the gas exchange occurs in leaves, plants can influence the conductivity of the pathway. However, it simultaneously influences the driving gradient of CO_2 inflow as the downstream concentration of CO_2 results from the balance between consumption in photosynthesis and inflow from atmosphere. As the driving downstream concentration of water vapor remains constant, the stomatal control also influences the ratio of carbon and water vapor exchange. We have shown (Hari and Mäkelä 2003, Mäkelä et al., 2004) that even in humid boreal climate optimizing the carbon gain relative to water use seem to predict well the stomatal action relative to environmental conditions. The optimization requires though that carbon cost of transpired water is defined.

The carbon cost of transpired water is related to tree structure as one of the main roles of branches and stems of trees is to transport water from soil to replace the water that is transpired from leaves. The water, or the sap, flow relies on metastable state of water and therefore requires specific structural properties to allow the transport. As water is lost from water surfaces to vapor at internal air spaces in leaves the surfaces become curved. Surface tension forces create a pull that the cohesive forces propagate throughout the transport structure. The viscous forces oppose the flow and tension gradients of several MPa can develop in the water transporting xylem. This means that the xylem structure has to be very strong to avoid collapsing under the tension. Under such negative pressure also air bubbles are easily formed and they spread readily threatening the water transport that relies on continuous chains of water molecules from leaves to soil. Xylem tissue consists of small conductive elements with thick walls that are connected to each other through small pits that have a filtering membrane in the middle. Such structure can withstand strong pressure gradients and efficiently hinder the spreading of the air bubbles. Downside of such structure is that the better filtering capacity, the more resistance there is for water flow. Our recent theoretical analysis suggests that the membrane pore sizes, the sizes of conductive elements and the macroscopic stem and branch structure and wood versus foliage relationships seem to be tightly and optimally connected relative to carbon cost of water transport (Hölttä et al., 2011).

The xylem structure and quantitative scaling between xylem and foliage (along with leaf properties) determine how large negative pressure develops per unit of transpired water. As mentioned, high tensions can be detrimental if they result into formation and spreading of air-bubbles in the xylem conducting tissue. But further, xylem tension influences also the trees ability to transport assimilated sugars from leaves to other parts. The transport of sugar is driven by positive bulk (turgor) pressure gradient of water that is osmotically created in the living cells of phloem that is a parallel transport system to xylem in the bark tissue. At the sites of sugar assimilation osmotic strength is high resulting into high turgor pressure while at the sites of sugar consumption it is the opposite case. Now if the water tension is high in the parallel xylem tissue, more sugars are needed to draw water from there to phloem and consequently sugar transport with the bulk flow is slower than it would be if xylem tension was lower. By opening and closing

of stomata, leaves control the water and carbon flows i.e. also xylem water tension and assimilation rate and hence the potential osmotic strength in the phloem. Incidentally, we recently showed that requiring the stomata open such that maximizes the sugar transport from leaves, produces observed behavior of stomata and leaf gas exchange (Nikinmaa et al., 2012). The result is naturally the same as with the previously introduced optimal stomatal control of gas exchange as both fit the data the same way but this recent formulation does not require assigning carbon cost for water but it directly links gas exchange with xylem and phloem transport properties and structural scaling.

Gas exchange of carbon and water is determined by structural properties and scaling of transport tissue relative to leaves but simultaneously they are the largest sinks of assimilated carbohydrates. This linking is further emphasized as the growth of new tissue requires positive cell enlarging pressure in the growing cells. So gas exchange, water pressures and growth need to match each other at any time but over extended periods their relationships determine the structural properties that in turn feed back to those fluxes. It is foreseeable that only specific combinations of these processes will thrive in given environment. Combining these with the tree stand and canopy dynamics builds up a coherent framework of understanding the role of trees in controlling water and carbon cycles.

At SMEAR stations one of our main goals is to understand how vegetation controls the carbon and water fluxes. The above theoretical framework that we have developed since 1980´s forms the basis for versatile tree measurements that aim to test and quantify our theoretical framework and the component processes dynamically under the full spectrum of long term environmental variation. We have measured the leaf gas exchange (with automated chambers (Hari et al., 1999) and eddy-covariance (e.g. Kolari et al., 2004)), xylem and phloem pressures, with diurnal diameter variation of xylem and bark tissue, (Perämäki et al., 2001, Sevanto et al., 2002 and 2003), sapflow rate in the xylem (with granier type sensors) and also dynamics of extension and thickness growth. We have also modeled xylem and phloem transport dynamics and their interaction with leaf gas exchange and growth (e.g. Hölttä et al., 2006 and 2010; Duursma et al., 2008; Nikinmaa et al., 2012).

The last fifteen years have included large variation of weather from cold and wet years to exceptionally warm and dry years which together with mathematical modeling of the theoretical framework will allow us to predict the forest behavior in the changing climate. The modeling can also be used to analyze the sensitivity of the outcome on specific structural or process features that can be experimentally tested. Finally the analysis can be extended easily to other species allowing us to build more comprehensive picture at landscape and larger levels.

RESEARCH ON PLANT PRODUCTIVITY AND ENERGY EXCHANGE (F. Berninger et al.)

Previously we have shown that the productivity of boreal evergreen forests depends largely on the length of the growing season (Suni et al., 2003, 2004, Mäkelä et al., 2004). Furthermore, the transitions between the winter and summer stages seem to be important for the emission of volatile organic carbon compounds and lead to frequent nucleation events during spring (Kulmala et al., 2004, Dal Maso et al., 2009).

From a research perspective we have been working towards a better understanding of how to better predict this "phenology of photosynthesis" on different scales (shoot, stand, region), to better understand the underlying physiological processes, including approaches that can be used for monitoring of photosynthetic production using present or future remote sensing methods. For, forest energy balances we tried to understand how changes in albedo affect the forest energy balance and the interactions of albedo changes with climate variability and land use changes.

It is well known that the photosynthesis of boreal trees is slowed down during the winter period due to environmental constraints as physiological adjustments of the trees. While the environmental constraints are reasonably well addressed by current models, models including physiological adjustments are rare and not well established. Porcar et al. (2008a, b) developed models of the recovery of photosynthetic production based on fluorescence. They demonstrated that the recovery under field conditions depends strongly on the light environment and developed new approaches for the quantification of long term

acclimation to cold using fluorescence. This slow recovery of photosynthesis is not well understood in present models of photosynthetic production but has received a lot of emphasis in our research group using models based on the work of Mäkelä et al. (2004). We tried to expand the analysis to a multisite comparison of eddy covariance sites (Mäkelä et al., 2008, Gea-Izquierdo et al., 2010) and found that slow physiological recovery processes are very important in boreal forests. While, ignoring this slow recovery from models of production in temperate forests will not bias photosynthesis models much, models for boreal forests will be seriously biased if slow physiological adaptations are ignored.

During 2011 we started with attempts to come to a more rigorous description of forest energy balances on the landscape scale. Using long time series from the SMEAR II station we arrived to quantify the variation of albedo in Scots pine forests under different snow conditions (Kuusinen et al., 2012). The work showed that the albedo during snow cover is variable. Highest albedo values seem to occur after snow fall and under cold, but cloudy conditions. This shows that the modelling of albedo, snow cover and its integration with remote sensed data should be used and designed with care, since satellite pictures, emphasizing clear sky conditions, will yield different albedos than ground data (that measures under all conditions). We are presently developing approaches to combine land cover data and satellite data for albedo estimation from satellites (Kuusinen et al., submitted).

REMOTE SENSING OF PHOTOSYNTHESIS: UNDERSTANDING THE SEASONAL SIGNALS
(A. Porcar-Castell et al)

Plants are constantly adjusting their photosynthetic performance to the environment. Adjustments take place during the day in response to the diurnal changes in illumination and temperature, but also at a much more slow temporal scale in response to water or temperature induced stress, and the seasonal pattern in light and temperature. These adjustments generate optical signals that have been widely used to study the short-term acclimation in photosynthetic energy partitioning at the leaf level. Optical signals include the emission of chlorophyll-a fluorescence as well as the reflectance spectra. The mechanisms linking these optical signals to photosynthesis are very well understood at the short-term (minutes-days). However, important questions at the seasonal time-scale remain, which need to be solved if we are to implement the approach to the remote sensing of photosynthesis.

During the last years our group has made significant advances in this field: (1) We have developed a theoretical model framework and generated a number of novel fluorescence parameters (Porcar-Castell et al. 2008a, Porcar-Castell 2011, Porcar-Castell, this issue) that allow us to study the seasonal acclimation of photosynthesis using chlorophyll fluorescence (Porcar-Castell et al. 2008b) or spectral reflectance indices (Porcar-Castell et al. 2012a). In addition (2) we are world pioneers in the implementation of long-term leaf-level chlorophyll fluorescence monitoring in the field (Porcar-Castell et al. 2008c), and the first to characterise the annual dynamics in photosynthetic energy partitioning at the light reactions of photosynthesis in situ (Porcar-Castell 2011). These advances are crucial to understand the signature of photosynthesis as we see it from space (Porcar-Castell 2012b), and the sun-induced fluorescence signal (Guanter et al, in review). In the present we are working with leaf-level bottom-up mechanistic models (remote sensing friendly) (Olascoaga et al. In prep, Olascoaga et al. manuscript), that once coupled with canopy and atmospheric radiative transfer models will facilitate the interpretation of the satellite passive fluorescence signal.

Last but not least, the most obvious application of this approach is the spatially explicit estimation of intra and interannual variability in ecosystem GPP, however, because the seasonal acclimation of the light reactions might also be linked to the seasonal dynamics in VOC emission (Porcar-Castell et al. 2009), the resulting synoptic maps of photosynthetic activity might be useful for modelling of large-scale VOC emission patterns.

MODELLING FOREST PRODUCTIVITY AND GROWTH (A. Mäkelä et al.)

The objective of our modelling work is to synthesize the empirical research in quantitative terms, in order to develop tools for the analysis of the interactions of the different material fluxes and the interactions between plant structure and function (Mäkelä 2012). The models also aim to offer tools for applications in forestry in a changing climate.

We have developed models combining tree and stand carbon fluxes with structural growth through functional balances since 1980s (e.g., Mäkelä 1986, Mäkelä and Hari 1986, Nikinmaa 1992, Mäkelä 1997). While a lot of our work has been directed towards a better understanding of the long-term structural dynamics of trees and stands (Mäkelä and Sievänen 1992, Valentine and Mäkelä 2005, Mäkelä and Valentine 2006) with applications to economic optimisation of forest management (Hyytiäinen et al. 2004, Niinimäki et al. 2012), the focus has more recently shifted to (1) incorporating spatial and temporal variation in environmental conditions quantitatively in the models, and (2) including a better description of nutrient and water dynamics alongside with carbon dynamics. These developments have made the approach more readily applicable to the analysis of climate change impacts and adaptation (e.g., Mäkipää et al. 2011, Nikinmaa et al. 2012).

A unique characteristic of our work is modularity based on scale. According to this, short-term processes and processes defined at high spatial resolution are modelled in relative isolation from those at the larger scale, however, defining the links between the scales carefully on the basis of process understanding. This allows for independent testing and calibration of the models at different scales, therefore increasing the transparency of the modelling process (Mäkelä 2003). Examples of this include models of canopy photosynthesis as driven by environmental variables (Mäkelä et al. 2008, Peltoniemi et al. 2012) and combining these with regional flux and stand growth predictions (Härkönen et al. 2010, 2011), as well as a modular model of wood quality with a hierarchical structure including tree, whorl, and branch levels (Mäkelä and Mäkinen 2003). Recently, we have further developed our earlier canopy photosynthesis model by adding ecosystem water fluxes (Peltoniemi et al., in preparation).

For the analysis of nitrogen and carbon relationships, we have developed an approach based on evolutionary optimisation and yielding optimal co-allocation of carbon and nitrogen in the forest stand. Our first approach focused on a quasi-steady state assuming slow height growth, resulting in realistic predictions of the impacts of carbon and nitrogen availability on stand structure (Mäkelä et al. 2008, Dewar et al. 2009). A further development of this model included height growth dynamics (Valentine and Mäkelä 2012). This approach is currently being combined with a model of soil carbon and nitrogen dynamics (Chertov et al. 2001), and applications to forest productivity and growth in a changing climate are underway (Nikinmaa et al. 2012). Preliminary results suggest that while canopy photosynthetic potential may increase in boreal forests due to increasing temperatures, precipitation and CO_2 levels, the degree to which this can be actually utilised by the canopy largely depends on the simultaneous increase in nutrient release from the soil, which may be accelerated less than the potential photosynthetic capacity.

PROCESS STUDIES WITH MANIPULATION AND MEASUREMENT SYSTEMS UNDER CONTROLLED CONDITIONS (J. Bäck et al)

We have conducted continuous gas exchange measurements (at both shoot and stand scales) in our field site for already 16 years. These are among the longest time series in the world. The field data has been used for calculating stand level budgets of carbon, water and nitrogen balances (e.g. Ilvesniemi et al., 2009, 2010, Kolari et al., 2006, 2009, Korhonen et al., 2012 submitted). These measurements give ample information on tree and stand physiological processes in prevailing and momentary environmental conditions, and on the seasonal and interannual patterns in the measured processes (Altimir et al. 2006, Mäkelä et al. 2006, Kolari et al. 2007, Launiainen et al. 2011).

The small-scale flux measurements have also been utilised in more theoretical studies of stand-scale flux measurements (Mammarella et al. 2007) and in studying the contribution of different CO_2 sinks and sources to observed stand-level CO_2 exchange (Alekseychik et al. submitted).

However, field measurements give information on the rates of physiological processes in prevailing conditions where the environmental driving factors are often correlated. Less understanding is obtained on e.g. the potential photosynthetic capacity in standard or optimal conditions, changes in photosynthetic parameters with environment, or separating the effects of whole-tree or belowground sink control from direct effects of environment on shoot photosynthetic responses (or vice versa). A two-year campaign of monthly measurements of gas exchange responses on pine shoots revealed that different drivers and mechanisms are responsible to the seasonality of photosynthesis (Juurola et al. this issue). Therefore we have been developing instrumented laboratory facilities, with a potential to manipulate the tree (branch, roots or whole tree) environment, and to measure instantaneous and delayed responses to these manipulations. The fast response photosynthesis measurement system with attached microcosms enable studies where dynamic interactions between above and below ground plant compartments can be efficiently analyzed.

As an example, the microcosms were used for testing the impact of soil temperature and three different boreal forest tree species on the archaeal populations in the bulk soil, rhizosphere, and mycorrhizosphere (Bomberg et al., 2011). The most commonly detected archaeal 16S rRNA gene sequences belonged to a group typically found in boreal and alpine forest soils. Interestingly, also one sequence belonging to group I.1b Crenarchaeota was detected from Scots pine mycorrhiza although sequences of this group are usually found in agricultural and forest soils in temperate areas. Tree and temperature-related shifts in the archaeal population structure were observed. The greatest diversity of archaeal DGGE bands was detected in Scots pine roots and mycorrhizas. No archaea were detected from humus samples from microcosms without tree seedling, indicating that the archaea found in the mycorrhizosphere and root systems were dependent on the plant host.

TOWARDS AN INTEGRATED APPROACH IN ECOSYSTEM STUDIES FROM THE SOIL POINT OF VIEW. (J. Pumpanen et al.)

The response of forest soil to rising atmospheric CO_2 concentration and rising temperature, and their feedback effects on the greenhouse gases and aerosols in the atmosphere, and in this way to the radiative forcing of the atmosphere, are key questions when predicting the climate conditions in the future.

Recent studies have shown that plants act as carbohydrate sources, by emitting root exudates which sustain mycorrhizal fungal symbionts, but also other groups of specialized micro-organisms (Högberg and Read 2006, Pumpanen et al., 2009; Heinonsalo et al., 2010, Pumpanen et al., 2012). The flux of carbon belowground stimulates the decomposition of soil organic matter and nitrogen uptake of trees (Drake et al. 2011, Phillips et al. 2011). It has been suggested that root exudates and other easily decomposable carbon could enhance the decomposition of old soil organic matter (Fontaine et al., 2007, Kuzyakov 2010) and turnover rates of nitrogen in the rhizosphere with possible vegetation growth enhancing feedback (Phillips et al., 2011). In our ongoing studies, we have also observed that the root exudates and other easily decomposable carbon increase mineralization of old recalcitrant soil organic matter which was shown both in the age of respired CO_2 from the soil and ^{15}N isotopic signal of the trees (Lindén et al., unpublished).

In coupled climate-carbon cycle models, biological activity of soils is usually driven by abiotic factors such as temperature and moisture (Conant et al., 2011). However, in the nature the effects of temperature are coupled with other environmental factors such as irradiation, and the allocation of carbon belowground (Reichstein et al. 2005), which are seasonally and geographically highly variable. Plant growth and carbon allocation in boreal forest ecosystems depend on the supply of recycled nutrients within the forest ecosystem, because the external inputs in the form of atmospheric deposition are very low compared to the total requirement. In nitrogen limited boreal forest ecosystems the biologically available nitrogen (NH_4 and NO_3) is in short supply although the amount of N bound to soil organic matter may be large. Upon the decomposition of lignocellulose, the proportion of compounds having higher nitrogen content increases while the proportion of compounds containing carbohydrates (hemicellulose and cellulose) decreases. Therefore, there is a large pool of immobilized nitrogen in the slowly decomposing SOM pool (Hättenschwiler and Vitousek 2000).

Nitrogen balance of boreal forests and peat lands have been one of the focal points of the soil research conducted in the FCoE. Korhonen et al. (submitted, 2012) showed that in the boreal forest stand at SMEARII station nitrogen uptake and retranslocation were as important sources of N for plant growth. Most of the uptaken nitrogen originated from decomposition of organic matter, and the fraction of nitrogen that could originate directly from deposition was about 30%. Dry deposition and organic nitrogen in wet deposition contributed over half of the input in deposition. Total outputs of nitrogen from the site were very small were 0.4 kg N ha^{-1} yr^{-1}, the most important outputs being N_2O emission to the atmosphere and organic nitrogen flux in drainage flow.

Recent studies have shown that the nitrogen mineralization is stimulated by the increases in the flux of carbon belowground resulting in feedbacks to nitrogen cycling and nitrogen uptake of the trees (Drake et al., 2011 and Phillips et al., 2011). This may further increase net primary productivity of the forest ecosystem (Hari and Kulmala 2008). However, the processes affecting these feedbacks are poorly known and not quantified so that they could be incorporated in coupled climate-carbon cycle models (Arneth et al., 2010, Drake et al., 2011, Conant et al., 2011). We are tackling the processes underlying nitrogen acquisition of trees and ground vegetation from old recalcitrant soil organic matter by using stable isotopes ^{15}N, ^{13}C, radiocarbon dating, mesocosm and field experiment and process modeling. According to our preliminary results, the amount of easily decomposable carbon (sugar) affects the source of nitrogen acquisition of the Pinus sylvestris (Lindén et al., unpublished). We have also observed that belowground carbon sink activity is reflected to the aboveground photosynthesis in the common boreal tree species in an experiment where tree seedlings of different tree species were grown under three different temperature regimes (Pumpanen et al., 2012). The photosynthesis rate was reduced by cold soil temperatures and increased at higher temperatures. The net CO_2 exchange and seedling biomass did not increase significantly with increasing temperature due to a concomitant increase in carbon assimilation and respiration rates. Highest biomass accumulation was observed in the medium temperature.

Fire and storm are the most important natural disturbances in the boreal forest influencing strongly the structure, composition and functioning of the forest. Although less than 1 % of the boreal forests burn each year, it is a significant land area when taking into account that boreal forests cover 15% of the Earth's land area. It is expected that with future climate change the fire frequencies in boreal forests will increase as a result of long drought events. Already now, large forest fires are common in Russia and Canada during summer months. During a fire, SOM, mostly carbon, is released from the forest biomass rapidly to the atmosphere through combustion, and simultaneously the mineralized N is released in the soil in the form of NO_3^- and NH_4^+ favoring the re-establishment of vegetation during the first years of succession. However, the long term consequences of fire on the C and N cycle are largely unknown. It is not well known how the turnover rate of the remaining SOM will change as a result of changes in the fire interval. In 2010, we have established a chronosequence study at SMEAR I station and its surrounding forests in Värriö Strict Nature Reserve for studying the processes underlying carbon and nitrogen cycle at taiga forests exposed to fire. We are conducting there soil CO_2 efflux measurements as well as above and below ground C- and N-pool inventories.

A chronosequence approach was also used for studying the role of ground vegetation in the carbon exchange of boreal forest ecosystems (Kulmala 2011). A process model for estimating the gross primary productivity (GPP) of the most common shrub species was developed by Kulmala et al. (2011), and used for determining the GPP of a chronosequence of clear-cut sites around Hyytiälä area (Kulmala et al., 2012). Ground vegetation plays on important role in the carbon exchange of boreal forest; its contribution to total annual GPP in forest ecosystem was highest in young 6-9-year-old forest sites (about 350 g C m^{-2}) and decreasing during the forest succession.

The role of aquatic systems as a net sink or a source for atmospheric CO_2 is presently under debate. In a recent Nature paper (Yvon-Durocher et al., 2012), we showed that the annual ecosystem respiration in aquatic ecosystems show a substantially greater temperature compared to those of terrestrial ecosystems. This can be due to differences in the importance of other variables beside temperature such as primary productivity and allochtonous/terrestrial carbon inputs to the aquatic systems. When precipitation or other processes pull large volumes of organic matter from the land into nearby lakes, this carbon effectively

disappears from the carbon budget of terrestrial ecosystems if gas fluxes over the lake surface are ignored, which they traditionally have been. We have tracked the flow of carbon into and out of a lake in Southern Finland over five years and found that the lake was a net source of carbon, emitting between 70 and 100 g $C\ m^{-2}$ each year. When compared against the role of surrounding forest, which was a net C sink, the lake's emissions were enough to offset about 10% of the forest's annual C sequestration (Huotari et al., 2011). It is obvious that fluxes of carbon within lacustrine ecosystems must be accounted for when estimating carbon fluxes at the regional level. This is especially true in the boreal zone where lakes are abundant (Hanson et al., 2004, Wetzel 2001). The CO_2 which is transported from aquatic ecosystems to the atmosphere originates from the surrounding soils and wetlands, from mineralization of organic carbon and from respiration of roots and mycorrhiza. This way the biological processes taking place in the terrestrial ecosystem (e.g. photosynthesis, respiration and decomposition) are interlinked. In our recent studies, we have observed that the CO_2 concentration in stream and lake indeed are controlled by the water flushing from the surrounding forest soil through the riparian zone during and after heavy rain events (Rasilo et al., 2011). For monitoring the CO_2 concentrations in the aquatic systems and in the soil profile, we have developed a novel method using non-dispersive infrared CO_2 sensors (Hari et al. 2008). The system has been successfully used in our group for measuring the photosynthesis and respiration of planctonic algae (Hari et al., 2008), vertical distribution of respiration in the soil profile and the seasonal pattern of root and rhizosphere respiration (Pumpanen et al. 2008) and changes in the CO_2 concentrations in the soil, riparian zone, stream and lake continuum following rain events (Rasilo et al., 2012).

Riparian zone, between the terrestrial and aquatic ecosystems is an important hotspot area having important implications both in the lateral transport of carbon and nitrogen and as a source of major important greenhouse gases CO_2, CH_4, N_2O and also biogenic volatile organic compounds (BVOCs). The concentration of greenhouse gases (CO_2, CH_4, N_2O) in the lake is accumulating during the winter and released after the ice has melted. The proportion of aromatic compounds in the water percolating through the soil profile increases as it passes through the riparian zone (Rasilo et al., submitted 2012) indicating that the riparian zone also acts as a source of aromatic and volatile compounds. However, the processes affecting the water quality in the pathway of the water from the terrestrial to the aquatic ecosystems are still relatively poorly known.

Soil can also be a substantial source of organic amine compounds due to the large pool of organic nitrogen in the soil. This is because the most common form of N in soils is amino acid N (20–50% of the total N as amino N) (Senwo and Tabatabai 1998). Recently, we carried out a mesocosm experiment where amine formation in forest soil was induced with different enzyme treatments and artificial glucose amendments. The preliminary results show that amine formation seems to have a close link with root system and its processes since the quality and quantity of amine compounds were different and dependent on the presence of root system.

To sum it up, soil plays an important and active role in controlling the greenhouse gas balance in the atmosphere and it also affects indirectly the radiative forcing of the atmosphere through various feedback effects. In the future, we will emphasize the process understanding in our studies by planning field and laboratory experiments for studying the connection between above and below ground parts of the forest ecosystem. We will also continue studying the role of lateral transport of greenhouse gases between the ecosystems e.g. the connection between aquatic and terrestrial systems. Finally, last but not least we will strengthen our already strong methodological skills in greenhouse gas flux measurements (Pumpanen et al., 2004, Pihlatie et al., submitted) by organizing a new campaign to quantify errors related to N_2O flux chamber measurements.

CONCLUSIONS

The comprehensive measurements and development of sophisticated theoretical frameworks on the boreal forest ecology and ecophysiology at the SMEAR stations have provided us important understanding on how the forest ecosystem works, how it reflects the variability in environment, and how it influences the surrounding atmosphere, soil and watershed. The development of measurements and theoretical

frameworks will be continued and the systems constantly upgraded, further enhancing the implementation of our results in models for predicting the responses of forests to future conditions. Further, truly novel understanding about the role of boreal ecosystems, especially forests, in global biogeochemical cycles and in atmospheric chemistry and physics will be emerging with these powerful methods and exceptionally long time series. Effective and open collaboration between different disciplines is a crucial factor in this work.

ACKNOWLEDGEMENTS

REFERENCES

Aaltonen H., Aalto J., Kolari P., Pihlatie M., Pumpanen J., Kulmala M., Nikinmaa E., Vesala T. & J. Bäck (2012b) Continuous VOC flux measurements on boreal forest floor. Submitted to Plant and Soil

Aaltonen H., Pumpanen J., Hakola H., Vesala T., Rasmus S. & Bäck J. (2012a). Snowpack concentrations and estimated fluxes of volatile organic compounds in a boreal forest. – Biogeosciences 9: 2033–2044

Aaltonen H., Pumpanen J., Pihlatie M., Hakola H., Hellén H., Kulmala L., Vesala T. & Bäck J. (2011) Boreal pine forest floor biogenic volatile organic compound emissions peak in early summer and autumn. - Agricultural and Forest Meteorology 151: 682-691

Altimir N, Kolari P, Tuovinen JP, Vesala T, Back J, Suni T, Kulmala M, Hari P 2006. Foliage surface ozone deposition: a role for surface moisture? Biogeosciences 3, 209-228.

Arneth A., Niinemets Ü., Pressley S., Bäck J., Hari P., Karl T., Noe S., Prentice IC., Serça D., Hickler T., Wolf A. & Smith B. (2007) Process-based estimates of terrestrial ecosystem isoprene emissions: incorporating the effects of a direct CO_2-isoprene interaction. - Atmospheric Chemistry and Physics 7, 31-53.

Arneth A., Harrison S.P., Zaehle S. et al. (2010). Terrestrial biogeochemical feedbacks in the climate system. Nature Geosci. 3(8): 525-532.

Arneth A., Schurgers G, Lathiere J., Duhl T., Beerling D. J., Hewitt C. N., Martin M., and Guenther A. (2011) Global terrestrial isoprene emission models: sensitivity to variability in climate and vegetation Atmos. Chem. Phys., 11, 8037–8052

Bomberg M., Münster U., Pumpanen J., Ilvesniemi H. and Heinonsalo J. (2011). Archaeal communities in boreal forest tree rhizospheres respond to changing soil temperatures. Microbial ecology. DOI: 10.1007/s00248-011-9837-4.

Bäck J., Aalto J., Henriksson M., Hakola H., He, Q. & Boy, M. (2012) Chemodiversity of a Scots pine stand and implications for terpene air concentrations. - Biogeosciences 9: 689–702.

Bäck J., Aaltonen H., Hellén H., Kajos M., Patokoski J., Taipale R., Pumpanen J. & Heinonsalo J. (2010) Variable emissions of microbial volatile organic compounds (MVOCs) from root-associated fungi isolated from Scots pine. - Atmospheric Environment 44: 3651-3659.

Bäck J., Hari P., Hakola H., Juurola E. & Kulmala, M. (2005). Dynamics of monoterpene emissions in Pinus sylvestris during early spring. - Boreal Environment Research 10: 409-424.

Chertov, O.G., Komarov, A.S., Nadporozhskaya, M., Bykhovets, S.S., and Zudin, S.L. (2001). ROMUL - a model of forest soil organic matter dynamics as a substantial tool for forest ecosystem modeling. Ecol. Model. 138: 289-308.

Conant R.T., Ryan M.G., Ågren G.I. et al.. (2011). Temperature and soil organic matter decomposition rates – synthesis of current knowledge and a way forward. Global Change Biol. 17: 3392 – 3404

Dal Maso, M., Hari, P. & Kulmala, M. (2009): Spring recovery of photosynthesis and atmospheric particle formation. Boreal Env. Res. 14: 711–721.

Dewar R.C., Franklin O., Mäkelä A., McMurtrie R.E., Valentine H.T. (2009). Optimal function explains forest responses to global change. Bioscience 59:127-139.

Drake J.E. Gallet-Budynek A., Hofmockel K.S. et al. (2011). Increases in the flux of carbon belowground stimulate nitrogen uptake and sustain the long-term enhancement of forest productivity under elevated CO2. Ecol. Lett. 14: 349-357.

Duursma R.A., Kolari P., Perämäki M., Nikinmaa E., Hari P., Delzon S., Loustau D., Ilvesniemi H., Pumpanen J. & Mäkelä A. (2008) Predicting the decline in daily maximum transpiration rate of two pine stands during drought based on constant minimum leaf water potential and plant hydraulic conductance. Tree Physiology 28, 265–276.

Fontaine S., Barot S., Barré P. et al. (2007). Stability of organic carbon in deep soil layers controlled by fresh carbon supply. Nature 450(8): 277-280.

Gea-Izquierdo G.,; Mäkelä A., Margolis H.,;Bergeron Y.,Black AT., Dunn A., Hadley J., Tha Paw U., Falk M. Wharton S., Monson R., Hollinger DY., Laurila T., Aurela M., McCaughey H., Bourque C., Vesala T. Berninger F. (2010) .Modelling acclimation of photosynthesis to temperature in evergreen boreal conifer forests. New Phytologist 10.1111/j.1469-8137.2010.03367.x

Ghirardo A., Koch C, Taipale R, Zimmer I, Schnitzler J.-P. and Rinne J. (2010) Determination of de novo and pool emissions of terpenes from four common boreal/alpine trees by 13CO2 labelling and PTR-MS analysis. Plant Cell Env. 33: 781–792 doi: 10.1111/j.1365-3040.2009.02104.x

Guanter L, Rossini M, Colombo R, Meroni M, Frankenberg C, Lee J-E, Porcar-Castell A (In Review). Using field spectroscopy to assess the retrieval of sun-induced fluorescence from solar Fraunhofer lines and its relationshipwith gross primary production. Under Review in Remote Sensing of Environment.

Guenther, A. B., Zimmerman, P. R., Harley, P. C., Monson, R. K., and Fall, R. (1993) Isoprene and Monoterpene Emission Rate Variability – Model Evaluations and Sensitivity Analyses, J. Geophys. Res.-Atmos., 98(D7), 12609–12617.

Guenther, A., Hewitt, C. N., Erickson, D., Fall, R., Geron, C., Graedel, T., Harley, P., Klinger, L., Lerdau, M., Mckay, W. A., Pierce, T., Scholes, B., Steinbrecher, R., Tallamraju, R., Taylor, J., and Zimmerman, P. A. (1995) Global-Model of Natural Volatile Organic-Compound Emissions, J. Geophys. Res.- Atmos., 100(D5), 8873–8892

Guenther A, Karl T., HarleyP., Wiedinmyer C., Palmer P.I., and Geron C. (2006) Estimates of global terrestrial isoprene emissions using MEGAN (Model of Emissions of Gases and Aerosols from Nature). Atmos. Chem. Phys., 6, 3181–3210

Hakola H., Hellén H., Tarvainen V., Bäck J., Patokoski J. and Rinne J., (2009). Annual variations of atmospheric VOC concentrations in a boreal forest. Boreal Env. Res. 14, 722–730.

Hakola H., Hellén H., Henriksson M., Rinne J. and Kulmala M. (2012). In situ measurements of volatile organic compounds in a boreal forest. Atmos. Chem. Phys. Discuss., 12, 15565-15596, 2012

Hakola H., Rinne J. and Laurila T., (1998). The hydrocarbon emission rates of Tea-leafed willow (Salix phylicifolia), Silver birch (Betula bendula) and European aspen (Populus tremula). Atmospheric Environment, 32, 1825-1833

Hakola H., Laurila T., Lindfors V., Hellén H. Gaman A., and Rinne J. (2001). Variation of the VOC emission rates of birch species during the growing season. Boreal Environment Research, 6, 237-249

Hakola, H, Tarvainen, V., Laurila, T., Hiltunen, V., Hellén H. and Keronen P. (2003). Seasonal variation of VOC concentrations above a boreal coniferous forest. Atmospheric Environment 37, 1623-1634

Hakola H., Tarvainen V., Bäck J., Ranta H., Bonn B., Rinne J. & Kulmala M. (2006). Seasonal variation of mono- and sesquiterpene emission rates of Scots pine. - Biogeosciences 3: 93-101.

Hanson. P. C., Pollard, A. I., Bade, D. L., Predick, K., Carpenter, S. R. & Foley, J. A. (2004). A model of carbon evasion and sedimentation in temperate lakes. Glob. Change Biol. 10: 1285-1298.

Hari, P., Keronen, P., Bäck, J., Altimir, N., Linkosalo, T., Pohja, T., Kulmala, M., Vesala, T., (1999). An improvement of the method for calibrating measurements of photosynthetic CO2 flux. Plant Cell Environ. 22, 1297–1301.

Hari P & Kulmala M (2005) Station for Measuring Ecosystem–Atmosphere Relations (SMEAR II). Boreal Env. Res. 10: 315–322

Hari P. and Kulmala L. (editors) (2008) Boreal Forest and Climate Change. Advances in Global Change Research, Vol. 34, Springer Verlag. Berlin.

Hari, P. and Mäkelä, A (2003): Annual pattern of photosynthesis in Scots pine in the boreal zone, Tree Physiology, 23, 145–155.

Heinonsalo J., Pumpanen J., Rasilo T., Hurme K.-R. and Ilvesniemi H. (2010). Carbon partitioning in ectomycorrhizal Scots pine seedlings. Soil Biol. & Biochem. 42 (9): 1614-1623

Huotari J., Ojala A., Peltomaa E., Nordbo A., Launiainen S., Pumpanen J., Rasilo T., Hari P. and Vesala T. (2011). Long-term direct CO_2 flux measurements over a boreal lake: Five years of eddy covariance data. Geophys. Res. Lett. doi: 10.1029/2011GL048753

Härkönen S., Pulkkinen M., Duursma R.A., Mäkelä A. (2010). Estimating annual GPP, NPP and stem growth in Finland using summary models. For. Ecol. Manage. 259: 524-533.

Härkönen, S., Lehtonen, A., Eerikäinen, K., Peltoniemi, M., Mäkelä, A. (2011). Estimating carbon fluxes for large regions in Finland based on process-based modeling, NFI data and Landsat satellite images. Forest Ecology and Management 262:2364-2377.

Hyytiäinen K., Hari, P. Kokkila T., Mäkelä A., Tahvonen O. and Taipale J. (2004). Connecting a process-based forest growth model to stand-level economic optimization. Canadian Journal of Forest Research 34:2060-2073.

Hättenschwiler S. and Vitousek P.M (2000). The role of polyphenols in terrestrial ecosystem nutrient cycling. Tree 15(6): 238-243.

Högberg P. and Read D.J. (2006). Towards a more plant physiological perspective on soil ecology. Trends in Ecol. and Evol.. 21 (10):548-554.

Hölttä T, Vesala T, Sevanto S, Perämäki M, Nikinmaa E (2006) Modeling xylem and phloem water flows in trees according to cohesion theory and Münch hypothesis. Trees - Structure and Function 20: 67-78.

Hölttä T, Mäkinen H, Nöjd P, Mäkelä A, Nikinmaa E (2010). A physiological model of cambial growth. Tree Physiology 30: 1235-1252.

Hölttä T, Mencuccini M, Nikinmaa E. (2011) A carbon cost–gain model explains the observed patterns of xylem safety and efficiency. Plant, Cell & Environment

Ilvesniemi, H., Levula, J., Ojansuu, R., Kolari, P., Kulmala, L., Pumpanen, J., Launiainen, S., Vesala, T. & Nikinmaa, E. (2009): Long-term measurements of the carbon balance of a boreal Scots pine dominated forest ecosystem. Boreal Env. Res. 14: 731–753.

Kolari P., Bäck J., Taipale R., Ruuskanen T.M., Kajos M.K., Rinne J., Kulmala M. & Hari P. (2012) Evaluation of accuracy in measurements of VOC emissions with dynamic chamber system. - Atmospheric Environment, accepted

Kolari, P., Kulmala, L., Pumpanen, J., Launiainen, S., Ilvesniemi, H., Hari, P. & Nikinmaa, E. (2009) CO_2 exchange and component CO_2 fluxes of a boreal Scots pine forest. Boreal Env. Res. 14: 761–783.

Kolari P, Lappalainen HK, Hänninen H, Hari P. (2007). Relationship between temperature and the seasonal course of photosynthesis in Scots pine at northern timberline and in southern boreal zone. Tellus B 59, 542-552.

Kolari, P., Pumpanen, J., Rannik, Ü., Ilvesniemi, H., Hari, P. & Berninger, F. (2004). Carbon balance of different aged Scots pine forests in Southern Finland. Global Change Biology 10: 1106–1119.

Kolari P, Pumpanen J, Kulmala L, Ilvesniemi H, Nikinmaa E, Grönholm T, Hari P (2006). Forest floor vegetation plays an important role in photosynthetic production of boreal forests. Forest Ecology and Management 221, 241-248.

Kulmala L. Pumpanen J., Hari P., and Vesala T. (2011). Photosynthesis of ground vegetation in different aged pine forests: Photosynthesis of ground vegetation in different aged pine forests: Ef¬fect of environmental factors predicted with a process-based mode. Journal of Vegetation Science 22: 96-110.

Kulmala L., Pumpanen J., Kolari P., Muukkonen P., Hari P. and Vesala T. (2011). Photosynthetic production of ground vegetation in different aged Scots pine forests. Canadian Journal of Forest Research 41(10): 2020-2030, 10.1139/x11-121

Kulmala M., Suni T., Lehtinen K.E.J., Dal Maso M., Boy M., Reissell A., Rannik Ü., Aalto P., Keronen P., Hakola H., Bäck J., Hoffmann T., Vesala T. & Hari P. (2004). A new feedback mechanism linking forests, aerosols, and climate. - Atmospheric Chemistry and Physics 4: 557-562.

Kuusinen, N., Kolari, P., Levula, J., Porcar-Castell, A., Stenberg, P., & Berninger, F. (2012). Seasonal variation in boreal pine forest albedo and effects of canopy snow on forest reflectance. Agricultural and Forest Meteorology, 164, 53-60.

Kuzyakov Y. (2010). Priming effects: Interactions between living and dead organic matter. Soil Biol. & Biochem. 42: 1363-1371.

Lappalainen H.K., Sevanto S., Bäck J., Ruuskanen T.M., Kolari P., Taipale R., Rinne J., Kulmala M. & Hari P. (2009) Day-time concentrations of biogenic volatile organic compounds in a boreal forest canopy and their relation to environmental and biological factors. - Atmospheric Chemistry and Physics 9: 5447-5459.

Lappalainen H.K., Sevanto S., Dal Maso M., Taipale R., Kajos M., Kolari P. & Bäck J. (2012) A source orientated approach for estimating day-time concentrations of biogenic volatile organic compounds in an upper layer of a boreal forest canopy. – Boreal Environment Research, in print

Launiainen S, Katul GG, Kolari P, Vesala T, Hari P (2011). Empirical and optimal stomatal controls on leaf and ecosystem level CO_2 and H_2O exchange rates. Agricultural and Forest Meteorology 151, 1672-1689.

Mammarella I, Kolari P, Rinne J, Keronen P, Pumpanen J, Vesala T (2007). Determining the contribution of vertical advection to the net ecosystem exchange at Hyytiälä forest, Finland. Tellus B 59, 900-909.

Mäkelä A. (2012). On guiding principles for carbon allocation in eco-physiological growth models. Tree Physiology 32:644-647.

Mäkelä A., Valentine H., Helmisaari H.-S. (2008). Optimal co-allocation of carbon and nitrogen in a forest stand at steady state. New Phytologist 180.

Mäkelä, A. (1986). Implications of the pipe model theory on dry matter partitioning and height growth in trees. Journal of Theoretical Biology 123, 103-120

Mäkelä, A. (1997) A carbon balance model of growth and self-pruning in trees based on structural relationships. Forest Science 43(1):7-24

Mäkelä, A. (2003). Process-based modelling of tree and stand growth: towards a hierarchical treatment of multi-scale processes. Canadian Journal of Forest Research 33:398-409

Mäkelä, A. and Hari, P. (1986). Stand growth model based on carbon uptake and allocation in individual trees. Ecological Modelling 33, 205-229.

Mäkelä, A., Hari, P., Berninger, F., Hänninen, H., Nikinmaa, E., (2004). Acclimation of photosynthetic capacity in Scots pine to the annual cycle of temperature. Tree Physiol. 24, 369–376.

Mäkelä A and Mäkinen H. (2003) Generating 3D sawlogs with a process-based growth model. Forest Ecology and Management 184:337-354

Mäkelä A., Pulkkinen M., Kolari P., Lagergren F., Berbigier B., Lindroth A., Loustau D., Nikinmaa E., Vesala T., Hari P. (2008) Developing an empirical model of stand GPP with the LUE approach: analysis of eddy covariance data at five contrasting conifer sites in Europe. Global Change Biology 14: 98- 108.

Mäkelä, A. and Sievänen, R. (1992). Height growth strategies in open-grown trees. Journal of Theoretical Biology 159, 443-467.

Mäkelä A. and Valentine H. (2006). Crown ratio influences allometric scaling in trees. Ecology 87:2967-2972

Mäkelä A, Kolari P, Karimäki J, Nikinmaa E, Perämäki M, Hari P. (2006). Modelling five years of weather-driven variation of GPP in a boreal forest. Agricultural and Forest Meterology 139, 382-398.

Mäkipää R., Linkosalo T., Niinimäki S., Komarov A., Bykhovets S., Tahvonen O. and Mäkelä A. 2011. How forest management and climate change affect the carbon sequestration of a Norway spruce stand. Journal of Forest Planning 16:107-120.

Niinimäki S., Tahvonen O., Mäkelä A. (2012). Applying a process-based model in Norway spruce management. Forest Ecology and Management 265:102-115

Nikinmaa E (1992) Analyses of the growth of Scots pine; matching structure with function. Acta Forestalia Fennica. 1992, 235, 68 p

Nikinmaa E., Mäkelä A., Kolari P., Valsta L., Mäkinen A., Cao T. and Tomppo E. 2012. Significance of adaptation to forest management and economic returns in forests under transition due to climate change. In: T.Carter, A. Perrels, M. Hilden (Eds): Second Nordic International Conference on Climate Change Adaptation, Helsinki, 29-31 August 2012. Programme and Abstracts. P. 42.

Nikinmaa E., Hölttä T., Hari P., Kolari P., Mäkelä A. Sevanto, S. & Vesala T. (2012). Assimilate transport in phloems sets conditions for leaf gas exchange. Plant, Cell &Environmmen. (Accepted).

Peltoniemi M., Pulkkinen M., Kolari, P., Duursma, R., Montagnani, L., Wharton, S., Lagergren, F., Takagi, K., Verbeeck, H., Christensen, T., Vesala, T., Falk, M., Loustau, D., Mäkelä, A. (2012). Does canopy mean N concentration explain differences in light use efficiencies of canopies in 14 contrasting forest sites? Tree Physiology, 32(2): 200-218

Perämäki M, Nikinmaa E, Sevanto S, Ilvesniemi H, Siivola E, Hari P, Vesala T. (2001). Tree stem diameter variations and transpiration in Scots pine: an analysis using a dynamic sap flow model. Tree Physiology 21(12-13): 889-897.

Phillips R.P., Finzi A.C.and Bernhardt E.S. (2011). Enhanced root exudation induces microbial feedbacks to N cycling in a pine forest under long-term CO_2 fumigation. Ecol. Lett. 14: 187-194

Porcar-Castell, A., Garcia-Plazaola, J.I., Nichol, C.J., Kolari, P., Olascoaga, B., Kuusinen, N., Fernández-Marín, B., Pulkkinen, M., Juurola, E. & Nikinmaa, E. (2012) Physiology of the seasonal relationship between the photochemical reflectance index and photosynthetic light use efficiency, Oecologia, pp. 1-11.

Porcar-Castell A, Juurola E, Nikinmaa E, Berninger F, Ensminger I, Hari P. (2008a). Seasonal acclimation of photosystem II in Pinus sylvestris. I. Estimating the rate constants of sustained thermal dissipation and photochemistry. Tree Physiology 28:1475-1482.

Porcar-Castell A, Juurola E, Berninger F, Ensminger I, Hari P, Nikinmaa E. (2008b) Seasonal acclimation of photosystem II in Pinus sylvestris. II. Studying the effect of light environment through the rate constants of sustained heat dissipation and photochemistry. Tree Physiology 28:1483–1491.

Porcar-Castell A, Pfündel E, Korhonen JFJ, Juurola E, (2008c).A new monitoring PAM fluorometer (MONI-PAM) to study the short- and long-term acclimation of photosystem II in field conditions. Photosynthesis Research 96:173-179.

Porcar-Castell A, Peñuelas J, Owen S, Llusià J, Munné-Bosch S, Bäck J. (2009). Leaf carotenoid concentrations and monoterpene emission capacity under acclimation of the light reactions of photosynthesis. Boreal Environment Research 14:794-806.

Porcar-Castell A. (2011). A high-resolution portray of the annual dynamics in photochemical and non-photochemical quenching in needles of Pinus sylvestris. Physiologia Plantarum 143: 139-153.

Porcar-Castell, A., Garcia-Plazaola, J.I., Nichol, C.J., Kolari, P., Olascoaga, B., Kuusinen, N., Fernández-Marín, B., Pulkkinen, M., Juurola, E. & Nikinmaa, E. (2012a) Physiology of the seasonal relationship between the photochemical reflectance index and photosynthetic light use efficiency, Oecologia (Early Online) Doi: 10.1007/s00442-012-2317-9

Porcar-Castell A (2012) Interactive comment on "Chlorophyll fluorescence remote sensing from space in scattering atmospheres: implications for its retrieval and interferences with atmospheric CO_2 retrievals" by C. Frankengerg et al. Atmospheric Measurement Techniques Discussions, 5, C969-C971.

Pumpanen J., Kolari P., Ilvesniemi H., Minkkinen K., Vesala T., Niinistö S., Lohila A., Larmola T., Morero M., Pihlatie M., Janssens I., Curiel Yuste J., Grünzweig J. M., Reth S., Subke J.-A., Savage K., Kutsch W., Østreng G., Ziegler W., Anthoni P., Lindroth A. and Hari P. (2004). Comparison of different chamber techniques for measuring soil CO_2 efflux. Agric. For. Met. 123: 159-176

Pumpanen J.S., Heinonsalo J., Rasilo T., Hurme K.-R. and Ilvesniemi H. (2009). Carbon balance and allocation of assimilated CO_2 in Scots pine, Norway spruce and Silver birch seedlings determined with gas exchange measurements and ^{14}C pulse labelling in laboratory conditions. Trees-Structure and Function 23: 611-621. doi:10.2136/sssaj2007.0199.

Pumpanen J., Heinonsalo J., Rasilo T. and Ilvesniemi H. (2012). The Effects of soil and air temperature on CO2 exchange and net biomass accumulation in Norway spruce, Scots pine and Silver birch seedlings. Tree Physiology 32(6): 724-736.

Rasilo T., Ojala A., Huotari J. and Pumpanen J. (2012). Rain induced changes in CO_2 concentrations in the soil – lake – brook continuum of a boreal forested catchment. Vadose Zone Journal. doi: doi:10.2136/vzj2011.0039.

Rasilo T., Ojala A., Huotari J., Starr M. and Pumpanen J.. (2012) Concentrations and quality of DOC along a boreal forested terrestrial-aquatic continuum. Submitted to Journal of Fresh Water Science.

Reichstein M., Falge E., Baldocchi D., Papale D., Aubinet M., Berbigier P., Bernhofer C., Buchmann N., Gilmanov T., Granier A., Grünwald T., Havránková K., Ilvesniemi H., Janous D., Knohl A., Laurila T., Lohila A., Loustau D., Matteucci G., Meyers T., Miglietta F., Ourcival J.-M., Pumpanen J., Rambal S., Rotenberg E., Sanz M., Tenhunen J., Seufert G., Vaccari F., Vesala T., Yakir D. and Valentini R. (2005). On the separation of net ecosystem exchange into assimilation and ecosystem respiration: review and improved algorithm. Global Change Biol. 11: 1-16.

Rinne J., Markkanen T., Ruuskanen T.M., Petäjä T., Keronen P., Tang M.J., Crowley J. N.,. Rannik U, and Vesala T. (2012) Effect of chemical degradation on fluxes of reactive compounds – a study with a stochastic Lagrangian transport model. Atmos. Chem. Phys., 12, 4843–4854

Senwo Z.N. and Tabatabai M.A. (1998). Amino acid composition of soil organic matter. Biol. Fertil. Soils 26(3): 235-242

Sevanto S, Vesala T, Perämäki M, Nikinmaa E. (2002). Time lags for xylem and stem diameter variations in a Scots pine tree. Plant Cell Environ 25(8): 1071-1077.

Sevanto S, Vesala T, Perämäki M, Nikinmaa E. (2003). Sugar transport together with environmental conditions controls time lags between xylem and stem diameter changes. Plant Cell Environ 26(8): 1257-1265.

Sjöblom H. (2011). Biogenic volatile organic compounds from lake Kuivajärvi in Hyytiälä. MSc thesis. University of Helsinki, Department of Environmental Sciences.

Suni T., Berninger F, Vesala T, Markkanen T, Hari P, Mäkelä A, Ilvesniemi H, Hänninen H, Nikinmaa E, Huttula T, Laurila T, Aurela M, Grelle A, Lindroth A, Arneth A, Shibistova O, Lloyd J (2003) Air temperature triggers the commencement of evergreen boreal forest photosynthesis in spring. Global Change Biology 9:1410-1426.

Suni T., Berninger F., Markkanen T., Keronen P., Rannik Ü., Vesala T., (2003) Interannual variability and timing of growing-season CO_2 exchange in a boreal forest. Journal of Geophysical Research. 108, 4265, doi:10.1029/2002JD002381

Tarvainen V., Hakola H., Hellen H., Bäck J., Hari P. & Kulmala M. (2005). Temperature and light dependence of the VOC emissions of Scots pine. - Atmospheric Chemistry and Physics 5: 6691-6718

Valentine H.T. and Mäkelä A (2005). Bridging process-based and empirical approaches to modeling tree growth. Tree Physiology 25:769–779

Valentine H.T, Mäkelä, A. (2012). Modeling forest stand dynamics from optimal balances of carbon and nitrogen. New Phytologist. 194: 961–971

Wetzel R. G. (2001). Limnology, Lake and River Ecosystems, Academic, 443 San Diego, California.

Yassaa N., Song W., Vanhatalo A., Bäck J., Williams J. (2012) Diel cycles of isoprenoids in the emissions of Norway spruce, four Scots pine chemotypes, and in Boreal forest ambient air during HUMPPA-COPEC-2010. - Atmospheric Chemistry and Physics, 12, 7215–7229.

Yvon-Durocher G., Caffrey J.M., Cescatti A., Dossena M., del Giorgio P., Gasol J.M., Montoya J.M., Pumpanen J., Staehr P.A., Trimmer M., Woodward G. and Allen A.P. (2012). Reconciling differences in the temperature-dependence of ecosystem respiration across time scales and ecosystem types. Nature. 7408 (vol.487): 472-476.

ACTIVITIES IN THE AEROSOL PHENOMENOLOGY GROUP

M. DAL MASO, N.L. PRISLE, H. LAPPALAINEN, H. JUNNINEN, T. NIEMINEN, L. LIAO, L. RIUTTANEN, E.-M. KYRÖ, B. MOLGAARD, M. PARAMONOV, V. KARSISTO, AND M. KULMALA

University of Helsinki, PO. Box 48, 00014 University of Helsinki, Finland

Keywords: AEROSOL, TRACE GASES, ATMOSPHERIC PROCESSES, ATMOSPHERIC TRANSPORT

INTRODUCTION

Atmospheric aerosol and trace gases are key factors in most processes affecting the properties of the atmosphere and its effect on the earth's biosphere. Changes in their concentrations and transport cause changes in eg. the radiative properties of the atmosphere, the water budget of the land-atmosphere interface, the oxidative capacity of the atmosphere, and many other processes. Such changes impact human and ecosystem welfare, for example via a changing climate or increases in aerosol concentrations causing adverse health effects. In addition, these changes cause changes in the atmospheric processes, which in turn can further change the concetrations of aerosols and trace gases, causing feedbacks in the system of ecosystems.

The aerosol phenomenology group is focused on studying these processes and the phenomena caused by them by making use of field data collected at various sites, and analysing them with a process-oriented view.

OBJECTIVES AND METHODS

The aerosol phenomenology group consists of 4 post-doctoral researchers and ca. 10 PhD and MSc students, and is lead by Miikka Dal Maso. The focus areas of the Aerosol Phenomenology group are

Aerosol particle birth and evolution of aerosol populations

Research on the atmospheric aerosol particle birth and evolution of aerosol population extends from molecular clusters to the activation of cloud condensation nuclei, and from biogenic aerosol precursor vapours to the evolution of aerosol population in urban areas.

One of the major research topics is atmospheric new particle formation. The group studies the formation of aerosol particles by nucleation and the growth of these nanosized particles towards cloud condensation nuclei (CCN) sizes, as well as relevant ambient vapours and aerosol particle loss processes. The background aerosol particle concentration in both urban and rural areas and the activation of aerosol particles to CCN are also researched, as well as indoor aerosol processes.

The characterisation of the physical and chemical properties of aerosol particles is imperative in improving our understanding of the processes that they are involved in and the potential influence on global climate and human health they exert. Our research spans several orders of magnitude of particle size, and considers both natural and anthropogenic, as well as primary and secondary,

aerosol. One of the specific interests of our group is concentrated on the aspect of urban aerosols and their health effects. Both field measurement data and atmospheric models are used as tools. The research in our group also focuses on the ability of aerosol particles to act as CCN, which is largely determined by the size and chemical composition of the particles. The main research objectives are the spatial and temporal variability of CCN properties, the role that CCN chemistry plays in cloud formation, and the evolution of aerosol populations through cloud processing.

Characterization of physical and chemical properties of aerosol particles

Research on the atmospheric aerosol particle birth and evolution of aerosol population extends from molecular clusters to the activation of cloud condensation nuclei, and from biogenic aerosol precursor vapours to the evolution of aerosol population in urban areas.

One of our major research topics is the atmospheric new particle formation. We study the formation of aerosol particles by nucleation and the growth of these nanosized particles towards cloud condensation nuclei (CCN) sizes, as well as relevant ambient vapours and aerosol particle loss processes. We also study the background aerosol particle concentration in both urban and rural areas and the activation of aerosol particles to CCN. Our study also includes indoor aerosol processes.

Advanced statistics and machine learning

The datasets from our SMEAR stations are large, and there is potential for deriving a lot of knowledge from them. However, the size and complexity of these datasets make it difficult and time consuming to extract more information. Helpful tools for this work are found in the fields of statistics and machine learning. For the study of new particle formation a tool based on self-organising maps has been developed. From a set of learning data it extracts information on the particle number size distributions on days with and without new particle formation. Given a new set of number size distribution data, it can tell us on which days new particle formation happened.

A forecast model for urban particle number concentration is another example. It is a parametric regression model implemented in a Bayesian framework. Through Bayesian inference it forecasts probability distributions of particle number concentrations. Also cluster analysis has been used in various contexts.

RESULTS

We will present a summary of recent results of the aerosol phenomenology group.

A study of aerosol transport between 3 stations in Northern Finland showed a consistent pattern of how aerosol grows as it arrives over land. The pseudo-Lagrangian methodology used allowed the determination of an overall average growth rate of aerosols, without selection bias towards days that are particle formation days; this led to lower values than previous estimates made from Euclidean point measurements, and the average growth rate of aerosols was shown to be around 1 nm/h (Väänänen *et al.*).

A air mass history study of aerosol formation in the Boreal clean sector that acts as a source area for the SMEAR I and II stations shows that the aerosol mass yield – and also their growth rate – from biogenic precursors is a) temperature-dependent for the SMEAR II station (see Fig. 1) and b) lower at the northern stations (Liao *et al.*). This is of interest to the organic aerosol community, as current efforts to model organic aerosol growth usually use a constant yield factor from precursors.

The long-term aerosol and trace gas time series measured at the SMEAR I and II stations have been utilized to perform an analysis of possible trends visible in the time series. For the SMEAR
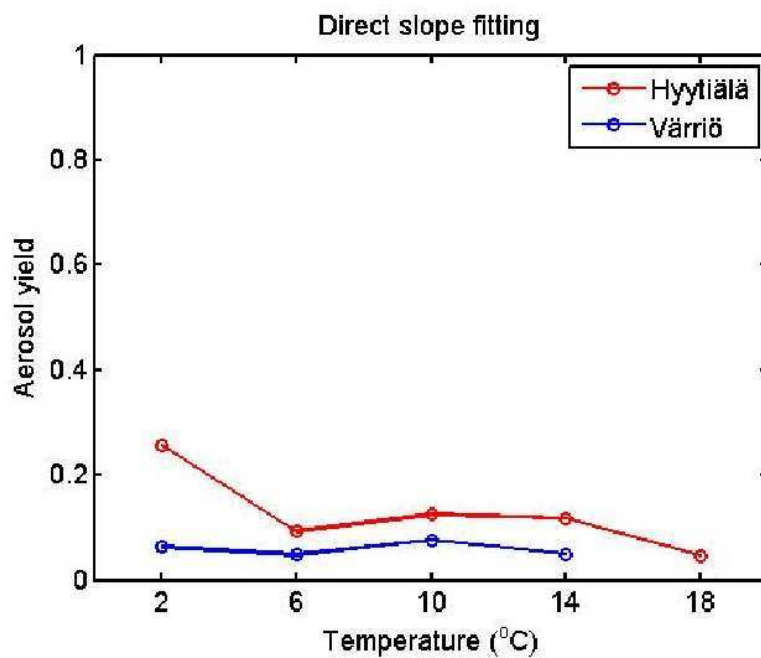
Figure 1: The aerosol mass yield as a function of temperature for air masses arriving at the SMEAR I and SMEAR II station.
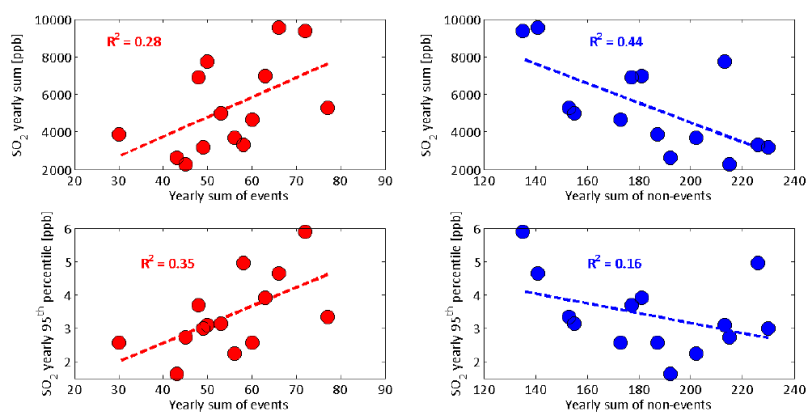
Figure 2: The correlation between measured SO_2 correlation statistics and observed particle formation event numbers at the SMEAR I station.
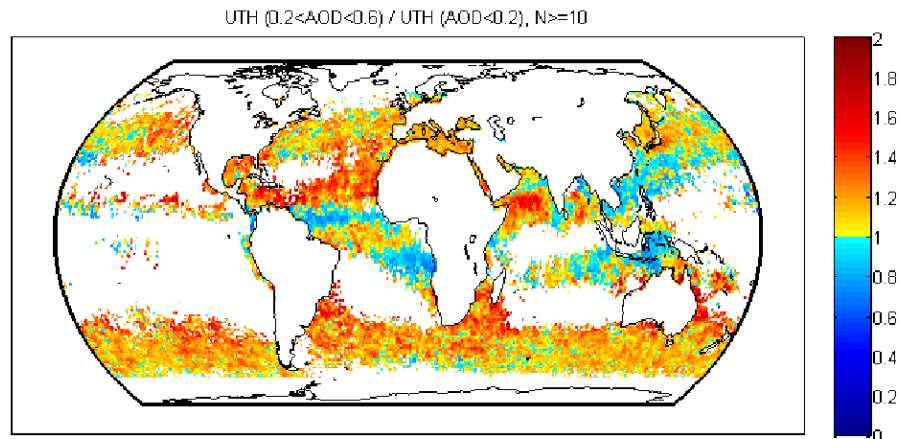
Figure 3: Change in upper tropospheric humidity (UTH) when aerosol optical depth (AOD) is high vs. low: UTH(0.2¡AOD¡0.6)/UTH(AOD¡0.2). White areas are areas with less than 10 data points. The study is done over ocean only.

I (Värriö) station, trend analysis showed a decreasing trend for SO_2, as expected, and also a decrease in total particle number and CCN number, but not nucleation mode particle nubmers. However, yearly sums show a correlation between the number of aerosol formation events and the SO_2 concentration sum (Fig. 2); this is certainly interesting but as the causal link between the two observations is compicated, a deeper study into this phenomenon is warranted (Kyrö *et al.*).

A similar trend analysis was performed for the SMEAR II data. The analysis revealed that formation rates of particles did not exhibit a significant trend; however, a 3% annual increase of particle growth rate relative to the 16-year trend was observable in the measurements. Trends in the condensation sink and an semi-empirical sulphuric acid proxy were found to be negative, which suggests that the increase in growth rates is not due to sulphuric acid, but eg. organic compounds.

In addition to SMEAR station data, data from measurement campaigns was also investigated. A campaign at the Aboa station in antarctica revealed particle formation occurring on several days. Deeper investigation of the formation periods revealed that the particles were formed as the air mass passed over liquid water ponds on Antarctica, but not when air was coming from the coast. This presents a new source for aerosol formation on the Antarctic continent, and based on the evidence organic emissions from the scarce Antarctic flora are involved (Kyrö *et al.*,b).

As demonstrated by some of the above studies, an important link between the biosphere and the atmosphere are organic compounds. Emission rates and concentrations of biogenic volatile organic compounds (BVOCS) are continuously measured at the SMEAR II station. To try to understand the variations of the concentrations of some BVOCs, these measurements were used to construct a statistical model of the concentrations. A model that included temperature, the mixed layer height and the ozone concentration was found to be the best fit to the observations (Karsisto *et al.*).

Studies of satellite data concerning atmospheric humidity and its connection to aerosol concentrations (Riuttanen *et al.*). Investigations showed an increase in the upper tropospheric humidity (UTH) when the aerosol optical depth was high (see Fig. 3). To study this potentially climatically important phenomenon, careful examination of the data is necessary, as it is affected by factors such as deep convection, seasonal changes in aerosol sources, wet scanvenging, meteorological patterns and possible cloud or humidity contamination of the AOD data.

As the secondary effect of aerosols on climate is largely based on the number of cloud condensation
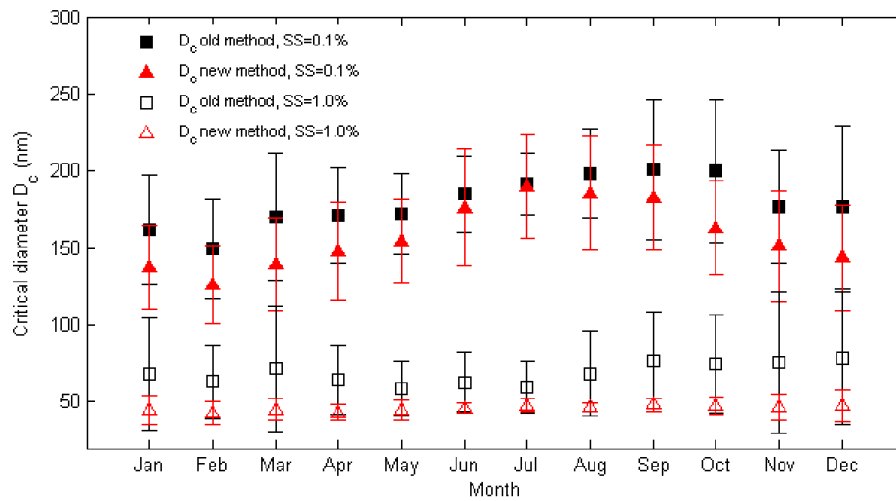
Figure 4: Monthly variation of differently derived Dc for two SS levels at SMEAR II
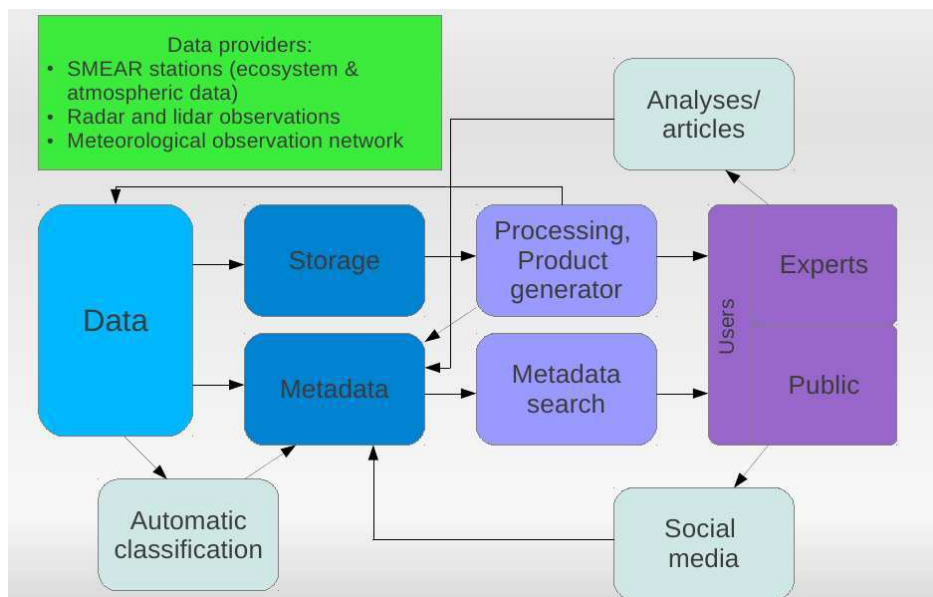
Figure 5: A schematic of the data findability and sharing solution being developed for the SMEAR stations.

nuclei (CCN) present in the atmosphere, we have also studied the 3-year time series of CCN measured at the SMEAR II station. The analysis of the data required methodology development, and a new method was developed to derive critical diameters. Using the new method, result point to higher hygroscopicity of boreal particles than previously thought. An annual variation of critical diameters was found (Fig 4.), the more hygroscopic particles found in winter (Paramonov *et al.*).

Members of the phenomenology group have also participated in the development of a data handling environment, aimed at facilitating the usage and sharing of data between researchers inside the Centre of Excellence and also the rest of the scientific community. The vision and basic outline of the planned data storage, search, and handling environment is shown in Fig. 5.

ACKNOWLEDGEMENTS

REFERENCES

Väänänen, R., Nieminen, T., Dal Maso, M., Virkkula, A., Svenningson, B., Kivekäs, N., Holst, T., Arneth, A., Kerminen, V.-M., and Kulmala, M. Analysis of aerosol dynamics between three sites in Northern Scandinavia *this collection*

Liao, L., Kulmala, M., and Dal Maso, M. Study the effect of temperature on natural aerosol production potentials over boreal forest *this collection*

Paramonov, M., Petäjä, T., Aalto, P.P., Dal Maso., M., Prisle, N., Kerminen, V.-M., and Kulmala, M. The analysis of size-segregated cloud condensation nuclei counter (CCNC) data from SMEAR II and its implications for aerosol-cloud relations *this collection*

Riuttanen, L., Bister, M., John, V., Dal Maso, M., Räisänen, J., De Leeuw, G., and Kulmala, M. Possible links between upper tropospheric humidity and aerosols *this collection*

Kyrö, E.-M., Virkkula, A., Kerminen, V.-M., Dal Maso, M., Parshintsev, J., Ruiz-Jimenez, J., Forsström, L., Manninen, H., Heinonen, P., Riekkola, M.-L., and Kulmala, M. Antarctic aerosol formation from continental biogenic sources *this collection*

Kyrö, E.-M., Dal Maso, M., Virkkula, A., Nieminen, T., Aalto, P.P., Keronen, P., Hari, P. and Kulmala, M. Long-term trends in air pollution and new particle formation in Eastern Lapland, Finland *this collection*

Karsisto, V., Junninen, H., Lappalainen, H., and Dal Maso, M. BVOC concentration modeling using environmental factors *this collection*

OVERVIEW OF THE STUDIES CONDUCTED BY THE UEF AEROSOL PHYSICS GROUP

ARI LAAKSONEN[1,2], SAMI ROMAKKANIEMI[1], JORMA JOUTSENSAARI[1], AMAR HAMED[1], JUSSI MALILA[1], IRSHAD AHMAD[1], ELHAM BARANIZADEH[1], LIQING HAO[1], ANTTI JAATINEN[1], HELMI KESKINEN[1], TAPANI KORHOLA[1], AKI KORTELAINEN[1], THOMAS KÜHN[1], ZUBAIR MAALICK[1], PASI MIETTINEN[1], SANTTU MIKKONEN[1], AKI PAJUNOJA[1], JAMES N: SMITH[1,3], PETRI VAATTOVAARA[1], PASI YLI-PIRILÄ[1], ANNELE VIRTANEN[1]

[1]University of Eastern Finland, Department of Applied Physics, Kuopio, Finland

[2]Finnish Meteorological Institute, Helsinki, Finland

[3]National Centre for Atmospheric Research, Boulder, CO 80305, USA

Keywords: aerosols, clouds

INTRODUCTION

The Aerosol Physics Group of the university of Eastern Finland has conducted studies on 1) Aerosol-Cloud-Climate interactions, 2) the properties – especially the phase state – of organic aerosols, 3) atmospheric new particle formation, and 4) theoretical nucleation studies.

AEROSOL-CLOUD-CLIMATE INTERACTIONS

One of the key issues in the quantification of the aerosol effect on climate change is the better understanding of aerosol-clouds interactions. UEF aerosol physics group is mainly working on the field of aerosol-cloud microphysics by developing theories and modelling tools, and conducting both experimental and modelling studies.

We have conducted both theoretical and experimental studies on the ability of particles to act as CCN in the atmospheric conditions. As shown in theoretical study by Sorjamaa and Laaksonen (2007), insoluble, but wettable, particles can act as cloud condensation nuclei, and their activation potential can be described by adsorption theory. The theory was tested with silica particles by Keskinen et al (2011) and it was found that the hygroscopic behaviour (measured by HTDMA) of these particles can be described by adsorption theory when the shape of the particles is taken into account. Recently we have conducted measurements of particles composed both of soluble and insoluble part, and based on the result the shape of particles is one of the key factors in analyzing the results from CCN-counter measurements also (Dalirian et al. 2012).

Beside laboratory studies we have also been active in the field. During 2010 Puijo cloud experiment campaign we measured the chemical composition of particles by aerosol mass spectrometer (AMS) (Hao et al., 2012). With the special inlet system we were able to measure composition of interstitial particles and all particles alternately in 14 minutes cycle. As a result we resolved, respectively, the chemical compositions of particles forming cloud droplets and those staying as unactivated interstitial particles. Three different distinct features was found: 1) Nitrate found in interstitial particles is mainly in the form of organic nitrate as ammonium nitrate was partitioned into cloud droplets, 2) organics found from interstitial particles were less oxidized than organics on average over the whole distribution, 3) Interstitial particles are clearly acidic compared to all aerosols, indicating that a fraction of ammonia is transferred from interstitial particles to cloud droplets (Hao et al. 2012).

As is well known, the dependence on cloud droplet number concentration (N_d) on aerosol number concentration (N_a) is not linear. We have studied this dependence both from experimental data and by modeling the aerosol effect on cloud. In Ahmad et al. (2012) we compared the in situ measured cloud droplet number concentration from Puijo measurement station to those retrieved from MODIS instrument onboard AQUA and TERRA satellites. We found good agreement between the measurements in both N_d as well as in aerosol cloud interaction parameter which describes the dependence of N_d on some aerosol parameter, in our case the number concentration (N_{acc}) of particles in the accumulation mode. Most interestingly, both direct measurement and satellite observation show similar dependence of Nd on N_{acc}, as Nd was increasing almost linearly with Nacc until Nd reaches $\sim 250 cm^{-3}$ and after that N_d increases very slowly as a function of N_{acc}. This can be explained by low updraft velocities prevailing in the measured clouds. In such conditions N_d is more dependent on updraft velocity than on N_{acc} after some limit is exceeded. Thus the kinetics of cloud droplet formation is limiting the aerosol effect. Similar effect can be seen in the more polluted conditions. In the early 1990's the aerosol concentration decreased substantially in the Central Europe and this could be seen for example in the measurements of aerosol optical depth. However, at the same time it was observed that radiation on the surface during overcast conditions did not change, indicating that aerosol is not affecting cloud properties. We studied this by taking the earliest European long term aerosol size distribution measurement available, from the city of Erfurt, and estimated composition of particles based on literature, and used this information in cloud parcel model to simulate the aerosol effect on the cloud droplet concentrations. We found that although the total aerosol concentration changed a lot, the shape of the aerosol size distribution changed in such a way that N_d did not change substantially. This was the case especially with updraft velocities less than 0.5 m/s, which are the conditions in which the aerosol indirect effect is expected to be the most important (Romakkaniemi et al . 2012).

As a joint effort with Finnish Meteorological Institute we are developing aerosol modules that can be used in large scale applications. Recently Bergman et al. (2012) presented the model development study where sectional aerosol module SALSA was tested and evaluated in atmospheric model ECHAM5.5. We are also evaluating the performance of widely used modal representation of aerosol size distribution. Usually in such a model different modes are forced to the certain width and also the mean size of modes is allowed to change only little. We are studying the effect of these restrictions both on cloud droplet concentration and extinction coefficient to see if there is some systematic bias due to the method used (Korhola et al 2012).

We have also continued the studies of semivolatile and surface active compounds affect on cloud droplet activation. We have conducted global scale simulations in which different methods to take account surface active species on cloud droplet formation were compared. We found that the effect of surface active compounds on global cloud droplet number burden is negligible if the behavior of surfactants during the activation is properly taken into account (Prisle et al. 2012). Thus in large scale modeling it is a good enough approximation to totally omit surfactants. It has been found in several previous studies that semivolatile gases, such as nitric acid, enhance the cloud droplet activation and thus they should have a negative radiative forcing on the climate. Previously we have constructed a parameterization describing the nitric acid effect on cloud droplet number concentration (Romakkaniemi et al. 2005) and now we have used the parametererization in global modeling framework (Makkonen et al. 2012). It was found that the nitric acid contribution to the present-day cloud albedo effect was $-0.32\pm0.01 Wm^{-2}$, and to the total indirect effect $-0.46\pm0.25 Wm^{-2}$ (compared to a nitric acid free atmosphere). Compared to the latest ICCP-estimate of aerosol direct forcing of -0.5±0.4 Wm^{-2}, the nitric acid effect can be considered high and it should motivate also experimental studies on the effect of semivolatile compounds on cloud droplet formation. In this issue we are also presenting the first modeling results on the possibility to use DMT CCN-counter to study the effect of semivolatiles on CCN-activity of particles (Romakkaniemi et al 2012).

There is no trend visible towards decreasing greenhouse gas emissions so researchers have started to plan optional methods to counteract the global warming. Most promising methods are related to aerosol, especially increasing the brightness of marine stratocumulus clouds and adding sulphate into atmosphere

to mimic volcanic eruptions. We have used global model ECHAM5.5 to study both geoengineering techniques. It was found in Partanen et al. (2012) that by artificial emission of sea salt particles on persistent stratocumulus regions (the most suitable 3.3% of total Earth surface chosen) -0.8Wm^{-2} radiative flux perturbation can be achieved. Even higher effect could be obtained by optimizing the size of emitted particles. However, it was highlighted that more information especially on the updraft velocities prevailing in the marine stratocumulus clouds is needed. To obtain more information about aerosol fluxes needed and dispersion of aerosol in marine boundary layer we have started cloud resolving study where we use UCLALES large eddy model coupled with SALSA to get realistic conditions (Maalick et al 2012). In Laakso et al. (2012) the possibility to use passenger aircrafts to increase the amount of particles in the stratosphere was studied. The basic idea was to increase the flying altitude and sulphur content of the fuel used on intercontinental flights. However, even with relatively high sulfur content (five-fold increase to current) the radiative flux perturbation was only -0.1 Wm^{-2}. Furthermore, the spread of particles to the stratosphere is not optimal as the intercontinental routes are generally far from the equator and flight altitude is still relatively low although within the stratosphere. Thus changing the flying altitudes does not appear a very promising tool in adding aerosol to stratosphere.

ORGANIC AEROSOL PROPERTIES

Formation of secondary organic aerosols (SOA), i.e., particle production from condensable oxidation products of volatile organic compounds (VOCs), in the troposphere is one of the main processes affecting composition and properties of atmospheric aerosols and thus influences the Earth's radiation balance and climate. Although formation and properties of SOA are widely studied to clarify their role in radiative forcing and climate, very limited information is, however, available on the morphology and phase state of SOA particles. Our recent plant chamber and field results show that atmospheric SOA particles from biogenic origin can be amorphous solid in their physical phase (Virtanen et al., 2010). The phase state of SOA particles has important implications for a number of atmospheric processes because the phase of particles may influence the partitioning of volatile compounds, reduce the rate of heterogeneous chemical reactions, affect the particles' ability to accommodate water and act as cloud condensation or ice nuclei, and change the atmospheric lifetime of the particle.

Recently, we have studies physical phase of small particle (Virtanen et al., 2011), developed a new method to resolve the phase state of aerosol particles (Saukko et al., 2012a) and the effect of humidity on physical state of the SOA particles from biogenic and anthropogenic precursors (Saukko et al., 2012b). Our results indicate (Virtanen et al., 2011) that particle bounce (i.e. effect of solid phase) clearly decreases with decreasing particle size in 10 - 30 nm size range for SOA particles. The results suggest difference in composition and phase of large (>30 nm) and smaller (17 and 30 nm) particles.

To study phase state of aerosol particles, a novel method based on impaction and subsequent counting of bounced particles by a condensation particle counter have been developed (Saukko et al., 2012a) and applied to study the effect of humidity on physical state of the particles (Saukko et al., 2012b). All the studied SOA systems, both form biogenic and anthropogenic precursors were amorphous solid or semi-solid in their physical state at RH <50 % and showed full or partial deliquescence when the humidity increased up to 65%. In the majority of cases the bounce behaviour of the various SOA systems did not show correlation with the particle O/ C ratio. Addition of hygroscopic sulphuric acid to the SOA liquefied the mixed particles at low RHs. We further note, that if sulphuric acid plays an important role in atmospheric nucleation processes, our results suggest that freshly nucleated particles containing appreciable amounts of sulphuric acid are initially liquid

In addition to studies of SOA phase, we have carried out plant chamber experiments to investigate mass yields of SOA from the oxidation of α-pinene and real plant emissions (Hao et al., 2011) and the effect of biotic stress on SOA formation and aerosol forcing of climate (Joutsensaari et al., 2012). For the SOA formation from real plant emissions, aerosol mass yields varied from 1.9% at Mo 0.69 μg m^{-3} to 17.7% at

Mo 26.0 µg m^{-3} were observed. Based on the results, the SOA mass yield of 10±2% can be recommended on global scale (Hao et al., 2011). Laboratory and field experiments showed that biotic stress (i.e. insect herbivory) increase VOC emissions significantly (ca. 10-fold), resulting in 200-1000 fold increases in SOA mass formed through ozonolysis at 50-200 ppb of O_3. The results from field and laboratory experiments, global modelling (GLOMAP), and satellite observations suggest that more frequent insect outbreaks in a warming climate could result in ample increase in biogenic SOA formation in the boreal zone and affect both aerosol direct and indirect forcing of climate at regional scales. The effect of insect outbreaks on VOC emissions and SOA formation should be considered in future climate model calculations (Joutsensaari et al., 2012).

ATMOSPHERIC NEW PARTICLE FORMATION

New particle formation (NPF) events have been observed frequently almost everywhere globally (*Kulmala et al., 2004* and references therein). However, the fundamental processes causing nucleation and subsequent growth into the size-range of a few nanometres are still not well understood. Most likely there is not just one mechanism that controls atmospheric nucleation processes. To improve the understanding of atmospheric NPF, numerous field measurements, laboratory experiments and models studies are devoted to monitor the gas-phase nucleating vapors and chemical compositions of new particle formation. Advanced field measurements are crucial to provide information about the spatial distribution of the rate coefficient in the nucleation parameterizations to assess the impacts of aerosols on climate, weather, air quality, and human health.

Recently, an intensive field campaign (PEGASOS) study was conducted at the San Pietro Capofiume (SPC) measurement station (44^0 39$^'$ N, 11^0 37$^'$ E, 11 m a.s.l) from June 3rd to July 12th 2012. During this summer campaign, a large number of different quantities were measured by several international research groups. During this campaign a large number of events were observed (from a total of 39 measurement days, 82% i.e. 32 days were new particle formation (NPF) days).

Particle formation events are observed at SPC measurement station on 80–150 days in a year, with maxima in event frequency in spring and summer (Hamed et al., 2007). However, the significant strong nucleation events are more frequent in summer season than spring season with maxima in June-July. Together with the PEGASOS collaboration, we are characterizing the nucleation events and the chemistry of particles during the growth phase of the frequently observed nucleation events in SPC. Particularly, we report (i) the temporal variations of particle size, number, and composition during the nucleation events; (ii) the dynamics of chemical species in the ultrafine particles; and (iii) the possible mechanisms responsible for the growth of ultrafine particles (Hamed et al., 2012a).

In addition to SPC station, we extended our analysis of NPF to the Bologna measurement site situated in the suburb of the city some 40 km from SPC; interestingly nucleation events always take place 1-2 hours earlier in SPC than in Bologna (see Fig. 1). This appears to be associated with the morning boundary layer development (start of vertical mixing) that starts earlier in SPC. The preliminary results show that regionally the BL development may triggers the nucleation events. In order to characterize the boundary layer evolution during the morning, the mixed layer height is modelled using the hig-resolution weather model HARMONIE.

Besides our NPF analysis during the campaign periods at SPC, the continuous measurements of the particle size distribution measurements, meteorological and gas data at SPC have been studied for the SPC site. (Laaksonen et al., 2005; Mikkonen et al., 2006; Sogacheva et al., 2007; Hamed et al., 2007; Jaatinen et al., 2009). The Particle size distribution measurements at the SPC measurement station were started on 24 March 2002 (Hamed et al, 2007). In addition to the continuous particle size measurements, several gas

and meteorological parameters are being measured at SPC: SO_2, NO, NO_2, NO_x, O_3, temperature, relative humidity, wind direction, wind speed, global radiation, precipitation, and atmospheric pressure. Unfortunately, in most long term measurements, sulphuric acid – the most important nucleation species - is not measured. We therefore have formulated statistical proxies (Mikkonen et al., 2011). For the EUCAARI sites, Mikkonen et al concluded that the best predictive proxy of H_2SO_4 at different European sites was achieved by multiplying combinations of global solar radiation, SO2 concentration, condensation sink and relative humidity
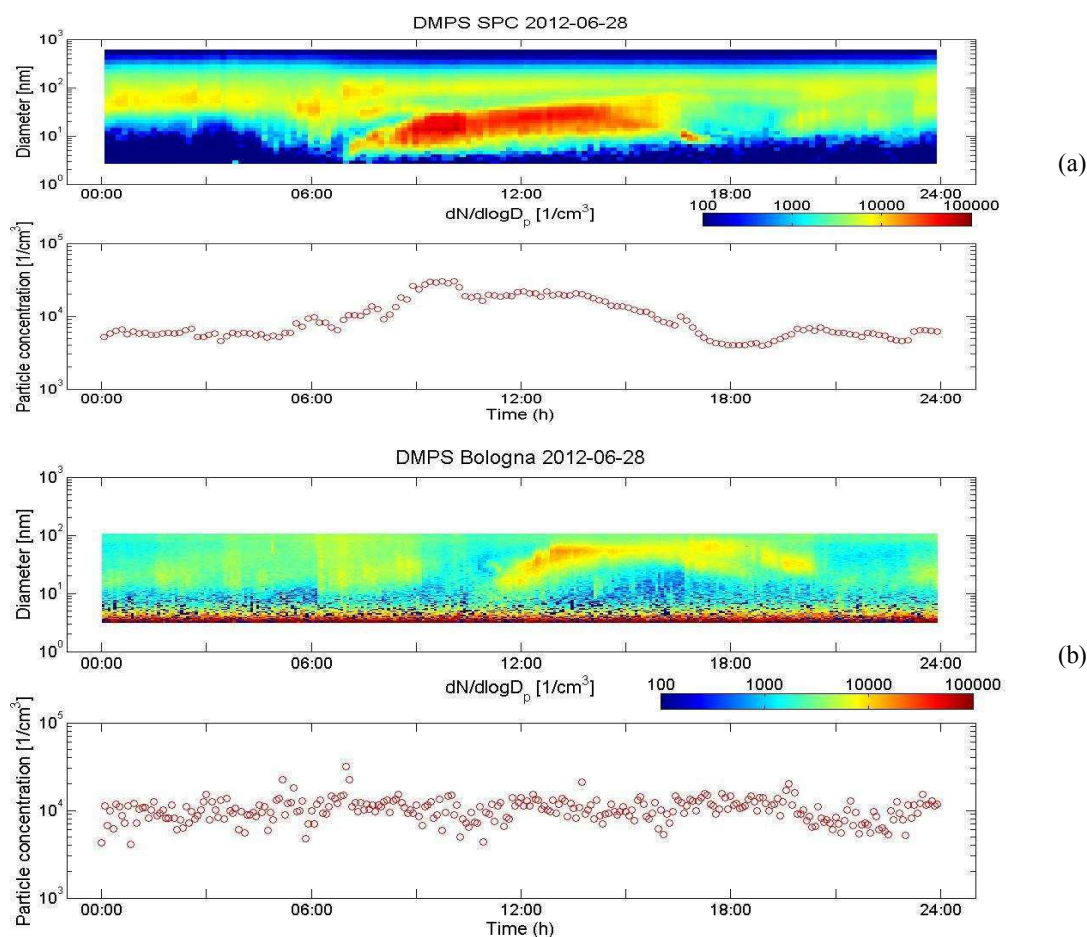
Figure 1. New particle formation day (28.06.2012) measured by DMPS systems at (a) rural site SPC station (40 km northeast the city of Bologna) and (b) at the Bologna (suburban site) measurement station.

.
Recently, Hamed et al (2012b) have extended the continuous NPF analysis for the SPC to span 10 years. Figure 2 shows the monthly frequency of new particle formation vents at SPC over the 10-year dataset. Unlike to many other stations, the maximum frequency of nucleation days occurs during summer (with maximum of 68% in July) while the lowest frequency (30%) occurs during autumn and winter (see Figure 2). These trends reflect the role of the radiation levels driving the photochemical reactions that result in formation of nucleating vapours. Comprehensive statistical analysis of the NPF with respect to meteorological and trace gases of nucleation events to elucidate the different process govern nucleation for the station are in progress and will be presented in our incoming publication.

Beside Po Valley, a long term aerosol monitoring is conducted on top of the Puijo tower in Kuopio (Leskinen et al, 2012; Portin et al., 2012; Mielonen et al., 2012). The monitoring was started in 2006, and provides an opportunity to study NPF statistics at a site which is located between a large rural forested area and a city with a population of ~ 90 000.. The station is on the top of the Puijo observation tower; 62° 54′ 32″ N, 27° 39′ 31″ E, 306 m a.s.l and 224 m above the surrounding lake and located about 2 km northwest of the center of Kuopio city, Eastern Finland. Details of the station can be found in Leskinen et al. (2009). The observations of aerosol nucleation at the Puijo research station presented here took place from June 2006 to November 2009. There are distinct sectors for cleaner and more polluted air, which give us a good opportunity to investigate the effects of local emission sources on aerosol particle formation. Our analysis uses the measured particle number size distribution (measurements were carried out using a twin DMPS system (Differential Mobility Particle Sizers) at the Puijo site, with particle size ranges of 7-800 nm), trace gas concentrations (SO_2 ,NO_x,O_3) and basic meteorological variables (T, RH, P, wind speed and wind direction).
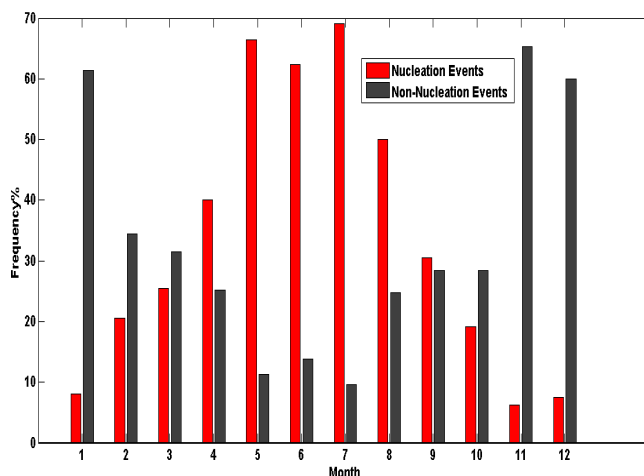
Figure 2. Monthly frequency of nucleation events at the (SPC) station over 10 years data (March 2002-March 2012).

In the process of the NPF analysis from Puijo research station, the particle formation events were identified and classified into three different categories according to the local emission sources; Class 1 includes normal nucleation days (similar to what has been observed in different environments) with very high number particle concentrations and clear growth of the newly formed particles that last for many hours; Class 2 includes clean nucleation days (with relatively very low growth rates and low concentrations of SO_2); and Class 3 includes polluted nucleation days (with high concentrations of SO_2 when the wind comes from N, NE directions). Hamed et al., (2011) showed that 12% of the measurement days were nucleation event days (i.e. class 1), 17% were non-nucleation days, 53% of the days were class 3. Moreover, Hamed et al study emphasizes the diversity of sources that exist in the Kuopio region, and the interplay between NPF events and local emissions motivated the ongoing comprehensive analysis.

According to the recent study by Leskinen et al. (2012), Baranizadeh et al (2012) divided the back trajectories into five air mass arrival sectors, named as Arctic (315-10□), Arctic\Kola (10-70□), East (70-160□), South (160-235□) and West (235-315□). Table 1 shows the numbers of classified days in different sectors. The results show that most dominant trajectory directions for nucleation days (Class 1) are coming from a clean sector (Sector 5).

Recently, Hamed et al (2012c) studied CCN production from nucleation events taking place at Puijo station. Methods and main findings are presented in this issue of FCoE 2012. Generally, 50% of the nucleation events at Puijo station were strong enough for a fraction of particles to survive to sizes of 50 nm

and larger. Overall, the NPF appears to be somewhat more important source of CCN in Puijo compared to Pallas in Lapland.

	total number of days	Sector 1	Sector 2	Sector 3	Sector 4	Sector 5
class 1	19	7	2	1	0	9
class 2	37	20	7	0	0	10
class 3	66	28	11	5	1	21
NE	168	17	35	24	28	64

Table 1. Number of nucleation event days and non-event (NE) days in the 5 sectors: Sector 1 is: Arctic (315-10□), sector 2 is: Arctic\Kola (10-70□), sector 3 is East (70-160□), sector 4 is South (160-235□) and sector 5 is West (235-315□) during time period June 2006 to November 2009.

THEORETICAL NUCLEATION STUDIES

To extract further information on the nucleation process behind observed NPF, the first nucleation theorem has been routinely used. This theorem links together the number of molecules in so-called critical nucleus, presenting bottleneck for vapour-to-particle transition, the rate of NPF and concentration of condensing species (e.g. sulphuric acid). Recently, we have demonstrated for a model systems that coagulation losses of clusters smaller than the critical size distort the results of this analysis (Malila et al., 2012a) towards larger sizes, while cluster-cluster interactions (Vehkamäki et al., 2012) have dominantly an opposite effect. Work to extend these results for atmospherically relevant systems is in progress (Malila et al., 2012b).

The 3nm particle formation rate (J_3) and the nucleation rate (J_1) are central quantities for nucleation and NPF analysis. The estimation of J_1 is usually extrapolated from the apparent formation rate of 3 nm particles (J_3), which is obtained from measured particle size distributions. Many of uncertainties around this issue were discussed lately in many publications (e.g. Korhonen et al., 2011). Lehtinen et al (2012) are developing a new method for estimating the nucleation rates from apparent particle formation rates and vice versa, taking into account the effect of size dependent growth rates as was recommended by latest study of Kuang et al., (2011).

REFERENCES

Ahmad I., T. Mielonen, H. Portin, A. Arola, S. Mikkonen, A. Leskinen, M. Komppula, K.E.J. Lehtinen, A. Laaksonen, S. Romakkaniemi (2012). Aerosol effect on Stratiform clouds: In situ vs. MODIS observations. Manuscript in preparation.

Baranizadeh E., A. Leskinen, A. Hamed, A. Virtanen, H. Portin, M. Komppula, A. Laaksonen (2012). New particle formation statistics at Puijo measurement station. Manuscript in preparation.

Baranizadeh E., A. Leskinen, A. Hamed, A. Laaksonen, A. Virtanen, H. Portin, M. Komppula (2012). New particle formation statistics at Puijo measurement station. Abstract is submitted to CRAAIC workshop, Oslo.

Bergman, T., Kerminen, V.-M., Korhonen, H., Lehtinen, K. J., Makkonen, R., Arola, A., Mielonen, T., Romakkaniemi, S., Kulmala, M., and Kokkola, H. (2012). Evaluation of the sectional aerosol microphysics module SALSA implementation in ECHAM5-HAM aerosol-climate model, Geosci. Model Dev.,5, 845-868

Dalirian M. et al., CCN activities of silica particles coated with various soluble substances (2012). Manuscript in preparation.

Hamed, A, J. Joutsensaari, S. Mikkonen, L. Sogacheva, M. Dal Maso, M. Kulmala, F. Cavalli, S. Fuzzi, M. C. Facchini, S. Decesari, M. Mircea, K. E. J. Lehtinen, and Laaksonen, A. (2007): Nucleation and growth of new particles in Po Valley, Italy. Atmos. Chem.Phys., 7,355-376, 2007.

Hamed, A. , Portin, H., Leskinen, A., Komppula, M. , Lehtinen, K.E. J. , Romakkaniemi, S., Smith, J.N. , Joutsensaari, J. and Laaksonen, A. (2011). Characterization of New Particle Formation Events in Kuopio, Finland Based on a three-year analysis, Proceedings of the 2011 European Aerosol Conference, 4-9 Sep 2011, Manchester, UK.

Hamed, A., et al. (2012a). Overview on the new particle formation events during the 2012 Pegasos campaign at the San Pietro Capofiume research station. Manuscript in preparation.

Hamed et al., (2012b). Secondary new particle formation in PoValley site between the years 2002 and 2012. Manuscript in preparation.

Hamed A., M. Komppula, H. Portin , Leskinen, A, Romakkaniemi, S., Lehtinen,K., Smith,J., Joutesnsaari,J,. Laaksonen, A., and Virtainen, A. (2012 c): CCN production from nucleation events at a semi-rural environment: Puijo station, Eastern Finland. Submitted to FCoE, 2012. Hyytiälä, September 19-21,2012.

Hao, L. Q., Romakkaniemi, S., Yli-Pirilä, P., Joutsensaari, J., Kortelainen, A., Kroll, J. H., Miettinen, P., Vaattovaara, P., Tiitta, P., Jaatinen, A., Kajos, M. K., Holopainen, J. K., Heijari, J., Rinne, J., Kulmala, M., Worsnop, D. R., Smith, J. N., and Laaksonen, A. (2011). Mass yields of secondary organic aerosols from the oxidation of alpha-pinene and real plant emissions. Atmos. Chem. Phys., 11, 1367-1378

Hao, L, S. Romakkaniemi, A. Kortelainen, A. Jaatinen, H. Portin, P. Miettinen, M. Komppula, A. Leskinen, A. Virtanen, J. Smith, D. Sueper, D. Worsnop, K. Lehtinen, A. Laaksonen (2012). Aerosol Chemical Composition in Cloud Event by High Resolution Time-of-flight Aerosol Mass Spectrometer. Environ. Sci. Tech., submitted

Joutsensaari J., P. Yli-Pirilä, H. Korhonen, A. Arola, J. D. Blande, J. Heijari, M. Kivimäenpää, L. Hao1, P. Miettinen, P. Lyytikäinen- Saarenmaa, A. Laaksonen, J. K. Holopainen (2012). Biotic stress accelerates formation of climate-relevant aerosols in boreal forests. Nature Climate Change, submitted

Jaatinen, A., Hamed, A., Joutsensaari, J., Birmili, W., Wehner,B., Spindler,G., Wiedensohler, A., Decesari, S., Mircea, M., Facchini, M., Junninen, H., Kulmala, M., Lehtinen, K., and Laaksonen, A: A comparison of new particle formation events at three different sites in the European boundary layer. *Boreal Env. Res. 14: 481-498, 2009.*

Keskinen H., S. Romakkaniemi, A. Jaatinen, P. Miettinen, E. Saukko, J. Joutsensaari, J. M. Mäkelä, A. Virtanen, J. N. Smith, and A. Laaksonen (2011) On-Line Characterization of Morphology and Water Adsorption on Fumed Silica Nanoparticles. Aerosol Science and Technology, Vol. 45, Iss. 12, 1441-1447

Korhola T., H. Kokkola, H. Korhonen, A.-I. Partanen, A. Laaksonen, T. Kuhn, and S. Romakkaniemi: Effect of modal representation of aerosol size distribution on aerosol activation and optical properties. This issue

Korhonen, H., Sihto, S.-L. , Kerminen, V.-M. and Lehtinen, K. (2011): Evaluation of the accuracy of analysis tools for atmospheric new particle formation. Atmos. Chem. Phys., 11, 3051-3066, 2011

Kuang, C., Chen, M., Zhao, J., Smith, J., McMurry, P.H., and Wang, J.(2012): Size and time-resolved growth rate measurements of 1 to 5 nm freshly formed atmospheric nuclei. Atmos. Chem. Phys., 12, 3573-3589, 2012

Kulmala, M., Vehkamäki, H., Petäjä, T., Dal Maso, M. Lauri, A., Kerminen, V.-M. W., Birmili, W., and McMurry. P. H.: Formation and growth rates of ultrafine atmospheric particles: a review of observations, J. Aerosol Sci., 35, 143–176, 2004.

Laakso A., A.-I. Partanen, H. Kokkola, A. Laaksonen, K.E.J. Lehtinen, H. Korhonen (2012). Stratospheric passenger flights likely an inefficient geoengineering strategy. Environ. Res. Lett, in press.

Laaksonen, A., Hamed A., Joutsensaari J., Hiltunen L., Cavalli F., Junkermann W., Asmi A., Fuzzi S. and Facchini M.C. ;Cloud condensation nucleus production from nucleation events at a highly polluted region. *Geophys Res Lett 32, 1-4, 2005.*

Lehtinen, K., Kerminen, V.M, and Korhonen, H (2012): Estimating nucleation rates from apparent particle formation rates and vice versa 2: effect of size dependent growth rates. Manuscript under preparation

Leskinen, A., Arola, A., Komppula, M., Portin, H., Tiitta, P., Miettinen, P., Romakkaniemi, S., Laaksonen, A., and Lehtinen, K. E. J. (2012). Seasonal cycle and source analyses of aerosol optical properties in a semi-urban environment at Puijo station in Eastern Finland. Atmos. Chem. Phys., 12, 5647-5659.

Leskinen , A. et al., 2009, Boreal Env. Res., 14, 576-590.

Maalick Z., H. Korhonen, H. Kokkola, A. Laaksonen, and S. Romakkaniemi: Large eddy simulations of marine stratocumulus geoengineering, This issue

Makkonen, R., Romakkaniemi, S., Kokkola, H., Stier, P., Räisänen, P., Rast, S., Feichter, J., Kulmala, M., and Laaksonen, A. (2012). Brightening of the global cloud field by nitric acid and the associated radiative forcing, Atmos. Chem. Phys., 12, 7625-7633.

Mielonen, T., H. Portin, M. Komppula, A. Leskinen, J. Tamminen, I. Ialongo, J. Hakkarainen, K.E.J. Lehtinen, A. Arola (2012. Biomass burning aerosols observed in Eastern Finland during the Russian wildfires in summer 2010 – Part 2: Remote sensing. Atmos. Environ. 47, 279-287.

Malila, J., R. McGraw, A. Laaksonen and K. E. J. Lehtinen (2012a). Losses of precritical clusters and the first nucleation theorem. Manuscript in preparation.

Malila, J., R. McGraw, A. Laaksonen and K. E. J. Lehtinen (2012b). Precritical cluster scavenging and nucleation theorems for binary H_2SO_4-H_2O nucleation. Submitted to FCoE, 2012. Hyytiälä, September 19-21,2012.

Mikkonen, S., Lehtinen, K. E. J. , Hamed, A., Joutsensaari, J. , Facchini, M. C. and Laaksonen, A..: Using discriminant analysis as a nucleation event classification method. *Atmos. Chem. Phys.6, 8485-8510, 2006.*

Mikkonen, S., Romakkaniemi, S., Smith, J. N., Korhonen, H., Petäjä, T., Plass-Duelmer, C., Boy, M., McMurry, P. H., Lehtinen, K. E. J., Joutsensaari, J., Hamed, A., Mauldin III, R. L., Birmili, W., Spindler, G., Arnold, F., Kulmala, M., and Laaksonen, A. (2011). A statistical proxy for sulphuric acid concentration. Atmos. Chem. Phys., 11, 11319-11334

Partanen, A.-I., H. Kokkola, S. Romakkaniemi, V.-M. Kerminen, K. E.J. Lehtinen, T. Bergman, A. Arola, and H. Korhonen (2012). Direct and indirect effects of sea spray geoengineering and the role of injected particle size, J. Geophys. Res., 117, D2

Portin, H. , T. Mielonen, A. Leskinen, A. Arola, E. Pärjälä, S. Romakkaniemi, A. Laaksonen, K.E.J. Lehtinen, M. Komppula (2012). Biomass burning aerosols observed in Eastern Finland during the Russian wildfires in summer 2010 – Part 1: In-situ aerosol characterization. Atmos. Environ. 47, 269-278

Prisle, N. L., Asmi, A., Topping, D., Partanen, A-I., Romakkaniemi, S., Dal Maso, M., Kulmala, M., Laaksonen, A., Lehtinen, K.E.J., McFiggans, G. and Kokkola, H. (2012) Surfactant effects in global simulations of cloud droplet activation, Geophys. Res. Lett., vol 39, L05802, doi:10.1029/2011GL050467

Romakkaniemi S., Kokkola H. and Laaksonen A. : Parameterization of the nitric acid effect on CCN activation. Atmos Chem Phys 5 879-885, 2005.

Romakkaniemi, S., A. Arola, H. Kokkola, W. Birmili, T. M. Tuch, V.-M. Kerminen, P. Räisänen, J. Smith, H. Korhonen, and A. Laaksonen (2012) Effect of aerosol size distribution changes on AOD, CCN and cloud droplet number concentration: case studies from Erfurt and Melpitz, Germany J. Geophys. Res., 117, D07202, 8 PP., doi:10.1029/2011JD017091

Romakkaniemi, S., A. Laaksonen and T. Raatikainen: Evaporation and condensation of semivolatile compounds in CCN-counter. 2012b, This issue

Saukko, E., Kuuluvainen, H., and Virtanen, A. (2012a) A method to resolve the phase state of aerosol particles, Atmos. Meas. Tech., 5, 259-265, doi:10.5194/amt-5-259-2012

Saukko, E., Lambe, A. T., Massoli, P., Koop, T., Wright, J. P., Croasdale, D. R., Pedernera, D. A., Onasch, T. B., Laaksonen, A., Davidovits, P., Worsnop, D. R., and Virtanen, A. (2012b) Humidity-dependent phase state of SOA particles from biogenic and anthropogenic precursors, Atmos. Chem. Phys., 12, 7517-7529

Sorjamaa, R. and Laaksonen A. (2007) The effect of H2O adsorption on cloud-drop activation of insoluble particles: a theoretical framework. Atmos Chem Phys 7 6175-6180.

Sogacheva, L., Hamed, A. , Facchini, M. C. , Kulmala, M., and Laaksonen, A.: Relation of air mass history to nucleation events in Po Valley, Italy, using back trajectories analysis. Atmos. Chem. Phys., 7,839-853, 2007.

Vehkamäki, H., M. J. McGrath, T. Kurtén, J. Julin, K. E. J. Lehtinen and M. Kulmala (2012). Rethinking the application of the first nucleation theorem to particle formation. J. Chem. Phys., 136, 094107.

Virtanen, A., Kannosto, J., Kuuluvainen, H., Arffman, A., Joutsensaari, J., Saukko, E., Hao, L., Yli-Pirilä, P., Tiitta, P., Holopainen, J. K., Keskinen, J., Worsnop, D. R., Smith, J. N., and Laaksonen, A. (2011)
Bounce behavior of freshly nucleated biogenic secondary organic aerosol particles,
Atmos. Chem. Phys., 11, 9313-9334

Virtanen, A., Joutsensaari, J., Koop, T., Kannosto, J., Yli-Pirilä, P., Leskinen, J., Mäkelä, J.M., Holopainen, J.K., Pöschl, U, Kulmala, M, Worsnop D.R. and Laaksonen, A. (2010). An amorphous solid state of biogenic secondary organic aerosol particles. Nature 467 824–827

OVERVIEW ABOUT ACTIVITIES IN AEROSOLS AND CLIMATE GROUP

H. LIHAVAINEN, T. ANTTILA, E. ASMI, D. BRUS, A. HIRSIKKO, R. HOODA, A. HYVÄRINEN, N. KIVEKÄS, J. LEPPÄ, K. NEITOLA, E. O'CONNOR, J. SVENSSON, O. TOLONEN-KIVIMÄKI and T. VISKARI

Finnish Meteorological Institute, Helsinki, PO.Box 503, 00101 Finland.

Keywords: Aerosol, Climate, Measurements, Modelling.

INTRODUCTION

Aerosol and climate research group carry out research on properties, processes and influences of aerosols to climate in the atmosphere, especially at northern latitudes. The research is based on continuous and campaign type measurements, laboratory experiments and modelling. The objective of the research is to answer following questions:

- what is the direct radiative forcing in our environment ?
- how does pollution in the atmosphere affect to the properties of clouds and indirect radiative forcing in northern latitudes ?
- what is the ratio between direct and indirect forcing in our environment ?
- what is the role of human activities to the radiative forcing by aerosols in our environment

Here we report the group's recent activities.

METHODS

The activities of the group can be divided into four categories: continuous in situ field measurements, modelling and data analysis, laboratory experiments and instrument development and campaign based measurements. In the following a more detailed insight to recent activities is given.

1. Continuous field measurements

Continuous field measurements of aerosol physical and optical properties are conducted in three different stations in Finland: In Pallas-Sodankylä Global Atmosphere Watch (GAW) station, Utö Atmospheric and Marine Research Station, and Virolahti measurement station. Utö and Virolahti are part of European Monitoring and Evaluation Programme (EMEP). In Pallas-Sodankylä GAW station we have studied aerosol long term properties, for example, time series new particle formation events (Asmi et al., 2011) and involved in study of long term trends of aerosol properties (Collaud Coen et al. 2012 , Asmi et al., 2012a, Asmi et al., 2012b). Data from all above mentioned three stations, along with two other stations, have been used to characterize black carbon aerosol properties in Finland, a gateway to Arctic (Hyvärinen et. al. 2011a).

Group is also involved in several measurement programs abroad. In India we have established a continuous measurement station, which has been operational since 2006. Currently we characterize the basic properties of aerosol, the effect of monsoon on aerosols properties (e.g Hyvärinen et al, 2011b, Hyvärinen et al., 2011c, Panwar et el. 2012) and new particle formation in rural background environment in northern India (Neitola et al., 2011).

We are also involved in collaboration to establish a state of the art long term measurement station to Siberia in Russia (Asmi et al. 2012). So far, direct year-round observations of important climate forcing agents have been inadequate within the Russian side of the Arctic. This is the reason why a new climate observatory was founded in Tiksi, Russia. Measurements of aerosol particles and greenhouse gases by

Finnish Meteorological Institute started in summer 2010 in Arctic Russia, Tiksi observatory. The year-round observations are used to pinpoint regional and global sources of these important climate forcing agents, and to study their interaction and feedback processes in this extreme Arctic climate. Importantly, up to now, very few direct observations from northern Siberian region have been available.

Finnish Meteorological Institute is in process of building a remote sensing instrument network which consists of Doppler lidars, a Raman lidar, ceilometers and a Doppler cloud radar. The sites in the network represent different environments and climate conditions from southern to northern Finland : 1) Helsinki, urban environment with marine influence, 2) Utö island, part of the Finnish archipelago, 3) Hyytiälä, continental background site, 4) Kuopio, continental urban site and 5) Sodankylä, arctic continental site. The aims for the network include monitoring and investigating aerosol, clouds and boundary layer wind and dynamics (Hirsikko et al., 2012) for weather forecast, air quality, aviation safety and climate change assessment purposes.

2. Modeling and data analysis

Models are developed to describe aerosol processes in the atmosphere. We use also process models to interpret of the aerosol measurements and new methodologies to analyse measurement data. Group also develops parameterizations to aerosol and cloud processes.

Modeling activities include studies on the relationships between aerosol properties (such as their physical size distribution, chemical composition and mixing state, i.e. the degree to which individual particles differ in their chemical composition among a particle population), aerosol CCN activity and clouds. We have developed a computational scheme that can be used to assess the influence of the particle hygroscopicity and mixing state on the cloud nucleating ability of particles. Additionally, the model provides an estimate for the peak supersaturation of water vapour reached during the formation of the observed clouds. The developed tools was applied to observations made during the Second and the Third Pallas Cloud Experiment (see field campaigns) in the Pallas – Sodankylä GAW station (Anttila et al., 2009, 2012). It was shown that the activated fractions and the total number of particles acting as CCN are were highly sensitive to the particle hygroscopic growth properties in the cloudy air masses sampled during the second Pallas cloud campaign (PaCE-2, Anttila et al., 2009). Also, size-dependent activation ratios of particles, which were determined from the measurements, were shown to carry information on the mixing state of particles. Further calculations done with the cloud model demonstrated that the observed variability in cloud droplet concentrations during PaCE-3 campaign was driven mainly by changes in the particle size distribution while variations in the meteorological conditions and in the particle hygroscopicity contributed to a lesser extent (Anttila et al., 2012a, b).

We have worked on a long-standing question in aerosol science about how to combine measurement data from several instruments. Current methods require limiting assumptions concerning the overlapping measurement ranges and have difficulties in properly accounting for measurement uncertainties. For this purpose, we have implemented an Extended Kalman Filter (EKF) and applied it to generate state estimates of the particle size distribution from multiple simultaneous measurements, namely from Differential Mobility Particle Sizer (DMPS), Aerodynamic Particle Sizer (APS) and nephelometer (Viskari et al, 2012a, b). The results indicate that the EKF is a very promising alternative to the instrument specific inversion techniques and seem to alleviate many deficiencies of the current techniques, such as unrealistic solutions in the over-lapping measurement ranges. The increased physical realism is due to the fact the a detailed microphysical aerosol model, the so-called UHMA model, is used to propagate the state estimation in time.

Methods that have previously been used to estimate the particle diameter growth rate and the proportion of ion-induced nucleation from measurements of aerosol charging state and fraction of charged particles have been developed to cover conditions in which the concentrations of negative and positive small ions are different (Gagné et al., 2012). Such conditions were observed at Helsinki, Finland, where aerosol charging

state was measured between December 2008 and February 2010, and the data was analyzed with these newly-developed methods (Gagné et al., 2012). The applicability of these methods in various atmospheric conditions was tested by conducting a set of aerosol dynamic simulations using an Ion-UHMA model and comparing the values from the simulations to those determined from the simulated data using the methods (Leppä et al., 2012a, b). It was found that the methods were able to provide reasonable estimates on the growth rate and the proportion of ion-induced nucleation, if the growth rate was high enough and if the charged particles did not grow much more rapidly than the neutral ones.

We are studying computationally cheap method to estimate and forecast the visibility in infrared wavelengths (Kivekäs et al., 2012). The study aims to improve the current estimations by taking a prescribed source region dependent shape of the dry aerosol size distribution and then scaling it by PM10 aerosol concentration and relative humidity.

3. Laboratory experiments and instrument development

In laboratory we have mainly studied nucleation, both unary and multicomponent nucleation. To the best of our knowledge, this is the first experimental work providing temperature dependent nucleation rate measurements using a high efficiency particle counter with a cutoff- size of 1.5 nm together with direct measurements of gas phase sulfuric acid concentration (Brus et al., 2011). A methods to produce constant amount of sulphuric acid into a gas flow and the effect of amines to nucleation in dry and at 30 % RH was studied (Neitola et al., 2012). The saturator method for producing sulphuric acid vapour is determined to perform well when comparing to the previous method of furnace. It produces constant sulphuric acid concentration with reproducible nucleation results. Total sulphate concentrations agree very well with prediction whereas the mass spectrometers measured monomer concentration is one to two orders lower than prediction. This difference between total sulphate and monomer concentration cannot be explained by formation of larger clusters (dimer, trimer, etc.) as the dimer concentration was always less than 1% of monomer, with decreasing trend when moving towards larger clusters. No clear enhancement to sulphuric acid –water nucleation rates of amines was observed.

In instrument development we have found an undercounting feature of black carbon in Multi Angle Absorption Photometer (MAAP). This was found during field experiments in polluted areas and occurs with high concentration. This was quantified with laboratory experiments and a method to correct for this has been proposed (Hyvärinen et al., 2012).

Finnish Meteorological Institute (FMI) in co-operation with Aalto University built a flying platform suitable for various surveillance and research applications (Brus et al., 2012). A Modified SHORT SC-7 Skyvan aircraft was equipped with isokinetic aerosol inlet and instruments to monitor aerosols and gases. The instrumentation is flexible and can be chosen according to purpose of the activity. First flight, so called demo flight, took place in July 2012.

4. Field campaigns

We have been conducting a series of cloud campaigns in Pallas-Sodankylä Global GAW station. The first Pallas Cloud Experiment (PaCE) was held in 2004 , second in 2005 and third one in 2009. The results of this campaign has been analysed and presented also here (Anttila et al., 2012).

We are conducting series of Soot on Snow (SoS) field campaigns targeting issue of the effect of deposited black carbon on snow albedo and melting (Kivekäs et al., 2012b). The SoS 2011 experiment demonstrates clearly that soot does have an effect on the albedo of snow, and that the effect in melting is also measurable. In SoS 2012 the weather was less favourable and masked all effects of the soot on the albedo and melting of snow, even though some effect on the snow structure remained.

In winter 2012, elemental carbon (EC) (also referred to black carbon depending on measurement technique) was investigated in Arctic Scandinavia (Svensson et al., 2012). The aim of the survey was to observe EC concentration differences throughout the Scandinavian Arctic, with the hypothesis that concentrations would increase the closer to the Russian border a sample was taken, due to higher emissions for the industrialized Kola Peninsula. Not obvious, but a tendency with higher concentrations the closer to Russia a sample was collected could be observed in the survey.

CONCLUSIONS

An overview has been presented of the group's activities. These supports the objectives of the group mentioned in the introduction, the collaborating universities and institutes and the goals of the Finnish Center of Excellence 'Physics, Chemistry, Biology and Meteorology of Atmospheric Composition and Climate Change' program. Our work contributes to achieve the objectives in Work Packages 1, 2, 3 and 4.

ACKNOWLEDGEMENTS

REFERENCES

Anttila, T., Vaattovaara, P., Komppula, M., Hyvärinen, A.-P., Lihavainen, H., Kerminen, V.-M., and Laaksonen, A. 2009Size-dependent activation of -aerosols into cloud droplets at a subarctic background site during the second Pallas Cloud Experiment (2nd PaCE): method development and data evaluation, Atmos. Chem. Phys., 9, 4841-4854, doi:10.5194/acp-9-4841-2009

Anttila, T., Brus, D., Jaatinen, A., Hyvärinen, A.-P., Kivekäs, N., Romakkaniemi, S., Komppula, M., and Lihavainen, H. (2012a) Relationships between particles, cloud condensation nuclei and cloud droplet activation during the third Pallas Cloud Experiment, Atmos. Chem. Phys. Discuss., 12, 13691-13732, doi:10.5194/acpd-12-13691-2012

Anttila, T., Brus, D., Hyvärinen, A.-P., Jaatinen, A., Kivekäs, N., Romakkaniemi, S., and Lihavainen, H. (2012b) Relationships between aerosols, cloud condensation nuclei and cloud droplets during the third Pallas Cloud Experiment, this issue

Asmi,E., N. Kivekäs, V.M. Kerminen, M. Komppula, A. Hyvärinen, J. Hatakka, Y. Viisanen, and H. Lihavainen (2011) Secondary new particle formation in Northern Finland Pallas site between the years 2000 and 2010, Atmos. Chem. Phys., 11, 12959-12972

Asmi E, T. Laurila, H. Lihavainen, D. Brus, M. Aurela1, A. Hyvärinen, J.Hatakka1, Y. Viisanen, V. Kondratyev, V. Ivakhov, A. Reshetnikov, T.Uttal, and A. Makshtas (2012) Measurement of erosol particles and greenhouse gases in Arctic Russia, this issue

Asmi,A., et al.,(2012a) Aerosol decadal trends – Part 2: In-situ aerosol particle number concentrations at GAW and ACTRIS stations, Atmos. Chem. Phys. Discuss., 12, 20849-20899

Asmi,A,. et al.,(2012b) Global trends of aerosol number concentrations, this issue

Brus, D., K. Neitola, A.-P. Hyvärinen, T. Petäjä, J. Vanhanen, M. Sipilä, P. Paasonen, M. Kulmala, and H. Lihavainen (2011) Homogenous nucleation of sulfuric acid and water at close to atmospherically relevant conditions, Atmos. Chem. Phys., 11, 5277-5287, doi:10.5194/acp-11-5277-2011

Brus, D., E. Asmi, S. Carbone[1], R. Hillamo, J. Hatakka, T. Laurila, H. Lihavainen, E. Rouhe, S.

Saarikoski, and Y. Viisanen (2012), New flying platform for atmospheric measurements, this issue

Collaud Coen, M., et al (2012), Aerosol decadal trends – Part 1: In-situ optical measurements at GAW and IMPROVE stations, Atmos. Chem. Phys. Discuss., 12, 20785-20848

Gagné, S., Leppä, J., Petäjä, T., McGrath, M. J., Vana, M., Kerminen, V.-M., Laakso, L., and Kulmala, M. (2012)Aerosol charging state at an urban site: new analytical approach and implications for ion-induced nucleation, Atmos. Chem. Phys., 12: 4647–4666

Hirsikko, A.E., E.J. O'Connor, C.R. Wood and L. Järvi: Wind observation strategies with a scanning Doppler lidar (2012), this issue

Hyvärinen,A.-P., P. Kolmonen, V.-M. Kerminen, A. Virkkula, A. Leskinen, M. Komppula, J. Hatakka, J. Burkhart, A. Stohl, P. Aalto,M. Kulmala, K. E. J. Lehtinen, Y. Viisanen, and H. Lihavainen (2011a) Aerosol black carbon at five background measurement sites over Finland, a gateway to the Arctic, Atmospheric Environment, 45, 24, 4042-4050, doi:10.1016/j.atmosenv.2011.04.026. 2011a.

Hyvärinen, A.-P., Raatikainen, T., Brus, D., Komppula, M., Panwar, T. S., Hooda, R. K., Sharma, V. P., and Lihavainen, H.: Effect of the summer monsoon on aerosols at two measurement stations in Northern India – Part 1: PM and BC concentrations, Atmos. Chem. Phys., 11, 8271-8282, doi:10.5194/acp-11-8271-2011, 2011a.

Hyvärinen, A.-P. ,Raatikainen, T., Komppula, M., Mielonen, T., Sundström, A.-M., Brus, D., Panwar, T. S., Hooda, R. K., Sharma, V. P., de Leeuw, G., and Lihavainen, H.: Effect of the summer monsoon on aerosols at two measurement stations in Northern India – Part 2: Physical and optical properties, Atmos. Chem. Phys., 11, 8283-8294, doi:10.5194/acp-11-8283-2011, 2011.

Hyvärinen, A.-P. , A. Petzold and H. Lihavainen (2012) Measurement artifact of the multi-angle absorption photometer (maap): laboratory quantification, this issue

Kivekäs, N., T. Mielonen, H. Portin, T. Kaurila, I. Rajakallio, K. Lehtinen and H. Lihavainen (2012a), Large particle climatology in finland – estimating the effect of aerosols in extinction of infrared radiation, this issue

Kivekäs, N., A. Virkkula, O. Järvinen, J. Svensson, A. Aarva, H. Lihavainen, D. Brus, A. Hyvärinen, O. Meinander, A. Heikkilä, R. Väänänen, J. Backman, and G. de Leeuw, (2012b) Measuring the effect of soot on physical and optical properties of snow, this issue

Leppä, J., Gagné, S., Laakso, L., Manninen, H. E., Lehtinen, K. E. J., Kulmala, M., and Kerminen, V.-M. (2012a) Using measurements of the aerosol charging state in determination of the particle growth rate and the proportion of ion-induced nucleation, Atmos. Chem. Phys. Discuss., 12, 21867-21922

Leppä, J., Gagné, S., Laakso, L., Manninen, H. E., Lehtinen, K. E. J., Kulmala, M., and Kerminen, V.-M. (2012b) Determination of the particle diameter growth rate and the proportion of ion-induced nucleation from the charged fraction, this issue

Neitola, K., E. Asmi, M. Komppula, A.-P. Hyvärinen, T. Raatikainen, T.S. Panwar, V.P. Sharma, and H. Lihavainen., 2011, New particle formation infrequently observed in western Himalayas – why?, Atmos. Chem. Phys., 11, 8447-8458, doi:10.5194/acp-11-8447-2011

Neitola, K., D. Brus, U. Makkonen, K. Kyllönen and H. Lihavainen, (2012) Findings from two nucleation campaigns; sulphuric acid monomer vs. total sulphate, enhancement of nucleation by amines, this issue

J. Svensson, D. Brus and H. Lihavainen (2012) Elemental carbon in snow from arctic scandinavia 2012, Preceedings of CRAICC (Cryosphere-atmosphere interactions in a changing Arctic climate) in September 26.-28., 2012

Viskari, T, Asmi, E, Kolmonen, P, Vuollekoski, H, Petäjä, T and H Järvinen, 2012a: Estimation of aerosol particle distributions with Kalman Filtering. Part I: Theory, general aspects and statistical validity. Atmos. Chem. Phys. Disc., 12, 18853-18887.

Viskari, T, Asmi, E, Virkkula, A, Kolmonen, P, Petäjä, T and H Järvinen, 2012b: Estimation of aerosol particle number distribution with Kalman Filtering. Part II: Simultaneous use of DMPS, APS and Nephelometer measurements. Atmos. Chem. Phys. Disc., 12, 18889-18925, 2012

AN OVERVIEW OF UNIVERSITY OF HELSINKI MEASUREMENT GROUP ACTIVITIES IN 2011-2012

T. PETÄJÄ, M. SIPILÄ AND THE UHEL MEASUREMENT GROUP

Department of Physics, FI-00014 University of Helsinki, Finland

Keywords:

ATMOSPHERIC AEROSOL PARTICLES, IONS AND OXIDANTS, TRACE GASES, LABORATORY AND FIELD MEASUREMENTS, MASS SPECTROMETRY, INSTRUMENT DEVELOPMENT.

INTRODUCTION

The last years have been active for the measurement group of Division of Atmospheric Science, University of Helsinki. Scientific achievements include breakthroughs in atmospheric oxidation (Mauldin et al. 2012), in nanoparticle and cluster formation (Petäjä et al. 2011, Kirkby et al. 2011, Kulmala et al. 2012), in aerosol growth (Riipinen et al. 2012) as well as in resolving climatic impacts of atmospheric aerosol particles and their mixing state (Cappa et al. 2012), all published within the last two years in a scientific collaboration with external partners as well as within the Finnish Center of Excellence.

The presented short synthesis is based mainly on the work published within years 2011-2012. Furthermore, some ongoing research activities are introduced shortly by refereeing to relevant extended abstracts in this issue of FCoE proceedings and to already published works in the scientific literature.

ADVANCES IN UNDERSTANDING ATMOSPHERIC OXIDATION

Sulfuric acid has been a long time one of the favourite molecules connected to atmospheric aerosol formation (Weber et al. 1996, Petäjä et al. 2009, Sipilä et al. 2010). This is linked to the tremendous decrease of saturation vapour pressure after the rapid oxidation steps after the initial OH attack on the precursor sulphur dioxide favouring either nucleation or condensation to pre-existing particles. The oxidation by OH is the rate limiting step. However, a recent laboratory study by Weltz et al. (2012) showed that also stabilized Criegee Intermediates (sCI) can oxidize SO_2 with a reaction rate orders of magnitude higher than assumed previously (Johnson, et al., 2001).

In the atmosphere, the sCI radicals originate from ozonolysis of alkenes. Ozone attacks the double bond of olefins producing an energy-rich primary ozonide, which decomposes very rapidly forming athe so-called Criegee Intermediate, CI. This energy-rich CI can either decomposes in a unimolecular reactions yielding OH and other products, or is can be collisionally stabilized by the media gaseous medium. This stabilized Criegee Intermediate (sCI) can further still decompose via in unimolecular reactions leading also to OH formation. However, besides the unimolecular reaction, the sCIs can react with several atmospheric constituents (Welz, et al., 2012, Taatjes et al., 2012, Mauldin et al., 2012, Berndt et al., 2012). This new pathway can potentially contribute to the atmospheric oxidation and budgets of various compounds. This can have large consequences of current knowledge on atmospheric oxidation capacity as well as new particle formation.

In our recent study we investigated oxidation of SO_2 by the sCIs formed in monoterpene ozonolysis and found that they react rapidly enough with trace amounts of atmospheric SO_2 to contribute to ambient sulphuric acid production and budget in a boreal forest environment (Mauldin et al. 2012). We showed that in the summertime boreal forest, with an extensive biogenic activity, the sCI chemistry can account even up to 50% of the sulphuric acid production in the surface layer. Further ramifications of this pathway are discussed in Sipilä et al. (2012).

ADVANCES IN UNDERSTANDING ATMOSPHERIC NUCLEATION

The atmospheric new particle formation is a complicated problem. Sometimes laboratory studies in controlled surroundings can resolve some of the complexities. A detailed study by Kirkby et al. 2011 in the CLOUD chamber shed light into the formation of aerosol particles both via neutral and ion induced pathways. One of the main outcomes of this study was that sulphuric acid – water system is not capable of reproducing the atmospheric new particle formation in the boundary layer. The role of ammonia in concentrations less than 100 pptv was crucial enhancing the nucleation rate considerably.

Ammonia is not in any way the only atmospheric base capable of stabilizing highly acidic sulphuric acid clusters. For example, amines (Ge et al. 2011) is a group of compounds identified as potential candidates for this stabilization (Kurtén et al. 2008). In order to explain our surprisingly high formation rates of sulphuric acid dimers (Petäjä et al. 2011) in a laminar flow tube setup in IfT, we proposed that amines are present even in ultra-clean laboratory experiments. The presence of the stabilizing compound prevented the dimer evaporation. Our results are in line with recent data obtained from CLOUD chamber.

However, understanding a process in a laboratory does not necessarily depict the whole phenomenon occurring in the real atmosphere. Our recent data from Hyytiälä (Arppe et al. 2012, this issue) for example shows that we regularly observe halogen containing compounds during daylight hours. Biogenic iodine has been identified being responsible for coastal nucleation (O'Dowd et al. 2002). Putting these findings together, we need examine further the role of the halogens also in the atmospheric chemistry and potentially aerosol formation in the boreal forest as well.

The key observation in the laboratory experiments and in the field was the Atmospheric Pressure interface Time-of-Flight mass spectrometer APi-TOF, Junninen et al. 2010, Ehn et al. 2010). This instrument is sensitive enough to resolve the nucleating clusters and follow their growth molecule by molecule, given that the process occurs at the measurement site. The Chemical Ionization APi-TOF utilizing nitrate ions to charge the ambient sample was introduced in Jokinen et al. 2011. The gas phase amine measurements with the CI-APi-TOF are described in Jokinen et al. 2012, this issue.

The added value of the capacity to characterize both the physical size and the chemical identity of the nucleating clusters is discussed in Kontkanen et al. 2012, this issue).

ADVANCES IN UNDERSTANDING NANOPARTICLE GROWTH

Organic vapours are thought to be responsible for a large fraction of the aerosol growth (Riipinen et al. 2012) as it cannot be typically explained with sulphuric acid alone. Riipinen et al. 2012 illustrated that a coherent picture can be drawn from the net effect of the organic condensation to nanoparticle growth for example in Hyytiälä. The results indicated that already at sizes around 5 nm more than half of the aerosol mass fraction is organic. The exact nature of these condensing vapors is unknown. Processes leading to formation of low-volatile organic compounds include 1) gas-phase oxidation, 2) organic salt formation and 3) polymerization / oligomerization in the growing clusters.

Laboratory study at a Teflon chamber at Paul Scherrer Institute, Switzerland revealed also the importance of organic condensable vapours to nucleation and growth. The results indicated that the organics contribute to the process already at 2 nm (Riccobono et al. 2012). Extremely oxidized organic molecules and their importance in the clustering process and aerosol formation was examined in Ehn et al. (2012). Based on this work we estimated concentration of these organic vapours in Hyytiälä to be in the range of 0.1-1 pptv (Ehn et al. 2012). Schobesberger et al. 2012, this issue, shows cluster evolution during sulphuric acid, ammonia, amines and pinanediol in the initial steps of nucleation and cluster formation in the CLOUD chamber. These observations indicate that the gas phase oxidation can rapidly produce also low volatile organic compounds.

In collaboration with the Analytical Chemistry group, we developed a methodology to collect atmospheric aerosol particles in the size range from 10 to 50 nm. We are able to separate the aerosol and gas phase collection enabling us to reduce the effect of positive artefact of the gas phase adsorption (Parshintsev et al.2011). Off-line analysis methods are developed and optimized e.g. for aliphatic and aromatic amines (Ruiz-Jimenez et al. 2012). In Hyytiälä for 30 nm particles, 13 different amines were quantified. Furthermore, 400 organic compounds were identified (Ruiz-Jimenez et al. 2011) from the atmospheric nanoparticle samples. These results are drawn together also in Riekkola et al. 2012, this issue.

ADVANCES IN UNDERSTANDING AEROSOL CLIMATIC EFFECTS

Understanding the processes and compounds participating in the new particle formation adds to our knowledge on aerosol climatic effects as this phenomenon frequently produces particles large enough that can activate as cloud droplets (Kerminen et al. 2012, Paramonov et al. 2012, this issue) in the boundary layer. However, in the real atmosphere this is not the only process. Another significant source of CCN sized particles is traffic and human actions. To further complicate the issue, e.g. diesel engines produce black carbon (BC) as well, which mixes to the pre-existing particulate population. Black carbon absorbs solar radiation and a BC layer in the lower troposphere can alter the temperature profile of the boundary layer and hinder mixing with atmospheric layers aloft.

To resolve the mixing state of BC in the atmospheric nanoparticles we developed a Hygroscopicity Volatility Tandem Differential Mobility Analyzer (HV-TDMA, Hakala (2012). This instrument is capable of probing to evaporation and hygroscopic growth of particles from 10 – 150 nm, where the former is connected to the BC concentration (Häkkinen et al. 2012) and the latter to cloud activation. In CalNex-project, the HV-TDMA was deployed onboard R/V Atlantis in a cruise along the Pacific coast in California in 2012 (Bates et al. 2012). The main impetus of this study was to probe into anthropogenic influences and aerosol aging as the emissions from California mix with clean marine air. The field data show that BC absorption enhancement is much less pronounced (6% at 532 nm) than earlier anticipated and only weakly affected by aerosol aging (Cappa et al. 2012). This can have dramatic consequences as typically the models assume the enhancement up to a factor of two potentially overestimating the effect of BC to the warming of the boundary layer.

The human influences on air quality and climate need a suite of high quality measurement data to facilitate the analysis. Recently, we have been conducting measurements around the world with a long-term commitment in mind. Currently we conduct aerosol measurements in Nanjing, China (Herrmann et al. 2012, this issue), South Africa (Vakkari et al., this issue) and in Saõ Paolo, Brazil (Backman et al. 2011). We also make targeted field studies to key areas, such as next to an oil refinery (Sarnela et al. 2012, this issue), Antarctica (Kyrö et al. 2012) and onboard an aircraft (Leino et al. 2012, this issue). We are also participating planning of the Pan Eurasian Experiment (Kulmala et al. 2012b, this issue). These kinds of measurements together with network of stations around the world (Kulmala et al. 2012c, this issue) provide a backbone e.g. for the assessment of aerosol particles in climate change (Asmi et al., this issue).

ADVANCES IN METHODOLOGIES AND TECHNOLOGICAL DEVELOPMENT

Kulmala et al. 2012 presents a complete methodology to characterize regional new particle formation events. This work was mainly done in collaboration with the FCoE. In Kulmala et al. 2012 we explain, how formation, nucleation and growth rates of atmospheric nanoparticles can be determined from state-of-the-art observational data. We introduce the relevant technologies for detecting these particles, explain needed data analysis techniques, provide the best practices to a wider community and even give troubleshooting advice. Furthermore, we underline the need for a long-term commitment of measurements, which is needed in order to resolve regional new particle formation and its consequences in various atmospheric environments.

Instrument development during the last few years has been productive. A crucial step in the development is building up an instrument characterization setup. Kangasluoma (2012) and Kangasluoma et al. (2012, this issue) describes a calibration and instrument verification setup capable of generating ions, clusters and charged particles from molecular standards, inorganic salts, metals and even fullerene in the size range 1-5 nm in a controlled and clean manner. The purity of the system has proven to be crucial in the success of instrument verification and development in the sizes below 3 nm.

The generation setup is important for ongoing development of chemical ionization methods for mass spectrometers (Adamov and Sipilä, 2012, Jokinen et al. 2012b, this issue) as a sample can be prepared with the same and known chemical composition increasing the repeatability and representativeness of the laboratory verifications (Lehtipalo et al. 2012, Hakala et al. 2012, this issue). The setup can be used also for transmission and fragmentation studies (Sundell et al. 2012, this issue) inside the mass spectrometers.

OUTLOOK

Our scientific understanding on the atmospheric nucleation, growth and aerosol effects on climate have expanded and strengthened during the last few years. The main findings have been obtained after teaming up with various research groups. The added value of the FCoE comes with the collaborative research. Excellent example is e.g. use of quantum chemical considerations to understand better chemical ionization processes (Kurtén et al. 2011). Breaking free from the methodological boundaries will evolve in a wider scientific understanding of the physical and chemical processes leading to secondary aerosol formation.

Together we can tackle grand challenges that are arising. In the atmospheric – surface interface the cycles of carbon, nitrogen, sulphur, water and energy are interconnected. These issues can only be solved jointly by in a large group, utilizing all the tools available in an open and coordinated research effort.

ACKNOWLEDGEMENTS

REFERENCES

Adamov, A and Sipilä, M. (2012) Non-radioactive ionization methods as alternatives for ^{241}Am in CI-APi-TOF, this issue.

Arppe, T., Junninen, H., Jokinen, T., Hakala, J., Schobesberger, S., Lönn, G., Sipilä, M., Kulmala, M., Worsnop, D.R. and Petäjä, T. (2012) Iodine-containing ions in Hyytiälä, this issue.

Asmi, A., and GAW, GUAN, EUSAAR and ACTRIS teams (2012) Global trends of aerosol number concentrations, this issue.

Backman, J., Rizzo, L.V., Hakala, J., Nieminen, T., Manninen, H.E., Morais, F., Aalto, P.P., Siivola, E., Carbone, S., Hillamo, R., Artaxo, P., Petäjä, T. and Kulmala, M. (2011) The variability of urban aerosol size distributions in São Paolo – Brazil: new particle formation events occur at the site, Atmos. Chem. Phys. Discuss. 11, 30419-30455.

Bates, T.S., Quinn, P.K., Frossard, A.A., Russell, L.M., Hakala, J., Petäjä, T., Kulmala, M., Covert, D.S., Cappa, C.D., Li, S.-M., Hayden, K.L., Nuaaman, I., McLaren, R., Massoli, P., Canagaratna, M.R., Onasch, T.B., Sueper, D., Worsnop, D.R. and Keene, W.C. (2012) Measurements of ocean derived aerosol off the coast of California. J. Geophys. Res. 117, D00V15, doi: 10.1029/2012JD017588.

Berndt, T., Jokinen, T., Mauldin III, R.L., Petäjä, T., Herrmann, H., Junninen, H., Paasonen, P., Worsnop, D.R. and Sipilä, M. (2012) Gas-phase ozonolysis of selected olefins: the yield of stabilized criegee intermediate and the reactivity toward SO2, J. Chem. Phys. (submitted).

Cappa, C.D., Onasch, T.B., Massoli, P., Bates, T.S., Gaston, C.J., Hakala, J., Petäjä, T., Hayden, K., Kolesar, K.R., Lack, D.A., Mellon, D., Li, S.-M., Nuaaman, I., Prather, K.A., Quinn, P.K., Song, C., Subramanian, R., Vlasenko, A., Worsnop, D.R. and Zaveri, R.A. (2012) On the magnitude of absorption enhancements due to mixing state of atmospheric black carbon, Science (published August 30, 2012).

Ehn, M., Junninen, H., Petäjä, T., Kurtén, T., Kerminen, V.-M., Schobesberger, S., Manninen, H.E., Ortega, I.K., Vehkamäki, H., Kulmala, M. and Worsnop, D.R. (2010) Composition and temporal behavior of ambient ions in the boreal forest. Atmos. Chem. Phys. 10, pp. 8513-8530.

Ehn, M., Kleist, E., Junninen, H., Petäjä, T., Lönn, G., Schobesberger, S., Dal Maso, M., Trimborn, A., Kulmala, M., Worsnop, D.R., Wahner, A., Wildt, J. and Mentel, Th.F. (2012) Gas phase formation of extremely oxidized pinene reaction products in chamber and ambient air, Atmos. Chem. Phys. 12, 5113-5127.

Ge, X., Wexler, A.S. and Clegg, S.L. (2011) Atmospheric amines – Part I, a review, Atmos. Environ. 45, 524-546.

Hakala, J. (2012) Hygroscopicity-Volatility Tandem Differential Mobility Analyzer, MSc. Thesis, University of Helsinki, Finland.

Hakala, J., Manninen, H.E., Petäjä, T. and Sipilä, M. (2012) Detection efficiency of a TSI environmental particle counter 3783, this issue.

Herrmann, E., Ding, A., Petäjä, T., Kulmala, M. (2012) Aerosol measurements in the Yangtse river delta, this issue.

Häkkinen, S.A.K., Äijälä, M., Lehtipalo, K., Junninen, H., Backman, J., Virkkula, A., Nieminen, T., Vestenius, M., Hakola, H., Ehn, M., Worsnop, D.R., Kulmala, M., Petäjä, T. and Riipinen, I. (2012) Long-term volatility measurements of submicron atmospheric aerosols in Hyytiälä, Finland, Atmos. Chem. Phys. Discuss. 12, 11201-11244.

Johnson, D., Lewin, A. G. & Marston, G. (2001) The effect of Criegee-intermediate scavengers on the OH yield from the reaction of ozone with 2-methylbut-2-ene. J. Phys. Chem. A 105, 2933–2935.

Jokinen, T., Sipilä, M., Junninen, H., Ehn, M., Lönn, G., Hakala, J., Petäjä, T., Mauldin III, R.L., Kulmala, M. and Worsnop, D.R. (2011) Atmospheric sulfuric acid and neutral cluster measurements using CI-APi-TOF, Atmos. Chem. Phys. 12, 4117-4125.

Jokinen T, Sipilä, M., Junninen, H., Ehn, M., Lönn, G., Hakala, J., Petäjä, T., Mauldin III, R.L., Kulmala, M. and Worsnop, D.R. (2012) Atmospheric amine measurements with CI-API-TOF, this issue.

Junninen, H., Ehn, M., Petäjä, T., Luosujärvi, L., Kotiaho, T., Kostiainen, R., Rohner, U., Gonin, M., Fuhrer, K., Kulmala, M. and Worsnop, D.R. (2010) API-ToFMS: a tool to analyze composition of ambient small ions. Atmos. Meas. Technol., 3, pp. 1039-1053.

Kangasluoma, J. (2012) Production and characterization of ions below 2 nm, MSc. Thesis (In Finnish), University of Helsinki, Finland.

Kangasluoma, J., Mikkilä, J., Lehtipalo, K., Vanhanen, J., Junninen, H., Attoui, M., Sipilä, M., Kulmala, M. and Petäjä, T. (2012) Effects of RH and composition on the detection of small ions in the Particle Size Magnifier, this issue.

Kerminen, V.-M., Paramonov, M., Anttila, T., Riipinen, I., Fountoukis, C., Korhonen, H., Asmi, E., Laakso, L., Lihavainen, H., Swietlicki, E., Svenningsson, B., Asmi, A., Pandis, S.N., Kulmala, M. and Petäjä, T. (2012) Cloud condensation nuclei production associated with atmospheric nucleation: a synthesis based on existing literature and new results, Atmos. Chem. Phys. Discuss. 12, 22139-22198.

Kirkby, J., Curtius, J., Almeida, J., Dunne, E., Duplissy, J., Ehrhart, S., Franchin, A., Gagné, S., Ickes, L., Kürten, A., Kupc, A., Metzger, A., Riccobono, F., Rondo, L., Schobesberger, S., Tsagkogeorgas, G., Wimmer, D., Amorim, A., Bianchi, F., Breitenlechner, M., David, A., Dommen, J., Downard, A., Ehn, M., Flagan, R.C., Haider, S., Hansel, A., Hauser, D., Jud, W., Junninen, H., Kreissl, F., Kvashin, A., Laaksonen, A., Lehtipalo, K., Lima, J., Lovejoy, E.R., Makhutov, V., Mathot, S., Mikkilä, J., Minginette, P., Mogo, S., Nieminen, T., Onnela, A., Pereira, A., Petäjä, T., Schnitzhofer, R., Seinfeld, J.H., Sipilä, M., Stozhkov, Y., Stratmann, F., Tome, A., Vanhanen, J., Viisanen Y., Vrtala, A., Wagner, P.E., Walther, H., Weingartner, E., Wex, H., Winkler, P.M., Carslaw, K.S., Worsnop, D.R., Baltensperger, U. and Kulmala, M. (2011) The role of sulfuric acid, ammonia and galactic cosmic rays in atmospheric aerosol nucleation, Nature, 476, pp. 429-433, doi:10.1038/nature10343.

Kontkanen J., Hakala, S., Nieminen, T., Lehtipalo, K., Manninen, H.E., Petäjä, T. and Kulmala, M. (2012) Neutral and charged sub-2nm clusters in boreal forest boundary layer, this issue.

Kulmala, M., Petäjä, T., Nieminen, T., Sipilä, M., Manninen, H.E., Lehtipalo, K., Dal Maso, M., Aalto, P.P., Junninen, H., Paasonen, P., Riipinen, I., Lehtinen, K.E.J., Laaksonen, A. and Kulmala, M. (2012) Measurement of the nucleation of atmospheric aerosol particles, Nature Protocols 7, 1651-1667, doi:10.1038/nprot.2012.091.

Kulmala, M., Lappalainen, H.K., Petäjä, T., Sipilä, M., Sorvari, S., Alekseychik, P., Paramonov, M., Kerminen, V.-M. and Zilitinkevich, S. (2012) Pan Eurasian Experiment (PEEX) – Towards a new multinational environment and climate research effort in Eurasia, this issue.

Kulmala, M., Lappalainen, H.K., Petäjä, T. and ACTRIS Finland team (2012) General overview: aerosols clouds, and trace gases research infrastructure network (EU-FP7-ACTRIS-I3 project), this issue.

Kurtén, T., Loukonen, V., Vehkam¨aki, H., and Kulmala, M. (2008) Amines are likely to enhance neutral and ion-induced sulfuric acid-water nucleation in the atmosphere more effectively than ammonia, Atmos. Chem. Phys., 8, 4095-4103.

Kurtén, T., Petäjä, T., Smith, J., Ortega, I. K., Sipilä, M., Junninen, H., Ehn, M., Vehkamäki, H., Mauldin, L., Worsnop, D. R., and Kulmala, M. (2011) The effect of H2SO4 - amine clustering on chemical ionization mass spectrometry (CIMS) measurements of gas-phase sulfuric acid, Atmos. Chem. Phys., 11, 3007-3019.

Kyrö, E.-M., Virkkula, A., Kerminen, V.-M., Dal Maso, M., Parshintsev, J., Ruiz-Jimenez, J., Forsström, L., Manninen, H.E., Heinonen, P., Riekkola, M.-L. and Kulmala, M. (2012) Antarctic aerosol formation from continental biogenic sources, this issue.

Lehtipalo, K., Vahanen, J., Toivola, T., Mikkilä, J., Petäjä, T. and Kulmala, M. (2012) Characterization of the Airmodus A20 Condensation Particle Counter, this issue.

Leino, K., Väänänen, R., Virkkula, A., Aalto, P.P., Pohja, T., Kortetjärvi, L., Krejci, R., Petäjä, T. and Kulmala, M. (2012) Airborne measurements of aerosol particles in the lower atmosphere of Southern Finland, this issue.

Mauldin III, R.L., Berndt, T., Sipilä, M., Paasonen, P., Petäjä, T., Kim, S. Kurtén, T., Stratmann, F., Kerminen, V.-M. and Kulmala, M. (2011) New atmospherically relevant oxidant, Nature, 488, 193-197, doi:10.1038/nature11278.

O'Dowd, C.D. Jimenez, J.L., Bahreini, R., Flagan, R.C., Seinfeld, J.H., Hämeri, K., Pirjola, L., Kulmala, M., Jennings, S.G. and Hoffmann, T. (2002) Marine aerosol formation from biogenic iodine emissions, Nature 417, 632-636.

Paramonov, M., Petäjä, T., Aalto, P.P., Dal Maso, M., Prisle, N., Kerminen, V.-M. and Kulmala, M. (2012) The analysis of size-segregated cloud condensation nuclei counter (CCNC) data from SMEAR II and its implications for aerosol-cloud relations, this issue

Parshintsev, J., Ruiz-Jiménez, J., Petäjä, T., Hartonen, K., Kulmala, M. and Riekkola, M.-L. (2011) Comparison of quartz and teflon filters for simultaneous collection of size separated ultrafine aerosol particles and gas phase zero samples. Anal. & Bioanal. Chem., 400, pp. 3527-3535, doi: 10.1007/s00216-011-5041-0.

Petäjä, T., Sipilä, M., Paasonen, P., Nieminen, T., Kurtén, T., Stratmann, F., Vehkamäki, H., Berndt, T. and Kulmala, M. (2011) Experimental observation of strongly bound dimers of sulphuric acid: application to nucleation in the atmosphere. Phys. Rev. Lett. 106, 228302.

Rantala, P., Hill, M., Kajos, M.K., Hellén, H., Hörger, C., Schallhart, S., Taipale, R., Patokoski, J., Ruuskanen, T.M., Petäjä, T., Reimann, S. and Rinne, J. (2012) Measuring VOCs: an intercomparison between PTR-MS and GC-MS in Hyytiälä in springtime, this issue.

Riccobono, F., Rondo, L., Sipilä, M., Barmet, P., Curtius, J., Dommen, J., Ehn, M., Ehrhart, S., Kulmala, M., Kürten, A., Mikkilä, J., Petäjä, T., Weingartner, E. and Baltensperger, U. (2012) Contribution of sulphuric acid and oxidized organic compounds to particle formation and growth, Atmos. Chem. Phys. Discuss. 12, 11351-11389.

Riekkola, M.-L., Ruiz-Jimenez, J., Hartonen, K., Parshintsev, J., Laitinen, T., Petäjä, T. and Kulmala, M. (2012) Analytical challenges and recent advances in atmospheric and aerosol chemistry, this issue.

Riipinen, I., Yli-Juuti, T., Pierce, J.R., Petäjä, T., Worsnop, D.R., Kulmala, M. and Donahue, N.M. (2011) The contribution of organics to atmospheric nanoparticle growth, Nat. Geo. Sci. 5, 453-458, doi: 10.1038/ngeo1499.

Ruiz-Jimenez, J., Parshintsev, J., Laitinen, T., Hartonen, K., Riekkola, M.-L., Petäjä, T., Virkkula, A. and Kulmala, M. (2011) A complete methodology for the reliable collection, sample preparation, separation and determination of organic compounds in ultrafine 30 nm, 40 nm and 50 nm atmospheric aerosol particles, Anal. Methods, 3, 2501-2509, doi:10.1039/C1AY05362K.

Ruiz-Jimenez, J., Hautala, S., Parshintsev, J., Laitinen, T., Hartonen, K, Petäjä, T., Kulmala, M. and Riekkola, M.-L. (2012) Aliphatic and aromatic amines in atmospheric aerosol particles: comparison of three ionization techniques in liquid chromatography-mass spectrometry and method development, Talanta, 97, 55-62.

Sarnela, N., Jokinen, T., Hakala, J., Taipale, R., Patokoski, J., Kajos, M., Lehtipalo, K., Schobesberger, S., Junninen, H., Sipilä, M., Teittinen, J., Westerholm, H., Larnimaan, K., Petäjä, T. and Kulmala, M. (2012) Aerosol and trace gas concentrations in the vicinity of Kilpilahti industrial area, this issue.

Schobesberger, S., Franchin, A., Junninen, H., Bianchi, F., Dommen, J., Donahue, N., Ehrhart, S., Ehn, M., Lehtipalo, K., Nieminen, T., Lönn, G., the CLOUD collaboration and Petäjä, T., Kulmala, M. and Worsnop, D.R. (2012) Measuring ion clusters of sulfuric acid, ammonia, amines, and pinanediol oxidation products in the CLOUD chamber by APi-TOF mass spectrometers, this issue.

Sipilä, M., Berndt, T., Petäjä, T., Brus, D., Vanhanen, J., Stratmann, F., Patokoski, J., Mauldin III, R.L., Hyvärinen, A.-P., Lihavainen, H. and Kulmala, M. (2010) The Role of sulfuric acid in atmospheric nucleation Science, 327, pp. 1243-1246.

Sipilä, M., Berndt, T., Makkonen, R., Jokinen, T., Paasonen, P., Mauldin, L., Kurtén, T., Junninen, H., Asmi, A., Worsnop, D.R., Kulmala, M. and Petäjä, T. (2012) SO2 oxidation by stabilized Criegee intermediates from forest emitted alkenes – contribution to global concentrations of sulfuric acid, CN and CCN, this issue.

Sundell, V.-M., Junninen, H., Kangasluoma, J., Schobesberger, S., Sipilä, M., Kulmala, M., Worsnop, D.R. and Petäjä, T. (2012) Characterization of an APi-TOF for transmission, this issue.

Taatjes, C. A., Welz, O., Eskola, A. J., Savee, J. D., Osborn, D. L., Lee, E P. F., Dyke, J. M., Mok, D.W. K., Shallcross, D. E. and Percival, C. J. (2012) Direct measurement of Criegee   intermediate   (CH2OO) reactions with acetone, acetaldehyde, and hexafluoroacetone, Phys. Chem. Chem. Phys., 14, 10391-10400.

Vakkari, V., Tiitta, P., Laakso, H., Venter, A., Jaars, K., Josipovic, M., Beukes, J.P., Van Zyl, P.K., Pienaar, J.J., Kulmala, M. and Laakso, L. (2012) Differences in physical and chemical properties of aerosol particles from Savannah fires in day and night time plumes, this issue.

Weber, R. J., Marti, J. J., McMurry, P. H., Eisele, F. L., Tanner, D. J, and Jefferson A.: Measured atmospheric new particle formation rates: Implications for nucleation mechanisms, Chem. Eng. Commun., 151, 53-64, 1996.

Welz, O., Savee, J.D., Osborn, D.L., Vasu, S.S., Percival, C.J., Shallcross, D.E. and Taatjes, C.A. (2012). Direct kinetic measurements of Criegee intermediate (CH2OO) formed by reaction of CH2I with O2. Science 335, 204-207.

ANALYTICAL CHALLENGES AND RECENT ADVANCES IN ATMOSPHERIC AND AEROSOL CHEMISTRY

M.-L. RIEKKOLA[1], J. RUIZ-JIMENEZ[1], K. HARTONEN[1], J. PARSHINTSEV[1], T. LAITINEN[1,2], T. PETÄJÄ[2] and M. KULMALA[2]

[1]Department of Chemistry, Laboratory of Analytical Chemistry
P.O. Box 55, FIN-00014 University of Helsinki, Finland.

[2]Department of Physics, Division of Atmospheric Sciences,
P.O. BOX 48, FIN-00014 University of Helsinki, Finland

INTRODUCTION

Qualitative and quantitative information about the compounds in aerosol particles is essential if we are to comprehend their role and effects in the atmosphere. To date, numerous analytical techniques, both on-line and off-line, have been developed in order to determine size-dependent chemical composition of ambient aerosol particles. However, still today chemical characterisation of aerosol samples can be plagued by significant errors in sampling, sample pre-treatment and in analytical procedures. Besides the artefacts of the sampling method, the sampling time to get enough particle mass for the analysis needs still often to be long so that rapid changes in concentration level of particular compounds might be difficult to track. In addition, before samples can be analysed by different methods, they must be pre-treated. Traditionally the sample pre-treatment steps are quite time-consuming, tedious, environmentally unfriendly and sometimes even a serious source of errors. The uncertainty of the data on organic compounds in aerosol particles is usually considerable because of bias in sampling and errors generated during sample pre-treatment.

The research of aerosol group of the Laboratory of Analytical Chemistry, University of Helsinki has been focused on the improvement of existing analytical methodologies and on the invention of new analytical approaches. This abstract compiles recent analytical advances achieved in the Laboratory. New methodologies for the determination of amines in atmospheric aerosols are presented. In addition, relatively new technique, called desorption atmospheric pressure photo-ionization mass spectrometry has been utilized for the semi-online analysis of aerosol particles, and laser desorption-ionization aerosol mass spectrometry has provided valuable information about chemical composition of ultra-fine aerosols. Moreover, methodologies for the determination of vapour pressures of even unknown compounds in mixtures have been developed. As well-recognized especially vapour pressures are important physicochemical properties in the aerosol formation.

METHODS

Aliphatic and aromatic amines in atmospheric aerosol particles

Although the chemical composition of atmospheric aerosols has been extensively studied during the last decades, only a few papers have focused on the determination of chemical composition of ambient nanometer size particles. Recent studies have demonstrated the relevance of the nitrogen containing organic compounds in the aerosol chemistry and their participation in particle growing processes.
The sampling of atmospheric aerosol particles is a highly challenging task, especially in the case of size segregated ultrafine particles. Two different devices such as, impactors and differential mobility analyzers

(DMA) can be utilized, but unfortunately the collection efficiency of the former tend to be poor for particles significantly smaller than 100 nm due to evaporation processes. The size-separated particles can be collected on the impactor plate or on a suitable filter, extracted and analyzed with chromatographic techniques utilizing mass spectrometric detection or directly transferred to a mass spectrometer. It is well known that a significant amount of gaseous compounds can be adsorbed on the filter, causing overestimation of particulate concentration of compounds, especially in the case of nanometer size aerosols. Two different approaches can be used in order to avoid or limit the presence of these artefacts. The first one is based on the removal of gas phase compounds before the collection of the particles in the filter using classical denuders. The second involves the use of new sampling systems based on particle size separation using a DMA and simultaneous collection of gas-phase zero samples allowing the quantification of these artefacts. It should be emphasized that this method is able to offset the adsorption of the gas phase on the filter but no other artefacts which can affect the concentration of the target analytes on the particles during the sampling step.

A complete methodology was developed for the determination of aliphatic and aromatic amines in atmospheric aerosol particles using liquid chromatography - tandem mass spectrometry. Derivatization of the target analytes using dansyl chloride as reagent was needed in order to improve the chromatographic and spectrometric properties. This step was accelerated by ultrasounds. The reaction vials were kept in dark while not in use. The chemical variables (pH, buffer and derivatization reagent concentrations) have the same optimal values in the classical derivatization procedure (Cohen, 1995) and the ultrasound assisted method. However, the reaction temperature was substantially lower in the case of the ultrasound assisted method (35 vs 60 °C), thus avoiding the most of the losses due to the evaporation and decomposition of the analytes (Cohen, 1995, Mao, 2009). The ultrasound assisted method shortened the derivatization time to the one fourth (15 vs 60 min) in comparison with the classical method (Cohen, 1995).

From three different ionization techniques tested in this research such as, electrospray ionization (ESI), atmospheric pressure chemical ionization (APCI) and atmospheric pressure photoionization (APPI), ESI was superior in terms of sensitivity, linearity, repeatability and reproducibility over atmospheric pressure chemical ionization and photoionization for the target analytes.

Two different instruments were tested for the determination of the target analytes in aerosol samples. An Agilent 1100 series liquid chromatograph furnished with an Waters Sunfire C18 column (150 mm × 2.1 mm i.d., 3.5 μm particle size), coupled to an Esquire 3000 plus ion trap mass spectrometer (Bruker Daltonics) for the detection; and an Agilent 1260 series liquid chromatograph furnished with an Agilent Poroshell 120 EC-C18 column (50 mm × 3 mm i.d., 2.7 μm particle size), coupled to an Agilent 6420 triple quadrupole mass spectrometer for the detection. The latter reduces the chromatographic analysis time to the half (15 min vs 30 min), improving the peak to peak resolution and reducing the ion suppression effect. In addition, this device improves the repeatability and sensitivity of the method and allows the determination of relatively important compounds such as methyl amine.

The developed method was fully characterized and validated using three different sample matrices such as gas phase collected onto the filter, ultrafine (30 nm) and total suspended particles (TSP). The accuracy of the method and the potential matrix effects were evaluated using standard addition at two concentration levels. An absence of significant differences between the concentrations added and those found in terms of mean, range, variance, and median, were proved by different statistical tests such as ANOVA, multiple ranges, Levene and Kruskal-Wallis, and Mood's median. The final step of the validation was the comparison of the results obtained by the developed methodology with those provided by our earlier validated method (Ruiz-Jimenez, 2011). The latter is also based on LC-MS but the analytes were analyzed without the derivatization. The same statistical tests used to establish the differences between the added concentrations and those found in the samples were used in this case. No significant differences were found in terms of mean, range, variance, and media.

Finally the method was applied for the determination of amines in natural aerosol samples. The results obtained for the atmospheric aerosol samples were in a good agreement with those provided by other methods found in the literature.

Partial least square regression as a tool for the quantification of amines identified by comprehensive two-dimensional gas chromatography coupled with time-of-flight mass spectrometry

Comprehensive two-dimensional gas chromatography coupled with time-of-flight mass spectrometry (GCxGC-TOF-MS) has already shown a great potential as screening tool in different fields. The superior resolution and sensitivity of GCxGC-TOF-MS compared to conventional GC-MS instruments allows the identification of hundreds or even thousands of compounds in the samples. The great potential of the technique could be considered also as a drawback, if the target of the analysis is the quantification of the identified compounds, due to the very limited variety of commercial standards available in the laboratories. This fact not only hinders the proper quantification of the identified compounds, but also limits GCxGC-TOF-MS to the semiquantification of minor and major components on the samples.

It is possible to find several approaches in the literature, based on the use of surrogates, for the quantification of compounds identified using MS (Claeys, 2004, Decesari, 2006), but frequently these approaches fall in a total lack of accuracy. In this study, a new approach based on partial-least-squares regression (PLSR) has been developed for the quantification of amino compounds. The peak areas and the mass spectra provided by the instrument for the individual reference compounds —tyramine, benzenepropanamine, cadaverine, dibutylamine, dipropylamine, and tripropylamine— were used for the development of the equations. Standard solutions, containing these compounds at eight different concentrations ranging from 0.5 to 30 ng μL^{-1}, were analyzed. All the samples were analyzed in triplicate. The total number of samples used for the equation development was 144. The individual response factors provided for the reference compounds were recalculated as a function of the different ions produced during their fragmentation (RFi (m/z)) using the mass spectra provided by the instrument.

The dataset was divided before the equation development into calibration and validation sets, which were defined independently and used for the model development and equation testing, respectively. 75% of the samples were in a calibration set and 25% in a validation set. The applicability of the model for the quantification of amines which were not included in the model, was evaluated using a procedure similar to cross-validation. The original samples were carefully divided into six training and validation sets containing 120 and 24 samples, respectively. All the samples from the same standard were included in a single validation set and the rest of the samples were included in the training set which was used for the recalculation of the equations. The results provided by these equations allowed the estimation of the prediction error for analytes not used in the development of the equations, which could be extended to other amines.

The reference data used for the equation development comprised 144 RFi (m/z) collected for 6 amines at eight concentration levels (mean concentration value 7.68 ng μL^{-1}, standard deviation 6.6 ng μL^{-1}). Standard laboratory error (SEL), which arises from standard solution preparation, was 0.3 ng μL^{-1}. Because the standard deviation of the samples used for the development of the PLSR equation was higher than SEL, the theoretical R^2 for the PLSR equation was 0.99 according to the Mark and Workman equation (Mark, 1987, 1996). Partial least squares regression (PLSR) was used to develop the calibration equation (main equation) based on the previously defined dataset. Maximum number of PLS factors was 13. This selection was based on the following rule: one PLS factor per ten samples of the training set plus two. Full cross-validation procedure was used to calibrate the equations. Minimum value of the standard error cross-validation determined the number of PLS factors in the equation, thus avoiding over-fitting problems. The criteria proposed by Shenk and Westerhaus (Shenk, 1996), based on the values of R^2 and standard error cross-validation (SECV), allow the evaluation of the developed equation. The values provided by the equation for R^2 prediction (0.99) and SECV (0.40 ng) indicated an excellent precision.

Calibration equation was tested using the validation set. Different parameters such as standard prediction error (SEP), R^2, slope and bias were studied for the evaluation of analytical quality of the equations (Table 2). The values of slope and bias were useful to distinguish systematic errors and study the correlation between the reference data and those provided by the proposed method. It was tested with a significance level of 99.5%, whether or not the slope was statistically equal to 1 and bias to 0. Non-significant ranges are shown in the slope and bias rows (values for these parameters were always within these ranges). The value for the slope was lower than 1 meaning that the values provided by the proposed method were systematically higher than the reference values, considering that the proposed method corresponded to the abscissa in the correlation plots. Because the SEP value was lower than 1.5×SECV, the developed equation was robust. The R^2 values for the correlation between the reference values and those obtained with the proposed method were always higher than 0.99. According to the R^2 criterion, amines can be determined with excellent precision using the developed equation.

Table 1. Statistical parameters for the evaluation of the PLSR equation.

Main equation		Tested equations	Prediction error (%)
Parameter	Value	Equation 1	7.339
SEP	0.405	Equation 2	8.259
R^2 prediction	0.994	Equation 3	8.659
Slope	0.994 (0.968 – 1.001)	Equation 4	7.775
Bias	0.004 (-0.028 – 0.068)	Equation 5	7.972
Prediction error (%)	**7.931**	Equation 6	7.584
		Mean	**7.931**

All the values obtained can be used to describe the developed equation and to evaluate the results derived from the determination of standard compounds, which were used for the development of the equation. However, no information was provided about the reliability of the results derived from the determination of unknown amines. Therefore, the samples were divided into six new training sets and their corresponding validation sets, which included all the different measurements of an excluded standard in different concentrations. Six equations were developed using the new training sets, and prediction errors were evaluated with the validation sets. Table 2 shows the prediction errors for the different tested equations and the mean prediction error (7.9 %), which can be associated with the error of the main equation.
The developed methodology was applied for the determination of amines in aerosol samples collected in SMEAR II station during 2011.

Desorption atmospheric pressure photoionization-mass spectrometry for the determination of chemical composition of atmospheric aerosols

Semi-on-line analysis, based on filter sampling of all-size ambient aerosols and desorption atmospheric pressure photoionization-mass spectrometry (DAPPI-MS, Figure 1) with consecutive DAPPI-MS[2] was developed. This approach allows the verification of structures of compounds found in aerosols by tandem mass spectrometry. The DAPPI-MS system gave linear response over the calibration range from 20 to 400 ng applied on filter for over 30 studied compounds (acids, aldehydes and amines). This allowed semiquantification of the compounds from the filter samples. Since no sample preparation was required and since the sampling system can be easily integrated to DAPPI-MS analysis, the method developed herein can be considered highly promising in the field of atmospheric research.
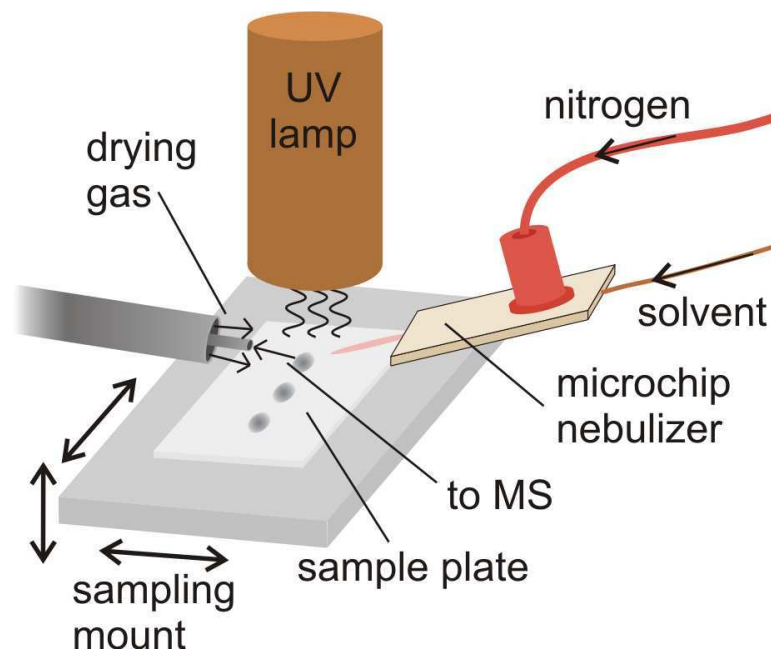
Figure 1. Schematic view of the DAPPI setup (Haapala, 2007).

Two-dimensional gas chromatography time-of-flight mass spectrometry (GC x GC-TOFMS) for the determination of vapor pressures of atmospherically relevant compounds from complex matrices

Four different approaches for the vapor pressure determination were studied. In the first one, isothermal runs were conducted for homologous series of alkanes by gas chromatography with flame ionization detection, followed by the runs under the same conditions for the compounds, for which vapor pressures were determined. The calculated retention indices were utilized to provide vapor pressures according to eq. 1, where p_z and $_{pz+1}$ are vapor pressures of alkanes eluting before and after the studied compound. The effect of column polarity and film thickness to the vapor pressure determination was also investigated. In the second approach, mass spectrometer was employed as a detector to get essential structural information for compounds needed e.g. in the chamber experiments. The third approach included gradient elution to speed up the process (eq. 2, t_1 and t_2 are retention times of compounds eluting before and after the studied compound (t_r), P_1, P_2 and P_0 are corresponding vapor pressures). In the last fourth approach, compounds of similar chemical nature as that of the studied compounds (alkanols, ketones and aldehydes) (Fig. 2) were selected as reference compounds to eliminate possible errors caused by the polarity differences between the analytes and alkane standards, and two-dimensional gas chromatography time-of-flight mass spectrometry was utilized.

$$\ln p_x = \ln p_z + \frac{(100_z - I_x)\ln\left(\frac{p_z}{p_{z+1}}\right)}{100}r^2 \quad (1)$$

$$\log P^\circ = \frac{\left(\log P_1^\circ - \log P_2^\circ\right)t_R + t_1 \log P_2^\circ - t_2 \log P_1^\circ}{t_1 - t_2} \quad (2)$$

Based on our studies, the most suitable column for the vapor pressure measurements was the nonpolar HP-1 column with 0.1 μm film thickness (30 m x 0.25 mm i.d.) (Hartonen, 2012). All four methodologies studied were compared and the fourth was the best for the compounds with different functionalities. Table

110

3 presents the final results. As expected, homologous series of compounds studied gave values comparable with the calculated ones. The procedure developed herein proved to be superior over all the existing methodologies in terms of sensitivity, analysis time, sample preparation and precision. In addition, the method allowed the structural elucidation of known and unknown compounds simultaneously with the vapor pressure determination in a single run. Vapor pressures of several atmospherically important compounds were determined for the first time.
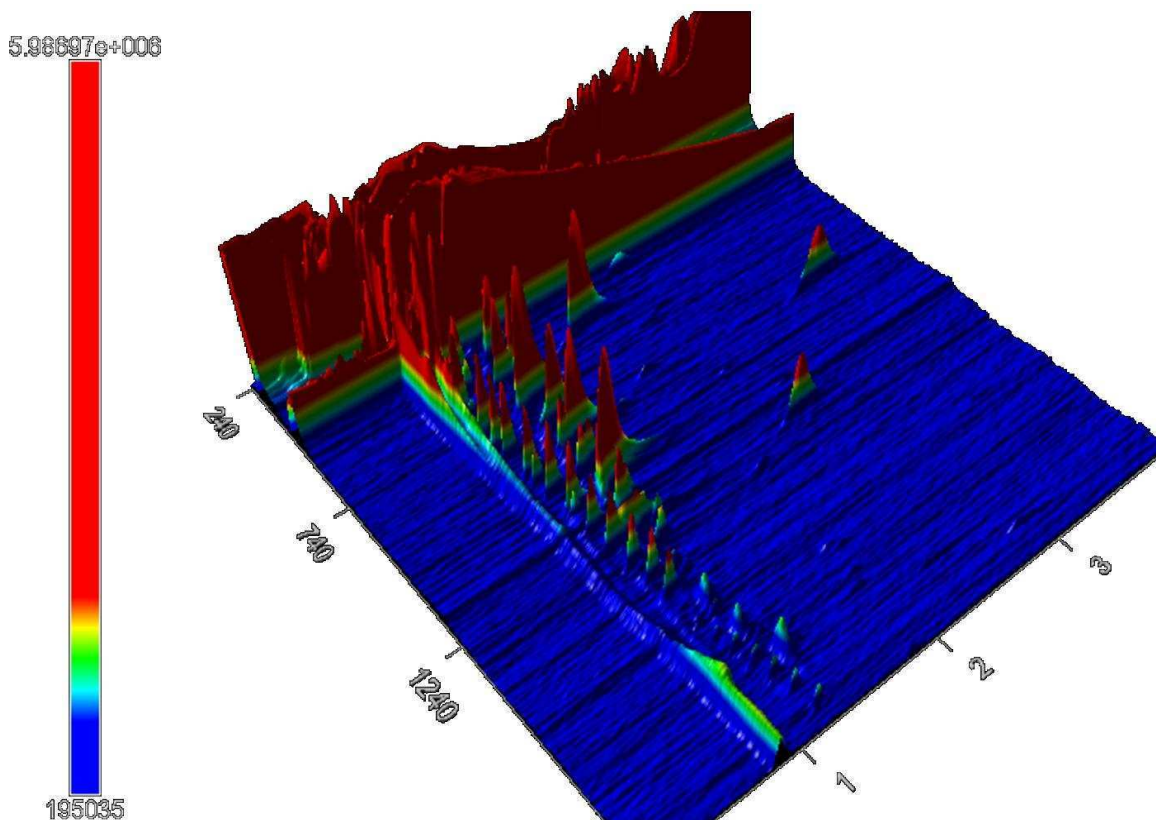
Figure 2. 3D plot (axes in seconds) of GC x GC-TOFMS experiment for the mixture of aldehydes (C3-C14, 12 compounds), alkanols (C6-C22, 14 compounds), 2-alkanones (C5-C16, 12 compounds), n-alkanes (C8-C20) and oxidation products of terpenes in Agilent 7890A gas chromatograph equipped with a split/splitless injector and a LECO Pegasus® 4D TOFMS system. An HP-1 column (30 m x 0.25 mm i.d., 0.1 μm film thickness) was used as the first-dimension column and an SLB™-IL 59 column (1 m x 0.1 mm i.d., 0.08 μm film thickness) as the second-dimension column (Parshintsev 2012).

Table 2. Vapor pressures (Pa) of studied compounds determined by gas chromatography (fourth approach), (Parshintsev 2012).

Analytes	Reference homologic series				
	alkanols	ketones	aldehydes	alkanes	theoretical value
caryophyllene aldehyde	0.01	0.08	0.13	0.07	1.55
nocaryophyllene aldehyde	0.01	0.06	0.09	0.05	0.20
pinonaldehyde	0.32	5.23	9.12	7.95	10.70
cis-pinonic acid	0.12	1.49	2.55	1.94	0.53

Identification of 1-(x-methylquinolin-x-yl) ethanone from 10 nm ambient aerosol particles

Measurements of 10 nm ambient aerosol particles were carried out in boreal forest environment at SMEAR II station Hyytiälä, Finland between 14th of March and 16th of May in 2011. Utilized instruments were the Laser AMS and aerosol filter collection system with off-line chromatographic analysis. The Laser AMS (Laitinen 2011) was used to determine different organic compounds, with focus on the nitrogen containing compounds, from 10 nm particles. The filter collection system was used to collect samples for quantitative chromatographic analysis of 18 carboxylic acids, 3 sugars, 18 aldehydes and 18 amines/nitrogen containing compounds from 30 nm and all-sized filter samples. Most interesting point in measurements was seen in mid-April 2011. On that time, the soil surface was uncovered from the heavy snow, temperatures went up and troposphere chemistry changed totally.

Two most abundant and interesting ions (m/z 143 and 185) in Laser AMS spectra after snow melted were further tested and identified together with filter samples (analyzed by HPLC-Ion Trap-MS) and additional analysis of filter samples with high resolution TOF instrument. The resulting compound for these studied Laser AMS ions was 1-(X-methylquinolin-X-yl)ethanone, $C_{12}H_{11}NO$, at molecular weight of 185.22 g/mol. The fragmentation of mother ion in HPLC-Ion Trap-MS of filters samples can be seen in figure 3.
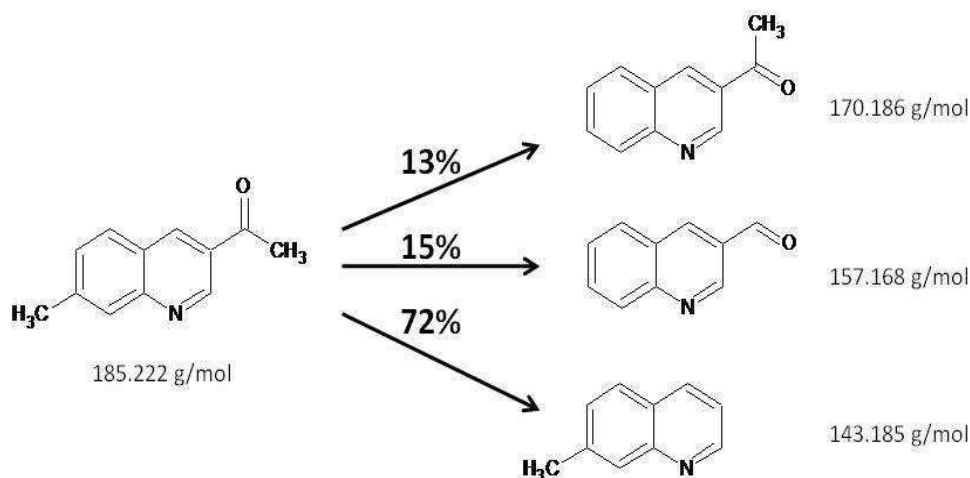
Figure 3. Fragmentation pattern of 1-(7-methylquinolin-3-yl)ethanone, with its intensities and exact masses of fragments, compared to the M+. This is one of the possible molecules for studied unknown nitrogen compound (Laitinen, 2012).

Within these techniques it is impossible to determine the exact structure of the molecule. Only HPLC-NMR could show the exact locations of substituents on the molecule, but sample amounts needed for that kind of analysis are several folds higher. This compound could also be determined by HPLC according to its retention times but that would require a standard solution of each possible molecule and synthesis of them in a laboratory.

CONCLUSIONS

The presented achievements in analytical chemistry of atmospheric aerosols bring us closer to the understanding of the complicated issue of aerosol formation and growth. Future developments are seeked from the special sampling valve that allows the size-selected particles to be introduced directly into the gas chromatography-mass spectrometry analysis. However, more research is needed in cooperation with scientist from other fields to draw a whole picture of aerosol life-cycle and effects on climate.

REFERENCES

Claeys, M., Graham, B., Vas, G., Wang, W., Vermeylen, V., Pashynska, R., Cafmeyer, J., Guyon, P., Andreae, M.O., Artaxo, P., Maenhaut, W. (2004). Science 303: 1173-1176.

Cohen, H., Armstrong, F., Campbell, H. (1995). J. Chromatogr. A, 694: 407–413.

Decesari, S., Fuzzi, A., Facchini, M.C., Mircea, M., Emblico, L., Cavalli, F., Maenhaut, W., Chi, X., Schkolnik, G., Falkovich, A., Rudich, Y., Claeys, M., Pashynska, V., Vas, G., Kourtchev, I., Vermeylen, R., Hoffer, A., Andreae, M.O., Tagliavini, E., Moretti, F., Artaxo, P. (2006). Atmos. Chem. Phys., 6: 375-402.

Haapala, M., Pol, J., Saarela, V., Arvola, V., Kotiaho, T., Ketola, RA, Franssila, S., Kauppila, T.J., Kostiainen, R. (2007). Anal. Chem., 79:7867-7872.

Hartonen, K., Parshintsev, J., Vilja, V.-P., Tiala, H., Knuuti, S., Lai, C.-K. and Riekkola, M.-L. (2012). Submitted to J. Phys. Chem. A.

Laitinen, T., Ehn, M., Junninen, H., Ruiz-Jimenez, J., Parshintsev, J., Hartonen, K., Riekkola, M.-L., Worsnop, D. and Kulmala, M. (2011). Atmos. Env., 45:3711-3719.

Laitinen, T., Junninen, H., Parshintsev, J., Ruiz-Jimenez, J., Hautala, S., Petäjä, T., Hartonen, K., Riekkola, M.-L., Worsnop, D., Kulmala, M. (2012). To be submitted to J. Mass. Spectrom.

Mao, M.H., Chen, B.G., Qian, X.M., Liu, Z. (2009). Microchem. J., 91: 176–180.

Mark, H. Principles and Practice of Spectroscopic Calibration, John Wiley & Sons Inc, 1996.

Mark, H., Workman, J. (1987), Spectroscopy 2: 38-42.

Parshintsev, J., Lai, C.-K, Hartonen, K. and Riekkola, M.-L. (2012). Submitted to Anal. Chem.

Ruiz-Jimenez, J., Parshintsev, J., Laitinen, T., Hartonen, K., Riekkola, M.-L., Petäjä, T., Virkkula, A., Kulmala, M. (2011). Anal. Methods, 3: 2501–2509.

Shenk, J.S., Westerhaus, M.O. in: A.M.C. Davies, P.C. Williams (Eds.), Near Infrared Spectroscopy: The Future Waves, NIR Publications, Chichester, West Sussex, U.K., 1996, pp. 198-202.

FINNISH CoE IN PHYSICS, CHEMISTRY, BIOLOGY AND METEOROLOGY OF ATMOSPHERIC COMPOSITION AND CLIMATE CHANGE IN THE EUROPEAN RESEARCH LANDSCAPE

S. SORVARI[1], H. LAPPALAINEN[2], M. BRUS[2], and M. KULMALA

[1]Finnish Meteorological Institute (FMI), Helsinki, Finland

[2]Department of Physics, University of Helsinki, Finland

Keywords: EUROPEAN RESEARCH AREA, EUROPEAN ENVIRONMENTAL RESEARCH INFRASTRUCTURES, JOINT PROGRAMMING

BACKGROUND

The Center of Excellence (CoE) is a significant funding scheme in the Finnish research system. By providing six-year funding, the programmes offer an excellent opportunity to create an innovative and target-oriented environment where the research is performed in interdisciplinary collaboration between research groups in different institutions and universities. The programme has enabled us to develop a unique infrastructure and make the scientific breakthroughs at the interfaces of scientific disciplines and research fields.

The large and sophisticated measurement network and the long-lasting research collaboration among the Finnish Center of Excellence (FCoE) partners enable a strong international research orientation to our work. Indeed, international collaboration is necessary for the strengthening of high level research, for attaining wider perspective of the scientific scope and exploitation of the results in global context.

Our CoE, the Center of Excellence on Atmospheric Composition and Climate Change, has large spectrum of international activities and stands at the forefront of on-going climate change research on European as well as Global level (Fig.1). Strong participation in the European Research Area (ERA) is a key part of this.

EUROPEAN RESEARCH LANDSCAPE

In 2008, Europe relaunched a vision for durable research integration, which is based on decision to create the common European Research Area (ERA). The ERA is carried through specific initiatives such as initiatives on Research Mobility, Research Infrastructures (RI's), Knowledge Sharing (IPR issues), Joint Programming (JPI), and International Science& Technology Cooperation. The ERA initiatives are mutually interlinked and for the specific research field it is necessity to develop the initiatives together in order to create such an overall research environment that enhance the excellence and new scientific breakthroughs. The FCoE structure, our position in science and our performance enable us to be an active partner in different ERA initiatives.

EUROPEAN ENVIRONMENTAL RESEARCH INFRASTRUCTURES

Research Infrastructures in the environmental sciences are necessary instruments for developing and securing environmental observations in research. They provide tools for scientists in their pursuit of understanding the principles of the climate change and its effects. The global nature of today's environmental challenges means that international collaboration among them is fundamental. Global, national as well as regional RI's will all contribute to the global network of research infrastructures, needed for environmental research.

The European Strategy Forum on Research Infrastructures, ESFRI, is a key instrument to support policy-making on research infrastructures. A major step took place in the ERA since 2006 with the publication of ESFRI Roadmap, which highlighted the key RI's necessary for European research in the next decades. Currently the ESFRI roadmap has 10 pan-European environmental infrastructures at the roadmap. FCoE is a member in many of these ESFRI infrastructures (e.g. in ICOS, COPAL, SIOS, LifeWatch, ANAEE) and in EC funded integrated infrastructure projects (ACTRIS, InGos and EXPEER). The backbone of our research infrastructure activities is our own efficient infrastructure, namely the network of stations like SMEAR's and Pallas-Sodankylä GAW stations. Our expertise, the research carried and data collected in these multifunctional, comprehensive measurement stations form the solid RI hard-ware, knowledge and expertise to contribute to the European level RI's in their construction and implementation phase.
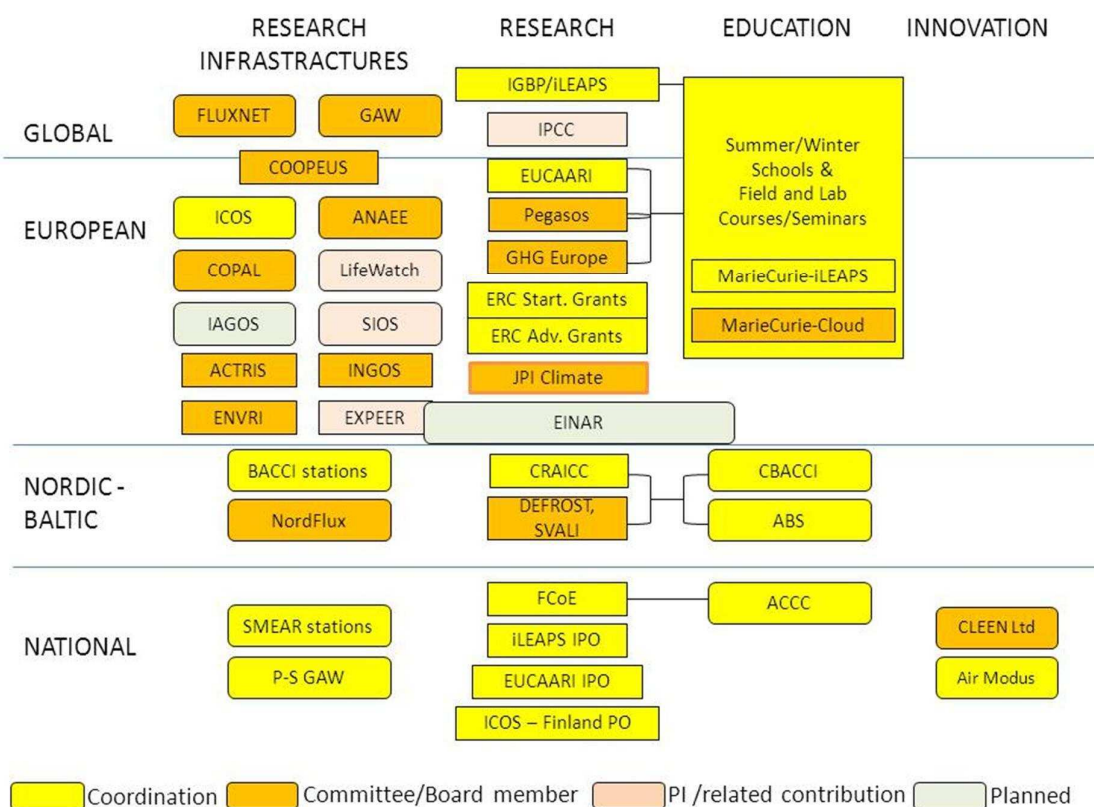
Figure 1. Coordination activities of the Finnish Center of Excellence in Physics, Chemistry, Biology and Meteorology of Atmospheric Composition and Climate Change

The development and financing of most infrastructures will remain in hands of science communities and the EU Member States, however strong cooperation amongst them, with the support of the EU, is needed to develop synergies and a common vision: this is a key element of the ERA vision and it has received consideration within the EU framework programmes, as well as in the forthcoming Horizon 2020.

Until now, EC has supported the ESFRI preparatory projects through cluster projects in a given scientific field. In environmental sciences, EC support has been provided through ENVRI and COOPEUS. These projects aim to enhance the interoperability of the data, methods, tools and services within the Environmental Research Infrastructure cluster. FCoE has a key role by leading the Work Packages on strategic planning and integration in both projects.

ENVRI

ENVRI "*Common Operations of Environmental Research infrastructures*" is gathering six ESFRI Environmental projects, to develop, with the support from ICT experts, common data and software components and services for their facilities.

The ESFRI-ENV projects are not starting from nothing. They all build upon many years of existing practice. All of them are currently working with some form of data infrastructures and contributing data and knowledge to international observation systems and for broad user communities. The ENVRI project is aiming to minimize the heterogeneity among environmental data infrastructures to offer common best practices and to provide technical tools to help ESFRI RIs to better fulfil their scientific remit.

The central goal of the ENVRI project is to implement harmonized solutions and draw up guidelines for the common needs of the environmental ESFRI projects. While the ENVRI infrastructures are very diverse, they face common challenges including data capture from distributed sensors, metadata standardization, management of high volume data, workflow execution and data visualization. The common standards, deployable services and tools developed will be adopted by each infrastructure as it progresses through its construction phase. Moreover, the ENVRI project aims to ensure that each infrastructure will fully benefit from the integrated new ICT capabilities beyond the project duration by adopting the ENVRI solutions as part of their ESFRI implementation plans. The projects period of ENVRI is 2011 - XX

COOPEUS

COOPEUS "*Strengthening the cooperation between the US and the EU in the field of environmental research infrastructure*" brings together scientists and users being involved in the ESFRI ENV preparatory projects with their US counterparts. The intention is that by interlinking the activities new synergies stimulating the creation of a truly global integration of existing infrastructures will be generated. The key of this integration process is the efficient access to and the open sharing of data and information produced by the environmental research infrastructures. This important crosscutting infrastructure category is subject to rapid changes, driven almost entirely outside the field of environmental sciences. Trends in this area include growing collaborations between computer and environmental scientists, leading to the emergence of a new class of scientific activity structured around networked access to observational information. Therefore links to running projects like ENVRI in Europe or EARTHCUBE in the US who are developing relevant architectures are indispensable. Considering this perspective the COOPEUS project will serve as a testbed for new standards and methods. Interoperability concepts and the development of e-infrastructures for the environmental ESFRI projects will beyond data also include the tools that scientist use for analyzing the data. The new term that describes this new quality in cooperation is "interworkability" which means that interoperability is extended to the exchange of concepts between individual scientists. The COOPEUS project will act as an incubation chamber for new sustainable concepts in this field. The main outcome will be to develop MoUs that will determine future cooperation strategies between the research infrastructures.

To avoid the duplication of work, collaboration of the projects is very important. We, as the leaders of working groups organizing External liaisons (ENVRI) and Common Research Infrastructure framework (COOPEUS) are strongly contributing to development of common strategies, networking and cooperation, which is necessary in order to bring the resources together and build the ERA.

JOINT PROGRAMMING INIATIVE AND JPI CLIMATE

The concept of Joint Programming (JPI) was introduced by the European Commission in July 2008. JPI is another initiative for implementing of ERA aiming to remedy the unwanted fragmentation in

environmental sciences. The idea of JPI is to increase the value of relevant national and EU R&D funding by concerted and joint planning, implementation and evaluation of national research programmes.

JPI Climate - Connecting Climate Knowledge for Europe – is one of the 10 initiatives launched so far. JPI Climate is a platform where the research funding policies of 12 countries, responsible for a large amount of climate research funding in Europe, can be aligned. Representing a funding volume of more than 200M€ per year by its member countries, JPI Climate has the potential to become a vital and important point of reference in the ERA landscape as well as on the international level.

JPI Climate has established its first Strategic Research Agenda (SRA) in June 2011. The Initiative is built upon four modules (M1: Moving towards decadal climate predictions, M2: Research for climate service development, M3: Understanding sustainable transformations of societies under climate change, M4: Improving models and scenario-based tools for decision-making under climate change), defined in SRA.

FCoE is strongly involved in JPI Climate and the members of the FCoE are committed in various tasks, such as being a member of the JPI Climate Management Board, co-chairing the Module 1: Moving towards decadal prediction, participating in Module work with several science experts as well as co-chairing the first JPI Climate implementation activities (e.g. Fast Track Activity (FTA) 1.3.: Changing cryosphere in the climate system – from observation to climate modeling). One of the first activities within the FTA 1.3. is a Pan-Eurasian Experiment (PEEX) workshop held in Helsinki in October 2012. The scope of the workshop is to set up a process for planning of a large-scale, long-term, coordinated observations and modeling experiment in the Pan-Eurasian region, especially to cover ground base, airborne and satellite observations together with global and regional models to find out different forcing and feedback mechanisms in the changing climate. The PEEX is described more in details in the PEEX Abstract by Kulmala et al. in this volume.

CONCLUSIONS

International research cooperation is crucial in Environmental sciences, given the fact that environmental challenges have international, regional and global dimensions. International cooperation is further motivated by the fact that a critical mass is needed given the scale, scope and high level of complexity of research. The FCoE acknowledge the importance of international collaboration and it has proven its capability to contribute and to be active partner in international cooperation and for further development of the European Research Area in the field of atmospheric and environmental sciences. For the future, the aim of the FCoE is to keep the current position in the forefront of the atmospheric science and continue to contribute to the building of a more coherent European environmental research landscape via various European RI and research projects.

OVERVIEW OF MOLECULAR MODELLING OF ATMOSPHERIC PARTICLE FORMATION

HANNA VEHKAMÄKI[1], NICOLAI BORK[1], HENNING HENSCHEL[1], KAROLIINA IGNATIUS[1], OONA KUPIAINEN[1], THEO KURTÉN[2], VILLE LOUKONEN[1], MATTHEW MCGRATH[3], ISMO NAPARI[1], TINJA OLENIUS[1], ISMAEL K. ORTEGA[1], KAI RUUSUVUORI[1] and NARCISSE TSONA TCHINDA[1]

[1]Department of Physics, Post Office Box 64, FI-00014 University of Helsinki, Finland
[2]Department of Chemistry, Post Office Box 55, FI-00014 University of Helsinki, Finland
[3]Department of Biophysics, Graduate School of Science, Kyoto University, 6068502, Kyoto, Japan

Keywords: particle formation, nucleation, molecular clusters, sulphuric acid, dimethylamine

INTRODUCTION

Experimental and theoretical data indicates that the formation of new particles in the atmosphere in most cases very likely involves sulphuric acid assisted with some base molecules. The role of ions in atmospheric particle formation is has been widely discussed during recent years. So far, there are no consistent theoretical approaches capable of explaining and predicting atmospheric neutral particle formation rates using realistic trace gas concentrations. All previous attempts (for example, binary H_2SO_4-H_2O and ternary H_2SO_4-NH_3-H_2O theories) have invariably predicted much too low formation rates for atmospheric conditions, apart from the Napari *et al.* 2002 ternary model, which is known to be internally inconsistent (Anttila *et al.* 2005). The diameter of the forming clusters is 1-2nm, falling between the smallest size where brute force quantum mechanical treatment is possible, and macroscopic size where bulk thermodynamics in applicable. A recent tutorial review (Vehkamäki and Riipinen, 2012a) summarizes current key questions in atmospheric particle formation.

METHODS

We have used a cost-effective multi-step computational chemistry method involving automated configuration sampling, density functional theory geometry optimizations and coupled-cluster energy calculations, to study the stability of charged and neutral sulphuric acid clusters containing ammonia and dimethylamine. We deduce fragmentation rates of the clusters from the computed formation free energies (Ortega *et al.* 2012). Collision and coagulation rates are computed from kinetic gas theory. We model cluster formation by explicitly simulating all possible collision, coagulation, evaporation and fragmentation reactions for a certain set of clusters. Dynamic simulations are carried out using the Atmospheric Cluster Dynamics Code model (ACDC; McGrath *et al.* 2012).

RESULTS

Our main line of study has been the formation of neutral and both positively and negatively charged clusters containing sulphuric acid, ammonia and DMA. We have modelled the formation and evaporation of clusters containing up to four sulphuric acid and four base molecules. The exclusion of larger cluster is a computational necessity rather than ideal choice at the moment. However, we predict that neutral clusters containing more than four acids and approximately the same number of stabilizing bases will evaporate very slowly, allowing their formation rate be used as justified approximation for the particle formation rate. We have show that clustering of DMA and sulphuric acid molecules at atmospheric vapour concentrations lead to particle formation rates comparable to those observed in the atmosphere. Our model also yields formation rates close to, although most somewhat above those observed in the CLOUD chamber experiment in CERN in the sulphuric acid, DMA and/or ammonia system. For computational reasons they model does not so far contain water molecules, although water is present both in atmosphere

and in the CLOUD chamber (Kirkby *et al.* 2011). Quantum chemical and thermodynamic test calculation imply that the clusters studies are fairly dry, and water present in the cluster does not alter the cluster dynamics significantly.

We studied the substitution of ammonia by dimethylamine in positively charged sulphuric acid – ammonia – dimethylamine clusters demonstrating a good agreement with an experimental study (Bzdek *et al.* 2010). Then we simulated base exchange in neutral clusters, which cannot be measured directly. Collisions of a dimethylamine molecule with an ammonia-containing positively charged cluster result in the instantaneous evaporation of an ammonia molecule, while the dimethylamine molecule remains in the cluster. According to our simulations, a similar base exchange can take place in neutral clusters, although the overall process is more complicated. Neutral sulphuric acid – ammonia clusters are significantly less stable than their positively charged counterparts, resulting in a competition between cluster evaporation and base exchange (Kupiainen *et al.* 2012).

We have shown that our quantum chemical methods produce consistent results with quadrupole-time-of-flight mass spectrometer experiments of small protonated pyridine/ammonia/water clusters and their reactions with ammonia. The pattern of the observed magic numbers suggest that $H^+(NH_3)(pyridine)(H_2O)_n$ have structures consisting of a $NH_4^+(H_2O)_n$ core with the pyridine molecule hydrogen-bonded to the surface of the core (Ryding *et al.* 2012).

We studied effect of cluster formation on the measurement of gas-phase sulphuric acid, predicting that a significant fraction of the gas-phase sulphuric acid molecules are clustered with amines if the amine concentration is even a few ppt. A small fraction of these acid-amine clusters may not be charged by the chemical ionization mass spectrometer (CIMS) instrument (Kurtén *et al.* 2011). The amine molecules will evaporate practically immediately after charging, thus evading detection. We also used our model to show that the observation of a close-to-collision-limited sulphuric acid dimer formation in atmospherically relevant laboratory conditions suggests that even in the ultraclean conditions there exist stabilizing compounds with concentration high enough to prevent the dimer evaporation (Petäjä *et al.* 2011). We have helped to rule out significant participation to particle formation of some oxidation products of sulphur dioxide other that sulphuric acid (Toivola *et al.* 2011)

To assist rigour interpretation of particle formation experiments, we studied how widely used nucleation theorems are affected by the existence of small stable clusters, whose collisions are the key pathway leading to overcritical clusters and thus stable particle. We conclude that if cluster-cluster collisions dominate over monomer cluster collisions, the nucleation theorems can not be used to infer the critical cluster size (Vehkamäki *et al.* 2012b).We have also developed theoretical tools for analysing novel experiments of heterogeneous nucleation on nanometre sized seeds (Winkler *et al.* 2012) and performed quantum chemical calculations on the interactions between the seed molecules and condensing vapour (Ruusuvuori et al. 2011).

CURRENT DIRECTIONS

Extensive analysis concerning the agreement of our computational results with CLOUD experiments and Hyytiälä field data is underway. We will use Markov chain Monte Carlo method to perform the error estimates in a more rigorous way, and to identify parameters whose feasible variations are most likely to result in significant changes ion our predicted cluster distributions and formation rates. We will further study the effect of water on cluster formation both using quantum chemistry and thermodynamic theories. Molecular dynamic studies based on quantum chemical molecular interactions are just becoming possible for smallest cluster relevant for atmospheric particle formation. Thus, we have started to study truly dynamic kinetic issues, such as steric hindrance, affecting cluster- cluster/molecule sticking in collisions. We continue to provide theoretical support for experiments and instrument development, such as a CIMS

aimed at measuring low concentrations on amines, and seek to improve and test our model by comparing to a wide selection of experiments.

ACKNOWLEDGEMENTS

REFERENCES

Anttila,T., Vehkamäki, H, Napari, I., Kulmala, M. (2005). Effect of ammonium bisulphate formation on atmospheric water-sulphuric acid-ammonia nucleation. *Boreal Environment Research* **10**, 511.

Bzdek, B. R., Ridge, D. P., and Johnston, M. V. (2010). Amine exchange into ammonium bisulfate and ammonium nitrate nuclei, *Atmospheric Chemistry and Physics* **10**, 3495.

McGrath, M.J., Olenius, T. I. K. Ortega, Loukonen V., Paasonen,P., Kurtén, T.,Kulmala, M., and Vehkamäki, H. (2012). Atmospheric Cluster Dynamics Code: a flexible method for solution of the birth-death equations. *Atmospheric Chemistry and Physics* **12**, 2345.

Kirkby, J. *et al.* (2011) Role of sulphuric acid, ammonia and galactic cosmic rays in atmospheric aerosol nucleation. *Nature* **476**, 429.

Kupiainen, O., Ortega, I.K., Kurtén, T. and Vehkamäki, H. (2012). Amine substitution into sulfuric acid – ammonia clusters. *Atmospheric Chemistry and Physics* **12**, 3591.

Kurtén, T., Petäjä, T., Smith, J. , Ortega, I.K., Sipilä, M., Junninen, H., Ehn, M.,Vehkamäki, H., Mauldin, L., Worsnop, D. R. and Kulmala, M. (2011). The effect of H_2SO_4 – amine clustering on chemical Ionization mass spectrometry (CIMS) measurements of gas-phase sulfuric acid. *Atmospheric Chemistry and Physics* **11**, 3007.

Napari,I. Noppel, M., Vehkamäki, H. and Kulmala, M. (2002).Parametrization of ternary nucleation rates for H2SO4-NH3-H2O vapors. *Journal of Geophysical Research – Atmospheres* **107**(D19), 4381.

Ortega, I.K., Kupiainen, O., Kurtén, T., Olenius, T., Wilkman, O., McGrath, M.J., Loukonen, V. and Vehkamäki, H. (2012). From quantum chemical formation free energies to evaporation rates. *Atmospheric Chemistry and Physics* **12**, 225.

Ruusuvuori, K., Kurtén, T., Ortega, I.K., Vehkamäki, H., Loukonen, V., Toivola, M. and Kulmala, M. (2011). Density-functional study of the sign preference of the binding of 1-propanol to tungsten oxide seed particles. *Computational and Theoretical Chemistry* **966**, 322.

Ryding, M., Ruusuvuori, K., Andersson, P., Zatula, A., McGrath, M.J., Kurtén, T., Ortega, I.K., Vehkamäki, H. and Uggerud, E. (2012). Structural Rearrangements and Magic Numbers in Reactions between Pyridine-containing Water Clusters and Ammonia. *Journal of Physical Chemistry A* **116**, 4902.

Toivola, M., Kurtén, T., Ortega, I.K., Sundberg, M., Padova, A. and Vehkamäki, H. (2011). Quantum chemical studies on peroxodisulfuric acid - sulfuric acid- water clusters. *Computational and Theoretical Chemistry* **967**, 219.

Vehkamäki, H. and Riipinen, I. (2012a) Thermodynamics and kinetics of atmospheric aerosol particle formation and growth. *Chemical Society Reviews* **41**, 5160.

Vehkamäki, H., McGrath, M.J., Kurtén, T., Julin, J., Lehtinen, K. E. J., and Kulmala, M.(2012b) Rethinking the application of the first nucleation theorem to particle formation. *Journal of Chemical Physics* **136**, 094107.

FROM WATER-AIR INTERFACES TO CARBON-WATER CYCLES

T. VESALA[1], I. MAMMARELLA[1], P. ALEKSEYCHIK[1], S. DENGEL[1], S. HAAPANALA[1], J. HEISKANEN[1], P. KERONEN[1], J. KUJANSUU[1], M. PIHLATIE[1], M. RAIVONEN[1], J. RINNE[1], M. TOMASIC[1,5], S. SMOLANDER[1], T. HÖLTTÄ[2], E. JUUROLA[1,2], P. KOLARI[1,2], T. AALTO[3], T. LAURILA[3], A. OJALA[4], E.-S. TUITTILA[5], J. LEVULA[6], J. BÄCK[2], E. NIKINMAA[2]

[1]Department of Physics, University of Helsinki

[2]Department of Forest Sciences, University of Helsinki

[3]Finnish Meteorological Institute, Helsinki

[4]Department of Ecological and Environmental Sciences, University of Helsinki

[5]University of Eastern Finland, Kuopio, Finland

[6]Hyytiälä Forestry Field Station, Finland

Keywords: Greenhouse gases, carbon cycle, water cycle, boreal forest, wetlands, lakes, Earth systems

BACKGROUND

Biosphere interacts with the atmosphere in the form of the exchange of mass, heat and momentum. Central for these processes is the tight coupling of transport phenomena, phase transitions and plant metabolism. The metabolic processes create sources and sinks, which act as driving forces for transport, either molecular (diffusion) or convective (bulk flow). Here three central research themes of biosphere-atmosphere interactions are discussed: whole-tree regulation of water circulation, gas exchange of aquatic ecosystems and methane emissions of peatlands. The common feature in the themes is that the mass transport phenomena occur at the presence of water-air interfaces, either extended flattish interfaces or curved interfaces such as in pores or bubbles. In this abstract, we overview the research themes and draft ideas and plans for future work on them.

METHODS

Whole-tree water circulation and stomatal regulation

Regulation of water circulation by trees has been under intensive study since 70's (see e.g. Mencuccini, 2003). Components of circulation are transpiration through stomata, sap flow in xylem, phloem flow and radial transport in the stem. These processes are tightly coupled. Trees regulate transpiration via stomatal action, which balances carbon uptake against water loss (e.g. Buckley, 2005) to match the transport capacity of xylem for replacing lost water while maintaining sufficient flux of water to phloem for transport of assimilated sugars (Hölttä et al. 2009). The so-called cohesion-tension theory (see e.g. Zimmermann, 1983) has been broadly accepted as a sound physico-biological framework for the ascent of sap, and there exists strong experimental support for the optimal stomatal control (e.g. Cowan and Farquhar, 1977). However, the understanding of the fundamental processes and mechanisms coupling these two, particularly with phloem transport of sugars is still far from complete. When the transport capacity of a tree is not enough, it tends to close stomata. Very intriguing question is related to embolism: Gas bubbles may form in the xylem conduits if water tension increases too much at high transpiration, reducing conductivity and potentially leading to desiccation of the plant (e.g. Sperry, 2000). However, plants are able to refill these gas-filled conduits (Salleo et al., 1996; Vesala et al., 2003), but how they do that, and in what conditions is still unknown despite the recent progress made in this field (Zwienicki and Holbrook, 2009). Understanding how embolism repair under tension occurs is critical for evaluating metabolic costs (Hölttä et al., 2009) and constraints of water transport (Hölttä et al., 2011).

To solve the problems, we formulate and test two new theoretical concepts related to the plant level regulation of stomatal opening, to water-use efficiency, to functioning of xylem and phloem

transport and to xylem embolism repair. The first theoretical concept is the hypothesis that there exists a stomatal opening that maximizes the sugar transport from leaves (Nikinmaa et al, 2012). The second one is the inclusion of the curvature of water surface in the physics of the plant gas exchange and water transport. Transpiration generates water tension, which via the surface tension produces curved surfaces in the pores. Beside the effects on the stomatal gas exchange, curved water surfaces may be involved reducing vulnerability of the water conduits to cavitation as well as in refilling of embolized water conduits. The gas bubble in the embolized conduits creates concave liquid surfaces, where the equilibrium vapour pressure is decreased. We utilize both new laboratory experiments and field observations.

Aquatic ecosystem gas exchange

The exchange of gases between the atmosphere and water bodies is controlled by the transport through a thin layer on the water-side of the surface (Jähne and Haussecker, 1998). To estimate the exchange rate, models are applied based on the measured CO_2 partial pressure difference between the air and water and parameterized bulk transfer coefficients, but the coefficient is difficult to determine experimentally (MacIntyre et al., 2010). Data on fluxes measured by the eddy-covariance (EC) technique over the lake can be also utilized in the quantification of the transfer coefficient. However, still only seven articles are reporting on EC measurements of CO_2 fluxes over lakes (see Vesala et al., 2012), and none over rivers, and the lengths of the records are rather short. Only one data set, which is longer than year, has been published (Huotari et al., 2011). There we presented the EC record over five consecutive open-water periods on a small lake Valkea-Kotinen (Finland). Nevertheless, inland waters, mostly being net heterotrophic and thus processing carbon of terrestrial origin, have a significant role in the sequestration, transport and mineralization of organic carbon (e.g. Battin et al., 2009). Although inland waters are especially important in lateral transporters of carbon, their direct carbon exchange with the atmosphere, so called outgassing, has also been recognized to be a significant component in the global carbon budget (Bastviken et al., 2011). There is a negative relationship between lake size and the gas saturation and especially small lakes are a relatively large source of CO_2 (e.g. Kortelainen et al., 2006). Beside EC, multiple other approaches to estimating air-water gas exchange exist (Cole at al., 2010), like floating chambers and profile methods. So far only one article has been published on EC measurements for CH_4 over the water body (Eugster et al., 2011). The water-side EC technique is becoming also an established method for estimating oxygen fluxes in natural aquatic ecosystems close to the bottom sediment (Lorrai et al., 2010).

To solve the problems, we address gas transfer coefficients for water-air exchange and they dependence on environmental variables and possible site-specific factors. We formulate new parameterizations to be tested against earlier ones and other data sets. There is a urgent need for more flux data from lakes and rivers of different size and type (like trophic status and water colour) over varying meteorological conditions and different seasons. We organise two campaigns with measurements of water velocities and turbulence accompanied by EC for CH_4. We carry out two EC campaigns over rivers (one large river and one smaller one) for CO_2.

Peatland methane emissions

Peatlands occupy a relatively small fraction, about 3%, of the Earth's land area, but they are a globally important carbon store due to their high carbon density (Frolking et al., 2011). Overall, undisturbed peatlands are currently a weak carbon sink and a moderate source of methane, emissions of which is a result from a balance between CH_4 production and CH_4 oxidation. The production results from metabolism of archaea (Vogels et al., 1988) degrading different carbon pools. Archaea require oxygen-free environments, found in waterlogged peatlands. The produced CH_4 can be transported to the atmosphere via diffusion through the peat matrix or through the gas-filled pore spaces of vascular plants or be released abruptly in the form of bubbles (ebullition) (e.g. Wania et al., 2010). The knowledge of the relative importance of different transport/released mechanisms is crucial, since it affects how much CH_4 may be oxidized before escaping to the atmosphere. Especially, the diffusion in the peat is prone to oxidization by methanotrophic aerobic bacteria (Hanson and Hanson, 1996), which may live in mutually beneficial loose symbiosis between mosses providing carbon to them (Kip et al., 2010; Putkinen et al., 2011). The processes that underlie CH_4 emissions are complex and depend on several climate- and

vegetation-related variables (such as inundation, vegetation composition and soil temperature). The inclusion of peatland methane emissions to terrestrial biosphere models and Earth System Models (ESM) have recently started. The model presented by Wania et al. (2010), simulating CH_4 emissions from northern peatlands, is suitable for large-scale applications and is broadly used, but several aspects of the model could be still improved.

To solve the problems, we address the description of the methane transport and release processes based on the fundamental physical principles coupled with the characteristics of vegetation and bacterial metabolic processes. The comparison of the model results to broad range of available observations are performed. We are establishing a long-term CO_2 and CH_4 EC measurement site at a boreal wetland, a raised bog with a strong characteristic pattern of hummocks and hollows with open water pools. Thus, together with data set from the nearby fen site, two long-term data sets from the same boreal wetland become available. New measurement methods for *in-situ* detection of methane bubbles in peat matrix will be developed and tested.

CONCLUSIONS

Comprehensive research of the phenomena discussed above requires theoretical frameworks, long-term field observations at different spatial and temporal scales, intensive measurement campaigns, laboratory experiments, process models and terrestrial biosphere models. We implement the new theoretical concepts, process model modules and parameterizations, into several terrestrial biosphere models and compare the model results against observations. We also carry out model intercomparisons and sensitivity tests. This leads to a new level of sophistication of understanding Biosphere-Atmosphere feedbacks concerning essential branches of carbon and water cycles. The results of the project are further utilized in process parameterizations of regional models or Earth System Models via international collaboration.

The research connects physical knowledge with ecophysiology, brings theoretical, experimental, observational and modeling aspects together and links various spatio-temporal scales (Fig.1).
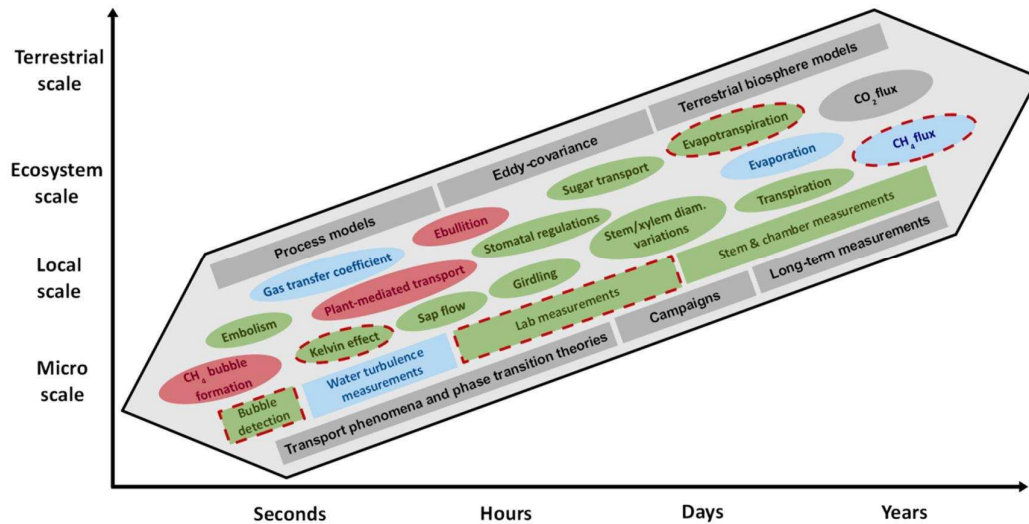
Fig. 1. Approximate scales of main processes and methods used. Ellipses refer to processes and boxes to methodologies. Green refers to trees/forests, red to peatlands, blue to lakes/rivers, red dashed line to peatlands jointly with trees or lakes and grey to joint item for all. Kelvin effect is the novel concept in plant physiology related to curved sub-stomatal water interfaces under high water tensions and consequent modification of the gas solubility to the water.

REFERENCES

Bastviken D et al. *Science* **331**, 50, 2011.
Battin TJ et al. *Nature Geoscience* **2**, 598, 2009.
Buckley TN *New Phytol*. **168,** 275, 2005.
Cole JJ et al. *Limnol. Oceanogr.: Methods* **8**, 285, 2010.
Cowan IR, Farquhar GD *Symposium Society for Experimental Biology* **31**, 471, 1977.
Eugster W et al. *Biogeosciences* **8**, 2815, 2011.
Frolking S et al. *Environ. Rev.* **19**, 371, 2011.
Hanson RS, Hanson TE *Microbiol. Rev.* **60**, 439, 1996.
Hölttä T et al. *J. Theor. Biol.* **259,** 325, 2009.
Hölttä T et al. *Plant Cell Environ*. **34**, 1819, 2011.
Huotari J et al. *Geophys. Res. Letters* **38**, L18401, doi:10.1029/2011GL048753, 2011.
Jähne B, Haussecker H *Annu. Fluid. Mech*. **30**, 443, 1998.
Kip N et al. *Nature Geoscience* **3,** 617, 2010.
Kortelainen P et al. *Global Change Biol.* **12**, 1554, 2006.
Lorrai C et al. *J. Atmos. Oceanic Technol.* **27**, 1533, 2010.
MacIntyre S et al. *Geophys. Res. Letters* **37**, L24604, doi:1029/2010GL0441164, 2010
Mencuccini M *Plant, Cell Environ.* **26,** 163, 2003
Nikinmaa E et al. *Plant, Cell Environ.* (in press) 2012
Putkinen A et al. *Frontiers in Terrestrial Microbiology* **3,** 15, 2011.
Salleo S et al. *New Phytol.* **132,** 47, 1996.
Sperry JS *Agric. Forest Meteorol*. **104,** 13, 2000.
Vesala et al. *Annals of Botany* **91**, 419, 2003.
Vesala et al. *Transport.* in: *Boreal Forest and Climate Change,* Eds. Hari H and Kulmala L. Springer, 2008.
Vesala T et al. *Eddy Covariance Measurements over Lakes*, in: *Eddy Covariance*, Eds. Aubinet M et al., Springer 2012.
Vogels GD et al. *Biogeohemistry of methane production*, in: *Biology of anaerobic microorganisms*, Ed. Zehnder AJB, Wiley, New York, 1988.
Wania R et al. *Geosci. Model Dev*. **3,** 565, 2010.
Zimmermann MH *Xylem structure and the ascent of sap.* Springer, New York, 1983.
Zwieniecki MA, Holbrook NM *Trends in Plant Science* **14**, 530, 2009.

SEASONAL VARIATION IN SCOTS PINE MONOTERPENE EMISSION POTENTIAL - INSIGHTS FROM THREE YEARS OF FIELD MEASUREMENTS

J. AALTO[1], J. BÄCK[2,3], H. AALTONEN[3], P. KOLARI[3], M. KAJOS[2], J. LEVULA[1] AND M. KULMALA[2]

[1]Hyytiälä Forestry Field Station, University of Helsinki, Juupajoki, Finland
[2]Department of Physics, University of Helsinki, Helsinki, Finland
[3]Department of Forest Sciences, University of Helsinki, Helsinki, Finland

INTRODUCTION

Estimates of biogenic volatile organic compound (BVOC) emissions are needed for atmospheric chemistry and climate change models. The majority of the BVOC emissions originate from plant biomass, especially from green leaves. Estimates of the BVOC emissions from the leaves are traditionally obtained for mature leaves or shoots under standard (steady-state) conditions to yield standard emission potentials (Guenther approach, G93, see e.g. Guenther *et al.* 1993, 1997), which then are used as model parameters for emission rates along the growing season. Temperature is the only driver for emissions of monoterpenes in the base model. However, in addition to the temperature-dependent volatility and the resulting emission rate, seasonality can also have an influence the monoterpene emission potentials due to changes in inherent biological processes involved in biosynthesis of the compounds (see critics to emission potential, Niinemets *et al.* 2010). The seasonal variations in emission potentials are not implemented in the G93 model approach, partially due to the lack of long term monitoring of emissions under natural conditions. Therefore we set up to study the temporal variability of the emission potential and the temperature dependency of the potential with high-resolution field data of Scots pine monoterpene emissions.

METHODS

We measured the monoterpene emission rates from mature Scots pine (*Pinus sylvestris* L.) shoots using fast online VOC analyzer (proton transfer reaction-mass spectrometer, model PTR-QMS high sensitivity, Ionicon Analytik G.m.b.H., Austria) coupled with a gas-exchange monitoring system based on dynamic chamber enclosures (Kolari *et al.* 2012). The measurements were conducted during years 2009, 2010 and 2011 at SMEAR II station, Hyytiälä, Finland. The shoot chambers had typically 32 measurement points (=closures) per day.

The description of the temperature based emission rate (G93) for monoterpenes is

$$E = E_{30}e^{\beta(T-T_{30})} \tag{1}$$

Where E is the monoterpene emission rate (ng g^{-1} s^{-1}), E_{30} is the steady-state emission rate under standard condition (T=30 °C), T is prevailing temperature (°C) and T_{30} is the standard condition temperature. The parameter β (°C^{-1}) describes the temperature dependence of the monoterpene evaporation from the monoterpene reserves, and it is based on the compound volatility as described in Henry's law (Copolovici

& Niinemets 2005). However, since the monoterpene emissions from Scots pine are partially light-dependent and originate also from recent assimilates (Shao *et al* 2001, Ghirardo *et al.* 2010), β includes also the effect of varying enzyme activity on de novo synthesis of monoterpenes (Niinemets *et al.* 2010). Although there clearly is variation in temperature dependency of monoterpene emissions (e.g. Tarvainen *et al.* 2005), in this calculation we used the constant, commonly used temperature dependency value, 0.09 °C^{-1} (e.g. Guenther *et al.* 1993.).

RESULTS AND DISCUSSION

Our data from three years (Figure 1) confirms the previously reported large variations in emission potentials of Scots pine over the seasons (e.g. Tarvainen *et al* 2005), but it also shows interesting, highly dynamic features that require further analyses. High maximum momentary monoterpene emission potentials (peaks up to 2-3 µg g(DW)$^{-1}$ h^{-1}) were seen in early spring, before the onset of shoot photosynthetic activity. The 10-day average emission potentials over the whole measurement period varied between 0.003 and 1µg g(DW)$^{-1}$ h^{-1}.
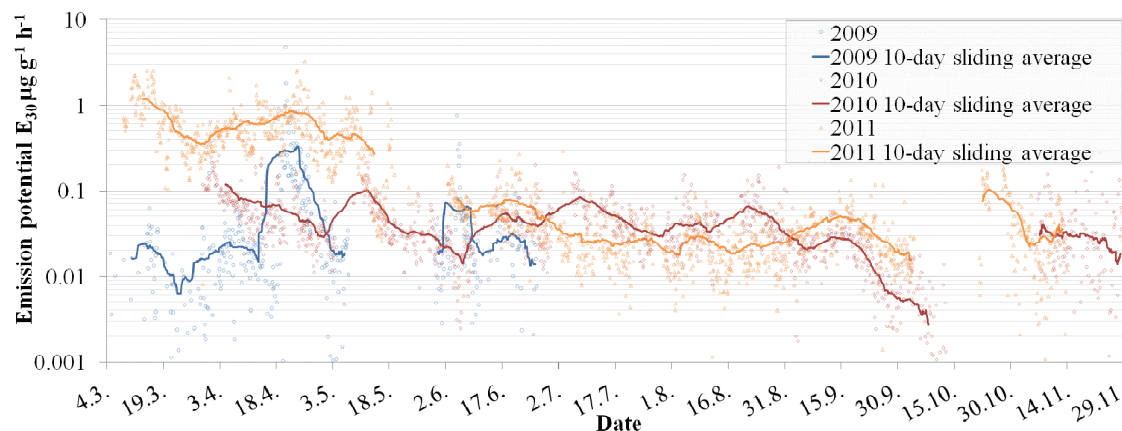
Figure 1. Scots pine monoterpene emission potential (µg g^{-1}(DW) h^{-1}) as momentary values (individual points) and 10-day sliding averages (lines).

There seems to be four distinct periods, differing in monoterpene emission potential over the year:

i) **Spring and early summer** are characterized by an order of magnitude variation in monoterpene emission potential. Variations exist both within and between years. The typical ambient conditions of this stage are characterized by large variations between daily maximum, minimum and mean temperature, increasing solar radiation intensity, and snow melt. The springtime recovery of photosynthetic apparatus coincides with this period so that at the end of this stage the photosynthesis is fully recovered.

ii) In **mid-summer** period, between early June and mid September, the emission potential is rather constant, but clearly lower than in springtime. The fairly constant emission potential is in line with the ambient conditions during high and late summer: the fluctuations in temperature within and between days and the changes in light conditions are not as drastic as during spring months.

iii) During **early autumn** (September) the monoterpene emission potential declines, together with the slowly cooling ambient temperatures and declining solar radiation intensity and

duration. However, the shoot photosynthesis rates are still high, which implies decoupling of processes related to monoterpene emissions from those related to carbon assimilation.

iv) **Late autumn**, October - November the emission potential returns back to summertime values.

The widely applied G93 approach takes temperature into account only when the temperature dependence of monoterpene evaporation is described, but abundant data implies that the emission potential itself also reflects temperature-dependent variations. Our long time series and fast time resolution measurements confirm these results, and provide an insight on the dynamical processes, such as photosynthesis and monoterpene biosynthesis, which influence the monoterpene emission potential. The results suggest that if model parameterization is based on a constant monoterpene emission potential, the resulting errors in atmospheric concentrations can be large, and therefore a dynamic emission potential should be used.

REFERENCES

Copolovici, L.O. and Ü. Niinemets. (2005). Temperature dependencies of Henry's law constants and octanol/water partition coefficients for key plant volatile monoterpenoids. *Chemosphere*, 61: 1390-1400.

Ghirardo, A, Koch, K, Taipale, R, Zimmer, I, Schnitzler, J, Rinne, J (2010) Determination of de novo and pool emissions of terpenes from four common boreal/alpine trees by $^{13}CO_2$ labelling and PTR-MS analysis. *Plant, Cell and Environment*, 33: 781-792.

Guenther, A., P. Zimmerman, P. Harley, R. Monson and R. Fall. (1993) Isoprene and monoterpene emission rate variability: model evaluation and sensitivity analysis. *J. Geophys. Res.*, 98D, 12609-12617.

Guenther, A. (1997) Seasonal and spatial variations in natural volatile organic compound emissions. *Ecol. Appl.*, 7(1): 34-45.

Kolari P., Bäck J., Taipale R., Ruuskanen T.M., Kajos M.K., Rinne J., Kulmala M. & Hari P. (2012) Evaluation of accuracy in measurements of VOC emissions with dynamic chamber system. *Atmospheric Environment*, submitted.

Niinemets Ü., Monson R. K., Arneth A., Ciccioli P., Kesselmeier J., Kuhn U, Noe S.M., Peñuelas J. and Staudt M. (2010) The leaf-level emission factor of volatile isoprenoids: caveats, model algorithms, response shapes and scaling. *Biogeosciences*, 7: 1809–1832.

Shao, M., Czapiewski, K. V., Heiden, A. C., Kobel, K., Komenda, M., Koppmann, R., and Wildt, J. (2001). Volatile organic compound emissions from Scots pine: mechanisms and description by algorithms, *J. Geophys. Res.*, 106: 20483–20491.

Tarvainen V., Hakola H., Hellen H., Bäck J., Hari P. & Kulmala M. (2005). Temperature and light dependence of the VOC emissions of Scots pine. *Atmos. Chem. Phys*. 5: 6691-6718.

BELOWGROUND CONCENTRATIONS OF VOLATILE ORGANIC COMPOUNDS IN BOREAL SCOTS PINE FOREST

H. AALTONEN[1], J. BÄCK[1,2], M. PIHLATIE[2], H. HAKOLA[3], H. HELLÉN[3], T.M. RUUSKANEN[2] and J. PUMPANEN[1]

[1]Department of Forest Sciences, University of Helsinki, P.O. Box 27, FI-00014 University of Helsinki, Finland
[2]Department of Physics, University of Helsinki, P.O. Box 64, FI-00014 University of Helsinki, Finland
[3]Air Quality Laboratories, Finnish Meteorological Institute, P.O. Box 503, FI-00101 Helsinki, Finland

Keywords: VOLATILE ORGANIC COMPOUNDS, TERPENES, BOREAL FOREST, SOIL

INTRODUCTION

Volatile Organic Compounds (VOCs) constitute the largest part of hydrocarbons produced and emitted by the biosphere (Kesselmeier & Staudt, 1999; Guenther et al., 2006). Terpenoids are a diverse group of maybe the most emitted biogenic VOCs, commonly divided into three parts: isoprene, and monoterpene and sesquiterpene groups. Also oxygenated hydrocarbons, like alcohols, aldehydes, alkenes and ketones, are common in biogenic VOC emissions.

Most of VOCs are emitted by flowers, fruits and green parts of plants and they function as inter- and intraspecific messenger compounds and as repellents or attractants for insects (Kesselmeier & Staudt, 1999; Dudareva et al., 2004; Schiestl, 2010). In addition to plant shoots, also roots (Hayward et al., 2001; Smolander et al., 2006) as well as decomposing processes and soil micro-organisms (Leff & Fierer, 2008; Bäck et al., 2010) have been found to produce VOCs, but the quantities and functions of these compounds in soils are largely unknown (Tholl et al., 2006).

VOCs have significant climatic effects, since in the troposphere VOCs react with ozone, and OH and NO_3 radicals and their reaction products may condense into aerosol particles (Kulmala et al., 1998, 2004). The branch- and canopy-level VOC emissions are rather well characterized (e.g. Kesselmeier & Staudt, 1999; Schnitzler et al., 2002; Hakola et al., 2003, 2006; Ruuskanen et al., 2005), but much less is known on volatiles originating from soils. Especially understanding on the dynamics of soil processes and the roles of different soil components such as roots, rhizosphere and decomposing organisms to VOC formation is limited (Asensio et al., 2007; Leff & Fierer, 2008; Gray et al., 2010). The VOC emissions from boreal forest field layer and soil have been observed to be highest in spring and autumn (Hellén et al., 2006; Aaltonen et al., 2011), but the processes behind seasonal variation are still uncertain. However, soil temperature and humidity conditions are important for many physical and biological processes related to VOC formation in soils (Asensio et al., 2007).

Since soil originating VOCs are poorly understood, we conducted measurements of belowground VOC concentrations during three consecutive years. The purpose was to identify and quantify the VOC compounds originating from boreal forest soil at different depths, as well as to determine the spatial and temporal changes in the respective VOC concentrations.

METHODS

Field measurement

The VOC concentrations in Scots pine (Pinus sylvestris L.) forest soil were measured at SMEAR II station (61°51´N, 24°17´E, 180 m a.s.l.), located in Hyytiälä Forestry Field Station in southern Finland (Hari and Kulmala, 2005). The measurements were performed during the snow free seasons starting in the autumn of 2008 and ending at the autumn of 2011. Samples were collected from cylindrical hydrophobic gas collectors (4 cm in diameter, 12 cm long) installed belowground permanently in spring 2008. The gas collectors were made of polytetrafluoroethylene (PTFE) by sintering with pore sizes of 5–10 μm. The pores in collectors allow diffusion of gases while keeping the liquid water outside.
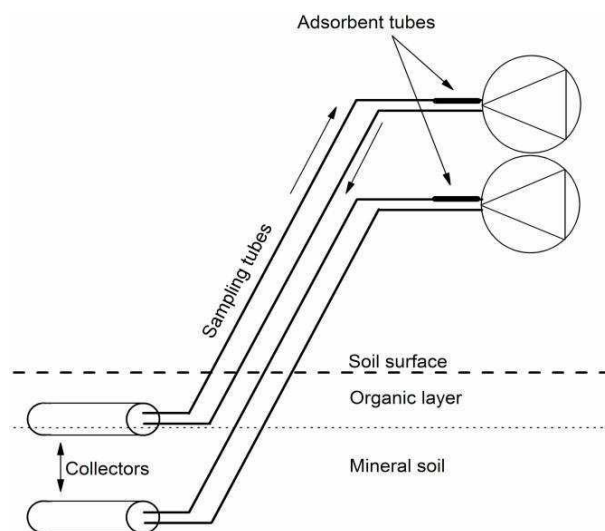
Figure 1. Measurement set-up for soil VOC concentration profiles.

Two collectors were installed at depths of 5 and 17 cm from soil surface in three places. The upper collectors were installed at the humus layer-mineral soil interface, the lower ones being completely in mineral soil (Figure 1). For sampling, two PTFE tubes (8 mm internal diameter) were connected to gas collectors. Samples were collected aboveground by circulating air from the gas collectors through Tenax–Carbopack-B adsorbent tubes at a flow rate ~100 ml min^{-1} using portable pumps. Air pumped through the adsorbent tube was returned to the collectors. Between the samplings the aboveground ends of the PTFE tubes were blocked. Each sample consisted of four 15 min sampling periods, with 15 min gaps between them. The amount of VOCs in the air volume inside the collector (~0.15 L) alone would not have been sufficient for analysis; thus, in order to get a sufficient sample volume the air samplings were prolonged to 60 min. Samplings were carried out in four 15 min periods to equilibrate the VOC concentrations between the collectors and the soil around them. During the four years, the samplings were performed 18 times in total. The samples were analysed using a gas-chromatograph with a mass selective detector. The detection limits varied from 0.04 to 0.60 ng per tube and the analytical error was ~6%, based on repeated analysis.

Laboratory test for the collector

The permeability of the gas collectors for VOCs was tested in laboratory conditions before installation to the field. The test was made for both dry and wetted collectors by using a gas mixture containing known concentrations of nine compounds (methanol, acetonitrile, acetaldehyde, acetone, isoprene, methyl vinyl ketone, 2-butanone, hexanal, and α-pinene) and proton transfer reaction-mass spectrometer (PTR-MS) for analysis (Figure 2).
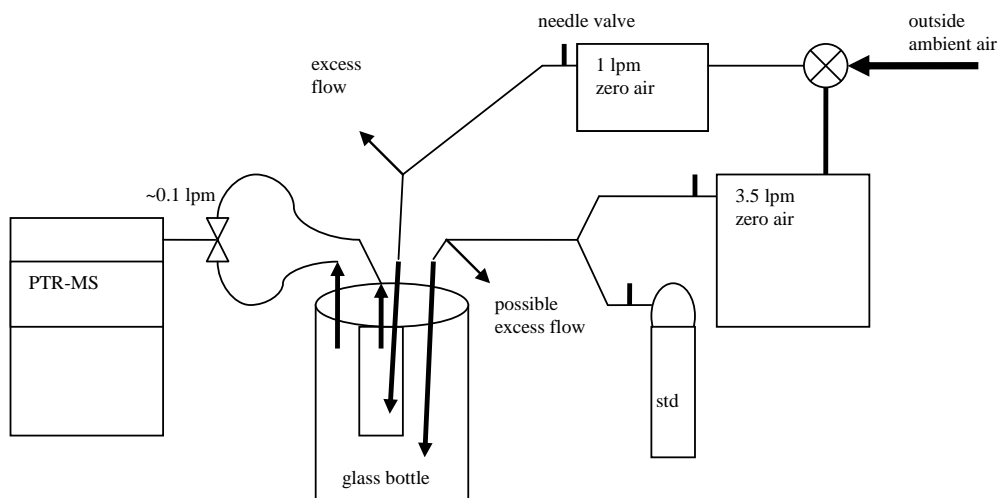
Figure 2. Set-up for the permeability tests of the sintered gas collectors.

RESULTS

Permeability test

All the compounds in the VOC standard permeate the collector easily, in order of minutes also with the wetted collector (Figure 3). α-Pinene was the heaviest compound in the gas mixture, and so was its diffusion through the wall of the collector the slowest. Methanol instead peaked immediately after introducing the gas mixture to the glass bottle, but after that it stabilised quickly.
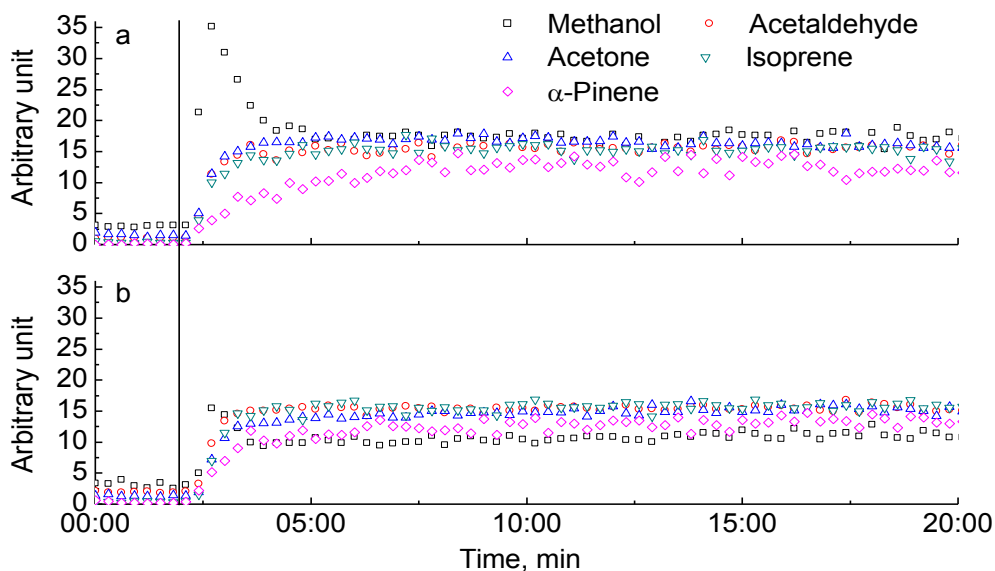
Figure 3. Results of the permeability tests with the five most relevant compounds for this study. Panel a) shows the results with dry collector and panel b) with a wetted one. Vertical line shows the time point when introduction of the VOC standard began.

Belowground VOC concentrations

We found 22 VOCs from the air in the soil layers and most of them belonged to mono- and sesquiterpene groups. Monoterpenes was the most abundant group, α-pinene, Δ3-carene and β-pinene having the highest concentrations of the single compounds. Monoterpenes constituted almost 90% of the total VOC concentration, sesquiterpenes accounting for less than 10%. The rest consisted of isoprene and oxygenated terpenoids. Monoterpenes were observed in every sampling, but sesquiterpenes and isoprene were absent in some sampling times. The average monoterpene concentration was 5200 ng m^{-3} in the organic layer and 4200 ng m^{-3} in mineral soil. Monoterpene concentrations were almost consistently higher in collectors located in the organic layer (Figure 4), while sesquiterpenes were always found in the lower collector in higher concentrations. Sesquiterpene concentration was on average 260 ng m^{-3} in the organic layer and 770 ng m^{-3} in mineral soil. The belowground concentrations of isoprene were low, only 31 and 14 ng m^{-3} in organic and mineral layer, respectively.
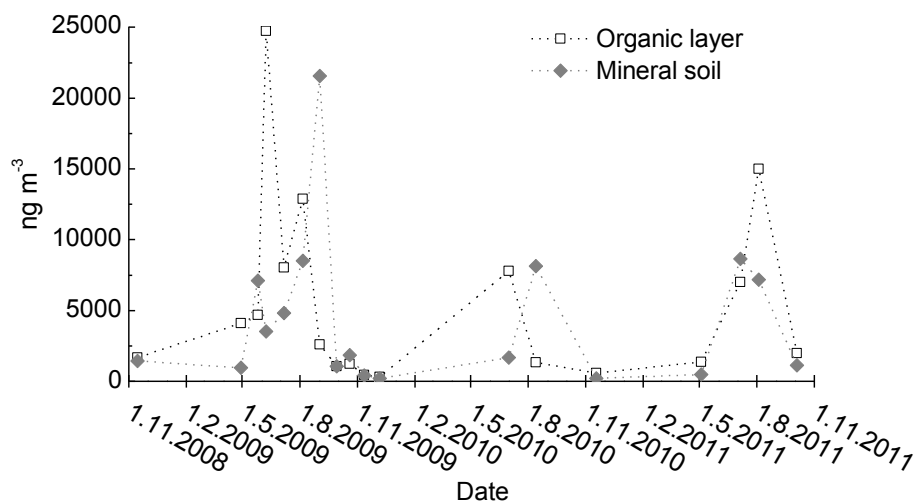
Figure 4. Belowground monoterpene concentrations in both depths (-5 and -17 cm) during the whole measurement period from autumn of 2008 to autumn of 2011. Dashed lines are just for guiding eyes.

The spatial variation in terpenoid concentrations between the three sampling places was substantial, even though the locations were chosen in order to minimize variations. The highest monoterpene concentrations were more than twofold the lowest in both depths. Sesquiterpene concentrations in the organic layer collectors were very similar, but in mineral soil the difference was again large. Also the ratio between terpenoid concentration in organic and in mineral soil layers changed between places. The average ratio between mineral soil and organic layer varied in monoterpenes between 0.60 and 0.82, and in sesquiterpenes between 1.3 and 3.6, respectively. The seasonal variations in belowground terpenoid concentrations were not as clear as those observed with terpenoid fluxes from forest floor (Hellén et al, 2006; Aaltonen et al., 2011). Monoterpene concentrations were generally higher in late summer/early autumn in the collectors in organic layer, while in mineral soil the concentrations peaked slightly later. However, with sesquiterpenes no seasonal trend was observable.

DISCUSSION AND CONCLUSIONS

The long-term measurements indicated noteworthy concentrations of terpenoids belowground. Especially the monoterpene concentrations in organic layer were high, in the same order of magnitude as observed inside snowpack during winter (Aaltonen et al., 2012). Sources of the forest floor/soil VOCs can differ depending on compound and/or soil layer. The decomposing litter has been assumed as being the main source for VOCs in the ground layer (Hayward et al., 2001; Hellén et al., 2006; Leff & Fierer, 2008; Gray

et al., 2010), and both decomposers and decomposing material can influence the VOC formation in the organic soil and decaying plant material. Another important source of belowground VOCs is roots (Smolander et al., 2006), and for compounds found deeper in soil, such as sesquiterpenes, roots are indeed a more feasible source.

A concentration peak in monoterpenes was measured in autumn; however this was missing with the other terpenoids. The forest at SMEAR II station is dominated by Scots pine, which drops the oldest age class of needles in autumn. The storages of monoterpenes in conifer needles are released during the decomposition. Thus the autumn peak in belowground monoterpene concentrations was most probably at least partly caused by decomposition of recently fallen needles. Also the delayed peak concentrations of monoterpenes in mineral soil compared to those in organic soil support theory of a source more distant from the deeper collectors. In addition to seasonal variation, also spatial variation in terpenoid concentrations was substantial, even though the forest at the site was fairly homogenous. This reflects the spatial heterogeneity in soil structure as well as processes observed also in many other measurements, and underlines the importance of sufficient numbers of samples.

Since these measurements showed such high terpenoid concentrations in soil layers, the next step is to study formation processes of these VOCs more carefully, applying also laboratory tests.

ACKNOWLEDGEMENTS

REFERENCES

Aaltonen, H., Pumpanen, J., Pihlatie, M., Hakola, H., Hellén, H., Kulmala, L., Vesala, T. and Bäck, J. (2011). Boreal pine forest floor biogenic volatile organic compound emissions peak in early summer and autumn. Agr. Forest Meteorol., 151: 682–691.

Aaltonen, H., Pumpanen, J., Hakola, H., Vesala, T., Rasmus, S. and Bäck, J. (2012). Snowpack concentrations and estimated fluxes of volatile organic compounds in a boreal forest. Biogeosciences, 9: 2033–2044.

Asensio, D., Peñuelas, J., Filella, I. and Llusià, J. (2007). Online screening of soil VOCs exchange responses to moisture, temperature and root presence. Plant Soil, 291: 249–261.

Bäck, J., Aaltonen, H., Hellén, H., Kajos, M.K., Patokoski, J., Taipale, R., Pumpanen J. and Heinonsalo, J. (2010). Variable emissions of microbial volatile organic compounds (MVOCs) from root-associated fungi isolated from Scots pine. Atmos. Environ., 44: 3651–3659.

Dudareva, N., Pichersky, E. and Gershenzon, J. (2004). Biochemistry of plant volatiles. Plant Physiol., 135: 1893–1902.

Gray, C.M., Monson, R.K. and Fierer, N. (2010). Emissions of volatile organic compounds during the decomposition of plant litter. J. Geophys. Res., 115, G03015, doi:10.1029/2010JG001291.

Guenther, A., Karl, T., Harley, P., Wiedinmyer, C., Palmer, P.I. and Geron, C. (2006). Estimates of global terrestrial isoprene emissions using MEGAN. Atmos. Chem. Phys., 6: 3181–3210.

Hakola, H., Tarvainen, V., Laurila, T., Hiltunen, V., Hellén, H. and Keronen, P. (2003). Seasonal variation of VOC concentrations above a boreal coniferous forest. Atmos. Environ., 37: 1623–1634.

Hakola, H., Tarvainen, V., Bäck, J., Ranta, H., Bonn, B., Rinne, J., and Kulmala, M. (2006). Seasonal variation of mono- and sesquiterpene emission rates of Scots pine. Biogeosciences, 3: 93–101.

Hari, P. and Kulmala, M. (2005). Station for Measuring Ecosystem-Atmosphere relations (SMEAR II). Boreal Environ. Res., 10: 315–322.

Hayward, S., Muncey, R.J., James, A.E., Halsall, C.J. and Hewitt, C.N. (2001). Monoterpene emissions from soil in a Sitka spruce forest. Atmos. Environ., 35: 4081–4087.

Hellén, H., Hakola, H., Pystynen, K.H., Rinne, J. and Haapanala, S. (2006). C_2-C_{10} hydrocarbon emissions from a boreal wetland and forest floor. Biogeosciences, 3: 167–174.

Kesselmeier, J. and Staudt, M. (1999). Biogenic Volatile Organic Compounds (VOC): An overview on emission, physiology and ecology. J. Atmos. Chem., 33: 23–88.

Kulmala, M., Toivonen, A., Mäkelä, J.M. and Laaksonen, A. (1998). Analysis of the growth of nucleation mode particles observed in Boreal forest. Tellus 50B: 449–462.

Kulmala, M., Suni, T., Lehtinen, K.E.J., Dal Maso, M., Boy, M., Reissell, A., Rannik, Ü, Aalto, P., Keronen, P., Hakola, H., Bäck, J., Hoffmann, T., Vesala, T. and Hari, P. (2004). A new feedback mechanism linking forests, aerosols, and climate. Atmos. Chem. Phys., 4: 557–562.

Leff, J.W. and Fierer, N. (2008). Volatile organic compound (VOC) emissions from soil and litter samples. Soil Biol. Biochem., 40: 1629–1636.

Ruuskanen, T.M., Kolari, P., Bäck, J., Kulmala, M., Rinne, J., Hakola, H., Taipale, R., Raivonen, M., Altimir, N. and Hari, P. (2005). On-line field measurements of monoterpene emissions from Scots pine by proton-transfer-reaction mass spectrometry. Boreal Environ. Res., 10: 553–567.

Schiestl, F.P. (2010). The evolution of floral scent and insect chemical communication. Ecol. Lett., 13: 643–656.

Schnitzler, J.-P., Bauknecht, N., Brüggemann, N., Einig, W., Forkel, R., Hampp, R., Heiden, A.C., Heizmann, U., Hoffmann, T., Holzke, C., Jaeger, L., Klauer, M., Komenda, M., Koppmann, R., Kreuzwieser, J., Mayer, H., Rennenberg, H., Smiatek, G., Steinbrecher, R., Wildt, J. and Zimmer, W. (2002). Emission of biogenic volatile organic compounds: an overview of field, laboratory and modeling studies performed during the 'Tropospheric research program' (TFS) 1997–2000. J. Atmos. Chem., 42: 159–177.

Smolander, A., Ketola, R.A., Kotiaho, T., Kanerva, S., Suominen, K. and Kitunen, V. (2006). Volatile monoterpenes in soil atmosphere under birch and conifers: Effects on soil N transformations. Soil Biol. Biochem., 38: 3436–3442.

Tholl, D., Boland, W., Hansel, A., Loreto, F., Röse, U.S.R. and Schnitzler, J.-P. (2006). Practical approaches to plant volatile analysis. Plant J., 45: 540–560.

NON-RADIOACTIVE IONIZATION METHODS AS ALTERNATIVES FOR ^{241}Am IN CI-APi-TOF

A. ADAMOV[1], and M. SIPILÄ[1]

[1]University of Helskinki, Department of Physics, P.O. Box 64, 00014, Helskinki, Finland

Keywords: chemical ionization, mass spectrometry, APi-TOF.

INTRODUCTION

Reported recently (Jokinen et al. (2012)), a nitrate ion based chemical ionization with atmospheric time-of-flight mass spectrometer (CI-APi-TOF) is a reliable and sensitive tool for sulfuric acid and neutral cluster detection. Primary ions in the CI-APi-TOF are produced by collisions between nitric acid containing clean air and alpha particles, which are generated by radioactive material (10 MBq ^{241}Am). ^{241}Am based ion source has excellent stability and requires no power for maintaining of the ion generation. However, transportation and using ^{241}Am material need special permission and often impossible due to local safety regulations. This work presents two non-radioactive alternatives for existing CI-APi-TOF instrument: corona discharge chemical ionization, and soft X-ray chemical ionization.

METHODS

Corona discharge atmospheric pressure chemical ionization (CD-APCI) is widely used non-radioactive alternative to radioactive atmospheric pressure chemical ionization (R-APCI)(Gross (2004)). When R-APCI produces positive and negative ions simultaneously, the CD-APCI has separate positive and negative modes, depending on corona needle polarity. Formation of the negative analyte ions in negative CD-APCI is analogous to ^{63}Ni or ^{241}Am based R-APCI. Replacing R-APCI by CD-APCI has been reported for similar chemical ionization mass spectrometer (CIMS)(Kürten et al. (2011)) and its application for H_2SO_4 measurements was found favorable over traditionally used for that applications R-APCI.

Soft X-ray is another alternative ion source, which can replace R-APCI in CI-APi-TOF set-up. A soft X-ray source with energy less then 9.5 keV can produce high concentrations of bipolar ions. Thus, X-ray ionize air molecules creating equal amount of positive and negative charges. And the ionization process is similar to ^{85}Kr, ^{210}Po and ^{241}Am R-APCI.

In order to confirm usage of the suggested alternative ionization methods, two version of CI-inlet set-up for CI-APi-TOF (described in details by Jokinen et al. (2012)) were build for this study. Modifications were done only to ionization part on CI-inlet. Figure 1 shows schematic diagram of both versions. ^{241}Am foil was replaced: by corona needle tip and by X-ray beam. The position of the corona tip and the X-ray beam were inside the gap between to concentric electrodes, where ^{241}Am foil was placed in original CI-APi-TOF. Also, required for corona needle and X-ray tube additional HV power supplies were installed on CI-APi-TOF set-up.

CONCLUSIONS

Two non-radioactive ionization alternatives to ^{241}Am were suggested for CI-APi-TOF. Corona discharge chemical ionization and soft X-ray chemical ionization sources were build and tested.
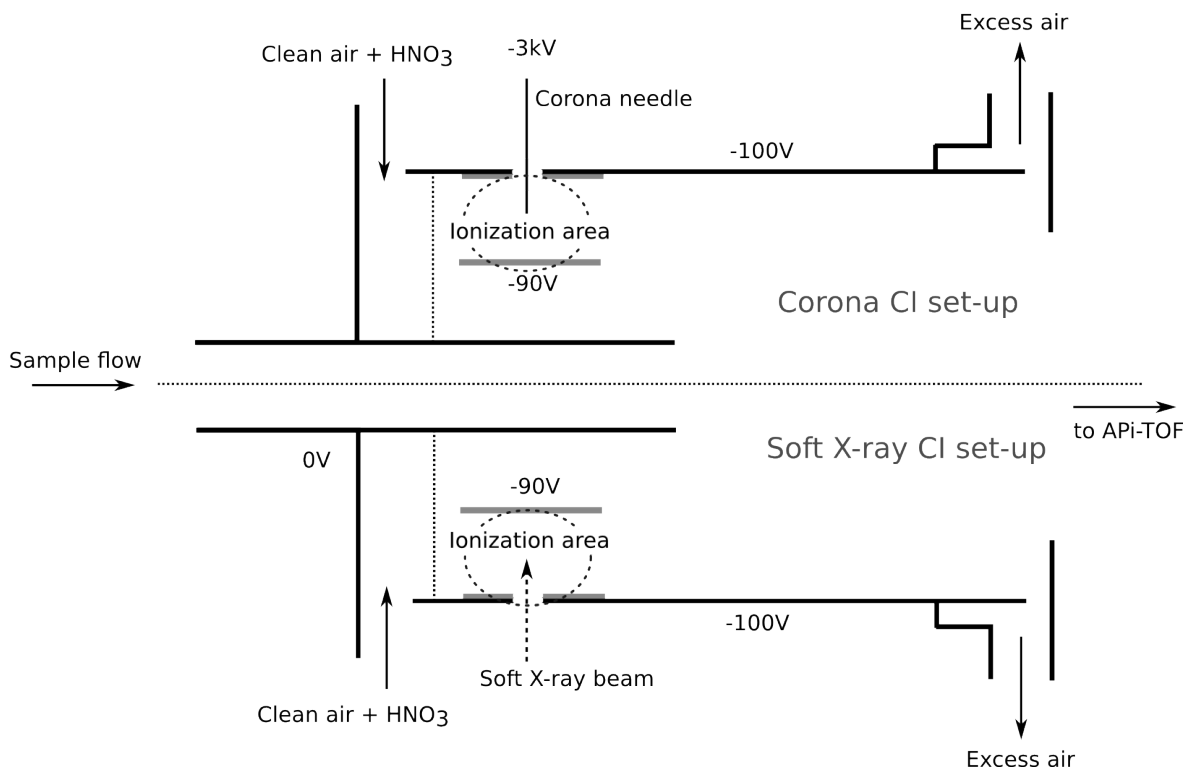
Figure 1: Corona CI-inlet set-up (above doted line) and soft X-ray CI-inlet set-up (below doted line).

REFERENCES

Gross, J. (2004). *Mass Spectrometry: A Textbook*. Springer.

Jokinen, T., Sipilä, M., Junninen, H., Ehn, M., Lönn, G., Hakala, J., Petäjä, T., Mauldin III, R. L., Kulmala, M., and Worsnop, D. R. (2012). Atmospheric sulphuric acid and neutral cluster measurements using ci-api-tof. *Atmospheric Chemistry and Physics*, 12(9):4117–4125.

Kürten, A., Rondo, L., Ehrhart, S., and Curtius, J. (2011). Performance of a corona ion source for measurement of sulfuric acid by chemical ionization mass spectrometry. *Atmospheric Measurement Techniques*, 4(3):437–443.

CLOUD DROPLET PROPERTIES FROM PUIJO MEASUREMENT STATION

I. AHMAD[1], H. PORTIN[1,2], M. KOMPPULA[2], J. JOUTSENSAARI[1], and S. ROMAKKANIEMI[1]

[1]Department of Applied Physics, University of Eastern Finland (Kuopio).
[2]Finnish Meteorological Institute, Kuopio Unit (Finland).

INTRODUCTION

The radiative properties of boundary layer stratus and stratocumulus clouds are dependent on their geometrical thickness (and liquid water profile), number of cloud droplets (N_d), effective cloud droplet size and the shape of cloud droplet size distribution. Geometrical thickness and vertical profile for liquid water content are mainly determined by the meteorology. Cloud droplet number concentration depends on aerosol particle size distribution, chemical composition, temperature, and on the updraft velocity at the cloud base (McFiggans *et al.*, 2006). According to Twomy (1977) for a given Liquid Water Content (LWC) the increase in Cloud Condensation Nuclei (CCN) results in decrease of cloud droplet size which increases the reflection of solar radiation back to space (First indirect effect (1st AIE)). The shape of cloud droplet size distribution can be described for example by the width or standard deviation σ (sigma – standard deviation of droplet diameter about mean diameter) of droplet size distribution. In several previous studies it has been shown that the width is dependent on the number of cloud droplet and also the number concentration of cloud condensation nuclei so that with air masses having marine or continental origin will have different cloud droplet properties. Thus for determination of 1st IAE and 2nd IAE (Albrecht, 1989), it is not enough to know N_d only but also information about cloud droplet size distribution is needed.

There exist several studies where cloud droplet properties are reported (see e.g. Miles *et al.*, 2000). However, usually many in situ measurements are conducted with aircraft flights providing thus only limited amount of data. Also, compared to ground based measurements, the high speed of flying aircraft might cause some averaging effect of properties measured. The aerodynamic of air flow around cloud droplet probes mounted on aircrafts could also affect the measurement. Thus the long term observations reported from ground based measurement stations are needed.

METHODS

In this work we have studied boundary layer clouds (Stratus/Stratocumulus) observed at Puijo measurement station (62º54'34" N, 27º39'19" E), in Kuopio (Finland). At the station cloud properties are measured using Cloud Droplet Probe (CDP) and aerosol properties by Differential Mobility Particle Sizer (DPMS) (Leskinen *et al*, 2009, Portin *et al*, 2009). Puijo tower has been found to be a good place for the observation of aerosol-cloud interactions as cloud events can be observed approximately during 15% of the days with different origin of air masses coming from very clean areas in the North and more polluted areas in the South.

Altogether, we will study the aerosol and cloud droplet size distribution data collected between the years 2005 and 2012. We will analyze dependence of cloud droplet size distribution parameters on the aerosol size distribution and origin of air masses, and meteorological parameters like rain intensity. We will study the effect of averaging time and wind speed to get an idea how much artificial widening can take place

because of spatial/temporal averaging. In this abstract we show a subset of the data with preliminary results.

<div align="center">RESULTS</div>

In this abstract we present results from the observations made in 2007. CDP gives droplet concentration in 30 different bins ranging from $3-50$ micron in diameter, and from the size distribution data we are able to calculate averages of total number concentration (263 cm^{-3}), liquid water content (0.046 g/m^3), standard deviation (2.78µm), and mean diameter (6 µm). The values of LWC, σ and mean droplet size are small as Puijo station is most of the time close to the base of the cloud. Usually these values increase as a function of altitude in the cloud as boundary layer clouds usually have close to adiabatic vertical profiles, while number concentration can be assumed to be constant.

In Figures 1 and 2 the standard deviation about the mean diameter and dispersion (σ/diameter) are presented as a function of cloud droplet number concentration for two different averaging times. Like expected, increase in the averaging time decreases the scatter. For example the cases with very low sigma are removed due to averaging. These could be cases where measured cloud droplets are just activated and these have not had time for mixing with other air parcels.
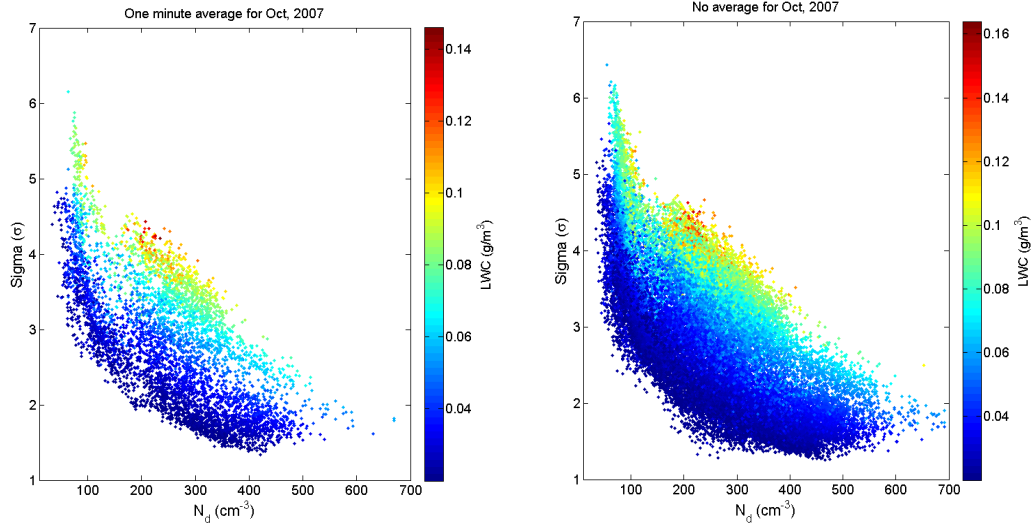
Figure 1: Standard deviation about mean diameter (σ) against droplet number concentration (N_d) measurement based on October 2007 (one minute average on the left and 10s average on the right) data from cloud droplet probe (CDP). Colorbar shows liquid water content.
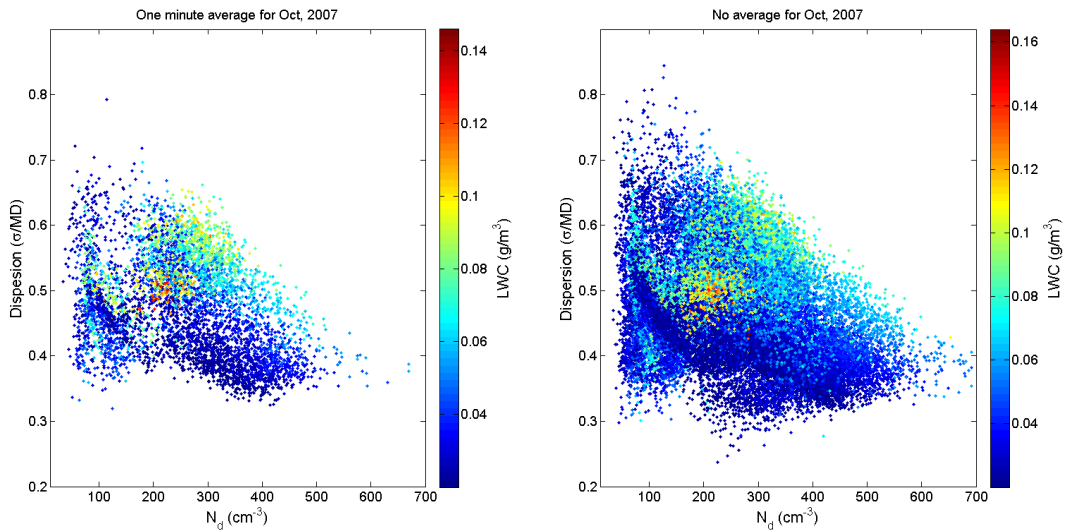
Figure 2: Dispersion (σ/ MD) vs. cloud droplet number concentration (N_d) measurement based on October 2007. One minute average is shown on the left and 10s average on the right. Colorbar shows liquid water content.
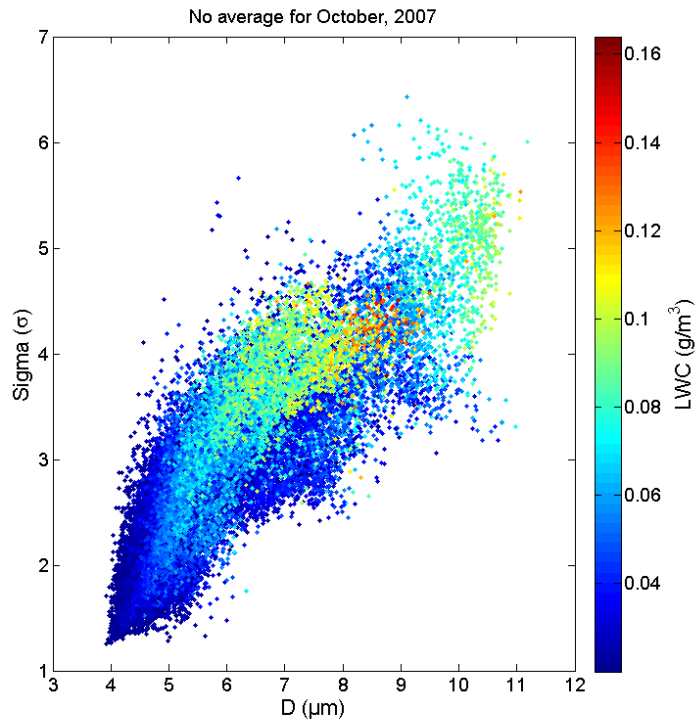
Figure 3: σ vs. mean diameter, for 12 second data over October 2007.

In Figure 3 the standard deviation is presented as a function of mean diameter, and here clearly distinct datasets can be seen. The reason for these is large particles present in the cloud droplet distribution increasing the liquid water content.

Overall, the values observed here agree well with those presented in other studies (see e.g. Miles *et al.,* 2000, Hudson *et al.,* 2012). We will continue the study by extending it to longer time period, and we will

divide the data according to air mass origin. We will also give special emphasis to time periods when we have measurement campaigns of aerosol-cloud interactions with CCN- measurements of aerosols available. The effect of temporal averaging on σ will also be the part of our future analysis, as it is expected to be changing with temporal averaging.

REFERENCES

Albrecht, B. A., Aerosols, Cloud Microphysics, and Fractional Cloudiness. *Science,* 245, 1227–1230, 1989.

Hudson, J. G., Noble, S., and V. Jha., Cloud droplet spectral width relationship to CCN spectra and vertical velocity, *J. of Geophy. Res*, vol. 117, D11211, doi:10.1029/2012JD017546,2012.

Leskinen, A., H., Portin, M. Komppula, P., Miettinen, A. Arola, H., Lihavainen, J. Hataka, A., Laaksonen, and K. E. J., Lehtinen., Overview of the research activities and results at the Puijo semi-urban measurement station, *Boreal Env. Res.,* 14, 576-590, 2009

McFiggans, G., P. Artaxo, U. Baltensperger, H., Coe, M. C. Facchini, G., Feingold, S. Fuzzi, M. Gysel, A. Laaksonen, U. Lohmann, T. F. Mentel, D. M. Murphy, C. D., O'Dowd, J. R. Snider, and E. Weingartner., The effect of physical and chemical aerosol properties on warm cloud droplet activation, *Atmos. Chem. Phys.,* 6, 2593–2649, doi:10.5194/acp-6-2593-2006.

Miles, N. L., Verlinde, J. and E. E., Clothiaux., Cloud droplet size distributions in low-level stratiform clouds. *J. Atmos. Sci.,* 57, 295-311, 2000.

Portin, J. H., M. Komppula, A.P. Leskinen, S. Romakkaniemi, A. Laaksonen, and K. E. J. Lehtinen., Overview of the aerosol-cloud interaction at the Puijo semi-urban measurement station, *Boreal Env. Res.,* 14: 641-653, 2009.

ARCTIC OCEAN WATER A SOURCE OF LIGHT ABSORBING PARTICLES TO THE ATMOSPHERE

F.R. ALEXANDER[1], J.O. NATHAN[2] and D.H. CHAPMAN[2]

J. STRÖM[1], J. ZÁBORI[1], R. KREJCI[1], A. M. L. EKMAN[2,4], P. TUNVED[1], and M. HANSSON[3]

[1]Department of Applied Environmental Science, Stockholm University, Sweden

[2]Department of Meteorology, Stockholm University, Sweden

[3]Department of Physical Geography and Quaternary Geology, Stockholm University, Sweden

[4)] Bert Bolin Centre for Climate Research, Stockholm University, Sweden

Keywords: POLAR, BUBBLES, NY-ÅLESUND, KONGSFJORDEN.

INTRODUCTION

The world's oceans are a very large source of aerosol particles to the atmosphere, and in the marine boundary layer sea salt particles may dominate the number of cloud forming nuclei. When waves break air bubbles are formed just below the water surface. When these bubbles burst, a spray of drops is formed which will remain as an aerosol in the atmosphere. Traditionally, research around these particles is motivated by their cloud forming properties and their ability to scatter solar radiation. In this study we have investigated the bubble bursting particles with respect their ability to absorb light. Specifically, we have investigated if the water temperature may influence the emission of light absorbing particles through this formation mechanism.

METHODS

The experiments were conducted in Ny-Ålesund, Svalbard in the local Marine Laboratory facility. Three types of winter water and three types of summer water were analyzed. "Deep" water was pumped from about 80 m depth out of Kongsfjorden directly into the Marine Laboratory (both during summer and winter). "Ocean" water was sampled at Kvadehuken, at the mouth of Kongsfjorden, from the coast line during wintertime and out of the fjord from a boat during the summer campaign. In addition a summer sample was taken in the middle of the fjord and a winter sample in the inner part of the fjord. These two fjord samples are simply termed "Fjord"

Approximately 55-140 L of sample water was contained in a stainless steel tank for each experiment. Water from this tank was pumped into a plastic container of approximately 20 L. A constant water level with a volume of about 10 L was maintained by a simple overflow system. Water was introduced from a ¼" stainless steel tube about 16 cm above the water surface at a rate of about 2 to 5 L per minute. When the recycled water hit the surface, this emulated the process of aerosol particle production from breaking waves. Water temperature, oxygen saturation, and salinity were monitored continuously. Cold sample-water was warmed by the ambient room temperature. To test reproducibility, experiments where the water was cooled down from room temperature to freezing temperature were also performed. Cooling was achieved by placing the storage tank outside the laboratory, but this was only done for the winter campaign.

During the experiment a suite of instruments was used to characterize the particles produced in the plastic container. The central for this study was the measurements of the particle light absorption that was conducted using a custom built Particle Soot Absorption Photometer (PSAP) (Krecl et al., 2007). In the PSAP instrument, sample air is drawn through a glass fiber filter with cellulose baking (Pall Corporation, Tissueglass E70-2025W) creating an approximately 3 mm diameter sampling spot by light absorbing

particles. A green LED at 525 nm wavelength is illuminating the filter area over the spot as well as a reference area that is not loaded with particles. Two detectors placed on the backside of the filter are used to measure the light transmitted through the filter. The rate of change of the transmitted light is a measure of the aerosol absorption coefficient (m^{-1}). To convert to a black carbon mass concentration equivalence, a specific absorption coefficient of 5 m^2 g^{-1} was used.

RESULTS AND CONCLUSIONS

The experiment results from using different water types are superimposed in Figure 1. Each water type is illustrated by a different color of the symbol. A clear systematic temperature dependence is evident, where colder water temperatures cause more light absorbing particles to be emitted. Traditionally the oceans have been regarded as a source of light scattering aerosols, but data presented in this study indicates that there might be a significant component of light absorbing aerosols in sea spray as well. At least this is true for the different Arctic waters tested here. Both surface water and water from 80 m depth were tested, during both winter and summer conditions and in all cases the results gave evidence of the ocean as a source of light absorbing aerosols. Although calculations are highly uncertain, the estimated mass fraction (not explained here) of the light absorbing particles may be on the same scale as the non-absorbing particle mass. Based on the observed size distribution, it is expected that the bulk of the light absorbing particles are found in the accumulation mode size range and larger. The source strength of light absorbing particles presents a clear dependence on water temperature. Decreasing the temperature from 10 to 0 °C increased the amount of light absorbed by the particles emitted to the atmosphere by about a factor of three.
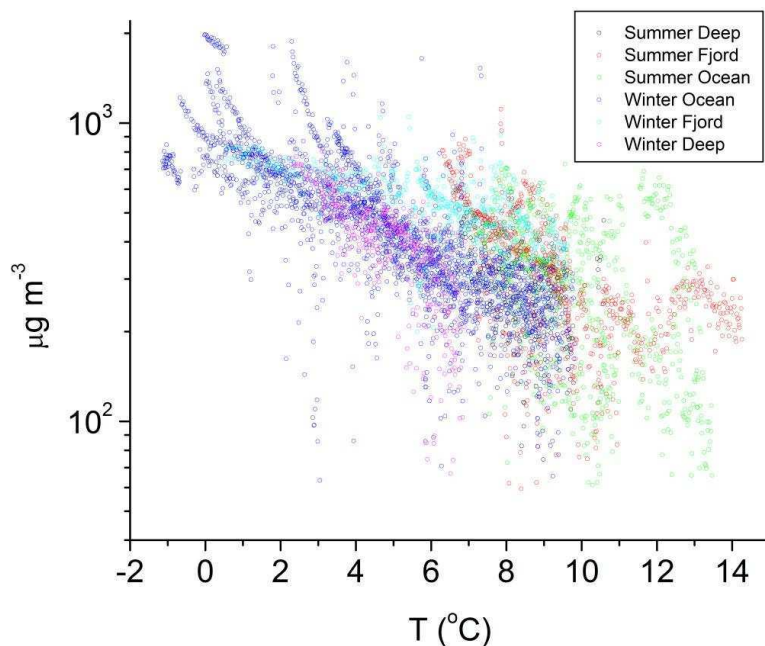
Figure 1. Mass concentrations of light absorbing particles as function of water temperature. Each data point represents a two minute average. Each color represents a different type of water.

ESTIMATING THE SURFACE ENERGY BALANCE OF BOREAL PEATLANDS

PAVEL ALEKSEYCHIK, IVAN MAMMARELLA, JANNE RINNE and TIMO VESALA

University of Helsinki, Department of Physics,
Helsinki, Finland.

INTRODUCTION

Wetlands and specifically natural peatlands represent important biomes on Earth. Besides covering a major fraction of the land surface, they contain vast amounts of organic carbon, which they have accumulated since the last glaciation era. There is a concern that the modern anthropogenic forcing can drive the climate towards warming, and the peatlands will get free of permafrost and climate constraints, emitting their carbon resources into the atmosphere. Wetlands remain undersampled and less understood compared to e.g. boreal forests, and some of their features have received little attention. Surface energy balance remains one of the most unexplored aspects in the wetland studies. The problem deserves more effort, since SEB connects such aspects as temperature, hydrology and carbon budget.

METHODS

Surface Energy Balance comprises the incoming and outgoing short- and long-wave radiation components, and in general form, it is often written as

$$R_n - G = H + LE + S, \qquad (Eq. 1)$$

where R_n is the net radiation, G the ground heat flux at the surface, H the sensible heat, LE the latent heat flux and S is the compound storage term. It can be said that the main problem is contained in finding the balance between the "available energy" ($R_n - G$) and H+LE. However, numerous complications arise when attempting to estimate SEB. On the one hand, instrumental systematic errors and uncertainties affect the measured fluxes; on the other hand, there always is a degree of incompatibility between the measurements leading to e.g. footprint mismatch, and no simple method exists for mitigation of such unwelcome effects.

AIM I: BOREAL PEATLAND RADIATION BALANCE STUDY

We intend to study SEB in several boreal peatlands, including Siikaneva (two sites of different trophicity), Loppi, Alkia and Linnansuo in Finland; Degerö Stormyr and Fajemyr in Sweden. The main points in the study are: compare the SEB closure at the said locations; determine the main controllers of the energy balance in peatlands; assess inter-and intra-site variation in SEB and the balance components; draw comparison between the boreal peatland and forest energy balance. This is a pioneering effort to present a compiled evidence of the boreal peatland energy balances.

AIM II: ASSESSMENT OF PEATLAND GROUND FLUX

The methodological problem relating to the ground flux estimation is of special importance for the case of wetlands. Just one aspect – the heat conduction in peat being a major determinant of CO_2 and CH_4 production – makes correct ground flux estimation one of the primary goals.

In wetlands, the water table depth (WTD) is probably the main determinant of the near-surface ground heat flux. Because of the high porosity and potential water content, the wetness of peat can range from near zero to near 100% (at saturation). The ground flux can be relatively easily estimated my measuring the flux at the depth z and correcting it by the storage flux at the surface in mineral soils, but the method is not completely established for wet environments such as peatlands (e.g. Kettridge and Baird, 2007). While most of the sites today are not equipped with heat plates, the direct G measurement faces complications

from hydrological and physical properties of peat. Correspondingly, the problem of G estimation from the standard measurements (T profile, WTD, RH) presents interest.

G can be presented as the total change in storage (S) of the top soil layer, if the lower reference level is deep enough that the temperature variation in the lower horizons is negligible. In wetlands, the reference depth for peatlands can in most cases be taken as -50cm. Despite the existence of seemingly simple strategies for S calculation from T profile, several problems remain unsolved: (a) thermal convection/advection by liquid and gaseous water in soil; (b) variation in thermal properties of peat caused by changes in water content.

Thus, we aim at constructing the most beneficial method for G estimation from standard measurements and examining the importance of (a,b).

RESULTS

Already the first results suggest importance of the thermal properties variation in peat. Thermal diffusivity, calculated from the time lag between the temperature series at different depths, exhibits correlation with the water table depth. Despite the scatter, two major periods are readily seen – high diffusivity at high water level, and low diffusivity at low water level. Since the linear relation between the heat capacity and thermal conductivity of poorly decomposed peat (Kettridge and Baird, 2007) implies constant thermal diffusivity, our observation suggests the change in the slope of that regression, probably due to the moisture content fluctuations related to water level.
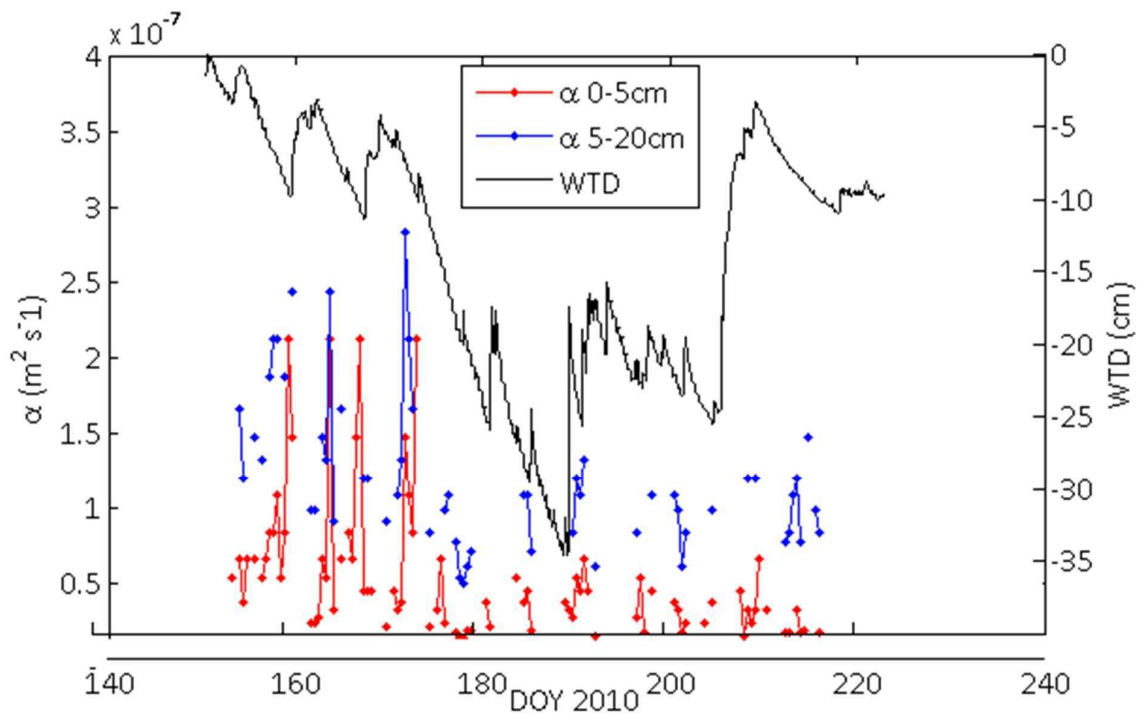
Figure 1. Thermal diffusivity (α) in two peat layers and the water table depth series, Siikaneva-1 site, summer 2010. A is smaller in the shallow layer than in the deeper layer, which can be explained by the bigger water content and higher degree of decomposition in the latter.

REFERENCES

N. Kettridge and A. Baird, 2007. In situ measurements of the thermal properties of anorthern peatland: Implications for peatland temperature models. *J. Geo. Res. 112,* doi:10.1029/2006JF000655.

RELATIONSHIPS BETWEEN AEROSOLS, CLOUD CONDENSATION NUCLEI AND CLOUD DROPLETS DURING THIRD PALLAS CLOUD EXPERIMENT

T. Anttila[1], D. Brus[1], A.-H. Hyvärinen[1], A. Jaatinen[2], N. Kivekäs[1], S. Romakkaniemi[2], H. Lihavainen[1]

[1] Finnish Meteorological Institute, Research and Development, Climate and Global Change, P.O. BOX 503, FI-00101 Helsinki
2 University of Eastern Finland, Kuopio Unit, Department of Physics, Finland.

INTRODUCTION

Representation of clouds in large scale models is a major source of uncertainty in climate change predictions (Forster et al., 2007). The uncertainty stems partly from the fact that global climate models have coarse spatial resolution due to the limited computing resources available, and therefore such models cannot resolve the microphysical processes involved in the cloud formation explicitly. Droplets that make up liquid phase clouds in the atmosphere are formed on aerosol particles called as cloud condensation nuclei (CCN) on air containing supersaturated water vapour. The size distribution and chemical composition of aerosols are the key properties that determine the number of CCN formed at a certain water vapour supersaturation. On the other hand, meteorological conditions influence the water vapour supersaturation levels reached in ambient clouds as well. Several microphysical parameterizations have been developed, implemented and tested in global models (Ghan et al., 2011) to tackle the problem of describing cloud formation on physical basis in large scale models. Despite these developments, further empirical and process level model studies on the relationships between aerosols, CCN and cloud microphysics are needed to increase our understanding on the climatic effects of aerosols (Ghan and Schwartz, 2007).

In this study, we focus on concurrent measurements of aerosols, CCN and cloud droplet activation that were carried out as a part of the third Pallas Cloud Experiment (PaCE-3). The campaign took place at a Pallas Global Atmospheric Watch station located in northern Finland (Hatakka et al., 2003) between September 11th and October 10th of 2009. The current study extends the work carried out during the first two PaCE campaigns (Lihavainen et al., 2008; Anttila et al., 2009; Kivekäs et al., 2009). Here we focus on comparing CDNC with various aerosol properties and CCN concentrations.

METHODS

Two differential mobility particle sizers (DMPS) were used to measure the aerosol number size distribution. Both instruments were operated as described by Komppula et al. (2005). One DMPS was attached to a so-called total air inlet, which lets in all particles including cloud droplets (but not rain drops). The cloud droplets were then evaporated, and the dry cloud condensing nuclei were measured among the non-activated particles. The other DMPS was attached to a PM 2.5 µm inlet which prevented the cloud droplets from entering the system and therefore this DMPS measured only the non-activated particles.

The Cloud Condensation Nuclei Counter (CCNC, DMT model CCN-100) was operated at a total flow rate of 0.5 lpm and at five different supersaturations (0.2, 0.4, 0.6, 0.8 and 1.0%), each set for 15 min. Data processing included skipping the first five minutes of data after changing the supersaturation to ensure that the CCNC column was operating at stable conditions. The total aerosol number concentration (CN) was measured by a condensation particle counter (CPC, TSI model 3772) connected to the same sampling line as the CCNC.

Presence of clouds on the measurement site was assessed with the approach taken in the previous study of Komppula et al. (2005). Briefly, a cloud event was judged to have taken place when the following conditions were met at least for an hour: relative humidity stayed around 100% and visibility was below 1000 meters. For further screening of the data we calculated the size distribution of activated particles (cloud residual particles) during the cloud events as described in Anttila et al. (2009). This allows for inferring the fraction of particles that activated into cloud droplets for each DMPS channel. The acquired data set was further screened according to the following criteria: no rainfall took place during the period and the fraction of activated particles was >80% at the diameter range >400 nm. As a result, the data set analyzed here consists of around 33 hours of measurements with five prominent cloud events.

RESULTS

Table 1 summarizes the key features of the considered cloud events which consist of around 33 hours of measurement data. The shortest event in duration, case B, covered only a single averaging interval while the longest case E lasted for around 11 hours and 45 minutes. The average total particle concentrations, CN_{tot}, varied from 385 to 1518 cm^{-3} between the events. Table 1 shows further that particles with dry diameters above 100 nm, $CN(>100$ nm$)$, made only a small contribution to the total number concentrations: the ratio between CN_{tot} and $CN(>100$ nm$)$ varied in the range 0.07 to 0.25, implying that Aitken mode sized particles dominated the total particle number concentrations. The average number of cloud droplets inferred from the dual-DMPS setup, CDNC, varied between 49 and 99 cm^{-3}. Such numbers are somewhat smaller than the average numbers obtained from an analysis of a longer data set from the site (Komppula et al., 2005) and are also generally smaller than observed in the previous campaign, PaCE-2 (Anttila et al., 2009).
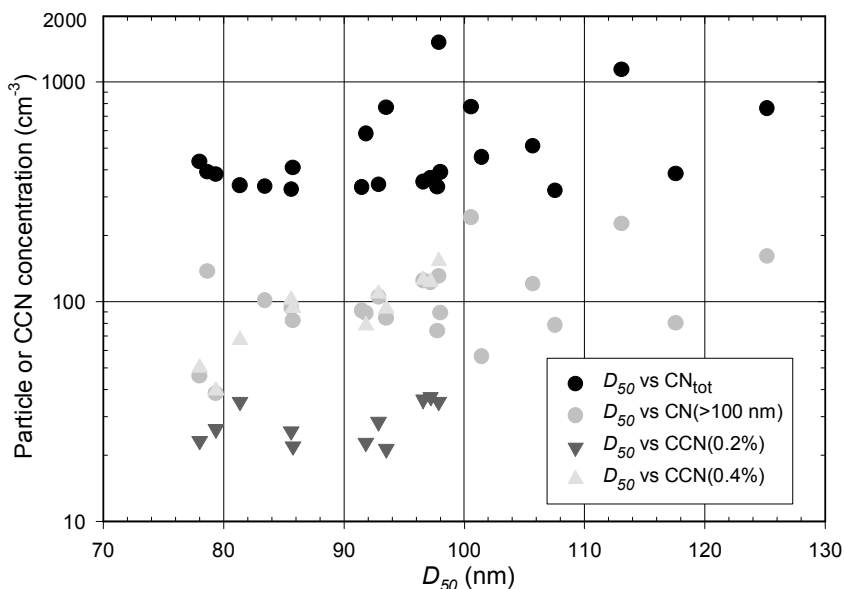
Figure 1. The diameter corresponding to 50% activation efficiency (D_{50}) versus particle and CCN concentrations (indicated in the legend).

The average value of the diameter at which 50% of the particles are activated into cloud droplets, D_{50}, varied in the range 80 to 102 nm between the cases. These numbers are slightly lower than observed in the previous campaign (Anttila et al., 2009) but compare well to those reported by Komppula et al. (2005). Figure 1 shows the correlation between D_{50} and CN_{tot} as well as between D_{50} and $CN(>100$ nm$)$. No

146

visible correlation can be seen which suggests that the observed variation in D50 was not driven by the aerosol number concentrations.

Table 1. Observed features of the analyzed cloud events. For each event, an average value of the quantity is shown followed by the value range during the event in parenthesis. Here CNtot is the total particle number concentration, CN(>100 nm) is the concentration of particles with dry sizes above 100 nm, CDNC is the inferred number of cloud droplets and D_{50} is the diameter corresponding to the 50% activation ratio. Also, measured CCN concentrations for supersaturation 0.2 and 0.4%, if available, are shown.

Case	A	B	C	D	E
Date and time	9.9. 08:00-13:45	22.9. 06:45-8:15	22.-23.9. 22:30-08:30	25.-26.9. 23:30-04:15	4.10. 01:30-12:15
CN_{tot} (cm^{-3})	531 (389-532)	1518	449 (325-768)	385 (339-434)	499 (321-1141)
CN(>100nm) (cm^{-3})	127 (56-242)	131	100 (82-125)	29 (14-46)	119 (74-226)
CDNC (cm^{-3})	93 (43-168)	97	89 (72-105)	49 (41-56)	99 (79-125)
D_{50} (nm)	101 (98-106)	98	92 (86-97)	80 (78-81)	102 (79-125)
Activated fraction	0.17 (0.09-0.22)	0.06	0.22 (0.09-0.29)	0.13 (0.11-0.17)	0.23 (0.13-0.37)
CCN(0.2%) (cm^{-3})	n/a	35	28 (21-37)	28 (23-35)	n/a
CCN(0.4%) (cm^{-3})	n/a	153	103 (78-126)	52 (39-67)	n/a

Overall, comparing the corresponding values of CN(>100 nm), CDNC and D_{50}, it can be concluded that Aitken mode particles made only a small contribution to the number of activated cloud droplets. This is further illustrated Figures 2 and 3: Figure 2 shows the correlation between CDNC and CN(>100 nm) while Figure 3 illustrates the average and overall variation of these quantities for each cloud event. Conversely, CN_{tot} and CDNC do not show any visible correlation (Figure 1) which further emphasizes the dominant role of accumulation mode particles played in the observed variation in CDNC. This finding is consistent with the previous cloud observations done at the site (Komppula et al., 2005). As also seen from Figure 2, the relationship between CDNC and CN(>100 nm) is approximately linear. This is in contrast with many other empirical data sets where sub-linear correlation between CDNC and accumulation mode sized particles is found (see e.g. Figure 5 in Lihavainen et al., 2008). As noted above, CDNC varied over a relatively small interval in the cloud cases considered here while the data set displayed in the aforementioned study covers a larger range of conditions. Also, the air masses sampled here were relatively clean while the "suppression effect", i.e. non-proportional increase in CDNC as a response to increasing aerosol concentrations, is more characteristic to polluted air masses.

CONCLUSIONS

Concurrent measurement of aerosols, cloud condensation nuclei (CCN) concentrations and cloud droplet activation were carried out as a part of the third Pallas Cloud Experiment (PaCE-3) which took place at a ground based site located on northern Finland during the autumn of 2009. Here we have focused on selected cloudy periods to investigate relationships between the aerosol properties, CCN and size resolved cloud droplet activation. The results suggest that the observed clouds were formed on the "aerosol-limited regime" where the number of CCN active particles largely determines CDNC. This is consistent with previous studies on the microphysics of clouds formed in clean air masses (e.g. Twohy et al., 2005). It should be noted, however, that the current study is based on a rather short intensive campaign where the range of atmospheric conditions encountered was limited. Therefore long term simultaneous measurements of aerosols, CCN and cloud droplet activation are desirable to investigate how the results obtained here compare to larger data sets containing results from different seasons and air mass types. As

a part of an ongoing research, the measurements observations reported here are further interpreted using modelling tools developed earlier (Anttila et al., 2009; Anttila, 2010).
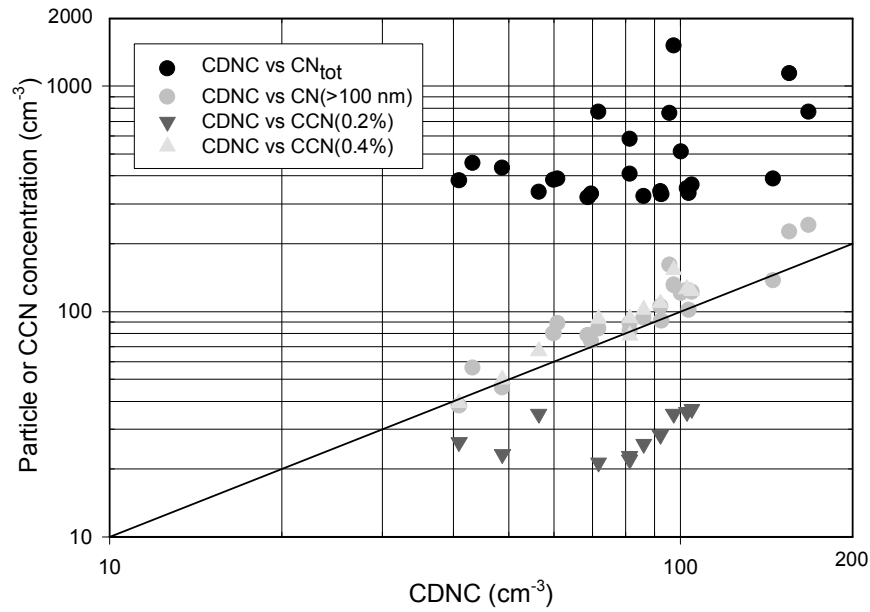
Figure 2. Cloud droplet concentration (CDNC) versus particle and CCN concentrations (indicated in the legend). A 1:1 line is included as a guide to the eye.
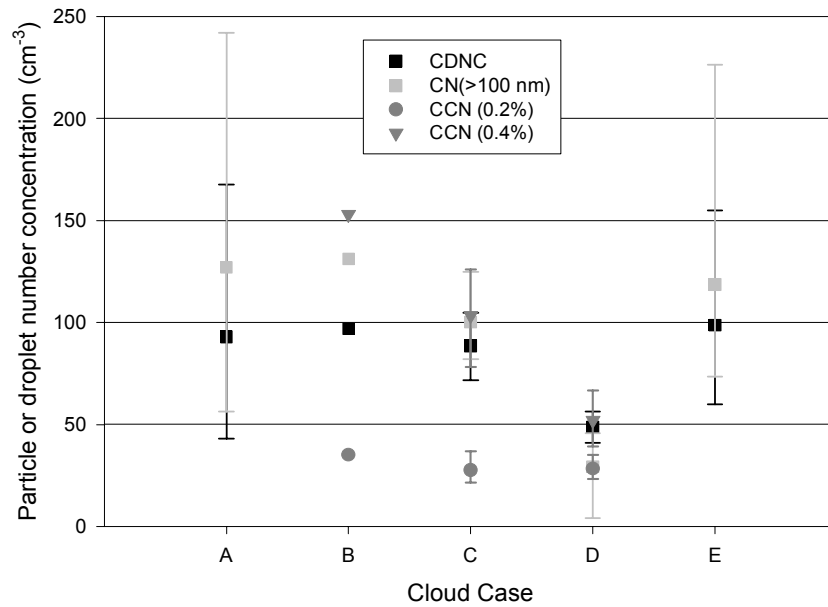
Figure 3. The comparison of the cloud droplet concentrations (CDNC), the number concentrations of particles with dry diameter above 100 nm, CN(>100 nm), and CCN concentrations at supersaturations 0.2 and 0.4% for each cloud case. Here the symbols represent average values and the bars indicate the range over which the quantity varied during the event.

ACKNOWLEDGEMENTS

REFERENCES

Anttila, T., P. Vaattovaara, M. Komppula, A.-P. Hyvärinen, H. Lihavainen, V.-M. Kerminen, and A. Laaksonen, (2009). Size-dependent activation of aerosols into cloud droplets at a subarctic background site during the second Pallas Cloud Experiment (2nd PaCE): method development and data evaluation, *Atmos. Chem. Phys.* **9**, 4841-4854, doi:10.5194/acp-9-4841-2009.

Anttila, T. (2010). Sensitivity of cloud droplet formation to the numerical treatment of the particle mixing state. *J. Geophys. Res.* **115**, D21205, doi:10.1029/2010JD013995.

Forster, P., et al. (2007). *Changes in Atmospheric Constituents and in Radiative Forcing.* In: Climate Change 2007: The Physical Science Basis. Contribution of Working Group I to the Fourth Assessment Report of the Intergovernmental Panel on Climate Change [Solomon, S., D. Qin, M. Manning, Z. Chen, M. Marquis, K.B. Averyt, M.Tignor and H.L. Miller (eds.)]. (Cambridge University Press, Cambridge, United Kingdom and New York, NY, USA,).

Ghan, S. J., and S. E. Schwartz (2007). Aerosol properties and processes – A path from field and and laboratory measurements to global climate models. *Bull. Am. Meteorol. Soc.* **88**, 1059-1083.

Ghan, S. J. et al (2011). Droplet nucleation: Physically-based parameterizations and comparative evaluation. *J. Adv. Model. Earth Syst.* **3**, M10001, doi:10.1029/2011MS000074.

Hatakka, J., et al. (2003). Overview of the atmospheric research activities and results at Pallas GAW station. *Boreal Environ. Res.* **8**, 365–384.

Kivekäs N., V.-M. Kerminen, T. Raatikainen, P. Vaattovaara, and H. Lihavainen (2009). Physical and chemical characteristics of the activating particles during the Second Pallas Cloud Experiment (Second PaCE). *Boreal. Env. Res.* **14**, 515-526.

Komppula, M., H. Lihavainen, V.-M. Kerminen, M. Kulmala, and Y. Viisanen (2005). Measurements of cloud droplet activation of aerool particles at a clean subarctic background site. *J. Geophys. Res.* **110**, D06204, doi:10.1029/2004JD005200.

Lihavainen, H. et al. (2008). Measurements of the relation between aerosol properties and microphysics and chemistry of low level liquid water clouds in Northern Finland. *Atmos. Chem. Phys.* **8**, 6925-6938, doi:10.5194/acp-8-6925-2008. '

Twohy, C. et al. (2005). Evaluation of the aerosol indirect effect in marine stratocumulus clouds: Droplet number, size, liquid water path, and radiative impact, *J. Geophys. Res.* **110**, D08203, doi:10.1029/2004JD005116.

IODINE-CONTAINING IONS IN HYYTIÄLÄ

T. ARPPE[1], H. JUNNINEN[1], T. JOKINEN[1], J. HAKALA[1], S. SCHOBESBERGER[1], G. LÖNN[1], M. SIPILÄ[1], M. KULMALA[1], D.R. WORSNOP[1,2] and T. PETÄJÄ[1]

[1]Department of Physics, University of Helsinki, Finland

[2]Aerodyne Research Inc., Billerica, MA, USA

Keywords: IODINE, BOREAL FOREST, MASS SPECTROMETRY.

INTRODUCTION

The role of iodine species in the formation of aerosols has been actively studied in recent years (O'Dowd et al., 2002a; Saiz-Lopez et al., 2012). The ions I^- and IO_3^- seem to be the inorganic iodine species to accumulate in aerosols, whereas the identity of soluble organic iodine, which is often thought to be a major fraction, is largely unknown (Vaattovaara et al., 2006). The influence of iodine on particle formation on a regional and global scale remains uncertain as most observations are from coastal locations (O'Dowd et al., 2002b; Kulmala et al., 2004). In this study, we investigate the occurrence of naturally charged iodine-containing ions in air at an inland site in Finland.

METHODS

The measurements were performed in August–October 2011 in a boreal forest area in Hyytiälä, Southern Finland in the SMEAR II station (Hari and Kulmala, 2005). The concentrations of negative ions in ambient air were monitored using an atmospheric pressure interface time-of-flight mass spectrometer APi-TOF (Junninen et al., 2010). The APi-TOF is an instrument capable of determining chemical composition of naturally charged atmospheric ions without any pre-treatment (Ehn et al., 2010). The instrument was located in a container approximately 100 m south of the main measurement mast at SMEAR II (see, e.g., Williams et al., 2011 for more details). The sample was taken from 2 m above ground level.

RESULTS

Many iodine-containing ions were observed, including I^-, IO^-, IO_2^- and IO_3^- and their water complexes. In addition, IO_3^- ion was present in the dimer $HIO_3 \cdot IO_3^-$ and acid complexes $HIO_3 \cdot NO_3^-$ and $HIO_3 \cdot HSO_4^-$.
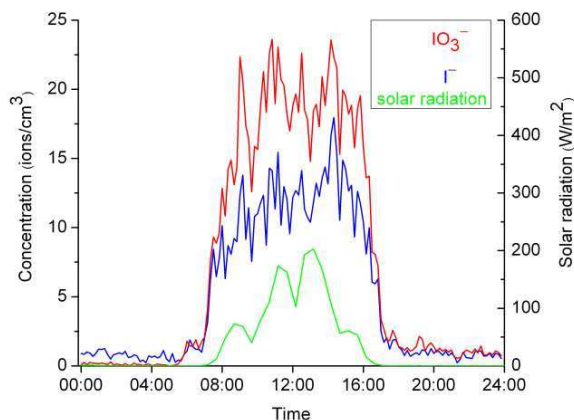
Figure 1. Concentrations of IO_3^- (uppermost curve, left scale) and I^- (middle curve, left scale) and intensity of solar radiation (lowermost curve, right scale) in Hyytiälä on 19 October 2011.

The iodate–malonic acid complex $C_3H_4O_4 \cdot IO_3^-$ was the clearest example of soluble organic iodine in these measurements. The major ionic iodine species was IO_3^-, closely followed by I^-. The diurnal cycle of IO_3^- and I^- was usually connected with solar radiation (Fig. 1). The presented preliminary results warrant a more thorough examination of the role of iodine in the particle formation in this non-marine environment.

ACKNOWLEDGEMENTS

REFERENCES

Ehn, M., H. Junninen, T. Petäjä, T. Kurtén, V.-M. Kerminen, S. Schobesberger, H.E. Manninen, I.K. Ortega, H. Vehkamäki, M. Kulmala and D.R. Worsnop (2010). Composition and temporal behavior of ambient ions in the boreal forest, Atmos. Chem. Phys. **10**, 8513–8530.

Hari, P. and M. Kulmala (2005). Station for measuring ecosystem–atmosphere relations (SMEAR II), Boreal Env. Res. **10**, 315–322.

Junninen, H., M. Ehn, T. Petäjä, L. Luosujärvi, T. Kotiaho, R. Kostiainen, U. Rohner, M. Gonin, K. Fuhrer, M. Kulmala and D.R. Worsnop (2010). A high-resolution mass spectrometer to measure atmospheric ion composition, Atmos. Meas. Tech. **3**, 1039–1053.

Kulmala, M., H. Vehkamäki, T. Petäjä, M. Dal Maso, A. Lauri, V.-M. Kerminen, W. Birmili and P.H. McMurry (2004). Formation and growth rates of ultrafine atmospheric particles: a review of observations, J. Aerosol Sci. **35**, 143–176.

O'Dowd, C.D., J.L. Jimenez, R. Bahreini, R.C. Flagan, J.H. Seinfeld, K. Hämeri, L. Pirjola, M. Kulmala, S.G. Jennings and T. Hoffmann (2002a). Marine aerosol formation from biogenic iodine emissions, Nature **417**, 632–636.

O'Dowd, C.D., K. Hämeri, J.M. Mäkelä, L. Pirjola, M. Kulmala, S.G. Jennings, H. Berresheim, H.-C. Hansson, G. de Leeuw, G.J. Kunz, A.G. Allen, C.N. Hewitt, A. Jackson, Y. Viisanen and T. Hoffmann (2002b). A dedicated study of new particle formation and fate in the coastal environment (PARFORCE): overview of objectives and achievements, J. Geophys. Res. **107**, 8108.

Saiz-Lopez, A., J.M.C. Plane, A.R. Baker, L.J. Carpenter, R. von Glasow, J.C. Gómez Martín, G. McFiggans and R.W. Saunders (2012). Atmospheric chemistry of iodine, Chem. Rev. **112**, 1773–1804.

Vaattovaara, P., P.E. Huttunen, Y.J. Yoon, J. Joutsensaari, K.E.J. Lehtinen, C.D. O'Dowd and A. Laaksonen (2006). The composition of nucleation and Aitken modes particles during coastal nucleation events: evidence for marine secondary organic contribution, Atmos. Chem. Phys. **6**, 4601–4616.

Williams, J., J. Crowley, H. Fischer, H. Harder, M. Martinez, T. Petäjä, J. Rinne, J. Bäck, M. Boy, M. Dal Maso, J. Hakala, M. Kajos, P. Keronen, P. Rantala, J. Aalto, H. Aaltonen, J. Paatero, T. Vesala, H. Hakola, J. Levula, T. Pohja, F. Herrmann, J. Auld, E. Mesarchaki, W. Song, N. Yassaa, A. Nölscher, A.M. Johnson, T. Custer, V. Sinha, J. Thieser, N. Pouvesle, D. Taraborrelli, M.J. Tang, H. Bozem, Z. Hosaynali-Beygi, R. Axinte, R. Oswald, A. Novelli, D. Kubistin, K. Hens, U. Javed, K. Trawny, C. Breitenberger, P.J. Hidalgo, C.J. Ebben, F.M. Geiger, A.L. Corrigan, L.M. Russell, H.G. Ouwersloot, J. Vilà-Guerau de Arellano, L. Ganzeveld, A. Vogel, M. Beck, A. Bayerle, C.J. Kampf, M. Bertelmann, F. Köllner, T. Hoffmann, J. Valverde, D. González, M.-L. Riekkola, M. Kulmala and J. Lelieveld (2011). The summertime boreal forest field measurement intensive (HUMPPA-COPEC-2010): an overview of meteorological and chemical influences, Atmos. Chem. Phys. **11**, 10599–10618.

GLOBAL TRENDS OF AEROSOL NUMBER CONCENTRATIONS

A. ASMI[1], and GAW, GUAN, EUSAAR and ACTRIS teams

[1] Department of Physics, University of Helsinki, Finland.

Keywords: Trends, Aerosol number concentrations, Time series.

INTRODUCTION

The long-term variability of aerosol particle number concentration is relevant for climate research, as it can reveal important feedback mechanisms that need to be accounted for in projection studies, provide important information on past drivers of climate change, and give a useful comparison parameter for long-term simulations of atmospheric chemistry. Analyses of the variability of aerosol number concentration and size have been performed by many studies, in particular from regionally representative stations of the Global Atmosphere Watch (GAW) network or affiliated to the EU-Infrastructure ACTRIS. The high seasonality can easily mask any other long-term variability, if not properly taken into account. Aerosol number concentration trends have not been so widely studied as trends in other aerosol properties, especially particulate matter (PM) and aerosol optical depth (AOD).

It is necessary to have access to time series over sufficient duration to distinguish between short-term variability and long-term trends. Continuous measurements of aerosol number concentration and size were initiated in the mid-70s at some stations, but it is only from the early 90s that reporting aerosol number concentrations or number size distributions have become more common. As of today, nearly 30 stations are regularly reporting number concentration information, many including the number size distribution information, to the World Data Center for Aerosols (WDCA) but very few records span over more than 5 years. Analyses of long-term trends for aerosol physical or optical properties require at least 10-year long records, which explains why very few studies have been published on aerosol particle number concentration trends.

We provide reliable information on aerosol number concentration decadal trends on both number concentration (Asmi et al., 2012) and on in-situ aerosol optical properties viewpoints (Collaud Coen et al., 2012). We study the similarities to aerosol optical properties trends and discuss potential causes for the long-term trends. We also evaluate the trends of aerosol number size distributions in locations where such information is available, and study the applicability of aerosol particle number concentration trends to CCN-sized aerosol properties in these environments. The results are meant to be consistent and robust for end-user groups from aerosol specialists to climate modellers.

METHODS

The aerosol particle number concentrations were measured with a variety of condensation particle counters (condensation nuclei counters), which differed significantly in type and performance from site-to-site. The main criterion for having a dataset of one station was at least 10 years of relatively continuous measurements.

The number size distribution measurements were obtained by custom-made mobility particle size spectrometers (differential mobility particle sizer, DMPS) systems, which stayed relatively unchanged during the whole measurement period. All of the stations included in the size distribution
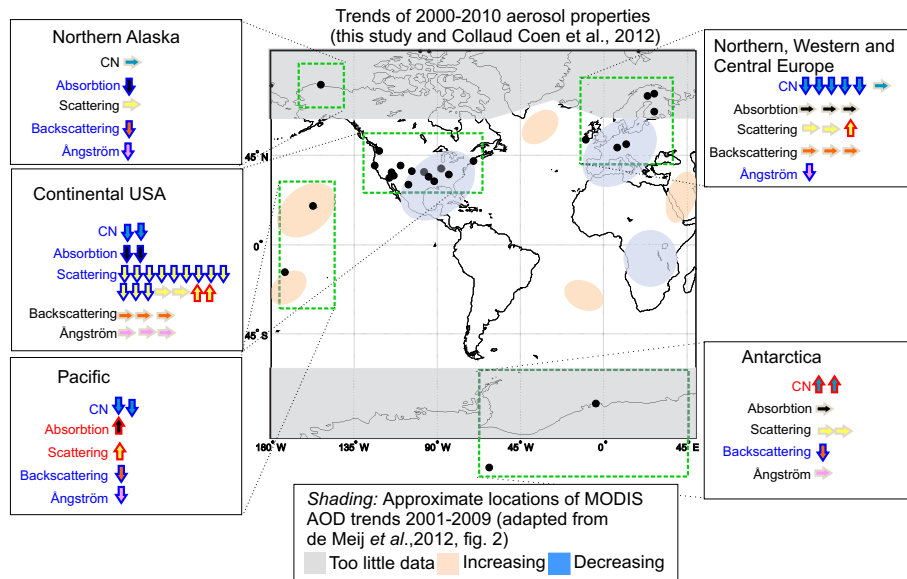
Figure 1: Direction of trends of number concentration (CN) (Asmi et al., 2012), aerosol optical properties (Collaud Coen et al., 2012) and, for comparison, satellite AOD (from de Meij et al. (2012)).

analyses had either constant monitoring of the instrument by measurement personnel (Hyytiälä) or effective site calibration routines.

Two methods for trend fitting were used: 1) The non-parametric Mann-Kendall trend analysis (MK) is based on rank and is associated with the Sen's slope estimator allowing detection of the presence of a trend and its magnitude, respectively. To correct for autocorrelation in the data, a pre-whitening procedure was applied to the data prior to the trend detection. Both methods were applied to linear space slope determination, which was then converted to relative trends by dividing by the sample median. 2) The generalized least square (GLS) trends, with either autoregressive or block bootstrap confidence intervals for statistical significance testing. The GLS approach is adapted from Mudelsee (2010) with minor modifications.

CONCLUSIONS

Trend analysis showed that the near-surface concentrations of atmospheric aerosol particles decreased at most observation points since the 1990s (Figure 1). These changes are visible and statistically significant in most locations studied in this paper, covering Northern Europe, North America, Antarctica, and the Pacific Ocean. The derived negative relative trends are generally slightly lower in magnitude than the reduction of anthopogenic SO_2 emissions over the last decades in EU and in US. However, the low number of stations with long datasets does not allow us yet to conclude that such decreasing trends are universal, regionally or globally.

Aerosol number concentration trends showed clear seasonal variations, with Northern European stations especially showing decreasing N trends during wintertime. At stations where size distribution measurements were available, the trends of number concentrations of over 20 nm particles and over 100 nm particles generally agreed very closely with each other, suggesting that, at least for Northern European conditions, the observed decreasing trends are happening for both N and CCN size ranges. Comparison with results from the companion paper do not show clear similarities

between the N and optical properties trends, although the locations where this comparison could be made was limited. The high level of agreement between the two fitting methods used in this paper demonstrates the technical reliability of the trend fitting procedures.

There is no real reason to assume that there is only one process affecting N trends at one station, or that the same process would be effective globally. The strongest support for the observed decrease in N during 2001-2010 period, of the limited set of potential reasons for these trends that was considered, is the reduction in the anthropogenic sources of aerosols and aerosol precursors, SO_2 in particular. Until the cause of the trends is better constrained, however, drawing strong conclusions about the future of aerosol number concentrations is not possible.

REFERENCES

Asmi, A., Coen, M. C., Ogren, J. A., Andrews, E., Sheridan, P., Jefferson, A., Weingartner, E., Baltensperger, U., Bukowiecki, N., Lihavainen, H., Kivekäs, N., Asmi, E., Aalto, P. P., Kulmala, M., Wiedensohler, A., Birmili, W., Hamed, A., Dowd, C. O., Jennings, S., Weller, R., Flentje, H., Fjaeraa, A. M., Fiebig, M., Myhre, C. L., Hallar, A. G., , and Laj, P. (2012). Aerosol decadal trends (II): In-situ aerosol particle number concentrations at GAW and ACTRIS stations. *Atmos. Chem. Phys. Discuss.*

Collaud Coen, M., Andrews, E., Asmi, A., Baltensperger, U., Bukowiecki, N., Day, D., Fiebig, M., Fjaeraa, A., Flentje, H., Jefferson, A., Jenning, S. G., Kouvarakis, G., Lihavainen, H., Myhre, C. L., Malm, W. C., Mihapopoulos, N., Molenar, J. V., O'Dowd, C., Ogren, J., Schichtel, B. A., Sheridan, P., Virkkula, A., Weingartner, E., Weller, R., , and Laj, P. (2012). Aerosol decadal trends (i): In-situ optical measurements at gaw and improve stations. *Atm. Chem. Phys. Discuss.* Submitted as companion paper.

de Meij, A., Pozzer, A., and Lelieveld, J. (2012). Trend analysis in aerosol optical depths and pollutant emission estimates between 2000 and 2009. *Atmospheric Environment*, 51(0):75 – 85.

Mudelsee, M. (2010). *Climate Time Series Analysis*, volume 42 of *Atmospheric and Oceanographic Sciences Library*. Springer, Heidelberg.

MEASUREMENTS OF AEROSOL PARTICLES AND GREENHOUSE GASES IN ARCTIC RUSSIA

E. ASMI[1], T. LAURILA[1], H. LIHAVAINEN[1], D. BRUS[1], M. AURELA[1], A.-P. HYVÄRINEN[1], J. HATAKKA[1], Y. VIISANEN[1], V. KONDRATYEV[2], V. IVAKHOV[3], A. RESHETNIKOV[3], T. UTTAL[4], and A. MAKSHTAS[5]

[1] Finnish Meteorological Institute, Climate Change Unit, Helsinki, Finland.

[2] Tiksi Hydrometeorological Service, Tiksi, Russia.

[3] Voeikov Main Geophysical Observatory, St. Petersburg, Russia.

[4] National Oceanic and Atmospheric Administration, Boulder, U.S.A.

[5] Arctic and Antarctic Research Institute, St. Petersburg, Russia.

INTRODUCTION

The Arctic and northern boreal regions of Eurasia are experiencing rapid environmental changes due to pressures by human activities. The largest anthropogenic climate forcings are due to aerosol particles and greenhouse gases (GHGs). Especially in the Arctic, there are also several possible amplifying feedpacks related to aerosols and GHGs which are expected to follow the changing climate. Of the most discussed, is for example release of methane from thawing permafrost soils with increasing temperatures. Also, methane emissions from the sea bottom of the Laptev and East Siberian seas have been reported recently (Shakhova *et al.*, 2010).

The Arctic environment is also highly sensitive to changes in aerosol concentrations or composition, largely due to the high surface reflectance for the most part of the year. Concentrations of aerosols in winter and spring Arctic are affected by 'Arctic Haze' (Shaw, 1995); a phenomenon suggested to arise from the transport of pollutants from lower latitudes e.g. (Stohl, 2006) and further strengthened by the strong stratification of the Arctic wintertime atmosphere. Sources and transport patterns of aerosols into the Arctic are, however, not fully understood. In addition, the polar front isolating the Arctic stratosphere makes it potentially very sensitive to emissions from inside the region. The latest studies show alarming indications that the long-term observed decreasing concentration trend has recently changed (McConnell *et al.*, 2007; Gong *et al.*, 2010).

In order to monitor the changes within the Arctic region, as well as to understand the sources and feedback mechanisms, direct measurements of aerosols and greenhouse gases within the Arctic are needed. So far, direct year-round observations of these important climate forcing agents have been inadequate especially within the Russian side of the Arctic. This is the reason why a new climate observatory was founded in Tiksi, Russia.

Tiksi meteorological observatory in northern Siberia (71°36′N; 128°53′E) on the shore of the Laptev Sea has been operating since 1930s. Recently, it was upgraded and joint in the network of the International Arctic Systems for Observing the Atmosphere (IASOA, www.IASOA.org), in the framework of the International Polar Year (IPY) Activity (#196) project (Fig. 1). The project is run in collaboration between National Oceanic and Atmospheric Administration (NOAA) with the support of the National Science Foundation (NSF), Roshydromet (AARI and MGO units), government of the Republic of Sakha (Yakutia) and the Finnish Meteorological Institute (FMI).

The research activities of FMI in Tiksi include continuous long-term measurements of aerosol physical properties as well as the fluxes and concentrations of the most important greenhouse gases (GHGs), carbon dioxide and methane. The measurements have been successfully running since summer 2010 and provide important additional information on the Arctic concentrations and processes, in addition to the FMI long-term Arctic measurements in northern Finland Pallas-Sodankylä station.

Figure 1: Map of IASOA observatories around the Arctic.

METHODS

Aerosol particle number size distributions are measured with a twin-DMPS system in the range of 7 to 500 nm using a TSI 3772 CPC as a particle counter in both of the systems. Larger particle size distributions are measured with a TSI APS 3321 between 0.5 and 10 μm. In addition, aerosol BC is measured by NOAA with a Magee Scientific Inc. 7-wl aethalometer. All aerosol data presented are cleaned from local influences using the additional available data sources and by removing the data measured during winds from polluted sector (mainly Tiksi town in north). It should be noted that prevailing wind directions are east and west.

Methane and carbon dioxide concentrations were measured by Los Gatos DLT100 laser spectrometer at sampling height of 10 m. Two calibration gases and one target gas were analysed every 50 hours. These cylinders were prepared at the WMO/GAW Central Calibration Laboratory in NOAA/ESRL, Boulder, CO. One target gas from MGO, St Petersburg was measured every 17 hours. Based on target gas measurements, methane concentrations were close to meet WMO/GAW compatibility goal of $\pm$ 2 ppm, but carbon dioxide compatibility was only around 1 ppm. Beginning from August 2011, weekly flask samples have been collected from the same mast and analysed in NOAA/ESRL, Boulder. Comparison between these flask samples and in-situ monitor indicated that methane observations were close to meet WMO compatibility target.

RESULTS

The aerosol number concentration shows a pronounced seasonal cycle with two maxima: early spring (March–April) and late summer (July–August) (Fig. 2). This is in agreement to that observed in lower latitutes in central Siberia (Heintzenberg *et al.*, 2011) although a highly more pronounced cycle is seen in high-Arctic in Tiksi. The spring maximum is likely related to appearance of sunlight together with very cold temperatures, favoring accumulation of pollutants near the surface. However, process of new particle formation was also seen to initiate with strong bursts of newly formed tiny particles already in the month of March. This suggests that transport of sufficient precursors from lower latitutes can indirectly increase the number concentration within the Arctic region during spring season.
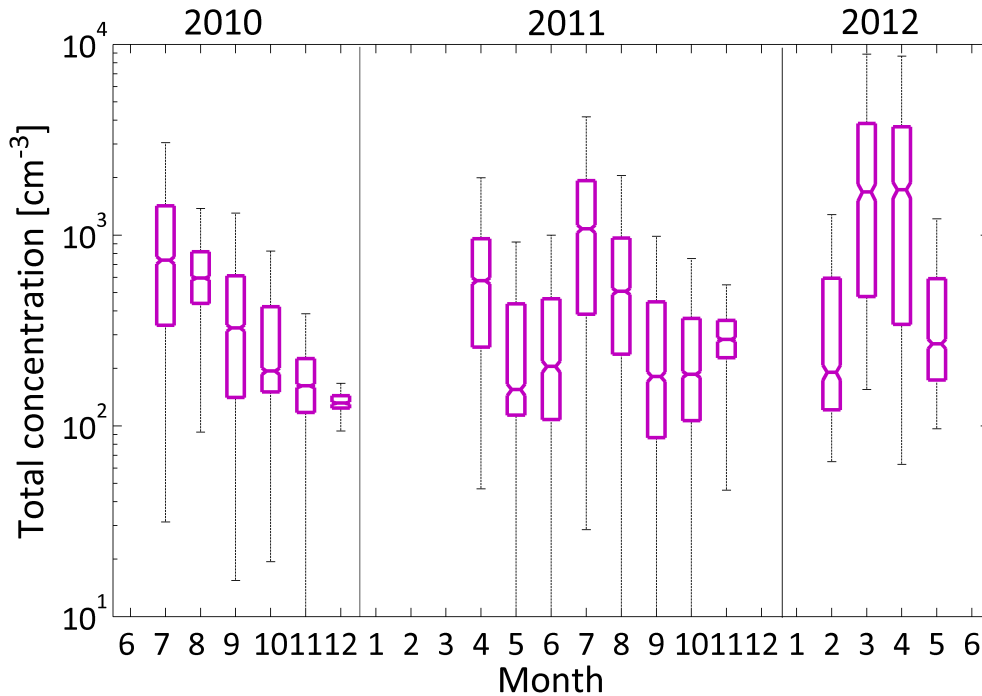
Figure 2: Total aerosol number concentration median with quartiles for each month with sufficient data coverage.

The summer maximum in concentrations is affiliated with increasing biogenic emissions over Siberia. In summer, the concentrations of CCN-sized (diameters > 100 nm) particles were the highest during continental winds while in contrast, the nucleation mode (diameters < 20 nm) aerosols were slightly favoured by marine or coastal clean air influences. Effect of biomass burning on summer aerosols is also studied using measured BC concentration.

In addition to differences by seasons and sources regions, local meteorological parameters presented clear patterns with aerosol number. A drastic increase of total (and also CCN-sized, > 100 nm) particle number was seen when temperature increased to over 15° C (Fig. 3). Concentrations were also elevated during the coldest temperatures observed, whereas the lowest number concentrations occured in temperatures between –10° C – 0° C. Clear patterns with other meteorological variables were also seen, such as continuous decline of concentrations with increasing RH. To find the reasons for these correlations, aerosols are separated by their source regions and studied together with other available precursors.
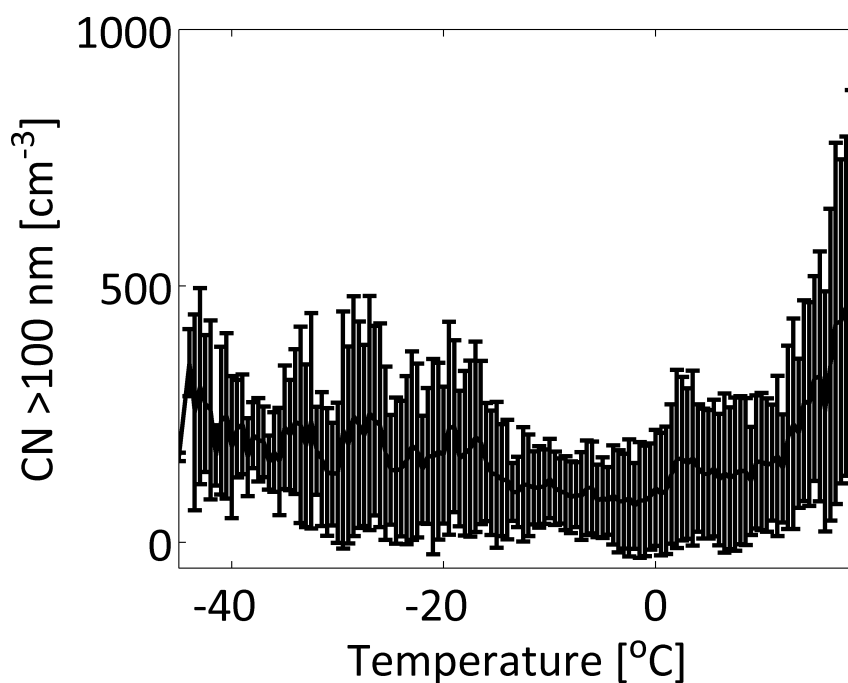
Figure 3: Dependance of > 100 nm particle concentration on temperature.

Methane concentrations showed seasonal winter maximum and early summer minimum because in wintertime the main sink process, photochemical destruction is diminished in the polar region (Fig. 4). On the average, methane concentrations in Tiksi were highest among the Arctic monitoring stations. This may be explained by vicinity of sources, stable boundary layer in the cold season and relatively low sampling height. Concentrations and their variability were high in June–October that is due to terrestrial and marine emissions. This period coincides with the period when topsoil temperature was close or above 0° C. Terrestrial methane emissions in this period were confirmed by nearby micrometeorological flux measurements. High concentrations in winter were observed when air mass advection was from the industrial areas of Siberia or European Russia.

CONCLUSIONS

Measurements of aerosol particles and greenhouse gases by Finnish Meteorological Institute started in summer 2010 in Arctic Russia, Tiksi observatory. The year-round observations are used to pinpoint regional and global sources of these important climate forcing agents, and to study their interaction and feedback processes in this extreme Arctic climate. Importantly, up to now, very few direct observations from northern Siberian region have been available.

The aerosol concentrations and size distributions, as well as the atmospheric methane concentrations and fluxes, were found to show clear seasonal patterns. Sources, sinks and local meteorological conditions were all shown to affect the concentrations. Natural aerosol particle production initiates relatively early in spring when soil is yet covered by snow. To which extend the aerosol concentrations can be explained by long-range transport, what are the main source regions as well as the role of local influeces, are currently studied.
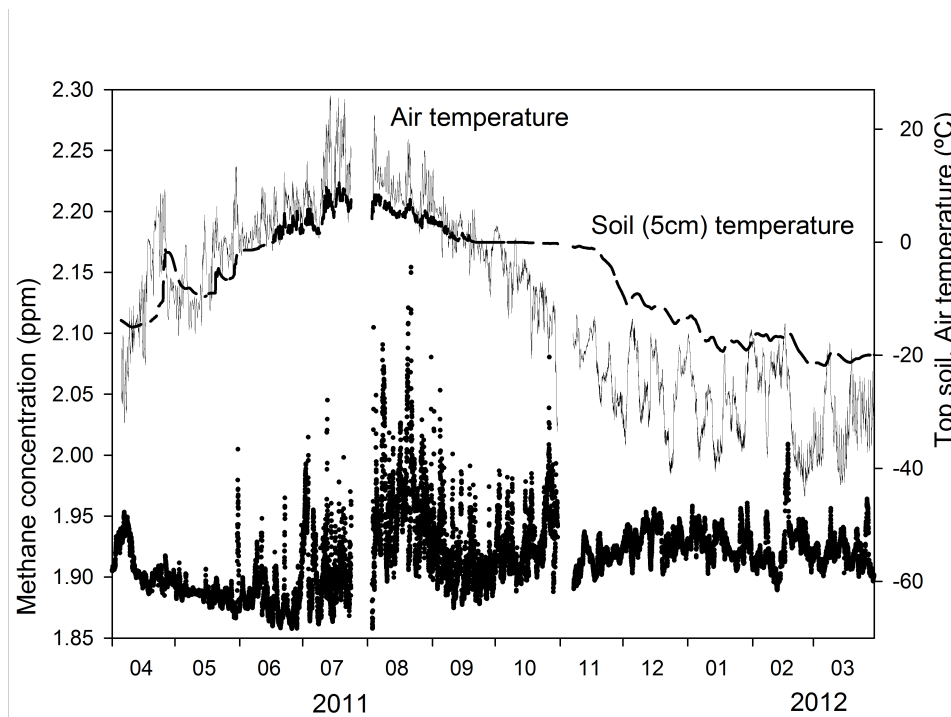
Figure 4: Half-hourly methane concentrations, air and top soil temperatures.

REFERENCES

Heintzenberg, J., W. Birmili, R. Otto, M.O. Andeae, J.-C., Mayer, X. Chi and A. Panov (2011). Aerosol particle number size distributions and particulate light absorption at the ZOTTO tall tower (Siberia), 2006–2009. *Atmos. Chem. Phys.*, **11**, 8703–8719.

Gong, S.L., T.L. Zhao, S. Sharma, D. Toom–Sauntry, D. Lavoué, X.B. Zhang, W.R. Leaitch and L.A. Barrie (2010). Identification of trends and interannual variability of sulfate and black carbon in the Canadian High Arctic: 1981–2007. *J. Geophys. Res.*, **115**, D07305, doi:10.1029/2009JD012943.

McConnell, J.R., R. Edwards, G.L. Kok, M.G. Flanner, C.S. Zender, E.S. Saltzman, J.R. Banta, D.R. Pasteris, M.M. Carter and J.D.W. Kahl (2007). 20th Century Industrial Black Carbon Emissions Altered Arctic Climate Forcing. *Science*, **317**, 5843, doi: 10.1126/science.1144856.

Shakhova, N., I. Semiletov, A. Salyuk, V. Yusupov, D. Kosmach and O. Gustafsson (2010). Extensive methane venting to the atmosphere from sediments of the East Siberian Arctic Shelf. *Science*, **327**, 1246–1250.

Shaw, G.E. (1995). The Arctic Haze phenomenon. *Bull. Am. Meteorol. Soc.*, **76**, 2403–2412.

Stohl, A. (2006). Characteristics of atmospheric transport into the Arctic troposphere. *J. Geophys. Res.*, **111**, D11306, doi:10.1029/2005JD006888.

TREND OF NORTHERN HEMISPHERE SEASONAL SNOW MASS AND ALBEDO FOR PERIOD OF 29 YEARS BASED ON SATELLITE DATA ANALYSIS COMBINED WITH ALBEDO MODELLING

K. ATLASKINA[1], J. PULLIAINEN[2], A. LAAKSONEN[2], K. LUOJUS[2], M. TAKALA[2], P. RÄISÄNEN[2], S. METSÄMÄKI[3], M. KULMALA[1], G. DE LEEUW[1,2]

[1]Department of Physics, University of Helsinki, Finland

[2]Finnish Meteorological Institute, Helsinki, Finland

[3]Finnish Environment Institute, Helsinki, Finland

Keywords: SNOW COVER ALBEDO, SNOW MASS, RADIATIVE FORCING, SATELLITE DATA.

INTRODUCTION

The seasonal snow cover governs the terrestrial surface albedo and thus the radiation balance of the climate system at high latitudes. Due to the large difference in albedo of snow-covered and snow-free surface, the snow albedo has the largest impact on the radiative balance during snowmelt period. We investigate trends in albedo and radiative forcing by applying novel observational datasets derived from space-borne measurements as input to the albedo formulation of ECHAM-5 General Circulation Model (GCM).

METHODS

The GlobSnow snow water equivalent (SWE) processing system (Takala et al. 2011) employs in an assimilation scheme passive microwave observations from Scanning Multichannel Microwave Radiometer (SMMR), Spectral Sensor Microwave/Imager (SSM/I), and Advanced Microwave Scanning Radiometer (AMSR-E) sensors and in situ snow depth observations, to produce maps of SWE estimates over the northern hemisphere (NH). The dataset covers the period from 1979 till present; however, in this work, only years from 1982 to 2010 are considered.

In the ECHAM-5 albedo formulation scheme (Roeckner et al. 2003) two dynamical variables for land grid points are considered: (a) the fractional snow cover and (b) surface temperature (Ts). The albedo of snow is parameterized as a linear function of Ts with a maximum of 0.8 at $T_s < -5$ °C and 0.3 at $T_s > 0$ °C. Among the static parameters are (a) surface topography, (b) forest coverage, (c) land type (GlobCover dataset) and (d) forest canopy transmissivity derived from MODIS-observations together with GlobCover land cover dataset (Metsämäki et al 2012, Bicheron et al. 2008).

RESULTS

Albedo changes show in general a negative trend with the most pronounced changes at areas with melting conditions (Fig.1). The magnitude of the trend is increasing from January to May. Positive trends are observed mainly over areas with negative temperature trends and mountain areas in North America. Mean trend values for Eurasia and North America separately are shown in the Table 1.
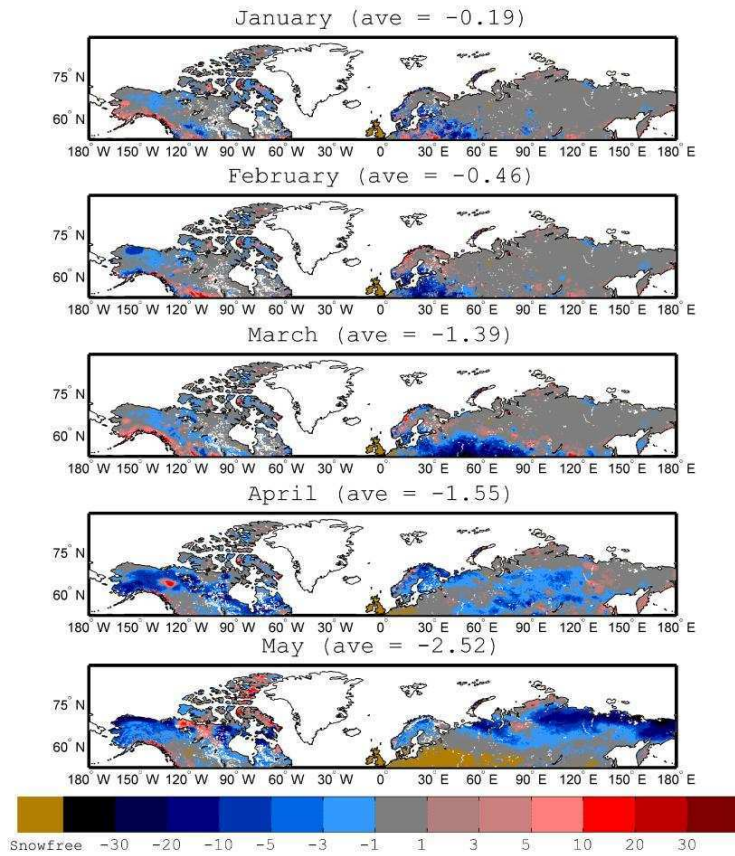
Figure 1. Modeled albedo trends [%] for years 1982-2010.

Month	Eurasia	North America	NH
January	-0.36	0.2	-0.19
February	-0.72	0.11	-0.46
March	-2.17	0.33	-1.39
May	-1.0	-2.76	-1.55
June	-3.0	1.62	-2.52

Table 1. Modeled albedo trends [%] for years 1982-2010 for Eurasia, North America and Northern Hemisphere.
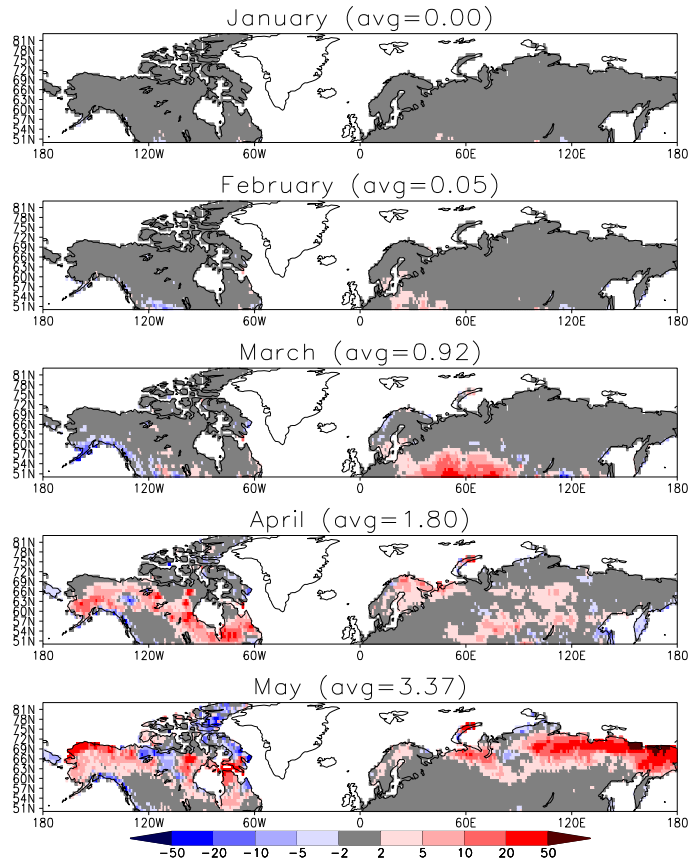
Figure 2. Trend for years 1982-2010 of top-of-the atmosphere (TOA) net shortwave flux (down-up) referred to albedo changes only [W/m2].

Radiative forcing (RF) associated with albedo changes was estimated by simulating short-wave radiative fluxes at the top of the atmosphere with ECHAM-5 and the CERES Energy-Balanced and Filled (EBAF) radiative flux dataset. RF has predominantly positive trend consistent with albedo changes, shifting from south to north as snow melting processes propagate.

REFERENCES

Bicheron, P., Defourny, P., Brockmann ,C., Schouten, L., Vancutsem, C., Huc, M., Bontemps, S., Leroy, M., Achard, F., Herold, M., Ranera, F., Arino, O. (2008). GLOBCOVER Product Description Manual, Issue 2, Rev. 2, 4/12/2008
Metsämäki, M., Mattila, O-P., Pulliainen, J., Niemi, K., Luojus, K., Böttcher K., (2012). An optical reflectance model-based method for fractional snow cover mapping applicable to continental scale. Remote sensing of environment; **123**: 508-521
Roeckner, E. et al 2003: The atmospheric general circulation model ECHAM5: Part I. Max Planck Institute for Meteorology Rep. 349, 127 pp.

162

Takala, M., Luojus, K., Pulliainen, J., Derksen, C., Lemmetyinen, J., Kärnä, J-P., Koskinen, J., Bojkob, B. (2011). Estimating northern hemisphere snow water equivalent for climate research through assimilation of space-borne radiometer data and ground-based measurements. Remote sensing of environment ; **115 (12):** 3517-3529

Wielicki, B., Barkstrom, B., Harrison, E., Lee III R., Smith G., Cooper J. (1996). Clouds and the Earth's Radiant Energy System (CERES): An Earth Observing System Experiment, Bull. Amer. Meteor. Soc., **77**, 853-868

A STUDY OF AEROSOL PRODUCTION AT THE CLOUD EDGE WITH DIRECT NUMERICAL SIMULATIONS

N. BABKOVSKAIA[1], M. BOY[1], S. SMOLANDER[1], S. ROMAKKANIEMI[2] and M. Kulmala[1]

[1] Division of Atmospheric Sciences, Department of Physics, University of Helsinki PO Box 48, Erik Palmenin aukio, 1, 00014 University of Helsinki, Finland.

[2] Department of Applied Physics, University of Eastern Finland, P.O.Box 1627, 70211 Kuopio, Finland.

INTRODUCTION

Aerosol clouds are dynamic systems with spatially and temporally varying properties. More cloud droplets may form due to in-cloud activation or due to entrainment of air from cloud edges that might lead to formation of fresh cloud droplets (J.-L., Brenguier, and W. W. Grabowski, 1993). On the other hand, cloud droplets may be evaporated because of mixing at cloud boundaries or in-cloud dynamics causing part of droplets to evaporate (S. Romakkaniemi et al., 2009). The latter of these can be important in stratus type clouds with long in-cloud residence time of air parcel. The mixing at cloud boundaries takes place in all clouds, and the type of mixing is dependent on the conditions and mixing time scales.

Different phenomena related to aerosol cloud interactions and cloud dynamics involve large range of scales. Microphysics of cloud aerosol interactions can be studied by process models, or so called box models, which are mainly used to study how and which aerosol particles are able to form cloud droplet. On the other end of scales are global models which are needed to assess how changes in cloud properties affect global radiation budget. Between these scales there are cloud resolving (CRM), or large eddy models (LES), that can be used to study cloud dynamics, and for example the effect of aerosol on drizzle formation. However, even in CRM the scale (resolution > 1 m) is such that all small scale turbulence needs to be parameterized. A tool to provide these parameterizations is direct numerical simulation (DNS), which can be used to study for example cloud boundaries in the scales from few centimeters up to few meters at most.

In this study we used the direct numerical simulation high-order public domain finite-difference PENCIL Code for compressible hydrodynamic flows. The code is highly modular and comes with a large selection of physics modules. It is widely documented in the literature and used for many different application (W. Dobler et al., 2006; Pensil Code, 2001). Recently, a detailed chemistry module has been implemented, including an accurate description of all necessary quantities, such as diffusion coefficients, thermal conductivity, reaction rates etc (N. Babkovskaia et al., 2011). This module was well tested by using the commercial code for calculation of the turbulent combustion process (Chemkin). The new developed aerosol-module coupled to the PENCIL Code now is prepared for calculating an evaporation and condensation processes of aerosol particles, which consists of a solid core covered by liquid water.

Since initially the PENCIL Code was elaborated for studying turbulent motions, it is well suitable to modeling the fluid mechanical processes in the atmospheric clouds. Additionally, due to an accurate description of the chemistry, the PENCIL Code is a powerful tool for studying the aerosol dynamics in a turbulent medium with complicated chemical composition. The scientific goals for
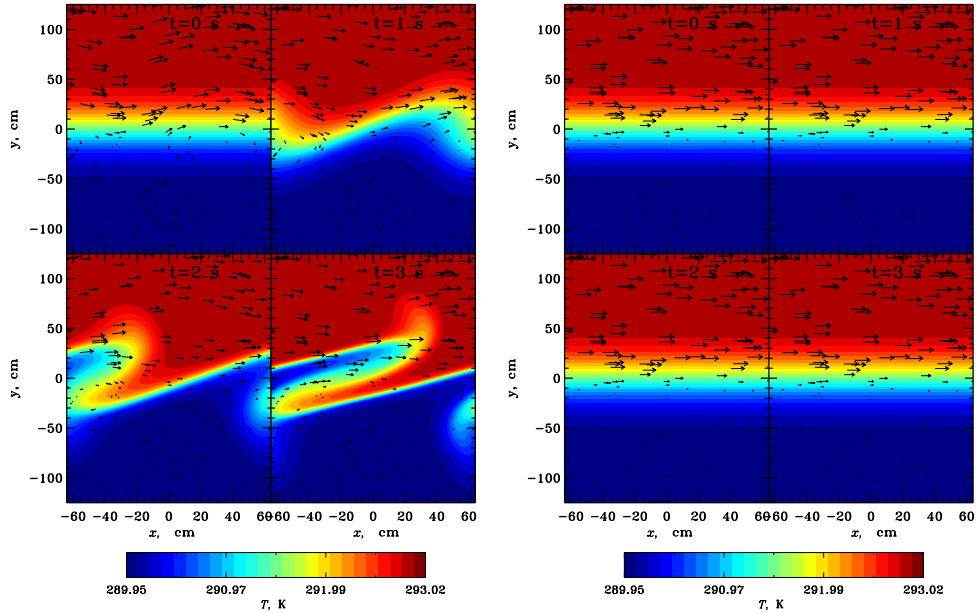
Figure 1: Velocity and temperature fields in the 2D calculated domain for inlet velocity $U_{in} = 20$ cm/s (*left panel*) and $U_{in} = 0$ cm/s (*right panel*) at $t = 0, 1, 2, 3$ s.

the construction of the new model are to investigate the spatial distribution of aerosol particles, turbulent mixing of clouds with the environment and the influence of turbulence on aerosol dynamics (and vice versa).

METHOD

In previous studies the direct numerical simulations are used to model micro-scale cloud-clear air mixing (M. Andrejczuk et al., 2004; M. Andrejczuk et al., 2004). They use the Boussinesq approximation where the density, kinematic viscosity and diffusivity of the temperature and water vapor in air are assumed to be constant. The temperature evolution is determined by the thermal flux and by the release/absorb of the energy due to evaporation/condensation of water droplets. Additionally, they neglect the solute effect in the aerosol dynamics (Seinfeld and Pandis, 2006) and consider 16 classes of the cloud droplets with the droplet sizes linearly distributed in the range from 0.78 to 24 μm.

In the proposed model we consider compressible gas; thermal conductivity and diffusion coefficients of every species and of a mixture are not constant and described by the accurate expressions (N. Babkovskaia et al., 2011); thermal flux, change of energy by evaporation/condensation and viscous heating are included in the energy equation, and the solute effect is taken into account. To study the activation of aerosol particles we take 80 classes of the cloud droplets with the droplet size logarithmically distributed in a range from 0.08 to 10 μm. Following Andrejczuk *et al.* (2004) we take the grid length of 2 cm, which is much larger than the estimated Kolmogorov scale of $O(1)$ mm, and use Smagorinski subgrid scale modeling with parameter for turbulent viscosity $C_s = 0.15$ (N. Haugen, A. Brandenburg, 2006; J. Kleissl et al., 2003).

For test purposes we start from a zero dimensional problem and take into account the condensation and evaporation of the aerosol particles covered by liquid water. We take the initial temperature $T = 293$ K, the air density $\rho = 8.6 \times 10^{-4}$ g cm^{-3}, the pressure $p = 1$ atm, and a lognormal distribution of 100 particles. In a general case the number density function $f(\mathrm{x}, m_s, r, t)$ is a
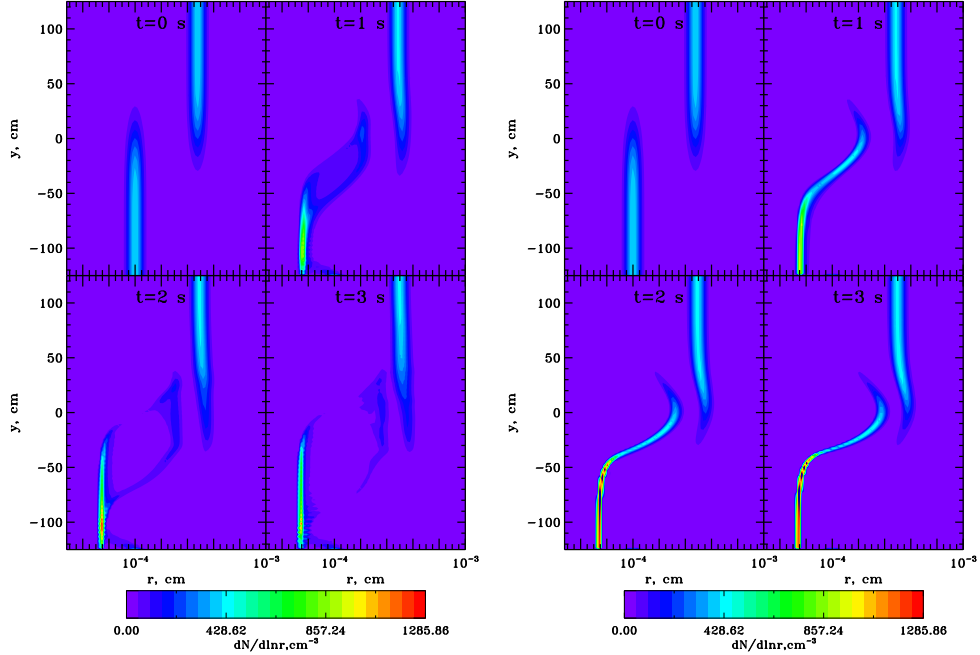
Figure 2: Distribution of particles avaraged over x for inlet velosity $U_{in} = 20$ cm/s (*left panel*) and $U_{in} = 0$ cm/s (*right panel*) at $t = 0, 1, 2, 3$ s.

function of the solute mass per particle m_s and the size of the particle r. We neglect by the dependence on m_s and assume that all particles have the same solute mass, which does not change with time. We make calculations for supersaturation $S = -0.1\%$ and 0.1 %, and show that for $S = -0.1\%$ the particles are evaporated and $S = 0.1\%$ they are activated.

Next, we consider one dimensional model. We take the size of the domain of 250 cm and 128 grid points. The air flux of the temperature $T = 290$ K with 100 particles, having the same parameters as in 0D model comes to the domain with the inlet velocity of 20 cm/c. In the middle of the domain there is a front (or cloud edge). Before the front the supersaturation is -0.1 % and behind it the supersaturation is 0.1 % and temperature $T = 293$ K. Analyzing the distribution of particles at different time moments we find that the larger particles are accumulated in the middle of the front, while the maximal concentration of smaller particles are at its edges. The maximum of S is in the middle of the front, and therefore, the most intensive growing of particles due to condensation of water happens there. Moreover, since the smaller the particles the larger the growth rate they have, at every time moment the largest particles appear in the middle of the front, while the smaller particles are accumulated at the edges. Since supersaturation is negative before the front and positive behind it, before the front the particles are evaporated and behind it they are activated.

Also, we study the structure and evolution of the cloud edge for different front thickness, inlet velocities and supersaturation. We conclude that qualitatively the results look quite similar, and no new features are found.

Finally, we consider a 3D domain of the size of 250 cm x 128 cm x 128 cm. The boundary conditions in y-direction is the same as in 1D model. In x- and z- directions we take periodic boundary conditions. The y - component velocity U_y as a function of x at $y = -125$ cm is taken to be $U_y(x) = 20$ cm/s $\times \cos(2\pi x/\Delta x)$, where $\Delta x = 128$ cm is horizontal size of the domain. In

the upper part of the domain there is a horizontal wind and vertical flux interacts with it at zero level ($y = 0$), i.e. $U_x(y \geq 0) = 50$ cm/s. The initial U_z is taken to be zero.

Analyzing the results of 3D simulation we find that for the first 5 s the z-component of velocity is still close to zero, i.e. 3D turbulence is not generated for such a time period. Therefore, for the next simulations we take 2D domain of the size of 250 cm x 128 cm and resolution 128 x 64 grid points. The time step is 3×10^{-5} s. Also, to study the effect of mixing on the particle distribution we compare the results of simulation for $U_{in} = 20$ cm/s and $U_{in} = 0$ cm/s. The temperature and velocity fields for these two cases at time moments $t = 0$ s, 1 s, 2 s and 3 s are presented in Fig. 1. In a case of zero inlet velocity U_{in} the shape of the front stays the same (flat), while for $U_{in} = 20$ cm/s it is significantly curved. However, the change of temperature before and behind the front appears to be smaller than 0.05 K.

In Fig. 2 we show distributions of particles averaged in x - direction at $t = 0$ s, 1 s, 2 s and 3 s. Both in a case of zero and in a case of non-zero inlet velocity before the front there is evaporation and behind the front particles are growing because of condensation (the same as in 1D approach). Also, for zero inlet velocity the most efficient growing of particles occurs inside the front (as it is in 1D model). In a case of non-zero inlet velocity, $U_{in} = 20$ cm/s, particles also intensively grow in the middle of the front, but additionally there is intensive evaporation near the front edges because of blowing water vapor away there.

Also, we analyze the distribution of supersaturation. We find that its distribution repeats the shape of the front. Moreover, the air mixing results in an increase of the supersaturation inside the front because of evaporation of particles there.

Finally, we study the effect of the air mixing on the particle activation. We compare a ratio of the amount of activated particles ($r > 5$ μm) to the total number $N_{in} = 20$ cm/s and without it. Note, that in a case of zero inlet velocity the shape of the cloud edge stays the same as initially at every time moment. A number of activated particles appears to be larger in a case of non-zero inlet velocity. The reason of that is in extension of the front where the activation occurs more efficiently (see Fig. 1).

CONCLUSIONS

In this paper we study the activation process at the cloud edge. We consider the flux of aerosol particles, which goes through the boundary between the dry and wet air. For a test purpose we start from a zero-dimensional problem and take into account the condensation and evaporation of the aerosol particles covered by liquid water. Initially we take a lognormal distribution of particles and supersaturation $S = \pm 0.1$ %.

Next, we consider a one dimensional problem to study a motion and evolution of the front between the dry and wet air. The dry air flux of 100 aerosol particles with the maximum of distribution at $r_m = 1$ μm and supersaturation $S = -0.1$ % is coming into domain with inlet velocity $U_{in} = 20$ cm/s and interacts with a wet cloud edge. The supersaturation behind the front is $S = 0.1$ %. This approach allows us to analyze the effect of the fluid mechanics on the aerosol dynamics (and vice versa) in a laminar regime. Using 1D approach we find that the most intensive activation occurs in the middle of the front, i.e. the distribution of the largest particles has a maximum there. Then such a single bump is splitting into two ones, and in turn, they shift toward the front edges.

Finally, we make 3D simulation with a more complicated velocity field at the cloud edge. We assume that the dry air flux is coming into the computational domain in its middle part and coming out near its boundaries. Wet air is moving in horizontal direction with velocity $U_x = 50$ cm/s. The third velocity component initially equals to zero, $U_z = 0$ cm/c. The maximum of particle distribution before the front is at $r_m = 1$ μm and behind the front is at $r_m = 3$ μm. The

other initial conditions are the same as in 1D case. After several seconds the cloud edge is curved and we analyze the final distribution of the aerosol particles there. We find that after 5 first seconds the z-component of velocity is still close to zero, i.e. for this time period the 3D turbulence is not developed, and for the next simulation we use 2D approach.

We study the effect of air mixing, comparing the results of simulation with zero, $U_{in} = 0$ cm/s, and non-zero, $U_{in} = 20$ cm/s, inlet velocity. We find that for $U_{in} = 0$ cm/s (no mixing) the most efficient growing of particles due to condensation occurs inside the front. In a case of $U_{in} = 20$ cm/s the intensive mixing of air results to evaporation and increasing of the supersaturation in the front area. Additionally, comparing the results of simulation for such two cases (with $U_{in} = 0$ cm/s and $U_{in} = 20$ cm/s) we conclude that the air mixing leads to increase of the number of activated particles (with the size larger than 5 μm). It happens because of extending of the front area where the most efficient growing of particles occurs. Also, we study the effect of the aerosol dynamics on the air motion. We conclude that its influence is very small and does not significantly change velocity field.

We should note that in this study the initial and boundary conditions are taken as typical parameters for the atmospheric conditions. Next we are planning to use the results of LES simulation for more detailed description of the boundaries. Also, the size distribution of the aerosol core and more detailed chemistry will be added in future.

REFERENCES

Andrejczuk, M., Grabowski, W., Malinowski, S., Smolarkiewicz, P. (2004). Numerical simulations of Cloud-clear air interfacial mixing. *J. of Atmospheric Sciences*, **61**, 1726.

Andrejczuk, M., Grabowski, W., Malinowski, S., Smolarkiewicz, P. (2006). Numerical simulations of Cloud-clear air interfacial mixing: Effects on cloud microphysics. *J. of Atmospheric Sciences*, **63**, 3204.

Babkovskaia, N., Haugen, N., Brandenburg, A. (2011). A high-order public domain code for direct numerical simulations of turbulent combustion. *J. of Computational Physics*, **230**, 1.

Brenguier, J.-L., W. W. Grabowski, (1993). Cumulus entrainment and cloud droplet spectra: A numerical model within a two-dimensional dynamical framework. *J. Atmos. Sci.*, **50**, 120.

Dobler W., Stix M., Brandenburg, A. (2006). Magnetic field generation in fully convective rotating spheres *Astrophys. J.*, **638**, 336.

Haugen N. E., Brandenburg, A. (2006). Hydrodynamic and hydromagnetic energy spectra from large eddy simulations *Phys. Fluids* , **18**, 1.

Kleissl, J., Meneveau, C., Parlange, M. B. (2006). On the magnitude and variability of subgrid-scale eddy-diffusion coefficients in the atmospheric boundary layer. *J. of Atmospheric Sciences*, **60**, 2372.

The PENCIL Code, http://pencil-code.googlecode.com, (2001).

Romakkaniemi, S., G. McFiggans, K. N. Bower, P. Brown, H. Coe, and T. W. Choularton (2009). A comparison between trajectory ensemble and adiabatic parcel modeled cloud properties and evaluation against airborne measurements. *J. Geophys. Res.*, **114**, D06214.

Seinfeld, J. H. and Pandis S. N., (2006). *Atmospheric chemistry and physics: From Air pollution to Climate Change.* (John Wiley & Sons, Inc).

NEW PARTICLE FORMATION STATISTICS AT PUIJO MEASURMENT STATION

E. BARANIZADEH[1], A. LESKINEN[2], A. Hamed[1], A. LAAKSONEN[1,3], A. VIRTANEN[1], H. PORTIN[2] and M. KOMPPULA[2]

[1]Aerosol Physics Group, Department of Applied Physics, University of Eastern Finland, Kuopio, Finland.

[2]Finnish Meteorological Institute, Kuopio Unit, P. O. Box 1627, FI-70211 Kuopio, Finland.

[3] Finnish Meteorological Institute, P. O. Box 503, 00101 Helsinki, Finland.

Keywords: New Particle Formation, Nucleation, Backrajectory, Puijo.

INTRODUCTION

New particle formation (NPF) in the atmosphere is a global phenomenon that has been shown to take place in a wide variety of environments. The newly formed 1-2 nm sized particles can further grow through condensation and coagulation up to a size range of > 100 nm and have a significant effect on our climate. Particles grown from NPF can affect the Earth's radiation balance directly by scattering sunlight and indirectly by having the potential to grow large enough to act as cloud condensation nuclei (CCN), and moreover, can activate to cloud droplets, resulting in even greater scattering of radiation which leads to a cooling effect on the climate (International Panel on Climate Change, IPCC 2007). However, the magnitude of aerosol indirect effects remains the single largest uncertainty in current estimates of anthropogenic radiative forcing (IPCC 2007) and causes large uncertainties in the calculations of future climate change.

Besides NPF, there are various natural and anthropogenic aerosol sources such as traffic, energy production, industry, biomass burning, wildfires, deserts, and oceans, which produce climatically active particles. Some of these particles (e.g. desert dust, sea-salt particles) are large enough that they can scatter sunlight and act as CCN, others (e.g. small particles from combustion processes) need to grow to larger sizes, similarly as the particles produced in NPF events, in order to have climatic relevance. At a given location, the fraction of different particle types depends on nearby particle sources and on meteorological conditions which govern NPF efficiency, particle removal processes, and the extent to which long range transport from distant particle sources contributes to the particle concentrations.

In this research we investigate the aerosol particle formation and evaluate the sources of different types of Arctic aerosols at Puijo station. The Puijo (62°54′32″ N, 27°39′31″ E) measurement station is on the top of an observation tower, 306 m a.s.l. and 224 m above the surrounding lake level. The tower is a 75 m high building on the Puijo hill, approximately 2 km northwest of the center of Kuopio. Several research groups at the Finnish Meteorological Institute (FMI) in Kuopio and Helsinki and at the University of Kuopio established the station in 2005. They instrumented the station for continues measurement of aerosols, cloud droplets, weather parameters and trace gases. They started measuring the weather parameters on 12 October 2005, the aerosol size distribution and total number concentration on 1 June 2006, aerosol optical properties (light absorption and scattering coefficient) on 26 August 2006, and concentrations of trace gases on 30 October 2006.

There are distinct sectors for cleaner and more polluted air, which enable us to investigate the effects of local emission sources on aerosol and cloud properties at Puijo (Figure 1). This study makes use of continuous 3 years of particle size distribution carried by Differential Mobility Particle Sizers with particle size ranges of 10-800 nm (Leskinen et al. ,2009).
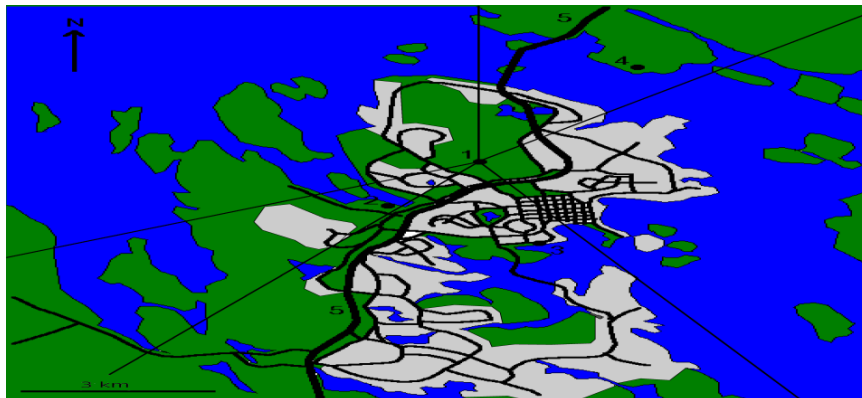
Figure 1. Surrounding of Puijo measurement site. 1= Puijo tower, 2 = Savilahti Campus, 3 = the peat-fired district heating plant, 4 = the paper mill, 5 = Highway. The blue area is water, green forest, and gray residential areas. The sectors in this figure are for local source emissions and are not the same as for the trajectories which will be shown in next part.
.

METHODS

In this research the nucleation event classification method adapted from Hamed et al., 2007 who have classified the new particle formation event using the particle size distribution. Therefore the nucleation classification here is base on event clarity, i.e. the number concentration of freshly formed particles, and their formation and growth rates. The nucleation event classes 1, 2 and 3 indicate strong, intermediate and weak nucleation event days respectively.

After classification of NPF events, to investigate the source and transport pathways of the air masses arriving to Puijo station during the time period from June 2006 to November 2009 we analyzed 120-hour back trajectories in 3-hour intervals from event and non-event days. According to Leskinen et al. (2009) who classified the trajectory into five air mass arrival sectors, named as Arctic (315-10°), Arctic\Kola (10-70°), East (70-160°), South (160-235°) and West (235-315°) which has been shown in Figure 2, we analyzed back trajectory arriving at noon time 12:00 from clear event and non-event days base on its main sector, i.e. the sector where it had spent most of the time during the last 120 hours.
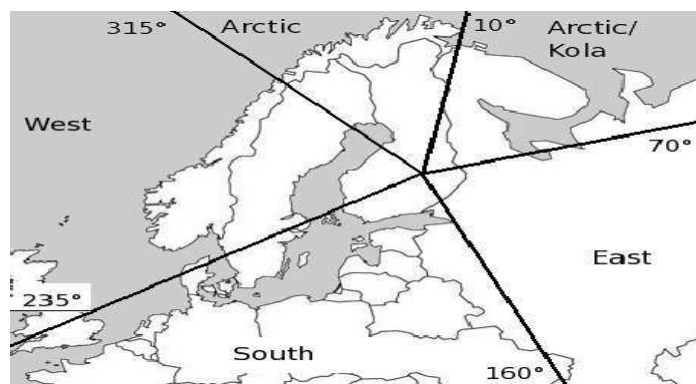
Figure 2. Location of Puijo measurement site in Kuopio, Finland. The lines define 5 sectors for trajectory calculations: sector 1 is: Arctic (315-10º), sector 2 is: Arctic\Kola (10-70º), sector 3 is: East (70-160º), sector 4 is: South (160-235º) and sector 5 is West (235-315º). The Marin areas are grey. This Figure adapted from Leskinen et al., 2009 renaming the marine sector as "West".

RESULT AND DISCUSION

Table 1 shows the number of normal new particle formation (NPF) days (class 1, 2 and 3) are the highest in spring times and the lowest in winter times which is a normal interpretation to the significant role of solar radiation in NPF processes, while the summer time events show moderate number of NPF. Furthermore, the maximum number of non-event days occurs during summer (Jun-July) and the minimum occurs during spring season (March-April).

Month	operational days	class 1	class 2	class 3	class 4	class0	NE	ND	BD
January	93	0	0	1	58	10	19	3	3
February	85	1	1	6	47	9	7	10	4
March	93	4	3	3	57	9	7	7	3
April	90	3	12	12	33	13	5	8	3
May	93	4	5	13	39	23	8	0	0
June	120	1	5	8	44	36	13	9	3
July	124	4	3	7	28	15	21	41	5
August	124	0	1	5	23	15	22	46	10
September	120	2	4	3	41	19	16	34	1
October	124	0	3	5	54	10	20	31	0
November	119	0	0	2	64	10	15	20	8
December	93	0	0	1	36	12	15	17	10
sum	1278	19	37	66	524	181	168	226	50

Table 1. numbers of nucleation event days (class 1, 2, 3 events), class 4, class 0, Non-Event (NE) and Missing Data (ND) from measurements for Puijo station during time period June 2006 to November 2009. (Operational Days=DMPS instrument was operational)

Figure 3 shows monthly frequency of nucleation event days in different classes. The maximum event frequency occurs during April with 30% of days and on May between 20 to 25% of days. Also, no class 1 and 2 events have been observed during November-January.
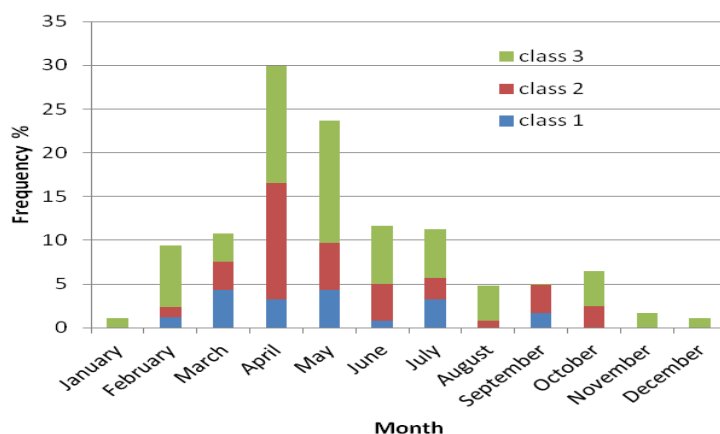
Figure 3. Monthly Frequency of nucleation event and non-event days at Puijo station.

Class 4 event is a new class that includes days with high effect of local emission sources (e.g. days that show high concentrations of SO_2 from the pulp mill and from south east direction where the power plant is). It is not clear for us whether the class 4 is a nucleation event or not, however it is not included in non-event cases. Figure 4 shows an example of class 4 on 26 June 2009. The highest frequency of class 4 occurs during September-March and the lowest frequency occurs in summer time (Figure 5).
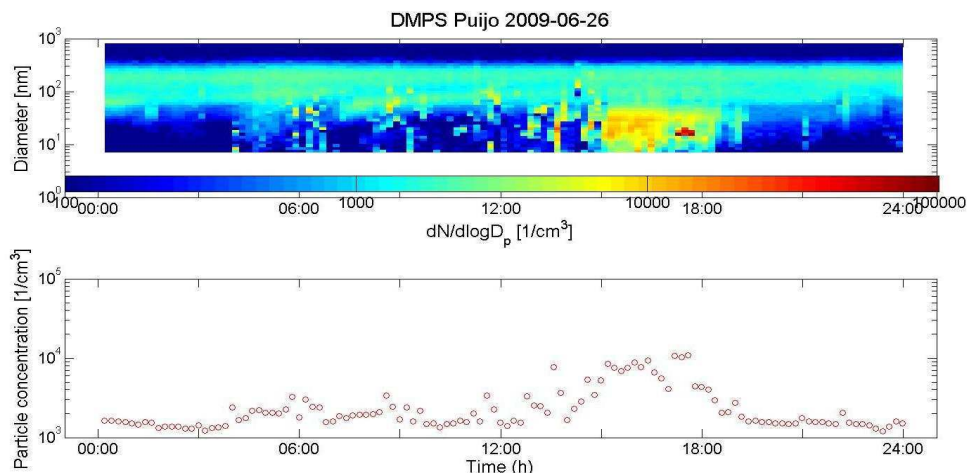
Figure 4. Example of class 4 on 26.06.2009
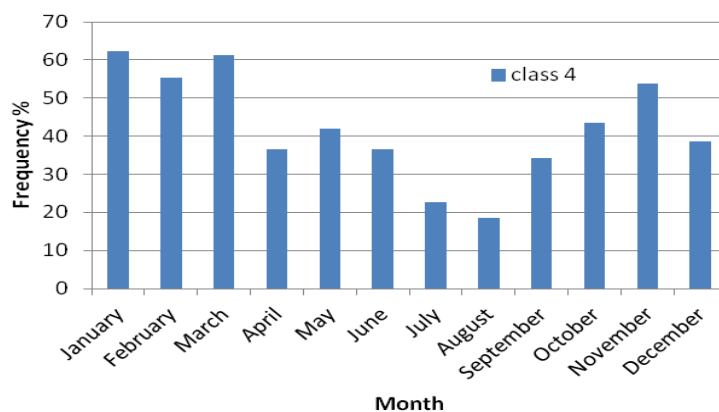
Figure 5. Monthly Frequency of class 4 event at Puijo station.

Table 2 summarizes the number of the event days in their main sectors which have been shown in Figure 2 numbered from 1 to 5. The results shows the air masses associated with nucleation events arrive mostly from Arctic sector and West sector where covers the northern Atlantic and the two Arctic sectors and the Arctic Ocean. In the resulting analysis clear nucleation events (classes 1, 2 &3) and non-events were only taken into consideration. Further study about class 4 is still ongoing and will be presented later.

	total number of days	Sector 1	Sector 2	Sector 3	Sector 4	Sector 5
class 1	19	7	2	1	0	9
class 2	37	20	7	0	0	10
class 3	66	28	11	5	1	21
NE	168	17	35	24	28	64

Table 2. Number of nucleation event days and non-event (NE) days in their main sector of the trajectory during time period June 2006 to November 2009. Sector 1 is: Arctic (315-10º), sector 2 is: Arctic\Kola (10-70º), sector 3 is East (70-160º), sector 4 is South (160-235º) and sector 5 is West (235-315º)

173

REFERENCES

Leskinen, A., H. Portin, M. Komppula, P. Miettinen, A. Arola, H. Lihavainen, J. Hatakka, A. Laaksonen, and K.E.J. Lehtinen (2009). Overview of the research activities and results at Puijo semi-urban measurement station. Boreal Environment Research **14**, 576-590.

Hamed, A., J. Joutsensaari, S. Mikkonen, L. Sogacheva, M. Dal Maso, M. Kulmala, F. Cavalli, S. Fuzzi, M.C. Facchini, S. Decesari, M. Mircea, K.E.J. Lehtinen and A. Laaksonen (2007). Nucleation and growth of new particles in Po Valley, Italy. Atmos Chem Phys **7**, 355-376.

BOREAL AND ARCTIC WATER BALANCE UNDER A CLIMATE CHANGE: COMBINING MULTIPLE SOURCE DATA TO DETECT TRENDS IN ECOSYSTEM FUNCTIONING

F. BERNINGER, V. KASURINEN, A. OJALA and E. NIKINMAA

Department of Forest Sciences, PL24 University of Helsinki

INTRODUCTION

Northern boreal and arctic ecosystems are undergoing multiple changes at different scales and different processes are occurring simultaneously. There is evidence that temperatures and potential evapotranspiration in the arctic has increased leading to more frequent droughts (Barber 2002). On the other hand on the average the runoff of arctic rivers has been increasing (Rennermalm 200x). Increases in winter precipitation, leading to a later activation of tree photosynthetic activity could be another major factor increasing runoff vs. evapotranspiration. Furthermore, changes in the atmospheric CO_2 concentration could lead to stomatal closure further reducing transpiration.

In this presentation of a "proof of concept" that combinations of different data sources, eddy covariance measurements from fluxnet, river runoff data, global meteorological data can result in powerful models that can be used to infer ecosystem functioning. Because of the close physiological connections between the different processes these models can be used to infer on ecosystem processes beyond water balance: as long term changes of gross primary production or changes in DOC export from the land.

MATERIALS AND METHODS

We developed a model of boreal photosynthesis and transpiration based on the works of Gea et al. (2010). The model includes slow processes of the recovery of photosynthesis from winter. It was assumed that the rate of photosynthesis and stomatal conductance are correlated. The recovery of maximum photosynthesis, determining the stomatal conductance was assumed to depends as a dynamical process on temperature. The time constant of this process is quite long (several days) and therefore photosyntheis as traspiration depend on the development of temperatures over longer periods. We found previously that northern forests are strongly temperature limited in their photosynthesis and hypothesize that the linkage of the plant canopy to the atmosphere as well as the transpiration rates in these ecosystem. The models showed a good fit to carbon exchange data on different time scales (Figure 1)
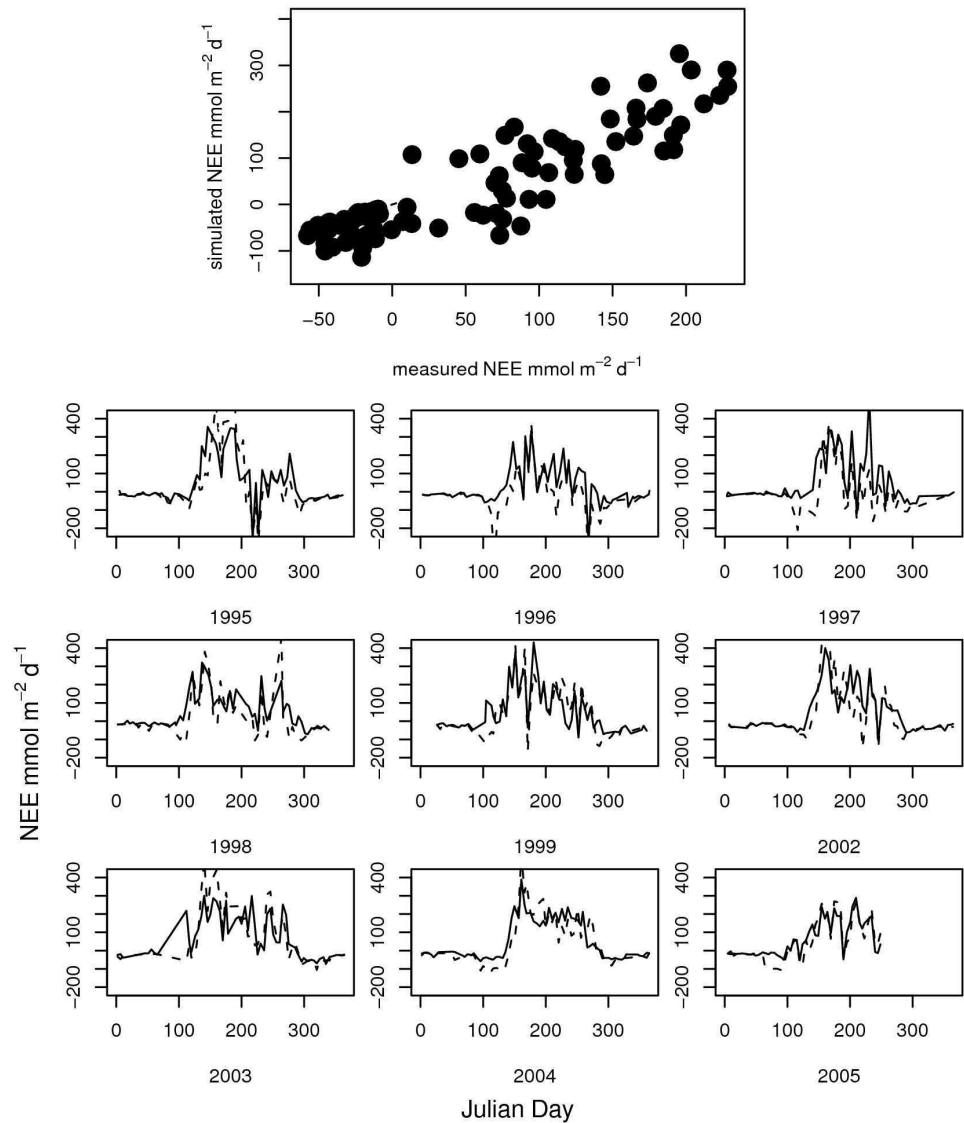
Figure 1) Observed and measured carbon flux from the model and for the Eddy Covariance site at NOBS.

To validate the model we used river debit data for this analysis, as a close correlation between the photosynthetic production and transpiration is expected on both theoretical (Wong et al. 1979) and empirical grounds (e.g. Monteith 1988). We used yearly debit data of the Caniapiscau River, which drains an area of 37380 km^2 above the gauging station. The basin and a climate station are in the eastern part of the experimental area. These data were measured from 1956 to 1985 and reconstructed thereafter using the water balance of the basin since the river was diverted for hydroelectricity in 1985. We validated the simulated transpiration by comparing percolation for the simulated site with the runoff of the Caniapiscau basin. We simply assumed that the simulated runoff from our sites equals the yearly runoff of the Caniapiscau basin. The comparison was performed at a yearly scale since we do not have a detailed runoff model of the basin. The results are shown in figure 2.

176
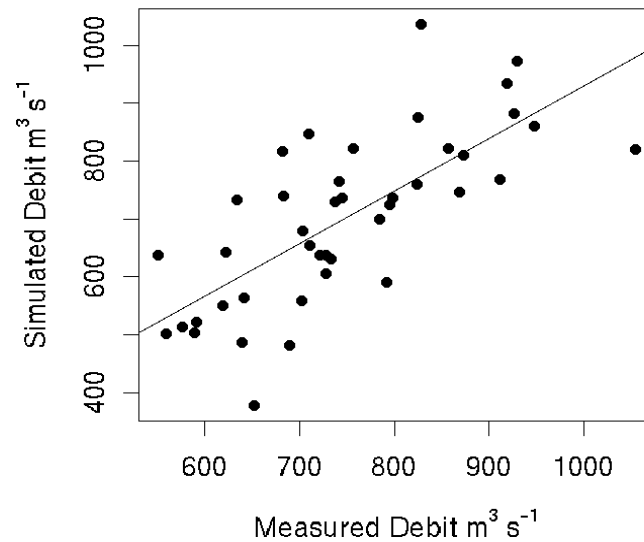
Figure 2) Measured and simulated debit of the Caniaspiscau basin.

DISCUSSION AND CONCLUSIONS

The project demonstrates that the use of physiological models has potential to explain and understand the water flow of northern rivers. The transitions from winter to spring seem to play an important role in the transpirational power of forests (as shown by Gea-Izquierdo for photosynthetic production.

The work will be used to predict water flows of northern rivers and to understand the influences of changing tree physiology on river debit in low internesity managed or unmanaged ecosystems.

ACKNOWLEDGMENTS

REFERENCES

Gea-Izquierdo G.,; Mäkelä A., Margolis H.,;Bergeron Y.,Black AT., Dunn A., Hadley J., Tha Paw U., Falk M. Wharton S., Monson R., Hollinger DY., Laurila T., Aurela M., McCaughey H., Bourque C., Vesala T. Berninger F. (2010) .Modelling acclimation of photosynthesis to temperature in evergreen boreal conifer forests. New Phytologist 10.1111/j.1469-8137.2010.03367.x

Monteith JL (1988) Does transpiration limit the growth of vegetation or vice versa? Journal of Hydrology,.100, 57–68.

Rennermalm, A. K., E. F. Wood, A. J. Weaver, M. Eby, and S. J. Dery ´ (2007), Relative sensitivity of the Atlantic meridional overturning circulation to river discharge into Hudson Bay and the Arctic Ocean, J. Geophys. Res., 112, G04S48,doi:10.1029/2006JG000330.

Wong SC, Cowan IR, Farquhar GD (1979) Stomatal conductance correlates with photosynthetic capacity. Nature, 282, 424–426.

A CHEMICAL VIEW OF SVALBARD SNOW

M. P. BJÖRKMAN[1,2], C. P. VEGA[3], V. A. POHJOLA[3] and E. ISAKSSON[1]

[1]Norwegian Polar Institute, Fram Centre, N-9296 Tromsø, Norway.

[2]Department of Geosciences, University of Oslo, P.O. Box 1047 Blindern, 0316 Oslo, Norway.

[3]Department of Earth Sciences, Uppsala University, Villavägen 16, SE-76236, Uppsala, Sweden.

Keywords: snow chemistry, Svalbard

INTRODUCTION

The chemistry of snow is a complex cocktail of ions that is a function of: 1) the origin of the air masses that produce the snow, 2) on the ambient exchange en route, 3) what ice nucleation processes that was operating, and 4) what the snow flake scavenged during the snow fall. Further, post depositional processes as photochemistry, evaporation, dry deposition, melt events and biological assimilation may alter the original signature from the snow fall. All these processes results in the chemical records found in ice cores and are used to evaluate past climates and atmospheric contents. However, it is also commonly known that the within snow chemical variability is large.

METHODS

To retrieve an overall picture of the chemical load to Svalbard snow nine glacier areas (Austre Brøggerbreen, Kongsvegen, Holtedalfonna, Slackbreen, Tellbreen, Nordenskiöldbreen, Lomonosovfonna, Austfonna and at Hartogbukta) was investigated in spring 2010. In total 16 snow pits was sampled with a resolution of 5 to 10 cm ranging from 100 to 1200 m in elevation and from the far west to the far east of the archipelago.

RESULTS

Large variation was found (e.g. from below detection to up to almost 1 mg/l for nitrate) within the layering of the snow pits indicating different origin of the air masses and different transport routes. This is in line with recent findings that a few episodic precipitation events might give up to 50 % of the annual load of nitrogen.

Data will also be used to model the main explanation parameters as: location, elevation and accumulation, for the data set.

Holtedahlfonna # 6, 2010
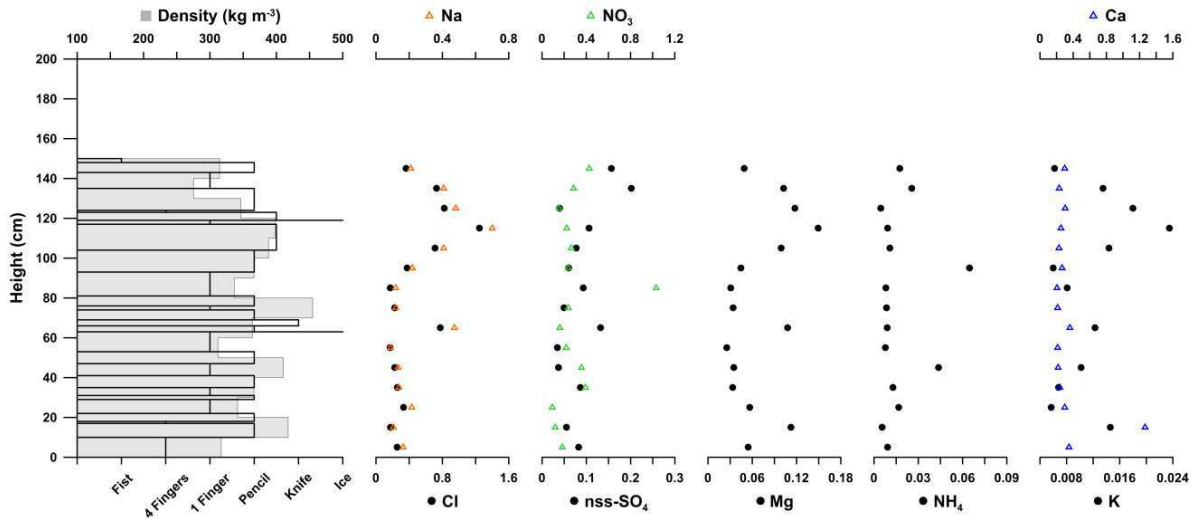
Figure 1. Snow pit stratigraphy and chemistry at Holtedahlfonna, 770 m a.s.l., on the west coast of Svalbard.

Austfonna Summit, 2010
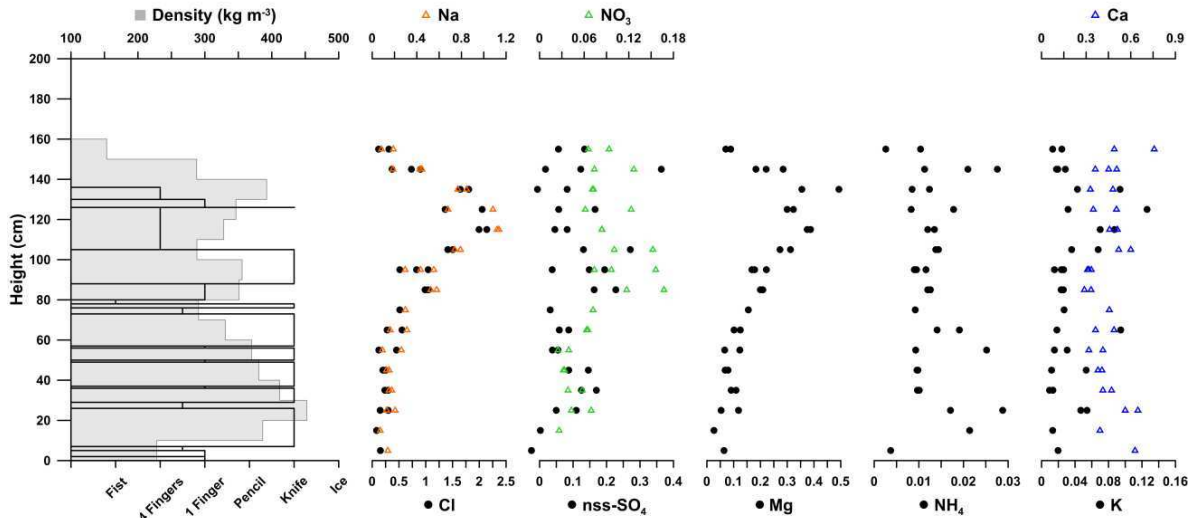
Figure 2. Snow pit stratigraphy and chemistry at Austfonna, 790 m a.s.l., on the east coast of Svalbard.

NEW FLYING PLATFORM FOR ATMOSPHERIC MEASUREMENTS

D. BRUS[1], E. ASMI[1], S. CARBONE[1], J. HATAKKA[1], R. HILLAMO[1], T. LAURILA[1], H. LIHAVAINEN[1], E. ROUHE[2], S. SAARIKOSKI[1], and Y. VIISANEN[1]

[1]Finnish Meteorological Institute, Erik Palménin aukio 1, P.O.Box 503, FI-00101, Helsinki, Finland

[2]Department of Radio Science and Engineering, Aalto University, P.O. Box 13000, FI-00076 Aalto, Finland

Keywords: Airborn particles, Mass spectrometry, CCN, CN, Green House Gasses, Scattering coefficient

INTRODUCTION

The Baltic Sea is a busy area for short-sea marine traffic. Nowadays shipping represents one of a major contribution to the international transportation sector which is unfortunately not well quantified in terms of global emissions and climate impacts (Petzold et al., 2008). In this context, gaseous and particulate matter emissions from seagoing ships are gaining increasing attention because of probable environmental and climate effects. Most of the existing methods to estimate emissions of ship traffic up to the present have unfortunately relied on very simplified information (Dentener et al., 2006) and are based on averages in terms of the number and size of vessels, the distances travelled between ports, engine power levels and/or the amounts of fuel. One of the key components of the particulate matter, sulphates, can be effectively reduced by using low-sulphur fuel in marine diesel engines. In this context there raised a need of a suitable infrastructure enabling direct comprehensive measurements of physical and chemical properties of boundary layer atmosphere over the Baltic Sea, its coast and over the inland.

Finnish Meteorological Institute (FMI) in co-operation with Aalto University built a flying platform suitable for various applications of such a kind. Basic funding to start the design became available in the end of 2011 by FMI, and the Measurement, Monitoring and Environmental Assessment programme (MMEA). The main goals within the programme are: The monitoring and direct measurements of ship emissions over the Baltic Sea (SA Bonus programme 2013 and forward), the direct comparison of remote sensing (Utö station) vs. airborne observations (Skyvan platform) and greenhouse gases (GHG) profiling in the boundary layer over the sea and Finland.

METHODS

In this study a modified SHORT SC-7 Skyvan aircraft (Short Brothers and Harland Ltd, Northern Ireland, UK) suitable for various research purposes was used. Currently, Skyvan is operated by Radio Science and Engineering Department of Earth observation group at Aalto University. It is a non-pressurized twin-engine turbo-propeller aircraft with a maximum operating distance of 1370 km and the maximum operating height of just over 3 km. Skyvan is equipped with the MIDG II INS/GPS, an Inertial Navigation System with Global Positioning System for recording of precise position and speed.

All the onboard instruments were connected to BMI Isokinetic Inlet System (Model 1200, Brechtel Manufacturing Inc., USA.). The inlet system is fully automated, with transmission efficiency > 90% for particle aerodynamic diameters < 10 µm. It is equipped with anti-icing system, Pitot tube for airspeed measurements and isokinetic flow control, also directly provides flow rate, pressure and temperature measurements of sample flow. Integrated data system records all parameters in 1 Hz resolution.

The Soot particle Aerosol Mass Spectrometer (SP-AMS, Aerodyne Research Inc., USA) is a modified version of High-Resolution Time-of-Flight Aerosol Mass Spectrometer (HR-ToF-AMS) (DeCarlo et al., 2006). The instrument consists of a particle sampling inlet, a particle sizing chamber and a particle composition detection section. The aerosol particles are sampled through aerodynamic lens, forming a narrow particle beam which is transmitted into the detection chamber where non-refractory species are flash vaporized upon impact on a hot surface (~600ºC) under high vacuum and chemically analyzed via electron impact ionization (70 eV) in the high resolution time-of-flight mass spectrometer. When equipped with an intracavity laser vaporizer (1064 nm), based on the Single Particle Soot Photometer (SP2) design, it measures online chemical composition of submicron particles containing refractory black carbon (Onasch et al., 2012).

The continuous-flow stream wise thermal-gradient cloud condensation nuclei counter (DMT-CCNC) was used in this study, model No. CCN-100 (Droplet Measurement Technologies, Inc., DMT, USA).
The design and operating principles of the instrument are based on Roberts and Nenes (2005). The CCN was operated behind the Constant Pressure Inlet (CPI, DMT Inc., USA) set to 700 or 615 mbar, together with a condensation particle counter (CPC, model 3010, TSI, St. Paul, Minnesota, USA). The CCN was set to sampling flow of 0.5 lpm and constant level of saturation ratio of 0.5% through the whole campaign. The total number of aerosol particles was monitored with second CPC 3010 connected to BMI isokinetic inlet.

The scattering and backscattering coefficients were measured with an integrating nephelometer (model 3563, TSI, Inc., St. Paul, Minnesota, USA). This instrument measures scattering by aerosols in three walengths; 450, 550 and 700 nm. The instrument measures scattering, sca, and backscattering coefficients, bsc, in three wavelengths, 450, 550, and 700 nm. The instrument illuminates the sample volume from the side and measures the light scattered by aerosol particles and gas molecules in the direction of the photomultiplier tube integrating the scattering over angle of 7–170°. The instrument is described in detail by e.g. Anderson et al. (1996). Calibration of the nephelometer is carried out using CO_2 (purity 4.0) as high span gas and filtered air as low span gas. Nonidealities due to nonlambertian and truncation errors in nephelometer were corrected using the method described by Anderson and Ogren (1998).

Picarro G1301-m (Picarro, Inc. Sunnyvale, CA USA) measures concentrations of CO_2, CH_4 and H_2O using near-infrared lasers and Cavity Ring-Down Spectroscopy (Crosson, 2008; Chen et al., 2010). This model is designed for measurements on mobile platforms such as airplanes. Measurement cycle is accelerated giving rise-fall time less than 2 seconds. Inlet gas flow is about 0.4 lpm and inlet pressure may vary between 1000 - 250 Torr. Precisions of the concentrations of CO_2, CH_4 and H_2O are 0.2, 0.0015, and 100 ppmv, respectively. Response of the instrument was checked before the flight campaign and it was calibrated after the campaign. Power consumption was around 250 Watts.

RESULTS

The airborne measurements consisted of two demonstrations flights, the first on July 30th from Helsinki-Vantaa airport towards town of Porvoo and back, and the second on July 31st from Helsinki-Vantaa towards town Perniö and then towards island Utö and back. Both flight-paths can be seen in figure 1. During both flights several ascents were done to monitor vertical profiles of measured properties, those can be seen as spirals in the flight-paths. The ranges of altitudes in first and second flight were from 300 to 2800 m and 300 to 3100 m, respectively.

The measured chemical composition of non-refractory particles (smaller than 1μm) by SP-AMS instrument can be seen on figure 2: nitrate, organics and sulfate mass concentration as function of altitude. Unfortunately during this demonstration flights the SP module was not operating due to electricity restrictions in Skyvan.

Figure 1. Flight-paths of two flights, the first flight from Vantaa (white line) only over land around town of Porvoo, the second from Vantaa (green line) over both land and Baltic Sea around Utö island. The spirals represent the vertical ascents from ~300 to ~3000 m.
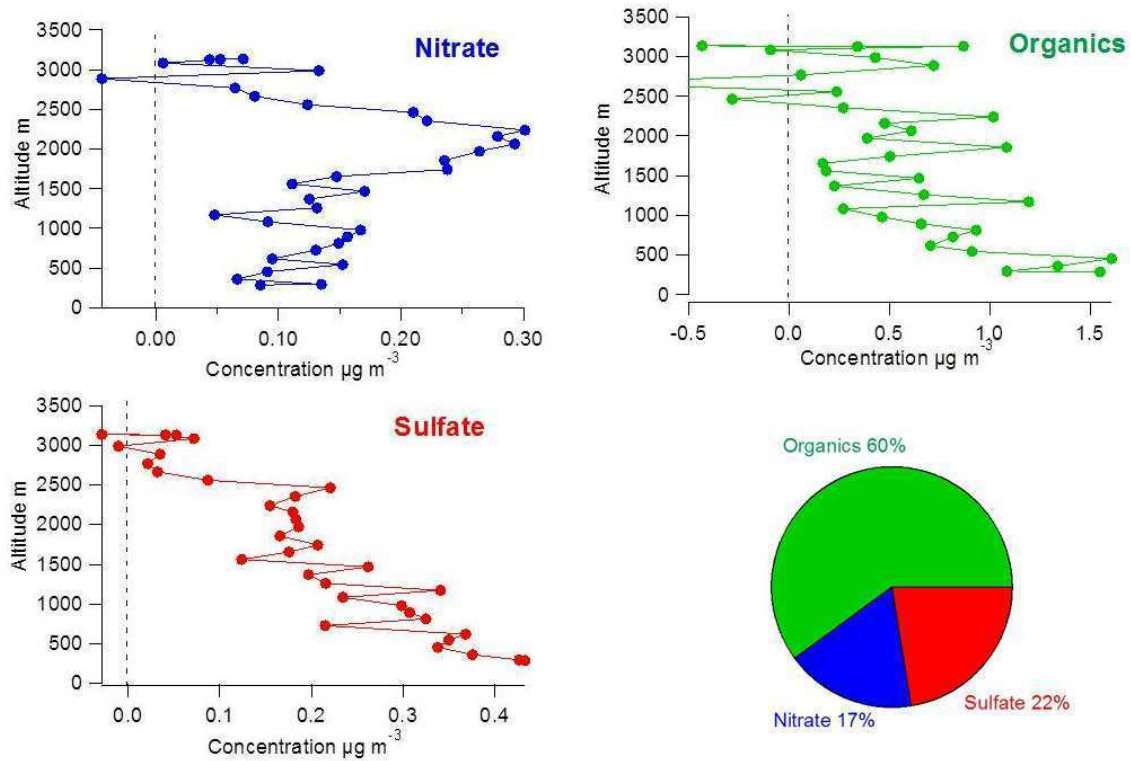
Figure 2. SP-AMS data from the ascent near Perniö, the contribution of nitrate, sulfate and organics composition during the flight as a function of altitude, and the averaged chemical composition data can be seen in the pie chart.

183

Example dataset of particle number concentration (CN) and number of cloud condensation nuclei (CCN) from the first demo flight over Porvoo can be seen in figure 3. The CCN number concentration data are corrected to ambient pressure, since operating CCN counter at constant pressure affects the particle concentration. Data has to be also corrected for the supersaturation since the instrument was calibrated at ambient pressure. Usually the applied correction is about 0.035% per 100 mb change in pressure, so the constant supersaturation set to SS=0.5% will change close to 0.4% at ambient pressure during the flight.
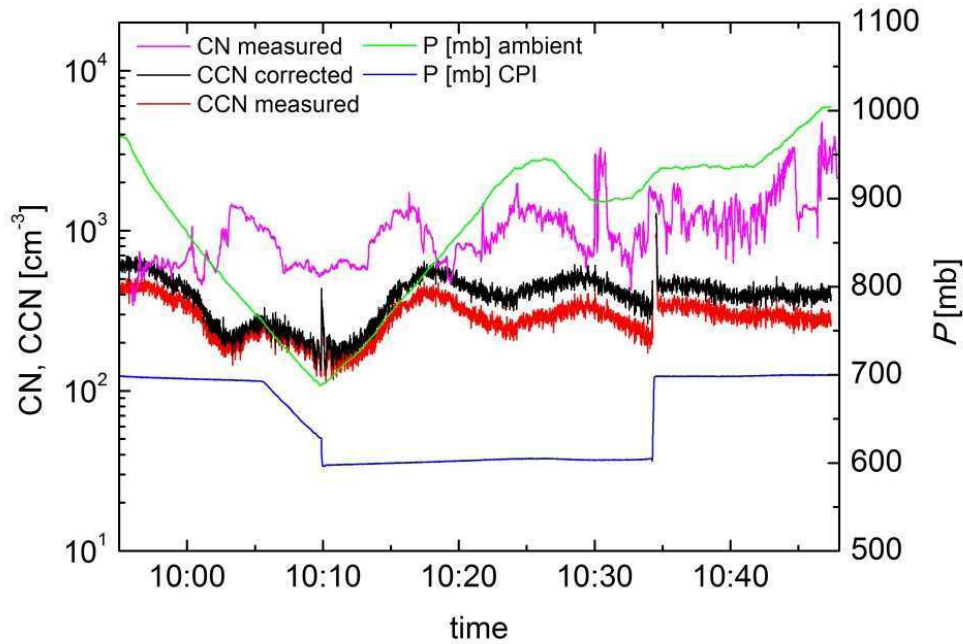
Figure 3. The timeline of first demo flight, particle number concentration (CN), number of cloud condensation nuclei (CCN) raw and corrected data, set pressure of constant pressure inlet (CPI) and ambient pressure in millibars.

In Figure 4 is example of results from the second demo flight, vertical profiles of scattering coefficient at 550 nm over land and over sea about 60 km south from the coast. Scattering values are reported in 0°C and at 1013 hPa.

Picarro measured successfully during the both flight days. As an example we present CO_2 and CH_4 concentrations during the flight path from the north of Utö island to Vantaa on July 31 (Figure 5). The flight altitude was 200-350 m. We observed marine boundary layer for 16 minutes in the beginning. The air advected from southwest, the Northern Baltic proper. Then the plane entered the island of Keimiö and we sampled boundary layer air over mainland. Over the Archipelago Sea CO_2 concentrations were relatively high being lower closer to the Utö island and coastline. Over the rural areas CO_2 concentrations were about 4 ppm lower and variability much higher than over the sea reflecting CO_2 uptake by terrestrial vegetation during the summer day. Closer to the Helsinki metropolitan area CO_2 concentrations increased probably due to anthropogenic emissions. Close to the city of Lohja we observed elevated CO_2 concentrations and slightly elevated CH_4 concentrations. Methane concentrations were on the same level over the sea and land but variations over land were double compared to those over the sea. Highest CH_4 concentrations were observed in the plume of the Ämmässuo landfill which is the largest municipal solid waste landfill in the Nordic countries. The plane passed this plume three times at a distance of about 4 km from the landfill.
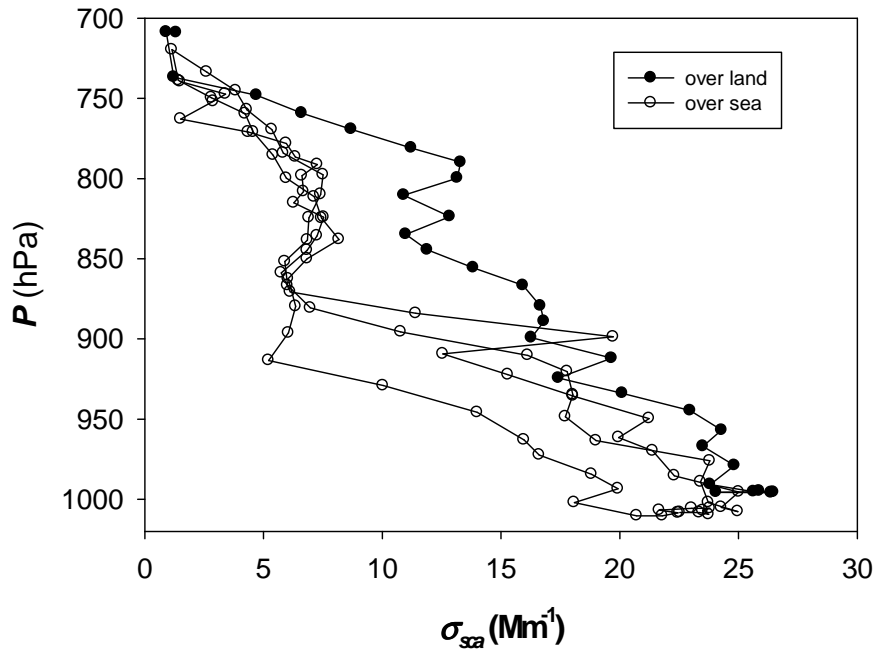
Figure 4. Vertical profiles of scattering coefficient at 550 nm. Scattering values are reported in 0°C and at 1013 hPa.
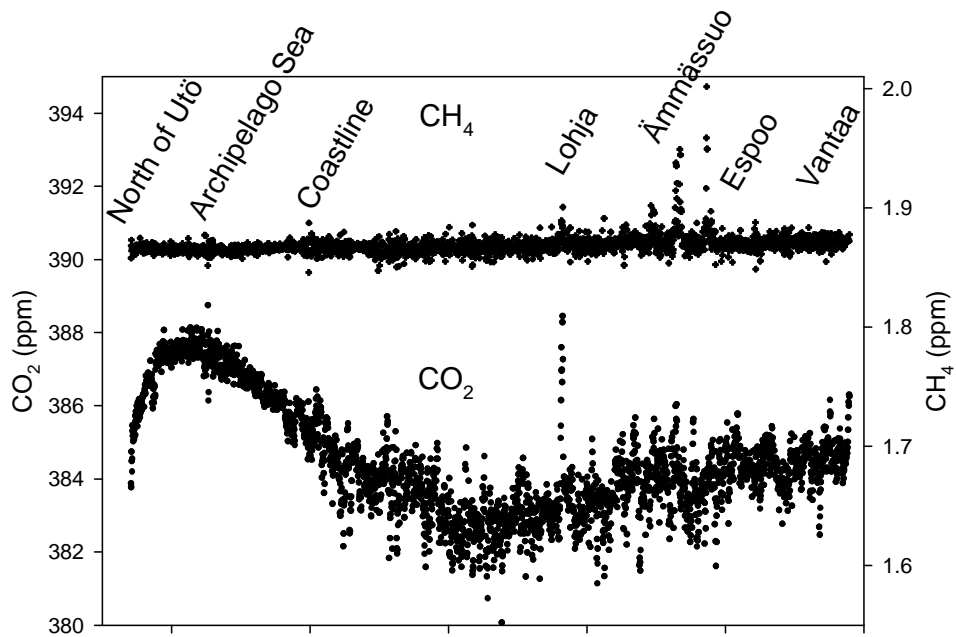
Figure 5. Measured concentrations of CO_2 and CH_4 in the boundary layer during the second flight path from Utö to Helsinki-Vantaa.

ACKNOWLEDGEMENTS

REFERENCES

Anderson, T. L., D. S. Covert, S. F. Marshall, M. L. Laucks, R. J. Charlson, A. P. Waggoner, J. A. Ogren, R. Caldow, R. L. Holm, F. R. Quant, G. J. Sem, A. Wiedensohler, N. A. Ahlquist, and T. S. Bates (1996), Performance characteristics of a high-sensitivity, three-wavelength, total scatter/backscatter nephelometer, *J. Atmos. Oceanic Technol.*, **13**, 967–986.

Anderson, T. L. and J. A. Ogren (1998), Determining aerosol radiative properties using the TSI 3563 integrating nephelometer, *Aerosol Sci. Technol.*, **29**, 57–69.

Chen, H., J. Winderlich, C. Gerbig, A. Hoefer, C. W. Rella, E. R. Crosson, A. D. Van Pelt, J. Steinbach, O. Kolle, V. Beck, B. C. Daube, E. W. Gottlieb, V. Y.Chow, G. W. Santoni, and S. C.Wofsy (2010): High-accuracy continuous airborne 10 measurements of greenhouse gases (CO_2 and CH_4) using the cavity ring-down spectroscopy (CRDS) technique, *Atmos. Meas. Tech.*, **3**, 375-386.

Crosson, E. R. (2008). A cavity ring-down analyzer for measuring atmospheric levels of 20 methane, carbon dioxide, and water vapor. *Applied Physics B*, **92** (3), 403-408.

DeCarlo, P.F., J.R. Kimmel, A. Trimborn, M. Northway, J.T. Jayne, A.C. Aiken, M. Gonin, K. Fuhrer, T. Horvath, K.S. Docherty, D.R. Worsnop and J.L. Jimenez (2006). Field-Deployable, High-Resolution, Time-of-Flight Aerosol Mass Spectrometer, *Anal. Chem.*, **78**, 8281-8289.

Dentener, F., S. Kinne, T. Bond, O. Boucher, J. Cofala, S. Generoso, P. Ginoux, S. Gong, J.J. Hoelzemann, A. Ito, L. Marelli, J. E. Penner, J.-P. Putaud, C. Textor, M. Schulz, G. R. van der Werf, J. Wilson (2006).. Emissions of primary aerosol and precursor gases in the years 2000 and 1750 prescribed data-sets for AeroCom. *Atmos. Chem. Phys.* **6**, 4321.

Onasch T.B., A.Trimborn, E.C. Fortner, J.T. Jayne, G.L. Kok, L.R. Williams, P. Davidovits and D.R. Worsnop (2012). Soot Particle Aerosol Mass Spectrometer: Development, Validation, and Initial Application, *Aerosol Science and Technology*, **46** (7), 804-817.

Petzold, A., J. Hasselbach, P. Lauer, R. Baumann, K. Franke, C. Gurk, H. Schlager, and E. Weingartner, (2008). Experimental studies on particle emissions from cruising ship, their characteristic properties, transformation and atmospheric lifetime in the marine boundary layer, *Atmos. Chem. Phys.*, **8**, 2387-2403.

Roberts, G. C. and A. Nenes (2005). A Continuous-Flow Streamwise Thermal-Gradient CCN Chamber for Atmospheric Measurements, *Aerosol Sci. Technol.*, **39**, 206–221.

MIXED-PHASE CLOUDS OBSERVATIONS AT PALLAS SUBARCTIC BACKGROUND SITE

D. BRUS, J. SVENSSON, K. NEITOLA, and H. LIHAVAINEN

Finnish Meteorological Institute, Erik Palménin aukio 1, P.O.Box 503, FI-00101, Helsinki, Finland

Keywords: mixed-phase clouds, arctic, CAPS, CCN

INTRODUCTION

The Arctic region is slowly heading towards a new climatic state with substantially less permanent ice cover. The Arctic environment is very specific and full of not very well understood feedbacks, thus very hard to be predictable with current global models. Central role in these feedback processes are supposed to play Arctic clouds (Vavrus, 2004).

METHODS AND RESULTS

The winter cloud experiment has been conducted in first week of February 2012 at Finnish Meteorological Institute's Pallas-Sodankylä Global Atmosphere Watch (GAW) station located in northern Finland. The measuring site - Sammaltunturi station (67°58′N, 24°07′E) - resides on a top of the second southernmost fjeld, a round topped treeless hill, in a 50-km-long north and south chain of fjelds at an elevation of 565 m above sea level. Sammaltunturi station is due to topography of the surrounding terrain a great place for ground-based observations of orographic clouds. Thus providing an opportunity to investigate not only the cloud droplet activation of aerosol particles but also directly the cloud particle phase (Komppula et al., 2005).
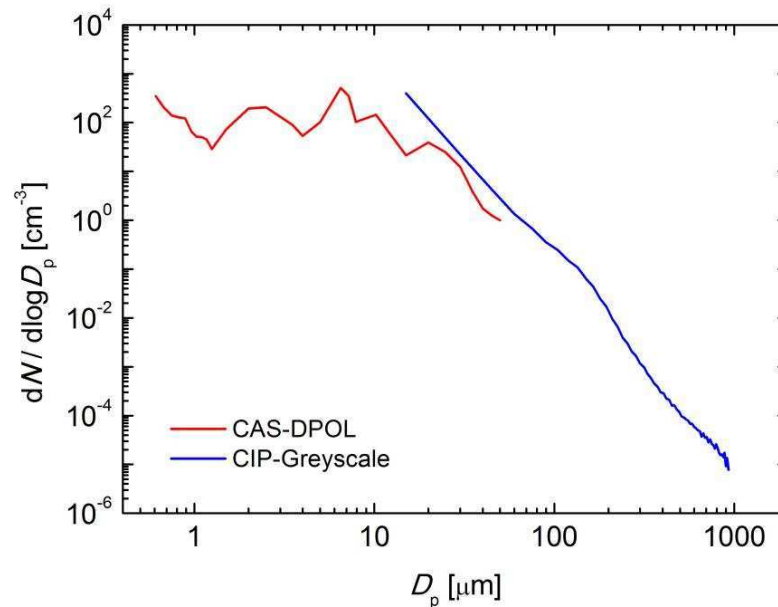
Figure 1. Example of raw size distributions obtained with CAS-DPOL and CIP-Greyscale probes during the campaign at Sammaltunturi, between 01:50-02:30, February 1st 2012.

The Cloud, Aerosol and Precipitation Spectrometer (CAPS, DMT, CO, USA) which includes three instruments: the Cloud Imaging Probe (CIP), the Cloud and Aerosol Spectrometer (CAS) with depolarization, and the Hotwire Liquid Water Content Sensor (Hotwire LWC), were used in this campaign together with Cloud Condensation Nuclei counter (CCN-100, DMT, CO, USA) and Hygroscopic Tandem Differential Mobility Analyser (HTDMA). The CAPS probe was equipped with tailored inhalator to make it suitable for ground-based measurements. The average airspeed in the system was approximately 22 ms^{-1}. The shattering (Schwarzenboeck et al., 2009) and thus overestimation of the concentrations of ice crystals obtained with the CIP probe is not expected to be observed. Within the one week of intensive campaign five arctic cloud or freezing fog events lasting several hours have been observed. The maximum and minimum temperature during the campaign was between -14 and -27°C. The maximum droplet concentrations were observed up to 100 cm^{-3} and 400 cm^{-3} for CIP-Greyscale probe and CAS-DPOL probe, respectively. Liquid water content was observed up to 1.5 g m^{-3}.

Figure 1 shows overlap of number concentration distributions obtained with CAS-DPOL and CIP-Greyscale probes in a range 0.5 µm – 1 mm. Images taken by CIP probe show both small spherical super-cooled drops together with larger irregular particles, figure 2.

The next step of the analysis will include all available experimental data on cloud particles together with physical and chemical properties, and activated fraction of aerosol particles (CCN and HTDMA).
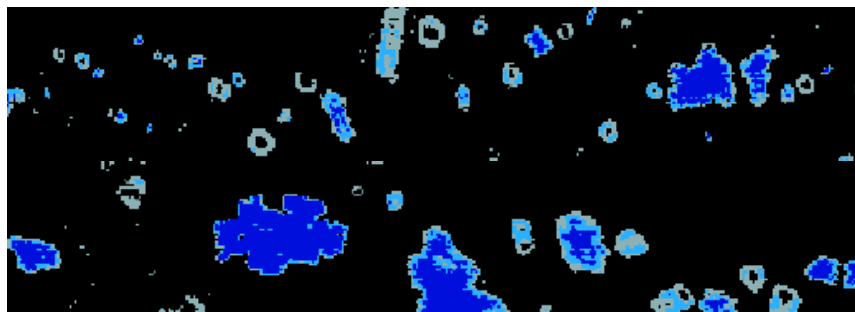
Figure 2. Example of image taken with CIP-Greyscale probe, particle sizes found on the picture are between 25- 850 µm.

ACKNOWLEDGEMENTS

REFERENCES

Vavrus, S. (2004), J. Climate, **17**, 603-615

Komppula, M., H. Lihavainen, V.-M. Kerminen, M. Kulmala, and Y. Viisanen (2005), J. Geophys. Res., **110**, D06204.

Schwarzenboeck, A, V. Shcherbakov, R. Lefevre, J.-F. Gayet, Y. Pointin, and C. Duroure, (2009), Atmos. Res. **92,** 220-228.

THERMODENUDER EXPERIMENTS FOR THE DETERMINATION OF THE SIZE DEPENDENT ORGANIC FRACTION OF SEA SPRAY AEROSOL

A.C. BUTCHER[1], S.M. KING[1,*], T. ROSENOERN[2], and M. BILDE[1]

[1] Copenhagen Center for Atmospheric Research, Department of Chemistry, University of Copenhagen, Denmark

[2]FORCE Technology, Park Allé 345, 2605 Brøndby

*Now at Haldor Topsoe, Lyngby, Denmark

INTRODUCTION

Sea spray aerosols play an important role in the Earth's climate system, representing a significant fraction of the total mass of aerosol in the atmosphere Seinfeld and Pandis (2006). Information on the chemical composition of these aerosols has been probed in previous studies Claeys et al. (2010); Rinaldi et al. (2010); O'Dowd et al. (2004); Kawamura et al. (2003) but the resolution has been limited to the cut-off diameter of the sampling instruments, to both secondary and primary aerosols sampled, and a large chemical matrix. Recent work focusing on the organic fractions of laboratory produced sea spray aerosols (SSA) from various groups has led to a characterization of the effects of organics on the CCN activity King et al. (2012); Fuentes et al. (2010); Moore et al. (2011); Wex et al. (2010). While these studies have elucidated the role of organics in the modification of the CCN properties of primary marine aerosols, little information has been elucidated on the preference of certain organic species to enter the aerosol phase via bubble bursting processes. We present preliminary results of a novel measurement system in the field of primary marine aerosols which consists of a thermodenuder (TD) operating with same principle as a VH-TDMA.

METHODS

For this study we present initial results of organic/inorganic mixtures to test our assumptions of fully evaporated and denuded organic components of laboratory generated aerosols. With this first phase complete, chemical compositions similar to those used in the atomizer will be introduced in a laboratory SSA tank where SSA are generated via bubble bursting at a simulated sea-air interface King et al. (2012). In principle, a plunging jet, which is similar to the plunging jet observed in a plunging breaker Deane and Stokes (2002), is continuously impacted on the surface of a sample solution, entraining bubbles which rise and burst on the surface releasing aerosols. Since aerosols produced by Continuous atomization will have the same composition as the atomized solution, the differences in aerosols produced via bubble bursting and continuous atomization will indicate which organic species are enriched in the aerosol phase relative to the tank solution. In addition, the CCN activity of aerosols produced via bubble bursting both before and after the TD will be measured to reinforce previous results King et al. (2012).

The aerosols generated, either by atomization or bubble bursting, are dried, size selected using DMA #1 (TSI 3080), passed through a TD, and finally an SMPS. Aerosols observed to decrease in Geometric Mean Diameter, measured as the difference between the inlet DMA mobility diameter and the geometric mean of the sample collected by the SMPS system at the outlet, are assumed to

have lost organic material in the TD. The change in diameter is then used to calculate the volume of inorganics remaining in the aerosol sample which also gives the size dependent fraction of organic material for the aerosol if the mobility diameter of aerosols introduced to the TD is varied at fixed temperatures. The TD employed in this study was produced by TOPAS GmbH (model TDD 590) and is designed to be operated with flows from 1-3 L min^{-1}. The residence time in the heating section, L = 143.5 cm, D = 12.7 mm, for 1 L min^{-1} flow is 1.0 s, while the residence time in the denuding section is approximately 4.4 s. Temperature ranges of 25 °C (298 K) to 400 °C (673 K) were tested.

A solution of 60.7 mg NaCl (Sigma Aldrich) and 62.7 mg Fructose ($C_6H_{12}O_6$, Fluka) in approximately 700 mL of Milli-Q Ultrapure De-ionized water was aerosolized in a TSI 3076 constant output atomizer. The aerosol sample was then directed through two diffusion driers (TSI), followed by a Kr-85 bi-polar charger, size selected by a TSI 3081 DMA (10:1 sheath to aerosol ratio) passed through the TOPAS TD at different temperatures, and finally sampled by a TSI SMPS. A second solution was prepared in the atomizer consisting of 37 mg NaCl (Sigma Aldrich) and 37 mg Sodium Laurate (NaLa, Lauric Acid Salt, $C_{12}H_{23}NaO_2$, Fluka) and a similar stepping of temperature and mobility diameter was performed.

A solution of 100 g NaCl and 1 g Sodium Laurate were prepared in 10 L of Milli-Q Ultrapure water in the SSA tank of King et al. (2012). A similar aerosol sampling system was devised as for the atomizer experiments with additional sweep air exhausted to achieve 1 L min^{-1} flow rates through the TD. The plunging jet system was used with a nozzle of 4 mm diameter, corresponding to a flow rate of 4.5 L min^{-1}.

<div align="center">RESULTS</div>

Results for the atomized NaCl and Fructose solution are given in Table 1. The first diameter D_1 indicates the diameter selected by DMA #1. The measured diameter, D_2, represents the geometric mean diameter of the aerosol population exiting the thermodenuder. Assuming NaCl is the only remaining constituent of the aerosol, the mass of the organic that has evaporated is calculated baed on the density of NaCl and the organic.

D_1 (nm)	D_2 (nm)	V_1 (nm^3)	V_2 (nm^3)	Volume % Remaining	Organic Mass Fraction
25	18.75	8.18×10^3	3.45×10^3	42 %	0.44
50	36.98	6.55×10^4	2.65×10^4	40 %	0.46
100	73.22	5.24×10^5	2.06×10^5	39 %	0.57

Table 1: Atomizer experiments with NaCl and Fructose indicating a loss of material through the thermodenuder (set to 200°C). The original mass fraction of organic to total mass of solute the atomizer was 0.508 (Fructose:NaCl).

The results for the experiment with a solution of NaCl and Sodium Laurate (NaLa) in the atomizer are shown graphically in Figure 1. For all diameters selected by DMA #1 a decrease in particle diameter with increasing TD temperature is observed. The diameter decrease is most pronounced for 100 nm particles when the TD was operated at 400 °C indicating a decrease in diameter of 33 %, while the smallest diameter decrease for the same temperature is measured for 30 nm particles where only 30 % of the particle is lost. The decrease in particle diameter may indicate the loss of organics during transit through the TD. A sample calculation of the volume change of the 100 nm particles indicates that the volume decreases by 70 %. Assuming the two constituents did not disrupt the crystalline structure of the other, a density of NaCl of 2.1 g cc^{-1} and a density of NaLa

of 1 g cc^{-1}, the mass fraction of organic for 100 nm particles is 52.4 wt. %. This is within the range of experimental error to the expected result of 50 % based on the solution in the atomizer.
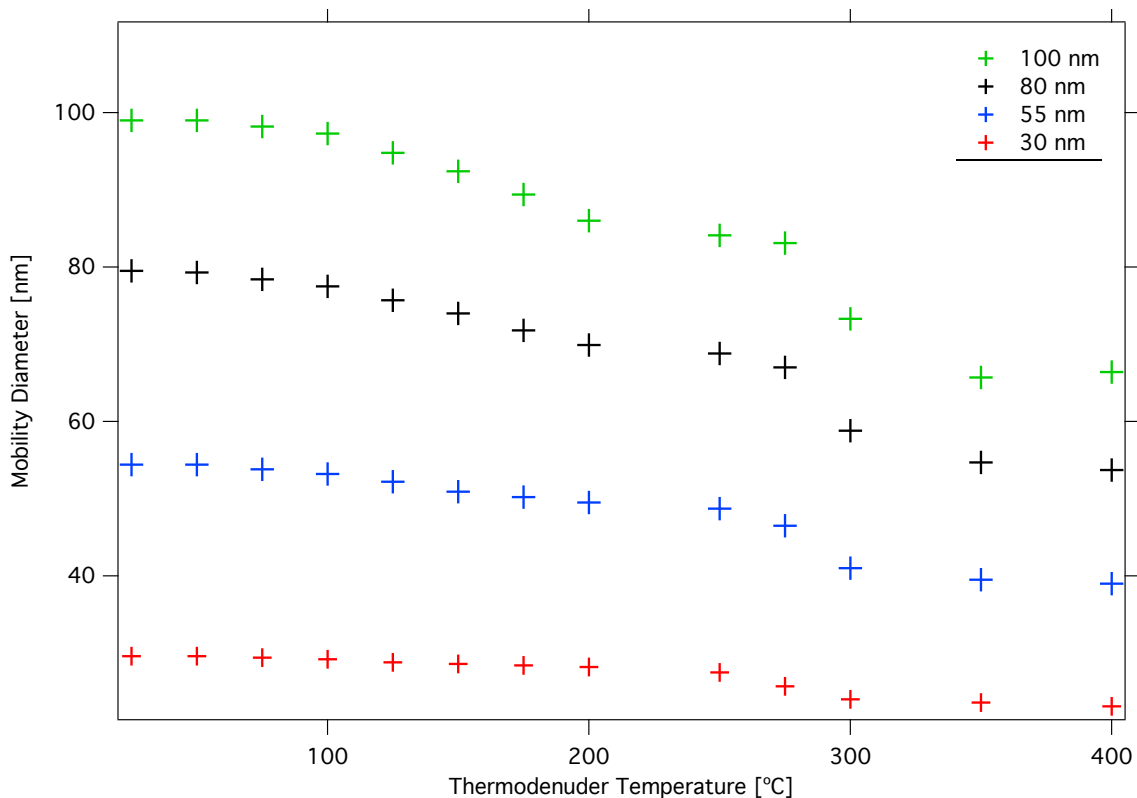
Figure 1: Series of temperature profiles for mobility selected diameters of aerosol produced from an atomizer containing a 50:50 solution of NaCl and NaLa.

The data indicates that sodium laurate volatilizes from aerosols generated from a mixture of sodium laurate and sodium chloride at roughly 350 °C (623 K) as indicated by a slight leveling off of the diameter in Figure 1. Seddon and Wood (1986) found that sodium dodecanoate (sodium laurate) lost 71.8 % of it's initial mass in the temperature range of 373-821 K using a Thermobalance while the residual was characterized as carbonaceous. This would indicate that thermodenuder evaporation studies must take into account the evaporation kinetics of the organic compound of interest. If the volatilization point of the organic compound of interest is higher than the maximum temperature of the TD or if complexes of organic:inorganics of higher volatilization are formed.

The results for the aerosol composition from the SSA tank are shown in Table 2. The results indicate a clear enrichment of the aerosols at 55 nm in organics, with the highest organic fractions found at higher TD temperatures where more organic has thermodenuded. The enrichment factor, or the ratio of organics to salts in the aerosol pause to that found in the parent bulk solution, for 300 °C TD temperatures is EF = 58.8. The effects of a char compound left over on the aerosol and perhaps a higher evaporating temperature need to be taken into account of a future error analyses.

Temperature ($^\circ$C)	D_2 (nm)	V_2 (nm^3)	Volume % Remaining	Organic Mass Fraction
25	54.08	8.28×10^4	100 %	0.00
250	48.76	6.07×10^4	73.3 %	0.148
350	34.24	2.10×10^4	25.3 %	0.583

Table 2: SSA tank experiment results for a solution of NaLa and NaCl (1:100 mass ratio, 0.01 (wt/wt) organic). DMA #1 was set to 55 nm giving a Geometric Mean Diameter in the SMPS after the TD at 25 $^\circ$C of 54.08 nm. DMA #1 remained set to 55 nm while the TD was set to 250 $^\circ$C and 300 $^\circ$C.

CONCLUSIONS

Preliminary results are presented for experiments with two solutions of organic and inorganic compounds which have been atomized and bubbled and then passed through a thermodenuder. The fraction of material remaining after passing through the TD for Fructose and NaCl mixtures for initial diameters of 25 nm, 50 nm, and 100 nm were 42%, 40%, and 39%, respectively. For experiments with Sodium Laurate and NaCl, similar results were obtained with higher temperature resolution, although for a 50:50 mixture of organic:inorganic. The results of the NaLa: NaCl experiment show that 70% of the original particle volume remains after transit through the TD, which corresponds to the 50:50 mixture of organics:inorganics in the atomizer solution within 2.5 %, which is within experimental error. The results for the SSA tank indicate that this method is sensitive to the organic enrichment of aerosols of approximately 55 nm, showing an enrichment of at least 58. These results are encouraging for further studies using the TD to investigate the organic fraction from our SSA tank, however the results will have to be analyzed for the possibility of aerosols not fully volatilizing which would affect the results significantly.

ACKNOWLEDGEMENTS

REFERENCES

Claeys, M., Wang, W., Vermeylen, R., Kourtchev, I., Chi, X., Farhat, Y., Surratt, J. D., Gómez-González, Y., Sciare, J., and Maenhaut, W. (2010). Chemical characterisation of marine aerosol at amsterdam island during the austral summer of 2006–2007. *Journal of Aerosol Science*, 41(1):13 – 22. Special Issue for the 9th International Conference on Carbonaceous Particles in the Atmosphere.

Deane, G. B. and Stokes, M. D. (2002). Scale dependence of bubble creation mechanisms in breaking waves. *Nature*, 418:839–844.

Fuentes, E., Coe, H., Green, D., de Leeuw, G., and McFiggans, G. (2010). On the impacts of phytoplankton-derived organic matter on the properties of the primary marine aerosol – Part 1: Source fluxes. *Atmospheric Chemistry and Physics*, 10(19):9295–9317.

Kawamura, K., Ishimura, Y., and Yamazaki, K. (2003). Four years' observations of terrestrial lipid class compounds in marine aerosols from the western north pacific. *Global Biogeochem. Cycles*, 17(1).

King, S. M., Butcher, A. C., Rosenoern, T., Coz, E., Lieke, K. I., de Leeuw, G., Nilsson, E. D.,

and Bilde, M. (2012). Investigating primary marine aerosol properties: CCN activity of sea salt and mixed inorganic–organic particles. *Environmental Science & Technology.*

Moore, M. J., Furutani, H., Roberts, G. C., Moffet, R. C., Gilles, M. K., Palenik, B., and Prather, K. A. (2011). Effect of organic compounds on cloud condensation nuclei (ccn) activity of sea spray aerosol produced by bubble bursting. *Atmospheric Environment*, 45(39):7462 – 7469.

O'Dowd, C. D., Facchini, M. C., Cavalli, F., Ceburnis, D., Mircea, M., Decesari, S., Fuzzi, S., Yoon, Y. J., and Putaud, J.-P. (2004). Biogenically driven organic contribution to marine aerosol. *Nature*, 431(7009):676–680.

Rinaldi, M., Decesari, S., Finessi, E., Giulianelli, L., Carbone, C., Fuzzi, S., O'Dowd, C. D., Ceburnis, D., and Facchini, M. C. (2010). Primary and secondary organic marine aerosol and oceanic biological activity: Recent results and new perspectives for future studies. *Advances in Meteorology*, 2010:1–10.

Seddon, A. B. and Wood, J. A. (1986). Thermal studies of heavy metal carboxylates: II. thermal behaviour of dodecanoates. *Thermochimica Acta*, 106(0):341–354.

Seinfeld, J. H. and Pandis, S. N. (2006). *Atmospheric Chemistry and Physics - From Air Pollution to Climate Change (2nd Edition)*. John Wiley & Sons.

Wex, H., Fuentes, E., Tsagkogeorgas, G., Voigtländer, J., Clauss, T., Kiselev, A., Green, D. H., Coe, H., McFiggans, G., and Stratmann, F. (2010). The influence of algal exudate on the hygroscopicity of sea spray particles. *Advances in Meteorology*, 2010:1–11.

CCN ACTIVATION OF INSOLUBLE SILICA AEROSOLS
COATED WITH SOLUBLE POLLUTANTS

M. DALIRIAN[1], H. KESKINEN[2], P. MIETTINEN[2], A. VIRTANEN[2], A. LAAKSONEN[2] and
I. RIIPINEN[1]

[1] Department of Applied Environmental Science (ITM) and Bert Bolin Centre for Climate research,
Stockholm University
[2] Department of Applied Physics, University of Eastern Finland (Kuopio campus)

Keywords: silica, coating, CCN activation

INTRODUCTION

Clouds are an important component of the Earth's radiation budget and hydrological cycle. Even small changes in cloud properties may have significant impacts on climate. According to the Intergovernmental Panel on Climate Change (IPCC, 2007), aerosol-cloud interactions represent the largest single uncertainty in predictions of future climate. Insoluble atmospheric particles, like mineral dust, soot and silica, can also act as efficient cloud condensation nuclei if they acquire some amount of deliquescent material. In recent years, some studies have been done on CCN activation of insoluble particles. Sorjamaa and Laaksonen (2007) studied cloud droplet activation of wettable insoluble compounds by assuming that droplet growth happens through multilayer adsorption. They combined adsorption isotherms and traditional Köhler theory to describe the equilibrium growth of insoluble particles and to find out their critical saturation ratios. Kumar et al. (2009) developed a cloud droplet formation parameterization where the CCN constitutes an external mixture of soluble aerosol (that follows Köhler theory) and insoluble aerosol (that follows FHH (Frenkel, Halsey and Hill) adsorption activation theory, FHH-AT). Kumar et al. (2011a) reported laboratory measurements of CCN activity and droplet activation kinetics of aerosols dry generated from clays, calcite, quartz, silica and desert soil samples. They used FHH adsorption activation theory for describing fresh dust CCN activity. Kumar et al. (2011b) studied particle size distributions, CCN activity, and droplet activation kinetics of wet generated aerosols from mineral particles.

In this study, laboratory measurements were conducted on the particle size distribution and CCN activation of insoluble silica particles coated with soluble and slightly soluble pollutants. The experimental results were analysed and compared to the theoretical calculations using the framework introduced by Kumar et al. (2011b).

MEASUREMENTS

Particles with insoluble core and soluble coating were generated and analysed in this study. Fumed silica (SiO_2, AEROSIL-90) was used as the insoluble particle. Three different kinds of species were used as soluble coatings: a salt (ammonium sulphate), a sugar (sucrose) and a protein (bovine serum albumin known as BSA). Particles were produced using the method introduced by Keskinen et al. (2011). The solid content (SiO_2+soluble coating) in the water suspension was set to 0.06 wt%. The ratios of coated component to silica were 1:19, 1:9 and 1:3, so soluble species were supposed to form 5%, 10% and 25% of total mass of the particles. Particle number distribution measurements were conducted using a

scanning mobility particle sizer (SMPS). The CCN instrument measures aerosol particles that can form cloud droplets. Size-resolved CCN activity is carried out using the Scanning Mobility CCN Analysis (SMCA), where the DMA used for aerosol classification is operated in scanning voltage mode with dry particle diameters from 30 to 200 nm in supersaturation (SS) range from 0.1 to 1.5.

THEORY

κ-Köhler theory (Petters & Kreidenweis, 2007) was used to estimate the critical supersaturation of pure ammonium sulphate, sucrose and BSA species. Critical supersaturation of pure silica particles, on the other hand, were calculated using the FHH adsorption theory (Sorjamaa and Laaksonen, 2007 and Kumar et al., 2009 & 2011a). For mixed soluble and insoluble particles Kumar et al. (2011b) introduced a shell-and-core model with the core representing insoluble dust and shell consisting of a layer of soluble salt. In this case the relationship between water saturation ratio S and particle size and composition can be expressed as:

$$s = \frac{4\sigma_w M_w}{RT\rho_w D_p} - \frac{\varepsilon_s D_{dry}^3 \kappa}{(D_p^3 - \varepsilon_i D_{dry}^3)} - A_{FHH}\left(\frac{D_p - \varepsilon_i^{1/3} D_{dry}}{2D_{H_2O}}\right)^{-B_{FHH}} \tag{4}$$

In which s is the saturation ratio, σ_w is the water surface, ρ_w is the water density, M_w is the molar mass of water, R is the universal gas constant, T is the temperature, D_{dry} is the dry particle diameter, D_p is the droplet diameter, D_{H2O} is the diameter of water molecule, κ is the hygroscopicity parameter of soluble particles, ε_i and ε_i are the insoluble and soluble volume fractions in the dry particle and A_{FHH} and B_{FHH} are the FHH adsorption isotherm parameters.

PRELIMINARY RESULTS

Aerosol particle size distributions

The SMPS measurements yielded the number size distributions for silica particles coated with $(NH_4)_2SO_4$, sucrose and BSA. Figure 1 shows the size distribution of particles made of pure fumed silica, pure sucrose and particles made of silica and different coating amounts of sucrose. Particles made of pure sucrose have a mean diameter of about 50 nm, and the particles made of pure silica around 100 nm. For the silica particles coated with different amounts of sucrose the size distribution show two peaks, one at less than 30 nm and the second one at around 150 nm.
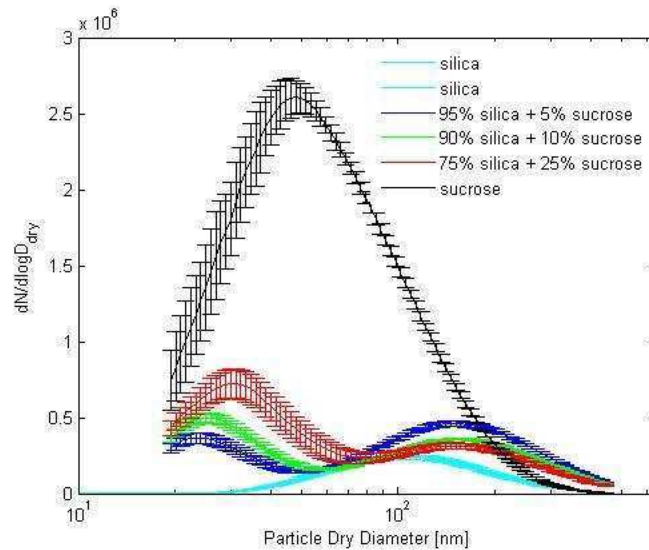
Figure 1: SMPS data on the number size distributions of silica particles coated with sucrose.

Particles which remained in the first peak of bimodal distribution curves are likely pure soluble particles, since their mean diameter is smaller than that of the pure silica particles. We therefore conclude that the second peak of the bimodal distribution curves represent the silica particles coated with the soluble species.

We calculated estimates on the coating thicknesses based on the SMPS results. For these calculations, we first assumed that all silica particles were coated and there were no pure soluble particles – thus yielding the maximum estimates for the coating thicknesses. The calculated coating thicknesses for the above assumption are presented in table 1 for particle with the dry diameters of 100, 150 and 250 nm. From a comparison with calculated coating thicknesses it became evident that a more careful treatment, accounting for the fraction of soluble material that formed pure particles instead of coating the silica, is needed (see Table 2 below). This is one of the next steps of the study.

Soluble mass fraction	$SiO_2+(NH_4)_2SO_4$			SiO_2+sucrose			SiO_2+BSA		
	$D_{dry} =$ 150nm	$D_{dry} =$ 200nm	$D_{dry} =$ 250 nm	$D_{dry} =$ 150nm	$D_{dry}=$ 200nm	$D_{dry} =$ 250 nm	$D_{dry} =$ 150nm	$D_{dry} =$ 200nm	$D_{dry} =$ 250 nm
25%	16.1	21.5	26.9	17.6	23.4	29.3	19.8	26.4	33.0
10%	6.2	8.3	10.4	6.9	9.2	11.5	7.9	10.5	13.2
5%	3.1	4.1	5.1	3.4	4.5	5.7	3.9	5.3	6.6

Table 1: Calculated coating thicknesses (in nm) assuming that all soluble material is distributed on top of the silica particles.

CCN activation results

Kumar et al. (2011a) (quartz silica) and Keskinen et al. (2011) (Fumed silica, AEROSIL-300) suggested quite different values for FHH adsorption parameters of silica. To compare our results (Fumed silica, AEROSIL-90) of the pure silica activation to these studies, we fitted the FHH adsorption parameters of silica. A_{FHH} and B_{FHH} values of 2 and 1.43 explained our results on the activation diameter vs. critical supersaturation (Fig. 2), although the fits were difficult to constrain uniquely. The results do indicate, however, that our results are a bit better in line with the work of Kumar et al. (2011a) than Keskinen et al. (2011). The main differences are most probably caused by different silica material used in each study (Figure 2). The experimental results showed that critical supersaturation of pure silica doesn't have the behavior as it was expected in calculations and in lower diameter (less than 150 nm) its relation with particles dry diameter is nonlinear. The reason for this apparent discrepancy between our experimental results and the FHH theory at the small particle sizes is not clear and a subject for further investigation.
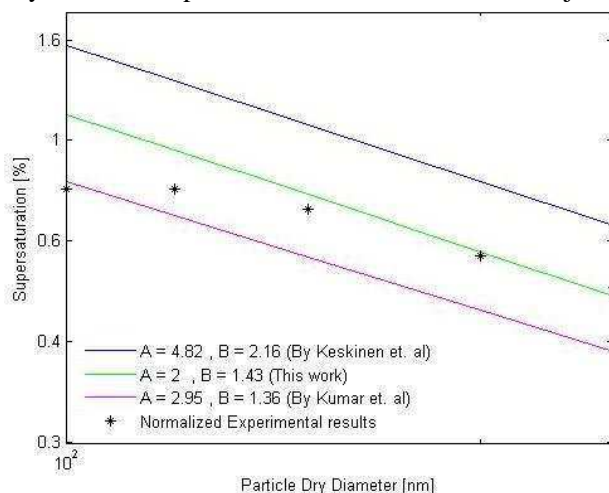
Figure 2: Critical supersaturations and activation diameters of pure silica particles with different FHH adsorption isotherm parameters.

For estimating the critical supersaturation of pure soluble particles, κ-Köhler theory was used. Lots of studies have been done on CCN properties of pure ammonium sulphate. So in this study we only investigated the CCN properties of pure sucrose and BSA particles. The calculated and experimental values of critical supersaturations of pure BSA and sucrose particles are shown in Fig. 3. κ-Köhler theory gave good results with the CCN activation of pure BSA and sucrose particles. The κ values for sucrose and BSA were calculated by the relation introduced by Petters & Kreidenweis (2007) using the observed pure soluble particles critical supersaturations obtained from the experiments. The estimated κ values for ammonium sucrose and BSA are 0.084 and 0.012, respectively.
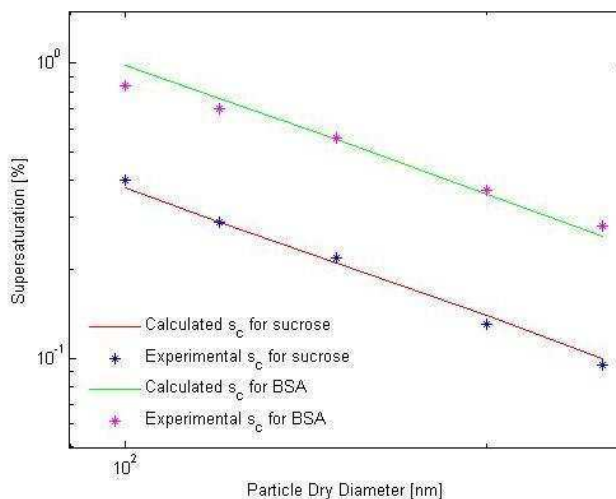
Figure 3: Critical supersaturation of pure sucrose and BSA particles in different diameters

As it was described in the previous part, most of the silica particles coated with $(NH_4)_2SO_4$, sucrose and BSA had mean diameters of around 150 nm. Theoretically, the coated particles had a maximum 5%, 10% or 25% of soluble coating. However, as it was described before, the SMPS data revealed that some particles were made of pure soluble species.

Particle composition	150 nm			200 nm			250 nm		
	calc. Sc	exp. Sc	AAD%	calc. Sc	exp. Sc	AAD%	calc. Sc	exp. Sc	AAD%
100% silica	0. 76	0.73	3.56	0.59	0.6	2.33	0.48	0.51	5.31
100% $(NH_4)_2SO_4$	0.071	-	-	0.052	-	-	0.037	-	-
25% $(NH_4)_2SO_4$, 75% silica	0.22	0.42	47.62	0.145	0.369	60.70	0.105	0.28	62.5
10% $(NH_4)_2SO_4$, 90% silica	0.3	0.46	34.782	0.2	0.39	48.72	0.145	0.33	56.06
5% $(NH_4)_2SO_4$, 95% silica	0.21	0.22	4.54	0.138	0.13	6.15	0.099	0.095	4.21
100% sucrose	0.21	0.22	4.55	0.14	0.13	6.15	0.1	0.095	4.21
25% sucrose , 75% silica	0.35	0.3	17.00	0.23	0.25	6.4	0.17	0.206	17.48
10% sucrose , 90% silica	0.48	0.44	9.32	0.33	0.38	12.89	0.25	0.31	20.97
5% sucrose , 95% silica	0.58	0.54	6.48	0.41	0.47	12.98	0.31	0.38	18.42
100% BSA	0.55	0.56	2.5	0.36	0.37	2.7	0.26	0.28	7.14
25% BSA , 75% silica	0.651	0.59	10.34	0.41	13.42	0.354	0.35	0.37	4.32
10% BSA , 90% silica	0.705	0.61	15.574	0.51	2.74	0.413	0.41	0.46	10.22
5%BSA , 95% silica	0.728	0.67	8.66	0.55	0.36	0.442	0.44	0.49	9.8

Table 2: experimental and estimated critical supersaturations (S_c) for 150, 200 and 250 nm particles made of pure and coated materials, assuming complete coating with all available soluble material. AAD is the average absolute deviation of the experimental and theoretical supersaturations.

In table 2, the estimated critical supersaturations of 150, 200 and 250 nm particles made of pure silica and pure soluble materials (calculated with the approach by Kumar et al., 2011) and particles made of silica and 5, 10 and 25% soluble species have been presented compared to results obtained from the experiments. The comparison between the experimental and calculated critical supersaturations showed that the theoretical values were systematically lower than the experimental ones. In fact, the average absolute deviation for coated particles is much more than the pure ones and in most cases by increasing the coating thickness the deviation is increasing. However here, we have overestimated the theoretical coating thicknesses by ignoring the separate mode of pure soluble particles (Figure 1) in calculations.

During the studies, the activation ratio curves (the ratio of cloud condensation nuclei to condensation nuclei) were prepared for particles with the dry diameters of 100, 120, 150, 200 and 250 nm and different ratios of soluble to insoluble materials.

Figure 4 represents the activation probabilities of silica particles coated with BSA. The coated particles behave similarly as the particles coated by $(NH_4)_2SO_4$ and sucrose: The activation diameter at a given supersaturation getting smaller with an increasing fraction of soluble material. The pure $(NH_4)_2SO_4$ and sucrose particles activated at a lower supersaturations than the coated particles – as predicted by the theory as well. In the case of pure BSA, however, different behaviour was observed: The pure BSA particles started to activate at higher supersaturations for a given particle size than the coated ones (see Fig, 4).The reason for this behaviour is not clear, but it has been shown that adsorption of BSA on the silica can affect the structural properties of BSA (Larsericsdotter et al., 2005).This might cause coated particles activate at lower supersaturations than the pure ones.
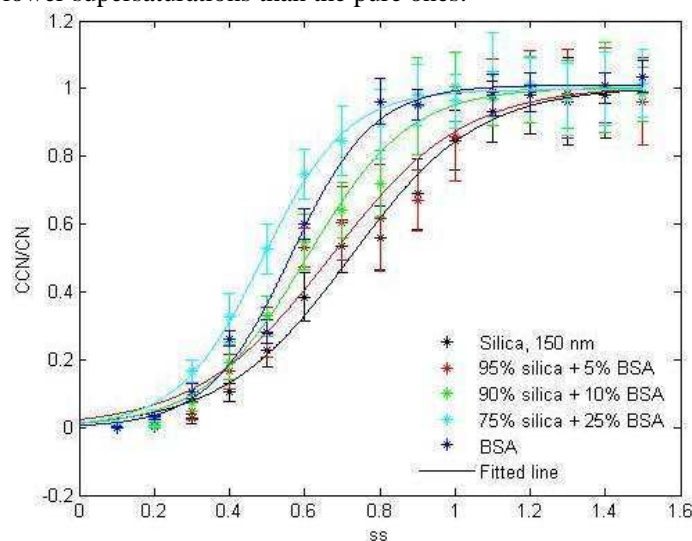
Figure 4: Activation ratios vs. supersaturation for silica + BSA particles of 150 nm dry diameter.

CONCLUSIONS

We measured the particle size distribution and CCN activation of insoluble fumed silica particles coated with $(NH_4)_2SO_4$, sucrose and BSA with an SMPS. Results showed that the size distributions of pure particles formed unimodal distribution curves, while the coated particles distributions behave as bimodal distribution curves. The SMPS measurements showed that the some of the particles consisted of pure soluble materials and the diameters of these particles were less than 100 nm. Also, some of the silica particles might remain uncoated but it couldn't be defined directly by SMPS experiments.

The CCN activity measurements were conducted in various supersaturations up to 1.5 and activation ratio curves were prepared for particles with the dry diameters of 100, 120, 150, 200 and 250 nm and different ratios of soluble to insoluble materials. The experimental data were compared to theoretical predictions using the FHH adsorption theory (e.g. Sorjamaa and Laaksonen, 2007) for the pure silica particles, the κ-Köhler theory (Petters and Kreidenweis, 2007) for the pure soluble particles, and the

combination of these two (Kumar et al., 2011a) for the coated particles. The first estimates on the coating thicknesses needed in the calculations were obtained by assuming that all the soluble material was distributed onto the insoluble silica particles.

The pure soluble particles, specifically sucrose and BSA, followed the predictions of κ-Köhler theory. The pure silica, however, showed a deviation from the FHH theory at particle sizes below 200 nm. The reason for this deviation is not clear and needs further investigation.

For the coated particles, at particle sizes > 150 nm the experiments showed that by increasing the thickness of soluble coating of the particles activated at lower supersaturations. In the case of BSA, however, abnormalities were observed. The pure BSA particles activated at higher supersaturations than the coated ones. Because of adsorption of BSA molecules by silica particles, their structural stability could have been influenced and it could be a reason for the different activation behaviour of coated particles compared to the pure BSA. Curiously, ammonium sulphate and sucrose showed similar behavior at the small (< 150 nm) particle diameters. The reason for this behaviour needs further investigation.

The next steps of this study include a more accurate calculation of the coating thicknesses based on the SMPS data, accounting for the formation of the separate mode of soluble particles. This proved to be critical for meaningful comparisons of theoretical and experimental data on the activation behaviour of the coated particles. Additionally, Transmission Electron Microscope (TEM) will be used to find out the structure of the particles and their effect on the size-dependence of the CCN activation behaviour of pure silica as well as the coated particles.

ACKNOWLEDGEMENTS

REFERENCES

Alley, R.B., Berntsen, T.,Bindoff, N.L., Chen, Z., Chidthaisong, A., Friedlingstein, P., Gregory, J.M., Hegerl, G.C., Heimann, M. and … , (2007), Summary for Policymakers, A report of Working Group I of the Intergovernmental Panel on Climate Change.

Keskinen, H., Romakkaniemi, S., Jaatinen, A., Miettinen, P., Saukko, E., Joutsensaari, J., Mäkelä, J.M., Virtanen, A., Smith, J.N. and Laaksonen, A., (2011), On-Line Characterization of Morphology and Water Adsorption on Fumed Silica Nanoparticles, Aerosol Science and Technology, 45,1441.

Kumar, P., Sokolik, I. N., and Nenes, A., (2009), Parameterization of cloud droplet formation for global and regional models: including adsorption activation from insoluble CCN, Atmos. Chem. Phys., 9, 2517.

Kumar, P., Sokolik, I. N., and Nenes, A., (2001a), Measurements of cloud condensation nuclei activity and droplet activation kinetics of fresh unprocessed regional dust samples and minerals, Atmos. Chem. Phys., 11, 3527.

Kumar, P., Sokolik, I. N., and Nenes, A., (2001b), Cloud condensation nuclei activity and droplet activation kinetics of wet processed regional dust samples and minerals, Atmos. Chem. Phys., 11, 8661.

Larsericsdotter, H., Oscarsson, S., Buijs, J., (2005), Structure, stability, and orientation of BSA adsorbed to silica., J Colloid Interface Sci., 289(1), 26.

Petters, M. D. and Kreidenweis, S. M. (2007), A single parameter representation of hygroscopic growth and cloud condensation nucleus activity, Atmos. Chem. Phys., 7, 1961.

Sorjamaa, R. and Laaksonen, A.(2007). The effect of H2O adsorption on cloud drop activation of insoluble particles: a theoretical framework, Atmos. Chem. Phys., 7, 6175.

USING SATELLITE DATA TO CREATE AEROSOL ESSENTIAL CLIMATE VARIABLES

G. DE LEEUW[1,2], T. HOLZER-POPP[3], P. KOLMONEN[2], L. SOGACHEVA[2] AND T.H. VIRTANEN[2]

[1]Department of Physics, University of Helsinki, Finland
[2]Finnish Meteorological Institute (FMI), Helsinki, Finland
[3]Deutsches Zentrum für Luft- und Raumfahrt (DLR), Deutsches Fernerkundungsdatenzentrum, Oberpfaffenhofen, Germany.

Keywords: Satellite remote sensing, Aerosols, ECV.

INTRODUCTION

Aerosol retrieval using satellite data was introduced at the Department of Physics of the University of Helsinki and the Finnish Meteorological Institute (FMI) in 2007. The instrument used is the Advanced Along Track Scanning Radiometer (AATSR) which was launched on the European Space Agency (ESA) Environmental Satellite ENVISAT in March 2002 and provided data until 6 April 2012 when contact with the satellite was lost. AATSR and its predecessor ATSR-2 (Along Track Scanning Radiometer) on ERS-2 were initially designed for measurements of land and sea surface temperatures. However, both instruments have two views (nadir and 55° forward) which, together with its seven wavebands at wavelengths from the visible to the thermal infrared, render it very suitable for aerosol retrieval over land (Veefkind et al., 2008a,b). Algorithms to achieve this were developed at the Netherlands Organisation for Applied Scientific Research TNO (Veefkind et al., 2008a,b, 2000; Robles-Gonzalez et al., 2000, 2003, 2006, 2008; Schmid et al., 2003) and transferred to Helsinki in 2007. The algorithms used are the dual view algorithm (ADV) used over land (Veefkind et al., 1998a; Curier et al., 2009; Kolmonen et al., 2012) and the single view algorithm used over water (Veefkind et al., 1998b; Kolmonen et al., 2012). After initial implementation problems a long period followed in which the algorithms were substantially improved and applied in a range of studies including forest fires (Sundström et al., 2008, 2009b; Sogacheva et al., 2011), absorbing aerosol (Sundström et al., 2009b) , AOD over Finland (Sogacheva et al., 2008) and the Boreal forest (Sogacheva et al., 2010b), the synergistic use of AATSR and MERIS for aerosol retrieval over ocean (Sogacheva et al., 2009) an studies over China (Sundström et al., 2010a; 2011a; 2012a; b), India (Sundström et al., 2010b, c; 2011) and Africa (Sogacheva et al., 2010a) estimates of the direct radiative effect of aerosol (Sundström et al., 2011b; 2012c), model evaluation (Hannukainen et al., 2011a), Volcanic ash detection (Virtanen et al., 2012a; b), Megacities studies (Rodriguez et al., 2010a; b; c; Hannukainen et al., 2011b; Beekmann et al. 2012), determination single scattering albedo (ssa) and surface albedo (Rodriguez, 2012a; b).

In this contribution we describe work undertaken to prepare for the use of satellite data to produce essential climate variables (ECVs) for aerosols, in particular the aerosol optical depth (AOD). Focus will be on work by the UHEL/FMI team using data from the Advanced Along track Radiometer (AATSR) flying on the European Space Agency (ESA) environmental satellite ENVISAT (2002-2012). This work contributes to Aerosol-cci project funded by the European Space Agency (ESA) as part of the ESA climate change initiative (CCI).

ESA CLIMATE CHANGE INITIATIVE

The goal of the ESA climate change initiative (CCI) is to produce essential climate variables (ECV) using satellite data, following requirements formulated by GCOS and potential users (mainly the climate modelling community). The ECVs cover 13 different areas, divided in three topics: atmosphere (aerosols, clouds, greenhouse gases, ozone), ocean and land. The focus is on the use of European satellites, but other satellites are used as needed. The ECVs are produced for use by the climate change community which is

involved in the initiative as advisors represented by the Climate Change User Group (CMUG), a consortium comprising the Met Office Hadley Centre, the Max Planck Institute for Meteorology, ECMWF and Météo-France. For more information see http://www.esa-cci.org/.

THE AEROSOL-CCI PROJECT

The Aerosol-cci project is a consortium including 14 partners coordinated by DLR and FMI providing the science co-leader. The consortium consists of three teams. The EO team is responsible for algorithm development and improvement, the validation team is responsible for the validation and evaluation of the retrieval products, and the system engineer team is responsible for the actual processing of the data series and system design. The validation team is independent from the EO team (different partners) which ensures an independent and unbiased evaluation of the EO products. Furthermore, the validation team includes representatives of the global climate modelling community through AEROCOM and their feedback ensures that products will indeed be useful for them. This aspect has proven to be of crucial value for the improvement of the retrieval algorithms. The system engineering team brings the experience of data centres and experience with data format and data access. The Aerosol-cci project started in July 2010 and has a duration of 3 years with a potential extension to 6 years.

AEROSOL RETRIEVAL ALGORITHMS

The aerosol retrieval algorithms included in the Aerosol-cci project use data from the Advanced Along Track Scanning Radiometer (AATSR), the MEdium Resolution Imaging Spectrometer (MERIS) both flying on ESA's Environmental satellite ENVISAT (2002-2012) and POLarization and Directionality of the Earth's Reflectances (POLDER / PARASOL) part of NASA's A-train constellation. Aerosol-cci includes both algorithms using one single instrument as well as synergistic use of two instruments (SYNAER). These algorithms provide information on column integrated aerosol properties such as AOD. In addition, the Ozone Monitoring Instrument (OMI) provides information on the aerosol absorbing index (AAI) and the Global Ozone Monitoring by Occultation of Stars (GOMOS) provides information on stratospheric aerosol profiles. The algorithms included in Aerosol-cci and the institutes developing these are:
- AATSR ADV (FMI / Univ. Helsinki)
- AATSR ORAC (Oxford University / RAL)
- AATSR SU (Swansea University)
- AATSR+SCIAMACHY SYNAER (DLR)
- MERIS standard (testing by HYGEOS)
- MERIS ALAMO (ocean only, HYGEOS; complimentary retrieval)
- MERIS BAER (Univ. Bremen)
- PARASOL (ocean only; LOA)

- OMI AAI (KNMI)
- GOMOS stratospheric extinction profile (BIRA)

The initial focus of the Aerosol-cci project was on understanding differences between different algorithms as a basis for their improvement. The baseline algorithms were those that existed at the start of the project and improvements were measured with respect to these, as measured by several different methods. Tests were made for data from a single month (September 2008) and the best version, as decided by the each EO team for their own algorithm, was used in a round robin (RR) test which encompassed four months in 2008 (March, June, September and December) representing the different seasons. Aerosol-cci brings together the most prominent European aerosol retrieval groups. Non-European groups are invited to attend workshops and discussion meetings to exchange information and advance aerosol observations from space.

Based on the RR exercise, the best possible algorithm, or combinations of algorithms will be selected to produce the global AOD for the whole year 2008. For more information on the aerosol-cci project, see: http://www.esa-aerosol-cci.org/.

VALIDATION AND EVALUATION

For validation and evaluation of the retrieval algorithms used in Aerosol-cci, three principal methods were used, based on statistics for Level 2 (L2) and Level 3 (L3) products, where in Aerosol-cci L2 products are the daily products as produced by the retrieval with a spatial resolution of $10x10km^2$ and L3 are daily or monthly aggregates provided on a spatial scale of $1^{o}x1^{o}$. These products are available globally. It is noted that using the FMI/UHEL other products are available as well such as for $1x1$ km^2 over limited areas. The principal validation methods include:

- Statistical inter-comparison of L2 products (scatterplots, LSQ fits and histograms of AOD and Ångström coefficients):
    - versus collocated AERONET sun photometer measurements
    - versus products from other satellites (MODIS, MISR)
- L3 comparison with daily AERONET data providing statistics (slope, bias, correlation) and histograms.
- Statistical analysis of satellite products with collocated or daily AERONET data gridded to 1° $x1^{o}$ (correlation, bias) to establish regional spatial and temporal correlations which are combined to a total score (= bias * spat.corr * temp.corr), and combination of the total regional scores to a global score

Other validation exercises include studies on uncertainty estimation and studies on the comparison with measurements of aerosol properties at ambient relative humidity (RH) (such as column integrated measurements with associated variations of ambient properties with height) with in situ measurements such as those made in the ground-based networks with controlled RH (cf. Zieger et al., 2011) .

ALGORITHM IMPROVEMENT

Aerosol retrieval is an underdetermined problem since the number of degrees of freedom is smaller than the number of observations. Hence assumptions need to be made. The most important assumptions made in aerosol retrieval concern:

- Aerosol optical properties and size distribution
- Cloud screening
- Surface treatment

Algorithm improvement in Aerosol-cci is based on an open discussion and interaction involving the European aerosol retrieval groups (EO partners) in which experts from outside (e.g. MODIS, MISR) are invited to participate. In addition, working groups have been established to work on the three topics identified above.

The aerosol properties workshop has resulted in a simple set of aerosol components with prescribed lognormal size distributions, defined by mode radius, effective radius, geometric standard deviation and variance, and complex refractive index for fine mode absorbing and non-absorbing particles and for coarse mode particles (sea spray aerosol and desert dust). These components can be mixed to provide an aerosol model described by a bimodal size distribution with any absorption.

Furthermore, a climatology of aerosol properties has been derived from 12 global models participating in AEROCOM which provides the median, monthly distribution of aerosol components, together with statistics derived from AERONET (Holben et al., 2008) data. This climatology is used as a priori for the occurrence of aerosol types /mixtures, per region and per month. Using the occurrence of aerosol types, the retrieval algorithm computes the radiances at the top of the atmosphere which are compared with the satellite measurements. Based on this comparison the aerosol mixtures are adjusted and the procedure is iterated until convergence is reach and the most likely aerosol model providing the measured radiance is

selected. With this model the AOD is computed. The FMI/UHEL dual view algorithm ADV provides as a bonus also the mixing ration of the various aerosol components and the surface reflectance (Kolmonen et al., 2012). It is noted that the surface reflectance can only be provided because ADV eliminates surface effects by using the AATSR dual view and hence no assumptions need to be made in the retrieval

The above aerosol retrieval can only be made for cloud-free sky because the high reflectance of clouds at wavelengths in the UV-NIR interferes with the aerosol reflectance and hence prohibits accurate retrieval of aerosol properties. Therefore, an accurate cloud mask has to be applied to screen all pixels for the occurrence of clouds and exclude them form retrieval. The Aerosol-cci cloud working group has studied various cloud detection methods and has provided a cloud mask for comparison of results from different satellites. This subject is still under study and no unique cloud detection method is currently in use. The FMI/UHEL algorithm ADV uses the cloud mask described by Robles-Gonzalez (2003) (see also Curier et al., 2009), with a post-processing method based on comparison of neighbouring pixels in a 3x3 pixels (L2) area which provides adequate results and has very much improved the retrieval products.

As indicated above, the ADV algorithm used at FMI/UHEL uses the two AATSR views to eliminate surface effects and retain only the atmospheric path radiance. However, other groups apply other principles and the effect of treatment of the surface is an on-going issue in aerosol retrieval over land (cf. Kokhanovsky and de Leeuw, 2009). Over ocean only a single view is used in the retrieval step. The ocean surface is dark at wavelengths in the NIR and an ocean reflectance model is used to correct for effects due to chlorophyll and whitecaps.

Algorithm improvement was measured by application of the validation and evaluation exercises described above. These exercises were made for only one month, September 2008, a necessary restriction because of time limitation and pressure to produce the results. Success was identified by comparison with the baseline algorithm and successive improvement after implementation of different aerosol models, the use of the AEROCOM median with different degrees of comprehensiveness (i.e. varying from completely free retrieval without any use of the climatology to a full prescription of the aerosol mixing and combinations thereof) and different cloud masks. In addition to these experiments, algorithms were also improved as regards coding and debugging and the retrieval products were improved by application of post-processing.

ROUND ROBIN EXCERSIZE

The round robin (RR) exercise was made for four months in 2008 (March, June, September and December), using global retrieval results from each of the algorithms indicated above (except GOMOS and OMI) providing AOD and Ångström coefficients. The versions of the algorithms used to provide these products were selected by each of the retrieval groups based on the exercises described above. The products were evaluated by the validation group which provided an advice as regards the statistical quality. Other considerations were data coverage and spatial patterns. Figure 1 shows a comparison of the global AOD which was provided or the RR exercise from the ADV algorithm, aggregated from the four months to an annual product and a similar map based on MODIS/Aqua Collection 5 data which is used as a reference. Also shown is the ADV baseline product.

Comparison of the RR results with the baseline shows the enormous improvement of ADV. The global mean AOD is 0.154 as compared with the MODIS / Aqua Collection 5 global mean AOD of 0.156. Some differences are still visible between MODIS and ADV, which are a subject of further study which should include both ground-based observations and comparison with other algorithms. Discrepancies may be due to either ADV or MODIS or both.
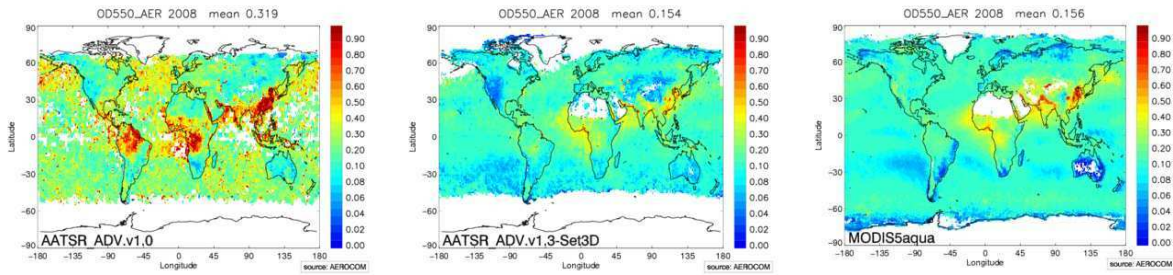
Figure 1. Global AOD maps aggregated from AATSR (baseline lADV v1.0; left, RR results ADV v1.3, set 3D; middle) and MODIS/Aqua Collection 5 (right) retrievals. The AATSR RR map shows the large improvement with respect to the baseline algorithm, in particular over ocean but also over land, resulting in a global mean AOD of 0.154 (upper right corner) as compared to the MODIS Aqua global mean of 0.156.

An obvious difference is the lower coverage of ADV than MODIS which is due to the restriction to a relatively low solar zenith angle in ADV (60°) which is currently enhanced to 75°. Furthermore, cloud screening over ocean is being improved leading to better coverage. Preliminary results including these two improvements in Figure 2 (note the different colour scale) show the effects of these on the coverage. Yet, AATSR is less mature than MODIS, as was concluded in the validation, mainly due to coverage problems associated with the smaller swath (500 km for AATSR vs 2330 km for MODIS). Nevertheless, the use of AATSR could be an advantage over MODIS since the RR validation scores for AATSR were somewhat better than those for MODIS over North America and similar over Europe. However, a firm conclusion can only be made after inspection of a larger data set, such as the one currently produced for the whole year of 2008.
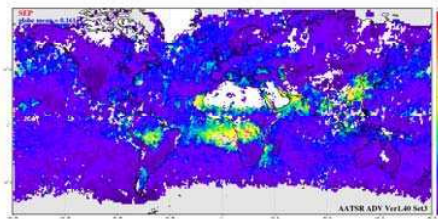
Figure 2. Global AOD map for September 2008 generated with AATSR v1.40, with a larger solar zenith angle and improved cloud screening over ocean, as compared to v1.3 (Figure 1 middle). Note that this is a preliminary results and that the colour scale is different. In particular note the strongly improved coverage with version 1.40.

CONCLUSIONS

The results presented above focused mainly on AATSR and the ADV algorithm. Similar results are available for all other algorithms and are described in de Leeuw et al. (in preparation). Results from algorithm improvement are described in Holzer-Popp et al. (in preparation).

Based on the RR exercise, algorithms were selected to produce a first set of Aerosol ECVs (AOD, Ångström coefficients and other parameters which may differ from each algorithm). For AATSR, ADV will provide the principal data set which will be merged with data from SU and ORAC for areas where these algorithms perform better (e.g. over desert). Other algorithms which are mature enough are PARASOL and MERIS ALAMO. Other algorithms need further development while also the selected algorithms will be further improved.

This first set of Aerosol ECV products will be offered to the climate modelling community for their validation and feedback as regards the use for climate studies. The cooperation of the EO community with the global modelling community has proven to be very important, in particular as regards the production of a data set and the data format in such a way that they are indeed useful .

The cooperation between the EO groups, which was the first time on a European level, has led to large improvement of almost all retrieval products. The initial gap with non-European products (in particular MODIS) has become much smaller.

The production of climate relevant data using satellites is relevant because satellites cover an extended period of time. The first ATSR instrument which can be used for aerosol retrieval was ATSR-2 (1995-2003), followed by AATSR (2002-2012) and a similar instrument (SLSTR) will be launched in 2014 aboard Sentinel 3. The retrieval of SLSTR data require some adjustment of the retrieval algorithm due to the geometry of the instrument (backward instead of a forward view), a wider swath in one of the views and an extra channel in the NIR which may prove important for several reasons such as surface correction in single view, or enhanced information on coarse aerosol particles

ACKNOWLEDGEMENTS

REFERENCES

Beekmann, M., A. S. H. Prevot, F. Drewnick, J. Sciare, S. N. Pandis, H. A. C. Denier van der Gon, M. Crippa, F. Freutel, L. Poulain, V. Ghersi, E. Rodriguez, S. Beirle, P. Zotter, S.-L. von der Weiden-Reinmüller, M. Bressi, C. Fountoukis, H. Petetin,S. Szidat, J. Schneider, A. Rossi, I. El Haddad, A. Megaritis, Q.J. Zhang, J.G. Slowik, S. Moukthar, P. Kolmonen, A. Stohl, S. Eckhardt, A. Borbon, V. Gros, N. Marchand, J.L. Jaffrezo, A. Schwarzenboeck, A. Colomb, A. Wiedensohler, S. Borrmann, M. Lawrence, A. Baklanov, U. Baltensperger: Will regional emissions control fine particulate matter levels in future megacities?, PNAS, 2012 submitted.

Curier, L., G. de Leeuw, P. Kolmonen, A. –M. Sundström, L. Sogacheva, Y. Bennouna (2009). Aerosol retrieval over land using the ATSR dual-view algorithm. In: A. A. Kokhanovsky and G. de Leeuw (Eds.), Satellite Aerosol Remote Sensing Over Land. Springer-Praxis (Berlin). ISBN 978-3-540-69396-3; pp. 135-159

de Leeuw, G., et al. (2012).Aerosol-cci: Aerosol retrieval algorithm improvement and evaluation. Inpreparation for submission to RSE.

Hannukainen, M., P. Kolmonen, A.-M. Sundström, L. Sogacheva, E. Rodriguez, G. de Leeuw (2011a). Comparison between the AOD derived from a global climate model HadGEM2 and from satellite observations. EGU 2011

Hannukainen, M., E. Rodriguez, M. Sofiev, J. Soares, W.J. Collins, P. Kolmonen, A-M. Sundström, L. Sogacheva, G. de Leeuw (2011b). Megacities inventory base on optical properties, using satellite and models results. 36 AM conference (August, 2011).

Holben, B.N., Eck, T.F., Slutsker, I., Tanre, D., Buis, J.P., Setzer, A., Vermote, E., Reagan, J.A., Kaufman, Y.J., Nakajima, T., Lavenu, F., Jankowiak, I. and Smirnov, A., 1998, Remote Sensing of Environment, 66, 1-16.

Holzer-Popp, T., et al., (2012). Extensive aerosol retrieval algorithm evaluation within ESA aerosol_cci project. In preparation for submission to AMT.

Kokhanovsky, A.A., and G. de Leeuw (Editors), 2009: Satellite Aerosol Remote Sensing Over Land. Springer-Praxis (Berlin). ISBN 978-3-540-69396-3, 388 pp.

Kolmonen, P., A.-M. Sundström, L. Sogacheva, E. Rodriguez, T.H. Virtanen, and G. de Leeuw (2012). Towards the assimilation of the satellite retrieved aerosol properties { the uncertainty characterization of AOD for the AATSR ADV/ASV retrieval algorithm. In preparation for submission to AMT

Veefkind, J.P., G. de Leeuw and P.A. Durkee (1998a). Retrieval of aerosol optical depth over land using two-angle view satellite radiometry during TARFOX. Geophys. Res. Letters. 25(16), 3135-3138.

Veefkind, J.P. and de Leeuw, G., 1998b, A new algorithm to determine the spectral aerosol optical depth from satellite radiometer measurements. *Journal of Aerosol Sciences,* **29**, 1237-1248.

Veefkind, J.P., G. de Leeuw, P.A. Durkee, P.B. Russell, P.V. Hobbs and J.M Livingston (1999). Aerosol optical depth retrieval using ATSR-2 and AVHRR data during TARFOX. J. Geophys. Res. 104 (D2), 2253-2260.

Veefkind, J.P., G. de Leeuw, P. Stammes and R.B.A. Koelemeijer (2000). Regional distribution of aerosol over land derived from ATSR-2 and GOME. *Remote sensing of the Environment,* 74 ,377- 386, 2000.

Robles-Gonzalez, C., J.P. Veefkind and G. de Leeuw (2000). Mean aerosol optical depth over Europe in August 1997 derived from ATSR-2 data. Geophys. Res. Lett. 27, 955-959.

Robles-Gonzalez, C., M. Schaap, G. de Leeuw, P.J.H. Builtjes and M. van Loon, Spatial variation of aerosol properties derived from satellite observations and comparison with model calculations, *Atmospheric Chemistry and Physics*, 3, 521-533, 2003.

Robles-Gonzalez, C., G. de Leeuw, R. Decae, J. Kusmierczyk-Michulec, and P. Stammes (2006), Aerosol properties over the Indian Ocean Experiment (INDOEX) campaign area retrieved from ATSR-2, *J. Geophys. Res.*, 111, D15205, doi:10.1029/2005JD006184.

Robles-Gonzalez, C., and G. de Leeuw (2008)., Aerosol properties over the SAFARI-2000 area retrieved from ATSR-2. J. Geophys. Res., 113, D05206, doi:10.1029/2007JD008636.

Rodriguez, E., P. Kolmonen, A.-M. Sundström, L. Sogacheva and G. de Leeuw (2010a). Satellite determination of regional aerosol properties over Paris and the surrounding area. EGU conference (April, 2010).

Rodriguez, E., P. Kolmonen, A.-M. Sundström, L. Sogacheva and G. de Leeuw (2010b). Aerosol properties comparison between Paris and other megacities, using AATSR and sun photometer. EAC conference (August, 2010).

Rodriguez, E., P. Kolmonen, A.-M. Sundström, L. Sogacheva and G. de Leeuw (2010c). Aerosol properties over Paris and the surrounding area obtained with satellite measurements. Conference: EUMESAT conference (September, 2010).

Rodriguez, E., P. Kolmonen, A.-M. Sundström, L. Sogacheva and G. de Leeuw (2012a). Satellite study over Europe to estimate the single scattering albedo and the aerosol optical depth. IRS conference, Berlin (August, 2012).

Rodríguez, E. , P. Kolmonen, A-M Sundström, L. Sogacheva, T. Virtanen, G. de Leeuw (2012b). Single scattering albedo and fine mode faction retrieved with AATSR satellite instrument. EAC conference (September, 2012).

Schmid B., J. Redemann, P. B. Russell, P. V. Hobbs, D. L. Hlavka, M. J. McGill, B. N. Holben, E. J. Welton, J. R. Campbell, O. Torres, R. A. Kahn, D. J. Diner, M. C. Helmlinger, D. A. Chu, C. Robles Gonzalez, and G. de Leeuw, Coordinated airborne, spaceborne, and ground-based measurements of massive, thick aerosol layers during the dry season in southern Africa, J. Geophys. Res, 108(D13), 8496, doi:10.1029/2002JD002297, 2003.

Sogacheva, L., Kolmonen, P., Sundsrtöm, A.-M., Curier, L., Aaltonen, V., and G. de Leeuw (2008). Aerosol retrieval over Finland using the dual-view AATSR algorithm. Proc. of the '2nd MERIS / (A)ATSR User Workshop', Frascati, Italy 22–26 September 2008 (ESA SP-666, November 2008)

Sogacheva, L., de Leeuw, G., Kolmonen, P., and L. Curier (2009). Combined AATSR/MERIS algorithm for aerosol optical depth retrieval. Proc. of the Workshop "Determination of Atmospheric Aerosol Properties Using Satellite Measurements, Bad Honnef, Germany ,August 16-19, 2009

Sogacheva, L., Kolmonen, P., Sundsrtöm, A.-M., Rodriguez, E., and G. de Leeuw (2010a). Aerosol Optical Depth over Africa from AATSR. Proc. of the EUMETSAT-2010, Cordoba, Spain, 20–24 September 2010

Sogacheva, L., Kolmonen, P., Sundsrtöm, A.-M., and G. de Leeuw (2010b). Aerosol Optical Depth Retrieval over Boreal Forests using AATSR - Case Studies . AGU 2010.

Sogacheva, L., Kolmonen, P., Sundsrtöm, A.-M., Rodriguez, E., Hannukainen, M., and G. de Leeuw (2011). Relation between aerosol optical depth and the occurance of fires over boreal forests using AATSR. Proc. of the IAC, Helsinki, Finland, 29 August–3 September 2010

Sundström, A-M., de Leeuw G., Kolmonen, P., Sogacheva, L., and Curier, L., (2008). Smoke plume detection with (A)ATSR over land. 2nd MERIS- AATSR workshop 22nd-26th September 2008, ESA/ESRIN Frascati (Rome), Italy.

Sundström, A-M., de Leeuw G., Kolmonen, P., and Sogacheva, L. (2009a). Detecting smoke aerosols over land with the AATSR Dual View algorithm. EUMETSAT Meteorological Satellite Conference, Sep. 21-25 2009, Bath, UK.

Sundström, A-M., de Leeuw G., Kolmonen, P., and Sogacheva, L. (2009b). Observing absorbing aerosols over land with the AATSR Dual View algorithm. Determination of Atmospheric Aerosol Properties Using Satellite Measurements, Aug. 16-19 2009, Bad Honnef, Germany.

Sundström, A-M., Kolmonen, P., de Leeuw, G., Sogacheva, L, and Rodriquez, E. (2010a). Monitoring aerosols over Asian megacities with the AATSR Dual-View Algorithm. European Geosciences Union General Assembly 2010, Vienna, Austria, 02 – 07 May 2010.

Sundström, A-M., Kolmonen, P., Hyvärinen, A., Sogacheva, L., Rodriquez, E., and de Leeuw G. (2010b). Aerosol retrievals in India with the AATSR Dual View Algorithm. International Aerosol Conference Aug. 29-Sep. 3 2010, Helsinki. Finland.

Sundström, A-M, (2011a). Aerosol optical properties over China observed with satellite remote sensing. Finnish Centre of Excellence in Physics, Chemistry, Biology and Meteorology of Atmospheric Composition and Climate Change Annual Workshop in Luostotunturi, May 18-20, 2011.

Sundström A-M, Huttunen J., Arola A., Kolmonen P., Sogacheva L., Virtanen T., Rodriguez E., and de Leeuw G. (2011b). Aerosol optical depth and direct radiative effect over China obtained from the satellite remote sensing measurements. Gordon Research Conference and seminar: Clouds, Aerosols, Precipitation and their Role in Climate and Climate Change. 9-15.7.2011 Waterville, Maine, US. Poster.

Sundström, A-M., Kolmonen, P., Sogacheva, L., and de Leeuw, G. (2012a). Aerosol retrievals over China with the AATSR Dual-View Algorithm. Remote Sensing of Environment, vol. 116, pp. 189-198.

Sundström, A-M., Kolmonen, P., Hyvärinen, A., Sogacheva, L., Rodriquez, E., and de Leeuw G. (2010c). Aerosol retrievals over India. EUCAARI annual conference 2010, 22.-26.11.2010, Helsinki, Finland.

Sundström A-M, Pekka Kolmonen, Meri Hannukainen, Larisa Sogacheva, Edith Rodriguez, Gerrit de Leeuw (2011). Aerosol retrievals over India with the AATSR Dual View Algorithm. Geophysical Research Abstracts Vol. 13, EGU2011-5647, 2011. EGU General Assembly 2011. Poster.

Sundström, A-M., Kolmonen, P., Sogacheva, L, Rodriquez E., Virtanen, T., Atlaskina K., Saponaro, G. and de Leeuw, G.(2012a). AATSR aerosol optical depth retrievals at high spatial resolution over Chinese megacities. MERIS- AATSR workshop 2012, ESA/ESRIN Frascati (Rome), Italy. Poster.

Virtanen, T.H., P. Kolmonen, L. Sogacheva, A-M Sundström, E. Rodriguez, K. Atlaskina, G. Saponaro and G. de Leeuw (2012a). Volcanic ash detection and ash plume height estimate using AATSR dual view, 9th Int. Symp. on Advanced Environmental Monitoring and Modeling.

Virtanen, T.H., P. Kolmonen, L. Sogacheva, A-M Sundström, E. Rodriguez, K. Atlaskina, G. Saponaro and G. de Leeuw (2012). Volcanic ash plume height estimate using AATSR dual view, 3rd MERIS/(A)ATSR & OLCI/SLSTR Preparatory Workshop.

Zieger, P., Weingartner, E., Henzing, J., Moerman, M., de Leeuw, G., Mikkilä, J., Ehn, M., Petäjä, T., Clémer, K., van Roozendael, M., Yilmaz, S., Frieß, U., Irie, H., Wagner, T., Shaiganfar, R., Beirle, S., Apituley, A., Wilson, K., and Baltensperger, U.: Comparison of ambient aerosol extinction coefficients obtained from in-situ, MAX-DOAS and LIDAR measurements at Cabauw, Atmos. Chem. Phys., 11, 2603-2624, doi:10.5194/acp-11-2603-2011, 2011.

CRAICC STUDIES ON SNOW SURFACE ALBEDO VARIABILITY AND EFFECTS OF DEPOSITION OF AEROSOLS

G. DE LEEUW[1, 2], O. MEINANDER[1], J. PULLIAINEN[1], K. ATLASKINA[2], A. VIRKKULA[1], N. KIVEKÄS[1], J. SVENSSON[1], A. HEIKKILÄ[1], H. LIHAVAINEN[1]

[1]Finnish Meteorological Institute (FMI), Helsinki, Finland
[2]Department of Physics, University of Helsinki, Finland

Keywords: snow, surface albedo, aerosols, remote sensing.

INTRODUCTION

Snow albedo has a large impact on the radiation balance at high latitudes. Hence it is important to know the short and long term variability of snow albedo in response to global change and associated changes in snow and ice cover, atmospheric transport and precipitation. CRAICC WP2, on cryosphere changes addresses such problems through application of satellite and ground-based remote sensing, in situ measurements and modelling. In situ measurements include long term observations of surface albedo and up-and down welling solar radiation at wavelengths in the UV and visible parts of the electro-magnetic spectrum as well as support measurements of environmental parameters. During campaigns the set of parameters is extended and intensive measurements are made of aerosol properties and spectral albedo and radiation, as well as snow properties and concentrations of black carbon in snow samples.

In this contribution an overview is provided of work on satellite remote sensing of the long term variation of seasonal snow cover using AVHRR data and it's implication for global modeling, as well as on experimental work in Finland on effects of black carbon (BC) on snow properties including snow melt and snow albedo.

EVOLUTION OF SEASONAL SNOW COVER AND ALBEDO TRENDS

The evolution of seasonal snow cover governs the behaviour of the terrestrial surface albedo, and thus the radiation balance, at high latitudes. This results from the large difference in albedo between the snow-covered and snow free terrain. The investigated key topic has been whether there are significant trends in long-term albedo and radiation forcing due to changes in snow conditions. This is accomplished by applying novel satellite data-derived observational data sets (GlobSnow data) as input to the albedo formulation of ECHAM5 General Circulation Model (Takala et al., 2011; Roeckner et al., 2003;2006).

The hemispheric GlobSnow data provide values of snow water equivalent (SWE), and snow extent, on a daily basis for a spatial grid of 625 km^2, and for a time period of 29 years, see Figure 1. These data are accompanied with other advanced data sets providing unique spatial information on land cover (GlobCover) and forest canopy transmissivity (Metsämäki et al., 2012). The application of these dynamic and static data as input to the albedo formulation of the ECHAM5 model enables the determination of the albedo trends in northern latitudes in an advanced manner. An example of modelled albedo is shown in Figure 2.

The results demonstrate the decline of the hemispheric snow mass and the resulting changes in surface albedo for the study period, see Figure 3. The albedo trend information is further applied to estimate the effects on top-of-the atmosphere (TOA) net shortwave radiation. The results show that the terrestrial albedo for different latitude zones is clearly declining, except for the high arctic. Consequently, the TOA radiation flux shows a clear increase in spring.

Results on trends in albedo and radiative forcing derived from the application of novel observational datasets obtained from space-borne measurements as input to the albedo formulation of the ECHAM-5 General Circulation Model will be presented by Atlaskina et al. (2012)
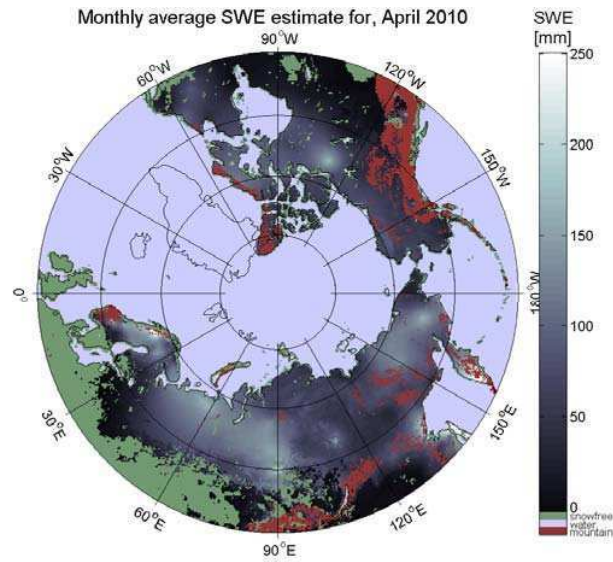
Figure 1. GlobSnow product on the snow water equivalent (SWE) and snow extent of the northern hemisphere for April 2010.
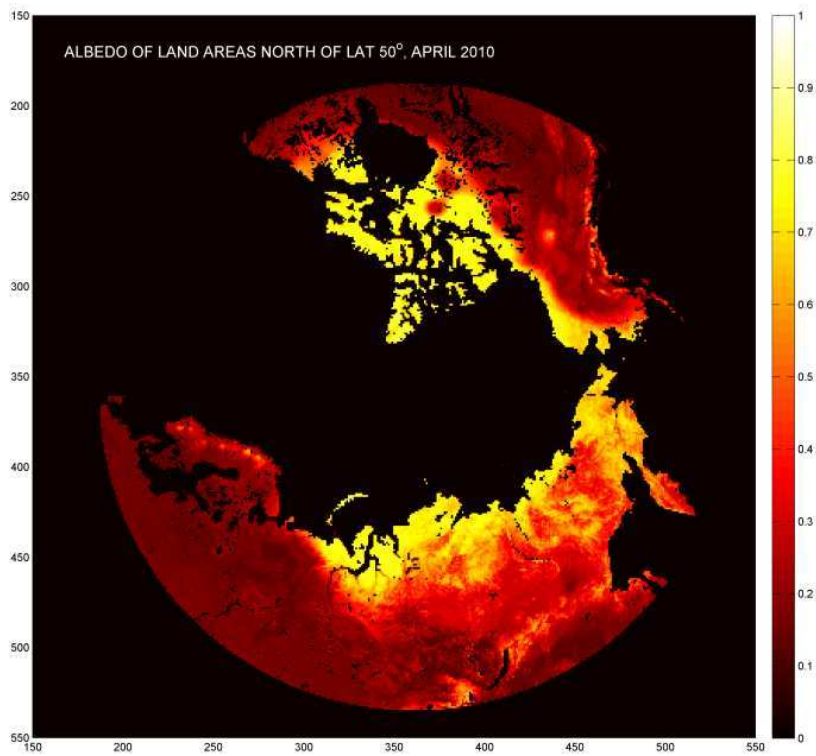
Figure 2. Predicted albedo of northern latitudes for April 2010. ECHAM-5 albedo formulation is applied using new observational data sets on snow (GlobSnow), land cover (GlobCover) and forest transmissivity as model input.

209
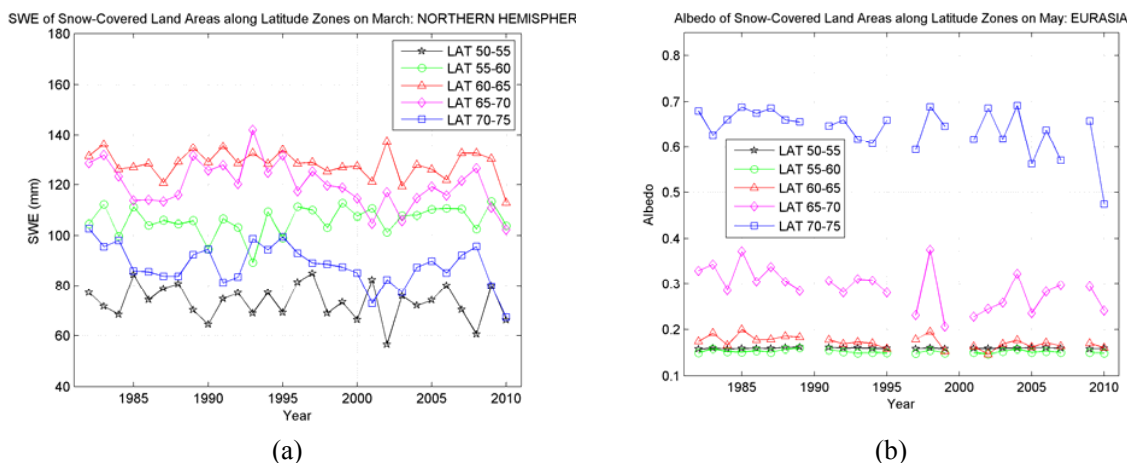
Figure 3. (a) Behaviour of Snow Water Equivalent (SWE) of different latitude zones of northern hemisphere for the period 1982-2010. (b) Zonal behaviour of terrestrial surface albedo for the regions seasonal snow cover during 1982-2010.

IN SITU MEASUREMENTS OF SEASONAL ARCTIC SNOW ALBEDO AND UV-VIS ALBEDO CHANGES INDUCED BY DEPOSITION OF SOOT

In situ measurements of snow albedo in the UV and VIS parts of the electromagnetic spectrum include:

a) variability of the seasonal broadband UV albedo of Arctic snow at the Sodankylä Arctic Research Centre (67°22'N, 26°39'E, 179 m asl), measured since the International Polar Year IPY-2007, with instruments mounted at a height of 2 m, at 1-min intervals. These measurements are combined with weekly analysis of the concentration of elemental carbon (EC) in snow.

b) Snow albedo and reflectance changes induced by soot: broadband, multiband and spectral surface albedo changes at wavelengths in the UV and VIS induced by the artificial deposition of soot to snow, within the SoS-2012 field campaign.

The Sodankylä data allow for studies of Arctic snow albedo in the UV on time scales ranging from a few days to 5 years (07-2012). The data show that the UV albedo of accumulating Arctic snow may be up to A_{UV}=0.8. For melting snow A_{UV} =0.5-0.7, while EC concentrations in snow were, e.g., up to EC_{max} = 40 ppb in 2009. For intensively melting snow, the diurnal decrease in albedo is ~10 % per day and asymmetric to the solar zenith angle (SZA).

To estimate the albedo effect of black carbon (BC) on snow and ice, the experiment Soot on Snow (SoS-2012) (see also Kivekäs et al., 2012), took place in 2012 at the Jokioinen Observatory, a synoptic FMI weather station in southern Finland. Soot was deposited on snow at three spots with different concentrations (one low and two high concentrations), with a reference spot where no snow was deposited. All soot concentrations were clearly above the background level. The experiments were conducted on a snow-covered agricultural field. The soot we used was produced in residential heating with wood and oil, and was collected by chimney cleaners. The soot concentration and size distribution were monitored during the deposition, and the concentration of elemental carbon was analysed from snow samples. The snow depth and snow albedo were measured throughout the melting period.

To measure the albedo, two erythemally weighted UV-B sensors (280-310 nm), together with pyranometers (310-2800 nm), were installed at about 20 cm above the snow surface to measure the UV albedo of the dirty snow continuously, until the end of snow melt. Also, periodical measurements were made of:

i) multichannel albedo using a NILU-UV radiometer at UV and VIS (400-700 nm) channels,

ii) spectral albedo using a Bentham spectrometer (300-600 nm),

iii) spectral reflectance using two different Analytical Spectral Devices spectrometers.

The NILU-UV results show that the initial albedo of clean snow (reference spot) were $A_{VIS} = 0.92$ and $A_{UV} = 0.70$. The surface elemental carbon content was EC = 87 ppb. Immediately after the application of soot, the albedo of the medium soot spot was $A_{VIS} = 0.29$ and $A_{UV} = 0.28$, while the mean amount of surface layer elemental carbon was EC = 4916 ppb.

Measurements with the Bentham spectroradiometer were used to follow the temporal evolution of snow albedo in the period after soot deposition unitl the snow had melted. Scans of spectral up-welling and down-welling irradiance were successively taken over each of the deposit spots. The ratio of the down-welling and up-welling irradiance yielded an estimate of the local albedo of each spot. Preliminary investigation of the data shows that the effect of the soot imbedded in the snow pack during the snow melt may be retrieved from the measurements. However, the differences are not very clear due to changing solar position and cloudiness during the spectral scans which took up to 12+12 minutes for the up-welling and down-welling irradiances. Therefore corrections need to be applied using a radiative transfer scheme.

Detailed results of the albedo measurements and SoS campaigns will be presented in the contributions by Meinander et al. (2012) and Kivekäs et al. (2012).

SPATIAL VARIATION OF ELEMENTAL CARBON IN SNOW

Elemental carbon (EC) (also referred to black carbon depending on measurement technique used) concentrations in snow in Arctic Scandinavia was investigated in an East-West transect. The hypothesis was that concentrations would increase as samples were taken further east due to the industrialized Kola Peninsula and associated higher emissions. To test this hypothesis, surface snow and bulk samples of the entire snow column were gathered, filtered and filters containing the impurities were analysed with an OCEC-analyser for their EC content.

With the exception of a few samples collected in the western Scandinavia, where EC concentrations in snow were relatively high, a trend in the EC concentrations in snow could be noticed in the data, with higher EC concentrations toward the Russian border. The high concentrations in the west were probably due to local pollution sources. Additional measurements are needed to further explore these results and a more extensive field campaign is planned for the winter of 2013.

Detailed results of this survey will be presented in the contribution by Svensson et al. (2012).

CONCLUSIONS

An overview has been presented of activities on the variability of snow albedo and the effects of BC deposition on snow. These activities contribute to achieving the following CRAICC WP2 objectives on the short and long term variability of the surface albedo, in particular deposition of aerosols and snow and ice cover changes, and on the evolution of snow and ice climatological zones.

ACKNOWLEDGEMENTS

REFERENCES

Atlaskina, K., J. Pulliainen, A. Laaksonen, K. Luojus, M. Takala, P. Räisänen, S. Metsämäki, M. Kulmala and G. De Leeuw (2012). Trend of Northern hemisphere seasonal snow mass and albedo for

period of 29 years based on satellite data analysis combined with albedo modeling. CRAICC Annual meeting Oslo, September 26-28, 2012.

Kivekäs, N., Virkkula, A., Järvinen, O., Svensson, J., Aarva, A., Lihavainen, H., Brus, D., Hyvärinen, A., Meinander, O., Heikkilä, A., Väänänen, R., Backman, J. and de Leeuw, G. (2012), Measuring the effect of soot on physical and optical properties of snow. Abstracts Of The Craicc Annual Meeting, Oslo, 26-28 September 2012.

Meinander, O., A. Heikkilä, A. Riihelä, A. Aarva, A. Kontu, E. Kyrö, H. Lihavainen, N. Kivekäs, A.Virkkula, O. Järvinen, J. Svensson and G. de Leeuw (2012). About seasonal Arctic snow UV albedo at Sodankylä and UV-VIS albedo changes induced by deposition of soot. Abstracts Of The CRAICC Annual meeting Oslo, September 26-28, 2012.

Metsämäki, S., Mattila, O.-P., Pulliainen, J., Niemi, K., Luojus, K. & Bötcher, K. An optical reflectance model-based method for fractional snow cover mapping applicable to continental scale. *Remote Sensing of Environment* **123**, 508-521 (2012).

Roeckner E., Bäuml G, Bonaventura L, Brokopf R, Esch M, Giorgetta M, Hagemann S, Kirchner I, Koernblueh L, Manzini E, Rhodin A, Schlese U, Schulzweida U, Tompkins A, 2003: The atmospheric general circulation model ECHAM5. Part I. Model description. Report 349, Max Planck Institute for Meteorology, Bundesstraße 53, 20146 Hambug, Germany, 127 pp.

Roeckner E, Brokopf R, Esch M, Giorgetta M, Hagemann S, Koernblueh L, Manzini E, Schlese U, Schulzweida U, 2006: Sensitivity of simulated climate to horizontal and vertical resolution in the ECHAM5 atmosphere model. *J. Climate*, **19**, 3771-3791.

Svensson, J., D. Brus, H. Lihavainen (2012). Elemental Carbon in Snow from Arctic Scandinavia 2012. Abstracts Of The CRAICC Annual meeting Oslo, September 26-28, 2012.

Takala, M., Luojus, K., Pulliainen, J., Derksen, C., Lemmetyinen, J., Kärnä, J.-P., Koskinen, J. & Bojkov, B. Estimating northern hemisphere snow water equivalent for climate research through assimilation of space-borne radiometer data and ground-based measurements. *Remote Sensing of Environment* **115**, 3517-3529 (2011).

UNDER ICE CO_2 DYNAMICS: IMPLICATIONS FOR A CHANGING CRYOSPHERE

B.A. DENFELD[1] and G. A. WEYHENMEYER[1]

[1] Department of Ecology and Genetics/Limnology, Uppsala University, Sweden

Keywords: Cryosphere, Climate Change, Carbon Dioxide, Lakes.

INTRODUCTION

The cycling of carbon (C) has been extensively studied globally due to its significant role as a climate regulator (i.e. Williamson *et al.,* 2009). Recently, inland waters have been included in estimates of the global carbon budgets due to their capacity to efficiently transform carbon, resulting in substantial emissions of carbon dioxide (CO_2) to the atmosphere. In addition to releasing CO_2 to the atmosphere, inland waters store terrestrial-derived (allochthonous) and newly produced (autochthonous) carbon in sediments and transport C to the ocean (Battin *et al.,* 2009; Cole *et al.,* 2007; Tranvik *et al.,* 2009). Regionally, estimating CO_2 evasion from inland waters in boreal landscapes, comprising 22% of global forest area, is of particular interests as boreal region have previously been considered to be net carbon sinks (Dunn, *et al.,* 2007). However, the high densities of humic lakes, covering 7% of the total land area (Kortelainen, 1993), combined with abundant streams (Koprivnjak, *et al.,* 2010), are potentially important conduits for carbon transformation, with a high proportion of CO_2 emitted via mineralization (Algesten *et al.,* 2003).

A defining aspect of high latitude regions (including boreal regions) is the cryosphere; the portion of the earth system containing water in its seasonally or perennially frozen state. Currently, annual CO_2 emission budgets do not account for the ice-cover period. Rather it is assumed that ice-cover does not change processes that control CO_2 dynamics, such that autumn CO_2 production rates can be applied for winter months and CO_2 accumulated under the ice is emitted as a one-time pulse emission at ice melt. However, aquatic ecosystems experience phenological and cyclical events in nature, thus, within a given system the abiotic and biotic conditions change seasonally (Wagner and Adrian, 2009). Sobek *et al.* (2003) found that variables explaining pCO_2 in lakes differ between winter and the open water season, suggesting that cryosphere dynamics influence annual CO_2 emissions during the winter. We argue that since most boreal and arctic lakes are covered by ice during substantial parts of the year, the influence of physical, chemical and biological processes on pCO_2 dynamics during ice cover are in need of further investigation. Understanding CO_2 dynamics during ice cover is of particular importance, as climate change will undoubtedly alter ice duration and formation on lakes (i.e. Prowse *et al.,* 2011a).

WORKING HYPOTHESES

It is known that during the open water season lake properties (e.g. Kortelainen et al., 2006), climatic variables (e.g. Tranvik & Jansson 2002) and lake biogeochemistry (e.g. Rantakari and Kortelainen, 2005) have direct and indirect effects on lake CO_2 dynamics. During the open water season, pCO_2 concentrations are mainly regulated by differences between lake respiration, photosynthesis, phototransformation and sedimentation which vary as a function of temperature, light and water currents. However ice cover reduces the temperature, light and water current regimes, allowing small processes such as river through-flow, heat flow from the sediments, solar radiation and induced oscillations to control the under ice conditions (Bengtsson, 1996; reference within). Thus, using the theory of findings during the open water period combined with knowledge of ice and snow dynamics, we formed testable hypotheses that explore ice cover CO_2 dynamics. Hypotheses are grouped into the following categories:

Lake morphology, the shape (shallow vs. deep) and size (small vs. large), influences material being sourced to the lake, how it is processed, and eventually transported. Generally, sediment respiration rates per square meter surface area and thereby CO_2 emission rates from lakes decrease with increasing

lake depth and increasing lake size (Hope et al.,1996; Humborg et al., 2010; Kortelainen et al., 2006; Pace and Prairie, 2005). Albeit, it is not known whether this is also the case during winter time when lakes are covered by ice we hypothesize that CO_2 is rapidly accumulated in small and shallow lakes, resulting in a significant impact of lake morphometry on winter pCO_2 values in lakes.

Hydrology, the flow path of C from the surrounding catchment, is a determinant of the fractional flow entering a lake via surface runoff (streams and precipitation) and subsurface flow (subsurface and ground water). During spring melt, the number of connecting streams, the amount of snow accumulated in the catchment and the ice and snow thickness on the lake, influences the hydrological flow of the lake and subsequent carbon processing. Thus, we hypothesize that isolated lakes and headwater lakes have highest pCO_2 and that pCO_2 will decline with lake order. Since dissolved organic carbon transported from terrestrial to aquatic ecosystems during short snowmelt period can be highly bioavailable and is used for mineralization (Finlay et al., 2006) we further hypothesize that small lakes with large catchments will have high pCO_2.

Ice dynamics, the timing of ice formation and ice thaw, is important in the context of regulating lake water carbon processing during the winter. In particular, ice thickness and snow depth can influence the processes that occur during ice melt. For example, in small lakes the spreading of surface melt water on the ice surface decreases surface albedo, indirectly advancing the radiation decay of the ice cover (Grenfell and Perovich, 2004). Further as ice begins to melt, phototransformation and photosynthesis can occur under the ice, reducing CO_2 concentrations at surface waters. We hypothesize that longer winter thermal stratification results in increased pCO_2 accumulation. Consequently, lakes that experience earlier ice break up will have lower pCO_2.

The biogeochemistry of lake water is regulated by the presence and interactions of available nutrients and organisms in the lake. In particular, terrestrial carbon inputs have been found to play an important role for the carbon cycle of boreal lakes, as most lakes have been reported as net heterotrophic due to metabolism of terrestrial organic carbon (Algesten et al., 2003). Sobek et al., (2003) found both the quantity (DOC) and quality (A250) of carbon and nutrients such as total phosphorus had a significant influence on pCO_2 during ice cover in 33 Swedish lakes. Thus we hypothesize that the presence of macronutrients and bioavailable carbon will lead to higher pCO_2 during winter.

METHODS

To test our hypotheses, lake water chemistry (available at http://www.slu.se/vatten-miljo), climate data (www.smhi.se) and GIS-derived lake morphology and catchment characteristics were retrieved for a diverse set of lakes in Sweden. Lake monitoring data were filtered to only represent lakes sampled during winter ice cover. This was done by selecting lake water samples with surface water temperatures less than 4°C and sampled during January-April, resulting in a total of 2400 samples from 300 lakes. pCO_2 for all lakes were calculated from water temperature, pH, alkalinity and altitude (according to Weyhenmeyer *et al.,* 2012). Total organic carbon, total phosphorus and total nitrogen data were included in the retrieved dataset. Using geographic information system (GIS), altitude, area, perimeter, depth, volume, runoff, lake hydrology and lake order were determined for each of the 300 lakes. Lake hydrology and lake order classification was based on Martin and Soranno (2006). Climate data retrieved from SMHI included ice on, ice thaw, radiation (during February), average annual precipitation, and average annual temperature. In GIS, an average value (1961 to 1990) for each climatic variable was extracted for all 300 lakes.

Statistical tests were carried out in JMP. To find important patterns for pCO_2 on a spatial scale we used Analysis of Variance (ANOVA), separating variables into categorical classes. A post-hoc (Tukey-Kramer) test was run to compare means between categories. To further investigate the strength of important drivers for pCO_2 during winter we used partial least squares regressions (PLS) (e.g. Sobek *et al,* 2003). PLS ranks *X*-variables according to their relevance in explaining *Y*, allowing the relative strength of each *X*-variable to be determined.

PRELIMINARY RESULTS

According to our expectations we found that pCO_2 differed significantly between lakes with varying lake depth, lake surface area and water volume ($p < 0.01$, Figure 1a). pCO_2 significantly declined with increasing lake depth, lake surface area and water volume.

In addition to lake morphometry we found a significant effect of lake order, lake hydrology and runoff on pCO_2 ($p < 0.01$, Figure 1b). pCO_2 decreased across the fluvial path with lake order; lakes with a lake order >3 had significantly different pCO_2 values than lakes with the lake order ≤ 2. Headwater lakes differed significantly between lakes with the order ≥ 1 but did not differ from isolated and inflow headwater lakes. Lake hydrology differed significantly between identified classes: headwater lakes were significantly different than inflow headwater and flow-through lakes but not isolated lakes. Runoff was significantly different between classes but the pattern was not as clear as for lake hydrology and lake order.

Unexpectedly the ice dynamics showed least impact on winter pCO_2 in lakes. Indeed we found a significant effect of freeze dates, thaw dates and ice duration on winter pCO_2 ($p < 0.05$) but the patterns were complex. pCO_2 was highest in lakes that freeze between Nov 1 to Nov 15. pCO_2 was significantly different from lakes that freeze between Dec 1 to Dec 15 and between Dec 15 to Jan 1 but not significantly different from lakes that freeze between Oct 15 to Nov 1 and Nov 15 to Dec 1. Concerning thaw dates pCO_2 was highest in lakes that thaw between May 15 to Jul 1 pCO_2 was significantly different from lakes that thaw between Jun 1 to Jun 15, Apr 1 to Apr 15, and Mar 15 to Apr 1 but not different from lakes that thaw between Apr 15 to May 1 and between May 1 to May 15. Lakes that thaw between Jun 1 and Jun 15 had the lowest pCO_2 and they were significantly different than all other thaw classes. Although pCO_2 varied between ice duration, none of the ice duration classes significantly differed between each other.

POTENTIAL IMPLICATIONS

From the preliminary results we conclude that lake water pCO_2 under ice cover is primarily dependent on lake morphology and hydrological conditions. Even ice cover dynamics play an important role but here patterns become complex. Of particular interest are thaw dates that are late in the year. Here surprisingly little CO_2 has been accumulated in the lake waters, suggesting that CO_2 is lost from lake waters via outflows rather than via the interface surface water – atmosphere. We argue that it is important to consider ice cover dynamics in understanding annual CO_2 budgets and further investigation is needed to be able to make more robust conclusion about the processes that affect CO_2 dynamics under ice. Further the processes must be compared so that the overall strength of the effect can be determined. Since artic and boreal regions are poised to experience significant changes to ice duration and dynamics and increase in winter precipitation (Prowse et al., 2011b), it is of utmost importance, in terms of understanding carbon dynamics in aquatic systems, that we advance the understanding of climate-induced changes to arctic and boreal freshwater ice and subsequent effects on lake CO_2 dynamics.
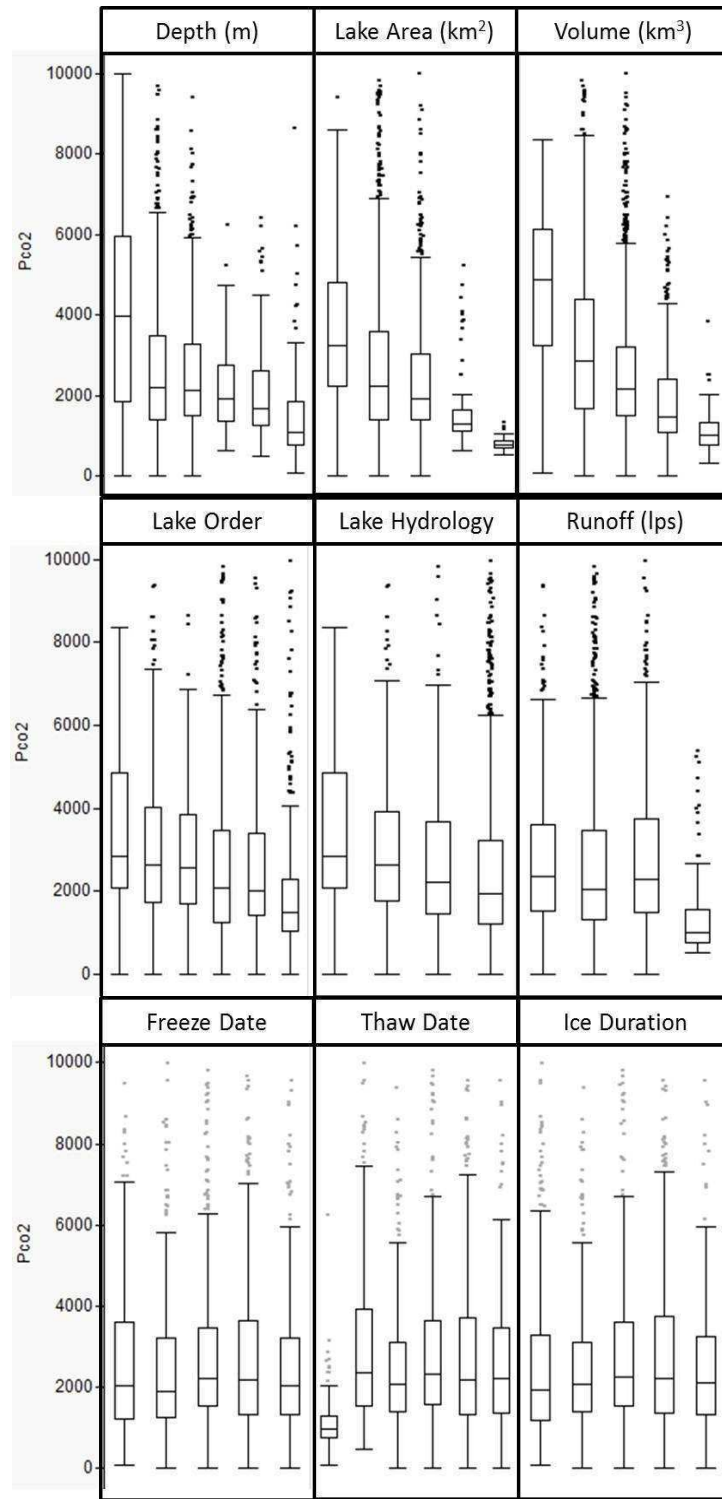
Figure 1. Box plots of pCO$_2$ in relation to **Lake morphology** (Depth (0-2, 2-4, 4-6, 6-8, 8-10, 10+); Lake Area (0.01-0.1, 0.1-1, 1-10, 10-100, 100-1000); Volume (0.1-1,1-10,10-100,100-1000, 1000+), **Lake Hydrology** (Lake Order (-1 (isolated), 0 (headwater), 1,2,3,4+); Lake Hydrology (Isolated, inflow headwater, headwater, flow through); Runoff (> 1, 1-10, 10-100, 100-1000)), and **Ice Cover** (Freeze Date (Oct15 to Nov 1, Nov 1 to Nov 15, Nov 1 to Dec 1, Dec 1 to Dec 15); Thaw Date (Jun1 to Jun 15, May 15 to Jun 1, May 1 to May 15, Arp 15 to May 1, Apr 1 to Apr 15, Mar 15 to Apr 1); Ice Duration (7 month, 6 months, 5 months, 4 months, 3 months).

216

ACKNOWLEDGEMENTS

REFERENCES

Algesten, G., Sobek, S., Bergström, A.-K., Ågren, A., Tranvik, L. J., & Jansson, M. (2003). Role of lakes for organic carbon cycling in the boreal zone. *Global Change Biology*, *10*, 141-147.

Battin, T. J., Luyssaert, S., Kaplan, L. A., Aufdenkampe, A. K., Richter, A., & Tranvik, L. J. (2009). The boundless carbon cycle. *Nature Geoscience*, *2*(9), 598-600.

Bengtsson, L. (1996). Mixing in ice-covered lakes. *Hydrobiologia*, *322*(1-3), 91-97.

Battin, T. J., Luyssaert, S., Kaplan, L. A., Aufdenkampe, A. K., Richter, A., & Tranvik, L. J. (2009). The boundless carbon cycle. Nature Geoscience, 2(9), 598-600. Nature Publishing Group. doi:10.1038/ngeo618

Cole, J J., Prairie, Y. T., Caraco, N. F., Mcdowell, W. H., Tranvik, L. J., Striegl, R. G., Duarte, C. M., et al. (2007). Plumbing the Global Carbon Cycle : Integrating Inland Waters into the Terrestrial Carbon Budget. *Ecosystems*, 171-184.

Dunn, A. L., Barford, C. C., Wofsy, S. C., Goulden, M. L., & Daube, B. C. (2007). A long-term record of carbon exchange in a boreal black spruce forest: means, responses to interannual variability, and decadal trends. *Global Change Biology*, *13*(3), 577-590.

Finlay, J., Neff, J., Zimov, S., Davydova, A., & Davydov, S. (2006). Snowmelt dominance of dissolved organic carbon in high-latitude watersheds: Implications for characterization and flux of river DOC. *Geophysical Research Letters*, *33*(10), doi:10.1029/2006GL025754

Grenfell, T. C., & Perovich, D. K. (2004). Seasonal and spatial evolution of albedo in a snow-ice-land-ocean environment. *Journal of Geophysical Research*, *109*, doi:10.1029/2003JC001866

Hope, D., TK, K., & JL, R. (1996). Relationship between pCO2 and dissolved organic carbon in northern Wisconsin lakes. *Journal of Environmental Quality*, *25*, 1442-1445.

Humborg, C., Mörth, C.-M., Sundbom, M., Borg, H., Blenckner, T., Giesler, R., & Ittekkot, V. (2010). CO2 supersaturation along the aquatic conduit in Swedish watersheds as constrained by terrestrial respiration, aquatic respiration and weathering. *Global Change Biology*, *16*(7), 1966-1978.

Koprivnjak, J.-F., Dillon, P. J., & Molot, L. a. (2010). Importance of CO 2 evasion from small boreal streams. *Global Biogeochemical Cycles*, *24*(4), doi:10.1029/2009GB003723

Kortelainen, P. (1993). Content of Total Organic Carbon in Finnish Lakes and Its Relationship to Catchment Characteristics. *Canadian Journal of Fisheries and Aquatic Sciences*, *50*(7), 1477-1483.

Kortelainen, P., Rantakari, M., Huttunen, J. T., Mattsson, T., Alm, J., Juutinen, S., Larmola, T., et al. (2006). Sediment respiration and lake trophic state are important predictors of large CO2 evasion from small boreal lakes. *Global Change Biology*, *12*(8), 1554-1567.

Pace, M. L., & Prairie, Y. T. (2005). Respiration in lakes. *Respiration in Aquatic Ecosystems* (pp. 103-121). Oxford University Press

Prowse, T., Alfredsen, K., Beltaos, S., Bonsal, B., Duguay, C., Korhola, A., McNamara, J., et al. (2011a). Arctic Freshwater Ice and Its Climatic Role. *Ambio*, *40*(S1), 46-52.

Prowse, T., Alfredsen, K., Beltaos, S., Bonsal, B. R., Bowden, W. B., Duguay, C. R., Korhola, A., et al. (2011b). Effects of Changes in Arctic Lake and River Ice. *Ambio*, *40*(S1), 63-74.

Rantakari, M., & Kortelainen, P. (2005). Interannual variation and climatic regulation of the CO2 emission from large boreal lakes. *Global Change Biology*, *11*(8), 1368-1380.

Sobek, S., Algesten, G., Bergstrom, A.-K., Jansson, M., & Tranvik, L. J. (2003). The catchment and climate regulation of pCO2 in boreal lakes. *Global Change Biology*, *9*(4), 630-641.

Tranvik, L. J., Downing, J. A., Cotner, J. B., Loiselle, S. A., Striegl, R. G., Ballatore, T. J., Dillon, P., et al. (2009). Lakes and reservoirs as regulators of carbon cycling and climate. *Limnology and Oceanography*, *54*(6), 2298-2314.

Tranvik, L., & Jansson, M. (2002). Terrestrial export of organic carbon. *Nature*, *415*, 861-862.

Wagner, C., & Adrian, R. (2009). Exploring lake ecosystems: hierarchy responses to long-term change? *Global Change Biology*, *15*(5), doi:10.1111/j.1365-2486.2008.01833.x

Weyhenmeyer, G. A., Kortelainen, P., Sobek, S., Muller, R., & Rantakari, M. (2012). Carbon dioxide in boreal surface waters - a comparison of lakes and streams . Ecosystems (in press).

Williamson, C. E., Saros, J.E., Vincent, W.F., Smol J.P. (2009). Lakes and reservoirs as sentinels, integrators, and regulators of climate change. Limnology and Oceanography, 54(6), 2273-2282.

APPLYING NEURAL NETWORKS AS A GAP-FILLING METHOD FOR CH_4 EDDY COVARIANCE FLUX DATA

S. DENGEL[1], D. ZONA [2], T. SACHS [3], M. AURELA [4], W. OECHEL [5, 6], T. VESALA [1]

[1] University of Helsinki - Department of Physics, P.O. Box 48, FI - 00014 University of Helsinki, Finland;
[2] University of Antwerp - Department of Biology, Campus Drie Eiken, D.B.034, Universiteitsplein 1, 2610 Wilrijk, Belgium;
[3] Helmholtz Centre Potsdam, GFZ German Research Centre for Geosciences, 14473 Potsdam, Germany;
[4] Finnish Meteorological Institute, P.O. Box 503, FI - 00101, Helsinki, Finland.
[5] San Diego State University, San Diego, CA. 92182, USA;
[6] Fondazione Edmund Mach (FEM), Centro Ricerca e Innovazione (CRI), Via Edmund Mach, 1, 38010 - San Michele, all'Adige, Italy.

Keywords: Neural Networks, Methane, gap-filling, eddy covariance.

INTRODUCTION

Methane (CH_4) is one of the most important greenhouse gases, second only to CO_2 (IPCC 2007) with natural wetlands thought to be the biggest individual source. Since the advancement in CH_4 gas analyser technology and its applicability to eddy covariance flux measurements (Hendriks *et al.* 2008; McDermitt *et al.* 2011), monitoring of CH_4 emissions is becoming more widespread in northern regions (Mastepanov *et al.* 2008; Sachs *et al.* 2008; Zona *et al.* 2009; Sturtevant *et al.* 2011). Such measurements contribute to a better understanding of the greenhouse gas balance of the Arctic. In order to accurately estimate annual greenhouse gas budgets, time series of high quality gap-free data are required (Falge *et al.* 2001; Rinne *et al.* 2007). Standardised methods are available for CO_2 flux data (Falge *et al.* 2001, Moffat *et al.* 2007) while there is still no consensus on CH_4 gap-filling methods. Studies where gap-filling was applied were site dependent and often applied to low resolution daily mean values (Hargreaves *et al.* 2001; Rinne *et al.* 2007; Riutta *et al.* 2007; Jackowicz-Korczyński *et al.* 2010; Long *et al.* 2010; Tagesson *et al.* 2012). Furthermore, large uncertainties in applied methods do still exist with no common protocol on missing data recovery of CH_4 eddy covariance flux data.

The application of neural networks (Jain *et al.* 1996; Saxén and Pettersson 2006) for data recovery and gap-filling (Aubinet *et al.* 2000; Papale and Valentini 2003; Ooba *et al.* 2006; Schmidt *et al.* 2008) has proven to be a very reliable tool in several scientific disciplines (Gardner and Dorling 1998; Lek and Guégan 1999; Lee and Jeng 2002; Toptygin *et al.* 2005). Neural networks are implemented as a simple gap-filling tool and they do not serve the purpose of disentangling the processes or drivers of methane fluxes. In the current study, we discuss the applicability of neural networks to gap-fill CH_4 flux data using data from northern high latitude ecosystems (wet sedge tundra, sedge fen and polygonal tundra).

Since CH_4 is the second most potent greenhouse gas in the atmosphere, it is becoming increasingly important to introduce a method that is capable in dealing with such high resolution data and auxiliary measurements and that is easy to implement across a variety of ecosystems. Regarding Arctic regions it is very important to work with time series where data gaps have been filled using reliable methods in order to accurately determine CH_4 emissions, annual budgets and prediction of future emissions under a changing climate (Anisimov 2007; IPCC 2007).

METHODS

Methane flux and meteorological data

The CH$_4$ eddy covariance flux data used in the current study originates from three distinctively different arctic ecosystems (Fig. 2, 3, 7): Barrow (Alaska) a wet sedge tundra in the northern part of the Arctic Coastal Plain (71°17'11.80'' N, 156°36'12.23'' W) (Zona *et al.* 2009); Lompolojänkkä, a nutrient-rich sedge fen located in the aapa mire region of north-western Finland (67°59.832'N, 24°12.551'E) (Aurela *et al.* 2009) and the wet polygonal tundra of Samoylov Island in the southern central Lena River Delta (72°22'N, 126°30'E) (Sachs *et al.* 2008, 2010). The CH$_4$ fluxes were measured by the eddy covariance (EC) method (Baldocchi, 2003). Data introduced in the current study was not previously gap-filled at 30 min / 1 hour resolution.

Pre-processing of data

The meteorological data, as well as the soil property data and CH$_4$ flux data consists of different magnitudes and units. In order to generalise the data, we have scaled all data from 0 to 1 which is necessary as we are applying a sigmoid activation function (Cybenko 1989), which has a range of 0 to 1. In order to examine all input variables and their effect on methane fluxes, we applied a simple stepwise regression in order to search for the best predictors or combinations of predictors from among all available 30 min (Barrow and Lompolojänkkä) and 1 h (Lena River Delta) resolution data. This method helped to pre-select the input variables and to prune the network by avoiding insignificant input data (Gunaratnam *et al.* 2003; Saxén and Pettersson 2006). Applying this procedure prior to running the neural network improved the overall performance of the network and simultaneously achieved higher results (better visual agreement and lower error values) during the training and testing phase.

Artificial Neural Networks

The neural network topology introduced in Figure 1 as an example shows the input variables (left side of the network) that are fed into the network with weights fitted and spread across the 2 layers with information flowing unidirectionally (blue arrows) to the nodes (marked in red) within the hidden layer, where a bias (offset) (marked with "b") are added. In this case the underlying function can be simply written as:

$$o = f\left(b + \sum_i w_i x_i\right),$$

where x_i represents the input variables ($x_1, ..., x_n$), w_i denotes the fitted weights ($w_1, ..., w_n$ - for each input variable) and b denotes the bias (or offset) that is added to the weighted sum ($\sum_i w_i x_i$) prior to applying the sigmoid activation function (f), leading further to the next layer, where a new set of weights are distributed, together with a bias and the sigmoid activation function before making an estimation of the output values. This output value also has a range of 0 to 1 which are than rescaled to their appropriate unit.
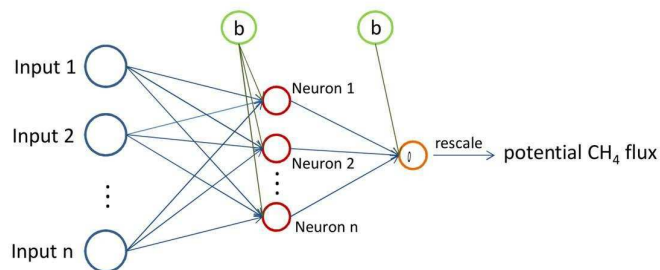
Figure 1: Example of a neural network topology. Input variables (left side of the network) are fed into the network with weights fitted (along blue arrows) with information flowing unidirectionally to the nodes (marked in red) within the hidden layer, where a bias (offset) (marked with "b") is added (along green arrows). Here a sigmoid function

(activation function) is applied to the weighted sum, leading further to the next layer, the "output" layer where a new set of weights are distributed, together with a bias and the sigmoid activation function before making an estimation for the output value. As the output still has a range of 0 to 1 it is rescaled prior to replacing missing data values. Weights are removed from the graph for clarity.

We found after applying the trial and error method that choosing rows of regular intervals gave a very good representation of the entire dataset. The remaining complete data pairs were then used for testing and validation purposes. Several learning algorithms are available for neural network training; in the current study we applied the resilient backpropagation algorithm (Riedmiller 1993). In order to test the network's performance various error functions can be applied, we chose the sum of squared errors (SSE), measuring the difference between predicted and observed output. In order to test the networks' performance (Fig. 2) the remaining complete data pairs (after rows used for training were removed) were used prior to applying the entire data set in order to recover missing data points.
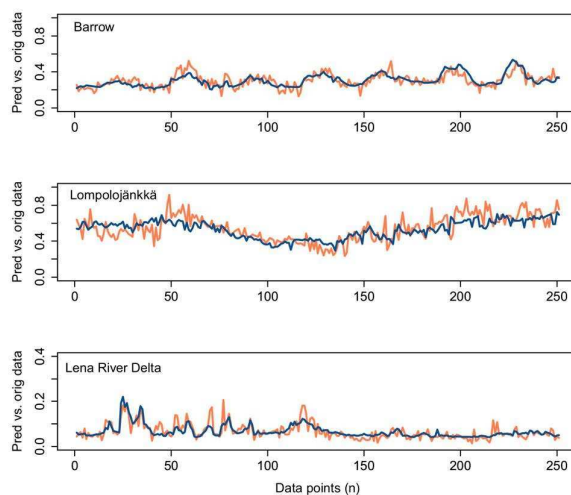
Figure 2: Visual representation of the performance of neural networks applied to Barrow, Lompolojänkkä and Lena River Delta CH_4 flux data. Data was scaled to the range of 0 to 1 in order to apply a sigmoid activation function. This visualisation gives a very good indication of well performing networks. Original data are marked in orange while predicted data are marked in blue. The scale in the Lena River Delta graph has been reduced for a better visual appearance. Data points shown represent 30-min values for Barrow and Lompolojänkkä and 1 h values for Lena River Delta.

Once we were satisfied with the performance of the networks (no further improvement could be realised in terms of goodness of fit) and their ability to predict relatively accurate CH_4 flux values we re-introduced the entire dataset of gap-free input variables to the networks in order to estimate flux values for those time periods where CH_4 flux values were missing.

CONCLUSIONS

We were able to apply artificial neural networks to high resolution 30-min (Barrow & Lompolojänkkä) and 1 hour (Lena River Delta) CH_4 flux data to predict CH_4 fluxes and proving their applicability as a gap-filling method for high resolution CH_4 flux data. Gaps in the original measured CH_4 flux data were replaced with flux values predicted by their respective network. Figure 3 shows the end result for the

month of July, seamlessly fitting into the original dataset, implying the great performance of these neural networks as a gap-filling method and their use in CH_4 flux studies. We find artificial neural networks to be recommendable as a reliable, robust and flexible gap-filling method for high resolution CH_4 flux data originating from various ecosystems.
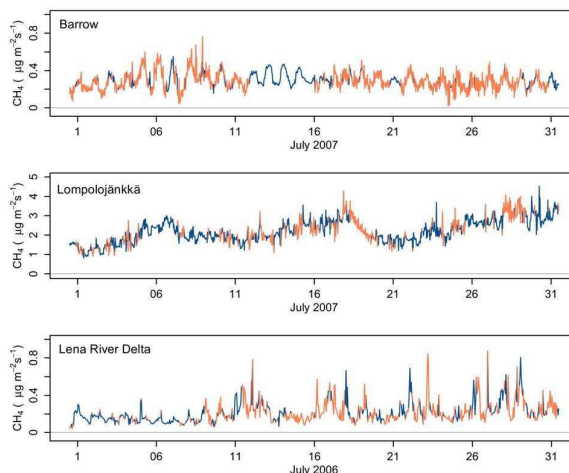
Figure 3: Data representing July (2007 and 2006 respectively) for all three sites, showing original measured data in orange and potential CH_4 flux values, estimated by applying neural networks, in blue.

ACKNOWLEDGEMENTS

REFERENCES

Anisimov, O.A. (2007). Potential feedback of thawing permafrost to the global climate system through methane emission. *Environmental Research Letters*, **2(4)**, 045016.

Aubinet, M., A. Grelle, et al. (2000). Estimates of the annual net carbon and water exchange of forests: The EUROFLUX methodology. *Advances in Ecological Research*, **30**, 113-175.

Aurela M., L. A., Tuovinen J.P., Hatakka J., Laurila T., Riutta T. (2009). Carbon Dioxide exchange on a northern boreal fen. *Boreal Environment Research,* **14**, 699 - 710.

Baldocchi, D.D. (2003). Assessing the eddy covariance technique for evaluating carbon dioxide exchange rates of ecosystems: past, present and future. *Global Change Biology*, **9(4)**, 479-492.

Cybenko, G. (1989). Approximation by superpositions of a sigmoidal function. *Mathematics of Control, Signals, and Systems (MCSS)*, **2(4)**, 303-314.

Falge, E., Baldocchi, D.D., Olson, R., Anthoni, P., Aubinet, M. et al. (2001). Gap filling strategies for defensible annual sums of net ecosystem exchange. *Agricultural and Forest Meteorology,* **107** (1 March), 43-69.

Gardner, M.W. & Dorling, S.R. (1998). Artificial neural networks (the multilayer perceptron)—a review of applications in the atmospheric sciences. *Atmospheric Environment*, **32(14–15)**, 2627-2636.

Gunaratnam, D.J., Degroff, T., Gero, J.S. (2003). Improving neural network models of physical systems through dimensional analysis. *Applied Soft Computing*, **2(4)**, 283-296.

Hargreaves, K.J., Fowler, D., Pitcairn, C.E.R., Aurela, M. (2001). Annual methane emission from Finnish mires

estimated from eddy covariance campaign measurements. *Theoretical and Applied Climatology*, **70(1)**, 203-213.

Hendriks, D.M.D., Dolman,A.J., van der Molen, M.K., van Huissteden, J. (2008). A compact and stable eddy covariance set-up for methane measurements using off-axis integrated cavity output spectroscopy, *Atmospheric Chemistry and Physics*, **8**, 431 – 443.

IPCC (2007). Summary for Policymakers. In: Climate Change 2007: The Physical Science Basis. Contribution of Working Group I to the Fourth Assessment Report of the Intergovernmental Panel on Climate Change [Solomon, S., D. Qin, M. Manning, Z. Chen, M. Marquis, K.B. Averyt, M.Tignor and H.L. Miller (eds.)]. Cambridge University Press, Cambridge, United Kingdom and New York, NY, USA.

Jackowicz☐Korczyński, M., Christensen, T.R., Bäckstrand, K., Crill, P., Friborg, T., Mastepanov, M., Ström, L. (2010). Annual cycle of methane emission from a subarctic peatland. *Journal of Geophysical Research*, **115(G2)**, G02009.

Jain, A.K., Mao, J., Mohiuddin, K.M. (1996). Artificial Neural Networks: A Tutorial. *Computer*, **29**, 31 - 44

Lee, T.L. & Jeng, D.S. (2002). Application of artificial neural networks in tide-forecasting. *Ocean Engineering*, **29(9)**, 1003-1022.

Lek, S. & Guégan, J.F. (1999). Artificial neural networks as a tool in ecological modelling, an introduction. *Ecological Modelling*, **120(2–3)**, 65-73.

Long, K.D., & Flanagan, L.B. (2010). Diurnal and seasonal variation in methane emissions in a northern Canadian peatland measured by eddy covariance. *Global Change Biology*, **16(9)**, 2420-2435.

Mastepanov, M., Sigsgaard, C., Dlugokencky, E.J., Houweling, S., Ström, L., et al. (2008). Large tundra methane burst during onset of freezing. *Nature*, **456(7222)**, 628-630.

McDermitt, D., Burba, G., Xu, L., Anderson, T., Komissarov, A. et al. (2011). A new low-power, open-path instrument for measuring methane flux by eddy covariance. *Applied Physics B: Lasers and Optics*, 1-15.

Moffat, A.M., Papale, D., Reichstein, M., Hollinger, D.Y, Richardson, A.D. et al. (2007). Comprehensive comparison of gap-filling techniques for eddy covariance net carbon fluxes. *Agricultural and Forest Meteorology*, **147(3-4)**, 209-232.

Ooba, M., Hirano, T., (2006). Comparisons of gap-filling methods for carbon flux dataset: A combination of a genetic algorithm and an artificial neural network. *Ecological Modelling*, **198(3–4)**, 473-486.

Papale, D. & Valentini, R. (2003). A new assessment of European forests carbon exchanges by eddy fluxes and artificial neural network spatialization. *Global Change Biology*, **9(4)**, 525-535.

Riedmiller, M. (1994). Rprop-description and implementation details. Technical Report, University of Karlsruhe, Germany.

Rinne, J., T. Riutta, Pihlatie, M., Aurela, M, Haapanala, S. et al. (2007). Annual cycle of methane emission from a boreal fen measured by the eddy covariance technique. *Tellus B*, **59(3)**, 449-457.

Riutta, T., Laine, J., Tuittila, E-S. (2007). Spatial variation in plant community functions regulates carbon gas dynamics in a boreal fen ecosystem. *Tellus B*, **59(5)**, 838-852.

Ryan, M., Müller, C. et al. (2004). The use of artificial neural networks (ANNs) to simulate N_2O emissions from a temperate grassland ecosystem. *Ecological Modelling*, **175(2)**, 189-194.

Sachs, T., Giebels, M., Boike, J., Kutzbach, L. (2010). Environmental controls on CH_4 emission from polygonal tundra on the microsite scale in the Lena river delta, Siberia. *Global Change Biology*, **16(11)**, 3096-3110.

Sachs, T., Wille, C., Boike, J., Kutzbach, L. (2008). Environmental controls on ecosystem-scale CH_4 emission from polygonal tundra in the Lena River Delta, Siberia. *Journal of Geophysical Research*, **113(G3)**, G00A03.

Saxén, H. & Pettersson, F. (2006). Method for the selection of inputs and structure of feedforward neural networks. *Computers & Chemical Engineering*, **30(6–7)**, 1038-1045.

Schmidt, A., Wrzesinsky, T., Klemm, O. (2008). Gap Filling and Quality Assessment of CO_2 and Water Vapour Fluxes above an Urban Area with Radial Basis Function Neural Networks. *Boundary-Layer Meteorology*, **126(3)**, 389-413.

Sturtevant, C. S., Oechel, W.C., Zona, D., Emerson, C.E. (2011). Soil moisture control over autumn season methane flux, Arctic Coastal Plain of Alaska. *Biogeosciences Discussions*, **8**, 6519-6554.

Tagesson, T., Mölder, M., Mastepanov, M., Sigsgaard, C., Tamstorf, M.P. (2012). Land-atmosphere exchange of methane from soil thawing to soil freezing in a high-Arctic wet tundra ecosystem. Global Change Biology, doi: 10.1111/j.1365-2486.2012.02647.x

Toptygin, A. Y., Gribanov, K.G., Imasua, R. Bleuten, W., Zakharovet, W.I. (2005). Seasonal methane content in atmosphere of the permafrost boundary zone in Western Siberia determined from IMG/ADEOS and AIRS/AQUA data, Honolulu, HI, USA, SPIE.

Zona, D., Oechel, W.C., Kochendorfer, J., Paw U, K.T., Salyuket, A.U. (2009). Methane fluxes during the initiation of a large-scale water table manipulation experiment in the Alaskan Arctic tundra. *Global Biogeochemical Cycles*, **23(2)**, GB2013.

FIRST OBSERVATIONS OF DROPLET AND ICE FORMATION IN THE CERN CLOUD CHAMBER

J. DUPLISSY[1], S. MATHOT[2], A. ONNELA[2], A. WASEM[2], R. GUIDA[2], L.P DE MENDEZ[2], J. KIRKBY[2], S. EHRHART[3], C. WILLIAMSON[3], C. FUCH[3], J. ALMEDIA[3], G. TSAGKOGEORGAS[4], T. SCHMITT[5], O. MOEHLER[5], F. BIANCHI[6], J. TROSLE[6], A. PRAPLAN[6], A. AMORIN[7], A. TOME[7], G. LLOYD[8], J. DORSEY[8] AND THE CLOUD COLLABORATION

[1]Helsinki Institute of Physics, University of Helsinki, Finland
[2]CERN, Geneva, Switzerland
[3]Goethe-University of Frankfurt, Institute for Atmospheric and Environmental Sciences, Frankfurt am Main, Germany
[4]Leibniz Institute for Tropospheric Research, Leipzig, Germany
[5]Karlsruher Institut für Technologie (KIT), Karlsruhe, Germarny
[6]Paul Scherrer Institute, Laboratory of Atmospheric Chemistry, Villigen, Switzerland
[7] SIM, University of Lisbon and University of Beira Interior, Lisbon, Portugal
[8]Centre for Atmospheric Science, University of Manchester, Manchester, United Kingdome

INTRODUCTION

The effect of aerosols and ions on cloud formation is crucial for the understanding of climate (Rosenfelf et al, 2008). How ions are influencing droplet or ice activation? How the chemical composition of the seed is influencing droplet and ice activation? After its first success on studying aerosol nucleation (Kirkby et al., 2011), the CLOUD chamber has now been upgraded to study droplet and ice formation in presence or not of ions. Here we present some of the CLOUD chamber modifications and prelimary observation of cloud formation performed during the CLOUD6 campaign in June-July 2012.

METHODS
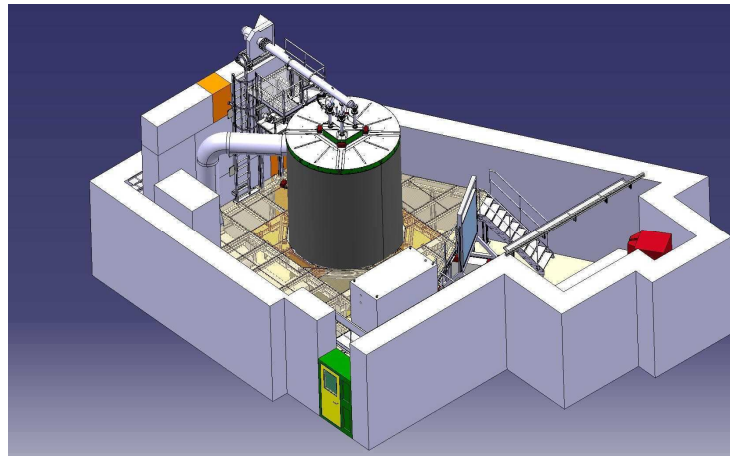
Figure 1: An illustration of CLOUD in the T11 experimental zone at the CERN PS. The de-focused particle beam exits a dipole magnet (right), crosses the hodoscope counter (middle) and then traverses the 3m-diameter CLOUD chamber. The new expansion system is installed on the top of the chamber.

The cloud chamber has been implemented with several new apparatus. A new control expansion system composed of a fast turbine pump, a fast pressure sensor, and a set of regulation valves have been installed on the top of the chamber (Figure 1). This new system precisely controls the expansion time, from seconds to hours. The starting pressure and ending pressure can be adjusted as well according to the needs of the experiment. A new temperature probe composed of a string of 5 fast thermo-sensors has been develop and used for the first time in the CLOUD chamber. A control heated system has been added to a standard CLOUD sampling probe for total water content measurement needs.

An aerosol population is first build up in the chamber from gas phase to particle conversion. The chamber pressure inside the chamber is raised (usually to +200 mbar above atmospheric pressure). The relative humidity and temperature are stable prior to start the expansion. The CERN beam is used to charge in a control manner the aerosol population. During neutral experiment, a clearing field inside the chamber is applied to remove all ions. An example of cloud formation can be seen in figure 2.
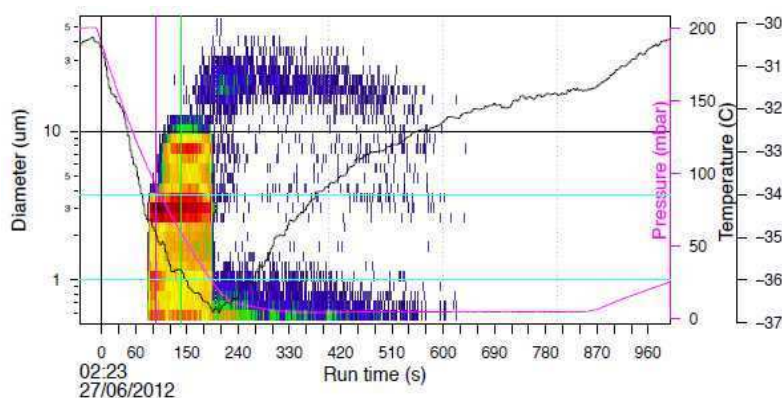
Figure 2: Droplet and ice formation measured by the CAPS. During an adiabatic expansion, the temperature decreases causing an increase of the RH. First a cloud made of liquid droplet is formed, followed by the formation of an ice cloud when the temperature reaches the homogeneous frizzing point.

CONCLUSIONS

CLOUD6 campaign was a successful commissioning of the CLOUD chamber. Ice and liquid clouds have been produced in a control manner. We have performed a set of experiments varying several parameters such as initial temperature, RH, ions concentration, expansion length, aerosol seed population. We have also learnt about technical improvements needs, such as instrumentation resistance for repeatedly pressure change.

ACKNOWLEDGEMENTS

REFERENCES
Rosenfelf et al (2008), *Flood or drought: How do aeorosol affect precipitation?*, Science
Kirkby et al. (2011), *Role of sulphuric acid, ammonia and galactic cosmic rays in atmospheric aerosol nucleation,* Nature

HYGROSCOPICITY AND CLOUD FORMING PROPERTIES OF ARCTIC AEROSOL DURING ONE YEAR

S. EKSTRÖM[1], U. WIDEQVIST[2], J. STRÖM[2], and B. SVENNINGSSON[1]

[1]Division of Nuclear Physics, Lund University, Lund, 22100, Sweden

[2]Department of Applied Environmental Science, Stockholm University, Stockholm, 10691, Sweden

Keywords: Arctic, CCN, hygroscopicity, aerosol chemistry.

INTRODUCTION

The Arctic aerosol has a strong seasonal variation in terms of number concentration. During the Arctic haze from February to May, aerosol numbers increase significantly. When the sunlight returns and the precipitation start, a period of cleaner air begins which lasts until fall. Long-term aerosol measurements of hygroscopicity and cloud forming properties are scarce in the Arctic region. Previous campaign studies suggest that local production of organic rich aerosol particles occur during the summer (Leck *et al.,* 2002) and model calculations have indicated that these could be important for cloud droplet formation (Lohmann and Leck, 2005). A relationship between the number of CCN and aerosol sulphate content have been shown by (Bigg and Leck, 2001). In addition, ice nuclei concentrations influence the CCN concentration (Lance et al., 2011).

We are now presenting the chemical composition, hygroscopicity, CCN activity of aerosols collected at the Zeppelin station during one year.

METHODS

From September -07 to August -08 twelve filters were collected with a high-volume sampler (PM10 cut-off) at the Zeppelin station, located at 474 m above sea level on Svalbard's west coast, a site that has been assessed as virtually free from local, anthropogenic particle emissions. The chemical composition was assessed from two additional smaller filters, with OC/EC analysis and ion chromatography (IC). The water-soluble fraction was extracted and analysed with respect to the ability to interact with sub- and supersaturated water. For this we used a Hygroscopic Tandem Differential Mobility Analyser (H-TDMA) coupled with Cloud Condensation Nuclei Counters (CCNC).

RESULTS AND DISCUSSION
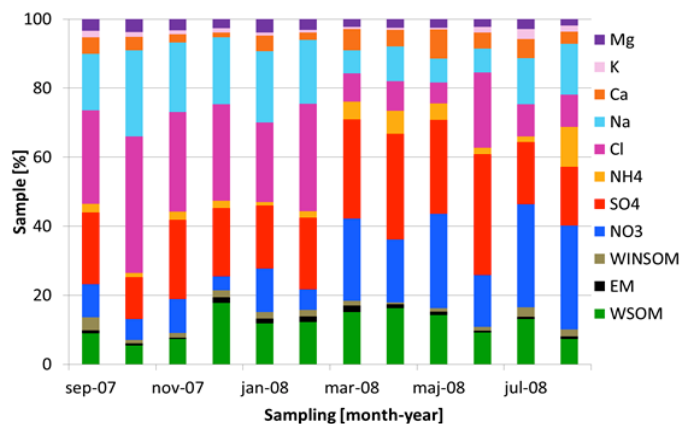
Figure 1. Chemical composition of Arctic aerosol.
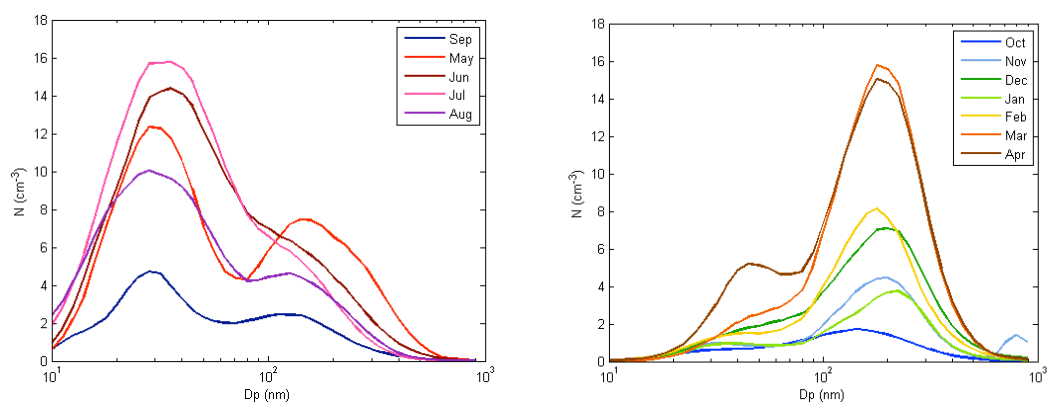
Figure 2. Monthly averages of the aerosol particle size distributions during the sampling period.

The results of the chemical analysis of the Zeppelin aerosol particle samples are shown in figure 1. The aerosol is dominated by the inorganic ions and the insoluble fraction, WINSOM and EM (EC or soot), is small. The aerosol particle size distributions are presented in figure 2. The seasonal variation is clearly seen.

The kappa values derived from CCNC measurements, hygroscopicity at 90% RH (H-TDMA data), and estimated from the chemical composition are shown in figure 3. They show that also the cloud forming properties vary during the year. The fall aerosol particles are clearly more efficient CCN than the spring aerosol. Both are periods dominated by accumulation mode particles in number concentrations. The summer months have size distribution shifted to Aitken mode and these particles are slightly more favourable as CCN than spring aerosol of same size. The kappa values based on hygroscopicity agrees in general well with those based on the CCNC measurements but the estimates based on chemistry gives slightly higher values.
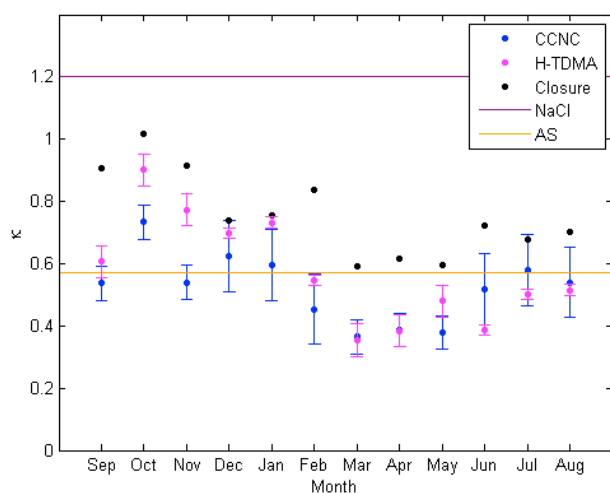
Figure 3. The κ values for each month from September 2007 to August 2008 derived from H-TDMA data, CCNC data and estimated based on chemical composition. The lines are representing reference values for pure ammonium sulfate (AS) and sodium chloride (NaCl) given by Petters and Kreidenweis (2007).

227
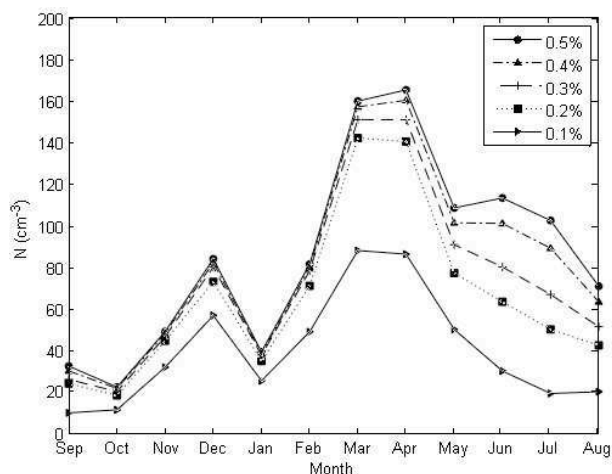
Figure 4. The CCN number concentration for several hypothetical supersaturations given for each month from September 2007 to August 2008.

To investigate whether sulphate and/or organics are important for the CCN population, we plotted concentration quotas against the kappa values. The influence of typical continental aerosol versus common marine was apparent. Sodium and chloride rich aerosol resulted in better CCN than sulphate and ammonium. However, in contradiction to previous findings no correlation between organic content and CCN efficiency was seen. IT should be noted that since we are using monthly samples, the correlations will be dominated by seasonal variations and correlations in day-to-day variability will not show at all.

In figure 4 the average number of CCN for each month is presented for a range of supersaturations. The CCN number is based on aerosol particle size distribution, where both size and number has an influence, as well as the results from the CCNC measurements. It can be seen that, in the period October to April, the number of CCN is almost independent of the supersaturation. This is interpreted as all particles being activated already at 0.2 % supersaturation and is consistent with the aerosol particle size distribution being dominated by accumulation mode particles (figure 2). However, for low supersaturations and when the size distribution is dominated by smaller particles, the kappa values makes a difference for the fraction of particles that can be activated to cloud droplets.

ACKNOWLEDGEMENTS

REFERENCES

Bigg and Leck (2001) *J. Geophys. Res.*, **106**, 32,155-32,166.
Lohmann, U. and Leck, C. (2005) *Tellus,* **57B**, 261–268.
Leck, C., Norman, M., and Bigg, E. K. (2002) *J. Geophys. Res.,* **107**, D12 4135.
Lance, S., Shupe, M. D., Feingold, G., *et al*. (2011) *Atmos. Chem. Phys.,* **11**, 8003–8015.

HOW WELL CAN WE SIMULATE LONG-TERM ARCTIC TREELINE CHANGES? A MODEL-DATA COMPARISON IN THE EUROPEAN TREELINE REGION

K. FANG[1,*], J. MORRIS[1], H. SEPPÄ[1], S. SALONEN[1], P. MILLER[2], H. RENSSEN[3]

1. Department of Geosciences and Geography, PO Box 64, 00014 University of Helsinki, Helsinki, Finland

2. Geobiosphere Science Centre, Department of Physical Geography and Ecosystems Analysis, Lund University, Sölvegatan 12, 223 62 Lund, Sweden

3 Department of Earth Sciences, Faculty of Earth and Life Sciences, VU University Amsterdam, NL-1081HV Amsterdam, The Netherlands

INTRODUCTION

The arctic region has received much attention in recent decades due to its rapid rate of warming. Amplified warming in the Arctic can have large impacts on the vulnerable ecosystems in the circumpolar regions, and enables treelines advances onto the tundra. Because of the sensitivity of Arctic ecosystems to climate warming and their potentials to provide feedbacks to the atmosphere, it is important to understand the drivers of forest/tundra ecotone dynamics. The Lund-Postdam-Jena-GUESS (LPJ-GUESS) model has been widely used to simulate the structure and dynamics of terrestrial ecosystems from landscape to global scales. Extensive investigations of Holocene treeline changes over northern Europe have been conducted using pollen, macrofossil and mega-fossil evidences. The objective of the research presented here is to compare LPJ-GUESS model output withproxy reconstructions of treeline locations in northern Europe and northwestern Russia over the last 9000 years and to make quantitative comparisons of biomass changes for selected treeline locations.

DATA and METHODS

The European arctic treeline region (55 °N - 65 °N, 10 °E - 70 °E) spans from the western coast of Norway eastward to the Ural Mountains, encompassing northern Fennoscandia, Kola Peninsula and northwestern Russia. The modern forest/tundra ecotone essentially mirrors the Arctic Ocean coastline between 60° to 70° N, spanning 5,500 km from the western coast of Norway eastward to the Ural Mountains. We employed the dynamic process-based LPJ-GUESS model to simulate regional vegetation dynamics of the plant functional types (PFT) (dominant species) with mechanistic representations of plant physiological and biogeochemical processes. LPJ-GUESS simulates vegetation dynamics of various PFTs using a number of replicated patches in each gridcell, allowing stochastic processes of establishment, mortality and disturbance to be considered. Two experiments were designed in our LPJ-GUESS simulation using climate data from the ORBGHG driven by orbital forcing and greenhouse gas forcing and OGMELTICE paleoclimate simulations including orbital forcing and greenhouse gas forcing but also includes forcings caused by the freshwater flux, albedo and topography of the Laurentide Ice Sheet. We assembled our fossil dataset from existing published pollen, macrofossil and mega-fossil records in the treeline regions to reconstruct the treeline shifts during the Holocene at 3000-year interval. We synthesized 29 pollen and 16 macrofossil records from the treeline regions in northern Fennoscandia and northwestern Russia.

CONCLUSIONS

Via comparisons between vegetation simulations and fossil pollen, macrofossil and mega-fossil data from northern Fennoscandia and northwestern Russia, we noticed that the model is limited in its ability to simulate species-level treeline dynamics; however LPJ-GUESS is able to simulate the coniferous treeline changes, particularly over the Scandes Mountains and Ural Mountains with a cutoff carbon biomass of 2 kg/m^2. The simulation is also able to capture the northward expansion of the boreal forest onto the tundra during the middle Holocene, and, consistently with data, show the major retreat of the arctic treeline in response to the climatic cooling during the last 3000 years. While there are mismatch with too northern or southern simulated treeline during the Holocene, which result from the temperature mismatches in the paleoclimate simulations. The modeling ability could be improved by considering the topographic features and the widespread peat land in, for example, Kanin peninsula. The simulated treeline appears to be too sensitive to climate, suggesting the current model may need to include potential ecological factors of, for example, microclimte conditions generated by forest. Temperature is the major driving factor for treeline changes and future global warming may have larger impacts over the northern European Russian regions with much tundra.

ACKNOWLEDGEMENTS

REFERENCES

MacDonald, G. M. 2010. Some Holocene palaeoclimatic and palaeoenvironmental perspectives on Arctic/Subarctic climate warming and the IPCC 4th Assessment Report. *Journal of Quaternary Science* 25, 39-47.

Miller, P. A., Giesecke, T., Hickler, T., Bradshaw, R. H. W., Smith, B., Seppä, H., Valdes, P. J. and Sykes, M. T. 2008. Exploring climatic and biotic controls on Holocene vegetation change in Fennoscandia. *Journal of Ecology* 96, 247-259.

Sitch, S., Smith, B., Prentice, I. C., Arneth, A., Bondeau, A., Cramer, W., Kaplan, J. O., Levis, S., Lucht, W. and Sykes, M. T. 2003. Evaluation of ecosystem dynamics, plant geography and terrestrial carbon cycling in the LPJ dynamic global vegetation model. *Global Change Biology* 9, 161-185.

Smith, B., Prentice, I. C. and Sykes, M. T. 2001. Representation of vegetation dynamics in the modelling of terrestrial ecosystems: comparing two contrasting approaches within European climate space. *Global Ecology and Biogeography* 10, 621-637.

RH DEPENDENCY OF THE ION-ION RECOMBINATION COEFFICIENT

A. FRANCHIN[1], S. SCHOBESBERGER[1], S. EHRART[2], H. E. MANNINEN[1], V. MAKHMUTOV[3], T. NIEMINEN[1], J. LEPPÄ[4], V. M. KERMINEN[2], THE CLOUD COLLABORATION, T. PETÄJÄ[1] AND M. KULMALA[1].

[1] Department of Physics, University of Helsinki, P.O. Box 64, FI-00014, Helsinki, Finland

[2] Institute for Atmospheric and Environmental Sciences, Goethe University, 60438, Frankfurt/Main, Germany

[3] Lebedev Physical Institute RAS, 119991, Moscow, Russia

[4] Finnish Meteorological Institute, P.O. Box 503, FI-00101, Helsinki, Finland.

Keywords: SMALL IONS, ION-ION RECOMBINATION, CLOUD CHAMBER.

INTRODUCTION

Ions are present in the atmosphere as part of the aerosol spectrum. They are usually classified in three groups: small ions, if their mass diameter is smaller than 1.6 nm; intermediate ions, if it is in the range [1.6 - 7.4 nm]; large ions, when it is bigger than 7.4 nm (Hõrrak *et al.*, 2000). They are continuously produced in the atmosphere from Galactic Cosmic Rays (GCRs) and terrestrial sources, such as Radon and gamma radiation from the soil and they are important because they play a fundamental role in many aspects of the electricity in the atmosphere, both in fair weather and during thunderstorms (Harrison and Carslaw, 2003). Air ions also enhance secondary aerosol production under certain conditions and, consequently, increase the number of cloud condensation nuclei, thus modify properties of clouds and, therefore, influence the climate (Kirkby *et al.*, 2011). Even though their net role in atmospheric new particle formation has been controversial and, in the literature, there are studies suggesting that their contribution is important or even dominant, whereas other studies indicate that their role is negligible (Hirsikko *et al.*, 2011).

METHODS

During the CLOUD (Cosmics Leaving OUtdoor Droplets) campaigns, several experiments of sulfuric acid-water neutral and ion induced nucleation were performed in an aerosol chamber. In this experiment, Galactic Cosmic Rays (GCR) and the Proton Syncrotron (PS) accelerator at CERN were used as sources to vary the ion production rate (IPR) to generate ions in the 26.1 m^3 CLOUD aerosol chamber under precisely controlled conditions. Both GCR and the PS pion beam were constantly monitored by a GCR counter and by an hodoscope, respectively. The ion concentration in the CLOUD chamber was measured with a Neutral cluster and Air Ion Spectrometer, (NAIS, Kulmala et al., 2007). The NAIS is able to measure air ion number size distributions in the mobility equivalent diameter range of 0.8 to 40 nm and correspondingly neutral particle number size distributions from 2 to 40 nm mobility diameter. In this study we limit our focus to ions with mobility diameter in the range 0.8 - 1.9 nm, measured in an aerosol-free environment. From the measured ion concentration and ion production rate we were able to determine the ion-ion recombination coefficient at different conditions. Here we present the measured recombination coefficient as a function of RH.

RESULTS

We observe an important dependency to RH (Figure 1). The rate at which ions recombine decrease at increasing RH.It should be noted that all the experiments were carried out at constant temperature, therefore, in this case RH corresponds to water vapour concentration. We don't fully understand the RH effect, although we think that it is related to the change in size of the small ions at increasing RH values. When more water vapour is available ions are hydrated and thus their diameter is bigger. This idea is supported by the indication given by Quantum chemistry calculations, that show that ions like to be clustered with water and the amount of water attached is dependent to RH (Husar *et al.*, 2012). It also known that bigger aerosol particles change in size according to the RH. In fact comparing the experimental data with the change of ion-ion recombination rate as a function of size in the range 1-2 nm calculated using Fuchs equations, we can see that there is a qualitative agreement.
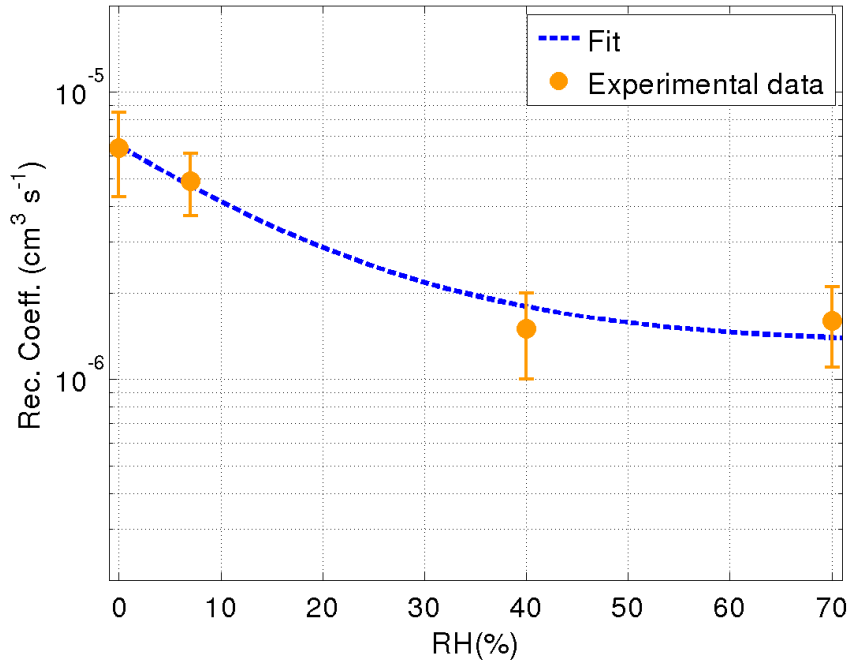
Figure 1: Ion-ion recombination coefficient as a function of RH, the temperature during the experiments was kept constant. The dashed line is an exponential fit to guide the eye.

REFERENCES

Harrison, R. G. and Carslaw, K. S. (2003). Ion-aerosol-cloud processes in the lower atmosphere. *Reviews of Geophysics*, **41**, 26 PP..

Hirsikko, A., Nieminen, T., Gagné, S., Lehtipalo, K., Manninen, H. E., Ehn, M., Hõrrak, U., Kerminen, V.-M., Laakso, L., McMurry, P. H. Mirme, A., Mirme, S., Petäjä, T., Tammet, H., Vakkari, V., Vana, M., Kulmala, M., (2011) Optical scattering from combustion aerosols. *Atmos. Chem. Phys.*, **11**, 767–798.

Hõrrak, U., Salm, J., Tammet, H., (2000). Statistical characterization of air ion mobility spectra at Tahkuse Observatory: Classification of air ions. *Journal of Geophysical Research*, 9291–9302.

Husar, Devon E. and Temelso, Berhane and Ashworth, Alexa L. and Shields, George C. Hydration of the Bisulfate Ion: Atmospheric Implications *The Journal of Physical Chemistry*,**21**, 5151–5163.

Kirkby, J. and Curtius, J., Almeida, J., Dunne, E., Duplissy, J., Ehrhart, S., Franchin, A., Gagne, S., Ickes, L., Kurten, A., Kupc, A., Metzger, A., Riccobono, F., Rondo, L., Schobesberger, S., Tsagkogeorgas, G., Wimmer, D., Amorim, A., Bianchi, F., Breitenlechner, M., David, A., Dommen, J., Downard, A., Ehn, M., Flagan, R. C., Haider, S., Hansel, A., Hauser, D., Jud, W., Junninen, H., Kreissl, F., Kvashin, A., Laaksonen, Ari, Lehtipalo, Katrianne, Lima, Jorge, Lovejoy, Edward R., Makhmutov, Vladimir, Mathot, Serge, Mikkilä, J., Minginette, P., Mogo, S., Nieminen, T., Onnela, A., Pereira, P., Petäjä, T., Schnitzhofer, R., Seinfeld, J. H., Sipilä, M., Stozhkov, Y., Stratmann, F., Tome, A., Vanhanen, J., Viisanen, Yrjo, Vrtala, Aron, Wagner, Paul E., Walther, Hansueli, Weingartner, Ernest, Wex, Heike, Winkler, Paul M., Carslaw, K. S., Worsnop, D. R., Baltensperger, U., Kulmala, M., (2011). Role of sulphuric acid, ammonia, galactic cosmic rays in atmospheric aerosol nucleation. *Nature* **476**, 429–433.

Kulmala, M., Riipinen, I., Sipilä, M., Manninen H. E., Petäjä, T., Junninen, H., Dal Maso, M., Mordas, G., Mirme, A., Vana, M., Hirsikko, H., Laakso, L., Harrison, R. M., Hanson, I., Leung, C., Lehtinen, K. E. J. and Kerminen, V-M. (2007). Toward Direct Measurement of. Atmospheric Nucleation. *Science*, **318**, 89-92.

SIMULATION OF LAKE ICE CHARACTERISTICS UNDER FUTURE CLIMATE

SOLOMON GEBRE[1], BOISSY THIBAULT[1] and KNUT ALFREDSEN[1]

[1]Department of Hydraulic and Environmental Engineering. Norwegian University of Science and Technology, NO-7491 Trondheim, Norway.

Keywords: MyLake Model, Lake Ice phenology, ice thickness, climate scenario.

INTRODUCTION

Lake ice is an important component of the cryosphere and its formation and decay play an important role in the energy balance of lakes in cold regions. Changes in lake ice cover characteristics due to anthropogenic causes will have significant ecological, hydrological, and socio-economic impacts (Prowse et al. 2011). Several one-dimensional (1D) thermodynamic lake-models have been developed over the years to evaluate the influence of climate and lake geometry on the lake thermodynamic balance and ice-phenology. Some of these studies had the objective of assessing the impact of anticipated climate change on lake thermal regimes (Fang and Stefan 2009; Saloranta et al. 2009), and ice cover characteristics (Stefan and Fang 1997; Fang and Stefan 1998; Fang and Stefan 2009). The coupling of 1D lake-models and gridded climate data over large areas is quite a recent phenomenon. Walsh et al. (1998) used a 1D lake-ice model called LIMNOS to produce ice phenology over the Northern Hemisphere on a 0.5° by 0.5° latitude-longitude grid for the period 1931-1960. The study was conducted on hypothetical lakes with mean depths of 5m and 20m using average monthly climate data as input. A few recent studies have also examined conditions of lake ice under a future warmer climate based on gridded simulations over a wide-area using daily input data (Brown and Duguay 2011; Dibike et al. 2011a; Dibike et al. 2011b). So far no detailed physically based modeling of lake-ice conditions has been carried out at a spatially high resolution over the Nordic and Baltic regions. Hence, the objective of this research is geared towards evaluating the sensitivity of lake ice conditions to anticipated climate change in these regions. A one-dimensional, physically-based model of lake-water temperature and ice-cover growth and ablation called MyLake is used to simulate lake ice phenology in the Nordic and Baltic regions on a spatial grid of 25km. Daily data from the ERA40 reanalysis data set downscaled to a 25km resolution using a regional climate model (RCM) was used to drive the model for the current climate. The future climate corresponding to the IPCC A1B, intermediate-level emission scenario, is modeled using an ensemble of two Global Climate Models (GCMs) downscaled to the same resolution. The potential changes to lake ice regimes for hypothetical lakes of various depths (5m, 10m, 20m and 40m) on a regional basis are evaluated for two time periods in the future: mid-century (2041-2070) and end of century (2071-2100).

DATA AND METHODS

The Lake Ice Model, MyLake (Saloranta and Andersen 2007) was first tested and validated using in situ observations on Lake Atnsjøen in South-Central Norway (Fig.1) which has long-term measured temperature profiles and ice phenology data. Meteorological input forcings for model simulations consists of 2m air temperature, precipitation, 2m relative humidity, 10m wind speed, surface air pressure and cloud cover on a daily time step. The meteorological data at nearby stations was obtained from the Norwegian Meteorological Institute (DNMI) whereas inflow discharge and temperature, lake temperature profiles, and ice phenology data were obtained from the Norwegian Water Resources and Energy Directorate (NVE). The model simulates a number of lake characteristics, notably water temperature profile, freeze-up and breakup dates as well as ice and snow thicknesses. The model was run keeping most of the model parameters at default values to ensure its applicability to a wide range of scenarios. Model sensitivity to input forcings was carried out to ascertain which meteorological variable(s) had a strong influence on the results. Data for the regional simulation was obtained from the online data portal of the EU ENSEMBLES

project (http://ensemblesrt3.dmi.dk/), maintained at the Danish Meteorological Institute. The control period (1961-1990) lake ice conditions were simulated using the ERA40 reanalysis data (Uppala et al. 2005) dynamically downscaled to a 25km resolution by using the the Rossby Centre Regional Climate Model (RCAO) developed by the Swedish Meteorological and Hydrological Institute. The Atnsjøen Lake model was also driven with the reanalysis data to evaluate how well the observed lake characteristics are reproduced. Hypothetical lakes of 5m, 10m, 20m and 40m depths were placed at every grid cell (25x25km) which gave 3708 grid cells over the study area; and MyLake simulations were carried out for every grid cell and the respective lake depths. The gridded control period simulation was also compared with historical lake ice observations (lakes of similar depth) from the Global Lake and River Ice Phenology Database (http://nsidc.org/data/lake_river_ice/) which are shown in Fig. 1. The future climate corresponding to the Inter-Governmental Panel on Climate Change (IPCC) SRES A1B scenario was derived from two different GCMs (ECHAM5, Max Planck Institute, GERMANY; HadCM3Q3, Hadley Center, UK) downscaled using the same RCAO RCM at 25km resolution. The delta-change approach (using mean monthly delta changes) was used to perturb the control period meteorological data using the mean monthly climate change signals. The potential changes to lake ice regimes on a regional basis are evaluated for two time periods in the future: mid-century (2041-2070) and end of century (2071-2100) by comparing model simulations of the future periods with the control period.
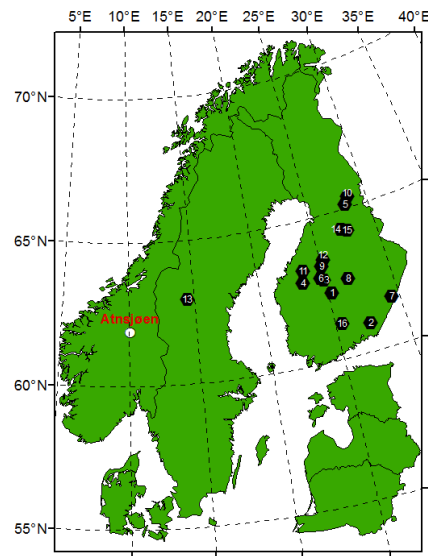
Figure1: Figure showing the study area domain, Lake Atnsjøen (white circle) used for detail model testing and the location of additional 16 lakes (black circles) used for validation of gridded simulation

RESULTS

Detailed model tests on Lake Atnsjøen revealed that MyLake can simulate temperature profiles; lake ice phenology as well as lake ice thickness with good accuracy (Fig. 2). This was done keeping most model parameters at default values which ascertains the applicability of the model for region-wide simulation. Model sensitivity analysis showed that air temperature is the most influencing factor on the model performance followed by relative humidity and inflow temperature. In addition the region-wide gridded simulations (using the downscaled ERA40 reanalysis data) were compared to observations at 16 sites obtained from the Global Lake and River Ice Phenology Database. These results also proved that the model reproduces ice-on and ice-off dates reasonably well with the gridded reanalysis data. These tests confirmed that the model can be employed to predict future ice conditions under anticipated climate change scenarios.
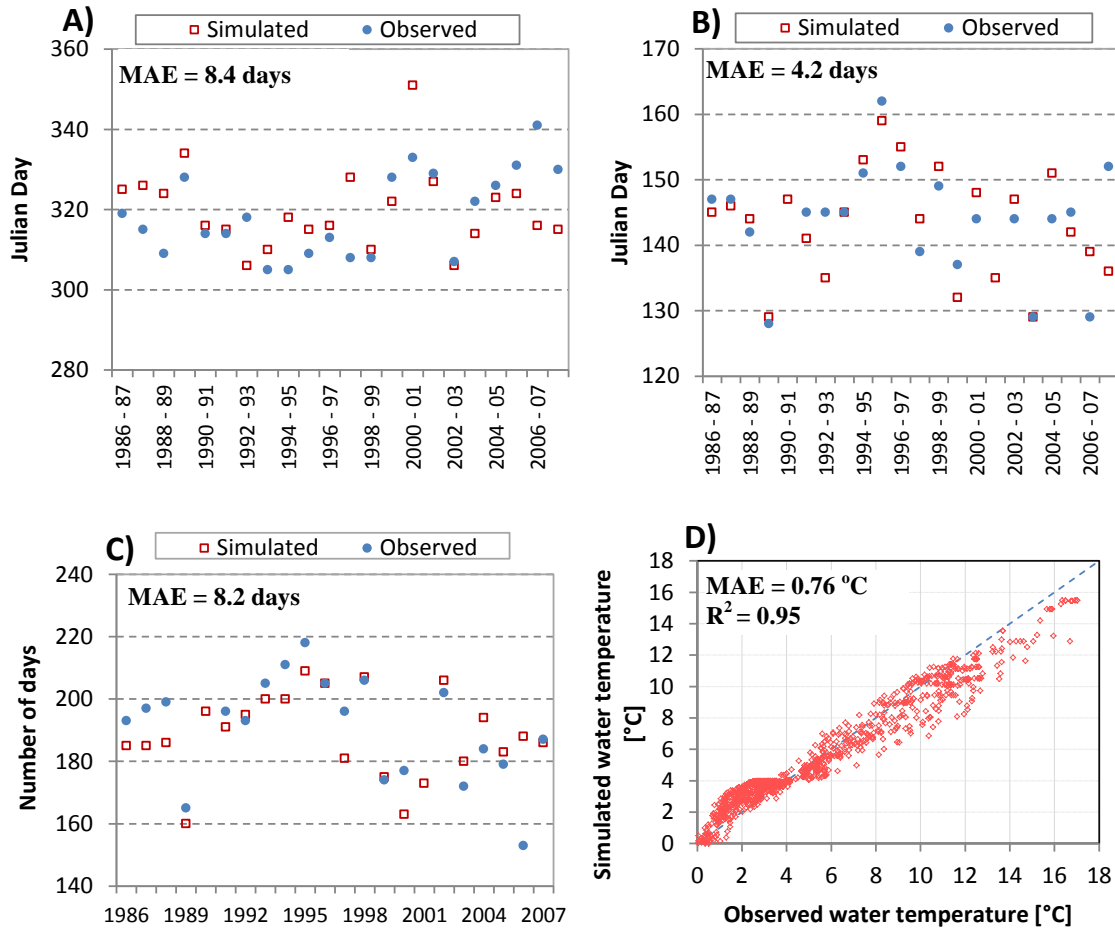
Figure 2: Partial results of model tests on Lake Atnsjøen based on observed meteorological forcing data; also shown are the Mean Absolute Error (MAE), and coefficient of determination (R^2)
A: Freeze-up date, B: Breakup date, C: Ice cover duration, and D: Lake water temperature

Mid-century (2041-2070) conditions
Figure 3 shows expected future changes in lake ice phenology and ice thickness for mid-century (2041-2070) compared to the control period (1961-1990), and for 20m deep lakes. Accordingly, freeze-up will be delayed by 2 to 22 days with the largest changes occurring in lower latitudes. Breakup timing, on the other hand, will advance on a larger margin of 8 to 74 days. The advance in breakup will also be larger in the lower latitudes. The delay in freeze-up and the advance in breakup will reduce the duration of ice cover by 12 to 68 days. The mean annual maximum lake ice thickness will show a marked reduction ranging from 3cm to 59cm and the largest diminution occurring along the Norwegian mountain ranges. The variability of the changes for various lake depths are compared as shown in Figure 4. The changes in ice phenology and thickness don't show a clear pattern with lake depths, though there are slight variations.

End-of-century (2071-2100) conditions
Figure 5 shows the changes in lake ice parameters for end-of-century (2071-2100) period. Freeze-up dates delay by between 5 and 26 days while breakup dates advance by between 11 and 73 days leading to a reduction in ice cover duration of 21 to 85 days (compared to 12 to 68 days for 2041-2070). The sensitivity of the expected changes to various lake depths is depicted in Figure 6, which shows that the expected changes do not show clear and significant dependency with lake depths.
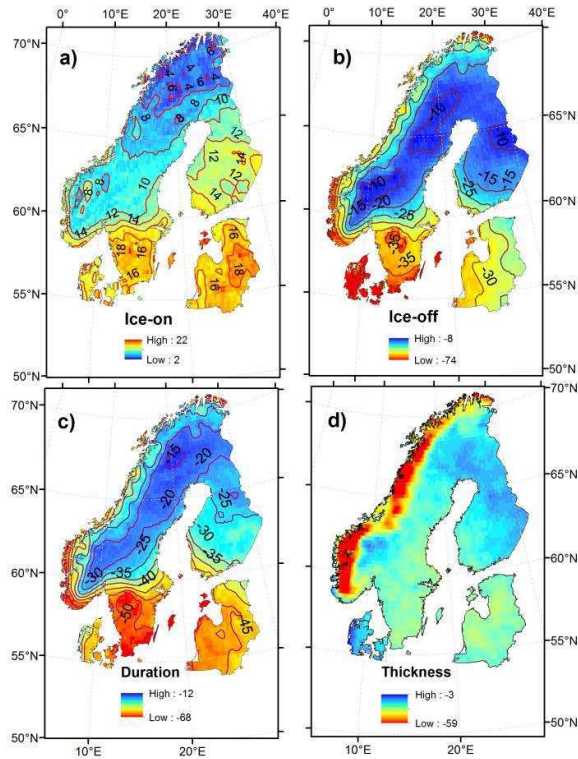
Figure 3: Changes in future ice conditions (2041-2070) compared to the control period (1961-1990) for 20m deep lakes: a) ice-on dates, b) ice-off dates, c) ice duration, and d) ice thickness. The results are derived from the mean simulations using the two GCMs (ECHAM5 and HadCM3Q3).
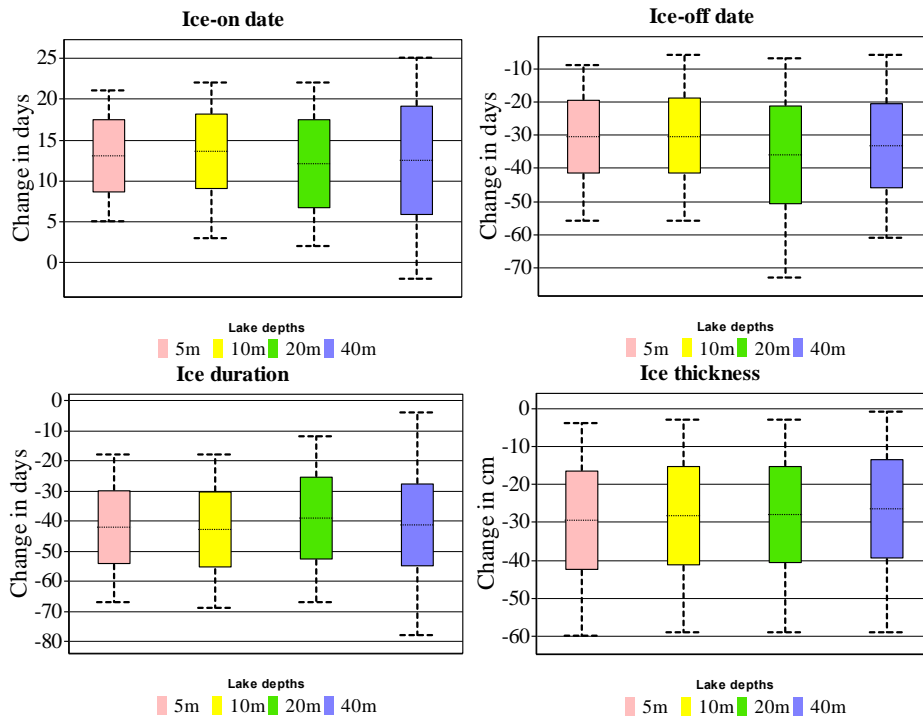
Figure 4: Box plot showing the variability of the future changes for 2041-2070 and for various lake depths
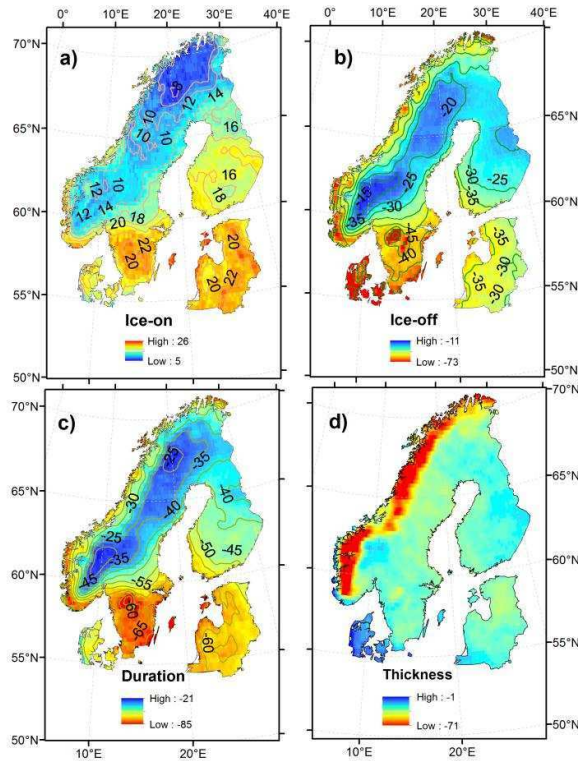
Figure 5: Changes in future ice conditions (2071-2100) compared to the control period (1961-1990) for 20m deep lakes: a) ice-on dates, b) ice-off dates, c) ice duration, and d) ice thickness (cm). The results are derived from the mean simulations using the two GCMs (ECHAM5 and HadCM3Q3).
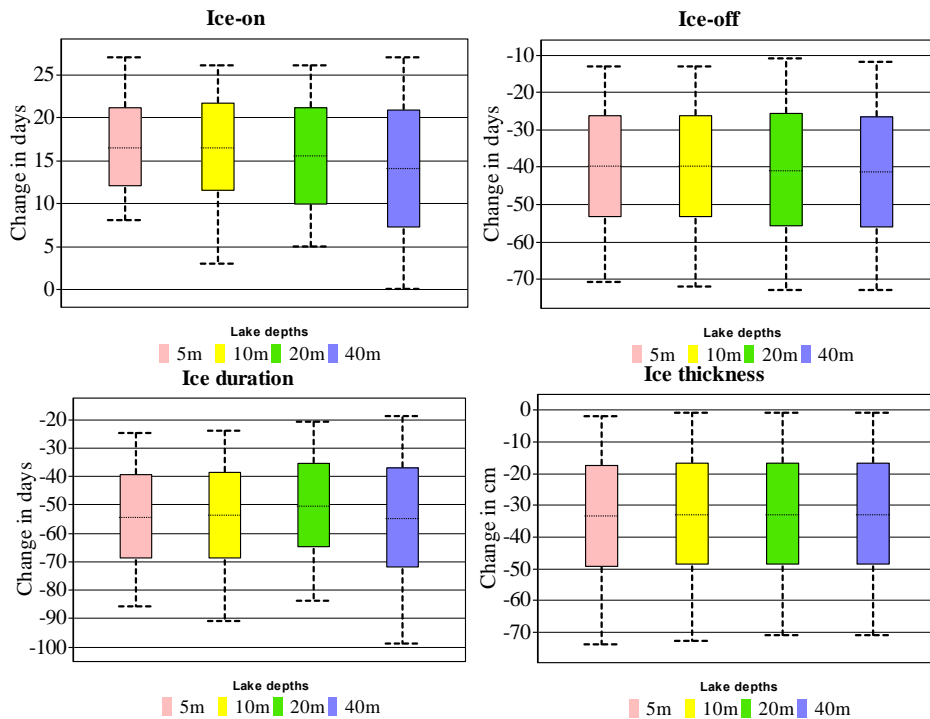
Figure 6: Box plot showing the variability of the future changes for 2071-2100 and for various lake depths

CONCLUSIONS

A one-dimensional, process-based model of lake-water temperature, ice-cover growth and ablation (MyLake) was used to simulate lake ice phenology in the Nordic and Baltic region on a spatial grid of 25km. The potential effects of climate change on lake-ice timing and thickness have been studied with the use of modeling results based on the RCAO RCM driven by two GCMs under SRES A1B emission scenario for two future periods: mid-century-2041-2070 and end-of-century-2071-2100. The results showed that freeze-up will delay by an average of 1 to 3 weeks in 2041-2070 and 1 to 4 weeks in 2071-2100. Breakup, on the other hand, will advance by between 1 to 10 weeks in 2041-2070 and by 2 to 10 weeks in 2071-2100. The combined effects of a delay in freeze-up and an advance in breakup will shorten the ice duration by 1 to 11 weeks in 2041-2070 and 3 to 14 weeks in 2071-2100. Ice thickness shows a reduction between 1 and 60 cm in 2041-2070 and 1 to 70 cm in 2071-2100. These changes in lake ice characteristics in the future can have significant consequences to the ecological and socio-economic functions of the lakes during the winter season.

ACKNOWLEDGEMENTS

REFERENCES

Brown, L. C. and C. R. Duguay (2011). "The fate of lake ice in the North American Arctic." The Cryosphere **5**: 869-892

Dibike, Y., T. Prowse, et al. (2011). "Simulation of North American lake-ice cover characteristics under contemporary and future climate conditions." International Journal of Climatology: 15.

Dibike, Y., T. Prowse, et al. (2011). "Response of Northern Hemisphere lake-ice cover and lake-water thermal structure patterns to a changing climate." Hydrological Processes **25**: 2942-2953.

Fang, X. and H. G. Stefan (1998). "Potential climate warming effects on ice covers of small lakes in the contiguous U.S." Cold Regions Science and Technology **27**: 119-140.

Fang, X. and H. G. Stefan (2009). "Simulations of climate effects on water temperature, dissolved oxygen, and ice and snow covers in lakes of the contiguous United States under past and future climate scenarios." Limonology And Oceanography **54**(6, part 2): 2359-2370.

Prowse, T., K. Alfredsen, et al. (2011). "Effects of Changes in Arctic Lake and River Ice." AMBIO **40**: 63-74.

Saloranta, T. M. and T. Andersen (2007). "MyLake—A multi-year lake simulation model code suitable for uncertainty and sensitivity analysis simulations." Eecological Modelling **207**: 45-60.

Saloranta, T. M., M. Forsius, et al. (2009). "Impacts of projected climate change on the thermodynamics of a shallow and a deep lake in Finland: model simulations and Bayesian uncertainty analysis." Hydrology Research **40**(2-3): 234-248.

Stefan, H. G. and X. Fang (1997). "Simulated climate change effects on ice and snow covers on lakes in a temperate region." Cold Regions Science and Technology **25**: 137-152.

Uppala, S. M., P. W. KÅllberg, et al. (2005). "The ERA-40 re-analysis." Quarterly Journal of the Royal Meteorological Society **131**(612): 2961-3012.

Walsh, S. E., S. J. Vavrus, et al. (1998). "Global patterns of lake ice phenology and climate: Model simulations and observations." J. Geophys. Res. **103**(D22): 28825-28837.

FIRST MODELLING STUDY ON NEW PARTICLE FORMATION AND GROWTH IN SOUTHERN AFRICAN SAVANNAH ENVIRONMENT

R. GIERENS[1], L. LAAKSO[1,2,3], V. VAKKARI[1], D. MOGENSEN[1], and M. BOY[1]

[1]Department of Physics, Division of Atmospheric Sciences, University of Helsinki, Helsinki, 00014, Finland.

[2]Finnish Meteorological Institute, Research and Development, P.O. BOX 503, FI-00101, Finland.

[3]School of Physical and Chemical Sciences, North-West University, Potchefstroom, South Africa.

Keywords: AEROSOL MODELLING, PARTICLE FORMATION AND GROWTH, BOUNDARY LAYER, SOUTH AFRICAN SAVANNAH.

INTRODUCTION

Africa is one of the least studied continents in respect to atmospheric aerosols. In this study measurements from a relatively clean savannah environment in South Africa were used to model new particle formation and growth. There are already some combined long-term measurements of trace gas concentrations together with aerosol and meteorological variables available (Laakso *et al.*, 2008), but to our knowledge this is the first time detailed simulations, that include all the main processes relevant to particle formation, were done.

METHODS

MALTE (Model to predict new Aerosol formation in the Lower TropospherE) is a one-dimensional model, which includes modules for boundary layer meteorology, emissions from the canopy as well as aerosol dynamical and chemical processes (Boy *et al.,* 2006, Lauros *et al.*, 2011). The aerosol dynamic processes are simulated with UHMA (University of Helsinki Multicomponent aerosol model) using two different nucleation approaches, the kinetic nucleation and organic induced nucleation. Previous studies indicate that this model is able to predict new particle formation events at the surface (Boy *et al.*, 2006 and Lauros *et al.*, 2011) and in the boundary layer with good agreement compared with measurements.

The measurements utilized in this study were done at a relatively clean background savannah site in central southern Africa (Laakso *et al.*, 2008). The location is characterized with relatively low pollutant concentrations with occasional polluted air masses from the industrial areas 100-300 km to the east. New particle formation at the site has been found to take place during most of the sunny days, 69 % of the days showing clear nucleation with additional 14 % of the days with non-growing nucleation mode (Vakkari *et al.*, 2011). The measurements include meteorological variables (temperature, relative humidity, wind speed and direction, precipitation, and radiation), trace gas concentrations (SO_2, NO_x, CO, and O_3), aerosol number size distribution, and concentrations of volatile organic compounds.

RESULTS

The observational data was used for input and comparisons with the simulations. We selected a couple of days of continuous data and varying conditions of clean and polluted background air. Figure 1 shows the measured and modelled particle size distributions for one day (the 10th of October 2007), during which a relatively polluted air mass was advected on the site. The model was able to reproduce the nucleation event and the growth of the particles, but the particles grow to the detected size, which is shown in the figure with a white line, later than observed. For this day the kinetic nucleation approach also underestimated the number concentrations.
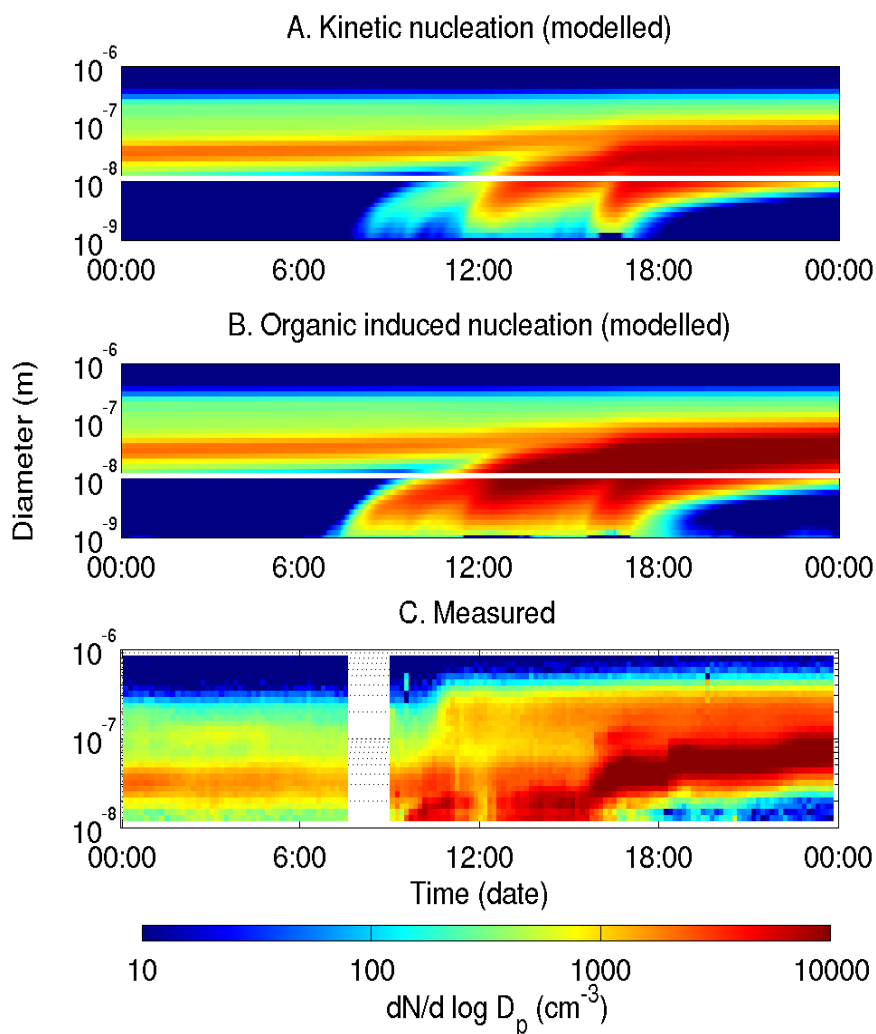
Fig 1. Particle number size distribution on the 10th of Oct assuming a) kinetic nucleation and b) organic induced nucleation in the simulation, and c) from the measurements. The white line in a and b show the detection limit of the instrument at 10nm.

CONCLUSIONS

The frequent new particle formation events and particle growth for the simulated days was evaluated in detail. We were able to simulate the aerosol number concentrations of newly formed particles with a reasonable good agreement with the measurements. This work will present new model results to give a better understanding on the new particle formation process in South Africa and discuss the reasons for high frequency of nucleation episodes observed

FUTURE PLANS

From May 2010 onwards the station in South-Africa has been located in Welgelund, 100 km west from Johannesburg. The instrumentation has been upgraded, for example sensible heat flux and soil temperature are now measured. The new location also allows studying different source areas. We are planning to use this improved data set to continue the work with the model SOSAA. SOSAA (Boy *et al*. 2011) is also a one-dimensional model to study chemistry and aerosol dynamics in the boundary layer, but has the advantage compared to MALTE, that it is parallized. This makes it possible to evaluate longer time series, and thus enables better statistics and investigation of annual cycles, among other things.

ACKNOWLEDGEMENTS

REFERENCES

Boy, M., Hellmuth,O., Korhonen, H., Nilsson, E. D. , ReVelle, D., Turnipseed, A., Arnold, F. , and Kulmala M. (2006). MALTE – model to predict new aerosol formation in the lower troposphere, *Atmos. Chem. Phys.*, **6**, 4499-4517.

Boy, M., Sogachev, A., Lauros, J., Zhou, L., Guenther, A. and Smolander, S. (2011): SOSA - a new model to simulate the concentrations of organic vapours and sulphuric acid inside the ABL - Part I: Model description and initial evaluation, Atmos. Chem. Phys. **11**, 43-51.

Laakso, L.,Laakso, H., Aalto, P. P. , Keronen, P., Petäjä, T., Nieminen, T., Pohja, T., Siivola, E., Kulmala, M., Kgabi, N., Molefe, M., Mabaso, D., Phalatse, D., Pienaar, K., and Kerminen,V.-M. (2008). Basic characteristics of atmospheric particles, trace gases and meteorology in a relatively clean Southern African Savannah environment, *Atmos. Chem. Phys.*, **8**, 4823–4839.

Lauros, J., Sogachev, A., Smolander, S., Vuollekoski, H., Sihto, S.-L., Laakso, L., Mammarella, I., Rannik, Ü., and Boy, M. (2010). Particle concentration and flux dynamics in the atmospheric boundary layer as the indicator of formation mechanism*, Atmos. Chem. Phys.* **11**, 5591-5601.

Vakkari, V., Laakso, H., Kulmala, M., Laaksonen, A., Mabaso, D., Molefe, M., Kgabi, N. and Laakso, L. (2011).New particle formation events in semi-clean South African savannah, *Atmos. Chem. Phys.*, **11**, 3333-3346.

OBSERVATIONS OF AEROSOL OPTICAL PROPERTIES IN ARCTIC BETWEEN 2003 AND 2010

P. Glantz[1], M. Tesche[1] and K. Stebel[2]

[1]Department of Applied Environmental Science (ITM), Stockholm University,
Svante Arrhenius väg 8, SE-11418, Stockholm, Sweden.

[2]Norwegian Institute of Air Research (NILU), Kjeller, Norway.

Keywords: AOD, Ångström exponent, Arctic haze

INTRODUCTION

Due to the ice-albedo-feedback the Arctic is expected to be the region on Earth that is most sensitive to global warming. The ice retreat has continued for more than a decade and shows no sign to stagnate. Climate models (GCM) have for many years predicted a decline in Arctic perennial sea ice due an enhanced green-house effect in combination with the ice-albedo-feedback. The Arctic summer sea ice has declined by approximately 40%, and snow is melting earlier in spring on the surrounding land. Due to more of open water surfaces emissions of sea salt and organic aerosols as well as DMS are expected to increase significant in future. Therefore, it is important to include these sources of aerosols in regional and climate model simulations in an attempt to estimate impacts on the radiation balance in this very sensitive environment. However, the models need to be validated and then against ambient conditions, which is possible based on remote sensing of aerosols in the atmosphere. In the present study aerosol optical thickness (AOT) simulated by the CAM-Oslo model for the subarctic marine region has been compared to AERONET (AErosol RObotic NETwork) sun photometer observations for the period 2003 - 2010. In addition, observed AOT as well as the Ångström exponent (α) are compared to in-situ measurements of aerosol particle size distribution and scattering coefficient, carried out at Mt Zeppelin station, Svalbard, for 2008. Finally, aerosol optical properties obtained with the MODIS (MODerate resolution Imaging Spectroradiometer) collection 5 (c005) standard aerosol product have been evaluated against the AERONET observations.

METHODS

AERONET level 2.0 (quality assured) sun-photometer data of AOT, at 440 and 500 nm, and the Ångström exponent (α), obtained for the wavelengths 440/675 nm, have been analysed for Longyearbyn and Hornsund and the years 2003-2004 and 2005-2010, respectively. The data were recorded every 15 min and automatically cloud screened (Smirnov et al. 2000). AERONET derived estimates of spectral AOT are expected to be accurate within ±0.02 (e.g., Holben et al., 1998).

The recently released MODIS Aqua Collection 5 (c005) Deep Blue level 2 column AOT and α, with the highest confidence level 3, on a 10 km grid at the wavelength 555 nm have be analyzed as well. The spectral observations are screened for thick and thin clouds according to a horizontal resolution of 500 m (Gao et al., 2002; Martins et al., 2002). MODIS Aqua has produce satellite scenes with a swath width of 2 330 km at the surface since 2002. The MODIS Aqua ocean c005 products are accurate to within prelaunch expectations of $\Delta AOT = \pm0.03 \pm0.05 \cdot AOT$ (Remer et al. 2008).

In addition, the aerosols have been characterized at the Mt Zeppelin station, Ny Ålesund, Svalbard, based on in-situ measurements of aerosol particle size distribution and light scattering at three wavelengths with a Differential Mobility Particle Sizing System (DMPS) and an integrating nephelometer, respectively. Measurements with these instruments were performed indoor and with dried samples at relative humidities of 10-30%.

Figure1 shows two MODIS Aqua scenes of AOT around Svalbard, the latter influenced by local and transported aerosols on the 7 July 2005 and 2 May 2006, respectively. Daily median values of AOT as well as α and corresponding one standard deviation have been calculated, according to the white box shown in the figure, for the comparison with the AERONET sites on Svalbard.
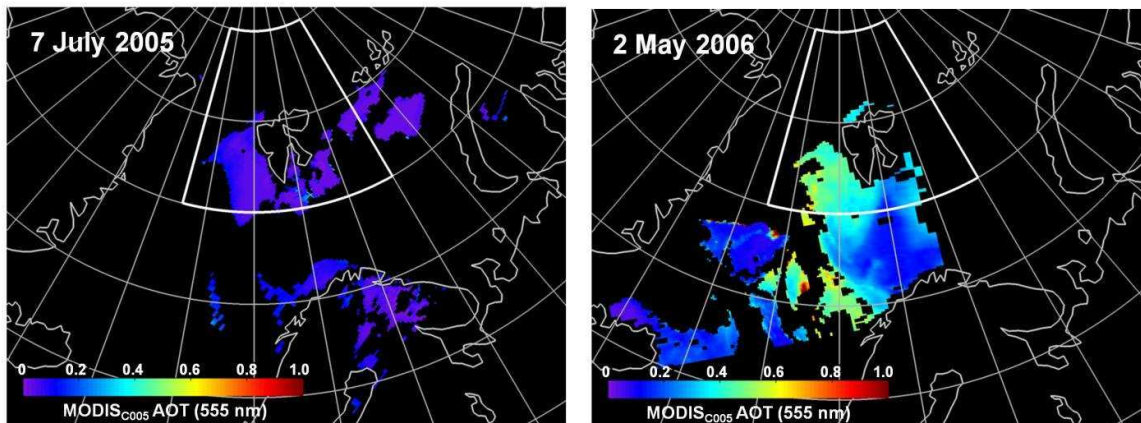
Figure 1. Retrievals of AOT according to MODIS Aqua for 7 July 2005 (left) and 2 May 2006 (right). MODIS median values and corresponding one standard deviation have been calculated according to aerosol pixels within the white box in comparison with AERONET observations (Hornsund/Longyearbyn, Svalbard).

In Figure 2, daily median AOT obtained with MODIS Aqua are compared to AERONET measurements for days of the years 2003 - 2010 where sun photometer data are available. The figure shows that the satellite retrievals of AOT on the whole agree well with the AERONET observations. In addition a clear
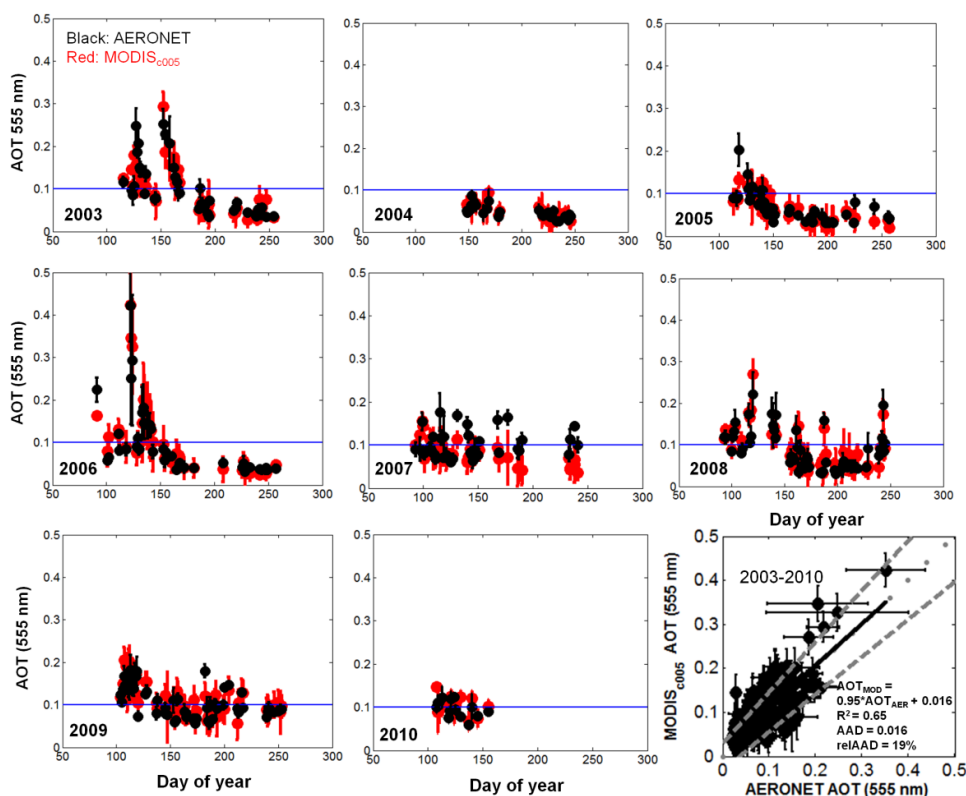
Figure 2. Time series of MODIS c005 and AERONET AOT for the period 2003 - 2010. Dashed lines in the scatter plot denote expected uncertainties for the MODIS retrievals. AAD is the absolute average deviation.

difference in AOT appears between spring (haze period) and summer for the years where enough of data are available. Note that the enhanced values that occur after 15 August 2008 (day 228) and 3 July 2009 (day 185) are caused by Kasatochi and Sarychev volcanic particles, respectively. Vertical profiles of aerosol extinction coefficient at the 532 nm wavelength were measured with the Koldewey Aerosol Raman Lidar (KARL) by Hoffmann et al. (2010) during summer 2008 and Hoffmann (2010) during summer 2009.
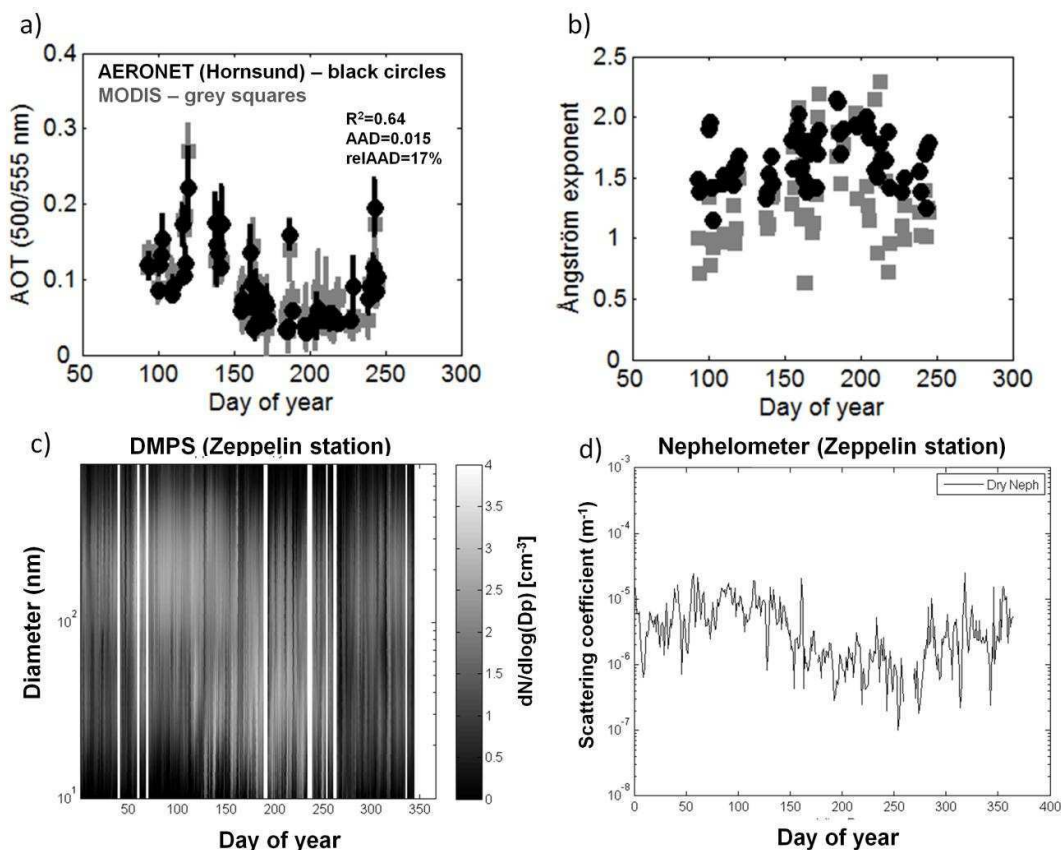
Figure 3. AOT (a) and Ångström exponent (b), retrieved with MODIS and AERONET, and aerosol particle size distributions (c) and aerosol scattering coefficient (d), measured with a DMPS and nephelometer, respectively, in the area around Svalbard for the year 2008.

Figure 3 shows ambient column AOT and α, retrieved by MODIS Aqua and AERONET for 2008. Aerosol microphysical and optical properties measured at the Mt Zeppelin station are also shown. These results are consistent in the sense that a clear seasonal variability appears (see above about influences from volcanic aerosols), although the dry nephelometer aerosol scattering coefficient values are very low in summer. This is probably explained by small aerosols present, which was also found during the summer season at Barrow, Alaska (Quinn et al., 2002). The presence of small aerosols in summer is also supported by MODIS and AERONET α as well as the DMPS values shown in Figure 3. Although the particle number concentrations at Barrow shows a maximum in the summer months the scattering coefficient was also here very low (similar to what is shown in Fig. 3d), indicating that the small particles were inefficient scatters of light (Quinn et al., 2002). By assuming a mean scattering coefficient of 10^{-6}, based on the summer values shown in Figure 3d, and a boundary layer of 2 km this give an AOT of only 0.002 (dry condition) for this layer. Although Figures 3b and 3c suggests that small particles appear in summer the ambient AOT is highly determined by hygroscopic growth, with relative humidity values frequently found to be around 80% or higher during this season (ECMWF). Consequently, it is important to measure aerosol optical properties under ambient conditions in Arctic to estimate radiative effects accurately.

Furthermore, we have compared the satellite and ground-based retrievals of AOT in ambient conditions for the period 2003-2010 (Figure 2) with estimates of AOT by the CAM-Oslo model in the arctic region (Struther et al., 2011). From these preliminary results we have found that the model simulation of total AOT (Figure 9 in Struther et al., 2011) is approximately a factor between 2 and 3 too high in summer for many of the years investigated (Figure 2). The most likely explanation for the discrepancy is an overestimation of the transport of organic aerosol in the model, from distant sources to the arctic region.

CONCLUSIONS

The following conclusions can be established based on the results obtained in this study.

- The validation with AERONET measurements for sites on Svalbard shows that results of AOT obtained with the MODIS Aqua c005 algorithm, for the wavelengths 555 nm, were generally found to vary within the expected uncertainty for one standard deviation of the MODIS retrievals ($\Delta AOT = \pm 0.03 \pm 0.05 \cdot AOT$). Even so, in order to include results of satellite retrievals of AOT for days where no AERONET data are available the deviations that have been found between MODIS and AERONET for some of the days shown in Figure 2 have to be explained.
- A clear seasonal variation was observed in AOT for several of the years investigated. A minimum in AOT appears during the summer season, related to small aerosol particles present (< 100nm) in the atmosphere. The maximum in AOT is observed during the haze season, explained by an increase in the concentration of aerosol particles larger than 100 nm particles.
- Although the number concentration of aerosols is high during the summer months the scattering coefficient was found to be very low, indicating that the small particles were inefficient scatters of light. Therefore, this study suggest that measurements obtained with a wet nephelometer instead of a dry one is required in an attempt to estimate radiative effects accurately.
- This study suggest that observations of aerosol optical properties from space and ground are very useful to evaluate regional and climate model simulations of aerosols in Arctic.

ACKNOWLEDGEMENTS

REFERENCES

Hoffmann, A. (2010). Lidar observations of volcanic aerosol layers in the Arctic. Oral presentation at the IPY Oslo Science Conference, June 11, 3010.

Hoffmann, A., Ritter, C., Stock, M., Maturilli, M., Eckhardt, S., Herber, A. and Neuber, R. (2010). Lidar measurements of the Kasatochi aerosol plume in August and September 2008 in Ny-Ålesund, Spitsbergen. J. Geophys. Res., **115**, D00L12. doi: 10.1029/2009JD013039.

Holben, B. N., Eck, T. F., Slutsker, I., Tanr´e, D., Buis, J. P., Setser, A., Vermote, E., Reagan, J. A., Kaufman, Y. J., Nakajima, T., Lavenu, F., Jankowiak, I., and Smirnov, A. (1998). AERONET – A federated instrument network and data archive for aerosol characterization, Remote Sens. Environ., 66, 1–16.

Gao, B., Kaufman, Y. J., Tanr´e, D., and Li, R. (2002). Distinguishing tropospheric aerosols from thin cirrus clouds for improved aerosol retrievals using the ratio of 1.38 μm and 1.24 μm channels, Geophys. Res. Lett., 29, 1890, doi:10.1029/2002GL015475,.

Martins, J., Tanre, D., Remer, L., Kaufman, Y., Mattoo, S., and Levy, R. (2002). MODIS Cloud screening for remote sensing of aerosols over oceans using spatial variability, Geophys. Res. Lett., 29, 1619, doi:10.1029/2001GL013252.

Quinn, P. K., Miller, T. L., Bates, T. S., Ogren, J. A., Andrews, E. and Shaw, G. E. (2002). A 3-year record of simultaneously measured aerosol chemical and optical properties at Barrow, Alaska, J. Geophys. Res., **107**, D11, 4130, 10.1029/2001JD00124248.

Remer, L. A., Kleidman, R. G., Levy, R. C., Kaufman, Y. J., Tanr´e, D., Mattoo, S., Martins, J. V., Ichoku, C., Koren, I., Yu, H., and Holben, B. N. (2008). Global aerosol climatology from the MODIS satellite sensors, J. Geophys. Res., 113, D14S07, doi:10.1029/2007JD009661.

Smirnov, A., Holben, B. N., Eck, T. F., Dubovik, O., and Slutsker, I. (2000) Cloud screening and quality control algorithms for the AERONET database, Remote Sens. Environ., 73, 337–349.

Struther, H., Ekman, A. M. L., Glantz, P., Iversen, T., Kirkevåg, A., Mårtensson, E. M., Seland, ∅. and Nilsson, E. D. 2011, The effect of sea ice loss on sea salt aerosol concentrations and the radiative balance, Atmos. Chme. Phys., **11**, 3459-3477, doi:10.5194/acp-11-3459-2011.

MESAURING CAMPAIGNS AT ST. NORD, JULY-AUGUST 2011 AND MARCH 2012, DESCRIPTION OF THE MEASUREMENTS AND THEIR ANALYSIS

S. E. GRYNING[1] and E. BATCHVAROVA[1,2]

[1]DTU Wind Energy, Roskilde, Denmark
[2]National Institute of Meteorology and Hydrology, Sofia, Bulgaria
.

AIM OF PROJECT

The project has as starting point measurements carried out at the high-Arctic Station Nord in Greenland which serves as a background station for air pollution. The site is at 81.6°N; 16.7°W, thus usually located north of the polar front.

It is part of a larger project on short lived greenhouse gases in the Arctic, lead by Aarhus University. The specific measurements of special interest here are:

1. Measurements of cloud cover and the height of the atmospheric boundary layer in the high Arctic (St. Nord). Feasibility study with a ceilometer.

2. Measurements of atmospheric fluxes of heat and momentum by a sonic anemometer.

3. Intensive campaigns to provide details on the vertical profile of the atmospheric boundary layer by use of radiosoundings.

The ceilometer measurements are performed continuously since 2011, two radiosonde campaigns has been carried, one 28 July to 5 August 2011 and the next 3 weeks in March 2012. Within CRAICC we will primarily analyze the meteorological measurements at Station Nord in order to:

1. clarify if the instruments (ceilometers, radiosounding) are useful and technical suitable for Arctic conditions.

2. improve the knowledge on the processes in the boundary layer in the high Arctic – what does the weak diurnal variation of the incoming solar radiation do to the atmospheric boundary-layer.

3. See how successful the WRF model will be in modelling the meteorology measured at St. Nord, especially during the intensive campaigns.

SOME EXAMPLES OF RADIOSOUNDINGS FROM THE SUMMERCAMPAIGN IN 2011.

It was generally found that there was more structure in the profiles of the wind speed and direction than we usually observe in Scandinavia. In Figure 1 and 2 some prominent examples are shown. In Figure 1 left panel a very pronounced oscillations in the wind speed profiles between the ground and 1000 meters height can be observe in combination with some very distinct shifts in the wind direction, which suggest a layering of the atmosphere. The clockwise change in wind direction between the ground and 1000 meters height is of the order of 300 degrees. Figure 1 right panel shows a low level jet at around a height of 200

meters. Below the low level jet the wind direction is nearly constant, above it gradually turns clockwise (veers) having a total turning of the wind direction between the ground and 1000 meters height of about 90 degrees.
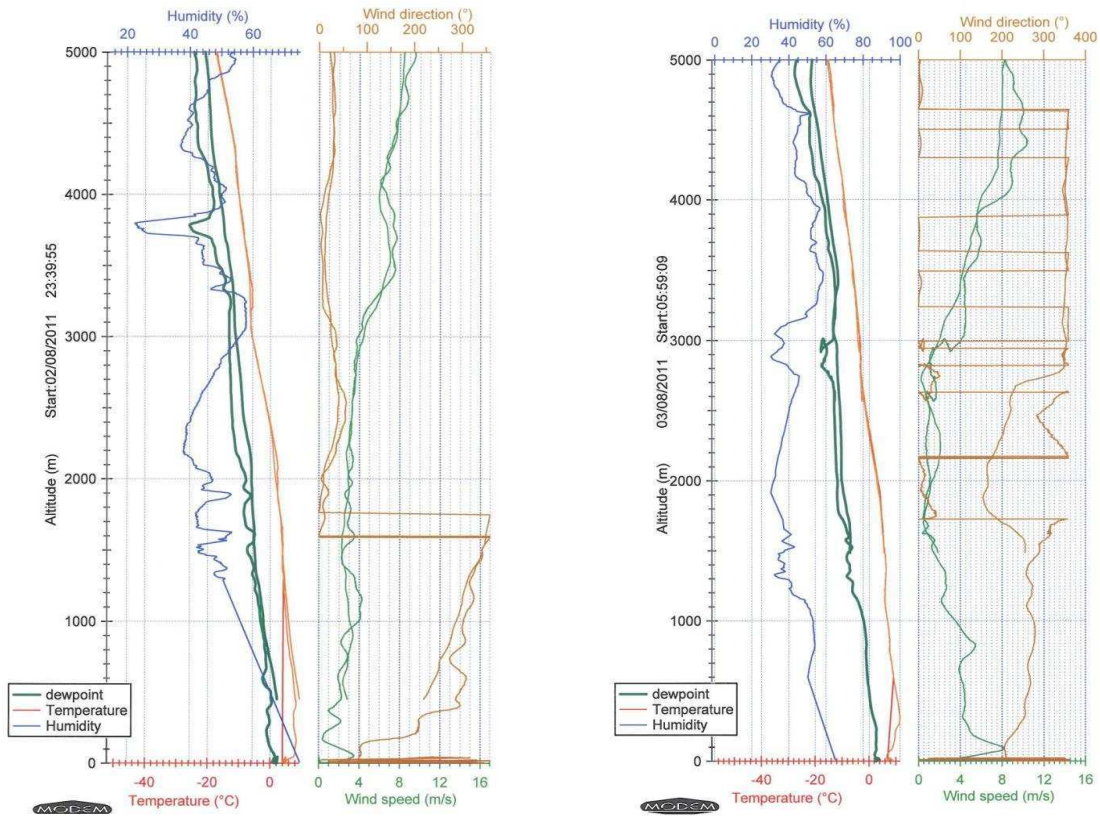
Figure 1. Examples of radiosoundings at St. Nord.

Figure 2 left panel is a fine example of a low level jet of about 14 ms^{-1} at about 400 meters height and a stronger jet of about 50 ms^{-1} at 8 km.. It is also interesting that the southerly wind direction is almost constant with height. It is noted that the upper jet is not westerly as is often observed south of the polar front. Figure 2 right panel is an example of a very shallow strong wind near the surface of about 8 ms^{-1} but being only 2 and 3 ms^{-1} at100 to 200 meters height. There is also a pronounced shift in wind speed and direction at 3 kilometers height but the shift is not associated by pronounced changes in the temperature and humidity profile.
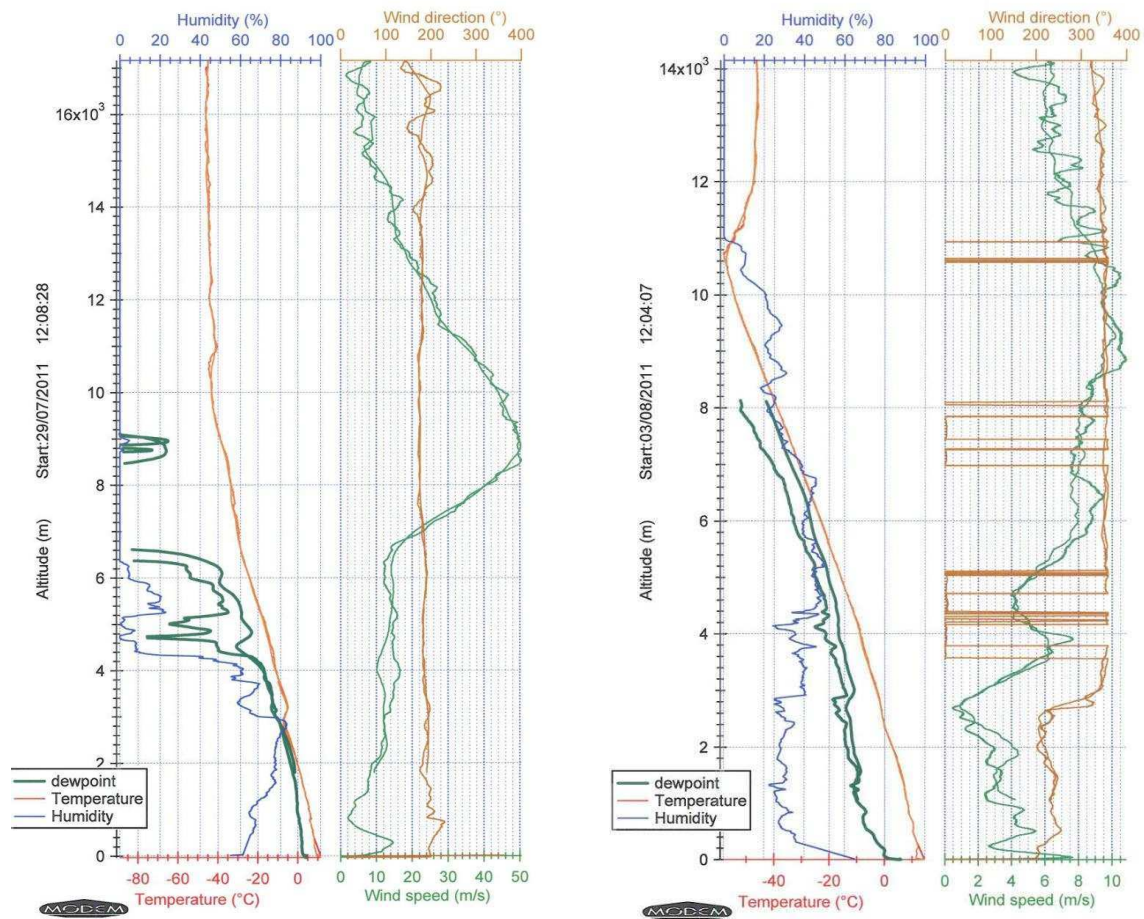
Figure 2. Same as for fig. 1.

CONCLUSION

Rather limited information is available on the formation of the weather in the Arctic air, north of the polar front, which makes the measurements at Station Nord very interesting and their study very challenging. The profiles of wind speed and direction that were measured by radiosoundings carried out at St. Nord during the summer of 2011 generally are quite different from those measured in Scandinavia in such a way that there generally is more structure in the profiles of wind speed and direction at St. Nord. An outline for further investigations on the details of the meteorology during the campaigns is provided.

ACKNOWLEDGEMENTS

EVALUATION OF SEA SPRAY AEROSOL SOURCE FUNCTIONS IN FLEXPART

H. GRYTHE[1,2,3] and A. STOHL[2]

[1]Department of Applied Environmental Science, Atmospheric Science Unit, Stockholm University, Svante Arrhenius väg 8 SE-11418 Stockholm Sweden

[2]NILU - Norwegian Institute for Air Research P.O. Box 100 N-2027, Kjeller, Norway

[3]Finnish Meteorological Institute Erik Palmenin aukio 1, P.O.Box 503, FI-00101 Helsinki, Finland

INTRODUCTION

Sea Spray Aerosol (SSA) is an important factor in the climate system. As atmospheric aerosols, SSA act as climate forcers both directly by reflecting and absorbing radiation and indirectly by affecting cloud microphysics as cloud condensation nuclei (CCN). Combined, the radiative effects of aerosols constitute the largest uncertainties in climate modeling. Thus a better quantification of aerosol sources and aerosol processing is an important task to improve our understanding of climate change (e.g. IPCC 2007).

In marine air, sea spray is generally the dominating source of particulate matter in the atmosphere. Even globally, SSA constitute the largest mass of particulate matter in the atmosphere together with mineral dust (Textor *et. al.* 2006). Production of SSA is primarily wind driven as surface stress forces waves to break and bubbles to form which in turn burst and release particles. A climate with different surface wind speeds will have different SSA production. Consequently SSA production can potentially provide a strong feedback mechanism in the climate system. Recent studies also suggest that warmer ocean temperatures may increase SSA production (Mårtensson *et. al.* 2003; Sofiev *et. al.* 2011). Thus understanding and quantifying the mechanisms responsible for SSA entering the atmosphere is an important task in limiting the uncertainties of the future climate.

METHODS

In this study, the Lagrangian particle dispersion model FLEXPART (Stohl *et. al.* 2005) is used to model SSA concentrations. It is applied to several suggested SSA source functions and compared to a global set of observations from both research ship cruises and measurement stations, spanning almost 30 years. The observed PM_{10} is compared to model masses of four $r < 10$ μm lognormal modes (size classes). The masses that are put into each class are determined by the shape and amplitude in that size range by the different source functions.

The model FLEXPART provides an unique tool to examine the source functions as they are easily implemented and exchanged. FLEXPART is run backwards for each observation. The resulting emission sensitivity is then coupled off-line (i.e., after the model run) with the independent wind (temperature & salinity)-dependent size resolved emitted mass to produce a model PM_{10} mass at the observation site. By applying all the source functions using exactly the same model output and comparing the results against a global set of data, it should be possible to evaluate the overall strengths and weaknesses of all the source functions. It should also be possible to examine the wind/production relationship and temperature and

salinity dependences and identify strengths and weaknesses of individual parameterizations under certain environmental conditions.

EXPECTED OUTCOME

Preliminary results indicate that there is more than an order of magnitude difference in mass produced by the different source functions and similar differences in the resulting concentrations. We also find evidence that there are only weak biases in the model between cold and warm source regions, which suggests a rather weak link between sea surface temperature and production, with warmer waters producing more SSA. A careful statistical analysis of parameters with possible influence on SSA production, including wind, sea surface temperature and salinity will be performed for each observational site. From this, characteristics of each observational site's source region characteristics will be known and can be used to evaluate each parameters influence. When possible, SSA size resolved observations will be compared to modeled size distributions.

ACKNOWLEDGEMENT

REFERENCES

IPCC, 2007: Fourth Assessment Report: Climate Change 2007. Cambridge Cambridge University Press, UK and New York, USA (eds.)

Mårtensson, E. M., E. D. Nilsson, G. de Leeuw, L. H. Cohen, and H. C. Hansson (2003), Laboratory simulations of the primary marine aerosol production, J. Geophys. Res., 108(D9), 4297, doi:10.1029/2002JD002263.

Sofiev, M., J. Soares, M. Prank, G. de Leeuw, and J. Kukkonen (2011), A regional-to-global model of emission and transport of sea salt particles in the atmosphere, J. Geophys. Res., 116, D21302, doi:10.1029/2010JD014713.

Stohl, A., Forster, C., Frank, A., Seibert, P., and Wotawa, G.: Technical note: The Lagrangian particle dispersion model FLEXPART version 6.2, Atmos. Chem. Phys., 5, 2461–2474, doi:10.5194/acp-5-2461-2005, 2005.

Textor, C., et al. (2006), Analysis and quantification of the diversities of aerosol life cycles within AeroCom, Atmos. Chem. Phys., 6, 1777–1813, doi:10.5194/acp-6-1777-2006.

INTERCOMPARISON OF GAS ANALYZERS FOR NITROUS OXIDE FLUX MEASUREMENTS

S. HAAPANALA[1], S. LIND[2], N. HYVÖNEN[2], M. ACOSTA[1,3], O. PELTOLA[1], I. MAMMARELLA[1], N. SHURPALI[2], and T. VESALA[1]

[1]Department of Physics, University of Helsinki, Finland
[2]Department of Environmental Science, University of Eastern Finland, Finland
[3]Global Change Research Centre, Academy of Sciences, Czech Republic

Keywords: EDDY COVARIANCE, NITROUS OXIDE.

INTRODUCTION

During the last years there has been a rapid development in application of laser spectroscopy for greenhouse gas measurements. The goals of this study are to compare the available equipment for N_2O flux measurements and to evaluate their reliability, need of maintenance, user friendliness, data coverage, data quality; and to determine the magnitude and dynamics of N_2O fluxes during the growing season of reed canary grass (Phalaris arundinaceae L.). The primary output from this campaign will be instrumentation suggestion for the European research infrastructure ICOS (Integrated Carbon Observation System). In addition, the methods for flux calculation using laser spectrometer data are evaluated and further developed.

Three gas analyzers, capable of measuring nitrous oxide (N_2O) concentration at a response time necessary for eddy covariance flux measurements, were operated in parallel during the growing season of 2011. The instruments were TGA100A (Campbell Scientific Inc.), CW-TILDAS-CS (Aerodyne Research Inc.) (see e.g. Zahniser et al., 2009; Lee et al., 2011), and N2O/CO-23d (Los Gatos Research Inc.) (see e.g. Provencal et al., 2005). Los Gatos instrument was operational only from the beginning of July.

The measurement site is a plantation of reed canary grass - a perennial bioenergy crop. The site is located on the rural area of Maaninka, Eastern Finland. The plantation is fertilized in the beginning of the growing season, resulting in large emission pulse of N_2O into the atmosphere. The emission dynamics of N_2O is of great importance in defining the greenhouse gas balance of the bioenergy production by reed canary grass (e.g. Shurpali et al., 2010).

RESULTS AND CONCLUSIONS

The preliminary results show great similarity among the instruments in both concentrations and fluxes. Figure 1 show turbulent fluxes of sensible heat, momentum and nitrous oxide measured in May 2011. N_2O fluxes were small in the beginning of the season, increased significantly after the fertilization and then decreased back to low, although clearly positive, level after a few weeks. Aerodyne CW-TILDAS-CS has clearly the lowest detection limit thanks to its low noise. Los Gatos N2O/CO-23d also provides sufficiently good data, while the old generation instrument, Campbell TGA100A suffers from clearly higher levels of noise and drift. There were some differences between the instruments in reliability and need on maintenance. However, these are difficult to evaluate quantitatively during that short period, and using just one instrument of a kind.
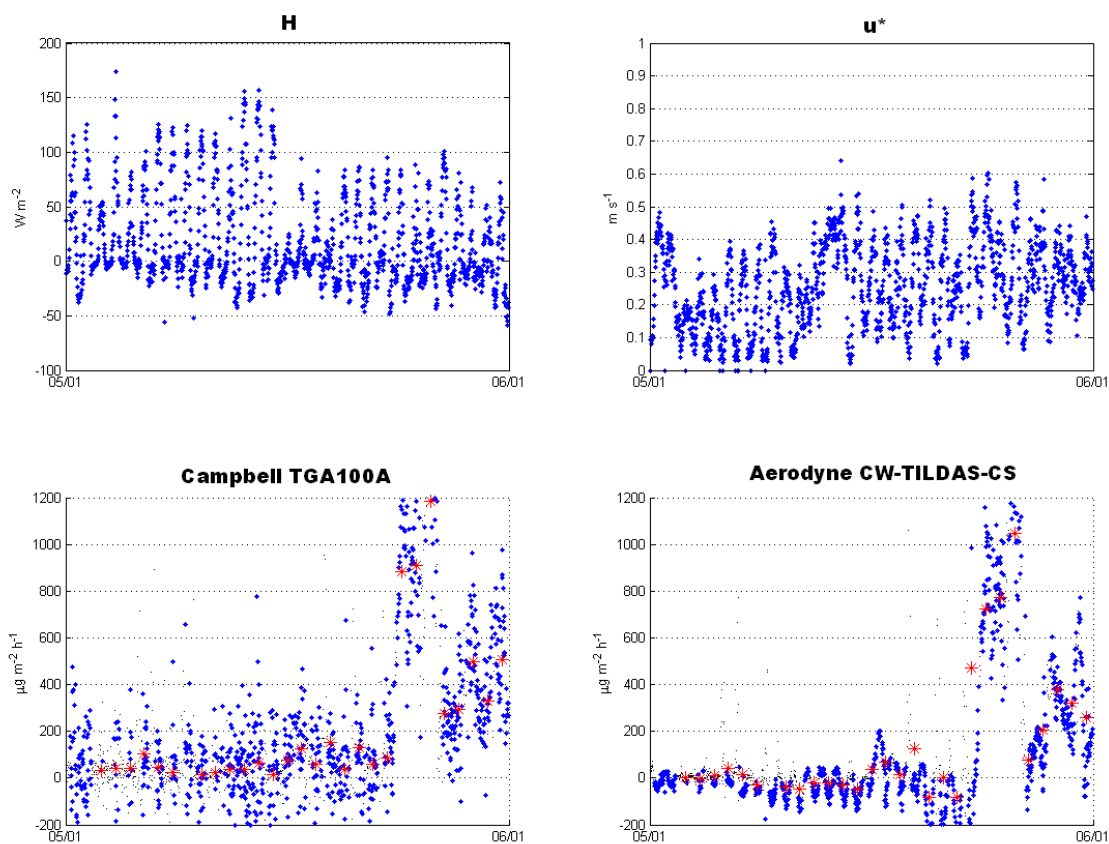
Figure 1. The two upper panels show sensible heat flux and friction velocity measured in May 2011. The two bottom panels show N_2O fluxes measured using Campbell TGA100A and Aerodyne CW-TILDAS-CS. The blue dots are ½ hour data while the red stars indicate the daily averages. The fertilization took place 23rd of May causing the strong emission peak.

Instrument	RMS noise (ppb)
Campbell TGA 100A	1.8
Los Gatos N2O/CO-23d	0.4
Aerodyne CW-TILDAS-CS	0.1

Table 1. Comparison between the RMS noises of different instruments measuring N_2O at 10 Hz.

REFERENCES

Lee, B. H., Wood, E. C., Zahniser, M. S., McManus, J. B., Nelson, D. D., Herndon, S. C., Santoni, G. W., Wofsy, S. C., and Munger, J. W. (2011). Appl. Phys. B, **102**, 417-423.

Provencal, R., Gupta, M., Owano, T. G., Baer, D. S., Ricci, K. N., O'Keefe, A., and Podolske, J. R. (2005). Appl. Optics, **44**, 6712-6717.

Shurpali, N. J., Strandman, H., Kilpeläinen, A., Huttu-nen, J., Hyvönen, N., Biasi, C., Kellomäki, S., and Martikainen, P. J. (2010). GCB Bioenergy, **2**, 130-138.

Zahniser, M. S., Nelson, D. D., McManus, J. B., Hern-don, S. C., Wood, E. C., Shorter, J. H., Lee, B. H., Santoni, G. W., Jimenez, R., Daube, B. C., Park, S., Kort, E. A., and Wofsy, S. C. (2009). Proc. SPIE, **7222**, 72220H.

DETECTION EFFICIENCY OF A TSI ENVIRONMENTAL PARTICLE COUNTER 3783

J. HAKALA[1], H.E. MANNINEN[1], T. PETÄJÄ[1] AND M. SIPILÄ[1]

[1]Department of Physics, University of Helsinki, PL 64, 00014 University of Helsinki, Finland.

Keywords: CPC, DETECTION EFFICIENCY

INTRODUCTION

Monitoring the number concentration of aerosol particles is one of the basic measures to characterize the air quality for health and climatological purposes. The Condensation Particle Counters (CPCs), which include the new water based TSI Environmental Particle Counter (EPC) 3783 under the study, are widely used for this purpose. In this study we present the experimental and simulated results of the performance of the EPC 3783 for hygroscopic and hydrophobic materials.

METHODS

The detection efficiency and cut-off diameter D_{50} for a TSI model 3783 were determined by particles produced by evaporating silver (Ag), ammonium sulphate ($(NH_4)_2SO_4$) and sodium chloride (NaCl) to passing nitrogen flow in a tube furnace. As the flow cooled down after exiting the furnace, the vaporized material nucleated forming polydisperse aerosol particles. A monodisperse fraction of a certain diameter was selected with a Differential Mobility Analyzer, and the detection efficiency of the EPC was determined by comparing the number concentration measured by EPC 3783 to the number concentration measured by an electrometer. The cut-off diameters for different materials with default saturator and growth tube temperatures (20°C and 60°C respectively) are presented in table 1.

Particle material	D_{50} [nm]
Ag	6.4
$(NH_4)_2SO_4$	4.8
NaCl	4.3

Table 1. The EPC 3783 cut-off diameters for particles of different chemical composition.

The supersaturation inside the growth tube is the key element affecting the detection efficiency of the laminar flow water based CPCs (Hering and Stolzenburg, 2005). It was calculated using Comsol Multiphysics 3.5a simulation software. Knowing the supersaturation, it was possible to calculate the contact angle best suited to replicate the detection efficiency curve for non-soluble particles using the heterogeneous nucleation theory (Fletcher, 1958). The Köhler-theory was used to simulate the detection efficiency for hygroscopic and water soluble salts.

CONCLUSIONS

Our experiment show an expected behavior for the cut-off diameters of particles of different chemical compositions; the more hygroscopic the particles are, the lower the cut-off diameter. The contact angle for silver particles retrieved from the simulation was 36°, which is in good agreement with results by Wagner *et al.*, 2003. In figure 1 are presented the simulated and experimental results for the detection efficiency of the EPC 3783 for silver particles. It can be seen from the figure that the contact angle alone can't be the only parameter for predicting the detection efficiency. It also turned out that the simulations overestimated the detection efficiency for NaCl and $(NH_4)_2SO_4$ particles. It seems that there are no experiments

256

published that study the hygroscopic growth and activation of NaCl particles below 6 nm and $(NH_4)_2SO_4$ particles below 8 nm to compare our results with.
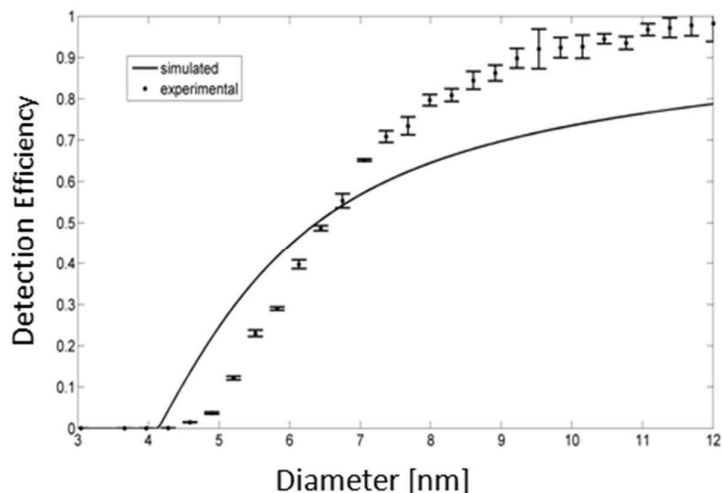
Figure 1. The simulated and experimental detection efficiency of the TSI EPC 3783 for silver particles.

ACKNOWLEDGEMENTS

REFERENCES

Fletcher, N. H. (1958). The Size Effect in Heterogeneous Nucleation. *J. Chem. Phys.* 29:572-577.

Hering, S. V. and Stolzenburg, M. R. (2005). A Method for Particle Size Amplification by Water Condensation in a Laminar, Thermally Diffusive Flow. *Aerosol Sci. Technol.* 39:428-436.

Köhler, H. (1936): The nucleus and the growth of hygroscopic droplets, *Trans. Farad. Soc.*, 32, 1152–1161.

Wagner, P. E., Kaller, D., Vrtala, A., Lauri, A., Kulmala, M., and Laaksonen, A. (2003) Nucleation Probability in Binary Heterogeneous Nucleation of Water-n-Propanol Vapor Mixtures on Insoluble and Soluble Nanoparticles. *Phys. Rev. E.* 67:021605.1–021605.12.

IN SITU MEASUREMENTS OF VOLATILE ORGANIC COMPOUNDS IN A BOREAL FOREST

H. HAKOLA[1], H. HELLÈN[1], M. HENRIKSSON[1], J. RINNE[2],
M. KULMALA[2]

[1]Finnish Meterological Institute, PL 503, 00101 Helsinki, Finland
[2]Helsinki University

Keywords: VOC, monoterpene, sesquiterpene, on-line GC

INTRODUCTION

The concentrations of biogenic VOCs have been measured in western Eurasian boreal forests using pumped sampling into the sample canisters (Laurila and Hakola, 1996; Hakola et al., 2006a), adsorbent tubes (Hakola et al., 2003 and 2009), and by online proton transfer reaction – mass spectrometry, PTR-MS (Rinne et al., 2005; Lappalainen et al., 2009). Often the measurements conducted by the two first-mentioned techniques, requiring laboratory analysis by gas chromatographic techniques, enable good compound identification but they lack the time resolution of the last-mentioned technique (PTR-MS). However, compound identification in PTR-MS measurements is less certain than with GC-MS, and PTR-MS cannot separate compounds with the same mass, e.g. monoterpenes, from each other.

As an example of earlier research, the solid adsorbent sampling measurements by Hakola et al. (2009) at a boreal forest site, SMEAR II, cover a uniquely long time-period, seven years, but samples were only taken at midday about twice a week. However, they reveal significant variations in annual patterns of concentrations, which are influenced by biological and meteorological factors. The measurements at the same site by PTR-MS (Rinne et al., 2005) show the contrasting diurnal cycles of e.g. isoprene and monoterpenes, but cannot separate the individual monoterpenes.

There is thus a need for well-identified VOC concentration data, especially speciated monoterpene concentration data, covering full annual cycles with a time resolution capable of revealing diurnal cycles. In the current study we conducted VOC measurements at the SMEAR II station using on-line gas-chromatograph.

METHODS

The VOCs were measured using an on-line gas-chromatograph-mass-spectrometer. Ambient air was drawn through a 3 or 5 metre long stainless steel tube (od 1/4 inch) at a flow rate of 1 l/min. According to the instructions given by Helmig et al. (1997) the tubes were heated to 120^oC to avoid any losses of sesquiterpenes. The recoveries were at least 89 % for the compounds found in the present study. The heated inlet also destroyed ozone, and no other ozone removal was needed (Hellén et al., 2012). The ozone removal by a heated inlet and subsequent VOC recoveries has been tested by Hellén et al., (2012). VOCs in a 38 ml/min subsample were collected in the cold trap of a thermal desorption unit (Perkin Elmer ATD-400) packed with Tenax TA. The trap was kept at $10\square C$ (after June 2011 at 20^oC) to prevent water vapour present in the air from accumulating into the trap. This allowed the analysis of mono- and sesquiterpenes, but not isoprene, since it needs lower temperatures or stronger adsorbents. Approximately 60 % of the isoprene was lost during collection. Also benzene was not retained totally in the cold trap at

20°C, and about 60 % of the benzene was lost. At 10°C there was no breakthrough of benzene, and thus benzene results are reliable until June. Sesquiterpene measurements were unreliable in June and in July due to the bad quality of the chromatography at the end of the chromatogramme, and these data were not used.   The thermal desorption instrument was connected to a gas chromatograph (HP 5890) with DB-1 column (60 m, i.d. 0.25 mm, f.t. 0.25 μm) and a mass selective detector (HP 5972). One 60-minute sample was collected every other hour. The system was calibrated using liquid standards injected on Tenax TA-Carbopack B adsorbent tubes and analyzed using the offline mode of the instrument. The detection limit was below 1 ppt for all of the analytes, much lower than in the corresponding off-line analysis.

The measurements did not cover the whole year, but at least one week was measured each month. In June and in July sesquiterpene data was lost due to chromatographic problems.

RESULTS AND DISCUSSION

Figure 1 shows the mean monthly concentrations of monoterpenes and aromatic hydrocarbons. Aromatic hydrocarbons are emitted from traffic and wood combustion (Hellén et al., 2006, 2008) and have maximum concentrations in winter due to slower sink reactions and larger emissions (e.g. heating with wood and cold starts of cars), whereas monoterpenes, in spite of their faster sink reaction, have maximum concentrations in summer due to larger emissions during the growing season. Sesquiterpenes have a summer maximum, but small amounts of sesquiterpenes were also measured in winter. The sesquiterpene summer maximum is in accordance with their emission rate maximum from Scots pine (Hakola et al., 2006b) and Norway spruce (Hakola et al., 2003).

During the winter months, concentrations of mono- and sesquiterpenes were low, very often below detection limits. Aromatic hydrocarbons were the main compound group; the mean winter concentration of all aromatics was 270 ppt, whereas mono- and sesquiterpene winter mean concentrations were 8 and 2 ppt, respectively (occasional episodes not included). Monoterpene concentrations increased gradually in spring and reached a maximum in August (520 ppt). In July, measurements covered only the first week, and therefore the maximum could have been reached earlier than in August. Sesquiterpene concentrations also had a maximum in August (2.3 ppt). Aromatic hydrocarbons were below 100 ppt after June, and stayed at a low level until the measurements were finished in October 2011.

The main monoterpene in winter was camphene, followed by p-cymene, α-pinene, and Δ^3-carene (Fig.2). The amount of p-cymene and camphene did not change much annually, the lowest concentrations being measured in February 2011, 1 ppt both, and the highest in summer 2011, 11 ppt in June for p-cymene and 28 ppt for camphene in June. As spring proceeded, the contribution of camphene and p-cymene became less important, and by February the main monoterpene was already α-pinene, followed by Δ^3-carene. Limonene, β-pinene and 1,8-cineol concentrations were only significant (monthly mean above 10 ppt) in summer and early autumn. The main sesquiterpenes measured were longifolene and isolongifolene (Fig. 3). The somewhat surprising sesquiterpene winter concentrations may be due to fluxes from the forest floor (Aaltonen et al., 2012).
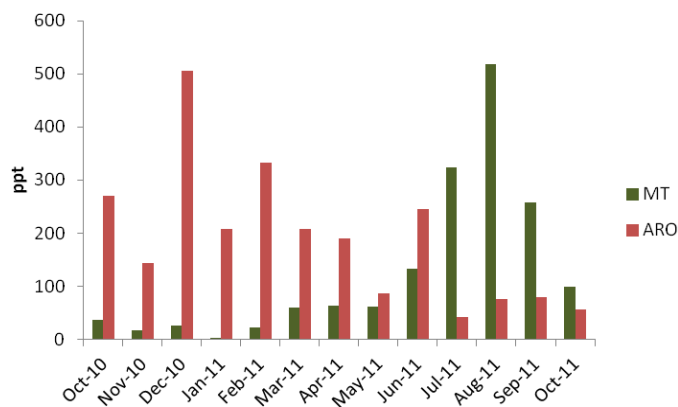
Figure 1: Monthly mean concentrations of monoterpenes and aromatic hydrocarbons at Hyytiälä.
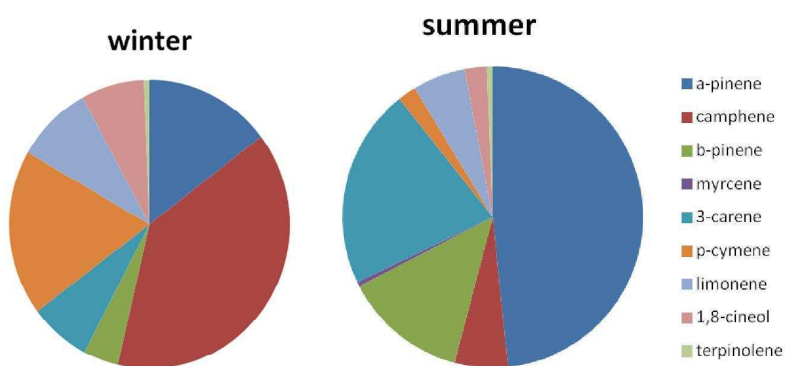
Figure 2: The monoterpene distribution in winter and in summer at Hyytiälä.
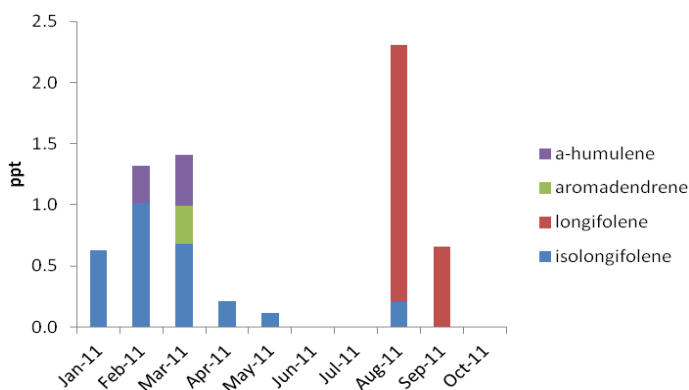
Figure 3: The monthly mean concentrations of different sesquiterpene species at Hyytiälä. June and July measurements are missing due to chromatographic problems.

During the winter months there was no diurnal variability in any of the VOCs. The monoterpene concentrations above detection limits were associated with occasional episodes. In the middle of April,

monoterpenes started to show a pronounced diurnal variation, maximum concentrations occurring during the night and minima during the day (Fig. 4). March is not included in the figure, because concentrations in March recalled the low winter concentrations with no diurnal variation. Even though the emissions from Scots pine (the main tree species in the vicinity) are higher during the day (Holzke et al., 2006; Rinne et al., 2005; Taipale et al., 2011), the ambient air concentrations measured during the day were at their lowest, due to increased mixing and faster photochemical reactions.

In summer, the diurnal variability was similar to that in spring, except that the concentrations were higher, the total monoterpene concentration being 670 ppt at night and 60 ppt in the daytime (Fig. 5). This is due to the higher emissions in summer. The highest hourly monoterpene concentrations in summertime were generally observed during periods with the lowest friction velocities, and vice versa (Fig. 6). As the friction velocity tends to be lower at night, the higher concentrations are mainly found at night-time. It is noteworthy that low daytime friction velocities are also often associated with high monoterpene concentrations. Friction velocity is a good estimate for mixing and boundary layer height. The smaller the friction velocity the smaller the BL heigh and vice versa. Each monoterpene species also showed similar behaviour separately. In contrast, isoprene concentrations did not show this kind of behaviour but were generally lowest in the night and highest in the afternoon.

Isoprene is formed and emitted only in light conditions and is not therefore emitted during the night. A significant part of the monoterpene emission originates from large storages, and is thus controlled by temperature via the saturation vapour pressure of monoterpenes (Ghirardo et al., 2010). This leads to significant night-time emission, albeit lower than daytime emissions. Thus the diurnal cycle of isoprene concentration is the opposite to that of the monoterpenes. Since sesquiterpene concentrations showed a similar diurnal profile to that of the monoterpenes (Fig. 7), emissions are not likely to be totally under the control of light.
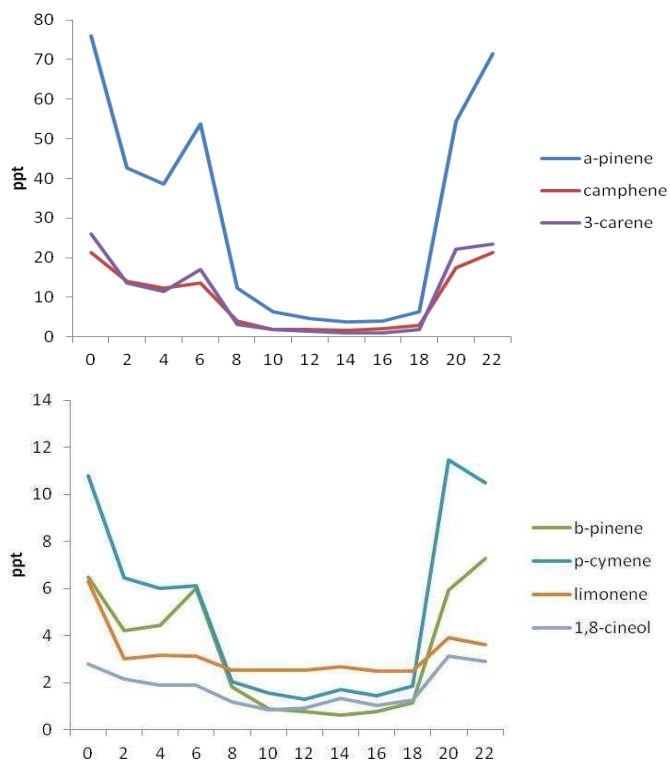
Figure 4: The mean diurnal variability of monoterpenes in spring (April, May). March is not included in the figure, because concentrations then are more like winter concentrations, with no diurnal variability.
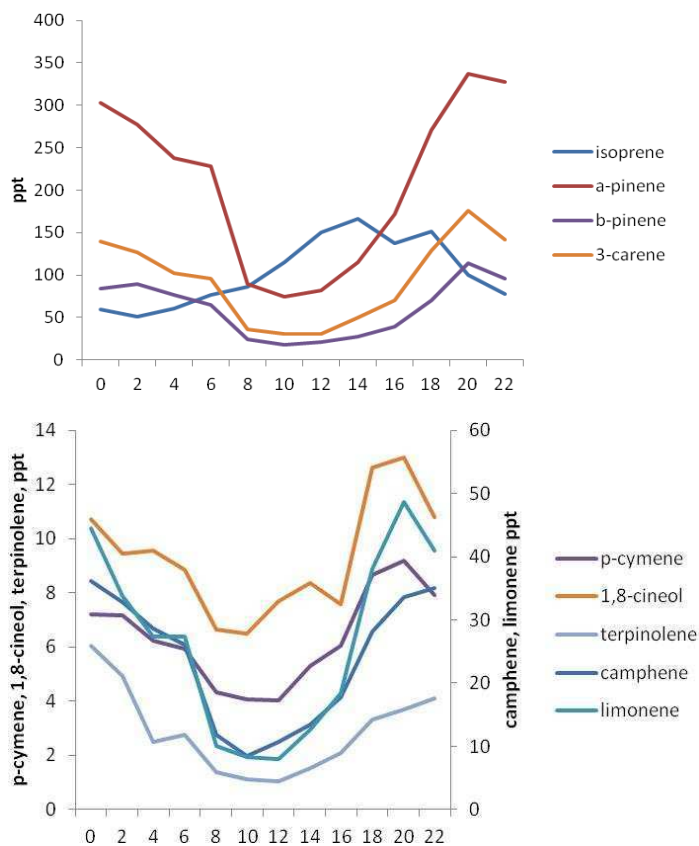
Figure 5: The mean diurnal variability of monoterpenes and isoprene in summer (Jun, July, Aug). (Isoprene concentrations are underestimates due to breakthrough of the cold trap)
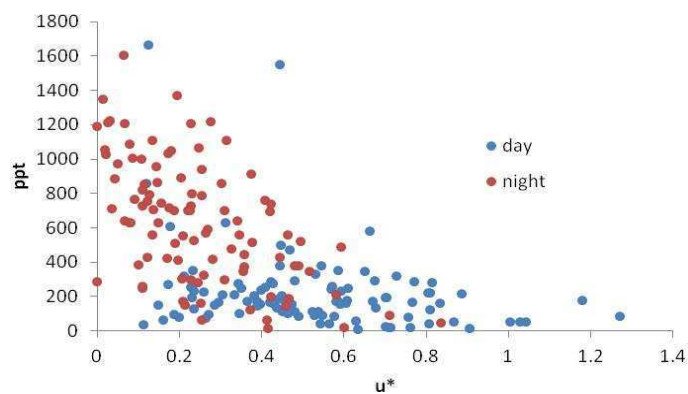
Figure 6: The monoterpene concentration dependence on friction velocity in June, July and August
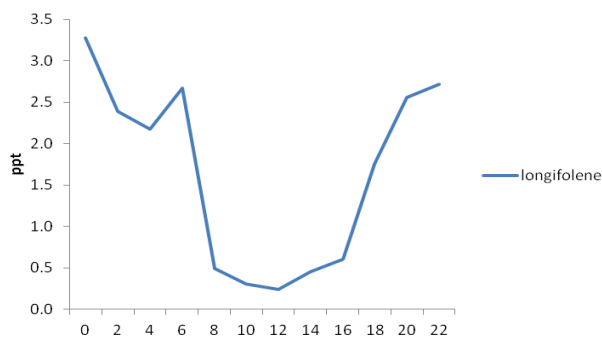
Figure 7: The mean diurnal variability of longifolene in August

ACKNOWLEDGEMENTS

REFERENCES

Ghirardo, A., Koch, K., Taipale, R., Zimmer, I., Schnitzler J.-P. and Rinne, J.: Determination of de novo and pool emissions of terpenes from four common boreal/alpine trees by $^{13}CO_2$ labeling and PTR-MS analysis. *Plant, Cell & Environment*, 33, 781-792. doi: 10.1111/j.1365-3040.2009.02104.x, 2010.

Hakola, H., Hellén, H. and Laurila T.: Ten years of light hydrocarbon (C_2-C_6) concentration measurements in background air in Finland. Atmospheric Environment 40, 3621-3630, 2006a.

Hakola, H., Tarvainen, V., Laurila, T., Hiltunen, V., Hellén, H., Keronen, P.: Seasonal variation of VOC concentrations above a boreal coniferous forest. Atmospheric Environment 37, 1623-1634, 2003.

Hakola, H., Tarvainen, V., Bäck, J., Rinne, J., Ranta, H., Bonn, B., and Kulmala, M.: Seasonal variation of mono- and sesquiterpene emission rates of Scots pine. Biogeosciences, SRef-ID: 1726-4189/bg/2006-3-93, 93-101, 2006b.

Hakola, H., Hellén, H., Tarvainen, V., Bäck, J., Patokoski, J. and Rinne, J.: Annual variations of atmospheric VOC concentrations in a boreal forest. Boreal Env. Res. 14, 722–730, 2009.

Hellén, H., Hakola, H., Pirjola, L., Laurila, T. and Pystynen, K.-H.: Ambient air concentrations, source profiles and source apportionment of 71 different C_2-C_{10} volatile organic compounds at urban and residential areas in Finland. Environmental Science and Technology 40, 103-108, 2006.

Hellén, H., Hakola, H., Haaparanta, S., Pietarila, H. and Kauhaniemi, M.: Influence of residential wood combustion on local air quality. Science of the Total Environment 393, 283– 290, 2008.

Hellén, H., Kuronen, P., Hakola, H.: Heated stainless steel tube for ozone removal in the ambient air measurements of mono- and sesquiterpenes. Atmospheric Environment 57 35-40, 2012

Helmig, D.: Ozone removal techniques in the sampling of atmospheric volatile organic trace gases, Atmospheric Environment 31, 3635-3651, 1997.

Holzke, C., Hoffmann, T., Jaeger, L., Koppmann, R., Zimmer, W.: Diurnal and seasonal variation of monoterpene and sesquiterpene emissions from Scots pine (Pinus sylvestris L.) Atmospheric Environment 40, 3174–3185, 2006.

Laurila T. and Hakola, H.: Seasonal Cycle of C2-C5 hydrocarbons over the Baltic Sea and Northern Finland. Atmospheric Environment, 30, 1597-1607, 1996.

Lappalainen, H., Sevanto, S., Bäck, J., Ruuskanen, T.M., Kolari, P., Taipale, R., Rinne, J., Kulmala, M. and Hari, P.: Day-time concentrations of biogenic volatile organic compounds in a boreal forest canopy and their relation to environmental and biological factors. Atmos. Chem. Phys. 9, 5447-5459, 2009.

Rinne, J., Ruuskanen, T.M., Reissell, A., Taipale, R., Hakola, H. and Kulmala, M.: On-line PTR-MS measurements of atmospheric concentrations of volatile organic compounds in a European boreal forest ecosystem. Boreal Env. Res.*10,* 425-436, 2005.

Taipale, R., Kajos, M.K., Patokoski, J., Rantala, P., Ruuskanen, T.M., Rinne, J.: Role of de novo biosynthesis in ecosystem scale monoterpene emissions from a boreal Scots pine forest. Biogeosciences, 8, 2247-2255, doi:10.5194/bg-8-2247-2011, 2011.

Comparison between the AOD derived from a global climate model HadGEM2 and from satellite observations

MERI HANNUKAINEN[1], PEKKA KOLMONEN[2], BILL COLLINS [3], ANU-MAIJA SUNDSTRÖM[1], LARISA SOGACHEVA[2], EDITH RODRIGUEZ[2], GERRIT DE LEEUW[1,2,4]

[1] Department of Physics, University of Helsinki
[2] Climate Change Unit, Finnish Meteorological Institute
[3] Atmospheric Composition and Climate, Hadley Centre
[4] TNO B&O, Utrecht, Netherlands

INTRODUCTION

Aerosols and atmospheric trace gases exert a large effect on climate. Radiative effects of aerosols are due to reflection and absorption of incoming solar radiation (direct radiative effect) and due to the effects which aerosols have on cloud physical properties affecting cloud albedo and the hydrological cycle (first and second radiative effects, respectively). Radiative effects of aerosols and trace gases are usually evaluated using chemical transport models (CTM) or global circulation models (GCM). These models are used to simulate the effects of atmospheric constituents and their effect is evaluated by comparison of the results with a situation in which no trace gases and/or aerosols are present (Collins, 2009). However, the uncertainties and the differences between different models are large because of the many assumptions that are needed as regards sources and removal. This particularly applies to aerosol particles having a wide variety of sources and source strengths for widely different chemical species. In the atmosphere physical and chemical processes take place which change the physical and chemical properties of the aerosol particles. These in turn change the optical properties.

Measurements are increasingly used to constrain the models. These include both ground-based and satellite measurements. However, measurements alone are not enough to estimate the radiative effects of aerosols. A review of measurement-based estimates of the aerosol direct radiative effects (Yu et al., 2006) shows that these estimates use a combination of observations and models. The over-ocean direct radiative effects using MODIS data (Remer and Kaufman, 2006) makes use of a radiative transfer model.

In this study satellite data have been used to retrieve global distributions of the spectral aerosol optical depth (AOD) from radiances measured at the top of the atmosphere (TOA) with the Advanced Along Track Scanning Radiometer (AATSR) flying on ENVISAT, for the year 2008. This was achieved by using updated versions of the single view algorithm over the ocean (Veefkind et al., 1998a) and of the dual view algorithm (Veefkind et al., 1998b) over land. These algorithms are continually updated and improved based on new insights and developments and intercomparison with independent ground-based data (mainly sun photometer data from the NASA network AERONET (Holben et al., 1998)), other satellite data and models.

Satellite data have been validated with independent ground-based observations from AERONET (Holben et al., 1998), but they are not perfect and deviation may occur because of assumptions made in the retrieval algorithm, in particular as regards the aerosol models used and the optical properties of the aerosol particles. Therefore, in this study we compare the AOD retrieved from AATSR and MODIS with the AOD computed using the HadGEM2 model (Collins et al., 2011). AERONET sun photometer data, which provides an independent and reasonable accurate estimate of the AOD, (Holben et al., 1998) are used for comparison.

METHODS

2.1. AATSR

The AATSR (Advanced Along Track Scanning Radiometer) on board ESA ENVISAT (ENVIronmental Satellite) was launched in March 2002 and provided data until 6 April 2012. AATSR is the successor other ATSR-2 instrument aboard ERS-2. Together these two instruments provide a 17-year data series from 1995 to 2012. (A)ATSR was originally designed to measure SST (Sea Surface Temperature), current applications cover atmosphere (clouds, precipitation), Land(vegetation) and Ocean & coast (Sea Surface Temperature). The AATSR has a dual view, one at nadir and another at 55° forward, with a spatial resolution of 1km x 1km. The swath width is 500 km, which covers the globe in 5-6 days. AOD over land is obtained from AATSR measurements using the ADV (Aerosol Dual View) algorithm for wavelengths 0.555, 0.659 and 1.61 μm. ADV doesn't use a surface model, as it eliminates surface reflectance by using the k-ratio (between. Over ocean the AOD is retrieved using the single view algorithm which is applied to both the nadir and forward view separately. Aerosol retrieval can be made at pixel level of 1x1 km^2, but the default resolution is 10x10 km^2. AATSR data can be downloaded from http://aatsraerosol.fmi.fi/

2.2. MODIS

MODIS (Moderate Resolution Imaging Spectroradiometer) is onboard the NASA Terra and Aqua satellites. Terra was launched in December 1999 and is in a descending orbit with an equator crossing time at 10:30. Aqua was launched in May 2002 and is in an ascending orbit with an equator crossing time at 13:30. MODIS acquires aerosol property information including AOD in five wavelength bands with swath width of 2330 km, and spatial resolution of 500m. MODIS achieves global coverage in 1-2 days. Measurements used here are from Terra. MODIS data is level 2 aerosol product. This data can be found in LAADS Web at http://ladsweb.nascom.nasa.gov/data/search.html. This data has a spatial resolution of 0.1 x 0.1 degrees and it covers both land and sea areas. MODIS database also provides information of forest fires.

2.3. AERONET

AERONET (Aerosol Robotic NETwork; Holben et al., 1998) is a federation of ground-based remote sensing aerosol networks which provides a long-term, continuous and readily accessible public domain database of aerosol optical, micro physical and radiative properties for aerosol research and characterization, validation of satellite retrievals, and synergism with other databases. The network imposes standardization of instruments, calibration, processing and distribution. AERONET data can be found at http://aeronet.gsfc.nasa.gov/. 107 AERONET stations were selected for comparison with AATSR and MODIS, on basis of having most and best quality data.

2.4. Model: HadGEM2

HadGEM2 (Hadley Centre Global Environmental Model version 2) is a climate model which has 38 levels extending to 40 km, with a horizontal resolution of 1,875 x 1,25 degrees. At the equator this equals to 208 x 139 km^2, at latitude of 55 degrees this is 120 x 139 km^2. The HadGEM2 family of models comprises a range of specific model configurations incorporating different levels of complexity but with a common physical framework. The HadGEM2 family includes a coupled atmosphere - ocean configuration, with or without a vertical extension in the atmosphere to include a well-resolved stratosphere, and an Earth-System configuration which includes dynamic vegetation, ocean biology and atmospheric chemistry. HADGem2 AOD data used here was provided by Dr. Collins from Met Office, UK (http://www.metoffice.gov.uk).

CONCLUSIONS

Comparisons have been made between computed and measured radiative effects of aerosols, where the AOD has been used as a proxy. All satellite data have a spatial resolution of 10 x 10 km^2 and were regridded to the HadGEM2 resolution of 1,875 x 1,25 degrees for comparison. The results show the spatial distribution of the global AOD for 2008, aggregated for the whole year and per season. Model and satellite derived AOD general compare reasonably well but in some cases large discrepancies are observed. Although these seem to be connected with the occurrence of fires in some areas, there is no consistent pattern. This conclusion is based on comparison of AODs for AERONET stations inside and outside areas affected by forest fires.

ACKNOWLEDGEMENTS

REFERENCES

Collins, W.J., (2009): Global radiative forcing from megacity emissions of long-lived greenhouse gases. MEGAPOLI Scientific Report 09-01.

The HadGEM2 Development Team: Martin, G. M., Bellouin, N., Collins, W. J., Culverwell, I. D., Halloran, P. R., Hardiman, S. C., Hinton, T. J., Jones, C. D., McDonald, R. E., McLaren, A. J., O'Connor, F. M., Roberts, M. J., Rodriguez, J. M., Woodward, S., Best, M. J., Brooks, M. E., Brown, A. R., Butchart, N., Dearden, C., Derbyshire, S. H., Dharssi, I., Doutriaux-Boucher, M., Edwards, J. M., Falloon, P. D., Gedney, N., Gray, L. J., Hewitt, H. T., Hobson, M., Huddleston, M. R., Hughes, J., Ineson, S., Ingram, W. J., James, P. M., Johns, T. C., Johnson, C. E., Jones, A., Jones, C. P., Joshi, M. M., Keen, A. B., Liddicoat, S., Lock, A. P., Maidens, A. V., Manners, J. C., Milton, S. F., Rae, J. G. L., Ridley, J. K., Sellar, A., Senior, C. A., Totterdell, I. J., Verhoef, A., Vidale, P. L., and Wiltshire, A.: The HadGEM2 family of Met Office Unified Model Climate configurations, Geosci. Model Dev. Discuss., 4, 765-841, doi:10.5194/gmdd-4-765-2011, 2011.

Holben B., Eck T., Slutsker I., Tanré D., Buis J., Setzer A., Vermote E., Reagan J. and Kaufman Y.: AERONET- a federated instrument network and data archive for aerosol characterization. Remote Sens. Environ., 66, 1-16, 1998.

Remer, L. A. and Kaufman, Y. J.: Aerosol direct radiative effect at the top of the atmosphere over cloud free ocean derived from four years of MODIS data, Atmos. Chem. Phys., 6, 237-253, doi:10.5194/acp-6-237-2006, 2006.

Veefkind, J.P. and de Leeuw, G. (1998a), A new algorithm to determine the spectral aerosol optical depth from satellite radiometer measurements. *Journal of Aerosol Sciences*, 29, 1237-1248.

Veefkind, J.P., G. de Leeuw and P.A. Durkee (1998b). Retrieval of aerosol optical depth over land using two-angle view satellite radiometry during TARFOX. Geophys. Res. Letters. 25(16), 3135-3138.

Yu, H., Kaufman, Y. J., Chin, M., Feingold, G., Remer, L. A., Anderson, T. L., Balkanski, Y., Bellouin, N., Boucher, O., Christopher, S., DeCola, P., Kahn, R., Koch, D., Loeb, N., Reddy, M. S., Schulz, M., Takemura, T., and Zhou, M.: A review of measurement-based assessments of the aerosol direct radiative effect and forcing, Atmos. Chem. Phys., 6, 613-666, doi:10.5194/acp-6-613-2006, 2006.

CARBOXYLIC ACIDS AND ORGANOSULFATES IN AEROSOLS FROM SVALBARD DURING A FULL ANNUAL CYCLE

A.M.K. HANSEN[1], K. KRISTENSEN[1], R. KREJCI[2,3], J. STRÖM[2], P. TUNVED[2], F. COZZI[1] and M. GLASIUS[1]

[1]Dep. of Chemistry, University of Aarhus, Langelandsgade 140, DK-8000 Aarhus C, Denmark
[2]Dep. of Environmental Science, Stockholm University, S 106 91 Stockholm, Sweden
[3]Dep. of Physics, University of Helsinki, P.O. Box 48, 00014 Helsinki, Finland

INTRODUCTION

Arctic areas are especially vulnerable to climate change, but unfortunately also most at risk, as documented by the higher rate of warming experienced in recent years. In order to understand important processes influencing radiative effects of aerosols, detailed knowledge on aerosol sources and composition in the Arctic is needed. In this study we collected aerosols at Svalbard during a full annual cycle for analysis of the carbonaceous fraction including total organic carbon (OC), elemental carbon (EC), carboxylic acids and organosulfates, as well as nitrooxy organosulfates. The chemical speciation analysis focused on biogenic oxidation products. Oxidation products of biogenic volatile organic compounds (VOC), such as monoterpenes and isoprene, contribute to biogenic secondary organic aerosol (BSOA). The organosulfate derivatives of isoprene and monoterpenes, as well as their oxidation products, have been identified in both laboratory and field studies where they are formed through heterogeneous reactions involving acidic sulfur aerosols (e.g. Surratt *et al*., 2008), primarily originating from anthropogenic sources. The aim of the study was thus to investigate the sources to carbonaceous aerosols including the presence of BSOA in Arctic aerosols.

METHODS

Aerosols (TSP) were collected as weekly samples using a low-volume sampler at Zeppelin Mountain, Svalbard, Norway (78.9°N; 11.9°E) during 2008. After extraction, the samples were analysed by HPLC coupled through an electrospray inlet to a quadrupole time-of-flight mass spectrometer (qTOF-MS) (Kristensen and Glasius, 2011). Carboxylic acids were identified and quantified using authentic standards. Organosulfates and nitrooxy organosulfates were identified from their characteristic MS-fragments (HSO_4^-, SO_3^- and HNO_3) and the isotopic patterns of sulphur and nitrogen, and quantified using a synthesized organosulfate standard derived from β-pinene (MW 250).

CONCLUSIONS

Figure 1 shows concentrations of carboxylic acids observed at Svalbard during 2008. All carboxylic acids are oxidation products of biogenic VOC, except adipic acid, which is thus a molecular marker of anthropogenic SOA. Generally the highest concentrations of carboxylic acids are observed in late winter, when biogenic VOC emissions are expected to be low. Arctic haze is prevalent during the same period and OC also peaks during late winter/spring.

One organosulfate of α-pinene and one of isoprene were identified in the samples together with three previously unidentified organosulfates and two nitrooxy organosulfates of monoterpenes (Table 1). A few of these compounds have previously been observed in particle samples from Denmark during spring and summer (Kristensen and Glasius, 2011), as well as Norway, Sweden and Finland during summer (Yttri *et al*., 2011).
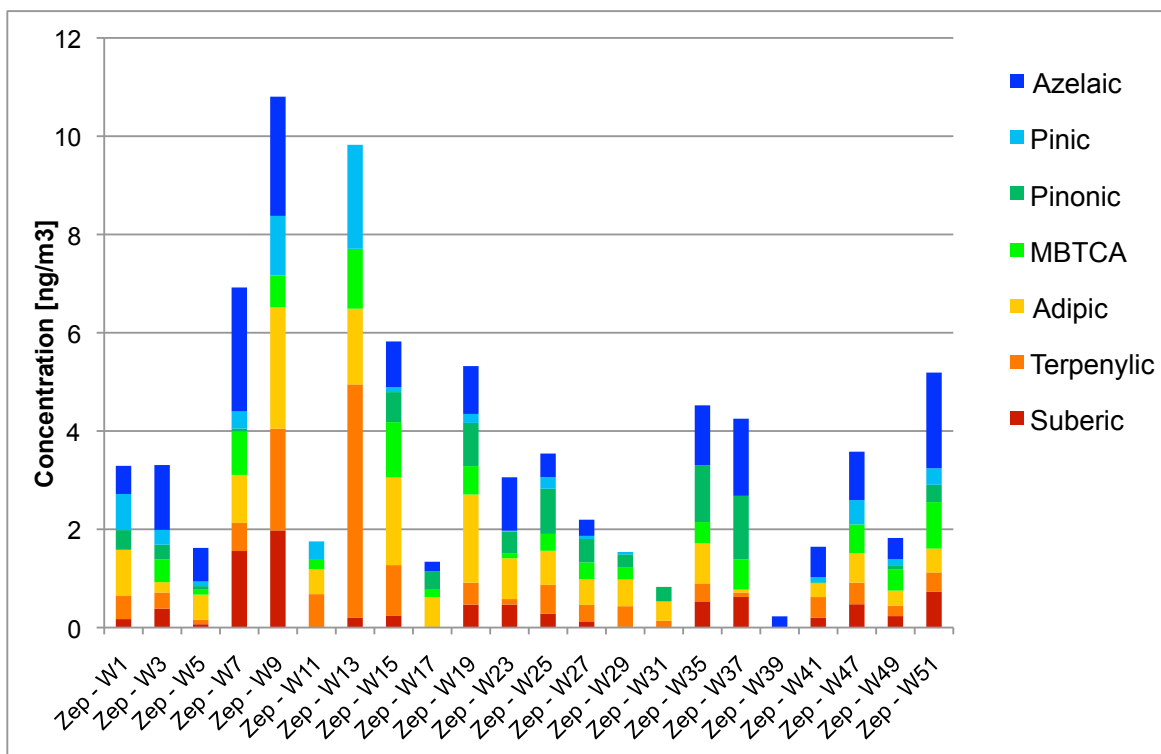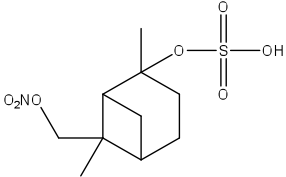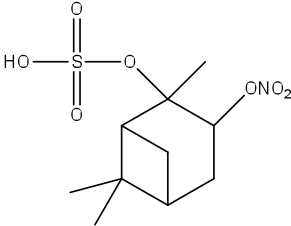
Figure 1. Carboxylic acids in aerosols collected at Svalbard during 2008. W is week number.

Table 1. Organosulfates and nitrooxy organosulfates identified in aerosol samples from Svalbard. MW is molecular weight.

	Molecular formula	Structure	Precursor
Organosulfate **MW 168**	$C_4H_8O_5S$		Not previously observed
Organosulfate **MW 170**	$C_3H_5O_6S$		isoprene
Organosulfate **MW 182_1**	$C_5H_{10}O_5S$	Unknown	α-pinene

268

Organosulfate **MW 196**	$C_6H_{12}O_5S$	Unknown	Unknown
Organosulfate **MW 210**	$C_6H_{10}O_6S$	Unknown	Unknown
Nitrooxy organosulfate MW 295_1	$C_{10}H_{17}O_7NS$		α-/β-pinene
Nitrooxy organosulfate MW 295_2	$C_{10}H_{17}O_7NS$		α-/β-pinene

The results show that molecular markers of BSOA are found in Arctic areas during winter and the sources and regional scale processes affecting their levels should be studied further.

REFERENCES

Kristensen, K. and M. Glasius (2011) Organosulfates and oxidation products from biogenic hydrocarbons in fine aerosols from a forest in North West Europe during spring. *Atmospheric Environment* **45**, 4546.

Surratt, J. D., Gomez-Gonzlez Y., Chan A. W. H., Vermeylen R., Shahgholi M., Kleindienst T. E., Edney E. O., Offenberg J. H., Lewandowski M., Jaoui M., Maenhaut W., Claeys M., Flagan R. C. and Seinfeld, J. H. (2008) Organosulfate Formation in Biogenic Secondary Organic Aerosol, *J. Physical Chemistry A* **112**, 8345.

Yttri K. E, Simpson D., Nøjgaard J.K, Kristensen K., Genberg J., Stenström K., Swietlicki E., Hillamo R., Aurela M., Bauer H., Offenberg J. H, Jaoui M., C. Dye, Eckhardt S., Burkhart J. F, Stohl A., and Glasius M. (2011) Source apportionment of summertime carbonaceous aerosol at Nordic rural background sites. *Atmospheric Chemistry and Physics Discussions*, accepted for discussion.

IMPORTANCE OF BIOGENIC VOLATILE ORGANIC COMPOUNDS IN URBAN AIR IN HELSINKI, FINLAND

HELLÈN H., TYKKÄ T. AND HAKOLA H.

Finnish Meteorological Institute, PL 503, 00101 Helsinki, Finland

E-mail: heidi.hellen@fmi.fi

Keywords: Air quality, monoterpenes, isoprene, urban air, receptor modeling, BVOCs

INTRODUCTION

There are lots of natural trees and other vegetation in many cities. Trees emit biogenic volatile organic compounds (BVOCs). These compounds are not toxic themselves, but they are very reactive and can therefore affect on atmospheric chemistry even at relatively low concentrations. In the presence of nitrogen oxides (NOx) they form ozone and their reaction products may take part into new particle formation. Sources, concentration levels and effects of isoprene and monoterpenes on local atmospheric chemistry were studied in urban background air in Helsinki, Finland. Ambient air concentration measurements were conducted using an in-situ gas chromatograph with a mass spectrometer at an urban background station station SMEARIII (Station for Measuring Ecosystem-Atmosphere Relations III, $60^{o}12´N$, $24^{o}58´E$, 26 m a.s.l.) during different seasons in 2011 (Hellén et al., 2012).

METHODS

Measurements were conducted at the 5th floor on the roof of Finnish Meteorological Institute in Helsinki, Finland, using a thermal desorpter (Markes Unity) with a gas chromatograph (Agilent 7890A) and a mass spectrometer (Agilent 5379N). Samples were taken every other hour during different months in 2011. Sampling time was 60 minutes and flow 30 ml min^{-1}. Samples were collected directly to the cold trap of the thermal desorpter. For studying source compositions and contributions multivariate receptor model EPA Unmix 6.0 (Norri et. al., 2007) was used.

RESULTS AND DISCUSSION

Highest concentrations of isoprene and monoterpenes were measured in summer (990 ng m^{-3}), but concentrations were clearly above detection limit also in winter (230 ng m^{-3}, Figure 1a). In winter and spring the urban background concentrations were higher than in a forested site in Finland indicating anthropogenic sources of isoprene and monoterpenes (Figure 1 b). Winter concentrations followed the diurnal pattern of traffic. In summer, the highest concentrations were measured in the early morning when mixing started. After that, concentrations decreased as photochemical reactions started to play an important role.

The concentrations of aromatic hydrocarbons were higher than BVOCs during all seasons (Figure 1 a), but hydroxyl radical (OH) reactivity scaled concentrations showed that also isoprene and monoterpenes have a strong influence on local atmospheric chemistry in urban air (Figure 2). High contribution of isoprene and monoterpenes to the OH-reactivity was detected also at other background site in Helsinki and in a residential area close to Helsinki.
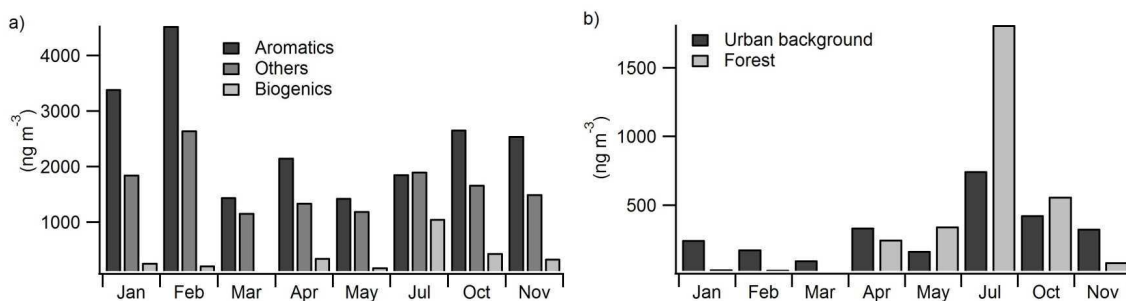
Figure 1. a) Concentrations of measured VOCs during different seasons at an urban background site in Helsinki in 2011 and **b)** monoterpene concentrations at the urban background site and in a forest 220 km north of Helsinki in 2011 (Hakola et al., 2012).

Large amounts of monoterpenes are emitted from vegetation, but this study showed that in urban areas there are also important anthropogenic sources. Unmix source estimates indicated, that traffic and wood combustion have the highest impacts on the concentration levels of monoterpenes in winter, spring and November (Figure 3). In July and October biogenic sources were dominant.

This study shows that when considering ways of improving air quality and the reduction of air pollution, isoprene and monoterpenes, usually understood to be mainly biogenic compounds, also have to be taken into account in urban areas. They can have a strong effect on local reactivity, especially in urban background air or in residential areas.
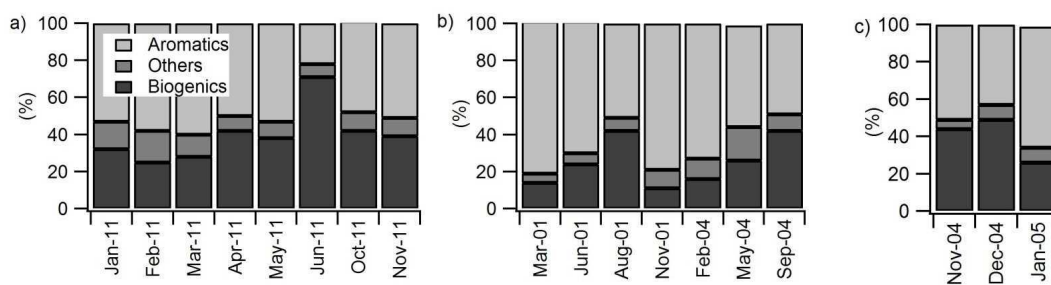
Figure 2. Relative contributions of aromatics and BVOCs to reactivity during different months **a)** at the urban background site (this study) in Helsinki in 2011, **b)** at an urban background station run by HSY in 2001 and 2004 and **c)** in a residential area in 2004 and 2005 (b and c were calculated from earlier data presented in Hellén et al. (2003 and 2006)).
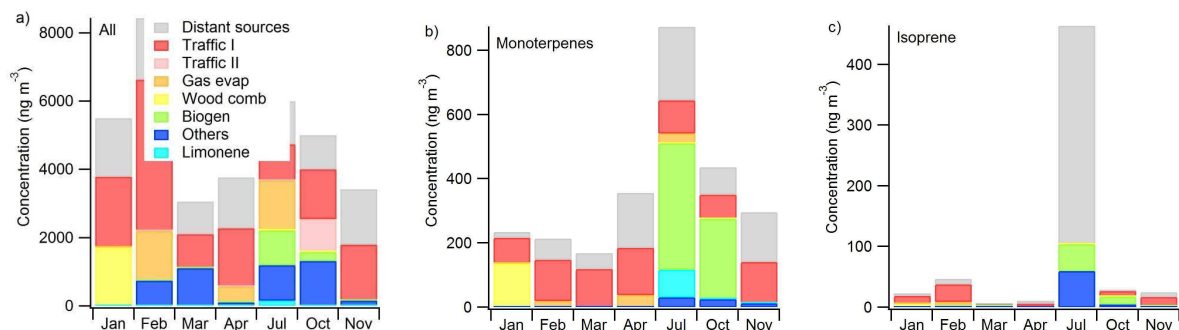
Figure 3. Contributions of different sources to the measured concentrations in urban background air in Helsinki in 2011.

REFERENCES

Hakola H., Hellén H., Henriksson M., Rinne J., and Kulmala M., 2012. In situ measurements of biogenic volatile organic compounds in Boreal Forest. Submitted to Atmospheric Chemistry and Physics.

Hellén H., Hakola H., Laurila T., 2003. Source contributions of NMHCs in Helsinki using chemical mass balance (CMB) and multivariate (Unmix) receptor models. *Atmospheric Environment*, 37, 1413-1424.

Hellén H., Hakola H., Pirjola L., Laurila T., Pystynen K.-H., 2006. Ambient air concentrations, source profiles and source apportionment of 71 different C2-C10 volatile organic compounds in urban and residential areas of Finland. *Environmental Science and Technology*, 40, 103-108.

Hellén H., Tykkä T. and Hakola H., 2012. Importance of isoprene and monoterpenes in urban air in Northern Europe. Atmospheric Environment, 59, 59-66.

Norris G., Vedentham R., Duvall R., 2007. EPA Unmix 6.0 Fundamentals & User Guide. U.S. Environmental Protection Agency, Office of Research and Development, Washington, DC 20460.

DEVELOPMENT OF CHAMBER METHOD FOR AMMONIA AND AMINE FLUX MEASUREMENTS

M. HENRIKSSON, H. HELLÉN, U. MAKKONEN and H. HAKOLA

Finnish Meteorological Institute, Finland

KEYWORDS: Ammonia, dimethylamine, chamber, MARGA

INTRODUCTION

Ammonia and amines are important gaseous species for new particle formation (Anttila et al., 2005; Smith et al., 2008). Particles that contain ammonia and sulphuric acid or amines and sulphuric acid can grow big enough to form cloud condensation nuclei (Kerminen et al., 2005).

The measurements of gaseous ammonia have faced difficulties especially due to problems in differentiation between gas-phase NH_3 and aerosol NH_4^+. We have used MARGA (Monitor for AeRosols and Gases in Ambient air) instrument for semi-continuous measurements for gaseous ammonia and amines in air with one hour time resolution (ten Brink et al., 2007; Makkonen et al., 2012). MARGA takes sample from the air. Airflow (16.7 l/min) goes through wet rotating denuder (WRD) and steam jet aerosol collector (SJAC). WRD takes the gases from the air flow, but particles continue to the SJAC. From WRD and SJAC sample lines go to the syringes, which collect the samples. From syringes the samples go to the IC-analysis.

In this work, we tested chamber systems to measure ammonia and dimethylamine (DMA). Our specific aim was to find a suitable chamber material for flux measurements.

METHODS

In the system there was a pump, a 12 meter long tubing from pump to chamber, and a HEPA-filter, an ammonia filter and some silica gel between the pump and the chamber. From the chamber to the MARGA there was a heated 12 meter long fluorinated ethylene propylene (FEP) tubing. Airflow to the chamber was 17 – 23 l/min and airflow from the chamber was 16.7 l/min. The relative humidity and the temperature were measured from the chamber.

We tried three different chamber materials: FEP, poly(methyl methacrylate) (PMMA) and stainless steel. Volumes of the chambers were 94 l, 288 l and 133 l, respectively. First we tested the blank values of the chambers.

After blank tests, we injected ammonia and DMA into the chambers with permeation oven. We tested both the chambers and the heated FEP-inlet with three different amount of ammonia (0.2, 1 and 2 μg), and three different amount of DMA (0.566, 2.83 and 5.66 μg).

RESULTS

Heated FEP-inlet gave too high ammonia concentrations (Figure 1, 2). We couldn´t find the reason for that. The recovery of DMA was only ~45% from the heated FEP-inlet (Figure 3).

$$y = 1.9189x - 0.0837$$
$$R^2 = 0.9992$$
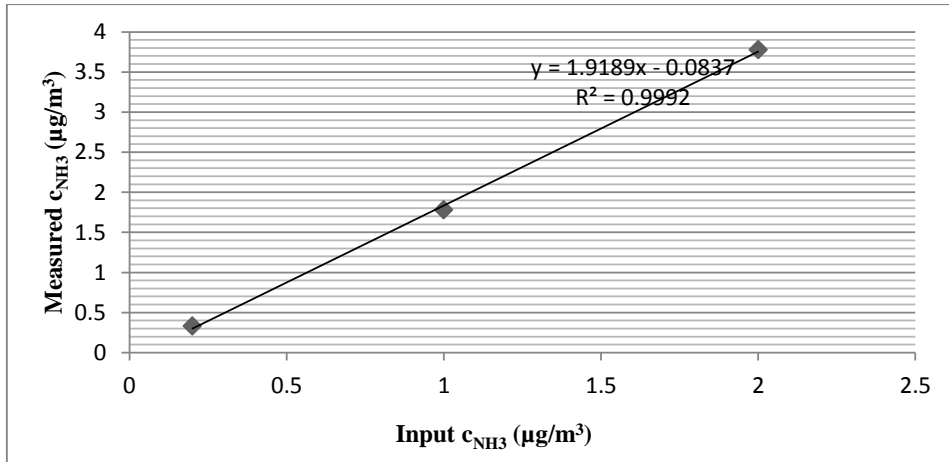
Figure 1. Measured concentration of ammonia from heated FEP-inlet compared to ammonia input.
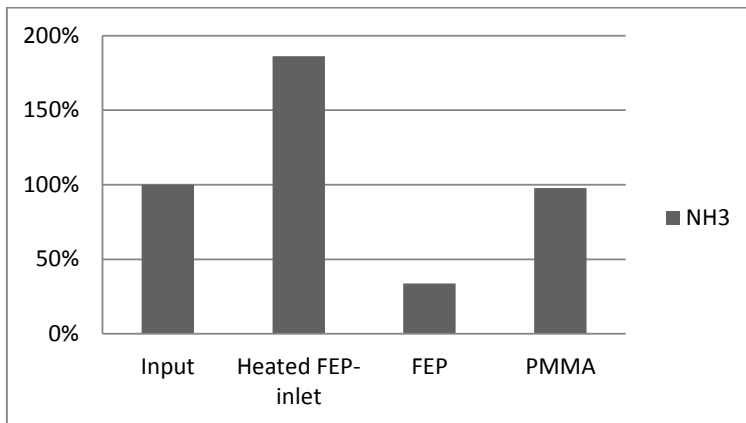
Figure 2. Recovery of ammonia from heated FEP-inlet, FEP-chamber and PMMA-chamber compared to input.
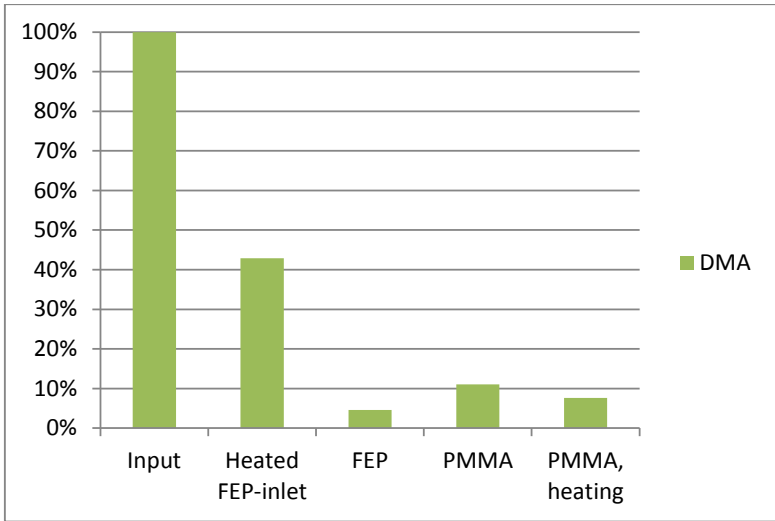
Figure 3. The recovery of DMA from heated FEP-inlet, FEP-chamber and PMMA-chamber compared to input. PMMA-chamber heating didn´t have significant effect to results.

The blank value of ammonia was best for FEP-chamber, and for stainless steel chamber it was too high. The stainless steel chamber wasn´t tested any further. Recovery of ammonia and DMA from FEP-chamber was poor even with highest concentrations (Figure 3). Therefore we didn´t test it any further.

The ammonia recovery from PMMA-chamber was good with different concentrations injected (Figure 2, 4). Concentration increase in the chamber was linear (Figure 4). Before calculating the recovery, we subtracted the blank value from the results. The DMA recovery was ~10% from PMMA-chamber (Figure 3). We tried to heat PMMA-chamber, but it didn´t have any significant effect to the results (Figure 3).
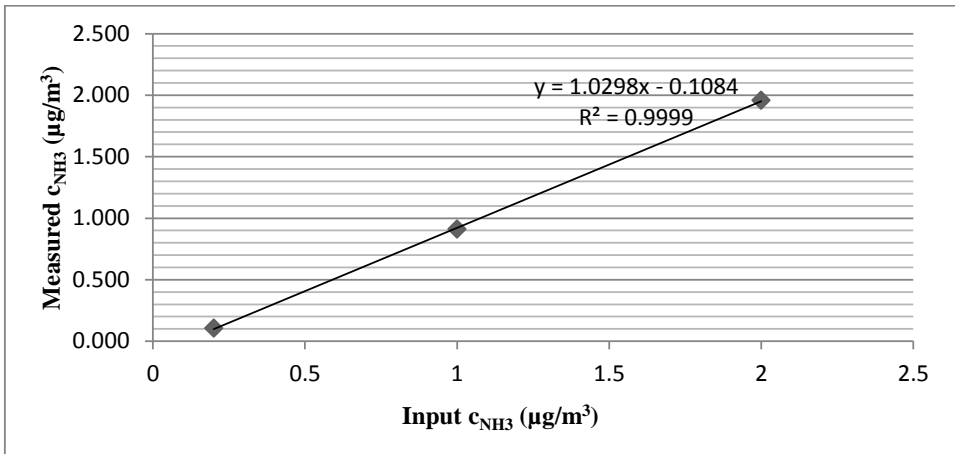
Figure 4. Measured concentration of ammonia from PMMA-chamber compared to ammonia input.

CONCLUSIONS

Best chamber material for the ammonia and DMA measurements was PMMA. Recovery for ammonia was OK, but for DMA it was only ~10 %. Heating of PMMA-chamber didn´t have remarkable effect to the DMA-results. It is not possible to study fluxes of DMA with this kind of system.

REFERENCES

Anttila, T.; Vehkamäki, H.; Napari, I.; Kulmala, M. (2005). Effect of ammonium bisulphate formation on atmospheric water-sulphuric acid-ammonia nucleation, Boreal Environment Research **10**, 511 – 523

Kerminen, V.-M.; Lihavainen, H.; Komppula, M.; Viisanen, Y.; Kulmala, M. (2005). Direct observational evidence linking atmospheric aerosol formation and cloud droplet activation, Geophysical Research Letters **32**, L14803

Makkonen, U., Virkkula, A., Mäntykenttä, J., Hakola, H., Keronen, P., Vakkari, V., and Aalto, P. P. (2012). Semi-continuous gas and inorganic aerosol measurements at a Finnish urban site: comparisons with filters, nitrogen in aerosol and gas phases, and aerosol acidity, Atmospheric Chemistry Physics, 12, 5617-5631

Smith, J.N.; Dunn,M. J.; VanReken, T.M.; Iida, K.; Stolzenburg, M.R.; McMurry, P.H.; Huey, L.G. (2008). Chemical composition of atmospheric nanoparticles formed from nucleation in Tecamac, Mexico: Evidence for an important role for organic species in nanoparticle growth , Geophysical Research Letters **35**, L04808

ten Brink, H. M., Otjes, R., Jongejan, P., and Slanina, J.(2007). An instrument for semi-continuous monitoring of the size-distribution of ammonium nitrate aerosol, Atmospheric Environment 41, 2768–2779

AEROSOL MEASUREMENTS IN THE YANGTSE RIVER DELTA

E. HERRMANN[1,2], A. DING[1], T. PETÄJÄ[2], M. KULMALA[2]

[1]School of Atmospheric Sciences, Nanjing University, Nanjing, PR China

[2]Division of Atmospheric Sciences, University of Helsinki, Helsinki, Finland

Keywords: aerosols, AIS, DMPS, atmospheric nucleation

INTRODUCTION

Atmospheric new particle formation has been observed all over the world (Kulmala et al. 2004). However, the details of the process and some of the vapors involved are still under discussion. Long-term measurements of aerosol distributions and other atmospheric data play a key role in understanding nucleation, but currently such data sets are available from very few locations that do not represent the global variation in conditions and circumstances (Hari et al. 2009). Nanjing University has recently established a comprehensive measurement station whose task it is to partly fill that gap in the long run. Here we present the first months of aerosol data from that site.
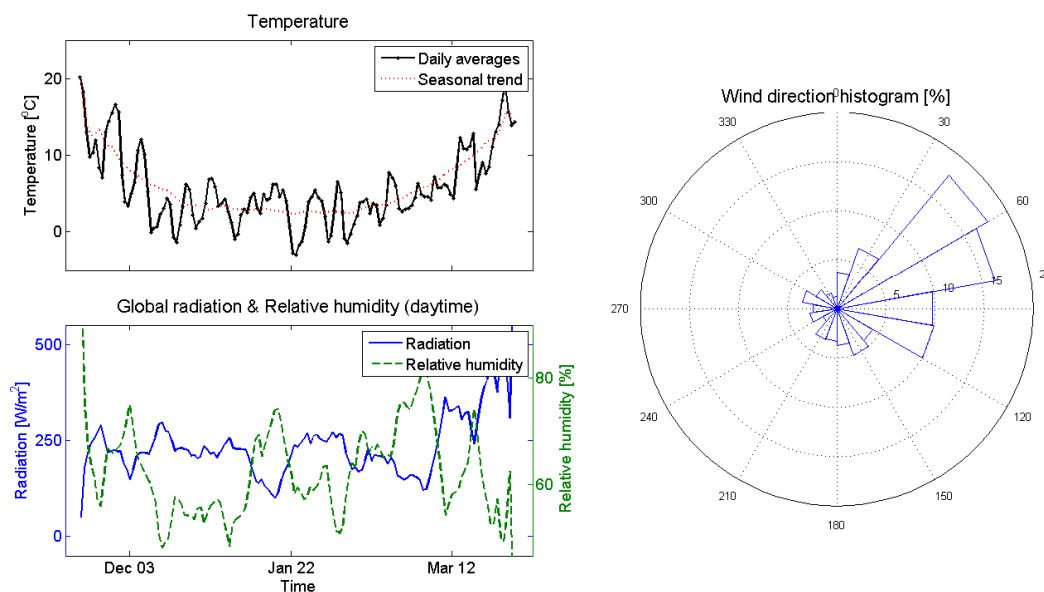
Figure 1. Conditions during the measurement period.

MEASUREMENTS

The Nanjing measurement station is located in the Yangtze River Delta (YRD), probably the biggest agglomeration of megacities in the world and a global pollution hotspot. The station is located some 20km east of Nanjing's city center, thus not measuring urban air but YRD background coming in from cities such as Shanghai and Suzhou.

The core of the aerosol measurements is formed by a DMPS an AIS (Mirme et al. 2007) which measure aerosols from 6 to 800 nm and air ions from 0.8 to 42 nm respectively. Combining these devices, it is possible to determine nucleation frequency, annual cycle, particle growth rates, formation rates, vapor

277

concentrations and vapor source rates. Besides aerosols and air ions, also trace gases, fluxes and various meteorological data are recorded at the station. The data presented here covers the period from 18 Nov 2011 to 31 March 2012, i.e. from late autumn to early spring. During this period, daily average temperatures varied between 20 and a few minus degrees Celsius. The clearly dominating wind direction is East-Northeast to East with very little contribution from the other direction.

RESULTS
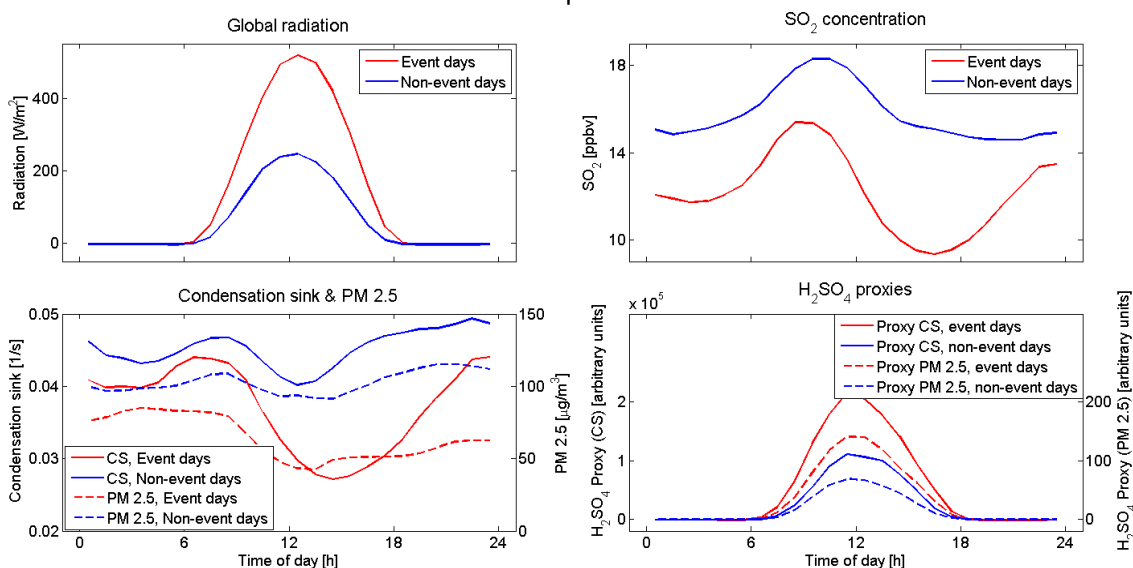
Figure 2. Dependency of event and non-event days on radiation, SO_2, CS, PM 2.5, and sulfuric acid proxies.

During the measurement period, the cluster band was populated by 800 ions cm^{-3} on average. The average total number concentration N was 20000 cm^{-3} with values ranging roughly from 10000 to 40000 cm^{-3}. PM 2.5 values were between 25 and 200 μm^{-3} with a median of 80. During a 4.5-month period, 25 particle formation events were observed, typically of type Ib.2 (classification according to Hirsikko et al. 2007) with a clear gap between the cluster band and the smallest observed aerosol particles. Nucleation activity was somewhat subdued only in December, with January to March showing similar nucleation probabilities. The growth rate from 6 to 30 nm was between 4 and 15 nm/h, with a median of about 7. The median observed formations rate J_6 was about 1 $cm^{-3}s^{-1}$. During the average event, about 4000 new accumulation mode particles were produced per cm^3.

According to current knowledge, particle formation is closely linked to the amount of sulfuric acid vapor available in the atmosphere. Since sulfuric acid is frequently not measured, a proxy has been developed to estimate its concentration: $[H_2SO_4] = k * [SO_2] * radiation / CS$ where k is a factor that depends on local conditions and has to be determined by actually measuring sulfuric acid concentrations. While such measurements have not been performed at the Nanjing site, the proxy without its pre-factor k can still give insight into the nucleation behavior.

Figure 2 shows the components of the proxy and the proxy itself and their average behavior for days with and without nucleation. As can be expected, strong radiation clearly favors particle formation; sunlight is needed to drive the necessary chemistry that produces sulfuric acid. The condensation sink CS on the other hand suppresses nucleation. PM 2.5 has been added to the same plot to show how closely related both values are. While SO_2 is necessary in the production of sulfuric acid, higher SO_2 concentrations do not go hand in hand with event days. Apparently, SO_2 is always available in abundance and not a limiting

factor. Instead, it can be considered a mere indicator of pollution which is supported by the fact that the SO_2 and the CS plot show very similar behavior. Since SO_2 and CS appear on different sides of the fraction line, the behavior of the proxy is reduced to that of radiation. In consequence, a revised proxy for polluted regions could be reduced to $[H_2SO_4]_{polluted} = k_{polluted} *$ radiation.
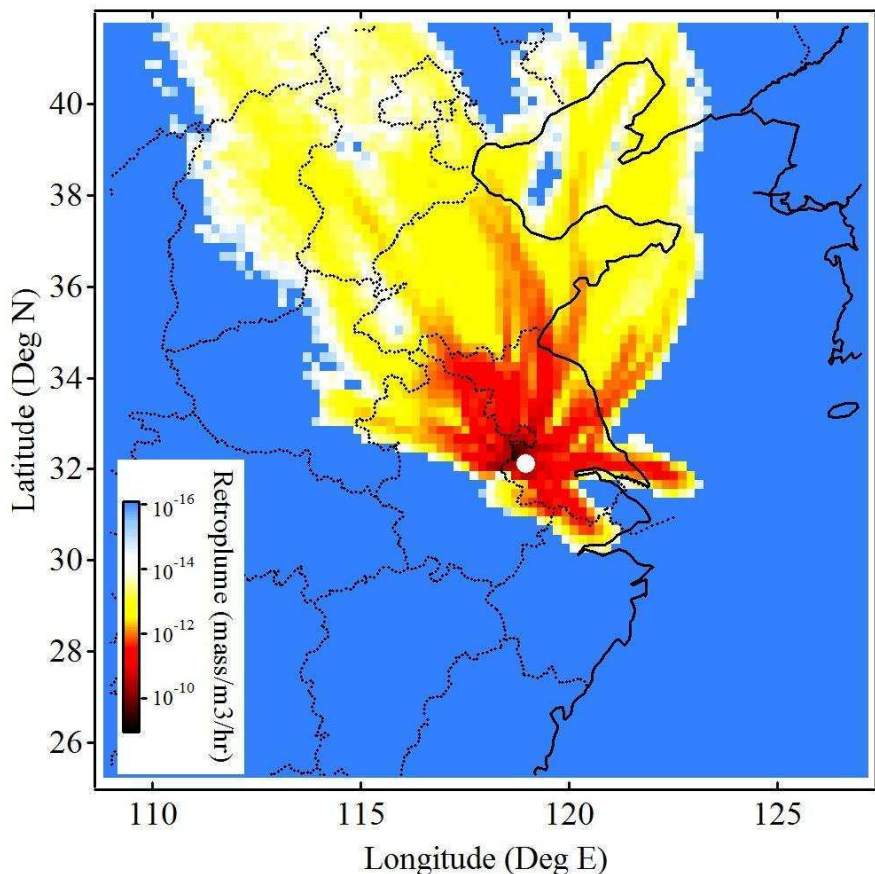
Figure 3. Retroplume (1 day) for event days.

Figure 3 shows the retroplume for a period for one day for event days, i.e. where the air masses have been during the day before the event. While it can be expected that events are more likely with colder, cleaner air coming in from the north, it is noteworthy that not a single event occurred with air masses coming in from the Shanghai direction along the Yangtze River and various large cities, despite the fact that air masses from that direction are quite a common occurrence.

	10nm-100nm	100nm-500nm	
Shanghai, CN	28511	1676	J. Gao et al.(2009)
Nanjing, CN	13000	6200	This work

Table 1. Comparison of particle concentration in Shanghai and Nanjing

Table 1 offers an explanation for this observation. While Shanghai has higher concentrations of total N, Nanjing has much more particles in the accumulation mode. With prevalent winds from the east, this is most likely imported pollution from the YRD, aged aerosol that has grown to larger sizes. This means a higher CS which apparently suffices to suppress nucleation.

279

ACKNOWLEDGEMENTS

REFERENCES

Hari, P. et al (2009). A comprehensive network of measuring stations to monitor climate change. *Boreal Env. Res.* **14**, 442-446.

Hirsikko, A. et al. (2007). Identification and classification of the formation of intermediate ions measured in boreal forest. *Atmos. Chem. Phys.* **7**, 201–210.

Kulmala, M. et al. (2004). Formation and growth rates of ultra$ne atmospheric particles: a review of observations. *J. Aerosol Sci.* **35**, 143-176.

Mirme, A. et al. (2007). A wide-range multi-channel Air Ion Spectrometer. *Boreal Env. Res.* **12**, 247-264.

WIND OBSERVATION STRATEGIES WITH A SCANNING DOPPLER LIDAR

A.E. HIRSIKKO[1], E.J. O'CONNOR[1,2], C.R. WOOD[1] and L. JÄRVI[3]

[1]Finnish Meteorological Institute, P.O. BOX 503, FI-00101, Helsinki, Finland
[2]Meteorology Department, University of Reading, Reading, UK
[3]Department of Physics, University of Helsinki, P.O. Box 64, University of Helsinki, 00014, Finland
Correspondence to: anne.hirsikko@fmi.fi

INTRODUCTION

Finnish Meteorological Institute (FMI) has recently established a Doppler lidar and Doppler cloud radar network (Hirsikko et al., 2012), which is to be completed within the coming year. The aim of the network is to investigate aerosol, cloud and boundary layer properties. Better understanding of wind and the turbulent nature of the boundary layer over a variety of surfaces enables us to 1) improve weather forecast models, 2) facilitate atmospheric research, since most of the atmospheric and surface interaction reactions are influenced by atmospheric dynamics, and 3) evaluate more accurately models of dispersion of pollution in the atmosphere, which among other things enables better planning of urban environment and buildings.

We focus on the urban environment, which comprises a rough and inhomogeneous surface. Due to varying and complex conditions, many measurement locations would be needed to characterise both prevailing meteorological parameters and microscale phenomena: much urban climate research has concentrated on the microscale (Barlow and Coceal, 2009). For similar reasons, processes taking place at the interface between atmosphere and open/ice covered sea surface make oceans a difficult study area. Recent developments of Doppler lidars enable us to investigate spatial and temporal evolution of wind and turbulence over any surface type and their interfaces (e.g. Pichugina and Banta, 2009; Collier et al., 2010). Recent studies have reported new techniques implemented for rather short campaigns. Consequently, our aim is to develop more complex scanning techniques, and subsequent data analysis methods, that are suitable for long-term data collection in a number of different environments in order to better describe the nature of air motions – particularly at the interface between rural/marine/urban environments to give a more comprehensive understanding of boundary layer meteorology beyond the microscale (e.g. Wood et al., 2012a). Here we present the current state of our surface wind and turbulence measurements with Doppler lidars, giving special focus for scanning strategies.

METHODS

The FMI has three full scanning pulsed Doppler lidars (HALO Photonics; Pearson et al., 2009) which have 30 m resolution along the beam and maximum range of about 7km. Our lidars are located on the shore of Baltic Sea at Utö island (59.49°N, 21.23°E), on top of FMI building in Helsinki (60.12°N, 25.58°E) and Kuopio (62.44°N, 27.32°E). The Utö island is part of Finnish southwest archipelago, the sites at Helsinki and Kuopio are in semi-urban environments. The Doppler lidars operate at 1.5 μm wavelength receiving backscattering signal from aerosol particles and hydrometeors. Unlike heavier hydrometeors, aerosol particles suspended in air have a small falling velocity (less than 1 cm/s) relative to air, and thus, serve as good tracers for air motions. Moving objects shift the wavelength of backscattered signal, known as Doppler shift, which enables us to obtain air velocity along lidar beam axis (called Doppler velocity).
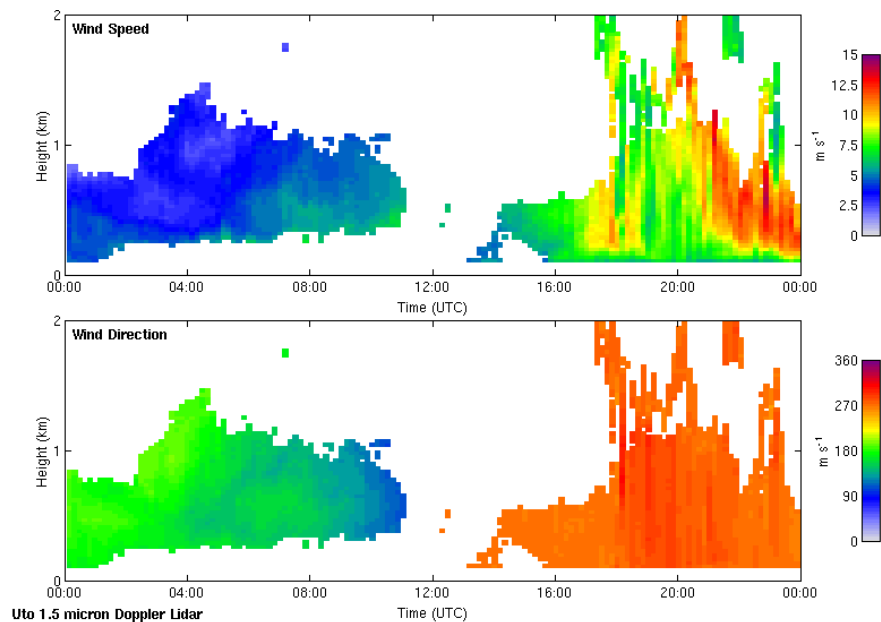
Figure 1. Profiles of horizontal wind speed and direction show temporal and spatial changes measured at Utö island on 25th April, 2012. The profiles are a measured snapshot (with the DBS scanning type) every 10 minutes.

The basic measurement strategy includes vertical staring for most of the time giving valuable information of vertical motion of air, in order to investigate boundary layer mixing and evolution (O'Connor et al., 2010; Barlow et al., 2011). By using the lidar scanning capability we are able to make more novel wind measurements, such as Doppler beam swinging (DBS), custom designed range height indicator (RHI) and vertical azimuth display (VAD) scans. The DBS (essentially a highly-simplified VAD scan) is a standard software application with the Doppler lidars from HALO Photonics and it gives vertical profiles of horizontal wind velocity (Fig. 1). The VAD scanning enables investigation of wind over a large horizontal surface (Fig. 2), while the RHI type of scanning allows investigation of wind on vertical-horizontal surface (Fig. 3). By using trigonometry and statistics we may analyse changes in wind speed, direction and turbulence caused by different roughness elements (e.g. Wood et al., 2012b).

OBSERVATIONS

Horizontal wind profiles throughout the boundary layer are one of the main products with Doppler lidars (Fig. 1). According to our current strategy one snapshot profile is measured every ten minutes (as part of a suite of scanning types operating intermittently); whereas in some other countries, Doppler lidars are used solely as boundary layer wind profilers. Currently we are in process of implementing wind information measured in Finland to weather forecast models.

Most of the time Doppler lidars are set to measure vertically in order to be able to respond to the aims to monitor and investigate aerosol, clouds and boundary layer dynamics. In between these operational tasks we have some time to investigate other processes, for example surface layer wind evolution. We are following the example of a simple duo-beam method introduced by Wood et al. (2012b) and are also testing more complex RHI and VAD strategies with different custom designed coordinate combinations. Fig. 2 shows the distributions of surface wind speed and direction retrieved using the duo-beam method (15° separation). These are preliminary examples, which show that with utilized setups at Utö wind speed
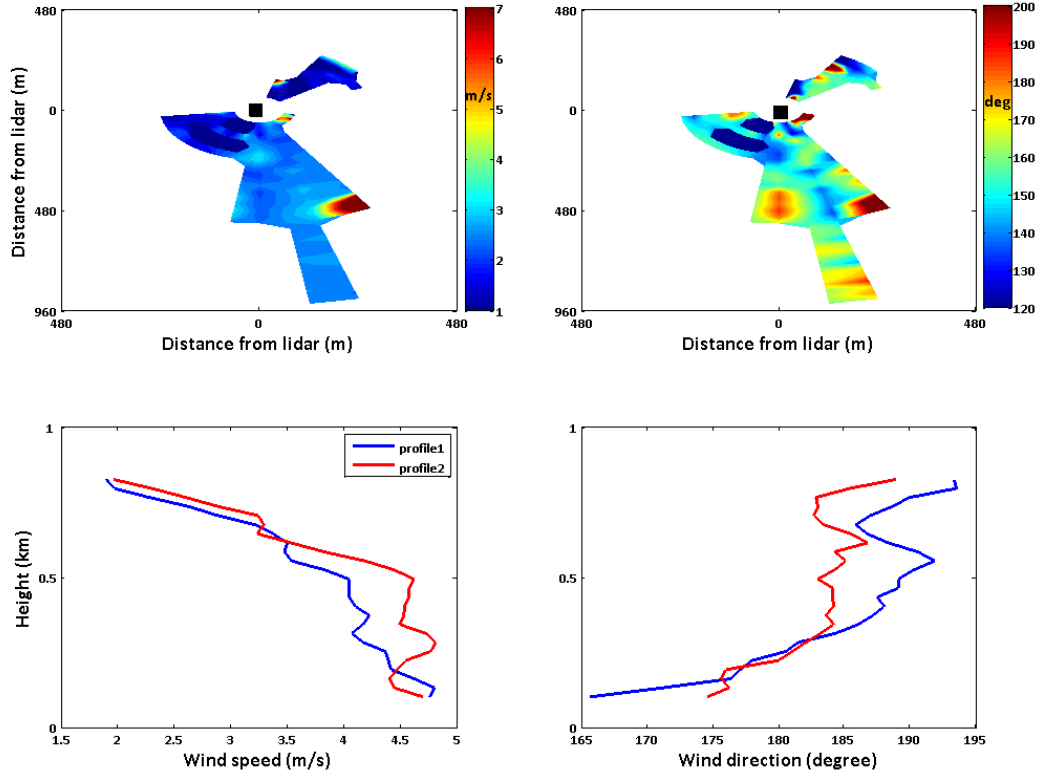
Figure 2. A VAD scan over land and sea interface measured at Utö on 25th April, 2012 at 00:15 am. Wind speed (top left panel) and direction (top right panel) over land and sea, and for method validation purposes vertical profiles of wind speed and direction using the DBS technique. The Doppler lidar is at (0,0) marked with black squares on top panel.

and direction are measured and retrieved quite accurately. Fluctuation in parameters is due to turbulence at the interface of air and variety of roughness elements, in this case sea and island surfaces. These retrievals are most representative with relative small angle between beam axis and mean wind direction. Thus, in the Fig. 2 accuracy is best closer to north-southward line than to east-westward line.

Air motions in urban environments have been difficult to model due to challenging morphology, and thus, most studies have concentrated on very simplified geometries of buildings and streets at the microscale (e.g. review by Barlow and Coceal, 2009). The RHI scanning (Fig.3), together with previously discussed VAD measurements, would allow sophisticated information on air motion over urban area with large spatial coverage at the neighborhood and city scales.

FINAL REMARKS

Doppler lidars measuring vertically or using different scanning routines provide valuable information on boundary and surface layer wind and turbulence. Some novel scanning and subsequent data retrieval strategies with Doppler lidars have been proposed (Pichugina et al., 2009; Wood et al., 2012b). Deployment of scanning Doppler lidars is young but will be continuous in Finland (Hirsikko et al., 2012). Therefore, besides the boundary layer structure and wind profile analysis (e.g. O'Connor et al., 2010;
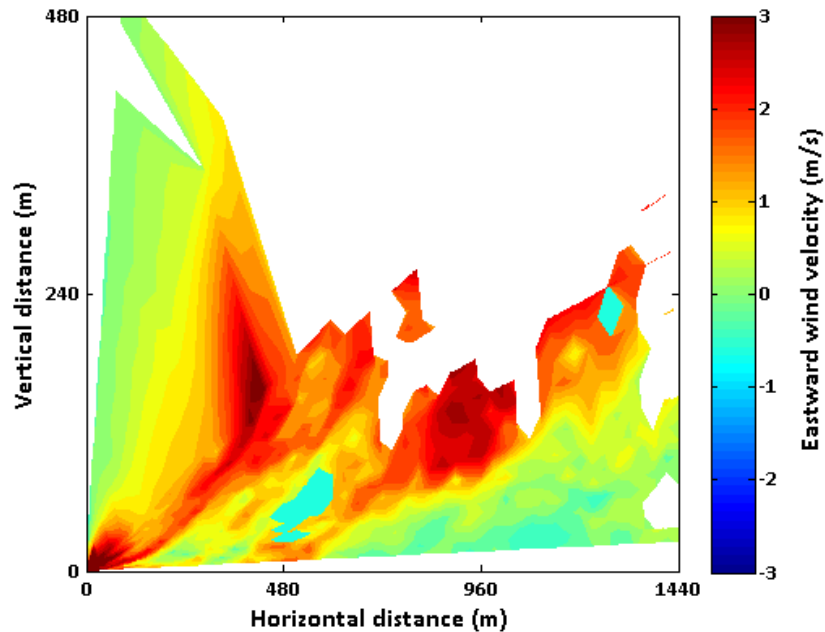
Figure 3. Wind speed scan from the FMI building on 15th March, 2012. The radial wind velocity is projected parallel to the horizontal surface. Negative velocity indicates that wind blows towards lidar at zero and positive velocity value that wind blows away from lidar.

Barlow et al., 2011) and implementation in dispersion and weather forecast models, we are in process of developing routines to investigate the effect of a number of surface roughness elements and combinations on air motion, and thus, facilitate our understanding of air ventilation in and around cities; and to study several meteorological and atmospheric phenomena. This development includes designing specific scanning routines to each environment, but also developing the data analysis and error estimation methods.

A full horizontal scan with zero elevation from lidar would be ideal. However, as shown in top part of Fig. 2, there are often some obstacles (i.e. trees, buildings) in the line of sight (see dark red spot in speed and direction distribution on southeast direction or missing data on northwest direction). To overcome this, we are testing several measurement strategies and data analysis methods beyond that proposed by Wood et al. (2012a). Temporal resolution of data integration is also an issue. Currently each individual beam is measured every 5 seconds, which causes additional challenges for data quality and interpretation. Due to low aerosol concentration, lidar sensitivity has to be increased by changing telescope focus (from infinity to just a few hundred metres) and increasing integration time (Hirsikko et al., 2012). The latter not being favorable, because scanning strategies become more time limited. Eventually some software modification allowing faster data collection would be one solution for discussed issues. Some of the data are very complex (Fig. 3), which motivate us to investigate in which meteorological conditions we receive sensible results with acceptable error. All the scanning has been done in between operation working of the lidars, which limits the data collection and statistical analysis. Therefore, we are planning to carry out short campaigns to collect more statistics for e.g. surface and mixed layer turbulence analysis.

REFERENCES

Barlow, J.F. and O. Coceal (2009). A review of urban roughness sublayer turbulence, Met Office
        Technical Report, Exeter, p. 68.

Barlow, J. F., T. M. Dunbar, E. G. Nemitz, C. R. Wood, M. W. Gallagher, F. Davies, E. J. O'Connor and R. M. Harrison (2011): Boundary Layer dynamics over London, UK, as observed using Doppler lidar, Atmos. Chem. Phys., 11, 2111-2125.

Collier, C.G., F. Davies and G.N. Pearson (2010). The land below the wind: Doppler LiDAR observations from the tropical rain forest of Sabah, Borneo, Malaysia, R Met S, 65, 45-50.

Hirsikko, A., E.J. O'Connor, M. Komppula, M. Bauer-Pfundstein, A. Poikonen, E. Giannakaki, M. Kurri, T, Karppinen, H. Lihavainen, A. Laaksonen, K.E.J. Lehtinen and Y. Viisanen (2012). A new lidar and cloud radar network in Finland, Proceedings of 26th International Laser Radar Conference, Porto Heli, Greece, 25-29 June 2012.

O'Connor, E.J., A.J. Illingworth, I.M. Brooks, C.D. Westbrook, R.J. Hogan, E. Davies and B.J. Brooks (2010). A method for the turbulent kinetic energy dissipation rate from a vertically-pointing Doppler lidar, and independent evaluation from balloon-borne in-situ measurements, J. Atmos. Oceanic Technol., 27, 1788-1812.

Pearson, G., F. Davies and C. Collier (2009). An Analysis of the Performance of the UFAM Pulsed Doppler Lidar for Observing the Boundary Layer, J. Atmos. Ocean. Tech., 26, 240-250.

Pichugina, Y.L and R.M. Banta (2009). Stable Boundary Layer Depth from High-Resolution Measurements of the Mean Wind Profile, J. Applied Meteorology and Climatology, 49, 20-35.

Wood, C.R., L. Järvi, R. Kouznetzov, A. Nordbo, A. Drebs, T. Vihma, A. Hirsikko, I. Suomi, C. Fortelius, E. O'Connor, D. Moisseev, S. Haapanala, J. Moilanen, M. Kangas, A. Karppinen, S. Joffre, T. Vesala and J. Kukkonen (2012a). An overview of Helsinki UrBAN, to be submitted to BAMS in the near future.

Wood, C.R., L. Pauscher, H.C. Ward, S. Kottsaus, J.F. Barlow, M. Gouvea, S.e. Lane and C.S.B. Grimmond (2012b). Wind observations above an urban river using a new lidar technique, scintillometer and anemometry, submitted to Science of Total Environment (http://www.met.reading.ac.uk/~bl_met/papers/Wood/Wood_etal_2012_STOTEN.pdf).

Hygroscopic, CCN and volatility properties of submicron atmospheric aerosol in a boreal forest environment during the summer of 2010

J. Hong[1], S. A. K. Häkkinen[1], M. Äijälä[1], J. Hakala[1], J. Mikkilä[1], M. Paramonov[1] and T. Petäjä[1], M. Kulmala[1]

[1]Division of Atmospheric Science, Department of Physics, University of Helsinki, Gustaf Hällströmin katu 2, 00014, Helsinki, Finland

INTRODUCTION

Hygroscopic properties of atmospheric aerosol particles describe the interaction between the particles with ambient water molecules at both sub and supersaturated conditions in the atmosphere. Although the size of the particle is dominant factor (Dusek et al. 2006) determining whether a particle is a potential cloud condensation nuclei (CCN), hygroscopicity plays a role at the size close to the limit of activation (e.g. Roberts et al. 2002). For example atmospheric oxidation of particles can modify the hygroscopicity of the particles making them CCN active (Petäjä et al. 2006, Massoli et al. 2010, and Chang et al. 2010). Furthermore, hygroscopicity can give essential information on particle composition (Swietlicki et al. 2008).

The aim of this study is to explore the hygroscopic and condensation nuclei properties of nucleation, Aitken and accumulation mode particles in sub- and supersaturation condition in a boreal forest (Hyytiälä, Hari and Kulmala, 2005) strongly affected by biogenic emissions from the forests during a period, which was exceptionally warm (summer 2010). The hygroscopicity parameters determined in sub- and supersaturations are compared with each other, and their information is coupled with the aerosol chemical composition data from an aerosol mass spectrometer. During the measurement period, the measurement site was also affected by occasionally by forest fires in Russia and anthropogenic emissions from Tampere area (Williams et al. 2011). The effects of these variable aerosol sources to the hygroscopicity and CCN concentrations are explored.

METHODS

This study was performed as a part of Hyytiälä United Measurement of Photochemistry and Particles – Comprehensive Organic Particle and Environmental Chemistry (HUMPPA-COPEC-2010) intensive field campaign (Williams et al. 2011). The study was hosted in Station for Measuring Ecosystem-Atmosphere Relations II, SMEAR II, Hari and Kulmala, 2005) field station in Hyytiälä, Finland between 12 June and 12 August, 2010.

Hygroscopicity of sub-micro aerosol particles were performed using a Hygroscopicity Volatility Tandem Differential Mobility Analyzer (HVTDMA, Hakala et al. 2010), while the CCN properties were measured with a commercial continuous-flow Cloud Condensation Nucleus Counter (CCNC, Roberts and Nenes, 2005, Sihto et al., 2011). The volatility properties were investigated using a Volatility Differential Mobility Particle Sizer (VDMPS, Häkkinen et al., 2012). The chemical information obtained from an Aerosol Mass Spectrometer (AMS) was used to support the interpretation of the results. The instrument parameters and size range is presented in Table 1. During the HV-TDMA measurements, the temperature of the thermal denuder was ramped from 25°C to 280°C. The relative humidity of the aerosol after the humidifier was set as 90% ±2% RH. The data of the aerosol passing through the whole systems were divided into 4 modes, one without going into the thermal denuder and humidifier called dry-mode, one going into the humidifier but without passing through the thermal denuder called H-mode, one flowing into the thermal denuder but without the humidifier called V-mode and the one entering both the thermal denuder and the humidifier called HV-mode. In the CCN counter operation, the supersaturation of the

CCN chamber was hold constant, while the diameters were scanned from 20 nm to 300 nm with a Vienna-type Differential Mobility Analyzer (Winkmayr et al., 1991). The volatility of the submicron population was monitored with a Volatility Differential Mobility Particle Sizer (VDMPS). In the VDMPS, the aerosol was heated up to a constant temperature of 280°C (Häkkinen et al., 2012).

Table 1. Instrument parameters during HUMPPA-COPEC 2010 intensive in Hyytiälä, Finland

Instrument	Description of data
CCNC	10 supersaturation levels were selected, particles were scanned from 20 nm to 300 nm
VHTDMA	RH=90%; Dp= 50, 75, 100, 110, 135, 150 nm; time resolution is around 3 min/dry size
VDMPS	Dp: 15-1000 nm, time resolution: ten minutes, temperature: 280°C

RESULTS

During the HV-TDMA measurements, the distribution of growth factors (GF) exhibited by the dry particles after exposure to a selected RH, also referred to as the growth factor probability density function (GF-PDF) was obtained. The spectra were fitted using the program TDMAinv-Tookit 3221 (Gysel et al., 2009). Average growth factor probability density function for different sizes is illustrated in Fig. 1 for H-mode. Williams et al (2011) characterized each sector, based on trajectories and local and regional influences observed on the site, into different time groups. The probability density function of each time group was analyzed to give better understanding of the hygroscopic properties of the ambient aerosols varying over time.

A hygroscopic parameter κ can be derived from the hygroscopic growth factor as a function of relative humidity, obtained from HVTDMA measurements. The κ value, coupling with the other physical chemical properties of particles was used to calculate the critical supersaturation of a certain size particles (Petters & Kreidenweis 2007). The results were compared with CCN results and previous study (Sihto et al., 2010). HVTDMA results agreed well with the oness obtained from CCNc and with the previous study within the uncertainty, shown in Fig. 2.

The volume fraction remaining of aerosol particles (VFR) was defined as the total volume of heated aerosol divided by the total volume of ambient aerosol. VFR is equivalent to the aerosol mass fraction remaining, which is a parameter to investigate the evaporation of ambient particles. VFR was obtained from both HVTDMA measurements during V-mode and VDMPS. The results were also compared with Häkkinen et al (2012), who performed long-term volatility measurements of submicron atmospheric aerosol in Hyytiälä. Figure 3 shows a good agreement of these results, but uncertainties need to be included for further analysis.

287
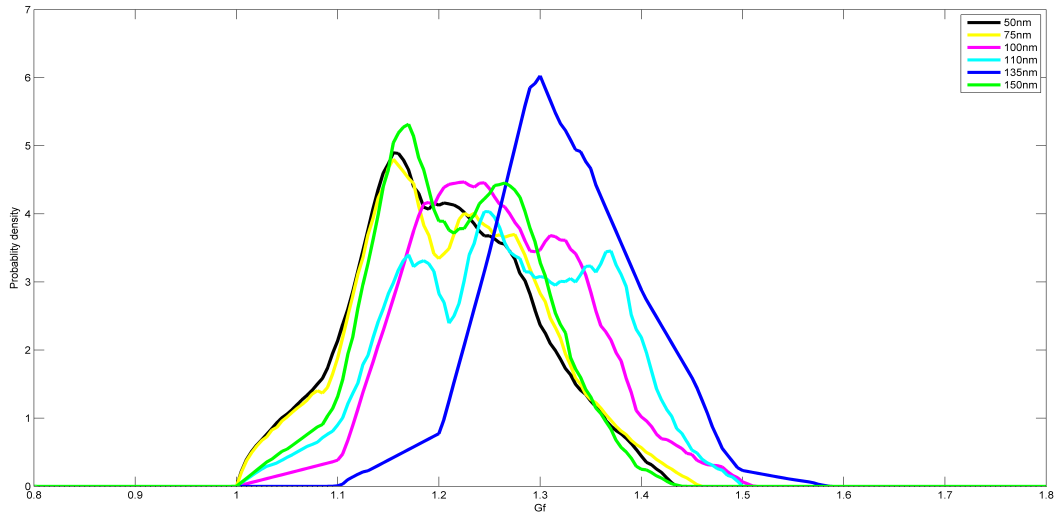
Figure 1. Probability density function as a function of growth factor for particles of different sizes during H-mode.
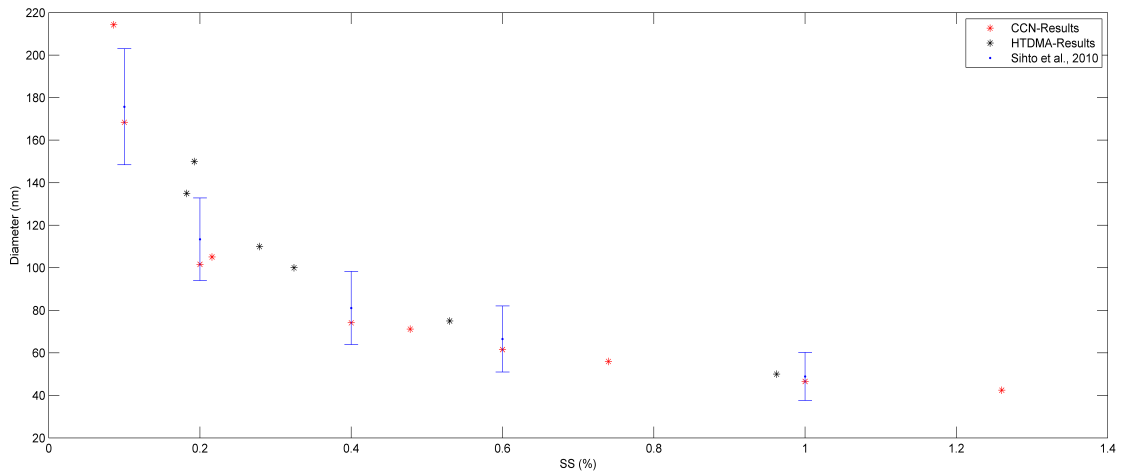
Figure 2: Critical diameter as a function of critical supersaturation from this study and Sihto et al (2010).
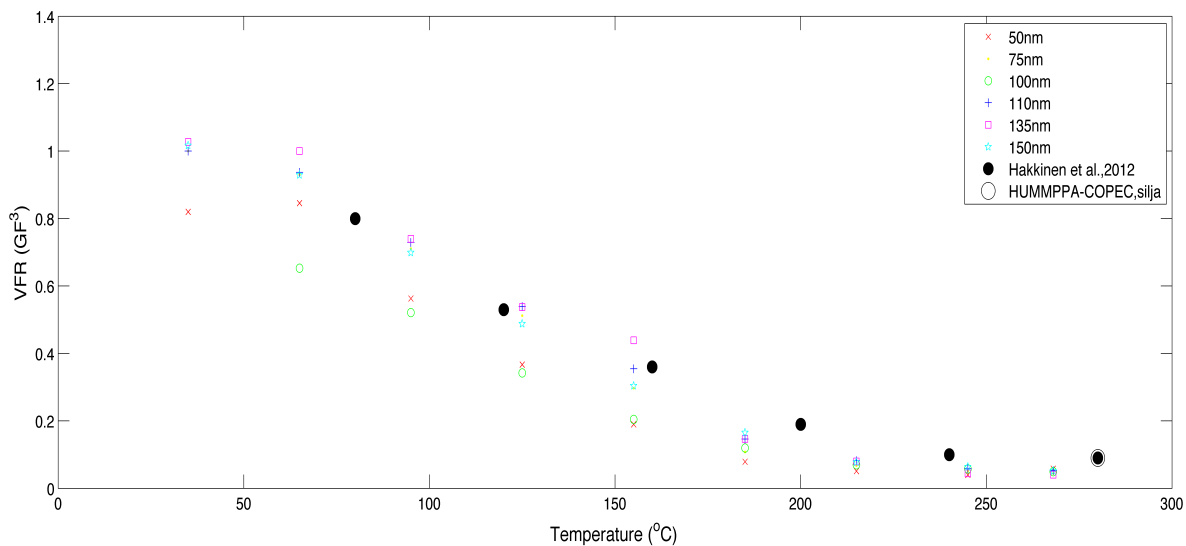
Figure 3: VFR as a function of temperature, obtained from HVTDMA and VDMPS, compared with Häkkinen et al (2012).

REFERENCES

Cerully et al (2011). Aerosol hygroscopicity and. CCN activation kinetics in a boreal forest environment during the 2007 EUCAARI campaign. *Atmo.Chem. Phys. Discuss* 11, 15029-15074.

Desuk et al (2011). Size Matters More Than Chemistry for Cloud-Nucleating Ability of Aerosol Particles. *Sciences* 312(5778), 1375-1378.

Ehn et al (2007). Hygroscopic properties of ultrafine aerosol particles in the boreal forest: diurnal variation, solubility and the influence of sulphuric acid. *Atmos. Chem. Phys* 7, 211-222.

Gysel M., McFiggans G. B., Coe H. (2009). Inversion of tandem differential mobility analyser (TDMA) measurements. *Aerosol Science* 40, 134-151, 2009.

Hari P. and Kulmala M. (2005). Station for Measuring Ecosystem-Atmosphere Relations (SMEAR II). Boreal Environment Research 10, 315-322.

Hakala J., Mikkilä J., Ehn M., Siivola E., Kulmala M., and Petäjä T. (2010) Indirect
aerosol chemical composition measurements with a VH-TDMA, Proceedings of the Finnish Centre of Excellence in Physics, Chemistry, Biology and Meteorology of Atmospheric Composition and Climate Change, Annual Workshop in Kuopio, May 17-19, 2010.

Häkkinen S., Äijälä M., Lehtipalo K., Junninen H., Backman J., Virkkula A., Nieminen T., Vestenius M., Hakola H., Ehn M., Worsnop D. R., Kulmala M., Petäjä T., and Riipinen I. (2012). Long-term volatility measurements of submicron atmospheric aerosol in Hyytiälä, Finland. *Atmos. Chem. Phys. Discuss* 12, 11201-11244, doi:10.5194/acpd-12-11201-2012, 2012.

Massoli et al (2010). Relationship between aerosol oxidation level and hygroscopic properties of laboratory generated secondary organic aerosol (SOA) particles. *Geo. Res. Lett* 37, L24801.

Petäjä et al (2006). Sub-micron atmospheric aerosol in the surroundings of Marseille and Athens: physical characterization and new particle formation. *Atmos. Chem. Phys. Discuss* 6,8605-8647.

Petters, M. D. and Kreidenweis, S. M (2007). A single parameter representation of hygroscopic growth and cloud condensation nucleus activity. *Atmos. Chem. Phys* 7, 1961-1971.

Roberts G. C. and Nenes A (2005). A Continuous-Flow Streamwise Thermal-Gradient CCN Chamber for Atmospheric Meausrements. *Aerosol Science and Technology* 39, 206-221.

Rose et al (2010). Cloud condensation nuclei in polluted air and biomass burning smoke near the mega-city Guangzhou, China-Part 1: Size-resolved measurements and implications for the modelling of aerosol particle hygroscopicity and CCN activity. *Atmos.Chem. Phys* 10, 3365-3383.

Riipinen et al (2011). Organic condensation: a vital link connecting aerosol formation to cloud condensation nuclei (CCN) concentrations. *Atmos. Chem. Phys* 11, 3865-3878.

Swietlicki et al (2008). Hygroscopic properties of submicrometer atmospheric aerosol particles measured with H-TDMA instruments in various environments-a review. *Tellus* 60B, 432-469.

Sihto et al (2010). Seasonal variation of CCN concentrations and aerosol activation properties in boreal forest. *Atmos. Chem. Phys. Discuss* 10, 28231-28272.

Williams et al (2011). The summertime Boreal forest field measurement intensive (HUMPPA-COPEC-2010): an overview of meteorological and chemical influences. *Atmos. Chem. Phys. Discuss* 11, 15921-15973.

THE ENERGY BUDGET OF FIRST-YEAR SEA ICE THROUGH THE MELT SEASON

S.HUDSON[1], M.GRANSKOG[1], D. DIVINE[1], C. POLASHENSKI[2], J. EHN[3],
C. PEDERSEN[1], A.SUNDFJORD[1], A. RENNER[1], S. GERLAND[1]

[1]Norwegian Polar Institute, Fram Centre, N-9296 Tromsø, Norway.

[2] ERDC-CRREL, Hanover, USA

[3] U. of Manitoba, Winnipeg, Manitoba, Canada

ABSTRACT

Over recent decades the age of sea ice covering the Arctic Ocean has decreased substantially, to the point that today first-year ice is the dominant ice type in much of the basin. Given that further warming is expected over the coming decades, we need an improved understanding of the processes that affect this younger ice cover; these can differ significantly from processes on the multi-year ice that was dominant in the past. To this end, we have carried out two field campaigns to observe the energy fluxes and processes affecting the melt of different types of seasonal sea ice. Near Barrow, Alaska (see Figure 1), we observed the spatial variability of the four components of the surface radiation budget along with measurements of the sensible and latent heat fluxes to the surface from the atmosphere
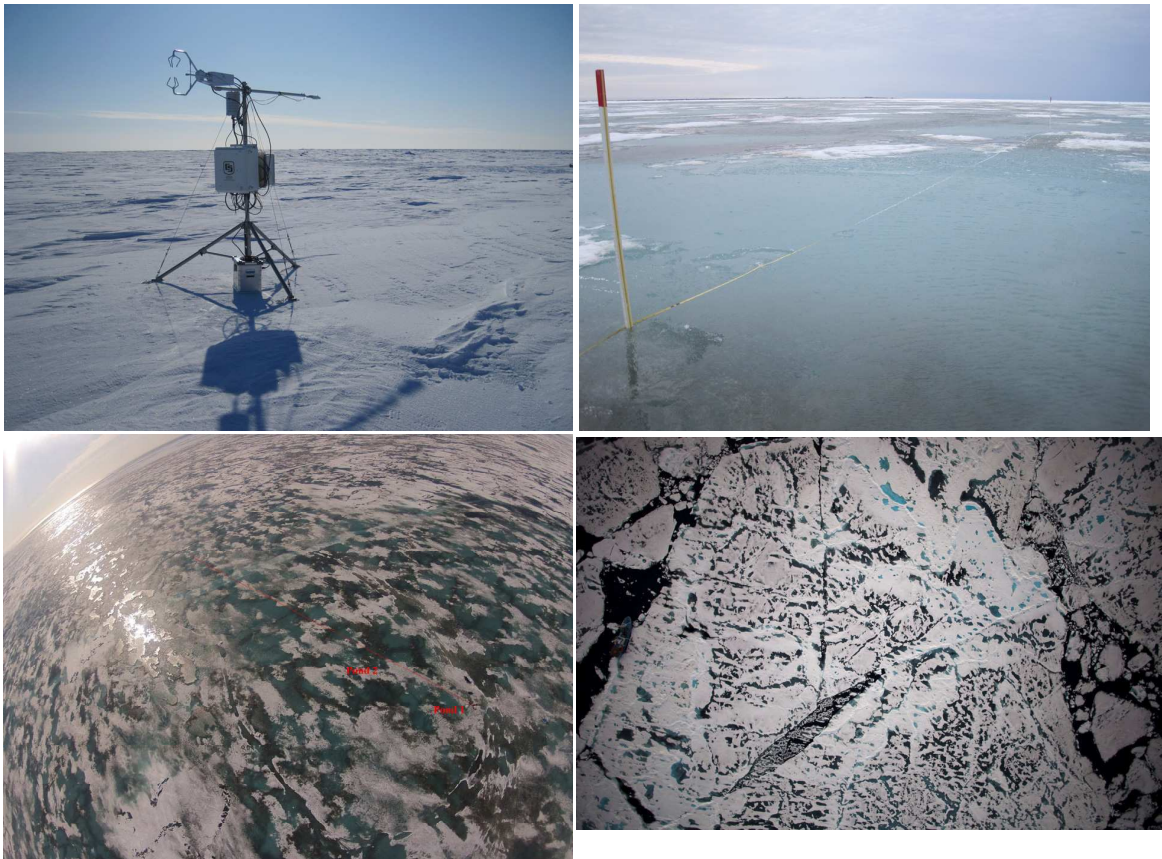
Figure 1. Images of the study areas. Top left: Barrow site in early April, showing the eddy covariance setup. Top right: Barrow site in early June, at the peak of surface flooding. Bottom left: Aerial view of the Barrow site in early June; radiation transect measurements were made along the 200-m line in red; Pond 1 and 2 are over the 45-m under-ice radiation transect. Bottom right: Aerial view of the July site on drift ice near 82.5° N, 21° E; the ship is visible at the left.

and the transmitted solar radiation below the ice, on relatively thick landfast ice. These observations were carried out from before the start of snow melt until melt ponds were well developed to see how the widely varying surfaces found on sea ice during the melt season affect the progression of the melt and the relative role played by atmospheric and radiative fluxes. A similar set of measurements was also carried out on seasonal drifting ice north of Svalbard (Figure 1) for a shorter period in July. Here, the surface measurements can be supplemented by more extensive observations of solar radiation under the ice and of turbulent heat fluxes from the ocean to the underside of the ice, allowing a complete view of the energy budget of Arctic seasonal sea ice in summertime.

Figure 2 shows the progression and spatial variability of the broadband albedo along a 200-m line on level ice in Barrow. There was relatively little variability before the snow melt began, when dry snow provided a fairly uniform surface. Warming in the second half of May caused the snow surface to become wet, lowering albedo and inducing increased variability. As ponds, which initially formed below a layer of intact ice, began to open up in early June, albedo dropped further, with another increase in spatial variability. A cooler period then stopped the progression for several days, before the ponds completely opened up and most of the ice was flooded, bringing the season's lowest albedos, with very few white areas. After this, the ice began forming holes that allowed the melt water to drain, reducing the area covered by melt water, leading to increased spatial variability and higher average albedos, though the darkest areas did not brighten during this period.

Figure 3 shows how this surface variability is also important beneath the ice. In this photo looking up from under the ice, areas with a white surface are clearly visible as dark regions between the ponds, which act as windows for the light to pass through the ice, heating the ocean and driving biological activity. With the help of divers, the spectral solar transmittance of the sea ice was measured along three 35-m profiles beneath the drifting floe studied during the July cruise. The results of one of these profiles are shown in Figure 4. Along this 35-m transect, which included a mix of light and dark ponds and white ice, transmittance of photosynthetically active radiation (PAR, 400–700 nm, roughly corresponding to visible light) varied from around 10% through the white ice up to over 60% through ponds overlying thin ice. Previous studies, generally from multiyear ice, reported pond transmittances closer to the pond over thick ice on the left end of this transect, and also showed less pond coverage overall. The increasingly transparent Arctic ice should be better understood if we are to know how future changes to the ice and ecosystem will unfold.
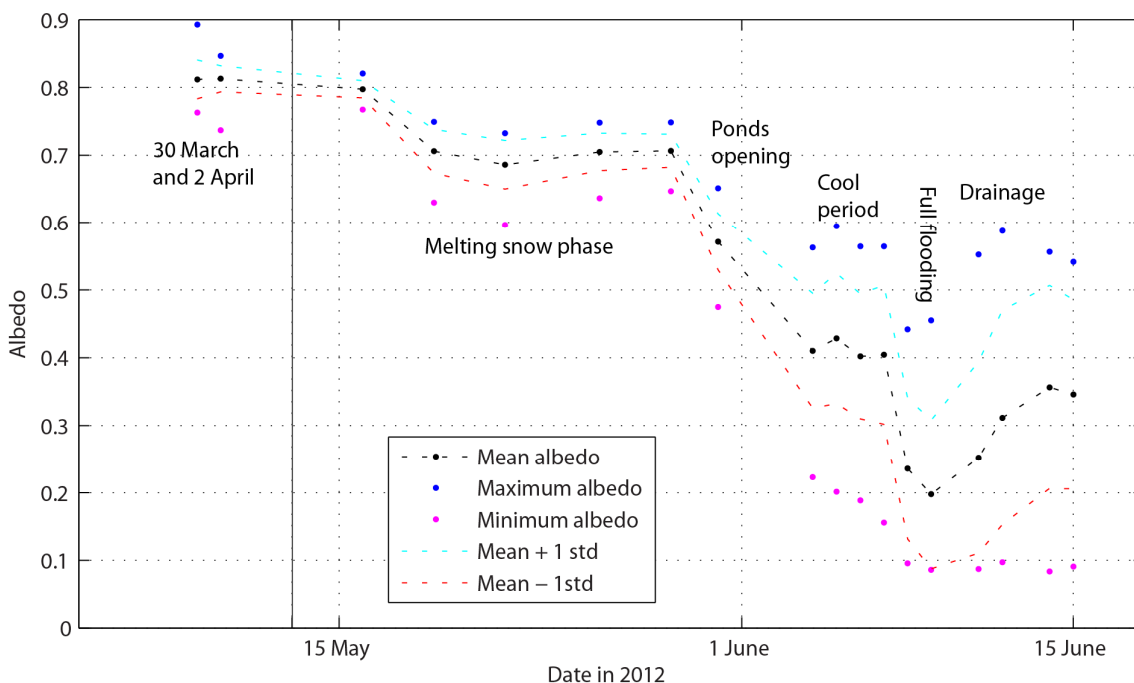
Figure 2. The seasonal progression of surface broadband albedo and its spatial variability on level ice near Barrow, Alaska.

Figure 3. A photograph of ponded sea ice in the Arctic Ocean in July 2012, taken from below. The light areas are melt ponds on the surface, while the darker areas have white ice on the surface.
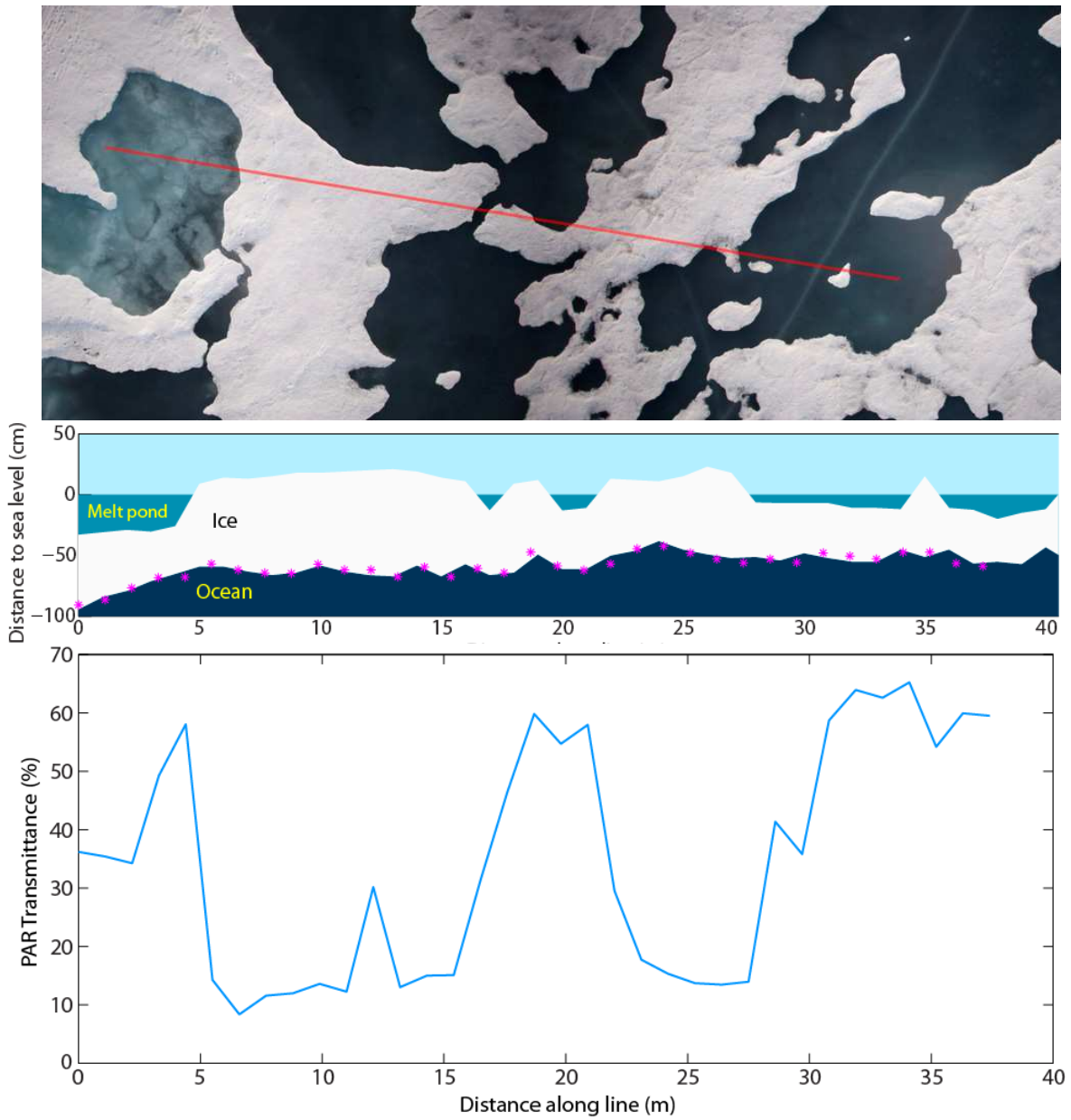
Figure 4. At the top is an aerial photograph of the region under which we conducted measurements of the transmittance of the sea ice in July, 2012, north of Svalbard; the transect follows the red line, starting at the left. In the middle is a sketch of the ice and pond thicknesses along the line, measured every meter; ponds had already drained to sea level. The measured transmittance of photosynthetically active radiation along the profile is shown at the bottom. The measurements were made at the purple marks on the middle drawing.

A MEASUREMENT ARTIFACT OF THE MULTI-ANGLE ABSORPTION PHOTOMETER (MAAP): LABORATORY QUANTIFICATION

A.-P. HYVÄRINEN[1], A. PETZOLD[2] and H. LIHAVAINEN[1]

[1] Finnish Meteorological Institute, Helsinki, FI-00101, Helsinki, Finland.

[2] Forschungszentrum Jülich GmbH, Institute of Energy and Climate Research IEK-8: Troposphere, 52425 Jülich, Germany.

INTRODUCTION

A widely used method for measuring atmospheric black carbon (BC) mass concentration involves the determination of absorption of an aerosol sample collected on an appropriate filter matrix. The most common instruments utilized today for this purpose are the filter-tape based instruments Aethalometer (Hansen et al. 1982), Multi-Angle Absorption Photometer (MAAP) (Petzold and Schönlinner 2004, Petzold et al. 2005), and the single-filter based instrument Particle Soot Absorption Photometer (PSAP) (e.g. Bond et al. 1999). Since BC by definition cannot be unambiguously measured with these instruments, it is customary to refer to the measured carbonaceous light absorbing aerosol constituent as equivalent BC (BCe) or light-absorbing carbon (LAC). For the sake of simplicity, we use the term BC throughout.

It is well known that filter-based BC measurements suffer from several artifacts. These include the filter loading effect that causes a decrease in the measured BC concentration with increasing filter load, and the sample matrix effect that causes scattering aerosols on the filter to increase the measured BC concentration. These artifacts can be corrected to some extent by using different numerical methods (e.g. Bond et al. 1999; Weingartner et al., 2003; Arnott et al., 2005; Virkkula et al., 2007; Coen et al., 2010). All of the correction schemes have their advantages and disadvantages under field conditions. Thus far, the MAAP has been deemed as the most reliable filter based instrument for measurement of BC, since the instrument design and software take the typical filter related artifact effects into account.

During aerosol field measurements in Gual Pahari, a highly polluted area in India (Hyvärinen et al. 2010), we observed that at high BC concentrations the MAAP is not free of measurement artifacts. The observed artifact is different from those seen with other filter based BC instruments. It occurs after a filter spot change: as BC is collected on a fresh filter filter spot, the concentration drops. This is followed by a gradual increase to the correct concentration level. Here, we quantify this artifact with the assistance of laboratory measurements utilizing two MAAPs operating at different flow rates. We present a method for correcting the results from the typical instrument print formats in the post-processing phase, and demonstrate how the artifact can be circumvented by logging the reflected photo detector signal.

METHODS

A laboratory test was conducted to accurately quantify the artifact. The basic assumption for designing the quantification experiment was that the observed artifact is closely related to the BC mass accumulation rate ΔBC in µg min-1. Hence, two MAAP instruments were set up to sample from the same aerosol but operated on different volume flow rates. This in turn resulted in different values for ΔBC.

Test aerosol was produced by atomizing (TOPAS ATM226 Atomizer) a water solution of "Aquadaq", a soot reference standard (Baumgartner et al. 2012), into a mixing volume of ~ 5 l. Two MAAP instruments sampled from this mixing volume – one (s/n 145) with a high flow rate ($16 - 20\,l\,min^{-1}$), and the other (s/n 87) with a low flow rate ($7 - 10\,l\,min^{-1}$). Make-up air was taken from the lab through a HEPA filter. The

concentration of BC was changed by changing the flow rate of the atomizer. The concentration- and flow rate- ratios were controlled so that the artifact occurred only in the high flow rate MAAP, thus utilizing the low flow rate MAAP as a reference instrument. MAAP flow rates were calibrated against a Gilibrator bubble flow meter.

RESULTS AND DISCUSSION

As the photo detector response (and thus the mass accumulation rate) depends both on the BC mass concentration and the flow rate Q of the instrument, we express the laboratory results in terms of $\Delta BC = BC \times Q$, i.e., BC accumulation rates. This notation is used, as both BC and Q can be logged with the MAAP standard print formats. The results indicate that at BC mass accumulation rates $> \sim 0.04$ µg min^{-1} the artifact can be identified from the data (Fig 1). The observed artifact is very systematic. After an initial drop, the BC signal increases with a rate proportional to the prevailing BC concentration. The artifact can be roughly divided in three distinct regions (Fig 1a):

(1) At moderately high mass accumulation rates (0.04 µg min^{-1} < BC$\times$Q < 0.08 µg min^{-1}) only the very first minutes experience a decrease of the signal, followed by a prominent increase above the initial signal level, before stabilization back to the correct level occurs.
(2) At high mass accumulation rates (0.08 µg min^{-1} < BC$\times$Q < 0.14 µg min^{-1}), the initial decrease of the signal becomes more apparent compared to the following overestimation. However, the point where the concentration stabilizes back to the correct level is still very distinct, as it is characterized by 1 or 2 minutes of clearly higher concentrations.
(3) At very high mass accumulation rates (BC$\times$Q > 0.14 µg min^{-1}), the initial signal decrease is so strong that the signal never recovers to the correct level before the next filter spot change, leading to an inevitable underestimation of the BC concentration. This reveals that an erroneous temporal response is not the only outcome of the artifact. At high enough BC concentrations, the MAAP underestimates BC values entirely (Fig 1b).
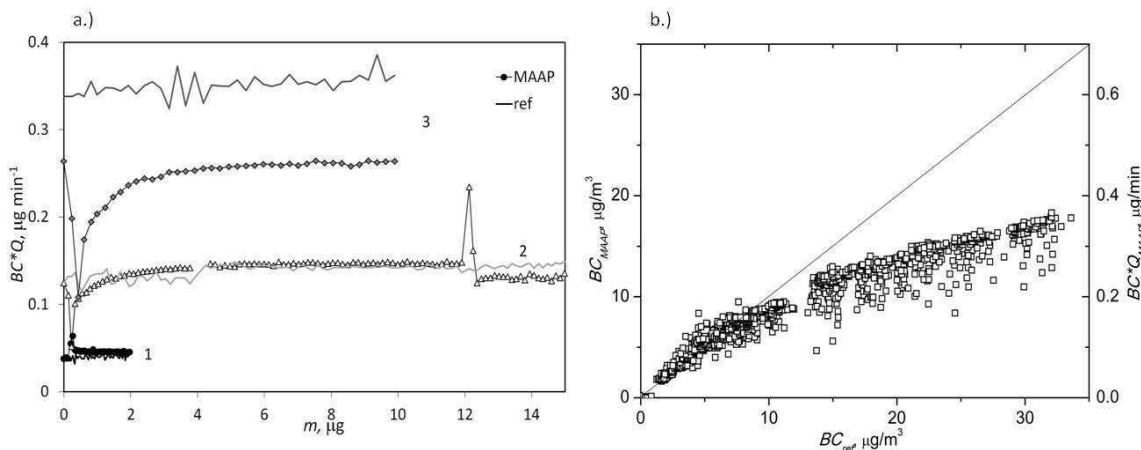
Figure 1. a.) Examples of the artifact temporal response. Symbol lines indicate data from the high flow rate MAAP, and solid lines data from the reference MAAP. Three regimes of different artifact behavior are indicated. See text for details. b.) Comparison of the low flow rate reference (BC$_{ref}$) and high flow rate (BC$_{MAAP}$) BC concentrations.

To compile a correction algorithm, we addressed the two principal problems present in the original data, i.e., (1) the overall concentrations which are underestimated when the rising MAAP signal cannot reach the true concentration (Fig 1b), and (2) the temporal response of the erroneous concentrations (Fig 1a).

(1) The overall correction was made by correlating the smoothed data from the high flow rate MAAP with the data from the reference low flow rate MAAP. The smoothed concentrations, BC_{smooth}, could simply be the last few minutes before the next filter spot change. The correlation can be described with a third level polynomial resulting in the corrected $BC_{CORR} \times Q$:

$$BC_{CORR} \times Q = 5.665 \pm 0.25(BC_{smooth} \times Q)^3 + 0.203 \pm 0.113(BC_{smooth} \times Q)^2 + 0.9363 \pm 0.0116(BC_{smooth} \times Q) \quad (1)$$

In conditions with changing concentrations, only considering data from a few minutes before each spot change might be misleading due to the poor time resolution.

(2) In order to smooth the temporal response, we assumed that the real concentration is a sum of the extracted artifact signal and real changes in the concentrations, and may thus be expressed as:

$$BC_{smooth} = BC_{ini} + (BC_{meas} - BC_{artifact}) \quad (2)$$

where BC_{ini} is the concentration before the spot change, BC_{meas} is the measured non-corrected concentration and $BC_{artifact}$ is the artifact signal dependent on the initial concentration described below. The shape of the MAAP artifact signal can be described with the so called Hill function as a function of the apparent accumulated mass on the filter spot, m:

$$BC_{artifact} \times Q = BC_{max} \times Q \frac{m^n}{m^n + k^n} \quad (3)$$

where $BC_{max} \times Q$ is the maximum plateau value simulated by the Hill function, and k and n are parameters describing the slope of the rising mass accumulation rate. The measured accumulated mass was chosen as the base for characterizing the artifact, as it is a reasonable assumption that the artifact is dependent on both the initial mass accumulation rate and the change of accumulated mass on the filter spot. The laboratory cases were fitted with this function, and the parameters $BC_{max} \times Q$, k and n were optimized. The parameters can be expressed with the following functions and constants:

$$BC_{max} \times Q = 0.8792 \times (BC_{ini} \times Q) + 0.0347$$
$$k = 1.6623 \times (BC_{ini} \times Q) + 0.0462$$
$$n = 20.02 \times (BC_{ini} \times Q)^2 - 4.6454 \times (BC_{ini} \times Q) + 1.428$$

where $BC_{ini} \times Q$ is the mass accumulation rate in $\mu g\ min^{-1}$ before the spot change. As noted earlier, when $BC \times Q < 0.14\ \mu g\ min^{-1}$, the artifact signal eventually makes an abrupt decrease back to the correct level (see Figure 1a). This point was found to follow the relation:

$$m_d = 0.1632 \times \exp(21.798 \times (BC_{ini} \times Q)) - 0.4 \quad (4)$$

The algorithm is not able to predict this decrease back to the real signal level, and should not be applied if the apparent accumulated mass from the spot change is greater than m_d (in μg).

An overall representation of the laboratory results is illustrated in Figure 2. The smoothed data (BC_{smooth}) corrects for the temporal response, but not the overall underestimation. However, the polynomial regression (eq. 1) brings the two datasets to a 1:1 ratio ($R^2 = 0.99$). Equation (1) is valid for the mass accumulation rate ($BC_{smooth} \times Q$) range of 0 - 0.39 μg min-1. The equation is nearly linear in the range of 0-0.14 $\mu g\ min^{-1}$ with an average relative difference of 3.8 % from a linear 1:1 correlation. The upper limit here is restricted by the artifact arising in the reference MAAP. The low flow rate data was used up to $BC \times Q = 0.14\ \mu g\ min^{-1}$ so that only the artifact–free data was chosen for the correlation. The average absolute deviation of the corrected measurement points of the high flow rate MAAP compared to the low flow rate MAAP was 0.49 $\mu g\ m^{-3}$, and the corresponding average relative deviation was 5.4 %. The highest individual deviations typically occur during the first 2-3 minutes after the filter spot change, due to the very steep signal increase of the artefact.

The BC concentrations were additionally determined from the MAAP by utilizing the instrument's photodetector measuring the reflected light (at 165°) from the filter sample (for details see Petzold and Schönlinner 2004). We see that this data follows the reference concentrations closely (Fig. 2), although with more scatter (R^2=0.96). Obviously the reflectance signal is not affected by the measurement artifact. This observation may indicate that the measurement artifact is occurring only in the processed transmission signal which then affects also the final MAAP output signal while the reflectance signal only, with appropriately applied corrections of the filter matrix effect (Petzold et al., 2005), is not affected by the artifact and reports BC mass concentration values at a correct level. This presents an opportunity to utilize the reflected signal from the MAAP when mass accumulation rates are high enough that the artifact appears. However, as most of the print formats of the MAAP do not give the raw signals as an output, the algorithm is a useful way for correcting the results.
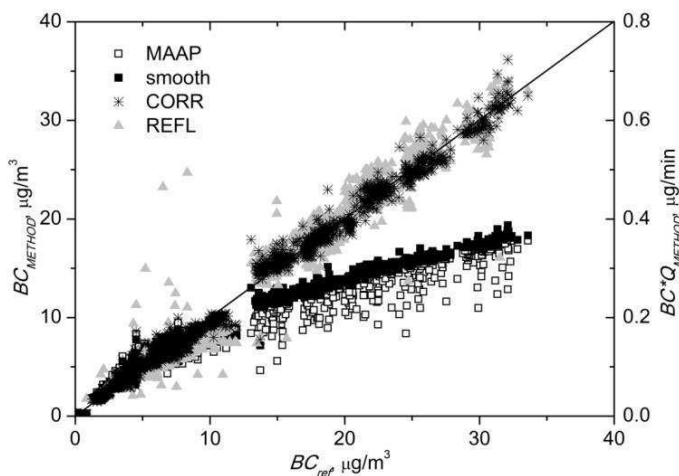
Figure 2. High flow rate MAAP BC concentrations as a function of the reference (low flow rate) MAAP concentrations. BC_{MAAP} is the original signal, BC_{smooth} is the smoothed signal without an overall concentration correction. BC_{CORR} is the smoothed signal with the overall concentration correction. BC_{REFL} is the original signal determined with the reflectance method. The 1:1 ratio line is also shown.

CONCLUSIONS

We have observed a measurement artifact in the MAAP at high BC concentrations. The artifact is related to the filter spot change – as mass is accumulated on a fresh filter spot, the photo detector response of the transmitted 0° light is lower than anticipated. However, the 165° photo detector signal is not compromised. The artifact seems to be related to erroneous dark counts in the transmitted light photo detector, in combination with an instrument internal averaging procedure of the photo detector raw signals. The artifact behavior however appears to be entirely related to the currently implemented data inversion algorithm, but not to any unknown physical processes. Using raw data on a 1 Hz basis and post-processing the data independently by an algorithm similar to that described by Petzold & Schönlinner (2004) shows no artifacts as described here (T. Onasch, private communication 2011). The artifact can be observed if the BC mass accumulation rate BC×Q exceeds 0.04 µg min^{-1}. At the typical flow rate of 1 m3 h^{-1}, this relates to a BC concentration of ~3 µg m^{-3}. Overall concentrations of uncorrected MAAP data are underestimated if BC×Q exceeds 0.14 µg min^{-1}. With increasing BC accumulation rate, the underestimation may be several tens of percent. We compiled an algorithm to correct the BC estimation from the typical most commonly used print formats of the MAAP. The algorithm is not dependent on the saving interval of the data and takes the instrument flow rate into account. It is strongly recommended that the algorithm is used for MAAP measurements at high concentrations. We also recommend the MAAP

users to switch to the scientific print format 12 in order to log the reflected signal of the MAAP. In the next step, we will test the different correction schemes for field observations.

ACKNOWLEDGEMENTS

REFERENCES

Arnott, W. P., Hamasha K., Moosmüller H., Sheridan P. J. and Ogren J. A.: Towards Aerosol Light-Absorption Measurements with a 7-Wavelength Aethalometer: Evaluation with a Photoacoustic Instrument and 3-Wavelength Nephelometer, Aerosol. Sci. Tech., 39, 17-29, 2005.

Coen, C. M., Weingartner, E., Apituley, A., Ceburnis, D., Fierz-Schmidhauser, R., Flentje, H., Henzing, J. S., Jennings, S. G., Moerman, M., Petzold, A., Schmid, O. and Baltensperger, U.: Minimizing light absorption measurement artifacts of the Aethalometer: evaluation of five correction algorithms. Atmos. Meas. Tech. 3:457-474, 2010.

Baumgardner, D., Popovicheva, O., Allan, J., Bernardoni, V., Cao, J., Cavalli, F., Cozic, J., Diapouli, E., Eleftheriadis, K., Genberg, P. J., Gonzalez, C., Gysel, M., John, A., Kirchstetter, T. W., Kuhlbusch, T. A. J., Laborde, M., Lack, D., Müller, T., Niessner, R., Petzold, A., Piazzalunga, A., Putaud, J. P., Schwarz, J., Sheridan, P., Subramanian, R., Swietlicki, E., Valli, G., Vecchi, R., and Viana, M.: Soot Reference Materials for instrument calibration and intercomparisons: a workshop summary with recommendations, Atmos. Meas. Tech. Discuss., 5, 2315-2362, doi:10.5194/amtd-5-2315-2012, 2012.

Bond, T. C., Anderson T. L., and Campbell D.: Calibration and intercomparison of filter-based measurements of visible light absorption by aerosols. Aerosol Sci. Tech. 30, 582-600, 1999.

Hansen, A. D. A., Rosen H., and Novakov T.: The aethalometer –an instrument for the real-time measurement of optical absorption by aerosol particles. Sci. Tot. Environ. 36, 191, 1982.

Hyvärinen, A.-P., Lihavainen H., Komppula M., Panwar T. S., Sharma V. P., Hooda R. K., and Viisanen Y.: Aerosol measurements at the Gual Pahari EUCAARI station: preliminary results from in-situ measurements. Atmospheric Chemistry and Physics, 10, 7241-7252, 2010.

Petzold, A. and Schönlinner M.: Multi-Angle Absorption Photometry—A New Method for the Measurement of Aerosol Light Absorption and Atmospheric Black Carbon. J. Aerosol Sci., 35, 421-441, 2004.

Petzold, A., Schloesser M., Sheridan P. J., Arnott W. P., Ogren J. A., and Virkkula A.: Evaluation of Multi-Angle Absorption Photometry for Measuring Aerosol Light Absorption. Aerosol Sci. Tech. 39, 40-51, 2005.

Virkkula, A., Mäkelä T., Hillamo R., Yli-Tuomi T., Hirsikko A., Hämeri K. and Koponen I. K.: A simple procedure for correcting loading effects of aethalometer data, Journal of the Air & Waste Management Association, 57, 1214-1222, 2007.

Weingartner, E., Saathoff H., Schnaiter M., Streit N., Bitnar B. and Baltensperger U.: Absorption of light by soot particles: determination of the absorption coefficient by means of aethalometers, J. Aerosol Sci., 34, 1445–1463, 2003.

SCALING OF XYLEM AND PHLOEM TRANSPORT CAPACITY AND RESOURCE ALLOCATION WITH TREE SIZE

T. HÖLTTÄ[1], M KURPPA[1], T. VESALA[2] and E. NIKINMAA[1]

[1] Department of Forest Sciences, University of Helsinki,, Finland
[2] Department of Physics, University of Helsinki, Helsinki, Finland.

Keywords: ALLOMETRICAL RELATIONS, NITROGEN, PHLOEM, XYLEM

INTRODUCTION

The long distance transport capacity of the xylem has to be high enough to be able to deliver water from the soil to the leaves at the rate that it is transpired. Similarly, the long distance transport capacity of the phloem has to match the production of carbon compounds assimilated by photosynthesis in the leaves. It is well recognized that xylem transport capacity will ultimately limit the photosynthetic production rate of a tree (Tyree & Sperry 1988). Similarly, when the transport rate of photosynthates through the phloem is not able to keep up with the photosynthetic production rate, carbohydrates will start accumulating in the leaves will cause down- regulation of photosynthesis and/or stomatal closure (e.g. Paul and Foyer 2001). At the same time, the transport tissues of the xylem and phloem constitute a large proportion of a trees carbon and nitrogen budget, and presumably even proportionally (compared to leaves and roots) with growing tree size. Thus the within tree scaling of both xylem and phloem tissue has important influence both on the gas exchange between forest canopy and the atmosphere and on the longevity of canopy captured carbon in organic pools. We measured allometric relations and nitrogen content of xylem and phloem tissue at different axial locations from four different boreal tree species. We then scaled these results to find out how total xylem and phloem tissue volume (representative of total carbon content), total nitrogen content, and hydraulic conductance vary with tree size.

METHODS

Eight trees were harvested at surrounding forests from Hyytiälä Forestry Field Station and two from Ruotsinkylä. Four tree species were measured: birch (Betula pendula), aspen (Populus tremula), pine (Pinus sylvestris) and spruce (Picea abies). Total and living bark diameters and xylem diameter were measured at various points along the conducting pathway from the branch tips to the stem bases. From the same samples we estimated also bark nitrogen contents. Estimates of xylem and phloem conduit radiuses and their densities plus the ratio of heartwood radius of the xylem were taken from the literature. In addition, the assumptions of the pipe model (Shinozaki et al. 1969) were used. Stem taper forms were estimated from the data. The values were used to derive equations of xylem and phloem scaling. These were used to estimate carbon and nitrogen requirements in different size trees.

RESULTS

Phloem volume was strongly concentrated towards the apex (Fig 1a), in contrast to the xylem, whose volume is very evenly distributed within a tree (not shown). The cross-sectional areas of the xylem and phloem were equal at branch diameters of 2.5 mm while lower down in the stem xylem cross-sectional area is many-fold.. Nitrogen concentration of both xylem (Fig. 1b) and phloem (Fig. 1c) increased with decreasing stem diameter, i.e. towards the transpiring leaf surfaces. The scaled volume (Fig. 2a) and nitrogen content (Fig. 2b) (expressed per leaf area) of the xylem increased much more sharply in comparison to the phloem with increasing tree size. Phloem conductance per leaf area (Fig. 2c) decreased much more sharply in comparison to the xylem.
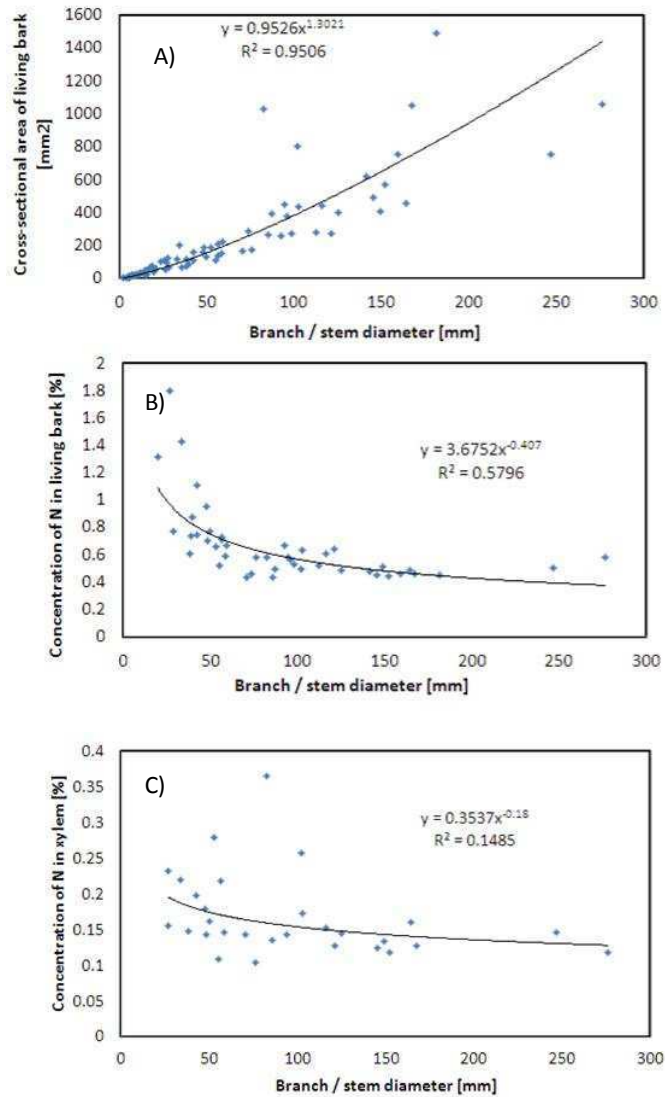
Figure 1. Stem/branch diameter vs phloem cross-sectional area (a), xylem nitrogen content (b), and phloem nitrogen content (c)

DISCUSSION

The study brings insight into discussion on the factors that limit tree water, carbon and nitrogen relations as trees grow in height. Xylem and phloem function can become a limiting factor for tree performance with growing tree size as their conductive capacity is predicted to decline strongly with tree size while they simultaneously consume a strongly growing proportion of the carbon and nitrogen balance of a tree. The empirically derived scaling would suggest that conductive capacity of phloem is strongly declining with tree size. The findings also highlight the question, which has been raised in previous studies (e.g. Thompson & Holbrook 2003), of how large trees are able to deal with phloem transport of photoassimilate products with tree size. The Münch hypothesis alone appears incomplete in explaining this. Our recent analysis (Nikinmaa et al. 2012) suggest that phloem transport capacity may be an important bottle neck also for leaf gas exchange. When compared with theoretical calculations of phloem conductive capacity, the measured scaling would suggest that it seems to be more than adequate in small trees, but declining

sharply as tree size grows. This may reflect the high mass specific nitrogen cost of phloem tissues. Our analysis also demonstrates that also the xylem would become a very large sink of nitrogen without the turnover of sapwood into heartwood (that contain very little nitrogen). Our study highlights the linkages between the carbon, water and nitrogen fluxes and more complicated connections between structural and functional properties of trees and ecosystem material fluxes. There is a clear need to conduct more measurements on the nitrogen content of both the xylem and phloem across a larger range of tree sizes to verify our predictions on nitrogen allocation to within a tree as a function of tree size.
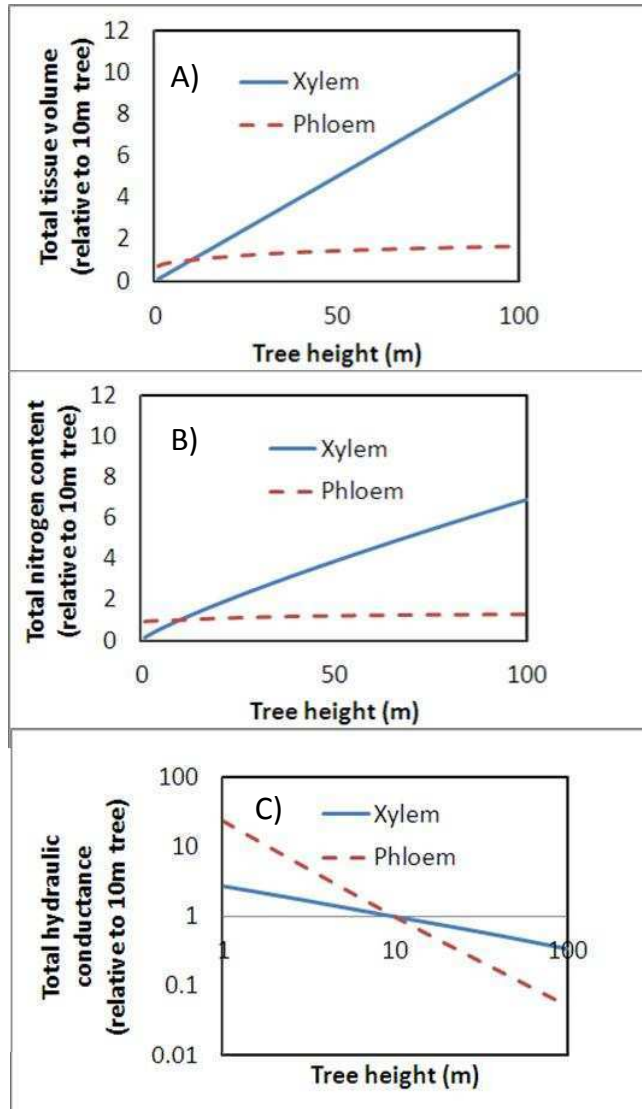
Figure 2. The predictions for the whole tree a) volume of xylem and phloem b) nitrogen content of xylem and phloem and c) hydraulic conductance of xylem and phloem as a function of tree height, and the same per leaf area in (d), (e), and (f).

ACKNOWLEDGEMENTS

REFERENCES

Nikinmaa E., Hölttä T., Hari P., Kolari P., Mäkelä A. Sevanto, S. & Vesala T. 2012. Assimilate transport in phloems sets conditions for leaf gas exchange. *Plant, Cell &Environmmen*. (Accepted).

Paul M.J. and Foyer C.H. (2001) Sink regulation of photosynthesis. *Journal of Experimental Botany* **52**,1383–1400.

Shinozaki K., Yoda K., Hozumi K. and Kira T.A. (1964) Quantitative analysis of plant form--the pipe model theory: I. Basic analysis. *Japanese Journal of Ecolology* **14**, 97-105.

Thompson M.V. and Holbrook N.M. (2003) Application of a singlesolute non-steady-state phloem model to the study of long-distance assimilate transport. *J Theor Biol.* **220**, 419–455.

Tyree M.T. & Sperry J.S. (1988) Do woody plants operate near the point of catastrophic xylem dysfunction caused by dynamic water stress? *Plant Physiology* **88**, 574–580.

ATMOSPHERIC AMINE MEASUREMENTS WITH CI-API-TOF

T. Jokinen[1], M. Sipilä[1], H. Junninen[1], M. Ehn[2], G. Lönn[1], J. Hakala[1], T. Petäjä[1], R. L. Mauldin III[1], M. Kulmala[1] and D.R. Worsnop[1,3]

[1]Department of Physics, University of Helsinki, Helsinki, 00014, Finland

[2] Institute for Energy and Climate Research, Forschungszentrum Jülich, 52425, Germany

[3] Aerodyne Research Inc., Billerica, MA 01821, USA

Keywords: AMINES, CHEMICAL IONIZATION, MASS SPECTROMETRY.

INTRODUCTION

Nucleation of new particles is one of the main sources of cloud condensation nuclei (CCN) in the atmosphere contributing even up to 50% to the global CCN budget (Merikanto et al., 2010). The initial steps of nucleation require the presence of sulphuric acid (SA) (e.g. Sipilä et al. 2010) but additional vapours are needed because SA does not nucleate itself at typical atmospheric conditions. Kirkby et al. (2011) found ammonia and dimethylamine (DMA) from charged clusters formed by ion induced nucleation and concluded that amines are plausible candidates for stabilizing neutral clusters at lower atmospheric conditions. The enhancing effect of amines on new particle formation was observed also in laboratory studies by Berndt et al, (2010). Amines can bind the cluster much more strongly (Kurtén et al., 2008) than ammonia and even ppt levels of amines can be enough to account for atmospheric nucleation rates (Petäjä et al., 2011).

EXPERIMENT

We have performed first ambient amine measurements using an acetone based Chemical Ionization Atmospheric Pressure interface Time-Of-Flight mass spectrometer (CI-APi-TOF). We previously used the exact same inlet for sulphuric acid measurements (Jokinen et al, 2011) but this time we used protonated acetone for the proton transfer reaction and ran the APi-TOF in the positive polarity mode. In this experiment acetone was ionized using a [241]Am bipolar charger to create positively charged acetone ions and clusters. In the proton transfer reaction only compounds that have higher proton affinity than acetone will get charged and detected by the APi-TOF.

RESULTS AND DISCUSSION

The data analysis is still ongoing and these results must be considered preliminary. We identified amine clusters by their exact masses and isotope patterns. So far two signals have been identified to correspond to the same chemical composition and exact mass as common aliphatic amines. These signals are $C_4H_{12}N^+$ (diethyl amine) and $C_6H_{16}N^+$ (triethyl amine). Timeseries of these signals are shown in figure 1. Figure 1 also demonstrates SA concentration (divided by 10 000) and it's seen that during a nucleation event, when SA concentration reaches its maximum, we only see a minimum amine signal. This may indicate that amines are reacting and/or clustering with freshly forming SA molecules or that as amines are emitted from the surface their concentrations are highest when the mixing layer is low during the night.

This setup has a few disadvantages that need to be further developed. First, one of the most interesting amine signals, trimethyl amine (TMA), is overlapped with the acetone isotope signal and it is almost impossible to separate from the spectrum. Second, this instrument consumes high amounts of acetone. The design of the inlet will be improved to consume less chemicals and the reagent ion may have to be changed before quantitative analysis of atmospheric amines can be done using the CI-APi-TOF.
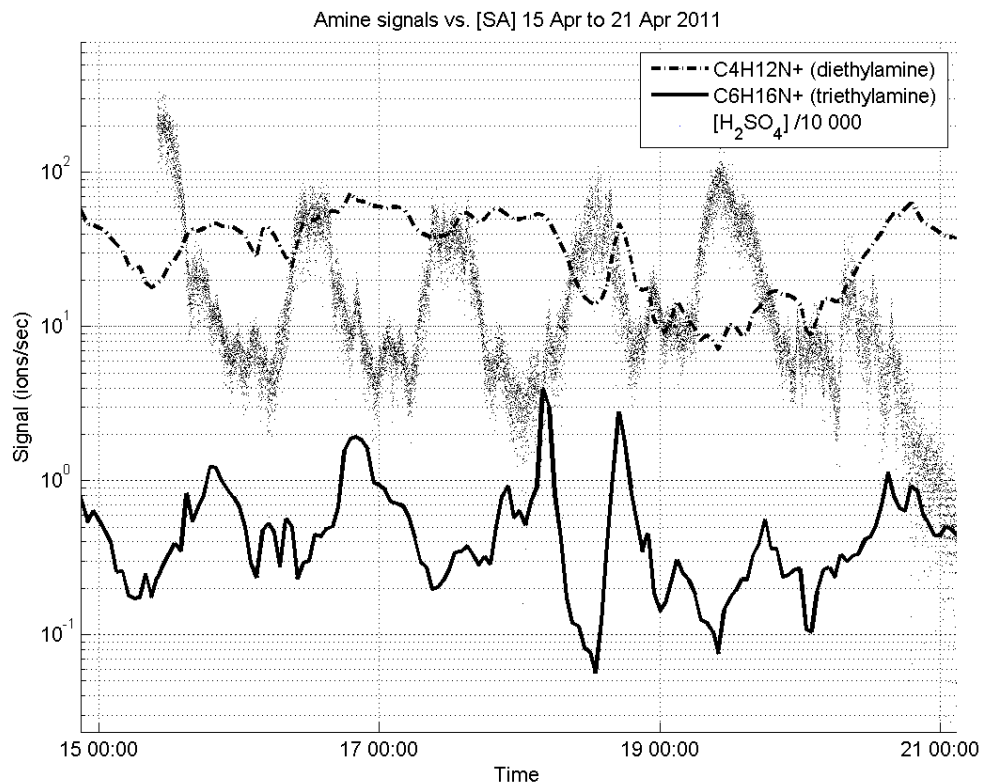
Figure 1. Diethyl and triethyl amine signals (ions/sec) and SA concentration (molec/cm^3) in Hyytiälä over six days of experiment.

REFERENCES

Berndt, T., Stratmann, F., Sipilä, M., Vanhanen, J., Petäjä, T., Mikkilä, J., Grüner, A., Spindler, G., Mauldin III, R.L., Curtius, J., Kulmala, M., and Heintzenberg, J. (2010). Laboratory study on new particle formation from the reaction OH + SO$_2$: influence of experimental conditions, H$_2$O vapour, NH$_3$ and the amine tert-butylamine on the overall process, Atmos. Chem. Phys., 10, 7101-7116.

Merikanto, J., Spracklen, D. V., Pringle, K. J., and Carslaw, K. S. (2010). Effects of boundary layer particle formation on cloud droplet number and changes in cloud albedo from 1850 to 2000, Atmos. Chem. Phys., 10, 695-705.

T. Jokinen, M. Sipilä, H. Junninen, M. Ehn, G. Lönn, J. Hakala, T. Petäjä, R. L. Mauldin III, M. Kulmala, and D. R. Worsnop (2011). Atmospheric sulphuric acid and neutral cluster measurements using CI-APi-TOF, Atmos. Chem. Phys., 12, 4117-4125.

Kirkby, J. et al. (2011). Role of sulphuric acid, ammonia and galactic cosmic rays in atmospheric aerosol nucleation, Nature, 476, 429-433.

Kurtén, T., Loukonen, V., Vehkamäki, H., and Kulmala, M. (2008). Amines are likely to enhance neutral and ion-induced sulfuric acid-water nucleation in the atmosphere more effectively than ammonia. Atmos. Chem. Phys. 8, 4095-4103.

Petäjä,T., Sipilä, M., Paasonen, P., Nieminen, T., Kurtén, T., Ortega, I. K., Stratmann, F., Vehkamäki, H., Berndt, T., and Kulmala, M. (2011). Experimental Observation of Strongly Bound Dimers of Sulfuric Acid: Application to Nucleation in the Atmosphere, Phys. Rev. Lett., 106, 228302.

Sipilä, M. et al. (2010). The role of sulfuric acid in atmospheric nucleation. Science 327, 1243–1246.

STATE-OF-ART TOOLBOX FOR HIGH RESOLUTION DE-CONVOLUTION OF ION-CLUSTER SIGNAL FROM TIME-OF-FLIGHT MASS SPECTROMETRY DATA

HEIKKI JUNNINEN[1], GUSTAF LÖNN[1], MIKAEL EHN[1], SIEGFRIED SCHOBESBERGER[1], TUUKKA PETÄJÄ[1], DOUGLAS R WORSNOP[1,2] AND MARKKU KULMALA[1]

[1]Department of Physics, University of Helsinki, Finland
[2]Aerodyne Research Inc., Billerica, MA, USA

Keywords: TIME-OF-FLIGHT MASS SPECTROMETRY, CHEMICAL COMPOSITION, TOFTOOLS.

INTRODUCTION

Recent developments in atmospheric measurement techniques that include a time-of-flight mass spectrometry (TOFMS) as a mean for separation and detection are increasing in number. Many of the application share the same mass spectrometer that is customizable for a specific needs and has been proven to be robust enough even for a field measurements. The TOFMS has the resolution power of 3000 to 6000 Th/Th, has mass accuracy less than 20 microTh/Th, and is built by Tofwerk AG.

Examples of application that are commercially available or built by research groups are; atmospheric pressure interface TOFMS (APiTOF - for measuring ambient ions, Ehn et al 2010), atmospheric pressure chemical ionization (NO3-CI-APiTOF - for sulphuric acid detection with nitrate ionization Jokinen et al 2011; H-CI-APiTOF – proton transfer for amine and ammonia detection), reduced pressure chemical ionization (Ac-CI-APiTOF – acetic acid ionization for detection of weak acidic molecules; PTR-TOF – proton transfer for VOC detection), aerosol instruments (TD-CIMS, thermal desorption aerosol collection of 10-30nm particles Smith et al 2004, laser-AMS – for laser desorption of 10-30nm particles Laitinen et al 2009, MOVI-CIMS – simultaneous sampling of aerosol and gaseous sample, Yatavelli et al 2010).

Common for the all techniques listed above is the same mass spectrometer and the same data format and thus, the same data analysis requirements and needs. Work presented here provides common tools for initial steps of data analysis of time of flight mass spectrometry data. Each sampling and ionization technique has a specific post-processing and calibrations but the raw data acquired by the mass spectrometer is the same for all.

Toolbox presented here features all the essential steps required for high resolution data analysis, including custom time averaging and filtering of raw data, robust mass calibration, defining instrument parameters, unit mass resolution stick calculations and high resolution peak fitting. The later includes custom peak shape and isotope locking. In the presentation these steps will be explained in detail and real world examples will be used to illustrate the process.

METHODS

The toolbox, tofTools is built in MatLab (newer than R2009b) environment. The first step after averaging raw data to working time resolution is the conversion of measured time of flight to mass-to-charge. The time of flight of ions is converted to mass/charge (m/Q) by an empirical mass-calibration function. The toolbox features three calibration functions; 2-parameter (Eq 1a with p=2), 3-parameter (Eq. 1a with p=1.999-2.001) and 2-parabola function (Eq1b, where p1and p2 are constrained between 1.999 and 2.001)

$$\frac{m}{Q} = \left(\frac{t-b}{a}\right)^p \qquad \text{1a} \qquad\qquad \frac{m}{Q} = \left(\frac{t-b_1}{a_1}\right)^{p_1} + \left(\frac{t-b_2}{a_2}\right)^{p_2} \qquad \text{1b}$$

where m/Q is the mass/charge ratio of the ion, t is the measured ion flight time, and a, b, p, a1, b1, p1, a2, b2 and p2 are instrumental parameters,

Measuring the peak location for calibration or identification purposes includes fitting a certain shape mathematical function to a measured peak. In most simple case the fitted peak is Gaussian, but in almost always the actual peak has a tail in front or back of the peak. Therefore, tofTools provides means to measure the peak shape and use this custom peak shape (Figu1A) for high resolution peak de-convolution (same method is used by DeCarlo et al 2008).
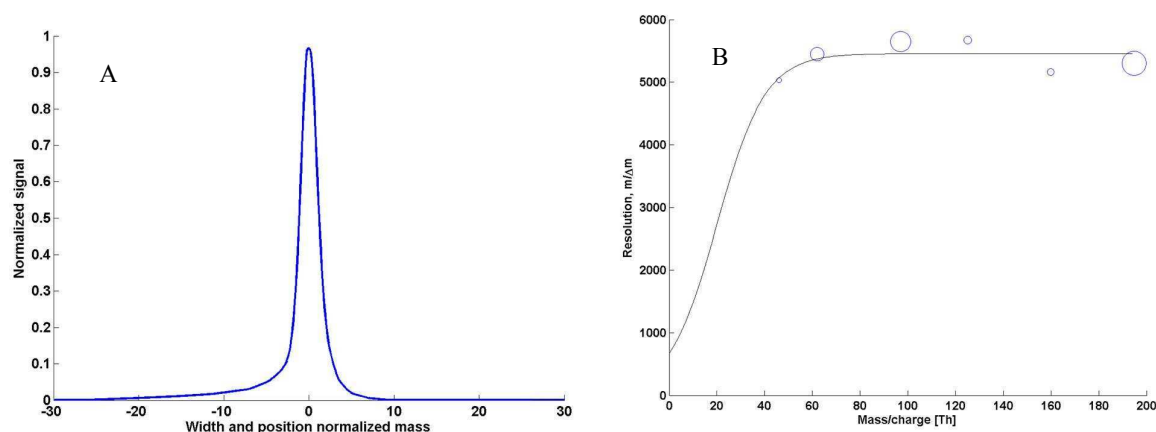
Figure 1. Instrumental parameters A) Custom peak shape, B) Resolution function, open circles are measured resolution of single peaks.

Another instrumental parameter that has to be measured before actual peak de-convolution is resolving power (Eq2a). Nominal resolving power (R_0) is constant throughout the mass range, but actual resolving power (R) has mass dependency that is described by equation 2b. Two parameters in Eq2b are fitted by measuring resolution of single peaks and minimizing root mean square error.

$$R_0 = \frac{\frac{m}{Q}}{FWHM} \qquad \text{2a} \qquad\qquad R = R_0 - \frac{R_0}{1 - \exp\left(\frac{\frac{m}{Q} - \frac{m}{Q_0}}{slp}\right)} \qquad \text{2b}$$

where, R_0 - nominal resolving power, R – actual resolving power, $FWHM$ – full width at half maximum, m/Q_0 and slp – are constants.

When peaks of known composition are used for de-convolution the isotopic abundances have to be taken into account by locking the isotopic intensities to main isotopic peak. So, if a peak is a combination of isotope of a previous peak and an unknown peak, the unknown peaks is effectively fitted to the residual what is remained by subtracting the isotope intensity. In practice all is done iteratively so that all peaks and isotopes are fitted simultaneously. Figure 2 illustrates a situation where intensity of an isotope of a previous peak is explaining almost half of the peak at 341Th.

308
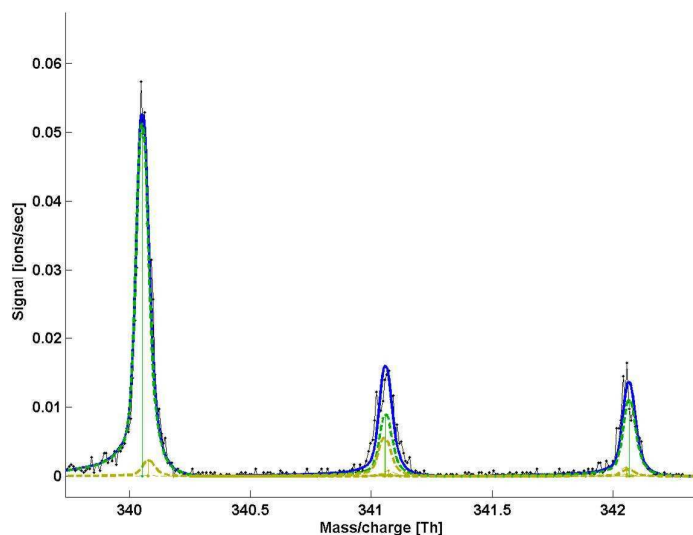
Figure 2. An example of high resolution peak de-convolution where custom shaped peaks of known composition are fitted. Black is measured data, blue is total fitted spectrum, green fitted main isotopic peak and brown minor isotopic peaks that are constrained to the main peak according isotopic abundances.

CONCLUSIONS

A reliable high resolution peak de-convolution has too many degrees of freedom to be executed purely on statistical bases. We present a toolbox, tofTools that featuring tools for constraining the de-convolution by instrumental parameters and natural isotopic abundances. Instrumental parameters have strong effect on final output of the de-convolution and therefore have to be defined carefully. The constraints for reliable de-convolution are custom peak shape, resolution function, isotopic locking for known peaks.

REFERENCES

Junninen, H., M. Ehn, T. Petäjä, L. Luosujärvi, T. Kotiaho, R. Kostiainen, U. Rohner, M. Gonin, K. Fuhrer, M. Kulmala and D.R. Worsnop (2010). A high-resolution mass spectrometer to measure atmospheric ion composition, *Atmos. Meas. Tech.* **3**, 1039–1053.

Ehn, M., Junninen, H., Petäjä, T., Kurtén, T., Kerminen, V.-M., Schobesberger, S., Manninen, H.E., Ortega, I.K., Vehkamäki, H., Kulmala, M. and Worsnop, D.R. (2010) Composition and temporal behavior of ambient ions in the boreal forest. Atmos. Chem. Phys. 10, pp. 8513-8530.

Jokinen, T., Sipila, M., Junninen, H., Ehn, M., Lonn, G., Hakala, J., Petaja, T., Mauldin, R. L., Kulmala, M. and Worsnop, D. R.: Atmospheric sulphuric acid and neutral cluster measurements using CI-APi-TOF, Atmos Chem Phys, 12, 4117-4125, 2012

Smith, J. N., Moore, K. F., Mcmurry, P. H. and Eisele, F. L.: Atmospheric measurements of sub-20 nm diameter particle chemical composition by thermal desorption chemical ionization mass spectrometry, Aerosol Sci Tech, 38, 100-110, 2004

Decarlo, P. F., Kimmel, J. R., Trimborn, A., Northway, M. J., Jayne, J. T., Aiken, A. C., Gonin, M., Fuhrer, K., Horvath, T., Docherty, K. S., Worsnop, D. R. and Jimenez, J. L.: Field-deployable, high-resolution, time-of-flight aerosol mass spectrometer, Anal Chem, 78, 8281-8289, 2006

Yatavelli, R. L. N. and Thornton, J. A.: Particulate Organic Matter Detection Using a Micro-Orifice Volatilization Impactor Coupled to a Chemical Ionization Mass Spectrometer (MOVI-CIMS), Aerosol Sci Tech, 44, 61-74, 2010

Laitinen, T., Hartonen, K., Kulmala, M. and Riekkola, M. L.: Aerosol time-of-flight mass spectrometer for measuring ultrafine aerosol particles, Boreal Environ Res, 14, 539-549, 2009

SEASONAL PATTERN OF PHOTOSYNTHETIC PARAMETERS IN SCOTS PINE

E. JUUROLA[1,2], P. KOLARI[1,2], T. CHAN[1], A. PORCAR-CASTELL[1], and E. NIKINMAA[1]

[1]Department of Forest Sciences, P.O. Box 27, FIN-00014, University of Helsinki, Finland.

[2]Department of Physics, University of Helsinki, Finland.

Keywords: Farquhar -model, Scots pine, photosynthesis.

INTRODUCTION

Conifers in Boreal zone have a clear annual pattern in their photosynthetic activity and they undergo several adjustments during frost-hardening period to maintain their functionality even in harsh winter conditions (e.g. Vogg *et al*., 1998). Observed seasonality of Boreal Scots pine has been reported extensively, and it has been explained by the temperature-driven   seasonal change (Mäkelä *et al.*, 2004; Kolari *et al.*, 2007). However, there is also evidence of the effect of light on the recovery of photosynthesis in spring and cessation in autumn (Porcar-Castell *et al.* 2008a; 2008b). In general, there has to be a correlation between photosynthetic capacity and performance. Having too high capacity necessarily means a trade-off, i.e. the resources could have been better used.

Continuous gas exchange measurements in the field give information on photosynthetic properties in prevailing and momentary environmental conditions, less so on the potential photosynthetic capacity in standard or optimal conditions. Furthermore, not all photosynthetic parameters can be determined from continuous measurements especially when the range of environmental driving factors is narrow (e.g. low light and small diurnal variation of T in autumn). Also, tree-scale effects on instantaneous photosynthetic rate (e.g. water supply, sink control) are embedded in the responses of photosynthetic rate to the environment. Determining the role of different environmental drivers in the seasonality is disturbed by these facts.

Comparison of continuous measurements on intact shoots in the field and campaign measurements of excised shoots in controlled conditions can give more information about the different drivers of seasonality. Tree-scale effects are also eliminated when studying excised shoots, instead there is standard water status and photosynthate transport capacity.

There is ample literature on seasonality of photosynthesis on deciduous tree species and on species growing at temperate climate (e.g. Xu and Baldocchi, 2003; Xu and Griffin, 2006; Ow *et al*. 2010). However the studies on seasonality of conifers acclimated to survive the severe winter conditions in boreal zone are scarce.

We studied the seasonal pattern of photosynthetic parameters for two full years at SMEAR II station in Hyytiälä. Our aim was to determine the seasonality of photosynthetic capacity (parameters) in Scots pine and to interpret field-observed photosynthetic parameters using measurements in controlled conditions. Furthermore, our aim was to reveal what are the most important driving factors for changes in photosynthetic capacity in Scots pine, how does the performance vs. capacity vary and could it be linked to some trade-offs in resource allocation.

METHODS

We conducted monthly measurements of photosynthetic light and CO_2 responses of 47-year-old Scots pine trees (*Pinus sylvestris* L.) at Helsinki University SMEAR II field measurement station in Hyytiälä, (61°51'N, 24°17'E, 181 m a.s.l). Gas exchange measurements were carried out in situ in needles from the upper canopy of Scots pine with a portable gas exchange fluorescence system (Walz GFS-3000,

Heinz Walz, Germany). The measurements were conducted from February 2010 to December 2011. During each characterization, six branches from pre-selected trees were cut and sampled in the laboratory. Five sets of measurements from each branch were executed for photosynthetic activity at varying conditions. Measurements were held at prevailing field temperature and at 18°C. For each temperature setting, a sample was measured by stepwise decrease (beginning at 600 µmol mol $^{-1}$, with a stabilization period between each step), then increase of saturating light (ranging from 0 to 1700 µmol mol $^{-1}$) with a stabilized CO_2 concentration of 380 ppm, and again at 1500ppm. An additional measurement at 18°C at 1300 µmol mol $^{-1}$ PAR (photosynthetically active radiation) was measured at nine CO_2 concentrations, ranging from 25-1200 ppm. Relative humidity and air flow were kept constant for all measurements, at 55% and 650 µmol mol $^{-1}$, respectively. After the sampling, the needles were collected and their projected areas were calculated with image analysis software (ImageAnalyzer mp.14.4.2005). The needles were then measured for their fresh weight, length, and width, and dried at 105°C for 24 hours, and measured for its dried weight.

We applied a well-known biochemical model of photosynthesis (Farquhar et al. 1980) for analysing the state of the photosynthetic machinery. Net CO_2 exchange A is determined as the minimum of light-limited and carbon-limited photosynthetic rates W_j and W_c minus respiration R_d:

$$A = \min\left\{W_c, W_j\right\} - R_d$$

Light-limited photosynthesis

$$W_j = \frac{J(C_i - \Gamma^*)}{4C_i + 8\Gamma^*}$$

Electron transport rate

$$J = \frac{\alpha I + J_{max} - \sqrt{(\alpha I + J_{max})^2 - 4\alpha\theta I J_{max}}}{2\theta}$$

Carbon-limited photosynthesis

$$W_c = \frac{V_{cmax}(C_i - \Gamma^*)}{C_i + K_C(1 + O_2/K_O)}$$

The environmental driving factors in the model are photosynthetically active radiation (I) and CO_2 concentration in the substomatal cavity (C_i). The maximum electron transport rate (J_{max}), maximum carboxylation rate (V_{cmax}) and apparent dark respiration during the day (R_d) were determined from the A-I and A-C_i data set by fitting the biochemical photosynthesis model. K_c, K_o and Γ^* were taken from literature (Aalto 1998 & original references in that paper).

$$A = \frac{\varepsilon I P_{max}}{\varepsilon I + P_{max}} - R_d$$

RESULTS

We found a clear seasonal pattern in photosynthetic parameters. Light saturated rate of electron transport (J_{max}) at standard temperature, reflecting the capacity for the light reactions, peaked quite early during the growing season, in 2010 already in May and in 2011, a bit later, in late June (Fig. 1). During winter J_{max} was clearly inhibited.
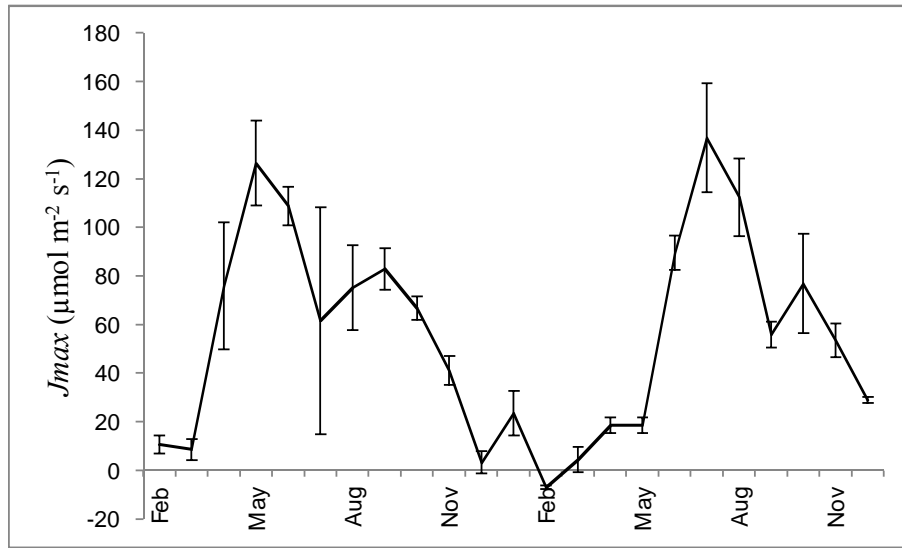
Figure 1. Light saturated rate of electron transport (J_{max}) at standard leaf temperature of 18 °C and photosynthetic active radiation of 1300 μmol mol^{-1}; measured at Hyytiälä, Finland from February 2010 – December 2011. The points are average of 5-6 replicate measurements with standard error of the mean.

Maximum rate of carboxylation capacity (V_{cmax}), measured at the standard temperature, showed a similar, very clear annual patter. In 2010, however, the V_{cmax} stayed pretty stable during the growing season, starting to decrease only in October.
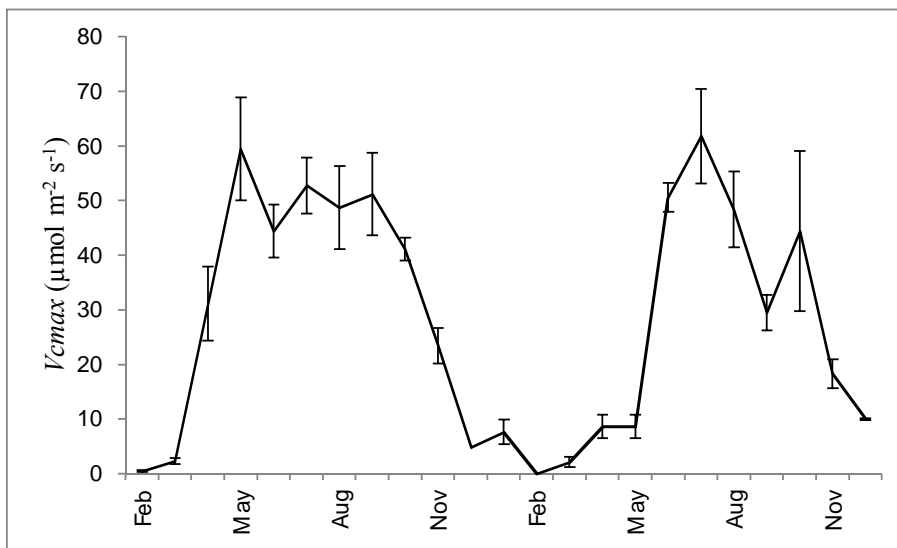
Figure 2. Maximum rate of carboxylation (V_{cmax}) at standard leaf temperature of 18 °C and photosynthetic active radiation of 1300 μmol mol^{-1}; measured at Hyytiälä, Finland from February 2010 – December 2011. The points are average of 5-6 replicate measurements with standard error of the mean.

CONCLUSIONS

This kind of annual pattern in the photosynthetic capacity cannot be revealed in field measurements. Also, in other parameters analyzed a clear annual pattern was observed. There seemed to be a

discrepancy in the recovery of photosynthetic light and dark reactions during spring. However, this was more pronounced in photosynthetic rate and photochemical efficiency than in V_{cmax} and J_{max}.

To our knowledge, this is the most extensive time series following the annual pattern of photosynthetic properties in boreal conditions, where trees undergo strong adjustments to survive the harsh winter. Some open questions that are possible to tackle with the help these results are: how does the ration of C_c/C_i change seasonally? Is the mesophyll conductance larger in winter? These are important factors affecting the analysis of the traditional photosynthetic parameters and thus our understanding on annual cycle.

ACKNOWLEDGEMENTS

REFERENCES

Aalto, T. (1998). Carbon dioxide exchange of Scots pine shoots as estimated by a biochemical model and cuvette field measurements. *Silva Fennica* **32,** 321.

von Caemmerer, S. and J.A. Berry (1980). A biochemical model of photosynthetic CO_2 assimilation in leaves of C_3 species. *Planta* **149,** 78.

Kolari, P., H.K. Lappalainen, H. Hänninen and P. Hari (2007). Relationship between temperature and the seasonal course of photosynthesis in Scots pine at northern timberline and in southern boreal zone. *Tellus B* **59,** 542.

Mäkelä, A., P, Hari, F. Berninger, H. Hänninen and E. Nikinmaa (2004). Acclimation of photosynthetic capacity in Scots pine to the annual cycle of temperature. *Tree Physiology,* **24**, 369.

Ow, L.F., D. Whitehead, A.S. Walcroft and M.H. Turnbull (2010). Seasonal variation in foliar carbon exchange in *Pinus radiata* and *Populus deltoides*: respiration acclimates fully to changes in temperature but photosynthesis does not. *Global Change Biology* **16,** 288.

Porcar-Castell, A., E. Juurola, E. Nikinmaa, F. Berninger, I. Ensminger and P. Hari (2008a). Seasonal acclimation of photosystem II in *Pinus sylvestris*. I. Estimating the rate constants of sustained thermal dissipation and photochemistry. *Tree Physiology* **28,**1475.

Porcar-Castell, A., E. Juurola, I. Ensminger, F. Berninger, P. Hari and E. Nikinmaa (2008b). Seasonal acclimation of photosystem II in *Pinus sylvestris*. II. Studying the effect of light environment through the rate constants of sustained thermal dissipation and photochemistry. *Tree Physiology* **28,** 1483.

Vogg, G., R. Heim, J. Hansen, C. Schäfer and E. Beck (1998). Frost hardening and photosynthetic performance of Scots pine (*Pinus sylvestris* L.) needles. I. Seasonal changes in the photosynthetic apparatus and its function. *Planta* **204,** 193.

Xu, C.Y. and K.L. Griffin (2006). Seasonal variation in the temperature response of leaf respiration in *Quercus rubra*: foliage respiration and leaf properties. *Functional Ecology* **20,** 778.

Xu, L.K. and D.D. Baldocchi (2003). Seasonal trends in photosynthetic parameters and stomatal conductance of blue oak (*Quercus douglasii*) under prolonged summer drought and high temperature. *Tree Physiology* **23,** 865.

ANNUAL PATTERN OF TERPENOID PRODUCTION IN BOREAL SCOTS PINE

E. JUUROLA[1,2], A. VANHATALO[1], J.-P. SCHNITZLER[3], A. GHIRARDO[3], I. ZIMMER[3], J. BÄCK[1,2]

[1]Department of Forest Sciences, P.O. Box 27, FIN-00014, University of Helsinki, Finland.

[2]Department of Physics, University of Helsinki, Finland.

[3]Helmholtz Zentrum München, Research Unit Environmental Simulation, Neuherberg, Germany

Keywords: monoterpenes, *Pinus sylvestris*, seasonality, enzyme activity.

INTRODUCTION

It is now well recognised that the synthesis and emissions of volatile organic compounds (VOCs) play an important role in tree – atmosphere interactions, especially because VOCs participate in aerosol formation which may act as cloud formation nuclei, eventually affecting the climate system. The most important compounds with respect to chemical reactions in atmosphere are terpenoids, i.e. isoprene, mono- and sesquiterpenes. They can be synthesized in both aerial and below-ground plant parts, and large storage pools of some compounds are found in e.g. conifer foliage, trunks and roots. The turnover rates of the terpenoid pools depend both on prevailing synthesis levels, and on factors controlling their evaporation. Their biosynthesis is regulated either by the supply of substrates, by the availability of energy, or by enzyme activities in the metabolic branching points of the biosynthetic pathways (Bohlmann *et al*., 1998; Fischbach *et al*., 2002; Dudareva *et al*., 2004).

The VOC synthesis is linked to photosynthesis through substrate availability. It has been hypothesized that, among other roles, VOC synthesis may act as a protective mechanism during periods when photosynthesis is depressed, especially in winter and spring. However, the direct linkage to active photosynthesis is often hidden behind the emissions from large storage pools.

Large seasonal variation in VOC emission rates and also in the emission blend has often been reported from coniferous trees such as Scots pine (*Pinus sylvestris*). The monoterpene emissions are high in spring, decrease slightly and stabilize during the summer growth period, whereas sesquiterpenes are being emitted only during the summer period (e.g. Tarvainen *et al*., 2005, Hakola *et al*., 2006). Further, tree-specific variation in the emission blend is large, with some trees emitting large amounts of carene, while in other trees this compound is totally missing from emissions (Thoss *et al*., 2007; Bäck *et al*., 2012).

Although the climate change will increase the length of the growing season, increasing winter temperatures may induce several risks to trees. This may have significant consequences on the balance between photosynthesis and VOC emissions as well as physico-chemical properties of leaves in evergreen trees.

We studied the linkage between photosynthesis and synthesis and emissions of terpenoids during the annual cycle of the trees. Here, we report the first results on the annual pattern in enzymatic activities of monoterpene synthases and total terpene content in needles. In addition, we followed also the VOC emission rates and other biochemical properties in needles that will be analysed later.

METHODS

We followed total terpene content and synthase activities in Scots pine needles for 1.5 years from winter 2009 to summer 2010 at SMEARII station in Hyytiälä Forest Field Station. Needle samples were collected from four 47-48 years old trees. A permanent scaffold was used to reach the topmost branches of the trees. 6 needle pairs from three different branches were collected as one pooled sample per tree. Samples from two needle age class (formed during 2008 and 2009) were collected separately. The samples were collected one to three times per month, so that in transient phases during spring the sampling interval was most intensive. In mid-winter there was a break in sample collection. The samples were immediately placed in a dry liquid nitrogen container and stored at -80 °C until analysis.

The analysis of total terpene content and enzyme activities were made in Munich at Helmholtz Zentrum with the method introduced in Fischbach *et al*. (2000) and Fischbach *et al*. (2002). For concentration assay monoterpenes from ground frozen samples were extracted to pentane and the extraction was analyzed with a gas chromatograph-mass spectrometer (GC-MS). For monoterpene synthase activity assay proteins from the samples were extracted and incubated for 60 min with geranyl diphosphate (GPP), a precursor of monoterpenes. The reaction products of the incubation were analyzed with GC-MS.

Here we present the time series of one of the four trees, that are now fully analysed, and one spring date, March 16th 2010 for all four trees.

RESULTS

The four trees differed clearly from each other in both in needle total monoterpene content (Fig 1); the consequent enzyme activities (Fig. 2) as well as in the blend (chemotype) and amount of needle monoterpene emissions (reported in Yassaa *et. al*., 2012). The total monoterpene content and compound blend in needles were rather stable both in 2008 and 2009 needles and no marked annual pattern was observed (Fig. 3). However, the total monoterpene content was always larger in the current year (2009) needles, the difference originating mainly from α-pinene.

Instead, in enzyme activities a clear annual pattern was observed (Fig. 4). Also, the effect of the aging of the needles was evident. Needles showed higher enzymatic activity for the first year, until July in the year following their formation. After this activities were lower for all the trees studied.
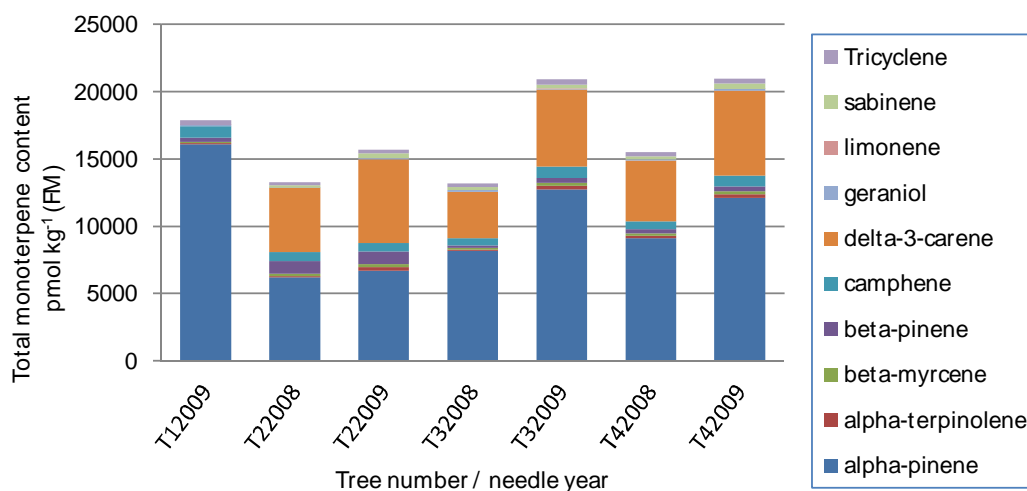
Figure 1. Total terpene content in needles of all four trees studied in March 16th 2010. The values are from one pooled needle sample per tree. Tree 1 suffered from insect damage on previous year needles, and thus samples were taken only from the youngest needle age class (2009).
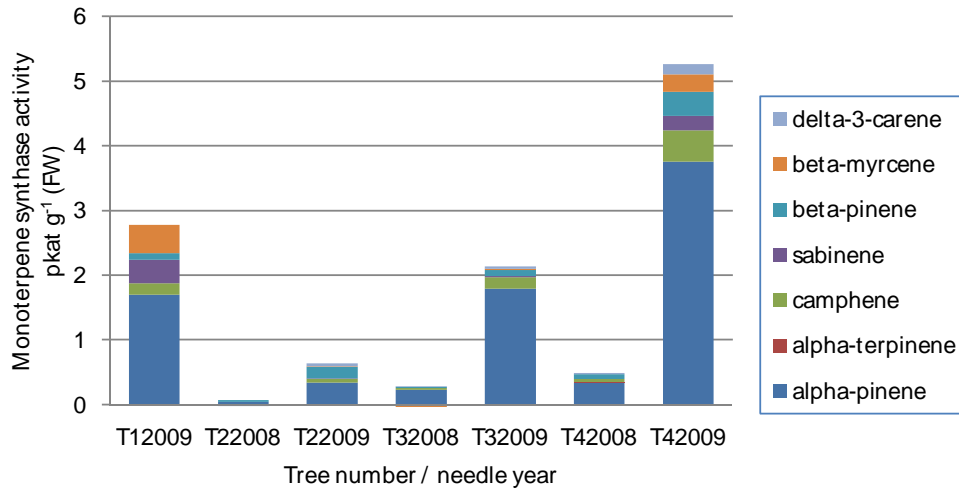
Figure 2. Monoterpene synthase activities in needles in March 16th 2010. The values are from one pooled needle sample per tree. Tree 1 suffered from insect damage on previous year needles, and thus samples were taken only from the youngest needle age class (2009).
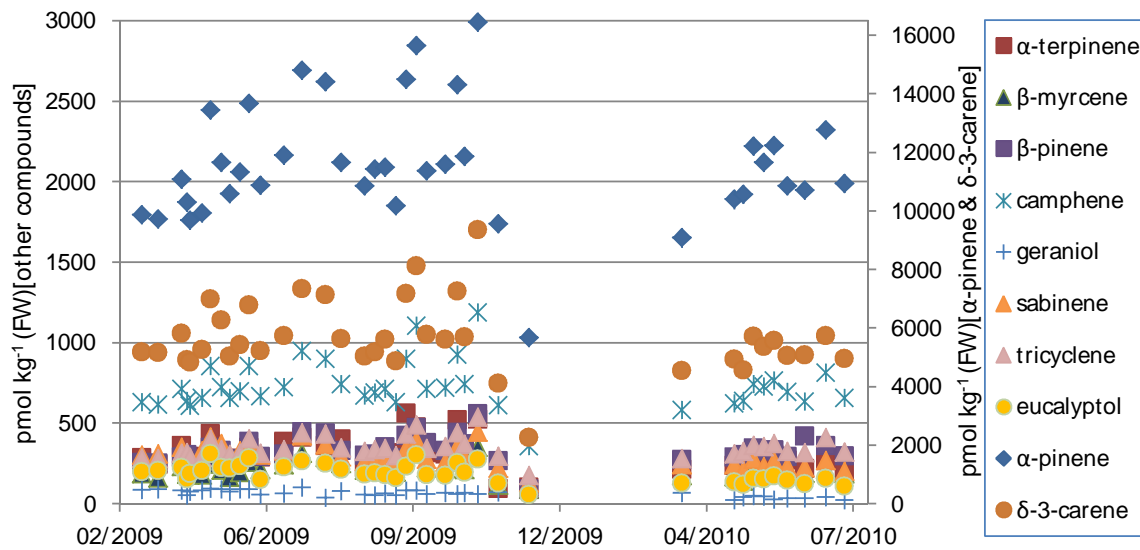
Figure 3. Time series of the total monoterpene content of tree 4. The needles were formed in the summer 2008.
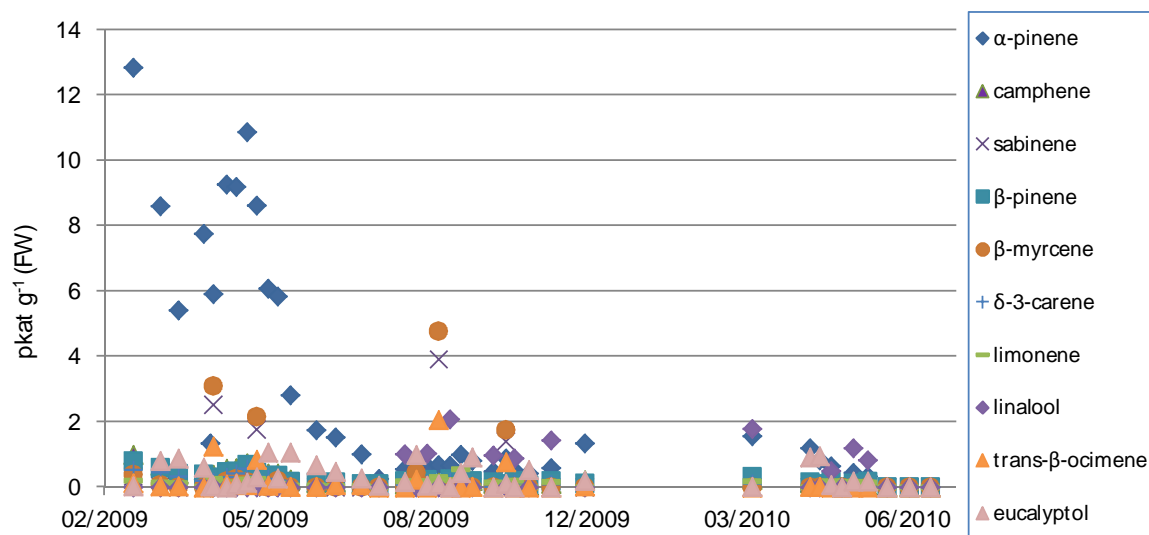
Figure 4. Time series of the monoterpene synthase activities of tree 4. The needles were formed in the summer 2008.

CONCLUSION

The time series is a unique data set providing information on the dynamics and origin of the monoterpene emissions in the field. First, in agreement with resent studies e.g. by Yassaa *et al.* (2012), the four trees differed clearly in their chemotype. Second, there were clear differences in the blend of monoterpenes when the emissions, storage and monoterpene synthase activities are compared. For example, tree 1 was totally lacking δ-3-carene both in concentration and in synthase activity, whereas the other trees had substantial storage of δ-3-carene. In those trees, although there was a substantial storage of δ-3-carene in the needles, there was very little or no enzyme activity. This suggests that any δ-3-carene emissions in mature Scots pine needles would originate from the storages, not from *de novo* synthesis. Third, we observed a clear effect of needle ageing in the monoterpene synthase activities, while the total monoterpene content remained rather stable. High activity e.g. in α-pinene in spring 2009 had no marked effect on the total α-pinene content. These results will be combined with the emission data from the same time period to get the full picture on the relationship between the monoterpene content in the needles, synthesis of monoterpenes and the emission pattern observed in the field.

ACKNOWLEDGEMENTS

REFERENCES

Bäck, J., J. Aalto, M. Henriksson, H. Hakola, Q. He and M. Boy (2012). Chemodiversity of a Scots pine stand and implications for terpene air concentrations. *Biogeosciences* **9,** 689.

Bohlmann, J., Meyer-Gauen G. and R. Croteau (1998). Plant terpenoid synthases: Molecular biology and phylogenetic analysis. *Proc. Natl. Acad. Sci. USA* **95,** 4126.

Dudareva, N., E. Pichersky and J. Gershenzon (2004). Biochemistry of Plant Volatiles. *Plant Physiology* **135,** 1893.

Fischbach, R. J., I. Zimmer, R. Steinbrecher, A. Pfichner and J.-P. Schnitzler (2000). Monoterpene synthase activities in leaves of *Picea abies* (L.) Karst. and *Quercus ilex* L. *Phytochemistry* **54,** 257.

Fischbach, R. J., M. Staudt, I. Zimmer, S. Rambal, and J.-P. Schnitzler (2002). Seasonal pattern of monoterpene synthase activities in leaves of the evergreen tree *Quercus ilex*. *Physiologia Plantarum* **114,** 354.

Hakola, H., V. Tarvainen, J. Bäck, H. Ranta, B. Bonn, J. Rinne and M. Kulmala (2006). Seasonal variation of mono- and sesquiterpene emission rates of Scots pine. *Biogeosciences* **3,** 93.

Tarvainen, V., H. Hakola, H. Hellen, J. Bäck, P. Hari and M. Kulmala (2005). Temperature and light dependence of the VOC emissions of Scots pine. *Atmos. Chem. Phys*. **5,** 6691.

Thoss, V., J. O'Reilly-Wapstra and G.R. Iason (2007). Assessment and Implications of Intraspecific and Phenological Variability in Monoterpenes of Scots Pine (*Pinus sylvestris*) Foliage. *J. Chem. Ecol.* **33,**477.

Yassaa, N., W. Song, J. Lelieveld, A. Vanhatalo, J. Bäck and J. Williams (2012). Diel cycles of isoprenoids in the emissions of Norway spruce, four Scots pine chemotypes, and in Boreal forest ambient air during HUMPPA-COPEC-2010. *Atmos. Chem. Phys.* **12,** 7215.

ANNUAL CO$_2$ FLUXES IN HELSINKI, FINLAND

L. JÄRVI[1], A. NORDBO[1], H. JUNNINEN[2], J. MOILANEN[1], ANU RIIKONEN[3], EERO NIKINMAA[3] and T. VESALA[1]

[1]Division of Atmospheric Sciences, Department of Physics, University of Helsinki, P.O. Box 48, University of Helsinki, Finland
[2]Division of Atmospheric Sciences, Department of Physics, University of Helsinki
[3]Department of Forest Sciences, University of Helsinki

Keywords: CARBON DIOXIDE, EDDY COVARIANCE, TURBULENT FLUX, URBAN.

INTRODUCTION

Urban areas act as hotspots for greenhouse gas emissions, one of the most important one being carbon dioxide (CO$_2$). The measurements of CO$_2$ flux have been carried out at the SMEAR III station (*Station for Measuring Ecosystem Atmosphere Relations*; Järvi *et al.*, 2009a) in Helsinki, Finland, since December 2005. So far these are one of the longest continuous CO$_2$ flux measurements ongoing in urban areas in addition to being the northernmost urban flux site, and therefore provide important information about the seasonal and annual variability of CO$_2$ fluxes. In this study we examined five full years of CO$_2$ flux data from 2006 to 2010.

METHODS

The CO$_2$ exchange is measured using the eddy covariance (EC) technique on top of 31 meter high lattice tower (60°12.17'N, 24°57.671'E, 26 m above sea level) situated at the university campus in Kumpula, Helsinki. Additional meteorological measurements are made on the roof of one of the University of Helsinki buildings at a height of 29 m. According to the prevailing wind direction, the measurement surroundings around the tower can be divided into three areas: built, road and vegetation, each representing the typical surface cover in the area (Järvi *et al.* 2012; Vesala *et al.* 2008). The built area is covered with university campus buildings and Finnish Meteorological Institute (mean height 20 m) in the vicinity of the measurement tower, and a single family house area behind. A heavily trafficked road with 44 000 vehicles per workday passes the road area with the closest distance between the road and the tower being 150 m. There are also large crossroads with several traffic lights located in the area. The area between the road and the tower is covered with deciduous forest and the area behind the road is covered with a combined mix of residential and commercial buildings. In the vegetation area the fraction of vegetation is high as the University Botanical Garden and City Allotment Garden are located in the area.

The EC measurement setup consisted of an ultrasonic anemometer (USA-1, Metek GmbH, Germany) to measure all three wind speed components and sonic temperature, and open- and closed-path infrared gas analyzers (LI-7500 and LI-7000, respectively, LI-COR, Lincoln, Nebraska, USA) to measure CO$_2$ density and mixing ratio, respectively. Data was recorded with 10 Hz and raw data were stored for later post-processing. 30-min fluxes according to the commonly accepted methodologies and quality screening were calculated. Detailed information about the measurements setup and data post-processing can be found in Järvi *et al.* (2012) and Nordbo *et al.* (2012). For the first 18 months, CO$_2$ flux measured with the open-path analyzer was used in the analysis whereas the closed-path analyzer was used for rest of the study period.

In addition to EC measurements, photosynthetically active radiation (PAR) and air temperature were measured at 31 m in the measurement tower using a photodiode sensor (PAR Lite, Kipp&Zonen, Delft, Netherlands) and a platinum resistance thermometer (Pt-100, home-made), respectively, using a one minute time step. A weighting rain gauge (Ott Pluvio, Ott Hydromet GmbH, Kempten, Germany) located on the roof of a nearby building was used to measure precipitation with a four minute time step. Hourly traffic counts were monitored by the city of Helsinki on a road located 4 km from the measurement period. These have been found to correlate well with traffic counts observed on a road next to the measurement site (Järvi *et al.* 2012).

The purpose of the study was to examine the annual CO_2 flux balances and for this, data needed to be gap filled. Three different methods were tested 1) median diurnal cycles (MDC), 2) an artificial neural network where traffic is used as an input variable ($ANN_{Traffic}$), and 3) and an artificial neural network without traffic rate as an input variable ($ANN_{Notraffic}$). In many cities traffic counts are not available and we wanted to test if ANN can be used without this knowledge. A feed-forward multilayer perceptron network was used as an artificial neural network. The network consisted of three layers: input layer, hidden layer and an output layer. Used input variables were traffic, air temperature, PAR, time of day, time of year and wind direction. Time variables were treated as fuzzy variables, whereas for wind direction the surrounding area was divided into nine wind direction sectors (0 - 40°, 40 - 80°,…, 320 - 360°). Each of the sectors was presented as a binary input variable for MLP (WD1, WD2,…,WD9), so that for each half hour only one of these wind direction variables would have a value one. Details of the artificial neural networks can be found from Järvi *et al.* (2012).

CONCLUSIONS

Artificial neural network where traffic is used as an input variable ($ANN_{Traffic}$) was found to give the best performance when compared with an independent dataset (Table 1). None of the three methods were able to simulate extreme CO_2 fluxes, which could be related to unstationary situations in the flux data or unidentified local short-time CO_2 sources. All three methods were used to calculate annual CO_2 emissions and differences between the different methods were found to be small. On average, both neural networks gave the same results 1760 g C m^{-2}, whereas MDC gave slightly lower average emissions of 1740 g C m^{-2} (Table 2). However, larger systematic errors are related to $ANN_{Notraffic}$ and MDC (-9.1 and -20.5 g C m^{-2}, respectively) than $ANN_{Traffic}$ (6 g C m^{-2}). Because of the slightly better performance, $ANN_{Traffic}$ was used in the final gap filling.

	a_1	a_0 (µmol m^{-2} s^{-1})	RMSE (µmol m^{-2} s^{-1})	R^2
$ANN_{Traffic}$	0.64	1.79	3.86	0.40
$ANN_{Notraffic}$	0.51	2.33	4.45	0.26
MCD	0.55	2.16	4.41	0.27

Table 1. The performance of the different gap filling methods for the independent dataset ($N = 11\ 516$). a_1 and a_0 are parameters from a fit $y = a_0 x + a_1$.

	Annual F_c (g C m^{-2})		
	All	Road	Vegetation
$ANN_{Traffic}$	1760 (6)	3500 (167)	870 (-14)
$ANN_{Notraffic}$	1760 (-9.1)	-	-
MCD	1740 (-20.5)	-	-

Table 2. Annual average CO_2 budgets calculated using different gap filling methods.

Annually the source area of the EC measurements was found to be a source for CO_2 with average yearly emissions of 1760 g C m^{-2}. The lowest annual emissions 1580 g C m^{-2} was observed in 2009 when 16% less CO_2 was emitted to the atmosphere than in 2006, when annual emissions of 1880 g C m^{-2} was observed (Fig. 1). The lower annual value in 2009 was mainly a result of lowered emissions in Aug-Sep when the dominant wind direction (occurrence of 70%) was from the area of high fraction of vegetation cover. On other years the occurrence from the same direction was only 50%. Therefore, the lower emissions in 2009 are rather related to synoptic conditions and the complex measurement surrounding than variations in emissions and sinks. The annual emissions are at the lowest end of the values given in other urban studies; particularly similar emissions have been observed in a suburban site in Montreal where half of the surface fraction was also vegetation cover (Bergeron and Strachan, 2011).
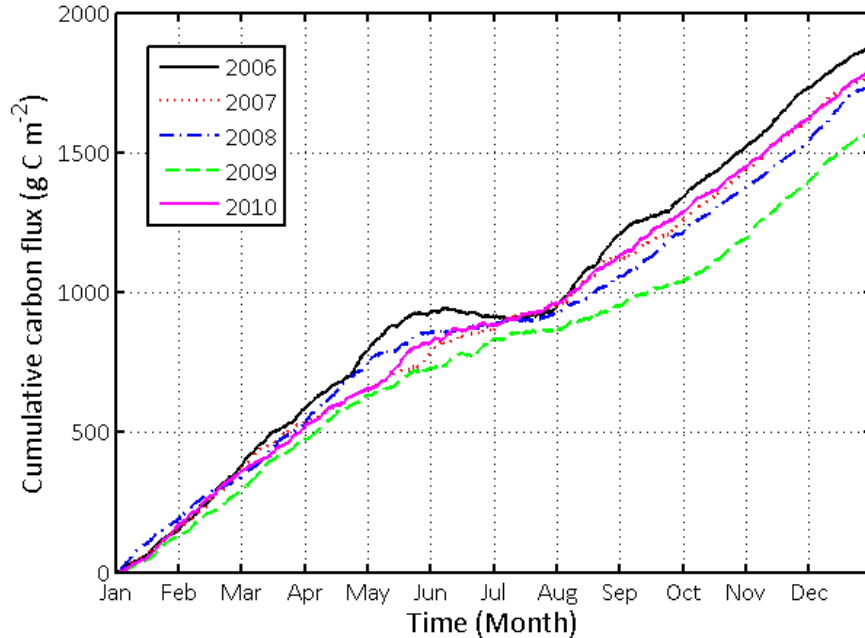
Figure 1. Cumulative carbon dioxide flux separately for different years.

In order to minimize the effect of heterogeneous measurement surrounding to the annual balances, $ANN_{Traffic}$ was used to generate artificial time series for the different wind direction sectors. If we use the meteorological input data and set one of the wind direction inputs to one (equals to an assuming that wind was from that particular sector during the whole measurement time), we can predict F_c for this certain wind direction using measured meteorological conditions. F_c was predicted for sectors WD3 (80 - 120°) and WD6 (200 - 240°) representing the road and vegetation areas, respectively. These sectors are in the middle of the surface areas so they can be assumed to be representative of them. The cumulative sums obtained for these two surface areas differ largely (by 75%) and annually the road area emits on average 3500 (170) g C m^{-2}, whereas from the vegetation area the annual emissions are on average 870 (-14) g C m^{-2}. Despite the high fraction of vegetation in the vegetation area, this direction was annually a net source for CO_2. From soil chamber measurements we estimated that soil respiration accounts 63% of the annual carbon emissions from the area. The rest 37% is a combination of other CO_2 sources in the area minus carbon uptake by vegetation. The high variability of CO_2 emissions from different directions shows that in order to get realistic estimates for CO_2 emissions in a city scale, several measurement points covering different urban surfaces are needed.

We can now examine how the annual emissions calculated for different surface cover areas have varied during the studied year as the effect of heterogeneous measurement site does now affect. In the road area, the predicted emissions decreased 8% between 2006 and 2010. At the same time the traffic rates have increased suggesting the decrease to be caused by improved technology to reduce vehicle CO_2 emissions.

EC measurements together with footprint analysis can be used to calculate emission factors for mixed fleet traffic. Indeed, the emission factors have decreased from 502 g km^{-1} in 2006 to 361 g km^{-1} in 2010 showing that this is likely to be the reason for the decreased annual emissions. Decreasing trend in annual balances is not observed in the vegetation area. On monthly level, the strongest sink of 90 g C m^{-2} is observed in June 2006 whereas the sink is only 60 g C m^{-2} in 2008. The strong sink in summer 2006 was observed in all wind directions and this was caused by the exceptionally warm and sunny weather observed in whole Europe. This shows how long-term measurements of F_c are needed in order to distinguish the effect of exceptional weather condition on carbon fluxes.

ACKNOWLEDGEMENTS

REFERENCES

Järvi, L., A. Nordbo , H. Junninen, A.Riikonen, J. Moilanen, E. Nikinmaa and T. Vesala (2012). Seasonal and annual variation of carbon dioxide surface fluxes in Helsinki, Finland, in 2006-2010. *Atmos. Chem. Phys.* **12**, 8355 - 8396.

Järvi L., H. Hannuniemi, T. Hussein, H. Junninen, P.P. Aalto, R. Hillamo, T. Mäkelä, P. Keronen , E. Siivola, T. Vesala and M. Kulmala (2009a). The urban measurement station SMEAR III: Continuous monitoring of air pollution and surface-atmosphere interactions in Helsinki, Finland, *Boreal Env. Research* 14 (Suppl. A), 86-109.

Nordbo, A., L. Järvi and T. Vesala (2012). Revised eddy covariance flux calculation methodologies – effect on urban energy balance. *Tellus B* 48, 18184, http://dx.doi.org/10.3402/tellusb.v64i0.18184.

Vesala, T., L. Järvi, S. Launiainen, A. Sogachev, Ü. Rannik, I. Mammarella,E. Siivola, P. Keronen, J. Rinne, A. Riikonen and E. Nikinmaa (2008). Surface-atmosphere interactions over complex urban terrain in Helsinki, Finland, *Tellus* **60**B, 188 – 199.

EVENT AND GROWTH RATE ANALYSIS AND MODAL STRUCTURE AT DOME C, ANTARCTICA

E. JÄRVINEN[1], A. VIRKKULA[1,2], T. NIEMINEN[1], P.P. AALTO[1], E. ASMI[2], C. LANCONELLI[3], M. BUSETTO[3], A. LUPI[3], R. SCHIOPPO[4], V. VITALE[3], T. PETÄJÄ[1], V.-M. KERMINEN[1] and M. KULMALA[1]

[1]University of Helsinki, Department of Physics, P.O. Box 64, 00014 Univ. of Helsinki, Finland.

[2]Finnish Meteorological Institute, P.O. Box 503, 00560 Helsinki, Finland.

[3]Institute of Atmospheric Sciences and Climate of the Italian National Research Council (ISAC-CNR), Via Gobetti, 101, 40129 Bologna, Italy.

[4]ENEA-UTA Unitá Tecnica Antartica, via Anguillarese 301, S.Maria di Galliera, Roma, Italy.

INTRODUCTION

Antarctica is an ideal continent for studying the natural aerosol processes. It is clean and there is practically no vegetation, so the oceans surrounding it are the main source of aerosols (e.g., Yu and Luo, 2010; Udisti et al., 2012) even though also some long-range transported pollutant aerosols from other continents have been observed (e.g., Fiebig et al., 2009). Aerosol number concentrations, size distributions and chemical composition have been studied at several stations around Antarctica. There exist long-term records of aerosol number concentrations (Weller et al., 2011) but aerosol number size distributions have been measured mainly during campaigns. The measurements presented here are the first step towards filling in this gap: particle number size distributions have been measured at the Dome C station (75°S, 123°E) in the upper plateau at about 3200 m amsl from December 2007 to November 2009. This study is also the first study to show that nucleation events occur in the central Antarctica and not only in the coastal area.

METHODS

Particle number size distributions in the size range 10-600 nm were measured with a differential mobility particle sizer (DMPS). Simultaneously with the aerosol measurements meteorological data were acquired. The wind data were used here to exclude data contaminated by the station itself. Different modes were identified from the DMPS data with an automatic algorithm (Hussein et al. 2005). This algorithm parameterizes aerosol particle number size distributions with a multi log-normal distribution function.

New particle formation event days were determined following the procedure of Dal Maso et al. (2005). The lower limit of the instrument, 10 nm particle diameter, created a challenge of interpreting both the event starting time and the event duration. We counted as an event day the days when growth occurred as well the days when growth could be followed.

Determining growth rates was not straightforward due to different nature of Antarctic events. Several methods were used depending on the event. For most of the clear and more rapid events (class 1 events, Dal Maso et al. 2005) the method of Hirsikko et al. (2005) was used. In some of the events the growth appeared as a burst, which did not grow in to the larger sizes. These events were called apple events (Vana et al. 2008). For apple events the growth rates were determined by fitting a curve to mode data or to

calculated geometric mean. Besides class 1 events and apple events, two more event classes were used. They were slowly growing events, when the growth could be followed several days and all the growth stayed under 30 nm, and winter events, when the event happened during winter. For these events growth rates were determined by fitting a curve to the calculated geometric mean values that were calculated for the size distribution data.

RESULTS AND DISCUSSION

A clear seasonal cycle was seen from the number concentration data. The concentrations were at their highest in Austral summer, when average number concentration was 324±197 cm-3 and the average volume concentration was 0.103±0.148 μm3 cm-3, and at their lowest in Austral winter, when the average number concentration was 21±37 cm-3 and the average volume concentration was 0.021±0.091 μm3 cm-3. The cycle in particle concentrations is similar to that observed at other Antarctic sites as well (Weller et al. 2011).

Also modal behaviour was studied for the first time at Dome C. When the concentration of particles was low (in winter), most of the time only one mode was present. When new particle formation took place or the air was more polluted, most often there were three modes. Figure 1 shows the relative frequency the modes calculated by the automatic algorithm and how they fit to the nucleation mode, Aitken mode and the accumulation mode size range. The relative frequency was calculated by summing up the occurrence of each of them and dividing this by the total number of modes in the nucleation, Aitken and accumulation size range in each month. The automatic algorithm fitted most of the modes in nucleation mode or Aitken mode range. The modes were mostly found in nucleation mode range from May to August when the total concentrations were the lowest and from Aitken mode size range in all other months. The fitted modes could be found in the accumulation mode size range in December and at the beginning of a year when nucleation was most frequently observed and the particles were also able to grow to bigger sizes. This all indicates that the particles on the high Antarctic East-plateau air are small and are not growing very fast or at all.
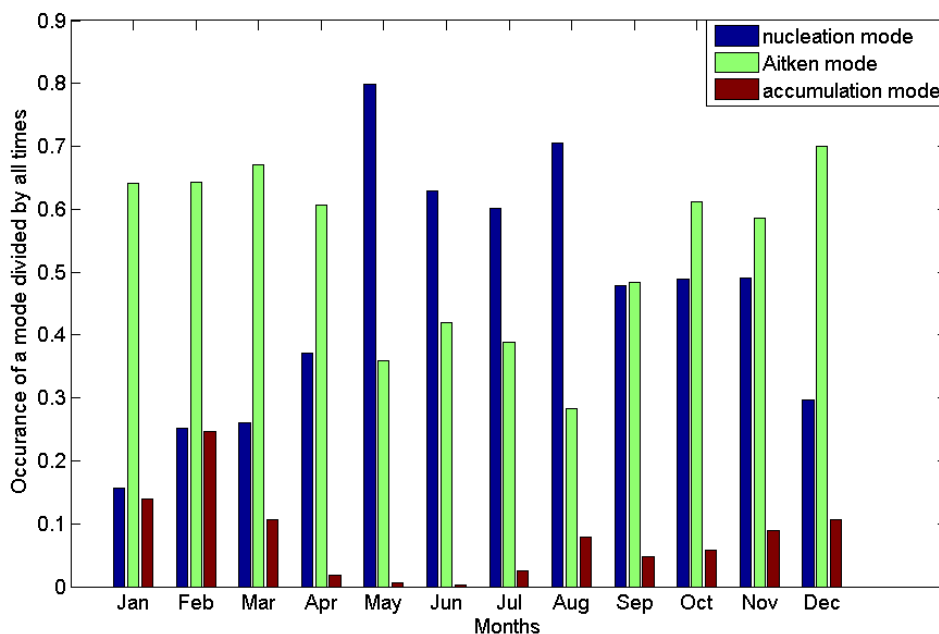
Figure 1: Relative frequency of the occurrence of the three fitted modes in each month. The fitted modes have been looked monthly, how many times modes are fitted to nucleation mode, to Aitken mode or to accumulation mode range.

New particle formation events occurred mainly in the Antarctic summer, peaking in November and February. In February almost 30 % of the days were new particle formation days. Almost 60 new particle formation days were found, from which growth rate for sizes 10-25 nm was able to be determined from 26 days. Most of the new particle formation events were class 1 events, meaning that the particle growth could be followed and the event took part within one day. Continuous growth of the nucleated particles during several hours suggests that the new particle formation occurs in an area that is from tens of kilometers up to hundreds of kilometers wide, depending on the wind conditions. Also apple events took place in February, March, June, September, October and November. Apple events were seen on 0-7 % of the month days. In Antarctica there were additionally two kinds of event types which are not often seen anywhere else. They were slowly growing events and winter-time events (fig. 2). From the slowly growing events, growth rates could be calculated. The growth of the event could be followed up to three days. The winter events happened in Antarctica winter time, when sunlight was not present and particle concentrations were extremely low. Another extraordinary quality of the observed events was that smaller particles seemed to grow more rapidly than larger particles. It has been observed in boreal forest (Yli-Juuti et al. 2011) and in continental European sites that larger particles tend to grow faster.
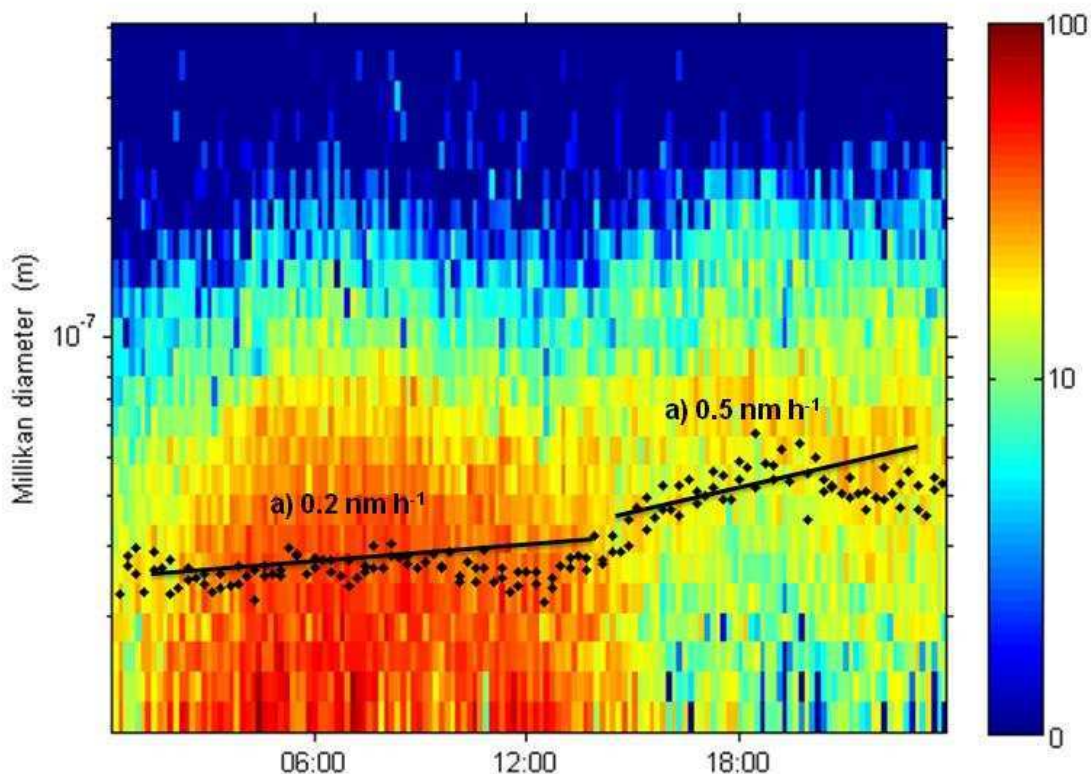
Figure 2. New particle formation event during dark time in Antarctic winter 11th June 2008. Black dots represent the calculated geometric mean diameter and black lines the fitted slopes where growth rate was determined. Slope a) is fitted to the first part of growth and slope b) to the second part. Normally growth is more rapid in the beginning and slows down, but here the case is other way round. Notice the color scale.

Growth rates and statistics were calculated for each event type. Statistics were calculated season-wise, but in some seasons there were only one or two growth rates, when statistics are not reliable. The median growth rate in size class 10-25 nm was 1.25 nm h^{-1} based on 26 events. In the class 1 events the median growth rates were from 2-3 nm h^{-1} in summer and autumn, which is comparable to most of the continental

rural or clean sites (e.g. Kulmala et al 2004; Asmi et al., 2011). In winter the growth rates in clear cases were below 1 nm h^{-1}. From spring the statistics could not be determined, because there were only two class 1 events. The median growth rate in size class from 25 nm to 100 nm was 0.83 nm h^{-1}. Statistics could be calculated for summer, when the median growth rate was 0.78 nm h^{-1}. For other seasons there were not enough days when growth rate could be determined. In the apple-type events, for which growth rates could be to determined, the median growth rate was 0.25 nm h^{-1}. The growth rate from the apple type events could be determined to be larger, if we could localize the event. For slowly growing events the median growth rate was 0.36 nm h^{-1}, which could indicate a low condensation sink. In every event type, the growth rates were larger in spring and summer than in winter and autumn, which is similar to most global observations. In winter there were only three events for which growth rate could be determined.

ACKNOWLEDGEMENTS

REFERENCES

Asmi, E., Kivekäs, N., Kerminen, V.-M., Komppula, M., Hyvärinen, A.-P., Hatakka, J., Viisanen, Y., and Lihavainen, H.: Secondary new particle formation in Northern Finland Pallas site between the years 2000 and 2010, Atmos. Chem. Phys., 11, 12959–12972, 2011.

Dal Maso, M., Kulmala, M., Riipinen, I., Wagner, R., Hussein, T., Aalto, P. P. & Lehtinen, K. E. J.,: Formation and growth of fresh atmospheric aerosols: eight years of aerosol size distribution data from SMEAR II, Hyytiälä, Finland. Boreal Env. Res. 10: 323–336, 2005.

Fiebig, M., Lunder. C.R., Stohl, A. Tracing biomass burning aerosol from South America to Troll Research Station, Antarctica. Geophys. Res. Lett., 36, L14815, 2009.

Hirsikko A., Laakso L, Hõrrak U., Aalto P.P., Kerminen V.-M. & Kulmala M.: Annual and size dependent variation of growth rates and ion concentrations in boreal forest. Boreal Env. Res. 10: 357–369, 2005.

Hussein T., Dal Maso M., Petäjä T., Koponen I., Paatero P., Aalto P., Hämeri K. & Kulmala M.: Evaluation of an automatic algorithm for fitting the particle number size distributions. Boreal Env. Res. 10: 337-355, 2005.

Kulmala M., Vehkamäki H., Petäjä T., Dal Maso M., Lauri A., Kerminen V.-M., Birmili W. and McMurry P. H. Formation and growth rates of ultrafine atmospheric particles: A review of observations. *J. Aerosol Sci.* **35**, 143-176. 2004.

Udisti, R., Dayan, U., Becagli, S., Busetto, M., Frosini, D., Legrand, M., Lucarelli, F., Preunkert, S., Severi, M., Traversi, R., Vitale, V.: Sea spray aerosol in central Antarctica. Present atmospheric behaviour and implications for paleoclimatic reconstructions, Atmos. Environ., 52, 109-120, 2012.

Vana, M., Ehn, M., Petäjä, T., Vuollekoski, H., Aalto, P., De Leeuw, G., Ceburnis, D., O'Dowd, C. D., and Kulmala, M.: Characteristic features of air ions at Mace Head on the west coast of Ireland, Atmos. Res., 90, 278-286, 2008.

Weller, R., Minikin, A., Wagenbach, D. and Dreiling, V.: Characterization of the inter-annual, seasonal, and diurnal variations of condensation particle concentrations at Neumayer, Antarctica, Atmos. Chem. Phys., 11, 13243–13257, 2011.

Yli-Juuti, T., Nieminen, T., Hirsikko, A., Aalto, P. P., Asmi, E., Hõrrak, U., Manninen, H. E., Patokoski, J., Dal Maso, M., Petäjä, T., Rinne, J., Kulmala, M., and Riipinen, I.: Growth rates of nucleation mode particles in Hyytiälä during 2003–2009: variation with particle size, season, data analysis method and ambient conditions, Atmos. Chem. Phys., 11, 12865–12886, 2011.

Yu, F. and Luo, G.: Oceanic dimethyl sulfide emission and new particle formation around the coast of Antarctica: a modeling study of seasonal variations and comparison with measurements, Atmosphere, 1(1), 34–50, 2010.

VOC EMISSIONS FROM HUMAN BREATH – DIFFERENCES BETWEEN TYPE 1 DIABETES PATIENTS AND HEALTHY CONTROL GROUPS

M. K. KAJOS[1], J. PATOKOSKI[1], P. RANTALA[1], A. RUSANEN[1], M. METSÄLÄ[2], O. VAITTINEN[2], T. PETÄJÄ[1] and M. KULMALA

[1]Department of Physics, University of Helsinki, Finland

[2]Department of Chemistry, University of Helsinki, Finland

Keywords: BREATH SAMPLE, PTR-MS, TYPE 1 DIABETES, VOCs

INTRODUCTION

Diabetes (*Diabetes mellitus*) is a group of autoimmune diseases that lead to a high blood sugar content. The reason can be that the body of the patient is not producing enough insulin or that the cells are not responding to the insulin which is produced. Insulin is a hormone which regulates sugar metabolism in the body (THL). Diabetes is one of the fastest growing diseases in the world. About 6% of all the 20-79 year olds in the world have diabetes, 80% of these people live in the developing countries (Tiede, 2006).

Diabetes mellitus is often divided into two types: type 1and type 2. The type 1 diabetes is characterized by a loss of the insulin-producing pancreatic beta cells in the islets of Lagerhans resulting to a partial or a complete lack of insulin. Thus the patients are dependent on insulin injections. Usually the type 1 diabetes occurs before 40 years of age although it can develop at any age. The disease has a tendency to be hereditary but also external factors can have an impact on the outbreak. In spite of abundant research, these environmental factors are still poorly known. One suspected triggering factor are viral infections. (Mustajoki, 2011).

In the type 2 diabetes insulin-regulated sugar transfer from the blood to cells is disturbed and the pancreas has to produce more insulin in order to transfer the sugar. Over time, the insulin producing cells in the pancreas fail to keep up leading to increase in blood sugar levels and eventually diabetes bursts. Approximately every third people have a hereditary tendency to the type 2 diabetes. However, the genetic tendency alone rarely leads to diabetes if a person maintains a healthy lifestyle but the tendency may initiate the diabetes due to obesity and a low physical activity (Mustajoki, 2011).

In Finland more than 200 000 people have diabetes and over 15 000 new diabetes cases are diagnosed every year. Since 1950's, diabetes has become alarmingly more common; a frequency of the type 1 diabetes has gone up four-fold and the type 2 ten-fold. The type 1 diabetes, which 10-15% of the Finnish diabetes patients are ailing, is relatively more common in Finland than anywhere else in the world. The reason for the increase in the abundance of the type 1 diabetes is unknown. (THL and Mustajoki 2011).

Both the type 1 and the type 2 diabetes are associated with serious additional diseases such as cardiovascular, kidney and eye diseases that develop slowly over time (Mustajoki, 2011). Thus, it is important to follow how the state of a diabetes patient wellbeing is evolving. One possible way to do this is to use breath air analysis. The advantage of sampling of the breath air is that it provides a non-invasive way to take samples from the patients (see eg. Lindinger et al., 1998). However the breath air analysis is still a relatively new branch of science and yet a lot of research on this topic needs to be conducted.

The aim of our study is to try to characterize volatile organic compound emissions of type 1 diabetics and further trying to identify possible VOC markers of diabetes and associated illnesses. This study was done as part of FinnDiane (The Finnish Diabetic Neuropathy Study), which is a national study aiming to identify genetic and environmental factors that predispose to diabetes and its additional illnesses. It was initiated to uncover the risk factors and mechanisms of diabetes and associated illnesses concentrating to the type 1 diabetes. FinnDiane is a collective study of the Helsinki University Central Hospital, Folkhälsan Research Center and nationwide hospital and health care network (see FinnDiane webpage for more information).

METHODS

For the analysis, diabetes patients and a control group each provided one single exhalation breath sample. The sample was collected by breathing directly into a sampling bag of 1300 cm^3 coated with aluminium (Wagner Analysen Technik, WT 8004). A second sampling bag of the same type was filled simultaneously with the room air where the subject was staying. The sampling system is described in more detail in Metsälä et al. (2010). Both the diabetics and the control people were required to stay in the room for a minimum of 10 minutes before the sampling and the samples were analyzed on the same day. In this study we analyzed 17 samples from the diabetes patients and 21 samples from the healthy control group.

The samples were analyzed for volative organic compounds with a quadrupole Proton Transfer Reaction Mass Spectrometer (PTR-quad-MS, Ionikon Analytik GmbH). The PTR-MS allows measurements of many VOCs with concentrations in the range of a few ppt. The method is based on chemical ionization of the analytes at a reduced pressure by hydronium (H_3O^+) ions, which perform a non-dissociative proton transfer to the most of the common volatile organic compounds but do not react with any of the main components present in the air. The instrument consists of a discharge ion source to produce the H_3O^+ ions, a drift-tube reactor, where the proton transfer reaction between H_3O^+ and VOCs take place, and a quadrupole mass spectrometer for the detection of reagent and product ions. The PTR-MS measures the mass to charge ratio with one atomic mass unit (Da) resolution and thus the different compounds with a same unit mass cannot be distinguished. (Lindinger *et al.*, 1998; de Gouw and Warneke, 2007). In order to find a suite of possibly interesting compounds which can be measured with the PTR-MS from the samples, the instrument was scanning all mass to charge ratios between 20 and 200 Da.

PRELIMINARY RESULTS

The preliminary results indicate that the breath samples from the type 1 diabetes patients differed in their VOC composition from the control group (Figure 1). A more detailed analysis will be presented in the annual workshop.
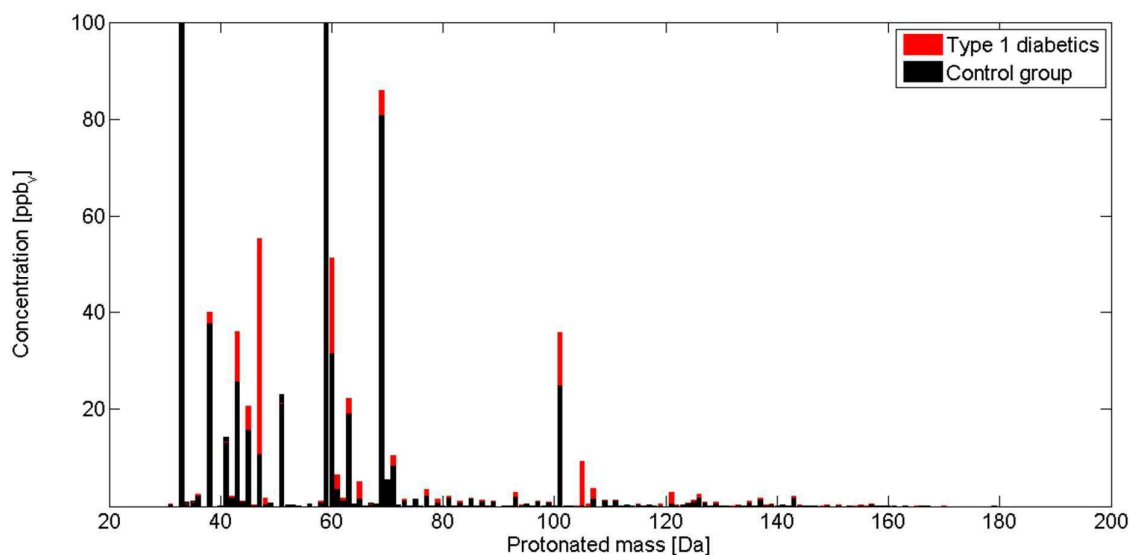
Figure 1: The median spectra of the exhaled VOCs for type 1 diabetes patients (red bars) and healthy control group (black bars). The concentrations of masses 33 Da and 59 Da are an order of magnitude higher than other concentrations thus height of those bars cannot be seen from the figure.

ACKNOWLEDGEMENTS

REFERENCES

de Gouw, J. and C. Warneke (2007). Measurement of volatile organic compounds in the earth's atmosphere using proton-transfer-reaction mass spectrometry. *Mass Spectrometry Reviews*, 26, 223-257.FinnDiane webpage: http://www.finndiane.fi/mission/, cited 20.8.2012, 9:10.

Lindinger, W., A. Hansel and A. Jordan (1998). On-line monitoring of volatile organic compounds at pptv levels by means of Proton-Transfer-Reaction Mass Spectrometry (PTR-MS) Medical applications, food control and environmental research. *Journal of Mass Spectrometry and ion processes*, 173, 191-241

Metsälä, M., F. M Schmidt, M. Skyttä, O. Vaittinen and L. Halonen (2010). Acetylene in breath: background levels and real-time elimination kinetics after smoking, *Journal of Breath Research*, 4

Mustajoki, P (2011). Duodecim Terveyskirjasto: http://www.terveyskirjasto.fi/terveyskirjasto/tk.koti?p_artikkeli=dlk00011, cited 20.8.2012, 9:10.

THL, Finnish National Institute for Health and Welfare (Terveyden ja hyvinvoinnin laitos), http://www.ktl.fi/portal/11825, cited 20.8.2012, 9:10.

Tiede, http://www.tiede.fi/uutiset/2760/diabetes_jo_6_prosentilla_maailman_aikuisista, cited 19.8.2012, 18:00.

BVOC CONCENTRATION MODELING USING ENVIRONMENTAL FACTORS

V.KARSISTO[1], H.JUNNINEN[1], H.K. LAPPALAINEN[1,2], M.DAL MASO[1]

[1]Department of Physics, P. O. Box 64, 00014 University of Helsinki, Finland

[2]Finnish Meteorological Institute, FI-00560, Helsinki, Finland

Keywords: BVOC concentration, statistical modeling

INTRODUCTION

The aim of this research was to find out how to model biogenic volatile organic compound (BVOC) concentrations in boreal forest as good as possible using environmental factors like temperature and mixing height. BVOCs affect to the formation and growth of aerosols and have an effect also to optical properties of the aerosols (Taipale et al.,2008). They react also with hydroxyl and nitrate radicals and affect to ozone formation in the troposphere (Bäck et al., 2012; Rinne et al., 2009). The biggest sources of volatile organic compounds (VOCs) are tropical forests, but also the forests of the northern areas emit those gases (Lappalainen et al., 2009). There are also anthropogenic sources of VOCs, but the biological emissions are ten times bigger than anthropogenic emissions (Taipale et al., 2008).

The estimates of VOC concentrations are needed to model atmospheric chemistry and climate, but it is challenging to model VOC gases because of complex emission and loss processes (Lappalainen et al., 2013). Many different methods have been used in BVOC modeling. Lappalainen et al. (2013) represented three models for methanol, acetaldehyde, acetone, isoprene and monoterpenes, which model day time concentration of those gases in boreal forest. Two of those models are represented later in this study. The two models have temperature related source terms but not loss terms at all.

This study continues the research of Lappalainen et al. (2013) extending the study from the variation of the day time concentrations to diurnal cycle using three hour medians of BVOC concentrations. Tested models contained also loss terms. Different dependence relations between factors are tested and the aim is to find the model which predicts the best BVOC diurnal and seasonal concentrations. In this abstract the results are represented for the monoterpenes and the isoprene, but also methanol and acetone are under the research.

METHODS

Statistical modeling was used in this research, because of BVOC concentrations in the air are dependent on many different factors and theoretical model developing would be very complicated. On the base of the models is theoretical knowledge about the behavior of the concentrations, but the model are optimized with statistical methods. The aim is to find the model which best fits to the measured concentrations.

BVOC and ozone concentration measurements and meteorological observations were conducted in the SMEAR II station of the University of Helsinki. The station is located in Hyytiälä (61°51´N, 24°17´E) about 200 north-west from Helsinki (Taipale et al., 2008). The nearest surroundings of the site were about 50 years old pine dominated forest (Ilvesniemi et al., 2009). 15 kilometers east-west from the station are located two sawmills and the pellet factory, which caused BVOC emissions (Lappalainen et al., 2009). To avoid error times when the wind was from that direction were deleted from BVOC concentration data. The meteorological data was taken from the height of 16.8 meters from the SMEAR II mast. The mixing height was taken from the Hysplit_4 -model (NOAA Air Resources Laboratory). BVOC concentrations

were measured using proton transfer reaction mass spectrometer (PTR-MS, Ionicon Analytik GmbH). The device was calibrated regularly and the data of the same device from the years 2006-2011 was used. For details of the device see Taipale et al., (2008).

The measurements between 12.6.2006-26.6.2009 were conducted from the cottage near the SMEAR II mast, where the air samples came via sampling lines from the tower. The measurement place was changed at the beginning of May 2010 and the time period 28.5.2010-5.7.2011 was measured from the SMEAR II mast. In this study the data from the previous place at the height of 14 m and the data from the mast at the height of 16.8 m were combined.

The modeling is based on local function minimization, where equation, dataset and the first guesses of the parameters are given to the model. BVOC concentrations were given as three hour medians and the other used variables were three hour averages. The model is searching for the parameters, which in the equation gives the results best suitable to the given measurement data. This is done with Nelder mead method. For more details, see Lagarias et al., (1998). RMSE (Root Mean Square Error) was used as the measure of the goodness of the model. It describes difference between the modeled data and the measured data.

The dataset was divided into two parts so that one part contained the one third of the data and the other part the rest of the data. The selection was done so that the both datasets would have equal proportions of data from all seasons. The bigger dataset was used to find the best model and the other to the validation of the results. Bootstrapping method was used in the modeling. The idea of the method is to calculate the error of the estimate calculated from the data using only the same data from which the estimate was calculated. Bootstrap sample is randomly generated from the original data and may contain some data points several times but may not contain some data points at all. Many bootstrap samples are taken and the estimate is calculated from the every of them. The error of the estimate is the standard deviation of the estimates calculated from the samples (Efron and Tibishirani, 1993). In this study the model generated bootstrap samples which were the size of 6 % of the original data and was correspond to the data of four weeks. Usually the number of taken samples was 3000, but to find out small differences between the models the amount of 6000 samples was used. The function minimization method was used to the every sample and the parameters which were got from the each sample were used to calculate the RMSE between the modeled and the measured data. The average of the different samples's RMSE values were used as the measure of the goodness of the models. The smaller the RMSE is the better are the results which model gives.

When executing the model it was noticed that using the RMSE average as the measure of the goodness is problematic for monoterpenes and isoprene, because of the distribution of the RMSE values wasn't Gaussian distribution. Instead it contained several spikes (Figure 1). This was the result of some remarkable big values, because of when those values were deleted the distribution did not have any
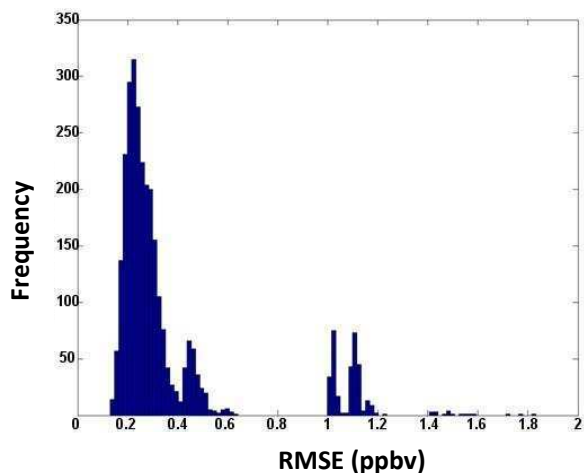
Figure 1. The distribution of modeled and measured monoterpene contentrations's RMSE when using model 1 and 3000 bootstrap samples. The RMSE in on the x-axis and the number of bootstrap samples which gave approximately the same values of RMSE when executing the model are on the y-axis.

additional spikes. Nevertheless, the big values can be real measurements and that's why those were included in the modeling. Instead of the average of all of the RMSE values, the median of the first RMSE distribution spike was used as the measure of the goodness of the model. To make different models comparable the same RMSE border was used to calculate the RMSE medians of the different models. When referring to the RMSE median in this study it means the RMSE median of the first RMSE distribution spike unless otherwise is said. The error of the median of the RMSE was calculated by using the bootstrap method. Bootstrap samples were taken from the each models RMSE data and then the medians were calculated from each sample. Number and size of the samples were the same as the size of the original RMSE data. The standard deviations of the RMSE medians were calculated from the each sample. The error was defined as the standard deviation multiplied by two.

RESULTS

The following results are calculated for monoterpenes. The number of the bootstrap samples was 3000. Models 1 and 2 were the same as the first two models of Lappalainen et al., (2013). Model 1 has the form

$$y = ae^{bT}, \tag{1}$$

where y is the concentration of the BVOC (ppbv), T is the temperature (K) and a and b are fitted parameters. Model 2 has the form

$$y = ae^{bT} + ce^{fS}, \tag{2}$$

where c and f are fitted parameters and S is the state of development, which descripes the photosynthetic efficiency of trees.

The RMSE median of the model 1 was (0.241±0.006) ppbv and the model 2 gave corresbondingly (0.241±0.05) ppbv. Those models were so near each other that it can't be said which one is better. In model 3 the mixing height was added to the equation:

$$y = \frac{e^{aT}}{bmix\_h}, \tag{3}$$

where mix_h is the mixing height (m) and a and b are fitted parameters. Mixing height affects to BVOC concentrations because of it represents the volume of the layer to which the gases can be mixed. The lower the mixing height is the bigger is BVOC concentration. However, the result for this model was weaker than for two previous models. The RMSE median was (0.279±0.007). In Model 4 the mixing height was placed in square root, which improved the results significantly. The RMSE median was (0.220±0.006) ppbv.

In model 5 also the ozone concentration was added to the equation:

$$y = \frac{e^{aT-bO_3}}{c\sqrt{mix\_h}}, \tag{4}$$

where O_3 is the ozone concentration (ppb) and a, b and c are fitted parameters. BVOCs react with ozone in the atmosphere and the ozone concentrations also affects to BVOC emissions from the plants. (Lappalainen et al., 2009; 2012) In model 6 the ozone concentration was also placed in the square root. The model 5 gives for the RMSE median value (0.214±0.006) ppbv and with the model 6 the RMSE median value was (0.208±0.007) ppbv. The models with ozone seem to be better than model 4, but it can't be said for sure since their error ranges overlap each other.

The temperature history has also an effect to the BVOC emissions. In models 7.1-7.4 temperature values from previous averaging periods were tested to the model 6. In the models 8.1-8.4 the same sets of the temperature data was tested to the model 1. The second numbers of model names refer to the averaging

period where the data was taken: 3 h past,6 h past, 9 h past and 12 h past in this order. The results are interesting, since between the models 8.1-8.4 the best results seems to give the model 8.3, where the temperature is taken from the averaging period 9 hour before other measurements. The RMSE median for the model 8.3 was (0.219±0.006) ppbv. Model 8.2, where temperature was from 6 hour previous averaging period, was quite close too since the RMSE median was (0.225±0.007)ppbv. Between the models 6 and 7.1-7.4 the models 6, 7.1 and 7.2 give results so near that it can't be said which one is the best. The median of the RMSE was (0,209±0.006) ppbv for the model 7.1 and (0.218±0.006) ppbv for the model 7.2.

In the models 9.1-9.9 and 10.01-10.14 the mixing height and the ozone concentration in the model 7.1 were tested with different powers. Many of these were so near each other that the results can't be separated with 3000 bootstrap samples, but the power of 0.3 for the mixing height seems to give good results. Different powers for ozone concentration were also tested in model 6 when the power of the mixing height was 0.3. Also one model without ozone were tested with temperature from 3 hour previous averaging period and models where there was PAR instead of ozone in the model were tested. To find out the best of the tested models, every model's RMSE median error range was compared to the smallest RMSE median's error range. The smallest RMSE median was (0.2006±0.0062) ppbv which were got with the model 10.01. It has the form

$$y = \frac{e^{aT_{past\_3} - bO_3^{0.1}}}{c mix\_h^{0.3}}, \tag{5}$$

where T_{past_3} is the temperature from the three hour previous averaging period. All of the models which RMSE median error range overlapped the error range of the model 10.01 and the model 10.01 were executed again with 6000 bootstrap samples. The comparison between the error ranges was conducted again, but there were still many models for which it was not possible to say which one was the best.

To find the best suitable model for monoteprenes of the tested models also the correlation coefficients of the different models were compared. Only the bootstrap samples of the model which gave RMSE value smaller than the border of the first spike were taken in to account when calculating the average of the correlation coefficient between the modelled and the measured data. The error of the correlation coefficient average was calculated using the same method as for the RMSE median. The comparison of the correlation coefficient error ranges gave the result that from the tested models the best results gives the model of the form:

$$y = \frac{e^{aT_{past\_3} - bO_3^{P1}}}{c mix\_h^{0.3}}, \tag{6}$$

where P1 is between 0.05-0.6. For example when the P1 was 0.05 the median of the RMSE was (2.008±0.0019) ppbv and the average of the correlation coefficient was 0.6886±0.0023. However, the model didn't catch big concentration spikes.

To define the parameters this model was executed with the smaller monoterpene dataset, which was put aside in the beginning. 0.05 was used as the P1 value. In figure 2 there are the distributions of the parameter. Only those parameters which are got from bootstrap samples which gave RMSE distributions first spike was taken into account. Geometric mean for parameter a was 0.12 and for parameter b 14. 68.3 % interval of confidence was for a 0.10- 0.15 and for b 10-19. Parameter c was defined separately giving value 0.12 for a and value 14 for b. Geometric mean of c was $9*10^5$ and the 68.3 % interval of confidence was (10-8) $*10^5$. The equation for monoterpenes can be now stated in form

$$y = \frac{e^{0,12\binom{+0,03}{-0,02} T_{past\_3} - 14\binom{+5}{-4} O_3^{0.05}}}{(9\pm1) mix\_h^{0.3}}. \tag{7}$$

In the figure 3 there is a plots of the values predicted with the model and the actual measurements from the time period 10.6 -10.7.2010 and in figure 4 A scatterplot of those datasets
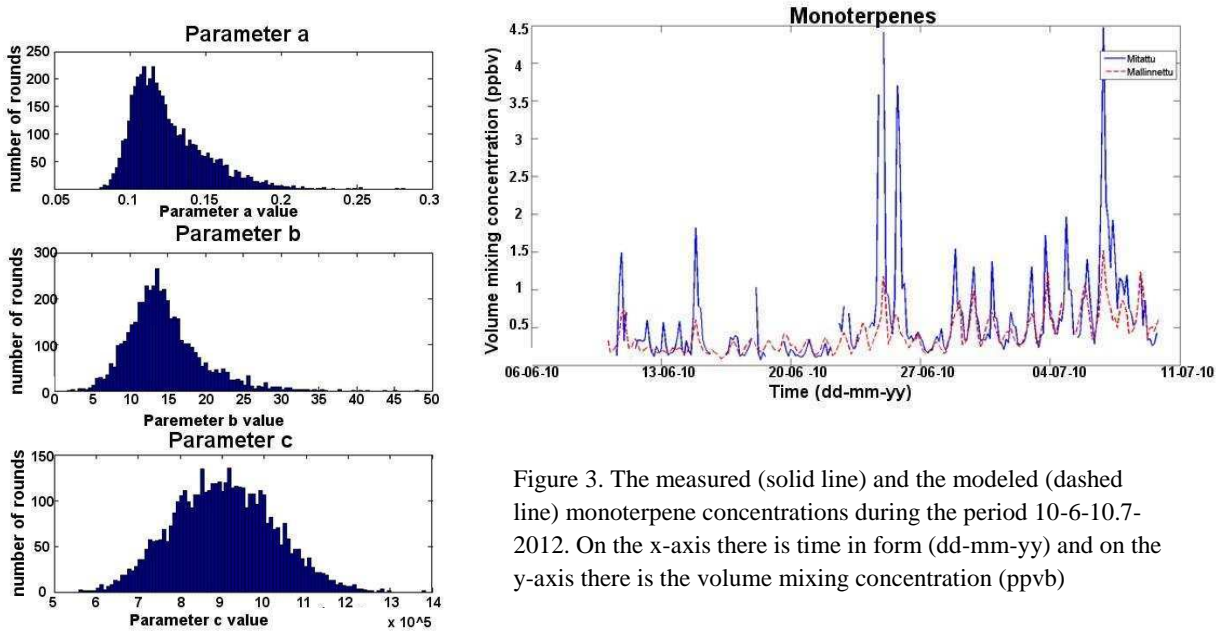
Figure 3. The measured (solid line) and the modeled (dashed line) monoterpene concentrations during the period 10-6-10.7-2012. On the x-axis there is time in form (dd-mm-yy) and on the y-axis there is the volume mixing concentration (ppvb)

Figure 2. The distribution of parameter values for the monoterpene model. a and b were defined together and c was defined separately. Parameter a is in the top, parameter b is in the middle and parameter c is in the bottom. The parameter values are on the x-axis and the number of bootstrap samples on the y-axis.

A   B
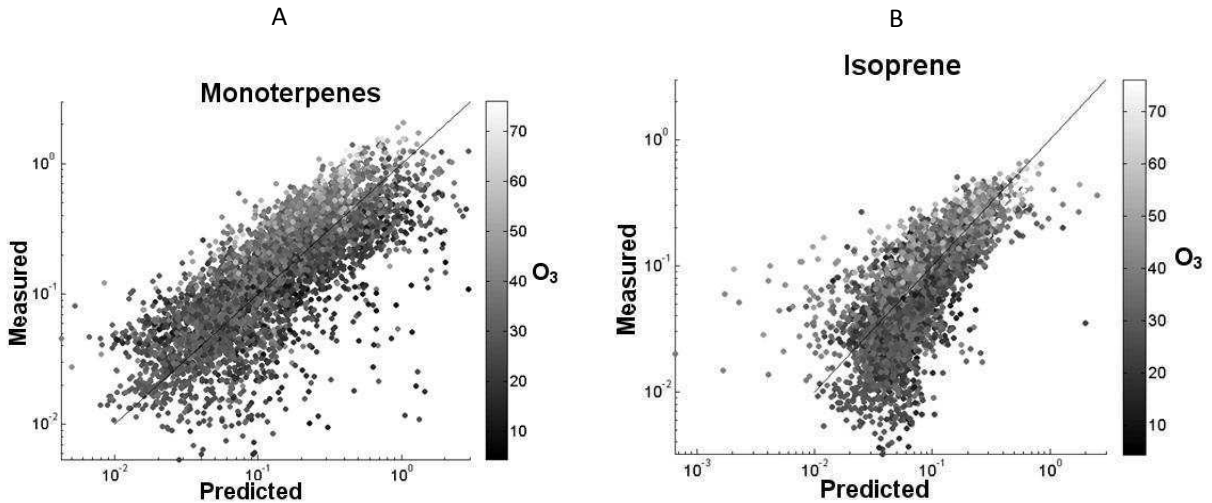
Figure 4. The measured and predicted concentrations of the monoterpene (A) and the isoprene (B). Predicted values are on the x-axis and measured values on the y-axis. The color of the spots refer to the ozone concentration. Linea presents where the spots would be if the models were perfect.

336

The same procedure was done to the isoprene, and the best results of the tested models gave the model:

$$y = \frac{e^{aT - b\sqrt{O_3}}}{cmix\_h^{0.2}}. \tag{8}$$

To get this result both the RMSE comparison and the correlation coefficient comparison were done. With this model and 6000 bootstrap samples the median of the RMSE was (0.0523±0.0003) ppbv and the average of the correlation coefficient was 0.759±0.004. The parameter values was defined in the same way as for monoterpenes, but because of the parameter b distribution had also negative values, the mean value was used instead of geometric mean value for that parameter. The geometric mean of the parameter a was 0.11 and the 68.3 % interval of confidence was 0.09-0.12. The mean value of the parameter b was 0.06 ppb$^{-0,5}$and the standard deviation was 0.07. The geometric mean of the parameter c was $0.260*10^{13}$ and the 68.3 % interval of confidence was $(0.246-0.274)*10^{13}$. In the figure 4 B there is a scatterplot of the values predicted with this model and the actual measurements.

ACKNOWLEDGEMENTS

REFERENCES

Bäck J., J. Aalto, M. Henriksson, H. Hakola, Q. He ja M. Boy (2012). Chemodiversity of a Scots pine stand and implications for terpene air concentrations. Biogeosciences **9**, 689-702.

Efron B., R.J. Tibshirani (1993). An introduction to the bootstrap,Monographs on statistics and applied probability, (Chapman & Hall, New York), 45-47.

Guenther A.B, P.R. Zimmerman, P.C. Harley, R.K. Monson and R. Fall (1993). Isoprene and Monoterpene Emission Rate Variability: Model Evaluations and Sensitivity Analyse. Journal of Geophysical Research **98**, NO. D7, 12 609-12 617.

Ilvesniemi H., J. Levula, R. Ojansuu, P. Kolari, L. Kulmala, J.Pumpanen, S. Launiainen, T. Vesala ja E. Nikinmaa (2009) Long-term measurements of the carbon balance of a boreal Scots pine dominated forest ecosystem. Boreal Environmental Research **14**, 731-753.

Lappalainen H.K., S. Sevanto, J. Bäck, T.M. Ruuskanen, P. Kolari, R. Taipale, J. Rinne, M. Kulmala ja P. Hari (2009). Day-time concentrations of biogenic volatile organic compounds in a boreal forest canopy and their relation to environmental and biological factors. Atmos. Chem. Phys. **9**, 5447-5459.

Lagarias J.C., J. A. Reeds, M. H. Wright, and P. E. Wright (1998). Convergence Properties of the Nelder-Mead Simplex Method in Low Dimensions, SIAM Journal of Optimization **9** No. 1, 112-147

Lappalainen H.K., S. Sevanto, M. Dal Maso, R. Taipale, M.K. Kajos, P. Kolari, J. Bäck (2012). A source orientated approach for estimating day-time concentrations of biogenic volatile organic compounds in a upper layer of a boreal forest canopy. Boreal Environmental Research, in press.

Rinne J., J. Bäck, H. Hakola, (2009). Biogenic volatile organic compound emissions from the Eurasian taiga: current knowledge and future directions. Boreal Environmental Research **14**, 807-826.

Taipale, R., T.M., Ruuskanen, J. Rinne, M.K. Kajos, T. Pohja ja M. Kulmala, 2008: Technical Note: Quantitative long-term measurements of VOC concentrations by PTR-MS – measurement, calibration, and volume mixing ratio calculation methods. Atmos. Chem. Phys. **8**, 6681-6698.

ENERGY EXCHANGE AND DOM PRODUCTION IN BOREAL FOREST IN RELATION TO CRYOSPHERE PROCESSES

V. KASURINEN[1], F. BERNINGER[1], and A., OJALA[2]
[1]University of Helsinki, Department of Forest Sciences,
[2]University of Helsinki, Department of Environmental Sciences

Keywords: DOM, WATER BALANCE, EDDY COVARIANCE, RIVERS

INTRODUCTION

Latest findings suggest that the discharge of boreal rivers has been increasing during the last decades. The driving processes behind the phenomenon are not well understood. Hydrological conditions as well as the interactions between cryosphere and biosphere are suggested to be potential explaining factors, although the regulation and variation of these processes are not fully discovered. The link between energy exchange and cryosphere processes is important, since a large part of the dissolved organic matter (DOM) is exported to aquatic systems during snowmelt and thus depends on winter conditions (both length of the winter and the amount of runoff). This may have implications for the carbon balance of north since dissolved organic matter (DOM) is transported to the ocean by these river systems. Laudon et al. (2004) reported that annual average export of total organic carbon (TOC) ranged from 36 to 76 kg ha^{-1} yr^{-1} and correlated positively with the areal extent of wetlands (R^2=0.72, p=0.03). In total, in the seven studied catchments the four week long spring period contributed from 50% to 68% of the annual TOC export suggesting that the leaching of organic carbon from the catchments strongly depends on the season.

While the global riverine discharge has decreased since 1948, the DOM discharge of the arctic rivers has increased by 12.8% (Dai et al 2012). This suggests that the DOM flux of boreal and Arctic rivers is increasing contrary to the decreasing trend at the global scale and in the Atlantic and Pacific Ocean systems. In addition, the average DOC concentrations in boreal and arctic rivers are naturally high because of the humic-rich soils. Biogeochemical recalcitrance of humic substances and the low mean temperatures suggest that degradation processes in Arctic streams might be ineffective when compared to temperate or tropical systems, and thus a relatively large fraction of organic carbon will be transported to the sea instead of in-stream consumption and production of CO_2 (del Giorgio and Pace 2008). During the in-stream transportation, only the labile fraction or organic carbon can be efficiently utilized, whereas a major fraction (80 ± 16%) of it is considered non-labile in a time scale of days to few weeks (Søndergaard and Middelboe (1995).

METHODS

In order to evaluate the energy exchange between bio- and cryosphere processes we will use the data collected by the present network of eddy covariance sites. The data have mostly been used in CO_2 flux measurements whereas energy exchange analysis has largely been neglected, thus the surface scheme is the main source of uncertainty in regional and global climate models. Furthermore, since a large part of the organic carbon export to aquatic ecosystems occurs during snowmelt, it depends on both the length of the winter and the spring conditions influencing the runoff. We aim at joining and combining the summary models of transpiration from different tower sites. The summary models will be based on the theoretical model of Mäkelä (2004) and they have been applied across a large dataset of eddy covariance sites in the boreal region by Grea et al. (2010). Although these studies were only about carbon, same models can be used for energy exchange.

At the first stage, we will analyse a large data set from the network of circumboreal and Arctic eddy covariance stations. Water flux and other components of the energy balance will be analysed and

explicitly modelled using simplified process based models as in Gea et al. (2010), and extended to energy and water exchange. The energy balance will be transferred into simple hydrological models. Currently we are developing an algorithm for the analysis of eddy covariance data. At the moment the data are covering measurements from Hyytiälä, southern Finland, in 1997-2011.We have also planned to compare modeled water balances between a boreal Scots pine forest and mire.

The energy balance models will address explicitly cryosphere processes like freezing, snow accumulation and melting of the soil and the water bodies. The energy balances will be adjusted for these and DOC export models will be derived from them. There are ample observations that snow-melt is associated with a peak in DOC export. Simulations of energy exchange will be made for a large number of weather stations (as for example the global summary surface of a day database of the WMO) and other selected long-term datasets (like the Soviet Meteorological Station data). Models are derived from the data and then spatialized to larger regions using gridded meteorological products. Although the monthly resolution in data might be problematic for hydrological scaling, we will try to give preference to high temporal resolution climate data (like the ANUSPLIN data of Environment Canada, the ECAC&D data for Europe). We probably have to use other spatial interpolation methods for Russia since reliable interpolated high frequency weather data are not available for Siberia. Simulated water balances for the large number of water sheds will be compared to runoff data from the GRDC database that provides the runoff data for over 2000 rivers in the boreal domain. DOM production and export will be estimated using existing models. We are currently reviewing the COUP model (Jansson 2011) and the DOC3 model (Jutras et al. 2011) as potential DOM models for the application. We are investigating how we can take into account changes in DOM due to changes in environmental pollution (e.g. Monteith et al. 2007). The DOC export will be tested agaÍnts existing datasets like the database from Finnish catchments (from the Finnish Environmental Institute) and from existing (lakes Kuivajärvi and Valkeakotinen) and planned data (Alfredson for rivers) of water chemistry and energy exchange.

Preliminary carbon isotopic results from the streams of Hyytiälä suggest that most of transported DOM derives from riparian zone and consists from relatively fresh carbon. These findings are in accordance with the results from five large arctic rivers were 50% exported DOM during the arctic spring thaw is 1-5 years old, 25% is 6-10 years, and 15% is 11-20 years old (Raymond et al 2007).

CONCLUSIONS / EXPECTED RESULTS

The proposed project aims at improved characterization of changes in boreal and Arctic energy balances and their influences on other biogeochemical processes. The effects of changing cryosphere processes will be quantified and the sensitivity of water export to changes in cryosphere processes, like ice formation, soil freezing and snow accumulation will be explicitly addressed.

While there is evidence for a widespread increase in the runoff of arctic-boreal rivers over the past century, the extent of these changes due to increases in precipitation and changes in evapotranspiration or possibly other changes (as changes in fire regimes) are not known. The proposed project will clarify the role of runoff changes in the framework of boreal-arctic climate change.

The proposed project will further look into the effect of changes in hydrology on aquatic systems by investigating changes in DOC export using models.

ACKNOWLEDGEMENTS

REFERENCES

Dai, M, Yin, Z., Meng, F., Liu, Q., Cai, W-F. (2012) Spatial distribution of riverine DOC inputs to the ocean: an updated global synthesis. Current Opinion in Environmental sustainability 4:170-178. Doi: 10.1016/j.cosust.2012.03.003

Del Giorgio, P. A and M. L. Pace (2008) Relative independence of dissolved organic carbon transport and processing in a large temperate river: The Hudson River as both pipe and reactor.

Gea-Izguierdo, G., Mäkelä, A., Margolis, H., Bergeron, Y, Black, A.T., Dunn, A., Hadley, J., Tha Paw, U., Falk, M., Wharton, S., Monson, R., Hollinger, D.Y., Laurila, T., Aurela, M., McCaughley, H., Bourque, C., Vesala, T., Berninger, F. (2010) Modelling acclimation of photosyhtesis to temperature in evergreen boreal conifer forests. New Phytologist 10.1111/j.14690-8137.2010.03367.x

Jansson, P.E., Karlberg, L. 2011 COUP Manual Coupled heat and mass transfer model for soil-plant-atmosphere systems. Official documentation. Pdf file http://www2.lwr.kth.se/CoupModel/index.html

Jonsson, A., Algesten, G., Bergström, A.-K., Bishop, K., Sobek, S., Tranvik L. J. and M. Jansson (2007) Integrating aquatic carbon fluxes in a boreal catchment carbon budget. Journal of Hydrology 334. 141-150.

Jutras, M-F., Nasr, M., Castonguay, M., Pit, C., Pomeroy, J., Smith, T. P., Zhang, C-f., Richie, C., Meng, F.-R., Clair, T., Arp, P. A. (2011) Dissolved organic carbon concentrations and fluxes in forest catchments and streams: DOC-3 model. Ecological Modeling 222: 2291-2313 doi:10.1016/j.ecolmodel.2011.03.035

Laudon, H., Köhler, S. and Buffman I. (2004) Seasonal TOC transport from seven boreal catchments in northern Sweden. Aquatic Sciences 66:223-230. Doi: 10,1007/s00027-004-0700-2.

Raymond, P. A, McClelland, J. W., Holmes, R. M., Zhulidov, A. V., Mull, K., Peterson, B. J., Striegel, R. G., Aiken R. G. and T. Y. Gurtovaya (2007) Flux and age of dissolved organic carbon exported to the arctic Ocean: A carbon isotopic study of the five largest arctic rivers. Global Biogeochemical cycles 21, GB4011. doi: 10.1029/2007GB002934, 2007

Søndergaard, M and Middelboe, M (1995) A cross-system analysis of labile dissolved organic carbon. Marine ecology progress series 118: 283-294.

ECOSYSTEM AND ATMOSPHERIC MEASUREMENTS IN ICOS-FINLAND

M. KAUKOLEHTO[1], T. LAURILA[2], L. KULMALA[1,3], E. JUUROLA[1,3], S. SORVARI[2], S. HAAPANALA[1], P. KERONEN[1], P. KOLARI[1,3], I. MAMMARELLA[1], M. KOMPPULA[4], K. LEHTINEN[4], J. LEVULA[5], S. JUUTI[4], T. AALTO[2], M. AURELA[2], L. LAAKSO[2], J. HATAKKA[2], A. LOHILA[2], T. MÄKELÄ[2], A. NORDBO[1], Y. VIISANEN[2] and T. VESALA[1]

[1]Department of Physics, PL 48, FIN-00014, University of Helsinki, Finland.

[2]Finnish Meteorological Institute, Helsinki, Finland.

[3]Department of Forest Sciences, University of Helsinki, Finland.

[4]University of Eastern Finland, Kuopio, Finland.

[5]Hyytiälä Forestry Field Station, Finland

BACKGROUND

The global mean temperature has increased and will continue to increase in the 21st century due to the increased concentrations of greenhouse gases such as carbon dioxide (CO_2), methane (CH_4) and nitrous oxide (N_2O) in the atmosphere (IPCC, 2007). Understanding about the driving forces of climate change requires full quantification of the greenhouse gas (GHG) emissions and sinks by long term and high precision observations in the atmosphere as well as on the land and ocean surfaces. There are major research challenges such as 1) what is the regional distribution of GHG fluxes, 2) how does environmental factors and human intervention impact the exchange of GHG, and 3) how will the sources and sinks of GHGes change in future.

Integrated Carbon Observation System (ICOS) has received funding by the EU to develop a strategic plan for constructing a European research infrastructure to provide the long-term atmospheric and flux observations required to understand the present state and predict the future behaviour of the global carbon cycle and GHG emissions as well as to monitor and assess the effectiveness of carbon sequestration in GHG emission reduction activities. The backbones of the ICOS research infrastructure are the national measurement networks for atmospheric, ecosystem and oceanic measurements. ICOS-Finland runs observation networks for atmospheric greenhouse gas concentrations and ecosystem fluxes.

The legal seat and the headquarters of the forthcoming ICOS organisation, European Research Infrastructure Consortium (ERIC), will be located in Finland, with secondary node in France. Finland has a role as a Nordic Hub and mobile laboratory operator of the Atmospheric Thematic Centre (ATC), which is led by France.

METHODS

The ICOS-Finland is established by three national partners: University of Helsinki (UH), Finnish Meteorological Institute (FMI), and University of Eastern Finland (UEF). ICOS-Finland will operate 14 ICOS measurement stations: four Level 1 atmospheric measurement sites; two Level 1 ecosystem measurement sites; one Level 2 ecosystem measurement site; and seven associate ecosystem measurement sites.

The Finnish sites represent the boreal and sub-arctic Eurasian environments with both east-west and south-north transitions in eco-climatic features. The Finnish SMEAR (station for measuring ecosystem-

atmosphere relationships) stations, especially the SMEAR II in Hyytiälä is an intensively equipped world-class observatory operating since 1995. The station is a full ecosystem station and being upgraded to become also an ICOS atmospheric station. Scots pine forest SMEARI in northern Finland and urban SMEARIII in Helsinki are associate ecosystem stations. The full measurement sites, Level 1 sites, will measure the full suite of parameters based on the definition by ICOS preparatory work. The Level 2 sites and associate sites will be measuring a subset of ICOS core parameters (see ICOS Stakeholder's handbook 2012[1]).

Atmosphere measurements include the precise determination of concentrations above the atmospheric surface layer. The spatial concentration variations measured the network of inter-calibrated towers together with the atmospheric transport models enables to estimate sinks and sources on the scale of 100–1000 km. The Pallas-Sodankylä is the most northern of the four Finnish Atmospheric stations. It has been operating since 1994. In the Sodankylä observatory, atmospheric concentration measurements are upgraded and a calibration gas cylinder filling station is running. New atmospheric site is running in the northern Baltic proper area (Utö).
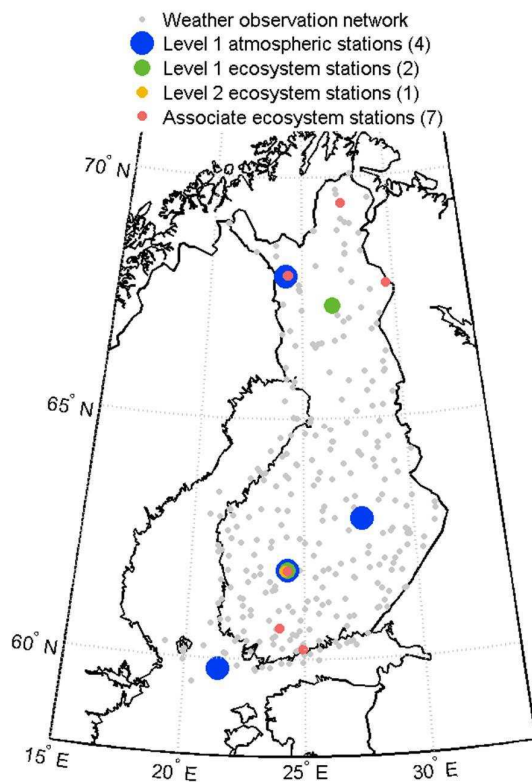
Figure 1: The research stations in Finland that contribute to the European ICOS. Pallas-Sodankylä, SMEARII Hyytiälä, Utö (Baltic Sea) and Puijo-Koli (SMEARIV) are the Finnish atmospheric stations of which Sodankylä and SMEARII Hyytiälä are also Level 1 ecosystem stations. SMEARI Värriö, SMEARIII Helsinki, Kaamanen, Tammela, Siikaneva, Lompolojänkkä (Pallas) and Kenttärova (Pallas) are associate ecosystem stations.

---

[1] http://www.icos-infrastructure.eu/docs/pub/PO_stakebook2012_ref_201205.pdf

In order to interpret the atmospheric concentrations above continents in terms of GHG cycle processes, additional measurements are needed at the surface. Eddy covariance (EC) techniques allow continuous monitoring of CO_2, H_2O and heat fluxes over vegetation canopies. These fluxes, typically calculated on ½ h basis, form the core of ecosystem measurements. The source area (footprint) extends 0.1–1 km away from the measuring tower. The utilization and interpretation of flux measurements require the observations of tens of other variables related to meteorology, hydrology, ecophysiology of vegetation and soil processes. CH_4 and N_2O can be also measured by EC although this is not yes as routine work as it is for CO_2.

Temporal resolution of a day for eddy flux towers is sufficient to capture the variability in terrestrial fluxes driven by changing weather patterns (e.g. the effect of frost or drought on forests) and transform them into operational systems. ICOS network aims at obtaining GHG balances in a high-resolution grid, ultimately in 10 km resolution. However, terrestrial ecosystem carbon fluxes are so heterogeneous and variable that it will be impossible to measure fluxes over all kinds of ecosystems continually over Europe and adjacent regions. The network of micrometeorological flux measurement sites should represent the most typical ecosystems. Other integrating parameters, such as biomass and soil carbon inventories are needed to upscale the flux data, in combination with satellite images.

The GHG balance is achieved by combining atmospheric concentration and ecosystem flux observations in a modelling system. Observations of net ecosystem CO_2 balances, using micrometeorological methods, will constrain simulations of CO_2 uptake by photosynthesis and emission by respiration. In addition, we should have flux observations from ecosystems for which the simulations rely more on observations. Managed peatlands are such an extensive ecosystem type in Finland. Soil respiration measurements by chambers will help in segregating soil processes from net ecosystem balance observations.

The full ecosystem stations, SMEARII in southern Finland and Sodankylä in northern Finland are ready and running. The eddy covariance measurements at SMEARI started in 2012. At some associate ecosystem sites, flux measurements still needs to be developed to reach ICOS standards. New sensors for ancillary measurements, such as radiation and soil temperature probes, are added to most sites. A new automated chamber measurement system has been developed for forest floor vegetation gas exchange (Lohila et al. 2010). At the Pallas node of the Global Atmosphere Watch site, a new flux site representing the arctic mountain vegetation started in autumn 2010.

One key area for FMI flux studies is northern ecosystems with presently ongoing measurements in two forest ecosystems on mineral soils (Sodankylä Scots pine forest and Kenttärova spruce forest) and on two pristine wetlands (northern boreal fen Lompolojänkkä and subarctic fen Kaamanen). Another focus for FMI is the carbon balance of different ecosystems on organic soils. The northern wetlands and one southern boreal fen, Siikaneva, that is run in co-operation with the UH serve as a good reference for the measurements on managed peatlands. Measurements at a nutrient-rich forestry-drained peatland (Lettosuo) were started in 2009.

Two sites of ICOS-Finland, Puijo atmospheric station and Hyytiälä ecosystem station, are currently participating in the ICOS demonstration experiment together with selected set of stations around Europe. The purpose is to evaluate the communications and interactions between the stations and the Thematic Centers, identify the critical aspect and problems in the data acquisition and data flow, evaluate if it is possible to acquire the 95% of the data as specified in the project, and to compare the data processed centrally with the site level version. The demonstration experiment was planned to last till October 2011, but it has been extended to gradually switch into the operative mode of the research infrastructure.

CONCLUSIONS

Climate change is one the most challenging problems that humanity will have to cope with in the coming decades. Long-term coordinated and standardized observations provided by ICOS help reduce the

uncertainties of future projections and predict the future behaviour of the global carbon cycle and GHG emissions. ICOS will monitor and assess the effectiveness of carbon sequestration and GHG emission reduction activities on global atmospheric composition levels, including attribution of natural and anthropogenic sources and sinks by region and sector. ICOS-Finland has the readiness to contribute to the European research infrastructure with four Level 1 atmospheric stations, two Level 1 and one Level 2 ecosystem sites, and seven associate ecosystem stations in the boreal and subarctic environments.

ACKNOWLEDGEMENTS

REFERENCES

IPCC: Contribution of Working Group I to the Fourth Assessment Report of the Intergovernmental Panel on Climate Change. In: Solomon, S., Qin, D., Manning, M., Chen, Z., Marquis, M., Averyt, K., Tignor, M.M.B. and Miller, H.L. (Eds.). (Cambridge University Press, Cambridge, UK and New York, USA.).

Lohila A., K. Minkkinen, P. Ojanen, T. Penttilä, M. Koskinen, M. Kämäräinen, M. Aurela, M. Linkosalmi, J. Hatakka, J.-P. Tuovinen, and T. Laurila. 2010. Lettosuo supporting ecosystem ICOS station: greenhouse gas flux measurements at a forestry-drained peatland. Poster abstract in the First ICOS-Finland Science Workshop, Hyytiälä, November 16-17, 2010.

CLOUD CONDENSATION NUCLEI PRODUCTION RESULTING FROM ATMOSPHERIC NUCLEATION: AN OVERVIEW

V.-M.. KERMINEN[1], M. PARAMONOV[1], T. ANTTILA[2], I. RIIPINEN[3] , C. FOUNTOUKIS[4], H. KORHONEN[5], E. ASMI[2], L. LAAKSO[2], H. LIHAVAINEN[2], E. SWIETLICKI[6], B. SWENNINGSSON[6], A. ASMI[1], S. N. PANDIS[4], M. KULMALA[1] and T. PETÄJÄ[1]

[1] Department of Physics, University of Helsinki, 00014 Helsinki, Finland

[2]Finnish Meteorological Institute, Research and Development, 00101 Helsinki, Finland

[3]Department of Applied Environmental Science & Bert Bolin Centre for Climate Research, Stockholm University, 11418, Stockholm, Sweden

[4]Institute of Chemical Engineering Sciences, Foundation for Research and Technology Hellas (ICEHT/FORTH), Patras, Greece

[5]Finnish Meteorological Institute, Kuopio Unit, 70211, Kuopio, Finland

[6]Division of Nuclear Physics, Lind University, P.O. Box 118, 22100 Lund, Sweden

INTRODUCTION

Understanding the relation between aerosol and their precursor emissions, atmospheric aerosol particle populations, clouds and, eventually, climate is not possible without quantification of the sources responsible for atmospheric cloud condensation nuclei (CCN) (Andreae and Rosenfeld, 2008; Carslaw et al., 2010). One such source is atmospheric nucleation and subsequent growth of nucleated clusters to larger sizes. Here we will synthesize the existing knowledge on CCN production associated with atmospheric nucleation (see Kerminen et al. (2012) for more details).

OBSERVATIONS

Field and laboratory measurements indicate that nucleated particles larger than about 50 and 100 nm of diameter are able to act as CCN in boundary-layer clouds. The initial size of freshly-nucleated particles is about 1–2 nm (e.g. Kulmala et al., 2007), which means that nucleated particles need to undergo significant growth before they can contribute to atmospheric CCN. Based on particle number size distribution measurements, nuclei growth rates have been determined in a large number of lower-troposphere environments (Kulmala and Kerminen, 2008, and references therein). The vast majority of the reported growth rates lie in the range 1–10 nm h^{-1}. Lower values have occasionally been observed in remote continental sites and in the marine boundary layer. Growth rates in excess of 10 nm h^{-1} have been reported in a few polluted environments, as well as in plumes from intense and localized sources of aerosol precursor vapours. We may conclude that the growth of nucleated particle to CCN sizes takes from a few hours up to about three days in the lower troposphere, with longer growth times more typical for remote locations.

During the last decade or so, regional nucleation events producing particles of several tens of nm in diameter have been found to be frequent in a large variety of lower-troposphere environments, including forested areas, many other remote continental regions, urban areas, and heavily-polluted environments (see Kulmala and Kerminen, 2008). Similar events have also been observed in several high-altitude sites in the mountains (e.g. Boulon et al., 2010), whereas in the marine boundary layer they appear to be rare (e.g. O'Dowd et al., 2010).

While regional nucleation events are clear indicators of atmospheric CCN production initiated by nucleation, relatively few experimental studies have attempted to quantify the strength of this source. Lihavainen et al. (2003) and later Asmi et al. (2011) analysed a large number of nucleation events measured at a remote site in Northern Finland, and found that number concentrations of 50, 80 and 100 nm particles were enhanced, on average, by the factors of 2.6, 1.7 and 1.5, respectively, from the beginning of a nucleation event to the end of the event. Slightly smaller CCN enhancement factors were reported by Sihto et al. (2011) for the SMEAR II station in Southern Finland. Laaksonen et al. (2005) found that nucleation significantly enhances the concentrations of CCN-size particles at a highly-polluted region of Po Valley, Italy, despite strong primary particle emissions there. Yue et al. (2011) reported average CCN enhancement factors between about 1.5 and 2.5 in Beijing, China, with larger values corresponding to nucleation events with higher particle growth rates. Kuang et al. (2009) derived an overall-average CCN enhancement factor of 3.8 for nucleation events recorded at three different continental sites, of which two (Boulder, CO and Atlanta, GA) were located in the USA and one in Mexico (Tecamac).

Only few investigators have linked nucleation measurements directly to corresponding CCN or cloud droplet number concentration measurements. Kuwata et al. (2008) measured aerosol number size distributions and CCN concentrations at four supersaturations at Jeju Island, Korea. They reported a few events where nucleation was followed by clear increases in CCN number concentrations after a few hours from the beginning of the event. Similar observations were made by Creamean et al. (2011) at a remote rural mountain site in California, USA, by Levin et al. (2012) at a forested site in Colorado, USA, and by Pierce et al. (2012) in a forested mountain valley in western Canada. Wiedensohler et al. (2009) and Yue et al. (2011) found rapid growth of nucleated particles to CCN in a highly-polluted region in Beijing, China, and high CCN concentrations resulting from nucleation. Sihto et al. (2011) analyzed a full year of simultaneous aerosol number size distribution and CCN concentration measurements at a forested site (SMEAR II station in Hyytiälä) in Southern Finland. They found that nucleation enhanced CCN number concentration by 70 to 110%, depending on the supersaturation level. Usually, CCN concentrations at highest supersaturations increased after a few hours from the beginning of the nucleation event, whereas CCN concentrations measured at low supersaturations tended to reach their maximum during the following night or next day (Sihto et al., 2011). Kerminen et al. (2005) observed that nucleated particles not only grew to CCN sizes, but also participated in cloud droplet formation at a remote continental site in Northern Finland.

MODEL RESULTS

The first model simulations on atmospheric CCN formation were zero-dimensional box model simulations that concentrated on the marine boundary layer. After realizing the importance of free-troposphere nucleation for marine CCN production and the high frequency of new particle formation in continental boundary layers, a clear need for large-scale model simulations emerged. Pioneering studies in this regard were those by Lucas and Arimoto (2006) and Spracklen et al. (2006), who demonstrated nucleation to be capable of enhancing aerosol number concentrations throughout the global troposphere. The first global model study on CCN production due to atmospheric nucleation was that by Spracklen et al. (2008), after which several other model investigations relying on different nucleation mechanisms were conducted. Some of these studies focused solely on CCN number concentrations in the global atmosphere (Spracklen et al., 2008; Merikanto et al., 2009, Pierce and Adams, 2009; Yu and Luo, 2009; Luo and Yu, 2011a), while others examined also changes in cloud droplet number concentrations and resulting climatic variables (Makkonen et al., 2009; Wang and Penner, 2009; Kazil et al., 2010; Merikanto et al., 2010). Regional-scale simulations of the contribution of nucleation to CCN number concentrations are scarce and cover mainly specific regions in Europe (Sotiropoulous et al., 2006; Fountoukis et al., 2012) and United States (Jung et al., 2010; Luo and Yu, 2011b).

Although the models simulating the production of CCN in the global atmosphere differ considerably in terms of how nucleation and other aerosol processes are treated, the results from the conducted model investigations share a number of common features. First, nucleation taking place in the upper free troposphere appears to be a major source of CCN in the global troposphere. After transport and growth, these particles dominate frequently CCN number concentrations in the remote marine boundary layer and contribute to CCN present in continental background areas. Second, boundary-layer nucleation enhances CCN number concentrations almost everywhere over the continents. The resulting enhancement, while rather small over areas with substantial primary particle emissions, may be several-fold in environments such as the summertime boreal forest. Third, organic compounds play a crucial role in the CCN production in continental boundary layers and, possibly, elsewhere due to their ability to grow nucleated particles effectively into larger sizes. Finally, the contribution of nucleation to the total CCN budget in the troposphere is definitely non-negligible, and it might be even larger than 50% at water vapor supersaturations approaching 1%.

Model simulations have pointed out that atmospheric CCN production due to nucleation depends in a non-linear way on the nucleation rate, subsequent growth of nucleated particles to larger sizes, and the presence of primary aerosol particles. Both nucleation and growth are very challenging processes to be simulated in large-scale modelling frameworks. In case of nucleation, this is due to our incomplete understanding of the atmospheric nucleation mechanisms and due to nucleation taking place in sub-grid scale plumes from sources such as major SO_2 emitters. In the case of nuclei growth, the main challenge is the proper treatment of the chemistry and gas-particle partitioning of organic compounds. Primary particles complicate the issue further by acting as a sink for low-volatile vapours and freshly-nucleated particles, and by providing additional CCN as a result of their aging during atmospheric transportation.

The effect of nucleation and resulting CCN production on atmospheric radiation fluxes and climate remain poorly constrained. Kazil et al. (2010) estimated that the total contribution of nucleation (including direct, semidirect and indirect effects) to the present-day net short-wave radiation at the top of the atmosphere (TOASW) is about 1% (-2.55 W m^{-2}). This is a significant contribution, and it is likely to have changed since the preindustrial times because emissions of gas-phase compounds responsible for nucleation and subsequent growth, as well as of primary particles acting as a sink for nucleated particles, have changed due to e.g. industrialization and land use changes. It is, therefore, probable that the nucleation process contributes to current aerosol radiative forcing (present-day aerosol effect compared to preindustrial time), and hence to climate change. This is supported by Makkonen et al. (2012a) who found the predicted aerosol forcing to increase from -1.03 to -1.61 W m^{-2} when nucleation was included in their model. Fatima et al. (2011) tested two ion-nucleation mechanisms and found a total indirect aerosol forcing of -1.42 and -1.54 W m^{-2}, while Wang and Penner (2009) obtained first indirect forcing estimates ranging from -1.22 to -2.03 W m^{-2} depending on their treatment of free tropospheric and boundary layer nucleation. The latter study also found that the effect of nucleation on the radiative forcing is highly sensitive to the relative change of primary particle and nucleation precursor emissions from the preindustrial times. In addition, Makkonen et al. (2012b) found that the simulated effect of nucleation on aerosol forcing depends also on the model used for biogenic volatile organic compound (BVOC) emissions. They estimated the shortwave cloud forcing to vary between -1.41 and -1.75 W m^{-2} depending on the nucleation mechanism and used BVOC emission model.

CONCLUSIONS

Based on available field measurements and large-scale model simulations, we conclude that cloud condensation nuclei (CCN) production associated with atmospheric nucleation is both frequent and widespread phenomenon in many types of continental boundary layers. The same is probably true over a large fraction of the free troposphere as well, but confirming this matter awaits further support from atmospheric measurements. The contribution of nucleation to the global CCN budget spans a relatively large uncertainty range, which, together with our poor understanding of aerosol–cloud interactions, results

in major uncertainties in the radiative forcing by atmospheric aerosols. In order to better quantify the role of atmospheric nucleation in CCN formation and Earth System behavior, more information is needed on i) the factors controlling atmospheric CCN production and ii) the properties of both primary and secondary CCN and their interconnections. In future investigations, more emphasis should be put on combining field measurements with regional and large-scale model studies.

ACKNOWLEDGEMENTS

REFERENCES

Andreae M. O. and Rosenfeld, D. (2008) Aerosol-cloud-precipitation interactions. Part 1. The nature and sources of cloud-active aerosols. *Earth Sci. Rev*. **89**, 13–41.

Asmi E. et al. (2011) Secondary new particle formation in Northern Finland Pallas site between the years 2000 and 2010. *Atmos. Chem. Phys*. **11**, 12959–12972.

Boulon J. et al. (2010) New particle formation and ultrafine charged aerosol climatology at a high altitude site in the Alps (Jungfraujoch, 3580 m a.s.l., Switzerland). *Atmos. Chem. Phys*. **10**, 9333–9349.

Carslaw K. S. et al. (2010) A review of natural aerosol interactions and feedbacks within the Earth system. *Atmos. Chem. Phys*. **10**, 1701–1737.

Creamean J. M. et al. (2011) Measurements of aerosol chemistry during new particle formation events at a remote rural mountain site. *Environ. Sci. Technol.* **45**, 8208–8216.

Fatima H. et al. (2011) On radiative forcing of sulphate aerosol produced from ion-promoted nucleation mechanisms in an atmospheric global model. *Meteorol. Atmos. Phys*. **112**, 101–115.

Fountoukis C. et al. (2012) Simulating ultrafine particle formation in Europe using a regional CTM: contribution of primary emissions versus secondary formation to aerosol number concentrations. *Atmos. Chem. Phys. Discuss.* **12**, 13581–13617.

Jung J., Fountoukis C., Adams P. J. and Pandis S. N. (2012) Simulation of in situ ultrafine particle formation in the eastern United States using PMCAMx-UF. *J. Geophys. Res*. **115**, D03203, doi:10.1029/2009JD012313.

Kazil J. et al. (2010) Aerosol nucleation and its role for clouds and Earth's radiative forcing in the aerosol-climate model ECHAM5-HAM. *Atmos. Chem. Phys*. **10**, 10733–10752.

Kerminen V.-M., Lihavainen H., Komppula M., Viisanen Y. and Kulmala M. (2005) Direct observational evidence linking atmospheric aerosol formation and cloud droplet activation. *Geophys. Res. Lett*. **32**, L14803, doi:10.1029/2005GL023130, 2005.

Kerminen V.-M. et al. (2012) Cloud condensation nuclei production associated with atmospheric nucleation: a synthesis based on existing literature and new results. *Atmos. Chem. Phys. Discuss*. (accepted)

Kuang C., McMurry P. H. and McCormick A. V. (2009) Determination of cloud condensation nuclei production from measured new particle formation events. *Geophys. Res. Lett.* **36**, L09822, doi:10.1029/2009GL037584.

Kulmala M. et al. (2007) Toward direct measurement of atmospheric nucleation. *Science* **318**, 89-92.

Kulmala M. and Kerminen V.-M. (2008) On the formation and growth of atmospheric nanoparticles. *Atmos. Res.* **90**, 132–150.

Kuwata M. et al. (2008) Cloud condensation nuclei activity at Jeju Island, Korea in spring 2005. *Atmos. Chem. Phys.* **8**, 2933–2948.

Laaksonen A. et al. (2005) Cloud condensation nuclei production from nucleation events at a highly polluted region. *Geophys. Res. Lett.* **32**, L06812, doi:10.1029/2004GL022092.

Levin E. J. T. et al. (2012) An annual cycle of size-resolved aerosol hygroscopicity at a forested site in Colorado. *J. Geophys. Res.* **117**, D06201, doi:10.1029/2011JD016854.

Lihavainen H. et al. (2003) Production of "potential" cloud condensation nuclei associated with atmospheric new-particle formation in northern Finland. *J. Geophys. Res.* **108**(D24), 4782, doi:10.1029/2003JD003887.

Lucas D. D. and Arimoto H. (2006) Evaluating aerosol nucleation parameterizations in a global atmospheric model. *Geophys. Res. Lett.* **33**, L10808, doi:10.1029/2006GL025672.

Luo G. and Yu F. (2011a) Sensitivity of global cloud condensation nuclei concentrations to primary sulfate emission parameterizations. *Atmos. Chem. Phys.* **11**, 1949–1959.

Luo G. and Yu F. (2011b) Simulation of particle formation and number concentration over the Eastern United States with the WRF-Chem + APM model. *Atmos. Chem. Phys.* **11**, 11521–11533.

Makkonen R. et al. (2009) Sensitivity of aerosol concentrations and cloud properties to nucleation and secondary organic distribution in ECHAM5-HAM global circulation model. *Atmos. Chem. Phys.* **9**, 1747–1766.

Makkonen R. et al. (2012a) Air pollution control and decreasing new particle formation lead to strong climate warming. *Atmos. Chem. Phys.* **12**, 1515–1524.

Makkonen R. et al. (2012b). BVOC-aerosol-climate interactions in the global aerosol-climate model ECHAM5.5-HAM2. *Atmos. Chem. Phys. Discuss.* 1**2**, 9195–9246.

Merikanto J. et al. (2009). Impact of nucleation on global CCN. *Atmos. Chem. Phys.* **9**, 8601–8616.

Merikanto J., Spracklen D. V., Pringle K. J. and Carslaw K. S. (2010) Effects of boundary layer particle formation on cloud droplet number and changes in cloud albedo from 1850 to 2000. *Atmos. Chem. Phys.* **10**, 695–705.

O'Dowd. C. D., Monahan C. and Dall'Osto M. (2010) On the occurrence of opean ocean particle production and growth events. *Geophys. Res. Lett.* **37**, L19805, doi:10.1029/2010GL044679.

Pierce J. R. and Adams P. J. (2009) Uncertainty in global CCN concentrations from uncertain aerosol nucleation and primary emission rates. *Atmos. Chem. Phys.* **9**, 1339-1356.

Pierce J. R et al. (2012) Nucleation and condensation growth to CCN sizes during a sustained pristine biogenic SOA event in a forested mountain site. *Atmos. Chem. Phys.* **12**, 3147–3163.

Sihto S.-L. et al. (2011) Seasonal variation of CCN concentrations and aerosol activation properties in boreal forest. *Atmos. Chem. Phys*. **11**, 13269–13285.

Sotiropoulus R. E. P. et al. (2006) Modeling new particle formation during air pollution episodes: impacts on aerosol and cloud condensation nuclei. *Aerosol Sci. Technol.* **40**, 557–575.

Spracklen D. V. et al. (2006) The contribution of boundary layer nucleation events to total particle concentrations on regional and global scales. *Atmos. Chem. Phys*. **6**, 5631–5648.

Spracklen D. V. et al. (2008) Contribution of particle formation to global cloud condensation nuclei concentrations. *Geophys. Res. Lett.* **35**, L06808, doi:10.1029/2007GL033038.

Wang M. and Penner J. E. (2009) Aerosol indirect forcing in a global model with particle nucleation. *Atmos. Chem. Phys*. **9**, 239–260.

Wiedensohler A. et al. (2009) Rapid aerosol particle growth and increase of cloud condensation nucleus activity by secondary aerosol formation and condensation: A case study for regional air pollution in northeastern China. *J. Geophys. Res.* **114**, D00G08, doi:10.1029/2008JD010884.

Yu F. and Luo G (2009) Simulation of particle size distribution with a global aerosol model: contribution of nucleation to aerosol and CCN number concentrations. *Atmos. Chem. Phys*. **9**, 7691–7710.

Yue D. L. et al. (2011): Potential contribution of new particle formation to cloud condensation nuclei in Beijing. *Atmos. Environ.* **45**, 6070–6077.

Evolution of nanoparticle composition in CLOUD in presence of sulphuric acid, ammonia and organics

H. Keskinen[1], J. Joutsensaari[1], G. Tsagkogeorgas[2], J. Duplissy[3], F. Bianchi[4], P. Miettinen[1], J. Slowik[4], M. K. Kajos[3], S. Schobesberger[3], F. Riccobono[4], E. Weingartner[4], M. Gysel[4], J. Dommen[4], A. Prevot[4], A. Praplan[4], K. Lehtipalo[3], S. Schallhart[3], T. Ruuskanen[3], H. Wex[2], F. Stratmann[2], U. Baltensperger[4], D. Worsnop[3], M. Kulmala[3], I. Riipinen[5], A. Virtanen[1], and A. Laaksonen[1,6] and CLOUD collaboration

[1] Dept. of Applied Physics, University of Eastern Finland, 70211 Kuopio, Finland.

[2] Dept. of Physics, Leibniz Institute for Trophospheric Research, Leipzig 04318, Germany.

[3] Division of Atmospheric Science, Dept. of Physics, University of Helsinki, Helsinki 00560, Finland.

[4] Paul Scherrer Institute, Laboratory of Atmospheric Chemistry, Villigen 5232, Switzerland.

[5] Finnish Meteorological Institute, 00560 Helsinki, Finland.

[6] Department of Applied Environmental Science & Bert Bolin Center for Climate Research, Stockholm University, Stockholm 114 18, Sweden.

Keywords: CLOUD, nanoparticles, hygroscopicity, composition

INTRODUCTION

The aim of this study is to predict the size-selected composition of the nucleated nanoparticles and their ability to act as a cloud condensation nuclei. Particles were produced in CLOUD (Cosmic Leaving Outdoor Droplets) experiment, whose aim is to study possible link between galactic cosmic rays and cloud formation.

METHODS

In the CLOUD experiment the atmospheric conditions were simulated in a chamber in which aerosols were formed. One can find detailed description of the CLOUD experiment elsewhere (Kirkby et al., 2011, Kupc *et al.,* 2011, Voigtlander *et al.,* 2012). For particle formation, ozone (O_3), sulphuric dioxide (SO_2), ammonia (NH_3), dimethylamine and pinanediol (PD) were introduced into the chamber. To study the chemical composition of the formed particles and the particle-water vapour interactions we used data from hygroscopic and organic ethanol tandem differential analyzers (H- and OETDMA) (Joutsensaari et al., 2001), cloud condensation nuclei counter (CCN-c) (Droplet Measurement Technologies, Roberts and Nenes, 2005) and Aerodyne high resolution time-of-flight aerosol mass spectrometer (HR-ToF-AMS) (DeCarlo *et al.*, 2006). The evolution of the particle mobility size distribution during nucleation and growth rates (GRs) of the particles were determined from the Scanning Mobility Particle Sizer (SMPS) measurements. The smallest measured size was 15 nm for H- and OETDMA, 30 nm for CCN-c 30 nm and 50 nm for HR-ToF-AMS. For results interpretation also the gas phase chemistry studied by Proton Transfer Reaction Time-of-Flight Mass Spectrometer (PTR-TOF) and the ions composition (up to 2 nm) measured by Atmospheric Pressure Interface Time-of-Flight Mass Spectrometer (APi-TOF, Junninen *et al.*, 2010) was used. Figure 1 illustrates the experimental system to analyze the nucleated nanoparticle properties during their growth.

From HTDMA and CCN-c measurements, we derived the hygroscopicity parameters (κ_{hgf} and κ_{ccn}, respectively) based on theory by Petters and Kreidenweis (2007). Same theory was also modified for calculating ethanol affinities (η):

$$\eta = (EGF^3 - 1) \cdot \left[\frac{1}{S} \cdot exp\left(\frac{4\sigma_e M_e}{RT\rho_e D_0 EGF} \right) - 1 \right]$$

where EGF is measured ethanol growth factor, S is the saturation ratio, σ_e is the ethanol surface tension, M_e is the molecular weight of the ethanol, R is the gas constant, T is the temperature, ρ_e is the density of the ethanol and D_0 is the selected dry particles size in DMA. From HR-ToF-AMS we can derive the oxidation level of the particles and connect that to their hygroscopic properties (Massoli et al. 2010, Raatikainen et al. 2010).

CONCLUSIONS

The analysis presented here will give valuable insight in the composition of the size-selected (from 15 nm) nucleated particles during their growth and further in their ability to act as cloud condensation nuclei in the atmosphere.
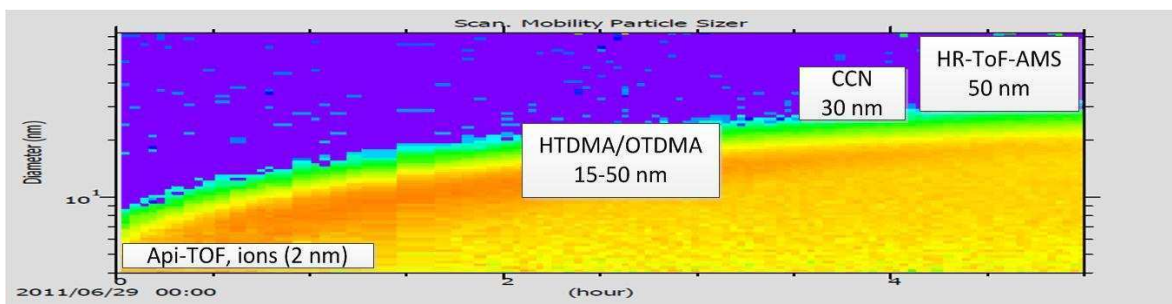
Figure 1. The experimental system to analyze the nucleated nanoparticles properties during their growth.

ACKNOWLEDGEMENTS

REFERENCES

DeCarlo, P. F. et al. (2006), *Analytical Chemistry*, 78, 8281-8289.
Joutsensaari J., *et al,* (2001), *ACP*, 1, 51-60.
Junninen *et al.* (2010), *Atmos. Meas. Tech*. 3, 1038-1053.
Kirkby, J., *et al.*, (2011) *Nature*, 476, 429-U77.
Kupc, *et al.*, (2011) *J. Aerosol Sci.* 42, 532– 543.
Massoli *et al.,* (2010) *GRL*, 37, L24801.
Petters M.D., and Kreidenweis S.M. (2007), *ACP*, 7, 1961-1971.
Raatikainen *et al.,* (2010) *ACP*, 10, 2063-2077.
Roberts, G. C. and Nenes (2005), *Aerosol Sci. Tech.,* 39, 206–2.
Voigtländer *et al.,* (2012) *ACP*, 12, 2205-2214.

ARTIFICIAL STIMULATION OF SOIL AMINE PRODUCTION BY ADDITION OF ORGANIC CARBON AND NITROGEN TRANSFORMING ENZYMES

A.-J. KIELOAHO[1,3], J. PARSHINTSEV[2], M.-L. RIEKKOLA[2], M. KULMALA[1], J.S. PUMPANEN[3] and J. HEINONSALO[1,3]

[1]Department of Physics, Division of Atmospheric Sciences,
P.O. BOX 48, FIN-00014 University of Helsinki, Finland

[2]Department of Chemistry, Laboratory of Analytical Chemistry
P.O. Box 55, FIN-00014 University of Helsinki, Finland

[3]Department of Forest Sciences,
P.O. Box 27, FIN-00014 University of Helsinki, Finland

Keywords: SCOTS PINE, BOREAL FOREST, SOIL, AMINES, ENZYMES.

INTRODUCTION

The major part of nitrogen (N) in boreal forest soil is in organic form (Soil Organic Nitrogen, SON) and largely in forms not directly available for plants or microbes (Knicker, 2011). Since the pools of nutritionally important inorganic N like NH_4^+ and NO_3^- are very low in forest soil (Korhonen et al. unpublished), the microbial transformations of SON into more readily available forms is of crucial importance for forest productivity.

One of the main pathways for amine production is the decay of organic matter in soil (Vranova *et al.*, 2011). In soil, amino acids react with specific decarboxylase enzymes which transform them to amines (Yan *et al.*, 1996, Näsholm *et al.*, 2001). Amino acid turnover time in forest soil is relatively fast (in hours) because amino acids can be used as N and C source by plants and especially by microbes (Jones and Kielland, 2012). Therefore, amino acid production by protease enzymes might be the critical step both for ecosystem productivity as well as for amine production and release from forest soil.

The aim of the study was to artificially introduce enzymes responsible for protein transformation into amino acids (proteases) as well as soil organic matter (SOM) decomposition (laccase and manganese peroxidase) in order to increase SON transformation and amine synthesis. Treatments were conducted both in Scots pine seedlings containing as well as non-planted microcosms. N transformations were examined, as well as amine concentration in soil and in volatile form.

METHODS

The experiment consisted of eight different treatments, two of which were regarded as controls concerning enzyme addition or stimulation. Four of the treatments were planted with one year old nursery grown Scots pine (*Pinus sylvestris* L.) seedlings and four were non-planted. The substrate additions and the overall experimental setup are shown in Table 1. The role of bovine serum albumin (BSA) was to act as control protein and equal the nutritional effect of enzyme additions. Proteases have the ability to degrade proteins into amino acids and laccase and manganese peroxidase induce SOM decomposition. Glucose addition has been shown to induce natural soil protease activity (Linden et al., unpublished).

	Scots pine	N	BSA	Protease	Lacc+MnP	Glucose
Humus+BSA	X	15	X			
Protease	X	15		X		
Protease +Lac+ MnP	X	15		X	X	
BSA+Glucose	X	15	X			X
Humus+BSA		5	X			
Protease		5		X		
Protease+Lac+MnP		5		X	X	
BSA+Glucose		5	X			X

Table 1. The experimental setup. Proteases, laccase and manganese peroxidise (Lacc+MnP) are functional enzymes and were added to induce SOM and SON transformations. Glucose has been shown to induce natural soil protease activities and bovine serum albumin (BSA) is added to equal the treatment from nutritional point of view (enzymes contain approx.. 15% N).

The experiment lasted approximately six months and the treatments with enzyme, protein and glucose additions were conducted within one more month. After the treatments, the experiment was continued for one extra month before being harvested for chemical analysis. All the analyses performed or under progress are listed in Table 2.

	Analysed	Under progress
Total soil N	X	
Dissolved N	X	
NH_4^+ in soil	X	
NO_3^- in soil	X	
Extractable proteins in soil	X	
Total proteins in soil		X
Amino acids in soil		X
Amines in soil	X	
Amines released from soil		X
Needle N (total)		X
Needle N (^{15}N)		X
Protease activity	X	
Biomass		X

Table 2. All the analyses performed or to be performed from the experiment.

RESULTS

The protease activity was discovered more commonly after the treatment with protease or glucose additions. In planted BSA-control some natural protease activity was found but not in non-planted controls. Different substrate additions did not cause any differences in total N percentage, but the presence of the seedlings diminished soil N% by approximately 20%. In addition, the same effect was clearly seen in dissolved N, NH_4^+ and NO_3^-, which is shown in Figure 1. Plant has exploited the soluble N forms almost entirely from the system, irrespective of the substrate treatment. However, the presence of the seedling changed the ratio of organic N - inorganic N from inorganic nitrogen towards organic nitrogen in the soil compared to the non-planted treatments which were dominated in inorganic nitrogen forms, NH_4^+ and NO_3^-.
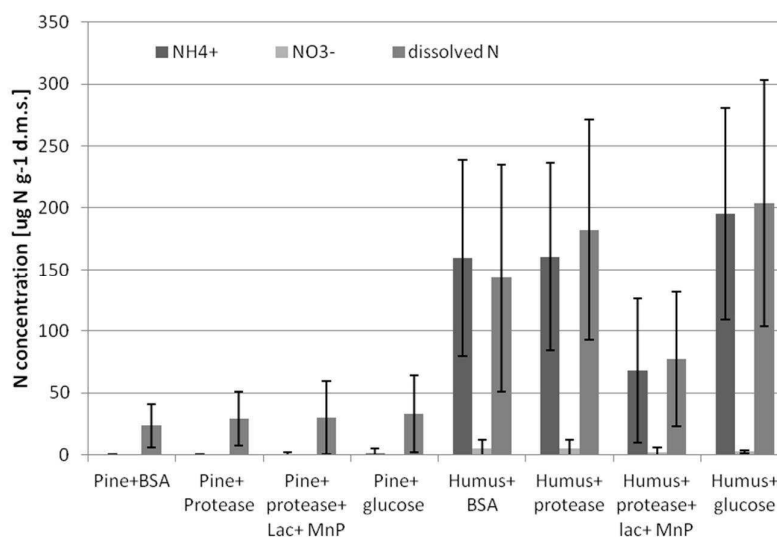
Figure 1. Soluble soil nitrogen concentrations after different treatments. Concentrations are in mass of nitrogen per dry mass of soil (μg N g^{-1} d.m.s.). Dissolved N includes soluble organic and inorganic soil N fractions.

The overall sums of the detected amines did not differ between any of the treatments although there was a trend of increased amine production in the absence of plants. Some amines in soil had a positive correlation with the presence (ethanol amine, spermidine, sec- and isobutylamine) or absence (dimethylamine) of plants. Concentrations of the most prominent amines in soil are shown in Figure 2 after different treatments.
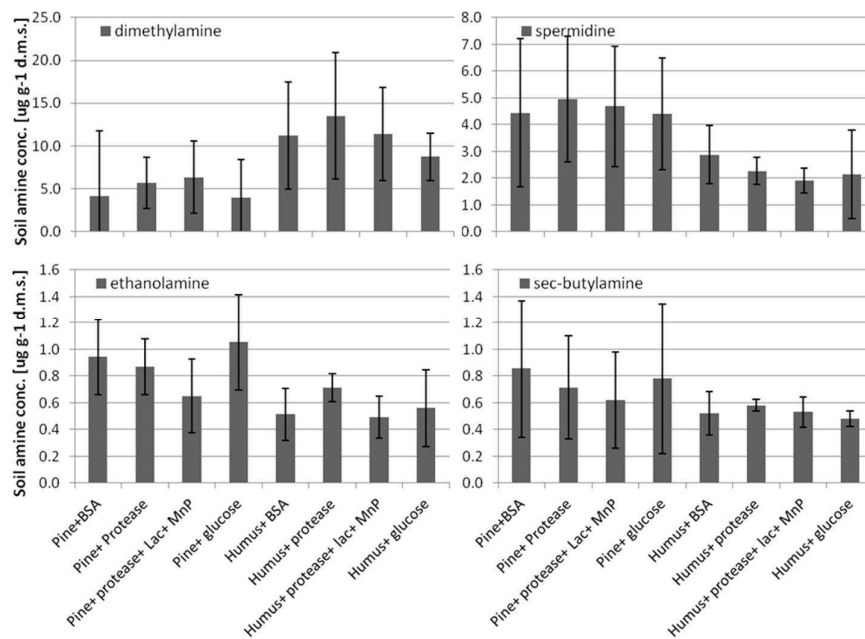
Figure 2. Concentrations of dimethylamine, spermidine, ethanolamine, and sec-butylamine in soluble fraction of soil after different treatments. Concentrations are in mass of amine per dry mass of soil (μg g^{-1} d.m.s.).

CONCLUSIONS

Based on the results obtained so far, it seems that artificial induction of amines in forest soil condition was not successful. However, we should keep in mind that large variations in natural forest soil conditions may mask the effects potentially caused by the enzyme and glucose additions. In addition, the reactions may be too fast for our sampling protocol.

However, it is evident that the effect of plant is crucial on many soil biochemical processes, and that soils did contain high quantities of certain amines and there were differences in amine compounds present and concentrations between planted and non-planted treatments. Therefore, the results confirm that if detected amines are volatilised, soils may be a significant source of amines in forest environment.

REFERENCES

Jones, D.L. and K. Kielland (2012). Amino acid, peptide and protein mineralization dynamics in a taiga forest soil. *Soil Biol. Biochem*. **55**, 60-69.

Knicker, H. (2011) Soil organic N – An under-rated player for C sequestration in soils? *Soil Biol. Biochem.* **43**, 1118-1129.

Nässholm, T., Huss-Danell, K., and Högberg, P. (2001) Uptake of glycine by field grown wheat. *New Phyt.* **150**, 59-63.

Vranova, V., Rejsek, K., Skene, K.R., and Formanek, P. (2011) Non-protein amino acids: plant, soil and ecosystem interactions. Plant Soil, **342**, 31-48.

Yan, F., Schubert, S., and Mengel, K. (1996) Soil pH increase due to biological decarboxylation of organic anions. *Soil Biol. Biochem*, **28**, 617-624.

LINKING AMBIENT AIR ALKYL AMINE CONCENTRATIONS, AEROSOL FORMATION AND SOIL IN A BOREAL FOREST

A.-J. KIELOAHO[1,3], H. HELLÉN[2], H. MANNINEN[1], H. HAKOLA[2] AND M. PIHLATIE[1]

[1]Department of Physics, Division of Atmospheric Sciences,
P.O. BOX 48, FIN-00014 University of Helsinki, Finland

[2]Air Quality Laboratories,
P.O. BOX 503, FIN-00560 Finnish Meteorological Institute, Finland

[3]Department of Forest Sciences,
P.O. Box 27, FIN-00014 University of Helsinki, Finland

Keywords: Amines, Aerosols, Soil, Forest.

INTRODUCTION

Alkyl amines are organic compounds that have common structure of R_3N, where R can be an alkyl group or a hydrogen atom. Amines have been shown to participate in atmospheric aerosol formation and growth into cloud condensation nuclei (Smith et al., 2009; Kurtén et al., 2008). This process of aerosol formation constitutes globally important source of cloud condensation nuclei, with potentially large implications on Earth's climate system (Wang and Penner, 2009; Merikanto et al., 2009; Andreae and Rosenfeld, 2008).

Alkyl amines can be emitted from a variety of sources, both antrophogenic and natural ones. Animal husbandry, industry, and combustion processes are main antrophogenic sources, and oceans, vegetation, biomass burning and soils are main natural sources of amines globally (Ge et al., 2010 and references therein).

Aim of the study is determine natural alkyl amine concentration in a boreal pine forest air, and find relations with aerosol concentrations and ecosystem variables.

METHODS

In this study a sample collection and analytical method for measuring ambient air concentrations of low molecular weight aliphatic amines have been developed for the following compounds: dimethylamine (DMA), ethylamine (EA), trimethylamine (TMA), propylamine (PA), diethylamine (DEA), butylamine (BA), and triethylamine (TEA), and measured in a boreal forest ecosystem from May to the end of October in 2011 in a boreal forest measurement station (Station for Measuring Ecosystem Atmosphere Relations, SMEAR2) in southern Finland.

In an amine sample collection, ambient air was pumped through a stack of filters. Samples were collected with an air flow of 16 L min^{-1}. The stack of filter consisted from a PTFE membrane filter (*Millipore: Fluoropore® 3.0 μm FS*) and from an acid impregnated glass fibre filter. The PTFE filter was used to collect particles before the impregnated filter. The impregnated filter was for trapping gas-phase amines as salts into the glass fibre filter. For the acid impregnated filters, the glass fibre filters were treated with phosphoric acid in methanol according to procedure introduced by Rampfl et al. (2005).

Duration of a sample collection was 24 hours in weekdays and 72 hours over weekends. During a week, samples were pooled, and pooled filters were extracted together. Measurement height was 2.5 m above the ground and a filter holder was shielded from rain and direct sunlight.

Analytical method for gas-phase amines is based on methods introduced by Rampfl et al. (2005). The extract was analysed by high performance liquid chromatography electro spray ionisation ion trap mass spectrometer (*Agilent 1100 series LC/MSD trap*). For quantitative analysis, 5 point external standard for all measured aliphatic amines were used. Analysis was repeated for each sample two times and final analyse results were calculated by averaging of two analysis. Uncertainty of analysis is reported as a standard error of results. Detection limits are three times of

standard deviations of field blanks. Because of insufficient chromatographical separation of DMA from EA, and TMA from PA, they were handled as a pairs.

Ambient air amine concentrations were compared with aerosol data and selected ecosystem variables measured in SMEAR2 station. For comparing data sets, weekly means were used. Aerosol data consists of NAIS and DMPS measurement data. For positive cluster ions sizes range from 0.8 to 3 nm and from DMPS data size range of 25 to 50 nm were used. Ecosystem variables consisted soil temperature and soil water content in A-horizon (0-10 cm depth), precipitation intensity, and air temperature measured in 4.2 m.

RESULTS

Ambient air concentration of the amines and their detection limits are shown in Table 1. EA+DMA and TMA+PA concentrations were over the detection limit throughout the measurement period, and the concentrations of DEA were over the detection limit for most of the measurement period. The highest concentrations were observed in July for DEA, and in the end of September and in the early October for EA+DMA and TMA+PA.

	TEA [ppt_V]	EA+DMA [ppt_V]	BA [ppt_V]	TMA+PA [ppt_V]	DEA [ppt_V]
Detection limits	3.2	0.2	8.9	0.4	6.7
Mean	>3.2	42.2	>8.9	21.1	>6.7
Standard deviation	-	29.4	-	23.2	5.6
Max conc.	3.2	156.8	>8.9	103.0	15.5
Min conc.	>3.2	12.2	>8.9	4.6	>6.7

Table 1. Detection limits and means, standard deviations maximums and minimums values for triethylamine (TEA), ethyl- and dimethylamines (EA+DMA), butylamine (BA), trimethyl- and propylamine (TMA+PA), and diethylamine during the measurement period from May to October. The concentrations are in parts per trillion (ppt_V).

Positive cluster ions and aerosol particle number concentrations followed DEA and EA+DMA concentrations during the measurement period, as shown in Figure 1. Concentrations of PA+TMA, and the number concentrations of positive cluster ions and aerosols did not peak at the same time periods.
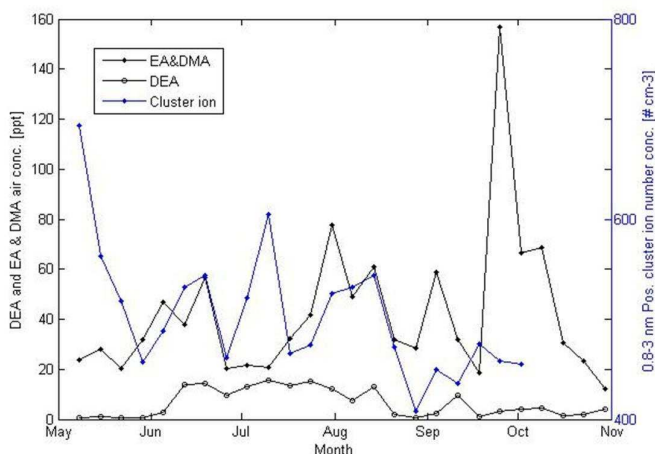
Figure 1. Diethylamine (DEA), and EA and DMA air concentrations and positive cluster ion number concentrations during the measurement period. The concentrations are in parts per trillion (ppt_V) for amines and in number per cubic centrimeter (# cm^{-3}) for positive cluster ions.

Soil temperature had positive correlated with DEA (r = 0.6; p < 0.05) and negative correlation with soil water content (r = -0.50; p < 0.05), shown in Figure 2. EA+DMA air concentrations were related to soil temperature and water content but not that strongly than for DEA.
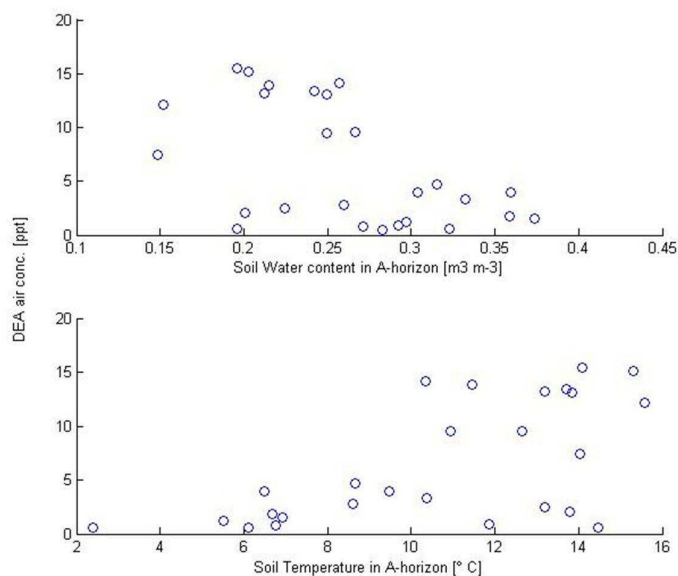
Figure 2. Diethylamine concentrations, soil water content (above) and soil temperature (below) in A-horizon. Diethylamine concentration is in parts per trillion (ppt_V), soil water content is in cubic meters per cubic meters ($m^3\ m^{-3}$), and soil temperature are in degrees of Celsius (°C).

CONCLUSIONS

In a boreal forest, high concentrations of measured amines we found to be in July and the highest concentrations we found in end of September. The most prominent amine compounds during the measurement period were the ethyl- and dimenthylamine, propyl- and trimethylamine, diethylamine. Positive cluster ions in size range of 0.8 to 3 nm and aerosol particles in size range 25 to 50 nm were following amine concentrations, especially of diethylamine, and ethlyl- and dimethylamine concentrations. Soil temperature had a positive and soil water content had a negative correlation with diethylamine concentrations. For the rest of amines, the relationship with soil temperature and water content were not clear.

ACKNOWLEDGEMENTS

REFERENCES

Andreae and Rosenfeld (2008) Earth-Sci. Rev., **89**, 13-41.
Ge, X., Wexler, A. S. & Cless S. L. (2011) Atmos. Environ., 45, 524–546
Kurtén et al. (2008) Atmos. Chem. Phys., 8, 4095-4103
Merikanto et al. (2009) Atmos. Chem. Phys., 9, 8601–8616.
Rampfl et al. (2005) Environ. Sci. Technol., **42**, 5217-522.
Smith et al. (2009) P. Natl. Acad. Sci., **107**, 6634-6639.
Wang and Penner (2009) Atmos. Chem. Phys., **9**, 239-260.

LARGE PARTICLE CLIMATOLOGY IN FINLAND – ESTIMATING THE EFFECT OF AEROSOLS IN EXTINCTION OF INFRARED RADIATION

N. KIVEKÄS[1], T. MIELONEN[2], H. PORTIN[2,3], T. KAURILA[4], I. RAJAKALLIO[4], K.E.J. LEHTINEN[2,3] AND H. LIHAVAINEN[1]

[1]Research and Development, Finnish Meteorological Institute, Helsinki, PO.Box 503, 00101 Finland

[2]Research and Development, Finnish Meteorological Institute, Kuopio, PO.Box 1627, 70211 Finland

[3]Department of Applied Physics,University of Eastern Finland, ,Kuopio, PO Box 1627,70211 Finland

[4]Technical Research Center of Finnish Defense Forces, Lakiala, Finland

Keywords: EXTINCTION, AEROSOL, INFRARED VISIBILITY

INTRODUCTION

Automatic measurements of visibility are often based on the scattering or extinction of infrared radiation in ambient air. In these applications there is a known source of infrared light and a sensor detecting the light a short distance away. Infrared radiation can also be used passively to detect signals caused by motors or electrical devices. In these applications it is crucial to know the rate of extinction of the signal in air to be able to estimate the distance to the signal source.

The extinction of infrared radiation consists of scattering and absorption of the radiation by gas molecules and aerosol particles. As the gaseous composition of the air does not vary much, the main source of uncertainty in extinction of infrared radiation in air are the number, size and composition of the aerosol particles.

Shettle and Fenn (1979) have developed a model for estimating the extinction of radiation in atmosphere by aerosols. The model was developed in military use. In their model there are four different shapes for the aerosol particle size distribution: Urban, rural, marine with continental origin, marine with oceanic origin and tropospheric. These size distributions are mostly unimodal, and they are characterized by the logarithmic standard deviation of the aerosol mode. The logarithmic mean diameter of the mode depends on both distribution type and ambient relative humidity. Finally, the number concentration of aerosol particles is parameterized by the distribution type and the ambient visibility.

In some cases this model greatly underestimates the aerosol effect on extinction in Scandinavian conditions (Kaurila et al., 2006; Mielonen et al., 2008). Kolmonen et al (2008) tried to solve this problem by making a more detailed source region analysis for Scandinavian background aerosol by positive matrix factorization. The work presented here aims to improve the estimation by taking a prescribed source region dependent shape of the dry aerosol size distribution and then scaling it by PM10 aerosol concentration and relative humidity.

METHODS

We have analysed continuous aerosol size distribution data from three station in Finland, Hyytiälä (61º 51' N, 24º 17' E), Puijo (62.54' N, 27.39' E) and Pallas (67º 58' N, 24º 07' E) from years 2007-2011. The data was measured from dried flow of ambient air using DMPS and APS (at Puijo DMPS and Grimm OPC), giving the aerosol size range 0.01 – 15 µm. The number size distributions were converted to volume size

distributions and normalized by the total volume concentration. Then the aerosol data was combined with FLEXTRA air mass back trajectories (Stohl et al., 1995).

Different combinations of marine and continental source areas were studied, but the differences between different continental areas as well as those between different marine areas were so small that in the end two simple source areas were used: marine and continental. The size distributions for these areas were somewhat different than those by Shettle and Fenn (1979) for the corresponding maritime and rural areas (figure 1).
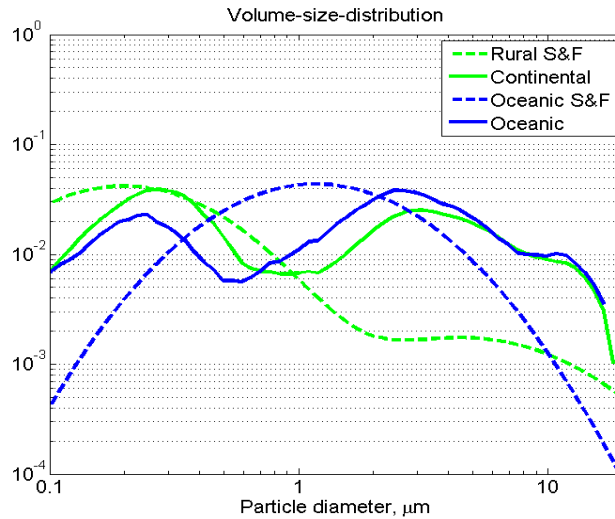
Figure 1. Aerosol volume size distributions in Shettle and Fenn (S&F) 1979 and in this work.

This leads to significant differences in extinction especially in the case of continental air, where the difference is more pronounced in the large particles (Figure 2). The extinction was calculated with the Mie theory assuming spherical $(NH_3)_2SO_4$ particles.
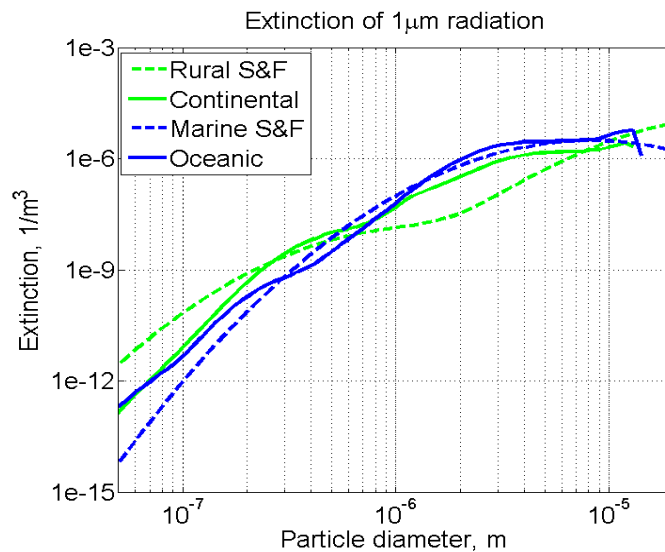
Figure 2. Extinction of 1 μm radiation caused by 1000cm^{-3} aerosol concentration in Shettle and Fenn (S&F) 1979 and in this work

For each trajectory the normalized aerosol size distribution was parameterized by taking an average of the continental and marine size distributions based on the weighted fraction of time the air had spent over land or ocean, respectively. The weighting was used to give more emphasis to the areas where the air had been more recently, as large particles have shorter lifetime in the atmosphere.

This method with assumed size distribution and no information on the chemical composition of the particles is definitely not accurate. The accuracy was tested by scaling the parameterized aerosol size distribution by the measured total volume concentration (representing PM10) and then comparing it to the actual measured aerosol size distribution. Extinction in infrared wavelengths were calculated to both distributions, and these were compared to each other in order to estimate the accuracy (Figure 3)
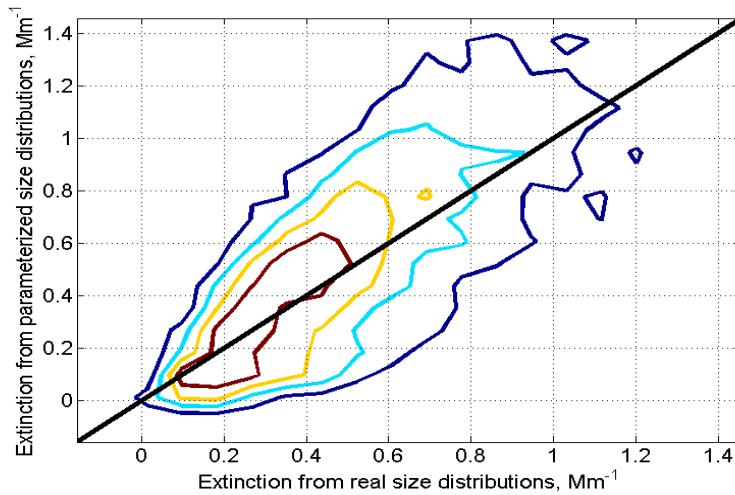
Figure 3. Extinction of 1 μm radiation based on real and parameterized aerosol size distribution. The fraction of all data points within each contour is (from in to out) 20%, 40%, 60% and 80%.

The parameterization was able to cope with significant variations in the particle volume (Figure 4), but as the details of the size distribution are not included, there are also periods when extinction values from parameterized and measured size distributions differ significantly.
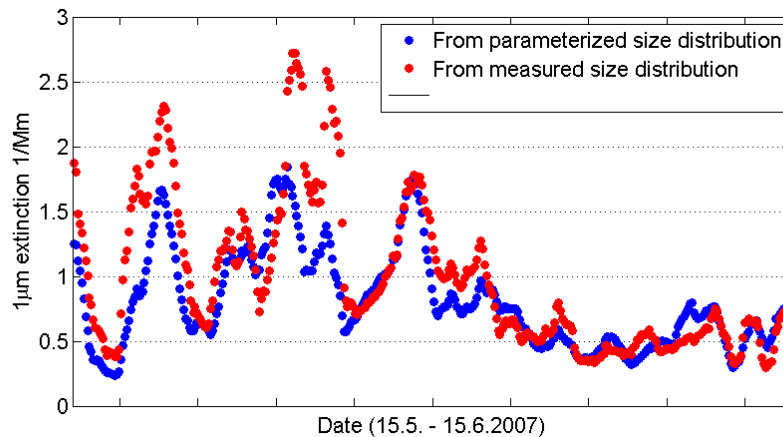
Figure 4. Extinction of 1 μm radiation in Hyytiälä based on real and parameterized dry aerosol size distributions. This is only an example period 15.5.-15.6.2006 of the whole data set.

CONCLUSIONS

The extinction values obtained from parameterized and measured aerosol volume-size-distributions agree in general, but there are cases when the error is significant. The error is further increased by the unkown factors in the hygroscopic growth of the particles. The errors, however, seem to me smaller than those obtained by using the Shettle & Fenn parameterization. The next step is to include the new aerosol size distributions into MODTRAN radiative transport model and compare the results of the model with those obtained using the Shettle & Fenn size distributions.

Kaurila, T., Hågård, A., and Persson, R. (2006), Aerosol extinction models based on measurements at two sites in Sweden, *Appl. Opt.* 45, 6750-6761.

Kneizys, F., Abreu, L., ., Anderson, G., Shettle, E., Berk, A., Bernstein, L., Robertson, D., Acharya, P., Rothman, L., Selby, J., Gallery, W. and Clough, S. (1996), The MODTRAN 2/3 Report and LOWTRAN 7 MODEL, Phillips Laboratory, Geophysics Directorate Hanscom AFB, Maine, USA

Kolmonen. P., Aaltonen, V., Hatakka, J. Hyvärinen, A. Kaurila, T. Lehtinen, K. and Lihavainen, H. (2007) European Aerosol Conference 2007, Salzburg, Austria, September 9-14 2007, Abstract T13A054.

Mielonen, T., Kaurila, T., Arola, A., Lihavainen, H., Komppula, M. & Lehtinen K. E. J. (2008) Effect of aerosols on the infrared transmission in Lakiala, Finland**,** *Atmospheric Environment* 42, 2603-2610.

Shettle, E. and Fenn, R. (1979), Models for the aerosols of the Lower Atmosphere and the Effect of Humidity Variations on the Optical Properties, *Environmental Research Papers* **676**, AFGL-TR-79-0214.

A. Stohl, G. Wotawa, P. Seibert, and H. Kromp-Kolb (1995): Interpolation errors in wind fields as a function of spatial and temporal resolution and their impact on different types of kinematic trajectories. *J. Appl. Meteor.* 34, 2149-2165.

MEASURING THE EFFECT OF SOOT ON PHYSICAL AND OPTICAL PROPERTIES OF SNOW

N. KIVEKÄS[1], A. VIRKKULA[1,2], O. JÄRVINEN[2], J. SVENSSON[1], A. AARVA[3], H. LIHAVAINEN[1], D. BRUS[1], A. HYVÄRINEN[1], O. MEINANDER[1], A. HEIKKILÄ[1], R. VÄÄNÄNEN[2], J. BACKMAN[2], and G. de LEEUW[1,2]

[1]Research and Development, Finnish Meteorological Institute, Helsinki, PO.Box 503, 00101 Finland.

[2]Department of Physics, Helsinki University, Helsinki, 00101, Finland.

[3]Weather and safety, Finnish Meteorological Institute, Helsinki, PO.Box 503, 00101 Finland.

Keywords: BLACK CARBON, ALBEDO, SNOW.

INTRODUCTION

Soot consists mainly of light absorbing carbon. When deposited on snow, it decreases the snow albedo, increases the absorption of radiation in snow and thereby enhances melting. This process has been studied for decades (e.g., Warren and Wiscombe, 1980; Clarke and Noone, 1985) and it has been recognized to be one of the major sources of warming in the Arctic regions (e.g., Flanner *et al.*, 2007; Quinn *et al.*, 2008). The link between soot, snow albedo, and climate change is still not understood in enough detail for quantitative analysis (Hansen and Nazarenko, 2004).

To provide more insight into these connections the Finnish Meteorological Institute with help of Helsinki University has started a series of Soot on Snow (SoS) measurement campaigns. In these campaigns soot is deposited on snow in the beginning of the melting season and then the properties of the snow pack are measured throughout the whole melting season until the snow is gone. SoS 2011 and SoS 2012 were held in southern Finland: SoS 2011at Nurmijärvi in the spring 2011 (Virkkula *et al*., 2011) and SoS 2012 at Jokioinen in spring 2012. SoS 2013 campaign is planned to take place at Sodankylä in Finnish Lapland in spring 2013.

METHODS

In SoS 2011 soot was produced by burning organics in a wood-burning stove. The purpose was to get as high soot concentrations in air as possible, so that the effects would become clear. The smoke was led through a pipe, cooled by snow surrounding the pipe, and led into a garage tent that was built on top of the snow. The smoke drifted out from the other end of the garage tent that was left open. This method produced a clear gradient of soot on the surface of snow. The campaign was held on agricultural field to avoid shading by trees and buildings.

Aerosol number concentration, size distribution, absorption and scattering were measured at the open end of the garage tent. After the tent was removed the snow measurements were set up. The snow albedo and snow pack thickness were measured continuously at two locations, one at the sooted area and one at the clean area. Snow samples were taken and analysed. Also the snow pack structure and temperature profile, as well as spectral transmittance through the snow were measured once during the melting period.

In SoS 2012 the soot was not produced at the site, but produced in domestic heating and collected by chimney cleaners in eastern parts of Helsinki. The soot was dispersed on the snow by blowing it through a cyclone into a specially manufactured cylindrical tent, 4 m in diameter (Figure 1). After the soot was blown into the tent for a pre-defined time it was let to settle before the tent was removed. This method

produced a uniformly distributed soot layer on the surface of snow. Three spots with different amounts of soot were produced this way. Again the measurements were done on an agricultural field.
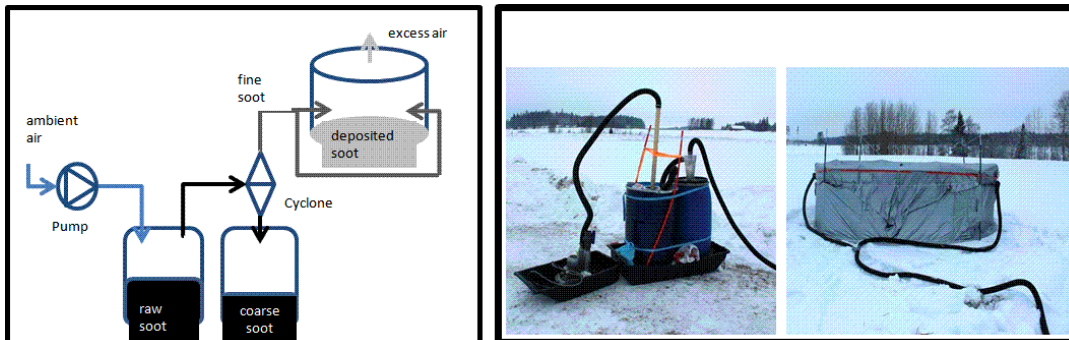
Figure 1. The schematic presentation (left) and photos (right) of the soot deposition system used in SoS 2012.

During the time when the tent was up, there were several instruments measuring air sampled from inside the tent. Particle number concentration and size distribution (15-10000 nm) were measured, as well as size distribution, scattering and absorption of the airborne soot. After the tent was removed, samples of the surface snow were taken from each spot, and samples at different depths were taken from a reference spot. These samples were later analysed for organic and elemental carbon (OC and EC) concentration. Another set of samples and snow temperature profiles were taken one month later. Snow thickness and albedo were measured continuously at each spot (plus the reference spot) through the whole melting season These albedo measurements are described in more detail in Meinander *et al*., 2012.

In SoS 2011 the effect of the soot was clearly observable. The mid-day albedo of the dirty snow was around 0.4 until the first snow fall, whereas the albedo of the clean snow was around 0.8 (Figure 2). After the snow fall the albedo of the dirty snow remained about 0.1 lower than that in the clean snow. The dirty snow area also melted 5 days before the clean area. In SoS 2012 there was a snow storm on the next day after the soot spots were made and another one a few days later. After the storm the albedo of all spots remained approximately equal throughout the melting season, and the melting rate and time of the snow depended mostly on how much snow had accumulated on the spot.

In both experiments the elemental carbon concentrations in the snow were analysed. The higher EC concentrations deposited on the top of snow were several tens of mg / m^2. When distributed evenly to the top 5 cm, this is several thousands of μg / l. In the reference spot the concentrations varied from 80 μg / l to 350 μg / l depending on the snow layer. When a new set of snow samples were taken one month later in SoS 2012, the EC concentrations in all four spots (including the reference spot) were 70 - 460 μg / l depending on the snow layer, the lowest concentrations being in the lowermost layers (Figure 3). In the lower snow layers in sooted spots were softer and consisted of visibly larger crystals than the layers above.
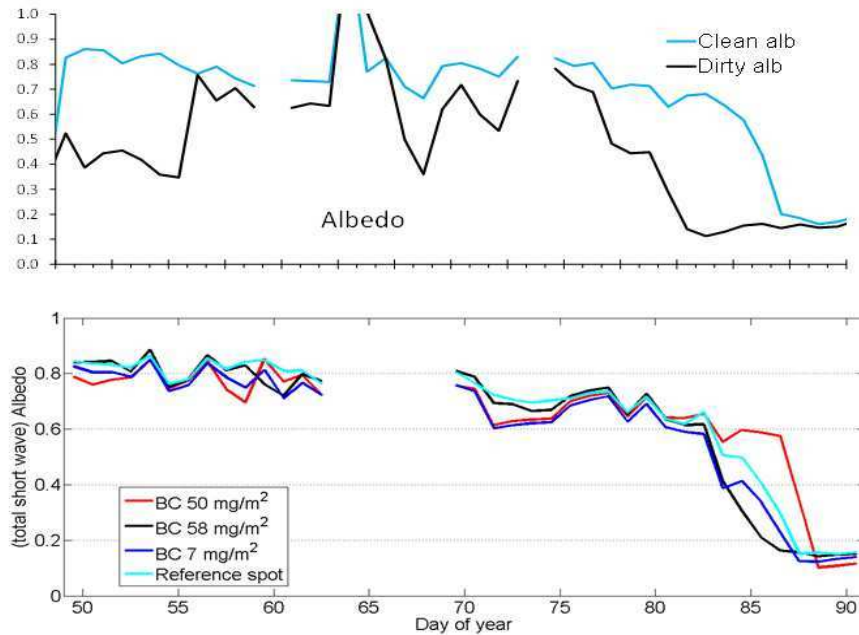
Figure 2. Mid-day (11-14 local time) albedo of clean and dirty snow in SoS 2011 (top) and SoS 2012 (bottom).
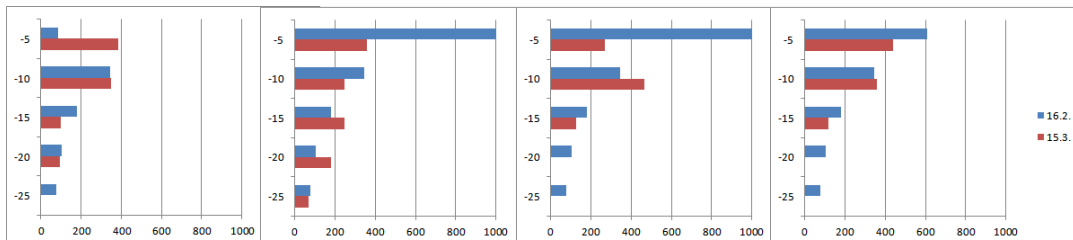
Figure 3. The concentrations of elemental carbon (μg/l) in different layers of snow from top to bottom in the different soot spots at 16.2. (blue) and at 15.3. (red). The spots are (in order from left to right) reference, 7μg/m^2 EC, 58 μg/m^2 EC, 50 μg/m^2 EC The lower layers at 16.2. were measured from the reference spot only, and the same values were used for the other spots. Note that the 16.2. values at the top layer of the two middle spots are over the scale.

CONCLUSIONS

The SoS 2011 experiment demonstrates clearly that soot does have an effect on the albedo of snow, and that the effect in melting is also measurable. In SoS 2012 the weather was less favourable and masked all effects of the soot on the albedo and melting of snow, even though some effect on the snow structure remained. The soot concentrations used in these experiments were at least an order of magnitude higher than those transported to Arctic by long range transportation. These findings illustrate that the effect of a single soot layer on snow might be much smaller than the effect of local weather patterns. On the other hand, even 10 μg / l of soot internally mixed in the snow have been calculated to decrease the snow albedo by 5%, which does produce a local climate forcing around 1 W/m^2 (Hansen and Nazarenko, 2004), so even small albedo changes are significant.

366

This set of experiments is planned to continue with a similar, but more closely followed experiment in Sodankylä, Finnish Lapland in 2013. The current experiments are not enough to quantify the effects of soot on snow. In Lapland the structure and behaviour of the snow pack are also closer to those at Arctic regions. In the future a similar experiment should be done with several layers of soot in the snow pack to better represent long range transport.

ACKNOWLEDGEMENTS

REFERENCES

Clarke, A. D. and Noone, K. J. (1985). Soot in the Arctic snowpack: a cause for perturbations in radiative transfer, *Atmos. Environ.*, **19**, 2045–2053.

Flanner, M. G., C. S. Zender, J. T. Randerson, and P. J. Rasch (2007). Present-day climate forcing and response from black carbon in snow, *J. Geophys. Res.*, 112, D11202, doi:10.1029/2006JD008003.

Hansen, J. and Nazarenko, L. (2004). Soot climate forcing via snow and ice albedos, *Proc. Nat. Acad. Sci.*, 101, 423–428, 2004.

Meinander O, Heikkilä, A., Riihelä A., Aarva A., Kontu A, Kyrö E, Lihavainen H, Kivekäs N, Virkkula A, Järvinen O, Svensson J, and de Leeuw G (2012), About Seasonal Arctic Snow UV Albedo at Sodankylä and UV-VIS Albedo Changes Induced by Deposition of Soot, Abstracts of the CRAICC Annual Meeting, Oslo, 26-28 September 2012.

Quinn, P. K., Bates, T. S., Baum, E., Doubleday, N., Fiore, A. M., Flanner, M., Fridlind, A., Garrett, T. J., Koch, D., Menon, S., Shindell, D., Stohl, A., and Warren, S. G. (2008). Short-lived pollutants in the Arctic: their climate impact and possible mitigation strategies, *Atmos. Chem. Phys.*, 8, 1723–1735, doi:10.5194/acp- 8-1723-2008.

Virkkula, A., Järvinen, O., Lihavainen, H., Hyvärinen, A., Mäkelä, T., Kivekäs, N., Väänänen, R., Backman, J., Heikkilä, A., Aarva, A., Kyrö, E-M. and de Leeuw, G. (2011), *Proceedings of the CRAICC annual meeting*, 10-14.10.2011.

Warren, S., and W. Wiscombe (1980). A model for the spectral albedo of snow. II: Snow containing atmospheric aerosols, *J. Atmos. Sci.*, 37, 2734– 2745.

NEUTRAL AND CHARGED SUB-2NM CLUSTERS
IN BOREAL FOREST BOUNDARY LAYER

J. KONTKANEN, S. HAKALA, T. NIEMINEN, K. LEHTIPALO, H. E. MANNINEN,
T. PETÄJÄ, AND M. KULMALA

Department of Physics, University of Helsinki, Finland

Keywords: molecular clusters, particle formation and growth, field measurements

INTRODUCTION

Atmospheric new particle formation is proposed to happen via the activation of the clusters in the size range of 1–2 nm (Kulmala et al., 2000; Kulmala et al., 2004; Kulmala et al., 2006). There are numerous observations of sub-2 nm charged clusters (e.g. Hirsikko et al., 2011 and references therein) and recent measurements have also proven the existence of neutral clusters (Kulmala et al., 2007; Lehtipalo et al., 2009). However, size-segregated measurements in the sub-2 nm size range are still needed to give more insight into the role of neutral and charged clusters in nucleation. In this work we present the results from the direct measurements of sub-2 nm clusters performed at the SMEAR II station in boreal forest boundary layer.

METHODS

The measurements were conducted during spring 2011 (14th March–16th May) and spring 2012 (27th March–15th May) at the SMEAR II station in Hyytiälä, Finland (Hari and Kulmala, 2005). The size distribution of neutral and charged clusters between 1 and 2 nm in mobility diameter was measured with the Particle Size Magnifier (PSM; Airmodus A09), which is a recently developed mixing-type condensation particle counter (Vanhanen et al., 2011). The ion mobility distribution was measured with the Neutral cluster and Air Ion Spectrometer (NAIS; Mirme et al., 2010) in the range from 3.2 to 0.0013 $cm^2 V^{-1} s^{-1}$, which corresponds to a mobility diameter range from 0.8 to 42 nm.

From PSM and NAIS measurements the total cluster concentration N_{tot} and ion concentration N_{ions} were calculated for different sub-2nm size classes. For the data measured in spring 2011 six sub-2nm size classes were used (0.9–1.1 nm, 1.1–1.3 nm, 1.3–1.5 nm, 1.5–1.7 nm, 1.7–1.9 nm, and 1.9–2.1 nm), while the spring 2012 data were divided into three size classes (1.1–1.3 nm, 1.3–1.5, and 1.5–2 nm). The concentration of neutral clusters originating from the recombination of oppositely-charged ions N_{rec} was estimated for each size class from the NAIS data. Finally, the concentration of neutral clusters N_n in each size class was calculated from

$$N_n = N_{tot} - N_{ions} - N_{rec} , \qquad\qquad\qquad\qquad (1)$$

where N_{tot} is the total concentration, N_{ions} is ion concentration and N_{rec} is the concentration of recombination products.

RESULTS AND DISCUSSION

In both spring 2011 and spring 2012 a continuously present population of sub-2nm clusters was observed in Hyytiälä. This cluster population seems to be dominated by neutral clusters, their concentration exceeding the concentration of ions and recombination products most of the time during both measurement periods. Especially during new particle formation events the dominance of neutral clusters was clear, which indicates a minor contribution of ion-mediated nucleation mechanisms to the total particle formation in Hyytiälä. On the other hand, during nighttime when the total cluster concentration was typically low ion concentration was often larger than the concentration of neutral clusters.

The median (and 5- to 95-percentile) concentration of sub-2nm neutral clusters was 4000 cm^{-3} (500–30 000 cm^{-3}) during spring 2011 and 3000 cm^{-3} (400–20 000 cm^{-3}) during spring 2012. The ion concentration was on average clearly lower and it also did not vary as strongly as the concentration of neutral clusters. During spring 2011 the median ion concentration was 800 cm^{-3} (500–1300 cm^{-3}) and during spring 2012 500 cm^{-3} (100–1000 cm^{-3}). The concentration of recombination products was observed to be small during both measurement periods. The differences in the cluster concentrations between spring 2011 and spring 2012 can at least partly be explained by the differences in the measured size range: in spring 2011 the smallest measured clusters were 0.9 nm in mobility diameter, while in spring 2012 the lowest size limit was 1.1 nm.

When studying the different sub-2nm size classes separately, the median concentration of neutral clusters can be observed to exceed the median ion concentration at all sizes (Figure 1). The concentration of neutral clusters was largest in the smallest size class (0.9–1.1 nm) and decreased with the increasing cluster size. This indicates that neutral clusters are continuously formed in the atmosphere, after which they grow to larger sizes or coagulate with the pre-existing larger particles. The concentration of ions was at its maximum between 1.1 nm and 1.3 nm, which is consistent with the earlier observations on the continuous population of small ions in the atmosphere (Hirsikko et al., 2005; Hirsikko et al., 2011). When comparing the cluster concentrations in different size classes measured in spring 2011 and spring 2012, it seems that during spring 2012 the concentrations of both neutral and charged clusters were on average slightly smaller than during spring 2011. However, especially in the largest size class (1.5–2 nm) this may be due to the differences in the measured size range.
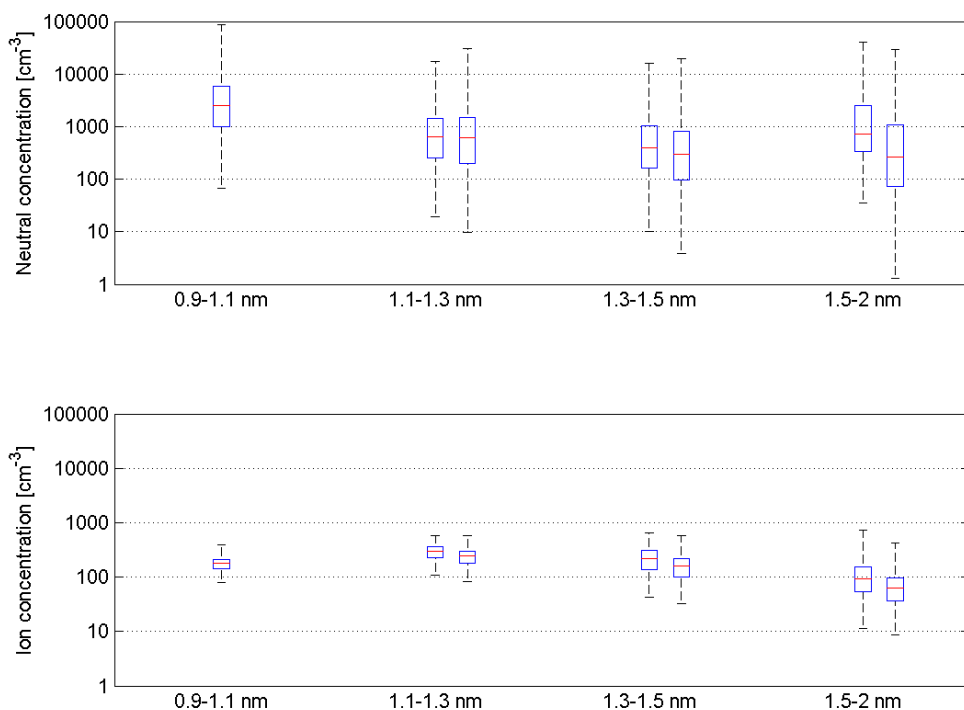
Figure 1. The concentrations of neutral and charged clusters in different size classes during spring 2011 (the boxes on the left-hand side) and spring 2012 (the boxes on the right-hand side). The red lines show the medians and the boxes indicate the 25- and 75-percentiles. For the smallest size class only data from the spring 2011 were used.

CONCLUSIONS

A continuous population of sub-2nm clusters was observed during spring 2011 and spring 2012 at the SMEAR II station in Hyytiälä. The cluster population was dominated by neutral clusters, especially during new particle formation events. This indicates that in boreal forest boundary layer the neutral nucleation mechanisms dominate over ion mediated ones. The continuous presence of clusters also implies that the formation and following growth of the clusters take place in the atmosphere all the time, not only during new particle formation events.

ACKNOWLEDGEMENTS

REFERENCES

Hari, P. and Kulmala, M.: Station for Measuring Ecosystem–Atmosphere Relations (SMEAR II), Boreal Environ. Res., 10, 315–322, 2005.

Hirsikko, A., Laakso, L, Hõrrak, U., Aalto, P. P., Kerminen, V.-M., and Kulmala, M.: Annual and size dependent variation of growth rates and ion concentrations in boreal forest, Boreal Environ. Res., 10, 57–369, 2005.

Hirsikko, A., Nieminen, T., Gagne, S., Lehtipalo, K., Manninen, H. E., Ehn, M., Hõrrak, U., Kerminen, V.-M., Laakso, L., McMurry,P. H., Mirme, A., Mirme, S., Petäjä, T., Tammet, H., Vakkari,V., Vana, M., and Kulmala, M.: Atmospheric ions and nucleation:a review of observations, Atmos. Chem. Phys., 11, 767–798, doi:10.5194/acp-11-767-2011, 2011.

Kulmala, M., Pirjola, L., and Mäkelä, J. M.: Stable sulphate clusters as a source of new atmospheric particles, Nature, 404, 66–69, 2000.

Kulmala, M., Kerminen, V.-M., Anttila, T., Laaksonen, A., and O'Dowd, C. D.: Organic aerosol formation via sulphate cluster activation, J. Geophys. Res., 109(D4), 4205, 2004.

Kulmala, M., Lehtinen, K. E. J., and Laaksonen, A.: Cluster activation theory as an explanation of the linear dependence between formation rate of 3 nm particles and sulphuric acid concentration, Atmos. Chem. Phys., 6, 787–793, 2006.

Kulmala, M., Riipinen, I., Sipilä, M., Manninen, H., Petäjä, T., Junninen, H., Dal Maso, M., Mordas, G., Mirme, A., Vana, M., Hirsikko, A., Laakso, L., Harrison, R. M., Hanson, I., Leung, C., Lehtinen, K. E. J., and Kerminen, V.-M.: Towards direct measurement of atmospheric nucleation, Science, 318, 89–92, 2007.

Lehtipalo, K., Sipilä, M., Riipinen, I., Nieminen, T., and Kulmala, M.: Analysis of atmospheric neutral and charged molecular clusters in boreal forest using pulse-height CPC, Atmos. Chem. Phys., 9, 4177–4184, doi:10.5194/acp-9-4177-2009, 2009.

Mirme, S., Mirme, A., Minikin, A., Petzold, A., Hõrrak, U., Kerminen, V.-M, and Kulmala, M.: Atmospheric sub-3nm particles at high altitudes, Atmos. Chem. Phys., 10, 437–451, doi:10.5194/acp-10-437-2010, 2010.

Vanhanen, J., Mikkilä, J., Lehtipalo, K., Sipilä, M., Manninen, H. E., Siivola, E., Petäjä, T., and Kulmala, M.: Particle size magnifier for nano-CN detection, Aerosol Sci. Tech., 45, 533–542, 2011.

EFFECTS OF MODAL REPRESENTATION OF AEROSOL SIZE DISTRIBUTION ON AEROSOL ACTIVATION AND OPTICAL PROPERTIES

T. KORHOLA[1], H. KOKKOLA[2], H. KORHONEN[2], A.-I- PARTANEN[2], A. LAAKSONEN[1,3], T. KÜHN[1]
S. ROMAKKANIEMI[1]

[1] Department of Applied Physics, University of Eastern Finland, Finland
[2] Finnish Meteorological Institute Kuopio Unit, Kuopio, Finland
[3] Finnish Meteorological Institute, Climate change, Helsinki, Finland

INTRODUCTION

Atmospheric aerosol size distributions usually follow log normal distribution. Thus it is tempting to use these functions also in atmospheric modelling to describe aerosol size distributions as they provide computationally efficient way to represent aerosols in large scale models. One, often used, way to describe an aerosol distribution is to list the number and mass of the aerosol particles in the mode in addition with the mode width. The average particle diameter can then be calculated for each compound with known density. This kind of approach has been used for example with MAM7, MAM3 and M7 aerosol modules (Sartelet et al., 2006, Vignati et al., 2003), which are largely used in several global scale applications.

In global modelling the atmosphere is divided into grid boxes, size varying from tens to hundreds of kilometres. Because of still limited computational power, calculations for these grid boxes are done separately during each time step. In the case of air mass mixing particles are moved between adjacent grid boxes. This can be done by transferring certain particle number and mass between corresponding modes in the grid boxes (accumulation mode particles to accumulation mode). If the average diameters of the corresponding to-be-transferred modes differ significantly the result of the transfer is a distribution that represents neither of the original distributions. To avoid this, the mode average diameters are restricted to predefined size ranges. The modes are kept under their threshold diameter by reallocating the number and mass corresponding to the largest particles in the mode to the larger mode (Binkowski and Roselle 2003). This reallocation decreases the average diameter of the (source)mode, and keeps it under desired size (Figure 1)
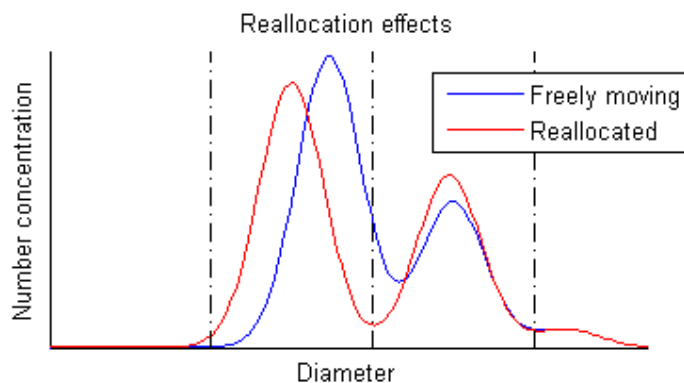
Figure 1: Figure showing a difference between reallocated and freely moving distribution. Vertical lines mark the threshold diameters for each mode.

By using reallocation routine, unrepresentative distributions are avoided when transferring particles between grid boxes. But it will cause problems under certain conditions when the distribution is growing, either within a grid box or as consequence of particle transfer. We studied the effects of reallocation on cloud droplet activation during cloud formation and extinction coefficient. These are the key parameters when the radiative effect of aerosol particles is estimated in global scale. Extinction coefficient is used in the calculation of aerosol direct effect, and changes in cloud droplet number concentration are causing the

so called indirect aerosol effect. We found out that reallocation can cause both under- and overestimation of the cloud droplet number concentration (CDNC) and extinction coefficient depending on the situation.

SIMULATIONS

We did two types of simulations to study the effects of reallocation to physically interesting parameters (CDNC and extinction coefficient). Both were box model simulations and had two separate aerosol distributions, one with freely moving modes and one with above described reallocation. The reallocation only affects the distribution if at least one mode is growing and has reached it threshold diameter. So both simulations have growth mechanisms (artificial and physical) for the particles. The purpose of the first simulation (case I) was to demonstrate the aerosol size and number/vertical velocity ranges where reallocation routine is causing over- or underestimation on either parameters. In case I we had a semi-realistic base distribution and we varied simultaneously the average diameter and number concentration/vertical velocity one mode at a time and calculated the CDNC and extinction coefficient for each value combination. In case II we included micro physical processes to simulate a simplified nucleation event. We were interested to see how reallocation affects the parameters during the particle growth after nucleation. The simulation included activation type nucleation, condensation, coagulation and water uptake. The particles in both simulations were composed from pure sulphate and the vertical velocity in case II for these simulations was 0.8 m/s. For CDNC calculation we used a parametrisation by Abdul-Razzak et al (2002), and libRadtran library was used for extinction coefficient calculations. In this abstract we present the second simulation and first results.

RESULTS FROM SECOND SIMULATION

Results from the case II simulation agree with the results from the case I, where we observed clear overestimation when the dominantly growing mode is in its entirety under the critical diameter. The difference of the distributions can be seen from figure 2. In the simulated nucleation event the strongest growth was in nucleation and Aitken mode and Figure 3 shows overestimation of CDNC by reallocated distribution. Figure 3 shows the CDNC and extinction coefficient in 24 hour nucleation event for freely moving and reallocated distribution. In the freely moving distribution the growth of the modes by condensation and coagulation is very slow, so the number of cloud droplets remains almost unchanged during the simulation. Small decrease in the beginning is caused by increase in the critical diameter, but the growth after five hours is fast enough to compensate that and results in slight increase of CDNC. The shape of the reallocated case is more interesting however. The first sharp increase is caused by the growth of the Aitken mode and its reallocation to accumulation mode. But the newly nucleated particles also grow and the nucleation mode reaches its threshold diameter just under five hours. The reallocation from nucleation to Aitken mode decreases the size of the Aitken mode faster than than condensation and coagulation increase its size and the reallocation to the accumulation mode stops. After ten hours the growth of the Aitken mode is again fast enough for it to grow to its threshold diameter and begin reallocating particles to accumulation mode, which is large enough to have part of its particles activated. The size range where changes happen in the distribution is small compared to the visible light wavelengths, because of this the changes in extinction coefficient are smaller but affected by the same mechanics as the cloud droplet number concentration. Slightly higher extinction coefficient from the reallocated distribution is due to higher number of accumulation mode particles.
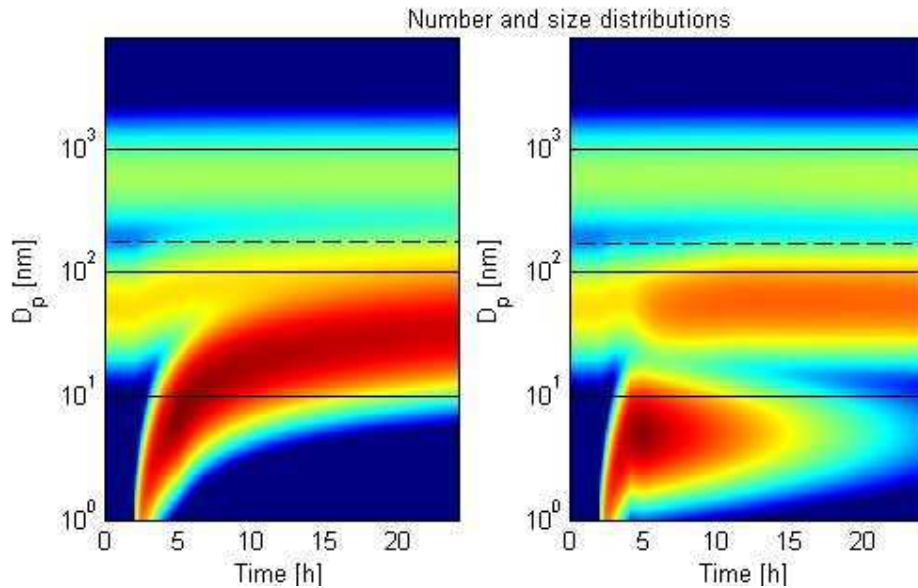
Figure 2: The number size distribution in the left panel is from the freely moving distribution, right side illustrates the effect of the reallocation. The solid lines mark the threshold diameters, and the dashed line shows the critical diameter.
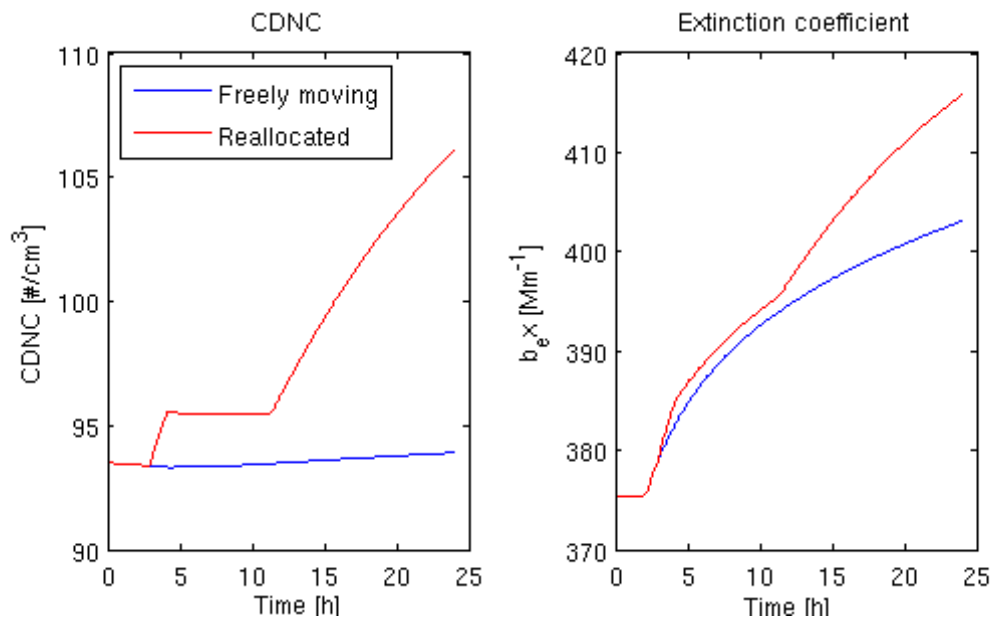
Figure 3: Left panel shows the CDNC calculated from the freely moving and reallocated distribution during 24 h simulated nucleation event. Right panel illustrates extinction coefficient for both distributions in the same event.

CONCLUSIONS

We studied the effects of reallocation of size distribution on the cloud droplet number concentration (CDNC) and extinction coefficient. We ran two different simulation types. The main difference between simulations was the growth mechanism of the particles. First simulation artificially altered the distribution and enabled us to find out how CDNC and extinction coefficient react to reallocation in wide variety of circumstances. Second simulation created a simplified nucleation event. Main motivation was to study

how CDNC and extinction coefficient behave during the growth of the particles after nucleation event. We found out that reallocation has strongest effect on the CDNC when particles in the accumulation mode are growing. The CDNC calculated from the reallocated distribution can be significantly lower compared to freely moving distribution. But relative difference in CDNC is not negligible during the Aitken mode growth either where the reallocation overestimates the number of activated particles. The changes in the extinction coefficient are strongly dependant on the initial distributions. In our simulations the relative difference of extinction coefficient varied between from -10% to 10% depending on the case. This research is not complete yet and it would be interesting to study the effects of simultaneous growth in several modes in detail to compare the opposing effects on CDNC. We haven't yet fully analysed the phenomena's affecting the extinction coefficient. Growth in large particles that affect the extinction coefficient strongly is still in progress. We are also planning to test methods to decrease the effect of reallocation, for example by allowing bigger overgrowth with the same threshold diameters, changing the definition of threshold diameters and the shape of the modes.

REFERENCES

Abdul-Razzak, H., Ghan, S. T., *A Parameterization of Aerosol Activation. Part 2: Multiple Aerosol Types.* J. Geophys. Res. D. (Atmospheres) 105:6,837-6,844, 2000

Binkowski, F., Roselle S., *Models-3 Community Multiscale Air Quality (CMAQ) model aerosol component 1. Model description.* J. Geophys. Res., 108, 4183, 18 PP, 2003

K. N. Sartelet, H. Hayami, B. Albriet & B. Sportisse, *Development and Preliminary Validation of a Modal Aerosol Model for Tropospheric Chemistry: MAM*, Aerosol Science and Technology, 40:2, 118-127, 2006

Vignati, E., J. Wilson, and P. Stier (2004), *M7: An efficient size-resolved aerosol microphysics module for large-scale aerosol transport models*, J. Geophys. Res., 109, D22202, doi:10.1029/2003JD004485, 2004

TOTAL NITROGEN DEPOSITION TO A BOREAL FOREST – ORGANIC DRY NITROGEN DEPOSITION ESTIMATED

J.F.J. KORHONEN[1], J. PUMPANEN[2] and M. PIHLATIE[1]

[1]Division of Atmospheric Sciences, Department of Physics, University of Helsinki
P.O.Box 48, FI-00014, University of Helsinki, Finland

[2]Department of Forest Sciences, P.O. Box 27, FI-00014, University of Helsinki

Keywords: WET DEPOSITION, DRY DEPOSITION, ORGANIC DEPOSITION, SCOTS PINE.

INTRODUCTION

Atmospheric deposition of nitrogen (N) has been studied intensively during the last decades. The deposition of reactive nitrogen (N_r) is linked with many environmental problems, such as eutrophication, loss of biodiversity, acidification of terrestrial and aquatic ecosystems, and health through air quality (NO_x) and quality of drinking water (NO_3^-; Sutton et al., 2011). Atmospheric N deposition is also an important source of N to forests near industrialized areas, altering the biogeochemical N cycle and boosting the forest growth.

Atmospheric N deposition consists of wet (D_w) and dry deposition (D_d), which both are within the same order of magnitude. Wet deposition is formed when water droplets scavenge aerosol particles and gas molecules from the atmosphere, and the water droplets are precipitated to ground. In dry deposition, aerosol particles or gas molecules collide with surfaces in the ground (such as plant surface). The measurement of wet deposition is challenging, because the measurement includes also some dry deposition, and thus the measured variable is often called bulk deposition (D_b). Unfortunately, D_b is not the same as the total deposition to the system, because the ratio of surface area to ground area, and other properties are different for the collector and the forest itself. Direct measurement of dry deposition is even more challenging, and usually dry deposition estimation is based on models (Flechard et al., 2011).

Traditionally the emphasis of research has been in mineral wet N deposition, although the importance of organic deposition is acknowledged and studied more recently (Neff et al., 2002; Mustajärvi et al., 2008). However, in case of dry deposition, the models are not advanced enough to include organic N deposition, and neither there are measurements of it. In this study, we present the estimation of total N deposition to a boreal Scots pine (*Pinus sylvestris*) forest in Hyytiälä, including estimation of organic dry deposition.

METHODS

We measured bulk deposition above the canopy of a young Scots pine (*Pinus sylvestris*) forest at SMEAR II station in Hyytiälä, Finland (61° 51′N, 24° 17′E). For estimating the wet-only and dry deposition, we used a time series of four years (2007-2010). Precipitation was collected to canisters via funnel, and canisters were emptied monthly in winter and once a fortnight in summer, or whenever they were getting full. No anti-microbial substances were used in the canisters. The water collection system is presented in more detail in (Ilvesniemi et al., 2010). Ammonium (NH_4^+), nitrate (NO_3^-) and total nitrogen concentrations (N_{tot}) were measured from the water samples at the Finnish Forest Research Institute, Vantaa Unit. Organic N (N_{org}) was determined using total nitrogen concentration in samples as follows

$$[N_{org}] = [N_{tot}] - [NH_4^+] - [NO_3^-], \qquad (1)$$

where the N_{org} consist of dissolved organic nitrogen (DON) and particulate nitrogen.

A simple model to fractionate the bulk deposition into wet and dry deposition was formulated based on the amount of precipitation and the period of time of dry deposition accumulation to the collector. As the result, the model gives an estimate of wet nutrient deposition to the ecosystem.

In the fractioning model the amount of nitrogen in the bulk deposition collector (D_{bc}; mg) is the sum of N in wet deposition (D_w) and N in dry deposition (D_d) and it is formulated as follows

$$D_{bc} = D_{wc} + D_{dc}, \qquad (2)$$

where subscript c refers to the chemical form of nitrogen (NO_3^--N, NH_4^+-N or N_{org}).

We assumed that nitrogen concentration in precipitation is constant and thus wet deposition collected into the sampling canister (D_{wc}; mg) is

$$D_{wc} = c_{wc}V_b, \qquad (3)$$

where unknown parameter c_{wc} is concentration of the nutrient in precipitation (mg dm^{-3}) and V_b is total water volume in the collector (dm^3) and subscript c refers to the chemical form of nitrogen (NO_3^--N, NH_4^+-N or N_{org}).

We further assumed that dry deposition (D_{dc}; mg) is only dependent on time and thus is

$$D_{dc} = \beta t, \qquad (4)$$

where unknown parameter β is dry deposition constant (mg day^{-1}), t is the length of the accumulation of dry deposition to the collector (days) and subscript c refers to the chemical form of nitrogen (NO_3^--N, NH_4^+-N or N_{org}). Vaisala DRD12 optical rain detector (Vaisala Oyj, Helsinki, Finland) was used to calculate t. Each moment in time any rain was measured, the days between the current and previous rain event were calculated. The amount of flushing events and accumulated days were calculated for each collection period

By combining Eqs. (2, 3 and 4), we can formulate the model as follows

$$D_{bc} = c_{wc}V_b + \beta t, \qquad (5)$$

In the equation the volume of the water sample (V_b), m_c and t were measured, and c_{wc} and β were the unknown parameters. Equation 5 was fitted to data from 2007 to 2010 for N_{org}, NH_4^+-N and NO_3^--N by changing c_{wc} and β. The fit and wet deposition calculation was done separately for summer and winter, because the collectors were different and in winter major part of the precipitation was snow. The wet deposition (D_w, kg N ha^{-1} yr^{-1}) amount was calculated as follows,

$$D_{wc} = \frac{c_{wc}V_b}{\beta t + c_{wc}V_b} D_{bc} \equiv \alpha D_{bc}, \qquad (6)$$

where α is the fraction of wet deposition of the bulk deposition (0…1).

A mean of the dry deposition of four models presented in Flechard et al. (2011) for Hyytiälä were used as an estimate of dry deposition. When this dry deposition data was used in conjunction with the measured bulk deposition data from this study, the modelled aerosol particle NH_4^+ and gaseous NH_3^+ deposition were coupled with the bulk NH_4^+ deposition, and modeled aerosol particle NO_3^- and gaseous NO_2 and HNO_3 deposition were coupled with the bulk NO_3^- deposition.

Organic N dry deposition was calculated by multiplying the ratio of organic and mineral dry deposition to the collector with the estimated mineral N dry deposition to the forest.

RESULTS AND DISCUSSION

The total atmospheric deposition was 7.4 kg N ha^{-1} yr^{-1} (Table 1). Approximately 60% of the deposition was dry deposition and approximately 40% was wet deposition. Although the deposition was mainly in mineral form, the organic fraction was also relatively high, being 0.32 and 0.24 of the total wet and dry N deposition, respectively.

Bulk deposition measurement overestimated wet deposition by 43%, and underestimated the total deposition by 34%. Thus, bulk deposition measurement is only indicative estimate of the total deposition. The underestimation was highest for NH_4^+ (and NH_3) and lowest for N_{org}.

Based on model predictions by (Flechard et al., 2011), NO_3^-, NO_2 and HNO_3 together comprise over 54% of the total dry deposition. The representative value of our analysis shows contribution of 45%. Respectively, the contribution of NH_4^+ and NH_3 is lower in our study. The results are not far from each other, taken into account the uncertainties in the measurements, our analysis, the input data and the models used in Flechard et al. (2011).

Table 1. The components of atmospheric nitrogen deposition. Wet deposition is estimated from bulk deposition measurement by linear regression (Eq. 6) assuming that dry deposition is independent from time, and that nitrogen concentration in wet deposition is constant. The estimated composition of dry deposition is based on the fractions of dry deposition collected in bulk deposition collector.

	NH_4^+	NO_3^-	N_{org}	Total
Measured bulk deposition (D_b; kg N ha^{-1} yr^{-1})	1.3	2.1	1.5	4.9
Estimated wet deposition ($D_w = \alpha D_b$; kg N ha^{-1} yr^{-1})	0.7	1.2	0.9	2.8
Modelled / estimated dry deposition (D_d; kg N ha^{-1} yr^{-1})*	1.0*	2.5*	1.1	4.6
Estimated total deposition ($D_{tot} = D_d + D_w$; kg N ha^{-1} yr^{-1})	1.7	3.7	2	7.4
Bulk deposition correction factor (α)	0.52	0.57	0.63	0.57
D_d overestimation of D_w ($(1-\alpha)D_b$; kg N ha^{-1} yr^{-1})	0.48	0.43	0.37	0.43
Estimated composition of dry deposition	32 %	45 %	23 %	100 %

*Flechard et al. (2011). NH_4^+ and NH_3 are combined as NH_4^+ and NO_3^-, NO_2 and HNO_3 are combined as NO_3^-.

Our simple model was able to predict nutrient concentrations in the collector relatively well (Fig. 1). The residual plots (not shown) do not show strong bias in the fit. There are other variables than time and amount of precipitation explaining the dry deposition to the bulk deposition sampler, and thus the model does not give accurate estimations for short periods of time. However, we assume that the model does give reasonably accurate average value for longer time periods. The calculation requires relatively many data points to be reliable, practically several years of data. The method is suitable for estimating deposition in time scale of a year or longer. For shorter time-scales it is quite useless.

The presented approach allows separating measured bulk deposition into wet deposition estimate. The approach also gives the composition of dry N deposition to the collector. The physical and chemical properties of the collector and the forest are different. This is not a problem, as long as the difference affects the measured compounds similarly. The method does not necessary require any changes to be made to the collection system, but the systematic errors can be reduced with correct material choices. In any case, the long datasets (such as the EMEP dataset) could be analyzed for more precise wet deposition estimations.

No anti-bacterial substances were used in the collectors. Therefore, it is possible that mineral N was transformed into organic N in the collector during the two-week collection period. If this was the case, the

N_{org} concentration in the collector should have increased at a higher rate than mineral N as a function of the length of the collection period. However, we did not observe this, and therefore we assume that the observation of s significant amount of organic dry N deposition was real.
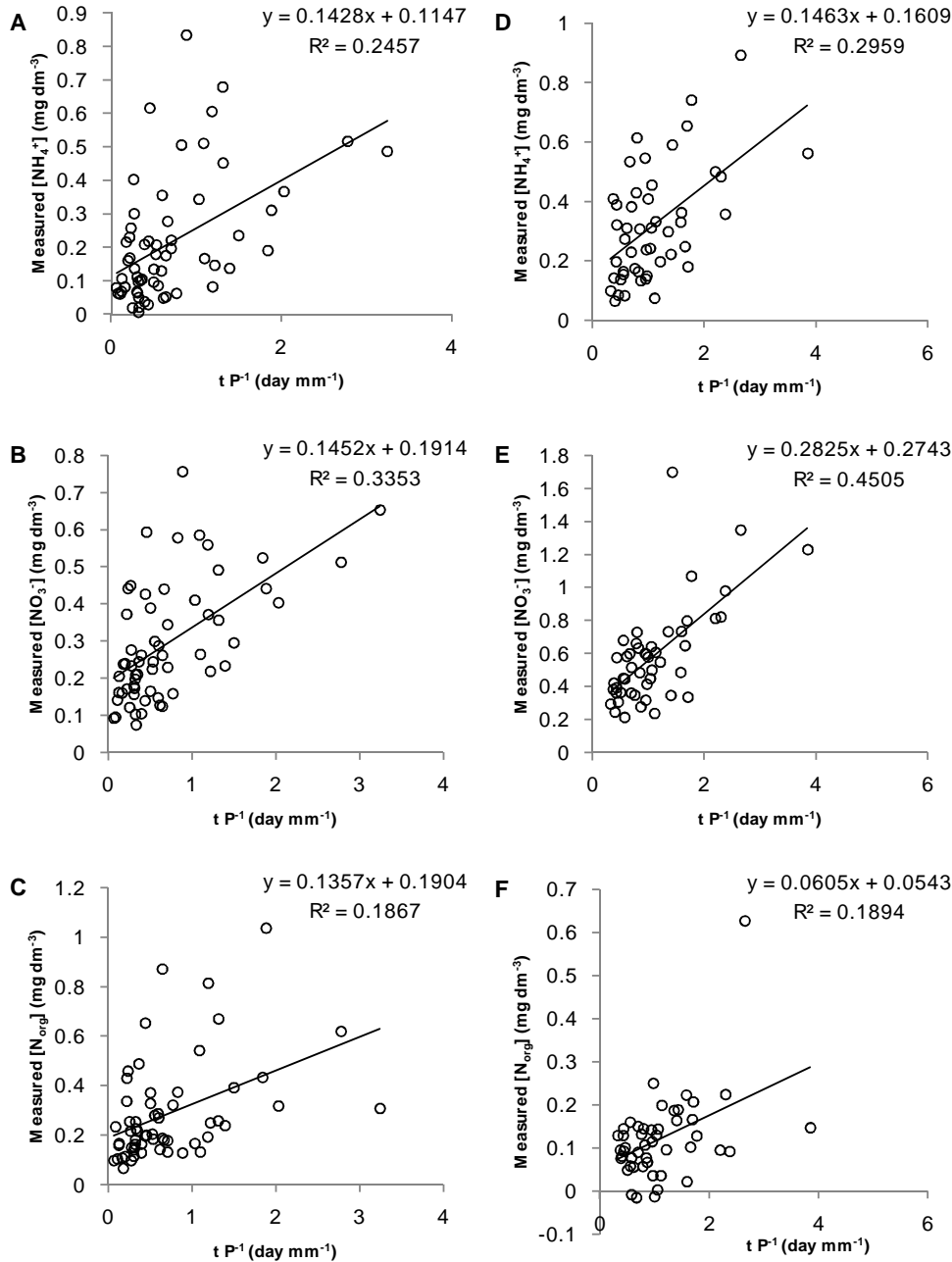
Figure 1. Modeled bulk deposition rate based on time (t) and precipitation (P). The column at left (A, B and C) is for summer deposition measurement, measured using a funnel. The column at right (D, E and F) is for winter (snow) deposition measured, measured using a bucket. First row (A and D) is NH_4^+-N, middle row (B and E) is NO_3^--N and the last row (C and F) is N_{org}. The first order parameter describes how much dry deposition contributes to the measured concentration and the zero order parameter is average concentration of NH_4^+-N, NO_3^--N or N_{org} in wet deposition. The negative values of N_{org} are due to measurement noise (see Eq. 1).

CONCLUSIONS

The bulk deposition measurement can overestimate wet nitrogen deposition markedly. Using the approach presented in this study, it is possible to quantify this overestimation. In addition, the approach gives information on the composition of dry deposition. With existing estimation of mineral N dry deposition rates, also organic N dry deposition can be estimated. The results suggest that organic N deposition can contribute significantly to the total N deposition. The method works on time scale of a year or longer. In combination with dry deposition models and long bulk deposition data-series, it could be used to improve the estimations of wet and total deposition in the past and present climate.

ACKNOWLEDGEMENTS

REFERENCES

Flechard, C. R., Nemitz, E., Smith, R. I., Fowler, D., Vermeulen, A. T., Bleeker, A., Erisman, J. W., Simpson, D., Zhang, L., Tang, Y. S., and Sutton, M. A.: Dry deposition of reactive nitrogen to European ecosystems: a comparison of inferential models across the NitroEurope network, Atmos Chem Phys, 11, 2703-2728, DOI 10.5194/acp-11-2703-2011, 2011.

Ilvesniemi, H., Pumpanen, J., Duursma, R., Hari, P., Keronen, P., Kolari, P., Kulmala, M., Mammarella, I., Nikinmaa, E., Rannie, U., Pohja, T., Siivola, E., and Vesala, T.: Water balance of a boreal Scots pine forest, Boreal Environ Res, 15, 375-396, 2010.

Mustajärvi, K., Merila, P., Derome, J., Lindroos, A. J., Helmisaari, H. S., Nojd, P., and Ukonmaanaho, L.: Fluxes of dissolved organic and inorganic nitrogen in relation to stand characteristics and latitude in Scots pine and Norway spruce stands in Finland, Boreal Environ Res, 13, 3-21, 2008.

Neff, J. C., Holland, E. A., Dentener, F. J., McDowell, W. H., and Russell, K. M.: The origin, composition and rates of organic nitrogen deposition: A missing piece of the nitrogen cycle?, Biogeochemistry, 57, 99-136, 2002.

Sutton M.A., Howard C.M., Erisman J.W., Billen G., Bleeker A., Grennfelt, P., van Grinsven, H., Grizzetti, B. (Eds). The European Nitrogen Assesment – Sources, Effects and Policy Perspectives. Cambridge University Press, Cambridge, U.K., 2011.

REAL-TIME CHEMICAL COMPOSITION ANALYSIS OF PARTICLE EMISSIONS FROM WOODCHIP COMBUSTION

A. KORTELAINEN[1], J. JOUTSENSAARI[1], A. JAATINEN[1], P. MIETTINEN[1], L. HAO[1], D. R. WORSNOP[1,3,4], J. JOKINIEMI[2], A. LAAKSONEN[1,3] and A. VIRTANEN[1]

[1]Department of Applied physics, University of Eastern Finland, Kuopio, 70211, Finland.
[2]Department of Environmental Science, University of Eastern Finland, Kuopio, 70211, Finland.
[3]Finnish Meteorological Institute, Climate change, Helsinki, 00101, Finland.
[4]Aerodyne Research Inc., Billerica, MA, 01821, USA.

Keywords: aerosol, wood combustion, chemical composition, aerosol mass spectrometer.

INTRODUCTION

Residential wood combustion produces high amounts of gaseous and particulate emissions into atmosphere. The crucial particulate products, ash, carbon and alkali metals (Tissari, 2009), cause commonly known climate and health effects, and therefore it is important to understand the evolution of different chemical compounds during wood combustion. In recent studies, the chemical composition of particulate emissions from residential wood combustion has been analyzed mainly using filter sampling. However, these methods have poor temporal information from aerosol composition in rapidly changing circumstances. This study's goal is to open the time-dependent knowledge of aerosol particles chemical composition in different combustion situations.

METHODS

The experiments were performed by burning wood chips in a grate fired burner (40 kW) under controlled combustion conditions, and measuring the emission products with dilution ratio of 600 to 1000 regulated by the emission yield. The experiments were divided into efficient, medium and poor combustion conditions by the emission rates of CO (low, elevated and high, respectively). Real-time size-dependent chemical composition of aerosol particles was measured by Aerodyne HR-TOF-AMS (High Resolution Time-Of-Flight Aerosol Mass Spectrometer) using typical 600°C vaporizer temperature (Decarlo et al., 2006). In addition O/H/V-TDMA (Organic/Hygroscopic/Volatilization-Tandem Differential Mobility Analyzer) and CCNC (Cloud Condensation Nuclei Counter) measurements were carried out for getting better approach to particulate properties (volatilization, hygroscopicity and organic content). Detailed descriptions from instruments can be found from Joutsensaari et. al., 2001 (O-TDMA), Hämeri et al., 2000 (H-TDMA), Burtscher et al., 2001 (V-TDMA) and Roberts and Nenes, 2005 (CCNC).

CONCLUSIONS

Aerosol mass spectrometer found nitrate, chloride, sulphate, polycyclic aromatic hydrocarbons (PAH) and organics, which were divided into smaller subgroups by positive matrix factorization (PMF) (Ulbrich, 2009). Organics were split into formerly reported factors HOA (Hydrocarbon-like Organic Aerosol) and OOA (Oxygenated Organic Aerosol) and new factors named "Aromatics" and "Benzene". The proportion of each chemical compounds are presented in table 1.

Compound	Med. Combustion (%)	Poor combustion (%)
HOA	43	8
OOA	15	6
Aromatics	0	24
Benzene	12	26
PAH	0	31
SO$_4$	23	0
Chl	7	5

Table 1. Relative abundance of the chemical compounds for experiments.

In the mass spectrum of HOA, highest peaks were C2H3O, C4H7, C4H9 and included notable hydrocarbon series (i. e. CnH2n±1) with O/C ratio of 0.1. For OOA, the highest peaks were CO and CO2, and O/C ratio was 0.75. Benzene spectrum had a remarkably high contribution of C6H5 and C5H3NO4 and O/C ratio was 0.19. The peak of C6H5 was thought to be originating from the particles produced from the split of aromatic hydrocarbons contained aromatic ring retaining products. Aromatics had high contribution in hydrocarbon series of Cn+5Hn+1,n = 1,..,4, which were thought to be doubly charged ions from PAH and O/C ratio was 0.23. Aromatics had good correlation with PAH compounds in poor combustion.

Particles were not detectable in AMS at efficient combustion conditions due to their small size and low mass concentration of vaporized products in 600°C. In medium combustion conditions main constituents were HOA, SO4, OOA, Benzene and Chl whereas in poor combustion there were also PAH and Aromatics present simultaneously with constantly occurring CO/NOx plumes. In the case of poor combustion, SO4 was almost negligible and small amounts of nitrate (mainly NO fragment) were found. No ammonium was detected, hence we conclude that NO was originated mainly from organics.

The mechanic operation of the grate fired burner added new wood chips at every 20 minutes and changed the burning conditions in a way that concentrations of gaseous CO/NOx rapidly increased to high values for approx five minutes. The chemical reactions occurring at the time had an influence on oxidation level and organic content of particles in way that oxidation increased at that time and also concentration of PAH got higher. The average composition of the particles in poor circumstances was investigated during the CO peaks and outside of the peaks, during regular burning conditions. It was found that Aromatics and PAH clearly formed during the CO peaks as shown in table 2. In addition, OOA and Chl are increasing at the same time, while they also exist outside the peak. Benzene is the only organic factor that is higher outside the peaks and therefore it may not depend that much on chemical reactions that happen during the addition of woodchips in grate fired burner.

Compound	Average mass conc., std and relative abundance.	
	during peak (µg/m^3)	outside of peak (µg/m^3)
HOA	1.9 ± 1.5 (7.1 %)	0.5 ± 1.0 (5.0 %)
OOA	3.2 ± 2.0 (12.0 %)	0.7 ± 0.5 (6.9 %)
Aromatics	7.6 ± 10.0 (28.6 %)	0.4 ± 0.4 (4.0 %)
Benzene	3.7 ± 3.7 (13.9 %)	7.1 ± 5.1 (70.3 %)
PAH	8.6 ± 14.0 (32.3 %)	0.6 ± 0.5 (5.9 %)
SO$_4$	0.3 ± 0.6 (1.1 %)	0.0 ± 0.2 (0 %)
Chl	1.3 ± 0.4 (4.9 %)	0.8 ± 0.4 (7.9 %)

Table 2. Average mass concentrations and standard deviations (std) of compounds during and outside of gaseous CO peaks in poor combustion.

Organic growth factors from 100 nm particles show that particulate organic content increase when the combustion conditions are getting worse from efficient to poor. Similar way the hygroscopisity of particles decrease from efficient to poor suggesting that the organic content increase. In efficient combustion CCNC show that particles form, activate, cloud condensation nuclei easily suggesting that the particles are inorganic salts. Also critical diameters of $(NH_4)_2SO_4$ are in good agreement with measured critical diameters of efficient combustion results. The most volatile particles are in poor combustion and growth factor of 0.95 suggests that roughly 15 % of particle mass evaporate in 280°C.

In efficient combustion the products are mainly inorganic salts, metals and ash compounds. In future it might be useful to measure efficient as well as the other burning conditions with AMSs 800°C vaporizer temperature to get more information from different inorganic salts, that didn't vaporize at the used temperature.

ACKNOWLEDGEMENTS

REFERENCES

Burtscher, H. et al., Separation of volatile and non-volatile aerosol fractions by thermodesorption: instrumental development and applications, Journal of Aerosol Science, 32:427-442, 2001.
DeCarlo P. F. et al., Field-Deployable, High-Resolution, Time-of-Flight Aerosol Mass Spectrometer, Analytical Chemistry, 78:8281-8289, 2006.
Hämeri, K. et al., Hygroscopic growth of ultrafine ammonium sulphate aerosol measured using an ultrafine tandem differential mobility analyzer, Journal of Geophysical Research, 105(D17), 22,231–22,242, 2000.
Joutsensaari J. et al.,A novel tandem differential mobility analyzer with organic vapor treatment of aerosol particles, Atmospheric Chemistry and Physics, 1, 51-60, 2001.
Roberts, G., and A. Nenes (2005), A continuous-flow streamwise thermalgradient CCN chamber for airborne measurements, Aerosol Sci. Technol., 39, 206–221.
Tissari, J. Atmospheric Environment, 42, 7862-7873, 2009.
Ulbrich, I.M. Atmospheric Chemistry and Physics , 9(9), 2891-2918, 2009.

ARCTIC OCEAN PRIMARY MARINE AEROSOL PROPERTIES

R. KREJCI[1,2], J.ZABORI[1], J. STRÖM[1], A. EKMAN[3], P. VAATTOVAARA[4], G. DE LEEUW[2,5], E.M. MÅRTENSSON[1,6] and E.D. NILSSON[1]

[1]Department of Applied Environmental Science (ITM), Stockholm University, S 106 91 Stockholm, Sweden.
[2]Department of Physics, University of Helsinki, FI-00014 Helsinki, Finland.

[3]Department of Meteorology, Stockholm University, S 106 91 Stockholm, Sweden.

[4]Department of Applied Physics, University of Eastern Finland, FI-70211 Kuopio, Finland.

[5]Finnish Meteorological Institute, Climate Change Unit, FI-00101 Helsinki, Finland.

[6]Department of Earth Sciences, Uppsala University, SE-752 36 Uppsala, Sweden.

Keywords: PRIMARY MARINE AEROSOL, ARCTIC, CLIMATE

INTRODUCTION

Primary marine aerosols (PMA) are an important source of cloud condensation nuclei and a key element of the remote marine radiative budget. Changes occurring in the rapidly warming Arctic, namely the decreasing sea ice extent, will alter PMA production and through a set of feedbacks will modulate the Arctic climate. There is not much known about the effects on sea spray emissions from changes in the physical properties of sea water in the Arctic Ocean region. In light of this, laboratory experiments with Arctic Ocean water during both Arctic winter and summer were conducted and focused on PMA emissions as a function of seasonality and sea water properties (Zábori et al, 2012).

METHODS

Laboratory experiments using Arctic Ocean sea water were carried out at Ny-Ålesund (78° 55´ N, 11° 56´ E), western Svalbard in a marine laboratory during late Arctic summer conditions (from the 24th August to the 7th of September 2009) and late Arctic winter conditions (from the 15th of February to the 7th of March 2010). Sampling locations were selected to account for outer and inner fjord conditions, where the latter was influenced by glacial melt water. During summertime, water outside the fjord mouth was sampled by boat, while the sampling took place from the coastline at the north-west side of the peninsula during winter conditions. In the inner part of Kongsfjorden, close to the glacier, water was sampled by boat during both seasons. In the laboratory, a deep water inlet is permanently installed. Thus, experiments with deep fjord water were also conducted during both campaigns.

Collected sea water was poured into a storage stainless steel tank situated in the laboratory. From the steel tank the water was pumped into a carefully sealed polyethylene bottle (Nalgene Labware) using an aquarium centrifugal pump. The water entered the bottle through a stainless steel nozzle producing a water jet mimicking a wave crest which entrains air into sea water. To avoid any contamination by room air, clean air was pumped through a particle filter resulting in particle free air into the PET bottle. The total aerosol number concentration was measured at 1 Hz for particles with a $D_p > 0.01$ μm using a TSI model 3010 Condensation Particle Counter (CPC) and for particles with a $D_p > 0.25$ μm using a GRIMM 1.109 Optical Particle Counter (OPC). The size distribution for the size range 0.01 μm $< D_p <$ 0.30 μm was determined using a closed-loop sheath air custom-built differential mobility particle sizer (DMPS) equipped with a TSI 3010 CPC. One scan covering 15 size bins was completed in 2.5 minutes. The aerosol size distribution in the range 0.25 $< D_p <$ μm 32 μm was determined every 6 seconds with a GRIMM 1.109 Optical Particle Counter (OPC), sizing particles in 31 bins. The relative humidity of the

sampled air was monitored in the sampling line prior to entering individual instruments. Due to the clean air supplied to the tank, the relative humidity during the experiments was lower than 40 % (winter and summer). For a comparison of the winter and summer total particle number concentration data, total particle number concentration medians were calculated for 1 °C temperature bins for each different water type. To compare summer and winter particle number size distributions, median number size distributions were calculated for overlapping water temperature (T_w) ranges for the different water types.

CONCLUSIONS

Median particle number concentrations for both $D_p > 0.01$ µm and $D_p > 0.25$ µm as a function of water temperature were compared for summer and winter measurements for the three different sampling locations (Figure 1).
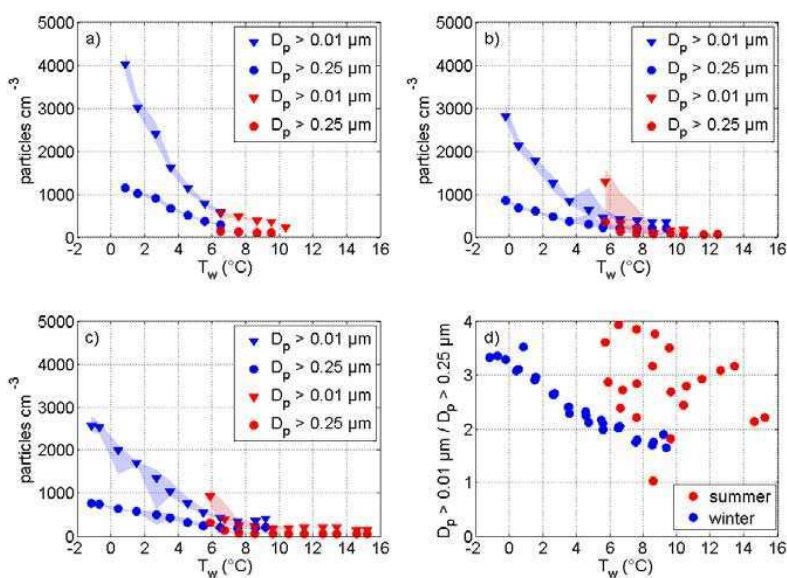
Figure 1. The median particle number concentrations as a function of water temperature (T_w). Blue data points represent winter data and red data points summer data with triangles for particles $D_p > 0.01$ µm and circles for particles with $D_p > 0.25$ µm. Blue and red shaded areas represent the interquartile ranges. Particle number concentrations resulted from bubble bursting in a) deep water b) water sampled close to glacier c) water sampled at the fjord mouth d) ratio between particle number concentration of particles $D_p > 0.01$ µm and $D_p > 0.25$ µm. The ratios were built for each data point shown in a – c.

In addition, the dependency on water temperature of the resulting ratio between particles $D_p > 0.01$ µm and $D_p > 0.25$ µm was compared for summer and winter conditions (Figure 1d). Three patterns can be observed: (i) particle number concentrations decrease with increasing T_w up to a water temperature of about 5 – 7 °C (4 – 5 time decrease from about 1 °C to 6 °C for all different water types and $D_p > 0.01$ µm) and stay relatively constant for higher water temperatures; (ii) in general, no distinct concentration shift for particles with $D_p > 0.01$ µm between the summer and winter measurements can be observed in the overlapping temperature bins; (iii) for overlapping water temperature ranges, summer measurements show on average a ratio of three and winter measurements a ratio of two for particle concentrations of $D_p > 0.01$ / $D_p > 0.25$ µm.

Even if the dependency of particle number concentrations on water temperature is consistent for winter and summer measurements, summer particle number concentrations for $D_p > 0.01$ µm are about $2 - 3$ times higher than the particle number concentrations recorded during winter for the lowest overlapping temperature bin (T_w between 5 °C and 6 °C). This is observed for water sampled close to the glacier and at the fjord mouth. However, it should be noted that the inter-quartile range is relatively large (Figure 1b,c). For overlapping water temperature bins, median particle number concentrations resulting from water sampled during summer time are similar or up to 70 % higher for particles with $D_p < 0.125$ µm. For $D_p > 0.125$ µm, the particle number concentrations during winter were mostly higher than in summer (up to 50 %). During both seasons, a decrease in the relative particle number concentration for D_p $0.100 - 0.300$ µm with increasing T_w is observed. At the same time, a relative increase of particles with $D_p > 1$µm and $D_p < 0.100$ µm is observed for winter and summer measurements, respectively.

The decrease in Arctic sea ice extent due to the current warming will be followed by changes in a number of different processes, which eventually will lead to different feedbacks. Figure 2 displays a potential feedback loop. It is likely far from showing the complete picture. Our ambition is to focus on processes related to PMA production and changes in sea ice cover. The impact of processes related to secondary marine aerosol production, e.g. changes in DMS emissions, is not considered.
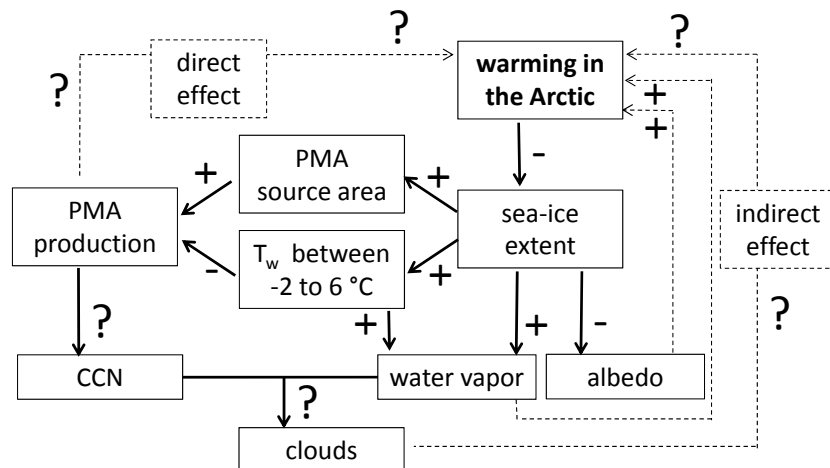
Figure 2. Potential feedback loop resulting from a warming in the Arctic. Plus signs indicate increases and minus signs indicate decreases.

ACKNOWLEDGEMENTS

REFERENCES

Zábori, J., R. Krejci, A. M. L. Ekman, M. Mårtensson, J. Ström, G. de Leeuw, E. D. Nilsson (2012): Wintertime Arctic Ocean sea water properties and primary marine aerosol concentrations, *Atmos. Chem. Phys. Discuss.*, 12, pp: 16085-16130

RESPONSES OF LARIX GMELINII RADIAL GROWTH TO CLIMATE IN CONTRASTING NORTH- AND SOUTH-FACING SLOPES IN CENTRAL SIBERIA

J. KUJANSUU[1,2], K. YASUE[2], T. KOIKE[3], A.P. ABAIMOV[4], T. VESALA[1] and Y. MATSUURA[5]

[1] Department of Physics, University of Helsinki, Finland

[2] Department of Forest Science, Faculty of Agriculture, Shinshu University, Japan

[3] Field Science Center for Northern Biosphere, Hokkaido University, Japan

[4] Sukachev Institute of Forest, Siberian Branch, Russian Academy of Science, Russia

[5] Forestry and Forest Products Research Institute, Tsukuba, Japan

INTRODUCTION

Siberian boreal forests account for 20% of the world forest area and are mainly dominated by deciduous *Larix* species. Thus, responses of Siberian larch forest to climate change can have a significant effect on carbon fixation in terrestrial ecosystem. We compared the growth responses of tree-ring widths and maximum densities to air temperature and precipitation on contrasting north- and south-facing slopes to clarify the impact of future changes in climate on the radial growth of *Larix gmelinii* (Rupr.) Rupr. growing on permafrost in central Siberia.

METHODS

Research was performed in Tura, central Siberia ($64^o19^{'}$N, $100^o16^{'}$E). An analysis was performed of the climatic responses of radial growth of *L. gmelinii* at two sites with the development of ring width and maximum density chronologies. Thirty sample trees per plot were chosen and two cores were extracted from each tree on site 1. Tree-ring width series were cross-dated visually and statistically to ensure that the correct date is assigned to each annual ring. Tree-ring widths were measured at 0.01 mm precision. Measurement series were standardized by fitting a cubic smoothing spline to extract climatic signals. Autoregressive modeling was used to remove the effect of autocorrelation from the standard series. Residual and standard chronologies were developed by averaging individual series. Relationships between chronologies and average daily mean temperatures for 10 consecutive days from 1930 to 1995 (n=65) were used in the analysis with 2 days lag starting from previous year 1st of May. Relationships between winter (October-

April) and May precipitation (divided to early, middle and late part of the month) and monthly precipitations from June to September from 1939 to 1995 (n=56) were also used.

To assess the climatic responses of maximum density and to confirm responses of ring width on the other location with different site conditions, site 2 was established at the following year on the north- and south-facing slope at 30 km away from site 1. Thirty dominant trees per plot were chosen and disks were cut. Ring widths and maximum densities were measured by X-ray densitometry for both sites, after which measurement series were cross-dated visually and confirmed statistically. Residual and standard chronologies of ring width and maximum density were developed for each slope on both sites. Responses of tree-ring parameters to air temperature and precipitation were analyzed by calculating the simple correlations between the chronologies and climate variables.

Ring widths were positively correlated with temperature from late May until mid June on all four slopes. Ring widths of standard chronologies were negatively correlated with precipitation during the winter and in May on the north-facing slope at site 1 and on the south-facing slope at site 2, respectively. Maximum densities of tree rings were positively correlated with temperature in early July on all four slopes. Maximum densities were also positively correlated with precipitation during August of the previous year on all the slopes with the exception of the north-facing slope of site 1.

Observation on snow-melt and leaf development revealed that snow-melt in the spring of 2004 occurred on 19 May on the south-facing slope and on 25 May on the north-facing slope of site 1. Leaf flushing occurred at the 25 May and leaf development continued until the middle of June.

CONCLUSIONS

Our results demonstrate that air temperatures from the middle of May through the middle of July are the most important determinant of the radial growth of *L. gmelinii* under central Siberian permafrost conditions. Neither ring widths nor maximum densities exhibited any major differences in terms of responses to air temperature between the north- and south-facing slopes, whereas both tree-ring parameters exhibited site-specific responses to winter precipitation. The period that revealed significant correlation between ring width and temperature coincided with the observed leaf flushing and subsequent stages of leaf development. The difference in response to precipitation between the slopes on site 1 can be attributed to one week difference in snow-melt date. Still, the responses of ring widths on site 2 are opposite to site 1. The results suggest that the effects of snow are likely to vary with topography and the accumulation of snow. The fore-casted increase in winter precipitation and spring and early summer temperatures possess high potential to influence carbon fixation of Siberian larch forest, however, the effect of each variable are in contrast.

ACKNOWLEDGEMENTS

REFERENCES

Kirdyanov, A.V., Hughes, M.K., Vaganov, E.A., Schweingruber, F.H. and Silkin, P. (2003). The importance of early summer temperature and date of snowmelt for tree growth in the Siberian subarctic. Trees 17, 61-69.

Kobak, K.I., Turchinovich, Y.E., Kondrasheva, Y.U., Schulze, E.D., Schulze, W., Koch, H. and Vygodskaya, N.N. (1996). Vulnerability and adaptation of the larch forest in eastern Siberia to climate change. Water, Air, and Soil Pollution 92, 119-127.

Koike, T., Mori, S., Matsuura, Y., Prokushkin, S.G., Zyranova, O.A., Kajimoto, T. and Abaimov, A.P. (1998). Photosynthesis and foliar nutrient dynamics in larch and spruce grown on contrasting north- and south-facing slopes in the Tura Experiment Forest in Central Siberia. In: Mori, S., Kanazawa, Y., Matsuura, Y. and Inoue, G. [eds.] Proceedings of the 6th symposium on the joint Siberian permafrost studies between Japan and Russia in 1997. pp. 3-10.

Schweingruber, F.H. (1996). Tree Rings and Environment: Dendroecology. Birmensdorf, Swiss Federal Institute for Forest, Snow and Landscape Research. Berne, Stuttgart, Vienna, Haupt.

Vaganov, E.A., Hughes, M.K., Kirdyanov, A.V., Schweingruber, F.H. and Silkin, P.P. (1999). Influence of snowfall and melt timing on tree growth in subarctic Eurasia. Nature 400, 149-151.

CHANGES IN PHYSICAL AND CHEMICAL SOIL PROPERTIES AFTER A CLEAR CUT AND PRESCRIBED BURNING OF SLASH IN A BOREAL SPRUCE FOREST

L. KULMALA[1], H. AALTONEN[1], J. KORHONEN[2], M. PIHLATIE[2], J. PUMPANEN[1], J. LEVULA[3] and E. NIKINMAA[1]

[1]Department of Forest Sciences, P.O. Box 27, FIN-00014, University of Helsinki, Finland.

[2]Department of Physics, University of Helsinki, Finland.

[3]Hyytiälä forestry field station, University of Helsinki, Juupajoki, Finland.

Keywords: pH, soil temperature, soil moisture, nitrate, ammonium

INTRODUCTION

Wildfire is a natural part of forest ecology disturbing forest succession. In Fennoscandia, wildfires are effectively eliminated during the life span of a forest stand, which possibly increases the amount of soil organic matter in the humus layer in the long run (Wardle *et al.*, 1997). The thick humus layer could result in inefficient seeding and seedling establishment upon forest regeneration. Therefore, prescribed burning of slash and other residuals from logging is sometimes used to ease the seedling establishment by reducing the competition of ground vegetation and releasing important nutrients in the soil. Nowadays, also biodiversity issue, i.e. creating habitat for endangered species, has become more important, because efficient fire protection has decreased the area of forest fires in Fennoscandia. Successional patterns and the carbon stocks after prescribed burning are well studied, but the consequences of prescribed burning and natural forest fires on the greenhouse gas fluxes following burning of slash are still relatively poorly known.

A clear cut removes trees and thereby eliminates most of the above- and belowground carbon input whereas a prescribed burning eliminates the ground vegetation and decrease the amount and alter the quality of organic matter in the soil. After the removal of the above canopy, soil is exposed to higher solar irradiation that increases soil temperature. The effect is even greater on the burnt surface due to lack of buffering ground vegetation and due to darkened colour leading to smaller albedo compared with a clear-cut site (O'Halloran *et al.*, 2012; Certini, 2005). Besides, wildfire or burning of slash is an enormous disturbance affecting also many other physical, chemical and biological soil properties such as the quantity and quality of organic matter (Certini, 2005), the availability of nutrients (Johnson *et al.*, 2007; Grady and Hart, 2006; Covington and Sackett, 1992), soil temperature (Takakai *et al.*, 2008), pH (Certini, 2005), moisture (Yoshikawa *et al.*, 2003), microbial biomass (Pietikäinen and Fritze, 1995) and microbial species composition (Malmström *et al.*, 2009). All of these are well-known factors determining soil greenhouse gas emissions.

The aim of this study was to quantify the changes taking place in soil following clear-cutting and prescribed burning. In order to study these effects, we measured soil temperature and moisture continuously and with regularity soil pH, the carbon and nitrogen content and the nitrogen compounds in 1) a mature spruce forest, 2) a clear cut spruce forest, and in 3) a clear cut and burnt spruce forest.

METHODS

The experimental site was a spruce (*Picea abies* (L.*)* Karst.) forest near the station for measuring ecosystem-atmosphere relations (SMEARII, Hari and Kulmala, 2005), southern Finland (61.52 N, 24.17 E). During the period from 1960 to 1990, the annual mean temperature was +2.9ºC and precipitation, 709 mm. January was the coldest month (mean −8.9ºC) and July the warmest (mean +15.9ºC). The

experimental site belongs to Myrtillus site type (MT) in the Finnish Classification system (Cajander,1926) with a sparse occurrence of peat. The stem volume was app. 400 m^3 ha^{-1}. Most common species on the forest floor are *Pleurozium schreberi*, *Maianthemum bifolium*, *Dicranum polysetum*, *Vaccinium myrtillus*, *Deschampsia flexuosa* and *Hylocomium splendens*.

1.5 ha of the site was clear cut in February 2009. The merchantable stem wood was collected but all slash was left on the site. The biomass of the above ground slash was 47 000 kg ha^{-1}. In June 2009, 0.81 hectare of the clear cut area was burnt resulting in three different treatments: a mature control forest, a clear cut site, and a clear cut and burnt site (Figure 1).

After burning we sampled the amount of unburned wood from 21 0.5m^2 plots. All the wood was collected from the plots, dried (24h, 105 °C) and weighted. The amount of burned tree biomass was calculated as extraction of the non merchantable tree biomass (tree tops, branches and non merchantable trees) and unburned wood biomass.

The soil temperature measurements started in early June 2008 before the treatments with two identical set of measurements, both including two PT100-sensors in humus layer and two in A-horizon. The other set was positioned on an area that was later clear cut whereas the other set was on an area that was clear cut, but also burnt. Data was gap-filled by linear relationship between the prevailing measurements and the soil temperature measurements under closed canopy at the SMEAR II station at the same depths. The linear relationship was determined for each year. The soil temperatures at the control site was measured with iButtons® (Maxim Integrated products Inc., Sunnyvale, CA). Soil moisture was estimated from a regression between the moisture content of manual soil samples and automatic soil moisture measurements of SMEARII site (Ilvesniemi et al. 2010).

Soil samples were collected from all study sites once before the treatments, once after the clear cut and seven times after the burning. We collected two separate samples from four different soil horizons (litter layer, humus layer, 0–10 cm and 10–30 cm deep in mineral soil) at two separate sample plot at each treatment (i.e. n=4). The soil samples for analysing total carbon and nitrogen content were pooled by layer and analysed by Vario MAX CN elementar analyser (Elementar Analysensysteme, Germany). The four individual samples of available ammonium nitrogen (NH_4-N), nitrate nitrogen (NO_3-N) and total nitrogen (Tot-N) from each soil layer were extracted with KCl-solution for flow injection analysis.
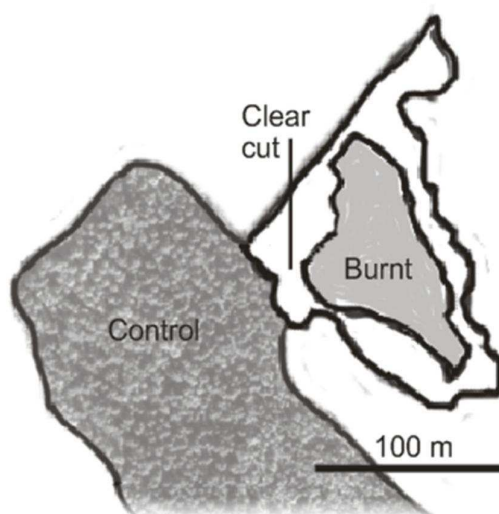
Figure 1: The different treatments: mature control forest, a clear cut site and a clear cut and burnt site

According to the sampling, 38 000 kg ha^{-1} (78%) of slash, 2 300 kg ha^{-1} (~100%) of ground vegetation, and 18 000 kg ha^{-1} (22%) of organic soil in litter- and humus layer were burnt during the prescribed burning.

The soil temperatures were identical before the treatments. After the clear cut and partial burning of the slash, temperature of humus and A-horizon were the highest in the burnt treatment and lowest in the control forest. The soil moisture in A and B-horizons decreased the most during rainless periods in the control forest and the least in the clear cut site.

The treatments increased pH in the organic layers in the burnt and clear cut site (Figure 2). The rise was the highest in the litter layer in the burnt site but the pH lowered to the initial level already two years after the treatments.

The C/N ratio was slightly decreased in the litter layer of the harvested sites due to an increased proportion of nitrogen while the carbon content stayed constant. In the humus layer of the clear cut site, both nitrogen and carbon content decreased being the lowest 1.5 years after the clear cut and increasing thereafter exceeding the pre-cut level. The C/N ratio in the humus layer was still two years after the burning and clear cut lower at the treated sites than at the control site but do not differ notably. In the mineral soil, the C/N ratio increased in the spring after the harvesting due to decreased nitrogen content, but C/N ratio decreased thereafter rapidly at both treatments due to a sharp increase in soil nitrogen, probably due to the death of tree roots. However, some differences between the sites existed already before the treatments and the results are fluctuating indicating an inadequate number of samples in the mineral soil.

The NH$_4$-N concentrations notably increased at the harvested sites in the litter and humus layers (Figure 3A1, B1). The NO$_3$-N content increased rapidly in the litter layer of the burnt site whereas at the clear-cut, the NO$_3$-N content started to increase more than year after the treatment (Figure 3A2). The increase in the NH$_4$-N and NO$_3$-N contents in the mineral soil was also delayed (Figure 3C1-2, D1-2). The percentage of the post-burn NH$_4$-N of the total available N increased from 3 to 78% in the litter layer and from 2 to 79% in the humus layer, respectively, being around 60–70 % two years after the treatments. Similarly, the NH$_4$-N content of the total nitrogen was maximally 82% and 77% in the litter and humus layers in the clear-cut site being 50–60% two years after the treatments.

Total available nitrogen content (Tot-N) decreased in the litter layer of the harvested sites (Figure 3A3), whereas in the topmost mineral soil at the burnt site, the amount of organic Tot-N peaked 0.5-1.5 years after the treatments (Figure 3C3).
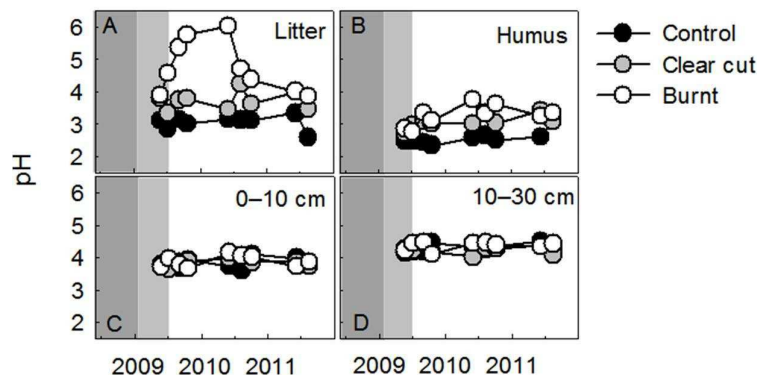
Figure 2. pH in different soil horizons from May 2009 to August 2011. The dark grey indicates the time before any treatments. The light grey indicates the time between the harvest in February 2009 and burning treatment in late June 2009.
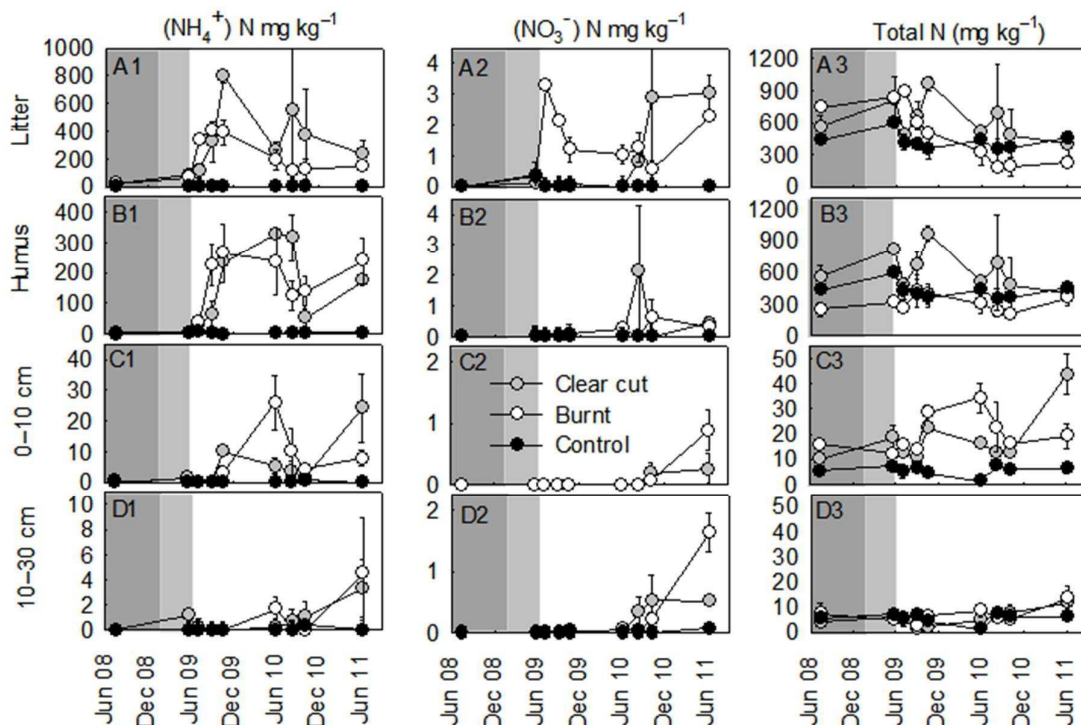
Figure 3. Ammonium nitrogen (NH₄-N), nitrate nitrogen (NO₃-N) and total nitrogen (Tot-N) content in the different treatments and in different soil layers. The dark grey indicates the time before the treatments and the light grey indicates the time between the harvest in February 2009 and burning treatment in late June 2009. Note the varying y-scales.

ACKNOWLEDGEMENTS

REFERENCES

Cajander, A.K. (1926). The Theory of Forests Types. *Acta Forestalia Fennica* **29**,1–108.

Certini, G. (2005). Effects of fire on properties of forest soils: a review, *Oecologia* **143**, 1–10.

Covington, W.W. and S.S. Sackett (1984). The effect of a prescribed burn in southwestern ponderosa pine on organic matter and nutrients in woody debris and forest floor, *Forest Sci*. **30**, 183–192.

Grady, K.C., and S.C. Hart (2006). Influences of thinning, prescribed burning, and wildfire on soil processes and properties in southwestern ponderosa pine forests: A retrospective study, *Forest Ecol. Manag.* **234**, 123–135.

Hari, P. and M. Kulmala (2005). Station for measuring ecosystem-atmosphere relations (SMEAR II), *Boreal Environ.Res*. **10**, 315–322.

Ilvesniemi, H., J. Pumpanen, R. Duursma, P. Hari, P. Keronen, P. Kolari et al. (2010) Water balance of a boreal Scots pine forest. *Boreal Environment Res*.**15**, 375–396.

Johnson, D., J. D. Murphy, R. F. Walker, D. W. Glass, and W. W. Miller. (2007). Wildfire effects on forest carbon and nutrient budgets, *Ecol. Eng.* **31**,183–192.

Malmström, A., T. Persson, J. Bengtsson, K. Gongalsky and K. Ahlström (2009). Dynamics of soil mesoand macrofauna during a 5-year period after clear-cut burning in a boreal forest, *Appl. Soil Ecol.* **43**, 61–74.

O'Halloran T.L, B.E. Law, M.L. Goulden, Z. Wang, J.G. Barr, C. Schaaf, M. Brown, J.D. Fuentes, M. Göckede, A. Black and V. Engel (2011). Radiative forcing of natural forest disturbances, *Glob. Change Biol.* **18**, 555– 565.

Pietikäinen, J. and H. Fritze (1995). Clear-cutting and prescribed burning in coniferous forest: comparison of effects on soil fungal and total microbial biomass, respiration activity and nitrification, *Soil Biol. Biochem.* **27**, 101–109.

Takakai F., A.R. Desyatkin, C.M.L. Lopez, A.N. Fedorov, R.V.R. Desyatkin and Hatano (2008). Influence of forest disturbance on CO_2, CH_4 and N_2O fluxes from larch forest soil in the permafrost taiga region of eastern Siberia, *Soil Sci. Plant Nutr.* **54**, 938–949.

Wardle, DA, O. Zackrisson, G. Hörnberg, and C. Gallet (1997). Influence of island area on ecosystem properties, *Science* **277**, 1296–99.

Yoshikawa, K., W.R. Bolton, V.E. Romanovsky, M.Fukuda and L.D. Hinzman (2003), Impacts of wildfire on the permafrost in the boreal forests of Interior Alaska, *J. Geophys. Res.*, **108**, 8148.

CARBONTREE VISUALIZES THE CO_2 UPTAKE AND RELEASE OF A SCOTS PINE

L. KULMALA[1], P. KOLARI[1,2], J. RASINMÄKI[3], T. HAAPOJA, IVAYLO DZHEDZHEV[3] and E. JUUROLA[1,2]

[1]Department of Forest Sciences, P.O. Box 27, FIN-00014, University of Helsinki, Finland.

[2]Department of Physics, University of Helsinki, Finland.

[3]Simosol Oy, Riihimäki, Finland.

Keywords: photosynthesis, respiration, popularization of science

INTRODUCTION

Since the 1980s, scientists have been interested in the role of forest in the mitigation to climate change. However, the interaction between atmosphere and biosphere is complicated and therefore, the popularizing of the obtained results has been problematic. CarbonTree, a co-operation between art, software development and science, has succeeded in transforming the novel scientific knowledge in a modern and experiential way to anyone interested in the action of forest ecosystems.

SMEARII station (Hari and Kulmala, 2005) is an intensively equipped world-class observatory in southern Finland measuring material and energy fluxes between the forest and the atmosphere. Many years of measurements have provided a lot of information on the behaviour of the forest: how a tree photosynthesizes and respires. We know more or less what to expect the tree will do according to the time of the year, the available light and CO_2, the air and soil temperature and the water availability in the soil. This knowledge is expressed by mathematical models that can forecast the overall behaviour of the tree.

CarbonTree presents the obtained ecophysiological knowledge to common people and schools. The core is a visually catching and appealing webpage (www.hiilipuu.fi) presenting the carbon exchange of a Scots pine forest at SMEAR II. In the summer 2012, a transferable, interactive CarbonTree was aldo launched for exhibitions.

METHODS

The photosynthesis
The animation on the web page is the result of models for canopy photosynthesis, soil and tree respiration. According to the real weather and soil conditions measured on-line at the SMEARII station, we use a model to calculate the photosynthesis rate. The photosynthesis, p (μmol m^{-2} s^{-1}), is a result of leaf area (LAI), air humidity (vapour pressure deficit, VPD), soil moisture (relative extractable water, REW), air temperature (T), CO_2 concentration (CO_2) and photosynthetically active radiation (PAR):

$$p = f_{lai} \, f_{par} \, Min\{f_{vpd}, \, f_{rew}^{tree}\} \, f_T \, f_{Tmin} \, f_S \, f_{CO2}. \tag{1}$$

Photosynthesis increases with increasing leaf area (*lai*):

$$f_{lai}(lai) = \frac{1}{k}(1 - e^{-k \, lai}). \tag{2}$$

In the equation, *lai*=8 m^2 m^{-2} and *k*=0.18. The effect of PAR (μmol m^{-2} s^{-1}) is saturating:

$$f_{par}(PAR) = \frac{p_{max} \, PAR}{PAR + b}. \tag{3}$$

In the equation, PAR is measured above canopy, $p_{max} = 9$ µmol m^{-2} s^{-1} and $b = 600$ µmol m^{-2} s^{-1}. Decreasing air humidity (increasing VPD) hinders the photosynthesis, modelled by the following equation:

$$f_{vpd}(VPD) = e^{-h\ VPD}, \tag{4}$$

where $h=0.02$. Low relative extractable soil water (REW) also decreases the rate of photosynthesis below a critical soil moisture value ($rew_{crit}^{tree} = 0.45$):

$$f_{rew}(REW) \begin{cases} 1, & \text{if } REW \geq rew_{crit}^{tree} \\ Max\left\{0, \frac{REW}{rew_{crit}^{tree}}\right\}, & \text{if } REW < rew_{crit}^{tree}. \end{cases} \tag{5}$$

REW is calculated using measured soil moisture (SM, m^3 m^{-3}), wilting point (wp) and field capacity (fc):

$$REW = \frac{SM - wp}{fc - wp}. \tag{6}$$

S (°C) describes the effect of temperature history i.e. state of development (Pelkonen and Hari, 1980; Mäkelä *et al.*, 2004; Kolari *et al.*, 2006). It follows temperature (T) with a time constant τ:

$$\frac{dS}{dt} = \frac{T(t) - S(t)}{\tau}. \tag{7}$$

The time constant $\tau=150$ h. The effect of S on photosynthesis is modelled by the equation (8):

$$f_S(S) = \frac{1}{1 + e^{c(s - T_s)}}, \tag{8}$$

where $c = -0.25$ and $T_S = 5.5$ °C. The effect of current temperature (T) follows the equation:

$$f_T(T) = 1 - e^{(c_T(T + T_0)}, \tag{9}$$

where $T_0 = -5$ °C and

$$c_T = \text{Min}\{-0.1, 0.5 * f_s(S) - 1\}. \tag{10}$$

In addition, recent possible frosts decrease the rate of photosynthesis:

$$f_{Tmin}(T_{min}) = \text{Max}\left\{0, \text{Min}\left\{1, \frac{(T_{0min} - T_{min})}{(T_{0min}}\right\}\right\}. \tag{11}$$

In the equation, T_{min} is the lowest temperature (°C) during previous 24 h and $T_{0min} = -10$ °C Increasing CO$_2$ concentration also increases photosynthesis:

$$f_{co2}(CO2) = \frac{CO2 - \gamma}{CO2 + \gamma + k_{CO2}} \frac{co2_{ref} + \gamma + k_{CO2}}{co2_{ref} - \gamma} \tag{12}$$

In the equation, $co2_{ref} = 400$ ppm, $\gamma =50$ ppm and $k_{CO2} = 500$ ppm.

Tree respiration

Above ground tree respiration (r_{tree}, µmol m^{-2} s^{-1}) is determined by soil moisture (REW) and air temperature (T) using the following equation:

$$r_{tree} = Max\{0, \ f_{rew}^{tree}(REW) \ r_0^{tree} \ q_{10}^{tree\frac{T}{10}} - c_r^{tree}, \tag{13}$$

where $r_0^{tree} = 1.6$ µmol m^{-2} s^{-1}, $q_{10}^{tree} = 1.5$, $c_r^{tree} = 0.8 * r_0^{tree}$ and

$$f_{rew}^{tree}(REW) = Min\{1, \ Max\left\{0, \ \frac{REW+d_{rew}^{tree}}{rew_{crit}^{treeresp}}\right\}\}, \tag{14}$$

where $d_{rew}^{tree} = 0.05$ and $rew_{crit}^{treeresp} = 0.35$

Soil respiration

Soil respiration (r_{soil}, µmol m^{-2} s^{-1}) is determined by soil moisture (REW) and soil temperature (T_{soil}) using the following equation:

$$r_{soil} = Max\{o, \ f_{rew}^{soil}(REW) \ r_0^{soil} \ q_{10}^{soil\frac{T_{soil}}{10}} - c_r^{soil}, \tag{15}$$

where $r_0^{soil} = 1.1$ µmol m^{-2} s^{-1}, $q_{10}^{soil} = 2.4$, $c_r^{soil} = 0.5$ µmol m^{-2} s^{-1} and

$$f_{rew}^{soil}(REW) = Min\{1, \ Max\left\{0, \ \frac{REW+d_{rew}^{soil}}{rew_{crit}^{soil}}\right\}\}, \tag{16}$$

where $d_{rew}^{soil} = 0.1$ and $rew_{crit}^{soil} = 0.60$.

Approaches

The idea of CarbonTree is an artistic animation that visualizes the carbon uptake and release by showing CO_2 molecules as visible particles moving towards and away from the tree and soil (Figure 1) with rates that depend on the current state of the environmental factors that are obtained by the on-line data from SMEAR II. On the web pages, the changes in the environmental factors and at the CO_2 exchange rates are presented also by traditional graphs over the past 24 h. Besides the on-line data, the web pages include interactivity: a user can change the state of the environmental factors and see the effect on the rate of CO_2 exchange. The web page is rebuilt in the autumn 2012 to include more spatial and temporal elements together with deeper knowledge about the measurements, models and the research process, for example.

During June and July 2012, an interactive CarbonTree was out in Think Corner in Helsinki city centre. The interactive piece of art consisted of a projection of the tree, soil and moving CO_2 molecules but used as an input the environmental factors near a visitor instead of the on-line data. A user could increase the temperature by hand, increase the CO_2 concentration by exhaling or decrease light intensity by his/her own shadow. The CO_2 exchange in the projected tree and soil reacted to these changes. The interactive work received widely positive feedback and during the autumn 2012, it will be present in exhibitions to increase the overall knowledge about forest-atmosphere relations.
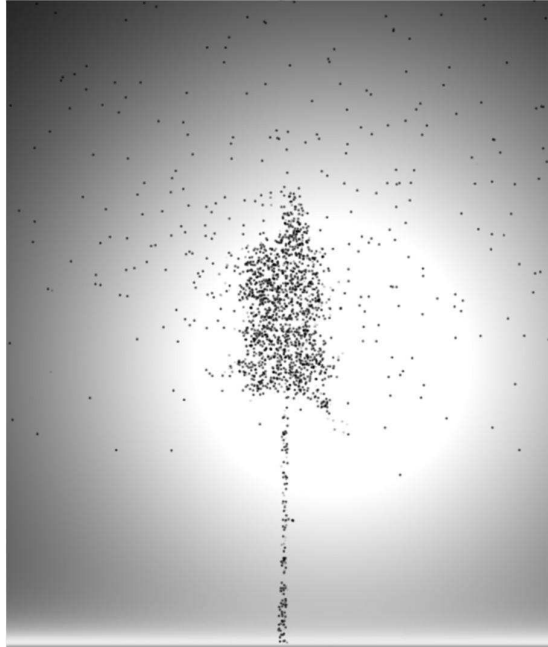
Figure 1: CO_2 molecules are visualized as particles moving towards and away from soil and the tree

REFERENCES

Hari, P. and M. Kulmala (2005). Station for measuring ecosystem-atmosphere relations (SMEAR II). *Boreal Environ.Res*. **10**, 315–322.

Hari, P., H. Hänninen, F. Berninger, P. Kolari, E. Nikinmaa, A. Mäkelä (2009). Predicting boreal conifer photosynthesis in field conditions. *Boreal Environment Research* **14**, 19–28.

Kolari, P., J. Pumpanen, L. Kulmala, H. Ilvesniemi, E. Nikinmaa, T. Grönholm, P. Hari (2006) Forest floor vegetation plays an important role in photosynthetic production of boreal forests. *Forest Ecology and Management* **221**, 241–248.

Mäkelä, A., P. Hari, F. Berninger, H. Hänninen E. Nikinmaa (2004) Acclimation of photosynthetic capacity in Scots pine to the annual cycle of temperature. *Tree Physiology*. **24**, 369–376.

ION-INDUCED VS. BASE-INDUCED SULFURIC ACID CLUSTER FORMATION

O. KUPIAINEN[1], T. OLENIUS[1], I.K. ORTEGA[1], T. KURTÉN[2], AND H. VEHKAMÄKI[1]

[1] Department of Physics, University of Helsinki, Gustaf Hällströmin katu 2 A, P.O. Box 64, FI-00014 Finland.

[2] Department of Chemistry, University of Helsinki, A.I. Virtasen aukio 1, P.O. Box 55, FI-00014 Finland.

Keywords: Sulfuric acid, cluster formation, ions, bases.

INTRODUCTION

A large fraction of atmospheric aerosols are formed in the atmosphere by gas-to-particle nucleation, but their birth-mechanism remains partly unclear. New-particle formation rates have been observed to correlate strongly with sulfuric acid concentrations in a wide range of conditions, suggesting that sulfuric acid would be involved in the first steps of nucleation. However, particle formation cannot be explained by homogeneous nucleation of sulfuric acid and water alone. Instead, some additional compound is needed to stabilize the small sulfuric acid clusters and enable them to grow into particles.

Since acids and bases bind strongly together, bases are likely to enhance sulfuric acid cluster formation. We have studied the role of ammonia, which is a weak base and abundant in the atmosphere, and dimethylamine (DMA), which is a stronger base but has a lower concentration.

Clustering can also be enhanced by ions through several mechanisms. Firstly, ions attract polar and polarizable molecules and clusters, which leads to higher collision rates compared to neutral cluster formation. Secondly, ionic clusters are more strongly bound, leading to lower evaporation rates and thus a higher probability for clusters to collide and grow before breaking. Finally, the recombination of oppositely charged clusters may enable the formation of neutral clusters even in conditions where purely neutral cluster formation would be negligible.

METHODS

We have computed formation Gibbs free energies of neutral and negatively and positively charged sulfuric acid – ammonia – DMA clusters up to four acids and four bases using a multi-step quantum chemistry method (Ortega *et al.*, 2012). These energies were used to calculate evaporation rates of the clusters, assuming classical collision rates and barrierless reactions. Cluster formation was then studied using the Atmospheric Cluster Dynamics Code (ACDC) (McGrath *et al.*, 2012), which solves the birth-death equations governing cluster collisions and evaporations.

RESULTS AND CONCLUSIONS

We have simulated the formation and growth of clusters at various concentrations of sulfuric acid, ammonia and DMA, and different ionization rates and temperatures. The formation rate of 1.3-1.6 nm cluster is shown in Figure 1 as a function of ionization rate and in Figure 2 as a function of temperature.
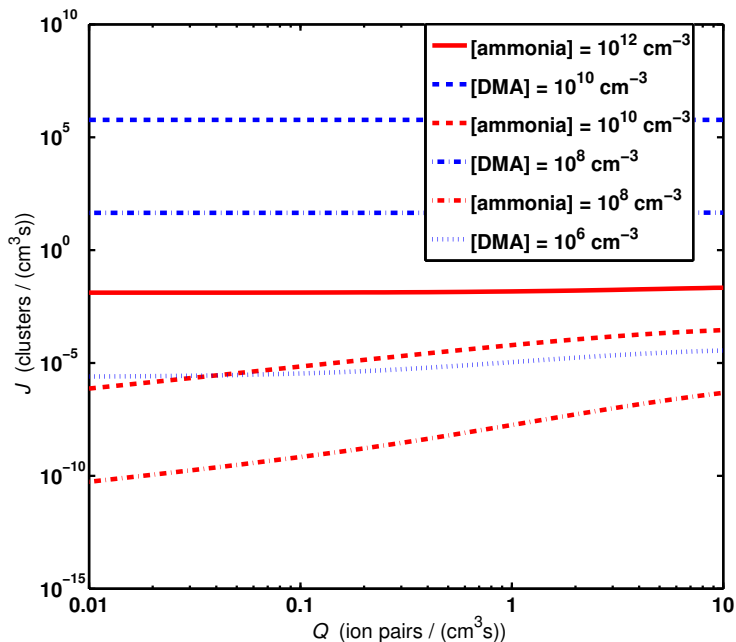
Figure 1: Formation rate of 1.3-1.6 nm clusters as a function of ion pair formation rate at 19 °C, a sulfuric acid concentration of 10^6 cm^{-3} and different ammonia and DMA concentrations.
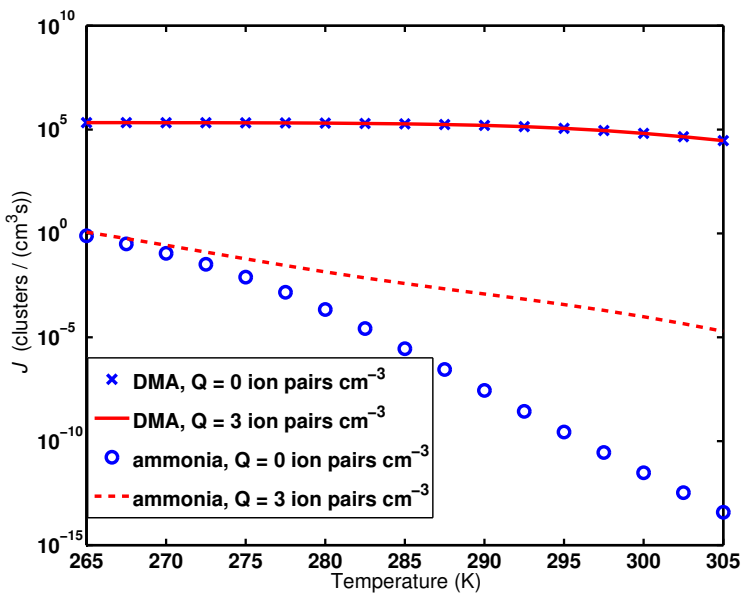
Figure 2: Formation rate of 1.3-1.6 nm clusters as a function of temperature at a sulfuric acid concentration of 10^7 cm^{-3} and an ammonia or DMA concentration of 2.5×10^8 cm^{-3}.

Sulfuric acid – DMA clusters are very stable in all charging states, although the optimal acid-base ratio varies depending on the charge. In ambient temperatures, cluster formation is mainly collision limited, as can be seen from the very weak temperature dependence of the formation rate (Fig. 2), noting that collisions rates increase slowly with temperature and evaporation rates increase rapidly

399

with temperature. At high DMA concentrations neutral cluster formation dominates (Fig. 1), but at low DMA concentrations the ionic pathway becomes important mainly due to higher collision rates of ionic clusters.

Sulfuric acid – ammonia clusters are overall more weakly bound than sulfuric acid – DMA clusters, and neutral clusters are less stable than charged clusters. Formation rates are several orders of magnitude lower than with DMA (Figs. 1 and 2) and decrease strongly with increasing temperature, showing that evaporation of clusters limits the formation and growth rates. Since ionic clusters are more stable than neutrals, ion induced cluster formation dominates at high temperatures and low ammonia concentrations.

ACKNOWLEDGEMENTS

REFERENCES

Ortega, I. K., Kupiainen, O., Kurtén, T., Olenius, T., Wilkman, O., McGrath, M. J., Loukonen, V. and Vehkamäki, H. (2012). From quantum chemical formation free energies to evaporation rates. Atmos. Chem. Phys. **12**, 225.

McGrath, M. J., Olenius, T., Ortega, I. K., Loukonen, V., Paasonen, P., Kurtén, T., Kulmala, M., and Vehkamäki, H. (2012). Atmospheric Cluster Dynamics Code: a flexible method for solution of the birth-death equations. Atmos. Chem. Phys. **12**, 2345.

ESTIMATING SUBPIXEL FOREST ALBEDOS BY LINEAR UNMIXING OF MODIS ALBEDO COMPOSITES

N. KUUSINEN[1], F. BERNINGER[1] and E. TOMPPO[2]

[1]Department of Forest Sciences, P.O. Box 27, 00014 University of Helsinki, Finland
[2]The Finnish Forest Research Institute, P.O. Box 18, 01301 Vantaa, Finland

Land cover changes are usually accompanied by changes in surface albedo, which determines the fraction of solar irradiance absorbed by the surface. Thus, instead of quantifying only the effects of changing carbon sequestration on radiative forcing, increasing attention is paid on the biophysical impacts of land cover change on climate trough albedo (Betts et al. 2007). Simulations of the impacts of land cover changes on climate need accurate estimates of surface albedo in various vegetation types. Spatially and temporally comprehensive albedo estimates are only derived from satellite observations. However, the spatial resolution of satellite albedo products is often too low to allow direct comparison of pixel albedo values to vegetation cover types in areas with fragmented vegetation cover. A possible approach to overcome this problem is to use the linear unmixing approach (Settle and Drake 1993) to derive subpixel albedos for a priori known land cover classes from a satellite albedo product.

We used MODIS BRDF/albedo subsets and local land cover/forestry maps form three different boreal locations (southern Finland, northern Finland and Quebec, Canada) to test the linear unmixing method. The MODIS pixel albedos were predicted by the cover fractions of the different land cover types (endmembers) present in the pixel area using linear least squares regression. Four years of MODIS 16-day composites for each location were selected and after quality filtering 57-77 composites per area remained for the analysis.

The albedo estimation yielded reasonable endmember albedos and the RMSEs of the prediction were similar in all three test areas. The prediction was more accurate in summer than in winter when changes in snow cover lead to uncertainties in the albedo estimation. R^2 values of the estimation were highest in the test areas with most distinct variations in the landscape (lakes, croplands, forest). However, the standard errors of predicted forest endmember albedos were similar in all areas. The forest albedo was mainly determined by tree species, and connection to the amount of growing stock after the initial young stand phase was not found. We also compared the albedos predicted for forest endmembers in southern Finland to mast measured forest albedos in the same area and noticed that the method tended to shift very high and very low endmember albedos slightly towards the average. Figure 1 shows an example of the results for southern Finland study area.

The method could be used to estimate areal average albedos for known vegetation types as well as to track changes in the vegetation type albedos caused by ecological, climatic or human induced factors such as phenology, snow, disturbances or forest management practices. Problems are caused for instance by the errors in the land cover/forestry map used and the mismatch between the true observation area and the predefined grid cells in MODIS data, causing the endmembers assigned to a pixel not quite to correspond the real proportions of cover types present in the signal area (Tan et al. 2006).
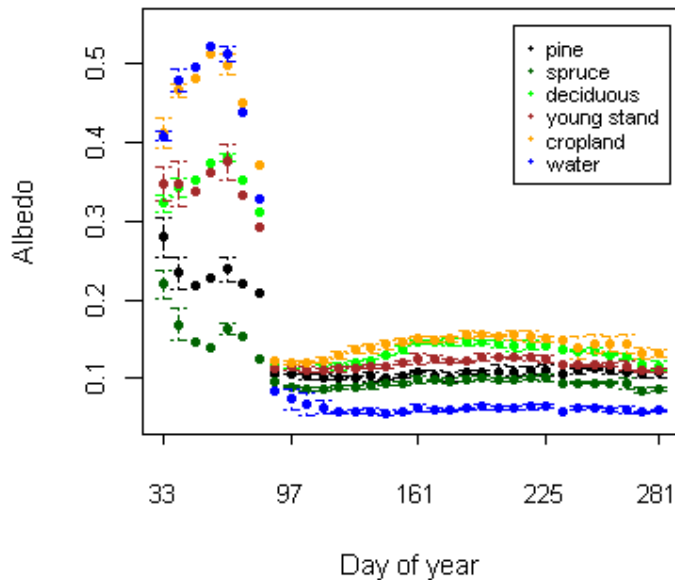
Figure 1. Annual course of the over four years averaged endmember albedos in Hyytiälä, southern Finland.

REFERENCES

Betts, R.A., Falloon, P.D., Goldewijk, K.K., Ramankutty, N. 2007. Biogeophysical effects of land use on climate: model simulations of radiative forcing and and large-scale temperature change. Agric. For. Meteorol. 142, 216–233.

Settle, J.J., Drake, N.A. 1993. Linear mixing and estimation of ground cover proportions. Int. J. Remote Sens. 14, 1159–1177.

Tan, B., Woodcock, C.E., Hu, J., Zhang, P., Ozdogan, M., Huang, D., Yang, W., Knyazikhin, Y., Myneni, W. 2006. The impact of griddling artifacts on the local spatial properties of MODIS data: Implications for validation, compositing, and band-to-band registration across solutions. Remote. Sens. Environ. 105, 98–114.

IMPACT OF AEROSOL EMISSIONS IN CHINA AND INDIA ON GLOBAL CLIMATE

T. KÜHN[1], H. KOKKOLA[2], H. KORHONEN[2], S. ROMAKKANIEMI[1], A. LAAKSONEN[1,3]

[1] University of Eastern Finland, Department of Applied Physics, Kuopio, Finland.

[2] Finnish Meteorological Institute, Kuopio Unit, Kuopio, Finland.

[3] Finnish Meteorological Institute, Climate Change, Helsinki, Finland.

Keywords: ECHAM, AEROSOL, CLIMATE.

INTRODUCTION

Existing surface temperature records show warming in the beginning of last century, followed by cooling starting from 1940 and again strong heating from 1975 until recent years. This behaviour has been attributed to increase in the greenhouse gas and aerosol emission as well as to natural variability of climate. Making a difference between these is crucial as climate predictions and international policy related to emission reductions are based on the models that are mainly evaluated against the historical temperature records.

While in Europe and North America the aerosol emissions have decreased since the late 1970s, the emissions in China and India have started to increase dramatically at about the same time and have only recently started to stagnate due to new regulations in China. Here we use emission scenarios from the years 1996 through 2010 to assess the effect that these emissions have on local aerosol properties and climate as well as on the global climate.

METHODS

We use the aerosol-climate model ECHAM5-HAM (Roeckner 2003; Roeckner 2004) to simulate the local aerosol properties in China and India in the years 1996 through 2010, and their impact on local as well as global climate. For anthropogenic aerosol greenhouse gas emissions we use the ACCMIP-MACCity Aerocom emissions (Aerocom 2) (Lamarque, 2010) in combination with the emissions for China and India after Lu et. al (Lu, 2011) for the mentioned period of time.

To test the performance of the model in combination with the used emission inventories, we compare aerosol properties, as obtained from a 15 year ECHAM5-HAM run on a T63L31 grid, with measurement data from MODIS (Acker, 2007) and AeroNet (AeroNet). The simulations use prescribed sea surface temperatures and are nudged after (Jeuken, 1996).

To assess the impact of anthropogenic aerosol emissions on earth's climate, we use the ECHAM-HAM model coupled to a mixed layer ocean on a T42L19 grid using three different scenarios:

1. with the combined Aerocom 2 - Lu et. al aerosol emissions of 1996 as a reference point

2. with the combined Aerocom 2 - Lu et. al aerosol emissions of 2010

3. with a hypothetical scenario where the global emissions of 2010 are combined with the emissions in China and India of 1996, i.e. combining Aerocom 2 for 2010 with Lu et. al for 1996

With each of these (fixed) scenarios, the model is run for about 70 to 100 years to simulate the atmosphere in equilibrium, and thereby assess the relative differences in local and global aerosol properties and temperatures.

CONCLUSIONS

The presented work is currently in progress. Preliminary results comparing the aerosol optical depth (AOD) as obtained from ECHAM-HAM and from MODIS are shown in Fig. 1.
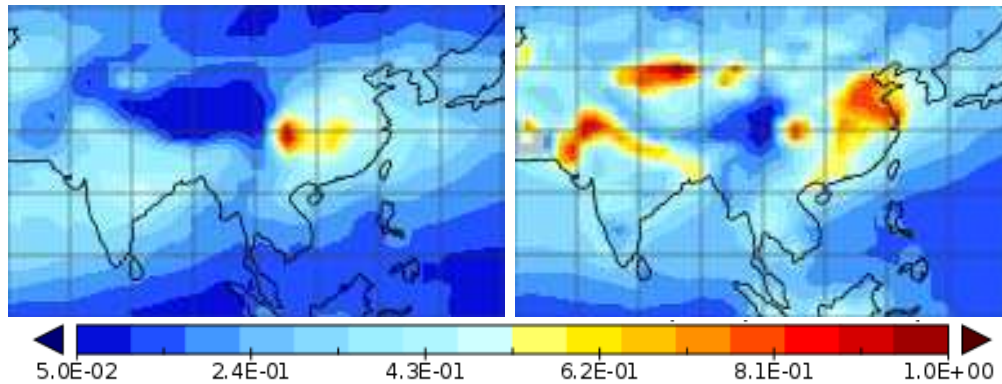
Figure 1: Aerosol optical depth (AOD) (one year average for 2002) as obtained with ECHAM-HAM (left) compared to MODIS AOD data obtained from Giovanni website (Acker, 2007)

ACKNOWLEDGEMENTS

REFERENCES

Roeckner, E., Bäuml, R., Bonaventura, L., Brokopf, R., Esch, M., Giorgetta, M., Hagemann, S.,Kirchner, I., Kornblueh, L., Manzini, E., Rhodin, A., Schlese, U., Schulzweida, U., and Tompkins,A (2003). The atmospheric general circulation model ECHAM5, Part I: Model description *Tech. rep., Max-Planck Institute for Meteorology, Hamburg, Germany*

Roeckner, E., Brokopf, R., Esch, M., Giorgetta, M., Hagemann, S., Kornblueh, L., Manzini, E.,Schlese, U., and Schulzweida, U. (2004). The atmospheric general circulation model ECHAM5, PartII: Sensitivity of simulated climate to horizontal and vertical resolution *Tech. rep., Max-PlanckInstitute for Meteorology, Hamburg, Germany,*

Jeuken, A. B. M., Siegmund, P. C., Heijboer, L. C., Feichter, J., and Bengtsson, L (1996). On thepotential of assimilating meteorological analyses in a global climate model for the purpose ofmodel validation *J. Geophys. Res.*, **101**, 16939

J. F. Lamarque, et. al (2010). Historical (1850-2000) gridded anthropogenic and biomass burning emissions of reactive gases and aerosols: methology and application *Atmos. Chem. Phys.*, **10**, 7017

Z. Lu, Q. Zhang, and D. G. Streets Sulfur dioxide and primary carbonaceous aerosol emissions in China and India, 1996-2010 (2011) *Atmos. Chem. Phys.*, **11**, 9839

J. G. Acker and G. Leptoukh (2007) Online Analysis Enhances Use of NASA Earth Science Data *Eos, Trans. AGU*, **88**, 14

AeroNet: See http://aeronet.gsfc.nasa.gov/new_web/index.html for details

ANTARCTIC AEROSOL FORMATION FROM CONTINENTAL BIOGENIC SOURCES

E.-M. KYRÖ[1], A. VIRKKULA[1,2], V.-M. KERMINEN[1], M. DAL MASO[1], J. PARSHINTSEV[3], J. RUIZ-JIMENEZ[3], L. FORSSTRÖM[4], H.E. MANNINEN[1], P. HEINONEN[5], M.-L. RIEKKOLA[3] and M. KULMALA[1]

[1] Department of Physics, University of Helsinki, P.O.Box 48, 00014 Helsinki, Finland

[2] Air Quality Research, Finnish Meteorological Institute, P.O.Box 503, 00101 Helsinki, Finland

[3] Department of Chemistry, University of Helsinki, P.O.Box 55, 00014 Helsinki, Finland

[4] Department of Biological and Environmental Sciences, University of Helsinki, P.O.Box 65, 00014 Helsinki, Finland

[5] Finnish Meteorological Institute, Finnish Antarctic Logistics, P.O.Box 503, 00101 Helsinki, Finland

INTRODUCTION

Antarctica is the cleanest continent. Being extremely isolated, especially during the winter, it has had no known sources of secondary aerosol particles on its surface (Ito, 1989) until present. However, during the Finnish Antarctic Research Program (FINNARP) 2009 expedition, the first evidence of Antarctic particle formation due to continental biogenic precursors was observed.

The Finnish Antarctic Research Station Aboa ($73°03'S$, $13°25'W$) is located in Western Dronning Maud Land. It is build on a nunatak (mountaintop) Basen, $500m$ a.s.l., some $130km$ from the open ocean. During the Antarctic summer, many meltwater ponds and trickles form to and around the nunataks (mountaintops) that are peaking out from the thick ice mass. These ponds hold a variety of biological activity in them (Jungblut *et al.*, 2005), e.g. cyanobacteria *Nostoc commune* (Vaucher), a species very tolerant for extreme conditions (Dodds *et al.*, 1995) and commonly found from Basen. Also the margin, where continental ice ends and shelf ice starts, is abundant with blue-ice, which experiences surface melting during the summer (Liston & Winther, 2005). Blue-ice and snow melting combined, as much as 11.8% of the Antarctic continent experiences surface melting during the summer (Liston & Winther, 2005). In summer $2009 - 2010$, the ponds on top of Basen were formed around Christmas.

During the campaign, several aerosol and atmospheric composition measurements were carried out. The measurement devices were kept inside a small container, approximately $200m$ upwind from the main station. In addition to these measurements, samples of the cyanobacterial mat and water from the meltwater ponds were taken. The ponds were approximately $2.5km$ upwind from the container.

METHODS

The concentrations of neutral and charged particles as well as their size distribution and quartz filter samples were taken from the atmosphere, about 3 m above the ground level. The filters were

changed three times a week. Different chemical compounds from the filter as well as water and *Nostoc commune* samples were analyzed later in Finland with a comprehensive two dimensional gas chromatography-time-of-flight mass spectrometry (GCxGC-TOF-MS). With this methodology, a great amount of different organic compounds can be detected (Ruiz-Jimenez *et al.*, 2011). The neutral particle size distribution from 10 to $500nm$ was measured using a Differential Mobility Particle Sizer (DMPS, (Aalto *et al.*, 2001)) and Air-Ion Spectrometer (AIS, (Hirsikko *et al.*, 2005)) was used to measure the charged particle size distribution from 0.8 to $42nm$. The samples of water and *Nostoc commune* were kept frozen until they were analyzed.

Growth- and formation rates (GR and J, respectively) were obtained for all new particle formation events from both charged and neutral particle size distributions. An additional estimation of apparent growth rates using a linear fit was applied to four apple- or bump-shaped events, where the traditional way of calculating the GR was not feasible due to the shape of the event. HYSPLIT back-trajectories were calculated to estimate the origin of regional new particle formation (NPF) events.

RESULTS AND DISCUSSION

During the campaign three periods of frequent new particle formation (NPF) and subsequent growth were observed. In two last periods, that we will now focus on - 1st to 3rd and 17th to 20th January 2010 - both local and regional particle formation was observed. On contrary to the first event period and observations by Virkkula *et al.* (2009), these events were not associated with intrusion of air from upper troposphere. The GR for the charged cluster ions as well as for neutral Aitken mode particles were high for Antarctica (Kulmala *et al.*, 2004) and comparable to those measured over vegetated areas. Also the formation rates of $1.6 - nm$ sized negative clusters were high, even up to $4.6cm^{-3}s^{-1}$.

During these event periods, that happened after the melting of the ponds, a total of seven apple- or bump-type (Manninen *et al.*, 2010) NPF events were observed. The shape of the events suggested that the formation happened on a small scale, close to the station and the particle formation was unusually intense for Antarctica. To our knowledge, this has not been observed earlier in Antarctica.

In addition to the local particle production, also regional NPF was observed during these periods. We used HYSPLIT back-trajectories to estimate the origin of the growing Aitken mode particles in the "banana-type" events. The results showed that the particles had originated from the large blue-ice zone in the margin of sheet and shelf ice, few hundreds of kilometres away from open ocean. This area experiences surface melting during the summer (Liston & Winther, 2005). Some of the regional NPF events were also originated from mountain ranges Gjelsvikfjella, Mühlig-Hofmannfjella, Heimefrontfjella and Vestfjella. This applies especially for the last event period.

Although the total surface area of the nunataks is quite small, combined with the blue-ice and snow melt area they may be important source regions for secondary organic aerosols during the summer in Antarctica. In the future, as the climate warms, it is likely that more meltwater ponds will open up during the summertime and they will exist longer. Also the snow and blue-ice melt is very sensitive to variations in atmospheric forcing (Liston, G.E. *et al.*, 1999). This could increase both the aerosol number concentrations and their condensational growth and finally CCN and cloudiness. We hope, that our results will help in estimating the climatic feedbacks of aerosols and future climate in Antarctica.

REFERENCES

Aalto, P., *et al.* (2001). Physical characterization of aerosol particles during nucleation events. *Tellus*, **53B**, 344-358.x

Dodds, W. K., *et al.* (1995). The Ecology of Nostoc. *J. of Phycology*, **31(1)**, 2-18.

Hirsikko, A., *et al.* (2005). Annual and size dependent variation of growth rates and ion concentrations in boreal forest. *Boreal Environ. Res.*, **10**, 357-369.

Ito, T. (1989). Antarctic Submicron Aerosols and Long-Range Transport of Pollutants. *Ambio*, **18(1)**, 34-41.

Jungblut, A.-D. (2005). Diversity within cyanobacterial mat communities in variable salinity meltwater ponds of McMurdo Ice Shelf, Antarctica. *Env. Microbio.*, **7(4)**, 519-529.

Kulmala, M. *et al.* (2004). Formation and growth rates of ultrafine atmospheric particles: a review of observations. *J. Aerosol. Sci.*, **35**, 143-176.

Liston, G.E. & Winther, J.-G. (2005). Antarctic Surface and Subsurface Snow and Ice Melt Fluxes. *J. Clim*, **18**, 1469-1481.

Liston, G.E. *et al.* (1999). Meltwater production in Antarctic blue-ice areas: sensitivity to changes in atmospheric forcing. *Pol. Rec.*, **18**(2), 283-290.

Manninen, H.E. *et al.* (2010). EUCAARI ion spectrometer measurements at 12 European sites - analysis of new particle formation events. *Atmos. Chem. Phys.*, **10**, 7907-7927.

Ruiz-Jimenez, J. *et al.* (2011). Comprehensive two-dimensional gas chromatography, a valuable technique for screening and semiquantitation of different chemical compounds in ultrafine 30 nm and 50 nm aerosol particles. *J. Environ. Mon.*, **13**,2994-3003.

Virkkula, A. *et al.* (2009) Review of Aerosol Research at the Finnish Antarctic Research Station Aboa and its Surroundings in Queen Maud Land, Antarctica. *Geophysica*, **45**, 163-181.

LONG-TERM TRENDS IN AIR POLLUTION AND NEW PARTICLE FORMATION IN EASTERN LAPLAND, FINLAND

E.-M. KYRÖ[1], M. DAL MASO[1], A. VIRKKULA[1,2], T. NIEMINEN[1], P.P. AALTO[1], P. KERONEN[1], P. HARI[3] and M. KULMALA[1]

[1] Department of Physics, University of Helsinki, P.O.Box 48, 00014 Helsinki, Finland

[2] Air Quality Research, Finnish Meteorological Institute, P.O.Box 503, 00101 Helsinki, Finland

[3] Department of Forest Sciences, University of Helsinki, P.O.Box 27, 00014 Helsinki, Finland

Keywords: Long-term trends, new particle formation, sulphur dioxide, air pollution

INTRODUCTION

The smelter industry in Kola peninsula is the most important source of air pollution in Eastern Lapland. During the past two decades, the sulphur emissions have decreased distinctively, yet they are still bigger than the emissions of whole Finland (Paatero *et al.*, 2008). SMEAR I station (Station for Measuring Ecosystem-Atmosphere Relations) (Hari *et al.*, 1994) was established in 1991 to measure trace gases alongside with aerosol concentration, photosynthesis and meteorology. The station is located only some $6km$ from the Russian boarder and is maintained from Värriö Research Station. Usually Värriö experiences South-Westerly winds (Ruuskanen *et al.*, 2003), but whenever the wind direction turns between North and East, the sulphur dioxide concentration increses drastically. The largest SO_2 concentrations are observed in late winter (Ruuskanen *et al.*, 2003).

Once emitted to the atmosphere, SO_2 forms sulphuric acid (H_2SO_4) via oxidizing reactions. Since sulphuric acid is known to be an essential factor in atmospheric new particle formation (NPF) (Sipilä *et al.*, 2010), we investigated, whether we can see the decrease in the Kola SO_2 emissions also in the frequency of NPF. Such a connection has previously been reported from Central Europe (Hamed *et al.*, 2010). Furthermore, we wanted to know, how much of the observed NPF the emissions explain. In addition, we tested a very simple approach to see what would be the presumable cloud condensation nuclei (CCN) concentration if the atmospheric SO_2 concentration would drop to pre-industrial level. In the analyses, we used data from $1998 - 2011$, since particle size distributions were available from 1998 onwards.

METHODS

At SMEAR I-station many atmospheric composition and aerosol properties are measured all-year-round. In this study, we used measurements of SO_2, aerosol size distribution and meteorological variables. The cut-off diameter of the size distribution measurements was changed from $8nm$ to $3nm$ in 2003. Sulphur dioxide is measured with a pulsed fluorescence analyzer and the aerosol size distribution with a DMPS (Differential Mobility Particle Sizer) system (Aalto *et al.*, 2001).

Particle formation events were classified based on the size distribution data (Dal Maso *et al.*, 2005) to events, non-events and undefined days. Particle formation rate was calculated by taking into account the time evolution of $3 - 25 - nm$ ($8 - 25 - nm$) sized particles and coagulation and the particle growth rate was obtained by following the nucleation mode mean diameter. Sulphuric acid proxy was calculated using the established parametrization (Petäjä *et al.*, 2009).
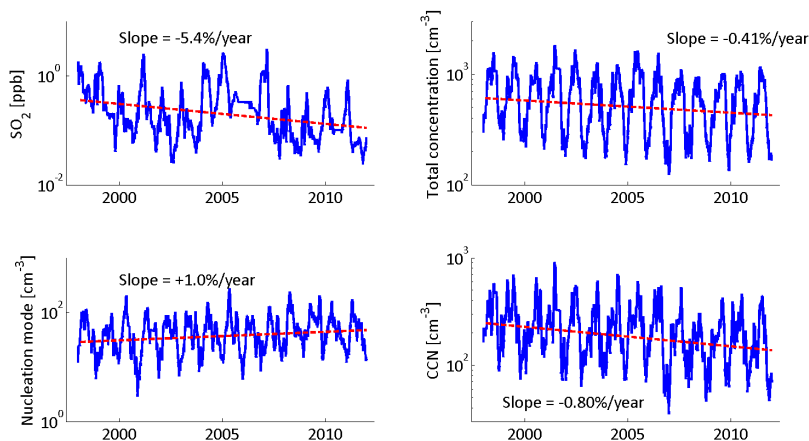
Figure 1: Timeseries of SO_2, total particle concentration, nucleation mode particle concentration and CCN concentration together with linear fits and slope percentages.

Sulphur dioxide concentrations are decreasing at SMEAR I on average $5.4\% yr^{-1}$ (Fig. 1). Similar decreasing trend is found in total particle concentration ($-0.41\% yr^{-1}$) and CCN concentration ($-0.8\% yr^{-1}$), however nucleation mode particle concentration is increasing ($+1\% yr^{-1}$).
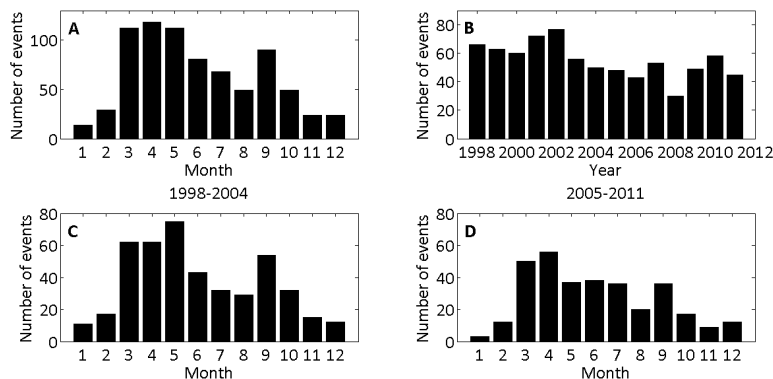
Figure 2: Monthly and yearly distributions of events during $1998 - 2011$ as well as monthly distributions during $1998 - 2004$ and $2005 - 2011$ at SMEAR I.

The number of events has a peak in April (Fig. 2A) and over the years the total number is clearly decreasing (Fig. 2B). If the timeseries is divided into two ($1998 - 2004$ and $2005 - 2011$), especially the late winter - early spring (March-May) values are clearly lower in the latter period. Since sulphur dioxide has also annual peak in late winter, the decrease in SO_2 concentration could be one reason for the lower amount of NPF in the $2005 - 2011$ period.

The correlations (R^2) with the yearly sum of events and non-events vs. the yearly sum and 95th percentile of SO_2 is presented in Fig. 3. The largest correlation ($R^2 = 0.44$) is found with the sum of non-events and sum of SO_2. Also the correlation with event sum and yearly SO_2 95th percentile has rather high correlation, 0.35. The median value over the whole time period is $0.2 ppm$. Thus,

410
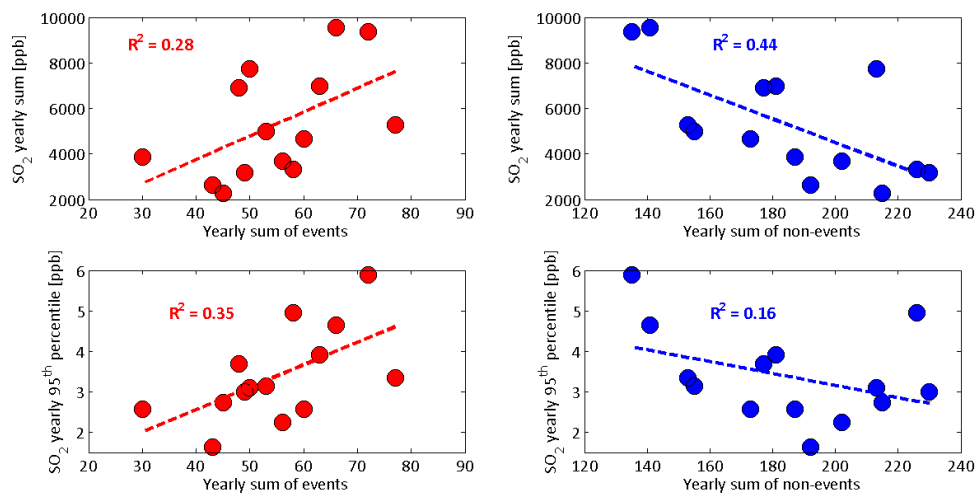
Figure 3: Correlations with yearly sum of events and non-events vs. yearly sum and 95th percentile of SO_2.

the sum and 95th percentile of SO_2 represents almost entirely the emissions coming from Kola peninsula. If the sulphur dioxide data is divided into "polluted" and "unpolluted" using the 95th percentile as a limit, the yearly sum of nucleation mode particles correlates very well with the yearly sum of SO_2 ($R^2 = 0.69$) in the values that are above 95th percentile. In unpolluted data there is no correlation ($R^2 = 0.02$).

If the amount of events during a timestep t is divided by the same t, we get a timeseries of the event fraction or event probability. In Värriö, the event probability is decreasing $0.8\% yr^{-1}$ and the non-event probability increases $1.4\% yr^{-1}$, correspondingly. Assuming, that the decrease in event probability is not linear, but logarithmic, with the current pace the events would decrease to 25% of the value in 1998 by the mid-2030s.

With similar, logarithmic approach, we can also estimate, how SO_2 explains of the new particle formation in Eastern Lapland and what would be the presumable CCN concentration with pre-industrial SO_2 concentration level. If both SO_2 and event fraction would decrease at the same pace as they are decreasing currently, at the time SO_2 would reach an average concentration $0.1 ppb$, which is the detection limit of the instrument and also the pre-industrial level (Stevenson et al., 2003), the event fraction would be decreased to 56% of the 1998 value. This would mean that the SO_2 pollution, that is mostly coming from Kola peninsula, would explain 56% of the events observed at SMEAR I. Similarly, with the pre-industrial SO_2 level, the CCN concentration would decrease down to $127 cm^{-3}$ from the 1998 value ($\approx 250 cm^{-3}$).

ACKNOWLEDGEMENTS

REFERENCES

Aalto, P., et al. (2001). Physical characterization of aerosol particles during nucleation events. Tellus, **53B**, 344-358.

Dal Maso, M., *et al.* (2005). Formation and growth of fresh atmospheric aerosols: eigth years of aerosol size distribution data from SMEAR II, Hyytiälä, Finland. *Boreal Environ. Res.*, **10**, 323-336.

Hamed, A., *et al.* (2010). Changes in the production rate of secondary aerosol particles in Central Europe in view of decreasing SO_2 emissions between 1996 and 2006. *Atmos. Chem. Phys.*, **10**, 1071-1091.

Hari, P., *et al.* (1994). Air Pollution in Eastern Lapland: Challenge for an Environmental Meaurement Station. *Silva Fennica*, **28**(1), 29-39.

Paatero, J., *et al.* (2008). Effects of Kola air pollution on the environment in the Western part of the Kola peninsula and Finnish Lapland - Final report. *Finnish Meteorological Institute Reports*, **6**, 1-26.

Petäjä, T., *et al.* (2009). Sulfuric acid and OH concentrations in a boreal forest site. *Atmos. Chem. Phys.*, **9**, 7435-7448.

Ruuskanen, T., *et al.* (2003). Atmospheric trace gas and aerosol particle concentration measurements in Eastern Lapland, Finland 1992-2001. *Boreal Env. Res.*, **8**, 335-349.

Sipilä, M., *et al.* (2010). The role of sulfuric acid in atmospheric nucleation. *Science*, **327**, 1243-1246.

Stevenson, D.S., *et al.* (2003) Atmospheric impact of the $1783 - 1784$ Laki eruption: Part I Chemistry modelling. *Atmos. Chem. Phys.*, **3**, 487-507.

RECOVERY OF SOIL CARBON POOLS IN A CHRONOSEQUENCE OF FOREST FIRES IN VÄRRIÖ STRICT NATURE RESERV, EASTERN LAPLAND.

K. KÖSTER[1,2], J. PUMPANEN[1], F.BERNINGER[1]

[1]Department of Forest Sciences, University of Helsinki, Finland.
[2]Institute of Forestry and Rural Engineering, Estonian University of Life Sciences, Estonia.

Keywords: SOIL CARBON, FIRE CHRONOCEQUENCE, SOIL CO_2 EFFLUX

INTRODUCTION

Boreal forests are a crucial part of the climate system since they contain about 60% of the carbon bound in global forest biomes. The temperature changes predicted for the future climate will be the most pronounced in boreal region (Kasischke, 2000).With increasing temperature there will be also changes in the disturbance regimes (intervals, intensity, severity). Fire is one of the most important natural disturbances in the boreal forest influencing strongly the structure, composition and functioning of the forests (Franklin et al., 2002). Fire is the primary process which organizes the physical and biological attributes of the boreal biome and influences energy flows and biogeochemical cycles, particularly the carbon and nitrogen cycle. It is expected, that with future climate change the fire frequencies in boreal forests will increase as a result of long drought events (Yakov, 2010).

Carbon fluxes between terrestrial ecosystems and atmosphere are large compared to anthropogenic emission, but they are currently in balance so that terrestrial ecosystems are a small net sink. The processes controlling the soil carbon pool play a substantial role in the terrestrial carbon balance. Even small proportional changes in the turnover of soil carbon stocks will reverse the terrestrial carbon sink to a source with consequent increase in the atmospheric CO_2 concentrations. For example, a decrease by 10% in soil organic carbon would be equivalent to all the anthropogenic CO_2 emitted during the last 30 years (Kirschbaum, 2000).

The aims of this study were to investigate the effect of fire on the decomposition of soil organic matter. More specifically, we studied the changes in the size and quality of soil carbon and nitrogen pools in boreal forests in the subarctic zone during different stages of forest succession after fire.

METHODS

The measurements were conducted in Värriö Nature Park (67°46' N, 29°35' E), which is located close to the Russian border in Lapland (Finland), in the northern boreal or subarctic coniferous forests. The sites are situated north of the Arctic Circle, near to the northern timberline at an average of 300 m altitude. Lowlands in the area are covered by taiga, where the main tree species is Scots pine (*Pinus sylvestris* L.). The soil in the area is moraine (with plenty of stones). Typical herbaceous plants*: Vaccnium myrtillus, Vaccinium vidis-ideae, Empetrum nigrum*, indicates also rather poor soil conditions. Treeline is around 470 m a.s.l. Annual mean precipitation in the area is about 600 mm and average annual mean temperature at Värriö research station (altitude 380 m) is around -1 °C. The climate in the area is subcontinental and the soil has no underlying permafrost. The snow covers the ground for around 200–225 days per year, and the length of the growing season is 105–120 days. The growing season in the area (mean monthly temperature more than 5 °C) lasts for 4 months and the average temperature during that period (from June to August) in the area is around 12 °C.

We have established 10 sample areas (with two replicate plots in each) in a chronosequence of 5 age classes (2 to 150 years since the last fire) during the summer 2011. The chronosequence consisted of four types of areas: (i) old areas, fire more than 150 years ago, (ii) fire around 60 years ago, (iii) fire around 40 years ago, (iv) fire 2 years ago. To characterize the stands we have established circular sample plots on areas with a radius of 11.28 m, where different tree characteristics were measured (diameter at 1.3 m height, height of a tree, crown height, crown diameter, stand age, etc.). A set of tree and ground vegetation

biomass measurements has been made. Five litter bags with Scots pine needles have been installed to each plot under the humus layer together with iButton temperature sensors (Maxim Integrated Products Ltd.) for soil organic matter (SOM) decomposition measurements. Age of trees and the time since last fire has determined from core samples taken from sample trees and analysed with WinDENDRO (Regent Instruments. Canada Inc., 2009). Ground vegetation biomass has been determined from 5 small sample plots (0.2 x 0.2 m in size) located systematically inside the circular sample plots.

Soil respiration was measured manually from all sample plots and continuous automatic soil air CO_2 concentration, temperature and water vapour measurements were taking place on one sample area. We measured soil air CO_2 by using Vaisala GMP343 (non-dispersive infrared sensor) diffusion type CO_2 probes (Vaisala OYj., Vaanta, Finland). We installed four sensors in August 2010 on the top of a soil (the air slot in the probe was pointing to the humus). The measurements were recorded with a data logger at 15-min intervals.

Manual chamber measurements were performed on 6 collars at each sample plot from June till August 2011 and will be performed from June till August 2012. The manual chamber was 0.24 m in high and 0.22 m in diameter. The CO_2 concentration (GMP343 Vaisala), air humidity and temperature (HM70, Vaisala) were recorded during a 4 minutes chamber closure time. The rate of CO2 exchange was estimated from linear regression that was fitted to the CO_2 readings.

To characterize the soil carbon (C) and nitrogen (N) content, and fine root biomass at the sites, we have taken 10 soil cores (0.1 m long and 0.05 m in diameter) from every sample plot. The soil cores were divided according to morphological soil horizons to litter and humus layers and the mineral layers to eluvial and illuvial horizons and sieved. Fine roots were separated from the soil. The soil C and N content was measured with elemental analyser (varioMAX CN elemental analyser, Elementar Analysensysteme GmbH, Germany) after drying the samples in an oven at 105 °C for 24 hours.

RESULTS AND CONCLUSIONS

The overall/total C and N contents in the first 10 cm of the topsoil (all soil layers taken into consideration) were highest on old areas (fire 150 years ago) and lowest on new areas (fire 2-40 years ago). The highest C pools (1071 g m-2) were measured on old areas from top soil horizons (consisting of decomposing litter). The total C pool at the old site was 2329 g m-2. The area where the fire was 2 years ago had the lowest total C pools, 1550 g m-2 respectively. The lowest C pools were measured from the area where the fire was 60 years ago. When we compared the total C pools, the newly burned areas (areas where the fire was 2 – 40 years ago) formed one group (had similar values of total C) and old areas (areas where the fire was 60-150 years ago) formed another group with similar values. Same tendencies occurred also in total N pools, where the lowest values occurred where the fire was recently and the highest values were observes in old areas. These results are also correlating to the soil respiration measurements, where we had the lowest values in areas where the fire was 2 years ago (0,047 mg CO2 s-1 m-2) and highest values were measured in old areas (0,144 mg CO2 s-1 m-2).

Our preliminary results show that forest fire has a substantial effect on the C and N pool in the litter layer decaying on the forest top soil layer, but not in the humus layer and in mineral soil layers. Soil respiration and biomass development showed similar chronological response to the time since the forest fire indicating that substantial proportion of the respiration was originating from the very top of the soil.

ACKNOWLEDGEMENTS

REFERENCES

Franklin, J.F., Spies, T.A., Pelt, R.V., Carey, A.B., Thornburgh, D.A., Berg, D.R., Lindenmayer, D.B., Harmon, M.E., Keeton, W.S., Shaw, D.C., Bible, K., Chen, J., 2002. Disturbances and structural development of natural forest ecosystems with silvicultural implications, using Douglas-fir forests as an example. Forest Ecology and Management 155, 399-423.

Kasischke, E.S., 2000. Boreal ecosystems in the global carbon cycle. In: Kasischke, E.S., Stocks, B.J. (Eds.), Fire, Climate Change, and Carbon Cycling in the Boreal Forests. Springer, New York, 461 p., pp. 19-31.

Kirschbaum, M.U.F., 2000. Will changes in soil organic carbon act as a positive or negative feedback on global warming? Biogeochemistry 48, 21-51.

Yakov, K., 2010. Priming effects: Interactions between living and dead organic matter. Soil Biology and Biochemistry 42, 1363-1371.

THE EFFECT OF SEA ICE CONDITIONS AND NORTH ATLANTIC OSCILLATION TO THE AEROSOL PROPERTIES IN NY-ÅLESUND, SVALBARD – PRELIMINARY RESULTS

M. LASSILA[1], E.-M. KYRÖ[1], R. KREJCI[1,2], P. TUNVED[2], J. STRÖM[2] and M. KULMALA[1]

[1]Department of Physics, University of Helsinki, P.O.Box 48, 00014 Helsinki, Finland

[2]Department of Applied Environmental Science, Stockholm University, S-106 91 Stockholm, Sweden

INTRODUCTION

Recent studies have documented evidence for dramatic decrease in both annual mean sea ice extent and sea ice thickness (Singarayer et al. 2006) in the Arctic Ocean. The record low sea ice extent was reached in 2007 (Lindsay et al. 2009). The concentrations of methanosulphnic acid (MSA) in the atmosphere and sea ice extent have been shown to correlate positively (Sharma et al. 2012). Therefore, it is likely that the aerosol production in the Arctic will increase with the declining sea ice cover.
The North Atlantic Oscillation (NAO) is an index that describes the atmospheric circulation in the North Atlantic region and is related to the semi-permanent pressure areas over Iceland and the Azores. Eckhardt et al. (2003) have shown that NAO strongly affects the pollution transport into the Arctic. During positive phases of the NAO, when the pressure difference is high, more pollution is transported into the Arctic compared to its negative phases. The aim of this study was to find out if aerosol properties (e.g. size distribution and concentration) over sea ice differ from properties over open ocean in Ny-Ålesund, Svalbard and whether NAO has an effect on aerosol properties.

METHODS

We used aerosol and meteorological data from Zeppelin, Ny-Ålesund and trajectories from HYSPLIT model (Draxler and Rolph, 2011) to track air parcel backward in time. We chose trajectories which came to Ny-Ålesund from sea and compared those with the sea ice extent to find trajectories which came to Ny-Ålesund over sea ice and under 500 meters. The height was chosen so that trajectories travelled over the ice inside the mixing height. We used sea ice data from the AMIP-project of Program for Climate Model Diagnosis and Intercomparison (PCMDI) (Hurrell et al., 2008). The ice concentration is reported as a percentage (0 to 100 percent). We used a threshold value of 15 percent, in dividing the open sea from ice covered sea. Same percentage is used at the National Snow and Ice Data Center. A total of 1016 trajectories fulfilled our criteria during 2000-2009. Later we will also take into our analysis the time that the air mass stays over the ice. In addition, we used black carbon (BC) data, which is available from 2005 onwards from Zeppelin station.

RESULTS

The mean temperature, wind speed and relative humidity during 2000-2009 and over the sea ice during the same period are shown in Table 1. The mean temperature during when the air mass is coming over sea ice is 20 °C lower than the overall mean value. The differences in wind speed and relative humidity between the air masses that are coming over sea ice compared to overall mean values are not large.

Nucleation and Aitken mode particle concentrations are clearly lower when the air mass has been over sea ice compared with the entire period 2000-2009 (Table 2). In accumulation mode concentration there is no difference. New particle formation (NPF) does not happen as often over sea ice as over sea (Fig. 1).

Also, the aerosol is more aged in air masses over ice than over sea, which can be seen as a shift from 160 nm to 180 nm in the peak value of the larger mode in Figure 1.

	2000-2009	Over sea ice 2000-2009
Temperature (^{o}C)	6.8	-14.0
Wind speed (m/s)	3.1	4.2
Relative humidity (%)	83.0	90.0

Table 1. Mean meteorological values in Ny-Ålesund during 2000-2009 and over the sea ice during the same period.

	2000-2009	Over sea ice 2000-2009
Nucleation mode	28.2	14.4
Aitken-mode	64.7	30.0
Accumulation mode	71.9	71.3
Total	156	115

Table 2. Mean aerosol concentrations at Zeppelin, Ny-Ålesund, during 2000-2009 and over sea ice during the same period
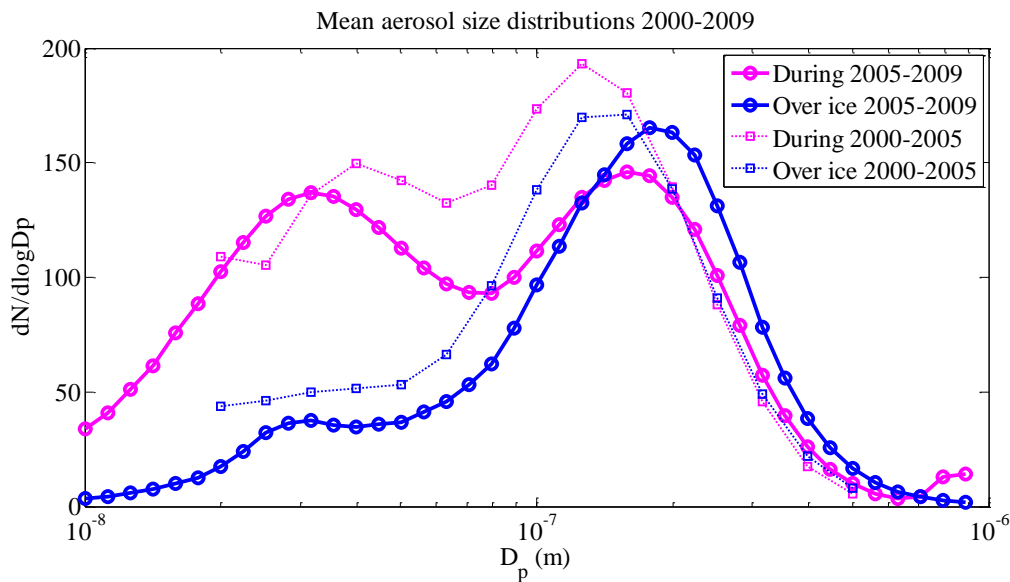
Figure 1. Mean aerosol size distributions during 2000-2009 and over sea ice during the same period.

	Positive NAO-index		Negative NAO-index	
	During 00-09	Over ice	During 00-09	Over ice
Nucleation mode	40.1	7.80	38.2	22.1
Aitken-mode	70.1	31.3	79.5	35.0
Accumulation mode	84.3	80.5	78.5	78.7
Total	193	119	195	135

Table 3. Mean aerosol concentrations in Ny-Ålesund, during positive and negative phases of NAO, 2000-2009 and over sea ice during the same period.

There are clear differences in the aerosol size distributions during the negative and positive phases of NAO. While during positive NAO the aerosol size distribution over sea ice is unimodal (Fig. 2A), it is

bimodal during negative NAO. The concentrations during 2005-2009 and over sea ice during the same period are shown in Table 3. These differences most likely reflect the different transport pathways of air masses during positive and negative phases of NAO.

The mean BC concentration when the air mass had been over sea ice was 0.05 µg cm^{-3}, which is clearly lower compared with entire period 2005-2009 (0.14 µg cm^{-3}). During NAO+ the values were few times larger (0.08 and 0.27 µg cm^{-3}, respectively) , than during NAO- (0.059 and 0.032 µg cm^{-3}, respectively).
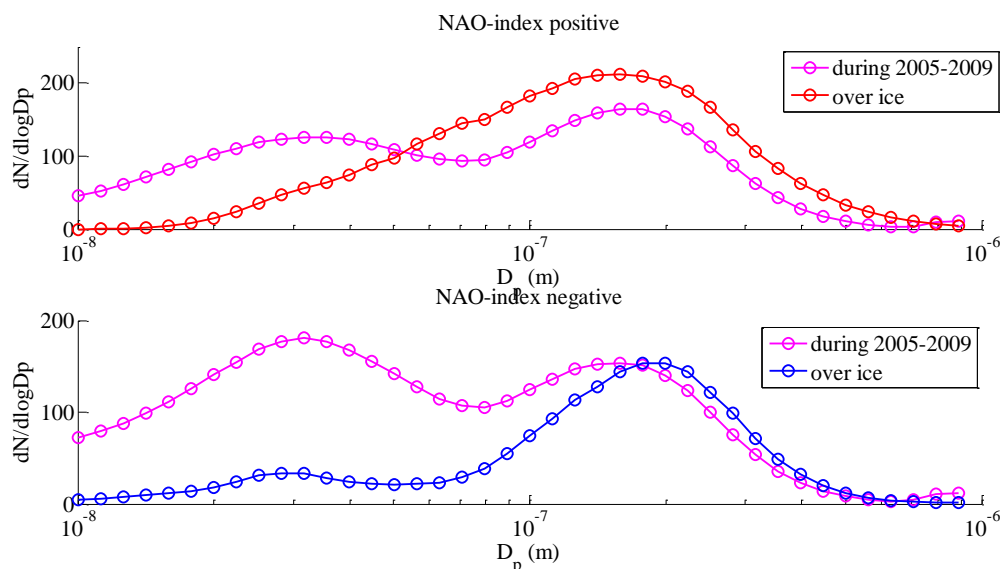
Figure 2. Mean values of aerosol size distributions during positive (A) and negative (B) phases of NAO, 2005-2009.

REFERENCES

Draxler, R. R. and Rolph, G. D. (2011). HYSPLIT (HYbrid Single-Particle Lagrangian Integrated Trajectory) model, http://ready.arl.noaa.gov/HYSPLIT.php, NOAA Air Resources Laboratory, Silver Spring, MD.

Eckhardt, S., et al. (2003). The North Atlantic Oscillation controls air pollution transport to the Arctic. Atmos. Chem. Phys.**3**, 1769–1778.

Hurrell, J.W., et al. (2008). A New Sea Surface Temperature and Sea Ice Boundary Dataset for the Community Atmosphere Model. J. Clim., **21**, 5145–5153.

Lindsay, R., et al. (2009). Arctic sea ice retreat in 2007 follows thinning trend, J. Clim., **22**, 165–176.

Singarayer, J. S., et al. (2006), Twenty-first-century climate impacts from a declining Arctic sea ice cover, J. Clim., **19**, 1109 –1125.

Sharma, S., et al. (2012). Influence of transport and ocean ice extent on biogenic aerosol sulfur in the Arctic atmosphere. JGR, **117**, D12209.

CHARACTERIZATION OF THE AIRMODUS A20 CONDENSATION PARTICLE COUNTER

K. LEHTIPALO[1,2], J. VANHANEN[1], T. TOIVOLA[1], J. MIKKILÄ[1], T. PETÄJÄ[2] AND M. KULMALA[2]

[1]Airmodus Oy, Helsinki, Finland

[2]Department of Physics, University of Helsinki, Helsinki, Finland

Keywords: AEROSOL INSTRUMENTATION, CONDENSATION PARTICLE COUNTERS

INTRODUCTION

Condensation particle counters (CPCs) are the basis of modern aerosol instrumentation in the sub-micrometer size range. CPCs can be used both as stand-alone instruments for measuring the total particle number concentration, and as counters in different kind of applications such as the differential/scanning mobility particle sizer (DMPS/SMPS).

Airmodus A20, a new laminar flow condensation particle counter, was launched in 2011. The A20 uses butanol as the condensing liquid and has a robust saturator design for durability. The aerosol flow rate is 1 LPM, achieved with a critical orifice and an external pump. Narrow pulse widths allow measuring at high concentrations. The A20 can be also combined to the Airmodus A09 Particle Size Magnifier (PSM; Vanhanen *et al.*, 2011) for decreasing the cut-off size even down to 1.5 nm.

METHODS

The performance of the A20 CPC was verified in the University of Helsinki laboratory calibration setup (*e.g.* Petäjä *et al.,* 2006) using silver particles produced in a tube furnace and size selected by a Hauke-type DMA. Nitrogen was used as carrier gas in the furnace, and the aerosol was neutralized with an Am241 source. The size-selected silver particles were used for determining the cut-off size of the new instrument, and for concentration calibrations. The reference instrument for the calibrations was a TSI 3068B aerosol electrometer with a sample flow rate of 5 LPM.

Additionally, we investigated the stability of the instrument in long-term measurement both in the laboratory and in field conditions at the Hyytiälä SMEAR II measurement station (Hari and Kulmala, 2005).
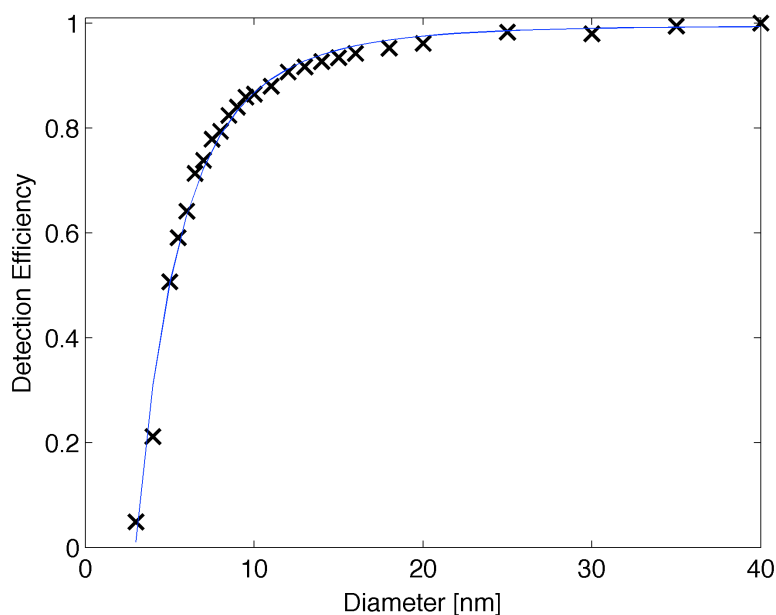
Figure 1. The detection efficiency as a function of particle size for A20.

CONCLUSIONS

Figure 1 presents the results of the cut-off size calibration. The 50% detection efficiency (cut-off size) of the Airmodus A20 CPC was about 7.1 nm for negatively charged silver particles.

Concentration calibrations were conducted using 35 nm charged silver particles. The single particle counting capability (with < 10% coincidence) of the A20 reached to about 25 000 #/cc. In higher concentrations the pulse rate started to decrease compared to the electrometer concentration due to co-incidence in the optics. Based on calibrations, a 4th order polynomial correction function was determined for correcting the concentration. Using this correction function to the measured pulses the concentration matches with the electrometer even above 10^5 #/cc (Figure 2).

The A20 bCPC was also tested in field conditions. It proved to be suitable for long-term field measurements over a large range of sizes and concentrations and compared well to other similar aerosol instrumentation.
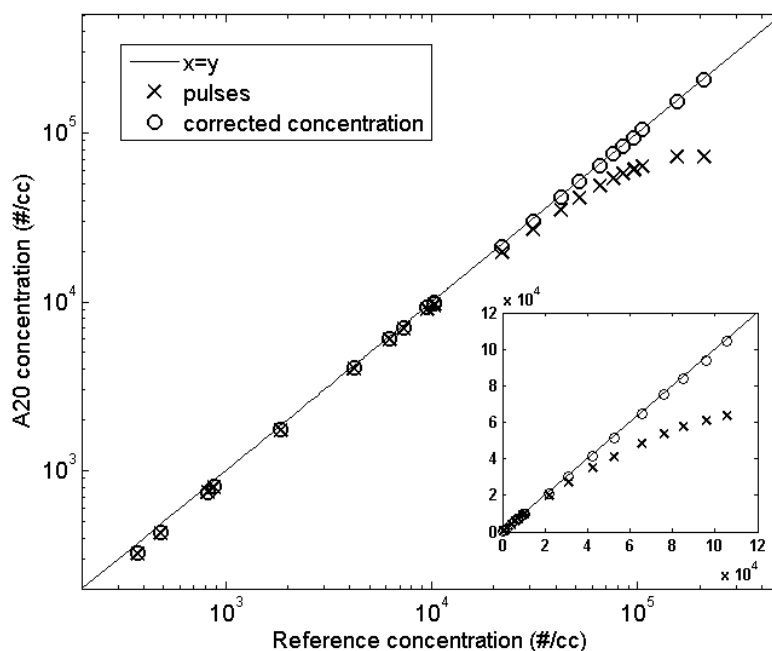
Figure 2. The concentration (raw pulse data and the corrected concentration) measured with the A20 against the concentration from the reference instrument, presented in log-scale (larger picture) and linear scale (small picture).

REFERENCES

Hari, P. and Kulmala, M. Station for measuring ecosystem-atmosphere relations (SMEAR II). *Boreal. Environ. Res.* **10**, 315-322, 2005.

Petäjä, T., Mordas, G., Manninen, H., Aalto, P.P., Hämeri, K., and Kulmala, M.: Detection efficiency of a water-based TSI condensation particle counter 3785. *Aerosol Sci. Technol.* **40**, 1090-1097, 2006.

Vanhanen, J., Mikkilä, J., Lehtipalo, K., Sipilä, M., Manninen, H. E., Siivola, E., Petäjä; T., Kulmala, M. (2011). Particle Size Magnifier for Nano-CN Detection. *Aerosol Sci. Tech.,* **45**, 4, 533-42.

AIRBORNE MEASUREMENTS OF AEROSOL PARTICLES IN THE LOWER ATMOSPHERE OF SOUTHERN FINLAND

K.E. LEINO[1], R. VÄÄNÄNEN[1], A. VIRKKULA[1,2], P.P. AALTO[1], T. POHJA[1], L. KORTETJÄRVI[1], R. KREJCI[1,3], T. PETÄJÄ[1] and M. KULMALA[1]

[1]Department of Physics, University of Helsinki, Helsinki, Finland
[2]Finnish Meteorological Institute, Helsinki, Finland
[3]University of Stockholm, Sweden

Keywords: Aerosol, airborne, wildfire.

INTRODUCTION

Atmospheric aerosol particles have significant climatic effects (IPCC, 2007). Depending on the environment and conditions, the atmospheric air contains different amounts of aerosol particles. One of the globally important sources of these particles is secondary new particle formation (Birmili et al., 2003; Kulmala et al., 2004; Dal Maso et al., 2005; Mönkkönen et al., 2005; Stolzenburg et al., 2005; Kulmala ja Kerminen, 2008). New particle formation (NPF) events, different growth mechanisms and composition of the particles are currently under an intensive investigation. Another important source of aerosol particles is primary sources, like wild fires (Niemi et al., 2005; Mielonen et al., 2011) and traffic (Kittelson et al., 2004).

To characterize both vertical and horizontal characteristics of the sub-micron particles, we performed several airborne measurement campaigns within the boreal atmosphere in Southern Finland during 2009–2012 (Schobesberger et al., 2012). In this study, the analysis concentrates on flights conducted in 29 – 30 July 2010. During this period there were intensive wildfire episodes in Russia. The aim of these studies was to investigate the total aerosol particle number concentration and carbon dioxide from ground level up to 3500 meters in eastern and southern Finland. The results are compared with the ground-level measurements in Smear III and observations in Mielonen *et al.,* 2011 around Kuopio area.

METHODS

The measurement flights were made using a small aircraft, Cessna FR172F. The instrumentation onboard the plane are described in more detail in Schobesberger et al. 2012. Shortly, the devices during these flights in question included an ultrafine particle counter TSI 3776 (Mordas et al., 2008) that was measuring total particle concentration with 3 nm cut-off size. There were also a CO_2/H_2O analyzer Li-Cor LI–840 and a pressure sensor inside the plane and a relative humidity and temperature sensor as well as the sample air inlet mounted outside the plane in the right wing of the aircraft. GPS receiver recorded the flight coordinates.

Overall, the measurement flights in the lower troposphere were carried out during three campaign periods in 2010 operated from and to Tampere-Pirkkala airport. The measurement areas covered mainly forest areas in the central and southern Finland, with the aim to look into new particle formation events. The exeption was the flights between 29.-30.7. 2010, when we probed into emissions of sub-micron particles from wildfires in Russia.

BIOMASS BURNING AEROSOLS FROM WILDFIRES

During summer 2010, the forest fire emitted particles were observed in Eastern Finland (Mielonen et al., 2012). July 29 2010 total number concentrations went up to $(8 \cdot 10^3 \text{ cm}^{-3})$ cm^{-3} at altitudes 2.5 – 3.8 km

over the Jämsä area in Finland. The total particle number concentration and also carbon dioxide concentration for four altitude profiles are shown below in fig 1. At next day July 30th we did not detected significantly elevated concentrations any more (fig 2). The flight tracks for both days are shown in fig 3. The CO_2 concentration was about 380-390 ppm during the all flights and it did not differ from usual values. Air masses came to Finland on 29July from Southeast at altitudes 3 km and from Southeast or East at altitudes 500 meters. On 30 July air masses came to Finland from Southwest or South at all altitudes according to backtrajectory analysis (Figure 4). The air mass trajectories are calculated using HYSPLIT4 model (Draxler, 1999) and the results are shown in fig 4 and 5.
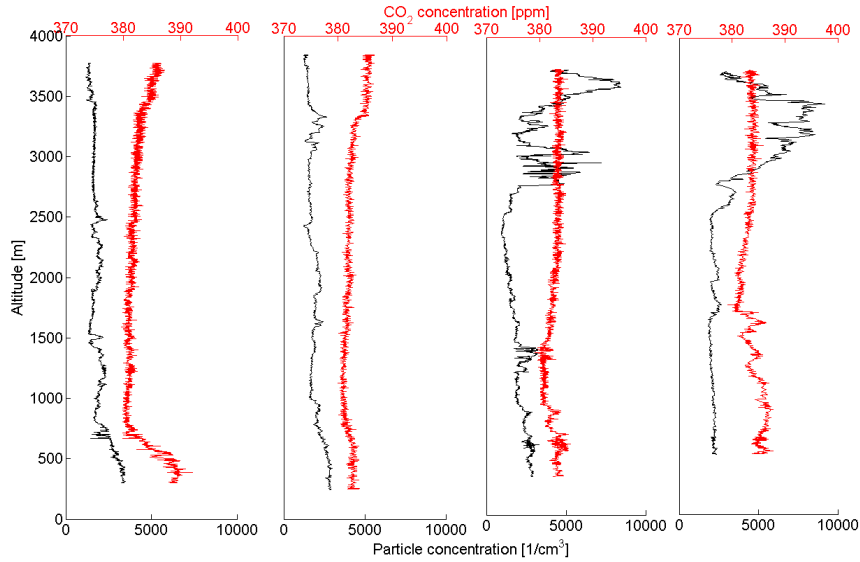
Figure 1. The total number concentration and CO_2 concentration during four altitude profiles in the evening on July 29th.

423
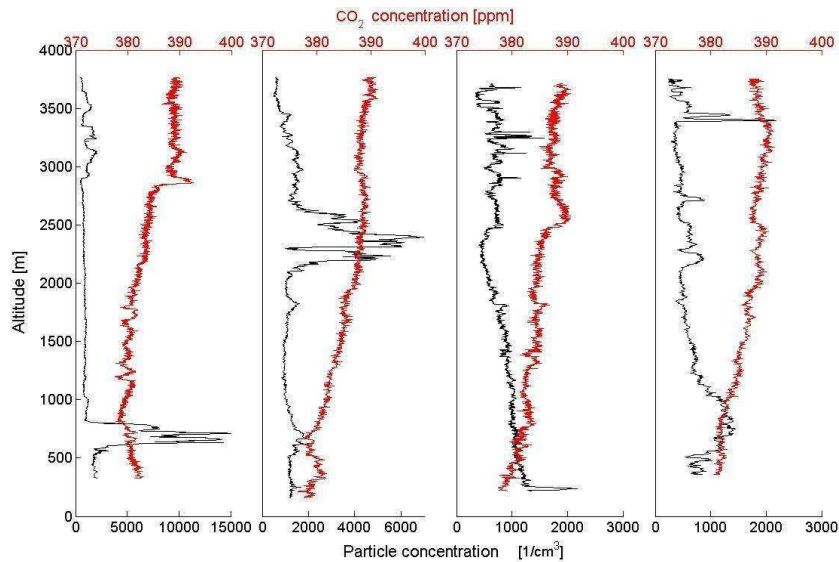
Figure 2. The total number concentration and CO_2 concentration during four altitude profiles in the morning on July 30th.
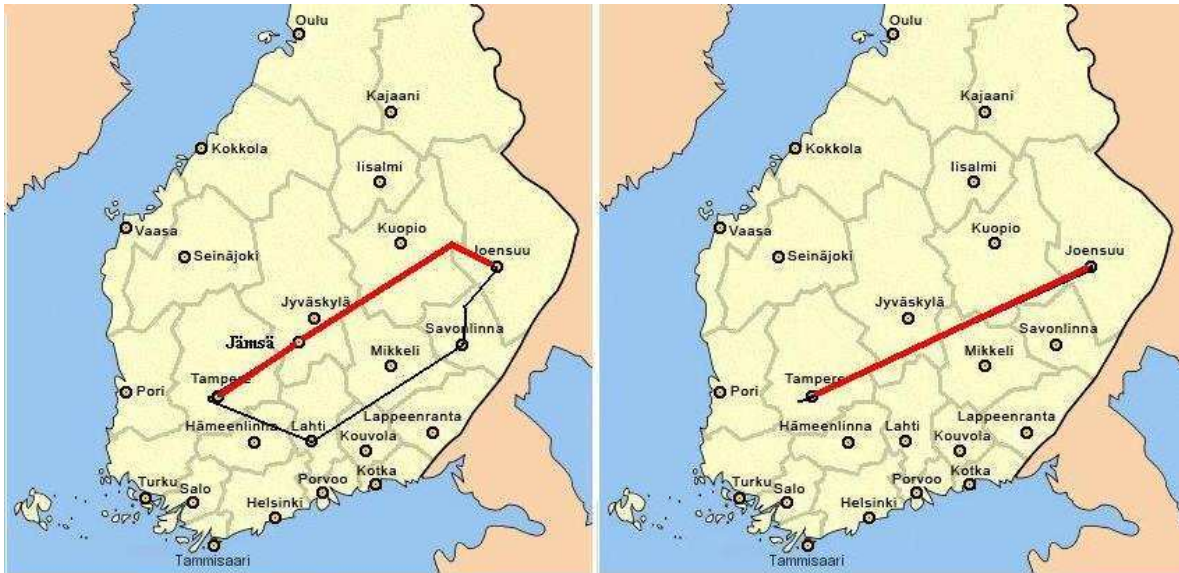
Figure 3. On the left side of this figure are described the flight tracks of two measurement flights on 29 July and on the right the flight tracks of two measurement flights on 30 July. The red lines are corresponding to the tracks for profiles considered in figures 1 and 2.

Air masses came to Finland on 29 July from Southeast at altitudes 3 km and from Southeast or East at altitudes 500 meters. On 30 July the sampled air mass onboard the Cessna came to Finland from Southwest or South at all altitudes.
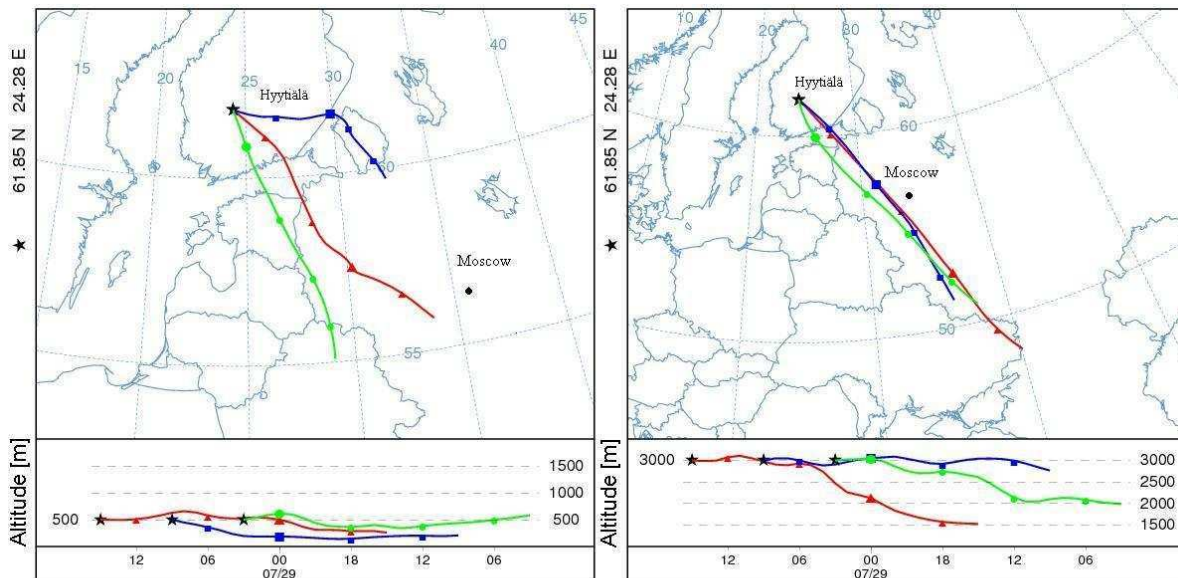
Figure 4. The trajectories for air masses arrived to Finland in two air levels on 29 July.
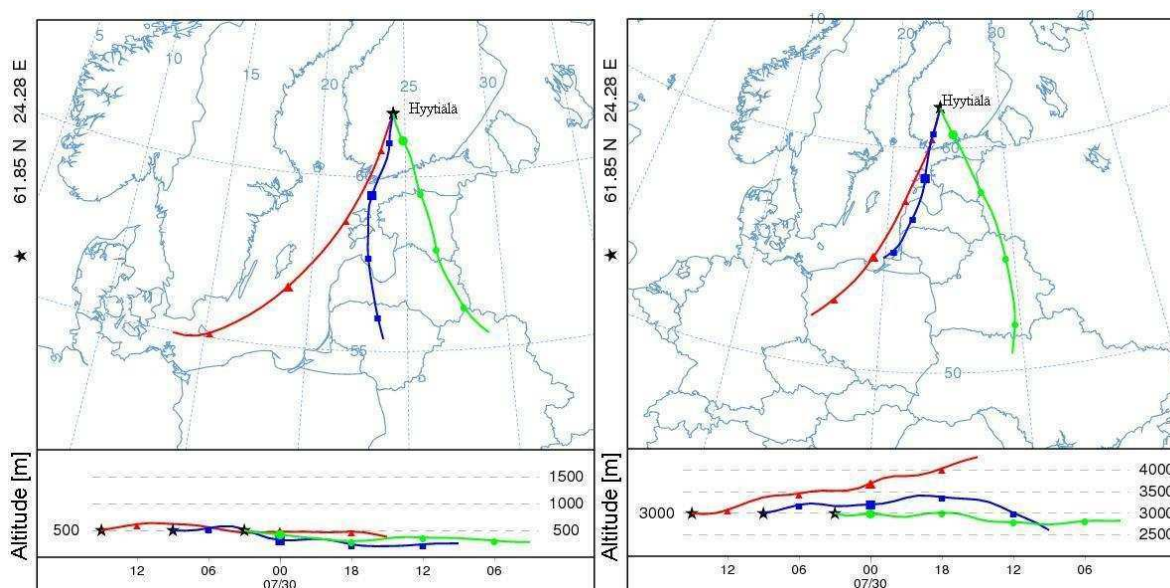
Figure 5. The trajectories for air masses arrived to Finland in two air levels at 500 m above mean sea level and at 3000 m (AMSL) on 30 July.

CONCLUSIONS

During summer 2010 measurement campaign was conducted revealing the aerosol particle total number concentration and carbon dioxide concentration in eastern and southern Finland during Russian peat bog and forest fires near to Moscow. July 29 was detected significant smoky layers at altitudes 2.5 – 3.8 km in the central of Finland. Also the visibility was weak during this measurement flight. Air masses came to Finland directly from wildfire areas and the smell of smoke was pungent. This kind of biomass burning measurement and other emitted particles on the air need more investigation to solving climatic problems for instance.

ACKNOWLEDGEMENTS

REFERENCES

Birmili, W., *et al.* (2003). The Hohenpeissenberg aerosol formation experiment (HAFEX): a long-term study including size-resolved aerosol, H_2SO_4, OH, and monoterpenes measurements. *Atmos. Chem. Phys.* 3: 361–376.

Dal Maso, M., *et al.* (2005). Formation and growth rates of fresh atmospheric aerosols: eight years of aerosol size distribution data from SMEAR II, Hyytiälä, Finland. *Boreal Env. Res.,* 10: 323–336. Draxler, R.R. (1999): *HYSPLIT4 user's guide*. NOAA Tech. Memo. ERL ARL-230

IPCC (the Intergovernmental Panel on Climate Change) (2007). Climate Change 2007: The Physical Science Basis. Summary for Policymakers. *Contribution of Working Group I to the Fourth Assessment*

Report of the Intergovernmental Panel on Climate Change [Solomon, S., D. Qin, M. Manning, Z. Chen, M. Marquis, K.B. Averyt, M.Tignor and H.L. Miller (eds.)]. Cambridge University Press, Cambridge, United Kingdom and New York, NY, USA. Available online at http://www.ipcc.ch/publications_and_data/ar4/wg1/en/spm.html.

Kittelson et al. (2004) Nanoparticle emissions on Minnesota highways, Atmos. Environ.

Kulmala, M., *et al.* (2004). Formation and growth rates of ultrafine atmospheric particles: a review of observations. *J. Aerosol Sci.* 35: 143–176.

Kulmala, M. and Kerminen, V.-M. (2008). On the formation and growth of atmospheric nanoparticles. *Atmos. Res.* 90: 132–150.

Mielonen, T., *et al.* (2011). Biomass burning aerosols observed in Eastern Finland during the Russian wildfires in summer 2010 - Part 2: Remote sensing. *Atmos. Env.,* 1–9.

Mordas, G., *et al.* (2008). Nanometer Particle Detection by the Condensation Particle Counter UF-02proto. *Aerosol Sci. Tech.,* 42: 7, 521–527.

Mönkkönen P., *et al.* (2005). Measurements in a highly polluted Asian mega city: Observations of aerosol number size distributions, modal parameters and nucleation events. *Atmos. Chem. Phys.* 5: 57–66.

Niemi, J.V., *et al.* (2005). Characterization of aerosol particle episodes in Finland caudes by wildfires in Eastern Europe. *Atmos. Chem. Phys.* 5, 2: 2469–2501.

Schobesberger S., *et al.* (2012). Airborne measurements over the boreal forest of southern Finland during new particle formation events in 2009 and 2010. *Bor. Env. Res.,* 18:00–00. In prep. http://www.borenv.net/BER/pdfs/preprints/Schobesberger.pdf

Stolzenburg, M.R., *et al.* (2005). Growth rates of freshly nucleated atmospheric particles in Atlanta. *J. Geophys. Res.* 110, D22S05.

STUDY THE EFFECT OF TEMPERATURE ON NATURAL AEROSOL PORDUCTION POTENTIALS OVER BOREAL FORESTS

L. LIAO[1], M. KULMALA[1] and M. D. MASO[1]

[1] Division of Atmospheric Sciences, Department of Physics, University of Helsinki, P.O.Box 48, 00014, Helsinki, Finland

Keywords: aerosol, temperature, BVOCs.

INTRODUCTION

Atmospheric aerosol has climatic influence, and affects air quality and human health. The source of atmospheric aerosols includes both natural and anthropogenic origins. Secondary aerosol formed via the oxidation of biogenic volatile organic compounds accounts for the most significant fraction among the global aerosol budget. The boreal forest emitted VOCs, in particular terpenes, have shown to be one of the important aerosol precursor sources linking to the secondary aerosol production in northern hemisphere (Tunved et al., 2006). The emission of biogenic VOCs is temperature dependent, thus it may influence the secondary aerosol production as well as the CCN loading (Tunved et al., 2008), which further forms the vegetation, aerosol and climate interaction system (Kulmala et al., 2004).

In this work, we investigate the potential and the order of magnitude of the temperature influence on the natural aerosol budgets; we discuss the natural aerosol growth at different size ranges in different temperature bins from back trajectory analysis.

METHODS

The research and data analysis were based on the measurements at two Finnish SMEAR (Station for Measuring Ecosystem-Atmosphere Relations stations: SMEAR I (67°46' N, 29°35' E, 400 m asl) in Värriö, and SMEAR II (61°51'N, 24°17'E, 170 m asl) in Hyytiälä, Finland. 13 year dataset from 1998 to 2010 at SMEAR I and 15 year dataset between 1996 and 2010 at SMEAR II have been used, including continuously DMPS measurements, temperature and backward trajectory data. The DMPS particle size spectrums were divided into three size modes: the nucleation mode in the particle size range of 3--25 nm, Aitken mode (25--100 nm), and accumulation mode (100--1000 nm). Particle number concentrations at each mode were calculated every one hour. Hourly particle volume concentrations were integrated from the DMPS size distribution assuming spherical particles. The hourly 96 hour backward trajectories arriving at 100 m a.g.l over both stations were calculated from the HYSPLIT4 model (Draxler et al., 1997).

Trajectories transporting 90% of time in one 180° transport sector 0ºN-180ºS relative Värriö, and travelled only above 60° North at the SMEAR I station, and one 180° transport sector 90ºW-90ºE relative Hyytiälä at the SMEAR II station, (seen in Figure 1), were extracted from the whole dataset. The travelling time over land for each trajectory was estimated from topographical data. The temperature along each trajectory was equally separated to 5 bins from 0 to 20 Celsius degrees.

CONCLUSIONS

The preliminary results suggest that temperature plays a strong role on controlling the growth of aerosol particles (see. E.g. Figure 2). First, temperature controls the precursor emissions of secondary aerosols, which will directly link to the volume and mass growth of aerosol particles. Second, temperature influences the gas/particle partitioning mechanisms. However, temperature has various influences on aerosol particles at different mode
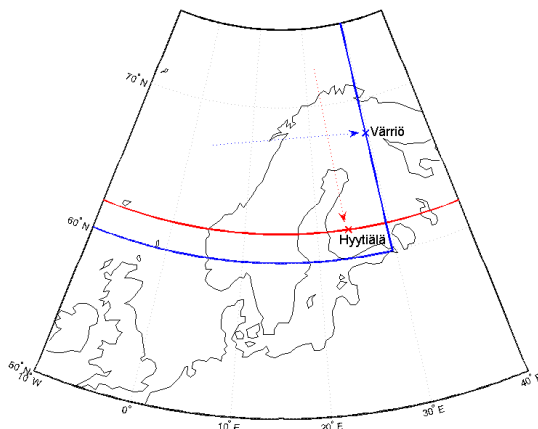
Figure 1. The transport sectors of back trajectories at the two stations. Area above red line is the travelling zone of selected trajectories arriving at Hyytiälä station. The blue sector covers the transport area of trajectories arriving at Värriö station. At both stations, each trajectory should spend at least 90% of travelling time inside the transport sectors.

(a)	(b)
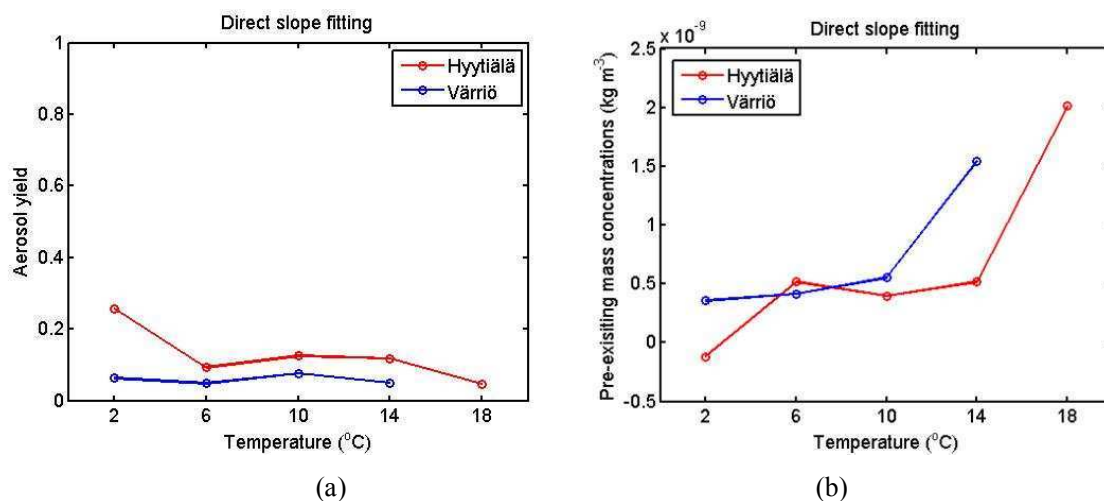
Figure 2. (a) The estimated aerosol yield (i.e. the direct fitting slope between aerosol mass and total MT emissions) in five temperature bins, and (b) the pre-existing aerosol mass defined from the y-intercept from the fitting at five temperature bins at both stations.

REFERENCES

Draxler, R. R. & G. D. Hess (1997) Description of the Hysplit_4 modelling system. *NOAA Tech Memorandum,* ERL ARL-224.

Tunved, P., H. C. Hansson, V. M. Kerminen, J. Strom, M. Dal Maso, H. Lihavainen, Y. Viisanen, P. P. Aalto, M. Komppula & M. Kulmala (2006) High natural aerosol loading over boreal forests. *Science,* 312**,** 261-263.

Tunved, P., J. Stroem, M. Kulmala, V. M. Kerminen, M. Dal Maso, B. Svenningson, C. Lunder & H. C. Hansson (2008) The natural aerosol over Northern Europe and its relation to anthropogenic emissions - implications of important climate feedbacks. *Tellus Series B-Chemical and Physical Meteorology,* 60**,** 473-484.

Kulmala, M., T. Suni, K. E. J. Lehtinen, M. Dal Maso, M. Boy, A. Reissell, U. Rannik, P. Aalto, P. Keronen, H. Hakola, J. B. Back, T. Hoffmann, T. Vesala & P. Hari (2004) A new feedback mechanism linking forests, aerosols, and climate. *Atmospheric Chemistry and Physics,* 4**,** 557-562.

A NEW APPROACH FOR USING NATURAL ISOTOPE RATIOS TO DESCRIBE CHANGES IN MICROBIAL CN POOLS WITHIN SOM

A.S. LINDÉN[1], J. HEINONSALO[1,2], E. SONNINEN[3], H. ILVESNIEMI[4], and J. PUMPANEN[1]

[1]Department of Forest Sciences, Faculty of Agriculture and Forestry, P.O.Box 56, FIN-00014 University of Helsinki, Helsinki, Finland
[2]Viikki Biocenter, Department of Food and Environmental Sciences, Faculty of Agriculture and Forestry, P.O.Box 56, FIN-00014 University of Helsinki, Helsinki, Finland
[3]Finnish Museum of Natural History, Dating Laboratory, P.O. Box 64, FI-00014 University of Helsinki
[4]Finnish Forest Research Institute, Vantaa Research Station, PO Box 18, FI-01301 Vantaa, FINLAND

INTRODUCTION

The transformation of soil organic matter (SOM) and its stabilization during decomposition processes is reflected in the ratio between the less abundant heavier isotopes ^{15}N and ^{13}C compared to the lighter isotopes ^{14}N and ^{12}C in SOM. The heavier isotopes tend to enrich in the compounds where the molecular bonds are strongest and therefore, their content becomes larger in the highly, often highly processed SOM fractions (Fry 2008). In many natural ecosystems, the availability of nitrogen, plays a crucial role in controlling net primary production and the response of plants on increasing CO_2 fertilization is very uncertain. In free air CO_2 enrichment (FACE) experiments, it has been shown that the trees can increase the nitrogen acquisition from soil by increasing belowground allocation of recent photosynthates (Drake *et al.* 2011). In this study, we wanted to examine the possible changes occurring in the natural isotopic composition of ^{15}N and ^{13}C in boreal topsoil SOM fractions.

The use of isotopic tracers has its limitations in monitoring the changes taking place in SOM in field conditions because the changes in natural isotope ratios in soils can be efficiently masked by the high variation within the heterogeneous soil matrix that is constantly varying under opposite microbial processes. Here, we developed a new approach for evaluating the changes occurring in SOM fractions during decomposition and nutrient acquisition by plants. Currently, the classification of soil into different density or chemical fractions has been widely utilized to separate different pools, but in practice these methods fail to account biological as well as structural properties of soils that represent important constraining factors for decomposition process. We have been examining way to combine good properties from both worlds by studying pools of material decomposition in a such way that polymeric chemical bonds are separated indiscriminately by their energetic principles and bond strength, rather than discriminating substances based solely on their density or chemical functionality. In our experiment, we were using SOM from our microcosm experiment, which was first separated into different fractions according to their solubility by using a pressurized hot water extraction (PHWE) method and subsequent radiocarbon dating as well as analysis of $\delta^{13}C$ and $\delta^{15}N$ values form the extracts separately.

METHODS

The SOM was separated by using the pressurized hot water extraction (PHWE) (Kronholm *et al.* 2007). Extractions were carried out at Finnish Forest Research Institute (METLA) by using 2 g SOM subsamples weighted into extraction chamber. The separated fractions and the left over material were freeze-dried for later isotope analysis of $\delta^{13}C$ and $\delta^{15}N$ at Finnish Museum of Natural History, Dating Laboratory. The preliminary results indicate that the PHWE extraction method could be utilized to separate ecologically relevant microbial pools to reduce natural variation within the whole soil matrix.

CONCLUSIONS

The method may be suitable for studying the connection between canopy level processes and rhizomicrobial processes in field conditions by using the natural abundance of isotope ratios of carbon and nitrogen. This enables

the observations of otherwise hidden and small transformations. Approach could be new promising way to utilize the natural abundance of ^{15}N and ^{13}C isotopes for monitoring and quantifying changes in forest soils. Currently, we are evaluating the reliability of this approach to identify how the selective degradation of recalcitrant SOM by fungal communities and subsequent C utilization by bacteria may be observed in field conditions without using additional isotopic tracers.

ACKNOWLEDGEMENTS

REFERENCES

Fry B 2008. Stable Isotope Ecology, (eds Fry B), pp. 10, 202. Springer Science / Business Media, New York.

Kronholm J., Hartonen K. and Riekkola M.L. 2007. Analytical extractions with water at elevated temperatures and pressures. Trends anal. chem. 26(5): 396-412.

Drake, J.E., Gallet-Budynek, A., Hofmockel, K.S., *et al.*, 2011 Increases in the flux of carbon belowground stimulate nitrogen uptake and sustain the long-term enhancement of forest productivity under elevated CO_2. Ecology Letters 14, 349-357.

XYLEM DIAMETER CHANGES IN TREES RELATED TO DRAUGHT AND FREEZING

A. LINTUNEN[1], L. LINDFORS and T. HÖLTTÄ

[1]Department of Forest Sciences, University of Helsinki,
P.O. BOX 27, FI-00014 University of Helsinki, Finland.

Keywords: xylem diameter, freezing, draught, Scots pine

INTRODUCTION

At the boreal forest zone, trees experience large seasonal variations in temperature: from +30°C in summer to -50°C in winter. At temperatures above freezing, changes of xylem diameter in stem have been reported in several papers and they are linked to transpiration-induced water tensions inside the stem (e.g. Simonneau *et al.*, 1993; Zweifel *et al.*, 2000; Sevanto *et al.*, 2006). Xylem diameter in trees is known to change also at freezing temperatures, it shrinks due to freezing (Zweifel and Häsler, 2000; Améglio *et al.*, 2001). It is not yet known what mechanism is behind the diameter changes in xylem at freezing temperatures. It has been suggested that consistently with summer diameter changes, diameter changes in xylem during freezing would be based on changes in xylem water tensions related to the proceeding of the ice front (Améglio *et al.*, 2001).

Also bark of tree stems is known to shrink due to freezing considerably more compared to xylem because of the higher elasticity of the living cells (Zweifel and Häsler, 2000;Améglio *et al.*, 2001). Shrinkage of bark due to freezing has been related to extracellular freezing, which protects the living cells from cell death (Burke *et al.*, 1976). In extracellular freezing (Fig. 1), the freezing of parenchyma cells is avoided as water is passively pulled out from the cells due to the difference in water vapour pressure between the unfrozen cell sap and proceeding ice front in the extracellular spaces. As a result of this, the cell shrinks and it's osmotic concentration increases thus lowering the freezing point (Burke *et al.*, 1976). When the bark has been autoclaved, no shrinking has occurred but swelling instead due to the larger volume of ice compared to liquid water (Améglio *et al.*, 2001).
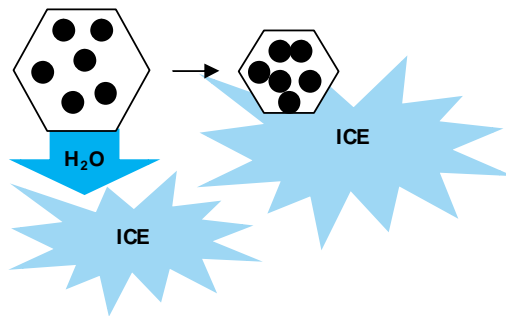
Figure 1. Schematic presentation of extracellular freezing. In extracellular freezing, the osmotic concentration inside the living cells increases as extracellular ice creates a water vapour pressure deficit that draws cell water out of the winter acclimated, elastic cells. This leads to shrinkage of the cells.

We hypothesize that the living parenchyma cells have a role in the diameter changes of xylem both in summer and winter time. Xylem contains approximately 5-8% parenchyma of its volume in conifers (Panshin and de Zeeuw 1980 in Spicer and Holbrook, 2004). There are three types of living parenchyma in xylem: parenchyma in wood rays, longitudinal wood parenchyma and parenchyma in resin ducts (Kärkkäinen, 2007). In order to understand the phenomena driving the xylem diameter changes better and

to assess the potential role of the living parenchyma cells, we measured diameter changes in living and killed samples in drying and freezing experiments.

MATERIAL AND METHODS

Eight 5cm long samples from branches of Scots pine (*Pinus sylvestris* L.) were cut during summer from six years old saplings for the drying experiment. For the freezing experiment, six 15cm long samples from cold acclimated branches of Scots pine and three 15cm long samples from cold acclimated branches of European aspen (*Populus tremula*) were cut during February. We also used three saplings of aspen grown in a greenhouse and thus they were not winter acclimated. There were two alternative killing-treatments for the samples before the drying or freezing experiments: heating and sudden freezing. In the heating treatment, the samples were wrapped in plastic film and insulation tape after which the samples were kept in 60°C oven for an hour in order to kill most of the living parenchyma cells in the xylem. In the sudden freezing treatment, the samples were protected from evaporation with aluminium foil and dipped into liquid nitrogen (LN_2). The reference samples had no treatment.

Xylem was reviled at the intact surface of the diameter sensors in order to detect only changes in xylem diameter. Before the drying experiment, water was run through the samples in order to flush the samples and to make sure they were fully hydrated before the experiment. The drying experiment was done in ambient room conditions by letting two samples dry on table, one killed sample (heated or suddenly frozen) and one reference sample. The freezing experiments were conducted in a weather chamber. The ambient temperature was decreased from approximately 20°C to -10°C in approximately two hours. Thermocouples were measuring the xylem- and ambient temperatures. Two diameter sensors were recording the changes in xylem ray diameter during drying or freezing.

In the drying experiment, the diameter change was defined as the total diameter change before the samples reached approximately -1.8MPa water potential. In the freezing experiment, xylem diameter change was defined as the maximum diameter change reached after the freezing.

RESULTS AND CONCLUSIONS

In the drying experiment, xylem diameter shrank more in the reference samples compared to the treated samples (Fig. 2a). We did not make difference between the two killing treatments among the treated samples. In the freezing experiment, xylem in the reference samples shrank, whereas in the case of treated samples, the diameter swelled (Fig. 2b). Also in the untreated aspen saplings that were grown in a greenhouse, the diameter swelled at freezing, because they died in the freezing experiment due to the lack of winter acclimation (Fig. 2b). It seems that the living cells do have a role in the diameter changes of xylem both in freezing temperatures, and in summer.
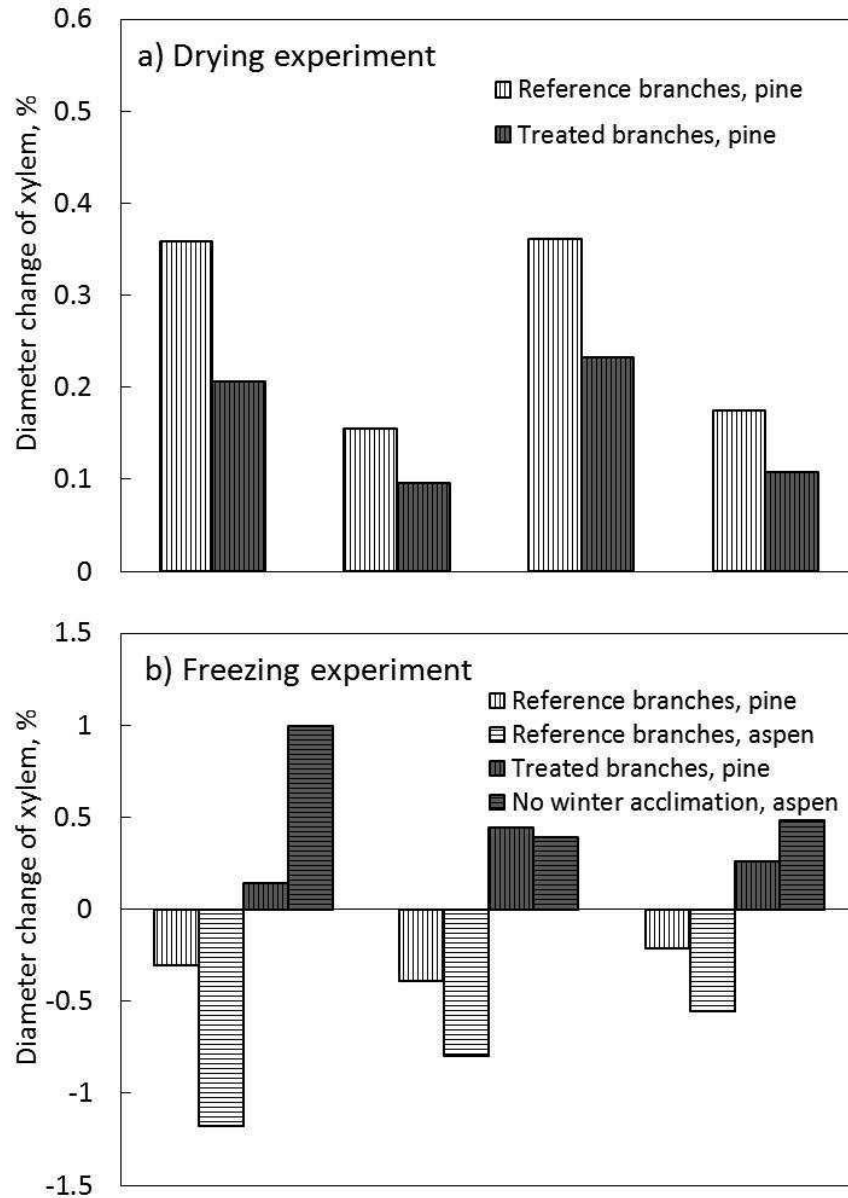
Figure 2. Relative change of xylem diameter during a) drying and b) freezing. Each repetition with different treatments is shown.

.

The mechanism of diameter shrinkage in the freezing experiment of the reference samples could be similar as hypothesized for the bark; extracellular freezing of parenchyma cells (Améglio et al. 2001). When the shrinkage of parenchyma cells was not possible, the samples swelled. Phase change of liquid water into ice increases the volume of water by 9%. Perhaps in the case of functioning parenchyma cells in xylem of the reference samples, the volume growth of freezing water uses the space released by the shrinking of the elastic parenchyma cells. But when the parenchyma cells have lost the elasticity due to the killing treatment and do not shrink, there is no space for the volume growth of water to expand than to outwards increasing the sample diameter. Similarly in the drying experiment, part of the xylem diameter change may be related to the water leakage out of the living cells due to high water potential differences between the living cells and the surrounding water conducting conduits.

The results of this study show that the changes in xylem diameter at freezing are a sum of extracellular freezing of living parenchyma cells and phase change of water in the xylem: the xylem conduits are expanding due to an increase in volume, and the parenchyma cells are shrinking due to extracellular freezing simultaneously. The latter change is larger as the net effect in the reference samples is xylem diameter shrinking. Thus the diameter changes cannot be directly used as indicators of xylem tensions related to the proceeding of the ice front. It seems that the living parenchyma plays a role also in the diameter changes of xylem at summer time, although the xylem diameter changes have been interpreted to represent solely the changes in the tension of water in conducting xylem elements.

REFERENCES

Améglio, T., H. Cochard and F.W. Ewers (2001). Stem diameter variations and cold hardiness in walnut trees. *J. Exp. Botany* **52**: 2135.

Burke, M.J., L.V. Gusta, H.A. Quamme, C.J. Weiser and P.H. Li (1976). Freezing and injury in plants. *Ann. Rev. Plant Phys.* **27**: 507

Kärkkäinen, M. (2007). *Puun rakenne ja ominaisuudet (Wood structure and characteristics)*. (Metsäkustannus, Hämeenlinna, Finland)

Sevanto, S., T. Suni, J. Pumpanen, T. Grönholm, P. Kolari, E. Nikinmaa, P. Hari and T. Vesala (2006). Wintertime photosynthesis and water uptake in a boreal forest. *Tree Physiol.* **26**: 749.

Simonneau, T., R. Habib, J.P. Goutouly and J.G. Huguet (1993). Diurnal changes in stem diameter depend upon variations in water content: direct evidence in peach trees. *J. Exp. Botany* **44**: 615.

Spicer, R. and N.M. Holbrook (2004). Within-stem oxygen concentration and sap flow in four temperate tree species: does long-lived xylem parenchyma experience hypoxia? *Plant, Cell, Environ.* **28**: 192.

Zweifel, R. and R. Häsler (2000). Frost-induced reversible shrinkage of bark of mature subalpine conifers. *Agricul. For. Meteor.* **102**: 213.

Zweifel, R., H. Item and R. Häsler (2000). Stem radius changes and their relation to stored water in stems of young Norway spruce trees. *Trees* **15**: 50.

CARBON DIOXIDE AND ENERGY FLUXES IN A NORTHERN BOREAL LAKE

A. LOHILA[1], J. HATAKKA[1], M. AURELA[1], T. PENTTILÄ[2] and T. LAURILA[1]

[1]Finnish Meteorological Institute, Climate Change Research, PO Box 503, FI-00101 Helsinki, Finland.

[2]Finnish Forest Research Institute, Vantaa Research Unit, PO Box 18, FI-01301
Vantaa, Finland.

Keywords: carbon balance, catchment, ecosystem-atmosphere exchange, eddy covariance method.

INTRODUCTION

Boreal forest soils and peatlands store a huge amount of carbon (C) and interact with the atmosphere by exchanging greenhouse gases (GHG) which are relevant to global warming. Besides the ecosystem-atmosphere exchange, the aquatic export has been recognized as a highly significant component of the C balance (Kindler *et al*., 2011). The lateral fluxes of C constitute a key link between the terrestrial and aquatic ecosystems: surface waters move C from terrestrial system into lakes and finally into oceans. In a boreal catchment with mature forest in Finland, for example, it has been estimated that about 10% of the terrestrial net ecosystem production may be emitted back to the atmosphere by a lake (Huotari *et al.*, 2011). This makes it necessary to reassess the previously estimated carbon balances, which are based on atmospheric fluxes only and thus are likely to overestimate the true terrestrial sink. For this purpose, we have established a new eddy covariance (EC) flux measurement site on lake Pallasjärvi. The lake receives water from the Pallaslompolo catchment, within which the carbon dioxide (CO_2) and methane (CH_4) fluxes have been continuously measured with the EC method above a spruce forest and a wetland (Aurela *et al.,* 2009). In addition, lateral fluxes of inorganic and organic C have been monitored. Now, the establishment of this new lake flux site will enable the quantification of the full catchment-scale carbon balance. Here we present the measurement setup and the first results from this site.

METHODS

The measurements were conducted on the border of Kittilä and Muonio municpalities, on lake Pallasjärvi (60.005°N, 24.205°E). The 2 m tall steel mast was erected on the tip of a small spit, in shallow water in the bottom of the lake. The spit is part of an esker gravel ridge which is partly located underwater. The ridge divides the area into a shallow and sheltered inlet where the surface waters from the Pallaslompolo catchment are discharged (sector 160–330° from the mast), and a deeper lake (348–33° through north). The mean depth of the lake is about 1.5 and 5 m in the inlet and deeper parts, respectively. Only data from these wind directions were used in further analysis, while the rest of the data represents flux from the forest sector, and were thus not used. In addition, we removed all data with friction velocity <0.05 m s^{-1}.

The measurement height was 2.5 m above the bottom of the lake, while the water level at the point of measurement varied from 30-60 cm during the measurement period. The EC flux measurement system consisted of a LI-7200 CO_2/H_2O analyzer (LI-COR Inc.) and a sonic anemometer (uSonic-3 scientific, Metek GmbH). In addition, meteorological variables such as air and water temperature (Pt 100), water level height (Trafag 8438.66.2646), net radiation (NR lite, Kipp&Zonen), and incoming and reflected PAR (PQS1, Kipp&Zonen) were measured at the site. Measurement period presented in this paper covers June 17–August 20, 2012.

RESULTS

The CO_2 fluxes were small and mainly positive during the summer. Mean emission was highest from the shallow sector dominated by grasses, 0.019 mg CO_2 m^{-2} s^{-1}, and half of that in the open water sectors. On

average, the flux rate in the open water sector equals a daily flux of nearly 1 g CO_2 m^{-2} (Table 1). The CO_2 emission from the open water sector was at the lower range of the results reported by Vesala *et al.* (2006) for summer season from a small boreal lake in southern Finland surrounded by a mainly forested catchment.

Wind direction	Median CO_2 flux $\pm$ SE (mg m^{-2} s^{-1})	Daily emission (g CO_2 m^{-2} d^{-1})
South, grass dominated sector	0.019 ± 0.003	1.7
South, open water	0.011 ± 0.001	0.9
North, open deep water	0.010 ± 0.001	0.8

Table 1. CO_2 flux from different sectors on lake Pallajärvi in June-August 2012.
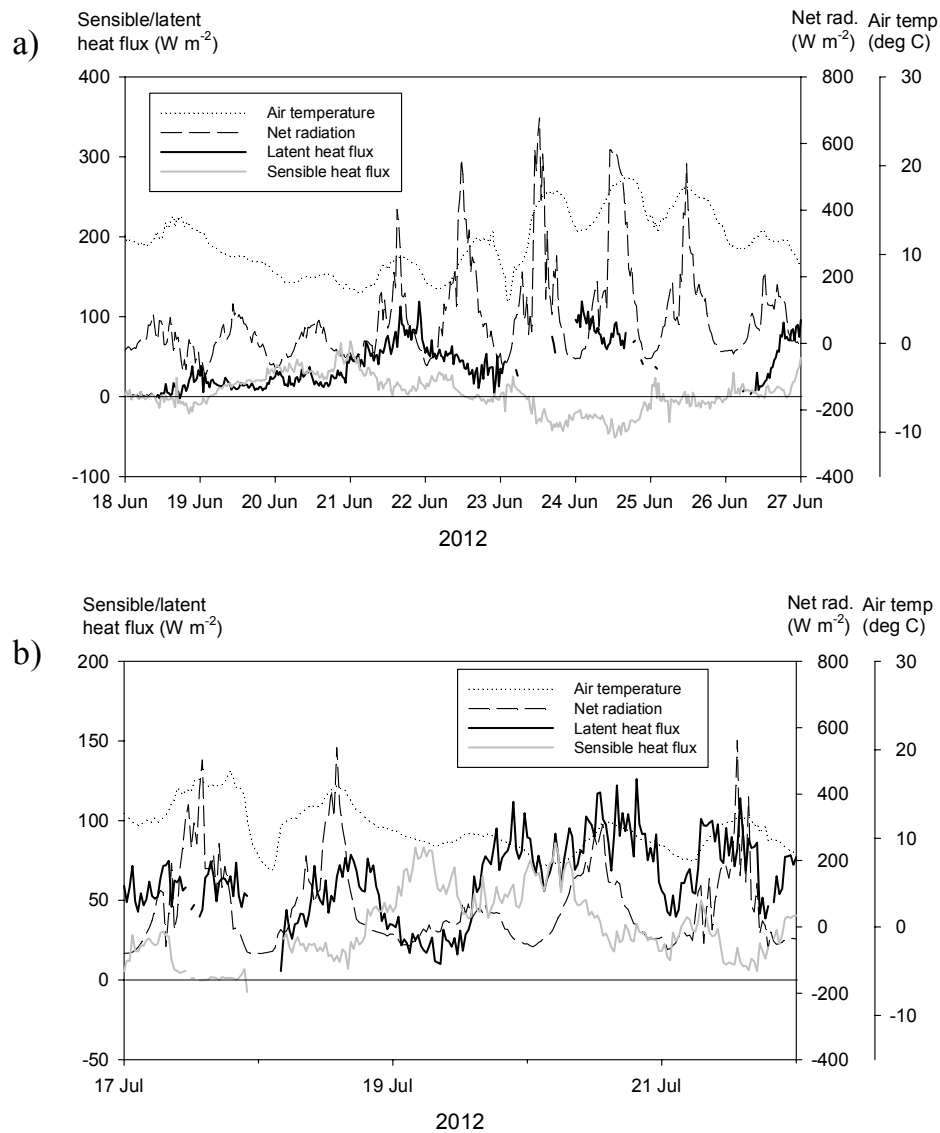
Figure 1. Latent and sensible heat fluxes together with net radiation on lake Pallasjärvi in a) June and b) July 2012.

Latent heat fluxes (LH) were small in June-August, below 150 W m^{-2}, and had no clear diurnal cycle. Sensible heat fluxes (SH) were within the same range with LH. SH fluxes varied from negative to positive values, and were controlled by the difference in air and water temperature. For example in June 23–27 with maximum air temperatures between 15–20 °C, the sensible heat flux was negative, indicating transfer of heat from the air into the lake. However in July 17–22, with lower air temperatures (around 10°C), the lake acted as a source of heat into the atmosphere.

ACKNOWLEDGEMENTS

REFERENCES

Aurela M., A. Lohila, J.-P. Tuovinen, J. Hatakka J., T. Riutta, and T. Laurila (2009) Carbon dioxide exchange on a northern boreal fen, *Boreal Environ. Res.* 14, 699–710.

Huotari J., A. Ojala, E. Peltomaa, A. Nordbo, S. Launiainen, J. Pumpanen et al. (2011) Long-term direct CO_2 flux measurements over a boreal lake: Five years of eddy covariance data, *Geophys. Res. Lett.* **38**, L18401.

Kindler R., J. Siemens, K. Kaiser, D.C. Walmsley, C. Bernhofer, N. Buchmann et al. (2011) Dissolved carbon leaching from soil is a crucial component of the net ecosystem carbon balance, *Global Change Biol.* **17**, 1167-1185.

Vesala, T., J. Huotari, Ü. Rannik, T. Suni, S. Smolander, A. Sogachev, S. Launiainen, and A. Ojala (2006) Eddy covariance measurements of carbon exchange and latent and sensible heat fluxes over a boreal lake for a full open-water period, *J. Geophys. Res.* **111**, D11101.

ELECTRIC DIPOLE MOMENTS OF SMALL SULFURIC ACID CONTAINING CLUSTERS FROM FIRST-PRINCIPLES MOLECULAR DYNAMICS SIMULATIONS

V. LOUKONEN[1], I-F. W. KUO[2], M. J. MCGRATH[3] and H. VEHKAMÄKI[1]

[1] Division of Atmospheric Sciences, Department of Physics, University of Helsinki, Helsinki, P.O. Box 64, FI-00014 University of Helsinki, Finland.

[2] Chemical Sciences Division, Lawrence Livermore National Laboratory, Livermore, California 94550, USA.

[3] Department of Biophysics, Graduate School of Science, Kyoto University, Kyoto 6068502, Japan.

Keywords: ELECTRIC DIPOLE MOMENT, ATMOSPHERIC CLUSTERS, FIRST-PRINCIPLES MOLECULAR DYNAMICS, SULFURIC ACID.

INTRODUCTION

Today, atmospheric new-particle formation is one of the most important research problems the scientific community faces. The numerous and interconnected feedback mechanisms ranging over several orders of magnitude in space and time make the phenomenon and its consequences very elusive to investigate as a whole. A more viable approach, it seems, is to concentrate on the specific details of the whole process separately. Here, we focus on the electric dipole moments of electrically neutral (sulfuric acid) · (ammonia) and (sulfuric acid) · (dimethylamine) clusters.

Sulfuric acid is probably the most important driving agent in atmospheric new-particle formation (e.g. Kulmala et al., 2004). However, during the very first clustering steps the participation of other species is probable. Recently, the role of various amines in this process has raised a lot of interest (e.g. Kurtén et al., 2008), whereas ammonia has been the standard clustering partner of sulfuric acid for years. A good understanding of the properties and formation of these clusters is a necessary prerequisite in the quest of finding out how the free molecules in the atmosphere form stable aerosol particles with potentially global consequences.

One interesting property these small molecular clusters possess is the electric dipole moment. In general, the dipole-dipole interaction is very weak in comparison with other types of electric interactions. Nevertheless, the electric dipole moment might very well have a role in the collision dynamics of neutral clusters, and, via the stronger charge-dipole interaction, the dipole moment most probably has an even bigger role if ions are present. However, we start by studying the electric dipole moment of stable and electrically neutral clusters.

METHODS

We chose to study the clusters of

$$(\text{sulfuric acid})_n \cdot (\text{dimethylamine})_n \quad \text{and} \quad (\text{sulfuric acid})_n \cdot (\text{ammonia})_{n-1}, \quad \text{where } n = 2, 3, 4 \text{ and}$$
$$(\text{sulfuric acid})_2 \cdot (\text{dimethylamine})_1 \quad \text{and} \quad (\text{sulfuric acid})_3 \cdot (\text{ammonia})_3,$$

as these clusters were found to be very stable in a recent theoretical study (Ortega et al., 2012).

First, we run first-principles molecular dynamics simulations in the NVT ensemble at the temperature of $T = 300$ K for 45 ps with a timestep of 0.5 fs. The simulations were performed using the CP2K program (`www.cp2k.org`) at the PBE/TZV2P level of electronic structure theory, using a simulation box of 20 Å and a plane-wave cutoff of 600 Ry. The simulations provided phase-space trajectories for all the atomic nuclei in the clusters. We then took "snapshots" from the trajectories with an interval of 5 fs, localized the electrons to obtain an approximation for the location of the negative charge, and finally calculated the dipole moments of the clusters.

The first ten pico-seconds of the simulations were used to equilibrate the clusters and equilibrium data was collected from the last 35 ps. The equilibrium is defined to be reached when the average of the potential energy stays constant (Loukonen et al., 2012). The only cluster that did not equilibrate during the first 10 ps was (sulfuric acid)$_4$ · (ammonia)$_3$. For this cluster the simulation was continued in order to obtain 35 ps of equilibration data.

<div align="center">RESULTS</div>

The time-development of the electric dipole moments for the studied clusters is shown in Figure 1: ammonia-containing clusters are in the left pane and dimethylamine-containing clusters in the right. Perhaps the most striking aspect to notice is the rather large oscillation in the dipoles. Firstly, there is faster, large-amplitude oscillation around the mean values. However, also the mean values do oscillate, but with a smaller magnitude. The likely cause for the oscillations is the thermal motion which keeps the clusters continuously moving, but is not large enough to break the clusters (Loukonen et al., 2012). However, the dipole moments seem to be much more affected by the thermal movement than e.g. the potential energy is. This is probably explained by the nature of the clusters: all the base molecules have accepted one proton from the sulfuric acid molecules, thus forming ion pairs between the acid and base molecules. These ion pairs largely dictate the bonding patterns that bound the clusters. Interestingly, the individual atoms forming the bonds changed during the simulations, even in equilibrium. In other words, the molecules do not only exhibit thermal vibrations but also rotations (Loukonen et al., 2012). As a consequence, the electric dipole moment reacts to this movement quite strongly.

The equilibrium values of the electric dipole moments are reported in Table 1.

Cluster	Electric dipole moment (Debye[†])
(sulfuric acid)$_2$ · (ammonia)$_1$	7.56 ± 1.13
(sulfuric acid)$_3$ · (ammonia)$_2$	8.54 ± 1.86
(sulfuric acid)$_3$ · (ammonia)$_3$	6.15 ± 1.48
(sulfuric acid)$_4$ · (ammonia)$_3$ [‡]	5.92 ± 1.83
(sulfuric acid)$_2$ · (dimethylamine)$_1$	8.47 ± 1.20
(sulfuric acid)$_2$ · (dimethylamine)$_2$	2.93 ± 1.16
(sulfuric acid)$_3$ · (dimethylamine)$_3$	8.11 ± 1.67
(sulfuric acid)$_4$ · (dimethylamine)$_4$	3.57 ± 1.43

Table 1: Mean values of the electric dipole moments from the first-principles molecular dynamics simulations, corresponding to the last 35 ps of simulations in Figure 1.
[†] Debye = 3.33564×10^{-30} C·m.
[‡] This value is obtained from an additional equilibrium simulation, not shown here.

It is interesting to notice that in the studied dimethylamine clusters with even number of acids and bases, the magnitude of the dipole is clearly smaller than in the odd amine-containing clusters. The ammonia clusters do not show similar characteristics. As one would expect, by adding a third ammonia molecule to 3:2-cluster yields a smaller dipole, but surprisingly, by adding an acid to
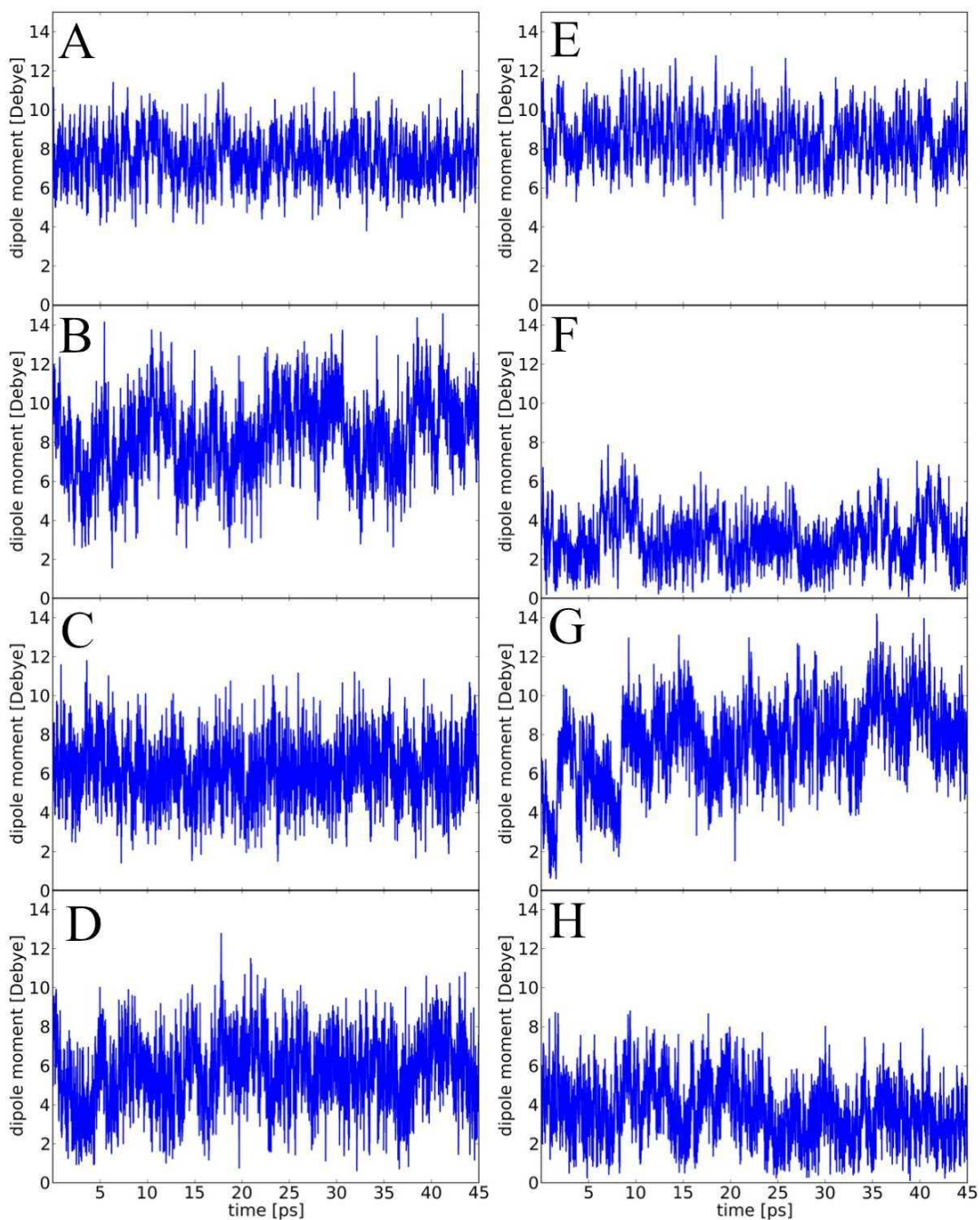
Figure 1: Electric dipole moments of the studied clusters as a function of time. A) 2A1N, B) 3A2N, C) 3A3N, D) 4A3N, E) 2A1D, F) 2A2D, G) 3A3D and H) 4A4D, where xAyN ≡ (sulfuric acid)$_x$ · (ammonia)$_y$ and mAnD ≡ (sulfuric acid)$_m$ · (dimethylamine)$_n$.

obtain 4:3-cluster further decreases the total dipole. Unfortunately, due to the scarcity of data points, one is not able to draw general conclusions. However, to our knowledge, this is the first

time the time-behavior of the electronic dipoles for atmospherically interesting clusters is presented.

The time-development of the electric dipole moment is also related to the vibrational spectrum of the cluster. In future work we will explore this relation further and more importantly, focus on the role of the dipole moment in the formation steps of small atmospheric clusters.

ACKNOWLEDGEMENTS

REFERENCES

Kulmala, M., Vehkamäki, H., Petäjä, T., Dal Maso, M., Lauri, A., Kerminen, V.-M., Birmili, W., and McMurry, P. H. (2004). Formation and growth rates of ultrafine atmospheric particles: a review of observations. *J. Aerosol Science*, **35**, 143.

Kurtén, T., Loukonen, V., Vehkamäki, H., and Kulmala, M. (2008). Amines are likely to enhance neutral and ion-induced sulfuric acid-water nucleation in the atmosphere more effectively than ammonia. *Atmos.Chem. Phys.*, **8**, 4095.

Loukonen, V., Kuo, I-F., W., McGrath, M. J., and Vehkamäki, H. (2012). *manuscript in preparation*

Ortega, I. K., Kupiainen, O., Kurtén, T., Olenius, T., Wilkman, O., McGrath, M. J., Loukonen, V., and Vehkamäki, H. (2012) From quantum chemical formation free energies to evaporation rates. *Atmos. Chem. Phys.*, *12*, 225.

PARAMETERIZATION OF BLACK CARBON AGING IN THE OSLOCTM2 AND IMPLICATIONS FOR REGIONAL TRANSPORT TO THE ARCTIC

M. T. LUND[1] and T. BERNTSEN[1,2]

[1]Center for International Climate and Environmental Research – Oslo (CICERO), Norway

[2]Department of Geosciences, University of Oslo, Norway

Black carbon (BC) has received increasing attention as an important contributor to global warming and can impact climate through several mechanisms. The lifetime, and hence transport and distribution, as well as cloud nucleating and optical properties of black carbon (BC) aerosols depend on the mixing state of the particles, and the parameterization of aging is an important element of global aerosol modelling. We compare two different parameterizations of BC aging in the Oslo chemistry transport model (CTM2). The effect on transport and distribution in general and on the contributions to Arctic BC from selected emission source regions is explored. The OsloCTM2 is a global 3-dimensional model with transport driven by meteorological data from the European Centre of Medium Range Weather Forecasts (ECMWF). Here, the model is run with a horizontal resolution of $2.8° \times 2.8°$ and 40 vertical layers. Fossil fuel and biofuel BC emissions are from Bond et al. (2004) and open biomass burning emissions for year 2004 are from the Global Fire Emissions Database (GFEDv2) (van der Werf et al., 2006). In the standard bulk parameterization BC aging is represented by a constant transfer from hydrophobic to hydrophilic mode and only the total mass of the aerosols is considered. The second parameterization is the microphysical aerosol module M7 (Vignati et al., 2004), which has been implemented in the OsloCTM2 to represent aerosol size distribution and interaction and the formation of mixed particles. The microphysical module captures seasonal and regional variations in BC aging by accounting for coating of the particles by sulfate, leading to differences in lifetime and distribution of BC in the OsloCTM2 compared to using the standard parameterization.

Using M7 generally leads to higher concentrations, and in particular the wintertime accumulation and seasonal cycle of BC in the Arctic is improved. Since the climate impact of BC aerosols can depend on their vertical location, it is important to both measure and model the vertical distribution of BC properly (Ban-Weiss et al., 2011; Koch & Del Genio, 2010). Comparison with measured vertical profiles shows that the model generally overestimates the BC concentration, especially at higher altitudes. Using M7 increases concentrations compared to the standard parameterization and, with the exception of high northern latitudes, exacerbates the overestimation. We consider contributions to Arctic BC from four separate emission surce regions; Europe, China, North America and Russia including former USSR. The regional contributions to Arctic BC depend both on the chosen parameterization and on whether we consider the atmospheric BC or the burden in snow/ice. However, both parameterizations show that emissions in Europe contribute most to atmospheric BC concentration and to BC in snow and ice north of 65°N. M7 leads to a pronounced seasonal pattern in contributions and contributions from Europe and Russia increase strongly during winter compared to the standard parameterization. There is generally a small increase in the amount of BC in snow and ice with M7 compared to the standard parameterization, but concentrations are still underestimated relative to measurements in several regions in the Arctic.

There are significant uncertainties related to the microphysics of BC. Future work will investigate the microphysical module in more detail and sensitivity tests for among other the coating thickness, interaction of BC with other soluble species and for assumptions about wet removal will be performed.

ACKNOWLEDGEMENTS

REFERENCES

Ban-Weiss G., Cao L., Bala G. & Caldeira K. 2011. Dependence of climate forcing and response on the altitude of black carbon aerosols. Climate Dynamics, 1-15, DOI: 10.1007/s00382-011-1052-y.

Bond T. C., Streets D. G., Yarber K. F., Nelson S. M., Woo J.-H. & Klimont Z. 2004. A technology-based global inventory of black and organic carbon emissions from combustion. J. Geophys. Res. 109(D14), D14203, DOI: 10.1029/2003jd003697.

Koch D. & Del Genio A. D. 2010. Black carbon semi-direct effects on cloud cover: review and synthesis. Atmospheric Chemistry and Physics. 10(16), 7685-7696, DOI: 10.5194/acp-10-7685-2010.

van der Werf G. R., Randerson J. T., Giglio L., Collatz G. J., Kasibhatla P. S. & Arellano A. F. 2006. Interannual variability in global biomass burning emissions from 1997 to 2004. Atmospheric Chemistry and Physics. 6, 3423-3441, DOI: 10.5194/acp-6-3423-2006.

Vignati E., Wilson J. & Stier P. 2004. M7: An efficient size-resolved aerosol microphysics module for large-scale aerosol transport models. Journal of Geophysical Research-Atmospheres. 109(D22), D22202, DOI: 10.1029/2003jd004485.

COMPARISON OF METHODS FOR GENERATING BIOAEROSOLS SUITABLE FOR IN AND CCN EXPERIMENTS

J. LÖNDAHL[1], O. NERBRINK[2], A. MASSLING[3], T. SANTL TEMKIV[3],
U. GOSEWINKEL KARLSON[3]

[1]Department of Design Sciences, Lund University, Lund, SE-22100, Sweden

[2]FOI, Umeå, Swedish Defence Research Agency, Umeå, SE-901 82, Sweden

[3]Department of Environmental Science, Aarhus University, Roskilde, DK-2000, Denmark

Keywords: BIOAEROSOL, IN, CCN, AEROSOL GENERATION

INTRODUCTION

Bioaerosols include viable bacteria, viruses, dead bacterial cells, pollen, fungi and cell fragments, as well as numerous organic compounds derived from biomolecules as, for example, sugars, amino acids and methyl-derivatives. It has been shown that airborne bacteria may be viable also in the harsh conditions at high altitudes in the atmosphere and act as cloud condensation nuclei (CCN) and ice nuclei (IN). Furthermore, they are able to influence cloud chemistry (Santl Temkiv, 2012).

In order to study the IN and CCN properties of bioaerosols in a laboratory setting it is necessary to use a generation methodology that preserves bacterial viability and minimize coating with redundant solvent impurities as this will increase particle size and distort chemical analysis. Few studies describe generation of bioaerosols, especially with respect to aerosol coating, background concentration and viability. The objective of this work is to compare various aerosol generators for bacteria, spores and vesicles.

METHODS

Six aerosol generators are investigated: atomizer (TSI Inc., Model 3075), Collison nebulizer (BGI Inc., 3-jet), bubbling aerosol disperser, sparging liquid aerosol generator (SLAG, CH Technologies), vibrating orifice aerosol generator (VOAG, TSI model 3450) and electrospray (TSI Inc., Model model 3480).

At this point, exclusively Bacillus subtilis, a common model for gram-positive bacteria, is studied. Particle number size distributions were measured with a scanning mobility particle sizer (SMPS, design: Lund University) and an aerodynamic particle sizer (APS, TSI Inc., Model 3321) in a stainless steel flow tube with controlled dilution (Figure 1). Bacteria are collected on tryptic soy agar plates with a rotating slit sampler.
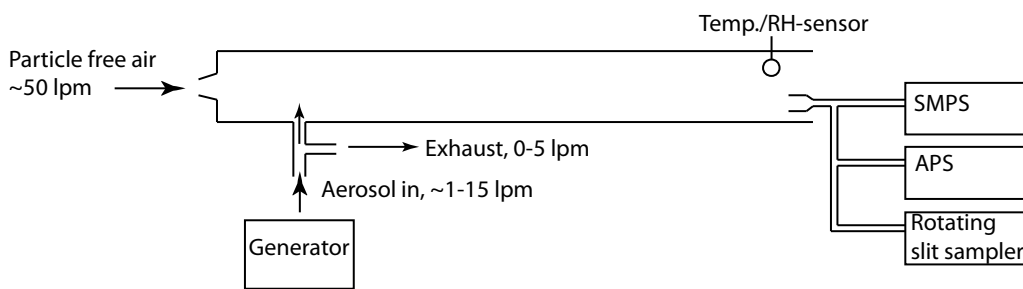
Figure 1. Experimental set-up.

Bacterial viability is analysed by counting colony forming units (CFU) and – in future studies – also by fluorescence with an UV-APS (FLAPS III). The initial droplet size from the generators is assessed by generating a solution with 1% mass ammonium sulphate and calculating the drop size from the mass of the dried particle.

RESULTS

The full matrix of generation methodologies is not yet available, but the preliminary results clearly show that many of the methods commonly used for generation of bioaerosols are unsuitable for examination of key properties of the particles such as CCN or IN ability. For instance the vibrating orifice aerosol generator (VOAG) produce uniform, but comparably large droplets (typically 20-40 µm). When dried, the background particles therefore had a size around 500 nm, while the bacteria had a peak at about 1.7 µm which indicates a significant coating. A surface coating of bioaerosols may significantly alter these abilities especially when soluble substances are involved.

Figure 2 shows the initial drop size from the Collison Nebulizer, the bubbling aerosol disperser and the sparging liquid aerosol generator (SLAG). The electrospray could not be used for bacteria, since they are too large, but may be appropriate for bacterial outer membrane vesicles and spores.
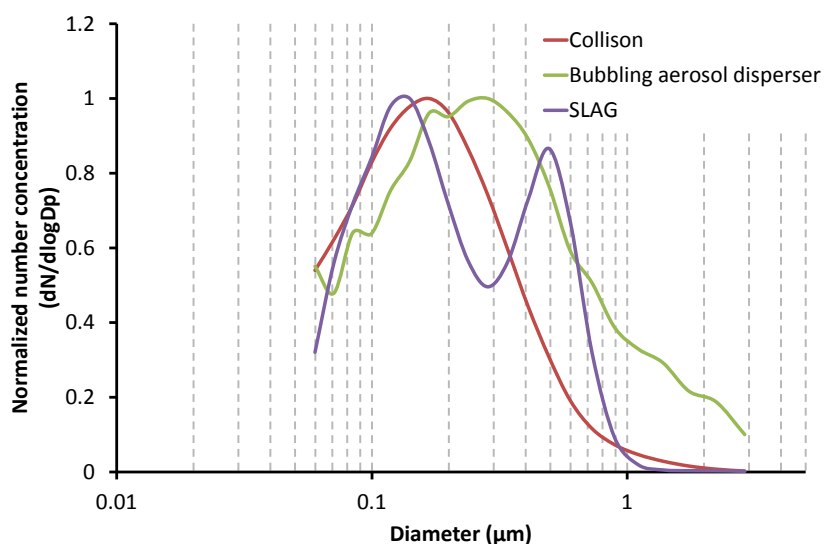
Figure 2. Initial drop size from the Collison Nebulizer, the bubbling aerosol disperser and the sparging liquid aerosol generator (SLAG).

All generators (possibly with exception for the electrospray) produce a substantial background of non-bacterial particles from impurities in the used liquid. The minimum background from Milli-Q water is shown in Figure 3.
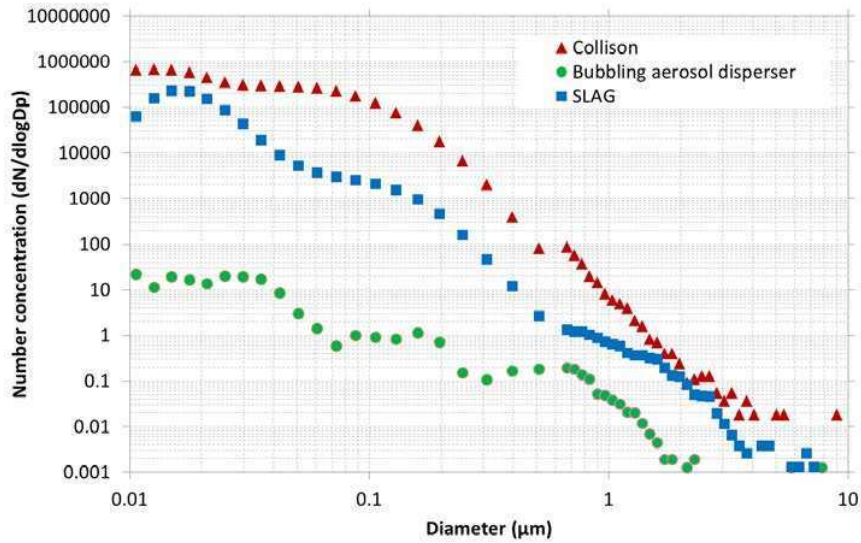
Figure 3. Minimum particle background from three of the generators.

The output of bacteria as colony forming units (CFU) was highest from the Collison nebulizer, but all generators showed a similar bacteria to background ratio (Figure 4 a and b).
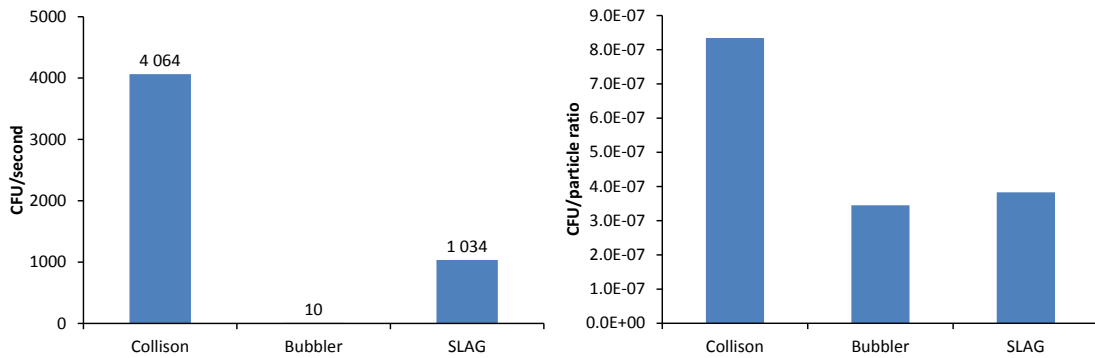
Figure 4. A, left) the total output of CFU per second and B, right) the CFU to background ratio.

Preliminary experiments show that all tested generators have a reasonable stability over time.

CONCLUSIONS

It is often difficult to provide bioaerosols from distilled water of high purity since the organism typically need some surrounding additives (salts etc.) for survival. It seems that the electrospray method is optimal for particles up to 200 nm (virus, spores and vesicles). This instrument leaves a minor surface coating due to a small initial droplet size. For larger particles it may be crucial to use a differential mobility analyser or a virtual impactor to reduce the background of unwanted particles.

Future experiments will include gram-positive bacteria that are not spore forming, gram-negatives and pure spores. In addition a UV-APS will be used to get a ratio between bacterial particles and CFU.

ACKNOWLEDGEMENTS

REFERENCES

Santl Temkiv, T., 2012, "Bacteria in clouds", PhD dissertation, Aarhus University, Denmark

CLOUD RESOLVING MODEL SIMULATIONS OF MARINE STRATOCUMULUS CLOUD BY SEA SALT INJECTIONS

Z. MAALICK[1], H. KORHONEN[2], H. KOKKOLA[2], A. LAAKSONEN[1,3] and S. ROMAKKANIEMI[1]

[1]Department of Applied Physics, University of Eastern Finland, Kuopio, 70211, Finland.

[2]Finnish Meteorological Institute, Kuopio Unit, Kuopio, 70211, Finland.

[3]Finnish Meteorological Institute, P.O.Box 503, Helsinki, 00101, Finland.

Keywords: STRATOCUMULUS CLOUDS, SEA SPRAY, AEROSOLS, CDNC.

INTRODUCTION

Increase in the anthropogenic green house emissions, followed by increase in the concentrations, is considered as a main reason for global warming. Need for an emission cut has been acknowledged, but there is no visible change in the emission trends. Thus, researchers are trying to develop some geo-engineering methods to control the climate conditions in order to reduce or counteract the effect of the greenhouse gas emissions. Many different methods of geo-engineering has been proposed so far but increasing the brightness of stratocumulus marine clouds and mimicking of volcano eruptions by adding aerosol particles to stratosphere are considered to be the quickest way to counteract the effect of anthropogenic emissions. It has been suggested that the albedo of marine boundary layer clouds can be increased enough to counteract warming from up to quadrupled CO2 concentrations by injecting high concentration of sea-salt particles in the air that will increase the number of cloud droplets (Latham 1990).

Studies has shown that marine stratocumulus geo-engineering is a potential candidate to counteract global warming but most of the studies has been conducted by using global climate models and without discussion of the detailed aerosol-cloud microphysical issues. Recent calculations using global models with size- resolved aerosol representations indicate that previously proposed sea spray producing vessel designs and emission fluxes are unlikely to lead to uniform cloud fields with high enough drop concentrations cooling (Korhonen et al. 2010, Partanen et al. 2011). This may have important implications on the size of the spray vessel fleet required to achieve desired effect. Also the study by Wang et al. (2011), using the cloud system resolving model, shown that this kind of geoengineering is efficient only in the cases where drizzle formation is suppressed by the increased number of cloud droplets and thus the cloud thickness is increased. They also concluded that this method is less effective in polluted and water-vapor-limited regimes. However, this study did not consider radiative effect of injected CCN particles, and also the representation of aerosol particles in the model was quite simple.

METHODS

In this study we have used large eddy model UCLALES (Stevens and Seifert 2007) with the aerosol module SALSA (Kokkola et al 2007) to study aerosol-cloud interactions in a cloud resolving scale. UCLALES model has been designed to study the marine stratocumulus clouds, and in this study we have coupled it with aerosol module to study aerosol-cloud-aerosol interaction at micro-physical level. With SALSA we are able to represent realistic aerosol size distribution found in marine environment. The number concentration of cloud droplet formed is parameterized as a function of updraft velocity in the cloud base and aerosol size distribution present in the air parcel forming the cloud. With the model we are able to study aerosol cloud interactions in realistic conditions with artificial sea salt injections. In the study we will use typical profiles for potential temperature and moisture content as well as surface fluxes to produce boundary layer dynamics with UCLALES.

UCLALES model simulations of marine stratocumulus geoengineering are performed by assuming the static vessel that emits sea spray particles with a predescribed flux. The aim is to see how well particles disperse in boundary layer before they enter the cloud or are removed through sedimentation. In the simulations we assume continuous boundary conditions in the horizontal direction.

Two simulations, sim1 and sim2, have been performed in a 2x4x1 km^3 domain for 4 hours with a grid spacing 30 m in horizontal and 15m in vertical. Wind speed of 3 m/sec is assumed with the emission rate of 5.3×10^{15} particles per second for about 10 minutes. Size of particles is 500 nanometers. This sea salt flux corresponds to the water flux of ~12 kg/s. The first simulation considers particles emissions without sedimentation, deposition, latent heat and coagulation. This means that emitted particles are behaving like passive scalar tracers in the model. In second simulation particles sedimentation, deposition, latent heat and coagulation processes have been taken into account to see how big fraction of particles is lost before they are dispersed evenly.

<div align="center">RESULTS</div>

Example of the simulation is presented in figure 1 where particle number concentration at different time steps at the emission level of 45m is shown. Emissions start at around 1.4 hr and lasts for 10 minutes. In Figure 1a the emission has lasted for 5 minutes. Particles spread in the domain with time (1b and 1c) till at around 3.7 hours they spread over the whole domain quite uniformly.
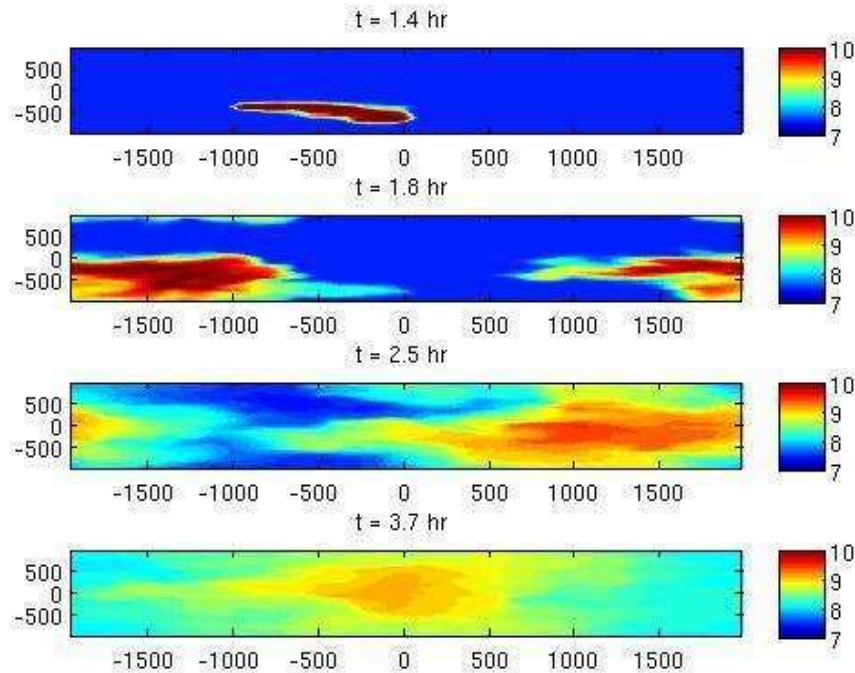
Figure 1. Particles number concentration at the emission altitude at different time steps. Colour is 10 base logarithm of number concentration. Size of the simulation area is 2x4km^2, and the wind is from left to right.

Figure 2 shows the comparison of particles emission of both simulations at time XX hours at cloud base. Sim2 in figure 2b shows that the number concentration of particles is lower at cloud base due to less

efficient mixing. This is caused by latent heat released form evaporating sea salt particles, which will cause negative buoyancy forming a pool of cold air close to the surface. Potentially this could increase the deposition on the surface. However, as can be seen by comparing Figure 2c and 2d, later the difference cannot be seen as clearly. It can be seen from the Figure 3, where the average number of particles in sim1 and sim2 is presented as a function of time, that the average concentration is lower in the sim2, and this is probably caused by coagulation and sedimentation during and soon after emission when concentrations are high. However, the change is small, and actually it seems like the inaccuracy in the calculation of aerosol advection is more important for aerosol concentration that the removal trough sedimentation or coagulation. This can be seen from Figure 3 as the average number concentration in sim1 should not decrease after injection as there is no process to remove aerosol particles from the system. Thus more work is needed to improve the numerical scheme.
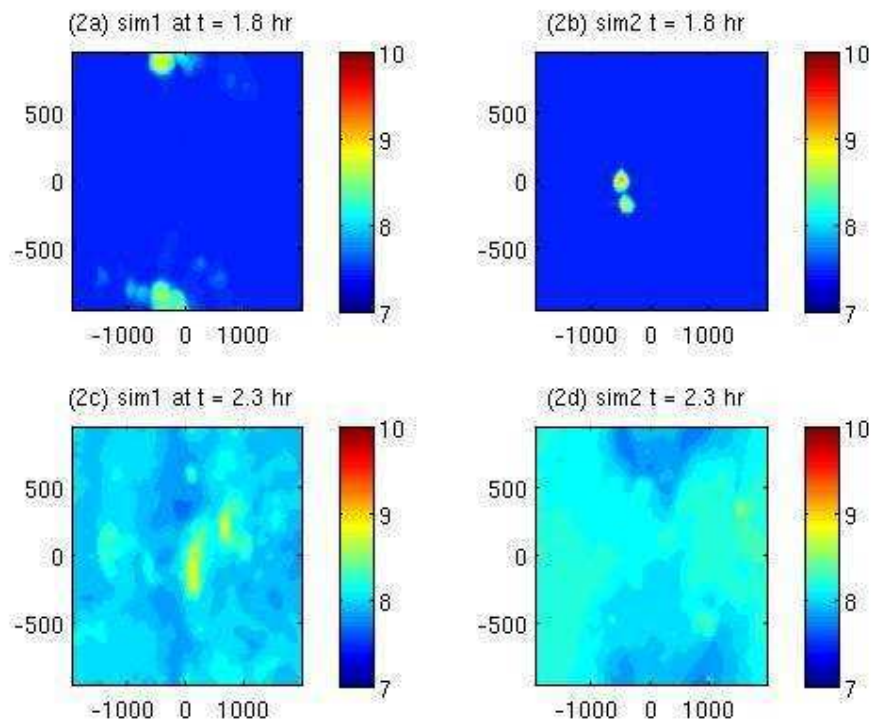
Figure 2. (2a) and (2b) shows particle emission in sim1 and sim2 at 1.8hr respectively. (2c) and (2d) shows dispersion of particle over the whole domain in sim1 and sim2 at 2.3 hr respectively.
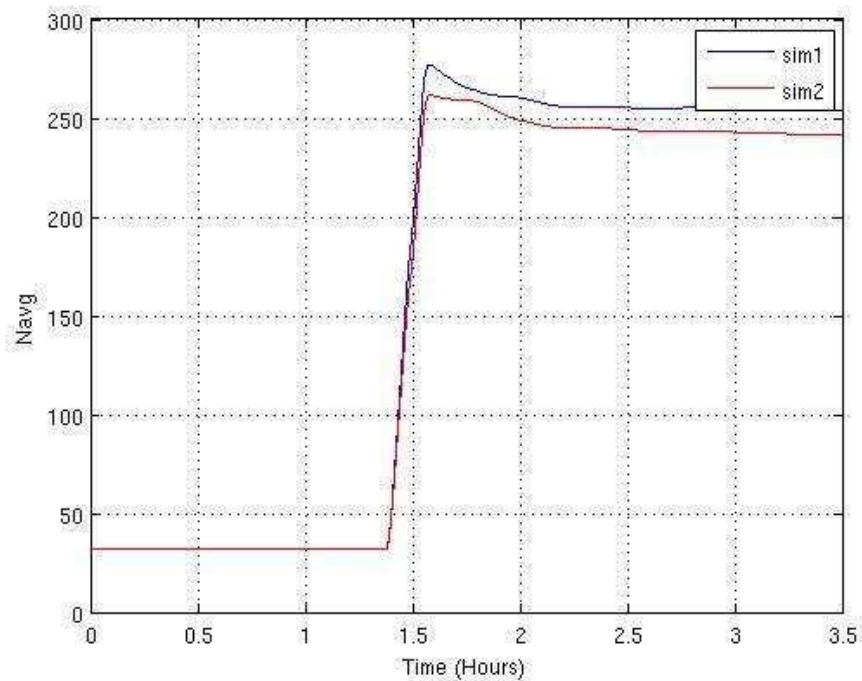
Figure 3. Comparison of average number of particles in sim1 and sim2

REFERENCES

Latham, J., P. Rasch, C. Chen, L. Kettles, A. Gadian, A.Gettelman, H. Morrison, K. Bower and T. Choularton (2008) "Global temperature stabilization via controlled albedo enhancement of low-*level maritime clouds"*, Phil. Trans. R. Soc. A 366, 3969-3987

Wang, H., P. J. Rasch, and G. Feingold (2011) "Manipulating marine stratocumulus cloud amount and albedo: a process-modelling study of aerosol cloud-precipitation interactions in response to *injection of cloud condensation nuclei"*, Atmos. Chem.Phys., 11, 885-916

Korhonen, H., K.S. Carslow. And S. Romakkaniemi (2010) "Enhancement of marine cloud albedo via controlled sea spray injections: a global model study of the influence of emission rates, *microphysics and transport"*, Atmos. Chem. Phys., 10, 4133-4143

Partanen, A.-I., H. Kokkola, S. Romakkaniemi, V. Kerminen, K. Lehtinen, T. Bergman, A. Arola and H. Korhonen (2012) "Direct and indirect effects of sea spray geoengineering and the role of injected *particle size"*. J. Geophysical research 117, 0148-0227

Kokkola, H., H. Korhonen, K. Lehtinen, M. Kulmula, A. Partanen and A. Laaksonen (2008) "SALSA- a sectional aerosol module for large scale application". Atmos. Chem. Phys., 8, 2469-2483

Stevens B. and A. Seifert (2008) "Understanding macrophysical outcomes of microphysical choices in simulations of shallow cumulus conve*ction"*, J. Met.Soc. Japan , 86A , 143_162

MODELING NEW PARTICLE FORMATION IN NORESM

R. MAKKONEN[1], J.E. KRISTJÁNSSON[1], Ø. SELAND[2], A. KIRKEVÅG[2] AND T. IVERSEN[1,2]

[1] Department of Geosciences, University of Oslo, Norway.

[2] Norwegian Meteorological Institute, Oslo, Norway.

Keywords: NUCLEATION, CLIMATE, ESM.

INTRODUCTION

Formation of new aerosol particles in the atmosphere is observed around the world (Kulmala et al., 2004). While many details of the atmospheric nucleation mechanism are still poorly understood, the increasing number of long-term and intense campaign observations of atmospheric particle size distributions has established several semi-empirical parameterizations of the nucleation process. It has been shown that including nucleation in global transport models significantly improves the simulated particle number concentrations (Spracklen et al., 2010). In global climate and earth system models (ESMs) accurate simulation of all aspects of the aerosol population is computationally impossible. However, these models require a description of the aerosol properties and associated processes which are relevant for quantifying their direct and indirect effects on climate.

Both observations (Kerminen et al., 2005) and model simulations (Makkonen et al., 2009; Merikanto et al., 2009) have indicated that atmospheric particle nucleation can increase the number of cloud condensation nuclei (CCN), provided that sufficient concentrations of condensing vapors are available to further grow the nuclei before they are lost by coagulation or removal. An increase in CCN can lead to an increase in cloud droplet number concentration (CDNC), which in turn may affect the albedo and lifetime of clouds. Hence, in order to fully capture both the natural background and the anthropogenic perturbation of the cloud forcing, the mechanisms behind new particle formation and the subsequent growth need to somehow be included in climate models and ESMs. Compared to the chemical transport models, the ESMs include dynamical and physical processes, such as climate-feedback mechanisms, and coupling of new particle formation with biogenic volatile organic compounds (BVOCs).

METHODS

NorESM (Bentsen et al., 2012; Iversen et al., 2012) is an Earth System Model based on the CCSM4 framework, including the land model CLM, the sea-ice model CSIM/CICE, the Bergen version of the ocean model MICOM including the ocean carbon cycle model HAMOCC. The atmospheric model component is the CAM4-Oslo (Kirkevåg et al., 2012), which includes parameterized aerosol chemistry and physics, aerosol-radiation, and aerosol-cloud interactions. Aerosols in CAM4-Oslo are represented by 14 modes. The modeled aerosol compounds are sulfate, black carbon, organic carbon, sea salt and dust. The aerosol number concentration is not a prognostic variable in CAM4-Oslo. The aerosol size distributions are constructed at each time step from calculated mass concentrations tagged according to the production mechanism. Primary particles are given in up to 4 log-normally size-distributed modes which are modified by the tagged concentrations.

For sulfate produced in gas phase, the current version of CAM4-Oslo assumes that after condensation on pre-existing particles has taken place, all remaining sulfuric acid immediately forms new

particles by nucleation. In this case, the gaseous sulfuric acid is not a historic variable.

This presentation discusses an extension of the aerosol scheme in CAM4-Oslo by introducing a nucleation mechanism. We have implemented binary sulfuric acid-water nucleation (Vehkamäki et al., 2002) throughout the atmosphere. The binary nucleation parameterization is a function of relative humidity, temperature and sulfuric acid concentration. While binary nucleation produces a large amount of new particles in the upper troposphere and lower stratosphere, it is known to be insufficient in the boundary layer. Hence, we have included additional nucleation schemes restricted to the boundary layer. There are several options available for the boundary layer nucleation mechanism, such as activation-type nucleation (Kulmala et al., 2006), kinetic nucleation (McMurry and Friedlander, 1979), or nucleation including organic vapours (Metzger et al., 2010). We have implemented several parameterizations from Paasonen et al. (2010). Together with the nucleation schemes, we have also implemented gas-phase sulfuric acid as a fully prognostic variable in the model. The calculation of sulfuric acid concentration available for nucleation is calculated following Kokkola et al. (2009).

The nucleated particles are typically of ∼1 nm in diameter, while the effective diameter of the nucleation mode in NorESM is 24 nm. Most of the newly formed particles can be lost by coagulation during the growth to nucleation mode size: the survival of particles is a competition between the coagulation sink and the particle growth rate. Including an additional mode between 1-24 nm would help to track nucleated particles, but with a considerable cost of computational efficiency. Instead, we use the parameterisation by Lehtinen et al. (2007) to model the apparent particle formation rate J_x

$$J_x = J_1 \cdot exp\left(-\gamma \cdot d_1 \cdot \frac{CoagS(d_1)}{GR}\right), \tag{1}$$

where J_x and J_1 (cm^{-3} s^{-1}) are the formation rates at simulated particle size and nucleation rate, respectively, γ is a parameter which depends on the existing particle population, d_1 is the diameter of nucleated particles, $CoagS(d_1)$ (s^{-1}) is the coagulation sink of nuclei and GR (nm h^{-1}) is the particle growth rate between size of nucleation and the nucleation mode. The coagulation sink needed by the parameterisation is calculated from the existing particle population at each time step. The particle growth due to both sulfuric acid and BVOCs is taken into account. The BVOC emissions can be taken from prescribed monthly emission maps, or from the coupled land model CLM which includes online MEGAN2 emissions of isoprene and monoterpene (Guenther et al., 2006). The NorESM does not include a separate model for secondary organic aerosol formation, and we assume that the BVOCs are distributed into the boundary layer to estimate the concentration of BVOC oxidation products available for particle growth.

RESULTS

The preliminary results shown are from 1-year simulations with activation-type nucleation in the boundary layer and year 2000 emissions of aerosols and precursors. Nuclei growth rates are calculated only from sulfuric acid.

The globally and annually averaged 10 nm particle formation rates are shown in Fig.1a. Binary sulfuric acid-water nucleation produces a distinct maxima around 250 hPa height due to favourable conditions, including low temperature and low coagulation sink. However, binary nucleation shows to be very weak below 700 hPa height. The activation-type nucleation is implemented across the boundary layer. Similar to sulfuric acid concentration, activation-type nucleation peaks in the second-lowest model level.
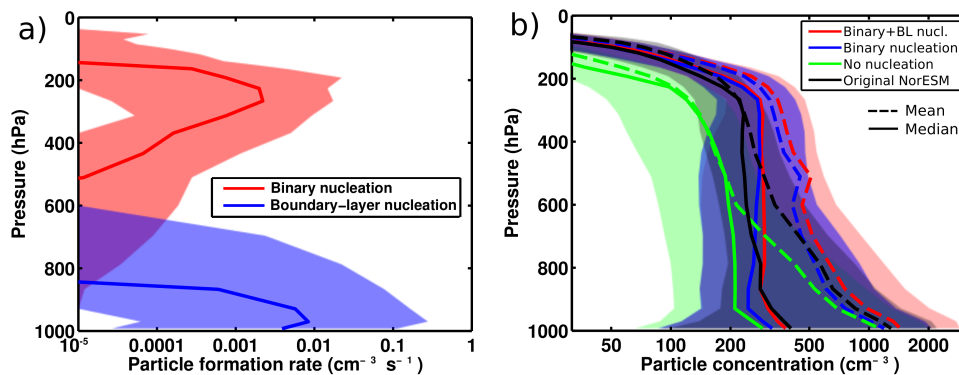
Figure 1: Vertical distributions of (a) annual global median 10 nm particle formation rates and (b) global median (solid lines) and mean (dashed lines) total particle number concentrations. The red line shows results including binary sulfuric acid-water nucleation, boundary layer nucleation and primary emissions. The blue line shows results from simulations where boundary layer nucleation is turned off. In the simulations shown in green, nucleation is turned off completely. Area between 10th and 90th percentiles is indicated with shading.

Compared to the original bulk nucleation scheme in NorESM, mechanistic nucleation implementations increase global average number concentrations by 10-20% below 700 hPa height. Due to active binary nucleation in the upper troposphere, the number concentrations between 200 and 500 hPa are increased globally by over 50%, compared to the original NorESM without mechanistic nucleation scheme.

We tested the sensitivity of aerosol concentrations to nucleation scheme by (1) switching boundary layer nucleation off, yet including binary nucleation and (2) switching nucleation off completely. With this setup, we can estimate the fraction of particles from primary emissions, binary nucleation and boundary layer nucleation as in Merikanto et al. (2009). Boundary layer nucleation increases global average aerosol concentrations by 20-40% between the surface and 800 hPa, compared to a simulation without boundary layer nucleation. The NorESM seems to be somewhat less sensitive to boundary layer nucleation than shown in other models (Merikanto et al., 2009; Makkonen et al., 2009). Globally, primary particles dominate number concentrations below 700 hPa.

The performance of NorESM to predict aerosol number concentrations is evaluated by compa in producing new particles and leads to similar number concentrations as the experiment without any nucleation. In Botsalano, including boundary layer nucleation improves the modeled number concentrations, while in Finokalia, the boundary layer nucleation even overshoots the number concentrations. In Puy de Dome (France), all experiments lead to results which are rather close to observations, and the effect of nucleation is almost invisible.

FUTURE WORK

We have implemented new particle formation mechanisms in the NorESM. Future work will include quantification of the effect of nucleation on cloud properties and aerosol indirect effect, and also studying the climate feedback mechanisms related to secondary aerosol formation.

455
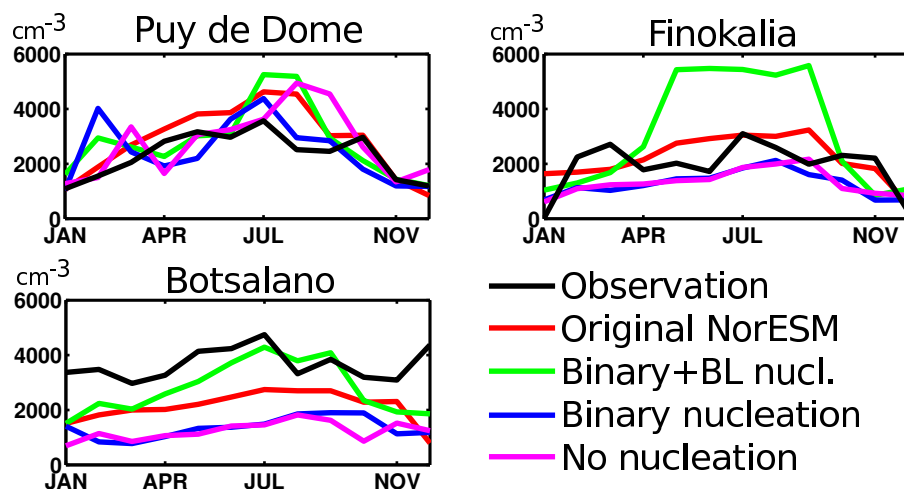
Figure 2: Monthly average particle number concentrations (cm^{-3}) in Puy de Dome (France), Finokalia (Greece) and Botsalano (South Africa). The observational data (black) is from Spracklen et al. (2010). The green line shows results including binary sulfuric acid-water nucleation, boundary layer nucleation and primary emissions. The blue line shows results from simulations where boundary layer nucleation is turned off. In the simulations shown in magenta, nucleation is turned off completely.

ACKNOWLEDGEMENTS

REFERENCES

Bentsen, M., Bethke, I., Debernard, J. B., Iversen, T., Kirkevåg, A., Seland, O., Drange, H., Roelandt, C., Seierstad, I. A., Hoose, C., and Kristjánsson, J. E. (2012). The Norwegian Earth System Model, NorESM1-M. Part 1: Description and basic evaluation. *Geosci. Model. Dev*, Submitted.

Guenther, A., Karl, T., Harley, P., Wiedinmyer, C., Palmer, P. I., and Geron, C. (2006). Estimates of global terrestrial isoprene emissions using megan (model of emissions of gases and aerosols from nature). *Atmos. Chem. Phys.*, 6(11):3181–3210.

Iversen, T., Bentsen, M., Bethke, I., Debernard, J. B., Kirkevåg, A., Seland, O., Drange, H., Kristjánsson, J. E., Medhaug, I., Sand, M., and Seierstad, I. A. (2012). The Norwegian Earth System Model, NorESM1-M. Part 2: Climate Response and Scenario Projections. *Geosci. Model. Dev*, Submitted.

Kerminen, V., Lihavainen, H., Komppula, M., Viisanen, Y., and Kulmala, M. (2005). Direct observational evidence linking atmospheric aerosol formation and cloud droplet activation. *Geophys. Res. Lett.*, 32:L14803.

Kirkevåg, A., Iversen, T., Seland, O., Hoose, C., Kristjánsson, J., Struthers, H., Ekman, A.,

Ghan, S., Griesfeller, J., Nilsson, E., and Schulz, M. (2012). Aerosol-climate interactions in the Norwegian Earth System Model - NorESM. *Geosci. Model Dev.*, Submitted.

Kokkola, H., Hommel, R., Kazil, J., Niemeier, U., Partanen, A.-I., Feichter, J., and Timmreck, C. (2009). Aerosol microphysics modules in the framework of the ECHAM5 climate model - intercomparison under stratospheric conditions. *Geosci. Model Dev.*, 2(2):97–112.

Kulmala, M., Lehtinen, K. E. J., and Laaksonen, A. (2006). Cluster activation theory as an explanation of the linear dependence between formation rate of 3 nm particles and sulphuric acid concentration. *Atmos. Chem. Phys.*, 6:787–793.

Kulmala, M., Vehkamäki, H., Petäjä, T., Dal Maso, M., Lauri, A., Kerminen, V.-M., Birmili, W., and McMurry, P. (2004). Formation and growth rates of ultrafine atmospheric particles: a review of observations. *J. Aerosol Sci.*, 35:143–176.

Lehtinen, K., Dal Maso, M., Kulmala, M., and Kerminen, V.-M. (2007). Estimating nucleation rates from apparent particle formation rates and vice versa: Revised formulation of the kerminen-kulmala equation. *Journal of Aerosol Science*, 38(9):988–994.

Makkonen, R., Asmi, A., Korhonen, H., Kokkola, H., Järvenoja, S., Räisänen, P., Lehtinen, K. E. J., Laaksonen, A., Kerminen, V.-M., Järvinen, H., Lohmann, U., Bennartz, R., Feichter, J., and Kulmala, M. (2009). Sensitivity of aerosol concentrations and cloud properties to nucleation and secondary organic distribution in ECHAM5–HAM global circulation model. *Atmos. Chem. Phys.*, 9(5):1747–1766.

McMurry, P. and Friedlander, S. (1979). New particle formation in the presence of an aerosol. *Atmos. Environ.*, 13(12):1635 – 1651.

Merikanto, J., Spracklen, D. V., Mann, G. W., Pickering, S. J., and Carslaw, K. S. (2009). Impact of nucleation on global CCN. *Atmos. Chem. Phys.*, 9(21):8601–8616.

Metzger, A., Verheggen, B., Dommen, J., Duplissy, J., Prevot, A. S. H., Weingartner, E., Riipinen, I., Kulmala, M., Spracklen, D. V., Carslaw, K. S., and Baltensperger, U. (2010). Evidence for the role of organics in aerosol particle formation under atmospheric conditions. *Proc. Natl. Acad. Sci.*

Paasonen, P., Nieminen, T., Asmi, E., Manninen, H. E., Petäjä, T., Plass-Dülmer, C., Flentje, H., Birmili, W., Wiedensohler, A., Hõrrak, U., Metzger, A., Hamed, A., Laaksonen, A., Facchini, M. C., Kerminen, V.-M., and Kulmala, M. (2010). On the roles of sulphuric acid and low-volatility organic vapours in the initial steps of atmospheric new particle formation. *Atmos. Chem. Phys.*, 10(22):11223–11242.

Spracklen, D. V., Carslaw, K. S., Merikanto, J., Mann, G. W., Reddington, C. L., Pickering, S., Ogren, J. A., Andrews, E., Baltensperger, U., Weingartner, E., Boy, M., Kulmala, M., Laakso, L., Lihavainen, H., Kivekäs, N., Komppula, M., Mihalopoulos, N., Kouvarakis, G., Jennings, S. G., O'Dowd, C., Birmili, W., Wiedensohler, A., Weller, R., Gras, J., Laj, P., Sellegri, K., Bonn, B., Krejci, R., Laaksonen, A., Hamed, A., Minikin, A., Harrison, R. M., Talbot, R., and Sun, J. (2010). Explaining global surface aerosol number concentrations in terms of primary emissions and particle formation. *Atmos. Chem. Phys.*, 10(10):4775–4793.

Vehkamäki, H., Kulmala, M., Napari, I., Lehtinen, K. E. J., Timmreck, C., Noppel, M., and Laaksonen, A. (2002). An improved parameterization for sulfuric acid/water nucleation rates for tropospheric and stratospheric conditions. *J. Geophys. Res.*, 107:4622–4631.

SEASONAL AND DIURNAL CYCLES OF NH3 IN HYYTIÄLÄ

ULLA MAKKONEN[1], AKI VIRKKULA[1,2], MARJA HENRIKSSON[1], JENNI MÄNTYKENTTÄ[1], HEIDI HELLÉN[1], HANNELE HAKOLA[1], PETRI KERONEN[2], VILLE VAKKARI[2], AND PASI P. AALTO[2]

[1] Finnish Meteorological Institute, FI-00560, Helsinki, Finland

[2] University of Helsinki, FI-00560, Helsinki, Finland

INTRODUCTION

A large campaign "Hyytiälä United Measurements of Photochemistry and Particles in Air - Comprehensive Organic Precursor Emission Concentration 2010 (HUMPPA – COPEC-10)", was conducted in Hyytiälä SMEAR II (Station for Measuring Ecosystem-Atmosphere Relationships) in July – August 2010. The general goal was to study links between gas phase oxidation chemistry and particle properties and processes. The Finnish Meteorological Institute contributed to the campaign with an on-line analyzer MARGA 2S for semi-continuous measurement of water-soluble gases and particles (ten Brink, 2007). After the campaign the MARGA instrument was kept running in Hyytiälä to study seasonal variation. Results with higher time resolution could be also used to evaluate models (Schaap, 2011).

METHODS

The MARGA 2S ADI 2080 (Applikon Analytical BV, Netherlands) consists of two sample boxes, one was used with a PM_{10}-inlet (Teflon coated) and in front of the other one there was also a $PM_{2.5}$ cyclone (Teflon coated) installed. Air was drawn (1 m^3/h) through the Wet Rotating Denuder (WRD) where water-soluble gases were diffused to the absorption solution (10 ppm hydrogen peroxide). After that particles were collected in a Steam Jet Aerosol Collector (SJAC) (Slanina et al., 2001). Hourly samples collected in syringes were analyzed every hour with a Metrohm anion and cation chromatograph using internal standard (LiBr). The instrument was described in detail in Makkonen et al 2012.

RESULTS

To study the temporal variations measurement data was divided into four seasons according to prevailing temperatures. On 15 August temperature decreased from 19°C to 14°C and on 24 August it was already below 10°C, therefore in this content autumn period started on 16 August. On 6 November temperature went below 0°C starting the winter period. On 4 March daily average temperature rose for the first time over 0°C, thought all the March was close to 0°C.

Summer	22 June, 2010 – 15 August, 2010
Autumn	16 August, 2010 – 5 November, 2010
Winter	6 November, 2010 – 3 March, 2011
Spring	4 March, 2011 – 30 April, 2011.

From the time series of the ammonia a clear seasonal cycle can be seen: the concentration were highest in summer 0.47 ppb in average (5% percentile was 0.15 ppb 95% percentile was 1.18 ppb) and decreased towards the winter (average 0.05 ppb, 95% percentile 0.096 ppb) and increasing slowly again in spring (Fig. 1), following the temperature profile of the same period. This is obvious, because at cold temperatures ammonia is in the form of ammonium: $NH_3 + HNO_3$ (g) $\leftrightarrow NH_4NO_3$ and at warm temperatures ammonium nitrate particles may volatilize. During the coldest months, when the temperature was below 0 ºC and the land covered with snow ammonia concentrations stayed near the detection limit. Also the main sources of ammonia e.g. the agricultural activities are most limited during winter period.
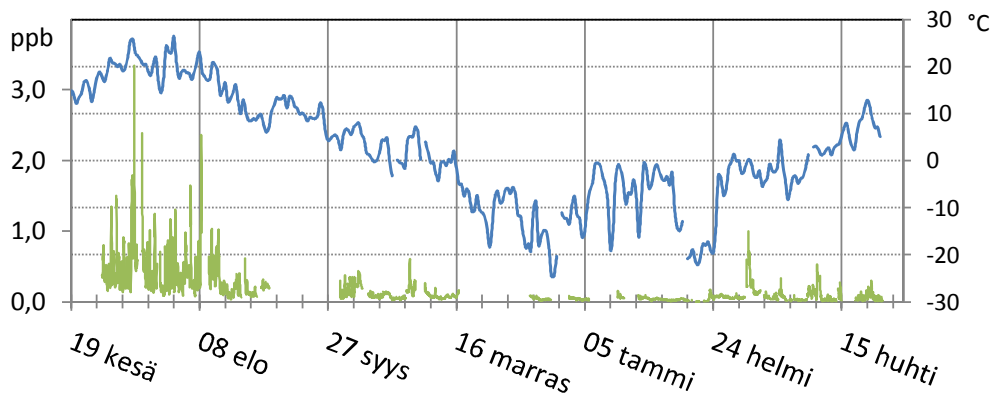
Figure 1. The hourly-averaged ammonia concentrations and the prevailing temperature in Hyytiälä in 2010-2011.
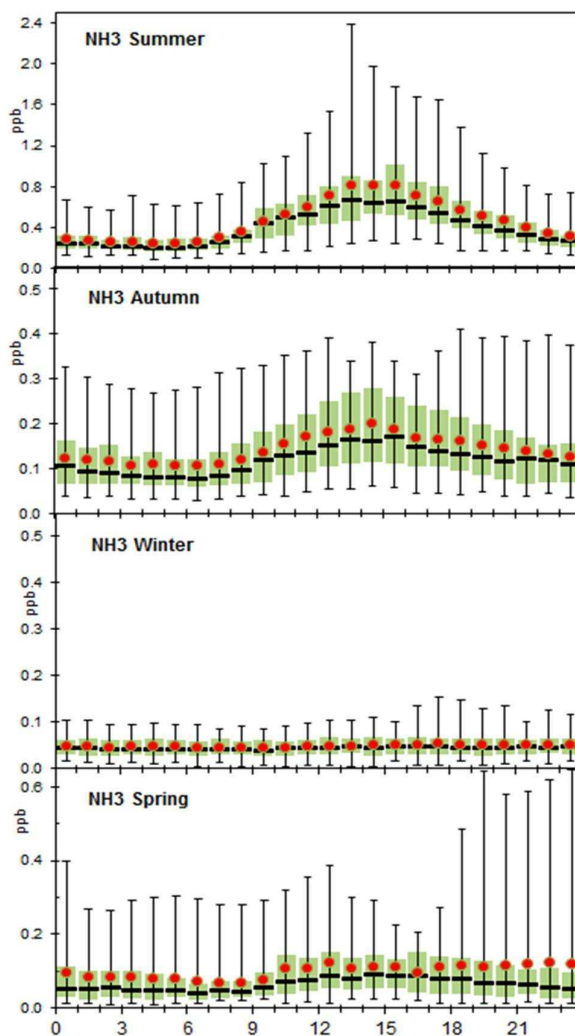
Figure 2. Diurnal cycle of ammonia during different seasons. The box represents the 25th to 75th percentile range. the bars the 90 percentile range (5th and 95th percentiles), the horizontal line the median and the red circle the averages of the hourly-averaged data of each hour.

The diurnal cycles of ammonia during different seasons are presented in Figure 2. In the summer there was a clear maximum during early afternoon hours, which can be seen in the autumn as well. For particulate ammonium and nitrate there were no diurnal cycles. In the summer the diurnal variation was larger than we expected, because there should not be any remarkable emission sources in the near surroundings. In the winter period ammonia stayed most of the time very low, mostly below 0.1 ppb. In March there was no diurnal variation, but the variation in the concentrations on the whole was strong, peaking up to 1 ppb. From the end of April diurnal variation in ammonia began again. Evidently, ammonia previously absorbed on leaf surfaces of trees and on vegetation during night time may be re-emitted as the leaf layers warms again in the warm summer morning. In addition, decomposition of leafs and mushrooms on forest soil may release ammonia.

CONCLUSIONS

In this study relevant hourly-averaged ammonia results could be achieved using a semi-continuous ion chromatograph, which is not possible with traditional filter methods. For ammonia clear seasonal and diurnal cycles were found in the boreal forest environment in Hyytiälä (SMEARII). It is likely that ammonia previously absorbed on leaf surfaces and on vegetation during night time may be re-emitted as temperature rise again in the warm summer morning. In addition, decomposition of leafs and mushrooms on forest soil may release ammonia. Further investigations are needed to find the reason for the diurnal variation of ammonia.

ACKNOWLEDGEMENT

REFERENCES

ten Brink, H., Otjes, R., Jongejan, P. and Slanina S. (2007). An instrument for semi-continuous monitoring of the size-distribution of nitrate, ammonium, sulphate and chloride in aerosol, *Atmos. Env.,* 41, 13, 2768-2779. Received 15 May 2006. Revised 10 November 2006. http://dx.doi.org/10.1016/j.atmosenv.2006.11.041

Makkonen, U., Virkkula, A., Mäntykenttä, J., Hakola, H., Keronen, P., Vakkari, V., and Aalto, P. P. (2012). Semi-continuous gas and inorganic aerosol measurements at a Finnish urban site: comparisons with filters, nitrogen in aerosol and gas phases, and aerosol acidity, *Atmos. Chem. Phys.*, 12, 5617-5631, doi:10.5194/acp-12-5617-201.

Schaap, M., Otjes, R. P., and Weijers, E. P. (2011). Illustrating the benefit of using hourly monitoring data on secondary inorganic aerosol and its precursors for model evaluation, Atmos. Chem. Phys., 11, 11041-11053, doi:10.5194/acp-11-11041-2011, 2011.

Slanina, J., ten Brink, H. M., Otjes, R. P., Even, A., Jongejan, P., Khlystov, S., Waijers-Ijpelaan, A., Hu, M., and Lu, Y. (2001). The continuous analysis of nitrate and ammonium in aerosols by the steam jet aerosol collector (SJAC): extension and validation of the methodology, *Atmos. Env.*, 35, 2319-2330, doi:10.1016/S1352-2310(00)00556-2.

PRECRITICAL CLUSTER SCAVENGING AND NUCLEATION THEOREMS FOR BINARY H₂SO₄–H₂O NUCLEATION

J. MALILA[1], R. McGRAW[2], A. LAAKSONEN[1,3] and K. E. J. LEHTINEN[1,4]

[1]Department of Applied Physics, University of Eastern Finland, P.O. Box 1627, FI-70211 Kuopio, Finland.

[2]Environmental Sciences Department, Brookhaven National Laboratory, Upton, New York 11973, USA.

[3]Finnish Meteorological Institute, Climate Change, P.O. Box 503, FI-00101 Helsinki, Finland.

[4]Finnish Meteorological Institute, Kuopio Unit, P.O. Box 1627, FI-70211 Kuopio, Finland.

INTRODUCTION

During last years, the first nucleation theorem has been applied on various experimental data reporting the dependence of the rate of a first order phase transition as a function of chemical potential difference between metastable and stable phases to give information on the size of the so-called critical nucleus. In case of vapour-to-liquid nucleation, several approximative forms have been used to link macroscopic measurements to give molecular-level insight of the nucleation processes, and in the form of "slope analysis," have been a major evidence to justify different hypothesis on the nature of new particle formation (NPF) in the atmosphere.

This theorem, on its commonly used form, $(\partial \ln J / \partial \ln S_a)_{T,\{S_b\}} \approx n_a^*$, linking the observed NPF rate J and saturation ratio (or concentration) of species a, S_a, to the number of a molecules in the critical cluster, n_a^*, has been noticed to suffer from shortcomings. We have recently provided a detailed analysis on one of those, losses of precritical clusters due various vapour phase inhomogeneities (Malila *et al.*, 2011). Here we discuss on the extension of this work into binary systems: We concentrate on binary sulphuric acid–water nucleation that provides an adequate description of nucleation processes relevant for the upper troposphere and stratosphere, where NPF inside clouds and volcanic plumes—with large coagulation sink for precritical clusters—has been observed.

MAIN RESULTS

For unary systems, the kinetic nucleation theorem (McGraw and Wu, 2003) is easily extended into case with losses: Number concentration of g-mers is given by a balance equation

$$\frac{\partial n_g}{\partial t} = J_g - J_{g+1} - Q_g. \tag{1}$$

Here J_g is the net growth rate from size $g-1$ to size g. Constrained equilibrium (N_g) and steady-state concentrations (f_g) can be obtained from Eq. (1); if the loss rate $Q_q = q_g n_g$ with q_g independent of n_g, we can actually obtain an analytical solution for all f_g and N_g. If now I is the nucleation rate at size $\bar{g} + 1$, where $\bar{g}$ is the kinetically defined critical size, when $Q_q = 0$ for all g, and J the corresponding rate when losses are accounted for, we have

$$\widetilde{g} = \frac{I}{J} \bar{g}, \tag{2}$$

where $\widetilde{g}$ is the apparent critical size from measured J.

The kinetic approach (McGraw and Wu, 2003) can be extended to Shugard–Heist–Reiss (SHR, 1974) scheme that gives a closed form solution for the binary nucleation rate:

$$I_{\mathrm{SHR}} = \left\{ \sum_{g_{\mathrm{H_2SO_4}}} \left[\sum_{g_{\mathrm{H_2O}}} \beta_a(g_{\mathrm{H_2SO_4}}, g_{\mathrm{H_2O}}) n(g_{\mathrm{H_2SO_4}}, g_{\mathrm{H_2O}}) \right]^{-1} \right\}^{-1}, \tag{3}$$

where β_a is a "hydrate-averaged" condensation rate of sulphuric acid on a cluster. Our previous treatment also carries over to the SHR scheme, and we have

$$\widetilde{g}_{\mathrm{H_2SO_4}} = \frac{I_{\mathrm{SHR}}}{J_{\mathrm{SHR}}} \bar{g}_{\mathrm{H_2SO_4}}, \tag{4}$$

and

$$\widetilde{g}_{\mathrm{H_2O}} = \frac{I_{\mathrm{SHR}}}{J_{\mathrm{SHR}}} (\bar{g}_{\mathrm{H_2O}} - 1) - 1. \tag{5}$$

HYDRATE DISTRIBUTION

As an example of the applications of the developed theory, we give the first results of sulphuric acid monomer hydrate distribution. For the SHR rate, these results are of great importance because they are needed for averaging over β_a. (Stable) equilibrium distribution was modelled after Noppel *et al.* (2002) in the scavenging-free case. The same calculation was repeated including scavenging using parameters corresponding a tropical Cirrus (Weigel *et al.*, 2011) observed to provide site for NPF. Results are given in Fig. 1.
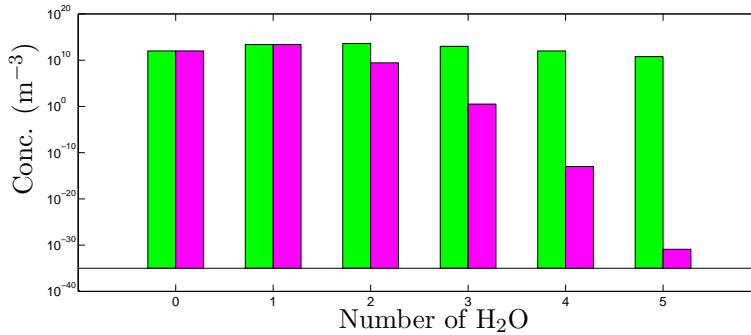
Figure 1: Change in the equilibrium population of the hydrates of sulphuric acid monomer when Brownian coagulation with cloud crystals is accounted for. Scavenging free concentrations are given in green/light and those with scavenging in pink/dark.

It should be noted that these results present only a preliminary account: To obtain the correct coagulation scavenging of clusters inside clouds, further processes besides simple Brownian coagulation needs to be taken into account (McGraw and McMurry, 1983; Jacobson, 2005). These calculations together with those for $\widetilde{g}_{\mathrm{H_2SO_4}}$ and $\widetilde{g}_{\mathrm{H_2O}}$ are in progress.

ACKNOWLEDGEMENTS

REFERENCES

Jacobson, M.Z. (2005). *Fundamentals of Atmospheric Modeling.* (Cambridge University Press, Cambridge, U.K.).

Malila, J., R. McGraw, I. Napari, K.E.J. Lehtinen and A. Laaksonen (2011). Coagulation scavenging of precritical clusters and the first nucleation theorem, in Proc. EAC 2011, Manchester (http://www.eac2011.com/files/Proc.zip), Abstract no. 921; also in preparation.

McGraw, R. and P. H. McMurry (1983). The coupling of nucleation and diffusion near an aerosol particle. *J. Colloid Interface Sci.*, **92**, 584.

McGraw, R. and D. Wu (2003). Kinetic extensions of the nucleation theorem. *J. Chem. Phys.*, **118**, 9337.

Noppel, M., H. Vehkamäki and M. Kulmala (2002). An improved model for hydrate formation in sulfuric acid–water nucleation. *J. Chem. Phys.*, **116**, 218.

Shugard, W.J., R.H. Heist and H. Reiss (1974). Theory of vapor phase nucleation in binary mixtures of water and sulfuric acid. *J. Chem. Phys.*, **61**, 5298.

Weigel, R., S. Borrmann, J. Kazil, A. Minikin, A. Stohl, J.C. Wilson, J.M. Reeves, D. Kunkel, M. de Reus, W. Frey, E.R. Lovejoy, C. M. Volk, S. Viciani, F. D'Amato, C. Schiller, T. Peter, H. Schlager, F. Cairo, K.S. Law, G.N. Suhr, G.V. Belyaev and J. Curtius (2011). In situ observations of new particle formation in the tropical upper troposphere: The role of clouds and the nucleation mechanism. *Atmos. Chem. Phys.*, **11**, 9983.

NUCLEATION MODE PARTICLE MEASUREMENTS ON BOARD ZEPPELIN

H.E. MANNINEN[1], S. MIRME[2], K. LEINO[1], E. JÄRVINEN[1], J. KANGASLUOMA[1], J. MIKKILÄ[1], T. PETÄJÄ[1], M. EHN[1,3], R. TILLMANN[3], TH. F. MENTEL[3] AND M. KULMALA[1]

[1]Department of Physics, University of Helsinki, PL 64, 00014 University of Helsinki, Finland.

[2]Institute of Physics, University of Tartu, Ülikooli 18, 50090 Tartu, Estonia.

[3]Institute for Energy and Climate Research (IEK-8), Forschungszentrum Jülich, 52425 Jülich, Germany.

Keywords: PARTICLE FORMATION, BOUNDARY LAYER, ZEPPELIN, PEGASOS

INTRODUCTION

The Zeppelin is observing radicals and aerosols in the atmospheric layers close to the ground over Europe. Within the PEGASOS project the aim is to quantify the magnitude of regional to global feedbacks between the atmospheric chemistry and the changing climate, and to reduce the corresponding uncertainty of the major ones. During campaigns the Zeppelin flights are divided into three categories: photochemistry, secondary organic aerosol, and nucleation flights. In nucleation studies, we are focusing on atmospheric interactions among chemical and physical processes during new particle formation (NPF). Our study consists of both airborne studies and ground based measurements. The main instruments used to study the onset of NPF in boundary layer are Particle Size Magnifier (PSM) and Neutral Cluster and Air Ion Spectrometer (NAIS).

METHODS

Within PEGASOS campaign following flights are planned and partly already performed (Fig 1.):

- Northbound campaign 2012: May 2012 over central Europe to Cabauw, Netherlands
- East mission transfer flight: June 2012 over Alps to Po Valley, Italy
- **Southbound campaign: June-July 2012 in Po Valley, Italy**
- West mission transfer flight: July 2012 over Alps via France to Friedrichshafen, Germany
- **Northbound campaign 2013: April-May 2013, heading for Hyytiälä, Finland**

There are three constellations, so-called cabin layouts, of instruments used for the Zeppelin flights. Some instruments are always on board (Fig. 2). Particle number size distributions from 1 nm to 20 µm (SMPS, UF-CPC and PSM), concentration of NO, NOx, O3, CO, OH, HO2, and OH lifetime are measured in every cabin layout as well as meteorological parameters. Other measurements are divided as follows

- **Nucleation layout:** Atmospheric pressure interface ToF mass spectrometer (API-TOF) for mass spectrometry of naturally charged ions, and Neutral cluster and Air Ion Spectrometer (NAIS) to measure nucleation mode particle and ion number size distribution.
- Photochemistry layout: the LOPAP instrument measuring nitrous acid (HONO) in the gas phase, a custom-built laser-induced fluorescence (LIF) instrument for the detection of gas-phase formaldehyde (HCHO), and a fast GC-MS system for VOC measurements
- Secondary Organic Aerosol layout: Aerosol mass spectrometer (AMS) for size resolved mass spectra of PM1, and black carbon and aerosol hygroscopicity measurements

During 11.06.-09.07.2012 Zeppelin was performing scientific flights in area of Po Valley, Italy, where total of 110 flight hours were used. Nucleation layout was flying on 5 days with different flight plans. Attention was given to nucleation occuring in Po Valley area, the development and breaks of the boundary layer and related photochemistry, and transects for aerosol composition and properties. We performed
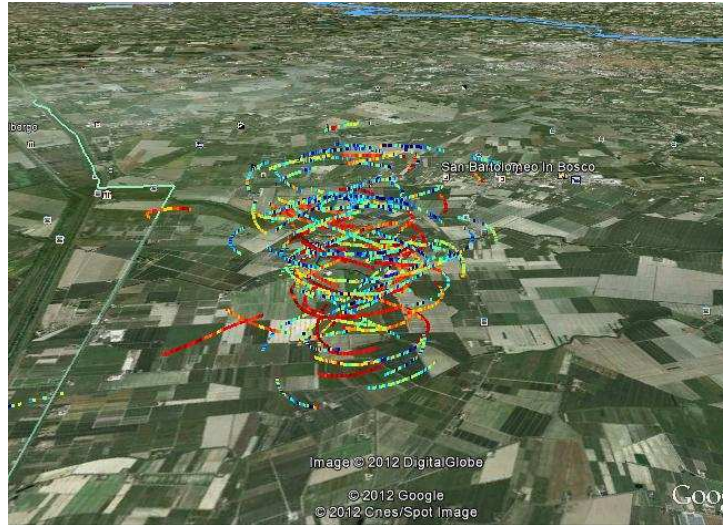
Figure 1. An example of 3-10 nm negative ions concentration measured along the flight track during 28.6.2012 when the Zeppelin was flying vertical profiles above the San Pietro Capofiume field site.
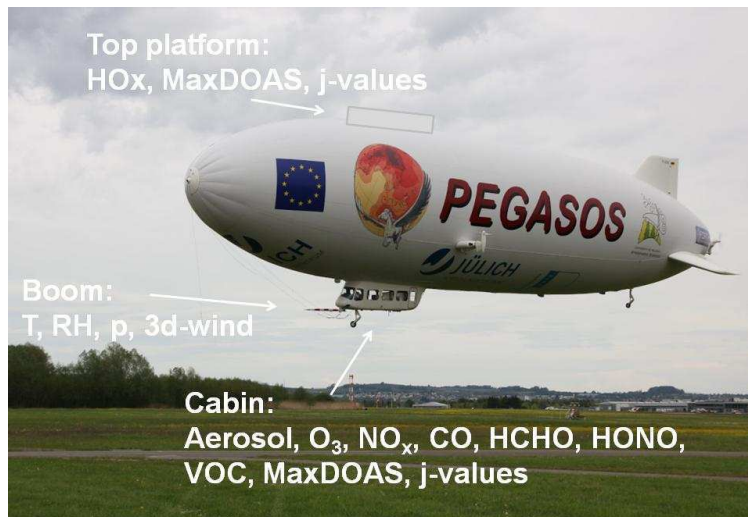
Figure 2l. PEGASOS Zeppelin and instrumentation on board.

additional ground based measurements at the San Pietro Capofiume field site to support the Zeppelin measurements. The NAIS, PSM, and DMPS was measuring continuously on ground the time evolution of particle number size distribution.

PRELIMINARY RESULTS

NPF was observed on 4 out of 5 nucleation layout flights during the Po Valley Zeppelin campaign. When particle formation was observed, it was seen both on airborne and ground based measurements. The preliminary results show that nucleation and particle growth takes place in the boundary layer not in free troposphere. To determine in which part of the boundary layer the onset of the particle formation actually takes place needs further data analysis.

CONCLUSIONS

Zeppelin measurements will provide an exceptional data package to study the vertical extension of NPF in the boundary layer. The detailed measurements of the mass spectra of the naturally charged ions provide evidence on the composition of these newly formed particles.

During next spring regional pollution gradients over Central and Northern Europe are studied. The main focus is on measurements of regional gradients of radical, trace gas, and aerosol concentration along transfer flights from Southern Germany to Southern Finland (via Pallas, Northern Finland). The Zeppelin flights will take place when the NPF frequency is the highest.

PEGASOS will conduct, for the first time, a fully integrated analysis of dynamically changing emissions and deposition, their link to tropospheric chemical reactions and interactions with climate, and emerging feedbacks between chemistry-climate and surface processes. PEGASOS will target both local and regional scales, taking into account chemistry and climate feedbacks on the global scale.

Blog for the EU PEGASOS Project:
http://eu-pegasos.blogspot.fi/

Link to TV feature on our work at PEGASOS Zeppelin project:
http://www.euronews.com/2012/06/14/zeppelin-led-research-into-climate-change/

ACKNOWLEDGEMENTS

ANNUAL CYCLE OF AIRBORNE POLLEN, FUNGAL SPORES AND PARTICLE MASS IN BOREAL FOREST

H.E. MANNINEN[1], V. HILTUNEN[1], J. BÄCK[2], H. LAAKSO[1], H. RANTA[3], A. RANTIO-LEHTIMÄKI[3], M. KULMALA[1] AND T. PETÄJÄ[1]

[1]Department of Physics, P.O.Box 64, FI-00014 University of Helsinki, Finland.

[2]Department of Forest Ecology, University of Helsinki, Finland.

[3]Department of Biology, University of Turku, FI-20014 Turku.

Keywords: BIOAEROSOLS, PM10/PM2.5, AIRBORNE POLLEN, FUNGAL SPORES

INTRODUCTION

We studied annual variation of particle mass, airborne pollen and spore concentration at the boreal forest site in Hyytiälä, Finland. Pollens were categorized into 16 genera and fungal spores to 25 genera, which represent majority of species observed in boreal forest. Biological particles (e.g. airborne pollen and fungal spores) play an important role as allergens; high airborne pollen and spore concentrations can cause allergic symptoms to sensitive people in particularly during spring season, when the concentrations are largest. The health effects are closely connected to the particle size as the respiratory deposition depends on the size of the pollen. Therefore, particle mass and size are included in this study. The aim of this study is to present annual cycles of different allergens at a boreal forest in Southern Finland.

METHODS

Burkard Spore Trap (Batterbee et al., 1996) is used to collect bioaerosol samples to tapes for later microscopy analysis. Particle mass distribution is measured with the Dekati PM10 impactor (Laakso et al., 2003) and particle size distribution of 0.5-20 μm with the TSI Aerodynamic Particle Sizer (APS). Years 2003 and 2004 are selected for closer studying.
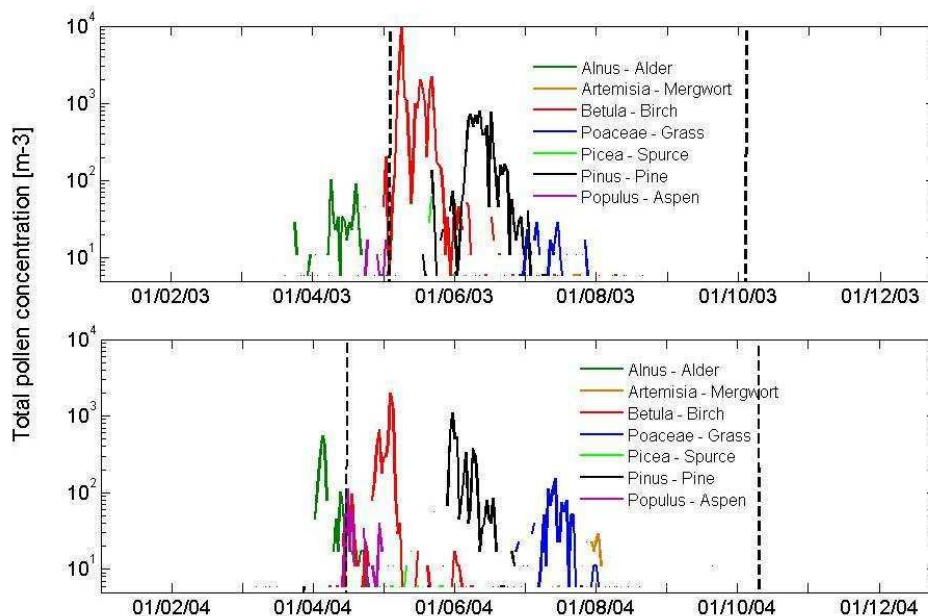
Figure 1: Annual airborne pollen concentrations (particles/m^3) during blossom seasons 2003 ans 2004.

RESULTS

In boreal forests, the most common pollen particles sources are the pine, birch and alder. Some of the more common fungal spore genera identified on the tapes belong to fungi imperfecti, basidiomycetes and ascomycetes. As expected pollen and fungal spore concentrations show a clear annual cycle. Fig. 1 presents airborne pollen concentrations on years 2003 and 2004.

In boreal area the highest concentrations of pollen in the atmosphere are on May and June (100-10000 m^{-3}). The first pollen observations on February are long transported particles from central Europe or Baltic countries, where the spring begins earlier. The highest peak in airborne spore concentrations is later in August and September. Although, the cycle on both years is the same, concentration levels do change. The spores could be called the "ever-present" bioaerosol component of the atmosphere. Meteorological factors affect atmospheric bioaerosol concentrations (Jones & Harrison, 2004).
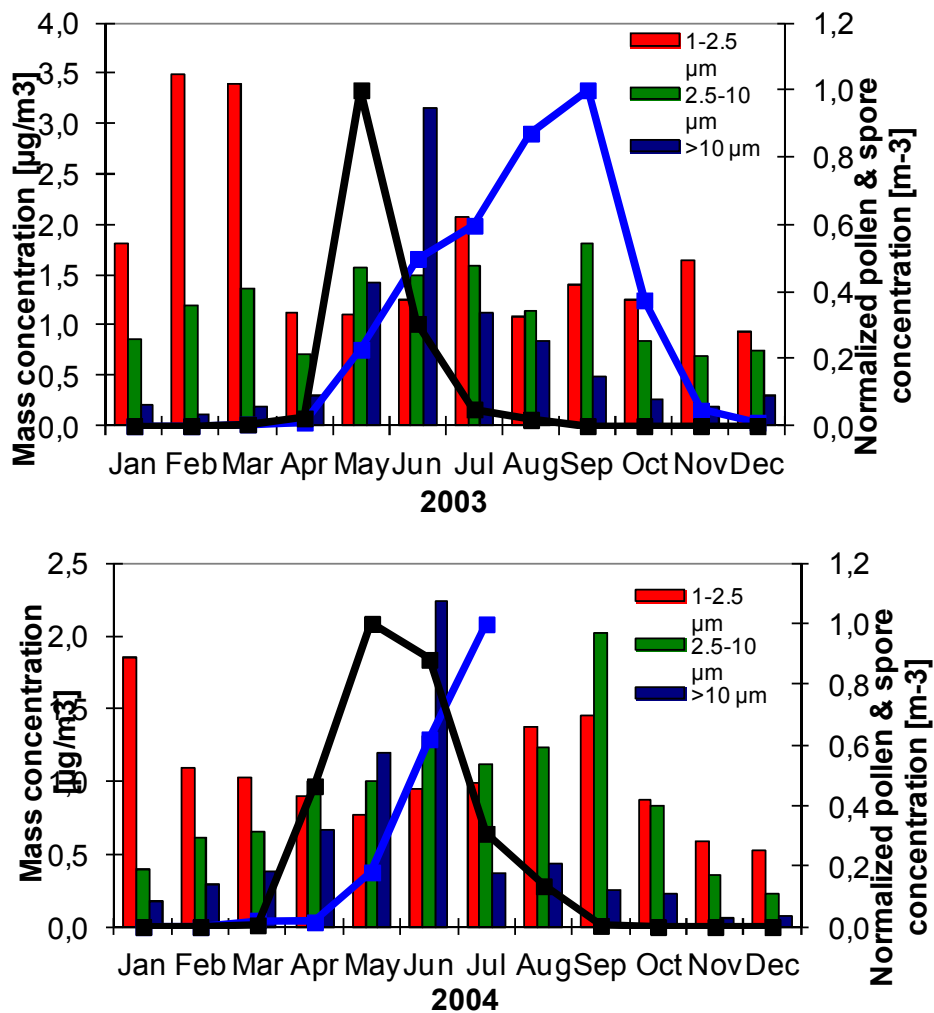
Figure 2: Mass concentration and normalized spore and pollen concentration measured in Hyytiälä in 2003 (top panel) and 2004 (bottom panel).

PM$_{2.5}$ and PM$_{10}$ has annual variation. The former peaks in autumn and the latter in summer (see Fig. 2.). The coarse mode particle mass seems to correlate partially with the bioaerosol concentrations measured with the spore trap (data not seen here). During the highest pollen season, impactor plates are visibly yellow out of t he pollen particles. Especially PM$_{2.5}$ correlates well with fungal spore concentrations. Both have clearly visible peaks in autumn. Based on literature fungal spores have typical diameter of 1-30 µm and pollens 20-60 µm in diameter. Airborne pollen and spore are not enough to explain particle mass peaks. Long-range transported pollution from urban areas covers a big fraction of PM$_{2.5}$.

Studied time series (2003-2004) are part of long-term measurements in Hyytiälä. The SMEARII measurement site provides also diverse meteorogical, vegetation activity, and aerosol data for comparison.

CONCLUSIONS

This study describes the quantitative, qualitative and temporal distributions of pollen and spore seasons. The ambient temperature, i.e. growing season, triggers the pollination. Though, the first pollen observations at Hyytiälä forest site are long transported particles from Central Europe or Baltic countries. In boreal forest fungal spores are present all the time. Most trees flower during spring and herbaceous species later in summer, and the flowering phenology is similar regardless of year. Bioaerosol concentration increases coarse mode particle mass during flowering but the effect in particle number is minor.

The next steps are to investigate 1) associations between meteorological parameters and the incidence different pollen and spore species, 2) diurnal cycle of pollen and spores, and 3) possible relationship with atmospheric new particle formation (connection between particle formation, biogenic volatile organic compounds, and biogenic factors in boreal forest).

ACKNOWLEDGEMENTS

REFERENCES

Batterbee, J. L., Rose, N. L. and Long, X. (1997) *Atmospheric Environment*, 31, 171-181.
Jones, A.M. and Harrison, R.M. (2004) The effects of meteorological factors on atmospheric bioaerosol concentrations - a review. *Science of the Total Environment*, 326: 151–180.
Laakso, L., Hussein, T., Aarnio, P., Komppula, M., Hiltunen, V., Viisanen, Y., ja Kulmala, M. (2003) Diurnal and annual characteristics of particle mass and number concentrations in urban, rural and Arctic environments in Finland. *Atmospheric Environment*, 37: 2629-2641.

ABOUT SEASONAL ARCTIC SNOW UV ALBEDO AT SODANKYLÄ AND UV-VIS ALBEDO CHANGES INDUCED BY DEPOSITION OF SOOT

O. MEINANDER[1], A. HEIKKILÄ[1], A. RIIHELÄ[1], A. AARVA[2], A. KONTU[3], E. KYRÖ[3], H. LIHAVAINEN[1], N. KIVEKÄS[1], A.VIRKKULA[1], O. JÄRVINEN[4], J. SVENSSON[1] and G. DE LEEUW[1,4]

[1]Research and Development, Finnish Meteorological Institute, Helsinki, PO.Box 503, 00101 Finland

[2]Weather and safety, Finnish Meteorological Institute, Helsinki, PO.Box 503, 00101 Finland

[3]Arctic Research Centre, Finnish Meteorological Institute, Tähteläntie 62, 99600 Sodankylä, Finland

[4]Department of Physics, University of Helsinki, P.O.Box 48, 00014 Helsinki, Finland

Keywords: SNOW, ALBEDO, ARCTIC, UV, VIS, BLACK CARBON.

INTRODUCTION

The albedo of snow on land varies, for example, with wavelength, place, time, environmental conditions, and properties of snow, like snow grain size and soot on snow (e.g., Wiscombe and Warren, 1980; Warren and Wiscombe, 1980). Our snow UV + VIS albedo activities within the NCoE CRAICC (Cryosphere-Atmosphere Interactions in a changing Arctic Climate, http://www.atm.helsinki.fi/craicc/), include: a) long-term UV albedo measurements on Arctic seasonal snow at Sodankylä, North-Finland, combined with weekly analysis of BC in snow; b) experimental field campaign measurements on snow albedo and reflectance changes, induced by artificial deposition of soot; including broadband, multiband, and spectral surface albedo and reflectance at UV and VIS wavelengths, within the SoS-2012 experimental field campaign, a continuation to SoS-2011 (Virkkula et al., 2011).

METHODS

Our long-term Arctic measurements on the local UV albedo of snow at the Sodankylä Arctic Research Centre (67°22'N, 26°39'E, 179 m asl), Finland, were planned and initiated as part of the International Polar Year IPY-2007 activities (IPY project ORACLE-O3) (Meinander et al., 2008). Two sensors of the UV Biometer Model 501from Solar Light Co. (SL501) with similar spectral and cosine responses are used, one facing upwards and the other downwards, mounted at a height of 2 m. The SL501 spectral response resembles the action spectrum for erythema, wavelengths in the UVB (280–310 nm) being most weighted. The albedo of snow (denoted as A) is calculated from the ratio of the up-welling UV irradiance to the down-welling irradiance (A = UVery↑/UVery↓) measured at 2π angle. Ancillary data at Sodankylä includes, e.g., data from an automatic weather station (AWS), BC on snow, and snow grain size diameter (D) estimated visually with a mm-grid (Figure 1).

For the Sodankylä carbon in snow results, the snow sample is melted, and the melt water is filtered through micro-quartz filters. A hand pump is attached to the filtering system to create a vacuum during filtering. The volume of melt water is noted and used for concentration conversions. Dried filters are thereafter analyzed in a Thermal/Optical Carbon Aerosol Analyzer (OCEC) (Sunset Laboratory Inc., Forest Grove, USA) for their apparent EC concentrations at the University of Stockholm, Sweden (J. Ström and P. Tunved).
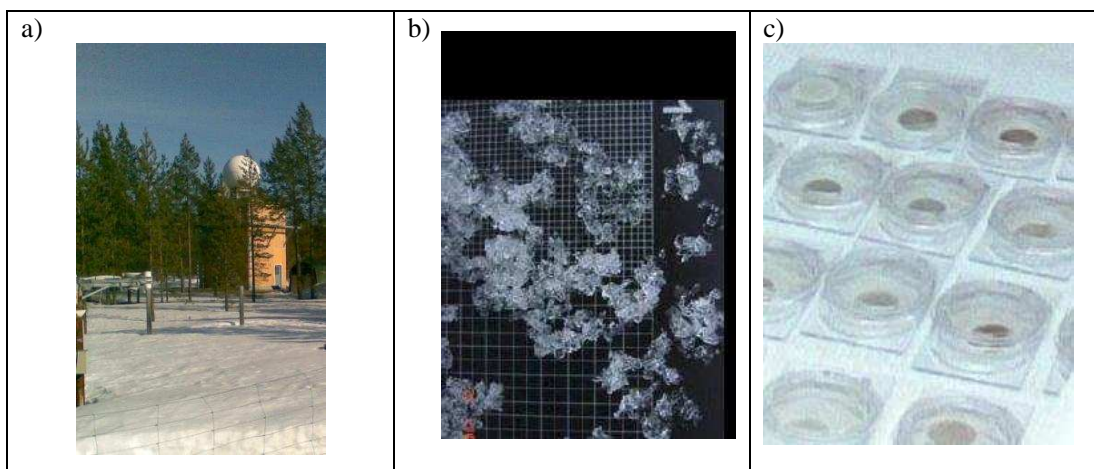
Figure 1. Our main methods at Sodankylä include: a) the continuous 1-min snow-time UV albedo measurements at Sodankylä Arctic Research Centre; b) snow grain size diameter detection with D=1mm and D=2 mm grids (center); and c) BC analysis of melted and filtered snow samples.

The experiment Soot on Snow (SoS-2012) to estimate the albedo effect of BC on snow and ice took place in 2012 at the Jokioinen Observatory, a synoptic FMI weather station in southern Finland (Figure 2). Three spots of different concentrations of soot (small, mid, and high) were generated by blowing soot on natural snow on an agricultural field. The soot was deposited only once to each spot, and thereafter the spots were monitored until the snow was melted. The sites were left to develop naturally, introducing as little disturbance as possible. A fourth measurement spot was a reference with no soot. The soot we used was produced in residential heating with wood and oil, and was collected by chimney cleaners. The soot deposition system is described more detailed in Kivekäs et al. (2012).

Figure 2. The SoS-2012 experiment with the mid-gray spot.

For albedo monitoring, two erythemally weighted UV-B sensors (280-310 nm), together with pyranometers (310-2800 nm), were installed at about 20 cm above the snow surface to continuously measure the UV albedo of the dirty snow, until the end of snow melt. Also, periodical measurements on i) multichannel albedo by a NILU-UV radiometer in the UV and VIS (400-700 nm) channels (measured by Meinander), ii) spectral albedo with a Bentham spectrometer (300-600 nm, measured by Heikkilä), and iii) spectral reflectance by two different Analytical Spectral Devices spectrometers (measured by Riihelä and Meinander) were applied.

CONCLUSIONS

With the Sodankylä data, we can study Arctic snow UV albedo over a time scale ranging from a few days to ~5 years (2007-2012). During one winter, the UV albedo of accumulating Arctic snow may be up to

$A_{UV}=0.8$, and for melting snow $A_{UV} =0.5$-0.7, the elemental carbon in snow being 15-106 ppb, and most of the winter up to $EC_{max} = 40$ ppb (in 2009, Table 1). During melt, the snow grain size diameter was then $D=-0.04t + 0.19Tmax -0.03h+4.98$, where D is grain diameter, t is time (the day of year), Tmax is the daily maximum temperature [^{o}C], and h is the height of the snowpack. (Meinander et al., 2008). For intensively melting snow, the diurnal decrease in albedo has been found to be ~10 % per day and asymmetric to the solar zenith angle (Meinander et al , 2010).

Date	Snow conditions	A (0-1)	D[mm]	EC [ppb]
10.4.	Accumulation	0.66	**0.25**	106
11.4.	Accumulation	0.74	-	-
12.4.	Snow melt starts	0.69	-	-
13.4.	Melting	0.67	-	-
14.4.	Melting	0.63	**2.5**	-
15.4.	Melting	0.59	-	-
16.4.	Rapid melt	0.58	-	-
17.4.	Rapid melt	0.57	-	16
18.4.	Rapid melt	0.58	-	-
19.4.	Rapid melt	0.60	-	-
20.4.	Rapid melt	0.59	**2.0**	-
21.4.	Melt	0.59	-	-
22.4.	Melt	0.56	**1.0**	-
23.4.	Melt	0.58	-	-
24.4.	Melt	0.55	-	87
25.4.	Melt	0.52	-	-
26.4.	Melt	0.51	**1.5**	-
27.5.	Melt	0.47	-	-

Table 1. An example of daily albedo avarage (A), snow grain size diameter (D), and the weekly-based elemental carbon (EC) values at Sodankylä natural snow (year 2009).

In the SoS-2012 experiment, the NILU-UV results show that the albedo values for the clean snow (reference spot) were $A_{VIS} = 0.92$ and $A_{UV} = 0.70$. The surface elemental carbon content was EC = 87 ppb. Immediately after application of the soot , the albedo of the mid-dark soot spot was $A_{VIS} = 0.29$ and $A_{UV} = 0.28$, while the mean amount of surface layer elemental carbon was EC = 4916 ppb (Table 2).

Albedo / BC	Reference spot Average (std)	Spot1 Average (std)
UV	0.70 (0.08)	0.28 (0.10)
VIS	0.92 (0.03)	0.29 (0.01)
EC(all)	160 (113)	4916 (1909)
EC (top)	87 (-)	4916 (1909)

Table 2. NILU-UV albedo (0-1) at UV and VIS, and elemental carbon (EC) [ppb] values of snow at SoS-2012 experiment. For the BC analysis from the reference spot, one surface sample and a vertical profile of every 5 cm were taken; for the sooted spot, three surface samples were taken.

Measurements with the Bentham spectroradiometer were used to follow the temporal development of snow albedo over the few weeks subsequent to the soot deposition. Scans of spectral up-welling and down-welling irradiance were successively taken over each deposit spot. The ratio of the up-welling and down-welling irradiance yielded an estimate representing the local albedo by each spot. Preliminary investigation of the data shows that the effect of the soot imbedded in the snow pack during the snow melt may be retrieved from the measurements. However, the analysis requires the application of radiative transfer calculation based corrections for changing solar position and cloudiness during the spectral scans covering up to 12+12 minutes for the up-welling and down-welling irradiances.

One of the most important tasks is the separation of the natural and anthropogenic effects of BC on snow albedo. For that, we need to know the natural variability of albedo and BC (or elemental carbon) of snow. Our data from Arctic Finland (Sodankylä) show that concentrations of up to 40 ppb BC in natural snow most of the winter results in UV albedo during melt time is 0.5-0.7, and 0.8 during accumulation time. At the same time the snow grain size diameter D varied from 0.2 mm (accumulating snow) up to several millimeters (melting snow). For comparison, we have measured that the clean Arctic Sea ice and snow at 87°N has $A = 0.91 - 0.92$ both in the UV and VIS (Paatero et al. 2008), consistent with the small absorption coefficient of ice. Our results show that in case of natural snow at southern Finland, albedo was A=0.92 in the VIS and A=0.70 in the UV. Introducing an amount of EC=4916 ppb soot on the surface of snow, decreased that albedo immediately into A=0.28-0.29 in both the UV and VIS. To complement these results with a study on the effect of artificial soot on Arctic snow albedo, the SoS-2013 campaign is planned to take place at Sodankylä in Finnish Lapland in spring 2013.

ACKNOWLEDGEMENTS

REFERENCES

Kivekäs, N., Virkkula, A., Järvinen, O., Svensson, J., Aarva, A., Lihavainen, H., Brus, D., Hyvärinen, A., Meinander, O., Heikkilä, A., Väänänen, R., Backman, J. And De Leeuw, G. (2012), Measuring the effect of soot on physical and optical properties of snow, Abstracts Of The Craicc Annual Meeting, Oslo, 26-28 September 2012.

Meinander, O., Kontu, A., Lakkala, K., Heikkilä, A., Ylianttila, L., and Toikka, M. (2008), Diurnal variations in the UV albedo of arctic snow, Atmos. Chem. Phys., 8, 6551-6563, doi:10.5194/acp-8-6551-2008, 2008.

Meinander, O, S. Kazadzis, A. Arola, R. Kivi, A. Kontu, H. Suokanerva, V. Aaltonen, T. Manninen, J.-L. Roujean, and O. Hautecoeur Spectral albedo of arctic snow during intensive melt period (2010),Atmos. Chem. Phys .Disc., 10, 27075-27098, 2010.

Paatero J, Vaattovaara P, Vestenius M, Meinander M, Makkonen U, Kivi R,Hyvärinen A, Asmi E, Tjernström M and Leck (2008), Finnish contribution to the Arctic Summer Cloud Ocean Study(ASCOS) expedition, Arctic Ocean 2008, Geophysica (2009), 45(1–2), 119–146, http://www.geophysica.fi/pdf/geophysica_2009_45_1-2_119_paatero.pdf

Virkkula, A., Järvinen, O., Lihavainen, H., Hyvärinen, A., Mäkelä, T., Kivekäs, N., Väänänen, R., Backman, J., Heikkilä, A., Aarva, A., Kyrö, E-M. and de Leeuw, G. (2011), Proceedings of the CRAICC annual meeting, 10-14.10.2011.

Warren, S., and W. Wiscombe (1980). A model for the spectral albedo of snow. II: Snow containing atmospheric aerosols, J. Atmos. Sci., 37, 2734– 2745.

Wiscombe, W, and Warren S. (1980). A model for the spectral albedo of snow. I:, J. Atmos. Sci., 37, 2712– 2733.

ION-INDUCED NUCLEATION OF SULFURIC ACID AND WATER: EXPERIMENTS AND ATMOSPHERIC IMPLICATIONS

J. MERIKANTO[1], J. DUPLISSY[2], H. VEHKAMÄKI[1], AND M. KULMALA[1]

[1]Division of Atmospheric Sciences, Department of Physics, University of Helsinki, Finland.

[2]CERN, PH Department, Geneva, Switzerland.

Keywords: Atmospheric nucleation.

INTRODUCTION

Atmospheric nucleation mechanisms are still poorly understood despite extensive research. While sulfuric acid is long considered to be involved in most of atmospheric nucleation phenomena, the role of other components, such as ions produced by cosmic rays, has remained unclear. Global models predict that approximately half of all global cloud condensation nuclei (CCN) originate from atmospheric nucleation (Merikanto et al., 2010). To better understand to role of humans in historical and future evolution of cloud albedo and lifetime, we need to understand the anthropogenic and natural influences to nucleation rates and subsequent CCN production rates. This research is impeded by the lack of high quality laboratory measurements of nucleation rates at atmospheric conditions. Such measurements have been produced at the CLOUD chamber in CERN for both homogeneous and ion-induced nucleation of sulphuric acid and water. The CLOUD experiment has already shown the enhancement of sulphuric acid nucleation rates due to presence of galactic cosmic rays and ammonia (Kirkby *et al.*, 2011). Here, we show some of the newest results from these experiments for the sulphuric acid-water-ion system, and show that improved theoretical calculations can predict the outcome of these experiments accurately. We will also discuss the atmospheric implications of these results.

METHODS

CLOUD experiments

Experiments have been performed in the CERN CLOUD chamber during the CLOUD5 campaign (October-December 2011). The chamber is a 3m-diameter electro-polished 316L stainless-steel cylinder (26.1 m^3). The chamber and gas supply were designed to achieve the highest standards of cleanliness. In the experiments, highly purified air of N_2 and O_2 with a mixing ratio of 79:21, clean de-ionized water, and trace amounts of SO_2 are lead to the chamber. The adjustable UV irradiation stimulates the oxidation of SO_2 to H_2SO_4. By varying the light intensity, the H_2SO_4 production can be adjusted as required.

Since the chamber is not underground, i.e. not shielded, it is continuously exposed to galactic cosmic rays. In addition to galactic cosmic rays, the chamber can be exposed to a 3.5 GeV/c secondary pion beam. This corresponds to the characteristic energies and ionization rates of cosmic ray muons in the lower troposphere. In the experiments with the beam turned on, the beam intensity was adjusted to produce the natural range of equilibrium ion-pair (i.p.) concentrations at the ground level (200 i.p cm^{-3}). The ion-pair concentration can also be reduced down to near zero using the clearing field inside the chamber, even though galactic cosmic rays are always present. Experimental runs can presently be performed at temperatures between 208 K and 310 K . The CLOUD chamber is described in detail in the supplementary material of Kirkby *et al.* (2011).
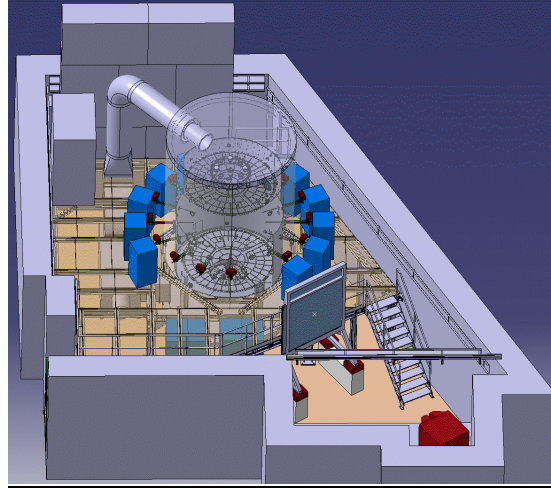
Figure 1: An illustration of CLOUD in the T11 experimental zone at the CERN PS. The de-focused particle beam exits a dipole magnet (bottom right), crosses the aluminium hodoscope counter (middle) and then traverses the 3m-diameter CLOUD chamber, before being stopped by the concrete wall (top left). The instruments (blue boxes) analyse the contents of the chamber via sampling probes. Precise control temperature air circulates between the chamber and the thermal housing. Clearing field for the removal of ions is shown by transparency (bottom and upper part of the chamber).

Nucleation theory

For the theoretical calculations we apply an improved form of Classical Nucleation Theory (CNT) following the work of Vehkamäki et al. (2002) presented for neutral sulphuric acid-water nucleation. In the improved theory, the size distribution of sulphuric acid hydrates is first solved using quantum chemistry based reaction rate coefficients given in Vehkamäki et al. (2002). This allows us to calculate the activity of sulphuric acid more accurately than within the basic CNT. We also generalize the approach of Vehkamäki et al. (2002) for the ion-induced case.

The nucleation rate in both the neutral and ion-induced nucleation is given by (Trinkaus, 1983; Vehkamäki et al., 2002)

$$J = \beta Z N^* = \beta Z N_{ref} \exp\left(\frac{\Delta W_{ref}^*}{kT} \right), \tag{1}$$

where β is collision rate of monomers and hydrates with the critical cluster, and Z is the Zeldovich non-equilibrium factor, N^* is the concentration of critical clusters, N_{ref} is the concentration of reference clusters such as a free ions, acid monomers or acid hydrates, and ΔW_{ref}^* is the work of formation of a critical cluster with respect to the reference cluster. According to CNT, a general expression for the work of formation of a cluster having a radius r is given by (Laakso et al. (2002))

$$W(r) = -n_a kT \ln\left(\frac{\rho_a^{free}}{\rho_{a,s}^{free}(x)} \right) - n_w kT \ln\left(\frac{\rho_w^{free}}{\rho_{w,s}^{free}(x)} \right) + 4\pi r^2 \gamma(x) + \frac{q^2}{8\pi\varepsilon_0}\left(1 - \frac{1}{\varepsilon_r} \right)\left(\frac{1}{r} - \frac{1}{r_0} \right), \tag{2}$$

where n_w is the total number of water molecules in the cluster (including bulk phase and surface excess molecules), n_a is the total number of molecules sulphuric acid molecules, ρ_i^{free} is the number concentration

of free molecules of component i in the nucleating vapour, $\rho_{i,s}^{free}(x)$ is the number concentration of free molecules in a saturated vapour above a solution with sulphuric acid mole fraction x, γ is the composition dependent surface tension of the solution, ε_0 and ε_r are the permittivities of the vacuum and the solution, respectively, and r_0 is the radius of the ion.

The critical cluster is located at the top of the energy barrier,

$$\left(\frac{\partial W(r^*)}{\partial r} \right)_{x=x^*,T} = 0. \qquad (3)$$

For neutral nucleation Eq. (3) has only one solution. In ion-induced nucleation the equation has two or zero real solutions. If the number of solutions is two, the smaller of the two values corresponds to a stable equilibrium cluster with $r_1^* \approx r_0$, and r_2^* is the radius of the critical cluster. If the number of real solutions is zero, particle formation takes place kinetically without any energy barrier. The work of formation of the critical cluster with respect to the reference cluster is obtained from

$$\Delta W_{ref}^* = W(r^*) - W(r_{ref}) \qquad (4)$$

where $r_{ref} = r_1^*$ and $r^* = r_2^*$ for ion-induced nucleation, so that the reference cluster is the free ion. For neutral homogeneous binary nucleation r^* is the only solution of Eq. (3), and take the reference cluster to be the sulphuric acid hydrate containing one sulphuric acid molecule and two water molecules as in Vehkamäki et al. (2002).
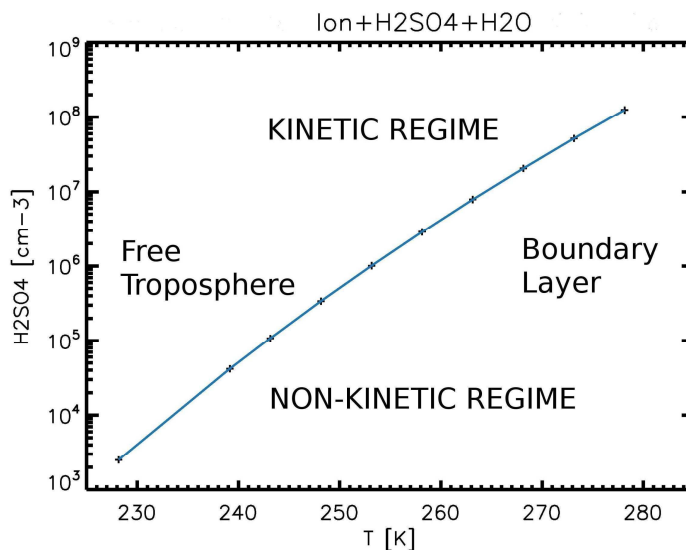
Figure 2: The required sulfuric acid concentration at which the ion-induced particle formation of sulphuric acid and water becomes kinetic. The kinetic regime extends to the conditions typically seen in the free troposphere, but not within the planetary boundary layer.

If the density of the sulphuric acid is high enough the energy barrier vanishes entirely, and particle formation is only limited by kinetics. Since the number of free ions in the atmosphere is always relatively

low, the ion-induced nucleation rates become atmospherically relevant only in the kinetic regime. The kinetic regime for ion-induced nucleation is illustrated in Figure 2.

RESULTS

The experiments were carried out at temperatures between 208 K and 278 K with ions removed from the chamber, with allowing ionization from galactic cosmic rays (GCR), and with the ionizing beam turned on. At 208K ionization did not have an effect on the nucleation rates at the tested sulfuric acid concentrations. At 248 K the nucleation rates were enhanced by the presence of ions, and at 278 K nucleation only took place when ions were present. This behavior is correctly predicted by the improved CNT. The measured and theoretical nucleation rates are in good agreement.
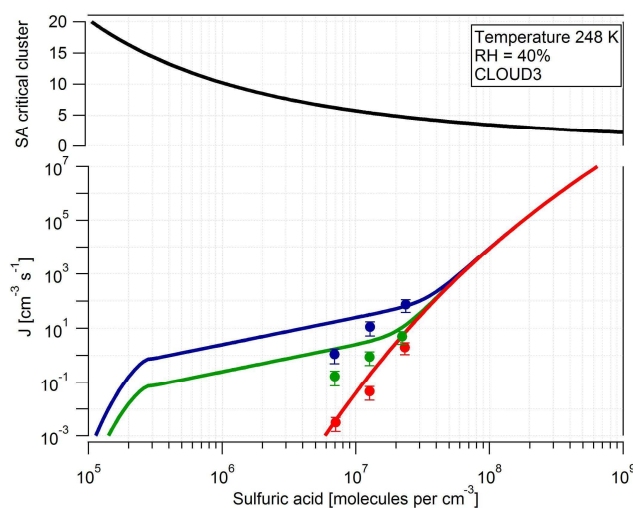
Figure 3: Upper panel: number of sulphuric acid molecules in the critical cluster. Lower panel: Measured (dots) and theoretical (lines) nucleation rates of neutral nucleation (red), neutral and ion-induced nucleation with galactic cosmic rays (green), and neutral and ion-induced nucleation with the ionization beam on (blue) at 248 K.
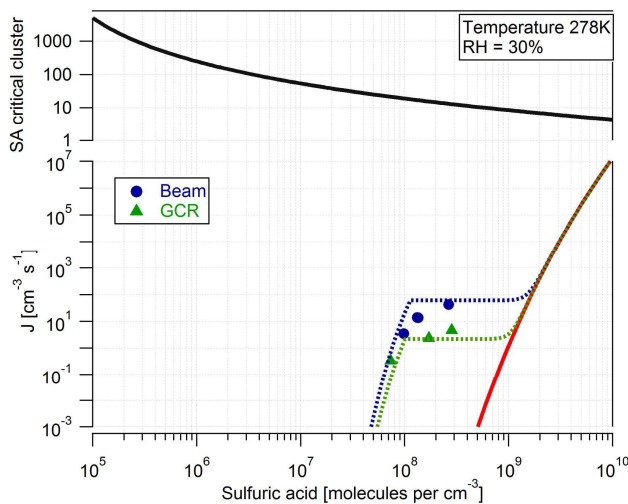
Figure 4: Upper panel: number of sulphuric acid molecules in the critical cluster. Lower panel: Measured (dots) and theoretical (lines) nucleation rates of neutral nucleation (red), nucleation with galactic cosmic rays (green), and with the ionization beam on (blue) at 278 K.

CONCLUSIONS

The neutral and ion-induced nucleation of sulphuric acid and water was measured with state-of-the-art equipment at the CLOUD chamber in CERN. The obtained nucleation rates match very precily with those predicted by the improved classical nucleation theory. This is somewhat surprising since classical nucleation theory is known to be far from accurate in its description of nucleation of many other substances. Nevertheless, the result is very encouraging given that parameterizations of homogeneous nucleation of sulphuric acid and water is widely used in global aerosol and climate models, where this mechanism is particularly active in the upper parts of the troposphere and contributes significantly to boundary layer through downward transport of nucleated particles. Furthermore, the experimental results show that ion-induced particle formation of sulphuric acid and water can dominate the neutral case at conditions corresponding to lower free troposphere. It is not likely that either neutral or ion-induced nucleation of sulphuric acid and water takes actively place within the planetary boundary layer.

ACKNOWLEDGEMENTS

REFERENCES

Kirkby, J., *et al.* (2011). Role of sulphuric acid, ammonia and galactic cosmic rays in atmospheric aerosol nucleation, *Nature* **476,** 429-433.

Laakso, L., J. M. Mäkelä, L. Pirjola, and M. Kulmala (2002), Model studies on ion-induced nucleation in the atmosphere, *J. Geophys. Res.*, 107, 4427, doi:10.1029/2002JD002140.

Merikanto, J., Spracklen, D. V., Mann, G. W., Pickering, S. J. & Carslaw, K. S. (2009). Impact of nucleation on global CCN. *Atmos. Chem. Phys.* **9**, 8601–8616

Vehkamäki, H., M. Kulmala, I. Napari, K. E. J. Lehtinen, C. Timmreck, M. Noppel, and A. Laaksonen (2002), An improved parameterization for sulfuric acid–water nucleation rates for tropospheric and stratospheric conditions, *J. Geophys. Res.*, 107, 4622, doi:10.1029/2002JD002184.

DETECTING RANDOM ERROR IN THE CLOUD DROPLET PROBE MEASUREMENT TIME SERIES

S.MIKKONEN[1], H. PORTIN[1,2], M. KOMPPULA[2], A. LAAKSONEN[1,3] AND S. ROMAKKANIEMI[1]

[1]Department of Applied Physics, University of Eastern Finland, POB 1627, FIN-70211 Kuopio, Finland
[2] Finnish Meteorological Institute, Kuopio unit, P.O.B. 1627, FIN-70211 Kuopio, Finland
[3]Finnish Meteorological Institute, P.O. Box 503, 00101 Helsinki, Finland

INTRODUCTION

Reliable measurements on cloud droplet concentration are needed in order to find the relationships between cloud properties and different meteorological parameters and aerosols. One of the instruments that can be used to measure cloud droplet concentration is Cloud Droplet Probe (CDP) manufactured by Droplet Measurement Technologies, Inc., Boulder, CO, USA.

Cloud droplet measurements can be subject to a wide variety of instrument biases, uncertainties and limitations (Lance at al., 2010). These biasing factors cause additional uncertainties in further analysis of the measurement data, e.g. computing the liquid water content or finding correlations between cloud droplet concentrations and the factors assumed to influence into the cloud formation. Our main goal is to find the factors affecting to the cloud droplet concentration and thus we have to reduce the bias of the measurements.

METHODS

The cloud droplet measurements were made in Puijo measurement station in the town of Kuopio in central Finland. The station is located on the top of an observation tower (306 m a.s.l.) and the station is detected to be in-cloud approximately 15% of the time. The station has produced continuous data on aerosol cloud interactions since June 2006 (Portin et al., 2009).

Lance et al. (2010) found out that the CDP underestimates high cloud droplet concentrations due to coincidence, when two or more droplets pass through the CDP laser beam within a very short time. In addition our results indicate that measured cloud droplet concentration time series contains random bias, which affects the interpretation of the time series.

The method used in reducing the bias in the measured data is called "Time series decomposition using eigenvector filtering" (EVF). The eigenvector filtering decomposes the signal by applying a principal component analysis (PCA) on the original signal and a certain number of copies of it incrementally lagged, collected in a multivariate matrix. Reconstructing the signal using only the most representative eigenvectors allows filtering it (Ibanez and Grosjean, 2009).

RESULTS

Figure 1 shows a 30 minute sequence of a measured time series within a cloud event which took place in March 6th 2009. The original measured time series in presented in the top panel, the filtered time series is in the middle and the residual time series, presenting the random bias, is shown in the lowest panel. The results indicate that the bias in a single observation may be as high as 50% of the measured cloud droplet concentration. The average bias of the measurements was around 10%.
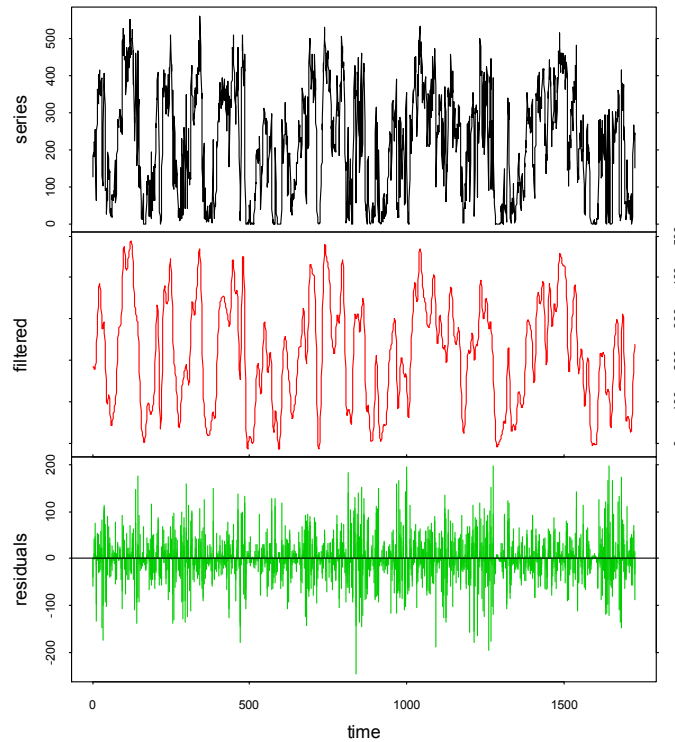
Figure 1. Original series in topmost panel, filtered series in the middle and the residual series in the bottom panel.

CONCLUSIONS

Proper filtering of the time series was found to increase the correlations between cloud droplet concentration and meteorological parameters suggested to influence in the cloud droplet concentration (e.g. wind conditions). The residual time series was found to be uncorrelated with these other parameters, which indicates that no information was lost in the filtering but all the information contained in the measured time series was passed to the filtered series. This indicates that the filtered time series can be used for example studying the effect of aerosol particles on the cloud formation.

ACKNOWLEDGEMENTS

REFERENCES

Ibanez, F. and Grosjean, P. (2009) pastecs: Package for Analysis of Space-Time Ecological Series. http://CRAN.R-project.org/package=pastecs

Lance, S., Brock, C. A., Rogers, D., and Gordon, J. A. (2010) Water droplet calibration of the Cloud Droplet Probe (CDP) and in-flight performance in liquid, ice and mixed-phase clouds during ARCPAC, Atmos. Meas. Tech., 3, 1683-1706, doi:10.5194/amt-3-1683-2010.

Portin, H. J., Komppula, M., Leskinen, A. P., Romakkaniemi, S., Laaksonen, A., and Lehtinen, K. E. J. (2009) Observations of aerosol-cloud interactions at the Puijo semi-urban measurement station, Boreal Env. Res., 14, 641–653.

GAS PHASE ATMOSPHERIC CHEMISTRY DURING THE HUMPPA-COPEC-10 CAMPAIGN

D. MOGENSEN[1,2], S. SMOLANDER[1], M. KULMALA[1], and M. BOY[1]

[1]Division of Atmospheric Sciences, Department of Physics, P.O. Box 48, University of Helsinki, 00014, Finland

[2]Helsinki University Centre for Environment, P.O. Box 27, University of Helsinki, 00014, Finland

Keywords: MODELLING, GAS PHASE CHEMISTRY, HUMPPA-COPEC-10, VOC, OH-REACTIVITY

INTRODUCTION

Boreal forest is one of the areas that are expected to heat most during the future climate warming (2 – 10° C predicted by IPCC 2006). The summer of 2010 was significantly warmer than usual, which gives us the possibility to study the future situation in a boreal forest during climate warming.

We present model–measurement comparison of gas phase chemistry during the extensive summertime boreal forest field campaign HUMPPA-COPEC-10 (Hyytiälä United Measurement of Photochemistry and Particles – Comprehensive Organic Particle and Environmental Chemistry 2010).

Our aim is to validate our 1D vertical chemistry transport model SOSA (Model to Simulate the concentrations of Organic vapors and Sulfuric Acid) (Boy *et al.*, 2011), and to explain the atmospheric chemistry that takes place in a boreal forest ecosystem during summer and during the future climate warming.

METHODS

The measurements were conducted at the SMEAR II (Station for Measuring Ecosystem-Atmosphere Relations), Hyytiälä, Finland (Hari and Kulmala, 2005) from 12 July – 12 August, 2010. Information about the campaign and measurements can be found in Williams et al. 2011. For model studies, we use the 1D vertical chemistry transport model SOSA (Model to Simulate the concentrations of Organic vapors and Sulfuric Acid) (Boy *et al.*, 2011). SOSA includes modules for meteorology (SCADIS), emissions (MEGAN) (Guenther *et al.*, 2006), and chemistry (MCM version 3.2 and KPP) (Damian *et al.*, 2002).

RESULTS AND DISCUSSION

With these extensive measurements we are able to characterise the fluxes, concentrations and compositions of VOCs (volatile organic compounds) emitted from the boreal forest zone during summer and investigate our lack of understanding of VOC chemistry. In order to support this investigation, total OH-reactivity was also measured, like total OH-reactivity and OH-reactivity caused by reaction with specific organic and inorganic compounds were modelled.

Soil emissions are normally not included into atmospheric models due to limited or no measured soil emission data, and no parametrisation of soil emissions are currently available. Soil emissions of isoprene, alpha-pinene, camphene, beta-pinene, carene, cineole, and limonene were measured during the campaign and we have investigated the effect of including soil emissions of these organic

compounds on OH-reactivity. In Figure 1 we show the ratio between OH-reactivity calculated with and without soil emissions into the SOSA model. The ratio is given as an 1 day average over July and August 2010. We quickly conclude that the soil emissions are crucial to include and the emissions have a dramatical effect especially near the forest floor (< 5 m) where we predict a more than 50 % increase of the total OH-reactivity. This information is very important to keep in mind, when comparing measured and modelled gas concentrations, since concentrations of atmospheric compounds are mostly conducted near ground (~ 1 m).
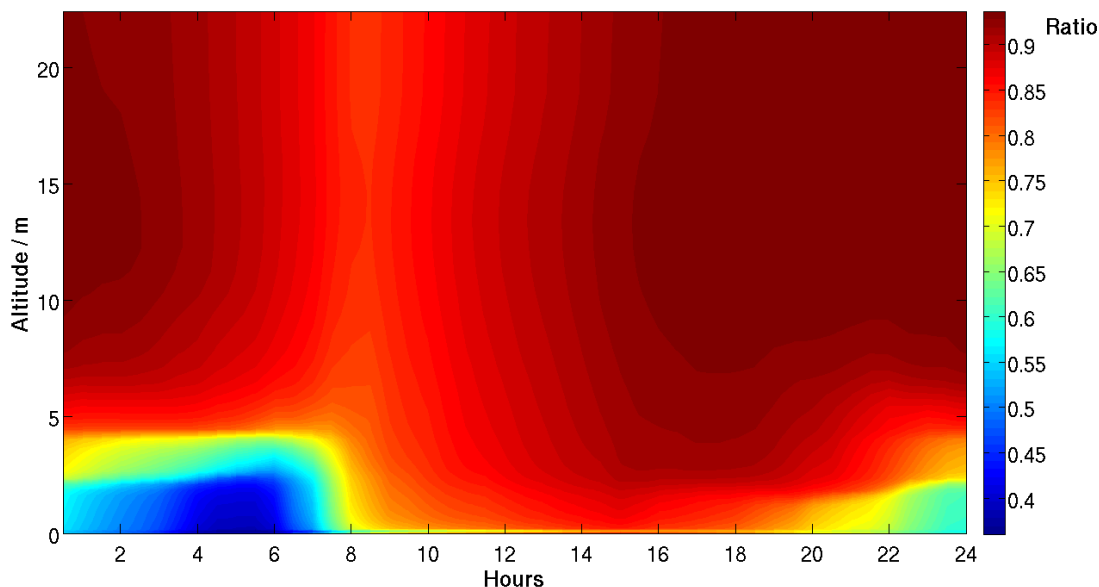
Figure 1: The ratio difference in OH-reactivity when including or not including soil emissions of organic compounds

We have also investigated the inorganic gas phase chemistry during the campaign, and we will present measurement-model comparison of; OH, H_2SO_4, H_2O_2, NO_3, N_2O_5. Also the oxidation capacity (importance of OH, O_3, and NO_3 at different times during day and night) was analysed.

ACKNOWLEDGEMENTS

REFERENCES

Boy, M., Sogachev, A., Lauros, J., Zhou, L., Guenther, A. and Smolander, S. (2011) SOSA – a new model to simulate the concentrations of organic vapours and sulphuric acid inside the ABL – Part I: Model description and initial evaluation *Atmos. Chem. Phys.*, **11**, 43.

Damian, V., Sandu, A., Damian, M., Potra, F., and Carmichael, G. R. (2002). The kinetic prepro-

cessor KPP – a software environment for solving chemical kinetics. *Comput. Chem. Eng.*, **26**, 1567.

Guenther, A., Karl, T., Harley, P., Wiedinmyer, C., Palmer, P. I., and Geron, C. (2006). Estimates of global terrestrial isoprene emissions using MEGAN (Model of Emissions of Gases and Aerosols from Nature) *Atmos. Chem. Phys.*, **6**, 3181.

Hari, P. and Kulmala, M. (2005). Station for measuring ecosystem-atmosphere relations (SMEAR II). *Boreal Env. Res.*, **10**, 315.

Williams, J., Crowley, J., Fischer, H., Harder, H., Martinez, M., Petäjä, T., Rinne, J., Bäck, J., Boy, M., Dal Maso, M., Hakala, J., Kajos, M., Keronen, P., Rantala, P., Aalto, J., Aaltonen, H., Paatero, J., Vesala, T., Hakola, H., Levula, J., Pohja, T., Herrmann, F., Auld, J., Mesarchaki, E., Song, W., Yassaa, N., Nölscher, A., Johnson, A. M., Custer, T., Sinha, V., Thieser, J., Pouvesle, N., Taraborrelli, D., Tang, M. J., Bozem, H., Hosaynali-Beygi, Z., Axinte, R., Oswald, R., Novelli, A., Kubistin, D., Hens, K., Javed, U., Trawny, K., Breitenberger, C., Hidalgo, P. J., Ebben, C. J., Geiger, F. M., Corrigan, A. L., Russell, L. M., Ouwersloot, H. G., Vila-Guerau de Arellano, J., Ganzeveld, L., Vogel, A., Beck, M., Bayerle, A., Kampf, C. J., Bertelmann, M., Köllner, F., Hoffmann, T., Valverde, J., Gonzalez, D., Riekkola, M.-L., Kulmala, M., and Lelieveld, L. The summertime boreal forest field measurement intensive (HUMPPA-COPEC-2010): an overview of meteorological and chemical influences *Atmos. Chem. Phys.*, **11**, 10599.

FINDINGS FROM TWO NUCLEATION CAMPAIGNS; SULPHURIC ACID MONOMER VS. TOTAL SULPHATE, ENHANCEMENT OF NUCLEATION BY AMINES

K. NEITOLA[1], D. BRUS[1], U. MAKKONEN[1], K. KYLLÖNEN[1] and H. LIHAVAINEN[1]

[1]Finnish Meteorological Institute, Erik Palménin aukio, P.O. Box 503, FI-00101 Helsinki, Finland

Keywords: nucleation, sulphuric acid, amine, total sulphate

INTRODUCTION

Sulphuric acid is known to be key component in atmospheric nucleation (Kulmala et al., 2006) but the exact mechanism of the first steps of nucleation are not yet known. Recent quantum chemical calculations suggest that sulphuric acid-water clusters are not thermodynamically stable and atmospheric nucleation needs a third species to stabilize the clusters (Ortega et al., 2012). Lately, laboratory studies of nucleation have moved towards finding other compounds involved in nucleation. Results from these studies show that ammonia and amines may enhance nucleation by several orders of magnitude (Benson et al., 2009; Erupe et al., 2010; Kirkby et al., 2011; Zollner et al., 2012). Here we present results of two campaigns where the effects of base substances to the sulphuric acid-water nucleation were studied.

METHODS

Laminar flow tube setup was used in this study and a schematic figure of the setup is presented in figure 1. Sulphuric acid vapour was produced by saturating purified, dry, particle free air in a thermally controlled saturator half filled with pure (97% w.t. baker analysed) sulphuric acid. The flow from the saturator was mixed with humidified clean air in the mixing unit. After the mixer, base substance was introduced to the flow. Nucleation and subsequent growth happens in the nucleation chamber. After the chamber relative humidity, temperature, particle concentration and size distribution were measured together with sulphuric acid concentration.
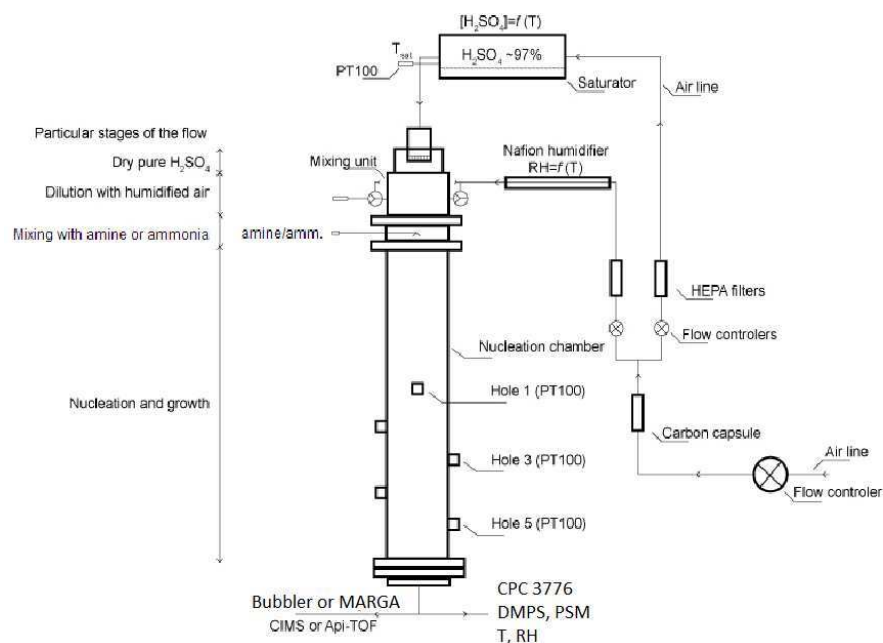

Figure 1. Schematic illustration of the setup.

Particle concentration was monitored with CPCs; Particle Size Magnifier (PSM, Vanhanen et al., 2011), TSI model 3776 or 3025A. The size distribution of the particles was measured in the range of 3-250 nm using a Differential Mobility Particle Sizer (DMPS) system. It consisted of radioactive neutralizer ([63]Ni), short HAUKE-type Differential Mobility Analyzer (DMA) and a CPC 3025A.

Sulphuric acid concentration was measured in the first campaign with mass spectrometers; Chemical Ionization Mass Spectrometer (CIMS, Eisele & Tanner, 1993; Mauldin et al., 1998; Petäjä et al., 2009) and Chemical Ionization Atmospheric pressure interface Time of Flight mass spectrometer (CI-Api-ToF, Tofwerk AG, Thun, Switzerland and Aerodyne Research Inc., USA, Junninen et al., 2010; Jokinen et al., 2012). These instruments used a similar chemical ionization inlet, where sulphuric acid molecules are ionized using nitrate ions (NO^-_3) produced from nitric acid using radioactive charger ([241]Am). For more details see above mentioned references.

In the second campaign an instrument for Measuring AeRosols and GAses (MARGA, Metrohm Applikon Analytical BV, Netherlands, ten Brink et al., 2007) was used to monitor sulphuric acid concentration. MARGA is an online ion chromatograph where the total sulphate concentration is measured. MARGA is able to measure concentration of base substances also. The main difference between the methods is that mass spectrometers measure the gas phase sulphuric acid monomer concentration compared to MARGA which measures total sulphate concentration including particle phase.

Two nucleation campaigns were conducted; first one with four bases (ammonia, trimethyl-, dimethyl- and monomethyl amine; NH_3, TMA, DMA, MMA) and the second one with three bases (ammonia, dimethyl- and monomethyl amine). First the output of the saturator was determined without the flow tube. After this, nucleation experiment with sulphuric acid and water only, was conducted. Amine experiments were done after the sulphuric acid-water experiment. The sulphuric acid concentration was kept constant during each base experiment. Base concentrations were increased in a stepwise in a range of 40-3500 ppt.

RESULTS

The measured output of the saturator is presented in figure 2 as a function of predicted concentration calculated from the vapour pressure using equation (33) from Kulmala & Laaksonen (1990). Total sulphate concentration measured with MARGA lies on top of the one-to-one line. Output was measured with mass spectrometers using several flow rates through the saturator and with two inlet flow rates. Dry and two humid conditions were used. Experiment with 1 meter tubing after the saturator was done to investigate the magnitude of the inlet losses after the saturator. Results from mass spectrometers lies from one to two orders of magnitude lower than the one-to-one line. RH and inlet flow rates do not influence the results. The flow rate through the saturator affects the results if it is too low as seen in the figure with flow rate of 0.05 and 0.2 lpm. Extended inlet has very little or no effect on the results.

Figure 3 presents the nucleation rates of sulphuric acid-water nucleation as a function of sulphuric acid monomer or total sulphate concentration, obtained in this study and from our previous studies, for comparison. The conditions in these measurements are exactly the same (T = 298K, RH ~30%, τ = 30s), which is evident from the nucleation rates. Data points measured using CIMS (squares, on the left) are done by using several CPC's. The green squares are measured using CPC 3776, which might be undercounting at low sulphuric acid concentration due to small sizes of the particles. This is supported by the results as the slope of the points is bending at lower sulphuric acid concentration. The black points in the figure represents measurements, where sulphuric acid was produced using furnace method (Brus, et al., 2010). The production method does not have any effect as the results lie in same space with both production methods. The stars presents results measured with ion chromatography methods, bubbler or MARGA. See Brus et al., (2010) for details of bubbler method. Main finding here is the one to three orders of magnitude difference between sulphuric acid monomer vs. total sulphate concentrations with similar nucleation rates.
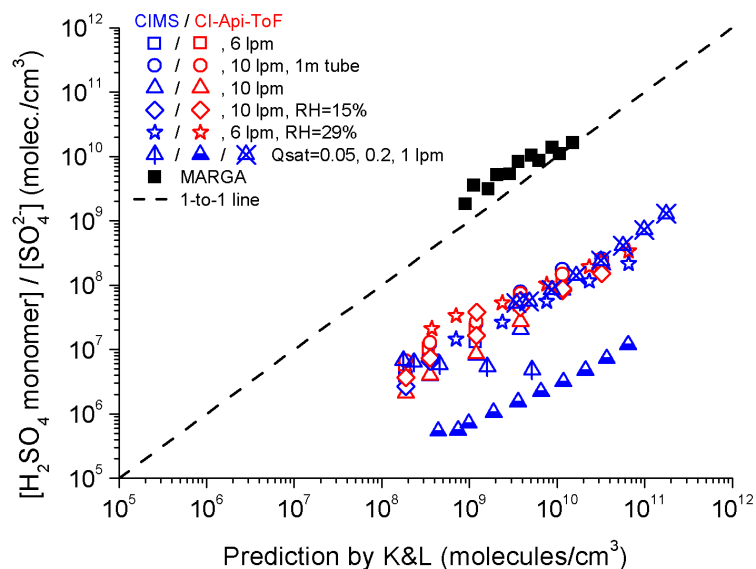
Figure 2. Output of the saturator as a function of prediction by Kulmala & Laaksonen (1990) measured with MARGA and mass spectrometers. Several saturator and two inlet flow rates were used with three (dry, RH 15% and RH 29%) humidity conditions.
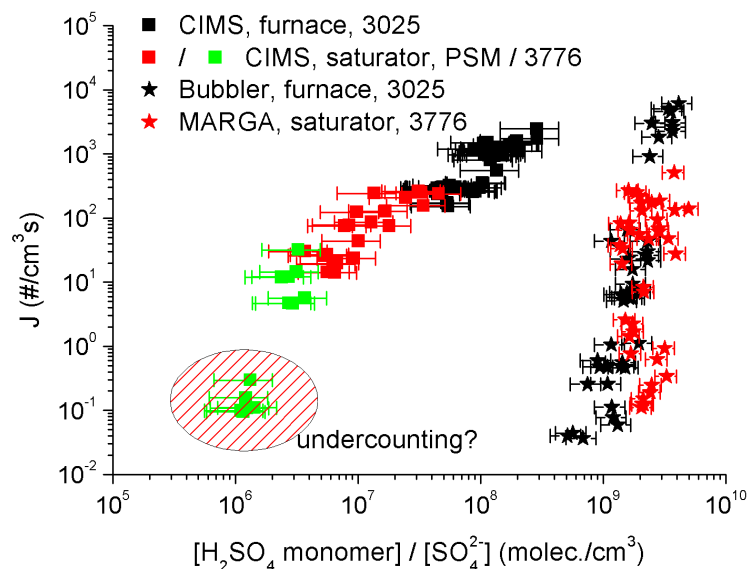
Figure 3. H_2SO_4-H_2O nucleation rates as a function of residual sulphuric acid monomer or total sulphate concentration. Black points are from our previous studies using furnace method.

Figure 4 shows the response of MARGA when adding base substances to the flow. Background of ammonia was measured before adding any bases and it is at 126 ppt when RH is ~30%. In dry conditions background ammonia concentration was found to be 60 ppt. Ammonia response is linear as it was expected but other amines not. This is probably due to oxidation of amines towards ammonia (TMA → DMA → MMA → NH_3). This causes the amines to be distributed in to several peaks in the MARGA spectra and the total concentration is almost impossible to get due to high detection limit.

486
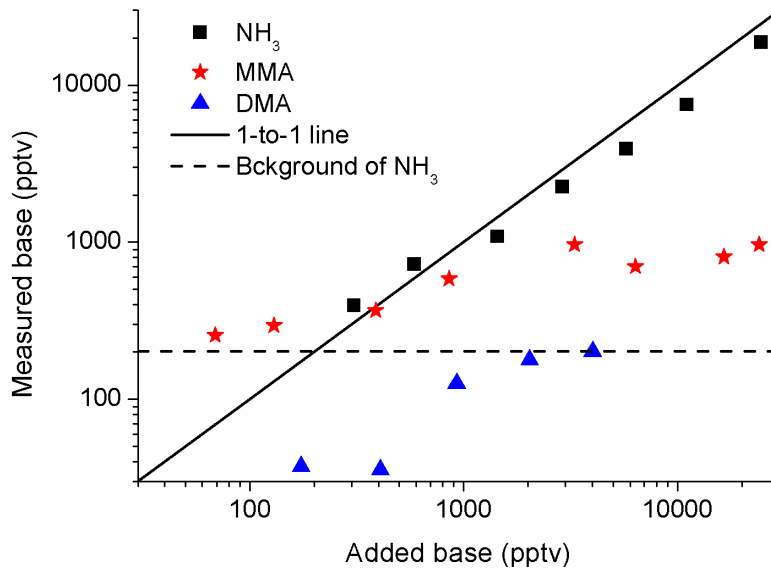
Figure 4. Measured base concentration as a function of added base, measured with MARGA. Background of ammonia (RH ~30%) is presented as dashed line.

In figure 5 are presented the measured particle concentration as a function of added or measured base concentration. Added means that output was not measured but a known amount was put in. The sulphuric acid concentration was kept constant when adding the bases. Enhancement of nucleation was observed only in first campaign when adding TMA (green stars), with a maximum enhancement factor of ~5.5.
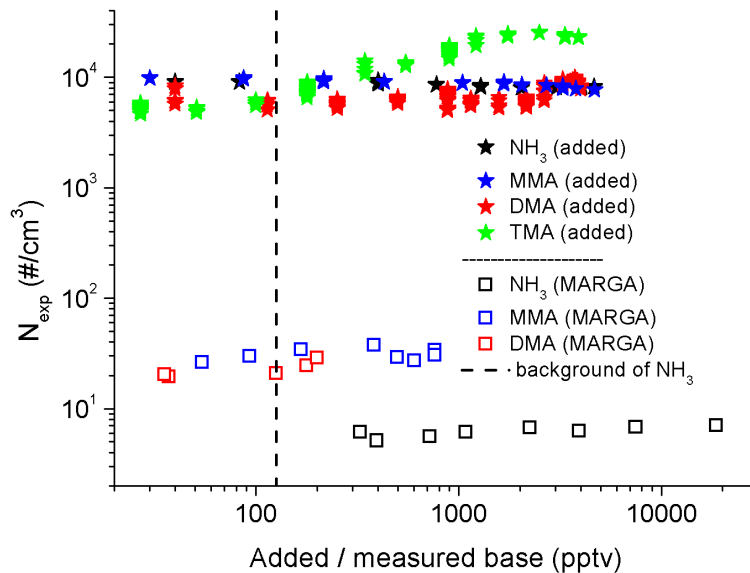
Figure 5. Measured particle concentration as a function of measured or added base concentration in two campaigns. Sulphuric acid concentration was kept constant during an experiment with each base. Enhancement was observed in the first campaign when adding TMA. Maximum enhancement factor ~5.5.

CONCLUSIONS

The saturator method for producing sulphuric acid vapour is determined to perform well when comparing to the previous method of furnace. It produces constant sulphuric acid concentration with reproducible nucleation results. Total sulphate concentrations measured with MARGA agree very well with prediction as the mass spectrometers measured monomer concentration is one to two orders lower than prediction. This difference between total sulphate and monomer concentration cannot be explained by formation of larger clusters (dimer, trimer, etc.) as the dimer concentration was always less than 1% of monomer, with decreasing trend when moving towards larger clusters. The nucleation rates also agree well when using similar instruments for sulphuric acid detection. When comparing similar nucleation rates between monomer and total sulphate concentration the difference in sulphuric acid concentration is from one to three orders of magnitude.

The background of ammonia is determined to be 60 ppt and 126 ppt for dry and RH ~30% conditions, respectively. MARGA responses linearly for adding ammonia but not for other bases. This is probably due to oxidation of amines and subsequent distributing the amines to several peaks in MARGA spectra.

The enhancement was observed only in the first campaign, when adding TMA with a maximum enhancement factor of ~5.5. Background of amines are below the detection limit (1 $\mu g/cm^3$). The background concentration of amines might still be high enough to saturate the influence of amines to sulphuric acid-water nucleation and this is the reason why enhancement was not observed with other bases than TMA.

Considering the results in this study, some important questions rises: Where is the rest of the sulphate? What is the "true" concentration of sulphuric acid involved in nucleation? What is the contribution of total sulphate to the growth of the particles?

ACKNOWLEDGEMENTS

REFERENCES

Benson, D. R., M. E. Erupe, and S.-H. Lee (2009). Laboratory measured H_2SO_4-H_2O-NH_3 ternary homogeneous nucleation rates: Initial observations, Geophys. Res. Lett, 36, L15818.

Brus, D., Hyvärinen, A.-P., Viisanen, Y., Kulmala, M. and Lihavainen H. (2010). Homogeneous nucleation of sulfuric acid and water mixture: experimental setup and first results, Atmos. Chem. Phys., 10, 2631–2641.

Eisele, F. and D. Tanner. (1993). Measurement of the gas phase concentration of H_2SO_4 and methane sulfonic acid and estimates of H_2SO_4 production and loss in the atmosphere, J. Geophys. Res., 98, D5, 9001-9010.

Erupe, M. E., D. R. Benson, J. Li, L.H. Young, B. Verheggen, M. Al-Refai, O. Tahboub, V. Cunningham, F. Frimpong, A. A. Viggiano, and S.-H. Lee, (2010). Correlation of Aerosol Nucleation Rate with Sulfuric Acid and Ammonia in Kent Ohio: An Atmospheric Observation, J. Geophys. Res., 115, D23216.

Jokinen, T., Sipilä, M., Junninen, H., Ehn, M., Lönn, G., Hakala, J., Petäjä, T., Mauldin III, R. L., Kulmala, M., and D. R. Worsnop, D. R. (2102). Atmospheric sulphuric acid and neutral cluster measurements using CI-APi-TOF. Atmos. Chem. Phys., 12, 4117–4125.

Junninen, H., Ehn, M., Petäjä, T., Luosujärvi, L., Kotiaho, T., R. Kostiainen, R., Rohner, U., Gonin, M., Fuhrer, K., Kulmala, M. and Worsnop, D. (2010). A high-resolution mass spectrometer to measure atmospheric ion composition, Atmos. Meas. Tech., 3, 1039–1053.

Kirkby, J., Curtius, J., Almeida, J., Dunne, E., Duplissy, J., Ehrhart, S., Franchin, A., Gagné, S., Ickes, L., Kürten, A., Kupc, A., Metzger, A., Riccobono, F., Rondo, L., Schobesberger, S., Tsagkogeorgas, G., Wimmer, D., Amorim, A., Bianchi, F., Breitenlechner, M., David, A., Dommen, J., Downard, A., Ehn, M., Flagan, R., Haider, S., Hansel, A., Hauser, D., Jud, W., Junninen, H., Kreissl, F., Kvashin, A., Laaksonen, A., Lehtipalo, K., Lima, J., Lovejoy, E., Makhmutov, V., Mathot, S., Mikkilä, J., Minginette, P., Mogo, S., Nieminen, T., Onnela, A., Pereira, P., Petäjä, T., Schnitzhofer, R., Seinfeld, J., Sipilä, M., Stozhkov, Y., Stratmann, F., Tomé, A., Vanhanen, J., Viisanen, Y., Aron Vrtala, A., Wagner, P., Walther, H., Weingartner, E., Wex, H., Winkler, P., Carslaw, K., Worsnop, D., Baltensperger, U. & Kulmala, M. (2011). Role of sulphuric acid, ammonia and galactic cosmic rays in atmospheric aerosol nucleation, Nature, 476, 429–433.

Kulmala M. & Laaksonen, A. (1990). Binary nucleation of water-sulfuric acid system: Comparison of classical theories with different H_2SO_4 saturation vapor pressures, J. Chem. Phys., 93 (1). 1.

Kulmala, M., K. E. J. Lehtinen and A. Laaksonen (2006). Cluster activation theory as an explanation of the linear dependence between formation rate of 3 nm particles and sulphuric acid concentration, Atmos. Chem. Phys., 6, 787–793.

Mauldin III, R. L., Frost, G., Chen, G., Tanner, D., Prevot, A., Davis, D., and Eisele, F. (1998). OH measurements during the First Aerosol Characterization Experiment (ACE 1): Observations and model comparisons, J. Geophys. Res., 103, 16713–16729.

Ortega, K., O. Kupiainen, T. Kurtén, T. Olenius, O. Wilkman, M. J. McGrath, V. Loukonen and H. Vehkamäki (2012). From quantum chemical formation free energies to evaporation rates. Atmos. Chem. Phys., 12, 225–235.

Petäjä, T., Mauldin, III, R., Kosciuch, E., McGrath, J., Nieminen, T., Paasonen, P., Boy, M., Adamov, A., Kotiaho, T. and Kulmala M. (2009). Sulfuric acid and OH concentrations in a boreal forest site, Atmos. Chem. Phys., 9, 7435–7448.

ten Brink, H., Otjes, R., Jongejan, P. and Slanina S. (2007). An instrument for semi-continuous monitoring of the size-distribution of nitrate, ammonium, sulphate and chloride in aerosol, Atmos. Env., 41, 13, 2768-2779.

Vanhanen, J., J. Mikkilä, K. Lehtipalo, M. Sipilä, H. E. Manninen, E. Siivola, T. Petäjä and M. Kulmala, (2011). Particle Size Magnifier for Nano-CN Detection. Aerosol Sci. & Tech., 45, 4.

Zollner, J. H., Glasoe, W. A., Panta, B., Carlson, K. K., McMurry, P. H. and Hanson, D. R. (2012). Sulfuric acid nucleation: power dependencies, variation with relative humidity, and effect of bases, Atmos. Chem. Phys., 12, 4399–4411.

SOURCE APPORTIONMENT OF ATMOSPHERIC PARTICLES AT STATION NORD USING COPREM AND PMF ANALYSIS

Q.T. NGUYEN[1,2], H. SKOV[1,3,4], L.L. SØRENSEN[1,4], B.J. JENSEN[1], A.G. GRUBE[1], A. MASSLING[1], M. GLASIUS[2] and J.K. NØJGAARD[1]

[1]Department of Environmental Science, Aarhus University, 4000 Roskilde, Denmark

[2]Department of Chemistry, Aarhus University, 8000 Aarhus, Denmark

[3]Adjunct Professor University of Southern Denmark, Institute of Chemical Engineering and Biotechnology and Environmental Technology, Niels Bohrs Allé 1, DK- 5230 Odense M, Denmark

[4]Arctic Research Centre, Aarhus University, 8000 Aarhus, Denmark.

Keywords: SOURCE APPORTIONMENT, ARCTIC, COPREM, PMF.

INTRODUCTION

In order to develop strategies for controlling and reducing Arctic air pollution, there is a need to understand the basic mechanisms for determining the fate of air pollution in the Arctic. Sources of atmospheric particles at the high Arctic site Station Nord in North East Greenland were evaluated based on measurements of elements, black carbon and inorganic ions for a two-year period from March 2008 to February 2010 using Positive Matrix Factorization (PMF) and Constrained Physical Receptor Model (COPREM).

METHODS

The measurement site "Flygers Hut" at Station Nord (81^o36'N, 16^o40'W, 30m asl) is located 2.5 km South East of the Danish military Station at North East Greenland. The location was selected due to the insignificant contribution from local air pollution (Heidam et al., 2004).

Parameter	Analytical method	Time resolution	Uncertainty
40 mm FP nitro cellulose filters			
Al, Si, S, K, Ca, Ti, V, Cr, Mn, Fe, Ni, Cu, Zn, Ga, As, Se, Br, Rb, Sr, Zr, Pb	Proton Induced X-ray Emission (PIXE)	7 days	18%
SO_2, SO_4^{2-}, Na^+, NH_4^+, NH_3, NO_3^-, HNO_3, Br^-, Cl^-	Ion Chromatography	7 days	20%
PSAP filters			
Black carbon	Particle Soot Absorption Photometer (PSAP)	15 min	20%
On-line gas monitors			
O_3, NOx, SO_2	Gas monitor	30 min	20%

Table 1. Analytical methods and sample frequency of measured parameters at Station Nord.

Source apportionment was performed using the receptor model PMF and COPREM, which is a hybrid receptor model unifying qualities from both PMF and Chemical Mass Balance (CMB) (Wåhlin, 2003). All species listed in Table 1 was included in source apportionment, with the exception of O_3, NOx and SO_2.

CONCLUSIONS

Source apportionment results by PMF and COPREM showed good agreement in general. Five sources were employed to adequately explain the measurements, including a *Marine* and a *Soil* source of natural origin and three anthropogenic sources, which were all largely influenced by metal industries namely *Cu/Ni*, *Combustion* and *Zn* source (Nguyen et al., 2012).
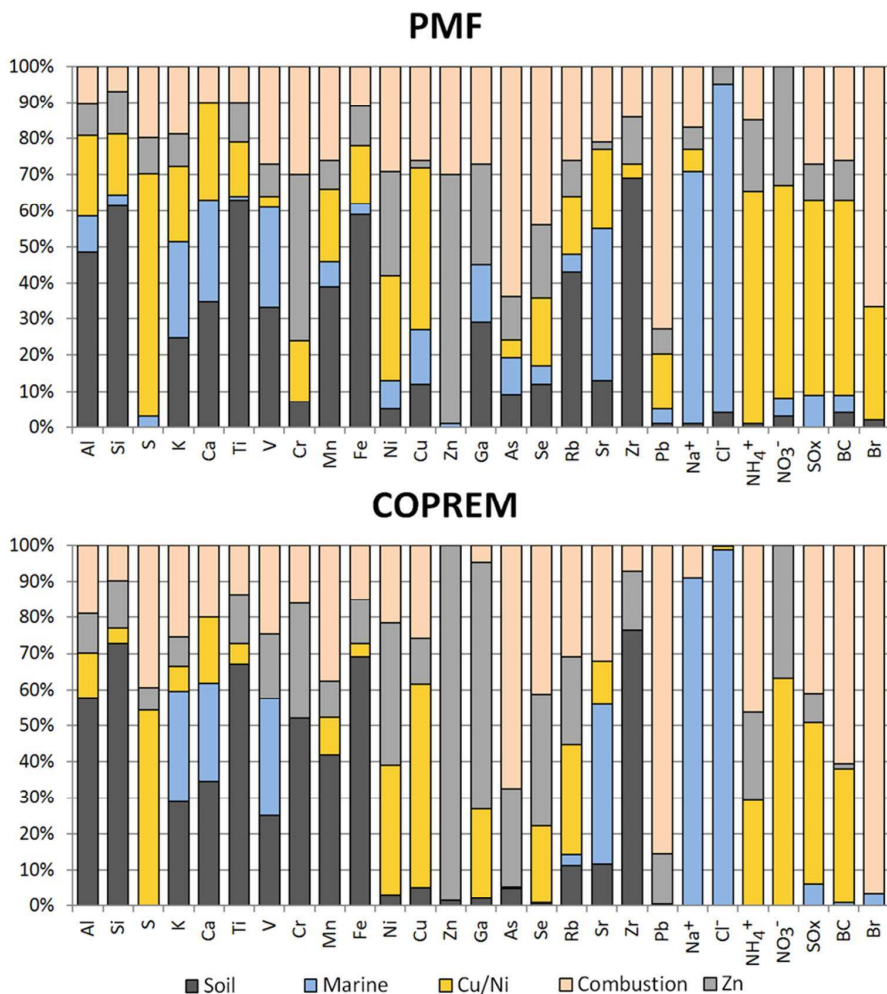
Figure 1. Source origin of chemical species apportioned by PMF and COPREM

The *Soil* source was dominated by Al, Si, Ca, Ti, Mn, V and Fe whereas Na and Cl dominated the *Marine* source. Source of sea salts possibly included frost flowers and marine snow pack (Fenger et al., 2012). The impacts of large-scale industry in Siberia, Russia were evident via large contribution of Cu to both the *Cu/Ni* and

Combustion source. Sources of black carbon were identified to be mainly anthropogenic and most probably of Siberian origin (80-98%). The *Combustion* source was also associated with high concentrations of Pb, As, V and Se, indicating contributions from oil and coal-fuelled industries being long-range transported to Station Nord. While the *Cu/Ni* and *Combustion* source followed the typical Arctic haze pattern with low concentrations in summer and elevated concentrations in winter, the *Zn* source accounts for episodes of high contribution of anthropogenic pollutants at Station Nord during summer. Air mass back trajectories using the Hybrid Single Particle Lagrangian Integrated Trajectory (HYSPLIT) model suggested a Canadian Arctic origin to this *Zn* source.

ACKNOWLEDGEMENTS

REFERENCES

Fenger, M., Sørensen, L. L., Kristensen, K., Jensen, B., Nquyen, Q. T., Nøjgaard, J. K., Massling, A., Skov, H., and Glasius, M.: Sources of anions in aerosols in northeast Greenland during late winter, Atmos. Chem. Phys. Discuss., 12, 14813-14836, 10.5194/acpd-12-14813-2012, 2012.

Heidam, N. Z., Christensen, J., Wahlin, P., and Skov, H.: Arctic atmospheric contaminants in NE Greenland: levels, variations, origins, transport, transformations and trends 1990-2001, Sci Total Environ, 331, 5-28, DOI 10.1016/j.scitotenv.2004.03.033, 2004.

Nguyen, Q.T., Skov, H., Sørensen, L.L., Jensen, B.J., Grube, A.G., Massling, A., Glasius, M. and Nøjgaard, J.K.: Source apportionment of particles at Station Nord, North East Greenland during 2008-2010 using COPREM and PMF analysis, Atmos. Chem. Phys. Discuss., submitted.

Wåhlin, P.: COPREM - A multivariate receptor model with a physical approach, Atmospheric Environment, 37, 4861-4867, DOI 10.1016/j.atmosenv.2003.08.032, 2003.

LONG-TERM TRENDS IN BOUNDARY LAYER NUCLEATION IN BOREAL FOREST

T. NIEMINEN[1], M. DAL MASO[1], T. PETÄJÄ[1], V.-M. KERMINEN[1], M. KULMALA[1]

[1]University of Helsinki, Department of Physics, P. O. Box 64, FI-00014 University of Helsinki, Finland

Keywords: new particle formation, sulphuric acid, long-term trends.

INTRODUCTION

Investigating new aerosol particle formation (NPF) in the atmosphere has been very active topic during the last two decades. This phenomenon has been observed in various environments around the world (Kulmala et al., 2004). One of the longest and most comprehensive data sets of atmospheric aerosol properties is available from the University of Helsinki SMEAR II station in Hyytiälä, southern Finland (Hari and Kulmala, 2005). Aerosol number concentration size distributions have been measured at Hyytiälä since January 1996 with a DMPS system covering particle size range 3 – 1000 nm (3 – 500 nm until end of 2004; see Aalto et al., 2001). Aerosol measurements are complemented by measurements of basic meteorological variables, trace gas concentrations (SO_2, O_3, CO, CO_2, NO, NO_x), and quantities related to the soil and forest surrounding the station.

METHODS

By the end of 2011 we have observed 1337 days when regional NPF is occuring at Hyytiälä. This means the formation of new 3 nm particles typically happening between 09–15 local time. The formation of particles is then followed by their growth to sizes of 40 – 100 nm usually within 10 – 20 hours. An example of an NPF event is shown in Figure 1. Most of the events occur at spring time from March to May, when as many as every second day can be an NPF day. The number of nucleation events detected at Hyytiälä varies from year to year in the range of 60 – 120 per year. The reasons behind this quite substantial variation are not yet found. We have, however, established that the variation of the galactic cosmic ray intensity due to the 11 year solar cycle is not connected to the particle formation intensity at Hyytiälä (Kulmala et al., 2010).

RESULTS AND CONCLUSIONS

Mean values and observed trends in the quantities relative to NPF are listed in Table 1. There is no statistically significant trend in the formation rates of 3 – 25 nm particles. In contrast, the growth rates are increasing by 3% per year relative to their 16 year mean value. Concentrations of sulphuric acid, which has in many studies identified as the most important precursor vapor in atmospheric NPF, can be approximated with a simple proxy model (Petäjä et al., 2009). This proxy takes into account the source from oxidation of SO_2 by OH radicals and the condensation sink by pre-existing particles. Both the SO_2 concentration and CS are decreasing in Hyytiälä, but the relative change in SO_2 is larger. This leads to a decreasing trend of 4% per year also in the H_2SO_4 proxy concentration, and suggests that the observed increase in the particle growth rates could be caused by increased concentrations of organic compounds and their oxidation products. As the emissions of these biogenic organic compounds are highly temperature dependent, increasing global temperatures can lead to a larger fraction of newly formed particles reaching cloud condensation nuclei sizes and this way NPF becoming more significant to climate.
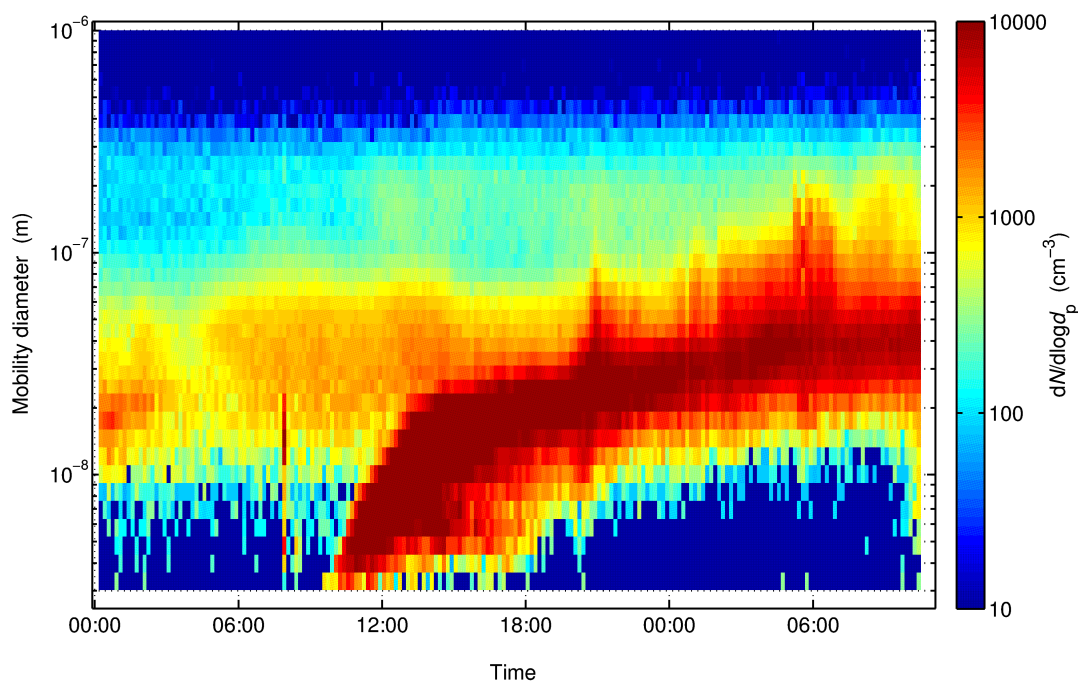
Figure 1. New particle formation event at Hyytiälä 15.3.2011.

Table 1. Mean values and trends of trace gas and aerosol quantities related to new particle formation in Hyytiälä during 1996 – 2011. Trend is calculated from linear least-squares fit to all the measurement data.

	1996 – 2011 mean value	Trend	
		absolute value	relative to 1996 – 2011 mean
SO$_2$	0.38 ppb	−0.02 ppb/year	−5.0%/year
Condensation sink	$5.1 \cdot 10^{-3}$ s^{-1}	$-1.5 \cdot 10^{-4}$ s^{-1}	−2.9%/year
H$_2$SO$_4$ proxy	$3.8 \cdot 10^{5}$ cm^{-3}	$-1.5 \cdot 10^{-4}$ cm^{-3}	−4.3%/year
Formation rate	0.84 cm^{-3} s^{-1}	no trend	–
Growth rate	3.1 nm/h	+0.1 nm/h	+3.2%/year

ACKNOWLEDGEMENTS

REFERENCES

Hari, P. and Kulmala, M. (2005). *Boreal Env. Res.* 10, 315–322.

Kulmala, M., Vehkamäki, H., Petäjä, T., Dal Maso, M., Lauri, A., Kerminen, V.-M., Birmili, W. and McMurry, P. H. (2004). *Journal of Aerosol Science* 35, 143–176.

Kulmala M., Riipinen, I., Nieminen, T., Hulkkonen, M., Sogacheva, L., Manninen, H. E., Paasonen, P., Petäjä, T., Dal Maso, M., Aalto, P. P., Viljanen, A., Usoskin, I., Vainio, R., Mirme, S., Mirme, A., Minikin, A., Petzold, A., Hõrrak, U., Plass-Dülmer, C., Birmili, W. and Kerminen, V.-M. (2010). *Atmos. Chem. Phys.* 10, 1885–1898.

Petäjä, T., Mauldin, R. L., Kosciuch, E., McGrath, J., Nieminen, T., Paasonen, P., Boy, M., Adamov, A., Kotiaho, T. and Kulmala, M. (2009). *Atmos. Chem. Phys.* 9, 7435–7448.

URBAN NET CO_2 EMISSIONS FROM LOCAL TO CONTINENTAL SCALE

A. NORDBO[1], L. JÄRVI[1], S. HAAPANALA[1], C.R. WOOD[2] and T. VESALA[1]

[1] Department of Physics, University of Helsinki, Helsinki, Finland.

[2] Finnish Meteorological Institute, Helsinki, Finland.

Keywords: CO_2 BUDGET, EDDY COVARIANCE, CARBON-NEUTRAL CITY.

INTRODUCTION

To date, over half of the world's population lives in cities (UN, http://esa.un.org/unpd/wup), and over 70% of global energy-related CO_2 emissions originate from cities (WEO, 2008; Rosenzweig et al., 2010). This makes cities hotspots of greenhouse gas (GHG) emissions and a main target in climate change mitigation (Kennedy et al., 2009). The development of mitigation strategies necessitate the direct quantification of GHG emissions from urban areas. The eddy-covariance method provides a means to determine the vertical surface–atmosphere exchange of CO_2, and it has been widely used in natural environments (Baldocchi et al., 2001; Valentini et al., 2000; Mizoguchi et al., 2009).

Extensive measurements in urban environments, to the contrary, have been conducted only during the past decade, allowing the calculation of annual CO_2 budgets (www.geog.ubc.ca/urbanflux). These budget estimates include direct emissions from the urban area in addition to vegetative photosynthetic uptake and respirative emissions. Thus, the budgets depart from indirect inventory-based estimates that exclude vegetation and include strong point sources, such as power plants. We denote the eddy-covariance-based budgets the net urban ecosystem exchange (NUE), which describes the in situ CO_2 budget of urban 'background activity', this has remained unresolved until now.

METHODS

The eddy-covariance method is based on simultaneous measurements of wind components and scalar concentrations, usually mounted on a mast above the desired terrain to be studied. The outcome is typically 30-minute average vertical turbulent fluxes. When turbulent exchange is considered the main means of vertical exchange, these fluxes can be assumed to be the surface fluxes. The source area of the method is several hectares depending upon the upwind surface type, measurement height and air flow properties (Vesala et al., 2008). The 14 sites (with 17 budget estimates) used in this study (Figure 1) provide over 16 000 days of measurements with a 58% data coverage. Data-loss is mainly caused by quality screening and thus the time series were gap-filled to provide annual budgets (typical gap-filling errors <5%, Järvi et al., 2012). Non-linear least-squares optimization is used for non-linear fits, and data coverage at each site is taken into account in fits by using a weighting function. Only sites with at least a year of measurements were included.

The fraction of natural land area (f_n) is the opposite of the fraction of urban area ($f_u = 1 - f_n$), which can be calculated from binary (urban/non-urban) data from the MODIS satellite (Schneider et al., 2009, 2010). These data have a spatial resolution of 500 m, and we aggregated the data into 4 km resolution to obtain a more continuous range of f_u with 65 possible values. We also compiled a set of GHG inventories from 56 urban areas in North America, Europe and eastern Asia. The

corresponding urban fractions were then extracted from the mapping of f_u using administrative boundaries (Database of Global Administrative Areas, www.gadm.org).

RESULTS AND DISCUSSION

Different predictors of NUE were analysed and f_n had the strongest explanatory ability. Figure 1 shows NUE from 14 urban eddy-covariance sites as a function of f_n, which here is the fraction of natural area within the source area of the turbulence measurements. This fraction is a very robust proxy for NUE (coefficient of determination $r^2 = 0.84$), especially when taking into account the large variety between city forms. The sites vary from the densely built-up metropolitan area of London (Helfter et al., 2011) to an urban park (Hiller et al., 2011), and all across the North America, Europe and eastern Asia. The largest urban emissions are forty times the uptake of grasslands (Soussana et al., 2007) and over ten times the global median terrestrial ecosystem uptake (Beer et al., 2010).

An urban area can be considered carbon-neutral when $f_n \approx 0.8$, which can be used as a first rule-of-thumb estimate in urban planning. It must be noted, though, that this is a carbon-neutrality estimate per square metre (ecosystem view) rather than per capita (political view), and it is well known that dense urban living has smaller per-capita GHG emissions compared to rural living (Dodman, 2009; Brown et al., 2009; Parshall et al., 2010). Thus, the estimate of $f_n \approx 0.8$ should not be used as a target in climate change mitigation. Increasing f_n has a mitigating effect only if it does not decrease living density, as with green roofs (Sailor et al., 2012).
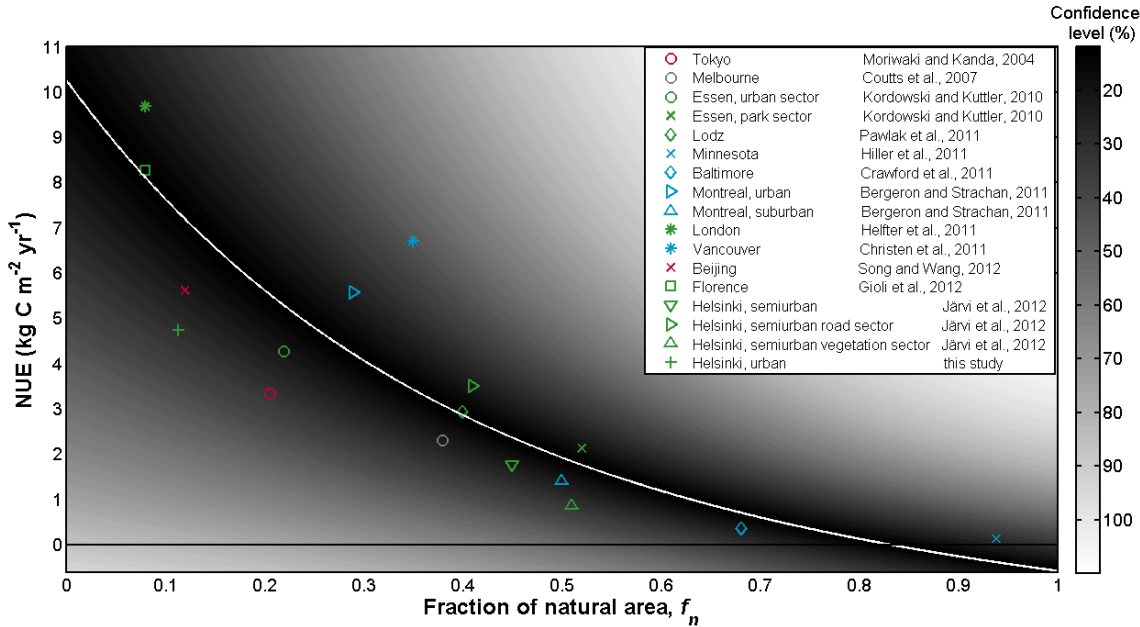
Figure 1: Net urban ecosystem exchange (NUE) from direct eddy-covariance flux measurements as a function of fraction of natural area (f_n). The colours show: North America (blue), Europe (green), eastern Asia (red), Australia (grey). The colourbar shows confidence intervals of the fit given in the legend. (Moriwaki and Kanda, 2004; Coutts et al., 2007; Kordowski and Kuttler, 2010; Pawlak et al., 2011; Hiller et al., 2011; Crawford et al., 2011; Bergeron and Strachan, 2011; Helfter et al., 2011; Christen et al., 2011; Song and Wang, 2012; Gioli et al., 2012; Järvi et al., 2012)

497

The robustness of f_n as a predictor of NUE (Figure 1) can be reasoned by the links f_n has to CO_2 exchange. If f_n is large, the road and population density are lower and thus the emissions from fossil-fuel combustion and human respiration are smaller. Large f_n may also cause daytime photosynthetic uptake and nigh-time respiratory release of CO_2. The relationship between NUE and f_n is non-linear perhaps due to the exponential growth of population density as a function of urban density (Pozzi and Small, 2005).

The strong explanatory power of f_n can also be used for parameterized estimates of NUE based on land-cover data. Figure 2a shows an example of f_u for Europe, where high urbanization dominates around the Benelux countries, Germany and southern England. This fraction is converted to NUE using the fit in Figure 1, resulting in Figure 2b, where areas with high f_u are interpreted as large CO_2 sources. The integrated NUE for the EU is 414 T g C yr^{-1}, which is half the inventory-based emissions (767 T g C yr^{-1} in 2006, WEO, 2008) and four times the uptake of CO_2 by biological fluxes (-102 ± 23 T g C yr^{-1}, Schulze et al., 2009). Similar analysis can be made for North-America and eastern Asia which are the areas where the eddy-covariance measurements in Figure 1 are from.
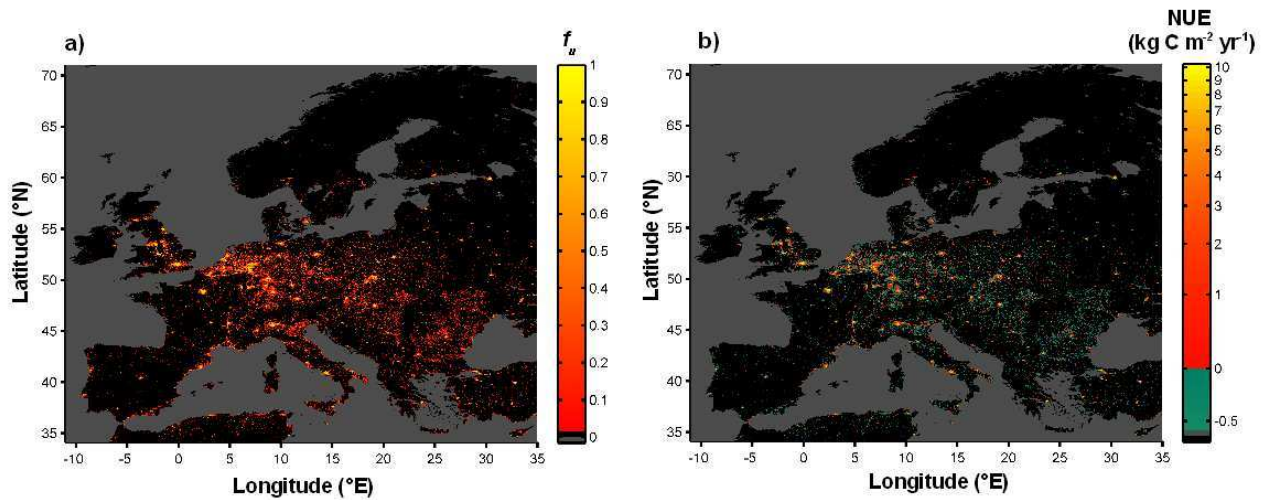
Figure 2: a) Urban fraction (f_u) based on satellite observations, b) Net urban ecosystem exchange (NUE, k g C yr^{-1} m^{-2}) based on a parameterization as a function of fraction of natural area (Figure 1).

Parameterized NUE estimates can be calculated for individual cities in a similar manner as for larger regions, like EU above. Figure 3 shows the parameterized NUE as a function of inventory-based estimates for 56 cities. The NUE estimates are systematically lower than the inventory-based estimates for all but Prague (slope 0.50), which is expected since NUE includes vegetation and excludes strong point sources. Nevertheless, there is a clear linear dependency ($r^2 = 0.72$, rms $= 1.42$ k g C yr^{-1} m^{-2}), which corroborates independently the usability of f_n as a proxy for NUE. A direct validation of the NUE parameterization method is not possible, since another method for providing CO_2 budgets of urban ecosystems does not exist.

CONCLUSIONS

This study shows that the fraction of natural area (f_n) is the strongest predictor of CO_2 emissions from cities (Figure 1). We also provide the first continental-scale estimates of CO_2 release from urbanized areas (Figure 2) based on direct eddy-covariance flux measurements. Individual cities
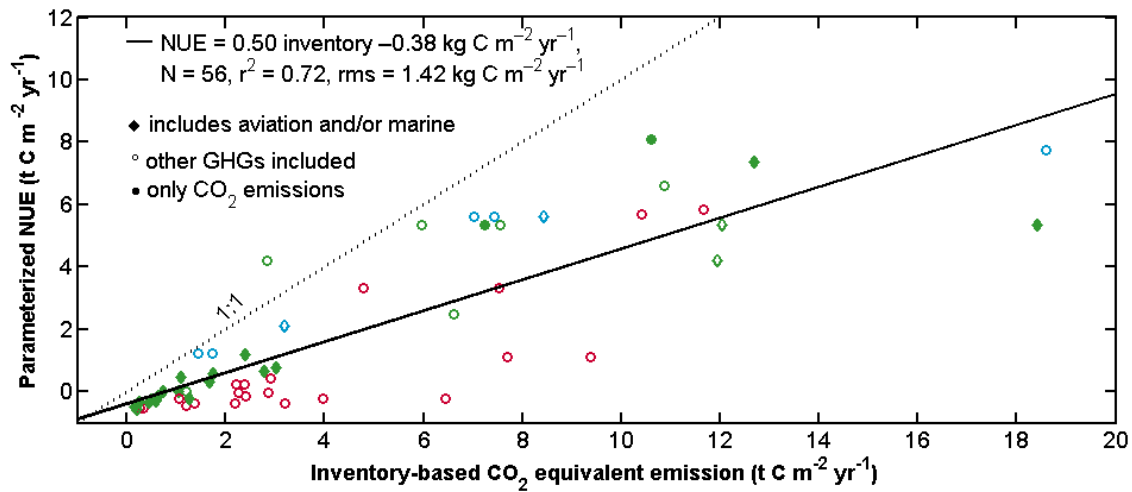
Figure 3: Parameterized net urban ecosystem exchange (NUE, k g C yr^{-1} m^{-2}) against inventory-based emissions (kg equivalent C yr^{-1} m−2). Inventory values contain only CO_2 (filled markers) or all GHGs (open markers); some contain aviation and/or marine emissions (diamond markers). Continents are distinguished by colours: North America (blue), Europe (green), eastern Asia (red)

were extracted from this type of mapping and their NUE estimates are shown to correspond well with inventory-based estimates (Figure 3), corroborating the robustness of f_n as a predictor of NUE.

Direct eddy-covariance measurements of CO_2 fluxes have just during the past two years become extensive enough to enable meta-analysis, such as the one presented here. Nevertheless, Europe and North-America are over-represented in the urban CO_2 budget measurements and studies are needed especially from Asia, Africa and South America. There is also a lack of studies to cover semi-continuously the whole f_n range.

ACKNOWLEDGEMENTS

REFERENCES

Baldocchi, D., Falge, E., Gu, L. H., Olson, R., Hollinger, D., Running, S., Anthoni, P., Bernhofer, C., Davis, K., Evans, R., Fuentes, J., Goldstein, A., Katul, G., Law, B., Lee, X. H., Malhi, Y., Meyers, T., Munger, W., Oechel, W., U, K. T. P., Pilegaard, K., Schmid, H. P., Valentini, R., Verma, S., Vesala, T., Wilson, K., and Wofsy, S. (2001). FLUXNET: A new tool to study the temporal and spatial variability of ecosystem-scale carbon dioxide, water vapor, and energy flux densities. *Bulletin of the American Meteorological Society*, 82(11):2415–2434.

Beer, C., Reichstein, M., Tomelleri, E., Ciais, P., Jung, M., Carvalhais, N., Roedenbeck, C., Arain, M. A., Baldocchi, D., Bonan, G. B., Bondeau, A., Cescatti, A., Lasslop, G., Lindroth, A., Lomas, M., Luyssaert, S., Margolis, H., Oleson, K. W., Roupsard, O., Veenendaal, E., Viovy, N.,

Williams, C., Woodward, F. I., and Papale, D. (2010). Terrestrial gross carbon dioxide uptake: Global distribution and covariation with climate. *Science*, 329(5993):834–838.

Bergeron, O. and Strachan, I. B. (2011). CO_2 sources and sinks in urban and suburban areas of a northern mid-latitude city. *Atmospheric Environment*, 45(8):1564–1573.

Brown, M. A., Southworth, F., and Sarzynski, A. (2009). The geography of metropolitan carbon footprints. *Policy and Society*, 27:285–304.

Christen, A., Coops, N. C., Crawford, B. R., Kellett, R., Liss, K. N., Olchovski, I., Tooke, T. R., van der Laan, M., and Voogt, J. A. (2011). Validation of modeled carbon-dioxide emissions from an urban neighborhood with direct eddy-covariance measurements. *Atmospheric Environment*, 45(33):6057–6069.

Coutts, A. M., Beringer, J., and Tapper, N. J. (2007). Characteristics influencing the variability of urban CO_2 fluxes in melbourne, australia. *Atmospheric Environment*, 41(1):51–62.

Crawford, B., Grimmond, C. S. B., and Christen, A. (2011). Five years of carbon dioxide fluxes measurements in a highly vegetated suburban area. *Atmospheric Environment*, 45(4):896–905.

Dodman, D. (2009). Blaming cities for climate change? an analysis of urban greenhouse gas emissions inventories. *Environment and Urbanization*, 21(1):185–201.

Gioli, B., Toscano, P., Lugato, E., Matese, A., Miglietta, F., Zaldei, A., and Vaccari, F. P. (2012). Methane and carbon dioxide fluxes and source partitioning in urban areas: The case study of Florence, Italy. *Environmental Pollution*, 164:125–131.

Helfter, C., Famulari, D., Phillips, G. J., Barlow, J. F., Wood, C. R., Grimmond, C. S. B., and Nemitz, E. (2011). Controls of carbon dioxide concentrations and fluxes above central London. *Atmospheric Chemistry and Physics*, 11(5):1913–1928.

Hiller, R. V., McFadden, J. P., and Kljun, N. (2011). Interpreting CO_2 fluxes over a suburban lawn: The influence of traffic emissions. *Boundary-Layer Meteorology*, 138(2):215–230.

Järvi, L., Nordbo, A., Junninen, H., Riikonen, A., Moilanen, J., Nikinmaa, E., and Vesala, T. (2012). Seasonal and annual variation of carbon dioxide surface fluxes in Helsinki, Finland, in 2006-2010. *Atmos. Chem. Phys. Discuss.*, 12:8355–8396.

Kennedy, C., Steinberger, J., Gasson, B., Hansen, Y., Hillman, T., Havranek, M., Pataki, D., Phdungsilp, A., Ramaswami, A., and Mendez, G. V. (2009). Greenhouse gas emissions from global cities. *Environmental science & technology*, 43(19):7297–7302.

Kordowski, K. and Kuttler, W. (2010). Carbon dioxide fluxes over an urban park area. *Atmospheric Environment*, 44(23):2722–2730.

Mizoguchi, Y., Miyata, A., Ohtani, Y., Hirata, R., and Yuta, S. (2009). A review of tower flux observation sites in Asia. *Journal of Forest Research*, 14(1):1–9.

Moriwaki, R. and Kanda, M. (2004). Seasonal and diurnal fluxes of radiation, heat, water vapor, and carbon dioxide over a suburban area. *Journal of Applied Meteorology*, 43(11):1700–1710.

Parshall, L., Gurney, K., Hammer, S. A., Mendoza, D., Zhou, Y., and Geethakumar, S. (2010). Modeling energy consumption and CO_2 emissions at the urban scale: Methodological challenges and insights from the United States. *Energy Policy*, 38(9):4765–4782.

Pawlak, W., Fortuniak, K., and Siedlecki, M. (2011). Carbon dioxide flux in the centre of Lodz, Poland - analysis of a 2-year eddy covariance measurement data set. *International Journal of Climatology*, 31(2):232–243.

Pozzi, F. and Small, C. (2005). Analysis of urban land cover and population density in the United States. *Photogrammetric Engineering and Remote Sensing*, 71(6):719–726.

Rosenzweig, C., Solecki, W., Hammer, S. A., and Mehrotra, S. (2010). Cities lead the way in climate-change action. *Nature*, 467(7318):909–911.

Sailor, D. J., Elley, T. B., and Gibson, M. (2012). Exploring the building energy impacts of green roof design decisions - a modeling study of buildings in four distinct climates. *Journal of Building Physics*, 35(4):372–391.

Schneider, A., Friedl, M. A., and Potere, D. (2009). A new map of global urban extent from MODIS satellite data. *Environmental Research Letters*, 4(4):044003.

Schneider, A., Friedl, M. A., and Potere, D. (2010). Mapping global urban areas using MODIS 500-m data: New methods and datasets based on 'urban ecoregions'. *Remote Sensing of Environment*, 114(8):1733–1746.

Schulze, E. D., Luyssaert, S., Ciais, P., Freibauer, A., Janssens, I. A., Soussana, J. F., Smith, P., Grace, J., Levin, I., Thiruchittampalam, B., Heimann, M., Dolman, A. J., Valentini, R., Bousquet, P., Peylin, P., Peters, W., Roedenbeck, C., Etiope, G., Vuichard, N., Wattenbach, M., Nabuurs, G. J., Poussi, Z., Nieschulze, J., Gash, J. H., and Team, C. (2009). Importance of methane and nitrous oxide for europe's terrestrial greenhouse-gas balance. *Nature Geoscience*, 2(12):842–850.

Song, T. and Wang, Y. (2012). Carbon dioxide fluxes from an urban area in Beijing. *Atmospheric Research*, 106:139–149.

Soussana, J. F., Allard, V., Pilegaard, K., Ambus, P., Amman, C., Campbell, C., Ceschia, E., Clifton-Brown, J., Czobel, S., Domingues, R., Flechard, C., Fuhrer, J., Hensen, A., Horvath, L., Jones, M., Kasper, G., Martin, C., Nagy, Z., Neftel, A., Raschi, A., Baronti, S., Rees, R. M., Skiba, U., Stefani, P., Manca, G., Sutton, M., Tubaf, Z., and Valentini, R. (2007). Full accounting of the greenhouse gas (CO_2, N_2O, CH_4) budget of nine European grassland sites. *Agriculture Ecosystems & Environment*, 121(1-2):121–134.

Valentini, R., Matteucci, G., Dolman, A. J., Schulze, E. D., Rebmann, C., Moors, E. J., Granier, A., Gross, P., Jensen, N. O., Pilegaard, K., Lindroth, A., Grelle, A., Bernhofer, C., Grunwald, T., Aubinet, M., Ceulemans, R., Kowalski, A. S., Vesala, T., Rannik, Ü., Berbigier, P., Loustau, D., Guomundsson, J., Thorgeirsson, H., Ibrom, A., Morgenstern, K., Clement, R., Moncrieff, J., Montagnani, L., Minerbi, S., and Jarvis, P. G. (2000). Respiration as the main determinant of carbon balance in European forests. *Nature*, 404(6780):861–865.

Vesala, T., Kljun, N., Rannik, Ü., Rinne, J., Sogachev, A., Markkanen, T., Sabelfeld, K., Foken, T., and Leclerc, M. Y. (2008). Flux and concentration footprint modelling: State of the art. *Environmental Pollution*, 152(3):653–666.

WEO (2008). *Chapter 16: Implications of the reference scenario for the global climate*, pages 381–406. World Energy Outlook. OECD/IEA.

COMPARING SIMULATED AND EXPERIMENTAL MOLECULAR CLUSTER DISTRIBUTIONS

T. OLENIUS[1], O. KUPIAINEN[1], I. K. ORTEGA[1] and H. VEHKAMÄKI[1]

[1]Department of Physics, University of Helsinki, P.O. Box 64, FI-00014 Finland

Keywords: MOLECULAR CLUSTERS, SULFURIC ACID, AMINES, MODELING.

INTRODUCTION

Formation of secondary atmospheric aerosol particles begins with individual molecules forming small molecular clusters. Today high-resolution mass spectroscopy enables the detection and unambiguous chemical characterization of electrically charged clusters from molecular scale upward, but direct experimental observation of electrically neutral clusters smaller than 1 nm in diameter still remains impossible. However, it is estimated that 90% of atmospheric particle formation is due to neutral particles (Kulmala et al., 2007). This results in a need for theoretical methods able to link the observed concentrations of charged clusters with the concentrations of neutral clusters.

METHODS

We have simulated a set of small molecular clusters containing sulfuric acid (H_2SO_4), dimethylamine (DMA, $(CH_3)_2NH$) and ammonia (NH_3) molecules with the kinetic code ACDC (Atmospheric Cluster Dynamics Code; McGrath et al., 2012) that solves the birth-death equations of the clusters. The code enables the monitoring of cluster concentrations and fluxes between the clusters and out of the simulated system. As an input for the code we have used evaporation rates of the clusters derived from quantum chemical calculations (Ortega et al., 2012).

We have included in the simulation both neutral clusters and negatively and positively charged cluster ions that contain up to four sulfuric acid and four base molecules, with the exception that the highly unstable clusters were not included. Since we have assumed that clusters that grow out will not re-evaporate, they have to be relatively stable, i.e. they must have reasonable numbers of acid and base molecules. We have set these boundary conditions to be as follows: 1) neutral clusters must have at least five acid and four base molecules 2) negative clusters must have at least five acid molecules and one base molecule 3) positive clusters must have at least four acid and five base molecules.

In the simulations we have used constant concentrations for DMA and ammonia monomers. However, we have taken the sulfuric acid concentration [H_2SO_4] to be the sum of all neutral clusters containing 1-2 acid molecules and 0-4 base molecules, since CIMS (chemical ionization mass spectrometer), the instrument used to measure acid concentration, can also detect them as acid monomers. The simulations were run in conditions relevant to the CLOUD experiment at CERN (Kirkby et al., 2011) at 5.5 °C, [H_2SO_4]=10^5-10^7cm^{-3}, [NH_3]=10 ppt, [DMA]=1 ppt and 10 ppt and with ion production rate of 3 ion pairs s^{-1} cm^{-3}.

We have examined the steady-state cluster distributions and compared the results for negatively charged clusters to concentrations measured experimentally in CLOUD. We have also studied the distribution of neutral clusters containing 1-2 sulfuric acid molecules to estimate what might actually be detected by CIMS.

RESULTS

Figure 1 shows the modeled and experimental concentrations of negatively charged sulfuric acid mono-, di-, tri- and tetramers as a function of sulfuric acid concentration. Concentrations of pure sulfuric acid i-mers and total concentrations of i-mers containing 0-4 DMA molecules in addition to the acid are shown

with separate lines and markers. Modeled distribution of neutral clusters containing 1-2 sulfuric acid molecules and 0-4 base molecules for different acid and DMA concentrations is shown in figure 2.

CONCLUSIONS

We have shown that ACDC is capable of qualitatively reproducing the results observed experimentally in CLOUD. ACDC can also be used to simulate the distribution of neutral clusters that cannot be directly measured, helping to evaluate the indirect measurement results and leading to a better understanding of atmospheric molecular cluster formation.
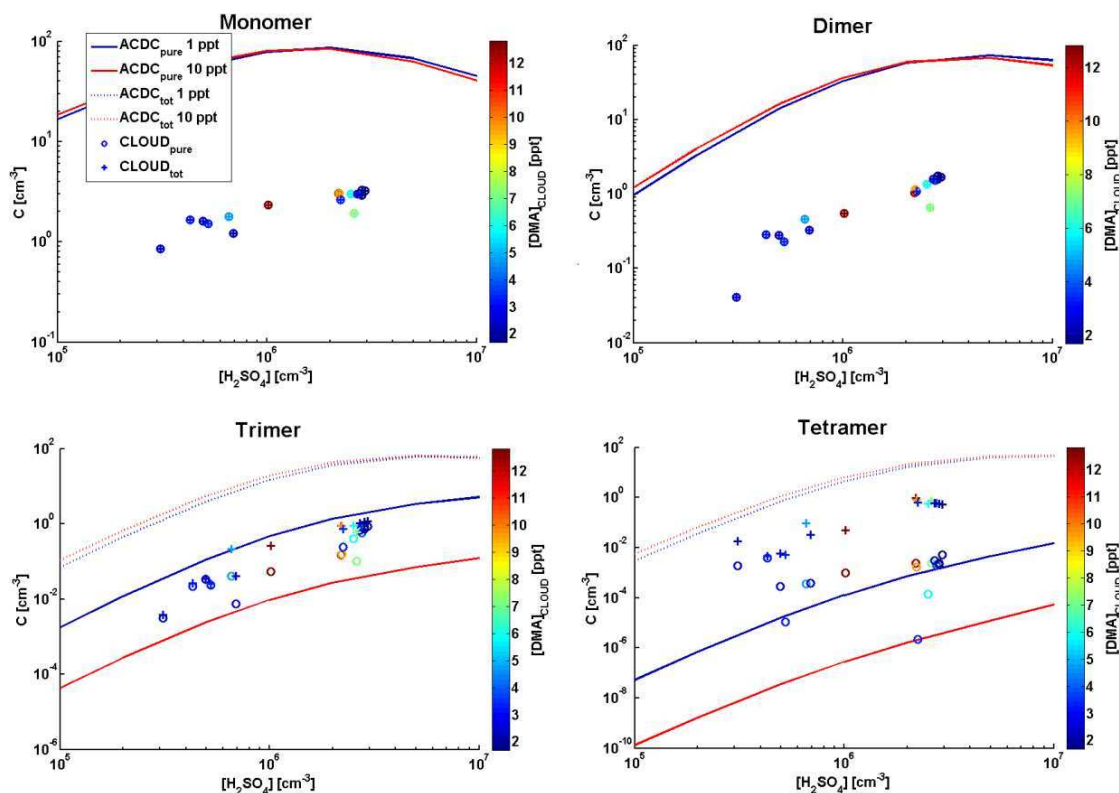
Figure 1. Modeled and experimental concentrations of negatively charged sulfuric acid mono-, di-, tri- and tetramers, pure or with DMA molecules, as a function of sulfuric acid concentration. Note the different scales in the y-axes.
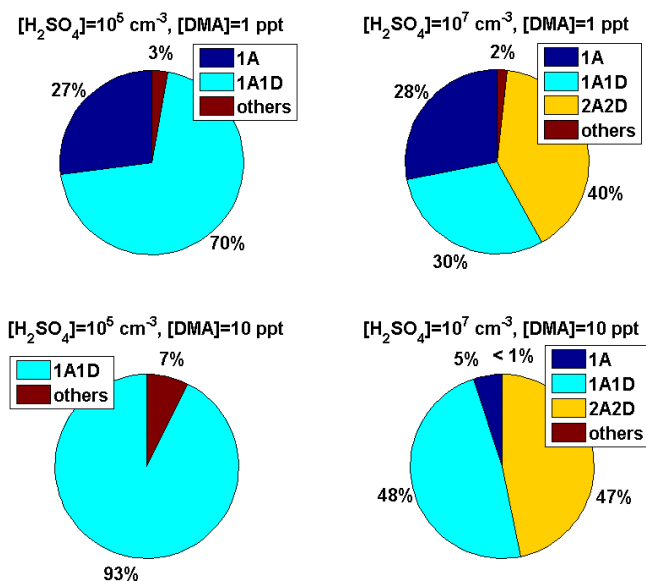
Figure 2. Modeled distribution of neutral clusters containing 1-2 sulfuric acid molecules and 0-4 base molecules for $[H_2SO_4]=10^5$ and 10^7 cm^{-3} and $[DMA]=1$ and 10 ppt. All clusters that have concentration less than 5% of the total concentration $[H_2SO_4]$ are under the label "others".

ACKNOWLEDGEMENTS

REFERENCES

Kirkby, J. et al. (2011). Role of sulphuric acid, ammonia and galactic cosmic rays in atmospheric aerosol nucleation, Nature **476**, 429–433.

Kulmala, M. et al. (2007). Toward direct measurement of atmospheric nucleation, Science **318**, 89–92.

McGrath, M.J. et al. (2012). Atmospheric Cluster Dynamics Code: a flexible method for solution of the birth-death equations, Atmospheric Chemistry and Physics **12**, 2345–2355.

Ortega, I.K. et al. (2012). From quantum chemical formation free energies to evaporation rates, Atmospheric Chemistry and Physics **12**, 225-235.

QUANTUM CHEMICAL STUDY OF PINONIC ACID - SULFURIC ACID - DIMETHYLAMINE CLUSTERS

I.K. ORTEGA[1] and H. VEHKAMÄKI [1]

[1]Department of Physics, University of Helsinki, Post Office Box 64, FI-00014, Helsinki, Finland.

Keywords: Quantum Chemistry, new particle formation, organic acids, sulphuric acid, dimethylamine

INTRODUCTION

Atmospheric new particle is an important source of aerosol particles that can act as cloud condensation nuclei in the atmosphere. Despite the numerous efforts to determine the compounds involved in new particle formation, some of these remain unknown. Sulphuric acid certainly has a key role in atmospheric new particle formation, but, in realistic atmospheric conditions, cannot explain the observed new particle formation rates on its own. Recently, state-of-the-art experiments in CLOUD chamber at CERN (Kirby et al. 2011), have showed how, although the presence of ammonia and ions can enhance new particle formation rates by a factor of 10000, the observed new particle formation rates are still far below those measured in the real atmosphere. This implies that other stabilizing compound(s), yet unknown, is involved in atmospheric new particle formation.

The participation of organic compounds in new particle formation is still under discussion. While some studies conclude that organics are only involve in particle growth (Laaksonen et al. 2008 ,and references therein), other studies conclude that they are also involved in the very first steps of new particle formation (Zhang 2010 and references there in). In the present study we have use quantum chemical methods to evaluate the stability of clusters containing sulfuric acid and different organic compounds. We have chosen dimethylamine ($(CH_3)_2NH$) as model compound for organic bases and cis-pinonic acid ($C_{10}H_{14}O_3$) as model compound for organic acids.

METHODS

We have used the method described by Ortega et al (2011) to calculate the formation Gibbs free energies and convert these in evaporation rates, so only relevant details are given here. The geometry optimizations and frequency calculations were performed with the Gaussian09 program (Frisch et al 2009) using the B3LYP hybrid functional and a CBSB7 basis set and a single- point electronic energy was then calculated with the TURBOMOLE program (Ahlrichs et al. 1989) using the RI- CC2 method and an aug-cc-pV(T+d)Z basis set.

CONCLUSIONS

The clusters included in this study are listed in Table 1 together with the formation Gibbs free energies from monomers, so for example, $H_2SO_4 + (CH_3)_2NH + C_{10}H_{14}O_3 \rightarrow H_2SO_4 \cdot (CH_3)_2NH \cdot C_{10}H_{14}O_3$.

Cluster	$\Delta G_{mon,298K}$ (kcal/mol)
$(C_{10}H_{14}O_3)_2$	-2.51
$C_{10}H_{14}O_3 \cdot H_2SO_4$	-9.56
$C_{10}H_{14}O_3 \cdot (H_2SO_4)_2$	-15.02
$(C_{10}H_{14}O_3)_2 \cdot H_2SO_4$	-13.23
$(C_{10}H_{14}O_3)_2 \cdot (H_2SO_4)_2$	-22.38
$C_{10}H_{14}O_3 \cdot (CH_3)_2NH$	-3.62
$C_{10}H_{14}O_3 \cdot H_2SO_4 \cdot (CH_3)_2NH$	-26.61

$C_{10}H_{14}O_3 \cdot H_2SO_4 \cdot ((CH_3)_2NH)_2$	-30.36
$C_{10}H_{14}O_3 \cdot (H_2SO_4)_2 \cdot (CH_3)_2NH$	-41.32
$C_{10}H_{14}O_3 \cdot (H_2SO_4)_2 \cdot ((CH_3)_2NH)_2$	-62.29

Table 1. Formation Gibbs free energies from monomers in kcal/mol for the clusters included in this study.

The formation of cis-pinonic acid dimmers is quite unfavourable, but the presence of sulfuric acid in the cluster enhances the addition of a second molecule of organic acid to the cluster (Table 2)

n	Addition energy (Kcal/mol)
0	-2.51
1	-3.67
2	-9.29

Table 2. Addition energy of $(H_2SO_4)_n \cdot C_{10}H_{14}O_3 + C_{10}H_{14}O_3 \rightarrow (H_2SO_4)_n \cdot (C_{10}H_{14}O_3)_2$

As can be seen, the presence of just one molecule of sulfuric acid, increases the addition energy by around 1 kcal/mol, but if a second molecule of sulfuric acid is present, the addition energy increases by 6.8 kcal/mol. This result is reasonable, since the addition of sulfuric acid to the cluster gives extra –OH and =O groups to form hydrogen bonds. The formation of a sulfuric acid-cis-pinonic acid dimer is almost 2 kcal/mol more favourable than the formation of a pure sulfuric acid dimer (-7.89 kcal/mol), Ortega et al. 2012). The addition of a sulfuric acid molecule to the sulfuric acid- cis-pinonic acid dimer is also around 2 kcal/mol more favourable, so the most probable pathway to the $(C_{10}H_{14}O_3)_2 \cdot (H_2SO_4)_2$ is the formation of $C_{10}H_{14}O_3 \cdot H_2SO_4$ cluster, addition of the second sulfuric acid molecule, and then the addition of the second cis-pinonic acid molecule to the $C_{10}H_{14}O_3 \cdot (H_2SO_4)_2$ cluster.

The formation of $C_{10}H_{14}O_3 \cdot (CH_3)_2NH$ cluster is quite unfavourable, but on the other hand the addition energy of cis-pinonic acid to $H_2SO_4 \cdot (CH_3)_2NH$ cluster is -11.2 kcal/mol, so to add one dimethylamine molecule to cis-pinonic acid, this dimethylamine should be coordinated to a sulfuric acid molecule. The addition of a second dimethylamine molecule to $C_{10}H_{14}O_3 \cdot H_2SO_4 \cdot (CH_3)_2NH$ cluster is not favourable. and the addition of a second sulfuric acid molecule is not favourable either, since the $(H_2SO_4)_2 \cdot (CH_3)_2NH$ cluster is really stable (Ortega et al. 2012) and the evaporation rate of cis-pinonic acid from $C_{10}H_{14}O_3 \cdot (H_2SO_4)_2 \cdot (CH_3)_2NH$ cluster is $2.3 \times 10^5 \, s^{-1}$.

The preliminary results reported in this work shows how cis-pinonic acid can be involved in new particle formation from the firsts steps. The presence of sulfuric acid seems crucial to allow the growth of clusters with cis-pinonic acid, since the addition of a second molecule of this acid to the cluster is not possible without sulfuric acid. Dimethylamine can stabilize cluster with one cis-pinonic acid but again, sulfuric acid is needed since cis-pinonic acid on its own cannot form stable cluster with dimethylamine. The addition of further dimethylamine or sulfuric acid molecules is not favourable, most probably cluster will grow by addition of a second molecule of cis-pinonic acid, this pathway will be studied in more detail in future studies.

REFERENCES

Kirkby J., Curtius J., Almeida, J., Dunne, E., et al.(2011). Role of sulphuric acid, ammonia and galactic cosmic rays in atmospheric nucleation. Nature **476**, 429.

Laaksonen A, et al. (2008) The role of VOC oxidation products in continental new particle formation. Atmos. Chem. Phys. **8**, 2657.

Zhang, R. (2010). Getting to the critical nucleus of aerosol formation. Science **328**, 1366.

Ortega, I. K., Kupiainen, O., Kurtén, T., Olenius, T., Wilkman, O., McGrath, M. J., Loukonen, V., and Vehkamäki, H. (2012). From quantum chemical formation free energies to evaporation rates, Atmos. Chem. Phys. **12**, 225.

Frisch, M. J., Trucks, G. W., Schlegel, H. B., Scuseria, G. E., Robb, M. A., Cheeseman, J. R., Scalmani, G., Barone, V., Mennucci, B., Petersson, G. A., Nakatsuji, H., Caricato, M., Li, X., Hratchian, H. P., Izmaylov, A. F., Bloino, J., Zheng, G., Sonnenberg, J. L., Hada, M., Ehara, M., Toyota, K., Fukuda, R., Hasegawa, J., Ishida, M., Nakajima, T., Honda, Y., Kitao, O., Nakai, H., Vreven, T., Montgomery Jr., J. A., Peralta, J. E., Ogliaro, F., Bearpark, M., Heyd, J. J., Brothers, E., Kudin, K. N., Staroverov, V. N., Kobayashi, R., Normand, J., Raghavachari, K., Rendell, A., Burant, J. C., Iyengar, S. S., Tomasi, J., Cossi, M., Rega, N., Millam, J. M., Klene, M., Knox, J. E., Cross, J. B., Bakken, V., Adamo, C., Jaramillo, J.,Gomperts, R., Stratmann, R. E., Yazyev, O., Austin, A. J., Cammi, R., Pomelli, C., Ochterski, J.W., Martin, R. L., Morokuma, K., Zakrzewski, V. G., Voth, G. A., Salvador, P., Dannenberg, J. J., Dapprich, S., Daniels, A. D., Farkas, ¨O ., Foresman, J. B., Ortiz, J. V., Cioslowski, J., and Fox, D. J.: Gaussian 09, Revision B01, Gaussian, Inc., Wallingford CT, 2009.

Ahlrichs, R., Bär, M., Häser, J., Horn, H., and Kölmel C.(1989). Electronic structure calculations on workstation computers: the program system TURBOMOLE, Chem. Phys. Lett. **162**, 165.

WATER INTERACTIONS WITH LIQUID AND SOLID ORGANICS OF ATMOSPHERIC RELEVANCE

P. PAPAGIANNAKOPOULOS [1,2], X. KONG[1], E.S. THOMSON [1], N. MARKOVIC[3], and J.B.C PETTERSSON[1]

[1]Department of Chemistry and Molecular Biology, Atmospheric Science, University of Gothenburg, SE-412 96 Gothenburg, Sweden

[2] Department of Chemistry, Laboratory of Photochemistry and Kinetics, 710 03 Heraklion, Crete, Greece

[3]Department of Chemical and Biological Engineering, Physical Chemistry, Chalmers University of Technology, SE-412 96 Gothenburg, Sweden

INTRODUCTION

Water interactions with organic phases play an important role for several atmospheric processes including the formation and transformation of organic aerosol. Here we investigate water interactions with both solid and liquid organics using the recently developed environmental molecular beam technique (EMB)(Kong, Andersson et al. 2011; Thomson, Kong et al. 2011; Kong, Andersson et al. 2012). Butanol (n-) is used as a model system and water uptake dynamics and kinetics are studied in the temperature range from 160 to 200 K. The n-butanol melts at 184.5 K and changes in alcohol surface structure influence water uptake over a 10 degrees range both above and below the melting point.

METHODS

Experiments were performed with an EMB apparatus (Kong, Andersson et al. 2011) in which a pulsed supersonic D_2O/He beam collides with a micrometer-thin n-butanol film on a flat substrate. D_2O was used instead of H_2O to enhance sensitivity. D_2O molecules collided with the butanol surface and inelastically scattered and thermally desorbed D_2O molecules were monitored with a quadrupole mass spectrometer (QMS). The D_2O flight time from the surface to the QMS ionization region was 1-10 ms, and time-resolved intensities were transformed into time-of-flight (TOF) distributions. The TOF distributions were subsequently deconvoluted into two components: a) the inelastically scattered (IS) and b) the thermally desorbed (TD) distributions, using a theoretical model that has been presented previously (Thomson, Kong et al. 2011).

Thin n-butanol multilayer films were prepared by condensation of low pressure (p(T) = 10^{-4} – 10^{-3} mbar) vapor for about 1 min with their buildup rate (70 MLs^{-1}) and thickness (1 μm), corresponding to ca. 3000 monolayers (ML). Their growth was controlled and measured by the reflections of a diode laser beam (1 mW, 670 nm) from the surface. Elastic scattering of helium atoms was also used to follow initial growth of butanol on the graphite substrate.

The theoretical fitting procedure (Thomson, Kong et al. 2011) yields the desorption rate coefficient (k_{des}) for water on butanol as a function of temperature. In addition, the absolute fraction of trapped and desorbed D_2O molecules (f_{TD}) was determined.

RESULTS

Three different types of experiments were performed according to the preparation method of butanol films: i) fresh vapor deposition at each temperature, ii) initial vapor deposition at 190 K and gradual cooling to 160 K (cooling process), and iii) initial vapor deposition at 160 K and gradual warming to 190 K (warming process). The temperature dependence of k_{des} was studied for all types of experiments. The behavior of k_{des} may be divided in three temperature regimes: (I) between 160 - 180 K, where desorption from solid butanol shows an activation energy E_a = 0.08 eV, (II) between 180-190 K, which includes the bulk melting point of n-butanol of 184.5 K, where the desorption rates undergo a gradual decrease with temperature that depends on the preparation method, and (III) above 190 K where water is rapidly lost by rapid diffusion into the butanol bulk and no trapping-desorption is observed. The data obtained with freshly prepared butanol interfaces are identical to those obtained with warming over the entire temperature range. On the other hand, the data obtained by cooling do not follow this behavior, especially in regime I, indicating the formation of supercooled liquid butanol layers during cooling. The crystallization or relaxation of supercooled liquid butanol was also investigated at 170 K, by performing experiments with films initially prepared at 190 K and subsequently supercooled to 170 K. The observed water desorption rate was constant for a period of 2 hours under these conditions indicating that n-butanol either remains as a supercooled liquid over longer times or that a polycrystalline phase with similar properties form.

DISCUSSION AND CONCLUSIONS

We have determined the water desorption rate on both liquid and solid n-butanol in the temperature range from 160 to 200 K. We conclude that water trap and rapidly desorb from solid butanol below 180 K, and that water is rapidly lost by diffusion into the bulk liquid butanol above 190 K. The most intriguing finding is the gradual change in water-butanol interactions around the 184.5 K melting temperature. The water residence time increases rapidly above 180 K suggesting that a liquid-like surface layer is formed below the melting temperature; a phenomenon known as surface melting and observed for many solids including water ice. Between 184.5 and 190 K, the surface remains more structured than the liquid bulk below. The crystallization of the surface layer has previously been observed for long-chain alcohols and alkenes (Sloutskin, Bain et al. 2005) and this unusual phenomenon has been termed surface freezing. We conclude that the short-chain n-butanol undergo both surface melting and surface freezing, and the transition from a solid to a liquid surface layer is a gradual process that takes place over 10 degrees, in sharp contrast to the

bulk transition at the melting point. This study illustrates the potential of the EMB method for molecular-level studies of organic surfaces of relevance to atmospheric processes.

ACKNOWLEDGEMENTS

REFERENCES

Kong, X., P. U. Andersson, et al. (2011). Environmental Molecular Beam Studies of Ice Surface Processes. Physics and Chemistry of Ice 2010. Y. Furukawa, Sazaki, G., Uchida, T., Watanabe, N., Eds., Hokkaido University Press: Sapporo, Japan, 2011**:** 79-88.

Kong, X., P. U. Andersson, et al. (2012). "Ice Formation via Deposition Mode Nucleation on Bare and Alcohol-Covered Graphite Surfaces." The Journal of Physical Chemistry C **116**(16): 8964-8974.

Sloutskin, E., C. D. Bain, et al. (2005). "Surface freezing of chain molecules at the liquid-liquid and liquid-air interfaces." Faraday Discussions **129**: 339-352.

Thomson, E. S., X. Kong, et al. (2011). "Collision Dynamics and Solvation of Water Molecules in a Liquid Methanol Film." The Journal of Physical Chemistry Letters **2**(17): 2174-2178.

THE ANALYSIS OF SIZE-SEGREGATED CLOUD CONDENSATION NUCLEI COUNTER (CCNC) DATA FROM SMEAR II AND ITS IMPLICATIONS FOR AEROSOL-CLOUD RELATIONS

M. PARAMONOV[1], T. PETÄJÄ[1], P.P. AALTO[1], M. DAL MASO[1], N. PRISLE[1], V.-M. KERMINEN[1] and M. KULMALA[1]

[1]Department of Physics, University of Helsinki, P.O. Box 64, FI-00014, Helsinki, Finland.

Keywords: CCN, aerosol, cloud, critical diameter, hygroscopicity.

INTRODUCTION

Aerosol particles are omnipresent in the atmosphere, and besides directly influencing the radiative balance of the Earth, they play a crucial role in cloud formation (Stevens and Feingold, 2009). Through a variety of microphysical processes aerosol particles influence the albedo, lifetime and precipitation patterns of clouds in what is known as indirect effects of aerosols on climate (Forster *et al*., 2007). The ability of aerosol particles to act as cloud condensation nuclei (CCN) is strongly linked to their physical and chemical properties, with the most important parameters being CCN number concentration, aerosol critical diameter D_c and hygroscopicity parameter κ (Seinfeld and Pandis, 2006).

METHODS

CCNC measurements have been conducted continuously at the SMEAR II (Station for Measuring Ecosystem-Atmosphere Relations) in Hyytiälä Forestry Field Station in Finland since June 2008, and they form a part of the comprehensive network of aerosol- and meteorology-related measurements in Southern Finland (Hari and Kulmala, 2005). The station (61° 50' 50.685"N, 24° 17' 41.206"E, 179 m a.m.s.l.) is located 220 km north-west of Helsinki on a flat terrain surrounded by a Scots Pine stand, and is, therefore, well representative of the boreal environment. The CCNC in question is a diffusion-type CCN counter, including a differential mobility analyzer (DMA), condensation particle counter (CPC), optical particle counter (OPC) and a saturator unit. Both non-size-segregated and size-segregated measurements are performed by the instrument, with the latter having started in February 2009 with an introduction of a DMA into the system. CCN concentrations are measured across 30 size channels, with particle diameters ranging from 20 to 300 nm for supersaturation levels of 0.1%, 0.2%, 0.4%, 0.6% and 1%. From July 2010 until May 2011 the instrument was operating at levels of SS different to those of factory calibration mentioned above, namely 0.0859%, 0.216%, 0.478%, 0.74% and 1.26%. The measurement setup allows for a direct determination of critical diameter D_c and the hygroscopicity parameter κ. The dataset consisted of data collected by CCNC from February 2009 up to April 2012.

Activated fractions A were calculated for each size channel in each spectrum by dividing the number concentration of CCN by the corresponding number concentration of CN. Each CCN efficiency spectrum was then fitted with a function proposed by Rose *et al*. (2008) in the form of

$$A = a\left(1 + \mathrm{erf}\left(\frac{D-D_a}{\sigma\sqrt{2}}\right)\right) \tag{1},$$

where a is half the maximum A for each spectrum, *erf* is error function, D is particle diameter, D_a is the particle diameter at $A = a$ and σ is the standard deviation of the cumulative Gaussian distribution function. In the function above the fit parameter D_a is the critical diameter of dry aerosol particles D_c, which in this study is defined as the diameter at which half of the incoming particles are activated at a certain level of supersaturation. The original fitting method was carried out as per Rose *et al*. (2008), in which A values were normalized to unity by multiplying every A in the CCN efficiency spectrum with $0.5/a$, and D_a and σ

were the fit parameters in the function. Since ambient aerosol is often externally mixed, any given CCN efficiency spectrum does not necessarily level out at the activated fraction $A=1$; this, in some cases, led to an inappropriate fit of the function to the data and the overestimation of D_c for all levels of SS. Therefore, another method was used, in which the observed activated fractions A are used (no normalization) and the value of a in Eq. 1 is also a fit parameter together with D_a and σ. Hereafter, the two methods are referred to as old and new methods.

Hygroscopicity parameter κ was then calculated for each pair of critical diameters and levels of SS using the following equation from Rose et $al.$ (2008):

$$s = \frac{D_{wet}^3 - D_s^3}{D_{wet}^3 - D_s^3(1-\kappa)} \exp\left(\frac{4\sigma_{sol}M_w}{RT\rho_w D_{wet}}\right) \tag{2}$$

where s is the water vapour saturation ratio, D_s is the dry particle diameter, substituted with D_c, D_{wet} is the droplet diameter, σ_{sol} is the surface tension of condensing solution (taken that of pure water), M_w is the molar mass of water, R is the universal gas constant, T is the absolute temperature, and ρ_w is the density of water. κ values were determined by varying κ and D_{wet} so that s is equal to the prescribed supersaturation and to the maximum of the Köhler model curve of CCN activation.

Critical diameters were calculated using both old and new methods, and hygroscopicity parameters κ were calculated for both sets of critical diameters (both also referred to hereafter as old and new).

RESULTS

As mentioned previously, the old method of calculating D_c produced consistently higher values than the new method; this was true for all SS levels (Table 1). Normalizing A to unity forced the function to level out at $A=1$, which in reality may not always be the case. In many instances, due to the aerosol being externally mixed, even the larger particles did not all activate completely and the observed A values reached a maximum of less than 1, e.g., 0.9 (Fig. 1).

Table 1. Critical diameter D_c from two methods at different supersaturations.

SS (%)	Old D_c	New D_c
0,0859	189,66	180,35
0,1	177,30	155,81
0,2	121,08	97,71
0,216	118,37	97,20
0,4	96,12	74,79
0,478	87,81	71,22
0,6	82,13	61,54
0,74	72,70	56,48
1	68,16	45,73
1,26	57,96	40,81

The old method was particularly inappropriate for higher SS levels due to a large scatter of A values. The new method produced the best fitting to the data, as discovered by the analysis of root mean square error (RMSE). However, it did not fit correctly in some cases of lowest SS, where the observed A reach their maximum at the largest sizes, and, therefore, no upper plateau existed. Since a was fit parameter in the new method, the function did not, as such, have an upper limit. Therefore, in cases described above, the function produced very high D_c values (although the RMSE was still better).
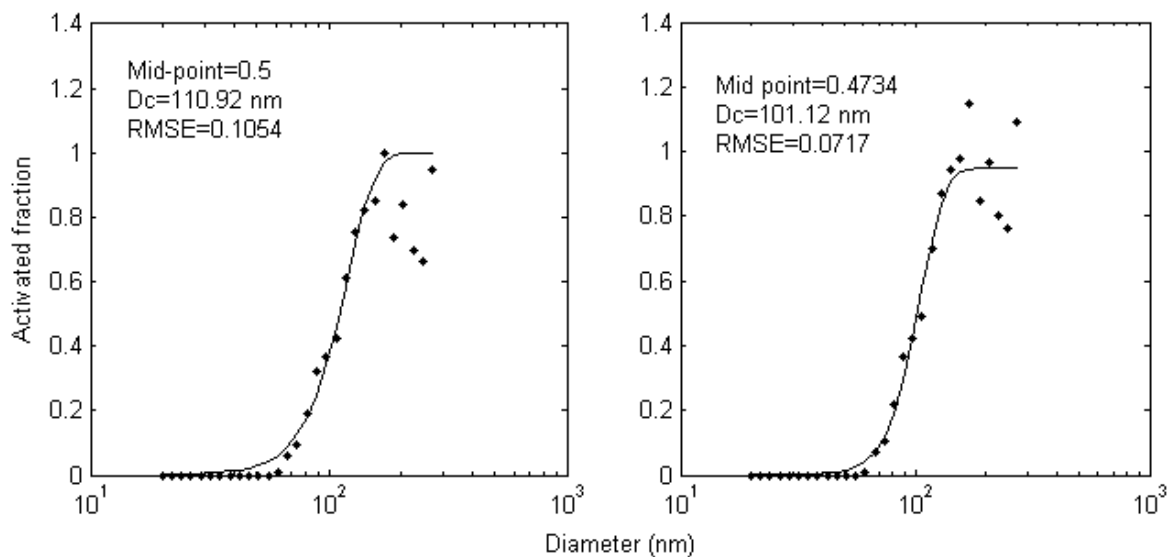
Figure 1. Sample CCN efficiency spectrum and two ways to determine D_c (left panel - old method, right panel - new method).

These two main differences of old and new fitting methods are clearly seen in Figure 2. The analysis of monthly variation of critical diameters clearly showed the annual trend for D_c at lowest SS (largest particles) (Figure 3). With a clear minimum at the end of winter, critical diameters increase to reach their maximum in late summer. This annual trend indicates that a particle of the same diameter is more hygroscopic in the winter than in the summer. This will later be shown in the monthly variation of κ. No diurnal variation of D_c was found.
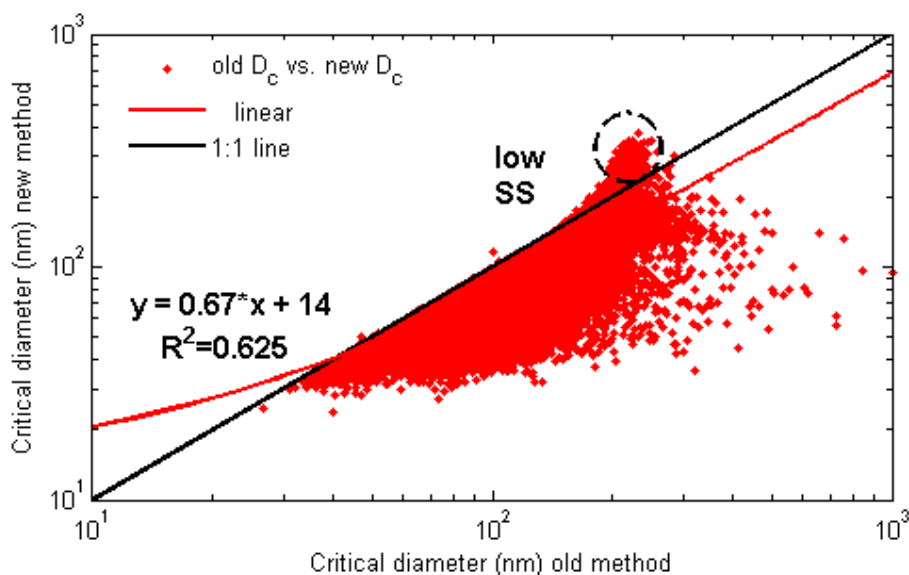
Figure 2. Critical diameters D_c from two methods.

An overall average κ for aerosol particles at SMEAR II was determined to be 0.17 and 0.30 for old and new methods, respectively, clearly indicating the presence of organic species within the particles. The old method produced a similar value as was reported by Sihto *et al*. (2010) for the same location; both of these values fall within the range of 0.27±0.21 reported by Pringle *et al*. (2010) for continental aerosol. While

513

the old method and the results by Sihto *et al.* (2010) indicate that aerosol particles in Hyytiälä are fairly non-hygroscopic, the new method, if considered appropriate, points to a higher hygroscopicity of aerosol particles in boreal environment than previously thought. The monthly variation of κ from old and new methods for two levels of SS points to the hygroscopicity of particles being largest in February and smallest in July-August, corresponding well with the observed monthly variation of D_c. The annual trend in D_c and κ is mostly pronounced for larger particles, indicating that over the course of the year the chemical composition of smaller particles remains the same, while larger particles exhibit changes in their chemical composition. Considering that typical levels of supersaturation inside the cloud are small (~0.1%) (Pruppacher and Klett, 1996) and, therefore, particles that activate as cloud droplets are the larger ones (>150 nm), the variation in their chemical composition throughout the year plays a crucial role in cloud formation and determination of their exact hygroscopicity becomes an important task. No diurnal variation of κ was found.
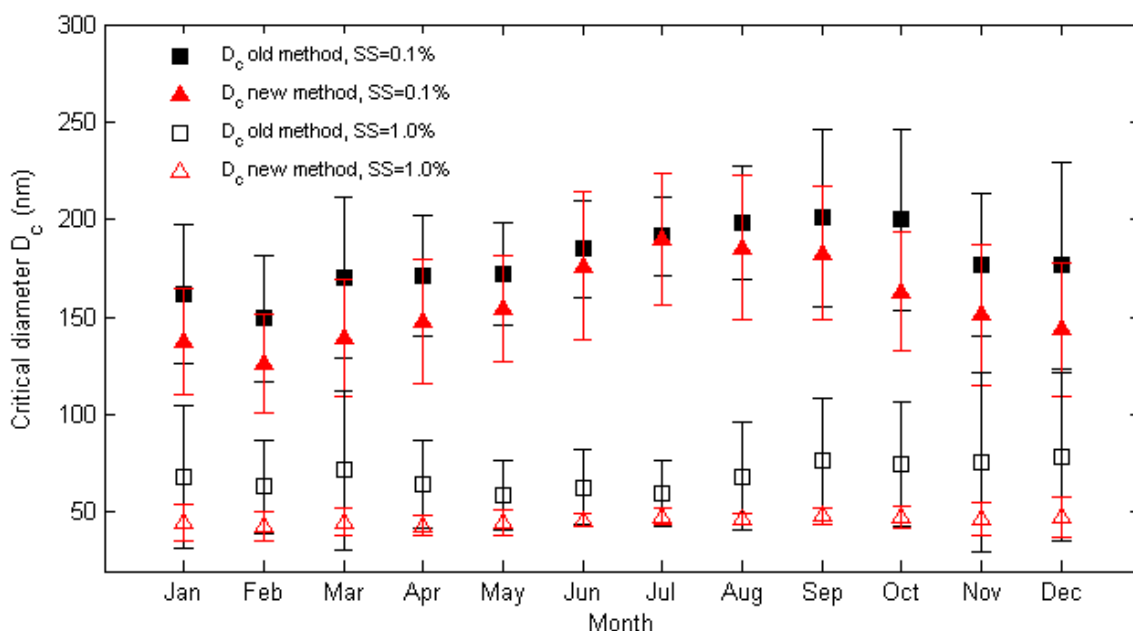
Figure 3. Monthly variation of differently derived D_c for two SS levels.

Particle critical diameters and their hygroscopicity were then examined with respect to potential particle sources. The analysis of corresponding black carbon BC concentrations revealed that κ is not affected by the combustion sources; this was the case for the whole dataset, as well as for separate seasons. It was also seen that κ does not have any dependence on the wind direction, indicating that long range transport does not affect the hygroscopicity of CCN-size aerosol. κ is likely determined by regional sources.

Since nucleation is often cited as one of the sources of CCN in the atmosphere (Kerminen *et al.*, 2012, accepted for publication in ACPD), it was attempted to see the effect of nucleation on κ. While κ for particles of all sizes was lower during event days, this trend was not significant. The diurnal behaviour of κ during event and non-event days also revealed no significant difference. It is hypothesized that nucleation affects particle hygroscopicity several hours, sometimes days, later, when nucleated particles reach relevant CCN sizes. However, since this time of growth to CCN sizes varies greatly, simply examining event and non-event days becomes implausible. A more rigorous analysis is required to determine the effect of nucleation on κ.

REFERENCES

Forster, P., V. Ramaswamy, P. Artaxo, T. Berntsen, R. Betts, D.W. Fahey, J. Haywood, J. Lean, D.C. Lowe, G. Myhre, J. Nganga, R. Prinn, G. Raga, M. Schulz and R. Van Dorland (2007): Changes in Atmospheric Constituents and in Radiative Forcing. *In: Climate Change 2007: The Physical Science Basis. Contribution of Working Group I to the Fourth Assessment Report of the Intergovernmental Panel on Climate Change* [Solomon, S., D. Qin, M. Manning, Z. Chen, M. Marquis, K.B. Averyt, M. Tignor and H.L. Miller (eds.)]. Cambridge University Press, Cambridge, United Kingdom and New York, NY, USA.

Hari, P. and M. Kulmala (2005). Station for measuring ecosystem-atmosphere relations. *Boreal Env. Res.* **10**, 315–322.

Pringle, K.J., H. Tost, A. Pozzer, U. Pöschl and J. Lelieveld (2010). Global distribution of the effective aerosol hygroscopicity parameter for CCN activation. *Atmos. Chem. Phys.Discuss.* **10**, 6301 6339.

Pruppacher, H.R. and J.D. Klett (1996). *Microphysics of Clouds and Precipitation* (2nd edition). (Springer, New York, USA).

Rose, D., S.S. Gunthe, E. Mikhailov, G.P. Frank, U. Dusek, M.O. Andreae and U. Pöschl (2008). Calibration and measurement uncertainties of a continuous-flow cloud condensation nuclei counter (DMT-CCNC): CCN activation of ammonium sulfate and sodium chloride aerosol particles in theory and experiment. *Atmos. Chem. Phys.* **8**, 1153–1179.

Seinfeld, J.H. and S.N. Pandis (2006). *Atmospheric Chemistry and Physics. from air pollution to climate change* (2nd edition). (John Wiley & Sons, New York, USA).

Sihto, S.-L., J. Mikkilä, J. Vanhanen, M. Ehn, L. Liao, K. Lehtipalo, P.P. Aalto, J. Duplissy, T. Petäjä, V.-M. Kerminen, M. Boy and M. Kulmala (2010). Seasonal variation of CCN concentrations and aerosol activation properties in boreal forest. *Atmos. Chem. Phys*. *Discuss.* **10**, 28231–28272.

Stevens, B. and G. Feingold (2009). Untangling aerosol effects on clouds and precipitation in a buffered system. *Nature* **461**, 607–613.

A CORRELATION ANALYSIS OF VOLATILE ORGANIC COMPOUND MEASUREMENTS DURING YEARS 2006-2008 IN SMEAR II

J. PATOKOSKI[1], R. TAIPALE[1], M.K. KAJOS[1], P. RANTALA[1], V.KARSISTO[1], J. AALTO[2], J. BÄCK[2], P. KERONEN, T.M. RUUSKANEN[1], T. PETÄJÄ and J.RINNE[1]

[1]Department of Physics, P.O. Box 64, University of Helsinki, Finland
[2]Department of Forest Ecology, University of Helsinki, Finland

Keywords: VOLATILE ORGANIC COMPOUNDS, LONG TERM MEASUREMENTS, RURAL SITE

INTRODUCTION

Volatile Organic Compounds (VOCs) have an important role in atmospheric chemistry because they react in the air with oxidants (O_3 and NO_3) and OH radicals and produce new oxidation products, which take part to chemical reactions in the atmosphere (Atkinson and Arey, 2003). The VOCs are also known to participate in the tropospheric ozone formation and destruction processes and to aerosol particle growth (Chameides, 1992; Tunved et al., 2006). Emissions of biogenic VOCs in a global scale are estimated to be an order of magnitude higher than anthropogenic ones (Guenther et al., 1995). In Finland the biogenic emissions are estimated to be two times higher than the anthropogenic ones (Lindfors et al., 2000).

In this study we aim to resolve connections between the VOC mixing ratios and other trace gases as well as meteorological variables as well as their long term trends. The volume mixing ratios (VMRs) of ambient VOCs were measured with a proton transfer reaction - mass spectrometer (PTR-MS, Ionicon Analytik GmbH) at SMEAR II (Station for Measuring Ecosystem - Atmosphere Relations, Hari and Kulmala, 2005), in Hyytiälä, Finland during years 2006-2008. More closely, the aim of our research was to study correlations and connection between certain VOCs, gases (NO_x, O_3, SO_2 and CO), temperature and radiation.

METHODS

SMEAR II is a rural site and it is located in Hyytiälä in Southern Finland ((61°51´N, 24°17´E, 180 m a.s.l.) 220 km from Helsinki. Tampere is a largest city near SMEAR II and its population is about 200 000. There are continuous long term measurements of trace gases, aerosol particles and micrometeorology(Hari and Kulmala, 2005). The VMRs of the VOCs were measured from 14 m height which is inside the canopy. The measurement set up, calibration procedure and volume mixing ratio calculations were presented in detail in Taipale et al. (2008). In this study a set of selected VOCs (methanol (M33), acetaldehyde (M45), acetone (M59), isoprene (M69), benzene (M79) and monoterpenes (137)) are discussed. In addition to the VOC data, we use data on mixing ratios of NO_x, O_3, SO_2, CO and temperature and photosynthetically active radiation (PAR) intensity.The trace gas data and temperature were measured at 16.8 m height level and the PAR data at 74 m (Hari et al., 2005).

PRELIMINARY RESULTS AND DISCUSSION

Time series of selected VOCs are presented in Figure 1.The VMRs of biogenic influenced VOCs such as methanol, isoprene and monoterpenes are clearly higher during summer than during winter. The compounds that are typically associated with anthropogenic emissions, such as benzene, had a lower seasonal variation. Comparing the summers with each other it seems that the VMRs were the highest during summer 2006. The winters resembled each other in terms of VOC mixing ratios. In Figure 2 we present time series of NO_x, O_3, SO_2, CO, temperature and PAR. Monoterpene signal correlated with a correlation coefficient between 0.44-0.53 with methanol, acetone, isoprene and acetaldehyde mixing ratios

tentatively indicating a common biogenic source. Benzene had only very low correlation coefficient of 0.02 with the monoterpenes, an anticorrelation (r = -0.33) with temperature, and a strong positive correlation coefficients (r = 0.89) with carbon monoxide and NO_x (r = 0.53). This indicates that high benzene mixing ratios were associated with trace pollutants with an anthropogenic origin.
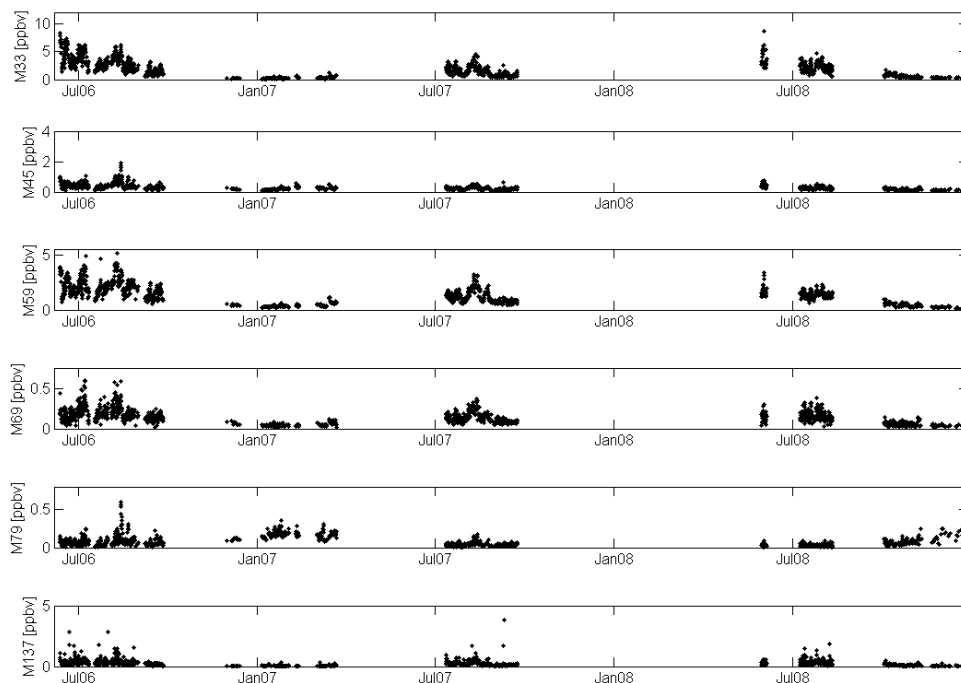
Figure 1. Time series of selected VOCs: methanol (M33), acetaldehyde (M45), acetone (M59), isoprene (M69), benzene (M79) and monoterpenes (M137) during years 2006-2008.
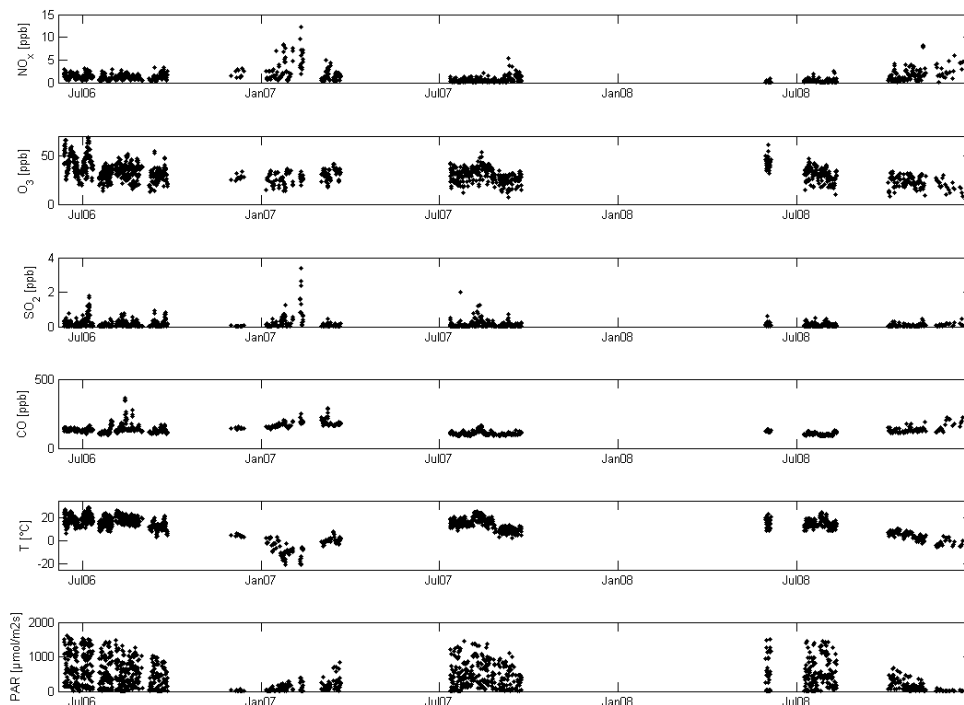
Figure 2. Time series of selected gases (O3, NOx, SO2 and CO), temperature and PAR during years 2006-2008.

REFERENCES

Chameides, W. L., Fehsenfeld, F., Rodgers, M. O., Cardelino, C., Martinez, J., Parrish, D., Lonneman, W., Lawson, D. R., Rasmussen, R. A., Zimmerman, P., Greenberg, J., Mlddleton, P., Wang, T., (1992). Ozone Precursor Relationships in the Ambient Atmosphere. J Geophys Res, 97, 6037-6055.

Guenther, A., Hewitt, C. N., Erickson, D., Fall, R., Geron, C., Graedel, T., Harley, P., Klinger, L., Lerdau, M., McKay, W. A., Pierce, T., Scholes, B., Steinbrecher, R., Tallamraju, R., Taylor, J., Zimmerman, P., (1995). A global model of natural volatile organic compound emissions. J Geophys Res, 100, 8873-8892.

Hari, P., and Kulmala, M. (2005). Station for Measuring Ecosystem–Atmosphere Relations(SMEAR II), Boreal Environ. Res.,10, 315–322.

Lindfors, V., Laurila, T., Hakola, H., Steinbrecher, R., Rinne, J., (2000). Modeling speciated terpenoid emissions from the European boreal forest. Atmos Environ, 34, 4983–4996.

Taipale, R., Ruuskanen, T. M., Rinne, J., Kajos, M. K., Hakola, H., Pohja, T., and Kulmala, M.: (2008). Technical Note: Quantitative long-term measurements of VOC concentrations by PTR-MS-measurement, calibration and volume mixing ratio calculation methods, ACP, 8, 6681-6698.

Tunved, P., Hansson, H.-C., Kerminen, V.-M., Ström, J., Dal Maso, M., Lihavainen, H., Viisanen, Y., Aalto, P. P., Komppula, M., Kulmala, M., (2006). High Natural Aerosol Loading over Boreal Forests. Science 312, 261-263.

INFLUENCE OF ORGANICS ON ICE FORMATION VIA DEPOSITION FREEZING

J.B.C PETTERSSON[1], X. KONG[1], N. MARKOVIĆ[2], P. PAPAGIANNAKOPOULOS [1,3] and E.S. THOMSON [1]

[1] Department of Chemistry and Molecular Biology, Atmospheric Science, University of Gothenburg, SE-412 96, Gothenburg, Sweden.

[2]Department of Chemical and Biological Engineering, Physical Chemistry, Chalmers University of Technology, SE-412 96, Gothenburg, Sweden.

[3] Laboratory of Photochemistry and Kinetics, Department of Chemistry, University of Crete, 71003 Heraklion, Crete, Greece.

INTRODUCTION

Volatile organic compounds (VOCs) are ubiquitous in the atmosphere and may modify the adsorption and desorption kinetics of coated atmospheric aerosols. For clouds such effects may result in changes in ice nucleation efficiency and rate, and could also affect ice growth morphology. In turn, changes in the physical properties of the ice in ice clouds will affect the cloud lifetime and its radiative properties, with implications for water cycling and global climate. Here we report on ice formation by water deposition on both organic and inorganic carbon substrates with a range of hydroscopic behavior. Ice nucleation and growth morphology are probed using helium and light scattering techniques at temperatures up to 213 K.

METHODS

Experiments were preformed using an environmental molecular beam (EMB) apparatus (Kong et al., 2011; Kong et al., 2012) that focuses a low density beam of molecules onto a graphite surface. The surface is housed within an environmental chamber that allows finite vapor pressures ($\leq 10^{-2}$ mbar) to be sustained. Thus in addition to the graphite, organic layers in dynamic equilibrium with their vapor can be condensed and used as ice nucleating substrates. The technique differs critically from other UHV systems in that it allows surfaces under atmospherically relevant temperatures and pressures to be directly probed.

Surface coverage and nucleation on the substrate is monitored with a beam of He atoms which is efficiently attenuated by ad-layers. Ice nucleation on layers of organic substrate is directly monitored using the surface reflections of a 670 nm laser. A surface roughness model is used to estimate surface morphology based on the attenuation of the scattered light signal (Kong et al., 2012).

The molecular flux and thus water vapor pressure within the chamber is measured using a rotatable quadrupole mass spectrometer (QMS). This allows the supersaturation required for ice nucleation to be determined as a function of temperature and surface properties.

RESULTS AND DISCUSSION

We observe that the nucleation of ice on a bare graphite crystal becomes increasingly inefficient as the surface temperature decreases from 200 to 155 K. The supersaturation over ice required for nucleation to occur increases from 130% at 200 K to 850% at 155 K. Adsorption of a monolayer of methanol on the graphite surface changes it from hydrophobic to highly hydrophilic. The methanol molecules provide sites for efficient hydrogen-bonding of water molecules, which stabilizes water on the surface compared to the bare graphite. Ice nucleation on the hydrophilic surface takes place at a lower supersaturation than on the hydrophobic surface, and the adsorbate thus influences the absolute nucleation rate at a given temperature. The supersaturation required for nucleation increases rapidly with decreasing temperature in the range 175-190 K, and the overall trend with temperature is similar for the bare and methanol-covered surfaces. Adsorption of a butanol monolayer results in an ice nucleation efficiency intermediate between the other two systems. Butanol forms a highly stable solid layer on graphite and water does not appear to efficiently wet the butanol layer. Again, the trend with temperature is similar to the other investigated systems. We conclude that the hydrophilicity of the surface influences the absolute nucleation rate, but the overall trend with temperature is qualitatively similar for the different systems. The results are also consistent with the limited data from the literature in the 150-200 K range. We conclude that the rapidly increasing supersaturation required for ice nucleation with decreasing temperature is qualitatively reproduced by classical nucleation theory. The implications for the description of heterogeneous ice nucleation in the upper troposphere and lower stratosphere are discussed.

ACKNOWLEDGEMENTS

REFERENCES

Kong, X., Andersson, P. U., Marković, N., and Pettersson, J. B. C. (2011). Environmental molecular beam studies of ice surface processes. In Furukawa, Y., Sazaki, G., Uchida, T., and N, W., editors, *Physics and Chemistry of Ice 2010*, pages 79–88, Sapporo, Japan. Hokkaido University Press.

Kong, X., Andersson, P. U., Thomson, E. S., and Pettersson, J. B. C. (2012). Ice formation via deposition mode nucleation on bare and alcohol-covered graphite surfaces. *The Journal of Physical Chemistry C*, 116(16):8964–8974.

THE EFFECT OF TEMPERATURE AND OXYGEN AVAILABILITY ON N_2 AND N_2O EMISSIONS FROM FORESTRY DRAINED BOREAL PEAT SOILS

M. PIHLATIE[1, 2], I. HONGISTO[1, 2], M. DANNEMNANN[2], G. WILLIBALD[2], R. GASCHE[2], and K. BUTTERBACH-BAHL[2]

[1]Department of Physics, University of Helsinki, P.O. Box 48, FI-00014 University of Helsinki, Finland.

[2]Karlsruhe Institute of Technology (KIT), Institute for Meteorology and Climate Research (IMK), Atmospheric Environmental Research (IMK-IFU), 82467 Garmisch-Partenkirchen Germany.

Keywords: DENITRIFICATION, PEAT SOILS, NITROGEN LOSSES.

INTRODUCTION

Emissions of molecular nitrogen (N_2) from terrestrial ecosystems have been identified to represent the largest uncertainty in the nitrogen cycle at all scales (Galloway *et al.*, 2004; Groffman *et al.*, 2006). This is largely due to difficulties in measuring the exchange of N_2 in the large background of atmospheric N_2. Peat soils contain large pools of carbon and nitrogen, and hence have a high potential of losing carbon and nitrogen to the atmosphere and water bodies. In Finland, 70% of the natural peatlands have been drained for forestry and agricultural use since the 1920s (Paavilainen and Päivänen, 1995; Joosten and Claarke, 2002). In drained peatland forests the fertility of the original peatland determines the rate of nutrient release into the soil, and gaseous emissions to the atmosphere. The emissions of nitrous oxide (N_2O) from fertile drained peatland forests can be very large (von Arnold *et al.*, 2005), however, information on N_2 emissions is practically non-existent due to the methodological difficulties.

Both N_2O and N_2 are by-products of microbial denitrification process. N_2 is produced in strictly anaerobic conditions from N_2O by the enzyme N_2O reductase. This enzyme is sensitive to oxygen and the reduction can only take place in fully oxygen deprived systems. Water table fluctuations and high decomposition activity in drained peat soils may lead to the creation of anaerobic conditions, where the most abundant product of denitrification is N_2. Hence, drained peatland soils have high potential of losing nitrogen in the form of N_2, however, there is no information available on the rates of N_2 emissions or the relations of N_2 to N_2O in these soils. Our aim was to quantify the N_2 and N_2O production rates from different drained peat soils under varying temperature and oxygen conditions.

METHODS

Soil samples were collected from two drained peatland forests differing in the fertility status and located in southern Finland, boreal zone. The site Kalevansuo is a nutrient-poor ombrotrophic dwarf-shrub pine bog and the Lettosuo site is a nutrient-rich myrtillus type peatland forest. Both measurement sites are part of measurement networks related to the measurements of greenhouse gas fluxes from drained peatland forests in Finland (GHG-Europe, Fluxnet, NitroEurope-IP).

Soil samples were collected in to stainless-steel soil cores in August 2010 and May 2011. The samples were shipped in cool-boxes to IMK-IFU, Garmisch-Partenkirchen, Germany, and stored at 4 °C until further analysis. Emissions of N_2 to N_2O from intact soil cores were measured using the helium gas flow soil core method described in detail by Dannemann *et al.* (2011), Butterbach-Bahl *et al.* (2002) and Dannenmann *et al.* (2008). In this method the soil cores are incubated in a N_2-reduced helium-oxygen atmosphere, in which the production or consumption of N_2 and N_2O are automatically measured. In the beginning of a measurement cycle the soil cores were flushed for 24-48 hours with He through the soil.

This was followed by an automatic gas sampling from the soil core headspace during the following 8 hours. The N_2 and N_2O as well as CO_2 concentrations in the headspace above the soil cores were analysed by gas chromatography.

In the Experiment 1, the contribution of different soil layers to the N_2 and N_2O production or consumption was studied. Soil samples collected from three peat layers were incubated at 15°C first under aerobic (20% oxygen, 80% Helium) and then under anaerobic (0% O_2, 100% He) conditions, and the N_2 and N_2O production or consumption were measured. The experiment 2 followed a schedule in which first soils were incubated in cold (2°C) aerobic (20% O_2, 80% He) until the N_2 and N_2O production or consumption was stabilized. Then the system was changed to a cold (2°C) anaerobic (0% O_2, 100% He), again until a stabilization was reached. Then the temperature was increased to 15°C under anaerobic conditions (warm anaerobic), and the N_2, N_2O and CO_2 dynamics were followed as long as the system was stabilized. Fluxes of N_2, N_2O and CO_2 were calculated by fitting a linear regression to the 6-8 concentration measurements in the headspace as described by Butterbach-Bahl *et al.* (2002). Fluxes were further presented in soil dry weight basis, after determination of the soil dry weight of the incubated soils.

In order to compare the gaseous dynamics to soil parameters, soil mineral N, microbial biomass N, dissolved organic N and C and pH were analyzed from the soil samples according to Dannenmann *et al.* (2010).

RESULTS

The top-most peat layer from both Kalevansuo and Lettosuo was the most active in N_2 and N_2O production or consumption. N_2 production and N_2O production / consumption in the deeper peat layers (10-15 cm and 30-35 cm) depth showed negligible emission rates at Kalevansuo and Lettosuo.

The two sites Kalevansuo and Lettosuo differed markedly both in N_2 and N_2O dynamics under varying temperature and oxygen availability. The nutrient-poor Kalevansuo had significantly lower emissions of N_2 and N_2O than the nutrient-rich Lettosuo. The N_2 dynamics in the nutrient-poor Kalevansuo peat soil did not respond to the changes in oxygen availability and temperature, while a small increase in the consumption of N_2O was observed in the anaerobic treatments (Table 1). In the nutrient-rich Lettosuo a change from the cold aerobic conditions to cold anaerobic induced marked N_2 and N_2O production. Furthermore, a change from a cold anaerobic (2°C) to a warm anaerobic (15°C) incubation stimulated N_2 emission, whereas, there was a clear switch from N_2O production towards N_2O consumption.

Site	Treatment	mean N_2 flux [min-max]	mean N_2O flux [min-max]
Kalevansuo	2°C, aerobic	7.5 [4.9-10.1]	-0.01 [-0.02-0.00)
	2°C, anaerobic	7.4 [4.5-11.0]	-0.1 [-0.4- -0.01]
	15°C, anaerobic	6.7 [3.0-9.7]	-0.2 [-0.6-0.00]
Lettosuo	2°C, aerobic	4.3 [2.4-5.5]	0.00 [-0.04-0.1]
	2°C, anaerobic	14.7 [7.1-29.8]	3.3 [-0.1-7.2]
	15°C, anaerobic	31.5 [5.6-123]	0.8 [-0.2-10.1]

Table 1. Mean N_2 and N_2O fluxes (μg N kg^{-1} SDW h^{-1}) and the flux range during different temperature and oxygen availability treatments at the Kalevansuo and Lettosuo peatland forests.

CONCLUSIONS

Nutrient status of the drained peatland forest determines the potential for N_2 and N_2O emissions. The N_2 and N_2O emissions in the nutrient-rich Lettosuo in this study responded markedly to anaerobicity and temperature, whereas both N_2 and N_2O production were small in the nutrient-poor peatland forest Kalevansuo, even under changing temperature and oxygen availability. We show that nutrient-rich

peatland forest may lose significant amounts of nitrogen into the atmosphere under conditions favourable for denitrification.

ACKNOWLEDGEMENTS

REFERENCES

Butterbach-Bahl, K., G. Willibald, H. Papen (2002). Soil core method for direct simultaneous determination of N_2 and N_2O emissions from forest soils. *Plant Soil* **240**, 105–111.

Dannenmann, M., K. Butterbach-Bahl, R. Gasche, G. Willibald, H. Papen (2008). Dinitrogen emissions and the N_2: N_2O emission ratio of a Rendzic Leptosol as influenced by pH and forest thinning. *Soil Biol. Biochem.* **40**, 2317–2323.

Dannenmann, M., G. Willibald, S. Sippel, K. Butterbach-Bahl (2011). Nitrogen dynamics at undisturbed and burned Mediterranean shrublands of Salento Peninsula, Southern Italy. *Plant Soil*. **343**, 5–15.

Galloway, J.N., F.J. Dentner, D.G. Capone, E.W. Boyer, R.W. Howarth, S.P. Seitzinger, G.P. Asner, C.C. Cleveland, P.A. Green, E.A. Holland, D.M. Karl, A.F. Michaels, J.H. Porter, A.R. Townsend, C.J. Vöösmarty (2004) Nitrogen cycles: past, present and future. *Biogeochemistry* **70**, 153–226

Groffman, P.M., M.A. Altabet, J.K. Böhlke, K. Butterbach-Bahl, M.B. David, M.K. Firestone, A.E. Giblin, T.M. Kana, L.P. Nielsen, M.A. Voytek (2006) Methods for measuring denitrification: diverse approaches to a difficult problem. *Ecol. Appl*. **16**, 2057–2063.

Joosten, H. and D. Claarke (2002). *Wise Use of Mires and Peatland*, (International Mire Conservation Group, Totnes., ISBN 951-97744-8-3).

Paavilainen, E. and J. Päivänen (1995). *Peatland Forestry – Ecology and Priciples*, (Springer, Berlin, 248 p.).

von Arnold, K., P. Weslien, M. Nilson, B.H. Svensson, and L. Klemedtsson (2005). Fluxes CO_2, CH_4 and N_2O from drained coniferous forests on organic soils, *Forest Ecol. Manag.,* **210**, 239–254.

ON THE INTERPRETATION OF SATELLITE CHLOROPHYLL FLUORESCENCE DATA: A THEORETICAL FRAMEWORK FOR THE ANALYSIS OF SEASONAL VARIATIONS IN LEAF-LEVEL CHLOROPHYLL FLUORESCENCE CONSIDERING BOTH PHOTOSYSTEMS

A.   PORCAR-CASTELL

Department of Forest Sciences , University of Helsinki, P.O.Box 27, 00014 FINLAND

INTRODUCTION

Terrestrial vegetation plays a crucial role in the operation of the global carbon cycle by acting as a pump that converts atmospheric carbon dioxide into biomass via the photosynthetic process. Consequently, precise and accurate quantification of ecosystem carbon fluxes is key to understand the interaction between terrestrial ecosystems and climate, and the global biogeochemistry as a whole. Carbon flux of an ecosystem can be directly measured using eddy-covariance techniques (Baldocchi *et al.,* 1988). However, logistic limitation aside, these measurements do not provide the required spatial continuity needed for upscaling ecosystem fluxes from the site to the landscape and regional levels. One indirect approach to bypass this limitation has been the use of land surface models to upscale site-level-observations (Williams *et al.,* 2009). However, current models retain a high level of uncertainty. A potential approach that has recently received very much interest is the use of remotely sensed satellite data as a direct proxy of photosynthetic performance in terrestrial ecosystems (Grace *et al.,* 2007; Hilker *et al.,* 2008). This direct approach, if proved successful, could dramatically reduce the level of uncertainty in these models since it would provide continuous spatial coverage, and near-real time data across the planet.

Two types of optical proxies linked to the regulation of photosynthesis are currently under very active scrutiny by the research community: 1) The use of the photochemical reflectance index (Gamon *et al.,* 1992), an index that is not only able to track the rapid but also the slow adjustments in leaf-level carotenoid pigments that typically take place together with the acclimation of photosynthesis (Filella *et al.* 2009; Porcar-Castell *et al.,* 2012). And 2) the use of the solar-induced chlorophyll fluorescence (SIF) emission from vegetation (Meroni *et al.,* 2009), a phenomena that is directly linked to the first steps of the photosynthetic process and therefore has the potential to provide very useful information. Both PRI and SIF have been successfully derived from currently available but non-*ad hoc* satellite platforms. For example, PRI has been retrieved using MODIS data (Drolet *et al.,* 2005), and recently global SIF has been obtained from GOSAT data (Joiner et al. 2011). These studies, together with a number of dedicated plot-level experiments provide important data towards the design and validation of future space missions, e.g. the FLEX mission currently under evaluation by the European Space Agency (Phase-A/B1).

This report presents some of the problematic behind the interpretation of leaf-level sun-induced ChlF data and suggests a tentative theoretical model that could be used as a framework to study the link between passive fluorescence data and the physiology of photosynthesis.

Since the discovery of the Kausty effect in the 30's (Kautsky and Hirsch, 1931), chlorophyll fluorescence has been intensively used to study several aspects of the organization and functioning of the light reactions of photosynthesis. The emission spectra of chlorophyll fluorescence expands from c. 660nm to 800nm and

although most of this fluorescence emanates from photosystem II (PSII), photosystem I (PSI) also contributes to the fluorescence emission in particular in the far-red regions (>700nm) (Genty *et al.,* 1990; Franck *et al.* 2002). Although the whole fluorescence spectra has been used for example in time-resolved fluorescence spectroscopy to follow the migration of excitation among different pigments within the antennae (Yamazaki *et al.* 1984), most fluorescence studies are based on data obtained with fluorometers that measure broadband fluorescence emission in a window around 690nm, or using a 700-710nm high-pass filter that integrates the far-red fluorescence. Commonly, field fluorometers use a low intensity modulated light that induces a modulated fluorescence signal which is registered by a detector (Schreiber *et al.,* 1986; Porcar-Castell *et al.,* 2008). These Pulse Amplitude Modulated (PAM) systems have allowed scientists to study the acclimation of the light reactions *in situ* since the resulting fluorescence signal does not suffer from interference caused by ambient light. In addition, in order to obtain information on the current energy partitioning at the level of photosystem between photochemical (photosynthetic electron transport), and non-photochemical (mainly thermal energy dissipation) processes, PAM fluorometers use a saturating light pulse technique that momentarily shuts down photochemistry and thus facilitates the quantification of the photochemical efficiency by comparing the fluorescence levels before (i.e. F_s, for stationary fluorescence) and after the pulse (i.e. F_m for maximal fluorescence) (Schreiber *et al.* 1986; Porcar-Castell, 2011). These type of measurements were previously done in the laboratory using chemicals (e.g. DCMU) or ultralow temperature (e.g. liquid nitrogen, 77K) to shut down photochemistry. Therefore, the modulated light combined with the saturating pulse technique have dramatically advanced the study of photosynthesis in field conditions, and the interaction between fluorescence, photosynthesis and environment as a whole.

However, because neither modulated light nor saturating pulses can be reasonably applied from a remote sensing platform (active fluorescence), passive systems that measure sun-induced fluorescence have been developed and recently tested in the field to prove the connection between this sun-induced fluorescence (SIF) and photosynthesis. The ultimate purpose is to probe and develop the required technology and knowledge to be able to derive information on photosynthetic acclimation using SIF. SIF has been recently measured within narrow solar or telluric atmosphere absorption bands (Hydrogen, Oxygen A- B-) that fall within the chlorophyll emission spectra with the help of sub-nanometer resolution spectrometers (Meroni *et al.,* 2009). However, although the linkage between active fluorescence parameters and photosynthesis is rather well understood, although questions remain open at the seasonal time-scale (Porcar-Castell, 2011), the mechanistic link between SIF and photosynthesis remains elusive.

On the first place, the absence of saturating pulse does not allow us to directly estimate the photochemical yield from the SIF signal, which calls for models that either integrate other sources of data such as the PRI (Meroni *et al.,* 2009, Porcar-Castell *et al.,* 2012), or integrate knowledge on basic molecular processes at the level of photosystem. On the second place, because SIF is often measured in the far-red region (Atmospheric Oxygen B-band absorption) where the contribution of PSI fluorescence can be very significant (e.g. 30-50%) (Genty *et al.,* 1990; Pfündel, 1998; Franck *et al.,* 2002) it is possible that the strong contribution to the measured SIF fluorescence by PSI interferes unexpectedly with our *a priori* knowledge gained from PSII fluorescence. The reason is that PSI fluorescence is expected to remain constant in response to the fast acclimation of photosynthesis, although in fact, very little is known on the seasonal changes in PSI, not to speak of its fluorescence. Overall, a new theoretical framework that encompasses both photosystems is needed to tackle these research questions.

In this report I introduce a theoretical model to interpret SIF data in terms of PSII and PSI components.

THEORETICAL MODEL

The fluorescence emanating from PSII, F(II) can be expressed following a lake model assumption where all de-exitation processes in the photosystem compete for excitation energy from a single pool as:

$$F(II) = I\,A\,\beta\,\frac{k_f}{k_f + k_{DII} + k_P + k_{II\to I}} \qquad \text{(Eq. 1)}$$

Where I is the intensity of the incident photosynthetically active photon flux (400-700nm), A is the leaf absorptance for the range 400-700nm, β is the absorption cross section of PSII (between 0 and 1, typically simplified as 0.5), k_f is the rate constant of fluorescence emission, k_{DII} is the rate constant of thermal energy dissipation in PSII that includes both the constitutive and regulated components, i.e. the latter being the diverse forms of reversible and sustained NPQ (Porcar-Castell, 2011), k_P is the rate constant of photochemistry which depends on the redox state of the primary electron acceptor pool as well as on the fraction of functional reaction centres (non photoinhibited), and finally $k_{II>I}$ is the rate constant of energy transfer from PSII to PSI (spillover). In turn the fluorescence emanating from PSI, F(I) can be expressed as:

$$F(I) = I\,A\left(\alpha + \frac{k_{II\to I}}{k_f + k_{DII} + k_P + k_{II\to I}}\right)\frac{k_f}{k_f + k_{DI}} \qquad \text{(Eq. 2)}$$

Where α is the absorption cross section of PSI (with $\alpha+\beta =1$), and k_{DI} is the rate constant of thermal energy dissipation for PSI.

Therefore, for a given wavelength, the measured fluorescence $F(\lambda)$ can be expressed as the sum of a PSII and a PSI contribution like:

$$F(\lambda) = \theta_{II}(\lambda)\,F(II) + \theta_I(\lambda)\,F(I) \qquad \text{(Eq. 3)}$$

Where θ_I and θ_{II} are wavelength-dependent photosystem contribution factors obtained experimentally (e.g. Franck *et al.* 2002), with $\theta_I + \theta_{II} =1$.

REFERENCES

Baldocchi, D.D., B.B. Hicks and T.P. Meyers (1988) Measuring biosphere atmosphere exchanges of biologically related gases with micrometeorological methods, *Ecology* **69**, 1331-1340.

Drolet, G., K. F. Huemmrich, F.G. Hall, E.M. Middleton, T.A. Black, A.G. Barr, H.A. Margolis (2005) A MODIS-derived photochemical reflectance index to detect inter-annual variations in the photosynthetic light-use efficiency of a boreal deciduous forest, *Remote Sensing of Environment,* **98**, 212-224.

Filella, I., A. Porcar-Castell, S. Munné-Bosch, J. Bäck, M.F. Garbulsky and J. Peñuelas (2009) PRI assessment of long-term changes in carotenoids/chlorophyll ratio and short-term changes in de-epoxidation state of the xanthophyll cycle. *International Journal of Remote Sensing* **30**, 4443-4455.

Franck, F., P. Juneau and R. Popovic (2002) Resolution of the Photosystem I and Photosystem II contributions to chlorophyll fluorescence of intact leaves at room temperature, *Biochimica et Biophysica Acta,* **1556**, 239-246.

Genty B., J. Wonders and N.R. Baker (1990) Non-photochemical quenching of F_o in leaves is emission wavelength dependent: consequences for quenching analysis and its interpretation, *Photosynthesis Research*, **26**, 133-139.

Grace J., C. Nichol, M. Disney, P. Lewis, T. Quaife and P. Bowyer (2007) Can we measure terrestrial photosynthesis from space directly, using spectral reflectance and fluorescence? *Global Change Biology* **13**, 1484-1497.

Hilker, T., N.C. Coops, M.A. Wulder, T.A. Black and R.D. Guy (2008) The use of remote sensing in light use efficiency based models of gross primary production: A review of current status and future requirements, *Science of the Total Environment* **404**, 411-423.

Kautsky, H. and A. Hirsch (1931) Neue Versuche zur Kohlensäureassimilation, *Naturwissenschaften,* **19**, 964-964.

Joiner, J., Y. Yoshida, A.P. Vasilkov, Y. Yoshida, L.A. Corp and E.M. Middleton (2011) First observations of global and seasonal terrestrial chlorophyll fluorescence from space, *Biogeosciences* **8**, 637-651.

Meroni M. M. Rossini, L. Guanter, L. Alonso, U. Rascher, R. Colombo, J. Moreno (2009) Remote sensing of solar-induced chlorophyll fluorescence: Review of Methods and applications. *Remote Sensing of Environment* **113**, 2037-2051.

Pfündel, E. (1998) Estimating the contribution of Photosystem I to total leaf chlorophyll fluorescence, *Photosynthesis Research,* **56**, 185-195.

Porcar-Castell, A., E. Pfündel, J.F.J. Korhonen and E. Juurola (2008) A new monitoring PAM fluorometer (*MONI-PAM*) to study the short- and long-term acclimation of photosystem II in field conditions, *Photosynthesis Research,* **96,** 173-179.

Porcar-Castell, A (2011) A high-resolution portrait of the annual dynamics of photochemical and non-photochemical quenching in needles of Pinus sylvestris, *Physoiologia Plantarum* **143**, 139-153.

Porcar-Castell, A., J.I. Garcia-Plazaola, C.J. Nichol, P. Kolari, B. Olascoaga, N. Kuusinen, B. Fernández-Marín, M. Pulkkinen, E. Juurola and E. Nikinmaa (2012) Physiology of the seasonal relationship between the photochemical reflectance index and photosynthetic light use efficiency. *Oecologia (early Online) doi:* 10.1007/s00442-012-2317-9

Schreiber U (1986) Detection of rapid induction kinetics with a new type of high-frequency modulated chlorophyll fluorometer, *Photosynthesis Research,* **9**, 261-272.

Yamazaki, I., M. Mimuro, T. Murao, I. Yamazaki, K. Yoshihara and Y. Fujita (1984) Excitation energy transfer in the light harvesting antenna of the red alga *Porphyridium cruentum* and the blue-green alga *Anacystis nidulans*. Analysis of the time-resolved fluorescence spectra, *Photochemistry and Photobiology* **39,**233-240.

Williams M., A.D. Richardson, M. Reichstein *et al.* (2009) Improving land surface models with FLUXNET data, *Biogeosciences* **6**, 1341-1359.

CHAMBER MEASUREMENTS OF SHOOT-LEVEL NO$_X$ FLUXES OF TREES: EFFECT OF TRANSPIRATION ON THE CHAMBER BLANK

M. RAIVONEN[1], J. JOENSUU[2], P. KOLARI[2], P. KERONEN[1], E. JÄRVINEN[1], N. ALTIMIR[3], T. VESALA[1], J. BÄCK[2], E. NIKINMAA[2]

[1]Division of Atmospheric Sciences, Department of Physics, P.O.Box 48, University of Helsinki, Finland
[2]Department of Forest Sciences, University of Helsinki, Finland
[3] Laboratory of Functional Ecology and Global Change Centre Tecnològic Forestal de Catalunya, Spain

INTRODUCTION

One of the processes underlying the atmospheric balance of nitrogen oxides (NO$_x$ = NO + NO$_2$) is their interaction with vegetation. NO$_x$ is deposited to and potentially also emitted from the foliage. Deposition may turn to emission at low enough ambient concentrations, i.e. below the compensation point. Existence of the compensation point is, however, controversial (Lerdau *et al.*, 2000). It has been detected in some studies but not in all, probably because the signal-to-noise ratio of NO$_x$ flux measurements at near-zero concentrations is low.

Leaf-level NO$_x$ fluxes of plants are measured with chambers. The plant or part of the plant is enclosed in a known volume of air, and NO$_x$ concentrations inside this chamber are monitored. Magnitude of the flux produced by the plant can be determined when one knows how much the other processes —e.g. sample air flow to a gas analyzer, airflow compensating for the air lost as the sample, or air-chemical reactions— change the concentration. With NO$_x$, one has to take into account the chamber blank: concentration change caused by interaction of NO$_x$ with the chamber surfaces. There are different ways to estimate it. Often there is another similar but empty chamber monitored alongside the plant chamber (Gut *et al.*, 2002). Sometimes the blank measurements are conducted before and after each leaf measurement with the same chamber (Hereid and Monson, 2001). Both methods have something in common: they assume the blank of a chamber is similar with and without a plant inside. However, the conditions in the chambers are somewhat different because plants change the composition of the chamber air by absorbing and emitting compounds. For example, they transpire water thus increasing the air humidity.

We monitor NO and NO$_2$ fluxes (along with fluxes of CO$_2$, H$_2$O, O$_3$ and BVOC) of Scots pine shoots in field conditions at the SMEAR II station in Southern Finland. The air there is relatively clean, thus the NO$_x$ fluxes are small and close to the detection limit of the instrumentation. We have used a separate, always empty chamber as an estimate for the blank. It has usually been a source of NO$_x$; for instance, we observed emission that depended on solar ultraviolet radiation (Raivonen *et al.*, 2003). The aim of this study was to improve the accuracy of our measurements by answering the question whether the chamber blank is similar with and without a transpiring plant. In practice, we tested if simulated transpiration affects the NO$_x$ fluxes in an empty chamber.

METHODS

In the chamber measurements of SMEAR II, the air compensating for the sample air (that is taken from the chambers to the gas analysers) is usually normal ambient air that flows into the chambers following the pressure gradient. However, it also is possible to use a system where compressed ambient air is fed into a chamber at a controlled flow rate. We created the simulated transpiration using this supply air system (Kolari *et al.*, 2004). The supply air as itself is drier than ambient, hence causing a negative water flux when fed into a chamber. To simulate transpiration, we added varying amounts of water vapor into

the supply air line. This was achieved by directing part of the supply air flow into a water tank and letting it bubble through, creating 100 % humidity in the air. The unheated and uninsulated water tank was outside and so its temperature followed ambient temperature. The humidity thus depended on ambient temperature, the airflow led through the tank, and the difference between ambient humidity and that of the supply air. There were two alternative ways to adjust the water flux. In the first set of experiments, we controlled the water vapor concentration in the supply air by adjusting the total supply flow and leading it through the tank. Additional replacement air got sucked into the chamber from ambient atmosphere. In the second set, we fed all replacement air into the chamber as supply air, and adjusted the supply air water vapor concentration. We used "transpiration" patterns that either imitated the diurnal variation of normal shoot transpiration, or differed from that, breaking the natural connection between radiation, temperature and evapotranspiration. Figure 1. illustrates how the created water fluxes imitated real transpiration.
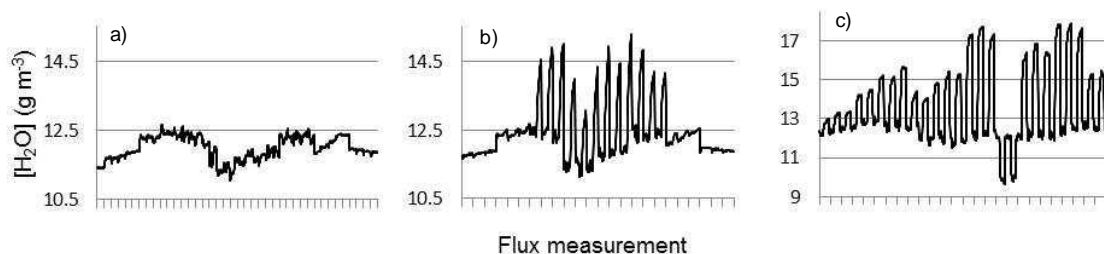
Figure 1. Water concentration in (a) an empty chamber when it has been measured as a normal reference, (b) a chamber enclosing a transpiring pine shoot, on the same day, and (c) the empty chamber on a water test day. In our measurement system, the chambers are most of the time open to the ambient air, and close only for the flux measurement. Thus, in the beginning of each flux measurement the gas concentrations equal the ambient but start to change when the chamber closes for the measurement. In (a) and (b), length of each flux measurement was 150 s, in (c) one measurement took 360 s. The concentrations are at T=273K and p=1013 hPa.

RESULTS

Analysing the NO and NO_2 flux data is under way. The preliminary result is that positive water fluxes (increasing humidity) do not seem to create any fatal artefacts in the NO_x flux measurements. However, a more detailed data analysis is necessary in order to find the possible smaller effects.

ACKNOWLEDGEMENTS

REFERENCES

Gut, A., M. Scheibe, S. Rottenberger, U. Rummel, M. Welling, C. Ammann, G.A. Kirkman, U. Kuhn, F.X. Meixner, J. Kesselmeier, B.E. Lehmann, W. Schmidt, E. Muller and M.T.F. Piedade (2002). Exchange fluxes of NO_2 and O_3 at soil and leaf surfaces in an Amazonian rain forest. *Journal of Geophysical Research* **107** (D20), Article Number: 8060.

Hereid, D.P. and R.K. Monson (2001). Nitrogen oxide fluxes between corn (Zea mays L.) leaves and the atmosphere. *Atmospheric Environment* **35**: 975–983.

Kolari, P., P. Keronen and P. Hari (2004). The accuracy of transpiration measurements with a dynamic cuvette system. *Report Series in Aerosol Science* 68: 112-114. ISBN 952-5027-48-1.

Lerdau, M.T., J.W. Munger and D.J. Jacob (2000).The NO_2 flux conundrum. *Science* 298: 2291-2293.

Raivonen, M., P. Keronen, T. Vesala, M. Kulmala, and P. Hari (2003). Measuring shoot-level NO_x flux in field conditions: the role of blank chambers, *Boreal Environment Research* **8**: 445-455.

MODELING THE METHANE EMISSIONS FROM BOREAL PEATLANDS

M. Raivonen[1], M. Tomasic[1], T. Hölttä[2], S Smolander[1], T Larmola[2,3], E-S. Tuittila[2,4], J. Rinne[1], S. Haapanala[1], A. Valdebenito[5], R.J. Schuldt[6], V. Brovkin[6], C. Reick[6], T. Vesala[1]

[1]Division of Atmospheric Sciences, Department of Physics, University of Helsinki, Finland
[2]Department of Forest Sciences, University of Helsinki, Finland
[3]Mount Holyoke College, Clapp Laboratory, South Hadley, Massachusetts, USA
[4]School of Forest Sciences, University of Eastern Finland, Joensuu, Finland
[5]Norwegian Meteorological Institute, Oslo, Norway
[6]Land in the Earth System, Max-Planck-Institute for Meteorology, Hamburg, Germany

Keywords: methane, wetlands, global modeling

INTRODUCTION

Methane (CH_4) is the second most important greenhouse gas after carbon dioxide (CO_2) and it has produced current radiative forcing of ~30% of that of CO_2. Although the total CH_4 emissions in the atmosphere are known relatively well, the contributions and trends of different sources are not. Most CH_4 (over 70%) is released from biogenic sources like rice cultivation, livestock and, above all, natural wetlands that are the largest single source of CH_4 in the atmosphere. (Denman *et al.*, 2007).

Wetlands release methane because the continually or intermittently high water table creates anoxic conditions in the soil layers that contain decomposable plant litter. Oxic decomposition produces only CO_2 but in anoxic conditions, both CO_2 and CH_4 are produced. CH_4 is a metabolic end product of strictly anaerobic methanogenic micro-organisms that belong to the domain Archeae. After being produced, a CH_4 molecule can have different fates. It can be transported to the atmosphere through the soil by diffusion in water- and air-filled soil pores. It can form gas bubbles with other molecules and be released to the atmosphere in ebullition. It can be transported via plants: in stems and roots of flood-tolerant plant species there are air spaces (*aerenchyma*) that enable atmospheric oxygen to move to the roots, and this route allows also CH_4 to move upwards. The molecule can also be destroyed: in the oxic parts of the soil there are methanotrophic bacteria that use molecular oxygen to oxidize CH_4 to CO_2 and cellular carbon.

Because of the anoxia, wetlands also are major terrestrial carbon stores. Decomposition rate in them is slow, slower than rate of biomass production. Therefore, a fraction of carbon accumulates as peat. Over millennial timescales, substantial carbon reservoirs have been formed in wetlands. Yu *et al.* (2010) estimated that wetlands have accumulated globally around 600 Gt of carbon. These reservoirs are vulnerable since climatic changes like temperature rise and consequent water level draw down can change the conditions so that the accumulated organic matter starts to decompose and to release CO_2.

As methane source and carbon sink, wetlands hence play an important role in the climate system. It would be essential to be able to estimate how the climatic change affects their carbon cycle. The large variation within climate change scenarios and the high structural and functional diversity of wetlands makes it quite impossible question to address empirically. However, this can be achieved via modeling. Several models for estimating the methane emissions from wetlands exist (e.g. Walter *et al.*, 2001; Kettunen, 2003; Wania *et al.*, 2010; Riley *et al.*, 2011).

We have been developing a model of the CH_4 cycle of boreal peatlands. The model is aiming to be a part of the CBALANCE carbon tool of the JSBACH (Jena Scheme for Biosphere-Atmosphere Coupling in Hamburg) land component of the MPI (Max Planck Institute) Earth System Model. In addition, we plan to use it as a tool to combine the diverse experimental studies related to the production and release of CH_4 that have been conducted at our measuring site Siikaneva, an ombrotrophic fen in southern Finland.

MODEL DESCRIPTION AND CURRENT STATUS

The starting point of our work has been to add a methane production and transport module into the CBALANCE of MPI-ESM. Other processes of the carbon cycle (carbon uptake and peat accumulation) of peatlands were modeled by the group at MPI (Kleinen *et al.*, 2012). Our model is based on the methane emission model of Wania *et al.* (2010); however, there also are several differences.

At this initial phase, the peat layer in our model reaches 2.5 m depth and is divided into 5 cm thick sub layers. Biomass of the roots of aerenchymatous plants decreases exponentially with depth (Wania *et al.*, 2010). This decay function is used, besides for estimating the amount of gas transporting plant roots in each 5 cm layer, for vertical distribution of the decomposing plant litter that is available for CH_4 production. We get the quantity of anoxically decomposing carbon as input from the other parts of the soil carbon model. The description of methane production is very simple: the anoxically decomposed carbon is divided into CO_2 and CH_4 using a constant ratio. The ratio of methane to CO_2 production in fully inundated conditions is now set to 20%.

Models for molecular diffusion in soil and diffusion via plants are applied for both CH_4 and oxygen (O_2). O_2 concentrations in the soil are necessary for estimating the oxidation of methane. The calculation of oxidation uses Michaelis-Menten equations adopted from Matthews *et al.* (2000).

The water table depth (that we get as input) determines the depth of the oxic part of the peat, and we assume all the soil pores above it are filled with air, below it they are filled with water. So the molecular diffusion within the peat matrix occurs either in water or air, depending on the location of the soil layer. We included also the possible water-air interface inside the numerical diffusion scheme: e.g. CH_4 produced in the bottom inundated layer must diffuse through all water-filled and air-filled soil layers before it gets released into the atmosphere.

The model of plant transport of CH_4 and O_2 differs from that of Wania *et al.* (2010). The overall transport through the plant is given with two processes: diffusion in water between the peat layer and the interior of the root, and diffusion in the air inside the plant, between the root and the atmosphere. The former is calculated taking into account the root surface area in one soil layer (approximated to be 10 m^2 per 1 m^2 of soil in total, for each layer it is weighted by the root fraction), and the distance of diffusion around the root (approximated to 1 cm).

The model of methane ebullition is the one formulated by Wania *et al.* (2010). It bases on calculating maximum quantity of CH_4 that can be dissolved in the water. If the CH_4 concentration exceeds that limit, the excess is released to the atmosphere as bubbles. We have also been developing an own ebullition model, in which heterogeneous nucleation of CH_4 bubbles occurs once dissolved CH_4 reaches high enough supersaturation.

The main parts of the methane module are ready and currently we are doing test runs with it. Some additional features need still to be implemented, for instance, seasonal variation to the abundance of aerenchymatous plants.

ACKNOWLEDGEMENTS

REFERENCES

Denman, K. L., G. Brasseur, A. Chidthaisong, P. Ciais, P. Cox, R.E. Dickinson, D. Hauglustaine, C. Heinze, E. Holland, D. Jacob, U. Lohmann, S. Ramachandran, P.L. da Silva Dias, S.C. Wofsy, and X. Zhang (2007). Chapter 7: Couplings between changes in the climate system and biogeochemistry, in: Climate Change 2007: The Physical Science Basis. Contribution of Working Group I to the Fourth Assessment Report of the Intergovernmental Panel on Climate Change, edited by: Solomon, S., Qin, D., Manning, M., Chen, Z., Marquis, M., Averyt, K., Tignor, M., and Miller, H., Cambridge University Press, UK and New York, NY, USA, 2007.

Kettunen, A. (2003). Connecting methane fluxes to vegetation cover and water table fluctuations at microsite level: A modeling study. *Global Biogeochemical Cycles* Vol. 17(2), doi: 10.1029/2002GB001958.

Kleinen, T., V. Brovkin and R.J. Schuldt (2012). A dynamic model of wetland extent and peat accumulation: results for the Holocene. *Biogeosciences* 9: 235-248.

Matthews, R., R. Wassmann and J. Arah (2000). Using a crop/soil simulation model and GIS techniques to assess methane emissions from rice fields in Asia. 1. Model development. *Nutrient Cycling in Agroecosystems*, 58: 141-159.

Riley, W.J., Z.M. Subin, D.M. Lawrence, S.C. Swenson, M.S. Torn, L. Meng, N.M. Mahowald and P. Hess (2011). Barriers to predicting changes in global terrestrial methane fluxes: analyses using CLM4Me, a methane biogeochemistry model integrated in CESM. *Biogeosciences*, 8: 1925-1953.

Walter, B.P., M. Heimann and E. Matthews (2001). Modeling modern methane emissions from natural wetlands 1. Model description and results. *J Geophys. Res*. Vol 106(D24), 34207-34219.

Wania, R., I. Ross and I.C. Prentice (2012). Implementation and evaluation of a new methane model within a dynamic global vegetation model: LPJ-WHyMe v1.3.1. *Geoscientific Model Development* 3: 565-584.

Yu, Z., J. Loisel, D.P. Brosseau, D.W. Beilman and S.J. Hunt (2010). Global peatland dynamics since the Last Glacial Maximum. *Geophysical Research Letters* 37, L13402, doi:10.1029/2010GL043584.

MEASURING VOCS: AN INTERCOMPARISON BETWEEN PTR-MS AND GC-MS IN HYYTIÄLÄ IN SPRINGTIME

P. RANTALA[1], M. HILL[2], M.K. KAJOS[1], H. HELLÉN[3], C. HÖRGER[2], S. SCHALLHART[1], R. TAIPALE[1], J. PATOKOSKI[1], T.M. RUUSKANEN[1], T. PETÄJÄ[1], S. REIMANN[2] and J. RINNE[1]

[1] Division of Atmospheric Sciences, Department of Physics, University of Helsinki, Finland.
[2] Empa, Laboratory for Air Pollution/Environmental Technology, Switzerland
[3] Air Quality Research, Finnish Meteorological Institute.

Keywords: VOCs, PTR-MS, GC-MS, Hyytiälä, spring.

INTRODUCTION

Volatile organic compounds (VOCs) are mostly emitted into atmosphere from natural sources (Guenther *et al.*, 1995). Some of the compounds, such as monoterpenes, are highly reactive and seem to have major contributions to aerosol particle formation and growth, thus these compounds are also connected to the global climate change (Kulmala *et al.*, 2004). Approximately 50 % of the biogenic emissions are coming from the tropical rain forests, 15-20 % from the boreal forests and the rest from the other sources such as fields and oceans.

In this study, we measured different VOC species in Hyytiälä at SMEAR II (61° 51' N, 24° 17' E, 180 m a.m.s.l.) using the proton-transfer-reaction mass spectrometer (PTR-MS, Lindinger *et al.*, 1998), and two gas chromatography-mass spectrometers (GC-MS). The PTR-MS was operated by University of Helsinki (UHEL) and the GC-MSs by Finnish Meteorological Institute (FMI) and EMPA (Eidgenössische Materialprüfungs- und Forschungsanstalt). FMI measurements were conducted using an in-situ thermal desorpter (Markes Unity) with a gas chromatograph (Agilent 7890A) and a mass spectrometer (Agilent 5379N, see Hellén *et al.*, 2012). Measurements by EMPA were done using Modified Adsorption/Desorption System (MADS) GC-MS. The measurement period was from 16.4.–15.5.2012 and it covered the time after snow melting as well as couple of weeks before that.

One of our aims was to do intercomparison between the PTR-MS and GC-MSs. We measured pure hydrocarbons, such as benzene (C_6H_6), as well as oxygenated hydrocarbons, such as acetaldehyde (C_2H_4O) and acetone (C_3H_6O). In this abstract, we present the first results of the intercomparison for acetone, benzene and toluene.

METHODS

The PTR-MS is a highly sensitive instrument for real-time measurements of VOCs. The instrument uses hydronium ions (H_3O^+) to ionize target compounds via proton transfer reaction and quadrupole technique as a mass analyzer. The PTR-MS measures with 1 amu (atomic mass unit) resolution and it does not identify isobaric compounds. The PTR-MS is still one of the best instruments to do fast real-time measurements of many VOCs, such as methanol, acetone, isoprene and monoterpenes. The calibration and volume mixing ratio calculation procedures for the PTR-MS have been described by Taipale *et al.* (2008).
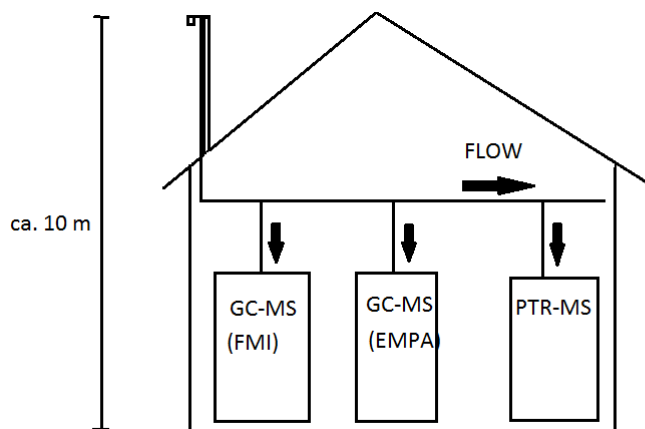
Figure 1: The measurement setup at SMEAR II during the campaign

The PTR-MS and both GC-MSs were connected to the same inlet line (PTFE, inner diameter 8 mm, total length 20 m., flow ca. 20 l/min). A schematic illustration about our measurement setup can be seen in figure 1. The inlet line was set above the roof of the measurement cottage and its altitude was about 10 m from the ground.

RESULTS AND DISCUSSION

The results show that there was a systematic difference in concentrations between the instruments. In most of the cases, the highest concentrations were detected with the PTR-MS which is predictable because the PTR-MS adds up all the molecules within 1 amu mass range. However, the background due to extra compounds should be much smaller than presented in the figures 2, 3 and 4. This could indicate an error, for example, in calibrations or instrumental background measurements. There were also significant differences in the results between the two GC-MSs (e.g. benzene, see figure 3) which might implicate that measurements at level near the detection limit are very sensitive for an instrumentation. Nevertheless, all three instruments had the results in the same magnitude and the concentrations of acetone, benzene and toluene seem to also correlate well.

During the campaign, benzene and toluene had very probably an anthropogenic origin, thus measuring those is important from the air quality research point view (e.g. Hellén, 2006). The PTR-MS has not been used widely for these purposes but this work indicates that it might be also a useable choice for monitoring some pollutants (especially when fast sampling is needed), also in high latitudes where concentrations are expected to be low.
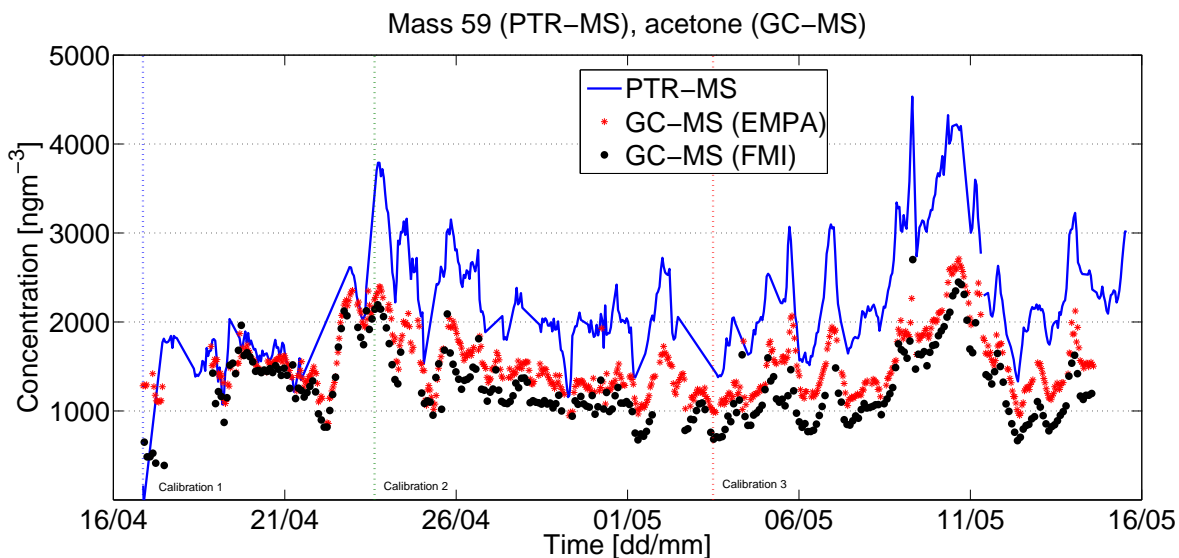
Figure 2: Concentration of acetone measured by the PTR-MS (solid blue line) and the GC-MSs (black and red dots). The calibration days of the PTR-MS have been marked in the figure using vertical dashed lines.
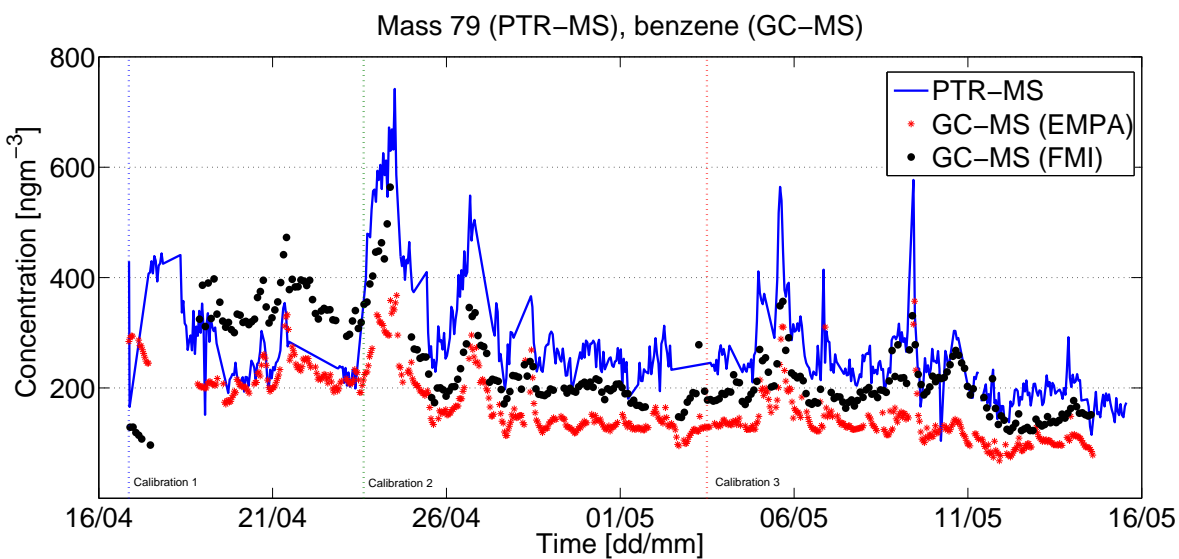
Figure 3: Concentration of benzene measured by the PTR-MS (solid blue line) and the GC-MSs (black and red dots). The calibration days of the PTR-MS have been marked in the figure using vertical dashed lines.
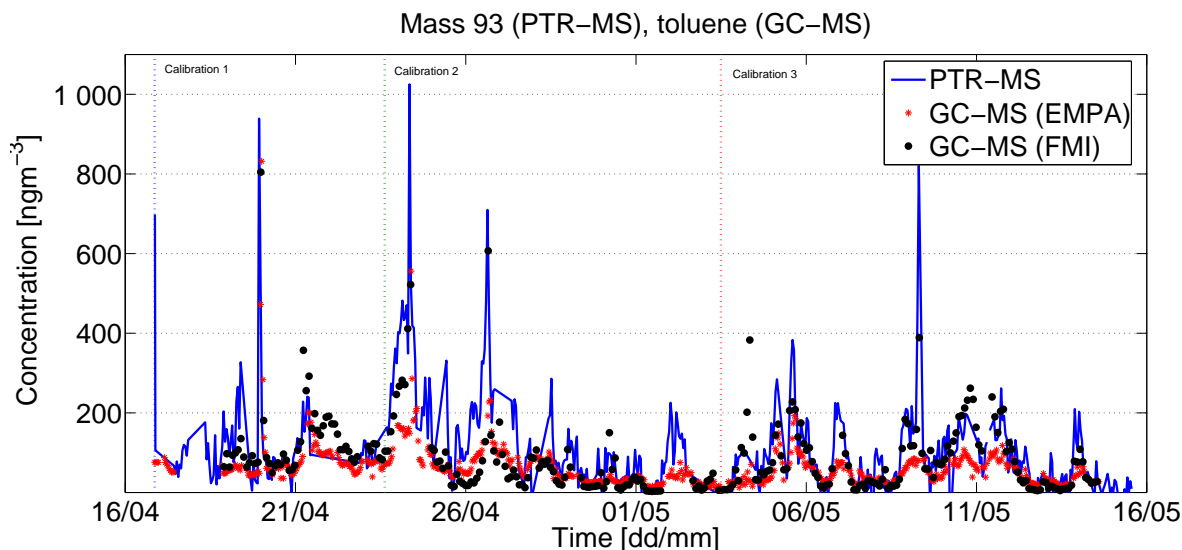
Figure 4: Concentration of toluene measured by the PTR-MS (solid blue line) and the GC-MSs (black and red dots). The calibration days of the PTR-MS have been marked in the figure using vertical dashed lines.

REFERENCES

Guenther, A., C. N. Hewitt, D. Erickson, R. Fall, C. Geron, T. G. P. Harley, L. Klinger, M. Lerdau, W. A. McKay, T. Pierce, B. Scholes, R. S. R. Tallamraju, J. Taylor and P. Zimmerman (1995). A global model of natural volatile organic compound emissions. *Journal of Geophysical Research*, **100**, 8873–8892.

Hellén, H. (2006). *Sources and concentrations of volatile organic compounds in urban air.* Academic Disseration, Finnish Meteorological Institute, Contributions 56.

Hellén, H., Kuronen, P. and H. Hakola (2012). Heated stainless steel tube for ozone removal in the ambient air measurements of mono- and sesquiterpenes. *Atmospheric Environment*, **57**, 35–40.

Kulmala, M., T. Suni, K. E. J. Lehtinen, M. D. Maso, M. Boy, A. Reissell, Ü. Rannik, P. Aalto, P. Keronen, H. Hakola, J. Bäck, T. Hoffmann, T. Vesala and P. Hari (2004). A new feedback mechanism linking forests, aerosols, and climate. *Atmospheric Chemistry and Physics*, **4**, 557–562.

Lindinger, W., A. Hansel and A. Jordan (1998). On-line monitoring of volatile organic compounds at pptv levels by means of Proton-Transfer-Reaction Mass Spectrometry (PTR-MS)—Medical applications, food control and environmental research. *Int. J. Mass Spectrom.*, **173**, 191–241.

Taipale, R., T. M. Ruuskanen, J. Rinne, M. K. Kajos, H. Hakola, T. Pohja and M. Kulmala (2008). Technical note : quantitative long-term measurements of VOC concentrations by PTR-

MS - measurement, calibration, and volume mixing ratio calculation methods. *Atmospheric Chemistry and Physics*, **8**, 6681–6698.

SOIL CO_2 CONCENTRATIONS AND FLUXES IN A BOREAL HEADWATER CATCHMENT

T. RASILO[1], J. PUMPANEN[1] and A. OJALA[2]

[1]Department of Forest Sciences, University of Helsinki,
P.O. Box 27, FI-00014 University of Helsinki, Finland.

[2]Department of Environmental Sciences, University of Helsinki, Niemenkatu 73, FI-15140 Lahti, Finland.

Keywords: carbon dioxide, riparian zone, boreal forest, soil

INTRODUCTION

Soil CO_2 flux forms a substantial part of the ecosystem respiration composing 46-62% of the annual ecosystem respiration (Wang et al., 2004). It is originated from CO_2 production by autotrophic (roots and mycorrhizae) and heterotrophic (decomposers) respiration (Hanson *et al*., 2000; Ryan and Law, 2005). The production of CO_2 is influenced mainly by changes in root density, microbial community composition, quality and quantity of soil carbon pools, and photosynthetic activity (Kuzyakov, 2006) whereas the transport of CO_2 by diffusion is affected by soil moisture, soil texture, and bulk density (Šimůnek and Suarez, 1993; Moldrup *et al*., 1999; Pumpanen *et al*., 2003). Thus, soil CO_2 flux, integrating biological CO_2 production in different soil layers and changes in soil CO_2 diffusivity in the soil profile, provides information about the interaction between soil processes and the atmosphere (Vargas *et al*., 2010).

Generally, the soil CO_2 flux is measured with chambers placed on the soil surface (e.g. Niinistö *et al.*, 2010). The soil temperature has been used to explain the variation of soil CO_2 flux and to estimate the annual soil CO_2 flux (*e.g.* Reichstein *et al*., 2003). The flux can also be modeled from CO_2 concentration differences between soil and the atmosphere and between different soil layers (Pumpanen *et al*., 2003; Pumpanen *et al*., 2008). Flux measurements on the soil surface do not give information on the vertical distribution of CO_2 sources and their seasonal dynamics, which can be significant *e.g.* in boreal forests (Pumpanen *et al*., 2008). Thus, the gradient method can provide a tool to study the processes underlying soil CO_2 fluxes and to determine the contribution of biological activity at different depths.

The riparian zone acts as an interface between terrestrial and aquatic ecosystems, and is a biogeochemical hotspot area where hydrological flow paths converge with substrates flow paths (McClain *et al*., 2003). For instance, riparian zones are known to be important sources of DOC to aquatic ecosystems (*e.g.*, Hinton *et al.*, 1998). In the boreal zone, inland waters form a substantial part of the landscape and in Finland, fresh waters cover 10% of the land area on average and the shoreline of lakes and rivers is approximately 215 000 km in length, emphasizing the importance of understanding the functioning of the riparian zone.

The aim of this study was to estimate the soil CO_2 flux in the riparian zone of a small forested catchment. We study its spatial and temporal variation and aim to determine the amount CO_2 released annually from the riparian zone soil. We compare results from chamber measurements, temperature calculations and gradient modeling.

METHODS

The study site was located in the Evo Nature Reserve area in the south boreal zone in southern Finland. The Valkea-Kotinen catchment (61°14' N, 25°04' E) has been part of the International cooperative programme on integrated monitoring of air pollution effects on ecosystems (ICP IM) since 1987; the only human influence to the area comes through the atmosphere deposition. This headwater catchment represents well the boreal zone, its outlines are easy to define and since the lake is the uppermost water body in the catchment area and thus without an inlet, it is convenient for studies on ecosystem effects. The catchment has been protected since 1955 and thus the forest is old and as natural as possible. The distance to the urban areas is over 40 km, which makes Valkea-Kotinen also suitable as a reference site. The small size of the catchment (ca. 30 ha) also hastens the response to variations in environmental conditions.

The catchment includes a headwater lake also called Valkea-Kotinen (4.1 ha, mean depth 3 m, 156 m a.s.l.) with a small outflow brook, coniferous forest (19.6 ha) and peatlands (7.9 ha). The annual mean temperature in the area is 3.1°C, the growing season (T > 5°C) lasts 112 days and the annual mean precipitation is 618 mm. The old growth forests are dominated by Norway spruce (*Picea abies* Karst.) with Scots pine (*Pinus sylvestris* L.) and birch (*Betula* sp.). The riparian zone, where the measurements were carried out, is histosol (peat depth > 60 cm) and dominated by old Norway spruce (1188 stems per ha), Scots pine (594 stems per ha), and birch (340 stems per ha). Bilberry (*Vaccinium myrtillus* L.), lingonberry (*Vaccinium vitis-idaea* L.), and Labrador-tea (*Rododendrum tomentosum* (L.) Harmaja) form the ground vegetation together with mosses (*Pleurozium schreberi* Mitt., *Hylocomium splendens* Schimp., *Sphagnum* spp.).

Soil temperature in the riparian zone was followed with automatic temperature sensors (DS1921G Thermochron iButton®, Maxim, San Jose, CA) placed at 2 cm depth. Three sensors were placed at 2 m from the lake shore and three at 12 m from the lake shore. The distance between each sensor was approximately 100 m.

To study CO_2 flux from the soil into the atmosphere, we used a closed dynamic chamber technique. The measuring system is comprised of a CARBOCAP GMP343 infrared diffusion type sensor (Vaisala Oyj, Finland) installed in the chamber (diameter 190 mm, height 240 mm). The chamber was covered with aluminium foil and equipped with a fan to ensure the air mixing inside the chamber. For measurements, plastic collars were installed in the soil at 5 cm depth. There were three collars at 2 m and three at 4 m from the lake shore considered as "shore" and three at 10 m and three at 12 m from the lake shore considered as "forest". For measurements the chamber was placed on one collar for four minutes and the increase of CO_2 concentration inside the chamber was recorded at 5 s interval. The soil CO_2 flux was calculated with a linear fitting from 60 to 280 seconds starting from the placement of the chamber. First minute, when the system was still stabilizing, was excluded as was the last minute to avoid the effect of possible saturation. To calculate the annual soil CO_2 flux, an exponential curve was fitted to the temperature and chamber measurement data and the obtained formula was used to calculate daily values from the continuous temperature measurements. These were then summed up to get the annual CO_2 flux.

To study the spatial variation of the soil CO_2 concentration, we installed gas sampling system in the riparian zone of the Lake Valkea-Kotinen. The sampling systems were located 2 m (three systems, "shore") and 12 m (three systems, "forest") from the shore. Each system consisted of steel tubes going to the measuring depths (2 cm, 10 cm, 30 cm and 50 cm), a silicon tube enabling the gas exchange with the soil air, three way valves to collect samples and one syringe connected permanently to the tubes to ensure that the volume of the sample was large enough. The sample was taken with a syringe and immediately pushed to a vacuumed vial. The vial (volume 11 ml) was over pressured with approximately 30 ml of the sample air. The samples were analysed with a gas chromatograph (Network GC systems 6890N, Agilent Technologies, Santa Clara, CA) for CO_2.

Soil CO_2 flux was also calculated with a dynamic model described in Pumpanen *et al.* (2003 and 2008). In the model, CO_2 moves in soil and from soil into the atmosphere due to diffusion, which depends on

porosity of soil, soil water content, and distance and concentration differences between the studied layers. Automatic continuous measurement of soil CO_2 concentration (GMP343 and GMM221, Vaisala Oyj, Finland) and soil humidity (EC-10 ECH2O Dielectric Aquameter sensors, Decagon Devices Inc., Pullman, WA) at 2, 10 and 30 cm depth were used to run the model and it was calibrated against the chamber measurements. The automatic measuring system is described in details in Rasilo *et al.* (2012).

For data analysis, the data were divided into four seasons with three months (spring=March–May, summer=June–August, autumn=September–November, winter=December–February). The differences between the locations during the whole year and the seasons were tested with Mann-Whitney U-test. Tests were done with SPSS 15.0 (SPSS Inc, IBM Corporation, Armonk, NY).

RESULTS AND DISCUSSION

Soil temperature varied throughout the year (Fig 1a). Even though the annual mean temperature was 4.7 °C both in the shore and in the forest, soil temperature between these two locations at 2 cm differed in summer and in winter (Mann-Whitney U, $Z=-1.968$, $P>0.05$ and $Z=-2.776$, $P<0.01$, respectively). The shore was warmer (13.2 °C) in summer and colder in winter (-1.7 °C) than the forest (12.8 and -1.2 °C, respectively).

CO_2 concentration at 10 cm depth was clearly higher in the forest (4769 ppm) than in the shore (896 ppm) (Mann-Whitney U $Z=-6.063$, $P<0.001$) (Fig 1b). The difference between the locations was significant during all the seasons expect for the spring (Mann-Whitney U $Z=-1.549$, $P>0.1$). Also at 2 cm, 30 cm and 50 cm depths, the difference between the shore and the forest was similar to that at 10 cm depth (data not shown). Both locations showed annual variation with highest values in summer. The soil CO_2 flux also was highest in summer (Fig 1c), but there were no differences between the locations, neither in the whole year, nor in a specific seasons. Our results are in accordance with soil CO_2 fluxes measured elsewhere in the boreal zone (e.g. Niinistö *et al.*, 2011).

Seasonal variation was present in CO_2 concentrations as well as in CO_2 flux. In the boreal zone, temperature varies widely and thus biological activity has a clear seasonal cycle. The temperature sensitivity of soil CO_2 flux can vary with the temperature and the substrate availability affects it, too (Kirschbaum, 2006). During the winter the vegetation is dormant and most of the produced CO_2 originates from the decomposition, whereas in summer the active vegetation produces fresh, easily decomposable carbon into the soil.

Exponential fitting between the soil CO_2 flux and temperature (Fig 2.) resulted in the following equations for the shore (s) and forest (f), respectively: $flux_S=0.0456*e^{0.1121Ts}$, $R^2=0.68$; $flux_F=0.0466*e^{0.1219Tf}$, $R^2=0.69$. Calculated with these equation and daily temperatures, the annual soil CO_2 flux was 0.87 and 0.95 kg C m^{-2} yr^{-1} in the shore and forest, respectively.

Preliminary results from the gradient modeling gives higher values of annual soil CO_2 flux (1.4 kg C m^{-2} yr^{-1}) than those based on soil temperature and chamber measurements (Fig. 3). However, they are in the same order of magnitude. Pumpanen *et al.* (2008) also determined the respiration of different soil horizons and estimated the contribution of recent photosynthates to total respiration. Humus layer and A-horizon contributed 69.9%, B-horizon 19.8%, and C-horizon 10.4% of the total CO_2 flux. However, the soil in the riparian zone of the Lake Valkea-Kotinen is histosol and thus, the clear layers present in podsol could not be determined.
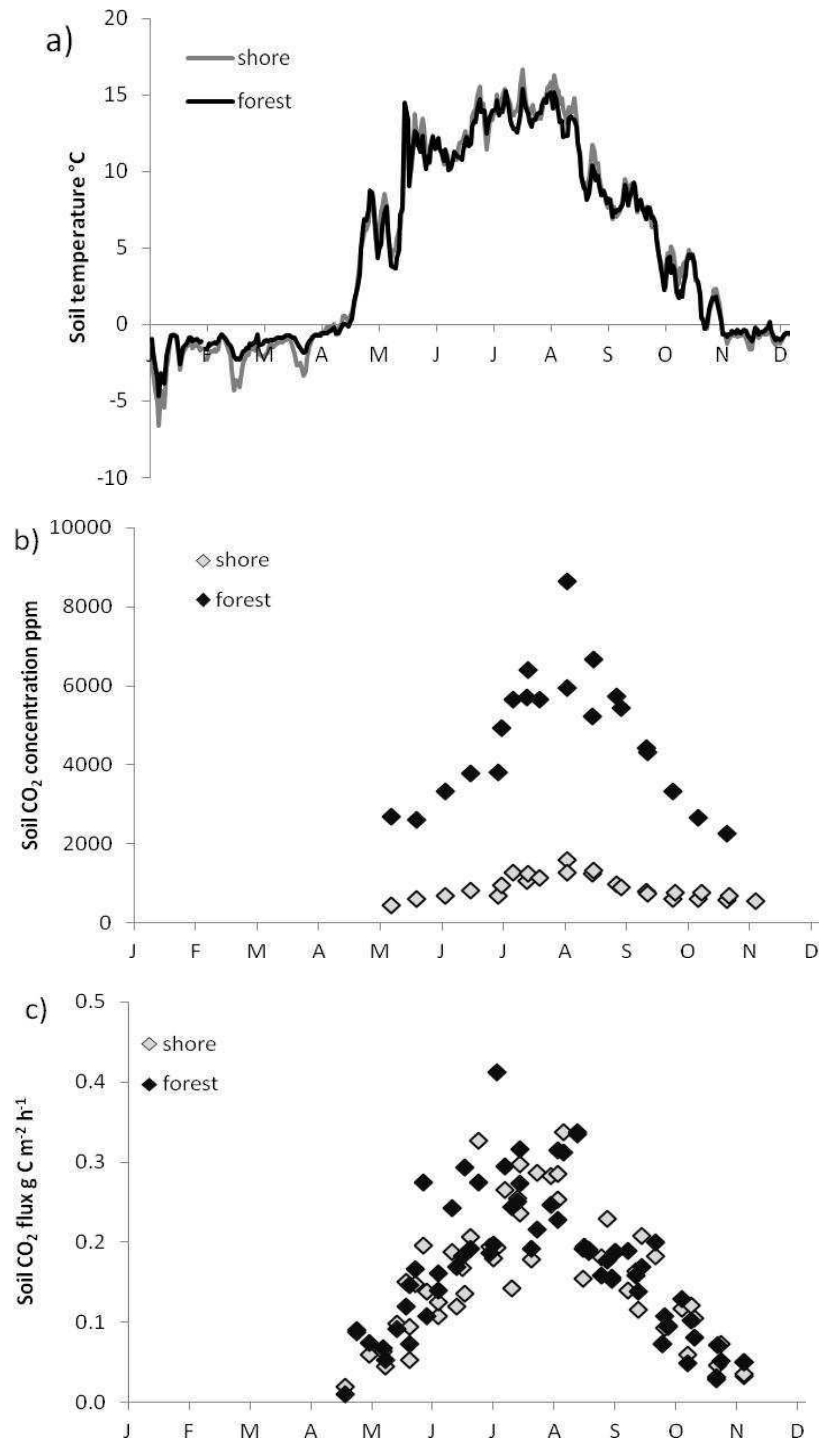
Figure 1. Measured daily mean soil temperature (°C) at 2 cm depth (a), measured soil CO_2 concentrations (ppm) at 10 cm depth (b) and CO_2 flux measured with chambers (c) in the Valkea-Kotinen catchment in 2007–2009. Shore = 2 m from the lake shore, forest= 12 m from the lake shore.
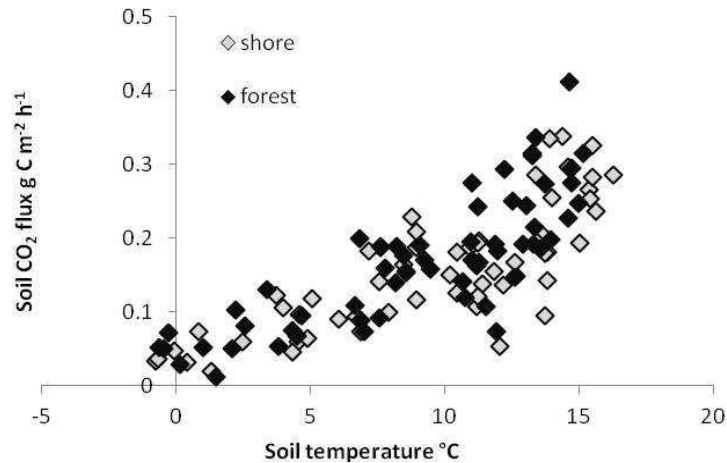
Figure 2. CO_2 flux (g C m^{-2} h^{-1}) vs. soil temperature (°C) in the Valkea-Kotinen catchment in 2007–2009. Shore = 2 m from the lake shore, forest= 12 m from the lake shore.
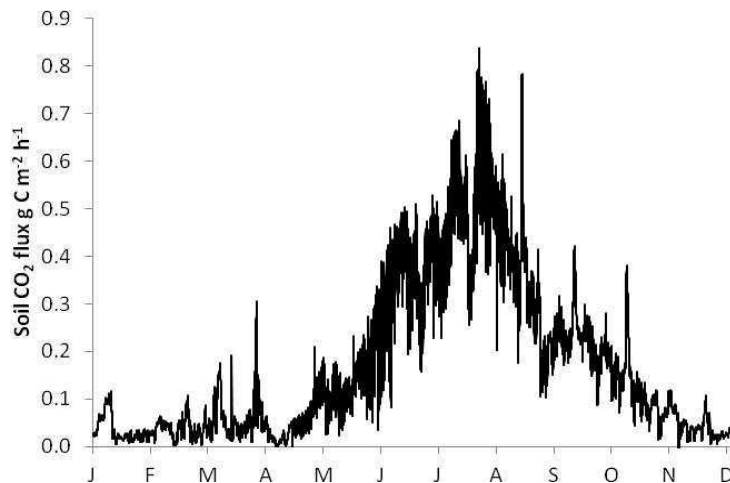
Figure 3. Modelled soil CO_2 flux (g C m^{-2} h^{-1}) based on the soil CO_2 concentration gradient in the Valkea-Kotinen catchment in 2008.

ACKNOWLEDGEMENTS

REFERENCES

Hanson, P. J., Edwards, N. T., Garten, C. T. and Andrews, J. A. (2000). Separating root and soil microbial contributions to soil respiration: a review of methods and observations. *Biogeochemistry* **48**:115–146.

Hinton, M.J., S.L. Schiff, and M.C. English. (1998). Sources and flowpaths of dissolved organic carbon during storms in two forested watersheds of the Precambrian Shield. *Biogeochemistry* **41**:175–197.

Kuzyakov, Y. (2006). Sources of CO_2 efflux from soil and review of partitioning methods. *Soil Biology and Biochemistry* **38**:425–448.

McClain, M.E., Boyer, E.W., Dent, C.L., Gergel, S.E., Grimm, N.B., Groffman, P.M., Hart, S.C., Harvey, J.W., Johnston, C.A., Mayorga, E., McDowell, W.H. and Pinay, G. (2003). Biogeochemical hot spots and hot moments at the interface of terrestrial and aquatic ecosystems. *Ecosystems* **6**:301–312.

Moldrup, P., Olesen, T., Yamaguchi, T., Schjonning, P. and Rolston, D. E. (1999). Modeling diffusion and reaction in soils. IX. The Buckingham-Burdine-Campbell equation for gas diffusivity in undisturbed soil. *Soil Science* **164**:542–551.

Niinistö, S.M., Kellomäki, S and Silvola, J. (2011). Seasonality in a boreal forest ecosystem affects the use of soil temperature and moisture as predictors of soil CO_2 efflux. *Biogeosciences* **8**:3169–3186.

Pumpanen, J., Ilvesniemi, H. and Hari, P. (2003). A processbased model for predicting soil carbon dioxide efflux and concentration. *Soil Science Society of America Journal* **67**:402–413.

Pumpanen J., Ilvesniemi H., Kulmala L., Siivola E., Laakso H., Helenelund C., Laakso M., Uusimaa M., Iisakkala P., Räisänen J. and Hari P. (2008). Respiration in boreal forest soil as determined from carbon dioxide concentration profile. *Soil Science Society of America Journal* **72**:1187–1196.

Reichstein, M., Rey, A., Freibauer, A., Tenhunen, J., Valentini, R., Banza, J., Casals, P., Cheng, Y., Grünzweig, J.M., Irvine, J., Joffre, R., Law, B.E., Loustau, D., Miglietta, F., Oechel, W., Ourcival, J.-M., Pereira, J.S., Peressotti, A., Ponti, F., Qi, Y., Rambal, S., Rayment, M., Romanya, J., Rossi, F., Tedeschi, V., Tirone, G., Xu, M. and Yakir, D. (2003). Modeling temporal and large-scale spatial variability of soil respiration from soil water availability, temperature and vegetation productivity indices. *Global Biogeochemical Cycles* **17**:1104.

Ryan, M. G. and Law, B. E. (2005). Interpreting, measuring, and modeling soil respiration. *Biogeochemistry* **73**:3–27.

Šimůnek, J. and Suarez, D. L. (1993) Modeling of carbon dioxide transport and production in soil. 1. Model development. *Water Resources Research* **29**:487–497.

Vargas, R,, Baldocchi, D.D., Allen, M.F., Bahn, M., Black, T.A., Collins, S.L., Yuste, J.C., Hirano, T., Jassal, R.S., Pumpanen, J., and Tang, J. (2010). Looking deeper into the soil: biophysical controls and seasonal lags of soil CO_2 production and efflux. *Ecological Applications* **20**:1569–1582.

Wang K.-Y., Kellomäki S., Zha T.S., and Peltola H. (2004). Component carbon fluxes and their contribution to ecosystem carbon exchange in a pine forest: an assessment based on eddy covariance measurements and an integrated model. *Tree Physiol.* **24**:19–34.

MODELING AEROSOL WATER UPTAKE IN THE ARCTIC AND ITS DIRECT EFFECT ON CLIMATE

N. RASTAK[1], S. SILVERGREN[4], P. ZIEGER[3], U. WIDEQVIST[1], J. STRÖM[1], B. SVENNINGSSON[4], A. EKMAN[2], P. TUNVED[1] and I. RIIPINEN[1]

[1]Department of Applied Environmental Science (ITM) and Bert Bolin Centre for Climate research, Stockholm University, Sweden
[2]Department of Meteorology (MISU), Stockholm University, Sweden
[3]Paul Scherrer Institute, Switzerland
[4]Division of Nuclear Physics, Lund University

INTRODUCTION

Hygroscopicity is one of the most fundamental properties of atmospheric aerosols. Aerosol particles containing soluble materials can grow in size by absorbing water in ambient atmosphere. Hygroscopic growth is described by the growth factor (GF), which is defined as the ratio of the wet diameter to the dry diameter of the particle. Hygroscopicity controls the size of an aerosol particle and therefore its optical properties in the atmosphere (see e.g. Petters and Kreidenweis 2007 and references therein). Hygroscopic growth depends on the dry size of the particle, its chemical composition and the relative humidity in the ambient air (Fitzgerald, 1975; Pilinis et al., 1995). One of the typical problems in aerosol studies is the lack of measurements of aerosol size distributions and optical properties in ambient conditions. The gap between dry measurements and the real humid atmosphere is filled in this study by utilizing a hygroscopic model which calculates the hygroscopic growth of aerosol particles at Mt Zeppelin station, Ny Ålesund, Svalbard during 2008. After using the hygroscopic model, the radiative properties and radiative influence of the aerosols on the Arctic environment are studied using a Mie scattering model and a radiative transfer model to address the following questions (see Fig. 1): 1) How big is the impact of relative humidity on the optical properties of aerosols and radiative balance of the atmosphere? 2) Is there a seasonal trend in optical properties of aerosol particles at Arctic? 3) How sensitive are the hygroscopic growth of aerosol particles at Arctic and thus their optical properties to 1) size of the particle 2) chemical composition of the particle and 3) relative humidity?
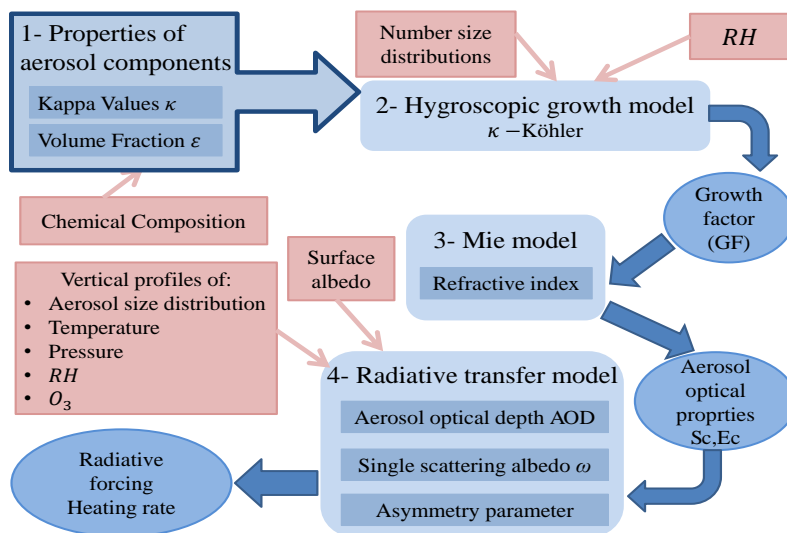
Fig.1. The models and inputs used in this study.

METHODS

The year 2008 was divided into 3 seasons based on the ratio of concentration of particles in the accumulation mode compared to the Aitken and nucleation modes (see Fig. 2), namely the haze season (Jan, Feb, Mar, Apr), the summer season (May, Jun, Jul, Aug), and the winter season (Sep, Oct, Nov, Dec).
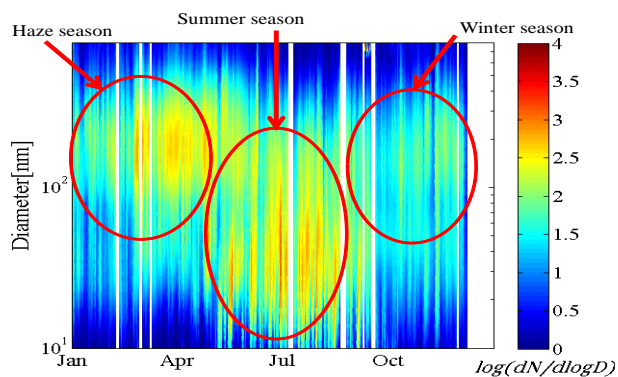
Fig. 2. Aerosol particle number size distributions during year 2008 at Zeppelin station and the classification of the data into 3 seasons.

A hygroscopic growth model was built on the κ-Köhler theory (Petters and Kreidenweis, 2007). The κ for a multicomponent particle with i components is given by the mixing rule $\kappa = \sum_i \varepsilon_i \kappa_i$, where ε_i is the volume fraction of i. The chemical composition of the aerosol particles was represented by observations of inorganic ions obtained from the Norwegian Institute for Air Research (NILU), sulfate $(NO_3^-, NH_4^+, SO_4^{2-})$ and sea salt $(Na^+, Cl^-, Ca^{2+}, Mg^{2+}, K^+)$ and filter sample analysis for the organic and elemental carbon (OC/EC) concentration (Silvergren et al., unpublished manuscript). The chemical composition was averaged over the seasons specified in the previous Section (see Fig. 3). The thermodynamic properties used for chemical components are listed in Table 1.
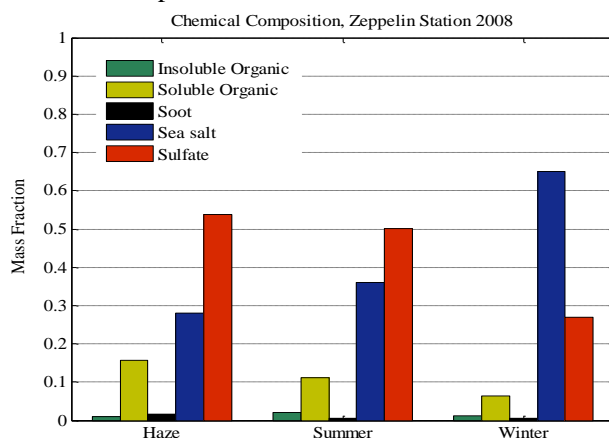
Fig. 3. The seasonally averaged chemical compositions for the aerosol particles.

Component	M [g]	ρ [g/cm3]	V_m [cm3]	κ
Sulfate (Ammonium Sulfate)	132.14*	1.77*	74.66	0.53
Sea Salt (Sodium chloride)	58.44*	2.17*	27	1.12
Water Soluble Organics	133**	1.56**	85.26	0.27
Water Insoluble Organics (SOA)	180***	1.5***	120	0.10
Soot	12	2	6	0.00

*(Svenningsson et al., 2006)/**(Koehler et al., 2006; Svenningsson et al., 2006)Mean value for glutaric acid, malonic acid, Succinic acid and Levoglucosan/***(Engelhart et al., 2008)/ κ values (Petters and Kreidenweis, 2007)Water Soluble Organics: mean value for glutaric acid, malonic acid and Levoglucosan

Table 1. Molecular mass, density, molecular volume and κ for considered chemical components.

To study the sensitivity of hygroscopic growth to particle dry size, RH and composition, the hygroscopic growth model was used for seven different simulation cases (Table 2). The base case was defined to resemble the ambient conditions at Svalbard as closely as possible. The variations from the base case were studied by means of the ratio

$$R_{GF} = \frac{GF_{estimated\ for\ each\ case}\ (annual)}{GF_{estimated\ for\ the\ base\ case}\ (annual)} .$$

	Chemical composition	RH	D_d
Base case (ambient RH)	seasonal varying	ambient RH	measured
Dry case (no RH)	seasonal varying	no RH	measured
Case 1 (ammonium sulfate)	pure ammonium sulfate	ambient RH	measured
Case 2 (high RH)	seasonal varying	ambient RH +10%	measured
Case 3 (low RH)	seasonal varying	ambient RH-10%	measured
Case 4 (high D_d)	seasonal varying	ambient RH	measured+10%
Case 5 (low D_d)	seasonal varying	ambient RH	measured-10%

Table 2. The hygroscopic model and Mie scattering model simulation cases.

The Mie scattering model, MIEV0 by Wiscombe (1979) was used. To compare the cases outlined in Table 3 we used the ratio

$$R_{Sc} = \frac{Sc_{estimated\ for\ each\ case}\ (annual)}{Sc_{estimated\ for\ the\ base\ case}\ (annual)} .$$

The Santa Barbara DISORT (discrete ordinate) Atmospheric Radiative Transfer model was used for the radiative calculations (SBDART, Ricchiazzi et al., 1998) with the wavelength range of 0.25-4 µm. The model is used with different surface albedos.

RESULTS AND CONCLUSIONS

The calculated growth factors in RH=90% for the size range of 80-120 nm show a good agreement with the HTDMA (Hygroscopic Tandem Differential Mobility Analyser) measurements, see Table 3.

Season	Measurements (GF)	Hygroscopic model (GF)
Haze	1.7±0.1	1.74
Summer	1.7±0.06	1.77
Winter	1.9±0.08	1.89

Table 3. The hygroscopic model calculations and the measured GF at Zeppelin station during 2008.

The calculated scattering coefficient (Sc) at 550 nm were compared to the humidified nephelometer measurements during a 90 days campaign at Zeppelin station (Zieger et al., 2010) and the dry nephelometer measurements operated by Stockholm University ($RH < 20\%$), and a good correspondence between the measured and modelled scattering was observed at both the dry and the wet conditions (see Fig. 4).
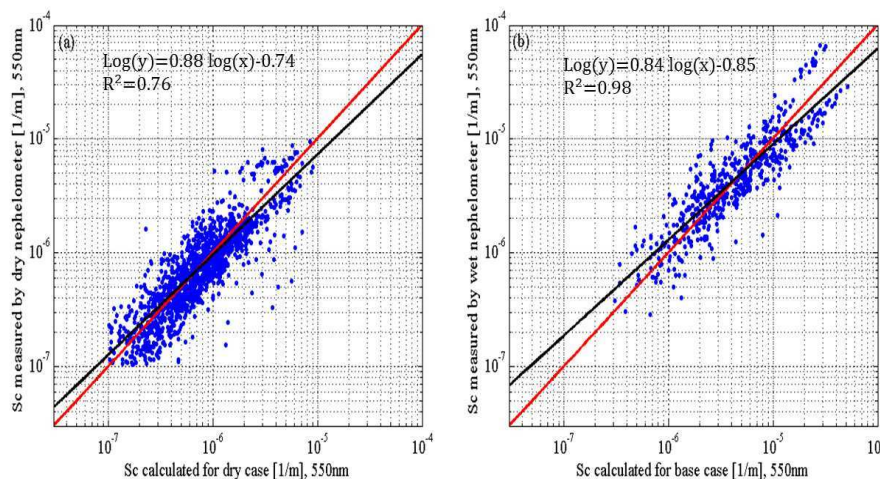
Fig.4. Hourly scattering coefficients (a) calculated for the dry case vs. dry nephelometer measurements. (b) calculated for the base case vs. wet nephelometer measurements during a campaign at the Zeppelin station (July 15th to October 12th, 2008). The red line is (y=x) and the black line is a fit to the data.

The calculated annual mean scattering coefficient was about 1.2×10^{-5} m^{-1}, and the annual mean growth factor GF was 1.56 ± 0.08. Considering the hygroscopic growth of aerosol particles in ambient atmosphere increases the scattering coefficient calculations by a factor of 4.2 ± 0.8, see Fig. 5. The annual mean radiative forcing calculated with measured surface albedo for the dry case was about -1.3 Wm^{-2} and for the wet case about -2.5 Wm^{-2}. The hygroscopic growth of aerosol particles results thus in almost two times larger negative forcing on the surface as compared with the dry case.

A clear seasonal trend was observed in the scattering coefficient (Fig. 5). Minimum values during the summer season, related to the domination of small aerosol particles (< 100nm), are followed by a moderate increase towards the winter, which coincides with the presence of more hygroscopic sea salt fraction with higher scattering efficiency (Fig. 3). The maximum scattering is observed during the haze season, associated with the increase in the concentration of > 100 nm particles (Fig. 2).
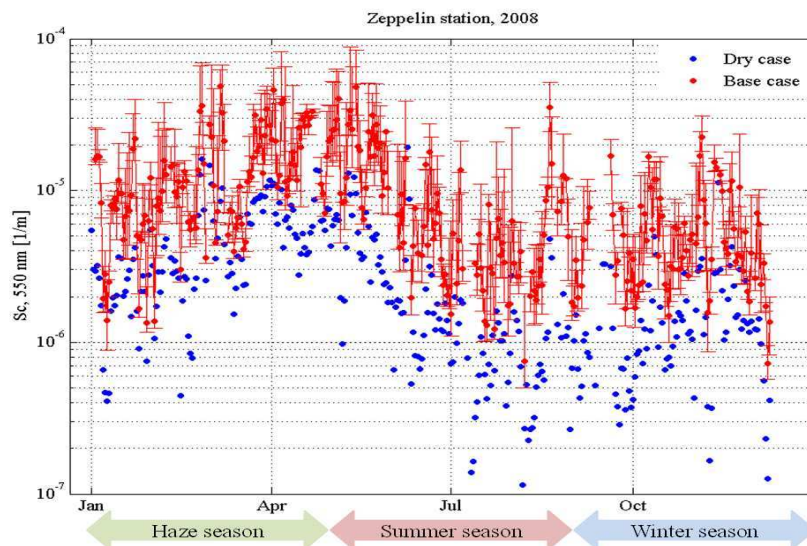
Fig.5. The daily calculated scattering coefficient (Sc) for the base case and the dry case at $\lambda = 550$ nm. At Zeppelin station during 2008.

Sensitivity of GF and SC to aerosol properties was studied using R_{GF} and R_{Sc}. Increasing the RH by 10% increases the annual mean Sc by 45%. Increasing the dry size of the particle by 10% increases the annual mean Sc by 36%. Replacing the seasonally varying chemical composition by pure ammonium sulfate decreases the annual Sc by only 10%. We thus conclude that the pin down of the aerosol optical properties, the size distribution and ambient relative humidity are critical to know with good accuracy.

REFERENCES

Engelhart, G.J. et al. Atmos. Chem. Phys. Discuss., 8, 95.

Fitzgerald, J. W., 1975, J. appl. Met., 14, 1044.

Koehler, K. A. et al. 2006, Atmos. Chem. Phys., 6, 795.

Petters, M. D., Kreidenweis, S. M., 2007, Atmos. Chem. Phys., 7, 1961.

Pilinis, C. et al., 1995, J. Geophys. Res., 100, 18739.

Richiazzi, P. et al. 1998, B. Am. Meteorol. Soc., 79, 2101.

Svenningsson, B. et al., 2006, Atmos. Chem. Phys., 6, 1937.

Wiscombe, W., 1979, Mie scattering calculations: Advances in technique and fast, vector speed computer codes, NCAR Technical Note NCAR/TN-140+STR, available from National Technical Information Service as NTIS PB 301388.

Zieger, P. et al. 2010, Atmos. Chem. Phys., 10, 3875.

KINETICS OF OXYGENATED CARBON CENTERED FREE RADICAL REACTIONS (CH$_2$OH, CH$_3$CHOH, CH$_2$CH$_2$OH AND CH$_3$OCH$_2$) WITH NO AND NO$_2$

M.P. RISSANEN[1,2] and R.S. TIMONEN[1]

[1]Laboratory of Physical Chemistry, Department of Chemistry, University of Helsinki, P.O. Box 55 (A.I. Virtasen aukio 1), FIN-00014 Helsinki, Finland

[2]Department of Physics, University of Helsinki, P.O.Box 64, FIN-00014 Helsinki, Finland

Keywords: Fundamental experimental radical kinetics, hydroxyalkyl radicals in combustion and atmosphere, photoionization mass spectrometry.

INTRODUCTION

Several oxygenated carbon centered free radical reactions with NO and NO$_2$ have been studied in direct time-resolved experiments. The reactions were investigated in temperature controlled tubular flow reactors connected to UV-laser photolysis and resonance gas lamp photoionization mass spectrometer (LP-PIMS) (Eskola and Timonen 2003).

The studied reactions were selected based on the sparse previous knowledge on their rate parameters and because of their probable relevance to energy production from alternative fuels. The investigation also concerns the reactions of three isomeric C$_2$H$_5$O species (CH$_3$CHOH, CH$_2$CH$_2$OH, and CH$_3$OCH$_2$), which could have theoretical interest as the radicals have the same molecular formula (C$_2$H$_5$O) but differ in their structural properties. From these, only the CH$_3$CHOH + NO reaction has been measured previously (Miyoshi et al. 1989) at room temperature and low pressure (2-4 Torr) using similar methods as in the present experiments.

Due to the growing need to decrease fossil fuel consumption (IPCC 2007), there is a sought for new "greener" fuel replacements and additives. Two possible candidates, that have received considerable attention, are ethanol (CH$_3$CH$_2$OH) (Goldemberg and Guardabassi 2009), currently the most used biofuel, and dimethylether (CH$_3$OCH$_3$) (Semelsberger et al. 2006). The abovementioned radicals can be formed from these in simple hydrogen abstraction reactions by the reactive species present (OH, Cl, etc.) and in this way the study may have some industrial importance as well.

METHODS

Reactions were studied in 6 to 17 mm i.d. tubular flow reactors with temperature control and pulsed UV laser photolysis (193 nm) along the axis of the reactor. To probe the time behavior of the produced radical concentrations in the gas mixture, the reactor was connected to a resonance gas lamp photoionization mass spectrometer through a small hole in the wall of the reactor. The schematic of the apparatus used is shown in Figure 1. All of the reactions were investigated at low pressures (0.5 to 10 Torr He) and under pseudo-first order conditions ([Reactant] >> [R]$_0$), which enabled us to isolate and study the reactions of interest with minimal interference from secondary chemistry.
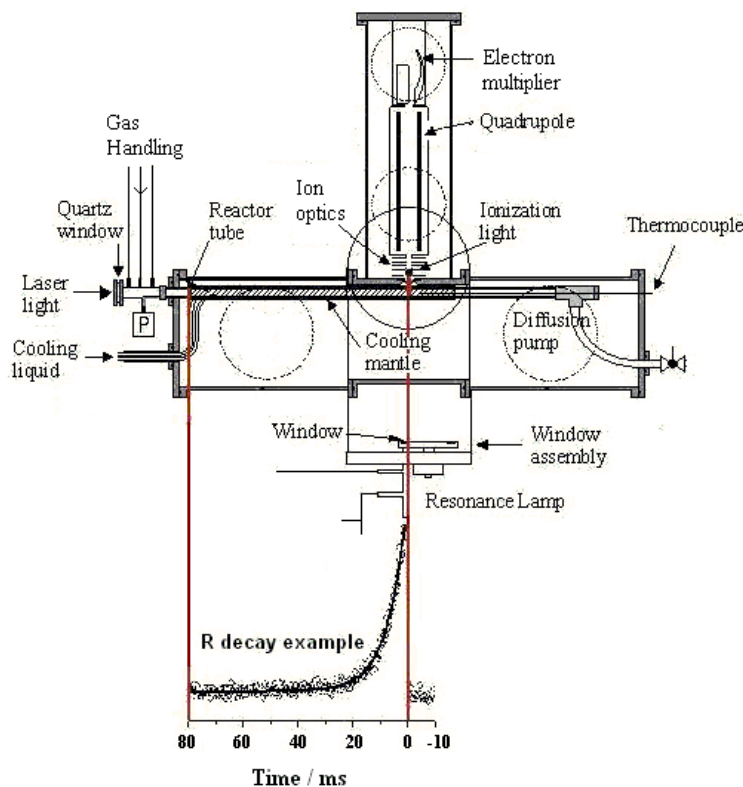
Figure 1. Schematic of the experimental apparatus used (Eskola and Timonen 2003).

The radicals were generated in direct photolysis reactions of suitable precursor species. For example, acetoin ($CH_3CHOHC(O)CH_3$) was used to produce the α-hydroxyethyl radicals (CH_3CHOH):

$$CH_3CHOHC(O)CH_3 + h\nu \text{ (193 nm)} \rightarrow CH_3CHOH + CH_3CO \qquad (1)$$
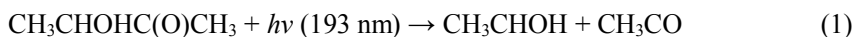
The initial radical concentrations of the experiments were estimated from gas flow rates, precursor vapour pressure at the precursor temperature, laser fluences and absorption cross section at 193 nm. If these parameters were not available, the initial radical concentrations were estimated from the precursor photodecomposition signal. Initial radical concentrations were estimated to be close to 1×10^{11} cm^{-3} in most of the measurements, and in the range 3×10^{10} cm^{-3} < $[R]_0$ < 1×10^{12} cm^{-3} in all of the measurements.

Selective ionization of the radicals and products was achieved using resonance gas discharge lamps by combining a specific lamp gas with a suitable window filter material. The kinetic experiments were performed using a Xe-lamp with a sapphire window or a Cl-lamp with a CaF$_2$-window, producing 8.4 eV or 9.1 eV radiation, respectively. In seeking the products, also H- (10.2 eV) and Ne-lamps (16.9 eV) with MgF$_2$ and CHS (Collimated hole structure plate) filters, respectively, were applied.

The radical signals, recorded under pseudo-first order conditions, could be described by a single exponential function $[R]_t = [R]_0 \times \exp(-k't) + a_0$, where $[R]_t$ is the radical signal at time t, k' is the pseudo-first-order rate coefficient describing the time dependence of the decaying radical concentration and a_0 is the pre-photolysis background signal. The bimolecular rate coefficients $k(R + NO)$ and $k(R + NO_2)$ were then obtained from the observed pseudo-first-order rate coefficients (k') according to a linear equation $k' = k(R + X) \times [X] + k_{wall}$ (Figure 2). In this equation, k_{wall} is the loss rate of the radicals in the reactor without added reactant X, k' is the rate coefficient obtained from the single exponential fitting, $[X]$ is the reactant (NO or NO$_2$) concentration and $k(R + X)$, the slope of the plot, is the bimolecular rate coefficient of the studied reaction.

551
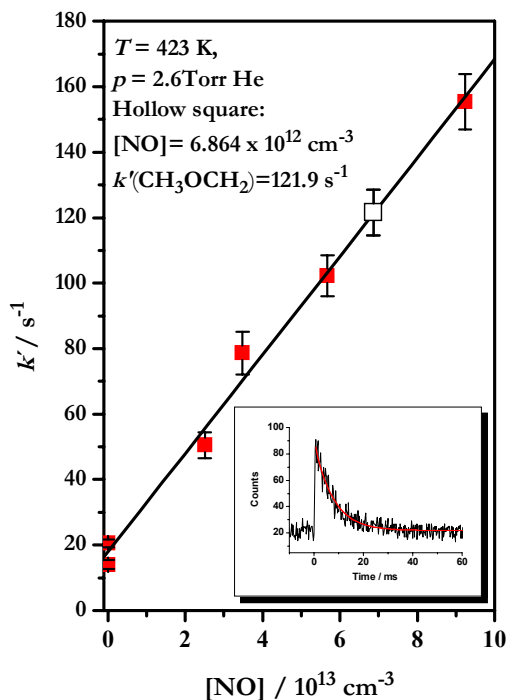
Figure 2. An example of a plot used to determine the bimolecular rate coefficient of the $CH_3OCH_2 + NO_2$ reaction. The inset shows a typical CH_3OCH_2 radical decay trace recorded in the measurements under the conditions of the hollow square in the plot.

An expression $k(T) = k_{300K}(T/300 \text{ K})^{-n}$ was fit to the temperature dependences observed in the R + NO$_2$ and CH_3OCH_2 + NO reaction rate coefficients (Figure 3). However, In the CH_3CHOH and CH_2OH reactions with NO, a clear curvature over this single exponential expression was observed and hence another parameter needed to be adopted for the equation, i.e. $k(T) = A \times (T/300 \text{ K})^{-n} \times \exp(B/T)$, to be able to express the results obtained.
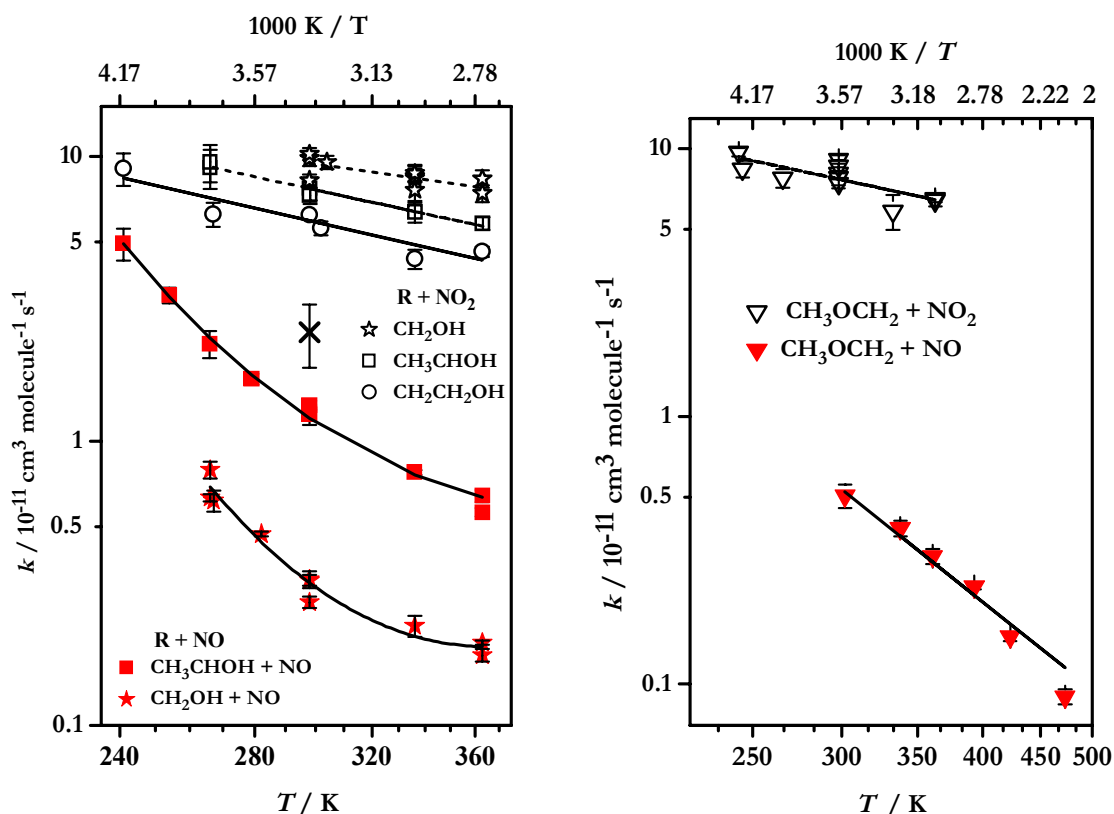
Figure 3. The R + NO and R + NO$_2$ rate coefficients determined in the current study shown as a function of temperature. Included is the previous determination of the CH$_3$CHOH + NO reaction at 298 K by Miyoshi et al. (Miyoshi 1989) shown with an x-symbol.

DISCUSSION

The determined R + NO and R + NO$_2$ rate coefficients are shown in Figure 3. All of the determined rate coefficients are fairly fast and display negative temperature dependence, that is, they speed up when temperature is lowered. This is typical for barrierless radical-radical addition reactions, where reaction collision cross section increases with decreasing temperature. Note that NO and NO$_2$ are also formally radical species with their unpaired valence electrons. Also the common trend observed previously, that R + NO$_2$ reactions are generally faster than R + NO reactions (Manion 2008), is observed again in the current results.

The CH$_3$CHOH + NO reaction rate coefficient determined by Miyoshi et al. (Miyoshi 1989) is in good agreement with the results obtained in the present investigation (see Figure 3). Similar comparison cannot be made with the rest of the reactions as the data for these is not available. All of the rate coefficients determined here are fast and can present a notable loss process for these radicals especially under combustion conditions and in highly polluted environments.

ACKNOWLEDGEMENTS

REFERENCES

Eskola, A. J., Timonen, R. S. (2003) Kinetics of the reactions of vinyl radicals with molecular oxygen and chlorine at temperatures 200–362 K. *Phys. Chem. Chem. Phys.,* **5**, 2557.

Goldemberg, J., Guardabassi, P. (2009) Are biofuels a feasible option? *Energy Policy,* **37**, 10.

IPCC, Intergovernmental Panel on Climate Change. (2007) http://www.ipcc.ch/.

Manion, J. A.; Huie, R. E.; Levin, R. D.; Burgess Jr., D. R.; Orkin, V. L.; Tsang, W.; McGivern, W. S.; Hudgens, J. W.; Knyazev, V. D.; Atkinson, D. B. et al. NIST Chemical Kinetics Database, NIST Standard Reference Database 17, Version 7.0 (Web Version), Release 1.4.3, Data version 2008. 12, (2008) National Institute of Standards and Technology, Gaithersburg, Maryland, 20899-8320. Web address: http://kinetics.nist.gov/

Miyoshi, A., Matsui, H., Washida, N. (1989) Reactions of hydroxyethyl radicals with oxygen and nitric oxide. *Chem. Phys. Lett., 160,* 291.

Semelsberger, T. A., Borup, R. L., Greene, H. L. (2006) Dimethyl ether (DME) as an alternative fuel. *J. Power Sources,* **156**, 497.

POSSIBLE LINKS BETWEEN UPPER TROPOSPHERIC HUMIDITY AND AEROSOLS

L. RIUTTANEN[1], M. BISTER[1], V. JOHN[2], M. DAL MASO[1], J. RÄISÄNEN[1], G. DE LEEUW[1,3] and M. KULMALA[1]

[1] Department of Physics, University of Helsinki, Finland.

[2] Met Office Hadley Centre, Exeter, UK.

[3] Finnish Meteorological Institute, Helsinki, Finland.

Keywords: aerosol-cloud interactions, remote sensing.

INTRODUCTION

Aerosols are a main source of uncertainty in our understanding of the current climate change. Especially their complex interactions with clouds and their effect to circulation of water are of high interest in climate research (Ramanathan et al., 2001; Tao et al., 2012). As water vapour is the most important greenhouse gas, any changes in its distribution are of great importance to climate (Held and Soden, 2006).

Main sources of aerosol particles are on the surface, and therefore aerosols are mainly located in the boundary layer. However, there may be a physical connection between humidity in the upper troposphere and aerosols when aerosols alter cloud microphysics in deep convection. To study this we have looked at aerosol optical depth (AOD) and upper tropospheric humidity (UTH) data from Aqua satellite and found changes in UTH when comparing high and low aerosol loadings. However, correlation does not mean causality, and there are also other than direct physical mechanisms causing correlations between AOD and UTH. In this abstract we look at the possible explanations for the correspondence found in AOD and UTH data.

UPPER TROPOSPHERIC HUMIDITY AND AEROSOLS

We have analysed upper tropospheric humidity from HSB instrument onboard Aqua satellite together with aerosol optical depth from MODIS instrument onboard the same satellite (Remer et al., 2005). HSB (Humidity Sounder for Brazil) was a microwave humidity sounder that measured mean relative humidity from 500 to 200 hPa during 180 days from August 2002 to February 2003. A microwave method developed by Buehler *et al.* (2008) and John *et al.* (2011) enables us to detect humidities also in the areas of anvil clouds. Only data over oceans has been used in this study.

Differences in UTH in case of high and low AOD are noticeable in Figure 1. In general there is a positive relationship between aerosol loading and humidity. In some regions the relative humidity is even twice as high when AOD is between 0.2 and 0.6 as when AOD is below 0.2. However, there are also regions, especially at low latitudes, where the relation is the opposite; namely high AOD is associated with lower relative humidity.

Main possible explanations to the observed changes are:

Deep convection To the authors' knowledge, the only physical connection between upper tropospheric humidity and major aerosol sources at the surface, is deep convection. Aerosol effect on

555

UTH (0.2<AOD<0.6) / UTH (AOD<0.2), N>=10
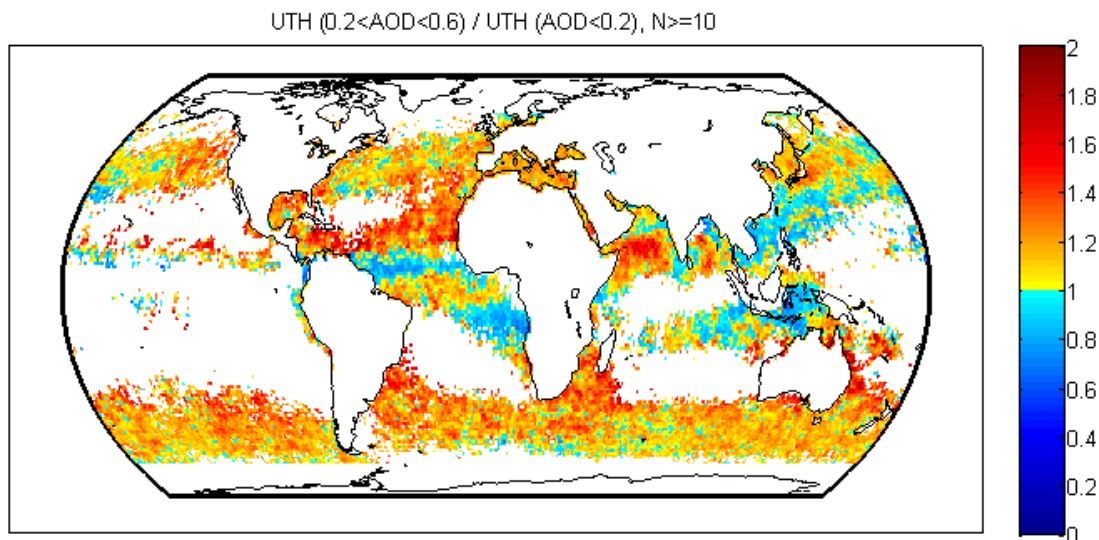
Figure 1: Change in upper tropospheric humidity (UTH) when aerosol optical depth (AOD) is high vs. low: UTH(0.2<AOD<0.6)/UTH(AOD<0.2). White areas are areas with less than 10 data points. The study is done over ocean only.

cloud microphysics has been studied recently and eg. Koren *et al.* (2005; 2010a) have found that clouds produce more extensive anvils in the presence of high aerosol loading. Bister and Kulmala (2011) propose that aerosols could affect the amount of water vapour left to upper troposphere after deep convection due to their effect on cloud microphysics leading to more ice precipitation and less warm rain.

Seasonality Seasonality in aerosol sources and general circulation pattern affect the result in Figure 1. Eg. biomass burning emissions are high during the dry season, when the descending motion is dominating and also upper troposphere is relatively dry. Seasonal patterns are likely to affect the results at least over the Atlantic west to Africa and perhaps also over the western Pacific.

Wet scavenging A negative connection is found between UTH and AOD in the area of the intertropical convergence zone (ITCZ). This can result from wet scavenging: when convection is most efficient, upper troposphere is humid and rain washes air from aerosols.

Meteorological patterns It is possible, that meteorological patterns affect both AOD and UTH causing spurious correlations (Koren et al., 2010). Convection in many regions is associated with convergence in the lower troposphere, which may cause an increase in AOD. The main meteorological parameter that has been noted to affect AOD is horizontal wind speed (Engström and Ekman, 2010), because the amount of sea salt is highly dependent on the wind speed. Also smoke and dust transport are governed by winds.

Cloud / humidity contamination of AOD data Aerosol optical depth and relative humidity have a strong connection. The effect may be both apparent and true - AOD detection is sensitive to high humidity, but aerosols also swell in humid conditions, especially hygroscopic aerosols, like sea

salt. However, as majority of aerosols are located in the lower troposphere, and we study humidity in the upper troposphere, we assume humidification effect not to be strong.

Cirrus contamination of AOD data may affect our results, as high cirrus concentration and high humidity are presumably connected. However, Kaufman *et al.* (2005) have estimated cirrus contamination in MODIS AOD data to be relatively small, 0.015 ± 0.003 at 0.55 m.

CONCLUSIONS

As all the mechanisms discussed above may affect the relation between aerosols and upper tropospheric humidity, it is challenging to separate the "real" microphysical effect of aerosols on upper tropospheric humidity.

Since this study covered only six months of data, definitely more data is needed to rule out purely seasonal effects on the analysis and to get statistically more significant results. To eliminate effect of meteorology to both AOD and UTH, the study should be done for binned vertical velocity classes separately. Satellite detections of deep convective clouds can be used to allocate our analysis to areas experiencing deep convection. In near future MetOp-A MHS UTH together with Terra/Aqua MODIS AOD will be analysed.

ACKNOWLEDGEMENTS

REFERENCES

Bister, M. and Kulmala, M. (2011) *Atm. Chem. Phys.*, vol. 11, no. 9, pp. 4577-4586.

Buehler, S., Kuvatov, M., John, V. O., Milz, M., Soden, B. J., Jackson, D. L., and J. Notholt (2008). *J. Geophys. Res.*, 113, D14110, doi:10.1029/2007JD009314.

Engström, A. and Ekman, A. M. L. (2010). *Geophys. Res. Lett.*, vol. 37, pp. L18814.

Held, I. M. and Soden, B. J. (2006). *J. Climate*, vol. 19, pp. 5686-5699.

John, V. O., Holl, G., Allan, R. P., Buehler, S. A., Parker, D. E. and Soden, B. J. (2011). *J. Geophys. Res.*, vol. 116, no. D14, pp. D14108.

Kaufman, Y., Remer, L., Tanre, D., Li, R., Kleidman, R., Mattoo, S., Levy, R., Eck, T., Holben, B., Ichoku, C., Martins, J. and Koren, I. (2005). *IEEE Transactions on Geoscience and Remote Sensing*, vol. 43, no. 12, pp. 2886-2897.

Koren, I., Kaufman, Y., Rosenfeld, D., Remer, L. and Rudich, Y. (2005). *Geophys. Res. Lett.*, vol. 32, no. 14, pp. L14828.

Koren, I., Remer, L. A., Altaratz, O., Martins, J. V. and Davidi, A. (2010). *Atmos. Chem. Phys.*, vol. 10, no. 18, pp. 8855-8872.

Koren, I., Feingold, G. and Remer, L. A. (2010). *Atmos. Chem. Phys.*, vol. 10, no. 10, pp. 5001-5010.

Ramanathan, V., Crutzen, P., Kiehl, J. and Rosenfeld, D. (2001). *Science*, vol. 294, no. 5549, pp. 2119-2124.

Remer, L., Kaufman, Y., Tanre, D., Mattoo, S., Chu, D., Martins, J., Li, R., Ichoku, C., Levy, R., Kleidman, R., Eck, T., Vermote, E. and Holben, B. (2005). *J. Atmos. Sci.*, vol. 62, no. 4, pp. 947-973.

Tao, W., Chen, J., Li, Z., Wang, C. and Zhang, C. (2012). *Rev. Geophys.*, vol. 50, pp. RG2001.

EVAPORATION AND CONDENSATION OF SEMIVOLATILE COMPOUNDS IN CCN-COUNTER

S ROMAKKANIEMI[1], A. LAAKSONEN[1,2], and T. RAATIKAINEN[2,3]

[1]Department of Applied Physics, University of Eastern Finland, Finland
[3]Finnish Meteorological Institute, Climate change, Helsinki, Finland
[3]School of Earth and Atmospheric Sciences, Georgia Institute of Technology, Atlanta, Georgia, USA

INTRODUCTION

Depending on the temperature, relative humidity and aerosol particle composition, semivolatile compounds can be found from the gas or particle phase in the atmosphere. Usually low temperature and high relative humidity, which increases liquid water content in the aerosol particles making them more dilute, favour partitioning to particles as both decrease effective Henry's law coefficient of gases.

Bahaviour of semivolatile compounds causes problems for both modellers and experimentalists. Beyond the condition dependent partitioning between the gas and particles, also the partitioning between particles of different size and composition needs be taken into account to fully address the effect of semivolatiles in direct and indirect aerosol forcing. For example, it has been shown in several modelling studies that semivolatile compounds enhance cloud droplet formation as they increase water soluble mass in particles before cloud droplet formation (Kulmala et al. 1993, Laaksonen et al. 1998, Romakkaniemi et al. 2005a). However, the effect is strongly dependent on the timescales available for condensation before maximum supersaturation is exceeded in the cloud base (Romakkaniemi et al. 2005b). Similarly the semivolatile compounds need to be carefully taken into account when the hygroscopic properties of particles are measured. This might be an issue for example in the measurements of aerosol hygroscopicity with the HTDMA. In the measurements ambient aerosol is first dried before it is size selected in the first DMA, and depending on the conditions, some of the semivolatiles might evaporate, and part of them might stay in the dry aerosol during water evaporation. After that aerosol is wetted, and depending on the relative humidity some semivolatiles might condense back to aerosol or they might condense on the walls of the instrument depending on the design of humidifier. Thus the hygroscopicity measured might be different than the actual hygroscopicity in the ambient air.

In this work we are studying how semivolatile compounds, especially ammoniumnitrate, behave in the CCN-counter. We will show that in the case of small particles, the evaporation rate is fast enough to affect the CCN-activity of particles containing high mass fraction of ammoniumnitrate. On the other hand we will show that with ambient concentrations the condensation of semivolatiles from gas to aerosol phase inside the CCN-column is not fast enough to affect CCN-activity of particles, but in the laboratory conditions with high concentration this might be an issue.

METHODS

To simulate condensation/evaporation dynamics of aerosol particles inside the CCN-column in the DMT-type CCN-counter, we have used a fluid dynamics model to calculate temperature and gas concentration profiles inside the CCN-column (Roberts and Nenes, 2005, Raatikainen et al., 2012), and a cloud parcel model (Kokkola et al., 2003, Romakkaniemi et al., 2005a) to simulate evaporation and condensation kinetics of aerosol particles more accurately. With this modelling setup we are able to study how the

semivolatiles are partitioned between the particles, gas phase and wetted walls in the CCN-column. The main assumption in the modelling is that the wetted walls act as an infinite sink for semivolatile gases, and with fluid dynamics model we are able to simulate spatial concentration of different gases in CCN-column and thus produce trajectories of particles in the column. These trajectories are used to run cloud parcel model to simulate time dependent partitioning with accurate thermodynamics.

RESULTS
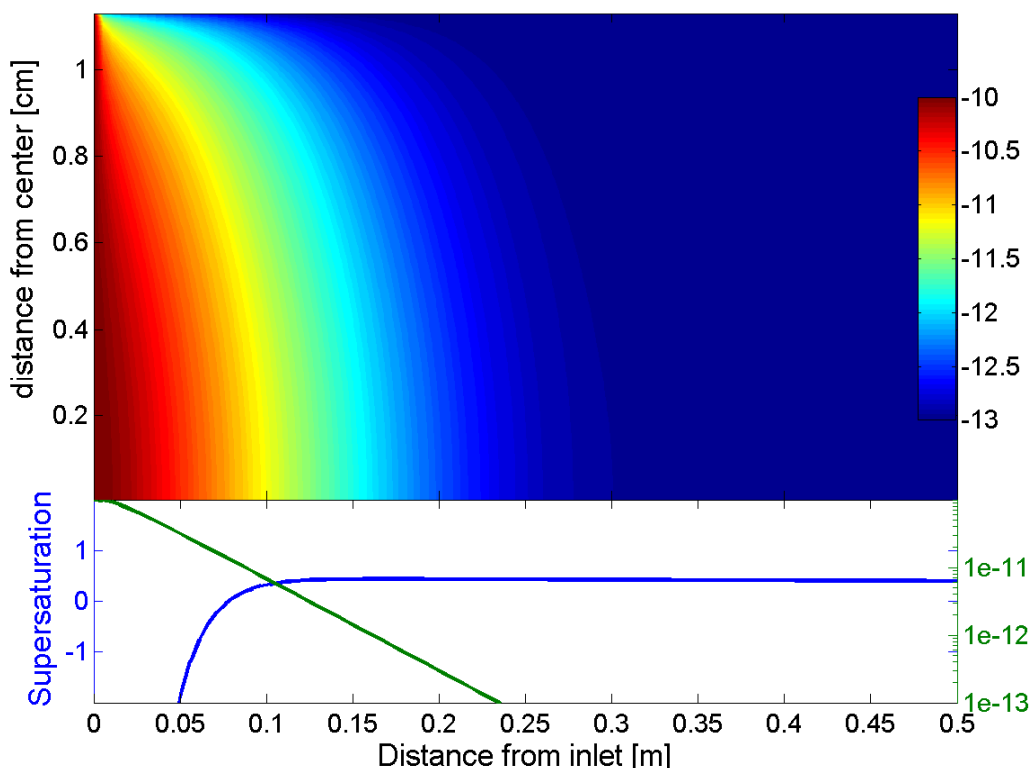
Figure 1. Upper panel: Gas phase concentration of nitric acid in the CCN-column. Lower panel: Gas phase concentration and water supersaturation in the centerline

From Figure 1 we can see the concentration of nitric acid inside the CCN-column. In the simulation we have assumed that the gas phase concentrations in the sample flow and in the sheet air are both 100ppt. It can be seen that before the water saturation reaches 1 (supersaturation 0) less than 10% of the gas phase concentration is left in the centerline (bottom in Figure 1) where aerosol particles are located. At maximum supersaturation this is decreased to ~1%. Based on this we can already conclude that with atmospheric concentrations having ppb levels of nitric acid at highest in the gas phase, the condensation of semivolatiles is not affecting CCN-results. Thus in the results presented in this abstract we concentrate more on the evaporation from aerosol before activation into cloud droplet.

Aerosol trajectories from centreline where fed to cloud parcel model, and dry sizes of particles are presented in the Figure 2 as a function of position in the CCN-column. In this case we have used aerosol particles composed mainly of ammoniumnitrate with 10% mass fraction of ammoniumsulphate. It can be seen that the evaporation of ammonia and nitrate decreases the size of all particles during the whole stay in the column. Naturally the evaporation is fastest before saturation reaches unity. After that evaporation slows done with particles growing to cloud particles. The size of the smallest particle activating is close to 51nm, but to activate these particles the initial dry size needs to be 63nm. Thus in this measurement the

activation potential of particles would have been underestimated, and the hygroscopicity would have been smaller than it would have been in the atmosphere where all semivolatiles would have condensed back to aerosol before cloud droplet formation.
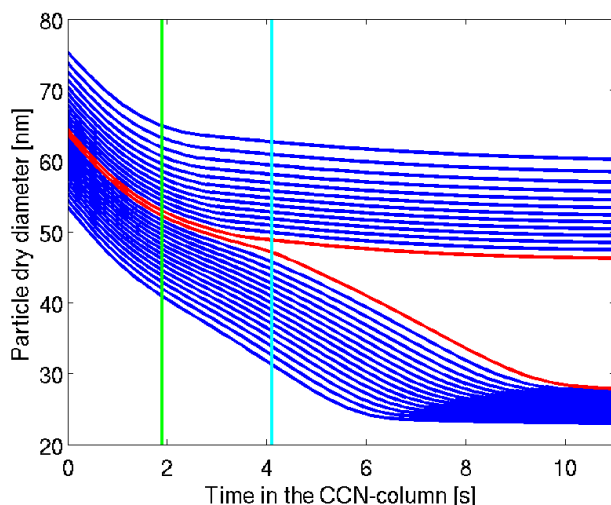
Figure 2. Dry size of particles composed of ammoniumnitrate (90mass%) and ammoniumsulphate (10mass%) inside the CCN-column. The particles closest to the activation limit are plotted with red lines. Also the times where S reaches 1 and maximum supersaturation are marked with green and cyan, respectively.

ACKNOWLEDGEMENTS

REFERENCES

Kokkola, H., S. Romakkaniemi, M. Kulmala, A. Laaksonen: A one-dimensional cloud model including trace gas condensation and sulfate chemistry. Boreal Environment Research, 8, 413-424, 2003.

Kulmala, M., A. Laaksonen, P. Korhonen, T. Vesala, T. Ahonen, J.C. Barrett: The effect of atmospheric nitric acid vapor on CCN activation. Journal of Geophysical Research (Atmospheres) 98, 22949-22958, 1993.

Laaksonen, A., P. Korhonen, M. Kulmala, R.J. Charlson: Modification of the Köhler equation to include soluble trace gases and slightly soluble substances. Journal of the Atmospheric Sciences 55, 853-862, 1998.

Raatikainen, T., Moore, R. H., Lathem, T. L., and Nenes, A.: A coupled observation – modeling approach for studying activation kinetics from measurements of CCN activity, Atmos. Chem. Phys., 12, 4227-4243, doi:10.5194/acp-12-4227-2012, 2012

Roberts, G. C. and Nenes, A.: A Continuous-Flow Streamwise Thermal-Gradient CCN Chamber for Atmospheric Measurements, Aerosol Sci. Tech., 39, 206–221, doi:10.1080/027868290913988, 2005.

Romakkaniemi, S., H. Kokkola and A. Laaksonen: The soluble trace gas effect on CCN activation: influence of initial equilibration on cloud model results. Journal of Geophysical Research (Atmospheres), 110:D15202 doi:10.1029/2004JD005364 , 2005b

Romakkaniemi S., Kokkola H. and Laaksonen A.Parameterization of the nitric acid effect on CCN activation. Atmos Chem Phys 5 879-885. SRef-ID: 1680-7324/acp/2005-5-879, 2005a

STUDYING THE LONG-TERM ACCUMULATION OF BLACK CARBON IN THE EUROPEAN ARCTIC

M. RUPPEL[1], E. ISAKSSON[2] and A. KORHOLA[1]

[1]Department of Environmental Sciences, University of Helsinki, Helsinki, Finland

[2]Norwegian Polar Institute, Tromsø, Norway

INTRODUCTION

Black carbon (BC) is a combustion derived aerosol with strong climate warming impacts in the Arctic (e.g. Baron et al., 2009). The role of BC in the regulation of Arctic climate and ecosystems is significant but still poorly understood. The origin, transportation, deposits and climate effect of BC is currently being studied e.g. by snow and satellite measurements (e.g. Hegg et al., 2009; Doherty et al., 2010). However, there has been only one publication on its long-term accumulation in the Arctic using the ice cores taken from the Greenland Ice Sheet. Information on the long-term accumulation of BC can unravel its climate effect in the past and help to make projections for future effects.

In addition to snow, satellite and ice core measurements, the deposition and accumulation of BC can be determined from lake sediments. Lake sediments are particularly important as a tool in retracing the deposition distribution history of BC, which can be made by their means with a 2-5 years resolution for hundreds and thousands of years into the past. When studying the accumulation of BC from archives it has to be kept in mind that at a specific point in space, local conditions, such as wind directions, topography and precipitation, can strongly affect the deposition. Thereby to get an overall view on the deposition of BC in the Arctic studies have to be conducted at various locations. While ice sheets are extremely valuable as archives of atmospheric pollutant deposition histories and record the concentrations with seasonal resolution for thousands of years, they are only found on very restricted areas in the Arctic. E.g. the Greenland ice sheet predominantly records the emission history of North America and partly Europe (McConnell et al., 2007) so that emissions from Asia have been left unresolved. Lake sediments however can be found all around the Arctic and thereby play an irreplaceable role in depicting the emission and deposition history of BC in the Arctic and beyond.

The aim of this project is to quantify the BC concentration in the European Arctic during the industrial era from lake sediments and assess its climate impact especially in connection to lake ice cover duration dynamics. In addition methods commonly used for BC measurements in lake sediments are tested for ice core samples in order to improve the comparability of results from these different archives.

METHODS

BC quantification
BC is not a specifically determined chemical component. Rather, the term is an operational one, dependent on the particular method of measurement (Goldberg, 1985). Traditionally BC is divided into char and soot BC but there are several subdivisions in the BC continuum (see Table 1).

Table 1. The black carbon combustion continuum. (Insprired by Masiello, 2004)

	Slightly charred biomass	Char	Charcoal	Spheroidal carbonaceous particles (SCP)	Soot BC	Graphite
Formation T	low	→→→→→→→→→→→→→→→			high	
Size	mm and larger		mm to µm	µm	nm	
Composition and formation	residue of burnt material (biomass and coals)			residue of fossil fuel combustion	combustion condensate	
Drift range	short (meters)		short (m to km)	intermediate (km to 1000s of km)	long (up to several 1000s of km)	

The methods for BC quantification are different between different matrices (e.g. atmosphere, snow, ice cores and sediments) and research groups, which makes comparison between these challenging. In order to ultimately infer the atmospheric and snow concentrations of BC in the past as well as its climate impact from lake sediments the BC content should be measured with same methods from all these matrices.

Here the BC concentration of four lakes from continental northern Europe will be compared with BC concentrations from a lake sediment core in Svalbard for the industrial era. The quantification will be made with three different methods:

1. Chemical extraction of Spheroidal Carbonaceous Particles (SCP), which result from fossil fuel combustion at high temperatures (Rose, 1994)
2. Chemothermal Oxidation at 375 °C (CTO-375 –method) for high refractory soot BC (Gustafsson et al., 1997, 2001)
3. Thermal Optical Transmittance (TOT) for elemental carbon (EC) (Chow et al., 1993)

The first two methods have been specifically developed for BC analysis from lake sediments, but both work for atmospheric samples as well (e.g. Zencak et al., 2007). However, they measure partially different parts of the BC combustion continuum, focusing on the high refractory part (see Table 2). The TOT method on the other hand, which quantifies a broader spectrum of BC (Tab. 2), has been originally developed for aerosol samples (Chow et al., 1993) but has been extended to be applicable also for snow samples (e.g. Forsström et al., 2009). The TOT method has also been converted for the purposes of sediment analysis (Husain et al., 2008) but this development is still continuing and the application may entail significant error sources.

Table 2. The analytical ranges of the methods used for BC quantification. The dashed lines indicate the uncertainty in the range of the BC continuum which each method measures. (Inspired by Hammes et al., 2007)

	Slightly charred biomass	Char	Charcoal	Spheroidal carbonaceous particles (SCP)	Soot BC
SCP analysis				———	
CTO-375			---------------———————----		
TOT/R		----———————————————----			

The TOT method seems to be most promising as a linking method between the different matrices. Therefore its application on ice core samples will be tested for samples from Svalbard. Also the CTO-365 method will be tested for the same ice samples. If the methods prove to be applicable for ice core samples further analysis of full ice core records from Svalbard for the last 200 years could be commenced and compared with the lake sediment results.

Calibration with atmospheric measurements

The past BC concentrations will be calibrated with atmospheric measurements. This will be made at a site in northern Finland (Utsjoki), where Professor Liaquat Husain (New York State Department of Health, USA) has undergone aethelometer measurements of atmospheric BC concentrations since 1963. He has developed a method of transferring the BC from the aethelometer filters to filters used in TOT measurements (Husain et al., 2008). These results will be compared to TOT results of BC concentrations from a nearby lake for the last 50 years.

Assessment of the climate impact of BC in the past

The deposition histories of BC in the Fennoscandian Arctic will be compared to meteorological time series of air temperatures and different kind of ice phenological data sets which refer to the formation and melting dynamics of lake ice (Prowse et al., 2011). Ice phenology can be reconstructed from lake sediments with help of diatom species analysis since different species are present and abundant in lakes depending on the length of the ice free season (Weckström et al., submitted). In Arctic lakes significant diatom species composition changes have been recorded and these are thought to be connected to variations ice phenology (Smol et al., 2005). According to the hypotheses of this study BC has strongly contributed to these variations by affecting the melt and freeze dynamics of Arctic lakes. The objective is to compare if these hitherto unexplained variations coincide with variations of BC concentrations which are not directly linked to climate. This way it is possible to study how BC affects the ice dynamics and starts a feedback process along with climate warming resulting in hastening ice melt and increasing air temperatures.

CONCLUSIONS

The project will strengthen our understanding on the past variations in BC concentrations in the Arctic, test new methods for BC quantification from different matrices and thereby enhance comparability of BC concentration results from different kind of studies. In addition the work will shed light on the sources, e.g. though the SCP analysis, and environmental impacts of BC in the past.

ACKNOWLEDGEMENTS

REFERENCES

Baron, R.E., Montgomery, W.D. & Tuladhar, S.D. (2009) An analysis of black carbon mitigation as a response to climate change. Copenhagen Consensus on Climate, CRA International, Washington DC.

Chow, J., Watson, J.G., Pritchett, L.C., Pierson, W.R., Frazier, C.A. & Purcell, R.G. (1993) The DRI Thermal/Optical Reflectance carbon analysis system: Description, evaluation and applications in U.S. air quality studies. Atmos. Environ., Part A **27**: 1185-1201.

Doherty, S.J., Warren, S.G., Grenfell, T.C., Clarke, A.D. & Brandt, R.E. (2010) Light absorbing impurities in Arctic snow. Atmos. Chem. Phys. **10**: 11647-11680.

Forsström, S., Ström, J., Pedersen, C.A., Isaksson, E. & Gerland, S. (2009) Elemental carbon distribution in Svalbard snow. J. Geophys. Res. **114**, D19112, doi: 10.1029/2008JD011480.

Goldberg, E.D. (1985) Black Carbon in the Environment. John Wiley & Sons. New York. 198pp.

Gustafsson, Ö., Haghseta, F., Chan, C., Macfarlane, J. & Gschwend, P.M. (1997) Quantification of the dilute sedimentary soot phase: Implications for PAH speciation and bioavailability. Environ. Sci. Technol. 31: 203-209.

Gustafsson, Ö., Bucheli, T.D., Kukulska, Z., Andersson, M., Largeau, C., Rounzaud, J-N., Reddy, C.M. & Eglinton, T.I. (2001) Evaluation of a protocol for the quantification of black carbon in sediments. Glob. Biogeochem. Cycles 15: 881-890.

Hammes, K., et al. (2007) Comparison of quantification methods to measure fire-derived (black/elemental) carbon in soils and sediments using reference materials from soil, water, sediment and the atmosphere. Global Biogeochem. Cycles **21**, GB3016, doi: 10.1029/2006GB002914.

Hegg, D.E. (2009) Source attribution of black carbon in Arctic snow. Environ. Sci. Technol. 43:4016-21.

Husain, L., Khan, A.J., Ahmed, T., Swami, K., Bari, A., Webber, J.S., Li, J. (2008) Trends in atmospheric elemental carbon concentrations from 1835 to 2005. J. Geophys. Res. 113: D13102.

Masiello, C.A. (2004) New directions in black carbon organic geochemistry. Marine Chemistry **92**: 201-213.

McConnell, J.R. et al. (2007) 20th century industrial black carbon emissions altered arctic climate forcing. Science 317: 1381-1384.

Prowse, T., Alfredsen, K., Beltaos, S., Bonsal, B., Duguay, C., Korhola, A., McNamara, J., Pienitz, R., Vincent, W., Vuglinsky, V. & Weyhenmeyer, G. (2011). Past and future changes in lake and river ice. Ambio 40: 53-62.

Rose, N.L. (1994) A note on further refinements to a procedure for the extraction of carbonaceous fly-ash particles from sediments. J. Paleolimn. 11: 201-204.

Smol, J.P., Wolfe, A.P., Birks, H.J.B., Douglas, M.S.V., Jones, V.J., Korhola, A., et al. (2005) Climate-Driven Regime Shifts in Arctic Lake Ecosystems. Proc. Nat. Acad. Sci. (PNAS) 102:4397-4402.

Weckström, J., Hanhijärvi, S., Forsström, L., Kuusisto E. & Korhola, A. (2011). Historical lake ice dynamics in subarctic Fennoscandia. Submitted to Geophysical Research Letters.

Zencak, Z., Elmquist, M., Gustafsson, Ö. (2007) Quantification and radiocarbon source apportionment of black carbon in atmospheric aerosols using the CTO-375 method. Atmos. Environ. **41**: 7895-7906.

MODEL STUDY ON THE PROPERTIES OF CONDENSING VAPOURS

A. RUSANEN[1], M. BOY[1], D. MOGENSEN[1,2] and S. SMOLANDER[1]

[1]Department of Physics, P.O. Box 48, University of Helsinki, 00014, Finland.
[2] Helsinki University Centre for Environment, P.O. Box 27, University of Helsinki, 00014, Finland

Keywords: aerosol dynamics, organic aerosols, aerosol modelling

INTRODUCTION

Detailed modelling of aerosol growth is possible with a variety of methods. In some cases it may be even possible to do all calculations analytically. Despite this, applying these models into non-trivial situations is not simple. This study tries to illustrate the sensitivity of an aerosol model to changes in input parameters.

In a simple chamber experiment the amount of produced compounds can be large. Same is true for more complicated setups, as encountered in field studies (Fuentes *et al.*, 2000). One must be able to predict the properties of these compounds, and mixtures of them, to determine their fluxes between the gas medium and particles. However measurement data is nonexistent for some compounds (Poling *et al.*, 2001). There are some methods to estimate these properties, for example those presented by Topping *et al.* (2007) , Nannonaal *et al.* (2008) and Poling *et al.* (2001). As they have explained, these estimates have errors. How does this affect the modelled results?

METHODS

This study used a simple fixed section aerosol model, University of Helsinki Aerosol Model (Korhonen *et al.*, 2004) now on abbreviated as UHMA, to model an initially monodisperse distribution of pure sulfuric acid particles.

The model included three vapours, sulfuric acid and two generic vapours. Vapour loss was not considered and the modelled situation was continuous growth, which means no evaporation happened in any of the model runs. The processes considered were condensation and coagulation.

The input values for temperature, pressure and the physical properties of one generic vapour were varied. In this study, this was done one variable at a time. The growth of the particles and the final state of the distribution after 24 hours of growth were observed.

CONCLUSIONS

The results of this study show that change in parameters of one vapour can, under some circumstances, have noticeable effects on the total aerosol distribution properties and the distribution of compounds within the aerosol. This also suggests that the effects of any possible errors in parameters may be significant. This study used a very wide range of parameters simply to see how large the effect could be. It should also be noted that the results of this study are specific to the modelled situation and numerical approach and thus they cannot directly be applied to other situations.

In the future we aim to extend on this study by modelling chamber experiments with explicit chemistry and vapour property determination by several methods.
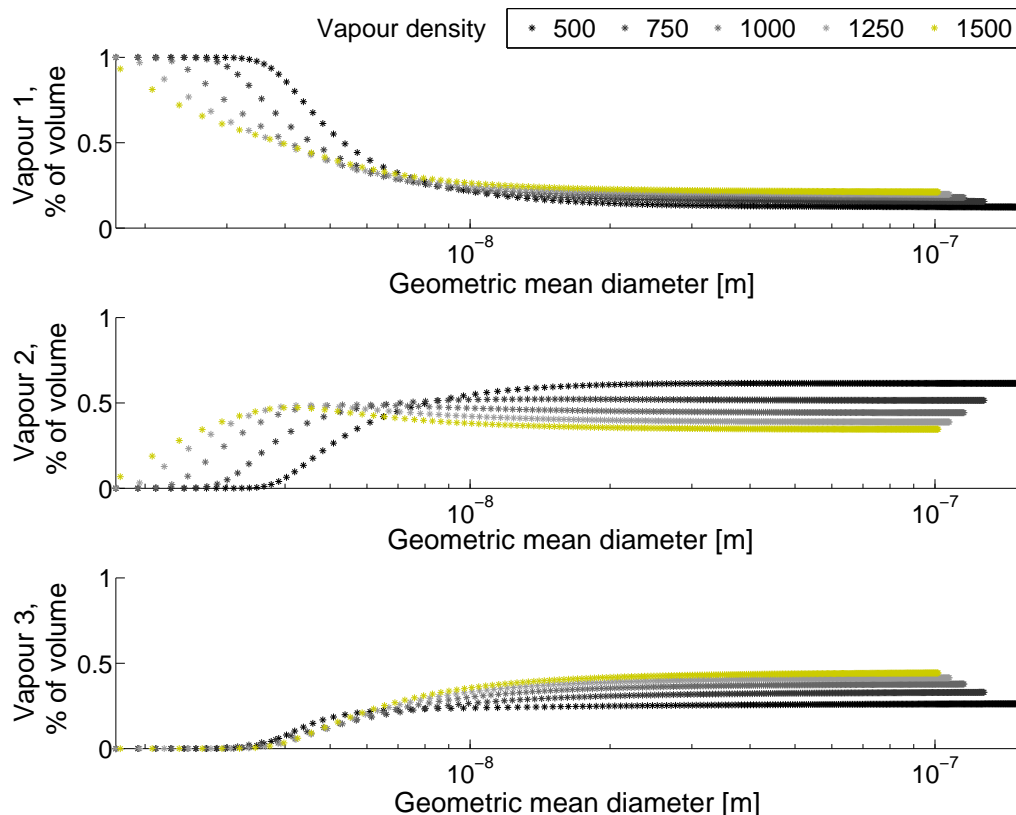
Figure 1: As an example of the results, the effect of variations in the density of vapour 2 are shown. Vapour 1 is sulfuric acid. The unit of vapour density is kg/m^3. The total aerosol volume fraction is shown as a function of the geometric mean diameter of the whole aerosol distribution. Each colour is a 24-hour simulation, where the points correspond to a different time. The values were calculated at constant time intervals. Since there is continuous growth, larger diameter means a later instant in time. This applies only within the same simulation. The delayed onset of condensation of vapour 2 is caused by the the kelvin effect. The figure also shows that higher vapour density reduces the total growth.

REFERENCES

Fuentes, J. D., Lerdau, M., Atkinson, R., Baldocchi, D., Bottenheim, J. W., Ciccioli, P., Lamb, B., Geron, C., Gu, L., Guenther, A., Sharkey, T. D., and Stockwell, W. (2000) Biogenic hydrocarbons in the atmospheric boundary layer: A review *Bulletin of the American Meteorological Society*, **81**, 1537-1575

Korhonen, H., Lehtinen, K.E.J. and Kulmala, M. (2004). Multicomponent aerosol dynamics model UHMA: model development and validation *Atmos. Chem. Phys.*, **4**, 757-771

Nannoolal, Y., Rarey, J., and Ramjugernath, D. (2008). Estimation of pure component properties - Part 3. Estimation of the vapor pressure of non electrolyte organic compounds via group contributions and group interactions *Fluid Phase Equilibria*, **269**, 117-133

Poling, B.E., Prauznitz, J.M and O'Connel J.P, (2001). *The properties of gases and liquids* 5th ed. (McGraw-Hill, New York)

Topping, D. O., McFiggans, G. B., Kiss, G., Varga, Z., Facchini, M. C., Decesari, S. and Mircea,M. (2007). Surface tensions of multi-component mixed inorganic/organic aqueous systems of atmospheric significance: measurements, model predictions and importance for cloud activation predictions *Atmos. Chem. Phys.*, **7**, 2371-2398

THE INFLUENCE OF MICROBIOLOGY ON SEA SPRAY PRODUCTION AT LOW TEMPERATURES: EXPERIMENTAL DESIGN

M.E. SALTER[1], E.D. NILSSON[1], M. BILDE[2], R. KREJCI[1], S.M. King[2], A.C. BUTCHER[2] and J. PINHASSI[3]

[1]Department of Applied Environmental Science, Stockholm University, Stockholm, Sweden.

[2]Department of Chemistry, University of Copenhagen, Copenhagen, Denmark.

[3]Department of Biology and Environmental Sciences, University of Kalmar, Kalmar, Sweden.

Keywords: PRIMARY MARINE AEROSOL, BUBBLE BURSTING, CLOUD CONDENSATION NUCLEI, MARINE MICRO-ORGANISMS.

MOTIVATION

Even if the ocean was composed simply of inorganic ions and sea spray consisted of little more than brine, the production of sea spray aerosol (SSA) would be complex. Winds build waves which break and in doing so entrain clouds of air bubbles. Due to their buoyancy these bubbles rise to the surface and break into "jet droplets" and "film drops". Thus on the microscale, physics drives primary marine aerosol production via viscosity and surface tension. However, the ocean is alive and can be envisaged as a complex "soup" of organic chemistry containing many surface-active compounds of biogenic origin which add complexity to bubble bursting and subsequent aerosol generation.

Dissolved organic matter (DOM) is the largest reservoir of reduced carbon in the ocean. It is mostly produced autochthonously by photosynthetic plankton in the surface ocean, and serves as a substrate to vast heterotrophic microbial populations. The least surface-active organic compounds from within this pool are likely to reach the atmosphere in proportion to their surface water concentration akin to the majority of inorganic ions. However, those that are most surface-active are likely enriched in SSA due to their ability to concentrate on both the surface of rising bubbles and the ocean surface. Importantly it is those compounds that are most surface-active that may have the largest effect on the ability of SSA to form clouds. Therefore this complex system offers a possible feedback link comparable to the famed CLAW hypothesis (Charlson et al., 1987) with primary SSA and their associated organics playing a role similar to that proposed for dimethylsulfide derived secondary aerosols in the aforementioned hypothesis (Struthers et al., 2011).

High latitudes are a region where the physical, chemical, and biological processes controlling bubble bursting and SSA generation are highly interlinked and most susceptible to climate change. SSA production is strongly controlled by changes to the cryosphere since a reduced sea ice area resulting from a warmer climate will result in larger SSA emissions. In addition to sea ice area and wind speed, water temperature is another strong physical forcing on SSA generation and there is increasing evidence that as sea surface temperatures increase SSA emissions are reduced (Zábori et al., 2012; Bowyer et al., 1990; Mårtensson et al., 2003). Although the feedbacks between climate, marine biology, and the physicochemistry of bubble bursting are unknown one can envisage that as sea surface temperatures increase in concert with a reduction in sea ice extent a positive climate feedback might ensue through a reduction in SSA emissions (Struthers et al., 2011; Mårtensson et al., 2003).

Despite the potential importance of sea surface temperature to SSA emissions, hysteresis effects

highlighted by previous work suggests that those studies investigating the temperature dependence of SSA emission have probably been conducted under unrealisiticly rapid temperature changes (Bowyer et al., 1990). It also appears that it is those temperatures closest to freezing where the largest changes to SSA emission may take place (Zábori et al., 2012) and such conditions have been difficult to achieve in previous laboratory work. With this in mind we are conducting a series of well defined experiments to test discreetly those parameters thought important under highly controlled temperature conditions.

METHODS

Recently there have been several attempts to quantify SSA production from laboratory-generated bubble plumes using both artificial and real seawater (*e.g.* Mårtensson et al., 2003; Keene et al., 2007; Tyree et al., 2007; Hultin et al., 2010; Hultin, 2010; Fuentes et al., 2010). These have highlighted the effects of salinity, temperature, means of bubble production, biology, and surfactants on resulting SSA size distributions. However given the complexity of results, especially for real seawater, it is now evident that greater understanding at process level and realistic parameterization of organic SSA for climate (or other large scale) models requires alteration of our fundamental experimental approach. Thus a number of tightly controlled experiments at Stockholm University and Copenhagen University have been designed to overcome this by using single, naturally occurring surfactants and monocultures of marine bacteria with the aim of bridging the gap between overly simplistic inorganic seawater experiments and measurements using chemically and biologically complex seawater.
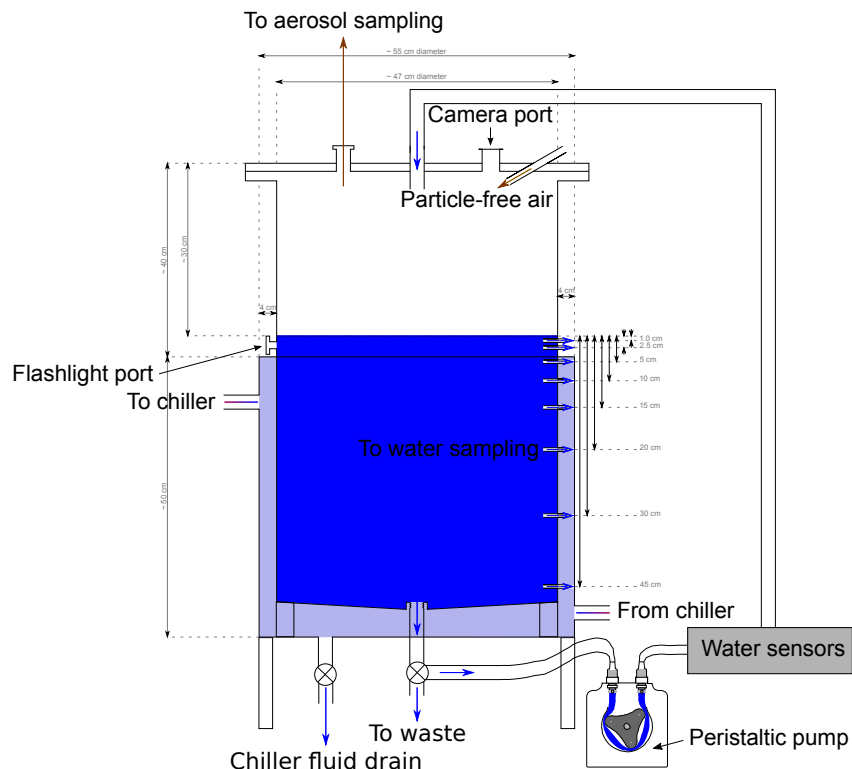

Figure 1: Schematic of the sea spray simulation tank.

The experiments will be conducted in a new sea spray simulation tank (Figure 1) incorporating a number of design features to enable systematic investigation of the physical, chemical, and biological

parameters that control SSA production. For example the system will i) allow control of the water-phase temperature to within 0.1 °C in the range −2 °C to 30 °C; ii) aim to remove contamination of organics using both chemically resistant, contact free pump technology and a PTFE tank coating for all wetted tank parts; iii) be designed in such a manner that bubbles can be generated using either a water jet or a frit using clean filtered air as well as allow water sampling at numerous depths to allow for adjustment of both the total volume of water-phase (and therefore the water-headspace volume ratio) and the bubble rise distance; iv) photograph and size the bubble spectra at the water surface, where the actual bursting takes place using a modern digital SLR camera with a dedicated macro lens.

A series of experiments will be conducted i) to evaluate our experimental setup in the context of previous studies by characterising the role of temperature, salinity and inorganic ion content on SSA production in this experimental system; ii) to evaluate the effect of both simple organics (*e.g.* humic substances and proteins such as tryptophan and tyrosine which are major end members of marine DOM) and complex "organic soups" on SSA production; iii) to evaluate the effect of micro-organisms through the addition of monocultures of the major bacteria found in the worlds oceans as well as those commonly found in the atmosphere, and iv) to evaluate potential climate effects by linking our sea spray simulator with a CCN counter from the University of Copenhagen.

ACKNOWLEDGEMENTS

REFERENCES

Bowyer, P. A., Woolf, D. K., and Monahan, E. C. (1990). Temperature dependence of the charge and aerosol production associated with a breaking wave in a whitecap simulation tank. *Journal of Geophysical Research*, 95:5313–5319.

Charlson, R., Lovelock, J., Andreae, M., and Warren, S. (1987). Oceanic plankton, atmospheric sulphur, cloud albedo and climate. *Nature*, 326:655–661.

Fuentes, E., Coe, H., Green, D., de Leeuw, G., and McFiggans, G. (2010). Laboratory-generated primary marine aerosol via bubble bursting and atomization. *Atmos. Meas. Tech.*, 3:141–162.

Hultin, K. A. H. (2010). *Primary marine aerosol production.* PhD thesis, ITM, Stockholm University, Sweden.

Hultin, K. A. H., Nilsson, E. D., Krejci, R., Mårtensson, E. M. Ehn, M., Hagström, A., and de Leeuw, G. (2010). In situ laboratory sea spray production during the marine aerosol production 2006 cruise on the northeastern atlantic ocean. *Journal of Geophysical Research*, 115.

Keene, W. C., Maring, H., Maben, J. R., Kieber, D. J., Pszenny, A. A. P., Dahl, E. E., Izaguirre, M. A., Davis, A. J., Long, M. S., Zhou, X., Smoydzin, L., and Sander, R. (2007). Chemical and physical characteristics of nascent aerosols produced by bursting bubbles at a model air–sea interface. *Journal of Geophysical Research*, 112.

Mårtensson, E. M., Nilsson, E. D., de Leeuw, G., Cohen, L. H., and Hansson, H. C. (2003). Laboratory simulations and parameterization of the primary marine aerosol production. *Journal of Geophysical Research*, 108.

Struthers, H., Ekman, A. M. L., Glantz, P., Iversen, T., Kirkevåg, A., Mårtensson, E. M., Seland, O., and Nilsson, E. D. (2011). The effect of sea ice loss on sea salt aerosol concentrations and the radiative balance in the Arctic. *Atmos. Chem. Phys.*, 11:3459–3477.

Tyree, C. A., Hellion, V. M., Alexandrova, O. A., and Allen, J. O. (2007). Foam droplets generated from natural and artificial seawaters. *Journal of Geophysical Research*, 112.

Zábori, J., Matisāns, M., Krejci, R., Nilsson, E. D., and Ström, J. (2012). Artificial primary marine aerosol production: a laboratory study with varying water temperature, salinity and succinic acid concentration. *Atmos. Chem. Phys. Discuss.*, 12:19039–19087.

VERTICAL PROFILES OF AEROSOL RADIATIVE FORCING – A COMPARISON OF AEROCOM PHASE 2 MODEL SUBMISSIONS

B.H.SAMSET[1], G.MYHRE[1]

[1]CICERO – Center for International Climate and Energy Research - Oslo, P.O. Box. 1129 Blindern, N-0318 Oslo, NORWAY

Keywords: RADIATIVE FORCING, AEROSOL DIRECT RADIATIVE EFFECT, BLACK CARBON

INTRODUCTION

Aerosols in the earth's atmosphere affect the radiation balance of the planet. The radiative forcing (RF) induced by a given aerosol burden is however sensitive to its vertical density profile, in addition to aerosol optical properties, cloud distributions and surface albedo.

Differences in vertical profiles are thought to be among the causes for the large intermodel differences in RF of the aerosol direct effect. In (Schulz et al, 2006) it was shown that even when the global aerosol models run with the same meteorological year and comparable emission datasets, there is significant variability in their calculated annual mean RF.

As part phase 2 of the AEROCOM direct radiative forcing experiment (Myhre et al, 2012), this study compares 3D concentration fields of black carbon from fossil fuel burning (BC) and sulphate (SO4) from a large set of major global climate models. The goal is to quantify the fraction of RF variability due to differences in assumption about the aerosol vertical profile, and to explore the mechanisms that link the Two.

METHODS

(Samset and Myhre, 2011) presented a set of vertical profiles of the direct radiative forcing per gram of aerosol for BCFF, i.e. the amount of top-of-atmosphere shortwave radiative forcing seen by a particular model (OsloCTM2) per gram of aerosols at a given altitude. Here we term these efficiency profiles (EP). For each model grid point and time step, we multiply the modeled BC concentration by the EP to get the contribution to the total shortwave, top-of-atmosphere BC radiative forcing. This gives us intercomparable 3D RF fields, something that is not immediately available from each model. Differences in model specific treatment of clouds, water uptake and microphysics are removed by this method, and we are left solely with variations due to the concentration profiles and the total aerosol burden.

Model differences due to the aerosol vertical profile can, via these EPs, be factored out from other differences such as aerosol physics, radiative transfer or ground albedo. This tool allows us to compare 4D (spatial + temporal) RF distributions from the AEROCOM models, and to quantify the fraction of the intermodel variability due to differences in aerosol vertical profiles.

In addition, we compare results using efficiency profiles for both all-sky and clear sky conditions, as well as for full 4D and for global, annual mean fields, to distinguish the contribution to the final variability from regional variations and cloud fields.

CONCLUSIONS

For BC, we show that between 20% and 50% of the model variability in RF can be attributed to differences in vertical profile alone. We also show preliminary results for sulphate aerosols.

Significant qualitative differences are found between primary BC emission regions such as China or mainland Europe, and pristine regions such as the Arctic where anthropogenic BC loads are due to transport from other regions. Future measurement campaigns aiming to constrain the vertical profile of BC should therefore focus on both these regions, as both give distinct contributions to the modeled variability of BC RF.

We find that models exert a significant fraction of their BC RF above 5km. In pristine regions such as the Arctic, this fraction may be as high as 70%, while for industrial emission regions it can be as low as 20%.

While the model treatment of cloud fields is clearly important for the variability due to RF vertical profiles, it is not the sole factor. We find significant residual variability even in the absence of clouds, due to the interplay between BC and Rayleigh scattering, water vapor and background aerosols as outlined in (Samset and Myhre, 2011).

ACKNOWLEDGEMENTS

REFERENCES

Schulz, M. et al. Radiative forcing by aerosols as derived from the AeroCom present-day and pre-industrial simulations. Atmospheric Chemistry and Physics 6, 5225-5246 (2006).

Myhre, G. et al. Radiative forcing of the direct aerosol effect from AeroCom Phase II simulations. (2012, Submitted to Atmospheric Chemistry and Physics).

Samset, B. H. & Myhre, G. Vertical dependence of black carbon, sulphate and biomass burning aerosol radiative forcing. Geophys Res Lett 38, doi:Artn L24802

MODELLING STUDIES OF THE INFLUENCE OF ATMOSPHERIC BC ON ARCTIC CLIMATE

M.SAND[1], T.K.BERNTSEN[1],J.E.KAY[2], J. F. LAMARQUE[2], Ø. SELAND[3], A. KIRKEVÅG[3] AND T. IVERSEN[3].

[1] Department of Geosciences, Meteorology and Oceanography Section, University of Oslo, Oslo, Norway.

[2] Center for Atmospheric Research, Boulder, Colorado, USA.

[3] Meteorological Institute, Oslo, Norway

INTRODUCTION

Arctic temperatures have increased at a rate about twice as fast as the global mean rate during the last decades (AMAP 2011). Many inter-related factors arising both from internal climate variability and external climate forcing could have contributed to this greater-than-global Arctic warming. These factors include local feedbacks (snow/ice-albedo, clouds), increased poleward heat transport, and enhanced forcing by absorbing aerosols (black carbon) (IPCC 2007). Accompanied by the temperature increase, the Arctic has experienced a longer melt season with an earlier spring melt and a decrease in the sea-ice extent (AMAP 2011). Black carbon (BC) aerosols absorb solar radiation and heat the surrounding air. This direct effect of BC may be potentially large in the Arctic, as the absorbing aerosols are located over highly reflective snow/ice surfaces (Pueschel and Kinne 1995; Hansen and Nazarenko 2004). In general added atmospheric heat will increase the downward fluxes of longwave radiation and sensible heat, and thus warm the underlying surface. However, models and measurements (Koch et al., 2009) indicate that BC aerosols are located mainly in the free troposphere and in may further stabilize the Arctic atmosphere, thereby limiting the downward flux of sensible heat and the potential surface warming.

BC aerosols in the Arctic originate from emissions mainly at mid-latitudes that are transported northwards (Barrie 1986; Law and Stohl 2007). Sources of BC include both anthropogenic sources (e.g. energy and industrial production, domestic combustion and transport) and natural sources (forest and grassfires induced from lightening). During winter the northward transport is strongest, and the lifetime of BC in the atmosphere is longer, causing a maximum BC concentration in the Arctic in late winter and spring (Sharma et al. 2006). The elevated BC concentrations also extend into the melting season, which could make BC particularly important in the Arctic. BC aerosols affect the atmospheric temperature gradients and can therefore change the atmospheric heat transport and the distribution of clouds. In addition, BC aerosols can have an indirect effect on clouds by acting as cloud condensation nuclei or ice nuclei and influence the cloud cover and cloud lifetime via microphysical interactions. BC can also affect the distribution of clouds by changing the stability of the atmosphere, often referred to as the semi-direct effect (Koch and Genio 2010).

BC affects the climate in numerous ways and there are large uncertainties in estimating the net BC forcing. Because of the short lifetime of BC compared to well-mixed greenhouse gases, BC has a potential for short-term climate control strategies (Hansen et al. 2000; Jacobson 2010). In order to identify the best options for emission reductions there is a need for improving the understanding of the role of BC aerosols in the Arctic (AMAP 2011) and how the response of the Arctic climate depends on the location of BC forcing. Shindell and Faluvegi (2009) perturbed forcings by enhancing the concentrations of BC aerosols

in different latitude bands and found that for the Arctic latitude band, the Arctic surface air temperature decreased, despite a positive forcing at the top of the atmosphere. Shindell and Faluvegi attributed this to a reduction in the pole-ward heat flux following increased absorption of incoming solar radiation by BC and strong local heating in the free troposphere. For positive direct forcing by BC aerosols in the mid-latitude band the Arctic surface temperature response was positive (warming).

The results from the study of Shindell and Faluvegi (2009) were somewhat unexpected, and with the increasing focus on the effect of BC aerosols on the Arctic climate, there is a need to verify that the results are robust by reproducing parts of the experiment with a different climate model; to analyze the Arctic climate response to BC perturbations in the Arctic (60N-90N) and northern mid-latitude (28N-60N) atmosphere respectively. To extend the study a bit further, we want to understand and quantify the contribution from the different processes that are important for BC forcing and response in the Arctic, including a comprehensive study of the Arctic heat budget. Idealized climate simulations with artificially increased BC concentrations in the two separate latitude bands have been performed with a fully coupled earth system model, the NorESM, to include feedbacks from sea ice cover and sea surface temperatures. The two experiments are compared with a control run to analyze the response in the Arctic temperatures to the two forcings, including changes in feedbacks from sea-ice, cloud cover and the meridional energy transport into the Arctic.

METHODS

The climate model used in this study is the Norwegian Earth System Model, NorESM (Iversen et al. (2012), Berntsen et al. (2012), Kirkevåg et al. 2012), to a large extent based on the Community Climate System Model CCSM4.0 (Gent et al. 2011), developed at the National Center for Atmospheric Research (NCAR). The model is run fully coupled with an atmospheric model, an ocean model, a land model, and a sea-ice model. The atmospheric part of NorESM, CAM4-Oslo, has applied aerosol and cloud droplet parameterization schemes. The prognostic aerosols and aerosol precursors in CAM4-Oslo include sea-salt, mineral dust, DMS, SO_2, SO_4, BC and particulate OM and they interact online with the cloud microphysics, radiation and dynamics in the model. Both the direct effect and the first and second indirect effects are calculated. The direct effect of aerosols is caused by the scattering and absorption of radiation, mainly in the shortwave spectrum. The indirect effects of aerosols are due to their interaction with clouds, by acting as cloud condensation nuclei or ice nuclei. The atmospheric model includes a comprehensive treatment of aerosol microphysics, accounting for aerosol nucleation, condensation, coagulation and cloud processing, and calculates the conversion of BC to a hydrophilic state where it can be scavenged by precipitation. The wet deposition is calculated in full integration with the cloud and precipitation schemes

3 simulations are run, one control simulation and 2 perturbed simulations. For each simulation the model is run 60 years from a 140 year spin-up with the same initial conditions and the same present-day emissions. In the two perturbed simulations the BC concentrations are multiplied by a factor of 10 in the Arctic (60N-90N; 'the ARC experiment') and mid-latitudes (28N-60N; 'the MID experiment'), respectively.

CONCLUSIONS

The influence of BC aerosols from lower latitudes provide extra warming and loss of sea-ice and snow in the Arctic. Using the NorESM model we find that when BC concentrations are scaled up in the Arctic according to its current vertical profile, the surface temperature response is negative despite a positive radiative forcing at TOA (fig 1). The surface cooling can be explained by a combination of changes in the vertical fluxes of heat and radiation and a reduction in the meridional heat transport from lower latitudes. There is an upper troposphere heating by absorption of SW radiation, a surface dimming effect that reduces the downwelling solar radiation and also seems to increase the static stability in the Arctic that

suppress the turbulent mixing of the heat to the surface and increases the cloud cover. We estimate that BC aerosols at mid-latitudes lead to increased transport of heat into the Arctic, causing a warming, both at the surface and in the whole atmospheric column. The largest increase in the temperatures is found in the upper troposphere during summer due to transport of heat along isentropic surfaces.
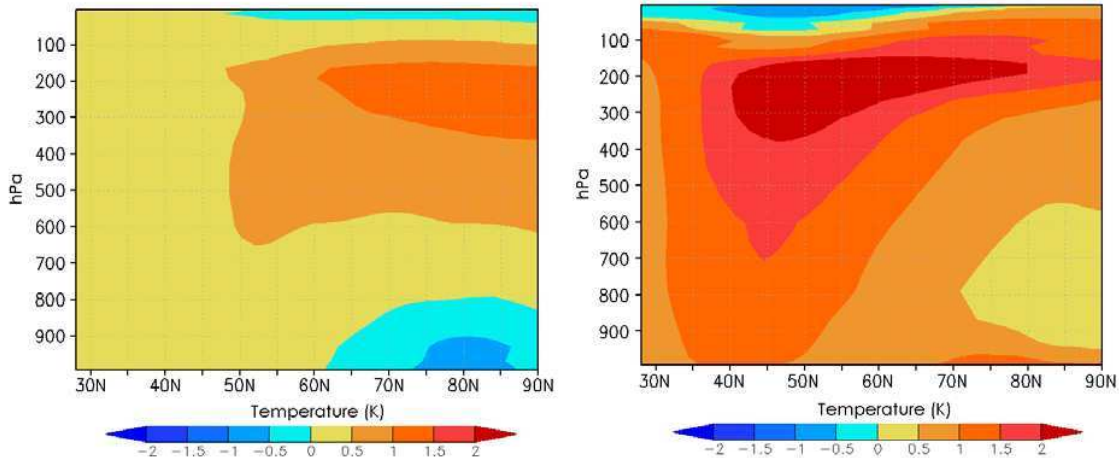
Figure 1. Zonal annual mean temperature change (in K) for the ARC-control run (left) and the MID-control run (right).

ACKNOWLEDGEMENTS

REFERENCES

AMAP: The Impact of Black Carbon on Arctic Climate, AMAP Technical Report No. 4, Arctic Monitoring and Assessment Programme (AMAP), Oslo, Norway, 2011.

Barrie, L. A.: Arctic air pollution: an overview of current knowledge, Atmos. Environ., 20, 643-663, 1986.

Bentsen, M., Bethke, I., Debernard, J. B., Iversen, T., Kirkev°ag, A., Seland, Ø., Drange, H., Roelandt, C., Seierstad, I. A., Hoose, C., Kristj´ansson, J. E.: The Norwegian Earth System 30 Model, NorESM1-M – Part 1: Description and basic evaluation, Geosci. Model Dev., in press, 2012.

Gent, P. R., Danabasoglu, G., Donner, L. J., Holland, M. M., Hunke, E. C., Jayne, S. R., Lawrence, D. M., Neale, R. B., Rasch, P. J., Vertenstein, M., Worley P. H., Yang, Z. –L. and Zhang, M.: The community climate system model version 4, J. Climate, 24, 4973-4991, 2011.

Hansen, J. and Nazarenko, L.: Soot climate forcing via snow and ice albedos, P. Natl. Acad. Sci. USA, 101, 423-428, 2004.

Hansen, J., Sato, M., Ruedy, R., Lacis, A. and Oinas, V.: Global warming in the twenty-first century: An alternative scenario, P. Natl. Acad. Sci. USA, 9875-9880, 2000.

IPCC (2007). Climate change 2007: the physical science basis: contribution of Working Group I to the
    Fourth Assessment Report of the Intergovernmental Panel on Climate Change, Cambridge Univ
Pr, 2007

Iversen, T., Bentsen, M., Bethke, I., Debernard, J. B., Kirkev°ag, A., Seland, Ø., Drange, H.,
    15 Kristjansson, J. E., Medhaug, I., Sand, M., and Seierstad, I. A.: The Norwegian Earth System
    Model, NorESM1-M – Part 2: Climate Response and Scenario Projections, Geosci. Model
    Dev., in press, 2012.

Jacobson, M. Z.: Short-term effects of controlling fossil-fuel soot, biofuel soot and gases, and methane on
    climate, Arctic ice, and air pollution health, J. Geophys. Res., 115, D14209, 2010.

Koch, D. and Genio, A. D. D.: Black carbon semi-direct effects on cloud cover: review and synthesis,
    Atmos. Chem. Phys. 10, 7685-7696, 2010.

Koch, D., Schulz, M., Kinne, S., McNaughton, C., Spackman, J., Balkanski, Y., Bauer, S., Berntsen, T.,

Law, K. S. and Stohl, A.: Arctic air pollution: Origins and impacts, Science, 315, 1537-1540, 2007.

Pueschel, R. F. and Kinne, S. A.: Physical and radiative properties of Arctic atmospheric aerosols, Sci.
    Total Environ., 160, 811-824, 1995.

Sharma, S., Andrews, E., Barrie, L., Ogren, J. and Lavoue, D.: Variations and sources of the
    equivalent black carbon in the high Arctic revealed by long-term observations at Alert and
    Barrow: 1989–2003, J. Geophys. Res., 111, D14208, 2006.

Shindell, D. and Faluvegi, G.: Climate response to regional radiative forcing during the twentieth century,
    Nat. Geosci., 2, 294-300, 2009.

AEROSOL AND TRACE GAS CONCENTRATIONS IN THE VICINITY OF KILPILAHTI INDUSTRIAL AREA

Nina Sarnela[1], Tuija Jokinen[1], Jani Hakala[1], Risto Taipale[1], Johanna Patokoski[1], Maija Kajos[1], Katrianne Lehtipalo[1], Siegfried Schobesberger[1], Heikki Junninen[1], Mikko Sipilä[1], Jukka Teittinen[2], Henrik Westerholm[2], Kai Larnimaa[2], Tuukka Petäjä[1] and Markku Kulmala[1]

[1]University of Helsinki, Department of Physics, P.O. Box 64, 00014 University of Helsinki, Finland

[2]Neste Oil Oyj, Porvoon jalostamo, PL 310, 06101 Porvoo, Finland

Keywords: industrial emissions, aerosol concentrations, on-line measurements

INTRODUCTION

Industrial activity is a major source of both gas and particulate phase pollution affecting the air quality in the vicinity of the industrial sites. These emissions are strongly regulated and controlled. Finland's environmental administration has given reference and limit values for the industrial emissions. The air quality in the surroundings of the Kilpilahti industrial area has been regularly monitored since 1970s. The monitoring includes sulfur dioxide, total concentration of reduced sulfur compounds, nitrogen oxides and ozone. The industrial emissions have decreased significantly in last twenty years due to adaptation of new technology and stricter regulations.

In the case of sulfur dioxide, it has both natural and anthropogenic sources. The Kilpilahti industrial area has yearly sulfur dioxide emissions of about 6000 tons. Sulfur dioxide oxidizes to sulfuric acid when adequate catalyst for example hydroxyl radical (OH^-) is present. OH^- has a strong diurnal cycle which causes the sulfuric acid concentrations to usually be lower during the night and the highest around the noon (Paasonen et al. 2010). Sulfuric acid has an important role in the initial steps of nucleation. In this study we examined the effects that industrial emissions cause to aerosol concentrations and behavior, and for example to the new particle formation in the vicinity of the Kilpilahti industrial park.

SITE DESCRIPTION AND INSTRUMENTATION

Measurements were performed in the Kilpilahti industrial area in Porvoo where chemical and plastics factories and an oil refinery are situated. The measurement campaign took place between 7 June and 5 July in 2012.

Aerosol particle size distribution and total concentrations were measured by a differential mobility particle sizer (DMPS Aalto et al. 2001). Two flow rates were used to cover particle sizes from 6 nm to 1000 nm. The particles sized between 6 and 200 nm were measured with a 4 liter per minute (lpm) flow rate and particles between 200 and 1000 nm with a 1 lpm flow rate. In DMPS the particles are categorized by their electric mobility and the number concentration of particles is recorded per sampled volume. In the instrument the sample passes through a differential mobility analyzer (DMA) in which the applied voltage is changed to select a certain particle size. The selected particles continue their way to the condensation particle counter (CPC). In the CPC the particles are introduced to a high butanol saturation ratio with the result that butanol molecules condense onto the particles. In that way the measured particles are grown to the size in which they scatter light and can be detected optically (McMurry, 2000).

The concentrations of the smallest aerosol particles were measured with a particle size magnifier (PSM). The PSM was used in scanning mode so that the saturator flow rate varied from 0.1 to 1 lpm. In the PSM

small sub-3nm aerosol particles are grown to the bigger size so that they can be detected optically with the CPC. The PSM produces a high saturation ratio by mixing a cooled aerosol sample with heated air that is saturated by diethylene glycol. After that the flow is cooled and guided to the CPC. In that way the particles grow approximately to the size of 90 nm (Vanhanen et al. 2011).

The chemical ionization atmospheric pressure interface time-of-flight mass spectrometer (CI-APi-TOF, Jokinen et al. 2012) was used to observe sulfuric acid and other acidic compounds. We installed an ion filter to the inlet of the CI-APi-TOF and took measurements while it was both switched off and on with voltages 50 and -50 V. The chemical ionization occurs at atmospheric pressure via proton transfer between nitrate ions and its clusters with nitric and sulfuric acid. The nitrate ions are created by alpha radiation from [241]Am source (Petäjä et al. 2009, Jokinen et al. 2012). The ionized sample enters the APi-TOF through a critical orifice and end up to the TOF after differentially pumped chambers (Junninen et al. 2010, Ehn et al. 2010).

A proton-transfer-reaction mass spectrometer (PTR-MS, Lindinger et al. 1998) was used to measure concentrations of volatile organic compounds. The PTR-MS was calibrated weekly during the measurement campaign. In the PTR-MS the sample is ionized in a soft ionization method by proton transfer reactions with hydronium ions (H_3O^+) at a reduced pressure. When using soft ionization methods the product ions are not usually fragmented. In the instrument the reagent and product ions are selected by a quadrupole mass spectrometer and detected by a secondary electron multiplier (Taipale et al. 2008). In addition to the data from our instruments Neste Oil provided us measured SO_2 concentrations from the site.

PRELIMINARY RESULTS, OUTLOOK

The measurement campaign succeeded well and data processing is currently in progress. Preliminary analysis indicated that the total sub-micron aerosol number concentrations varied from $1\times10^3 - 1\times10^5$ cm^{-3} in one hour median concentrations. Secondary aerosol formation and growth events (Kulmala et al. 2004) were observed on few days during the campaign.

A preliminary analysis indicated that the observed mixing ratios for volatile organic compounds and sulfur dioxide were typically below 10 ppbv and below 5 ppbv, respectively. The mixing ratio of benzene was most of the time below 1 ppbv. The measured values are comparable to values obtained from urban areas (Filella and Peñuelas 2006). On few occasions the trace gas concentrations increased, indicating that during certain times the industrial emissions were higher than usual. This is valid for example for SO_2, sulfuric acid, methanol, acetone and benzene.

The concentrations of SO_2 and sulfuric acid are correlated with each other and are higher than the ones measured in Hyytiälä (Petäjä et al. 2009, Mikkonen et al. 2011) but comparable to concentrations measured in urban areas for example in the SMEAR 3 station in Helsinki. The diurnal cycles of SO_2 and sulfuric acid seem to have two maximum points. We are going to further examine the connections between the measured compounds and their diurnal behavior in more detail.

REFERENCES

Aalto, P., Hämeri, K., Becker, E., Weber, R., Salm. J., Mäkelä, J. M., Hoell, C., O'Dowd, C., Karlsson, H., Hansson, H-C., Väkevä, M., Koponen, I., Buzorius, G. and Kulmala, M. (2001). Physical characterization of aerosol particles during nucleation events. Tellus **53**, 344-358

Ehn, M., Junninen, H., Petäjä, T., Kurtén, T., Kerminen, V.-M., Schobesberger, S., Manninen, H. E., Ortega, I. K., Vehkamäki, H., Kulmala, M. and Worsnop D. R. (2010) A high-resolution mass spectrometer to measure atmospheric ion composition. Atmos. Meas. Tech. **3**, 1039-1053

Filella, I. and Peñuelas J. (2006) Daily, weekly, and seasonal time courses of VOC concentrations in a semi-urban area near Barcelona. Atmos. Environ. **40**, 7752-7769

Jokinen, T., Sipilä, M., Junninen, H., Ehn, M., Lönn, G., Hakala, J., Petäjä, T., Mauldin III, R.L., Kulmala, M. and Worsnop, D.R. (2012) Atmospheric sulphuric acid and neutral cluster measurements using CI-APi-TOF. Atmos. Chem. Phys. **12**, 4117-4125

Junninen, H., Ehn, M., Petäjä, T., Luosujärvi, L., Kotiaho, T., Kostiainen, R., Rohner, U., Gonin, M., Fuhrer, K., Kulmala, M. and Worsnop, D. R. (2010) Atmos. Meas. Tech. **3**, 1039-1053

Kulmala, M., Vehkamäki, H., Petäjä, T., Dal Maso, M., Lauri, A., Kerminen, V.-M., Birmili, W. and McMurry, P. H. (2004) Formation and growth rates of ultrafine atmospheric particles: a review of observations. Aerosol Sci. **35**, 143-176

Lindinger, W., Hansel, A. and Jordan, A. (1998) Proton-transfer-reaction mass spectrometry (PTR-MS): On-line monitoring of volatile organic compounds at pptv levels. Chem. Soc. Rev. **27**, 347-354

McMurry, P. H. (2000) The history of condensation nucleus counters. Aerosol Sci. Tech. **33**, 297-322

Mikkonen, S., Romakkaniemi, S., Smith, J. N., Korhonen, H., Petäjä, T., Plass-Duelmer, C., Boy, M., McMurry, P. H., Lehtinen, K. E. J., Joutsensaari, J., Hamed, A., Mauldin R. L., Birmili, W., Spindler, G., Arnold, F., Kulmala, M. and Laaksonen A. (2011) A statistical proxy for sulphuric acid concentration. Atmos. Chem. Phys. **11,** 11319-11334

Paasonen, P., Nieminen, T., Asmi, E., Manninen, H. E., Petäjä, T., Plass-Dülmer, C., Flentje, H., Birmili, W., Wiedensohler, A., Hõrrak, U., Metzger, A., Hamed, A., Laaksonen, A., Facchini, M.C., Kerminen, V.-M. and Kulmala, M. (2010) On the roles of sulphuric acid and low-volatility organic vapours in the initial steps of atmospheric new particle formation. Atmos. Chem. Phys. **10**, 11223-11242

Petäjä, T., Mauldin III, R. L., Kosciuch, E., McGrath, J., Nieminen, T., Paasonen, P., Boy, M., Adamov, A., Kotiaho, T. and Kulmala, M. (2009) Sulfuric acid and OH concentrations in a boreal forest site. Atmos. Chem. Phys. **9**, 7435-7448

Taipale, R., Ruuskanen, T.M., Rinne, J., Kajos, M. K., Hakola, H., Pohja, T. and Kulmala, M. (2008) Technical note: Quantitative long-term measurements of VOC concentrations by PTR-MS - Measurement, calibration, and volume mixing ratio calculation methods. Atmos. Chem. Phys. **8**, 6681-6698

Vanhanen, J., Mikkilä, J., Lehtipalo, K., Sipilä, M., Manninen, H.E., Siivola, E., Petäjä, T. and Kulmala M. (2011) Particle Size Magnifier for Nano-CN Detection. Aerosol Sci.Technol. **45**, 533-542

Release of VOCs from cattle

S. SCHALLHART[1], J. SINTERMANN[2], M. K. KAJOS[1], A. MÜNGER[3], A. NEFTEL[2], T. M. RUUSKANEN[1] and M. KULMALA[1]

[1] Department of Physics, University of Helsinki, Finland

[2] Agroscope Reckenholz Tänikon Research Station, CH-8046 Zürich

[3] Agroscope Liebefeld-Posieux Research Station ALP, CH-1725 Posieux

INTRODUCTION

Volatile amines play an important role in aerosol formation, and they are likely to be more important in the gas-to-particle conversion than ammonia (Kurtén et al., 2008). Still, the sources and atmospheric abundance of amines are not well known and the information available on this topic is sparse.

In previous measurements in animal housings, the main component emitted by animal husbandry was trimethylamine (TMA). The source of TMA was assumed to scale with the emission of NH_3 (Schade and Crutzen 1995. However, a more recent study (Kuhn et al., 2011), indicated that rumination could be the main source of the amines and that emissions from stored slurry are negligible. In addition it suggested that an universally agricultural TMA-NH_3 emission ratio is not valid.

METHODS
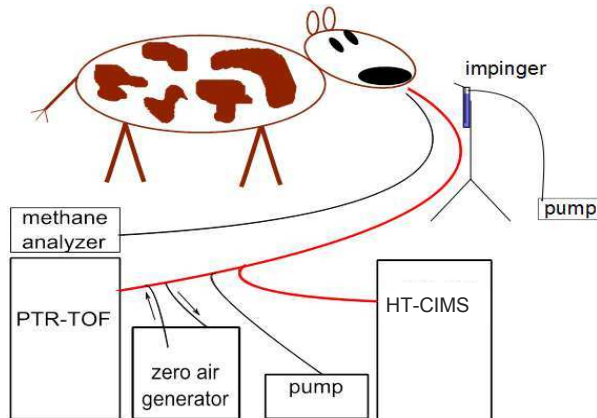
Figure 1: Schematic sketch of the inlet. Heated lines are shown in red, whereas black lines resemble tubing at ambient temperature.

In the CATTLE (Cow originated Amines/Ammonia, Towards True Levels of Emissions) campaign volatile organic compounds (VOCs), ammonia, methane and amines were measured in a research stable in Agroscope Liebefeld-Posieux, Switzerland. The campaign was carried out between 25.07 and 6.08.2011 using (Figure 1) a PTR-TOF (Proton Transfer Reaction Time Of Flight), a HT-CIMS (High Temperature Chemical Ionization Mass Spectrometer), a commercial methane analyzer and impinger samples, which were later analyzed by ion chromatography. The campaign included measurements of air inside the cow stables, as well as air exhaled by individual ruminating cows. A video camera was recording the animal activities, so that it was later possible to attribute concentration changes to the animal activity. Furthermore, headspace air above dung and urine samples was recorded.

The high mass resolution of the PTR-TOF allows separation of the isotope of acetone (breath marker) from the TMA ($\Delta m = 0.03$ amu), as well as to identify various VOCs. The combination of PTR-TOF with other high time resolution instruments allowed recording time traces of methane, ammonia, amines and acetone with one hertz resolution and to correlate them with other 500 mass peaks found in the TOF spectra.

CONCLUSIONS

New measurements, with a combination of fast and sensitive analyzers to trace volatile organic compounds, indicate that rumination and exhaled air are not the main sources of amines. The main compounds in breath air were acetone and methane. The highest concentrations of TMA were measured above dung and urine mixtures. Dung contains the enzyme urease that catalyzes the hydrolysis of urea in the urine. This process leads to an elevated pH in the urine/dung mixture that enables the volatilization of the dissolved TMA.

ACKNOWLEDGEMENTS

REFERENCES

Kuhn, U., Sintermann, J., Spirig, C., Jocher, M., Ammann, C. and Neftel, A. (2011). Basic biogenic aerosol precursors: Agricultural source attribution of volatile amines revised. Geophysical Research Letters 38: L16811.

Kurtén, T., Loukonen, V., Vehkamäki, H. and Kulmala, M. (2008). Amines are likely to enhance neutral and ion-induced sulfuric acid-water nucleation in the atmosphere more effectively than ammonia. Atmospheric Chemistry and Physics 8(14): 4095-4103.

Schade, G. W. and Crutzen P. J. (1995). Emission of Aliphatic-Amines from Animal Husbandry and Their Reactions - Potential Source of N2O and HCN. Journal of Atmospheric Chemistry 22(3): 319-346.

MEASURING ION CLUSTERS OF SULFURIC ACID, AMMONIA, AMINES, AND PINANEDIOL OXIDATION PRODUCTS IN THE CLOUD CHAMBER, BY API-TOF MASS SPECTROMETERS

S. SCHOBESBERGER[1], A. FRANCHIN[1], H. JUNNINEN[1], F. BIANCHI[2], J. DOMMEN[2], N. DONAHUE[3], S. EHRHART[4], M. EHN[1,5], K. LEHTIPALO[1], T. NIEMINEN[1], G. LÖNN[1], THE CLOUD COLLABORATION, T. PETÄJÄ[1], M. KULMALA[1] and D.R. WORSNOP[1,6]

[1]Department of Physics, University of Helsinki, Helsinki, 00014, Finland

[2]Laboratory of Atmospheric Chemistry, Paul Scherrer Institut, Villigen, 5232, Switzerland

[3]Department of Chemical Engineering, Carnegie Mellon University, Pittsburgh, PA 15213-3890, USA

[4]Institute for Atmospheric and Environmental Sciences, Goethe University, 60438, Frankfurt/Main, Germany

[5]Forschungszentrum Jülich GmbH, Jülich, 52428, Germany

[6]Aerodyne Research, Inc., MA 01821-3976, USA

INTRODUCTION

Atmospheric aerosols have direct and indirect effects on the Earth's radiation balance, and therefore on climate, as well as effects on air quality and human health. Nucleation from gaseous precursors is an important source of aerosol particles in the atmosphere. Sulfuric acid (H_2SO_4) has been found to play a crucial role in the nucleation process (Kulmala et al., 2004, Riipinen et al., 2007). Other compounds hypothesized as important are water, ammonia (NH_3), and yet unidentified organic compounds (e.g. Metzger et al., 2010).

The CLOUD (Cosmics Leaving OUtdoor Droplets) experiment at CERN provides exceptionally clean and well-defined experimental conditions for studies of atmospheric nucleation and initial growth, in an experimental setup centered on a 26.1 m^3 stainless-steel chamber (Kirkby et al., 2011). In addition, the influence of cosmic rays on nucleation and nanoparticle growth can be simulated by exposing the chamber to a pion beam produced by the CERN Proton Synchrotron. The research at CLOUD has so far focused on investigating nucleation at different conditions, including varying concentrations of H_2SO_4, NH_3, varying beam intensity, relative humidity, temperature, etc. In more recent experiments, dimethyl amine (C_2H_7N) was added as well as pinanediol ($C_{10}H_{18}O_2$). The latter was expected to yield oxidation products similar to those of monoterpenes ($C_{10}H_{16}$) which are naturally abundant volatile organic compounds.

METHODS

A key to understanding the mechanism by which nucleation proceeds in the CLOUD chamber is the use of state-of-the-art instrumentation (Kirkby et al., 2011), including novel condensation particle counters with cut-off sizes < 2 nm, and the Atmospheric Pressure interface Time-Of-Flight (APi-TOF) mass spectrometer.

The APi-TOF is developed by Tofwerk AG, and Aerodyne Research, Inc, and a detailed description of the instrument can be found in Junninen et al. (2010). It typically obtains resolutions between 4000 and 6000 Th/Th and mass accuracies < 10 ppm. Sampling occurs directly from atmospheric pressure through a critical orifice. Ions are then focused and guided to the time-of-flight mass spectrometer, while passing

through differentially pumped chambers. Note that no ionization of the sampled aerosol is performed; only ions charged in the CLOUD chamber are detected in the current configuration.

Using the APi-TOF, the composition of ions can be determined based on their exact masses and isotopic patterns (Ehn et al., 2012). Current versions of the MATLAB-based software package tofTools, being developed at the University of Helsinki, have been used for processing and analyzing the data.

RESULTS

During experiments at CLOUD, nucleation events were usually triggered in the chamber by switching on UV light, enhancing photolytic oxidation processes (particularly the oxidation of SO_2 to H_2SO_4). Depending on conditions, nucleation occurred mainly or partly by ions. Before adding any organics into the chamber, cluster ions were found to always contain H_2SO_4 (Kirkby et al., 2011). They also contained NH_3 molecules, with the $NH_3:H_2SO_4$ ratio depending on cluster size and experimental conditions (e.g. Fig. 1). To a lesser extent, they also contained organic contaminant compounds, mainly amines.
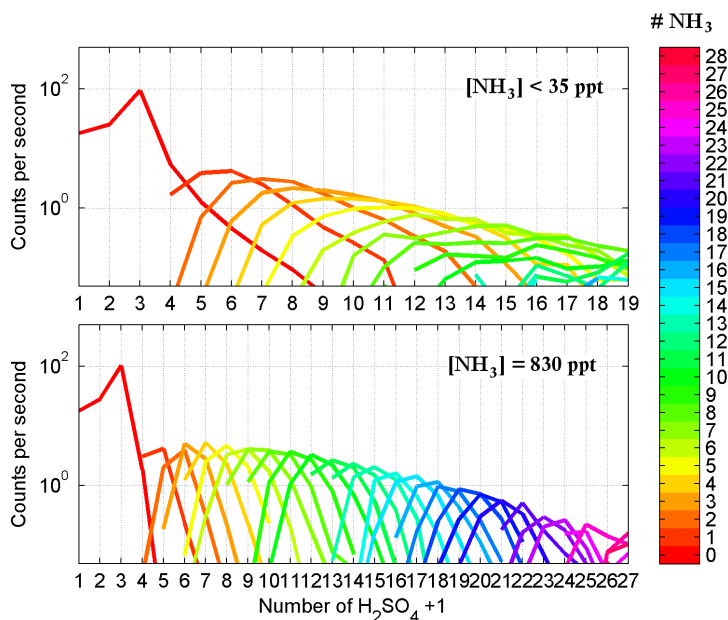
Figure 1. Counts from ion clusters of the form $(NH_3)_m(H_2SO_4)_nHSO_4^-$ vs. n+1, with m color-coded, for two different concentrations of NH_3 (in gas-phase) in the CLOUD chamber.

In later experiments, two organics (first dimethyl amine, later pinanediol) were added into the chamber. Their addition altered nucleation and growth, and the chemical compositions of the observed ion clusters changed accordingly. Cluster growth then included mixtures of sulfuric acid and dimethyl amine and/or a wide range of pinanediol oxidation products. Particularly with adding pinanediol into the CLOUD chamber, the ion mass spectra complicated: Many of the main peaks in the spectra were from multiple compounds, i.e. their masses were only partly resolvable. Yet we were able to deconvolute many such multiple peaks (e.g. Fig. 2), enabling us to obtain a good understanding of the chemical composition of the observed ions and ion clusters. We expect correlations between the abundances of individual clusters and various experimental variables to give detailed insights into the early steps of new (charged) particle formation in the CLOUD chamber.

Also, for all chemical systems studied, the initial growth of clusters/particles could be studied from smallest clusters upwards, using a range of employed instrumentation. The APi-TOF recorded ion spectra every 5 s; and time series for ion cluster appearance could usually be obtained at a practical time

resolution of about 30 s. Therefore, the initial growth of ions could be resolved molecule by molecule, while the largest observable ion clusters corresponded to mobility equivalent diameters of 1.8-2.1 nm.
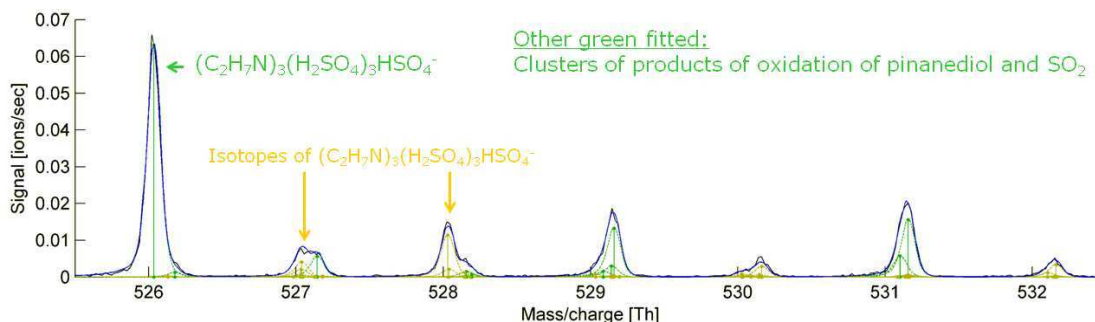
Figure 2. Parts of an anion mass spectrum, showing an example situation of peak identification for ion spectra during experiments when dimethyl amine and pinanediol were added into the CLOUD chamber.

ACKNOWLEDGEMENTS

REFERENCES

Ehn, M., E. Kleist, H. Junninen, T. Petäjä, G. Lönn, S. Schobesberger, M. Dal Maso, A. Trimborn, M. Kulmala, D.R. Worsnop, A. Wahner, J. Wildt, and Th.F. Mentel (2012). Gas phase formation of extremely oxidized pinene reaction products in chamber and ambient air, Atmos. Chem. Phys. **12**, 5113-5127.

Junninen, H., M. Ehn, T. Petäjä, L. Luosujärvi, T. Kotiaho, R. Kostiainen, U. Rohner, M. Gonin, K. Fuhrer, M. Kulmala and D.R. Worsnop (2010). A high-resolution mass spectrometer to measure atmospheric ion composition, Atmos. Meas. Tech. **3**, 1039–1053.

Kirkby, J., J. Curtius, J. Almeida, E. Dunne, J. Duplissy, S. Ehrhart, A. Franchin, S. Gagné, L. Ickes, A. Kürten, A. Kupc, A. Metzger, F. Riccobono, L. Rondo, S. Schobesberger, G. Tsagkogeorgas, D. Wimmer, A. Amorim, F. Bianchi, M. Breitenlechner, A. David, J. Dommen, A. Downard, M. Ehn, R.C. Flagan, S. Haider, A. Hansel, D. Hauser, W. Jud, H. Junninen, F. Kreissl, A. Kvashin, A. Laaksonen, K. Lehtipalo, J. Lima, E.R. Lovejoy, V. Makhmutov, S. Mathot, J. Mikkilä, P. Minginette, S. Mogo, T. Nieminen, A. Onnela, P. Pereira, T. Petäjä, R. Schnitzhofer, J.H. Seinfeld, M. Sipilä, Y. Stozhkov, F. Stratmann, A. Tomé, J. Vanhanen, Y. Viisanen, A. Vrtala, P.E. Wagner, H. Walther, E. Weingartner, H. Wex, P.M. Winkler, K.S. Carslaw, D.R. Worsnop, U. Baltensperger and M. Kulmala (2011). Role of sulphuric acid, ammonia and galactic cosmic rays in atmospheric aerosol nucleation, Nature **476**, 429-433.

Kulmala, M., H. Vehkamäki, T. Petäjä, M. Dal Maso, A. Lauri, V.-M. Kerminen, W. Birmili and P.H. McMurry (2004). Formation and growth rates of ultrafine atmospheric particles: a review of observations. J. Aerosol Sci. **35**, 143-176.

Metzger, A., B. Verheggen, J. Dommen, J. Duplissy, A.S. Prevot, E. Weingartner, I. Riipinen, M. Kulmala, D.V. Spracklen, K.S. Carslaw and U. Baltensperger (2010). Evidence for the role of organics in aerosol particle formation under atmospheric conditions. P. Natl. Acad. Sci. **107**, 6646–6651.

Riipinen, I., S.-L. Sihto, M. Kulmala, F. Arnold, M. Dal Maso, W. Birmili, K. Saarnio, K. Teinilä, V.-M. Kerminen, A. Laaksonen and K.E.J. Lehtinen (2007). Connections between atmospheric sulphuric acid and new particle formation during QUEST III–IV campaigns in Heidelberg and Hyytiälä, Atmos. Chem. Phys. **7**, 1899–1914.

SO2 OXIDATION BY STABILIZED CRIEGEE INTERMEDIATES FROM FOREST EMITTED ALKENES – CONTRIBUTION TO GLOBAL CONCENTRATIONS OF SULFURIC ACID, CN AND CCN

M. SIPILÄ[1], T. BERNDT[2], R. MAKKONEN[1], T. JOKINEN[1], P. PAASONEN[1], L. MAULDIN[1,3], T. KURTEN[4], H. JUNNINEN[1], A. ASMI[1], D. WORSNOP[1,5,6], M, KULMALA[1] and T. PETÄJÄ[1]

[1]Department of Physics, University of Helsinki, Finland

[2]Leibniz-Institute for Tropospheric Research, Leipzig, Germany

[3]University of Colorado at Boulder, Boulder, CO, USA

[4]Department of Chemistry, University of Helsinki, Finland

[5]University of Eastern Finland, Kuopio, Finland

[6]Aerodyne Research Inc., Billerica, MA, USA

INTRODUCTION

Sulphuric acid (H_2SO_4) plays a key role in Earth's atmosphere triggering secondary aerosol formation (Sipilä et al., 2010) and thus connecting anthropogenic SO_2 emissions to global climate via indirect aerosol effects on radiative forcing. In the atmosphere, gas phase H_2SO_4 forms in a reaction chain initiated by the reaction of SO_2 with hydroxyl radical, OH. OH has two major sources, photochemical reaction involving O_3 and H_2O, and ozonolysis of biogenic alkenes. Until very recently, SO_2 oxidation by OH was considered as the only important source of gaseous H_2SO_4 in the atmosphere. However, recent study by Weltz et al. (2012) showed, basing on the laboratory experiment, that stabilized Criegee Intermediates (sCI) can oxidize SO_2 with a reaction rate orders of magnitude higher than assumed earlier (Johnson, et al., 2001). In the atmosphere, sCI radicals origin from ozonolysis of alkenes. Ozone attacks the double bond of olefins producing an energy-rich primary ozonide which decomposes very rapidly forming the so-call Criegee Intermediate, CI. This energy-rich CI either decomposes in unimolecular reactions yielding OH and other products, or is collisionally stabilized by the media gas. This stabilized Criegee Intermediate (sCI) can still decompose in unimolecular reactions leading also to OH formation. Besides the unimolecular reaction sCIs can react with several atmospheric constituents (Welz, et al., 2012; Taatjes et al., 2012; Mauldin et al., 2012; Berndt et al., 2012).

In our recent study, we investigated the oxidation of SO_2 by sCI formed in monoterpene ozonolysis and found those reacting fast enough with SO_2 to contribute to atmospheric sulphuric acid production in boreal forest environment (Mauldin et al. 2012). We showed that in the summertime boreal forest, with the extensive biogenic activity, sCI chemistry can account even up to 50% of the sulphuric acid production in surface layer. In that study we were not able to experimentally determine the sCI lifetimes or yields, required to derive the reaction rate coefficient. Thus we estimated those parameters relaying on theoretical considerations. In the present study we investigated experimentally sCI yield, lifetime as well as rate coefficient for reaction with SO_2 for sCIs from ozonolysis of isoprene and a number of monoterpenes. Applying knowledge of those, we assessed the contribution of sCI + SO_2 reaction to the total H_2SO_4 burden in Earth's atmosphere using ECHAM5.5-HAM2 global aerosol – climate model.

EXPERIMENTAL YIELDS, LIFETIMES AND REACTION RATE COEFFICIENT FOR SCI+SO2.

Laboratory experiments were conducted in Leibniz-Institute for Tropospheric Research Laminar Flow Tube (IfT-LFT) at T = 293 ± 0.5 K, RH = 50%. We measured sCI and sCI lifetimes in presence of water vapour (RH=50%) representing an upper limit for the sCI lifetime against unimolecular self-reaction that

results in sCI decomposition. Reaction rate coefficients for sCI+SO_2 were also measured. Results will not be reported here.

ROLE OF MONOTERPENE ORIGINATING SCI'S IN GLOBAL H_2SO_4 ,CN AND CCN BUDGET

We implemented the new SO2 oxidation pathway by sCIs in the global aerosol-climate model ECHAM5.5-HAM2 (Zhang 2012). We performed simulations with present-day aerosol and precursor emissions. The control simulation included SO2 oxidation only by hydroxyl radical in the gas while the second simulation included the additional oxidation pathway by sCIs form monoterpene ozonolysis in the gas phase. The model was integrated for 16 months, and the last 12 months were used for the analysis.

The implementation of monoterpene oxidation leads to surface-level sCI concentrations in Hyytiälä of $1.0 \cdot 10^6$ and $0.9 \cdot 10^6$ cm^{-3} in July and August, respectively. This is in accordance with our field measurements (Mauldin et al., 2012) where we observed sCI concentrations ranging between few times 10^5 and few times 10^6 cm^{-3}. We found that including sCI oxidation pathway in the model increases sulphuric acid concentrations throughout the continents and that sCI+SO_2 pathway contributes to H_2SO_4 budgets in lowest simulation levels (boundary layer). The increased sulphuric acid concentrations result also in increased concentrations of secondary aerosol particles (CN) and cloud condensation nuclei (CCN) especially in summertime Eurasian boreal forest.

CONCLUSIONS

We investigated the kinetics of sCI from ozonolysis of boreal forest relevant alkenes. We measured the yields of sCI formation, sCI lifetimes and reaction rate coefficients for sCI + SO_2. Reaction rate coefficients were considerably higher than assumed before (Johnson et al., 2001), but in line with our earlier estimates (Mauldin et al., 2012). On the other hand, we found the reaction rate coefficients to be smaller than suggested by Welz et al. (2012) for the simplest sCI in low pressure system.

We implemented the kinetics of sCI formation, loss and reaction with SO_2 to global aerosol – climate model. We found sCI to have a contribution to H_2SO_4, CN and CCN concentrations in lowest simulation levels. It should be noted that thus far we considered only monoterpenes as the source of sCI in the model simulations. Implementing the sCI from ozonolysis of isoprene as well as from yet not experimentally investigated sesquiterpenes into model would most likely increase the H_2SO_4, CN and CCN concentrations in the model simulations. Running the simulations in the future increased temperatures and VOC emissions might reveal a new negative natural feedback mechanism possibly attenuating the climate warming at least in the forested areas of the globe. Besides the contribution of sCI to H_2SO_4 formation, also other reactions might be important from CN and CCN formation point of view.

ACKNOWLEDGEMENTS

REFERENCES

Dentener, F., Kinne, S., Bond, T., Boucher, O., Cofala, J., Generoso, S., Ginoux, P., Gong, S., Hoelzemann, J. J., Ito, A., Marelli, L., Penner, J. E., Putaud, J.-P., Textor, C., Schulz, M., van der Werf, G. R., and Wilson, J. (2006). Emissions of primary aerosol and precursor gases in the years 2000 and 1750 prescribed data-sets for AeroCom, Atmos. Chem. Phys., 6, 4321-4344, doi:10.5194/acp-6-4321-2006.

Johnson, D., Lewin, A. G. & Marston, G. The effect of Criegee-intermediate scavengers on the OH yield from the reaction of ozone with 2-methylbut-2-ene. J. Phys. Chem. A 105, 2933–2935 (2001).

Kulmala, M., Lehtinen, K. E. J., and Laaksonen, A. (2006). Cluster activation theory as an explanation of the linear dependence between formation rate of 3nm particles and sulphuric acid concentration, Atmos. Chem. Phys., 6, 787-793, doi:10.5194/acp-6-787-2006.

Mauldin III, R. L., Berndt, T., Sipilä, M., Paasonen, P., Petäjä, T., Kim. S., Kurtén, T., Stratmann, F.,

Kerminen, V.-M. and Kulmala, M. (2012). A new atmospherically relevant oxidant of sulphur dioxide. Nature, 488, 193-196.

Paasonen, P., Nieminen, T., Asmi, E., Manninen, H. E., Petäjä, T., Plass-Dülmer, C., Flentje, H., Birmili, W., Wiedensohler, A., Hõrrak, U., Metzger, A., Hamed, A., Laaksonen, A., Facchini, M. C., Kerminen, V.-M., and Kulmala, M. (2010). On the roles of sulphuric acid and low-volatility organic vapours in the initial steps of atmospheric new particle formation, Atmos. Chem. Phys., 10, 11223-11242, doi:10.5194/acp-10-11223-2010.

Sipilä, M. et al. (2010). The role of sulfuric acid in atmospheric nucleation. Science 327, 1243–1246.

Taatjes, C. A., Welz, O., Eskola, A. J., Savee, J. D., Osborn, D. L., Lee, E P. F., Dyke, J. M., Mok, D. W. K., Shallcross, D. E. and Percival, C. J. (2012). Direct measurement of Criegee intermediate (CH2OO) reactions with acetone, acetaldehyde, and hexafluoroacetone, Phys. Chem. Chem. Phys., **14**, 10391-10400.

Welz, O. et al. (2012). Direct kinetic measurements of Criegee intermediate (CH2OO) formed by reaction of CH2I with O2. Science 335, 204–207.

Zhang, K., O'Donnell, D., Kazil, J., Stier, P., Kinne, S., Lohmann, U., Ferrachat, S., Croft, B., Quaas, J., Wan, H., Rast, S., and Feichter, J. (2012). The global aerosol-climate model ECHAM-HAM, version 2: sensitivity to improvements in process representations, Atmos. Chem. Phys. Discuss., 12, 7545-7615, doi:10.5194/acpd-12-7545-2012.

TOWARDS A GLOBAL DATA BASE OF FORESTS AND TREE SPECIES AND THE IMPLICATION FOR ATMOSPHERIC MODELLING OF BVOCS

C.A.SKJØTH[1,2], D. ODERBOLZ[3], H.SKOV[2] and A.MASSLING[2]

[1]Department of Earth and Ecosystem Sciences, Division of Physical Geography and Ecosystems Analysis,

Lund University, Sölvegatan 12, 223 62 Lund, Sweden

[2]Faculty of Science and Technology,Department for Environmental Science, Aarhus University, P.O.Box 358, Frederiksborgvej 399, 4000 Roskilde, Denmark

[3]Laboratory of Atmospheric Chemistry (LAC), Paul Scherrer Institut (PSI), CH-5232 Villigen, PSI, Switzerland

Keywords: forests, inventories, tree species, ecosystems

INTRODUCTION

Forest areas are sources for gasses and particles that are relevant in atmospheric chemistry and physics. Emissions include isoprene and groups of monotherpenes or sesquiterpenes. Isoprene as well as other biogenic volatile compounds is known to be important in atmospheric chemistry and with respect to climate change. The capacity to release these gasses varies between tree species at the species level (Simpson et al., 1999). A good example is the difference between two common European oaks: Cork oak (*Quercus suber*) and Sessile oak (*Quercus petraea*). The emission potential of isoprene between these two species spans several orders of magnitude (Simpson et al., 1999). Detailed data on e.g. tree species of forests and their capability to release gasses (e.g. precursors of aerosols) and aerosols is therefore relevant in the context of atmospheric science.

Dynamic Vegetation Models can be used to describe the evolution of forest cover, the important feed-back processes between the biosphere and the climate system (Jones et al., 2009) as well as the release of VOCs such as isoprene and terpenes to the atmosphere (Arneth et al., 2011). The impact of these emissions go beyond continental scale as they take part in a number of feed-back mechanisms in the climate system (Arneth et al., 2011). However, many processes in relation to VOC production are still poorly understood and it has also been shown that these Dynamic Vegetation Models are sensitive to underlying vegetation fields. Furthermore, the forest composition is often influenced by management processes (Skjøth et al., 2008), making it difficult to predict tree species composition using vegetation models. Finally, it is considered to be nearly impossible using an accurate model to predict tree species composition, when the geographical coverage goes beyond continental scale such as in Europe (Hickler et al., 2012). Mapping of tree species in forests on either hemispheric or global scale are therefore relevant to improve our understanding of the climate system. However data gathering from a number of different regions on earth can be very challenging due to regional conflicts such as war or due to the fact that some regions such as rain forests remains to be fully explored. The aim of this paper is twofold: 1) To document current progress with respect to provide a global data base of tree species and 2) to show

591

the impact of data from this data base when data are used for BVOC calculations in an atmospheric chemistry transport model that covers most of Europe.

METHODS

Statistical data on forest compositions have been obtained from national statistical offices from a large number of countries by using a similar approach as in Skjøth et al (2008. About 80% of the globe is currently covered, corresponding to about 1030 statistical regions (Fig. 1). Few areas in Africa remain to be investigated as well as e. g. China and other nearby countries. Furthermore, data from USA needs additional calculations before this area can be considered as fully analysed.
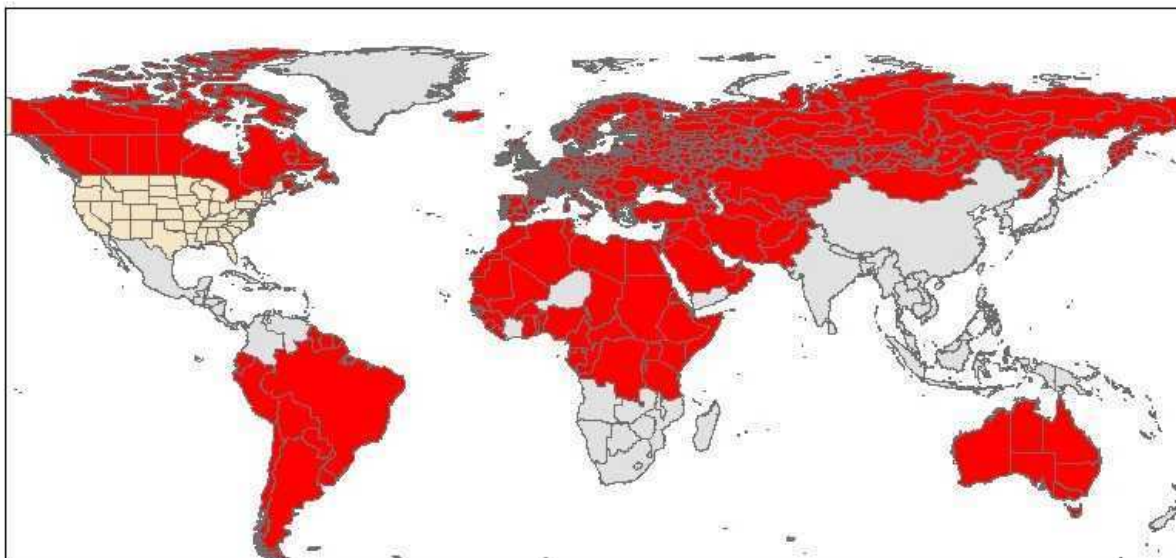
Fig 1. Current data coverage in the tree species database. Grey areas are not yet analysed. Pink areas have been analysed, but additional data is needed to achieve more sufficient data coverage. Red areas are fully analysed.

Data from the database is then extracted for the BVOC modelling over Europe and harmonised for use with grid based models. The harmonised data has then been analysed with three different land cover data sets USGS-land cover, GLC2000 and Globcover ver 2.2. Furthermore, it has been used by the BVOC model by Steinbrecher et al (2009) for CTM model calculations with the CAMx model (Oderbolz et al., 2012). Additionally, the data set is compared to two other European data sets with tree species information.

RESULTS

The data extraction show that most areas in Europe are well covered with respect to tree species information for BVOC modelling. However a few areas like Germany have limited knowledge as

information from the highly emitting oak species is only available at the genus level.
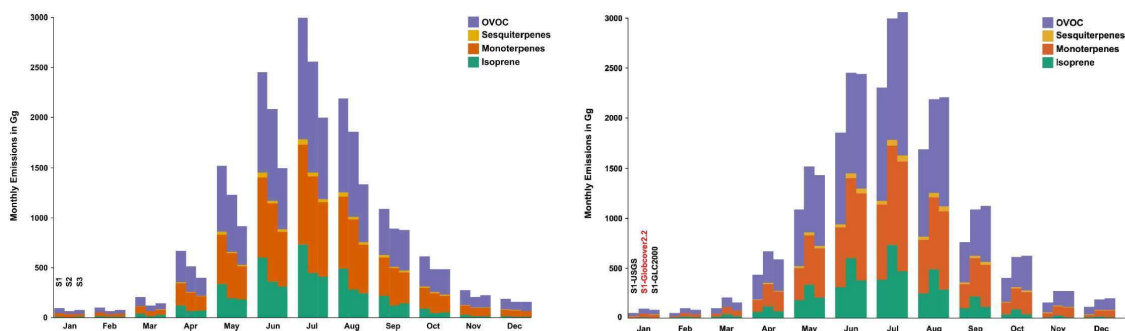
Fig. 2 (left) shows the result when the database is tested with three different tree species data sets and combining this with the Globcover 2.2 land cover data set. (right) shows the test of the tree species database by Simpson et al (1999), Skjøth et al (2008) and Köble and Seufert (2001) and combining this with three different land cover databases: USGS Landover, GLC2000 and Globcover 2.2, respectively. Highest emissions are in general found during summer and by including the most detailed information with respect to tree species information.

Model calculations on the extracted data are sensitive to the choice of tree species database. Highest emissions are observed during summer and lowest during winter. The tree species in this study provides higher emissions than the two other data sets, primarily due to the higher emissions for certain oak species. The model calculations also show that the choice of land cover affects the emissions. USGS in general results in lower emissions and globcover ver 2.2 provides the highest emissions.

Top emitters at the species level are for isoprene *Quercus* species and for monotherpenes *Pinus sylvestris* and various *Quercus* species and for sequiterpenes *Betula* is bar far the most dominating species.

CONCLUSIONS

We have here expanded the tree species database to near global coverage. The quality of the database varies highly, with the highest quality data in Europe and no data in certain areas of Africa, primarily due to the fact that regional conflicts permit access and data gathering. The tree species database has been shown to affect model calculations over Europe (Oderbolz et al., 2012) by using the CAMx model in connection with a dedicated BVOC model by Steinbrecher et al. (2009). Here Oderbolz et al. suggest, that BVOC model calculations are generally improved by making calculations at the species level and that the database in this study seems to be the best compromise among three different European data sets. However, it is also pointed out that the database needs improvements over certain areas such as Germany.

The results here shown that for global or near global usage, modellers need to be able to deal with data spare areas or areas without any information at all. The model results by Oderbolz et al (2012) also show, that minor species like e.g. Eucalyptus can have a large impact on the overall emissions. The reason to this is a combination of climate and high emission factors for that particular tree specie.

Additionally, the investigation shows, that the final model results are sensitive to the chosen land cover data set such as USGS landcover, GLC2000 or Globcover 2.2. The main reason is, that forest cover among these data sets does not entirely agree. This of course affects the distribution of trees at the species level.

The overall results suggest that a global database of tree species is a highly relevant product for studies in relation to climate and atmospheric chemistry. However, it seems that data users must accept data gaps or that the at least must be prepared to replace data gaps with supplementary information. It is therefore highly relevant, that the database is provided as an open data set that can be used and improved by all users including modellers that are interested in BVOCs and atmospheric chemistry.

ACKNOWLEDGEMENTS

REFERENCES

Arneth, A., Schurgers, G., Lathiere, J., Duhl, T., Beerling, D. J., Hewitt, C. N., Martin, M., and Guenther, A., 2011, Global terrestrial isoprene emission models: sensitivity to variability in climate and vegetation: Atmos. Chem. Phys., **11,** 8037-8052.

Hickler, T., Vohland, K., Feehan, J., Miller, P. A., Smith, B., Costa, L., Giesecke, T., Fronzek, S., Carter, T. R., Cramer, W., Kuhn, I., and Sykes, M. T., 2012, Projecting the future distribution of European potential natural vegetation zones with a generalized, tree species-based dynamic vegetation model: Global Ecology and Biogeography, **21,** 50-63.

Jones, C., Lowe, J., Liddicoat, S., and Betts, R., 2009, Committed terrestrial ecosystem changes due to climate change: Nature Geosci, **2,** 484-487.

Köble, R. and Seufert, G., 2001, Novel maps for forest tree species in Europe.

Oderbolz, D. C., Aksoyoglu, S., Keller, J., Barmpadimos, I., Steinbrecher, R., Skjøth, C. A., Plaß-Dülmer, C., and Prevot, A. S. H., 2012, A novel approach to emission modelling of biogenic volatile organic compounds in Europe: improved seasonality and land-cover: Atmos. Chem. Phys. Discuss., **12,** 19921-19985.

Simpson, D., Winiwarter, W., Borjesson, G., Cinderby, S., Ferreiro, A., Guenther, A., Hewitt, C. N., Janson, R., Khalil, M. A. K., Owen, S., Pierce, T. E., Puxbaum, H., Shearer, M., Skiba, U., Steinbrecher, R., Tarrason, L., and Oquist, M. G., 1999, Inventorying emissions from nature in Europe: J. Geophys. Res. , [Atmos.], **104,** 8113-8152.

Skjøth, C. A., Geels, C., Hvidberg, M., Hertel, O., Brandt, J., Frohn, L. M., Hansen, K. M., Hedegaard, G. B., Christensen, J., and Moseholm, L., 2008, An inventory of tree species in Europe - an essential data input for air pollution modelling: Ecological Modelling, **217,** 292-304.

Steinbrecher, R., Smiatek, G., Koble, R., Seufert, G., Theloke, J., Hauff, K., Ciccioli, P., Vautard, R., and Curci, G., 2009, Intra- and inter-annual variability of VOC emissions from natural and semi-natural vegetation in Europe and neighbouring countries: Atmos. Environ., **43,** 1380-1391.

MONOTERPENE EMISSIONS FROM BOREAL PINE FOREST IN SOUTHERN FINLAND: COMRARISON OF MEASUREMENTS AND TWO MODELS

S. SMOLANDER[1], Q. HE[2], D. MOGENSEN[1,3], L.ZHOU[1], J. BÄCK[1], T. RUUSKANEN[1], S. NOE[4], A GUENTHER[5], M KULMALA[1] and M. BOY[1]

[1]Department of Physics, University of Helsinki, Finland

[2]Institute of Earth Environment, Chinese Academy of Sciences, Xi'an, China

[3]Helsinki University Centre for Environment, University of Helsinki, Finland

[4]Department of Plant Physiology, Institute of Agricultural and Environmental Sciences, Estonian University of Life Sciences, Estonia

[5]Atmospheric Chemistry Division, National Center for Atmospheric Research, Boulder, Colorado, USA

Keywords: MONOTERPENE, BVOC, EMISSION.

INTRODUCTION

Biogenic volatile organic compounds (BVOCs) are essential in atmospheric chemistry because of their chemical reactions that produce and destroy tropospheric ozone, their effects on aerosol formation and growth, and their potential influence on global warming. As one of the important BVOC groups, monoterpenes have been a focus of scientific attention in atmospheric research. Detailed regional measurements and model estimates are urgently needed to study emission controls and the monoterpene budget on a global scale. However, since physical and biological factors such as genetic variation, temperature and light, water availability, seasonal changes, and environmental stresses have complex impacts on monoterpene emissions, comprehensive inventories are not reliably defined. To further track monoterpene concentrations and their chemical transformations, the model SOSA was applied to investigate Scots pine (*Pinus sylvestris*) emissions in the boreal coniferous forest at SMEAR II in Hyytiälä, Finland. Results indicate that modeling and observations agreed reasonably well. The predominant species were α-pinene, followed by 3-carene, which is consistent with previous research at SMEAR II. Seasonal and diurnal variations were demonstrated in both quantity and quality of emitted compounds. SOSA is also employed to test the influence of using different monoterpene chemotypic blends in order to reduce the uncertainties in the future.

The aim of the study is to verify the reliability of the atmospheric chemistry-transport model SOSA (model to simulate the concentrations of organic vapours and sulphuric acid) and to compare the performances of three different emission modules implemented. SOSA is also employed to test the influences to monoterpene simulations by using different chemotypic characterization blends input in order to reduce the uncertainties in the future.

METHODS

For estimating the robustness of SOSA's emission module, we used three different emission modules: "Old MEGAN" (Model of Emissions of Gases and Aerosols from Nature, Guenther *et al.,* 1995), "New MEGAN" (Guenther *et al.,* 2006) and "SIM-BIM" (Seasonal Isoprenoid synthase Model-Biochemical Isoprenoid biosynthesis Model, Grote *et al.,* 2006).

MEGAN coupled with SOSA provides on-line estimates of the landscape-averaged emission rates of monoterpenes and other BVOCs from terrestrial ecosystems into the above-canopy atmosphere at a specific location and time (Guenther *et al.,* 2006). The emissions of organic vapours from the canopy were calculated as:

$$\text{Emission} = [\varepsilon] * [\gamma] * [\rho] \qquad \text{(Eq. 2)}$$

where ε (μg m^{-2}h^{-1}) is an ecosystem-dependent emission factor representing the emission of a compound into the canopy at a photosynthetically active radiation (PAR) flux of 1000μmol m^{-2}s^{-1} and leaf temperature of 303.15K, referred to as standard emission potential. We assumed Scots pine to be the main tree species in our boreal forest ecosystem, and the seasonal standard monoterpene emission potentials used in the model were from Tarvainen *et al.,* 2005 and Hakola *et al.,* 2006. γ (normalized ratio) is a non-dimensional activity adjustment emission factor that accounts for emission changes due to deviations from standard conditions, and ρ (normalized ratio) is a factor that accounts for production and loss within plant canopies (Guenther *et al.,* 2006). The surface emission flux from the vegetation, $F_{vegetation}$, was calculated in the model as (Guenther *et al.,* 1995):

$$F_{vegetation} = D_m * [\varepsilon] * [\gamma] \qquad \text{(Eq. 3)}$$

where D_m (kg dry matter m^{-2}) is the foliar density obtained from the leaf area index (LAI) with 0.538 kg m^2 adopted as the constant value at SMEAR II (Ilvesniemi *et al.,* 2009). ε (μg m^{-2}h^{-1}) and γ are the same as mentioned above.

The new MEGAN takes into account emissions of also other VOC's than monoterpenes. Driving variables such as temperature and light in the past days were also recorded when calculating current emissions. Emissions of methanol, formaldehyde, acetone and sesquiterpenes, which may contribute significantly to atmospheric concentrations of VOC were estimated by the new MEGAN but were not discussed in the study due to a lack of continuous high-resolution observation data for these compounds. The emission activity factor γ in the new MEGAN was improved, and it accounted for the effects of soil moisture, leaf age and the canopy environment as (Guenther *et al.,* 2006):

$$\gamma = \gamma_{age} * \gamma_{SM} * \gamma_{CE} \qquad \text{(Eq. 4)}$$

where γ_{age} makes adjustments for effects of leaf age and is calculated from a leaf age algorithm that assigns different emission activities to new, growing, mature, and old leaves. γ_{SM} accounts for direct changes in γ due to changes in soil moisture. γ_{CE} describes variation due to LAI and light, temperature, humidity and wind conditions within the canopy environment and is estimated as:

$$\gamma_{CE} = C_{CE} * \gamma_{PT} * LAI \qquad \text{(Eq. 5)}$$

where C_{CE} is a factor that sets the emission activity to unity at standard conditions, γ_{PT} is the weighted average of the product of a temperature emission activity factor (γ_T) and a photosynthetic photon flux density (PPFD) emission activity factor (γ_P), *LAI* is the leaf area index. The new MEGAN extended algorithms to estimate γ_T and γ_P instead of using the constant values recommended by Guenther *et al.,* 1999, which improved the simulated variations in emission associated with past temperature and PPFD conditions (Guenther *et al.,* 2006). Previous researches show that measured terpenoid standard emission potentials are higher when warm sunny conditions have occurred during the previous days and are lower if there were cool shady conditions (Sharkey *et al.,* 2000). The impact on vegetation emissions by exposure to different temperature and light could last for several weeks (Pétron *et al.,* 2001). The factors controlling these variations may operate over a continuous range of time scales, but for modelling purposes the new MEGAN currently considers only 24 and 240 h (Guenther *et al.,* 2006).

Since neither the old or the new MEGAN versions consider the ability of plants to adapt their isoprenoid biosynthesis capacity dynamically according to changes of environmental parameters (Pétron *et al.,* 2001; Staudt *et al.,* 2003), a process-based model SIM-BIM was also used as an emission module. SIM-BIM takes into account the physiological/phenological state of the leaves and the biochemical processes like the available carbon and energy resources leading to the formation of volatile isoprenoids (Grote *et al.,* 2006). SIM-BIM presented is a combination of the seasonal isoprenoid synthase model SIM (Lehning *et al.,* 2001) that dynamically describes the seasonal development of isoprenoid synthase and daily step enzyme activity and the biochemical isoprenoid emission model BIM (Zimmer *et al.,* 2000) that mechanically simulates stand-level volatile isprenoid production in relation to instantaneous as well as integrated environmental conditions.
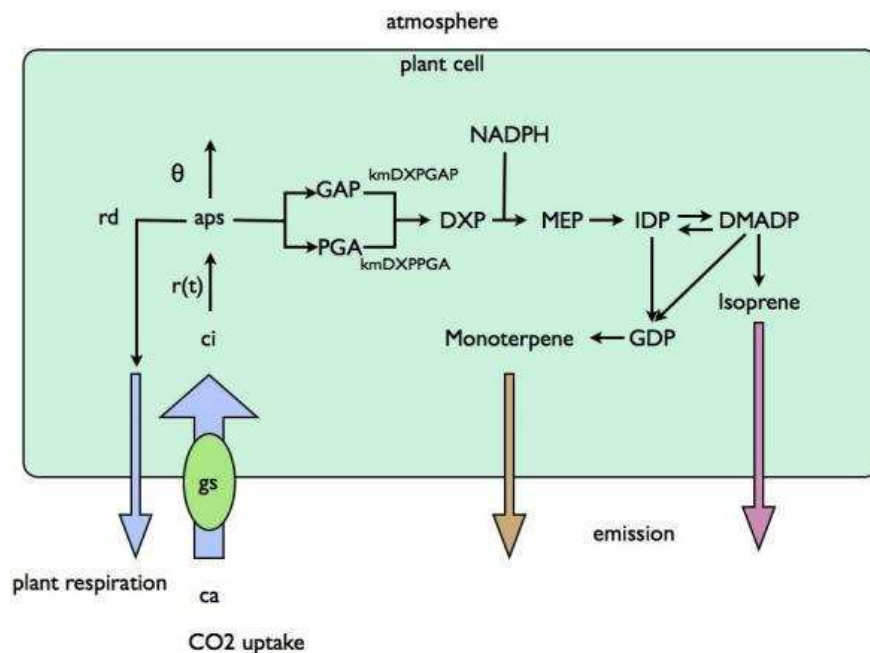
Figure 1. A simple scheme of the SIM-BIM in SOSA with ca = CO_2 concentration in the air; ci = intercellular CO_2 concentration; gs = stomata conductance; aps = taken up carbon pool; r(t) = photosynthesis rate as a function of light; rd = dark respiration rate; θ = the fraction of carbon used in plants metabolism; kmDXPGAP & kmDXPPGA = Michaelis-Menten reaction coefficients; GAP = glyceraldehydes-3 -phosphate; PGA = 3-phosphoglyceric aldehyde; DXP = 1-deoxy-D-xylulose 5-phosphate; MEP = 2-C-methyl-D-erythritol 4-phosphate; NADPH = nicotinamide adenine dinucleotide phosphate; IDP = isopentenyl diphosphate; DMADP = dimethylallyl diphosphate; GDP = geranyl diphosphate.

The SIM-BIM module calculates changes in the concentrations of a number of isoprene and monoterpene precursors within the chloroplast, assuming the absence of specific storage structures and neglecting the effect of unspecific storages (Grote, 2006). It basically consists of a sequence of first-order Michaelis-Menten enzymatic reactions that depend on instantaneous temperature (Grote *et al.,* 2010). As shown in Figure 1, primary substrates for the emission model are provided by photosynthesis. The C_i/C_a ratio is a sensitive indicator of stomatal conductance (gs), which is very important for water-use efficiency in photosynthesis. The basic carbon input is controlled by light intensity, humidity and temperature, the function *r(t)* by light. The taken up carbon (*aps*) is divided into three parts: the use of the carbon in respiration (loss to atmosphere), the use of the carbon in the plants metabolism (θ), and the use for isoprenoid production. *GAP* and *PGA* are made of 3 carbon atoms, so *aps* used for isoprenoid production

is divided by 3 to achieve one of these molecules. There is a fraction in the model that decides how much of *GAP* and *PGA* are built up, and those that would be transformed into *DXP* under different reaction rates (*kmDXPGAP* and *kmDXPPGA*). *DXP* then produces *MEP* with the presence of *NADPH* which is considered to be constant in our model. *MEP* reacts further to *IDP*. *IDP* and *DMADP* are both 5 carbon atoms and in equilibrium, with a certain equilibrium constant. When *IDP* and *DMADP* build together to form the 10 carbon monoterpene backbone molecule *GDP*, monoterpene will be emitted. The potential production rates are determined by activities of isoprenoid biosynthesis-related enzymes (Grote *et al.*, 2010). The proportion of carbon used for emission increases particularly rapidly if temperature increases beyond the optimum for carbon assimilation up to the optimum temperatures of the kinetic reactions involved in isoprenoid production (Zimmer *et al.*, 2000; Grote, 2006). Another notable advantage of this biochemical/physiological approach is that plant stresses such as drought can be additionally introduced without laborious re-parameterisation assumptions required (Niinemets *et al.*, 1999; Grote *et al.*, 2010).

RESULTS

With the consideration of chemotypic characterization, we selected the average case as our input data for model simulations. The differences among the three emission modules and their estimation for monthly mean monoterpene concentrations are shown in figure 2. As seen in this figure, all the modules could give similarly reasonable values in relative to the available measured monoterpene concentration data. Seasonal variations from modelling clearly correspond to the measurement distributions with the highest concentrations in the summer. The comparison with SIM-BIM indicates that MEGAN is slightly more expressed by seasonality, which agrees with a previous study in southern France (Grote, 2006; Grote *et al.*, 2010). SIM-BIM module results in smaller emissions and less variability in spring and autumn could attribute to slow response of synthase activity to unfavourable environmental conditions. However, MEGAN directly and immediately responding to light and temperature would lead to the stronger seasonality. Interestingly, a larger discrepancy with measurement values could be found in the months of April, May, August and September. We deduce that emissions from forest floor may play a role in these months but it was not taken into account in this figure. Previous research (Hellén *et al.*, 2006; Aaltonen *et al.*, 2011) also proves that in boreal forest soil, BVOC emissions are highest in spring and autumn. During the snow-free time from April to May when soil is unfrozen, plant roots and microbial population are in the active stage, while in August and September, with needles falling to the forest floor, the storage components of litter fall could also release a certain amount of monoterpenes.
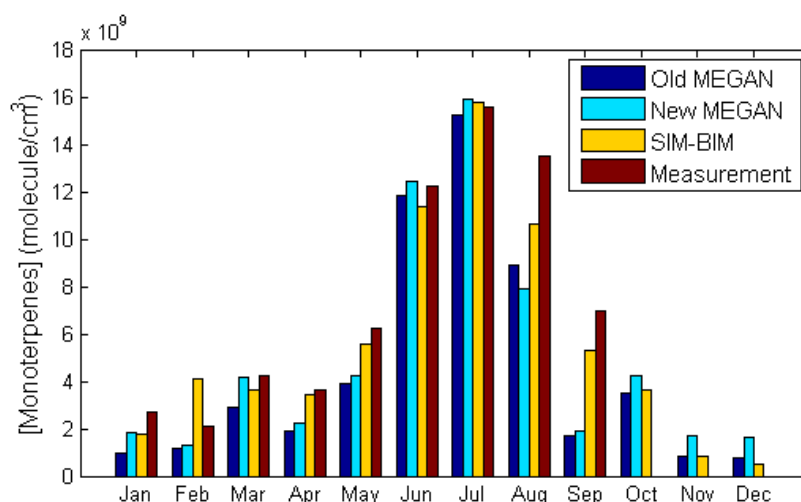

Figure 2. Modelled and measured monthly mean monoterpene concentrations at 4 m for 2007.

REFERENCES

Aaltonen, H., Pumpanen, J., Pihlatie, M., Hakola, H., Hellén, H., Kulmala, L., Vesala, T., Bäck, J.: Boreal pine forest floor biogenic volatile organic compound emissions peak in early summer and autumn, Agric. Forest Meteorol., 10,1016, 2011.

Grote, R., Mayrhofer, S., Fischbach, J. R., Steinbrecher, R., Staudt, M., Schnitzler, J.-P.: Process-based modelling of isoprenoid emissions from evergreen leaves of Quercus ilex (L.), Atmos. Environ., 40, S152-S165, 2006.

Grote, R., Keenan, T., Lavoir, A.-V. and Staudt, M.: Process-based simulation of seasonality and drought stress in monoterpene emission models, Biogeosicences., 7, 257-274, 2010.

Guenther, A., Hewitt, C. N., Erickson, D., Fall, R., Geron, C., Graedel, T., Harley, P., Klinger, L., Lerdau, M., McKay, W. A., Pierce, T., Scholes, B., Steinbrecher, R., Tallamraju, R., Taylor, J., Zimmerman, P.: A global model of natural volatile organic compound emissions, J. Geophys. Res., 100, 8873-8892, 1995.

Guenther, A., Baugh, B., Brasseur, G., Greenberg, J., Harley, P., Klinger, L., Serca, D., and Vierling, L.: Isoprene emission estimates and uncertainties for the Central African EXPRESSO study domain, J. Geophys. Res.-Atmos., 104(D23), 30625-30639, 1999.

Guenther, A., Karl, T., Harley, P., Wiedinmyer, C., Palmer, P. I. and Geron, C.: Estimates of global terrestrial isoprene emissions using MEGAN (Model of Emissions of Gases and Aerosols from Nature), Atmos. Chem. Phys., 6, 3181-3210, 2006.

Hakola, H., Tarvainen, V., Bäck, J., Ranta, H., Bonn, B., Rinne, J. and Kulmala, M.: Seasonal variation of mono- and sesquiterpene emission rates of Scots pine, Biogeoscience., 3, 93-101, 2006.

Hellén, H., Hakola, H., Pystynen, K.-H., Rinne, J., Haapanala, S.: C_2-C_{10} hydrocabon emissions from a boreal wetland and forest floor, Biogeosciences, 3, 167-174, 2006.

Ilvesniemi, H., Levula, J., Ojansuu, R., Kolari, P., Kulmala, L., Pumpanen, J., Launiainen, S., Vesala, T., Nikinmaa, E.: Long-term measurements of the carbon balance of a boreal Scots pine dominated forest ecosystem, Boreal Env. Res., 14, 731-753, 2009.

Lehning, A., Zimmer, W., Zimmer, I., Schnitzler, J.-P.: Modelling of annual variations of oak (Quercus robur L.) isoprene synthase activity to predict isoprene emission rates, J. Geophys. Res., 106, 3157-3166, 2001.

Niinemets, Ü., Tenhunen, J.D., Harley, P.C., Steinbrecher, R.: A model of isoprene emission based on energetic requirements for isoprene synthesis and leaf photosynthetic properties for Liquidambar and Quercus, Plant Cell Environ., 22, 1319-1335. 1999.

Pétron, G., Harley, P., Greenberg, J., and Guenther, A.: Seasonal temperature variations influence isoprene emission, Geophys. Res. Lett., 28(9), 1707-1710, 2001.

Sharkey, T. D., Singsaas, E. L., Lerdau, M. T., and Geron, C.: Weather effects on isoprene emission capacity and applications in emissions algorithms, Ecol. Appl., 9, 1132-1137, 2000.

Staudt, M., Joffre, R. and Rambal S.: How growth conditions affect the capacity of Quercus ilex leaves to emit monoterpenes, New Phytologist., 158, 61-73, 2003.

Tarvainen, V., Hakola, H., Hellén, H., Bäck, J., Hari, P. and Kulmala, M.: Temperature and light dependence of the VOC emissions of Scots pine, Atmos. Chem. Phys., 5, 989-998, 2005.

Zimmer, W., Brüggemann, N., Emeis, S., Giersch, C., Lehning, A., Steinbrecher, R., Schnitzler, J.-P.: Process-based modelling of the isoprene emission by oak leaves, Plant Cell Environ., 23, 585-595, 2000.

THE INFLUENCE OF CHANGING GREENHOUSE GAS CONCENTRATIONS AND AEROSOL EMISSIONS ON THE ARCTIC CLIMATE: 1970 TO 2000

H. STRUTHERS[1,2], A. M. L. EKMAN[1], A. LEWINSHAL[1], T. IVERSEN[3,4], A. KIRKEVÅG[3] and Ø. SELAND[3]

[1] Department of Meteorology, Stockholm University, Stockholm, SE-10691, Sweden.

[2] Department of Applied Environmental Science, Stockholm University, Stockholm, SE-11418, Sweden.

[3] Norwegian Meteorological Institute, Oslo, Norway.

[4] Department of Geosciences, Oslo University, Oslo, Norway.

INTRODUCTION

Since the 1970's, there has been a rapid change in the magnitude and spatial distribution of anthropogenic aerosol particle and precursor emissions with a significant decrease over e.g. Europe and North America and a substantial increase over large parts of Asia (Lamarque *et al.*, 2010). During the same time period, there has been a significant increase in global greenhouse gas concentrations. The Arctic climate is particularly sensitive to both the local and remote perturbations of the radiative budget associated with anthropogenic aerosol emissions (Shindell and Faluvegi, 2009) and thus we might expect to be able to detect the fingerprint of changes in anthropogenic aerosol emissions in the recent record of Arctic climate change.

In the present study, the global climate model CAM-Oslo (Seland *et al.*, 2008) is used to examine whether the shift in aerosol emissions between 1970 and present day results in a clear fingerprint in the modeled atmospheric circulation, temperature and surface pressure change patterns. CAM-Oslo includes a comprehensive module of the atmospheric aerosol cycle as well as descriptions of the direct and indirect effects of aerosol particles on radiation, cloud reflectivity and precipitation. We examine if the temperature, circulation and surface pressure response patterns differ when aerosol effects are considered separately or simultaneously with a change in greenhouse gas concentration.

METHODS

CAM-Oslo

CAM-Oslo is based on the CAM3 general circulation model (Collins *et al.*, 2006) and includes a detailed aerosol module as described by Seland *et al.* (2008). The aerosol module considers five prognostic aerosol compounds: sulfate (SO_4), particulate organic matter (OM), black carbon (BC), sea salt (SS) and mineral dust (DU) as well as two gaseous aerosol precursors (dimethylsulfide (DMS), and sulfur dioxide (SO_2)). The primary aerosol size distributions are approximated using a superposition of 11 log-normal modes which are subsequently modified via condensation and coagulation using a 44 sectional bin framework. All prognostic compounds, except DMS, are subjected to production, transport and dry and wet deposition (Iversen and Seland, 2002) with the mixing state of the aerosol components determined via a process-level description of aerosol dynamics. When the relative humidity is below 100%, the hygroscopic growth, dry deposition and

601

optical properties of the aerosol particles are approximated using extensive pre-calculated lookup tables (Kirkevåg and Iversen, 2002). Köhler theory is used to calculate the number of CCN at a given supersaturation which is assumed to be 0.1% for stratiform clouds. For convective clouds, the supersaturation is assumed to be 0.25% over ocean and 0.8% over land.

The aerosol fields and the direct and indirect aerosol radiative effects simulated by CAM-Oslo and its predecessor CCM-Oslo have been comprehensively evaluated through the AeroCom (Aerosol Comparisons between Observations and Models) aerosol modeling initiative (Kinne *et al.* 2006; Penner *et al.*, 2006; Schulz *et al.*, 2006; Textor *et al.*, 2006; Koch *et al.*, 2009). On a global scale, the general characteristics of the aerosol fields and radiative forcings simulated by CAM-Oslo and CCM-Oslo are within the range of the other models included in the AeroCom project (Kinne *et al.* 2006; Schulz *et al.*, 2006; Quaas *et al.*, 2009).

AEROSOL EMISSIONS

In CAM-Oslo, natural SO_2 emissions from volcanoes are considered as well as anthropogenic sources from combustion of fossil fuel and biomass burning. SO_2 is also produced from oxidation of DMS. A minor fraction of the anthropogenic sulfur emissions is assumed to be sulfate, produced catalytically during or immediately after combustion. This primary particulate sulfate is emitted with a modal radius of 75 nm, based on Stier *et al.* (2005).

BC and OM aerosols emitted from fossil fuel combustion are assumed externally mixed. When emitted from biomass burning, OM and BC are assumed internally mixed, as recommended in Dentener *et al.* (2006). Externally mixed BC is assumed fully hydrophobic whilst OM is assumed to be 25% as hygroscopic as ammonium sulfate. Both BC and OM are gradually converted into fully hydrophilic, internally mixed aerosols due to condensation of gaseous sulfuric acid, or by coagulation with sulfate or SS. Biogenic SOA is presently treated as OM emissions and is assumed internally mixed with BC when emitted in the same area.

Monthly varying mineral dust emissions are prescribed as area-sources on the ground and are thus not dependent on e.g. the modeled meteorology. The modeled sea salt emissions on the other hand depend on both the modeled SST and surface wind speed according to Mårtensson *et al.* (2003).

		1970	2000
GHG conc.	CO_2 (ppm)	325.0	368.9
	CH_4 (ppb)	1386	1751
	N_2O (ppb)	295.2	315.9
	CFC11 (ppt)	49.1	266.7
	CFC12 (ppt)	138.6	535.0
Aerosol and precursor emiss. ($Tg\ yr^{-1}$)	DMS	18.1	18.1
	$SO_2 + SO_4$	126.7	107.6
	OM	27.2	35.9
	BC	5.52	7.76
	DU	1671	1671

Table 1: 1970 and 2000 greenhouse gas concentrations and DMS and aerosol emissions (global total) used in CAM-Oslo. Note that sea salt aerosol emissions are calculated on-line by the model.

The magnitude of the anthropogenic aerosol and precursor gas emissions employed in the model follows the work by Lamarque *et al.* (2010) and is summarized in Table 1. Air pollution regulations in e.g. Europe and North America have resulted in a clear decrease of globally average SO_2 emissions of about 15%. At the same time, increased fossil fuel and biomass burning emission over Asia has

resulted in an increase of BC and OM emissions of approximately 40% and 32%, respectively. See also Figure 1 which depicts the change in the emission of anthropogenic aerosols (sulfur, OM and BC) from 1970 to 2000 as a function of latitude.
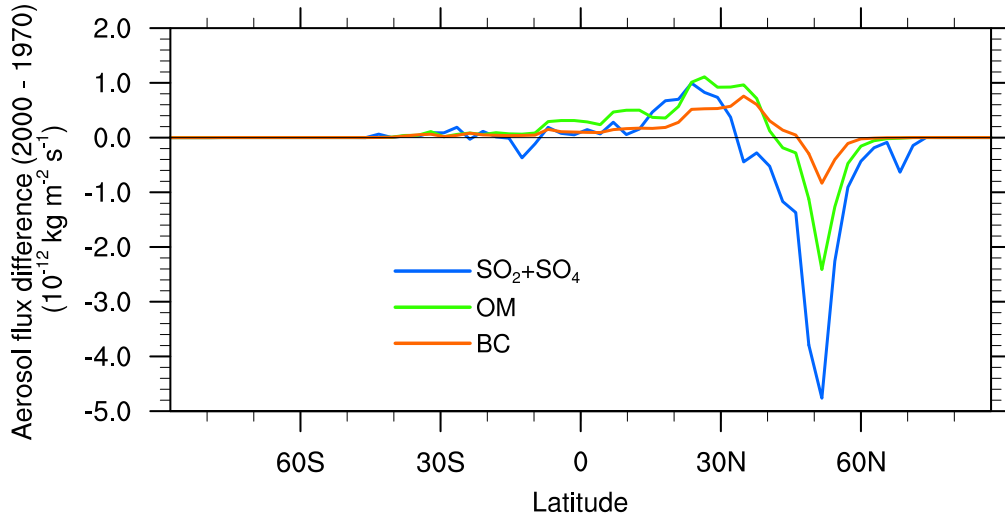
Figure 1: Zonally averaged changes (2000 - 1970) in the emission rates of anthropogenic aerosols. Note the $SO_2 + SO_4$ change has been reduced by a factor of 10.

SIMULATION SETUP

70 years of equilibrium simulations for the year 1970 and 2000 were performed using CAM-Oslo coupled to a slab ocean. The last 40 years of the simulation were utilized in the analysis.

To isolate the aerosol effect on different climate variables in the model, we conducted four sensitivity simulations (Table 2); one for present-day conditions (PD) using greenhouse gas (GHG) concentrations and aerosol particle and precursor emissions representative for the year 2000 (Lamarque *et al.*, 2010), one simulation using GHG concentrations representative for the year 2000 and aerosol particle and precursor emissions representative for the year 1970 (1970_AERO), one simulation using GHG and aerosol particle and precursor emissions representative for the year 1970 (1970_AEROGHG) and one simulation using aerosol particle and precursor emissions representative for the year 2000 and GHG concentrations representative for the year 1970 (1970_GHG).

Simulation label	GHG conc.	Aerosol emiss.
PD	2000	2000
1970_AERO	2000	1970
1970_GHG	1970	2000
1970_AEROGHG	1970	1970

Table 2: Description of the four sensitivity simulations performed using CAM-Oslo.

Despite applying the same anthropogenic aerosol emissions in 1970_GHG and PD, the predicted aerosol concentrations may still differ significantly between the two simulations, partly due to changes in natural sea salt emissions (which are dependent on the modeled sea surface temperature and wind speed) and partly due to changes in aerosol processing (e.g. condensational and coagulational growth, wet scavenging).

603

Changes (2000 - 1970) in the annually averaged, modeled aerosol optical thickness (AOT) (Figure 2) are strongly related to the changes in anthropogenic aerosol emissions prescribed in the model (Table 1 and Figure 1). Clear reductions in AOT over Europe are evident when changes in aerosol emissions are applied in the model (ie. 1970_AERO and 1970_AEROGHG). Relatively small changes in AOT are evident in the PD - 1970_GHG fields, these changes being driven by changes in in-situ processing of the emitted aerosol in response to changes in GHG concentrations.
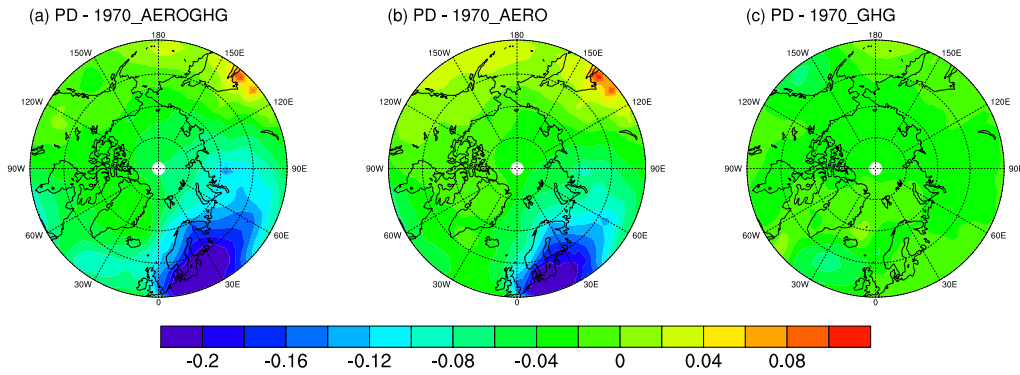
Figure 2: Annual average AOD (550nm) changes (2000 - 1970).

The Arctic climate response (MSLP, two metre temperature and 300 hPa geopotential height) to the different sensitivity simulations are shown in Figures 3, 4 and 5 respectively. Note that a climate response derived from equilibrium climate simulations, such as the ones conducted here using CAM-Oslo, is exaggerated compared to a corresponding transient simulation for the same time period.
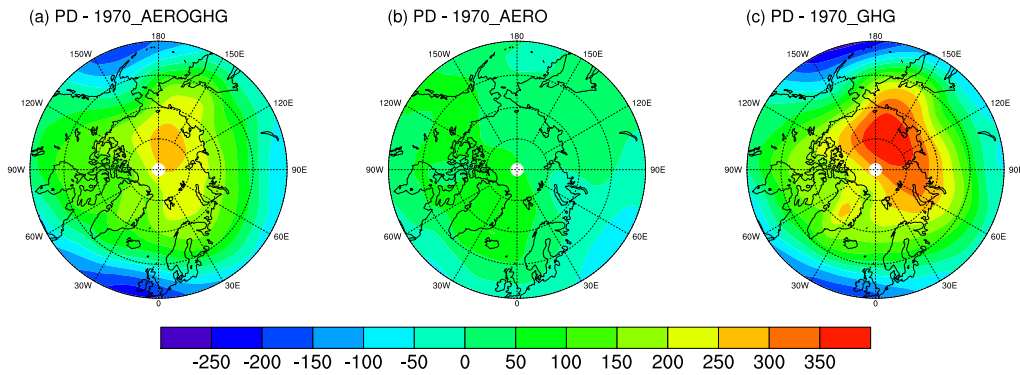
Figure 3: Annual average mean sea level pressure changes (2000 - 1970).

In CAM-Oslo, increasing GHG concentrations tends to enhance the the MSLP in the Arctic region (Figures 3(a) and 3(b)). When both GHG and aerosol changes are included in the model the Arctic MSLP response is significantly reduced compared to GHG changes alone. This model characteristic of a strong Arctic response due to increases in GHG concentrations being modulated by the inclusion of changes in aerosol emissions is also evident in the two metre temperature (Figure 4) and 300 hPa geopotential height (Figure 5) results.
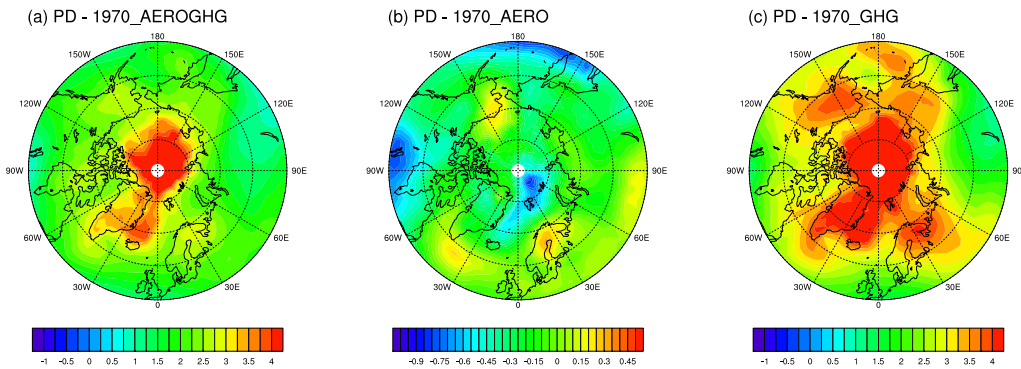
Figure 4: Annual average two metre temperature changes (2000 - 1970). Note the change of scale.
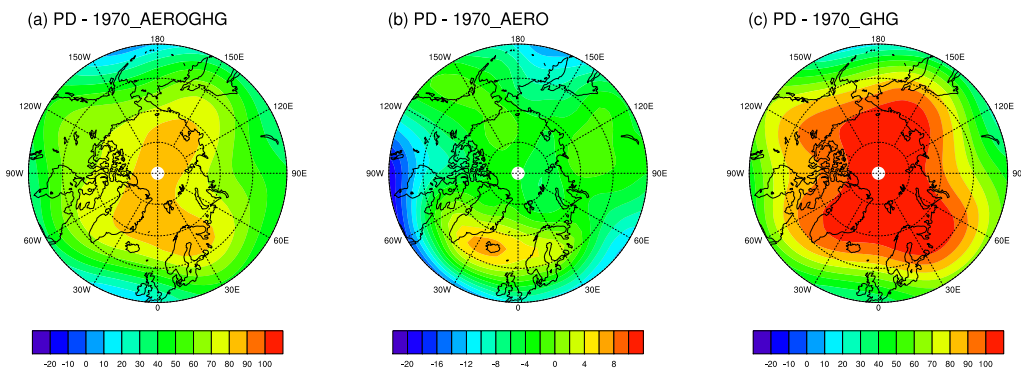
Figure 5: Annual average 300 hPa geopotential height changes (2000 - 1970). Note the change in scale.

SUMMARY AND OUTLOOK

The preliminary results demonstrate the presence of strong non-linearities in the climate response to combined changes in GHG and aerosol emissions. Understanding how the Arctic climate responds to changes in GHG and aerosol emissions is critical for accurate projections of climate in the northern mid- and high-latitudes. Studying the mechanisms via which the prescribed aerosol changes are influencing the model's Arctic climate response is a first step in this regard. Further sensitivity simulation results are available (e.g. including only the direct aerosol effect) and will be included in the analysis.

To evaluate the simulations, we will make use of observations and re-analysis data. We will determine if the modeled patterns of atmospheric change over the period 1970 to 2000 correlate better or worse with the observations when aerosol and greenhouse effects are included or excluded.

One limitation of the current model setup is that the oceanic DMS emissions are not calculated online and thus do not respond to changes in climate. Results demonstrate that this effect is important for the simulated sea salt aerosol emissions and so we plan to implement an on-line DMS emission scheme in the Norwegian Earth system model, NorESM.

ACKNOWLEDGEMENTS

REFERENCES

Collins, W. D., et al. (2006). The Formulation and atmospheric simulation of the Community Atmospheric Model Version 3 (CAM3). *J. Clim.*, **19**, 2144-2161.

Dentener, F. et al. (2006). Emissions of primary aerosol and precursor gases in the years 2000 and 1750 prescribed data-sets for AeroCom. *Atmos. Chem. Phys.*, **6**, 4321-4344.

Iversen, T. and Seland, Ø. (2002). A scheme for process-tagged SO_4 and BC aerosols in NCAR CCM3: Validation and sensitivity to cloud processes. *J. Geophys. Res.*, **107**, 4751.

Kinne, S., et al. (2006). An AeroCom initial assessment of optical properties in aerosol component modules of global models. *Atmos. Chem. Phys.*, **6**, 1815-1834.

Kirkevåg, A. and Iversen, T. (2002). Global direct radiative forcing by process-parameterized aerosol optical properties. *J. Geophys. Res.*, **107**, 4433.

Koch, D., et al. (2009). Evaluation of black carbon estimations in global aerosol models. *Atmos. Chem. Phys.*, **9**, 9001-9026.

Lamarque, J, -F., et al. (2010). Historical (1850–2000) gridded anthropogenic and biomass burning emissions of reactive gases and aerosols: methodology and application. *Atmos. Chem. Phys.*, **10**, 7017-7039.

Mårtensson, E. M., et al. (2003). Laboratory simulations and parmaeterization of the primary marine aerosol production. *J. Geophys. Res.*, **108**, 4297.

Penner, J. E., et al. (2006). Model intercomparison of indirect aerosol effects. *Atmos. Chem. Phys.*, **6**, 3391-3405.

Quaas, J., et al. (2009). Aerosol indirect effects: general circulation model intercomparison and evaluation with satellite data. *Atmos. Chem. Phys.*, **9**, 8697-8717.

Schulz, M., et al. (2006). Radiative forcing by aerosols as derived from the AeroCom present-day and pre-industrial simulations. *Atmos. Chem. Phys.*, **6**, 5225-5246.

Seland, Ø., Iversen, T., Kirkevåg, A. and Storelvmo, T. (2008). Aerosol-climate interactions in the CAM-Oslo atmospheric GCM and investigation of associated basic shortcomings. *Tellus*, **60A**, 459-491.

Shindell, D. and Faluvegi, G, (2009). Climate response to regional radiative forcing during the twentieth century. *Nature Geoscience*, **2**, 294.

Stier, P., et al. (2005). The aerosol-climate model ECHAM5-HAM. *Atmos. Chem. Phys.*, **5**, 1125-1156.

Textor, C., et al. (2006). Analysis and quantification of the diversities of aerosol life cycles within the AeroCom models. *Atmos. Chem. Phys.*, **6**, 1777-1813.

Characterization of an APi-TOF for transmission

V.-M. SUNDELL[1], H. JUNNINEN[1], J. KANGASLUOMA[1], S. SCHOBESBERGER[1], M. SIPILÄ[1], M. KULMALA[1], D.R. WORSNOP[1,2] AND T. PETÄJÄ[1]

[1]Department of Physics, University of Helsinki, Finland
[2]Aerodyne Research Inc., Billerica, MA, USA

INTRODUCTION

Naturally charged ions are part of the atmospheric mixture. In continental conditions typical concentrations range between 200 and 2500 cm^{-3} for positive and negative ions in size range < 1.6 nm (Hirsikko et al. 2011). While observation of physical number size distribution of the ions have been performed in a continental scale (Manninen et al. 2010), the spatial variability of the chemical identity of these ions is not yet known. An emerging technique to resolve this is time-of-flight mass spectrometry based instruments have been entering the field of aerosol science. At its most simple form the instrument, APiTOF (atmospheric pressure time of flight mass spectrometer) can sample naturally charged ambient clusters directly from atmosphere without any pre-treatment (Junninen et al, 2010, Ehn et al 2010). As an example, in the boreal environment the natural negative ion population is dominated by strong acids (sulfuric acid during daytime and nitric acid during night-time) while strong bases govern the positive ion population with a less diurnal variability (Ehn et al. 2010). In marine conditions halogen ions contribute to the ambient ion population (Lönn et al. 2011), which are also seen in a boreal environment (Arppe et al. 2012).

A side-by-side deployment of air ion spectrometers and the APi-TOF can be used to evaluate the transmission efficiency of the APi-TOF instrument (Ehn et al. 2011) in the field conditions. However, detailed laboratory experiments which include cluster generation, size selection and detection with reference instrument, are required to address the transmission in more detail. This is the aim of this study. Here we explore the variability of the APi-TOF settings to the transmission efficiency. These results are needed in order to convert the APi-TOF mass spectra in various field and laboratory deployments to reveal the total ion concentration in the atmosphere.

METHODS

Calibration substance in this study was ammonium sulphate that was evaporated in tube furnace at temperature of 200-300C, carrier gas was 5.0 grade nitrogen and cluster formation was taken place in water cooled tube at 4C. Formed clusters were charged by [241]Am and mobility classified by Herrman-type DMA (differential mobility analyser, Herrman et al 2000). The HDMA itself was calibrated using mobility standard THAB (tetraheptylammonim bromide, Ude et al. 2005), which was electrosprayed directly into the HDMA.

For determination of transmission for APiTOF 2 and 3 the voltages of DMA were scanned from 100V-1500V in 300 logarithmic steps that lasted for 0.5 seconds. For APiTOF 1 the voltages were changed in 10 steps each last for 5-15min, the duration was defined by the signal strength of APiTOF.

Reference instrument sampling the total ions classified by DMA was an electrometer. Sampling lines from DMA to electrometer and APiTOF were equal in length and shape.

Transmission value was obtained by diving APiTOF signal by electrometer signal.

RESULTS

We tested seven different settings in APiTOF 1 and eleven different settings in APiTOF 2 and APiTOF 3. The results are shown in table 1.

	1-500Th	500-1000Th	1000-2000Th	2000-3000Th	3000-4000Th	4000-5000Th
API1, setting1	0.26-0.43%	0.29-0.45%	0.04-0.29%	0.01-0.04%	0.00-0.01%	0.00%
API1, setting2	0.14-0.51%	0.51-0.67%	0.18-0.64%	0.11-0.18%	0.11-0.05%	0.01-0.05%
API1, setting3	0.18-0.63%	0.63-0.83%	0.25-0.78%	0.15-0.25%	0.08-0.15%	0.02-0.08%
API1, setting4	0.08-0.24%	0.04-0.24%	0.00-0.04%	0.00%	0.00%	0.00%
API1, setting5	0.06-0.10%	0.03-0.08%	0.01-0.03%	0.00-0.01%	0.00%	0.00%
API1, setting6	0.03-0.10%	0.07-0.11%	0.01-0.07%	0.00-0.01%	0.00%	0.00%
API1, setting7	0.01-0.38%	0.08-0.42%	0.01-0.08%	0.01%	0.00-0.01%	0.00%
API2, setting1	0.28-1.88%	1.88-2.92%	1.28-3.71%	0.11-1.28%	-	-
API2, setting2	0.19-1.20%	1.20-3.26%	3.26-5.82%	4.44-5.75%	2.29-4.44%	0.48-2.29%
API2, setting3	0.73-2.74%	2.74-3.82%	-	-	-	-
API2. setting4	0.21-1.45%	1.12-1.59%	0.89-1.59%	0.27-0.89%	0.06-0.27	-
API2, setting5	0.25-1.71%	1.23-1.76%	0.65-1.83%	0.18-0.65%	0.08-0.18%	-
API2, setting6	0.18-2.31%	0.33-1.36%	0.00-0.33%	0.00%	-	-
API2, setting7	0.17-2.10%	0.70-1.82%	0.00-0.70%	0.00%	0.00%	-
API2, setting8	-	-	-	-	-	-
API2, setting9	0.20-1.85%	0.10-0.51%	-	-	-	-
API2, setting10	0.23-2.33%	0.87-2.32%	0.07-0.87%	-	-	-
API2, setting11	0.42-3.41%	0.54-2.02%	0.07-0.54%	-	-	-
API3, setting1	0.82-2.82%	1.09-2.82%	0.06-1.09%	-	-	-
API3, setting2	1.12-3.54%	0.31-1.44%	0.04-0.31%	-	-	-
API3, setting3	0.24-1.08%	0.98-1.28%	0.08-1.16%	-	-	-
API3, setting4	0.89-1.86%	1.04-1.37%	0.05-1.04%	-	-	-
API3, setting5	-	-	-	-	-	-
API3, setting6	1.00-2.79%	0.15-1.30	0.02-0.15%	-	-	-
API3, setting7	0.93-3.24%	0.72-2.86%	0.05-0.72%	-	-	-
API3, setting8	1.80-4.37%	0.72-2.99%	0.05-0.72%	-	-	-
API3, setting9	0.22-1.10%	0.33-1.10%	0.01-0.33%	-	-	-
API3, setting10	0.57-1.37%	0.31-1.02%	0.03-0.31%	-	-	-
API3, setting11	1.56-5.31%	1.56-2.56%	1.38-2.80%	0.54-1.38%	-	-

Table 1. Transmission in different setting in different mass charge ratio.

ACKNOWLEDGEMENTS

REFERENCES

Arppe, T., H. JUNNINEN[1], T. JOKINEN[1], J. HAKALA[1], S. SCHOBESBERGER[1], G. LÖNN[1], M. SIPILÄ[1], M. KULMALA[1], D.R. WORSNOP[1,2] AND T. PETÄJÄ[1] (2012) IODINE-CONTAINING IONS IN HYYTIÄLÄ, this issue.

Ehn, M., Junninen, H., Petäjä, T., Kurtén, T., Kerminen, V.-M., Schobesberger, S., Manninen, H.E., Ortega, I.K., Vehkamäki, H., Kulmala, M. and Worsnop, D.R. (2010) Composition and temporal behavior of ambient ions in the boreal forest. Atmos. Chem. Phys. 10, pp. 8513-8530.

Ehn, M., Junninen, H., Schobesberger, S., Manninen, H.E., Franchin, A., Sipilä, M., Petäjä, T., Kerminen, V.-M., Tammet, H., Mirme, A., Mirme, S., Hõrrak, U., Kulmala, M. and Worsnop, D.

(2011) An instrumental comparison of mobility and mass measurements of atmospheric small ions Aerosol Sci. Technol., 45, pp. 522-532.

Junninen, H., M. Ehn, T. Petäjä, L. Luosujärvi, T. Kotiaho, R. Kostiainen, U. Rohner, M. Gonin, K. Fuhrer, M. Kulmala and D. R. Worsnop (2010). A high-resolution mass spectrometer to measure atmospheric ion composition, Atmos. Meas. Tech. 3, 1039–1053.

Hirsikko, A., Nieminen, T., Gagné, S., Lehtipalo, K., Manninen, H.E., Ehn, M., Hõrrak, U., Kerminen, V.-M., Laakso, L., McMurry, P.H., Mirme, A., Mirme, S., Petäjä, T., Tammet, H., Vakkari, V., Vana, M. and Kulmala, M. (2011) Atmospheric ions and nucleation: a review of observations. Atmos. Chem. Phys. 11, pp. 767-798.
Herrmann, W., Eichler, T., Bernardo, N., and Fernández de la Mora, J. (2000). Turbulent Transition Arises at Reynolds Number 35,000 in a Short Vienna Type DMA with a Large Laminarization Inlet. Abstract AAAR Conference, 15B5.

Lönn G., McGrath M.J., Junninen H., Schobesberger S., Franchin A., Petäjä T., Worsnop D.R. and Kulmala M. (2011) Chemical composition and correlation of ions in a marine atmosphere, Proceedings of FCoE Annual workshop, May 18-20, 2011, Luosto, Finland, 4 pp.

Manninen, H.E., Nieminen, T., Asmi, E., Gagné, S., Häkkinen, S., Lehtipalo, K., Aalto, P., Vana, M., Mirme, A., Mirme, S., Hõrrak, U., Plass-Dülmer, C., Stange, G., Kiss, G., Hoffer, A., Törö, N., Moerman, M., Henzing, B., de Leeuw, G., Brinkenberg, M., Kouvarakis, G.N., Bougiatioti, K., Mihalopoulos, N., O'Dowd, C.D., Ceburnis, D., Arneth, A., Svenningsson, B., Swietlicki, E., Tarozzi, L., Decesari, S., Facchini, M.C., Birmili, W., Sonntag, A., Wiedensohler, A., Boulon, J., Sellegri, K., Laj, P., Gysel, M., Bukowiecki, N., Weingartner, E., Wehrle, G., Laaksonen, A., Hamed, A., Joutsensaari, J., Petäjä, T., Kerminen, V.-M. and Kulmala, M. (2010) EUCAARI ion spectrometer measurements at 12 European sites – analysis of new-particle formation events. Atmos. Chem. Phys., 10, pp. 7907-7927.

Ude, S. and Fernandez de la Mora, J. (2005) Molecular monodisperse mobility and mass standards from electrosprays of tetra-alkyl ammonium halides, J. Aerosol Sci. 36, 1224-1237.

ESTIMATION OF THE DIRECT AEROSOL RADIATIVE EFFECT OVER CHINA BASED ON SATELLITE REMOTE SENSING MEASUREMENTS

A-M. SUNDSTRÖM[1], J. HUTTUNEN[2], A. AROLA[2], P. KOLMONEN[3], L. SOGACHEVA[3], T. VIRTANEN[3], E. RODRIGUEZ[3] and G. de LEEUW[3],[1]

[1] Department of Physics, University of Helsinki, Helsinki, Finland.

[2]Finnish Meteorological Institute, Kuopio, Finland.
[3]Finnish Meteorological Institute, Helsinki, Finland.

Keywords: Aerosol direct radiative effect, remote sensing, China.

INTRODUCTION

Aerosols influence the radiative budget of the Earth-atmosphere system directly by scattering and absorbing solar and thermal infrared radiation, and indirectly by modifying the microphysical, and hence the radiative properties and lifetimes of clouds. However, the quantification of aerosol radiative effects is complex and large uncertainties still exist, mainly due to the high spatial and temporal variation of the aerosol concentration and mass as well as their relatively short lifetime in the atmosphere (e.g. Hatzianastassiou *et al.*, 2007). The clear-sky direct aerosol radiative effect at the top of the atmosphere ($ADRE_{TOA}$) is defined as the difference between the net solar flux (difference between downward and upward fluxes) defined with (F_{aer}) and without (F_0) aerosols. The negative values of $ADRE_{TOA}$ correspond to increased outgoing short wave (SW) radiation and planetary cooling, whereas positive values correspond to decreased outgoing SW radiation at the TOA and increased atmospheric warming.

Satellites offer an opportunity to observe the spatial distribution of aerosol properties with adequate resolution and coverage from regional to global scales. The Moderate Imaging Spectroradiometer onboard (MODIS) NASA's Terra and Aqua platforms offer global observations of aerosol and cloud optical properties nearly on a daily basis. Both platforms also carry the Clouds and the Earth's Radian Energy System (CERES) instruments that measure TOA broadband fluxes with three different detectors in the shortwave (0.3-5 μm), IR-window (8-12 μm) and total (0.3-200 μm) channels. In this work a method is tested where collocated multisensor satellite observations are used to estimate $ADRE_{TOA}$ over eastern China. This approach has been previously used e.g. by Zhang *et al.* (2005) for defining SW aerosol radiative effect over cloud-free oceans and Patadia *et al.* (2008) for studying biomass burning effects over Amazon (CERES flux, MISR AOD). The advantage of this satellite observation based method is that a priori information about the aerosol type and surface properties are not needed, unlike when using the radiative transfer simulation based methods. However, when testing this method radiative transfer simulations are used for comparison and study e.g. the effect of changing aerosol type.

METHODS

The aerosol direct radiative effect ADRE at TOA for cloud-free sky is defined as the difference between the SW fluxes in the absence (F_0) and presence (F_{aer}) of aerosols;

$ADRE_{TOA} = F_0\text{-}F_{aer}$

And further, the aerosol direct radiative effect efficiency $ADRE_{TOA}^{eff}$ is defined as:

$$ADRE_{TOA}^{eff} = ADRE_{TOA}(\text{sza})/AOD_{550}(\text{sza})$$

where sza is the solar zenith angle and AOD_{550} aerosol optical depth at 550 nm wavelength.

For a cloud-free pixel, the CERES measurement represents the instantaneous value of F_{aer}. Since aerosols are always present in the atmosphere, it is not possible to obtain the value for F_0 directly from the satellite measurements. In this work we test the method where F_0 is estimated using collocated SW flux and AOD retrievals from CERES and MODIS instruments (CERES SSF data). It is assumed that over a month in one grid cell (0.5·0.5 deg.), the aerosol mixture and surface properties do not vary significantly, and the changes in F_{aer} are mainly caused by changes in the aerosol loading (AOD). When the aerosol loading is not extremely high (≥ 2.5), the relationship between F_{aer} and AOD is close to linear. Hence, for each grid cell the regression between the AOD and F_{aer} observations is defined, and the value for F_0 is obtained as the y-intercept of the regression line (AOD = 0). The LibRadtran radiative transfer code is used to model the diurnal variation of $ADRE_{TOA}$, and to convert the obtained instantaneous satellite observations to 24h averages over a month (Remer and Kaufman, 2006).

CONCLUSIONS

The aerosol radiative effect was defined monthly from March to November 2009 over Eastern China. Figure 1 shows the estimate of diurnally averaged seasonal mean of $ADRE_{TOA}$ for autumn (Sept.-Nov.) and Figure 2 the corresponding values of $ADRE_{TOA}^{eff}$. The estimate for the diurnally averaged $ADRE_{TOA}$ over Eastern China for Mar.-Nov. 2009 is -6 Wm^{-2}. It should be noted that the values obtained in this study are representing only completely cloud free cases.
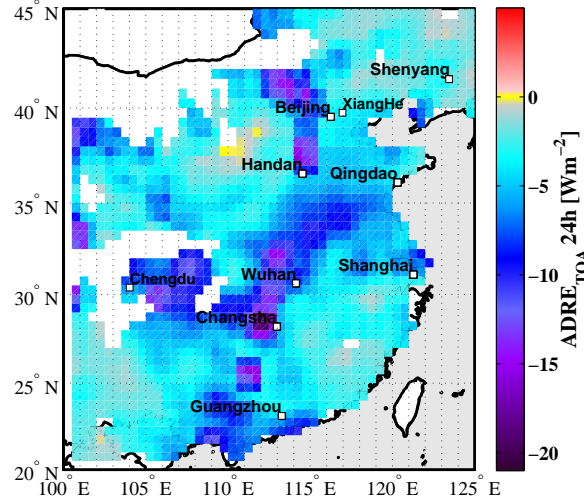

Figure 1: Diurnally averaged seasonal mean of $ADRE_{TOA}$ for autumn (Sept.-Nov.) defined from the satellite observations. White areas are places where the regression was not succesfull due to low number of observations.
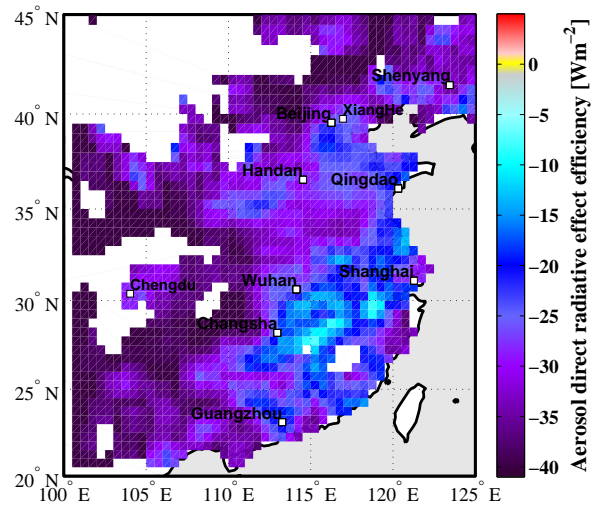
Figure 2: Seasonal average of $ADRE_{TOA}^{eff}$ for autumn 2009.

The aerosol radiative effect at TOA can be either negative or positive. The positive $ADRE_{TOA}$ requires dark (absorbing) aerosols over very bright surface. Especially during the summer months the method used in this study show some areas where the correlation between AOD and F_{aer} is negative resulting in positive values of $ADRE_{TOA}$. However, radiative transfer simulations reveal that surface is not bright enough to cause strong positive effect at TOA, and hence the positive values of $ADRE_{TOA}$ are most likely method artifact. Most of these cases can be related to areas where the AOD is systematically very low (≤ 0.1) and the fitting is not working well. However, there are also areas where the AOD loading over one month is varying from about 0.2 to 1.0, and the values of F_{aer} are decreasing with increasing AOD. For this specific case radiative transfer simulations were carried out. The simulations showed that one possible explanation for this negative dependence of AOD and F_{aer} is the change of aerosol type from highly scattering aerosol (when AOD is lower than 0.4) to highly absorbing aerosol (when AOD is higher than 0.5).

Even though the fitting method is giving reasonable results over China, the method include high uncertainties. More radiative transfer simulations, studies about changes in aerosol types as well as surface properties are needed to estimate the uncertainties.

ACKNOWLEDGEMENTS

REFERENCES

Hatzianastassiou, N., C. Matsoukas, E. Drakakis, P.W. Stackhouse Jr., P. Koepke, A. Fotiadi, K.G. Pavlakis and I. Vardavas. (2007). The direct effect of aerosols on solar radiation based on satellite observations, reanalysis datasets, and spectral aerosol optical properties from Global Aerosol Data Set (GADS), *Atmos. Chem. Phys*, **7**, 2585-2599.

Patadia, F., P. Gupta, S.A. Christopher, and J.S. Reid (2008). A Multisensor satellite-based

assesment of biomass burning aerosol radiative impact over Amazonia, *J. Geophys. Res.*, **113**, D12214.

Remer, L. and Y. Kaufman, (2006). Aerosol direct radiative effect at the top of the atmosphere over cloud free ocean derived from four years of MODIS data, *Atmos. Chem. Phys*, **6**, 237-253.

Zhang, J., S. A. Christopher, L. Remer, and Y. Kaufman (2005). Shortwave aerosol radiative forcing over cloud-free oceans from Terra: 2. Seasonal and global distributions, *J. Geophys. Res.*, **110**, D10S24.

THE SIGNIFICANCE OF LAND-ATMOSPHERE PROCESSES IN THE EARTH SYSTEM - iLEAPS PERSPECTIVE

T. SUNI[1], A. GUENTHER[2] and M. KULMALA[3]

[1] iLEAPS International Project Office, Division of Atmospheric Sciences, Department of Physics, University of Helsinki, Helsinki, Finland
[2] National Center for Atmospheric Research, Boulder, Colorado, USA
[3] Division of Atmospheric Sciences, Department of Physics, University of Helsinki, Helsinki, Finland

INTRODUCTION

The land-atmosphere interface is where humans primarily operate. Humans modify the land surface in many ways that influence the fluxes of energy and trace gases between land and atmosphere. Their emissions change the chemical composition of the atmosphere and anthropogenic aerosols change the radiative balance of the globe directly by scattering sunlight back to space and indirectly by changing the properties of clouds. Feedback loops among all these processes, land, the atmosphere, and biogeochemical cycles of nutrients and trace gases extend the human influence even further (Fig. 1).

iLEAPS (Integrated Land Ecosystem – Atmosphere Processes Study), a core project of IGBP (International Geosphere-Biosphere Programme), is an international cross-disciplinary research program aimed at improved understanding of processes, linkages and feedbacks in the land-atmosphere interface affecting the Earth System. iLEAPS facilitates scientific collaboration as well as synthesis and distribution of results to scientific, politic and public audiences. The main activities is iLEAPS include 1) highlighting and advertising important scientific results (newsletters, bulletins, website, synthesis reports and articles); 2) organising science conferences, workshops and trainings around LEAP science; 3) organising and co-sponsoring sessions at conferences; 4) organising the iLEAPS Science Conference that gathers together the latest findings and breakthroughs of the iLEAPS science community all over the world, and most importantly 5) developing LEAP science by starting off new initiatives and projects that focus on land-atmosphere-society interactions and take steps towards global sustainability.

EVOLUTION OF iLEAPS

Phase I (2004 – 2014) has been a time of awareness-raising and establishing a united community of land-atmosphere scientists. Science conferences held in Helsinki (2003), Boulder (2006), Melbourne (2009), and Garmisch-Partenkirchen (2011) brought to light the importance of land-atmosphere processes and feedbacks in the Earth System, and a number of publications have shown the crucial role of the terrestrial ecosystems as regulators of climate and emphasised both the long-term net impacts of aerosols on clouds and precipitation. Furthermore, the iLEAPS community has drawn attention to the importance of realistic land-use representation in land surface modelling and to that of other feedback processes and regional characteristics in current climate models and recommended actions to improve them.

Human influence has always been an important part of iLEAPS science but in Phase II (2014-2024), iLEAPS will work hand in hand with social science / economics groups and use fields such as economics, agricultural economics, social sciences, globalization research, and behavioural sciences to produce realistic estimates of land use and anthropogenic emissions by analysing future population increase, migration patterns, food production allocation, land management practices, energy production, industrial development, and urbanization. Phase II will see the foundation of new types of research groups such as

the BASC (Biodiversity, Agroecosystems, Society, Climate) Laboratory of Excellence in France led by iLEAPS SSC member Nathalie de Noblet-Ducoudré, a consortium of thirteen laboratories with expertise in climate sciences, genetics and genomics, evolutionary biology, ecology, agronomy, social sciences and economics. In the boreal zone, the Pan-Eurasian Experiment (PEER) will include large-scale, long-term, coordinated observations and modelling in the Pan Eurasian region, especially to cover ground base, airborne and satellite observations together with global and regional models to find out different forcing and feedback mechanisms in the changing climate, taking into account the simultaneous societal and cultural change. PEER aims to gather all the European and Russian key players in the field of climate and Earth system science to plan jointly in coordinated manner future research activities in the Pan-Eurasian region.
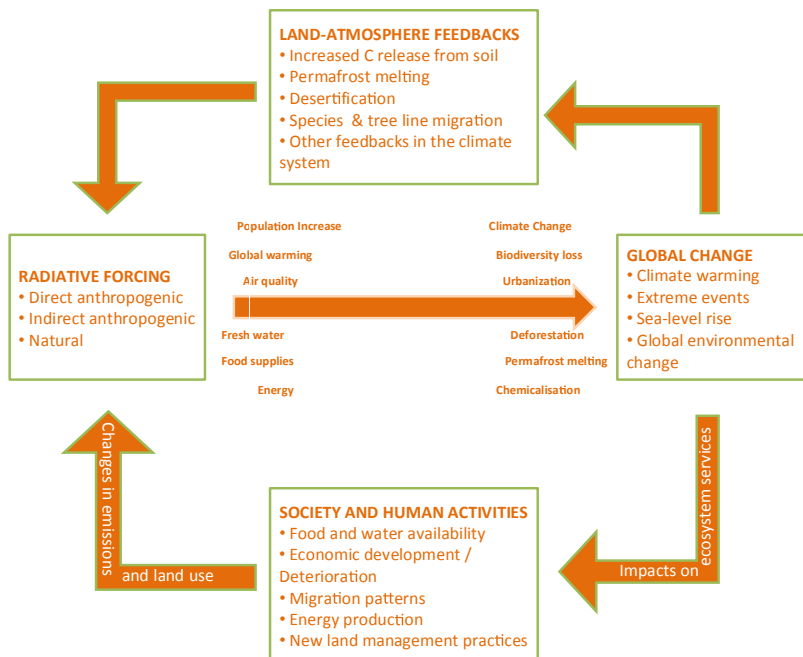
Figure 1. Land-atmosphere-society processes under global change.

CLIMATE REGULATION

Over the last decade, the importance of land-atmosphere processes and feedbacks in the Earth System has been shown on many levels and with multiple approaches, and a number of publications have shown *the crucial role of the terrestrial ecosystems as regulators of climate* (Ciais et al. 2003, Kulmala et al. 2004, Arneth et al. 2010, Ganzeveld et al. 2010, Teuling et al. 2010). Modellers have clearly shown the effect of missing land cover changes and other feedback processes and regional characteristics in current climate models and recommended actions to improve them (Arneth et al. 2010, Bonan et al. 2011, Davin and Seneviratne 2011, Pitman et al. 2011a, de Noblet-Ducoudré et al. 2012). For instance, Arneth et al. (2010) showed that although research into land–atmosphere exchange processes in climate science has traditionally focused on the surface radiation budget and its effects on sensible and latent heat fluxes, and more recently on carbon-cycle–climate interactions, many more bidirectional land–atmosphere fluxes modulate atmospheric composition and climate. They highlighted three principal pathways along which biogeochemical cycles interact with the atmosphere and climate: 1) climate change alters the biogeochemical cycling of greenhouse gases, which act directly as radiative forcing agents (CO_2, CH_4, influenced by N); 2) changes in atmospheric composition influence the biogeochemistry of radiatively active compounds (for instance, changes in O_3 levels influence photosynthesis); 3) climate change alters the biogeochemistry of substances that are not radiatively active in themselves (O_3, NO_x, BVOC), but that

affect the atmospheric concentration of other climatically active compounds (CO_2, CH_4, aerosols). The international initiative Aerosols, Clouds, Precipitation, Climate (ACPC) was founded during iLEAPS Phase I and it provided unprecedented insights of the long-term net impacts of aerosols on clouds and precipitation (Rosenfeld et al. 2008, Stevens and Feingold 2009, Li et al. 2011). The climatic relevance of aerosol formation has been confirmed in countless observations around the world within intensive initiatives such as EUCAARI (European Integrated project on Aerosol Cloud Climate and Air Quality Interactions, EUCAARI 2007-2011; Kulmala et al. 2011) or at established and new continuous observation platforms founded in climatically important locations such as remote boreal forest (SMEAR II research station in southern Finland), cities (SMEAR III in Helsinki, Finland) and in semi-clean areas (Welgegund observation platform in South Africa).

LAND USE AND LAND-COVER CHANGE

Land-cover change has become one of the key research priorities in iLEAPS as new important results have emerged from model intercomparison projects that showed that realistic land-use representation was essential in land surface modelling, and that the soil-plant continuum was not something that could be treated as a simple, constant block in the hydrological cycle (Pitman et al. 2009, de Noblet-Ducoudré et al. 2012). These findings led to the new Land Use and Land Cover Change (LULCC) synthesis project undertaken by iLEAPS and the Global Land Project (GLP) in collaboration with the International Human Dimensions Programme (IHDP). Furthermore, Ganzeveld et al. (2010) studied the influence of future land use and land cover changes on atmospheric chemistry-climate interaction with the aim of looking further than at merely the changes in physical climate and the carbon cycle. Using the chemistry-climate model EMAC (ECHAM5/MESSy Atmospheric Chemistry) constrained with present-day and 2050 land cover, land use, and anthropogenic emissions scenarios, they found that future LULCC may, among other things, result in an increase in global annual soil NO emissions and a decrease in isoprene emissions. However, compensating effects were also found, and the main conclusion was that the simulated impact of LULCC on atmospheric chemistry depends on a consistent representation of emissions, deposition, and canopy interactions and their dependence on meteorological, hydrological, and biological drivers to account for these compensating effects. As part of the iLEAPS LULCC project, Pitman et al. (2011b) showed the importance of background climate in determining the impact of land-cover change on regional climate: increased greenhouse-gas-driven changes in snow and rainfall affect the snow–albedo feedback and the supply of water, which in turn limits evaporation. These changes largely control the net impact of LULCC on regional climate. Capturing whether future biophysical changes due to LULCC warm or cool a specific region therefore requires an accurate simulation of changes in snow cover and rainfall geographically coincident with regions of LULCC. The authors state that is is a challenge to current climate models, but it also provides potential for further improving detection and attribution methods.

LONG-TERM LAND-ATMOSPHERE OBSERVATION PLATFORMS

Throughout Phase I, the iLEAPS community has invested in creating new ways to observe and model the land-atmosphere continuum: observation systems have developed to networks of long-term flux stations and large-scale land-atmosphere observation platforms and, more recently, to combining remote sensing techniques with ground observations (Baldocchi et al. 2005, Hari et al. 2009, Guenther et al. 2011, de Leeuw et al. 2011, Jung et al 2011). A major focus within the iLEAPS community are long-term observations of micrometeorological fluxes of carbon dioxide, water vapour, ozone, aerosol particles, and energy between land ecosystems and the atmosphere. Recent advances in upscaling and data integration across multiple data streams have enabled iLEAPS scientists to produce gridded datasets of regionally and globally explicit flux products. The sites that comprise the flux and spectral measurement networks FLUXNET and SPECNET have become an important source for "bottom-up" inputs to models that upscale flux quantities from canopies to landscapes and from landscapes to the globe. Data from tower measurements also serve as a validation tool for top-down modeling based on satellite and aircraft optical measurements. These capabilities have brought climate and ecosystem scientists within reach of quantifying carbon, water and energy fluxes on a continuous basis all around the world. They have also

enabled insights into climate-ecosystem interactions and trends over a range of spatial and temporal scales; and particularly at the largest scales. Global datasets such as these have been used to reveal important connections among plant physiology and atmospheric composition: Mahecha et al. (2010) found marked differences in the long-term fate of carbon taken up through photosynthesis, as well as in the availability of this carbon for respiration, across a number of sites in different biomes. The sensitivity of respiration to changes in temperature, however, fell within a narrow range, and proved to be independent of the mean annual temperature and biome. The global mean temperature sensitivity was also significantly lower than previous estimates. The authors attribute the difference to the exclusion of confounding processes in their analysis, such as the seasonal variability of biological activity. This finding could help to explain recent observations of feedbacks between climate and the carbon cycle that are weaker than those suggested by numerical models.

Global comprehensive measurement networks are essential in land-atmosphere interactions research. Hari et al. (2009) suggested a way to improve and organise existing observation platforms into a hierarchical system to cover spatial and temporal variations. The network should include stations of i) basic level ii) flux level, and iii) "flag-ship" level. The aim of the *basic stations* would be to provide information for spatial characterization, and the number of stations globally (~8000) should be large to obtain global coverage. The *flux stations* would provide information on fluxes in the ecosystem, and the approximately 400 global stations suggested would represent different ecosystems and climates; the number would be restricted by the infrastructure and instrumentation required. Finally, the *flag-ship* level stations (~20 globally), whose number would be limited because of the required scientific and technical level, would provide information on processes generating the fluxes, develop instrumentation, and serve to train scientists and technical staff. Building on this recommendation by Hari et al. (2009), Guenther et al. (2011) conducted a thorough review of current land ecosystem – atmosphere measurement capabilities and presented the status and needs for global observational networks (Fig. 2).
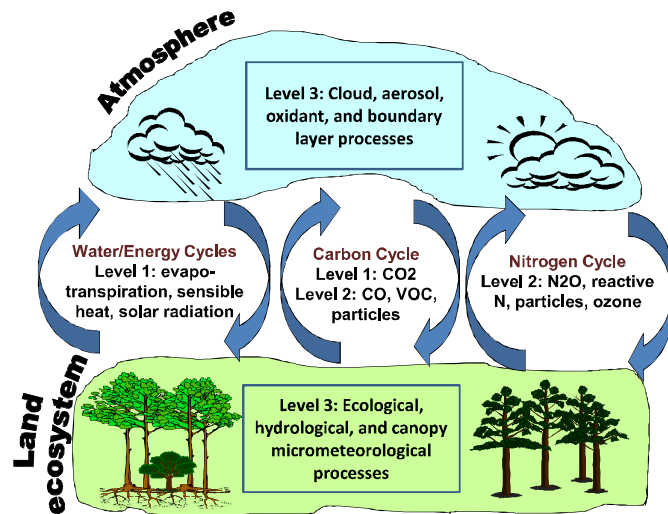
Figure 2. Schematic of land ecosystem – atmosphere interactions and hierarchical observational levels that include basic (1), advanced (2), and comprehensive measurements at flagship sites (3). Adopted from Guenther et al. (2011).

THE iLEAPS APPROACH

An innovative, comprehensive, multi-scale, multidisciplinary approach to land-atmosphere processes is a key element of iLEAPS observations and modelling. For the past two decades, the Amazon basin has been the focus of intensive, multidisciplinary measuring efforts within the ambitious study LBA (Large Scale Biosphere-Atmosphere Experiment in Amazonia) (Artaxo 2012). The project was one of the first in the

617

world to encourage cooperation among physicists, chemists, meteorologists and biologists to dive to the bottom of the complex Amazonian biogeochemical and ecological system. To account for the human influence, also economists and social scientists were brought into the research. In a recent LBA review article, Davidson et al. (2012) showed how agricultural expansion and climate variability have become important agents of disturbance in the Amazon basin: interactions between deforestation, fire and drought potentially lead to losses of carbon storage and changes in regional precipitation patterns and river discharge. In the boreal zone, similar efforts took place already in the late 90's in the BIOFOR campaign (Biogenic aerosol formation in the boreal forest, special issue appeared in Tellus 2001, Kulmala et al. 2001). Some 50 scientists from 11 research groups in Finland, Sweden, Estonia, Germany, Ireland, Australia, UK and USA participated in the project. In 2005, the SMEAR (Station for Measuring Forest Ecosystem – Atmosphere Relations) research program was launched in southern Finland. The SMEAR II station subsequently became one of the world's leading state-of-the-art observation platforms with the first continuous, comprehensive measurements of fluxes, storages and concentrations in the land ecosystem–atmosphere continuum (Hari & Kulmala 2005).

The iLEAPS community serves as an example of innovative thinking where the borders among disciplines and often very isolated measuring and modelling communities are crossed and fruitful collaboration produces excellent results. One of the main tasks of the iLEAPS community is to inform policy-makers that no climate-related phenomenon exists in isolation; all are linked to several processes on land and in the atmosphere, and sometimes improving one aspect will deteriorate another. All these different viewpoints and factors must be taken into account in impact studies and especially when designing solutions towards sustainable development.

NEXT STEP FOR ILEAPS RESEARCH: GLOBAL SUSTAINABILITY

In order to respond to the new challenges of global sustainability reflected, for instance, by Future Earth, the 10-year initiative that will reorganise ICSU's global environmental change (GEC) programmes IGBP, DIVERSITAS, and IHDP, closer ties with social science and economics groups will be necessary. They will be indispensable partners for natural sciences on the road to solving the equation of one Earth and a growing human population. Emphasis in the future work of iLEAPS should be placed on, for instance, new observation networks incorporating remote sensing techniques with ground-based observations; the role of land-cover changes in modulating carbon, nitrogen, and hydrological cycles and, consequently, atmospheric chemistry, aerosol dynamics, and climate; regional (high-latitude) processes and their influence on global simulations; and interactions among anthropogenic and biogenic aerosols, clouds, and climate.

ACKNOWLEDGEMENTS

REFERENCES

Arneth, A., et al. (2010). Terrestrial biogeochemical feedbacks in the climate system. *Nature Geoscience* 3, 525 – 532.
Artaxo P. (2012). Break down boundaries in climate research. *Nature* 481, 239.
Baldocchi, D.D., et al. (2005). Predicting the onset of net carbon uptake by deciduous forests with soil temperature and climate data: a synthesis of FLUXNET data. *Int J Biomet* 49, 377-387.
Bonan, G.B., et al. (2011). Improving canopy processes in the Community Land Model version 4 (CLM4) using global flux fields empirically inferred from FLUXNET data. *J Geophys Res* 116, G02014.

Ciais Ph., et al. 2005. Europe-wide reduction in primary productivity caused by the heat and drought in 2003. *Nature* 437, 529-533.

Davidson E., et al. (2012). The Amazon basin in transition. *Nature* 481, 321-328.

Davin, E.L. and S.I. Seneviratne (2011). Role of land surface processes and diffuse/direct radiation partitioning in simulating the European climate. *Biogeosciences Discuss* 8, 11601-11630.

de Leeuw, G., et al. (2011). On the use of satellites to obtain information on the occurrence of natural and anthropogenic aerosols over the boreal Eurasian forest. iLEAPS special issue in *Biogeosciences Discuss*. 8, 8451-8483.

de Noblet-Ducoudré, N., et al. (2012). Determining robust impacts of land-use induced land-cover changes on surface climate over North America and Eurasia; Results from the first set of LUCID experiments, *J Clim*, doi: http://dx.doi.org/10.1175/JCLI-D-11-00338.1.

Ganzeveld, L. et al. (2010). The impact of future land-use and land-cover changes on atmospheric chemistry-climate interactions. *J Geophys Res*, doi:10.1029/2010JD014041.

Ghehi, N. et al. (2011). Spatial variations of nitrogen trace gas emissions from tropical mountain forests in Nyungwe, Rwanda, *Biogeosciences Discuss* 8, 11631-11660.

Guenther, A. et al. (2011) Integrated land ecosystem - atmosphere processes study (iLEAPS) assessment of global observational networks, *Bor Env Res* 16, 321-336.

Hari, P,. and M. Kulmala 2005. Station for Measuring Ecosystem-Atmosphere Relations (SMEAR II). *Bor Env Res* 10, 315–322.

Hari, P., et al. 2009. A comprehensive network of measuring stations to monitor climate change. *Bor Env Res* 14, 442–446

Jung M, et al. (2011). Global patterns of land-atmosphere fluxes of carbon dioxide, latent heat, and sensible heat derived from eddy covariance, satellite, and meteorological observations. *J Geophys Res* 116, G00J07.

Kulmala, M. and T. Petäjä 2011. Soil nitrites influence atmospheric chemistry. *Science* 333, 1586-1587.

Kulmala, M., et al. (and 124 other co-authors) 2011. General overview: European Integrated project on Aerosol Cloud Climate and Air Quality interactions (EUCAARI) – integrating aerosol research from nano to global scales. *Atm Chem Phys* 11, 13061-13143.

Kulmala, M., et al. 2001. On the formation, growth and composition of nucleation mode particles. Special issue on BIOFOR, *Tellus* B53, 479–490.

Kulmala, M., et al 2004. A new feedback mechanism linking forests, aerosols, and climate. *Atm Chem Phys* 4, 557–562.

Li, Z. et al. 2011. Long-term impacts of aerosols on the vertical development of clouds and precipitation. *Nature Geoscience*, doi:10.1038/ngeo1313

Mahecha, M.D., et al. 2010. Global convergence in the temperature sensitivity of respiration at ecosystem level. *Science* 329, 838.

Pitman, A.J., et al. 2011a. Regionalizing global climate models. *Int J Clim*, doi: 10.1002/joc.2279

Pitman, A.J. et al. 2011b. Importance of background climate in determining impact of land-cover change on regional climate. *Nature–Climate Change*, doi:10.1038/NCLIMATE1294

Pitman, A.J., et al. 2009. Uncertainties in climate responses to past land cover change: First results from the LUCID intercomparison study. *Geophys Res Lett* 36, L14814.

Rosenfeld, D., et al. 2008. Flood or Drought: How Do Aerosols Affect Precipitation? *Science* 322, 1309-1313.

Stevens, B. and G. Feingold 2009. Untangling aerosol effects on clouds and precipitation in a buffered system. *Nature* 461, 607-613.

Su, H., et al. 2011. Soil Nitrite as a Source of Atmospheric HONO and OH Radicals. *Science* 333, 6049, 1616-1618.

Teuling, A., et al. 2010. Contrasting response of European forest and grassland energy exchange to heat waves. *Nature Geoscience* 3, 722–727.

ELEMENTAL CARBON IN SNOW FROM ARCTIC SCANDINAVIA 2012

J. SVENSSON[1], D. BRUS[1] and H. LIHAVAINEN[1]

[1]Climate Change Unit, Finnish Meteorological Institute, Helsinki, PO.Box 503, 00101 Finland.

Keywords: Black Carbon, Snow Albedo, Arctic Scandinavia.

INTRODUCTION

Impurities in snow, such as black carbon (BC), have been known for some time to have negative effects on snow albedo, hence perturbing the climatic system, especially in the vast snow-covered Arctic (Warren and Wiscombe, 1980; Hansen and Nazarenko, 2004). Measurements of BC concentrations in snow have increased in recent years (e.g. Doherty *et al.*, 2010; Forsström *et al.,* 2009; Aamaas *et al.,* 2011), however, the spatial coverage of measurements still remain sparse in many areas. In this pilot study, elemental carbon (EC) (also referred to black carbon depending on measurement technique) was investigated in Arctic Scandinavia. The aim of the survey was to observe EC concentration differences throughout the Scandinavian Arctic, with the hypothesis that concentrations would increase the closer to the Russian border a sample was taken, due to higher emissions coming from the industrialized Kola Peninsula.

METHODS

Snow samples were collected along a transect ranging from western Sweden to eastern Finland (latitude 67° 7'-69° 4' and longitude range 18° 6'- 26° 7'). Surface snow and bulk samples of the whole snow column were sampled from each site a certain distance away from the road travelled to avoid local pollution from the roads. Samples were kept frozen until filtration, in which micro-quartz filters were used to collect the impurities. Dried filters were analysed with an OCEC-analyser (Sunset Instruments Inc., USA) for their EC-content using the EUSAAR_2 protocol (Cavalli *et al.*, 2010). Methods followed the procedures previously used by Forsström *et al.* (2009) and Aamaas *et al.* (2011).
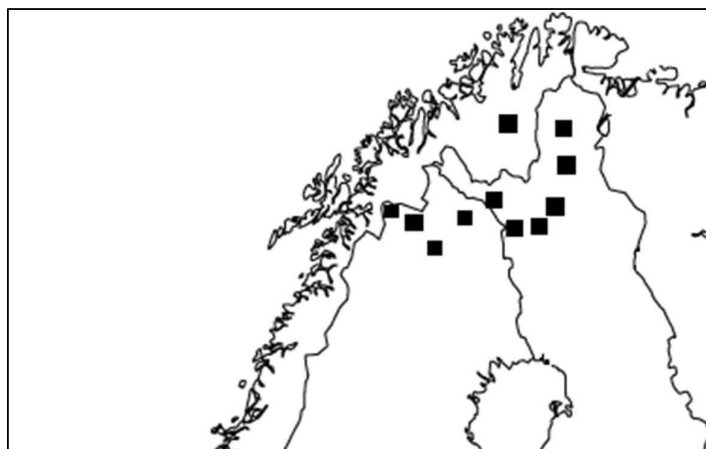
Figure 1. Location of samples collected in this Arctic Scandinavian survey.

CONCLUSIONS

Although not obvious, a tendency with higher concentrations the closer to Russia a sample was collected could be observed in the survey (fig. 2). We suspect that the sample taken south of Kiruna (higher concentration by a factor of at least two compared to the other samples) was affected by local pollution in the area (town of Svappavaara). This sample was therefore not included in figure 2. Additionally the two easternmost samples are questionable. One of the easternmost sample locations had a surface sample with

a very high concentration (it also had a factor of two difference from the rest of the samples) compared to the bulk sample, and its representativeness is consequently questioned. The other easternmost sample location had especially low concentrations, which could be due to a possible north-south concentration gradient, as these samples were gathered at higher latitude compared to the other samples. Without the easternmost and the Kiruna samples a gradient in the Scandinavian Arctic with higher concentrations to the east can be observed.

Bulk concentrations from each site generally agree with surface samples, with lower surface concentrations than the bulk samples. The two outliers are the samples described above, from south of Kiruna and the high surface concentration from eastern Finland.

This pilot study showed some promising results with an east-west gradient and also a potential north-south gradient. Additional measurements are needed to further support these hypotheses, and a more extensive field campaign is planned for the winter of 2013.
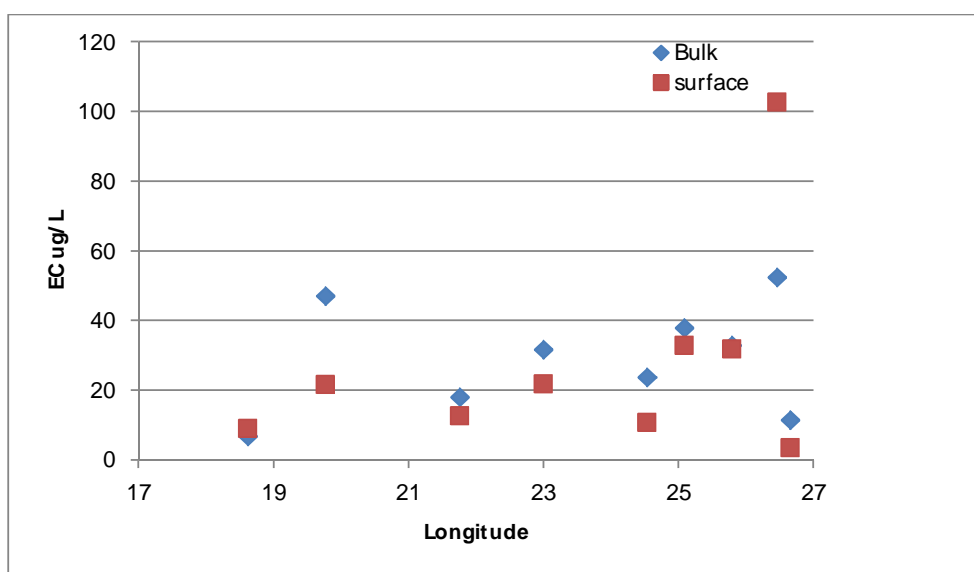

Figure 2. Sample concentrations plotted as a function of their location eastwards.

ACKNOWLEDGEMENTS

REFERENCES

Aamaas, B., C. E. Bøggild, F. Stordal, T. Berntsen, K. Holmén, and J. Ström (2011), Elemental carbon deposition to Svalbard snow from Norwegian settlements and long-range transport, *Tellus*, *63B*, 340-351.

Cavalli F., M. Viana, K. E. Yttri, J. Genberg, and J.-P. Putaud (2010), Toward a standardised thermal-optical protocol for measuring atmospheric organic and elemental carbon: the EUSAAR protocol, *Atmos. Meas. Tech*., 3, 79-89.

Doherty, S. J., S. G. Warren, T. C. Grenfell, A. D. Clarke, and R. E. Brandt (2010), Light-absorbing impurities in Arctic snow, *Atmos. Chem. Phys., 10*, 11,647–11,680.

Forsström S., J. Ström, C. A. Pedersen, E. Isaksson, S. Gerland (2009), Elemental carbon distribution in Svalbard snow, *J. Geophys. Res., 114,* D19112.

Hansen, J. and L. Nazarenko (2004). Soot climate forcing via snow and ice albedos, *Proc. Nat. Acad. Sci.*, 101, 423–428, 2004.

Warren, S. and W. Wiscombe (1980). A model for the spectral albedo of snow. II: Snow containing atmospheric aerosols, *J. Atmos. Sci.*, 37, 2734– 2745.

ICE NUCLEATION STUDIES IN THE CRAICC FRAMEWORK

E.S. THOMSON [1], J.B.C PETTERSSON[1], M. BILDE [2], E. SWIETLICKI, [3], B. SVENNINGSSON, [3], M. SIPILÄ[4], J. HAKALA[4] and H-C. HANSSON[5]

[1] Department of Chemistry and Molecular Biology, Atmospheric Science, University of Gothenburg, SE-41296, Gothenburg, Sweden.

[2] Department of Chemistry, University of Copenhagen, 2100 Copenhagen, Denmark.

[3] Division of Nuclear Physics, Department of Physics, Lund University, SE-22100, Lund, Sweden.

[4] Division of Atmospheric Sciences, Department of Physics, University of Helsinki, FIN-00014, Helsinki, Finland.

[5]ITM Department of Applied Environmental Science, Stockholm University, SE-10691, Stockholm, Sweden.

Keywords: ICE, NUCLEATION

INTRODUCTION

The main objectives of CRIACC's work package five (WP5) can be summarized shortly as, the aim to contribute detailed scientific understanding to the interrelation of clouds, aerosols, and climate in the Arctic environment. Specifically this is to be done in a number of ways, including as stated in the CRAICC proposal, "Ice Nuclei counters are developed and deployed as part of this project". Due to the cold temperatures most Arctic clouds form when ice particles nucleate in the atmosphere. Although, nucleation is an extensively studied phenomenon, the atmosphere is a unique environment where the physical and chemical characteristics of aerosol particles can serve to enhance and/or diminish the efficiency of ice nucleation. Furthermore, although they are of great interest there is a lack of environmental measurements of atmospheric ice nucleation. Currently, several CRAICC partners are collaborating with multiple outside-of-CRAICC partners to bring ice nucleation measurements to the Nordic community.

One primary aspect of this effort is the development of continuous flow diffusion chamber (CFDC) Ice Nuclei Counters (INCs), for use by CRAICC partners in both laboratory and field measurement campaigns. The INCs will be based on designs of a Portable INC (PINC) from ETH in Zurich and the project will be coordinated by CRAICC partners at the University of Gothenburg.

Simultaneous with the CFDC development, a substrate measurement method will be used to initiate long term ice nuclei (IN) measurements, with the central goal of establishing a baseline of continuous IN measurements within the Nordic area. The substrate method is similar to filter collection methods, whereby aerosols are electrostatically deposited onto silicon substrates which are subsequently analyzed using a freezing procedure in an static vapor diffusion chamber (FRIDGE). The sampling substrates, procedure, and FRIDGE apparatus have been refined by scientists at the Goethe-University in Frankfurt, Germany, who have agreed in principle to participate in CRAICC led measurements.

Here we give an overview of the development of the IN project to date, and outline the plans for building and deploying CRAICC INCs and for deploying and analyzing FRIDGE substrates.

The difficulty of formulating complete theoretical descriptions of heterogeneous ice nucleation has helped to motivate the development and deployment of INCs, with the parallel goals of contributing to the fundamental understanding and modeling efforts of Ice Nuclei (IN). The underlying principle of INC techniques is to collect an aerosol and in a controlled manner expose that air sample or aerosol particle to humidity and cooling. When exposed to cold and moist conditions some of the aerosol particles will facilitate ice particle nucleation. In most INCs the fraction of those particles that are "activated" for given conditions is measured. Ideally in systems using ambient air sampling the composition of the dry aerosol is also assessed. On the other hand, by analyzing known samples created in the laboratory nucleation properties for known particles can be determined. Almost all current INCs have evolved from technologies originally developed between the 1950s and 1970s. Much of the fundamental measurement techniques have simply gotten more accurate since that time period.

The most widely used INC devices are of the CFDC variety (DeMott et al., 2011). These instruments flow a focused sample aerosol between warm and cold ice coated surfaces which provide an established temperature and vapor field that is supersaturated with respect to ice (and water if desired). Ice nucleation in CFDCs is typically detected optically, either by an Optical Particle Counter (OPC) mounted at the chamber outflow after an evaporation section, or by using some type of depolarization detection. The primary benefits of CFDC chambers are the lack of substrate effects coupled with flexible temperature and relative humidity ranges and high time resolutions. Their relatively small size allows them to be transported and used for field and airborne measurements, but also limits the aerosol flow rate to $\approx 1 - 2$ L/min. They do not assess contact-freezing nucleation.

The filter and substrate collection techniques like FRIDGE traditionally suffered from unquantified substrate effects. However, the new electrostatic deposition technique used for FRIDGE shows good agreement with measurements made with continuous flow machines (Klein et al., 2010). Thus, although these methods still lack the time resolution of online techniques like CFDC machines they do benefit from being relatively easy to deploy in the field and provide a robust temporal average of IN. Furthermore, deposited IN are more readily microscopically analyzed. Still other IN characterization techniques include droplet levitation (Duft and Leisner, 2004; Svensson et al., 2009), expansion chambers (Möhler et al., 2005; Möhler et al., 2007) and others (Bundke et al., 2007; Hartmann et al., 2011). Each technique has specific merits and demerits, which encourages a plurality of measurement methods and inter-comparison. In an effort to obtain a full picture of the INC field and to best formulate a united Nordic INC effort, CRAICC has organized multiple workshops.

The first ice nucleation workshop was held in Copenhagen in April 2011 with the aim of establishing a baseline of scientific knowledge concerning active IN and INC research. Multiple outside visitors with technological and measurement expertise were invited and the direction of CRAICCs effort was actively discussed. In February 2012, a second INC workshop was held at ETH in Zurich in order to specifically discuss INC technology and to formulate a strategic plan for the development and deployment of such technology across the Nordic and Arctic region. At this meeting CRAICC partners decided on a two pronged approach which will include the development and deployment of CFDC chambers modeled on PINC in collaboration with ETH and the Leibniz Institute for Tropospheric Research (IFT). The decision to develop a Nordic CFDC machine was made based upon the opportunities to collaborate widely within Europe and throughout the world and also in the interest of the CFDC technology, which is considered to be the most mature online INC technique, with the most opportunity for direct inter-comparison with other measurements. Furthermore, with access to the design details of an existing apparatus (PINC) the collaboration with

ETH can be mutual beneficial as the INC is further developed. The utilization of FRIDGE is seen to be the best opportunity for quickly establishing a continuous and field deployable measurement campaign, that can benefit all future IN research.

DEVELOPMENT SCHEDULE

At the February 2012 workshop it was deemed necessary to draft a technology sharing agreement between all of the interested parties regarding the exchange of design and operational details of ETH's PINC. This agreement has been through multiple drafts and as of August 10, 2012 was agreed to in principle. It is currently being finalized and circulated for signatures. With this agreement each party will be protected and obligated to protect the other's intellectual property. It will also allow ETH to share the complete design details of the PINC instrument, including machine blueprints, technical specifications, software etc. This is expected to proceed no later than September 1, 2012.

In addition to the workshop and technology transfer agreement Jani Hakala from Helsinki University and Erik Thomson from Gothenburg University visited ETH for one week in June to gain practical user experience with the PINC machine. During this week they were able to examine the PINC and ZINC machines in detail and operate the PINC machine. With partners at ETH potential improvements for the next generation INC were discussed.

Currently, a detailed production plan for CRAICC INCs is expected to be completed shortly after the technology sharing agreement has been fully implemented and CRAICC partners receive technical specifications from ETH.

Discussions are currently in progress with the Goethe-University regarding establishing Nordic FRIDGE monitoring stations. The primary topics concern station locations and substrate analysis.

OUTLOOK

The goal for INC development by CRAICC is to have working INCs within one year. This includes time for planning, acquiring materials, machining, assembly, and testing. As they are completed each working prototype will also be benchmarked against ETH's PINC. Because the PINC has already been inter-compared with many other apparatuses (DeMott et al., 2011) this will also provide a baseline for data comparisons with existing measurements.

Prior to field deployment the INC will be tested extensively in the laboratory. Furthermore, many currently used experimental apparatuses within CRAICC would benefit from adding IN measurements. Targeted apparatuses include flow tube reactors, sea-salt aerosol generators, and aerosol chambers.

Additionally, a short (2 to 3 month) field season of FRIDGE substrate collection is anticipated in the fall of 2012. The goal of this field season is to develop procedures and strategies for substrate collecting, transport, and analysis with the cooperation of the Goethe-University.

A second, long-term, phase of field deployment is anticipated for the INCs developed within the CRAICC framework. Field studies will include deployment within the Arctic and sub-Arctic to assess the IN potential within these unique environments.

ACKNOWLEDGEMENTS

REFERENCES

Bundke, U., Bingemer, H., Nillius, B., Jaenicke, R., and Wetter, T. (2007). *Nucleation and Atmospheric Aerosols*, chapter The FINCH (Fast Ice Nucleus Chamber counter). Springer.

DeMott, P. J., Möhler, O., Stetzer, O., Vali, G., Levin, Z., Petters, M. D., Murakami, M., Leisner, T., Bundke, U., Klein, H., Kanji, Z. A., Cotton, R., Jones, H., Benz, S., Brinkmann, M., Rzesanke, D., Saathoff, H., Nicolet, M., Saito, A., Nillius, B., Bingemer, H., Abbatt, J., Ardon, K., Ganor, E., Georgakopoulos, D. G., and Saunders, C. (2011). Resurgence in ice nuclei measurement research. *Bulletin of the American Meteorological Society*, 92(12):1623–1635.

Duft, D. and Leisner, T. (2004). Laboratory evidence for volume-dominated nucleation of ice in supercooled water microdroplets. *Atmospheric Chemistry and Physics*, 4:1997–2000.

Hartmann, S., Niedermeier, D., Voigtlaender, J., Clauss, T., Shaw, R. A., Wex, H., Kiselev, A., and Stratmann, F. (2011). Homogeneous and heterogeneous ice nucleation at lacis: operating principle and theoretical studies. *Atmospheric Chemistry and Physics*, 11(4):1753–1767.

Klein, H., Haunold, W., Bundke, U., Nillius, B., Wetter, T., Schallenberg, S., and Bingemer, H. (2010). A new method for sampling of atmospheric ice nuclei with subsequent analysis in a static diffusion chamber. *Atmospheric Research*, 96(2-3):218–224.

Möhler, O., Buttner, S., Linke, C., Schnaiter, M., Saathoff, H., Stetzer, O., Wagner, R., Kramer, M., Mangold, A., Ebert, V., and Schurath, U. (2005). Effect of sulfuric acid coating on heterogeneous ice nucleation by soot aerosol particles. *Journal of Geophysical Research-Atmospheres*, 110(D11):D11210.

Möhler, O., DeMott, P. J., Vali, G., and Levin, Z. (2007). Microbiology and atmospheric processes: the role of biological particles in cloud physics. *Biogeosciences*, 4(6):1059–1071.

Svensson, E. A., Delval, C., von Hessberg, P., Johnson, M. S., and Pettersson, J. B. C. (2009). Freezing of water droplets colliding with kaolinite particles. *Atmospheric Chemistry and Physics*, 9(13):4295–4300.

EVALUATION OF FLUX FOOTPRINT OVER IDEALIZED URBAN SURFACE BY LARGE EDDY SIMULATION MODEL

S.M. TU[1], F. KANANI[2] , A. HELLSTEN[3] , T. MARKKANEN[3] , S. RAASCH[2] , L. JÄRVI[1] , A. NORDBO[1] and T. VESALA[1]

[1]Department of Physics, University of Helsinki, Helsinki, Finland.

[2]Department of Meteorology and Climatology , University of Hannover, Hannover, Germany.

[3]Finnish Meteorological Institute, Finland.

Keywords: FLUX FOOTPRINTS, LAGRANGIAN TRAJECTORY SIMULATION, LARGE EDDY SIMULATION.

INTRODUCTION

Knowledge of source/sink area is critical for understanding the data collected in the measurement site as well as the planning the site configuration. In principle, sensor must be placed warily in an sufficient height for the purpose of enclosing representative sample information throughout the site. Since every point or area source will potentially contribute to the concentration or flux profile downwind to a degree that varies with various elements such as distance from the source, elevation of observation, as well as with characteristics of the turbulent boundary layer and atmospheric stability (Schuepp *et al.*,1990), for any observation at an specific elevated point, the conman issues are the accuracy and the effect on the upwind source area sensed by the measurement.

Footprint analysis has won its reputation for revealing the spatial context of micrometeorological measurement with defining the surface information which the measurements represent as well as being considered for supporting the interpretation of measurements. Applying a footprint model can help examining the quantity obtained from measurements at different heights especially for the heterogeneous surface. Since the earth surface is characterised by thermal as well as aerodynamical inhomogeneities in a wide range of scales, the existence of these inhomogeneities makes footprint evaluations important (Steinfeld *et al.*, 2008).

For many obvious reasons such as highly growing proportion and human comforts, there is increasing interests in studying and predicting air flow and particles dispersion within urban canopy, especially the centre region. However, due to the complex structure of urban surface, to analyse the airflow becomes a challenging task with regard to the geometries and unsteady buoyant flow conduction. Recently, based on the benefits of numerical analyse; it is possible to study turbulent fluid transport and boundary condition by using numerical models. Large eddy simulation (LES) model stands on a vantage position in its ability to evaluate the details of subgrid-scale (SGS) turbulence symptom by simulating relevant fluid dynamic processes, furthermore, the complex building vortex shedding. Even though LES belongs to the group of high resource cost, today's computational resources allow us to use large eddy simulation (LES) models that explicitly resolve all relevant scales of turbulence.

METHODS

The large eddy simulation model that has been used for this study is the parallelised LES model PALM (Raasch and Etling, 1998; Raasch andSchroter, 2001). Detailed information on PALM is given by Raasch (2009). PALM has been applied for a wide variety of LES studies, such as the investigation of homogeneous (Schroter *et al*., 2000) and heterogeneous heated CBLs (e.g. Inagaki *et al*., 2006). In the

study, temperature profile was constant with height and humidity is completely omitted. Also, cyclic boundary conditions have been applied at the lateral boundaries of the model domain and Monin-Obukhov similarity theory has been applied between any rigid boundary. The neutral stratification was kept until the end of the simulation by avoiding heating and cooling of the simulated boundary layer. Coriolis force was omitted in this simulation.

The domain of this study was chosen to be 256 m in both x- and y-direction as well as 800 m for the vertical direction. A grid spacing of 2.5 m was used in the two horizontal and the vertical direction. All together 1024 cuboids with a side length of 37.5 m and with a height of 40 m were distributed in a regular pattern at the bottom of the model domain. The horizontal distance between two adjacent cuboids was 42.5 m.

10 hours after the start of simulation, when the flow had reached a quasi-stationary state, about 500000000 particles start to be released in interval time of 120s at 5 m height where is below the building top for 30 minutes and their life time last for 3 hours for the statistics reason. For the purpose of footprint calculations, this study only consider the effective number of particles which been taken into account that not all of the particles release in the simulation can really contribute to the footprint evaluation for a certain distance but only particles with sources in the sensor location area. Moreover, for the purpose of statistics, the extension of the sensor area is used here instead of the single sensor point. The evaluation of flux footprints was carried out at sensor heights 50 m and 10 m, respectively.

Pages should not be numbered. You may arrange your text under headings, in capitals and centred. Figures and Tables may be included in the abstracts, but please make sure that they all have a caption, and that they are numbered consecutively using Arabic numerals. The font used in captions can be smaller than used elsewhere, but be advised that anything smaller than 10pt may become illegible when reduced (slightly) for printing. Make sure that the caption fully describes all the features in the Figure or Table. Vertical lines in tables should be avoided.

RESULTS

Figure 1 shows the velocity components u, v and w as well as the subgrid kinetic energy, respectivly, after averaging over 1 hour with the averaging period starting after 12 hours of the simulation and ending after 13 hours of the simulation. It can be see clearly that in the same location with respect to the cuboid, the flow patten is similar. Figures 2 and 3 are the flux footprints with the height at 50 m and 10 m, respectively. The sensor place is in the intersection of dash line which divide into 8 different locations with respect to the buildings (sensor in the centre of building, behind the building, in the centre of canyon, in front of the building, in the north of building, in the centre of open street, in the south of building and in the intersection of street). The maximum value can seen in both figures located in the upstream of sensor location. Fig. 2 shows the classic pattern of footprint when the sensor location is above the buildings. Moreover, Fig. 3 shows the clear picture for the flow pass through the buildings. Furthermore, the sink location in the footprint can be study by the relationship with the sensor location.

CONCLUSIONS

This study carried out large eddy simulations for evaluating flux footprint over idealized urban surface. The footprint maximum is clearly situated upstream of the sensor position. The heterogeneity of the surface is clearly reflected in the footprints for different sensor positions within an idealized urban canopy.
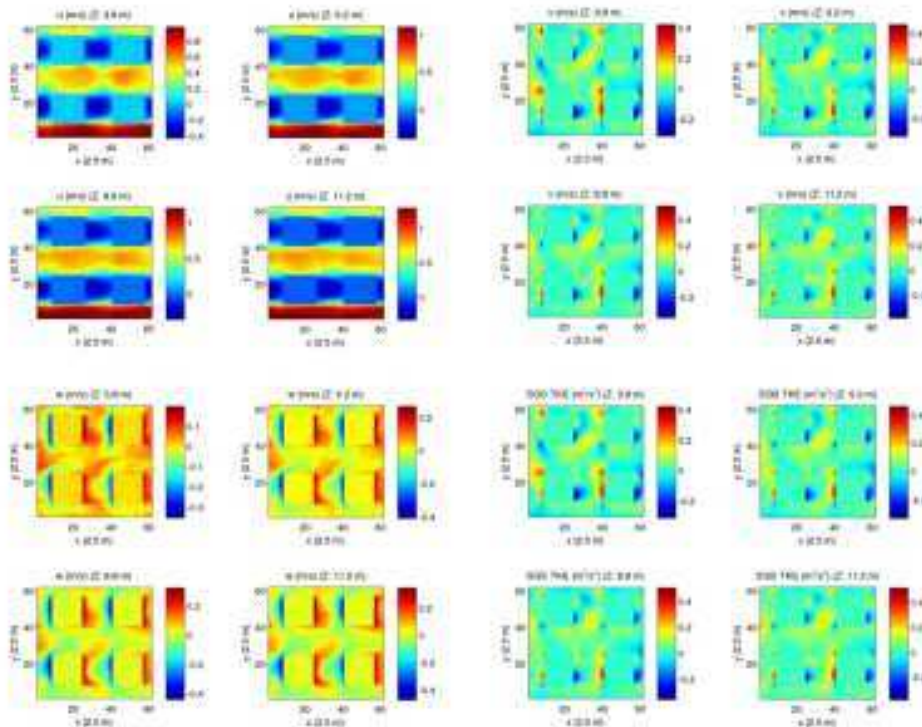
Figure 1. Hourly averaged u-, v- and w-component of wind speed as well as subgrid scale turbulence kinetic energy at 46800s.
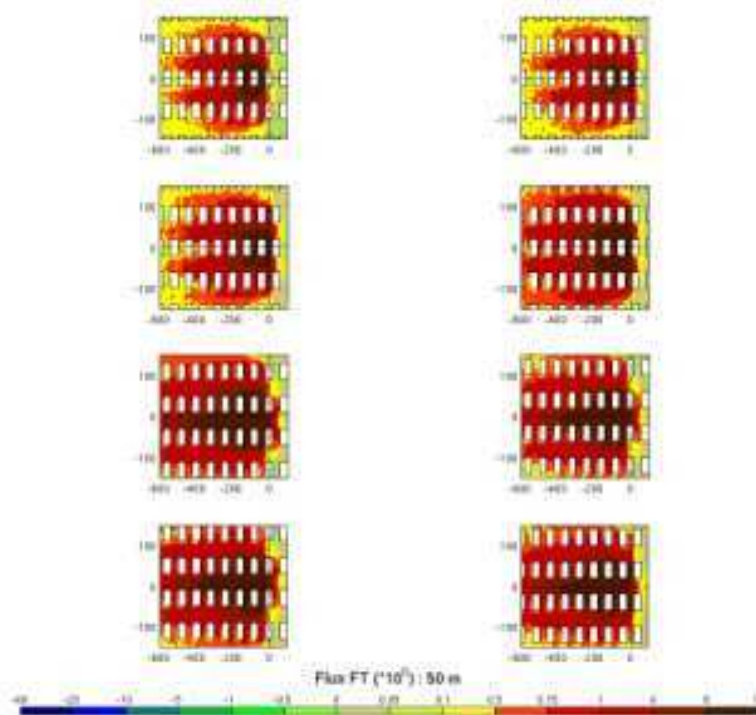

Figure 2. X-y cross section of flux footprint for the sensor height at 50 m.
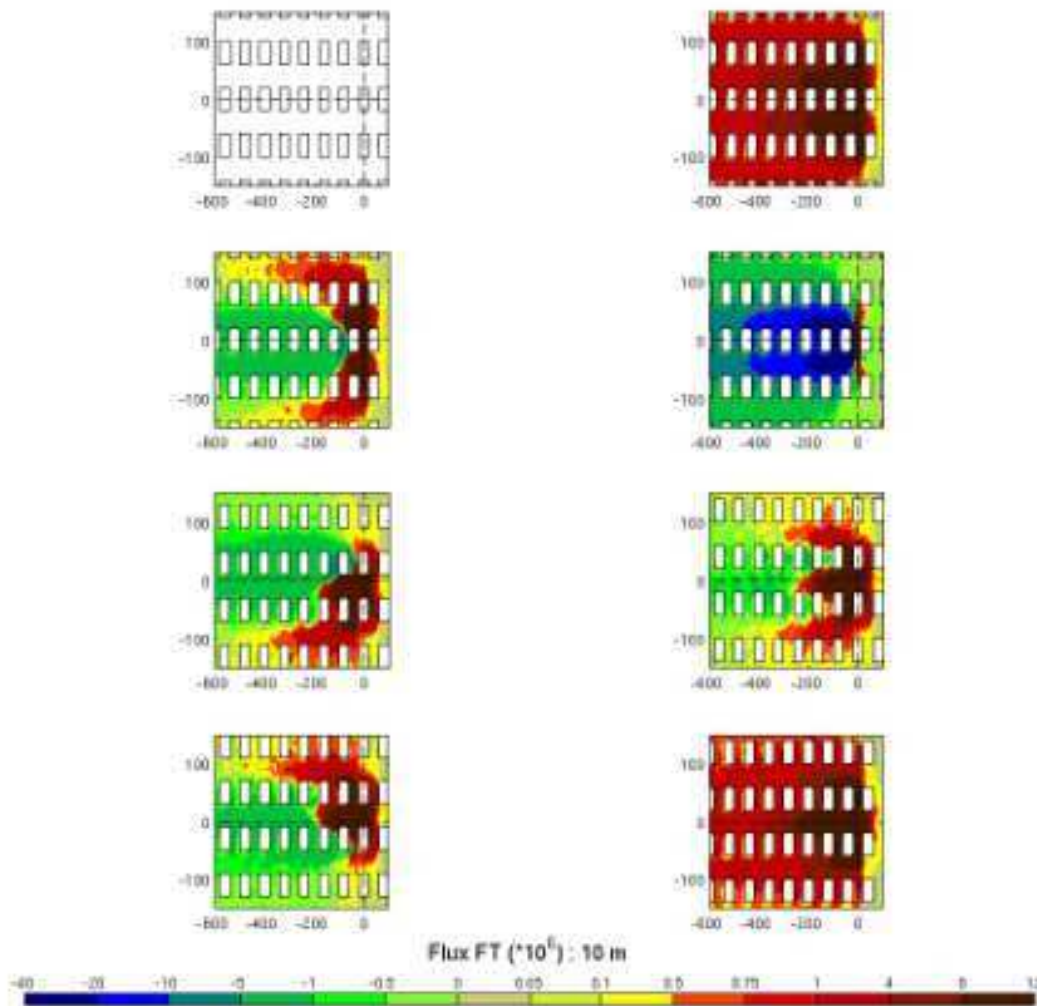
629

Figure 3. X-y cross section of flux footprint for the sensor height at 10 m.

ACKNOWLEDGEMENTS

REFERENCES

Inagaki A., Letzel M.O., Raasch S. and Kanda M. (2006). Impact of surface heterogeneity on energy imbalance: a study using LES. *J Meteor Soc Japan* **84**, 187-198.

Raasch S. (2009) PALM group. [Available online at http://www.muk.uni-hannover.de/ ˜raasch/PALM group/]

Schröter M., Bange J. and Raasch S. (2000). Simulated airborne flux measurements in a LES generated convective boundary layer. *Boundary-Layer Meteorol.* **95**, 437-456.

Schuepp, P. H., Leclerc, M. Y., McPherson, J. I., and Desjardin, R.L. (1990). Footprint prediction of scalar fluxes from analytical solutions of the diffusion equation, *Boundary-Layer Meteorol.* **50**, 355-374.

Steinfeld G., Raasch S., and Markkanen T. (2008). Footprints in homogeneously and heterogeneously driven boundary layers derived from a Lagrangian stochastic particle model embedded into large-eddy simulation, *Boundary-Layer Meteorol.* **129**, 225-248.

DROUGHT EFFECT ON CO_2, CH_4, AND N_2O FLUXES ALONG BOREAL FOREST/MIRE ECOTONE

B. ŤUPEK[1], K. MINKKINNEN[1], P. KOLARI[1], M. STARR[1], J. ALM[2a], T. VESALA[1], J. PUMPANEN[1], F.BERNINGER[1], J. LAINE[2b] and E. NIKINMAA[1]

[1]Department of Forest Sciences, P.O. Box 27, 00014 University of Helsinki, Finland.

[2a]Finnish Forest Research Institute, P.O. Box 68, 80101 Joensuu, Finland.

[2b]Finnish Forest Research Institute, Kaironiementie 54, 39700 Parkano, Finland

Keywords: Carbon dioxide, Methane, Nitrous oxide, Hydrological gradient.

INTRODUCTION

Soils, drainage, and carbon storage of boreal forest varies between well drained upland forests and poorly drained peatlands (Hartshorn et al. 2003, Seibert et al. 2007, Weishampel et al. 2009). Trace gas fluxes such as CO_2, CH_4, and N_2O of upland and peatland soils change especially along the wide range of moisture conditions (Solondz et al. 2008, Pihlatie et al. 2004). Upland forest soil is typically a large source of CO_2 into atmosphere, a small source or sink of N_2O, and a small sink of atmospheric CH_4 (Moosavi and Crill 1997, Kolari et al. 2009, Pihlatie et al. 2007, Ullah and Moore 2011). Natural peatland soil is typically a large source of CO_2 into atmosphere, a small source or sink of N_2O, and a large or small source of atmospheric CH_4 (Martikainen et al. 1995, Nykänen et al. 1995, Silvola et al. 1996, Alm et al. 1997, D'Angelo and Reddy, 1998, Riutta et al. 2007, Ullah and Moore 2011).

The field studies of spatiotemporal comparison of boreal forest CO_2 dynamics along wide range of moisture conditions became recently more common (Hartshorn et al. 2003, Solondz et al. 2008, Ťupek et al. 2008), however synergic CO_2, CH_4, and N_2O studies of natural boreal forest/mire ecotones are few (e.g. Ullah and Moore 2011). The ecotone represents an ecological tension between well drained upland forests and poorly drained peatlands connected on the toe of the slope by the forest/mire transition. The transition between forests and peatlands is an ecological switch, where vegetation of forests and soils of peatlands coincide and frequently undergo fluctuations in water level position (Hartshorn et al. 2003). The CO_2, CH_4, and N_2O dynamics of forest/mire transition may be expected to differ from typical forests and peatlands.

The aim of our study was to evaluate variation in the forest floor CO_2, CH_4, and N_2O fluxes during exceptional moisture conditions along the boreal forest/mire ecotone in relation to site specific environmental conditions.

In spatiotemporal variability of greenhouse gas dynamics and in the upscaling into the landscape level carbon and nitrogen balances the forest/mire transitions may act as a 'hotsposts' (McClain et al. 2003, Ullah and Moore 2011). Not including them into a consideration of the greenhouse gas assessment may lead to a biased landscape level estimate.

MATERIAL AND METHODS

The Vatiharju-Lakkasuo ecotone of nine forest and mire stations ECOGRAD forms a gradient in vegetation distribution, soil moisture and nutrient conditions in Central Finland (61° 47', 24° 19') (Ťupek et al. 2008). The ECOGRAD forests are situated along 450 m transect with a relative relief of 15 meters and a 3.3 % slope facing NE (Fig.1). The forest types range from well-drained upland forests, trough forest/mire transitions, to poorly-drained sparsely forested mires (Fig. 1). Catena of soils is formed by well drained haplic podzols on the hillsope, through intermediately drained histic and gleyic-histic podzols in forest/mire transitions on the toe of the slope, and permanently wet hemic histosols downslope.
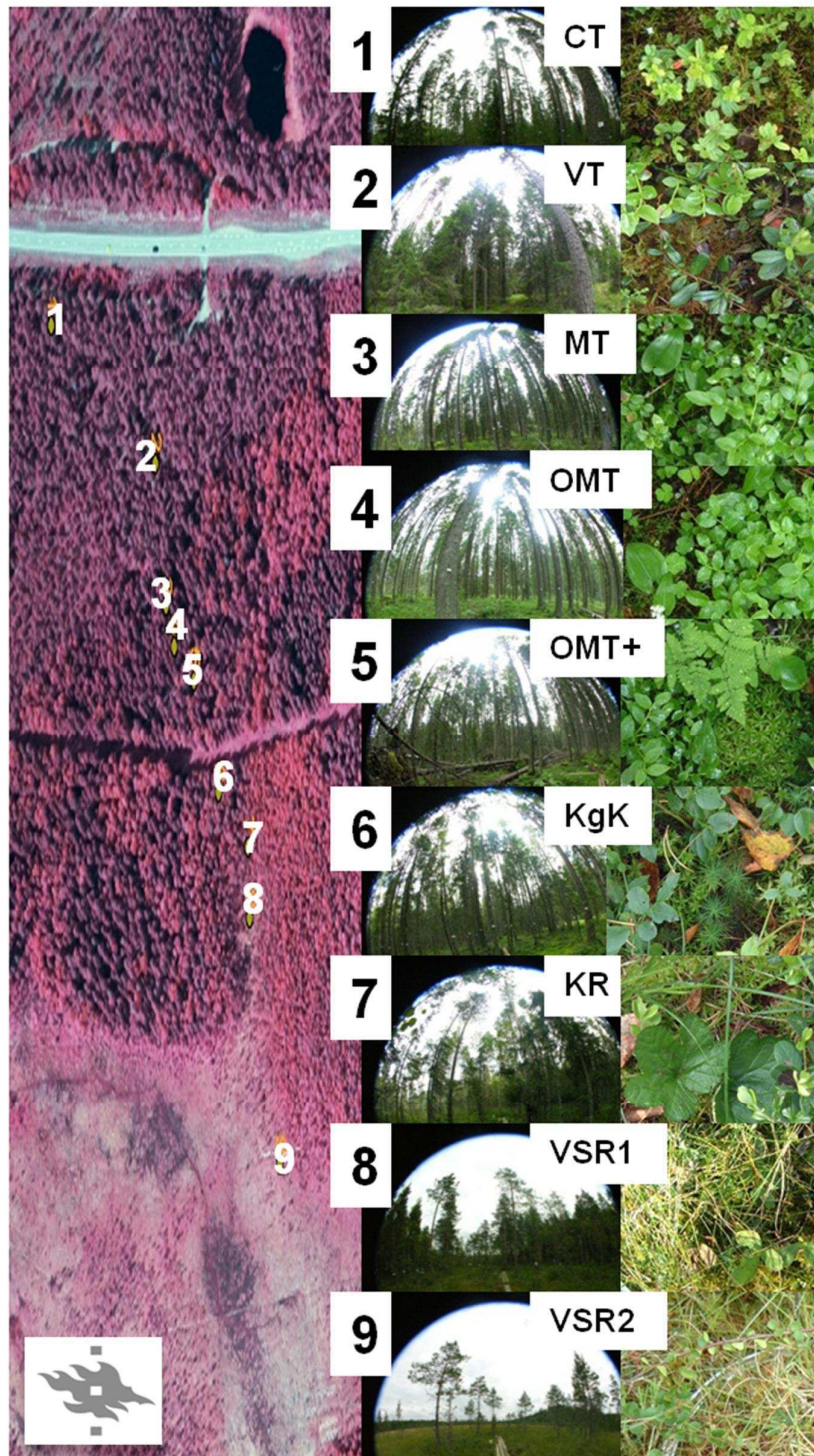
Figure 1. Left) Airborne infrared photograph show a 450 m long Vatiharju - Lakkasuo forest/ mire ecotone in Finland. Middle) Fish eye photographs show tree stands of upland xeric, subxeric, mesic and herb-rich forest types (1 CT - Calluna, 2 VT - Vitis Idea, 3 MT - Myrtilus, 4 OMT - Oxalis-Myrtillus); paludified forest - mire margin types (5 OMT+ - Oxalis-Myrtillus Paludified, 6 KgK – Myrtillus Spruce Forest Paludified); sparsely forested wet mire types: 7 KR – Spruce Pine Swamp, 8 VSR1 and 9 VSR2 - Tall Sedge Pine Fen). Right) Photographs show ground vegetation of 9 forest/mire types. Forest/mire types were classified according to classification system of Cajander (1949), and Laine *et al.* (2004).

The ECOGRAD micrometeorological and gas exchange measurements were taken weekly during summers of 2004 (July-November), 2005 (May-November), 2006 (May-September), and occasionally during winters. The measurements of the forest floor soil temperatures in 5 cm depth (T_5), the volumetric soil water content in 10 cm depth, the depth of water level, the forest floor respiration (R_{ff}) followed the same procedure as described by Ťupek *et al.* (2008).

The field gas sampling was conducted weekly during 2004 and 2005 season and bi-weekly during 2006 season. The occasion of the gas sampling was at the same day ±one day as the occasion of the micrometeorological and CO_2 flux measurements. The samples were taken from 3 opaque, vented, closed, static chambers (ø 315 mm, h 295 mm) placed on collars air tightly. For each measuring occasion one ambient gas and four 15 ml samples were drawn in syringes from each of three chambers at intervals of 5, 10, 15, 20 min totalling into 13 samples for each site. Chamber temperature was monitored during the sampling. After the sampling event, the gas samples were stored in coolers +4°C and analysed within 36 hours in laboratory by using gas chromatograph. Gas chromatograph (Hewlett-Packard, USA) was fitted with a flame ionisation detector (FID) for CH_4 and an electron capture detector (ECD) for N_2O detection. The CH_4 ($mgm^{-2} h^{-1}$) and N_2O ($\mu gm^{-2} h^{-1}$) fluxes were calculated from the slope of linear regression between the set of 4 gas concentrations and chamber closure time. Fluxes were verified against the standard and ambient gas concentration adopting criteria as used in Alm et al. (2007). Due to disturbance during the field gas sampling and due to poor gas chromatograph precision 17% of CH_4 and 49% of N_2O fluxes were discarded in total.

RESULTS

In comparison between dry year 2006 and previous wetter years, the seasonal medians of the forest floor CO_2 effluxes (Rff) showed clear reduction in all forest types (1 CT, 2 VT, 3 MT, 4 OMT, 5 OMT+, 6 KgK, and 7 KR) except mires (8 VSR1, 9 VSR2) (Figure 2a). In dry year the mean of seasonal medians of sites with the Rff reduction dropped almost by ½ and differences between forest types diminished. The Rff of mires during dry year was enhanced for the 9 VSR2 more abundant with hummocks than lawns, and remained similar for the 8 VSR1 more abundant with lawns. Exceptionally wet summer 2004 caused large enhancement of the Rff in less fertile xeric upland forest 1 CT and in fertile herbrich spruce forest 4 OMT. In general median Rff values were larger in wet year 2004 than in intermediate and dry year 2005 and 2006.

The Rff values during intermediate and wetter soil moisture conditions along the forest/mire ecotone were largest in the most fertile herb rich spruce forest 4 OMT. During wet year 2004, seasonal forest/mire site Rff values showed increase in sites with the water table depth deeper below the surface (Figure 2b). During dry year 2006, the opposing pattern of forest/mire Rff values were showing decrease as ground water levels of all sites dropped deeper. During intermediate year 2005 the Rff values showed hillslope maximum at around 30 cm water level depth. The 30 cm WT depth corresponds to the prevailing depth found in forest/mire transitions. The monthly medians of 5 OMT+, 6 KgK and 7 KR show clear Rff reduction in dry year 2006 and enhancement in wet year 2004 from the anticipated exponential response to soil temperature.

The seasonal medians of forest/mire types CH_4 dynamics showed small consumptions for upland forests on mineral soils (1 CT, 2 VT, 3 MT, 4 OMT), and small consumption/production for the forest/mire transitions (5 OMT+, 6 KgK, 7 KR) (Figure 2c). The sparsely forested mires 8 VSR1 and 9 VSR2 showed CH_4 production during all years. In comparison to rather stable consumption levels between the years along the forest/mire ecotone, the mire productions showed large difference between high CH_4 emissions in 2005 and low CH_4 emissions in 2006.

The CH_4 dynamics showed along the forest/mire ecotone an exponential trend from consumptions to productions in relation to the ground water levels rising from the deeper horizons towards the surface and

saturating the soil (Figure 2d, Figure 2b). Evaluation of CH_4 production/consumption in the forest/mire transitions (5 OMT+, 6 KgK, 7 KR) showed weak linear increase in CH_4 consumption with lowering ground water levels.

The seasonal medians of N_2O fluxes showed insignificant variation between intermediate and dry year and along forest/mire types (Figure 2e). The N_2O fluxes fluctuated between small consumptions and productions for each site. Although, the median values showed N_2O production along the forest/mire ecotone. Water levels did not explain the N_2O flux variation among the forest/mire types (Figure 2f).
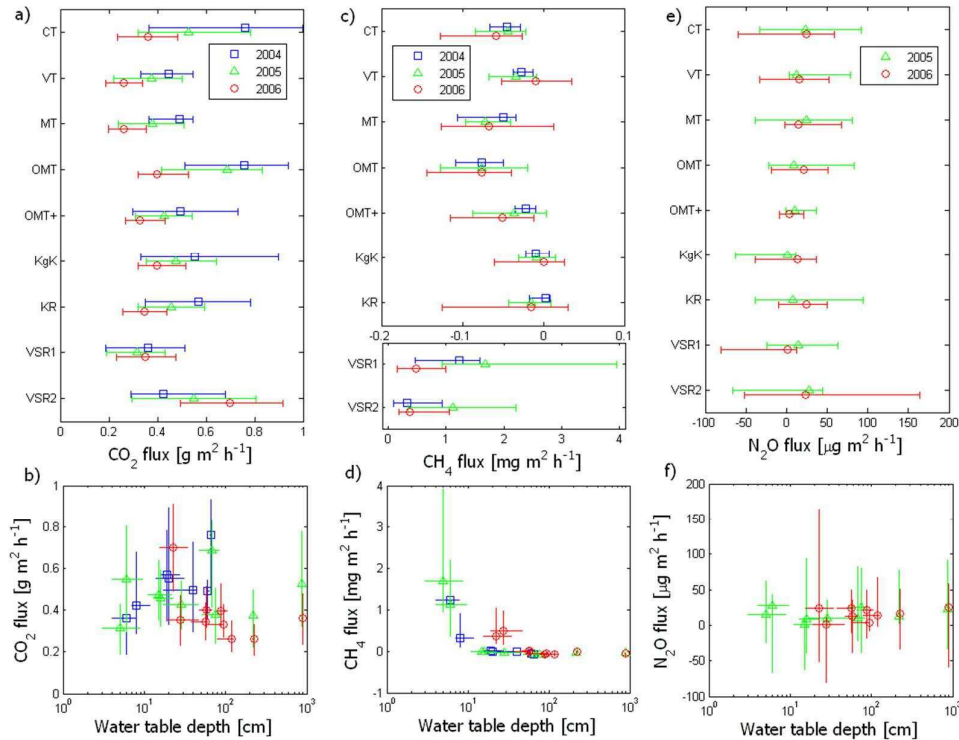

Figure 2. The monthly medians of the forest/mire types a) forest floor CO_2 efflux, c) methane flux, e) nitrous oxide flux during wet 2004, intermediate 2005, and dry year 2006. The panels b, d, f show forest/mire respective fluxes. For forest/mire types see Fig. 1. The error bars represent 25th and 75th percentile.

REFERENCES

Alm, J., Talanov, A., Saarnio, S., Silvola, J., Ikkonen, E., Aaltonen, H., et al. (1997). Reconstruction of the carbon balance for microsites in a boreal oligotrophic pine fen, finland. *Oecologia*, **110**(3), 423-431. doi:10.1007/s004420050177

Alm, J., Shurpali, N. J., Tuittila, E., Laurila, T., Maljanen, M., Saarnio, S., et al. (2007). Methods for determining emission factors for the use of peat and peatlands - flux measurements and modelling. *Boreal Environment Research*, **12**(2), 85-100.

Cajander, A. K. (1949). Forest types and their significance. *Acta Forestalia Fennica* **56**, 1–69.

D'Angelo, E., and Reddy, K. (1999). Regulators of heterotrophic microbial potentials in wetland soils. Soil *Biol Biochem*, **31**(6), 815-830. Retrieved from http://ukpmc.ac.uk/abstract/AGR/IND22042851

Hartshorn, A. S., Southard, R. J., and Bledsoe, C. S. (2003). Structure and function of peatland-forest ecotones in southeastern alaska.. *Soil Sci Soc Am* J, **67**, 1572-1581.

Kolari P, Kulmala L, Pumpanen J, Launiainen S, Ilvesniemi H, Hari P, Nikinmaa E (2009). CO_2 exchange and component CO_2 fluxes of a boreal Scots pine forest. *Boreal Environment Research* **14**, 761-783.

Laine, J., Komulainen, V.-M., Laiho, R., Minkkinen, K., Rasinmäki, A., Sallantaus, T., Sarkkola, S., Silvan, N., Tolonen, K., Tuittila, E-S., Vasander, H., and Päivänen, J. (2004) Lakkasuo, a guide to mire ecosystems. Helsingin Yliopiston Metsäekologian Laitoksen Julkaisuja, 31. Helsinki, Finland. 123 p.

Martikainen, P. J., Nykanen, H., Crill, P., & Silvola, J. (1993). Effect of a lowered water table on nitrous oxide fluxes from northern peatlands. *Nature*, **366**(6450), 51-53. Retrieved from http://dx.doi.org/10.1038/366051a0

McClain, M. E., Boyer, E. W., Dent, C. L., Gergel, S. E., Grimm, N. B., Groffman, P. M., et al. (2003). Biogeochemical hot spots and hot moments at the interface of terrestrial and aquatic ecosystems. *Ecosystems*, **6**(4), pp. 301-312. Retrieved from http://www.jstor.org/stable/3659030

Moosavi, S. C., & Crill, P. M. (1997). Controls on CH_4 and CO_2 emissions along two moisture gradients in the canadian boreal zone. *J.Geophys.Res.*, **102**, 29261-29277. doi:10.1029/96JD03873

Nykänen, H., Alm, J., Silvola, J., Tolonen, K., & Martikainen, P. J. (1998). Methane fluxes on boreal peatlands of different fertility and the effect of long-term experimental lowering of the water table on flux rates. *Global Biogeochemical Cycles*, **12**(1), 53-69. doi:10.1029/97GB02732

Pihlatie, M., Pumpanen, J., Rinne, J., Ilvesniemi, H., Simojoki, A., Hari, P., et al. (2007). Gas concentration driven fluxes of nitrous oxide and carbon dioxide in boreal forest soil. *Tellus B*, **59**(3), 458-469. doi:10.1111/j.1600-0889.2007.00278.x

Pihlatie, M., Syväsalo, E., Simojoki, A., Esala, M., & Regina, K. (2004). In (Ed.), Contribution of nitrification and denitrification to N_2O production in peat, clay and loamy sand soils under different soil moisture conditions (Trans.). Springer Netherlands. doi:10.1023/B:FRES.0000048475.81211.3c

Riutta, T., Laine, J. & Tuittila, E.-S. 2007. Sensitivity of CO_2 exchange of fen ecosystem components to water level variation. *Ecosystems* **10**: 718-733.

Seibert, J., Stendahl, J., & Sørensen, R. (2007). Topographical influences on soil properties in boreal forests. *Geoderma*, **141**(1–2), 139-148. doi:10.1016/j.geoderma.2007.05.013

Silvola, J., Alm, J., Ahlholm, U., Nykanen, H., & Martikainen, P. (1996). The contribution of plant roots to CO_2 fluxes from organic soils. *Biology and Fertility of Soils*, **23**(2), 126-131. doi:10.1007/BF00336052

Solondz, D. S., Petrone, R. M., and Devito, K. J. (2008). Forest floor carbon dioxide fluxes within an upland-peatland complex in the Western Boreal Plain, Canada. *Ecohydrology*, **1**(4), 361-376. doi:10.1002/eco.30

Ťupek, B., Minkkinen, K., Kolari, P., Starr, M., Chan, T., Alm, J., Vesala, T., Laine, J. and Nikinmaa, E. (2008), Forest floor versus ecosystem CO_2 exchange along boreal ecotone between upland forest and lowland mire. *Tellus B*, **60**: 153–166.

Ullah, S., and Moore, T. R. (2011). Biogeochemical controls on methane, nitrous oxide, and carbon dioxide fluxes from deciduous forest soils in eastern canada. Journal of Geophysical Research-*Biogeosciences*, **116**, G03010. doi:10.1029/2010JG001525

Weishampel, P., Kolka, R., and King, J. Y. (2009). Carbon pools and productivity in a 1-km(2) heterogeneous forest and peatland mosaic in minnesota, USA. *Forest Ecology and Management*, **257**(2), 747-754. doi:10.1016/j.foreco.2008.10.008

PARTICLE FORMATION FROM GREAT BARRIER REEF CORALS

P. VAATTOVAARA[1], E. DESCHASEAUX[2], G. JONES[2,3], H. SWAN[2], B. MILJEVIC[4] AND Z. RISTOVSKI[4]

[1]University of Eastern Finland, Kuopio, Finland

[2] School of Environment, Science and Engineering, Southern Cross University, Lismore NSW, Australia

[3] Marine Ecology Research Centre, Southern Cross University, Lismore NSW, Australia

[4]Queensland University of Technology, Brisbane QLD, Australia

Keywords: CORALS, PACIFIC OCEAN, AEROSOLS, CLIMATE

INTRODUCTION

Marine biologically active regions are known to produce a range of compounds that interact with the atmosphere directly and indirectly affecting particle production, composition, and properties in marine atmosphere. While the CLAW hypothesis (Charlson et al., 1987) suggests the importance of secondary sulfate production, this hypothesis doe s not take into account the secondary organic fraction in the composition of the formed particles. To date, observations of the presence of a marine origin secondary organic fraction have been indicated down to nucleation mode size particles (d< 15 nm) in Atlantic waters (Vaattovaara et al., 2006), ice edge open ocean waters in the Arctic (Vaattovaara et al., ICNAA, 2009), in central Arctic Ocean during summertime (Paatero et al., 2009), and sub-tropical Pacific Ocean waters (Modini et al., 2009). In spite of the importance of secondary particles to atmospheric radiatively active particle sizes, the composition of those marine produced particles is still uncertain in other marine biologically active environments around the world. This study about the composition of nucleation (d<15nm) and the lower end of Aitken (20nm<d<60nm) mode particles was focused on particle production at one such marine region located on Great Barrier Reef (Australia) in sub-tropical Pacific Ocean.

METHODS

From May 26th to June 14th 2011 during austral winter, the CORACE-1 (COral Reef Aerosol Characterization Experiment-1) campaign measurements were conducted on Heron Island coral cay (23°26'35.80"S/151°54'44.23"E) very close to the Tropic of Capricorn and nearby the southern end of the Great Barrier Reef. The study was a co-operation research project between UEF (University of Eastern Finland, Kuopio, Finland), QUT (Queensland University of Technology, Brisbane, Australia), and SCU (Southern Cross University, Lismore, Australia). The purpose was to find out whether coral reefs could contribute to aerosol particle formation and hence potentially influence local climate (Swan et al. 2012) during bubble bursting and under O_3 and UV radiation. The experiments were carried out at the Heron Island Reef flat where Acropora pulchra, a widely spread coral in the Indo-Pacific and Great Barrier Reef (GBR) (Veron, 2012) is commonly living in a sympiotic relationship with algae.

The ultfafine particle composition was studied using the UFO-TDMA (ultrafine organic tandem differential mobility analyzer) and the VH-TDMA (volatility hygroscopicity tandem differential mobility analyzer) methods on the newly established atmospheric research platform on the Heron Island marine research station. Auxiliary data were collected from the marine station regular observations and the Heron Island weather station. The particle size distribution was measured with the SMPS (scanning mobility particles sizer).

In addition to atmospheric measurement, the instruments were also placed in-line with the reaction chamber and bubbling chamber. This was because bubble bursting from breaking waves in the ocean is a primary source of sea-air exchange and sea spray aerosol production in the atmosphere, constituting a possible source for CCN formation. Hydroxyl radicals in the chamber were formed as a consequence of photodissociation of ozone (O_3) by solar UV in order to mimic atmospheric conditions and to get reference data for atmospheric measurements. In this report, we concentrate on the chamber measurements. A more detail description of these chamber experiments including gas phase sulphur analysis is available in Deschaseaux et al. (2012; e.g. Figure 1).
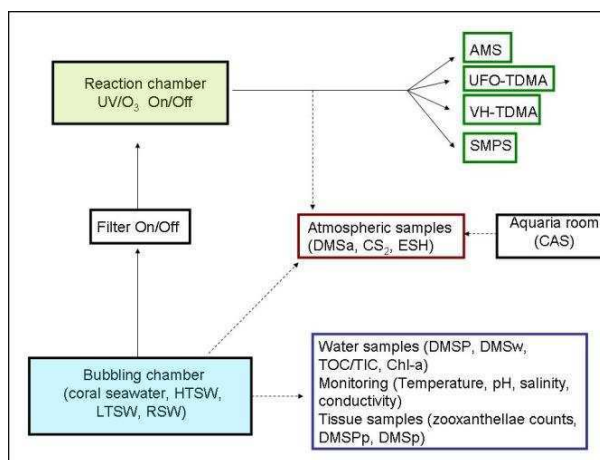

Figure 1. Experimental design of the bubbling chamber experiment conducted on coral seawater at Heron Island, May-June 2011.

RESULTS AND CONCLUSIONS

The SMPS data showed that new particle formation occurs when gaseous components released into the chamber headspace upon bubbling were exposed to UV and O_3. These newly formed particles were too small to be measured by the AMS (aerosol mass spectrometer) and therefore their chemical composition has not been determined in more detailed. The hygroscopicity and volatility profiles of these particles were lower and greater than for sulphates, respectively. The UFO-TDMA measurements when bubbling, particle filtration, UV and O_3 were applied, showed that the freshly formed secondary particles included at least 50% oxidised organic compounds. The formed ultrafine particles were quickly further oxidised (aged) when they grew bigger in size, due to the production of high level of oxidants into the air. In the coming analysis, these results will be compared to atmospheric coral reef measurements also done during the CORACE-1 campaign.

ACKNOWLEDGEMENTS

REFERENCES

Charlson RJ, Lovelock JE, Andreae MO, Warren SG (1987) Oceanic phytoplankton, atmospheric sulfur,

cloud albedo and climate. Nature 326:655-661.

Deschaseaux E., G. Jones, B. Miljevic, Z. Ristovski, H. Swan and P. Vaattovaara. Can corals form aerosol particles through volatile sulphur compound emissions? Proceedings of the 12th International Coral Reef Symposium, 2012 Cairns, Australia.

Modini RL, Ristovski ZD, Johnson GR, He C, Surawski N, Morawska L, Suni T, Kulmala M (2009) New particle formation and growth at a remote, sub-tropical coastal location. Atmos. Chem. Phys. 9:7607-7621.

Paatero J., Vaattovaara, P., Vestenius, M., Meinander, O., Makkonen, U. and co-authors. 2009. Finnish contribution the Arctic Summer Cloud Ocean Study (ASCOS) expedition, Arctic Ocean 2008. Geophysica, **45** (1-2), 119-146.

Swan HB, Jones GB, Deschaseaux ESM (2012). Dimethylsulfide and coral reef ecosystems. In: Proceedings of the 12th International Coral Reef Symposium, 2012 Cairns.

Vaattovaara P, Huttunen PE, Yoon YJ, Joutsensaari J, Lehtinen KEJ, O'Dowd CD, Laaksonen A (2006) The composition of nucleation and Aitken modes particles during coastal nucleation events: evidence for marine secondary organic contribution. Atmos. Chem. Phys. **6**, 4601-4616.

Veron J. (2000). Corals of the world. Australian Institute of Marine Science, Townsville.

VOC EMISSION MEASUREMENTS FROM LIVING SCOTS PINE TRUNK AND BRANCH

A. VANHATALO[1], J. AALTO[1], P. KOLARI[1,2], H. HAKOLA[3], T. HÖLTTÄ[1] and J. BÄCK[1,2]

[1]Department of Forest Sciences, University of Helsinki, Finland.

[2]Division of Atmospheric Sciences, Department of Physics, University of Helsinki, Finland.

[3]Finnish Meteorological Institute, Helsinki, Finland

Keywords: BVOC EMISSION, SCOTS PINE, LIVING TRUNK.

INTRODUCTION

Boreal forests are a significant source of biogenic volatile organic compound (VOC) emissions (Guenther *et al.*, 1995; Tarvainen *et al.*, 2007; Rinne *et al.*, 2009). Scots pine (*Pinus sylvestris* L.), Norway spruce (*Picea abies* (L.) Karsten), and birches (*Betula* spp.) are dominant tree species in Finnish boreal forests. Their BVOC emissions have been measured in campaign and/or continuous manner (Hakola *et al.*, 2001; Grabmer *et al.*, 2006; Hakola *et al.*, 2006; Bäck *et al.*, 2012). Most of these studies have been carried out with dynamic enclosures containing a shoot: leaves or needles, buds and a part of a wooden twig. Emissions are usually given per leaf mass or leaf area with an assumption that buds and wooden twig do not affect emission. Still, leaves and needles comprise only a small proportion of the total biomass of a boreal forest stand. Helmisaari *et al.* (2002) have calculated that 65,5 % of the biomass of a 15-year-old Scots pine stand was in stem wood, living and dead stem bark and living and dead branches. In 35- and 100-year-old stands the corresponding values were 70,1 % and 82,3 %, respectively. When a forest stand ages, the proportion of stem wood from the total biomass increases and that of the needles decreases (Helmisaari *et al.*, 2002). At SMEAR II stand total tree biomass was 13,7 kg ha^{-1} in year 2008, and needle biomass comprised only less than 1 kg ha^{-1} (Ilvesniemi *et al.*, 2009). Leaves and needles are physiologically active, but their biomass is low. Vice versa, woody tissue in trunk and branches has a lot of biomass, but its activity is low. At SMEAR II stand in 2002–2006 the respiration of tree foliage including twigs varied between 218–282 g C m^{-2} and the CO2 efflux from the stems and branches between 57–67 g C m^{-2} (Kolari *et al.*, 2009). Aboveground woody tissues were estimated to contribute less than 10 % to the total ecosystem respiration (Kolari *et al.*, 2009).

A big share of Scots pine VOC emissions originate from oleoresin storage pools in both needles and woody tissues, and the rest comes directly from *de novo* synthesis (Ghirardo *et al.*, 2010). Oleoresin is a liquid viscous mixture of volatile terpenes and non-volatile resin acids. It is a physical and chemical defense of coniferous trees against pathogenic fungi and wood-boring insects. The composition of oleoresin depends on e.g. tree species, age, provenance, health status, and environmental conditions (Manninen *et al.*, 2002; Turtola *et al.*, 2003). Oleoresin is under pressure in resin ducts in wood and needles. It flows out from a damaged site to protect the tree. Once in contact with air, volatile parts of oleoresin evaporate, and residual compounds, resin acids aka diterpenes, harden to make a solid protective seal over damaged tissues. The hardening time of resin depends on evaporation rate of the volatiles which in turn depends on temperature.

The knowledge on VOC emissions from living tree trunks is very scarce. Heijari *et al.* (2011) has studied how herbivory increased VOC emissions of 2-year-old Scots pine seedling stems, but otherwise studies on living stem VOC emissions are missing. Flux measurements from living Scots pine shoots and ambient air have been done before, but in spring 2012 we started VOC flux measurements from Scots pine trunk. The aim was to find out 1) how big is the flux from wooden parts of a tree i.e. trunk and thick branches, 2) are there seasonal variations, 3) how large is the flux from the trunk compared to flux from a shoot with needles and 4) are there qualitative differences between trunk, branch and shoot+needle emissions.

The sample tree, a 18,6-m-tall Scots pine (*Pinus sylvestris* L.), grows at the SMEAR II forest stand in Southern Finland. The 51 year old stand is dominated by Scots pine. A closer description of the site can be found for example at Vesala *et al.* (2005). Altogether four chambers were installed onto this pine in the spring 2012. The pine grows next to measurement tower so that the entire trunk is accessible from the scaffolding.

A stem cuvette consisted of a FEP foil tightened around a stem at both ends. Inside the chamber, there is an aluminium inlet/outlet port covered with FEP tape for mounting inlet and outlet pieces and a tube spiral preventing the foil touching the stem in the middle. A branch chamber is similar except that it is smaller and installed horizontally. Heights and diameters of the chambers vary so that the bark area inside the cuvette is 0,011–0,044 m^2. The chamber system is dynamic: supply air to the chambers is sucked from above the canopy and sample air is conducted via FEP tubing to H_2O and CO_2 analyzers and to a proton transfer reaction mass spectrometer (PTR-MS) in the measurement cabin.

On 26th March 2012 two chambers were installed (Figure 1, coding from the lowest chamber towards the top of the tree): chamber D around a branch at a height of about 14 m, 55 cm away from the trunk, and another (B) around the trunk at a height of about 12 m. The diameter of the branch was 1,8 cm and the diameter of the trunk at the cuvette 8,4 cm. Two more chambers were installed on 8th May. The upper one (C) is about 1,5 m below tree top at a diameter of 3,5 cm. The other (A) was installed to the lower part of the canopy at a height of about 7 m which is a couple of meters below the limit of living canopy. Sample air from these two latter chambers was not sampled online with PTR-MS due to limited measurement resources, but it was analyzed with H_2O and CO_2 analyzers.

2,5 months of VOC emission data was collected during the measurement campaign between late March and mid-June. As PTR-MS can not distinguish between compounds with same molecular mass, the online emission data was supplemented with adsorbent samples in order to obtain also compound-specific data on emissions. Tenax-adsorbent-samples were collected during one week in the beginning of May and one week in mid-July. The adsorbent collections from the chambers B and D were done in daytime for 20–40 min.
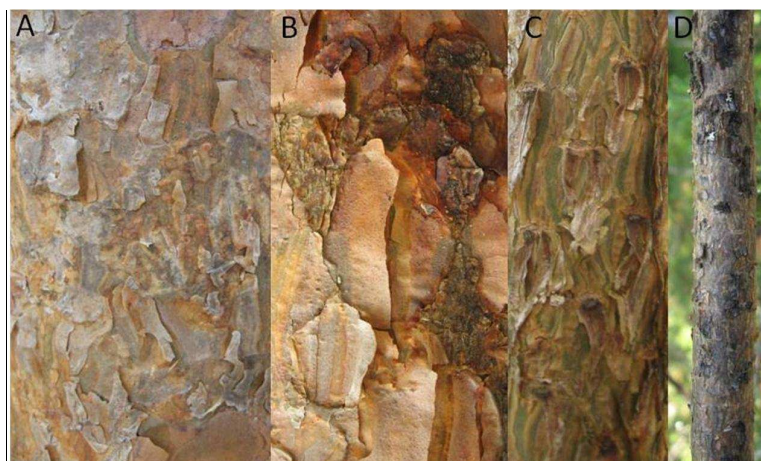

Figure 1. Different structure of pine bark. Tree height grows from left to right: chamber A at 7 m, B at 12 m, C at 17 m, and D branch bark at 14 m.

PRELIMINARY RESULTS AND CONCLUSIONS

Only preliminary results can be obtained at the moment as the growing season and measurement period is currently continuing. They show that significant VOC emissions from pine stem can be detected, and that they exhibit a diurnal cycle. Mass 137 (monoterpenes) have the strongest signal, but also e.g. masses 33 (methanol) and 59 (acetone) have been detected. M137and M33 fluxes from the trunk were large even very early in the spring, in the end of March. They seemed to follow the daily pattern of temperature in the chamber. Results from adsorbent samples also suggest that there would be a qualitative difference between monoterpene emissions from pine trunk and thick branches. For instance, more δ-3-carene was found in emissions from the branch than from the trunk and terpinolene was found from all the samples from the branch but it was absent in those from the trunk. Still, this issue deserves more investigation.

Most of the tree biomass is in the lower part of the trunk. As tissues there are biologically comparatively inactive and green photosynthesizing tissue is practically missing, VOC emissions from there are assumed to be low. Measuring VOC emissions from there is hard as the rugged bark on lower stem makes it difficult to get the chamber airtight without harming the bark. All cuts and other damages would result in resin flow and hence in increased VOC emissions. Measurement setup will be further improved based on the experience during this season.

REFERENCES

Bäck, J., J. Aalto, M. Henriksson, H. Hakola, Q. He and M. Boy (2012). Chemodiversity in terpene emissions at a boreal Scots pine stand. *Biogeosciences* **9**, 689–702.

Ghirardo, A., K. Koch, R. Taipale, I. Zimmer, J.-P. Schnitzler and J. Rinne (2010). Determination of *de novo* and pool emissions of terpenes from four common boreal/alpine trees by $^{13}CO_2$ labelling and PTR-MS analysis. *Plant, Cell and Environment* **33**, 781–792.

Grabmer, W., J. Kreuzwieser, A Wisthaler, C. Cojocariu, M. Graus, H. Rennenberg, D. Steigner, R. Steinbrecher and A. Hansel (2006). VOC emissions from Norway spruce (Picea abies L. [Karst]) twigs in the field – Results of a dynamic enclosure study. *Atmospheric Environment* **40**, S128–S137.

Guenther, A., C.N. Hewitt, D. Erickson, R. Fall, C. Geron, T. Graedel, P. Harley, L. Klinger, M. Lerdau, W.A. McKay, T. Pierce, B. Scholes, R. Steinbrecher, R. Tallamraju, J. Taylor and P. Zimmerman (1995). A global model of natural volatile organic compound emissions. *Journal of Geophysical Research* **100**, 8873–8892.

Hakola, H., T. Laurila, V. Lindfors, H. Hellen, A. Gaman and J. Rinne (2001). Variation of the VOC emission rates of birch species during the growing season. *Boreal Environment Research* **6**, 237–249.

Hakola, H., V. Tarvainen, J. Bäck, H. Ranta, B. Bonn, J. Rinne and M. Kulmala (2006). Seasonal varoation of mono- and sesquiterpene emission rates of Scots pine. *Biogeosciences* **3**, 93–101.

Heijari, J., J.D. Blande and J.K Holopainen (2011). Feeding of large pine weevil on Scots pine stem triggers localised bark and systemic shoot emission of volatile organic compounds. *Environmental and Experimental Botany* **71**, 390–398.

Helmisaari, H.-S., K. Makkonen, S. Kellomäki, E. Valtonen and E. Mälkönen (2002). Below- and above-ground biomass, production and nitrogen use in Scots pine stands in eastern Finland. *Forest Ecology and Management* **165**, 317–326.

Ilvesniemi, H., J. Levula, R. Ojansuu, P. Kolari, L. Kulmala, J. Pumpanen, S. Launiainen, T. Vesala and E. Nikinmaa (2009). Long-term measurements of the carbon balance of a boreal Scots pine dominated forest ecosystem. *Boreal Environment Research* **14**, 731–753.

Kolari, P., L. Kulmala, J. Pumpanen, S. Launiainen, H. Ilvesniemi, P. Hari and E. Nikinmaa (2009). CO_2 exchange and component CO_2 fluxes of a boreal Scots pine forest. *Boreal Environment Research* **14**, 761–783.

Manninen, A.-M., S. Tarhanen, M. Vuorinen and P. Kainulainen (2002). Comparing the variation of needle and wood terpenoids in Scots pine provenances. *Journal of Chemical Ecology* **28**, 212–228.

Rinne, J., J. Bäck and H. Hakola (2009). Biogenic volatile organic compound emissions from the Eurasian taiga: current knowledge and future directions. *Boreal Environment Research* **14**, 807–826.

Tarvainen, V., H. Hakola, J. Rinne, H. Hellén and S. Haapanala (2007). Towards a comprehensive emission inventory of terpenoids from boreal ecosystems. *Tellus* **59B**, 529–534.

Turtola, S., A.-M. Manninen, R. Rikala and P. Kainulainen (2003). Drought stress alters the concentration of wood terpenoids in Scots pine and Norway spruce seedlings. *Journal of Chemical Ecology* **29**, 1981–1995.

Vesala, T., T. Suni, Ü. Rannik, P. Keronen, P. Markkanen, S. Sevanto, T. Grönholm, S. Smolander, M. Kulmala, H. Ilvesniemi, R. Ojansuu, A. Uotila, J. Levula, A. Mäkelä, J. Pumpanen, P. Kolari, L. Kulmala, N. Altimir, F. Berninger, E. Nikinmaa and P. Hari (2005). Effect of thinning on surface fluxes in a boreal forest. *Global Biochemical Cycles* **19**, 1–11.

IN SITU AEROSOL MEASUREMENTS AT DOME C, ANTARCTICA IN 2007 - 2011

A.VIRKKULA[1,2], E. JÄRVINEN[2], T.NIEMINEN[2], R.VÄÄNÄNEN[2], H. MANNINEN[2], P.P. AALTO[2],
E. ASMI[1], J.BACKMAN[2], M. BUSETTO[3], C. LANCONELLI[3], R. SCHIOPPO[4], A. LUPI[3], V. VITALE[3],
R. HILLAMO[1] AND M.KULMALA[2]

[1]Finnish Meteorological Institute, Research and Development, FI-00560, Helsinki, Finland
[2]Department of Physics, University of Helsinki, FI-00014, Helsinki, Finland
[3]Institute of Atmospheric Sciences and Climate of the Italian National Research Council, Bologna, Italy
[4]ENEA Area Sperimentale di Monte Aquilone, Manfredonia (FG), Italy

INTRODUCTION

Aerosol number concentrations, size distributions and chemical composition have been studied at several stations around Antarctica. There exist long-term records of aerosol number concentrations, for instance from Neumayer and South Pole but aerosol number size distributions have been measured mainly during campaigns both at coastal stations and in the upper plateau at South Pole. The Norwegians recently started long-term size distribution measurements at the Troll station in Queen Maud Land (Hansen et al. 2009) but there are no long-term size distribution measurements from the upper plateau. Also light absorption measurements on the upper plateau are limited to campaigns. For instance at the South Pole Observatory there are no continuous absorption measurements.

In situ aerosol measurements have been conducted at the Dome C station (75°S, 123°E) on the upper plateau at about 3200 m amsl since December 2007. Part of these measurements have been continuous since then, part of them only for shorter periods. Particle size distributions have been measured ranging from the subnanometer to supermicron sizes and light absorption at three wavelengths. This work gives an overview of the data collected so far, Järvinen et al. (this issue) present a more detailed study on seasonal cycles of particle size distributions, modal structure, and new particle formation at Dome C.

METHODS

The size distributions in the size range 10 – 600 nm have been measured with a differential mobility particle sizer (DMPS) and with a Grimm Model 1.108 optical particle counter in the size range 0.3 – 15 μm. They were first stopped at the end of year 2009 due to technical problems but they were continued again in December 2010, and the goal is to continue these measurements. In December 2010 also a new instrument, an Air Ion Spectrometer (AIS), that measures charged particle size distributions in the size range of about 0.8 – 40 nm, was installed at the station. The AIS produced good data until May 2011.

Light absorption by particles has been measured at Dome C with a Radiance Research 3λ Particle Soot Absorption Photometer (PSAP). The PSAP reports absorption coefficients with a 0.1 Mm⁻¹ accuracy. This is not good enough since most of the time absorption coefficients are below that at Dome C. Therefore all absorption coefficients were calculated from the raw signal and reference counts of the PSAP by taking long enough integration time between subsequent measurements of signal and reference. This makes it possible to get essentially indefinitely low detection limits – at the cost of time resolution, however (Springston and Sedlacek, 2007). The PSAP data processing also needs scattering coefficients. These are not being measured at Dome C. However, the measured size distributions in the size range 0.01 – 15 μm have been used to calculate light scattering coefficients in the same wavelengths as the PSAP measures. To do this a Mie code has been used, assuming spherical particles and varying refractive indices from that of sulfuric acid to ammonium sulfate and sea salt.

RESULTS AND DISCUSSION

There was a clear seasonal cycle in the number concentration data. The concentrations were at their lowest around July and August and at highest around January, which is in agreement with the data from all other stations in Antarctica. New particle formation events did occur all year round, even in the darkest and coldest months June and July. These events were weak but not nonexistent, which is a new and interesting phenomenon, not reported earlier from the upper plateau of Antarctica. The AIS measurements show that often these particles do not grow to sizes larger than approximately 10 nm. An example of a period with almost daily formation of new particles that do not grow larger than 10 nm is given in Figure 1.
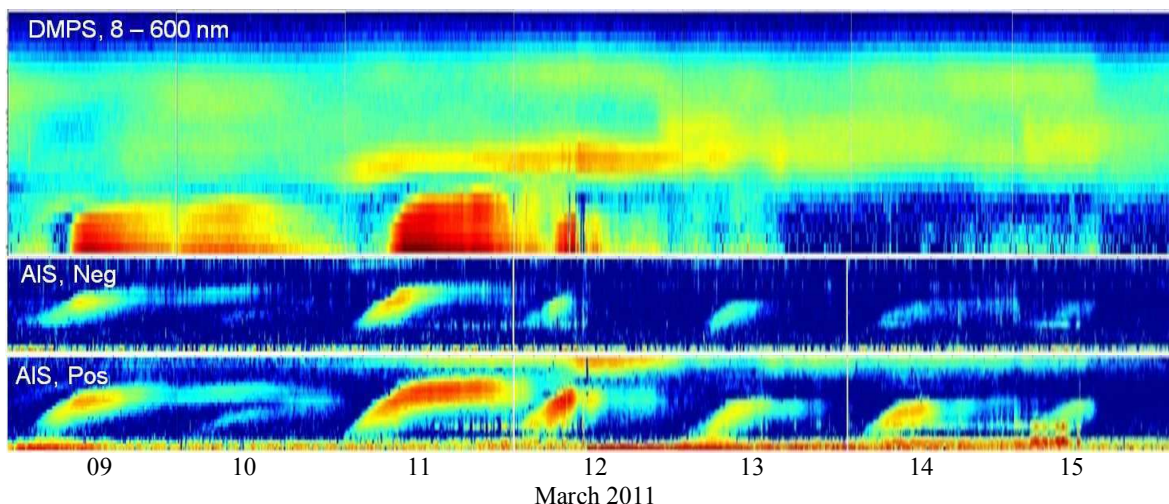

Figure 1. A one-week period of active particle formation in the Antarctic autumn 2011.

The median scattering and absorption coefficients in the period when the DMPS, the OPC and the PSAP were all operational are presented in Table 1. The scattering coefficients and thus also the absorption coefficients in Table 1 were calculated using the refractive index of sulphuric acid ($n_r = 1.426$). The aerosol seems to be weakly absorbing ($\omega_0 < 0.95$) and thus over bright snow surfaces potentially the radiative forcing is positive.

Table 1. Median scattering (σ_{sp}) and absorption (σ_{ap}) coefficients at the PSAP wavelengths in Dome C in December 2007 to November 2009.

	467 nm	530 nm	660 nm
$\sigma_{sp}(\text{Mm}^{-1})$	0.31	0.25	0.17
$\sigma_{ap}(\text{Mm}^{-1})$	0.019	0.017	0.015
ω_0	0.94	0.94	0.92

ACKNOWLEDGEMENTS

REFERENCES

Järvinen, E., A. Virkkula, T. Nieminen, P.P. Aalto, E. Asmi, C. Lanconelli, M. Busetto, A. Lupi, R. Schioppo, V. Vitale, T. Petäjä, V.-M. Kerminen, and M. Kulmala (2012) Event and growth rate analysis and modal structure at Dome C, Antarctica, *Abstracts of the annual CRAICC meeting*, Oslo, 2012.

IN SITU AEROSOL MEASUREMENTS AND SNOW SAMPLING DURING CHINARE 5 CRUISE THROUGH THE ARCTIC SEA

A. VIRKKULA[1,2], R. VÄÄNÄNEN[2], I. JÓNSDÓTTIR[3], J. HAKALA[2], T. PETÄJÄ[2], O. JÄRVINEN[2], J. SVENSSON[1], J. BACKMAN[2], P.P. AALTO[2], R. LEI[4], and M.KULMALA[2]

[1]Finnish Meteorological Institute, Research and Development, FI-00560 Helsinki, Finland
[2]Department of Physics, University of Helsinki, FI-00014 Helsinki, Finland
[3]Institute of Earth Sciences, University of Iceland, IS-101 Reykjavík, Iceland
[4]Polar Research Institute of China, Shanghai 200136, China

Keywords: Arctic aerosol, Number concentration, Optical properties, Snow reflectance.

INTRODUCTION

The Arctic sea-ice extent over the modern satellite record, from 1979 to present, shows a decreasing trend in all months and it largest at the end of summer, in September (e.g., Serreze et al. 2009; Flanner et al., 2012; Stroeve et al., 2012). The Arctic climate warming has been linked both to increased concentrations of atmospheric greenhouse gases and concentrations of light absorbing, i.e., black carbon (BC) aerosols (Shindell and Faluvegi 2009). BC, when deposited on snow, decreases the reflectivity and increases absorption of solar radiation and thus accelerates melting which further decreases reflectivity, leading to a positive feedback and positive radiative forcing (e.g., Doherty et al., 2010).

The fifth Chinese National Arctic Expedition (CHINARE 5) takes place in late summer and autumn of 2012 and it is still going on during writing the present abstract. The expedition is conducted onboard the Chinese polar research vessel Xue Long ("Snow Dragon" in English), the largest non-nuclear-powered icebreaker in the world. The cruise consists of two legs: the first approximately 15,000 km and six-week leg from China to Iceland through the Northeast passage and the second, somewhat shorther leg from Iceland straight through the North Pole back to China (Figure 1). The expedition's general goal is to study marine conditions in the Arctic and the rapid changes in marine environment and their impact on climate. Several stops are made to collect samples on meteorological, geological and chemical quantities.
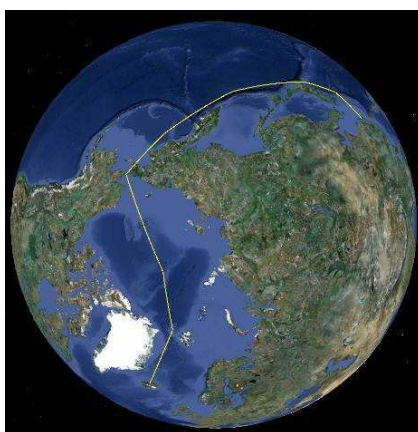

Figure 1. The tentative route of the second leg of the CHINARE 5 expedition.

For the second leg, aerosol measurements were added to the earlier setup. The aim of these is to study aerosol concentrations and the links between BC concentrations in air and snow and the reflectivity in the sea ice of the Arctic Sea. These measurements are conducted as a cooperation between the University of Helsinki, the University of Iceland, the Polar Research Institute of China, and the Finnish Meteorological Institute.

METHODS

The aerosol measurements consist of three instruments. Number concentrations are measured with a TSI Model 3010 condensation particle counter in the size range $D_p > 10$ nm. Light absorption by particles is measured with a Radiance Research 3λ Particle Soot Absorption Photometer (3λ PSAP) at λ = 467 nm, 530 nm, and 660 nm. Light scattering by particles is measured at λ = 545 nm with a Radiance Research Model M903 nephelometer. These instruments were installed in a rack on the bridge of the ship, the sample air is taken through a $PM_{2.5}$ cyclone inlet above the bridge (Figure 2).
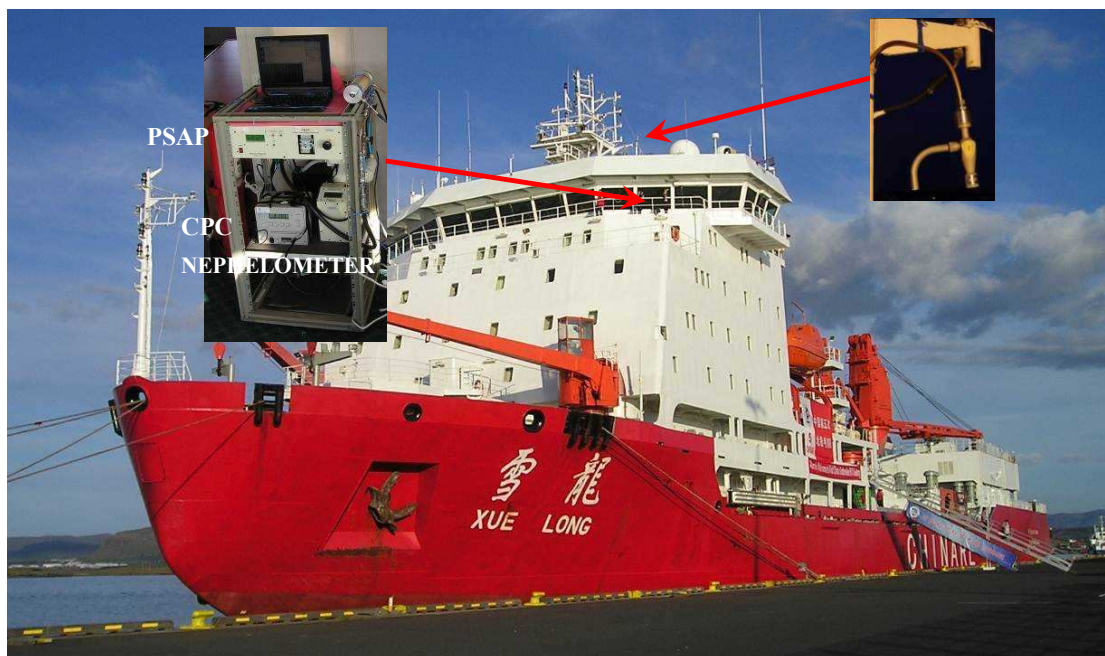

Figure 2. The research vessel Xue Long a Reykjavik harbour on 18 August 2012. The insert on the left shows the instrument rack, the insert on the right the inlet; the arrows show their locations on the bridge.

In other words, no size distributions are measured. Some indication of size distribution can be obtained, however. The bulk of light scattering is due to particles in the accumulation and coarse modes. So, the ratio of scattering coefficient to number concentration gives a rough indication of the size of the particles. The scattering and absorption coefficients will be used to calculate single-scattering albedo, the measure of the darkness of the particles.

In addition to the aerosol measurements, snow samples will be taken every time the ship stops by the sea-ice. These samples will be stored in a freezer, melted later, and drawn through quartz filters. These filter samples will be analyzed for organic and elemental carbon (OC and EC). EC is approximately the same concept as BC. On the sea-ice also albedo, i.e., the ratio of reflected to incoming radiation will be measured. This makes it possible to study the relationship between albedo and EC concentration.

RESULTS AND DISCUSSION

At the time of writing the present abstract, the ship has just left the harbour of Akureyri in Iceland, so no results are available.

REFERENCES

Doherty S.J., S.G. Warren, T.C. Grenfell, A.D. Clarke, and R.E. Brandt (2010) Light-absorbing impurities in Arctic snow, *Atmos. Chem. Phys.*, **10**, 11647–11680.

Flanner M.G., K.M. Shell, M. Barlage, D.K. Perovich and M.A. Tschudi (2011) Radiative forcing and albedo feedback from the Northern Hemisphere cryosphere between 1979 and 2008. *Nature Geoscience* **4**, 151–155, DOI:10.1038/ngeo1062.

Serreze MC, Barrett AP, Stroeve JC, Kindig DM, Holland MM (2009) The emergence of surfacebased Arctic amplification. *Cryosphere* **3**, 11–19.

Stroeve J.C., M.C. Serreze, M.M. Holland, J.E. Kay, J.M. Andrew, and P. Barrett (2012) The Arctic's rapidly shrinking sea ice cover: a research synthesis, *Climatic Change*, DOI 10.1007/s10584-011-0101-1.

ACIDIC REACTION PRODUCTS OF MONO- AND SESQUITERPENES IN ATMOSPHERIC FINE PARTICLES IN BOREAL FOREST IN FINLAND

VESTENIUS M.[1], HELLÈN H.[1], LEVULA J.[2], KURONEN P.[1] AND HAKOLA H.[1]

[1]Finnish Meteorological Institute, PL 503, 00101 Helsinki, Finland
[2]Hyytiälä Forestry Field Station, University of Helsinki, Hyytiäläntie 124, 35500 Korkeakoski, Finland

E-mail: mika.vestenius@fmi.fi

INTRODUCTION

A large amount of biogenic VOCs (monoterpenes and sesquiterpenes) is emitted to the atmosphere by vegetation, especially in the densely forested boreal regions (Hakola et al., 2006; Tarvainen 2005 and 2007; Hellén et al., 2006a; Wiedinmyer et al., 2004). In the atmosphere these compounds are oxidized producing reaction products, which may take part in the formation and growth of new particles (Tunved et al., 2006). Even though organic compounds account for 20-90 % of the total fine particle mass concentration in a wide variety of atmospheric environments (Kanakidou et al., 2005), only little is known about their detailed composition.

In smog chamber studies the secondary organic aerosol (SOA) yields for different hydrocarbons and even for different monoterpenes have been found to vary considerably (Lee et al., 2006, Griffin et al., 1999). For many sesquiterpenes atmospheric lifetimes are so short that their concentrations in the air cannot even be measured. Therefore knowledge about real atmospheric concentrations of the reaction products of terpenes is essential for different kind of aerosol studies.

There are some studies on concentrations of pinonic and pinic acids in real atmospheres (Zhang et al. 2010), but very little is known about ambient concentrations of other biogenic acids. There have been some short campaigns, where concentrations of some of these other acids have also been measured (Warnke et al. 2006). However, in those studies they did not have authentic standards for these compounds and they were identified only by their mass spectra and quantified by relative methods.

In this study acidic reaction products of biogenic VOCs, which affect the formation and growth of fine particles, were analyzed from aerosol samples taken at the SMEAR II station (Station For Measuring Forest Ecosystem-Atmosphere Relations) in Finland.

METHODS

The measurements were conducted at the SMEAR II station (Station For Measuring Forest Ecosystem-Atmosphere Relations) at Hyytiälä, in southern Finland. The nearest vegetation consists of a homogeneous Scots pine forest with some birches and Norway spruces growing nearby. In 2010 samples were collected few meters outside the forest in a small opening and in 2011 inside the forest.

The aerosol samples were collected using pumped sampling from the PM 2.5 fractions in air on to quartz filters. Before sampling filters were heated to ~500 °C for over 24 hours. Air flow through the filters was 16 L min^{-1}. Collection times were typically 1-7 days per filter. Gases were removed from the air flow using parallel plate carbon denuder (Sunset Laboratory Inc.). Efficiency of the denuder was checked by taking samples of more volatile organic compounds (aromatic hydrocarbons and monoterpenes) than measured in this study using pumped adsorbent sampling.

Samples were extracted with acetonitrile using ultrasonic extraction and evaporated to 100 μl. Camphoric acid was used as an internal standard and samples were analyzed using high performance liquid chromatography (Agilent 1100 Series) and electro spray ionisation ion trap mass spectrometer (*Agilent 1100*

Series LC/MSD Trap). LC column used in this study was Waters XTerra ® MS C_{18} (3.5 µm, 2.1 x 150 mm). The main components of the mobile phase were acetonitrile and MilliQ water. The pH of the mobile phase was adjusted to ~3 with acetic acid.

Of the measured bio acids only pinonic and pinic acids were commercially available. Other acids were synthesized at the Laboratory of Organic Chemistry at the Department of Chemistry of the University of Helsinki. Compounds to be synthesized were chosen based on their precursor emissions, concentrations and expected importance in formation of new particles. Relative yields of the reaction products in the aerosol were studied and those with highest yields were chosen to be synthesized.

RESULTS AND DISCUSSION

Highest concentrations for all studied compounds were measured in summer, except pinonic acid in 2010. (Table 1). Concentrations peaking in summer are most clear for caryophyllic acid. It is known to be emitted from typical boreal trees only in July and August (Hakola et al. 2006). Limonic acid concentrations increased already in spring. However, there were only four one week samples from spring. Pinonic acid is showing relatively high concentrations also in winter. Since pinonic acid is most volatile of the studied acids and it has been found with much higher concentrations in gas phase (Hellén et al. 2008, Zhang et al. 2010), cold winter temperatures may have more effect through gas-particle distribution or through positive artifacts if denuder did not work with 100% efficiency. In summer 2010 concentrations of pinonic and pinic acids were clearly lower than in 2011. In 2010, measurements were conducted at different site at the SMEAR II station than in 2011 and this can explain at least part of the difference.

Table 1. Average concentrations of bio acids during different seasons (summer 2010 - summer 2011).

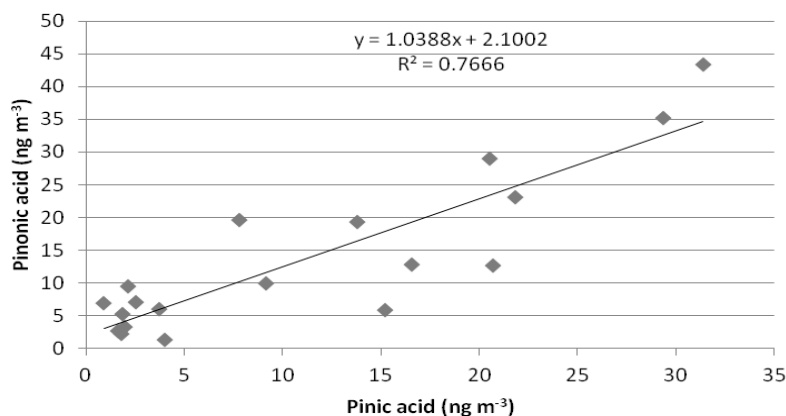| Bio acid	Precursor	Average concentrations (ng m^{-3})					
		sum-10	aut-10	win-10/11	spri-11	sum-11	aut-11
Pinonic acid	α-pinene	5.7	7.4	9.5	5.8	14.8	8.8
Pinic acid	α-pinene	2.6	4.4	1.5	0.8	10.1	2.0
Caric acid	3-carene	7.0	2.1	2.5	3.5	7.3	4.0
Limonic acid	limonene	1.0	0.9	0.5	1.8	1.7	1.2
β-caryophyllinic acid	b-caryophyllene	3.3	0.8	0.5	0.6	2.8	1.2

Figure 1. Comparison of pinic and pinonic acid concentrations during summer months (Jun-Aug 2010 and 2011). (Values below detection limits were excluded)
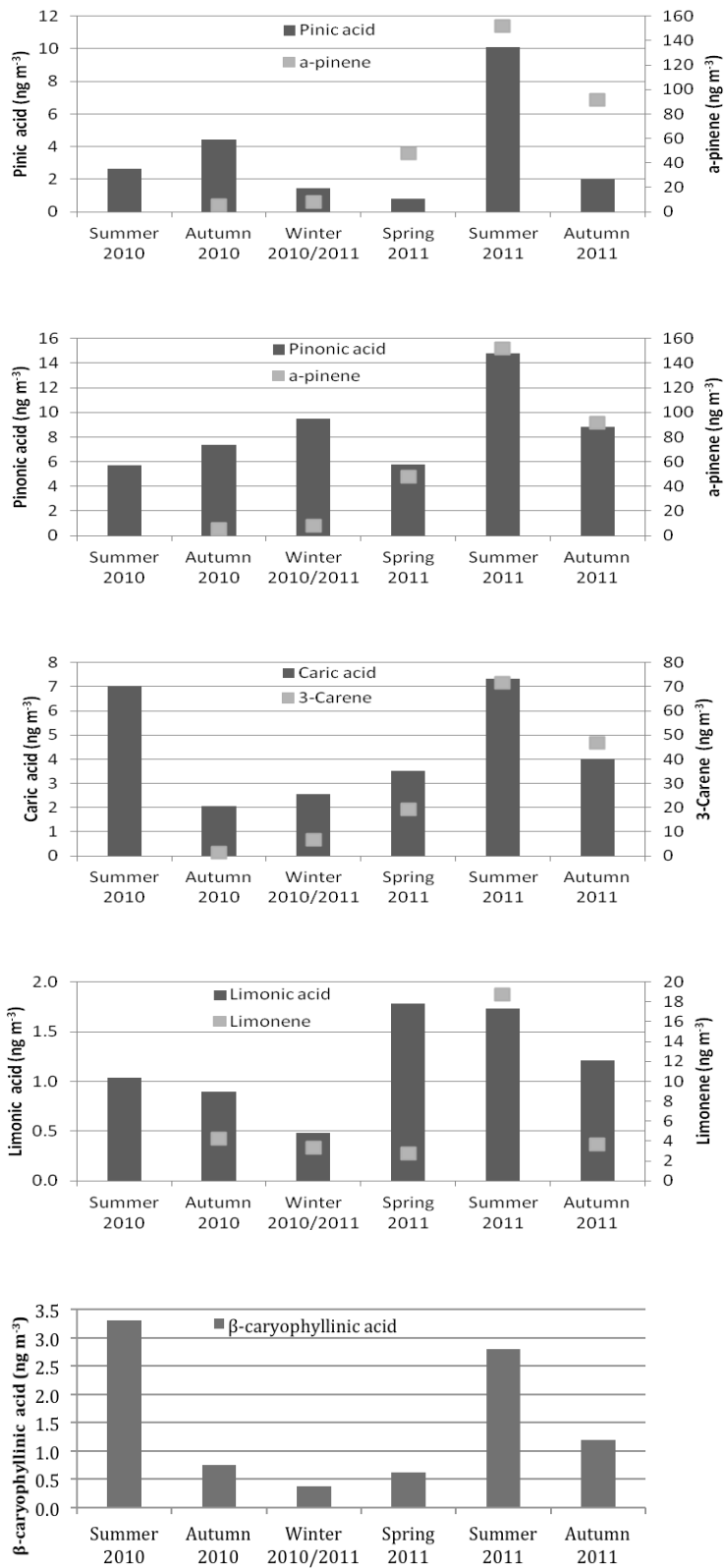
Figure 2. Seasonal variation of bio acids and their precursor monoterpenes

651

Concentrations of pinonic and pinic acids had relatively good correlation during summer months (Figure 1). This was expected since they have same precursors i.e. they are both reaction products of a- and b-pinene. Average concentrations for pinonic acid were 40% higher than for pinic acid.

Ambient monoterpene concentrations were measured at the same site from October 2010 until November 2011 close to the filter sampling site by in-situ thermo desopter-gas chromatograph-mass spectrometer. Detailed description of the monoterpene measurements can be found in Hakola et al. (2012). Pinic and caric acids show clearly the highest concentrations during summer months concomitant with their precursors (Figure 2). Also β-caryophyllinic acid has highest concentrations in summer, but since the precursor is very reactive, it cannot be found in ambient air. Limonic acid concentrations increase already in spring eventhough limonene concentrations are still low. Bioacids and their precursors show a similar trend, α-pinene and its reaction products (pinic acid+pinonic acid) having the highest concentrations and limonene and its reaction product (limonic acid) the lowest.

ACKNOWLEDGEMENTS

REFERENCES

Griffin R.J., Cocker III D.R., Flagan R.C., Seinfeld J.H., 1999. Organic aerosol formation from the oxidation of biogenic hydrocarbons. Journal of Geophysical Research, 104, 3555-3567.

Hakola H., Tarvainen V., Bäck J., Rinne J., Ranta H., Bonn B., and Kulmala M., 2006. Seasonal variation of mono- and sesquiterpene emission rates of Scots pine. Biogeosciences, SRef-ID: 1726-4189/bg/2006-3-93, 93-101.

Hakola H., Hellén H., Rinne J., Henriksson M., and Kulmala M., 2012. In situ chromatographic measurements of volatile organic compounds in a Boreal Forest. Atmospheric Chemistry and Physics Discussion, 12, 15565-15596.

Hellén H., Hakola H., Pystynen K.-H., Haapanala S., Rinne J., 2006. C_2-C_{10} hydrocarbon emissions from boreal wetland and forest floor. Biogeosciences, SRef-ID: 1726-4189/bg/2006-3-167, 167-174.

Hellén H., Dommen J., Metzger A., Gascho A., Duplissy J., Tritscer T., Prevot A.S.H. and Baltensperger U., 2008. Using Proton Transfer Reaction Mass Spectrometry for Online Analysis of Secondary Organic Aerosols. Environmental Science and Technology, 42, 7247-7353.

Kanakidou M., Seinfeld J.H., Pandis S. N., Barnes I., Dentener F. J., Facchini M.C., Van Dingenen R., Ervens B., Nenes A., Nielsen C. J., Swietlicki E., Putaud J.P., Balkanski Y., Fuzzi S., Horth J., Mootgat G.K., Winterhalter R., Myhre C. E. L., Tsigaridis K., Vignati E., Stephanou E. G., Wilson J, Organic aerosol and global climate modelling: a review. Atmos. Chem. Phys. 2005, 5, 1053-1123

Lee A., Goldstein A.H. Kroll J.H., Ng N.L., Varutbangkul V., Flagan R. C. and Seinfeld J.H., 2006. Gas-phase products and secondary aerosol yields from the photooxidation of 16 different terpenes. Journal of Geophysical Research, 11, D17305.

Tarvainen V. Hakola H., Rinne J., Hellén H. and Haapanala S., 2007. Towards a comprehensive emission inventory of the Boreal forest. Tellus, 59 B, 526-534

Tunved P., Hansson H.-C., Kerminen V.-M., Ström J., Dal Maso M., Lihavainen H., Viisanen Y., Aalto P.P., Komppula M., and Kulmala M., 2006. High natural aerosol loading over boreal forests. Science 312, 261-263.

Wiedinmyer, C., Guenther, A., Harley, P., Hewitt, N., Geron, C., Artaxo, P., Steinbrecher, R., and Rasmussen, R., 2004. Global organic emissions from vegetation. In: Emissions of atmospheric trace compounds, Granier, C. et al. (eds), Kluwer Academic Publishers, Dordrecht, 115-170.

AN EIGENVECTOR-BASED APPROACH FOR AUTOMATIC CLASSIFICATION OF NEW PARTICLE FORMATION EVENTS

H. VUOLLEKOSKI, H. JUNNINEN, M. DAL MASO, V.-M. KERMINEN and M. KULMALA

Division of Atmospheric Sciences, Department of Physics, University of Helsinki, 00014 Helsinki, Finland

Keywords: new particle formation, classification, eigenvectors.

INTRODUCTION

Atmospheric new particle formation is a frequent, globally observed phenomenon that depends on various factors. The study of these factors is facilitated by classification of new particle formation events according to certain criteria. Often this procedure is based on visual inspection of daily measurements of particle size distribution, which requires manual labor from several researchers (e.g. Buenrostro Mazon *et al.*, 2009). Efforts have been made to automatize the classification process by e.g. searching for specific features of new particle formation, such as the existence of a "continuous band" of particles all the way from detection limit to the accumulation mode. Here, we apply an information theoretical concept previously used in computer vision, and aim to develop an algorithm that could be used to

1) automatically repeat the classification process from a different perspective,
2) classify and predict new particle formation in real-time,
3) reconsider the classification schemes and
4) benefit other data analysis, such as interpolation of missing data.

The "eigenfaces" method (Turk and Pentland, 1991) is computationally fast and, with some limitations, reliable for human face recognition. Although our algorithm is still in early development, we expect the "eigenevents" to prove useful in atmospheric sciences as well.

THEORY

Particle size distributions from different days and different sites share common characteristics. One way to describe a particular measurement is to tell how it differs from the others. A set of measurements with similar characteristics can be decomposed into its principal components, namely the eigenvectors of the set's covariance matrix in a very high-dimensional space. Depending on the degree of similarity among the measurement data, only some of these eigenvectors will have a (relatively) significant eigenvalue, and therefore any practical significance. This smaller set of eigenvectors forms a basis set, whose linear combinations can then be used to approximately reconstruct the original measurements, and, assuming the learning set was representative enough, any given measurement. The measurement is then classified by e.g. minimizing its Euclidean distance from a vector of weights defining a class.

METHOD

Particle size distribution data from e.g. a differential mobility particle sizer (DMPS) is often represented as a surface plot: particle diameter vs. time, with color indicating the particle concentration. These are straightforward to plot directly from the DMPS data files. If one removes the size, time and total concentration vectors from the data matrix, one is left with a concentration matrix, which can be interpreted as an image with resolution of the number of particle size bins times the number of measurements of the whole size range. The particle concentration is the color of the "pixel". By using this analogy, it is straightforward to use the "eigenface" approach described by Turk and Pentland (1991):

1) define a learning set of DMPS measurements
2) reshape the daily measurement matrices to vectors
3) form a matrix comprising of the vectors of the learning set
4) calculate the eigenvectors of the covariance matrix
5) discard the eigenvectors with insignificant eigenvalues
6) define the event classes in terms of eigenvectors
7) classify data by minimizing the distance of their weight vector from the class vectors

DISCUSSION

The algorithm is still in early development, and its performance is uncertain. However, the eigenface method is known to recognize human faces reliably (with limitations unimportant for our consideration). It is also very fast: calculating the eigenevents for a whole year of measurement data takes only 5 seconds with the current algorithm. The main challenge will likely be in defining the weight vectors for different new particle formation event classes. On the other hand, the principal component analysis is not the optimal solution for class analysis, and a future version of our algorithm may have to be upgraded to accommodate linear discriminant analysis. Some noise filtering may also be necessary.

ACKNOWLEDGEMENTS

REFERENCES

Buenrostro Mazon, S., I. Riipinen, D. M. Schultz, M. Valtanen, M. Dal Maso, L. Sogacheva, H. Junninen, T. Nieminen, V.-M. Kerminen and M. Kulmala (2009). Classifying previously undefined days from eleven years of aerosol-particle-size distribution data from the SMEAR II station, Hyytiälä, Finland, *Atmos. Chem. Phys.* **9**, 667-676.
Turk, M. and A. Pentland (1991). Eigenfaces for Recognition, *J. Cognitive Neurosci. 3, 1.*

ANALYSIS OF AEROSOL DYNAMICS BETWEEN THREE SITES IN NORTHERN SCANDINAVIA

R. VÄÄNÄNEN[1], T. NIEMINEN[1], M. DAL MASO[1], A. VIRKKULA[1,2], B. SVENNINGSSON[3,4], N. KIVEKÄS[2], T. HOLST[4], A. ARNETH[5], V-M. KERMINEN[1], M. KULMALA[1]

[1]Department of Physics, University of Helsinki, P.O. Box 64, FIN-00014 University of Helsinki, Finland
[2]Finnish Meteorological Institute, P.O. Box 503, FIN-00101 Helsinki, Finland
[3]Department of Physics, Lund University, Box 118, SE-221 00 Lund, Sweden
[4]Division of Physical Geography and Ecosystems Analysis, Sölvegatan 12, 223 62 Lund, Sweden
[5]Karlsruhe Institute of Technology, Institute of Meteorology and Climate Research/Atmospheric Environmental Research, Kreuzeckbahn Str. 19, 82467 Garmisch-Partenkirchen, Germany

INTRODUCTION

Atmospheric aerosols play an important role in the climate systems via several mechanisms (IPCC, 2007). They affect the radiation budget indirectly by acting cloud condensation nuclei and directly by absorbing and scattering solar and infrared radiation. The overall result of these processes is estimated to be cooling. In high-latitudes, the deposition of black carbon particles onto snow has also contributing the positive snow-albedo feedback mechanism (Flanner et al., 2009). The cooling potential of secondary particles produced by boreal forests is connected tightly with aerosol dynamical processes taking place during atmospheric transportation, especially the particle growth, since secondary particles need to reach diameters larger than about 50-100 nm in order to participate in cloud droplet activation (Kerminen et al., 2005).

METHODS

We analyzed how particle size distribution evolves when airmasses travel hundreds of kilometres, and also examined the new particle formation in three measurement sites at Northern Scandinavia.

Two of the measurement sites, Värriö SMEAR I station and Pallas GAW stations are situated in Finland and the last one, Abisko in Sweden near the border of Norway. The sites are located roughly along a straight line from west to east on latitudes 67-68 °N. The distance from Abisko to Värriö is 440 km. The Abisko area is dominated by subarctic mires surrounded by birch woodland and mountain tundra, whereas Pallas and Värriö are surrounded by boreal forest. The Pallas station itself is situated above the tree line.

Our aerosol size distribution data were collected between Aug-2005 - Dec-2007. The data was measured using Differential Mobility Particle Sizers (DMPS) with a cutoff sizes of 3 and 7 nm in Värriö and Pallas, respectively, and using a Scanning Mobility Particle Sizer (SMPS) with a cutoff size of 10 nm in Abisko. The measurements at Pallas and Värriö are continuous, whereas the Abisko data were collected during campaigns of several months.

We analyzed and compared NPF events from each site according to the schema created by Dal Maso et al. (2005). The days were classified as events, non-events and undefined days. For event days we fitted the particle number-size distribution data to sum up to three lognormal distributions, and calculated the growth and formation rates of the nucleating particles.

 Tunved et al. (2006) had shown that boreal forests are a source of secondary organic aerosols via emission of biogenic volatile organic compound precursors. Here we repeated and broadened their analysis to cover also Abisko, and compared the growth of particles as a function of time the corresponding airmass had spend over land for all three measurement station. The HYSPLIT trajectory model (Draxler and Hess, 1998) was used to calculate the passing-times over-lands.

Particle size distribution data from several measurement stations combined with the calculated airmass trajectory information allowed us to study regionally the dynamical changes of aerosol particle populations. For this, we concentrated on the airmasses that passed more than one of the stations and compared the aerosol properties between different stations. The data describing the aerosol dynamics in atmosphere are multidimensional, containing the initial and final states, as well as the conditions between them. The data mining and data reduction is necessary.

When studying the aerosol dynamics, the initial states need to be comparable. For this, we clustered the particle size distributions measured at the upwind station to obtain a set of different initial states.

RESULTS

In Fig. 1a is shown the growth of the particle diameter when the airmasses arrive from sea to over land. As a comparison, during the NPF events the observed growing rate is about 3-4 times larger than these rates. The difference can be explained by noting that during NPF events the rates were only from a subset days with the most prominent growth, which was very likely to bias the results. Figure 1b) shows how the trajectories diverse for new particle formation event days, non-event days and undefined days. The results from Värriö and Pallas support the assumption that nucleation happened more probably when the air had shortly come from the ocean, and had thus small particle concentration and low condensation sink.
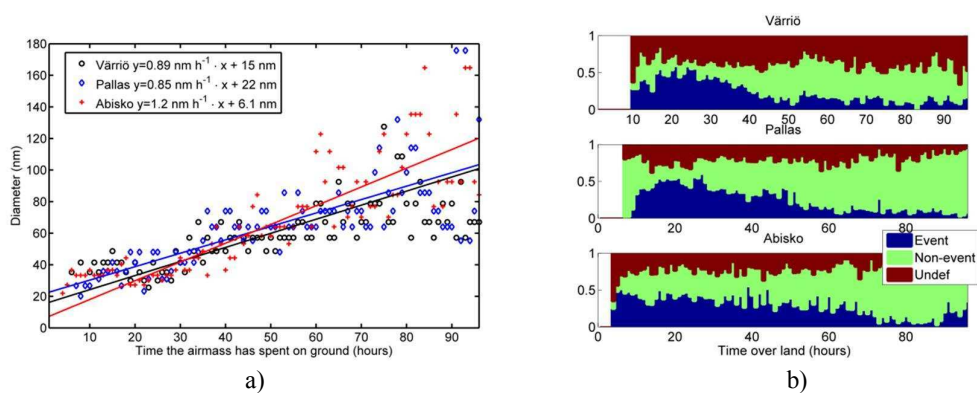

a)   b)

Figure 1: a) Particle diameters as a function of time the corresponding airmass has spent on-land. The growth coefficients calculated from time values of <80 h. b) Fractions of trajectories entering to each site on NPF event day, non-event day, and undefined day.

Three measurement sites located along a straight line enabled us to use a pseudo-Lagrangian approach to examine the dynamics of the aerosol during transport. Among other features, we studied shifts in the modes of the particle size distributions, when the airmasses are drifting between a measurement site pair.

We found that during the summer time, for both west-to-east pairs, i.e. for Abisko-to-Pallas and Pallas-to-Värriö, the most dominant cluster had an initial state with bi-modal structure. When the airmass drifted to the next station, the mode with smaller peak diameter grew in both peak diameter and concentration. The mode with the larger peak diameter remained relatively unaltered. For Abisko-to-Pallas route, during the transport, the first mode grew at size from 29 nm to 37 nm, and in concentration from 240 cm^{-3} to 415 cm^{-3}. With an average transport time of 15 hours, this corresponds to an apparent rates of 0.5 nm/h and 0.003 cm^{-3}/s. For Pallas-to-Värriö route, the corresponding apparent rates were 0.87 nm/h and 0.014 cm^{-3}/s.

These apparent rates were again mainly smaller than the typical Euclidian growth and formation rates measured during the new particle formation days in the Northern Scandinavia, and also the apparent growth rate was smaller than the one obtained from the analysis made with the method introduced in Tunved et al. (2006).

During the summertime, the opposite routes, i.e. Pallas-to-Abisko and Värriö-to-Pallas had a mutually similar, but different pattern when compared to the west-to-east routes. For the east-to-west transport it was common that the predominant cluster in the upwind station had a tri-modal structure with relatively low concentrations. When studying Värriö-to-Pallas route, this modal structure remained nearly unchanged, whereas for Pallas-to-Abisko route the total concentration grew, but the peak diameters of the modes remained the same. Since the peak diameters of the modes had not shifted, the dynamical aerosol processes during the transport were in quasi-equilibrium. We do not have yet clear explanation for this.

CONCLUSION

We studied aerosol dynamical processes related to secondary particle formation over boreal forests in Northern Scandinavia. We used three different approaches, each of them provided mutually supportive information of the processes. The analysis of the new particle formation events gives only a restricted view to the strength of the grow and formation, since it concentrates only to the most evident days. When analysing weaker effects, statistical and data mining tools are needed. An analysis according to method introduced in Tunved et al. (2006) reveals the averages of all days, whereas statistical special cases can be found for example by clustering the initial states and studying the average changes of each cluster.

ACKNOWLEDGEMENTS

REFERENCES

Dal Maso, M., Kulmala, M., Riipinen, I., Wagner, R., Hussein, T., Aalto, P. P., and Lehtinen, K. E. J. (2005), Formation and growth of fresh atmospheric aerosols: eight years of aerosol size distribution data from SMEAR II, Hyytiälä, Finland. *Boreal Environ. Res.*, **10**, 323–336.

Draxler, R.R. and G.D. Hess (1998), An overview of the HYSPLIT_4 modelling system for trajectories, dispersion and deposition, *Aust. Meteor. Mag.* **47**, 295-308.

Flanner M. G., Zender C. S., Hess P. G., Mahowald N. M., Painter T. H., Ramanathan V., and Rasch P. J. (2009), Springtime warming and reduced snow cover from carbonaceous particles, *Atmos. Chem. Phys.*, **9**, 2481–2497.

IPCC report, International Panel on Climate Change, Assessment report (2007). Cambridge University Press.

Kerminen, V.-M., H. Lihavainen, M. Komppula, Y. Viisanen, and M. Kulmala (2005), Direct observational evidence linking atmospheric aerosol formation and cloud droplet activation, *Geophys. Res. Lett.*, **32**, L14803.

Tunved, P., Hansson, H.-C., Kerminen, V.-M., Ström, J., Dal Maso, M., Lihavainen, H., Viisanen, Y., Aalto, P.P., Komppula, M, Kulmala, M. (2006), High natural aerosol loading over boreal forests, *Science*, **312**, 261-263.

MODEL FOR ACID-BASE CHEMISTRY IN NANOPARTICLE GROWTH

T. YLI-JUUTI[1], K. BARSANTI[2], L. HILDEBRANT RUIZ[3], A.-J. KIELOAHO[1], U. MAKKONEN[4], T. PETÄJÄ[1], M. ÄIJÄLÄ[1], M. KULMALA[1] and I. RIIPINEN[5]

[1]Department of Physics, University of Helsinki, Helsinki, PL64, Finland.

[2]Department of Civil & Environmental Engineering, Portland State University, Portland, OR, USA.

[3]Atmospheric Chemistry Division, National Center for Atmospheric Research, Boulder, CO, USA.

[4]Finnish Meteorological Institute, Helsinki, Finland

[5]Department of Applied Environmental Science and Bert Bolin Center for Climate Research, Stockholm University, Stockholm, Sweden

Keywords: PARTICLE GROWTH, ATMOSPHERIC AEROSOL, ORGANIC AEROSOL, AEROSOL CHEMISTRY.

INTRODUCTION

Atmospheric aerosol particles affect the Earth's climate both directly by scattering the solar radiation and indirectly by serving as cloud condensation nuclei. These effects have on average cooling effect for the climate but the level of scientific understanding of related processes is still relatively low. Significant fraction of atmospheric aerosol particles is formed in the air from vapors through gas-to-particle phase transition. These nanoparticles need to grow tens of nanometers in order to affect the climate effectively.

Sulfuric acid is found to be the key compound in atmospheric nucleation, the first step of formation of new particles. For the particle growth the role of sulfuric acid seems to be smaller. Instead, at many environments organic compounds are found to make most of the nanoparticle growth. However, the exact identification of these compounds is not established yet.

Gas phase processes affect the amount of vapors available for condensation but also particle phase processes can affect the growth rate of particles (Riipinen *et al*., 2012). Particle phase processes, like salt formation and polymerization, change the composition of particle and as a result affect the equilibrium vapor pressure of condensing vapor. It is found that vapors condensing on the atmospheric nanoparticles need to be very low-volatile with saturation vapor pressure 10^{-7} Pa or less in case the condensing compound does not take part in particle phase processes (Pierce *et al*., 2011). However, in recent experimental studies small organic acids and organic bases, both with saturation vapor pressures larger than this, have been found from atmospheric particle phase (Smith *et al*., 2010). Explanation of the existence of these compounds in nanoparticles has been suggested to be salt formation.

Here we are studying the effect of formation of organic and inorganic salts of the nanoparticle growth using thermodynamical condensation model. For this we have developed Model for Acid-Base chemistry in NAnoparticle Growth (MABNAG).

METHODS

Model for Acid-Base chemistry in NAnoparticle Growth (MABNAG) is a condensation model which includes particle phase acid-base chemistry in addition for gas phase transport. MABNAG is a single particle condensation model which calculates the time evolution of particle size and composition

based on gas phase concentrations of condensing vapors and initial particle composition. The particles are assumed to be liquid.

In this study we apply MABNAG for a system that has six vapors in the gas phase: two acids, two bases, one neutral organic compound and water. The acids are sulfuric acid and an organic di-acid, here chosen to be malonic acid. The base compounds are ammonia and an amine, here dimethylamine (DMA). The neutral organic compound used in addition for the five individually included vapors represents the sum of all the rest of the condensing compounds.

The condensation of the acids and the neutral organic compound on the particle are calculated based on the mass fluxes of these compounds

$$I_i = \frac{2\pi d_p p D_i M_i}{RT} \ln\left(\frac{1 - \dfrac{p_{eq,i}}{p}}{1 - \dfrac{p_{\infty,i}}{p}} \right) \tag{1}$$

where d_p is particle diameter, p is total pressure, D_i is diffusion coefficient of vapor molecule i in air, M_i is molar mass, R is gas constant, T is temperature, $p_{eq,i}$ is equilibrium vapor pressure above the particle and $p_{\infty,i}$ is the ambient vapor pressure. The subscript i refers to the vapors.

The bases and water are assumed to be constantly in equilibrium between gas and particle phase. Therefore, the amount of bases and water in particle are calculated based on

$$p_{eq,i} = p_{\infty,i} = c_i k_B T \tag{2}$$

where c_i is the ambient molecular concentration of vapor i.

The equilibrium vapor pressure of compound i depends on the particle size and composition

$$p_{eq,i} = X_i \cdot \gamma_i \left(X_j, T \right) \cdot \exp\left(\frac{4 M_i \sigma}{\rho d_p RT} \right) \cdot p_{sat,i}(T) \tag{3}$$

Here X_i is the molar fraction of i, σ is surface tension and $p_{sat,i}$ is saturation vapor pressure of i. Activity coefficient of i (γ_i) depends on the molar fractions of all the compounds in the particle.

Once the molecules have condensed on the particle they are exposed to acid-base chemistry which will affect the molar fractions of the compounds in the particle phase. To account for particle phase acid-base chemistry the condensation model was coupled with thermodynamic phase equilibrium model E-AIM (Extended aerosol inorganic model, Clegg $et\ al.$ 1992; Wexler and Clegg 2002; Clegg and Seinfeld, 2006a; 2006b; Ge $et\ al.$, 2011). E-AIM considers dissociation for acids and protonation for bases. Di-acids (H_2A) can dissociate twice producing single and double charged ions

$$H_2A \rightarrow HA^- + H^+$$

$$HA^- \rightarrow A^{2-} + H^+ .$$
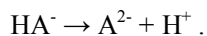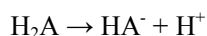
The bases (B) protonate and produce single charged ions

$$B + H^+ \rightarrow BH^+.$$
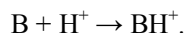
Also the dissociation of water is taken in to account in the model

$$H_2O \rightarrow OH^- + H^+.$$
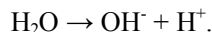
Sulfuric acid is strong acid and therefore all of it is assumed to get dissociated in E-AIM. Thus, the model includes in particle phase 13 different chemical species.

E-AIM was also used for calculating activity coefficients of all the condensing compounds.

RESULTS

We have applied MABNAG for a case study day 23.7.2010 when clear new particle event was observed at Hyytiälä, Southern Finland. This day was selected for case study as there were extensive gas phase data available: sulfuric acid, malonic acid, ammonia and amine concentrations were all measured. Total condensable organic vapor concentration is unknown and therefore the concentration of neutral organic vapor was estimated based on the observed particle growth rate. Thus, neutral organic compound represents all unknown compounds that contribute to the growth.

The model calculates condensation from particle size of approximately 3 nm in diameter. The initial composition of particles at this size is not known and we assumed that in the beginning of the model run particle contained 20 molecules of sulfuric acid, malonic acid and neutral organic compound accompanied with the amount of bases and water that corresponds to equilibrium.

In the base case model run the organic acid was malonic acid and amine was DMA. Base case values for vapor concentration were taken from the measurements except for DMA for which vapor concentration was somewhat overestimated. The base case values for vapor concentrations are given in Table 1.

Vapor	Concentration
Sulfuric acid	$3*10^6$ cm^{-3}
Malonic acid	$2*10^6$ cm^{-3}
Ammonia	$2*10^{10}$ cm^{-3}
Dimethylamine	$1*10^8$ cm^{-3}
Water	Equivalent conc. for RH = 60%

Table 1.Ambient conditions used as input for model in base case.

Figure 1 shows the MABNAG prediction for particle diameter and composition as a function of time in the base case. In the base case the model predicts that most of the growth is due to the neutral organic and there is very little growth due to the organic acids and bases. However, most of the malonic acid that condensed on particle was predicted to exist in the particle phase as its second dissociation product and almost all the DMA condensing on the particle got protonated. Therefore, for the condensation of malonic acid and DMA acid-base chemistry plays an important role according to the model.

When vapor concentration of both acids and bases were increased by an order of magnitude from base case values keeping concentrations of the neutral organic compound and water same as in vase case the GR increased by 20% for the particles in diameter range 7-20 nm. Also with these increased acid and base ambient vapor concentrations most of the growth was caused by the neutral organic compound. However in this case sulfuric acid caused almost similar fraction of particle growth as water. Also the condensation of malonic acid was enhanced as its mass fraction increased to 1 %.

Although our first results from MABNAG seem to predict little organic salt formation with the given ambient vapor concentrations they also suggest that in suitable ambient conditions or favorable properties of organic acid and bases salt formation may play an important role on the growth of particles. Next, more extensive study by varying ambient conditions and properties of condensing vapors will be done to map the conditions when organic salt formation is significant.
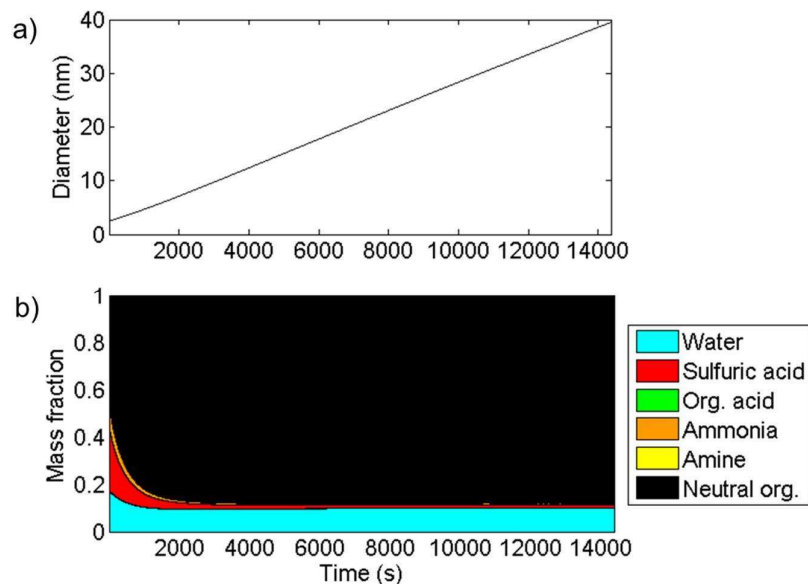

Figure 1. a) Particle diameter and b) mass fractions of compound as a function of time predicted with MABNAG. Mass fraction of each compound mentioned in the legend consists here of the mass fraction of the named compound as well as its dissociation/protonation product(s).

REFERENCES

Clegg, S. L., K. S. Pitzer, and P. Brimblecombe (1992). Thermodynamics of multicomponent, miscible, ionic solutions. II. Mixtures including unsymmetrical electrolytes. *J. Phys. Chem.* **96**, 9470.

Clegg, S. L. and J. H. Seinfeld (2006a). Thermodynamic models of aqueous solutions containing inorganic electrolytes and dicarboxylic acids at 298.15 K. I. The acids as non-dissociating components. *J. Phys. Chem. A* **110**, 5692.

Clegg, S. L. and J. H. Seinfeld (2006b). Thermodynamic models of aqueous solutions containing inorganic electrolytes and dicarboxylic acids at 298.15 K. II. Systems including dissociation equilibria. *J. Phys. Chem. A* **110**, 5718.

Ge, X, A. S. Wexler, and S. L. Clegg (2011). Atmospheric amines - Part II. Thermodynamic properties and gas/particle partitioning. *Atmos. Environ.* **45**, 561.

Pierce, J. R., I. Riipinen, M. Kulmala, M. Ehn, T. Petäjä, H. Junninen, D. R.Worsnop and N. M. Donahue (2011). Quantification of the volatility of secondary organic compounds in ultrafine particles during nucleation events. *Atmos. Chem. Phys.* **11**, 9019.

Riipinen, I., T. Yli-Juuti, J. R. Pierce, T. Petäjä, D. R. Worsnop, M. Kulmala and N. M. Donahue (2012). The contribution of organics to atmospheric nanoparticle growth. *Nature Geoscience* 5, 453.

Smith, J. N., K. C. Barsanti, H. R. Friedli, M. Ehn, M. Kulmala, D. R. Collins, J. H. Scheckman, B. J. Williams, and P. H. McMurry (2010). Observations of aminium salts in atmospheric nanoparticles and possible climatic implications, *PNAS* **107**, 6634.

Wexler, A. S. and S. L. Clegg (2002). Atmospheric aerosol models for systems including the ions H+, NH4+, Na+, SO42−, NO3−, Cl−, Br− and H2O. *J. Geophys. Res.* **107**, No. D14, art. no. 4207.

LONG TERM MODELLING OF NEW PARTICLE FORMATION AND GROWTH IN A BOREAL FOREST SITE

L. ZHOU[1], M. BOY[1], D. MOGENSEN[1], T. NIEMINEN[1], S. SMOLANDER[1] and M. KULMALA[1]

[1]Division of Atmoshperic Sciences, Department of Physics, University of Helsinki, Finland.

[2]Wind Energy Division, Risø National Laboratory for Sustainable Energy, Technical University of Denmark, Denmark

Keywords: Nucleation, particle growth, VOC, PBL, Atmospheric Modelling

INTRODUCTION

Natural and anthropogenic aerosols may have a great impact on climate as they can directly interact with solar radiation and indirectly affect the Earth's radiation balance and precipitation by modifying clouds. In order to quantify the direct and indirect effect, it is essential to understand the complex processes that connect an aerosol particle to a cloud droplet. However, while modern measurement techniques are able to detect particle sizes down to nanometre all the way from ground up to the stratosphere, the data does not serve for all of our needs for understanding the processes. Hence we will demonstrate a modelling approach to investigate the complex processes of aerosols in the atmospheric boundary layer (ABL).

METHODS

SOSAA (model to Simulate the concentration of Organic vapours, Sulphuric Acid, and Aerosols) is a 1D chemical-transport model with detailed aerosol dynamics. It was constructed to study the emissions, transport, chemistry, as well as aerosol dynamic processes in the PBL in and above a canopy [Boy et al., 2011].

As a first application of the model after the aerosol dynamics module was implemented, we tested different nucleation theories by simulating the new particle formation events in year 2010 at SMEAR II station, Finland. Since there has been numerous evidence that condensable organic vapours are the dominant contributors to the aerosol particle growth particularly in regions where biogenic volatile organic compound emissions are high, we also simulated the concentrations of a set of organic compounds and their first reaction products from oxidation [e.g. Kerminen et al. (2000); Sellegri et al. (2005); Boy et al. (2005); Allan et al. (2006); Laaksonen et al. (2008)].

CONCLUSIONS

The results have showed the ability of SOSAA to reconstruct the general behaviour of atmospheric trace gases and new particle formation in a boreal forest environment with reasonable uncertainties. The underestimation in H_2SO_4 concentration during nighttimes supports the view that other production mechanisms of H_2SO_4 exist. It also gives us a hint that the missing mechanisms are not likely to be photochemical driven. The simulations about particle nucleation emphasize the complexity of the phenomenon since there is no single nucleation theory that works all the time. The model also confirmed the importance of organic vapours to particle growth in spite of uncertainties.

As a column model, SOSAA has turned out to be a good tool to study the vertical profile of new particle formation events (Figure 1). Scavenging of background particles before a nucleation event has been observed regularly in the simulations. The deposition velocity has been estimated as strong in the model.
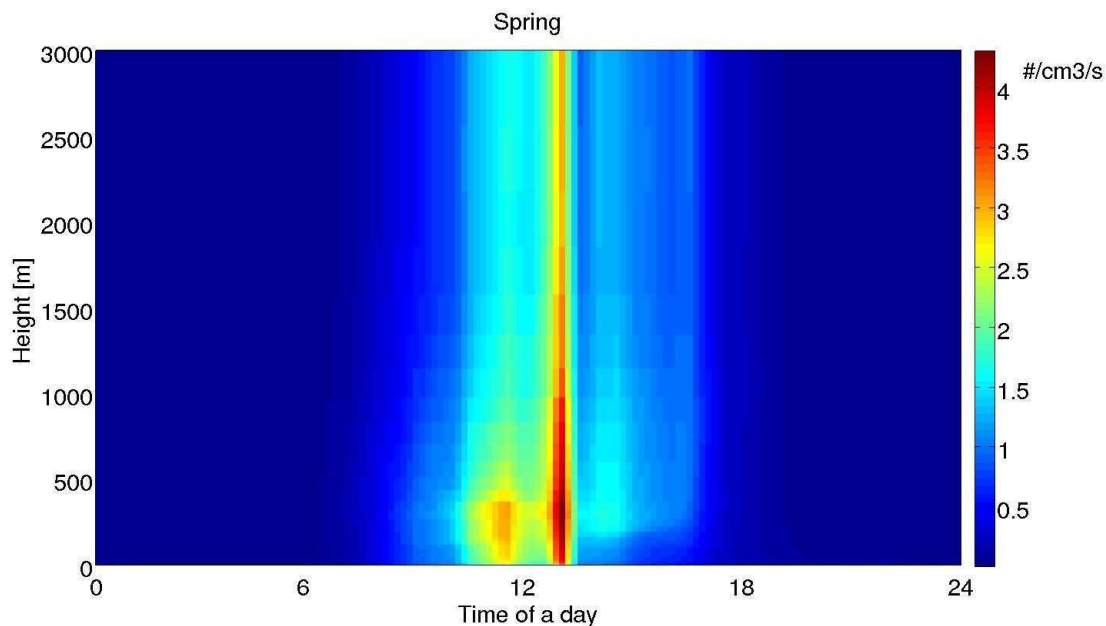
Figure 1: The average nucleation rates in a spring day. The results are from simulations based on kinetic nucleation theory.

REFERENCES

Allan, J. D., M. R. Alfarra, K. N. Bower, H. Coe, J. T. Jayne, D. R. Worsnop, P. P. Aalto, M. Kulmala, T. Hyötyläinen, F. Cavalli, and A. Laaksonen (2006). Size and composition measurements of background aerosol and new particle growth in a Finnish forest during QUEST 2 using an Aerodyne Aerosol Mass Spectrometer, *Atmos. Chem. Phys.* 6, 315-327.

Boy, M., M. Kulmala, T. M. Ruuskanen, M. Pihlatie, A. Reissell, P. P. Aalto, P. Keronen, M. Dal Maso, H. Hellen, H. Hakola, R. Jansson, M. Hanke, and F. Arnold (2005). Sulphuric acid closure and contribution to nucleation mode particle growth, *Atmos. Chem. Phys*. 5, 863{878.

Boy, M., A. Sogachev, J. Lauros, L. Zhou, A. Guenther, and S. Smolander (2011). SOSA - a new model to simulate the concentrations of organic vapours and sulphuric acid inside the ABL - Part1: Model description and initial evaluation, *Atmos. Chem. Phys.* 11, 43-51.

Kerminen, V.-M., A. Virkkula, R. Hillamo, A. S. Wexler, and M. Kulmala (2000). Secondary organics and atmospheric CCN production*, J. Geophys. Res.* 105, 9255 - 9264.

Laaksonen, A., M. Kulmala, C. D. O'Dowd, J. Joutsensaari, P. Vaattovaara, S. Mikkonen, K. E. J. Lehtinen, L. Sogacheva, M. Dal Maso, P. Aalto, T. Petⱥajⱥa, A. Sogachev, Y. J. Yoon, H. Lihavainen, D. Nilsson, M. C. Facchini, F. Cavalli, S. Fuzzi, T. Homann, F. Arnold, M. Hanke, . Sellegr, K., B. Umann,

W. Joukermann, H. Coe, J. D. Allan, M. R. Alfarra, D. R. Worsnop, M.-L. Riekkola, T. Hyøotyløainen, and Y. Viisanen (2008). The role of VOC oxidation products in continental new particle formation, *Atmos. Chem. Phys*. 8, 2657 - 2665.

Sellegri, K., B. Umann, F. Arnold, and M. Kulmala (2005). Measurements of organic gases during aerosol formation events in the boreal forest atmosphere during quest, *Atmos. Chem. Phys*. 5, 373 - 384.

A METHOD FOR ASSIGNING AMS MEASURED NITRATES AND SULPHATES INTO MOLECULAR SUBGROUPS

M. ÄIJÄLÄ[1], H. JUNNINEN[1], M. EHN[1,2], S. HÄKKINEN[1], J. HONG[1],
T. PETÄJÄ[1], M. KULMALA[1] and D. WORSNOP[1,3]

[1]Department of Physics, University of Helsinki, P.O. Box 64, FI-00014 Helsinki, Finland
[2] Institute for Energy and Climate Research (IEK-8), Forschungszentrum Jülich, 52425 Jülich, Germany
[3]Aerodyne Research Inc, Billerica, MA 01821

INTRODUCTION

The chemical composition of aerosols determines their physiochemical properties, which in turn affect e.g. their effects on climate and human health.

The Aerodyne Aerosol Mass Spectrometer (AMS, Canagaratna et al., 2007) is a useful instrument for analysis of chemical composition and quantification of basic aerosol chemical species. However, this important ability of the AMS to quantitatively measure mass comes at a price: the 70 eV electron impact ionization fragments the sampled molecules, often leaving little trace of original molecular composition of the sample compound. The quality of AMS chemical analysis therefore depends significantly on data analysis methods, particularly on the reconstruction of a picture of the original molecular composition.

METHODS

Typical AMS results provide concentrations of the main aerosol chemical species: nitrates, sulphates, ammonia, organics and chlorides. This classification is useful for many general purposes, but for studying aerosol physiochemical properties like particle hygroscopicity or volatility, additional molecular composition information is often required. In this study we present a simple method for assigning AMS main inorganic compounds – sulphates, nitrates and ammonia – into chemically more specific subgroups of sulphuric acid (SA), ammonium sulphate (AS), ammonium nitrate (AN) and organic nitrate. This can provide a way to better connect AMS measured aerosol chemical composition with observations of physiochemical properties from other aerosol instrumentation.

An estimate of ammonium sulphate and ammonium nitrate mass loadings can be derived using some basic chemical assumptions on acid-base reactions in forming salts, and assuming the aerosol is well mixed externally and internally. The latter assumption is often not fulfilled in ambient aerosol, but is a necessary first step in this type of analysis. The calculation itself is inspired by, and closely related to, AMS collection efficiency (CE) estimations (Quinn et al., 2006) and may prove to be of use in trying to better understand AMS CE dependencies on particle properties.

Based on the relative molar amounts of ammonium and sulphate ions ($NH4+$ and $SO4+$) measured by the AMS, all observations can be divided into three distinct cases:

Case 1: the concentration of ammonium ions is lower than the concentration of sulphate ions ([NH4] < [SO4]). All available ammonia is taken up by sulphate to form ammonium bisulphate $NH4HSO4$. The rest of the sulphate ions are assigned to liquid phase sulphuric acid in particles. All nitrate signal is assumed to be from organic sources.

Case 2: [SO4] < [NH4] < 2*[SO4]. All sulphate and ammonia is assigned to ammonium bisulphate or ammonium sulphate. All nitrate signal is attributed to organic nitrate.

Case 3: ([NH4] > 2*[SO4]). The leftover ammonium reacts with nitrogen condensed from gas phase to form ammonium nitrate $NH4NO3$. The rest of nitrate is assumed to be organic.

The estimate was tested on a month-long unit m/z resolution AMS dataset from the SMEAR II station in Hyytiälä, Southern Finland. The obtained inorganic-to-organic nitrate ratio was observed to correlate with the measured NO2+/NO+ fragmentation ratio (Figure 1), commonly used as a marker for the presence of inorganic nitrates. Further comparisons with instruments such as hygroscopicity and volatility tandem DMAs are ongoing to corroborate the results obtained using this method.
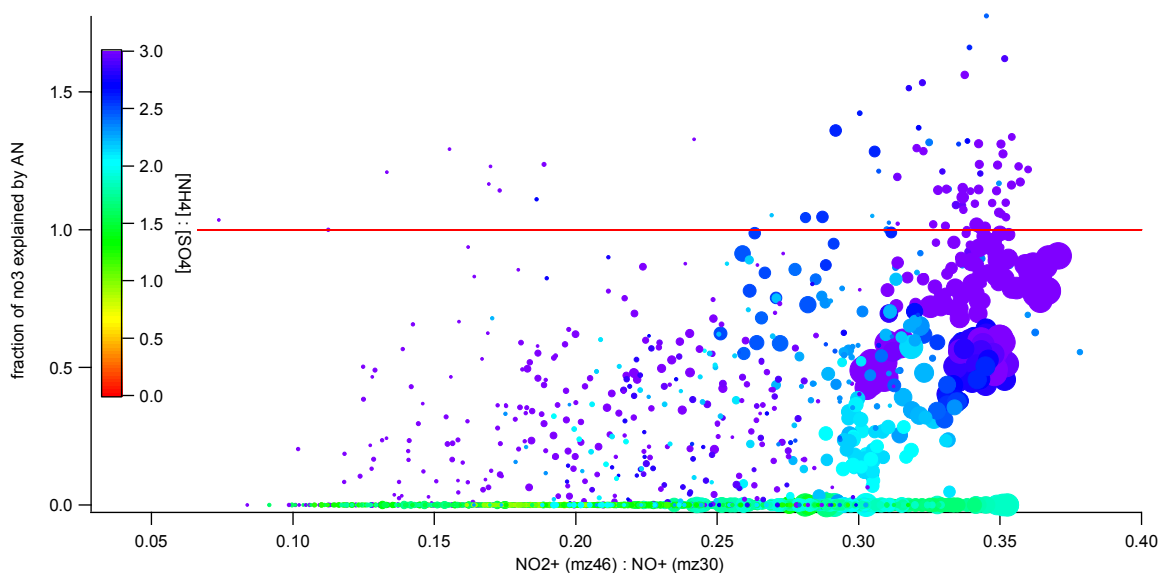

Figure 1. Fraction of nitrate signal explained by calculated ammonium nitrate loading, as a function of NO_2^+ /NO^+ ion ratio. A high NO_2^+/ NO^+ ratio is used as an indication of inorganic nitrate. Marker size describes AMS total nitrate concentration and colour the ratio of $[NH_4]$ to $[SO_4]$.

CONCLUSIONS

In this work we present a simple method for assigning AMS measured sulphates, ammonia and nitrates into more specific subgroups of sulphuric acid, ammonium sulphate, ammonium nitrate and organic nitrate. So far especially the comparison of the calculated organic nitrate amounts to AMS NO_2^+ to NO^+ ratio indicates a promising correspondence. The process of comparing the calculated results with data provided by other aerosol instrumentation is ongoing.

ACKNOWLEDGEMENTS

REFERENCES

Canagaratna M., Jayne J., Jimenez J., Allan J., Alfarra M., Zhang Q., Onasch t., Drewnick F., Coe H., Middlebrook A., Delia A., Williams L., Trimborn A., Northway M., DeCarlo P., Kolb E., Davidovits P., ja Worsnop D.,(2007). Chemical and microphysical characterization of ambient aerosols with the aerodyne aerosol mass spectrometer. *Mass Spectrometry Reviews*. Vol. 26, Issue 2: 185–222.

Quinn P., Bates T., Coffman D., Onasch T., Worsnop D., Baynard T., de Gouw J., Goldan P., Kuster W., Williams E., Roberts J., Lerner B., Stohl A., Pettersson A. and Lovejoy E. (2006). Impacts of sources and aging on submicrometer aerosol properties in the marine boundary layer across the Gulf of Maine. *Journal of Geophysical Research - Atmospheres*. Vol. 111,   Issue D23.